Neuroimaging in Schizophrenia

Marek Kubicki
Martha E. Shenton
Editors

Springer

Neuroimaging in Schizophrenia

Marek Kubicki • Martha E. Shenton
Editors

Neuroimaging in Schizophrenia

Springer

Editors
Marek Kubicki
Department of Psychiatry and Radiology
Brigham and Women's Hospital
Boston, MA
USA

Martha E. Shenton
Department of Psychiatry and Radiology
Brigham and Women's Hospital
Boston, MA
USA

ISBN 978-3-030-35205-9 ISBN 978-3-030-35206-6 (eBook)
https://doi.org/10.1007/978-3-030-35206-6

This Springer imprint is published by the registered company Springer Nature Switzerland AG
The registered company address is: Gewerbestrasse 11, 6330 Cham, Switzerland

Preface

Present-day imaging techniques are powerful diagnostic tools that are routinely employed in many areas of medicine. In most applications, imaging techniques play a more secondary role to the first line of medical care, such as clinical examination or laboratory tests, that guide clinical diagnosis. However, when the organ of interest is less accessible, imaging techniques play a more primary role. This is particularly true for the brain, arguably the most complex of human organs. Indeed, over the last three decades neuroimaging has been the only noninvasive technique to provide insight into the living brain's structure and function. Moreover, these techniques, particularly in the context of neuroscience research applications, have provided an unparalleled ability to study the human brain in both health and disease.

Many of the most advanced neuroimaging techniques have been applied to the study of neuropsychiatric disorders. The application of imaging techniques to neuropsychiatric disorders has not been limited to addressing more traditional research questions (i.e., case–control comparisons in brain structure or function)— many of which could not be addressed prior to the development of such tools—but have also now expanded to encompass studies that are aimed at identifying imaging-based markers for diagnosis, prognosis, or treatment efficacy. Modern-day scanners have the capacity to visualize brain structures with close microscopic precision, in a manner heretofore not possible, allowing advances in the measurement of underlying biological mechanisms such as molecules that can penetrate blood–brain barrier or individual cellular organelles. There is also a strong emphasis to establish big data repositories that would facilitate clinical and/or imaging queries, as well as an emphasis on machine-learning approaches that are capable of learning and improving data analysis iteratively, without supervision. These are just a few of the examples of advances in the field of neuroimaging over the last 30 years, which have changed the landscape of what is possible with respect to understanding the brain.

Neuroimaging techniques have been applied to schizophrenia more than any other psychiatric disorder. In the past, imaging approaches could not quantify the subtle alterations in the brains of individuals with schizophrenia because more sensitive tools were needed. With the advent of advanced imaging tools, we now know a great deal more about schizophrenia. However, the multitude of methods used, in addition to the large number of publications, have made the field quite complex to navigate for clinicians and scientists. Further, at this time, little effort has been made to map these research findings

into a thoughtful and easily accessible library that can succinctly capture the state of the field of neuroimaging in schizophrenia, along with some of the promising inroads for understanding the neurobiology of this devastating disease. In the chapters that follow we highlight some of these efforts. This book is intended to provide an overview of neuroimaging findings in schizophrenia. The target audience includes clinicians, PhD students in psychology or neuroscience, medical students, residents in psychiatry, as well as experienced researchers, who, in the quest for understanding schizophrenia, want an overview in areas in which they have not specialized themselves, but want to understand the state of other imaging modalities.

This book is divided into two parts—Part I provides detailed synopses of imaging techniques that have been employed in schizophrenia research, paired with the conclusions that have been drawn regarding how changes in brain structure and/or function may contribute to schizophrenia. In contrast, Part II provides representative examples of applications in which the use of neuroimaging techniques have made a significant impact. We end with a chapter that, while highlighting the existing shortcomings of the field, suggests possible solutions in the form of formulating future directions for the field of schizophrenia in general and neuroimaging in schizophrenia in particular.

The chapters are written by world-renowned experts in the field whom we asked to address the newest and most important developments in neuroimaging research in schizophrenia. We asked these experts to place these developments within the context of the last 30 years of research. Our purpose was to bring the reader closer to understanding the intricacies, advantages, and disadvantages of various imaging techniques, and to provide a greater understanding of how researchers in the field are using these techniques to test clinical hypotheses, or to develop clinically relevant biomarkers of disease onset, treatment response, or long-term prognosis. Our purpose was also to demonstrate, and to discuss, a path forward that merges imaging and non-imaging measures to build and to test hypotheses that may lead to a more comprehensive understanding of the neurophysiology, neurobiology, or neurotransmission pathologies involved in the clinical picture of schizophrenia. We hope that by showcasing many of the new challenges that the field of neuroimaging in schizophrenia now face, we could provide a roadmap for the future generation of researchers that will guide them toward finding solutions to many of today's questions.

We would like to acknowledge several people without whom this book would not have come to fruition. First of all, we are grateful to all the authors and co-authors of the chapters who agreed without hesitation to be part of this endeavor, and we are grateful also for delivering their thoughtful, comprehensive, and innovative contributions. We would like also to acknowledge our family members: our spouses Zuzanna and George, and our children: Michalina, Anthony, and Jessica for support and inspiration (often scientific). We would also like to thank Elizabeth Rizzoni for her help with editing and formatting. Finally, we acknowledge Harvard Medical School and the Department of Psychiatry at Brigham and Women's Hospital and

Massachusetts General Hospital for supporting our work, the National Institute of Health, and the VA for funding our research, and Springer for giving us the opportunity to showcase the state-of-the-neuroimaging techniques in schizophrenia research.

Boston, MA, USA Marek Kubicki
Boston, MA, USA Martha E. Shenton

Contents

Part I

Imaging Modalities and Their Findings in Schizophrenia

Structural Methods in Gray Matter

1

René C. W. Mandl, Hugo G. Schnack,
Rachel M. Brouwer, and Hilleke E. Hulshoff Pol

Contents

R. C. W. Mandl
Department of Psychiatry, University Medical Center
Utrecht Brain Center, Utrecht, The Netherlands

University Utrecht, Utrecht, The Netherlands

Center for Clinical Intervention and Neuropsychiatric
Schizophrenia Research, Mental Health Centre
Glostrup, Copenhagen University Hospital,
Copenhagen, Denmark
e-mail: r.mandl@umcutrecht.nl

H. G. Schnack · R. M. Brouwer
H. E. Hulshoff Pol (✉)
Department of Psychiatry, University Medical Center
Utrecht Brain Center, Utrecht, The Netherlands

University Utrecht, Utrecht, The Netherlands
e-mail: h.e.hulshoff@umcutrecht.nl

M. Kubicki, M. E. Shenton (eds.), *Neuroimaging in Schizophrenia*,
https://doi.org/10.1007/978-3-030-35206-6_1

1.1 Introduction

The human brain is a complex organ comprising various substructures and has been extensively studied both *in vivo* and *ex vivo*. Before the advent of more recent imaging techniques, knowledge about the possible relation between brain structure and function was primarily based on lesion studies revealing a level of functional specialization for various structures and their connecting networks. It is this structural-functional relationship that forms the basis for the interest in brain structures because by studying various aspects of brain morphology, we obtain a better understanding of the etiology of schizophrenia. The imaging studies in schizophrenia that have been performed since, and the numerous magnetic resonance imaging (MRI) studies in particular, have resulted in important new insights into the disorder. These new insights required acquisition and processing methodology that are described for gray matter in this chapter.

The main strength of MRI is the ability to distinguish between brain gray matter and white matter. Human brain tissue is mainly made up from two types of neuronal cells, namely neurons (including projection neurons and interneurons) and neuroglia (e.g., oligodendrocytes, astrocytes and microglia). Human brain tissue has approximately 10 times more glial cells than neurons. Neurons form large networks and communicate with each other using electrical signals (action potentials). Gray matter predominantly consists of the brain's neuronal cell bodies, glial cells, synapses and capillaries, while white matter predominantly consists of the brain's long-range myelinated axons connecting the distant neuronal cell bodies together forming neural networks. The first imaging studies in schizophrenia used pneumoencephalography and subsequently computerized tomography. However, it was the introduction of MRI in the 1980s that enabled the visualization of the gray and white matter in greater detail.

Another major advantage of MRI over most other medical imaging modalities is that it is non-invasive as the imaging contrasts are based on magnetic properties of water protons (abundant in brain tissue), which can be manipulated using harmless non-ionizing radio-frequency pulses in combination with varying magnetic fields. This makes MRI well-suited to study the brain in large groups of subjects. Different types of imaging contrasts can also be obtained by using various pulse combinations on the same scanner, rendering MRI as one of the most versatile medical imaging modalities to date. Indeed, MRI has been used for more than 30 years, but it is still the subject of active research with new types of acquisitions developed every day.

MRI brain scans are frequently interpreted by the expert judgment of the radiologist to identify possible abnormalities. While this is very successful for the identification of many neurological abnormalities such as vascular anomalies, space occupying lesions, and severe atrophy, the clinical interpretation of brain scans from patients with schizophrenia is usually normal. It thus requires sophisticated image analysis and subsequent quantification of large image datasets to detect the subtle yet clear changes in brain structures in schizophrenia. In addition, comparison with MRI brain scans of healthy individuals is needed to distinguish disorder-related changes from those of normal age and sex related influences. A key issue in such group comparisons is to define the feature(s) of interest in a valid and reliable manner.

In this chapter, we briefly introduce the anatomy of gray matter, MRI methodology, and the

most frequently used MRI contrasts in structural brain imaging. Next, we discuss gray matter tissue in more detail and focus on how gray matter brain structures can be (in part) delineated from MRI images, ranging from laborious manual delineation to modern fully-automated segmentation techniques. For the latter we will pay particular attention to the non-linear transformation step (warping) that is needed to align individual scans with the template brain. This warping is a crucial step in voxel-based and surface-based analysis techniques. This is then followed by a discussion of more complex study designs, and a discussion of the use of machine learning in structural gray matter brain imaging.

1.2 Magnetic Resonance Imaging

Until the 1970s, making 'pictures' of the human brain *in vivo* was limited to the use of pneumoencephalography (an X-ray-based method), which, when applied to schizophrenia research, lead to the important finding that patients had larger ventricles when compared to healthy individuals (Johnstone et al. 1976). The invention of computed tomography (CT) was a major step forward, because of the possibility to reconstruct parts of the human body (including the brain) in three dimensions. However, the quality was still limited because the skull severely hinders the radiation, which carries the information from the brain, to the receiver. The introduction of the use of nuclear magnetic resonance (NMR) in the field of medicine in the 1980s, leading to magnetic resonance imaging (MRI) of the human body, was a major breakthrough. Using MRI, pictures with higher resolution and better contrast between gray and white matter in the brain could be obtained. This led to many important findings, including the finding that a lower gray matter volume of the left superior temporal cortex is associated with a higher degree of thought disorder in patients with schizophrenia (Shenton et al. 1992).

In MRI the signals are created and carried by electromagnetic fields and radio waves. All (brain) matter is made of molecules, which, in turn are formed by atoms (e.g., hydrogen (H), carbon (C), oxygen (O)). Each atom consists of a core, the nucleus, and a 'cloud' of electrons, which determine the chemical properties, i.e., the way the atom forms bonds with other atoms. It is the atom's nucleus that is relevant for MRI. Almost all of the atom's mass is contained in its nucleus, which consists of protons (charged +1) and neutrons (electrically neutral). Although nuclei of several atoms can be used for NMR, we will focus on hydrogen-based NMR, the most widely used form in medical MRI. The hydrogen's nucleus is a single proton and can be thought of as a tiny sphere that rapidly rotates around its axis (Fig. 1.1). Because the proton is electrically charged, this so-called spin causes the nucleus to have a magnetic moment; it can be viewed as a little magnet, with a north pole and a south pole. When not inside a strong magnetic field, the nuclear spins are randomly oriented. When, however, the spins are exposed to the strong magnetic field of the MRI scanner (typically 1.5 or 3 T), they tend to align with it (compare with a compass

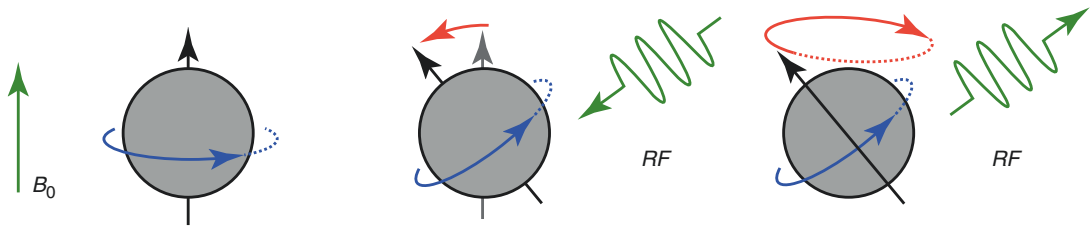

Fig. 1.1 Basic MRI physics. A proton rotates (blue arrow) around its axis (black arrow); its spin is aligned to the external magnetic field (green arrow, B0; left). A radio pulse (green, RF) makes the spin turn away from its alignment (over a certain 'flip angle', red; middle). The proton sends back a radio signal ('echo'), which can be received by the scanner (right)

needle pointing to the earth's magnetic north pole). If an electromagnetic (*cf* FM radio) pulse, produced by an antenna in the scanner, reaches the tissue, the nuclei 'feel' this as a force and the spins are tipped away from alignment, called excitation. Depending on the duration of the pulse, they now point in a direction at a certain angle (the so-called flip angle) with respect to the scanner's magnetic field, and start to make a precession, i.e., a rotating motion around the scanner's magnetic field. The frequency of this precession is called the Larmor frequency. This changing magnetic field produces electromagnetic (radio) waves, so the spin sends back a signal that can be received by an antenna in the scanner. This is in a nutshell how we can obtain signals, i.e., information, from brain matter by MRI. Note that it is a simplified picture of what is truly happening when a scan is made. Since, for now, all nuclei send their signals simultaneously, it would be impossible to trace back the origin of each individual signal. (Parenthetically, one can compare this to locating someone by his/her voice in a large room with many people, when all of them are talking simultaneously). Hence, we need to solve two issues: (1) can we discriminate between signals from different tissue types? and (2) can we discriminate between signals from different sources, i.e., different locations in the brain?

MRI can discriminate between signals from different tissue types. Spins are not alone. They are in an environment packed with other molecules containing atoms with nuclei with spins, all of them behaving like tiny magnets. Interactions between these—moving—particles cause spins to show relaxation: after a while, a spin will return to its original orientation, i.e., aligned with the magnetic field. Not all spins will return at the same moment (*cf.* radioactive decay); after a certain time that we call T1, 63% of the spins return to alignment. T1 relaxation times differ between different tissues and this causes signal strength differences. Collecting the signals at a well-chosen moment after excitation (the so-called echo-time (TE)), will lead to an optimal contrast between two tissues. Optimizing contrast between any pair of tissues will need tuning TE (and other parameters) differently, and not all contrasts can be optimal in one acquisition protocol. T1-weighted scans can provide good contrast between gray and white matter. Of course, this assumes the existence of pure gray and white matter, which is not the case, not biologically (see next section) nor technically (see voxels, below, leading to partial voluming, see Sect. 1.4.1). Another contrast can be made by the so-called T2-weighting, which arises from de-phasing of the precession between the spins in a piece of tissue, due to between-tissue differences in Larmor frequency, caused by local differences in magnetic field strength. T2 is the time after which the spins' in-phase component reduces to 37% of the original value. T2-weighted scans can, for example, be used to provide good contrast between cerebro-spinal fluid (CSF) and brain tissue. Finally, if signals are recorded very fast after excitation, relaxation effects do not play a role and the signal strength is a measure of the proton density (PD-contrast) in the tissue.

MRI can discriminate between signals from different sources, i.e., different locations in the brain. The Larmor frequency depends on the field strength. This dependency can be used to discriminate between signals coming from spins at different locations in the brain. Apart from the big coil producing the static magnetic field, the scanner contains several other coils that can be switched on and off to produce small, rapidly changing magnetic fields, or gradients, the strength of which varies with location, e.g., from left to right. When switched on, the spins' Larmor frequency will vary from left to right, and thus their precession frequency will vary. By tuning to a certain frequency, the receiver can 'listen' to signals originating from a certain location in the brain (*cf.* listening to a certain radio station). The scanner can tune to many different frequencies simultaneously and map the signals to their place of origin. The strength of the signals (see point 1) is converted to brightness values, and the result is an image containing (location, intensity) combinations.

Altogether, making an MRI scan is a complicated task consisting of many, repeated broadcasting of radio pulses and switching on/off

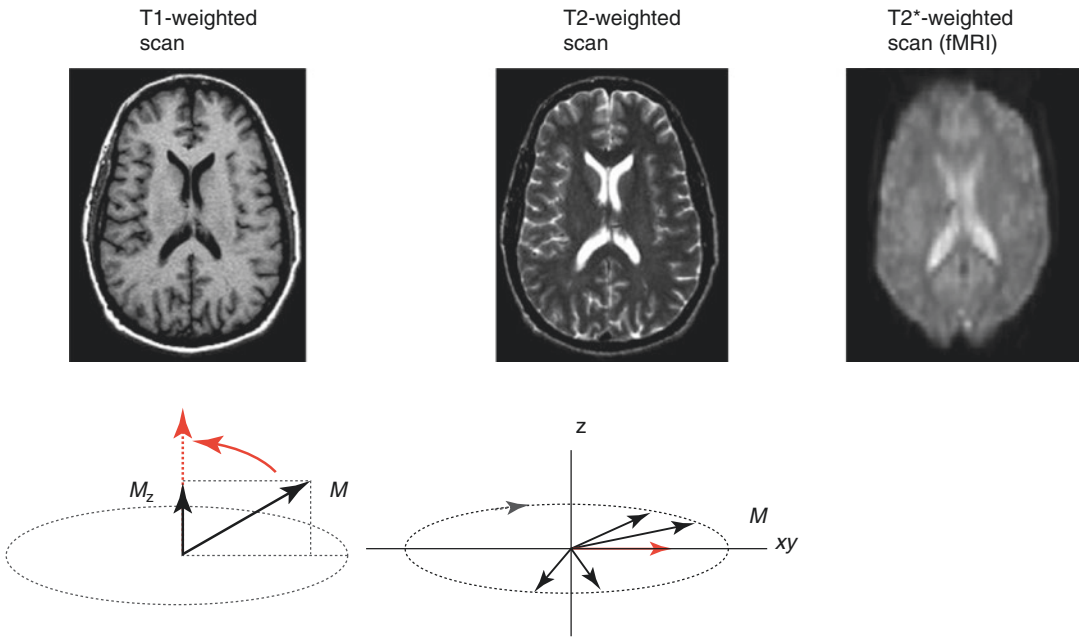

Fig. 1.2 Examples of a T1-weighted scan (left), a T2-weighted scan (middle) and a T2∗-weighted scan (right). The bottom row shows the relaxation process related to T1-relaxation (spins realigning to the scanner magnetic field; left) and T2-relaxation (spins dephasing; right). Differences in relaxation times between tissues lead to different signal strengths at time of measurement (echo time, TE) and thus to tissue contrast

gradient fields (see Stark and Bradley, 1999) for a more detailed description of the physics behind MRI). Moreover, acquisition of signals from different locations is a stepwise procedure, so signals are attributed to elements from a discrete 3-dimensional grid. The resulting image is therefore composed of elements of finite size (typically ~1 mm), the so-called voxels (from volume elements, *cf.* pixels from picture elements). When an acquisition protocol is developed, the MRI technician has to set parameters so as to obtain certain tissue contrasts (e.g., flip angle, echo time (TE), number of echos) and voxel size (Fig. 1.2). It is important to realize that all parameter settings have consequences. For instance, measuring more echos can improve signal-to-noise, but at the cost of longer scan time. Having more detailed images, i.e., with smaller voxels, will decrease signal-to-noise and/or increase scan time. Scanners with higher field strength give larger signals, which can thus be used for either improving contrast-to-noise, decreasing voxel size, or decreasing scan duration.

1.3 Brain Tissue

In the human brain, various types of neurons exist but all neurons have a number of properties in common. They have a cell body (soma), dendrites, and, most frequently, one single axon (Fig. 1.3 left). The cell body of a neuron can generate an action potential, which is transported via the axon to other neurons, sometimes over long distances. This electrical signal is then chemically transferred from the axon's endpoint via synaptic transmission of neurotransmitters to the dendrites, which are extremities (or processes) of other neurons. The axons are often sheathed by a fatty substance named myelin, which enables fast and efficient signal transport. In the central nervous system this myelin sheath is formed by the oligodendrocytes. It is this myelin that is responsible for the white color of the white matter tissue.

Indeed, the gray and white matter in the human brain (Fig. 1.3 right) do not represent different types of neuronal cells but instead represent two

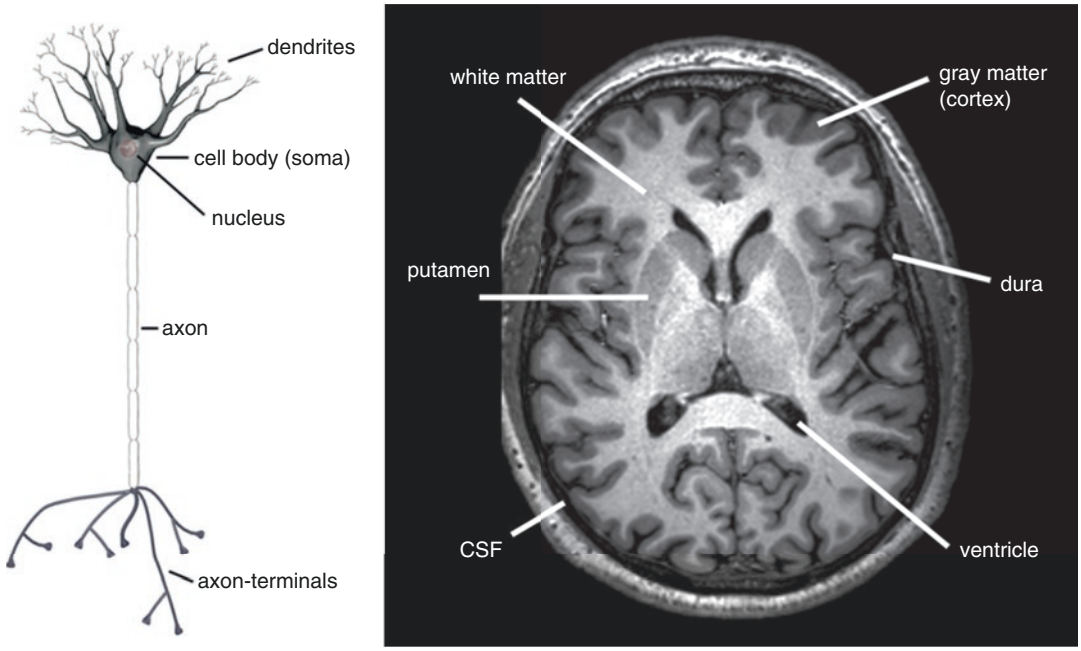

Fig. 1.3 Brain tissue (right), cartoon of a neuron (left). The electrical signal is generated in the cell body. This signal (or action potential) is then transported along the axon. The axon-terminals connect to dendrites from other neuronal cells. From the axon terminals the electrical signal is chemically transmitted to the dendrites of other cells. On the right a T1-weighted image of the brain (transverse view) is shown with gray matter showing up in gray, white matter in white, and cerebrospinal fluid in black

different parts within the neurons, namely the cell bodies (gray matter) and high concentrations of myelinated axons (white matter). This apparent difference in tissue is not only visible by the naked eye in brain slices but can also be observed in conventional MRI scans as several MRI contrasts are highly sensitive to myelin concentration. According to Eickhoff and colleagues (2005a), 77–84% of the T1 and T2 MR signal variation reflects variation in myelin (sheathing the axons) and only 9–16% reflects variation in size and packing density in cell-bodies. The fact that this gray/white matter distinction does not reflect a difference in neuronal cell types but merely a difference in myelin concentration should always be kept in mind when interpreting the results of MR imaging studies reporting differences or changes in gray matter tissue. For instance, when thinning of regions of cerebral cortex is reported during development this could reflect a reduction in the amount of neurons/connections between neurons—known as pruning (Huttenlocher et al. 1982). Alternatively, it may reflect a maturation-related increase in myelination of the axons close to the cortex (so-called encroachment (Paus et al. 2001)), or a combination of both. The brain's gray matter comprises the cerebral cortex, subcortical brain structures, including (amongst others) the putamen, caudate nucleus, thalamus and the limbic system, including the hippocampus and amygdala.

1.3.1 Cerebral Cortex

The cerebral (or neo) cortex is the highly curved, thin (ranging between 1.5 and 5 mm) outer layer of the cerebrum consisting of gray matter (Fig. 1.4). The ridges are called gyri and the grooves or fissures are referred to as sulci. The cellular makeup of the cortex has a clear laminar structure, where each layer can be defined based on the dominant cell type. Based on cytoarchitecture, six major different layers are recognized in

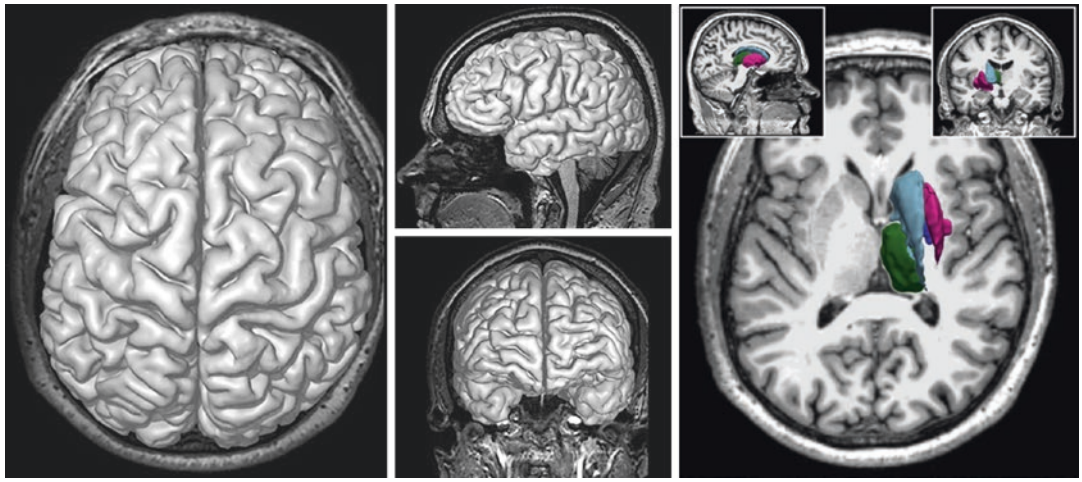

Fig. 1.4 Cortex and subcortical structures. The left pane shows the cortex from three different views. The right pane shows three different views for a few subcortical structures that have been frequently studied in schizophrenia: the right thalamus (green), right caudate (purple), right putamen (light blue) and right pallidum (dark blue)

the human cerebral cortex (with the exception of the motor cortex, which only has five layers) with layer I being the most outer layer and layer VI being the layer adjacent to the white matter.

These six layers (Fig. 1.5) are (I) the molecular layer, (II) the external granule cell layer, (III) the external pyramidal cell layer, (IV) the internal granule cell layer, (V) the internal pyramidal cell layer and (VI) the multiform layer (Kandell 2012: 326). The cytoarchitecture is not constant over the whole cerebral cortex but varies spatially. Regions with a similar architecture can be defined (e.g. Brodmann areas (1909)). Using various post-mortem staining techniques both the cyto- and myeloarchitecture can be studied in detail allowing identification of the regions, which can then be used to construct so-called brain atlases. There is a clear structural-functional relationship between these regions and various brain functions (Zilles and Amunts 2015). Some of these relations have been extensively studied (e.g. visual system, motor system, sensory system), but for higher order functions less information is available and this structural-functional relationship is part of active research.

At present, it is not possible to use MRI *in vivo* to measure cytoarchitecture in detail because conventional MRI contrasts like T1, T2 and PD predominantly provide myeloarchitectonical information rather than cytoarchitectonical information (Zilles and Amunts 2015). Indeed, there does exist a clear relation between myeloarchitecture and cytoarchitecture, but this relationship is not one-to-one (see Fig. 1.5). Also, there appears to be no clear relationship between macroscopic landmarks in the brain (such as locations of sulci and gyri, which can be detected with MRI) and the boundaries of these regions (Zilles and Amunts 2010, 2015). Thus, although MRI can be used to determine the boundaries between white matter and the pial boundary (i.e., the boundary between the most outer cortical layer (layer 1) and the CSF), in general it cannot be used to directly identify the boundaries between the cortical regions as these boundaries *within* the gray matter are defined by differences in cytoarchitecture. To estimate this part of the boundary for these cortical regions, a so-called brain atlas can be used (which will be discussed in the next section).

1.3.2 Subcortical Structures

Compared to the cerebral (neo)cortex, the subcortical brain structures are the evolutionary older brain structures and many of the subcortical structures of the brain have been studied in rela-

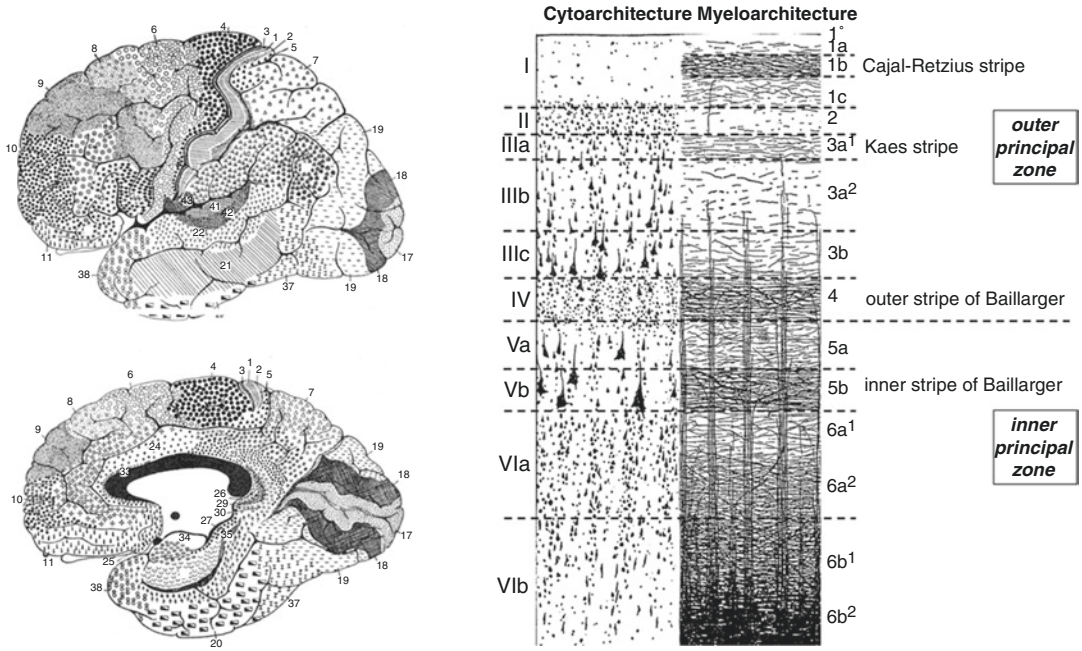

Fig. 1.5 Brodmann atlas and relation between cyto- and myeloarchitecture. The left pane shows the Brodmann areas for human neocortex (illustration from Brodmann (1909: 131)). The right pane shows an example of the relation between cyto- and myeloarchitecture (illustration from Palomero-Gallagher and Zilles (2019) https://creativecommons.org/licenses/by/4.0)

tion to schizophrenia (e.g., thalamus, caudate nucleus). In contrast to the cerebral cortex, the subcortical structures (except for the lateral geniculate nucleus and the superior colliculus (Zilles and Amunts 2015)) have no laminar architecture, albeit some of these substructures can be split up into constituent parts (Kandell 2015). In general, the boundaries of these subcortical structures are based on gray-white/gray-CSF borders only, which makes it relatively easy to reliably detect these borders using MRI.

1.3.3 Limbic System

The limbic system consists of brain structures that have been referred to as paleomammalian cortex. The limbic system is involved in emotion and long-term memory and has been extensively studied in relation to schizophrenia (Roalf et al. 2015; White et al. 2008; Fuller Torrey and Peterson 1974; Bogerts et al. 1985; Aleman and Kahn 2005). The definitions of these structures vary and include both cortical (e.g., hippocampus, para-hippocampal gyrus, and entorhinal cortex) and subcortical structures (e.g., amygdala). Whether the limbic system can be considered a separate system is, however, challenged. Anatomically, it combines a number of structures that lie directly under the cerebral hemispheres that are sometimes challenging to reliably measure with MRI (e.g., the amygdala, which is notoriously complex to delineate).

1.4 Analyses

1.4.1 Tissue Classification

An important part in all the different image analysis methods is tissue classification.

First, it is important to distinguish brain from non-brain tissue (e.g., dura, skull) and within brain matter to distinguish between gray matter, white matter, and CSF. For this task *a priori* knowledge such as location in stereotactic space

and geometric information can be used to determine what is brain tissue and what is not. For example, the location of gray/white matter boundary and the knowledge about the thickness of the cortex and smoothness are constraints used as *a priori* information to define the pial boundary. As the dura (at some locations and especially in younger individuals) may be very close to cortical gray matter, the resolution of the T1-weighted scan should contain sufficiently detailed information to enable successful separation of brain from non-brain tissue. One obvious way to improve the quality of the segmentation is to increase the resolution of the scan. Another solution is to combine T1-weighted scan with scans containing other types of contrast i.e., T2-weighted scans. In T2-weighted scans the main contrast is not found between gray and white matter (as in T1-weighted scans) but between CSF and brain tissue. If the T2-weighted scan is of a sufficiently high resolution then even very narrow gaps (filled with CSF) between dura and gray matter show up as detectable increases in signal intensity thereby aiding in the segmentation of brain tissue.

Tissue classification of brain tissue usually includes some form of (global) histogram separation or clustering of intensities, where differences in signal intensity are used to classify tissue into gray matter, white matter, and CSF. An important requirement, however, is that in the brain region of interest, the intensity values within the tissue classes are much more alike than the intensity values between the tissue classes. For standard T1 acquisitions, this requirement can only be met if the main magnetic B0 field is sufficiently homogeneous. Obtaining a homogeneous B0 field over large regions becomes increasingly difficult with increased magnetic field strengths. Therefore, when this region is large (e.g., the whole brain) additional preprocessing may be required (such as a B0 field inhomogeneity correction (Sled et al. 1998)) to obtain similar intensities within tissue types. Even when the tissue types can be separated by their intensity values there is still the problem of so-called partial voluming. Partial voluming refers to the case where a voxel contains more than one type of tissue yielding an 'in between' intensity value and typically occurs at the boundaries. Depending on the application, one can assign the voxel to one particular tissue type. A solution for instance is to simply assign the voxel to the tissue whose mean signal intensity is closest to that of the voxel. More sophisticated solutions also take information from surrounding voxels into account. Alternatively, one can estimate the fraction of each tissue type in a voxel. Increasing the resolution reduces the relative amount of partial volume voxels but does not completely eliminate them, so the problem of partial voluming will always be there.

1.4.2 Segmentation

Segmentation refers to the process of delineating the brain structure of interest. In some cases (e.g., subcortical structures) a large part of the boundary is defined by tissue type but in other cases (e.g., cortical regions) a part of the boundary is found within gray matter and additional information (e.g., cytoarchitecture) is needed. Because studies in the majority of neuropsychiatric disorders including schizophrenia are often characterized by small effect sizes (requiring large groups to obtain sufficient statistical power), automatic segmentation methods are clearly favored over manual segmentation for reasons of time and resources and often also for reasons of reliability. However, in some cases manual segmentation is required, for instance when creating new brain atlases (Despotović et al. 2015) (see Sect. 1.4.3) or when expert knowledge is needed to manually adjust the boundaries in order to increase the sensitivity of the analysis. In both cases, however, care must be taken that the level of reproducibility of the resulting segmentation is sufficient and (perhaps more importantly) that no bias is introduced. A way to ensure the former is to standardize the delineation or to adjust the automatic delineation (known as editing) as much as possible, to train and test the persons who perform the delineating/editing for consistency, and to discuss and decide on 'problem cases' together with other experts (known as consenting). Blinding the experts for group status is also one way to

minimize the risk of introducing bias. But if, for example, the comparison also includes left versus right brain regions, then it is also necessary to blind the experts for hemisphere (for instance by randomly swap the left and right side) because the quality of manual editing may depend on the location in the image.

To assess the reliability of the manual delineation/editing performed by two-or more image analysts, the inter-rater reliability can be computed using intraclass correlation coefficients (ICC) (Bartko 1966; Koo and Li 2016). To compute an ICC, each of the analysts process the same random subsample of the scans. In addition to a standard correlation an ICC typically also takes bias into account. This bias could be due to one analyst consistently including more tissue into the structure than the other. ICCs can also be used to assess the reliability of a single analyst (i.e., intra-rater reliability). In that case the analyst has to process the data set two or more times. Other possible solution to assess reliability include bland-altman plots (Bland and Altman 1986), providing similar information.

It may seem that systematic bias is only a potential problem in manual segmentation/editing, but this is certainly not the case. For instance, schizophrenia patients tend to move more during MRI acquisition (Pardoe et al. 2016) which may result in more motion artifacts (e.g., blurring, ghosting). These artifacts can lead to poorer segmentation results for the patients and hence a systematic bias. On the other hand, disease-related cortical atrophy in patients leads to a larger space between cortex and dura, which makes separation of the two easier in patients than in healthy controls. Thus in automatic segmentation studies, a careful checking of the analyses and interpretations is necessary. This can be done by comparing overall trends within and between studies.

1.4.3 Brain Atlases

Many of the automatic segmentation pipelines make use of atlases to incorporate *a priori* information (Evans et al. 2012; Toga 1999; Beckmann et al. 2001; Eickhoff et al. 2005b). For instance, when segmenting the cortex in separate regions for which the boundaries cannot be detected from conventional T1 and T2 contrast MRI scans. The basic idea is that a brain to be segmented is mapped to a model brain (or template) for which a segmentation (atlas) is available (See Fig. 1.6), and segmentation rules from the atlas are applied to the target brain. Currently, many different atlases are available where the parcellation may be based on histology, cortical folding, or the topography of the white matter tracts. Unlike the much-used Talairach atlas (Talairach and Tournoux 1988), which was based on the post-mortem dissection of a single human brain, more recent model brains and atlases are based on a set of subjects (usually healthy) in order to take population variability into account (e.g., MNI152, ICBM452 please see Mandal et al. (2012) for an overview). Also, different atlases can be used in a multi-atlas approach to increase segmentation accuracy (Iglesias and Sabuncu 2015).

The choice of model brain can avoid bias in certain population studies. For example, child templates have been developed (Fonov et al. 2011; Sanchez et al. 2012) because using an adult template in a pediatric population would allow for easier warping in the older subjects, thereby introducing bias. Alternatively, study-based atlases that include all subjects in a study can be built, providing a warping that is unbiased for example for disease status (Mazziotta et al. 2001). Additionally, a study-based atlas will have the same contrast as the individual subjects, which should allow for easier warping. In addition to the choice of the atlas, the quality of the mapping (or transformation) is crucial for the quality of the final segmentation as no two brains are alike. Note that this atlas approach assumes that there is a meaningful relationship between macroscopic features (used to steer the warping) and the information contained in the atlas.

1.4.3.1 Linear and Non-linear Transformations

Various types of transformations are applied for which the most basic are linear transformations. Linear transformations are a combination of global transformations such as translation,

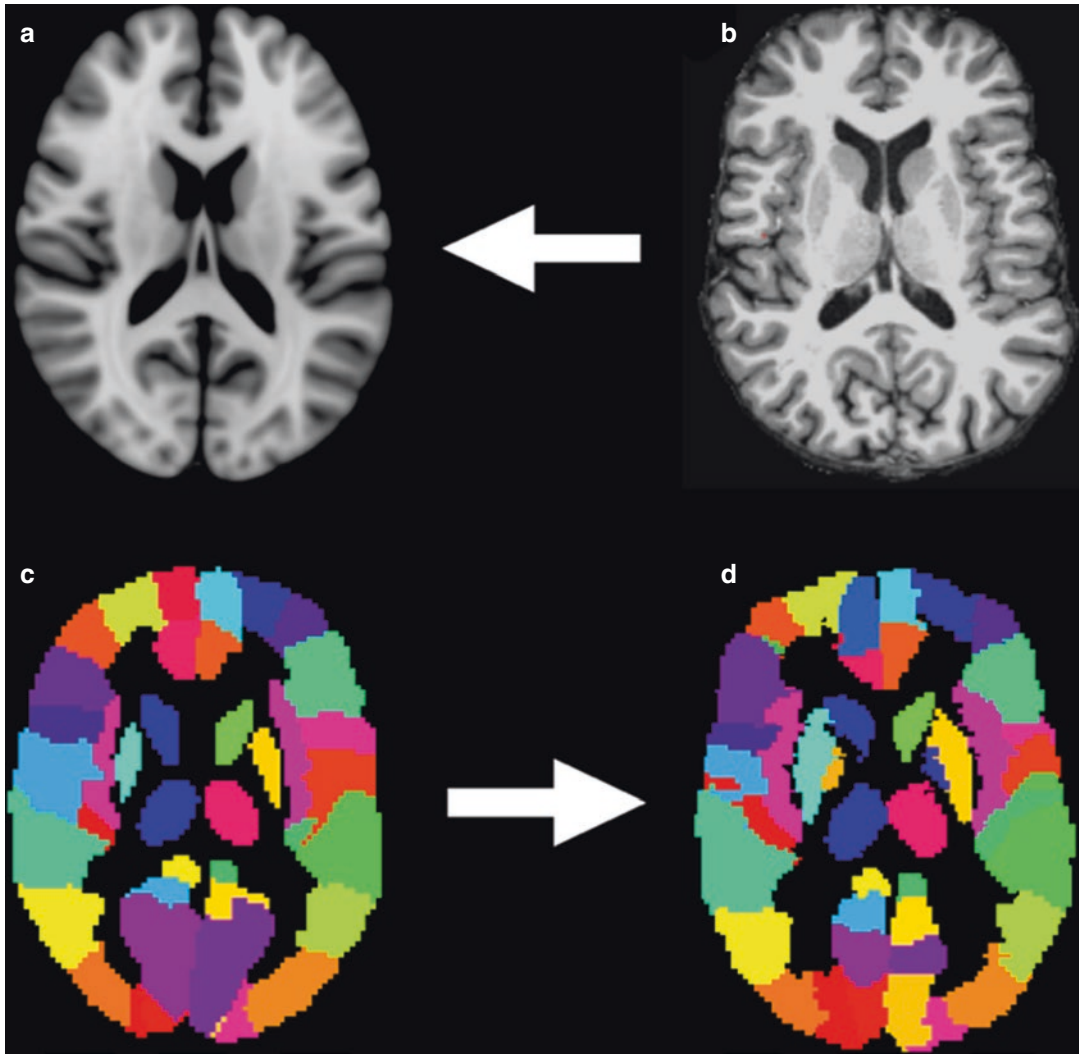

Fig. 1.6 Example of brain atlas application. First, the transformation is computed between an individual brain in native space (**b**) and the model brain (MNI152 (Fonov et al. 2011)) (**a**). The inverse of this transformation is then used to map the model brains atlas (in this example the AAL2 atlas (Tzourio-Mazoyer et al. 2002)) (**c**) to the native space of the individual brain resulting in a segmentation (**d**) for the individual brain

scaling, rotation, and shearing (See Fig. 1.7). These linear transformations only provide a crude mapping between brains, and usually an additional non-linear (warping) transformation is required to increase the quality of the mapping. With warping it is possible to apply local deformations (e.g., shrinking and stretching) to obtain a better mapping. Different types of warping transformations exist, but for this type of image analysis the most frequently used warping is the so-called elastic (or rubber-sheet) warping, where the warping transformation is subject to a smoothness constraint. This means that there are no abrupt differences in deformations between neighboring points allowed (much like a rubber sheet) guaranteeing a (topology-preserving) point-to-point mapping. The latter is important as it ensures that there exists an inverse of a transformation mapping image A to image B, that can be applied to map image B to image A. If the mapping is not one-to-one (as may be the case in

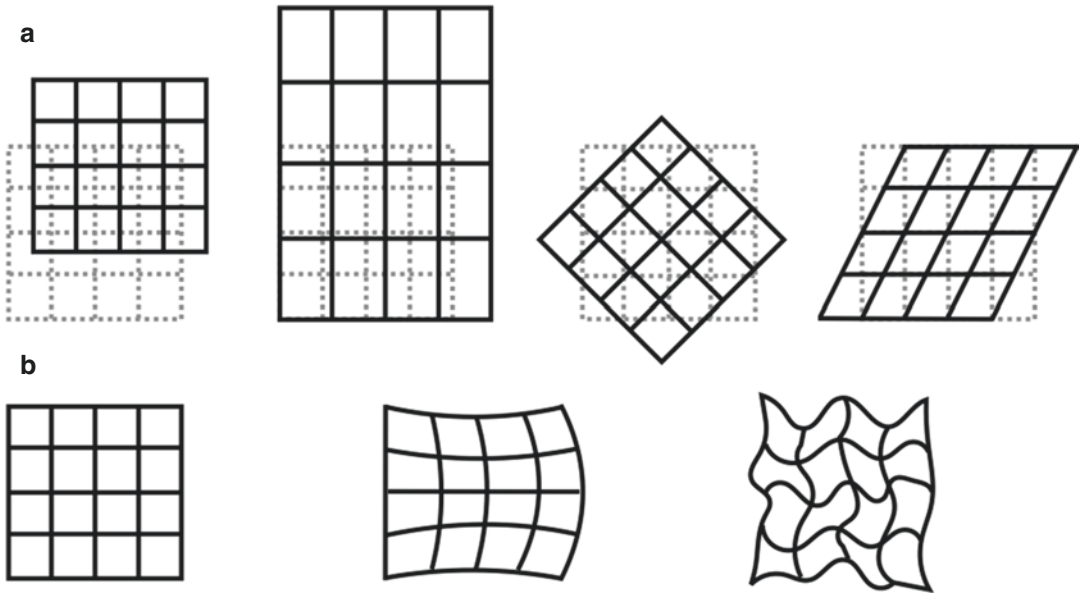

Fig. 1.7 Linear and nonlinear transformations. Examples of 2 dimensional linear transformations are shown in (**a**): translation, scaling, rotation and shearing. In (**b**) examples of non-linear transformations are shown in the middle and right figures. Note that the smoothness constraint is higher in the middle figure than in right figure

so-called fluid-transformations) then two or more points in image A can map to a single point in image B, and, as a consequence, one point in image B should then map to more than one point in A. Compared with the linear transformations, the non-linear transformations allow for a more tailor-made mapping due to the higher number of degrees of freedom but this comes at the price of higher computational workload when searching for the best possible mapping.

A key issue in determining the best possible mapping is to define a similarity metric to rate the quality of the mappings. This similarity metric must be based on macroscopic features (i.e., the features that can be visually detected by an operator) that can be determined in both the model image (in model space) and the image to be transformed to model space. For example, to manually put a brain in so-called Talairach space (Talairach and Szikla 1967) (one of the first stereotactic atlases originally developed for stereotactic neurosurgery) the operator needs to determine features including positions of the anterior commissure (AC) and posterior commissure (PC) on the sagittal mid-slice and the top, front and back of the brain. These features are then used to rotate and piecewise scale the brain to fit the Talairach space. This is a basic procedure including (piecewise) linear transformations only, and the identification of the features can easily be performed by hand. More sophisticated approaches, however, require many more features to compute the high-dimensional non-linear transformations needed to further increase the quality of the fit between the individual brain and the model. Here manual identification of the features is no longer possible simply because of the large number, and because reliable detection of these features by the naked eye is also no longer possible. Examples of such features include voxel intensity values (or higher order features based on these values) and shape characteristics of structures in the brain that can be automatically delineated. An example for the latter are the axon fiber bundles that form the white matter which can be detected by a combination of diffusion-weighted imaging and fiber tracking (see Chap. 3). The shape and begin and end points of the reconstructed tracts can be used as features of interest to guide the mapping.

1.4.4 Voxel-Based Morphometry

If tissue classification provides a measure of the brain structure of interest, the above techniques are sufficient to study patient—control differences. An alternative option is provided by using a voxel-based morphometry (VBM) approach, which does not require an *a priori* hypothesis. Similar to the atlas-based approaches, with VBM all brains are warped to a model brain (Fig. 1.8). Under the assumption of a perfect warping, all brains perfectly fit to the model brain (and to each other) resulting in a true point-by-point (or voxel-by-voxel) correspondence between all the brains (in model space).

However, there are (at least) two reasons why, in practice, the applied warping is less than perfect and the voxel-by-voxel correspondence is not complete. The first reason is that the variability between brains is more complex (for instance due to differences in topology rather than topography) and cannot be mitigated using local stretches. A second reason is that (at least with the VBM approach) we want to keep possible pathologies untouched (i.e., the group differences between patients and controls). Removing these group differences by the warping would defeat its purpose (but see DBA analysis below). This raises the question about the definition of a perfect warping. In the case of VBM, a "perfect" warping would remove all differences that are not of interest and leave all differences of interest untouched.

1.4.4.1 Blurring Kernel

One solution to restore the one-to-one correspondence is to apply a blurring kernel to each of the brain images. When applying a blurring kernel, the information in a voxel is spread out over its neighboring voxels (effectively reducing the image resolution and therefore the degrees of freedom). This averaging over voxels/leaking of information into neighboring voxels mitigates effects of small misalignments because at least part of the information is now available in the right place. Of course, in this way the sensitivity is reduced but robustness is gained. Note, however, that this action only (partly) restores the one-to-one correspondence if it can be assumed that neighboring voxels are

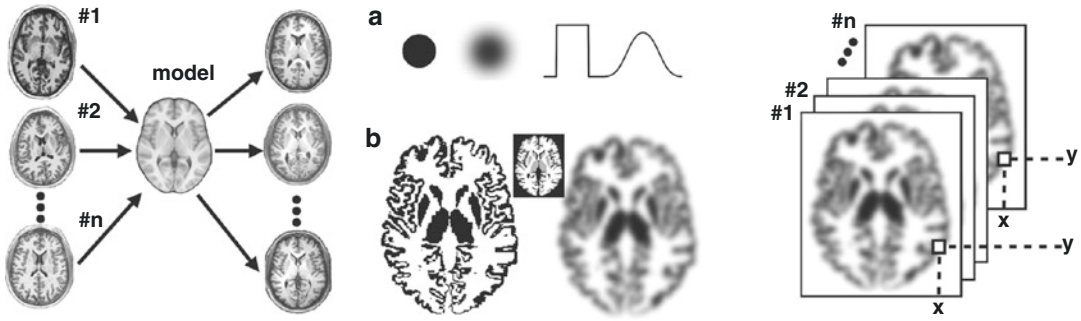

Fig. 1.8 Voxel based analysis (VBM). Left: VBM starts with placing the brains of all n subjects in the study in model space. For each of the n subjects the nonlinear transformation is computed that aligns the subject's brain with the model. By applying the non-linear transformation each brain is warped from native space to model space. Middle: Example of the effect of blurring. When blurring is applied, the signal is spread out over the immediate vicinity (the larger the applied blurring kernel the larger the spreading out of the signal). In A the effect of blurring is shown from the top (left) and a cross-section (right). Note that the total amount of signal does not change. After blurring the signal is spread out over a larger region and, thus as a consequence, the signal in the original region is lower. In B, the effect of blurring is shown when applied to the gray matter segmentation mask. Because the information is spread out over a larger region, the effect of small misalignments is mitigated. Right: After blurring, which (partly) restores the voxel-by-voxel correspondence, it is possible to perform statistics per voxel (e.g., voxel at (x, y)) to detect differences between schizophrenia and healthy comparison subjects. The result of this VBM analysis is a statistical map showing voxels for which there is a significant group difference found in gray matter tissue concentration

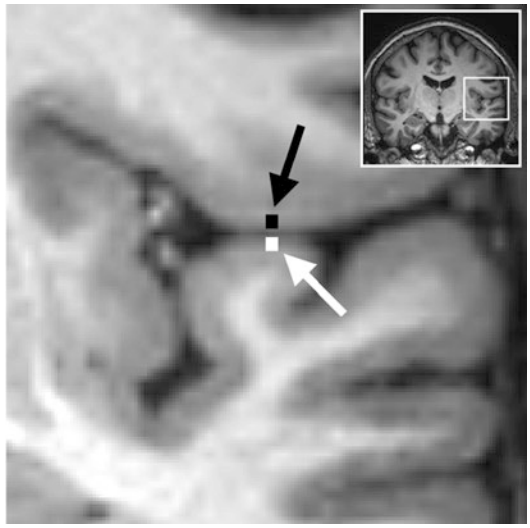

Fig. 1.9 Example for which two neighboring voxels are not functionally related. The Euclidean distance between the black and the white voxel is very small and the application of a 3D blurring kernel would therefore mix the signals from these voxels. However, these voxels are part of different lobes and despite their Euclidean proximity they are not structurally/functionally related

structurally/functionally related (which is not always the case, see Fig. 1.9).

1.4.4.2 Mass Statistical Tests

Given the point-by-point (in this case a voxel-per-voxel) correspondence, one can now perform a statistical test per voxel to test for differences between patients and controls. This does however result in a large number of statistical tests and therefore some form of correction for multiple comparisons (Lindquist and Mejia 2015) is required to keep the type II error (false positives) within bounds. One solution is to use the conservative Bonferroni correction. This correction is—especially after applying a blurring kernel—considered to be too conservative as it assumes that the degrees of freedom is equal to the number of tests (voxels) in the image while the real number of degrees of freedom is much lower (for instance due to the application of the blurring kernel). Therefore, more sophisticated correction methods, such as methods based on the random field theory (Worsley 2007) and the false discovery rate (Benjamini and Hochberg 1995) are often utilized.

1.4.5 Deformation-Based Analysis

An alternative analysis that is still closely related to VBM is deformation-based analysis (DBA). The main difference between the two methods is that with DBA we study group differences in the warping transformations themselves instead of in the warped images. For this approach we simply try to use a warping transformation that removes all the differences. Any group-related differences are then 'captured' in the transformations. In this way one avoids the problem of choosing a proper warping transformation, i.e., a transformation that removes all differences except for the differences of interest, such as is used in VBM. The problem of distinguishing between differences of interest and nuisance is, however, merely shifted to the interpretation part, and as a consequence, the interpretation of the results is more difficult. This may be one of the reasons why VBM is more popular than DBA.

1.4.6 Surface-Based Analysis

VBM and DBA can (and have been) used to analyze the neocortex, but the fact that these analytic techniques are volume based (3D) makes them probably not the best choice because of the highly curved nature of this gray matter structure, combined with the application of the 3D blurring kernel to mitigate the effects of small imperfections in warping. For structures with a high curvature there are regions where the assumption of structural/functional relations between neighboring voxels is violated. In Fig. 1.9 it can be seen that two points on the cortex may be very close to each other in terms of Euclidian distance, but in terms of geodesic (over the surface) distance they are far apart.

For these cases, surface-based analysis (SBA) methods such as FreeSurfer (Fischl et al. 1999) and CIVET (June et al. 2005; MacDonald et al. 2000) are better suited. In contrast to VBM (which is a whole brain analysis), SBA is used specifically to study the cortex. With SBA the cortex is considered a folded sheet where at each point (vertex) information on thickness and curvature is

available, determined from the pial surface and the surface determined by the gray and white matter boundary. Similar to VBM a vertex-by-vertex correspondence can be obtained by warping these folded sheets to a model, which also requires the application of a warping transformation and a blurring kernel. The main difference with VBM, however, is that both the warping and blurring are performed in 2D. The warping is based on information on locations of both gyri and sulci. Using a series of preprocessing steps, a spherical representation of sulci and gyri information is obtained for both the model and brain in native space (see Fig. 1.10). The warping transformation is determined by mapping the surface of the native sphere to the surface of the model sphere in such a way that the gyri and sulci information overlap as much as possible. As with VBA a smoothness constraint is forced on the solution.

Besides vertex-based group comparisons it is also possible to define regions of interest by using an atlas. Note however that this assumes that there is a meaningful relationship between the positions of the gyri and sulci (macroscopic information) and the cytoarchitecture, a relationship that is questionable (Zilles and Amunts 2015).

As there is considerable evidence (e.g., functional specialization) that geodesic proximity is related to functional similarity, the application of 2D blurring can be expected to do a better job in restoring the assumed (now) vertex-by-vertex correspondence required for group analysis. In Fig. 1.10 the various steps of SBA are depicted.

1.4.7 Statistical Shape Analysis of Subcortical Structures

While VBM provides information about local differences, it does not provide any information about differences in more global features of the structure such as volume and shape. While the computation of volume is straightforward once the segmentation for a specific structure is available, the shape analysis requires more sophisticated approach. Analogous to surface-based analysis it may be beneficial to use a more tailor-made type of analysis when studying one or more of cerebral gray matter subcortical structures (Roalf et al. 2015; Shenton et al. 2002; Styner et al. 2004; Coscia et al. 2009; McClure et al. 2013; Johnson et al. 2013; Chakravarty et al. 2015). Luckily, most of these substructures typically have a convex shape with a smooth surface and automatic delineation is therefore relatively easy.

Statistical shape analysis can be loosely divided into two categories, namely those based on local shape descriptors and those based on global shape descriptors (Niethammer et al. 2007). In the first category, similar to SBA, the structure is transformed to a standard coordinate system to obtain a one-to-one correspondence between the structures to be analyzed. Like SBA, this requires the definition of salient features (in SBA the locations of major sulci and gyri) to determine the transformation. These salient features do not have to be part of the structure per se but could also be marked features found in surrounding tissue. This is of particular importance when the structure itself does not hold sufficient marked features to determine the transformation. Of further note, compared to SBA, the transformation is usually of lower degrees of freedom (in many cases a linear transformation will suffice), hence requiring a fewer number of salient features. The shape of the object is then usually represented by a regular grid placed over the structure (similar to the vertices in SBA). Here the features of interest are the positions of the grid elements and group analysis can be performed to detect local differences in shape.

The second category includes descriptors that represent the structure's shape at a global level in a compact way. Often these global descriptors are invariant under translation, rotation, and scaling and can therefore directly be computed without the need to place the structure in standard coordinate system. Examples of such shape descriptors are invariant moments, shape indices, spherical harmonics, and Laplace-Beltrami spectrum (Niethammer et al. 2007). A possible disadvantage of these global descriptors is that the group-differences found are less simple to interpret compared to those found with local shape descriptors.

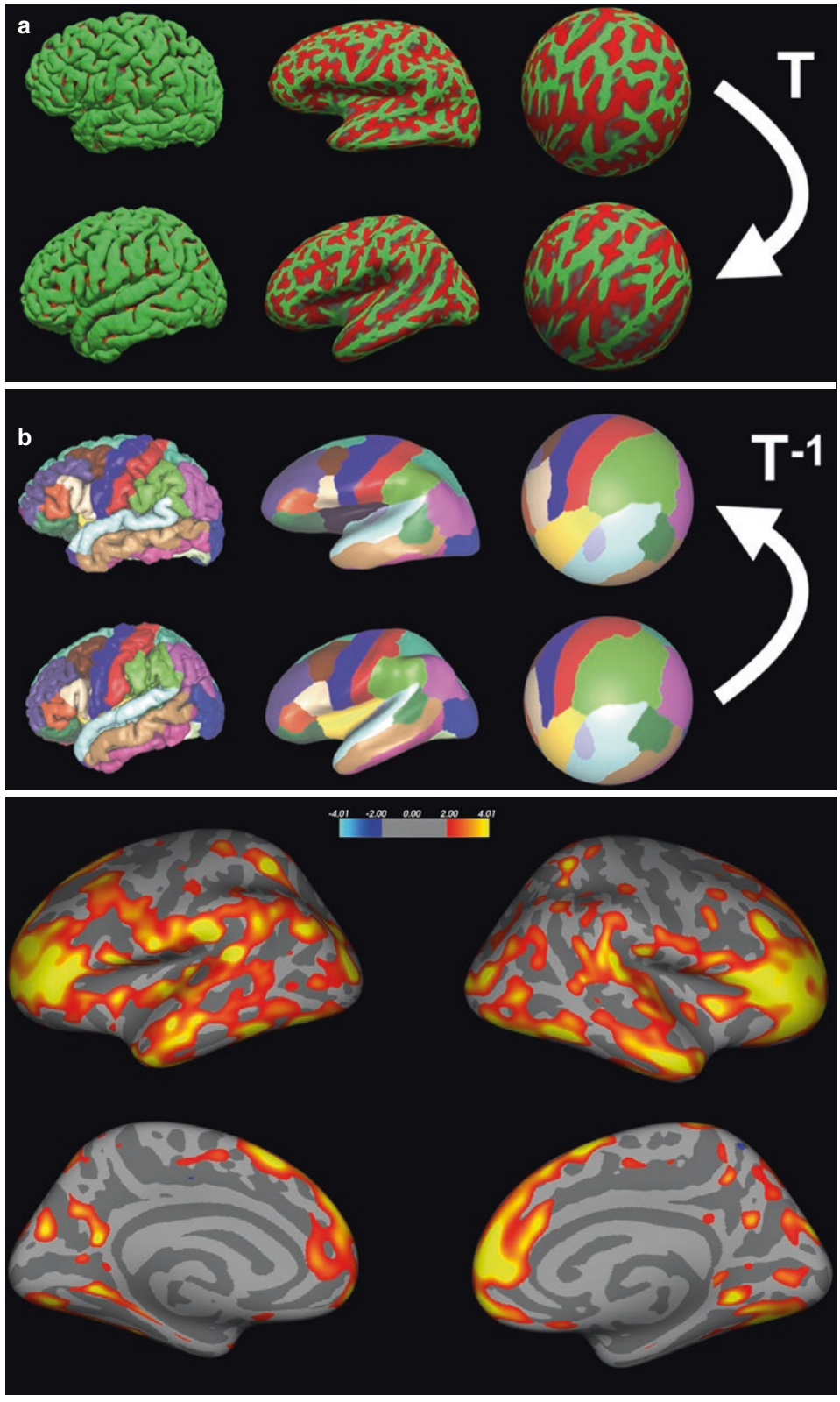
a
T
b
T-1
-4.01
-2.00
0.00
2.00
4.01

Fig. 1.10 Examples of surface-based analysis. In the top pane the computation of the surface-based warping transformation (**a**) and warping of the atlas information on the individual brain is shown (**b**). The computation of the transformation is based on the gyri/sulci pattern and requires the determination of the inner and outer cortical surface (left) for both the individual brain (upper row) and the model brain (lower left). Based on the surface information the gyri/sulci patterns for both the individual brain and the model brain are computed and placed on an inflated version of the brain (middle). Note that the inflated brains for the individual brain and model brain are not the same. Next, the inflated brains are transformed to a sphere allowing efficient computation of a nonlinear transformation (T) that registers the gyri/sucli patterns. To project the atlas information from the model brain to the individual brain the reverse route is followed (**b**). The atlas information available for the model brain (lower left) is projected onto the sphere (lower right) via the inflated brain (lower middle). Using the inverse of the transformation T, the atlas information is transformed to the sphere for the individual brain (right). Finally, this information is projected via the individual inflated brain (upper middle) to the individual brain in native space (upper left). In the bottom pane, an example (unpublished data) of the results of a vertex-based equivalent of a VBM are shown. Here cortical thickness information computed with FreeSurfer in 50 patients with schizophrenia and 50 healthy controls was warped to an average brain and vertex-wise compared. The red-yellow regions depict vertices where the cortex was significantly thinner in patients

1.4.8 Within Gray Matter Imaging

In the previous section we discussed analyses that focus on shape and size characteristics of gray matter structures. There are, however, new techniques that aim to look within the gray matter. Within the field of schizophrenia research, the focus is on the cortex because disease-related cortical thinning is a frequently reported finding, but it is not clear which layers are implicated. One 'obvious' possibility is to use ultra-high field MRI and/or high-performance gradient systems in order to increase image resolution for the standard imaging contrasts (e.g., T1, T2, PD, T2$*$). Given the relation between cytoarchitecture and myeloarchitecture, a finer resolution will allow us to measure variations in myelin content within, for example, the cortex, which can be used to infer cytoarchitectural properties.

In Fig. 1.11 an example of a high-resolution T1-weighted scan is shown that was acquired using ultra-high field (7 T) MRI where the line of Gennari can be detected in the visual cortex. To increase contrast within the cortex, T1-weighted scans can be optimized to be most sensitive to variations in myelin concentrations within in gray matter (Fracasso et al. 2016).

Increasing image resolution to study cortical layers, however, does not always require the use of ultra-high field MRI. Several approaches based on MRI scans at conventional field strengths were developed to study gray matter in more detail. For example, processing techniques can be used to compute so-called average cortical profiles from standard MRI scans acquired at 3 T and are therefore particularly useful in studies where the expected effect size is small and where large groups are required (such as in psychiatric diseases). A recently proposed technique uses a combination of deconvolution and profile alignment to compute one highly detailed profile per cytoarchitecture-based cortical region (Ferguson et al. 2018). In this method, resolution is 'exchanged' in the sense that resolution perpendicular to the cortex becomes higher (the detailed profile) and the resolution parallel to the cortex becomes lower (only one profile per area). See Fig. 1.12 for an example.

Another way to extract more information from gray matter is to use an MRI acquisition with multiple T1 values (Lifshits et al. 2018). The idea behind this approach is that due to differences in cellular makeup, the layers not only differ in signal intensity, but also in T1 relaxation time. By acquiring a series of T1 scans with different echo times it is possible to compute the T1-decay curve in each voxel allowing for computing the actual T1. Another MRI technique, not primarily sensitive to myelin concentration, makes use of the fact that the differences in cellular makeup also lead to differences in the diffusion profiles of water molecules, as can be measured with diffusion weighted imaging. Diffusion weighted imaging is most frequently used to image the brains' white matter, but can also be used to study the gray matter's microarchitecture (Assaf 2019) as the shape and size of the diffusion profile depends on the configuration of cell types in the

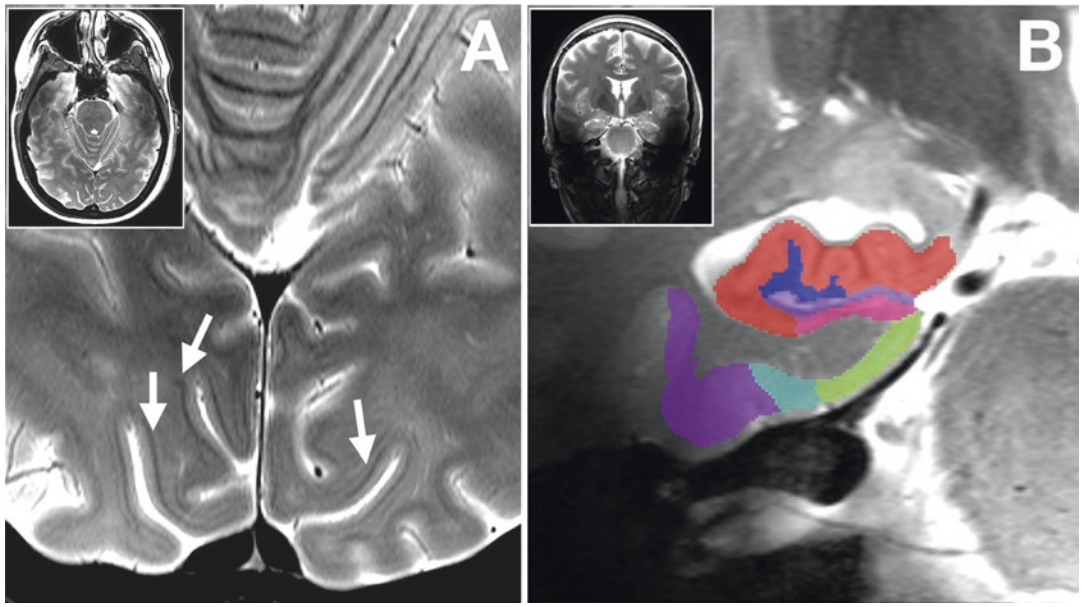

Fig. 1.11 Examples of ultra-high resolution MRI. Left: High-resolution whole brain scan of a T2-weighted image (voxel size 0.5 mm isotropic) showing primary visual cortex acquired at 7 T. Here the line of Gennari, which is a heavily myelinated outer band of Baillarger (exclusive for the visual cortex), is clearly visible as a dark band (white arrows). Right: Example of a high-resolution T2-weighted scan (voxel size, $0.28 \times 0.28 \times 2.0$ mm^3) designed to study the subfields of the hippocampus at 7 T. Automatic segmentation of the hippocampal subfields was obtained using the ashs software package (Yushkevich et al. 2015)

brain tissue. By studying various shape characteristics of the diffusion profile, information about the microstructure from the underlying brain tissue can be inferred. Although the resolution of the last two methods described is usually lower than conventional contrasts, and is currently too low to be used to accurately define cytoarchitectonical boundaries, the fact that these methods may have a more direct connection with cytoarchitecture makes them promising lines of research to pursue.

1.5 Complex Study Designs

1.5.1 Multicenter Studies

There have been several successful attempts to boost power for imaging studies in schizophrenia by combining data collected at different sites throughout the world. Several approaches have been explored. First, imaging data from schizophrenia patients have been made available to the public (e.g., SchizConnect (Wang et al. 2016)) which can be downloaded and explored. Second, imaging (and other types of data) has been brought together in consortia, either by pooling the original data (e.g., GENUS—Genetics of Endophenotypes of Neurofunction to Understand Schizophrenia (Blokland et al. 2018)) or through meta-analysis (e.g., ENIGMA—Enhancing NeuroImaging Genetics through Meta-Analysis; schizophrenia working group (Van Erp et al. 2016)) (see also Chap. 21). All of these approaches have the advantage that data that were first acquired at the individual sites can be reanalyzed in a larger context, making optimal use of the time and money that have been expended for these studies. The mega-analytic approach additionally allows researchers to answer more detailed questions, but harmonization of the different instruments used at each individual site can be a problem. A meta-analytic approach partly solves this problem when each individual site is well-balanced in terms of cases and controls. Finally, there are currently several multi-site collaborations ongoing (e.g., Psyscan (psyscan.edu), Prism (prism-project.eu/en/prism-

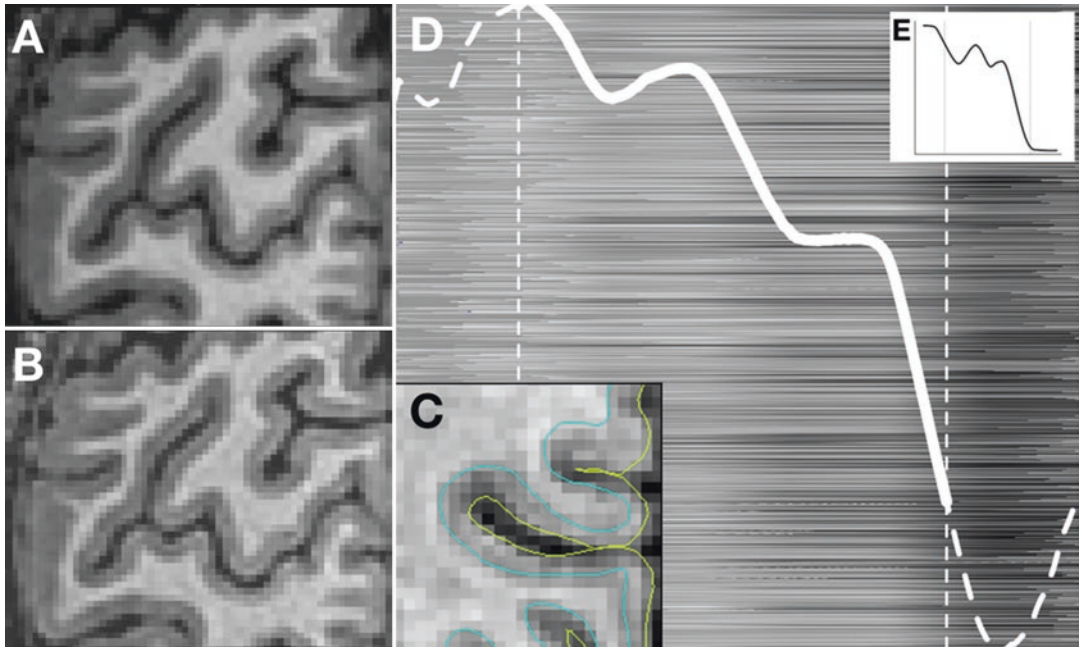

Fig. 1.12 Average cortical profiles. Example of an average cortical profile computed for area V1 from a standard T1-weighted image acquired at 3 T. First, 3D-deconvolution is applied to the original T1-weighted scan (**a**) resulting in a scan with increased detail but also with increased noise levels (**b**). Using information on the inner (white matter/gray matter boundary) and the outer (pial) surface (shown in **c**) obtained with FreeSurfer from the original T1 scan, average profiles can be computed for the complete region. We note that the inner and outer boundaries are computed in 3D and that the result shown on a 2D-slice (as in **c**) appears sub-optimal. All individual profiles (shown in **d**) are then aligned to correct for effects of small misalignments at the boundaries. The vertical white dashed lines represents the white matter/gray matter boundary (left) and the pial boundary (right). Finally, the aligned profiles are averaged yielding one average cortical profile (white profile in shown in **d**). In (**e**) the expected profile for the same region is shown that was created on ultra-high resolution imaging. See Ferguson et al. (2018) for a more detailed explanation of the method

study/)) that collect data as part of collaborations, thereby allowing for harmonization of imaging protocols before the data are collected.

1.5.2 Longitudinal Measurements

Given that the effect sizes in schizophrenia are usually modest, the differences between subjects are often larger than the group differences between patients and controls. It is therefore hard to separate meaningful brain differences from the individual differences that are not related to disease. This is especially the case in questions about whether there are progressive changes in the brain which are more easily answered in longitudinal studies (Brans et al. 2008; van Haren et al. 2007; Hulshoff Pol and Kahn 2008). A powerful design is the use of repeated measures in the same subjects in order to detect changes related to illness duration or ageing effects. In addition, longitudinal studies reduce measurement noise. That said, it is generally challenging to keep subjects willing to participate for longer periods of time in such studies. Also, scanner stability (see above) becomes even more important. Careful randomization of patients and controls can partly solve the latter problem.

1.5.3 Family Designs

1.5.3.1 Family Designs

Understanding the relative influences of genes and environment on differences in human brain structure are important for understanding the

dynamics of brain development and disease risk (see also Chap. 15). The family design, and in particular the twin model, is a powerful approach for determining the relative contributions of genetic influences and common and unique environmental influences on variation in brain structures and their common origin with disease liability (Rijsdijk et al. 2005). Moreover, morphologic findings in twins can be extended to singleton populations (Hulshoff Pol et al. 2002).

Using the family design, important insight into the contributions of familial influences to brain structure in schizophrenia have been revealed (Moran et al. 2013). Gray matter deficits observed in schizophrenia patients are in part also found in their first-degree relatives, and to a larger extent in monozygotic co-twins than in dizygotic co-twins (Moran et al. 2013; Baare et al. 2001; Hulshoff Pol et al. 2012; Bohlken et al. 2015), suggesting a shared genetic basis for both the liability for schizophrenia and gray matter deficits. Importantly, age-related *changes* in brain structures, such as in cortical thickness, are also partially genetically determined (Brans et al. 2010; Brouwer et al. 2017; Teeuw et al. 2019). This is relevant to schizophrenia where the extent of brain tissue loss over time based on longitudinal MRI is supported by findings from post-mortem studies (Hulshoff Pol and Kahn 2008). Longitudinal modeling of brain measures in twin pairs discordant for schizophrenia has also shown that genes for schizophrenia overlap with genes for brain volume *change* (Brans et al. 2008) and cortical thickness *change* (Hedman et al. 2016). These findings provide important directions for further research into the specific genetic and environmental factors implicated in schizophrenia.

1.6 Analysis of Derived Measures

1.6.1 Which Brain Measures Should Be Used?

We have reviewed a multitude of different ways in which structural MRI scans can be processed to obtain information about the brain's gray matter. This information ranges from global measures, where the gray matter properties are summarized into a single variable, e.g., total gray matter volume, to local measures, where the latter provide detailed information about gray matter, e.g., gray matter thickness at a certain position on the cortex. It should be clear by now that all of these quantitative measures are estimates, with different precision and accuracy. For instance, estimates of local cortical thickness from high-resolution MRI scans can be influenced by noise in the scan, which can interfere with the triangular net reconstruction of the cortical interfaces from which the distance is calculated. Conversely, local voxel-based gray matter volumetric information might be less accurate, since the procedure does not lead to well-defined measures ('concentration', 'density', 'presence' of gray matter, depending on a number of parameters such as kind of non-linear transformation technique and amount of deformation; amount of blurring).

Global measures, or more generally, measures of larger regions of the brain, are more reliable (or stable), than local measures, due to the summation (or averaging) effect that tends to cancel out (random) noise. The measures that need more complex reconstructions (shape analysis, cortical surface), however, tend to be less reliable (Schnack et al. 2010). A measure such as local cortical thickness has the advantage that it is clear what it is estimating: the distance from the cortical surface to the gray/white matter interface, while the shape of the hippocampus or gray matter density at some point in the brain is a much less clear measure. The bottom line is that from the many possible ways information can be retrieved from the brain image, the researcher should choose the 'best' one by balancing the advantages and disadvantages of the different approaches. This decision should be based on which measure is best suited to answer the research question, and on whether or not the sample is large enough to afford high-resolution measures.

1.6.2 From Group Analysis to Individual Predictions: Statistics and Machine Learning

Until now, when examining different image processing techniques, we referred to whether or not there would be a difference between patients and controls for a certain measure without actually stating what we meant by 'a difference between patients and controls'. Here, what is generally meant is a difference at the group-level, that is, a difference between the mean of patient values and the mean of control values. However, if there is large variation in values for the individual subjects—more precisely, if the spread of the values is large compared to the mean difference—this difference is quite meaningless. One needs statistics, e.g., a t-test, to determine whether or not the observed difference is 'significant' or could have happened by chance. If there is a large overlap in values between patients and controls, the measure used is not suitable as a marker for discriminating between patients and controls. It is, in other words, not a biomarker. However, why should we investigate only one measure (be it a voxel or total volume) at one time? In brain disorders, such as schizophrenia, morphological differences have been found throughout the brain (Haijma et al. 2013) and one could analyze brain measures in a multivariate way to detect patterns in brain morphology that are different between patients and controls. Examples of such multivariate techniques are principal component analysis (PCA), linear discriminant analysis (LDA), and partial least squares (PLS). The next step is to use an algorithm and have the computer detect which combination of measures ('features'), or pattern, best discriminates patients from controls. Such a procedure of training an algorithm and testing it—in data not used for training—is incorporated in machine learning. When applied to local (e.g., voxel-wise or vertex-wise) gray matter measures of a set of patients and controls, the result can be a discriminative 'map' in which each feature has been attributed a weight, reflecting its relative importance in the classification of patients and controls. Most popular machine learning algorithms include support vector machines (SVM) and random forests. In addition to being a multivariate technique to assess differences between patients and controls, machine learning models can also predict disease status for the individual patient. The application of machine learning methods to anatomical brain scan data to separate schizophrenia patients from healthy subjects has yielded accuracies between 70 and 90% (Kambeitz and Koutsouleris 2014). However, some studies used small datasets, and the classification models built from these sets are prone to overfitting. Indeed, a negative effect of sample size on accuracy has been found (Schnack and Kahn 2016). Large, multicenter datasets are thus needed to build accurate and reliable classification models using machine learning. Recently, using such approaches, imaging markers were found to predict functional outcome in patients (Koutsouleris et al., 2018), thus holding promise for potential future clinical applications of such methods in patients to aid in prevention, treatment and hopefully recovery.

Summary

- MRI is a brain image modality that allows for the inclusion of large groups of subjects which are needed to obtain sufficient statistical power to compare patients and healthy comparison subjects even if the effect sizes are small.
- With T1-weighted MRI, differences in myelin concentration are more predominantly observed than differences in cell types. Thus in this context, gray and white matter brain tissue refer to tissue with high and low concentrations of myelin.
- The relation between brain structure and brain function forms the basis for interest in brain structures because by studying various aspects of the structures we obtain a better understanding of the etiology of schizophrenia.

- Where there are large datasets, fully automatic analysis of the various gray matter structures is preferred.
- Multi-center initiatives are instrumental for obtaining sufficiently large subject samples.
- Machine learning may be used to translate group findings to individual predictions.

References

Aleman A, Kahn RS. Strange feelings: do amygdala abnormalities dysregulate the emotional brain in schizophrenia? Prog Neurobiol. 2005;77:283–98.

Assaf Y. Imaging laminar structures in the gray matter with diffusion MRI. Neuroimage. 2019;197:677–88.

Baare WFC, Hulshoff-Poll HE, Boomsma DI, Posthuma D, de Geus EJC, Schnack HG, et al. Quantitative genetic modeling of variation in human brain morphology. Cereb Cortex. 2001;11(9):816.

Bartko JJ. The intraclass correlation coefficient as a measure of reliability. Psychol Rep. 1966;19(1):3–11.

Beckmann N, Mueggler T, Allegrini PR, Laurent D, Rudin M. Maps of the brain. Anat Rec. 2001;265(2):37–53.

Benjamini Y, Hochberg Y. Controlling the false discovery rate: a practical and powerful approach to multiple testing. J R Stat Soc Ser B. 1995;57(1):289–300.

Bland JM, Altman DG. Statistical methods for assessing agreement between two methods of clinical measurement. Lancet. 1986;327:307–10.

Blokland GAM, del Re EC, Mesholam-Gately RI, Jovicich J, Trampush JW, Keshavan MS, et al. The Genetics of Endophenotypes of Neurofunction to Understand Schizophrenia (GENUS) consortium: a collaborative cognitive and neuroimaging genetics project. Schizophr Res. 2018;195:306–17.

Bogerts B, Meertz E, Schönfeldt Bausch R. Basal ganglia and limbic system pathology in schizophrenia: a morphometric study of brain volume and shrinkage. Arch Gen Psychiatry. 1985;42(8):784–91.

Bohlken MM, Brouwer RM, Mandl RCW, Van den Heuvel MP, Hedman AM, De Hert M, et al. Structural brain connectivity as a genetic marker for schizophrenia. JAMA Psychiat. 2015;73(1):1–9.

Brans RGH, Van Haren NEM, Van Baal GCM, Schnack HG, Kahn RS, Hulshoff Pol HE. Heritability of changes in brain volume over time in twin pairs discordant for schizophrenia. Arch Gen Psychiatry. 2008;65(11):1259–68.

Brans RGH, Kahn RS, Schnack HG, van Baal GCM, Posthuma D, van Haren NEM, et al. Brain plasticity and intellectual ability are influenced by shared genes. J Neurosci. 2010;30(16):5519–24.

Brodmann K. Vergleichende Lokalisationlehre der Grosshirnrinde. Leipzig: Johann Ambrosius Barth; 1909.

Brouwer RM, Panizzon MS, Glahn DC, Hibar DP, Hua X, Jahanshad N, et al. Genetic influences on individual differences in longitudinal changes in global and subcortical brain volumes: results of the ENIGMA plasticity working group. Hum Brain Mapp. 2017;38(9):4444–58.

Chakravarty MM, Rapoport JL, Giedd JN, Raznahan A, Shaw P, Collins DL, et al. Striatal shape abnormalities as novel neurodevelopmental endophenotypes in schizophrenia: a longitudinal study. Hum Brain Mapp. 2015;36(4):1458–69.

Coscia DM, Narr KL, Robinson DG, Hamilton LS, Sevy S, Burdick KE, et al. Volumetric and shape analysis of the thalamus in first-episode schizophrenia. Hum Brain Mapp. 2009;30(4):1236–45.

Despotović I, Goossens B, Philips W. MRI segmentation of the human brain: challenges, methods, and applications. Comput Math Methods Med. 2015;2015:450341.

Eickhoff S, Walters NB, Schleicher A, Kril J, Egan GF, Zilles K, et al. High-resolution MRI reflects myeloarchitecture and cytoarchitecture of human cerebral cortex. Hum Brain Mapp. 2005a;24(3):206–15.

Eickhoff SB, Stephan KE, Mohlberg H, Grefkes C, Fink GR, Amunts K, et al. A new SPM toolbox for combining probabilistic cytoarchitectonic maps and functional imaging data. Neuroimage. 2005b;25(4):1325–35.

Evans AC, Janke AL, Collins DL, Baillet S. Brain templates and atlases. Neuroimage. 2012;62:911–22.

Ferguson B, Petridou N, Fracasso A, van Den Heuvel MP, Brouwer RM, Hulshoff Pol HE, et al. Detailed T1-weighted profiles from the human cortex measured in vivo at 3 Tesla MRI. Neuroinformatics. 2018;16(2):181–96.

Fischl B, Sereno MI, Dale AM. Cortical surface-based analysis: II. Inflation, flattening, and a surface-based coordinate system. Neuroimage. 1999;9:195–207.

Fonov V, Evans AC, Botteron K, Almli CR, McKinstry RC, Collins DL. Unbiased average age-appropriate atlases for pediatric studies. Neuroimage. 2011;54(1):313–27.

Fracasso A, Van Veluw SJ, Visser F, Luijten PR, Spliet W, Zwanenburg JJM, et al. Lines of Baillarger in vivo and ex vivo: myelin contrast across lamina at 7 T MRI and histology. Neuroimage. 2016;133:163–75.

Fuller Torrey E, Peterson MR. Schizophrenia and the limbic system. Lancet. 1974;304:942–6.

Haijma SV, Van Haren N, Cahn W, Koolschijn PCMP, Hulshoff Pol HE, Kahn RS. Brain volumes in schizophrenia: a meta-analysis in over 18 000 subjects. Schizophr Bull. 2013;39(5):1129–38.

Hedman AM, van Haren NEM, van Baal GCM, Brouwer RM, Brans RGH, Schnack HG, et al. Heritability of cortical thickness changes over time in twin pairs discordant for schizophrenia. Schizophr Res. 2016;173(3):192–9.

Hulshoff Pol HE, Kahn RS. What happens after the first episode? A review of progressive brain changes in chronically ill patients with schizophrenia. Schizophr Bull. 2008;34:354–66.

Hulshoff Pol HE, Posthuma D, Baare WF, De Geus EJ, Schnack HG, van Haren NE, et al. Twin-singleton differences in brain structure using structural equation modelling. Brain. 2002;125(Pt 2):384–90.

Hulshoff Pol HE, Van Baal CM, Schnack HG, Brans RGH, Van Der Schot AC, Brouwer RM, et al. Overlapping and segregating structural brain abnormalities in twins with schizophrenia or bipolar disorder. Arch Gen Psychiatry. 2012;69(4):349–59.

Huttenlocher P, de Courten C, Garey L, Van der Loos H. Synaptogenesis in human visual cortex-evidence for synapse elimination during normal development. Neurosci Lett. 1982;33(3):247–52.

Iglesias JE, Sabuncu MR. Multi-atlas segmentation of biomedical images: a survey. Med Image Anal. 2015;24(1):205–19.

Johnson SLM, Wang L, Alpert KI, Greenstein D, Clasen L, Lalonde F, et al. Hippocampal shape abnormalities of patients with childhood-onset schizophrenia and their unaffected siblings. J Am Acad Child Adolesc Psychiatry. 2013;52(5):527–36.e2.

Johnstone E, Frith CD, Crow TJ, Husband J, Kreel L. Cerebral ventricular size and cognitive impairment in chronic schizophrenia. Lancet. 1976;308(7992):924–6.

June SK, Singh V, Jun KL, Lerch J, Ad-Dab'bagh Y, MacDonald D, et al. Automated 3-D extraction and evaluation of the inner and outer cortical surfaces using a Laplacian map and partial volume effect classification. Neuroimage. 2005;27(1):210–21.

Kambeitz J, Koutsouleris N. Neuroimaging in psychiatry. Multivariate analysis techniques for diagnosis and prognosis. Nervenarzt. 2014;85(6):714–9.

Kandell ER, Schwartz JH, Jessel TM. Principles of neural science. International edition. New York: McGraw-Hill; 2012.

Kandell. The effects of brief mindfulness intervention on acute pain experience: an examination of individual difference. In: Principle of neural science. Vol. 1. 2015. p. 1689–99.

Koo TK, Li MY. A guideline of selecting and reporting intraclass correlation coefficients for reliability research. J Chiropr Med. 2016;15(2):155–63.

Koutsouleris N, Kambeitz-Ilankovic L, Ruhrmann S, Rosen M, Ruef A, Dwyer DB, et al. PRONIA consortium. Prediction models of functional outcomes for individuals in the clinical high-risk state for psychosis or with recent-onset depression: a multimodal, multisite machine learning analysis. JAMA Psychiatry. 2018;75:1156–72. https://doi.org/10.1001/jamapsychiatry.2018.2165.

Lifshits S, Tomer O, Shamir I, Barazany D, Tsarfaty G, Rosset S, et al. Resolution considerations in imaging of the cortical layers. Neuroimage. 2018;164:112–20.

Lindquist MA, Mejia A. Zen and the art of multiple comparisons. Psychosom Med. 2015;77(2):114–25.

MacDonald D, Kabani N, Avis D, Evans AC. Automated 3-D extraction of inner and outer surfaces of cerebral cortex from MRI. Neuroimage. 2000;12(3):340–56.

Mandal PK, Mahajan R, Dinov ID. Structural brain atlases: design, rationale, and applications in normal and pathological cohorts. J Alzheimers Dis. 2012;31:S169–88.

Mazziotta J, Toga A, Evans A, Fox P, Lancaster J, Zilles K, et al. A probabilistic atlas and reference system for the human brain: International Consortium for Brain Mapping (ICBM). Philos Trans R Soc B Biol Sci. 2001;356:1293–322.

McClure RK, Styner M, Maltbie E, Lieberman JA, Gouttard S, Gerig G, et al. Localized differences in caudate and hippocampal shape are associated with schizophrenia but not antipsychotic type. Psychiatry Res. 2013;211(1):1–10.

Moran ME, Pol HH, Gogtay N. A family affair: brain abnormalities in siblings of patients with schizophrenia. Brain. 2013;136:3215–26.

Niethammer M, Reuter M, Wolter F-E, Bouix S, Peinecke N, Ko M-S, et al. Global medical shape analysis using the Laplace-Beltrami-Spectrum. In: MICCAI07, 10th International Conference on Medical Image Computing and Computer Assisted Intervention. 2007. p. 882.

Palomero-Gallagher N, Zilles K. Cortical layers: cyto-, myelo-, receptor- and synaptic architecture in human cortical areas. Neuroimage. 2019;197:716–41.

Pardoe HR, Kucharsky Hiess R, Kuzniecky R. Motion and morphometry in clinical and nonclinical populations. Neuroimage. 2016;135:177–85.

Paus T, Collins DL, Evans AC, Leonard G, Pike B, Zijdenbos A. Maturation of white matter in the human brain: a review of magnetic resonance studies. Brain Res Bull. 2001;54:255–66.

Rijsdijk FV, van Haren NEM, Picchioni MM, McDonald C, Toulopoulou T, Pol HEH, et al. Brain MRI abnormalities in schizophrenia: same genes or same environment? Psychol Med. 2005;35(10):1399–409.

Roalf DR, Vandekar SN, Almasy L, Ruparel K, Satterthwaite TD, Elliott MA, et al. Heritability of subcortical and limbic brain volume and shape in multiplex-multigenerational families with schizophrenia. Biol Psychiatry. 2015;77(2):137–46.

Sanchez CE, Richards JE, Almli CR. Age-specific MRI templates for pediatric neuroimaging. Dev Neuropsychol. 2012;37(5):379–99.

Schnack HG, Kahn RS. Detecting neuroimaging biomarkers for psychiatric disorders: sample size matters. Front Psychiatry. 2016;7:50.

Schnack HG, Van Haren NEM, Brouwer RM, Van Baal GCM, Picchioni M, Weisbrod M, et al. Mapping reliability in multicenter MRI: voxel-based morphometry and cortical thickness. Hum Brain Mapp. 2010;31(12):1967–82.

Shenton ME, Kikinis R, Jolesz FA, Pollak SD, LeMay M, Wible CG, et al. Abnormalities of the left temporal lobe and thought disorder in schizophrenia. A quantitative magnetic resonance imaging study. N Engl J Med. 1992;327(9):604–12.

Shenton ME, Gerig G, McCarley RW, Székely G, Kikinis R. Amygdala-hippocampal shape differences in schizophrenia: the application of 3D shape

models to volumetric MR data. Psychiatry Res. 2002;115(1–2):15–35.
Sled JG, Zijdenbos AP, Evans AC. A nonparametric method for automatic correction of intensity nonuniformity in MRI data. IEEE Trans Med Imaging. 1998;17(1):87–97.
Stark DD, Bradley WG. Magnetic resonance imaging. St. Louis: Mosby; 1999.
Styner M, Lieberman JA, Pantazis D, Gerig G. Boundary and medial shape analysis of the hippocampus in schizophrenia. Med Image Anal. 2004;8(3):197–203.
Talairach J, Szikla G. Atlas d'anatomie steroptaxique du telencephale: etudes anatomo-radiologiques. Paris: Masson & Cie; 1967.
Talairach J, Tournoux P. Co-planar stereotaxic atlas of the human brain. New York: Thieme; 1988.
Teeuw J, Brouwer RM, Koenis MMG, Swagerman SC, Boomsma DI, Hulshoff Pol HE. Genetic influences on the development of cerebral cortical thickness during childhood and adolescence in a Dutch longitudinal twin sample: the Brainscale Study. Cereb Cortex. 2019;29(3):978–93.
Toga AW, editor. Brain warping. New York: Academic; 1999.
Tzourio-Mazoyer N, Landeau B, Papathanassiou D, Crivello F, Etard O, Delcroix N, et al. Automated anatomical labeling of activations in SPM using a macroscopic anatomical parcellation of the MNI MRI single-subject brain. Neuroimage. 2002;15(1):273–89.
Van Erp TGM, Hibar DP, Rasmussen JM, Glahn DC, Pearlson GD, Andreassen OA, et al. Subcortical brain volume abnormalities in 2028 individuals with schizophrenia and 2540 healthy controls via the ENIGMA consortium. Mol Psychiatry. 2016;21(4):547–53.
van Haren NEM, Hulshoff Pol HE, Schnack HG, Cahn W, Mandl RCW, Collins DL, et al. Focal gray matter changes in schizophrenia across the course of the illness: a 5-year follow-up study. Neuropsychopharmacology. 2007;32(10):2057–66.
Wang L, Alpert KI, Calhoun VD, Cobia DJ, Keator DB, King MD, et al. SchizConnect: mediating neuroimaging databases on schizophrenia and related disorders for large-scale integration. Neuroimage. 2016;124:1155–67.
White T, Cullen K, Rohrer LM, Karatekin C, Luciana M, Schmidt M, et al. Limbic structures and networks in children and adolescents with schizophrenia. Schizophr Bull. 2008;34:18–29.
Worsley K. Random field theory. In: Friston K, Ashburner J, Kiebel S, Nichols T, Penny W, editors. Statistical parameter mapping: the analysis of funtional brain images. London: Academic; 2007.
Yushkevich PA, Pluta JB, Wang H, Xie L, Ding SL, Gertje EC, et al. Automated volumetry and regional thickness analysis of hippocampal subfields and medial temporal cortical structures in mild cognitive impairment. Hum Brain Mapp. 2015;36(1):258–87.
Zilles K, Amunts K. Centenary of Brodmann's map—conception and fate. Nat Rev Neurosci. 2010;11(2):139–45.
Zilles K, Amunts K. Anatomical basis for functional specialization. In: Uludag K, Ugurbil K, Berliner L, editors. fMRI: from nuclear spins to brain functions. Biological magnetic resonance, vol. 30. Boston, MA: Springer; 2015.

2 Gray Matter Involvement in Schizophrenia: Evidence from Magnetic Resonance Imaging Studies

Sophia Frangou and René S. Kahn

Contents

2.1 Schizophrenia-Related Gray Matter Alterations

A number of analytical approaches have been used to assess case-control differences in structural MRI studies (see Chap. 1 for more details). Univariate analyses of group differences in neuroimaging typically employ either a region-of-interest (ROI) approach or voxel-based morphometry (VBM). In the former, case-control differences are estimated at the level of anatomical regions defined using brain atlases while the latter involves a voxel-wise comparison of

S. Frangou
Department of Psychiatry, Icahn School of Medicine at Mount Sinai, New York, NY, USA

R. S. Kahn (✉)
Department of Psychiatry and Behavioral Health System, Icahn School of Medicine at Mount Sinai, New York, NY, USA
e-mail: rene.kahn@mssm.edu

M. Kubicki, M. E. Shenton (eds.), *Neuroimaging in Schizophrenia*,
https://doi.org/10.1007/978-3-030-35206-6_2

brain tissue concentration or density between two groups. In meta-analyses of ROI-based studies, the pooled effect size of case-control differences is commonly expressed either as Cohen's *d* (Cohen 1977) or Hedges' *g* (Hedges 1981). Meta-analyses of VBM studies examine whether the brain-coordinates of case-control differences derived from the primary literature are statistically likely to cluster within specific brain regions. The Anatomical Likelihood Estimation (ALE) (Eickhoff et al. 2012) and Signed Differential Mapping (SDM) (Radua and Mataix-Cols 2009) are the most widely used algorithms for VBM-based meta-analyses. Univariate analyses, although informative, ignore potential covariation among brain regions or voxels. By contrast multivariate analyses are concerned with the identification of case-control differences in the spatial patterns of brain structural covariation. Several multivariate methods have been employed and these mainly include source based morphometry and machine learning algorithms. Source-based morphometry (SBM) (Xu et al. 2009) extracts spatially independent components (i.e., clusters) from MRI-derived voxelwise measures of gray matter concentration or volume. Machine learning approaches examine the predictive value of brain phenotypes in discriminating patients from healthy individuals and commonly include a recursive feature elimination framework (Guyon et al. 2002; Saeys et al. 2007). Multiple machine learning algorithms are available with support vector machines (SVM), discriminant and sparse canonical analyses, multiple kernel learning, deep learning and multiview learning being the most popular choices (Arbabshirani et al. 2017; Veronese et al. 2013).

2.1.1 Cross-Sectional Studies

2.1.1.1 Univariate Analyses in Patient Samples Unselected for Illness Duration

The consortium for Enhancing NeuroImaging Genetics through Meta-Analysis (ENIGMA) (http://enigma.ini.usc.edu/) is the largest international collaborative initiative in brain imaging. ENIGMA is organized in disorder-specific working groups which aim to quantify case-control differences in brain phenotypes extracted from MRI data using harmonized analysis and quality assurance protocols across all participating sites (Thompson et al. 2014, 2017). The ENIGMA schizophrenia working-group has leveraged the data within the consortium to create one of the largest datasets of gray matter ROIs in patients with schizophrenia and healthy individuals. Studies from the ENIGMA consortium (Chap. 21) have established that schizophrenia is associated with replicable but subtle case-control differences in the volume of subcortical structures (patients = 2028 and healthy individuals = 2540) (van Erp et al. 2016) (Fig. 2.1) and in regional cortical thickness and area (patients = 4474 and healthy individuals = 5089) (van Erp et al. 2018) (Fig. 2.2). Specifically, compared to healthy individuals, patients had smaller hippocampus ($d = -0.46$), amygdala ($d = -0.31$), thalamus ($d = -0.31$), accumbens ($d = -0.25$) and intracranial volumes ($d = -0.12$) and larger pallidum ($d = 0.21$) and lateral ventricles ($d = 0.37$) and global bilateral reductions in cortical thickness (left: $d = -0.53$; right: $d = -0.51$) and surface area (left: $d = -0.25$; right: $d = -0.25$) (Fig. 2.1). When controlling for these global effects, patients showed further regional changes in cortical thickness but not area. This accentuated regional cortical thinning was most pronounced in the fusiform gyrus, but was also present in multiple temporal regions (inferior, middle and superior temporal gyri and parahippocampal gyrus), in the ventrolateral prefrontal cortex (PFC; lateral orbitofrontal and inferior frontal gyrus), in the insula, and in the posterior anterior cingulate cortex (ACC) (Fig. 2.3). Notably, the motor (precentral gyrus), somatosensory (postcentral gyrus), and parietal (superior and inferior parietal cortex and paracentral lobule) cortices as well as the rostral ACC were significantly thicker in patients than in healthy individuals (Fig. 2.3). The findings of ENIGMA have been replicated in an independent Japanese sample of 884 patients with schizophrenia and 1680 healthy individuals from the consortium of the Cognitive Genetics Collaborative Research Organization (COCORO) (Okada et al.

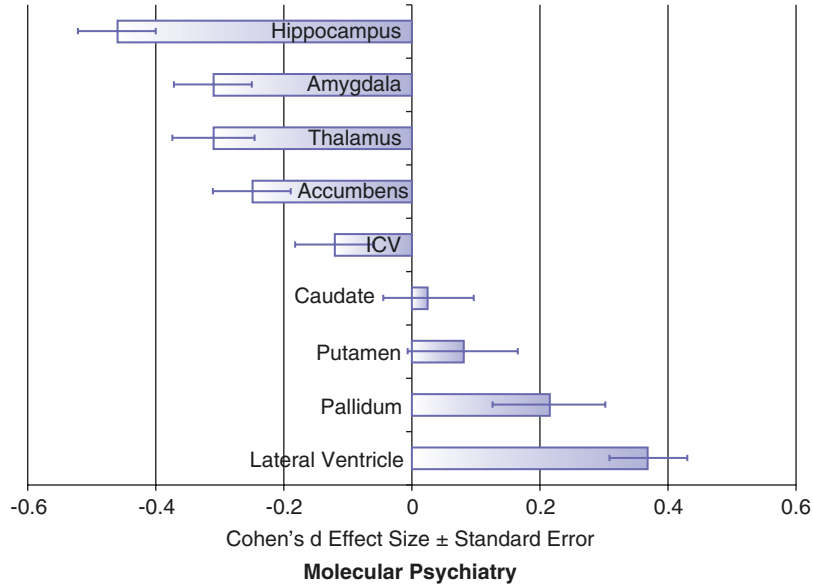

Fig. 2.1 Subcortical volume differences between patients with schizophrenia and healthy individuals. Mean and standard error of the effect size (Cohen's d) of regional case-control differences in subcortical volume (van Erp et al. 2016). The effect size for each subcortical volume was corrected for sex, age and intracranial volume (ICV). The effect size for ICV was corrected for sex and age. (From https://www.ncbi.nlm.nih.gov/pubmed/26283641)

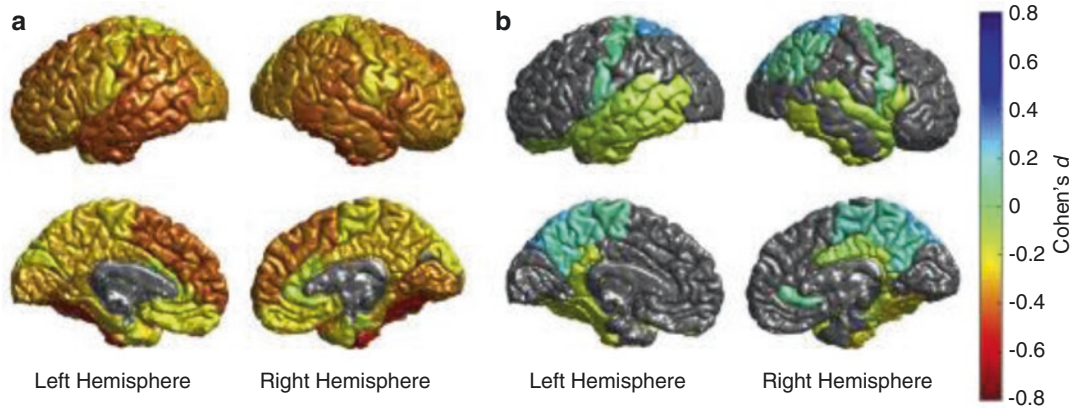

Fig. 2.2 Cortical map of differences in cortical thickness between patients with schizophrenia and healthy individuals. Cortical map of regional effect size (Cohen's d) of case-control differences in regional cortical thickness controlling for age and gender (**a**) and age, sex, and global cortical thickness (**b**) (van Erp et al. 2018). (From https://www.ncbi.nlm.nih.gov/pubmed/29960671)

2016) and are aligned with meta-analyses based on pooled effect size of case-control differences from 317 studies comprising over 18,000 patients (Haijma et al. 2013).

Two meta-analyses, published a year apart used ALE to map gray matter changes in schizophrenia. Glahn et al. (2008) used data from 31 VBM studies, comprising 1195 patients with schizophrenia and 1262 healthy volunteers, while Fornito et al. (2009) used data from 37 VBM studies that collectively compared 1646 patients to 1690 healthy individuals. Not surprisingly the primary studies in these two meta-analyses showed significant overlap, which extended to the results reported. Schizophrenia-related reductions were more consistent for gray matter concentration than for volume although the findings largely converged (Fornito et al. 2009). The regions where gray matter density reductions in patients were most likely to be reported comprised the ACC, the parahippocampal, middle frontal and postcentral gyri, and the thalamus;

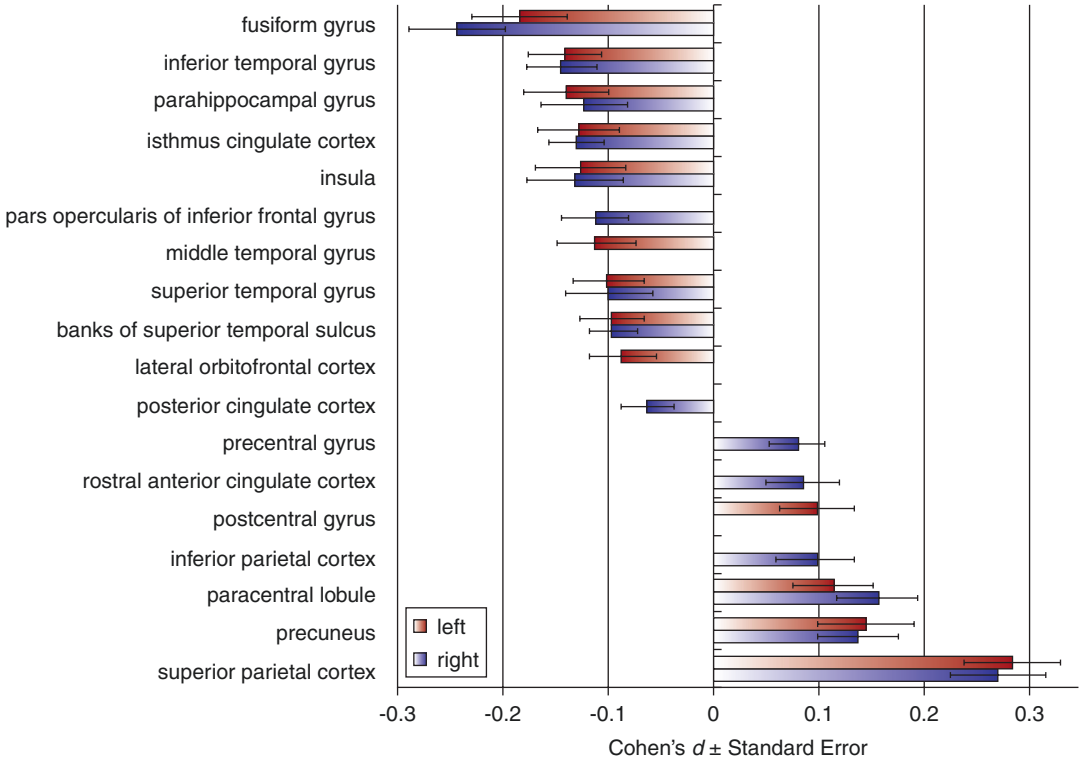

Fig. 2.3 Regional differences in cortical thickness between patients with schizophrenia and healthy individuals. Mean and standard error of the effect size (Cohen's d) of regional case-control differences in cortical thickness after controlling for age, sex, and global mean cortical thickness (van Erp et al. 2016). (From https://www.ncbi.nlm.nih.gov/pubmed/29960671)

conversely, patients had increased gray matter density in striatal regions (Fornito et al. 2009; Glahn et al. 2008). These findings were updated by Bora et al. (2011) who applied SDM to MRI data from 49 VBM studies comparing 1999 patients with schizophrenia and 2180 healthy individuals. Gray matter volume reductions were more likely to be located bilaterally in the ACC, the medial and inferior PFC, the superior temporal gyrus, the precentral gyrus and insula. Amongst the subcortical regions, schizophrenia-related reductions were also noted in the thalamus and the amygdala extending to the red nucleus in the midbrain.

2.1.1.2 Univariate Analyses in First-Episode Patients

Three separate meta-analyses have identified brain changes seen in patients with first-episode schizophrenia. Vita et al. (2006) and Steen et al. (2006) examined case-control differences in a very limited number of volumetric ROIs. The former study used data from 21 studies involving 551 first-episode patients with an approximate mean age of 25 years and 680 demographically matched healthy individuals. The latter extracted data contrasting 1424 patients with first-episode schizophrenia, with an approximate average age of 26 years, to 1315 matched healthy individuals. Although both studies found larger ventricles and smaller hippocampi, effect sizes were only provided by Vita et al. (ventricles: $d = 0.39$; hippocampi right $d = -0.47$ and left: $d = -0.65$). Radua et al. (2012) used SDM to analyse data from 25 VBM studies, contrasting 965 patients with first-episode psychosis, with an approximate mean age of 24 years, to 1040 matched healthy individuals. In patients, gray matter volume decrements clustered in the insula, operculum, the superior temporal gyrus and the medial

frontal and anterior cingulate cortices while gray matter increased clustered in the precentral gyri.

2.1.1.3 Univariate Analyses in Early-Onset Schizophrenia

A relatively small number of studies primarily conducted by the National Institutes of Mental Health (NIMH) in the USA and centres in the Norway, Spain, and the UK have examined brain alterations in patients with childhood-onset (onset before the age of 13 years) or adolescent-onset (onset between the ages of 13–18 years) schizophrenia, henceforth jointly referred to as early onset psychosis (EOP). Although EOP patients represent less than 4% of schizophrenia cases arising from any birth cohort (Cannon et al. 1999), their study has the potential to provide information about the interaction between schizophrenia-related mechanisms and developmental processes that occur during adolescence (Giedd et al. 1999).

Studies in adolescent-onset schizophrenia have found reductions in total brain volume (Collinson et al. 2003; Matsumoto et al. 2001) and gray matter volume particularly within the frontal lobe (Moreno et al. 2005; Reig et al. 2011; Yoshihara et al. 2008) but no such differences in subcortical volumes (James et al. 1999; Juuhl-Langseth et al. 2012; Matsumoto et al. 2001).

Nearly all studies on childhood-onset schizophrenia derive from the NIMH cohort and collectively have found that patients, compared to age-matched healthy children, have lower total brain and thalamic volumes and larger caudate and globus pallidus (Frazier et al. 1996a, b; Jacobsen et al. 1996; Kumra et al. 2000).

2.1.1.4 Multivariate Pattern Analyses in Patients Unselected for Illness Duration

The study of Gupta et al. (2015) is of particular interest as they applied SBM to the largest MRI dataset to date comprising 936 healthy individuals and 784 patients with schizophrenia. Following age and sex regression, both decrements and increments in gray matter concentration were observed in schizophrenia. Decrements clustered within the superior, middle, medial and inferior frontal gyri, the superior and inferior temporal gyri, the fusiform gyrus, the insula, the cuneus and precuneus, and the cerebellar vermis and declive while increments were located in the brainstem (pons and ventral tegmental area).

Further, Kambeitz et al. (2015) conducted a meta-analysis of studies (n = 20) that applied machine learning to MRI data from patients with schizophrenia from healthy individuals. They found that, regardless of the specific algorithm, patients with schizophrenia could be distinguished from healthy individuals with a sensitivity of 76.4% and a specificity of 79.0%.

Similar findings were reported in two of the largest studies conducted to-date that applied machine learning algorithms to structural MRI data to discriminate healthy individuals from patients with first episode schizophrenia (n = 127) and from patients with schizophrenia (n = 387) at different stages of their illness (Rozycki et al. 2018; Squarcina et al. 2017). In both studies, regions within the medial prefrontal, temporolimbic and peri-Sylvian cortex, together with ventricular and pallidal enlargement, showed the higher discriminative power but the accuracy of diagnostic classification was modest and ranged from 72 to 77% (Rozycki et al. 2018).

2.1.2 Longitudinal Studies

Several studies have assessed gray matter morphometry in patients with a first episode psychosis or chronic schizophrenia at multiple time points after illness onset as well as examined the association of the longitudinal changes identified to clinical outcome. The challenge in this line of research is to disentangle brain alterations related to disease mechanism versus those that may be more closely associated with medication exposure and side-effects, substance use, and suboptimal lifestyle choices.

2.1.2.1 First-Episode Psychosis

Multiple research groups, mostly based in Australia, Europe, and North America have contributed to the literature on brain alterations following the first psychotic episode in adult

(Andreasen et al. 2011; Cahn et al. 2002; DeLisi et al. 1997, 2004; Haukvik et al. 2016; Lieberman et al. 2001; Nakamura et al. 2007; Puri et al. 2001; Takahashi et al. 2009; Whitworth et al. 2005) and in EOP patients (Arango et al. 2012; Fraguas et al. 2012; Jacobsen et al. 1998; James et al. 2004; Keller et al. 2003; Reig et al. 2009; Sporn et al. 2003; Thompson et al. 2001). There is significant variability in the results reported, even between studies using cohorts with similar characteristics. Nevertheless, key meta-analyses of the literature have identified some consistent findings.

Fraguas et al. (2016) focused specifically on early onset psychosis. Their meta-analysis included longitudinal MRI studies (with a mean inter-scan of 2.46 years) that collectively involved 156 EOP patients (mean age at baseline 13.3–16.6 years) and 163 demographically matched healthy youth. They used a ROI approach to derive the effect size of case-control differences in longitudinal changes in total brain volume, total gray matter volume and in the gray matter volume of each cerebral lobe. Compared to healthy youth, EOP patients showed accelerated volume reduction in all the gray matter ROIs examined; the largest effect sizes were noted for the gray matter volume of the frontal ($g = -0.43$) and the occipital lobes ($g = -0.79$). These results resonate with the longitudinal changes in cortical thickness reported by Greenstein et al. (2006) in the NIMH cohort which only comprises youth with childhood-onset schizophrenia (n = 70) and healthy youth (n = 70) scanned repeatedly between the ages of 14 and 22 years. At younger ages, patients showed greater cortical thinning in anterior and posterior cortical regions. This pattern became more localized in the superior, middle, medial, and lateral orbital frontal gyri and in the superior and middle temporal gyri when the patients reached adulthood. Additionally during the follow-up period, the rate of cortical thinning in the superior parietal and postcentral gyri "normalized" while that in the superior and middle temporal gyri did not. Collectively, these findings have been interpreted as an exacerbation of the developmental changes taking place during adolescence (Thompson et al. 2001); in typically developing youth, there is a posterior-to-anterior wave of reduction in cortical volume and thickness which is assumed to reflect brain maturational processes in frontal and occipital regions that precede similar maturational changes in the lateral temporal cortex (Giedd et al. 1999; Gogtay et al. 2004).

Although EOP studies are informative, the typical onset of schizophrenia is in the third decade of life and therefore adult-onset datasets are more representative of the clinical population with schizophrenia. A meta-analysis by Vita et al. (2012) identified nine longitudinal studies of adults patients scanned within the first 24 months from onset that provided ROIs measures of gray matter of the whole-brain, the cerebral lobes and the auditory cortex on Heschl's gyrus (HG). Compared to healthy individuals (n = 337), patients (n = 341) showed reduction of moderate effect size (range of d: −0.30 to −0.58) in all the gray matter measures examined with the exception of the HG where the effect size of case-control differences was large (right: $g = -1.13$; left: $g = -1.33$).

We also highlight the contribution of the Iowa Longitudinal Study that stands out based on sample size and duration of follow-up. The Iowa Longitudinal Study was conducted between 1987 and 2007 that recruited 542 patients at their initial psychotic presentation at a mean approximate age of 24 years. Repeated MRI scans (minimum 2 and maximum 5 scans) were available from 202 patients and 125 healthy individuals; the mean interval between first scan and last available scan was 7.2 years (Andreasen et al. 2011). Patients showed accentuated decrease in whole-brain and regional gray and white matter volume and increased enlargement of the lateral ventricles. With regards to gray matter volume, the slope of decline in patients was greater for the frontal lobe and the thalamus (Andreasen et al. 2011). However, progressive brain changes did not occur uniformly in patients or in healthy individuals. For example, 47% of patients were losing at least 0.5% and 34% were losing at least 1% of frontal gray matter volume (as compared with 36% and 23% in healthy individuals, respectively). The interaction between time and

diagnostic group on all brain measures was statistically significant at the first inter-scan interval, which was at 2 years after intake, but not thereafter. Increased attrition with longer follow-up may have reduced the power to detect case-control differences. However, these findings raise the possibility that disease-mechanisms affecting brain integrity may indeed be most active during the early stages of schizophrenia. This interpretation may need to be considered in the context of a study by Schaufelberger et al. (2011) who conducted a 1-year follow-up of 39 patients with first-episode psychosis and 52 healthy individuals enrolled in a population-based case-control study. Although the sample size was small and the follow-up period was brief, the authors reported a significant group by time interaction in the superior temporal gyrus and the hippocampus due to gray matter increase in patients in these brain regions while no change was observable in the control group. This "gain" in patients was associated with prolonged remission suggesting that if disease mechanisms are indeed active in the early stages of the illness this effect may be limited to a subset of patients likely to have a more severe illness.

2.1.2.2 Patient Samples Unselected for Illness Duration

Several studies have examined progressive brain changes in patients of schizophrenia at different stages of their illness beyond the first episode (Mathalon et al. 2001; Mitelman et al. 2009; van Haren et al. 2008, 2011, 2016; Veijola et al. 2014; Wood et al. 2001) as have several reviews (Hulshoff Pol and Kahn 2008; Zipursky et al. 2013). Several meta-analyses have also provided a synthesis of the emerging patterns (Haijma et al. 2013; Kempton et al. 2010; Olabi et al. 2011).

More specifically, Kempton et al. (2010) focused their meta-analysis on the issue of lateral ventricular enlargement as an indirect measure of progressive brain loss; they included 13 studies that had measured the lateral ventricles or entire ventricular system at a minimum of two time points in a cumulative sample of 473 patients and 348 healthy individuals. Patients showed greater progressive ventricular enlargement than healthy individuals with a mean effect size $g = 0.45$; the effect size of case-control differences was similar for early stage ($g = 0.49$) and chronic ($g = 0.41$) patients.

Olabi et al. (2011) conducted a meta-analysis using data from 27 patient cohorts comprising 928 patients and 867 healthy individuals for whom baseline and follow-up a ROI volumetric data were available. The mean duration of illness at the baseline scan was 6.2 years (range: 0.3–18.7 years) and the mean inter-scan interval was 3.49 years. Greater progressive changes in patients were noted for the whole brain volume ($d = -0.40$) and the ventricular volume ($d = 0.53$). The slope of decline was steeper in patients for all gray matter ROIs but reached significance for the whole-brain ($d = -0.52$) and frontal lobe ($d = -0.34$). No significant time by diagnosis interaction was noted for subcortical structures although the reported confidence intervals were large, suggesting significant inter-study heterogeneity.

The results of these meta-analyses resonate with the findings from one of the largest longitudinal MRI datasets of patients with schizophrenia at the University Medical Center Utrecht (Hulshoff Pol et al. 2001). At baseline, the cohort comprised 159 patients with schizophrenia (with a mean duration of illness of 13.7 years) and 158 healthy participants. At intake, patients had smaller amygdala, hippocampus and thalamus and larger caudate and globus pallidus. They also showed evidence of cortical thinning in the inferior frontal, superior temporal and ventral occipital regions and in the precuneus, insula and posterior cingulate cortex (Hulshoff Pol et al. 2001) and greater volume in the superior parietal lobule and occipital pole (van Haren et al. 2011). After a mean interval of approximately 5 years, 96 patients and 113 healthy individuals were rescanned. At follow-up, both diagnostic groups showed progressive reductions in whole-brain and cerebral lobe gray matter volume (van Haren et al. 2008) and thickness, but the slope was steeper in patients particularly in frontal and temporal regions (van Haren et al. 2011). Subcortical progressive volumetric reductions

were more pronounced in patients' caudate, putamen, hippocampus, and amygdala (van Haren et al. 2016).

2.2 Associations Between Gray Matter Morphometry and the Clinical Features of Schizophrenia

Gray matter alterations in schizophrenia are thought to underpin disease expression but this association is complex. Several clinical features seem to correlate with symptom severity in cross-sectional investigations and the prognostic value of neuroimaging for clinical and functional outcomes. Outcomes were commonly defined using consensus criteria for clinical remission (e.g., Andreasen et al. 2005), type of course (e.g., non-remitting versus remitting) or overall function based on the General Assessment of Functioning (GAF) score. We focus on associations between gray matter morphometry and disease expression that were reported in the studies discussed in the preceding sections when such information was available. Additionally we highlight notable findings from the wider literature.

2.2.1 Cross-Sectional Studies

2.2.1.1 Associations Between Gray Matter Changes and Symptom Severity

In the ENIGMA studies, the association between gray matter ROIs and symptoms was assessed using both whole-brain and hypothesis-led ROI methods. In the whole-brain analyses, greater positive symptom severity correlated with cortical thickness in the left fusiform gyrus ($r = 0.60$), the left pars triangularis ($r = -0.08$), the left superior frontal gyrus ($r = -0.07$), the right inferior ($r = -0.07$), and the bilateral middle frontal gyrus (left $r = -0.08$; right $r = -0.10$) and middle temporal gyrus (left $r = -0.07$; right $r = -0.06$) (van Erp et al. 2018). Greater negative symptom severity correlated with widespread cortex thinning bilaterally (left and right $r = -0.08$) and larger lateral ventricular volume (van Erp et al. 2016, 2018). The hypothesis-led analyses focused on the superior temporal gyrus (STG) given its involvement in auditory hallucinations (Lee et al. 2018) and on PFC regions because of their association with negative symptoms (Millan et al. 2014). In these analyses, positive symptom severity was negatively related to STG thickness bilaterally (left: $\beta std = -0.05$; right: $\beta std = -0.07$) (Walton et al. 2017) while negative symptom severity negatively related with the thickness of the left medial orbitofrontal cortex ($\beta std = -0.07$) and to a lesser extent with the thickness of the left lateral orbitofrontal gyrus and the pars opercularis (Walton et al. 2018).

However, the ENIGMA findings are only partially supported by other meta-analyses. The meta-analysis by Bora et al. (2011) reported a link between negative symptom severity and reduced gray matter density in the medial and lateral orbital PFC (as well as the insula) but only in chronic patients. Fusar-Poli et al. (2012), who focused on first-episode mediation-naïve patients, found a negative between reduced STG gray matter volume and overall psychopathology. Therefore the magnitude of the associations between gray matter changes and psychopathology is generally small and perhaps it is not surprising that such associations have not been always detectable (e.g., Gupta et al. 2015).

The complexity of the links between gray matter phenotypes and psychopathology is highlighted by the contradictory findings from machine learning studies. Kambeitz et al. (2015) found that diagnostic accuracy based on machine learning analysis of structural MRI data was better for patients with predominantly positive symptoms while Rozycki et al. (2018) reported better diagnostic classification accuracy for patients with greater negative symptom severity.

2.2.1.2 Associations Between Gray Matter Changes and Outcome

In childhood-onset schizophrenia, whole-brain mean cortical thickness at baseline was positively associated with remission at 3 months post-scan (Greenstein et al. 2008). This finding was partially confirmed by Doucet et al. (2018) who

used a machine learning approach to evaluate the predictive value of gray matter phenotypes for symptomatic improvement at 6-months in adult patients (n = 100) in the early stages of schizophrenia (duration of illness <5 years). Although symptomatic improvement showed moderate correlations with global cortical thickness and subcortical volumes, none of these phenotypes had significant prognostic value.

Two notable studies attempted to test whether machine learning applied to brain structural features can distinguish between patients with remitting versus non-remitting outcomes (also see Chap. 17). Zannetti and colleagues (2013) used MRI data from 62 patients with first-episode of schizophrenia and an equal number of matched healthy individuals; the diagnostic accuracy of the classifier was modest in distinguishing cases from controls (73.4%), but failed to discriminate between patients with remitting and non-remitting course, as the diagnostic accuracy achieved was marginally above chance (58.3%). Nieuwenhuis et al. (2017) expanded upon this effort by using data from a substantial sample of patients with first episode psychosis (n = 386) from centres in Australia, Brazil, the Netherlands, Spain, and the UK. Classification accuracy according to outcome was modest in some of the participating centres but did not generalize across centres; in fact when data from all the centres were analyzed into one model, the classification accuracy was at chance level.

2.2.2 Longitudinal Studies

None of the major meta-analyses of longitudinal studies have addressed the association with clinical outcome (Fraguas et al. 2016; Olabi et al. 2011; Vita et al. 2012) so we focus on the findings of the two largest longitudinal studies, the Iowa Longitudinal Study, which followed-up first-episode psychosis (Andreasen et al. 2011, 2013), and the study coordinated by the University Medical Center Utrecht that examined patients with schizophrenia at different stages of their illness (Hulshoff Pol et al. 2001; van Haren et al. 2008, 2011, 2016). The Iowa Longitudinal Study focused on the association between remission (defined as in Andreasen et al. 2005), relapse (defined as in Csernansky et al. 2002) and the rate of progressive brain changes in patients (n = 202). Over an average period of 7 years, the mean duration of relapse was 1.34 years. The early phases of the illness were characterized by multiple relapses of relatively short duration; as time progressed, the number of relapses decreased while their length increased. The length of the period spent in relapse (but not the number of relapses) was associated with greater loss in whole-brain and frontal gray matter volume (Andreasen et al. 2013). In the cohort from the University Medical Center Utrecht, patients (n = 96) were followed-up for an average period of 5 years at which point the median GAF score was used to divide patients into those with good (GAF = 66.7) and those with poor outcome (GAF = 38.2). The outcome groups did not differ in age, sex, scan interval, socioeconomic status, illness duration, or antipsychotic medication intake. However, compared to patients with good outcomes, those with poor outcomes showed more pronounced progressive cortical thinning in multiple temporal regions (superior and middle temporal and Heschl gyri), in the ACC and in the visual cortex (cuneus).

2.3 Potential Moderators

2.3.1 Sex

There are no consistent reports of a differential effect of sex on schizophrenia-related brain structural alterations either in cross-sectional or longitudinal studies. Whenever an effect of sex has been found it has been associated with greater brain structural deviance in male patients. For example, the ENIGMA studies found no interaction between diagnosis and sex on subcortical volume when correcting for multiple comparisons; at a nominal uncorrected statistical threshold, the proportion male patients was associated with more pronounced case-control differences in the accumbens and the amygdala (van Erp et al. 2016). Moreover, meta-analyses that examined

the effect of sex found no interactions with diagnosis (Fraguas et al. 2016; Haijma et al. 2013; Kempton et al. 2010; Olabi et al. 2011) with the exception of Bora et al. (2011), who reported that male sex was associated with greater deviance in the gray matter of the PFC, the insula, the amygdala and the thalamus.

2.3.2 Age

Age and illness duration are commonly highly correlated and their independent contribution to schizophrenia-related gray matter morphometry can be difficult to disentangle. Age is a significant determinant of gray matter morphometry; a substantial body of literature suggests that gray matter regions cortical thickness and volume peak during late childhood and decrease thereafter (Ducharme et al. 2015; Good et al. 2001; Raz et al. 2005, 2010). The association between age and brain morphometry in schizophrenia is likely to involve complex interactions between age-related brain changes, primary effects of disease mechanisms, and secondary effects of prolonged medication exposure and patients' suboptimal lifestyle. There is some evidence that the magnitude of case-control differences in schizophrenia may be influenced by developmental age (Chap. 15). As previously noted, the slope of cortical thinning was steeper in adolescence in the NIMH cohort of childhood-onset schizophrenia but became similar to that of healthy youth as patients approached adulthood (Greenstein et al. 2006). The evidence for older adults is somewhat conflicting. Kambeitz et al. (2015) found that machine learning algorithms attained better diagnostic sensitivity for chronic compared to first-episode patients indicating that case-control differences in schizophrenia may become more distinctive with age. By contrast, in the University Medical Center Utrecht cohort, excessive gray matter volume decrease in patients with schizophrenia over a 5-year follow-up was significant for those aged 18–46 years but not in older patients (van Haren et al. 2008). This observation has not been replicated in other studies including a further study from the same cohort that examined cortical thickness (van Haren et al. 2011).

2.3.3 Antipsychotic Medication

The effect of antipsychotic medication on brain morphology is subject to intense scrutiny and debate (See also Chap. 18). Antipsychotic drugs are the mainstay pharmacological treatment of schizophrenia and reduce dopaminergic neurotransmission albeit to a variable degree. The first-generation antipsychotics (FGA) are high-affinity antagonists of dopamine D_2 receptors while the second-generation (SGA) antipsychotics have lower affinity for D_2 receptors but different affinities for serotonergic, adrenergic, acetylcholine, and histamine receptors (Miyamoto et al. 2005). Antipsychotic exposure and illness severity are not independent because patients with a more severe illness are more likely to receive medication for longer periods and at higher doses. Disambiguating the effects of medication on gray matter integrity from those attributable to primary disease mechanism is the greatest challenge as most MRI studies include medicated patients.

2.3.3.1 Effect of Antipsychotic Medication on Striatal Volumes

Striatal enlargement has been associated with antipsychotic treatment in multiple studies (Gupta et al. 2015; Ho et al. 2011; van Haren et al. 2016) and meta-analyses (Haijma et al. 2013) and is absent in studies of medication-naïve patients (Fusar-Poli et al. 2012, 2013). The first indication that antipsychotics may causally affect striatal structure was provided by Chakos and colleagues in 1994 who reported an increase in the volume of the caudate nucleus in patients with first-episode schizophrenia following initiation of treatment with haloperidol, a prototypical FGA. Subsequent studies found that caudate enlargement can be reversed following withdrawal of antipsychotic medication or substitution of FGAs with SGAs (Chakos et al. 1995; Frazier et al. 1996b; Corson et al. 1999). Because the caudate is rich in dopamine D_2 receptors, this FGA-induced enlargement has been attributed

to remodelling caused by strong dopaminergic blockade which can induce ultrastructural changes in striatal neurons (Benes et al. 1985; Chakos et al. 1998; Meshul et al. 1992) and alterations in the dendritic morphology of cortical neurons (Lidow et al. 2001; Selemon et al. 1999) and in fronto-striatal connectivity (Tost et al. 2010).

Antipsychotics may also influence progressive striatal changes. In the University Medical Center Utrecht cohort, the cumulative annual intake of FGAs was inversely associated with progressive volume loss in the putamen (rho = 0.46) and caudate (rho = 0.38) over a 5-year period (van Haren et al. 2016); similarly, in the Iowa Longitudinal Study, higher antipsychotic doses were inversely associated with progressive volume loss in the caudate and putamen over a 7-year period (Ho et al. 2011).

2.3.3.2 Antipsychotic Treatment and Volume Changes in Other Subcortical Regions

The most convincing evidence for an association between antipsychotic exposure and subcortical volumes derives from the ENIGMA dataset (van Erp et al. 2016). Specifically, the proportion of medication-naive patients was negatively associated with the effect size of case-control differences in hippocampal volume. The effect size of case-control difference in ventricular enlargement was negatively associated with the proportion of patients treated with SGA and positively associated with the mean current antipsychotic dose in chlorpromazine equivalents (CPZE).

2.3.3.3 Antipsychotic Treatment and Changes in Cortical Thickness or Volume

Preclinical studies suggest several mechanisms that may lead to cortical thinning following exposure to both FGAs and SGAs. These include antipsychotic-induced microstructural changes in dendritic morphology (Dorph-Petersen et al. 2005; Vernon et al. 2011), which can be reversed upon discontinuation (Vernon et al. 2012). FGAs may compromise gray matter integrity by reducing cerebral flow and metabolism (Goff et al. 1995; Lahti et al. 2004; Miller et al. 1997; Molina et al. 2003; Wright et al. 1998) and by increasing oxidative stress and excitotoxicity (Goff et al. 1995; Wright et al. 1998). Conversely, SGAs (such as olanzapine and clozapine) may preserve cortical gray matter integrity by reducing excitotoxicity (Duncan et al. 2000) while enhancing dendritic resilience (Wang and Deutch 2008), neurogenesis (Halim et al. 2004; Wakade et al. 2002; Wang et al. 2004), and neurotrophic factor expression (Bai et al. 2003; Fumagalli et al. 2003). The association between antipsychotic dose and class has therefore been examined in multiple MRI studies comparing patients to healthy individuals and patients treated with FGAs or SGAs.

The ENIGMA consortium found evidence for an association between antipsychotic exposure and mostly global measures of cortical thickness (van Erp et al. 2018). In particular, mean hemispheric cortical thickness was inversely associated with exposure to FGAs or combinations of FGAs and SGAs. In addition, higher dose in CPZEs inversely correlated with cortical thickness in almost all cortical regions but more prominently in the superior frontal gyrus, the pars triangularis, the superior, middle and inferior temporal gyri, and the supramarginal gyrus. The magnitude of these associations however was small ($|r| < 0.2$). The meta-analysis by Radua et al. (2012) has provided further information about the localization of cortical changes associated with antipsychotic medication in first-episode patients. In a series of meta-regression analyses they found that the gray matter volume in medial PFC, the ACC, and the insula were significantly lower in medicated patients compared to healthy individuals. This reduction was greater than that observed in the same regions in a subgroup analysis that included only samples with antipsychotic-naïve patients. The meta-analysis by Haijma et al. (2013) focused on more global measures and reported that higher antipsychotic dose at the time of scanning was associated with lower whole-brain gray matter volume for both FGAs and SGAs. Importantly, a sub-analysis of antipsychotic-naive samples found that the effect-size of case-control differences was approxi-

mately 75% of that seen in medicated samples, indicating that the most significant reduction in whole-brain gray matter volume may predate treatment initiation.

Two key single-cohort studies have examined the association between antipsychotic exposure and progressive cortical changes. In the Iowa Longitudinal Study, patients were divided into those that received high (mean dose, 929.4 CPZE mg), intermediate (mean dose, 391.7 CPZE mg), and low daily antipsychotic dose (mean dose, 111.5 CPZE mg) (Ho et al., 211; Andreasen et al. 2013). Patients in the top tertile had smaller frontal gray matter volume compared to those in the lowest tertile; this association however was independent of follow-up duration. Conversely, in the University Medical Center Utrecht longitudinal cohort, cortical thickness reduction over the 5-year follow-up period was associated with antipsychotic class (van Haren et al. 2011), being more pronounced in those treatment with FGAs. The main SGA prescribed in this cohort was olanzapine; higher exposure to olanzapine over the follow-up period (in mg per year) was associated with a non-significant increase in whole-brain gray matter volume. A different pattern was observed in patients with emergent treatment resistance that were prescribed clozapine at any point during the follow-up period. These patients showed more pronounced cortical thinning in the left superior temporal cortex compared to all other patients, and those prescribed higher doses of clozapine (in mg per year) showed further thinning in the PFC and ACC.

Similar results were reported by Vita and colleagues who examined the association between antipsychotic dose and class (FGA or SGA) on ROIs involving whole-brain, frontal, temporal, and parietal gray matter volume derived from 18 longitudinal studies (range of follow-up: 1–7 years) yielding a cumulative sample of 1155 patients with schizophrenia and 911 healthy individuals (Vita et al. 2015). Patients treated with FGAs or a combination of FGAs and SGAs showed reductions in all gray matter measures over time; the greater the exposure to FGAs during the inter-scan period, both in terms of cumulative and mean daily dose, the greater the reduction in whole-brain gray matter volume. By contrast, the higher the mean daily dose of SGAs during the follow-up, the lower the reduction in whole brain gray matter volume. A larger ROI-based meta-analysis by Fusar-Poli et al. (2013) of 30 studies comprising MRI data from of 1046 schizophrenia patients and 780 controls over a median follow-up period of over 1-year, also confirmed that progressive whole-brain gray matter volume decreases and lateral ventricular enlargement were associated with greater cumulative exposure to higher antipsychotic doses. This meta-analysis however did not consider antipsychotic class.

The study by Lieberman et al. (2005) merits special attention because their sample of patients with first-episode schizophrenia (n = 263) was randomized to double-blind treatment with the SGA olanzapine, 5–20 mg/day, or the FGA haloperidol, 2–20 mg/day, for up to 104 weeks. This random assignment enabled investigators to disentangle the effect of antipsychotic class from patient- and physician characteristics that may drive medication regimes in clinical settings. Patients were assessed by MRI at weeks 0 (baseline), 12, 24, 52, and 104 and were compared to 58 healthy study participants. At study end, the sample with available data comprised 239 patients with a baseline MRI, and 161 patients with at least one follow-up assessment. By week 12, patients' rate of whole-brain gray matter volume reduction was steeper in the haloperidol- versus the olanzapine-treatment group and the magnitude of this difference remained largely constant to the study end. These group differences were driven by volume loss in haloperidol-treated patients, which was absent in the olanzapine-treated patients. The same pattern was noted for frontal, temporal, and parietal gray matter volumes. The volume of the caudate showed greater enlargement in the haloperidol- compared with the olanzapine-treatment group beginning at week 24.

2.3.3.4 Gray Matter Alterations in Medication-Naïve Patients

Studies on medication-naïve patients are particularly useful in disentangling disease- versus medication-related brain structural changes.

Fusar-Poli et al. (2012) identified 14 studies with structural MRI data, collectively contrasting 206 antipsychotic-naive patients with first-episode psychosis (mean age of 26.4 years) to 202 healthy individuals. They found consistent and significant gray matter reductions ($g = 0.83$) (but no increases) in patients compared to healthy individuals that clustered within the superior temporal gyrus, the insula, and the cerebellum. These findings were largely replicated in a further meta-analysis by Haijma et al. (2013) who also found that medication-naïve patients, compared to healthy individuals, had smaller intracranial ($d = -0.14$), whole-brain ($d = -0.21$), whole-brain gray matter ($d = -0.36$), thalamic (d = −0.68), and caudate (d = −0.38) volumes.

2.3.4 Substance Use

Substance use, and particularly cigarette smoking, cannabis and alcohol, is highly prevalent in schizophrenia, affecting approximately 40% of patients (de Leon and Diaz 2005; Hunt et al. 2018). In MRI studies of non-psychotic populations, cannabis (Martín-Santos et al. 2010), cigarette smoking (Gallinat et al. 2006), and alcohol abuse (Zahr and Pfefferbaum 2017) have all been associated with diminished brain tissue volumes. Therefore substance abuse has the potential to exacerbate volume reductions in schizophrenia. Supporting evidence has been provided mainly from the University Medical Center Utrecht cohort, by Rais et al. (2008) who reported that first-episode patients who continued to use cannabis over the 5-year follow-up period showed greater reduction in gray matter volumes and increased ventricular enlargement compared to those that did not abuse cannabis. The effect of cannabis was most pronounced in regions rich in cannabinoid receptors (CB1) within the dorsolateral PFC, the ACC, and the occipital cortex (Rais et al. 2010). However, in a review of the literature, Malchow et al. (2013) cautioned that the effect of cannabis on brain structure in patients with schizophrenia is inconsistent and is likely to be small. Finally, a meta-analysis of the relevant literature, showed that alcohol abuse in patients with schizophrenia was associated with thinner cortex and enlarged ventricles but the magnitude of this effect was commensurate to that seen in non-psychotic individuals (Lange et al. 2017).

2.3.5 Stress and Cardiometabolic Risk Factors

There is substantial support for elevated baseline activity of the hypothalamic-pituitary-adrenal (HPA) axis, the central stress response system, in patients with psychosis (Borges et al. 2013; Walker et al. 2008). It is generally known that HPA hyperactivity is associated with microstructural abnormalities and volume loss in the hippocampus, which is a key target region for glucocorticoids (Sapolsky 2003). At present, the link between hippocampal volume reduction and HPA activity is based on a sample of 24 patients with first-episode schizophrenia where an inverse association was found with cortisol levels both cross-sectionally and at 3-month follow-up (Mondelli et al. 2010).

Patients with schizophrenia are at risk of developing cardio-metabolic disease for several reasons including genetic predisposition to diabetes (Ryan et al. 2003), reduced physical activity (Rosenbaum et al. 2014), and the metabolic side-effects of antipsychotic medications (Mitchell et al. 2013). It has been estimated that at least a quarter of all medicated patients meet criteria for metabolic syndrome (Mitchell et al. 2013). In non-psychotic populations (Doucet et al. 2018; Medic et al. 2016; Yates et al. 2012), the presence of metabolic syndrome (comprising insulin resistance, obesity, dyslipidemia and hypertension), or merely increased body mass index (BMI), is associated with cortical thinning. There are only two studies that have addressed the effect of BMI on brain morphometry in patients with schizophrenia. Jørgensen et al. (2017) obtained MRI data from patients with first-episode schizophrenia (n = 78) and healthy individuals (n = 119) at intake and then 1 year later. Increases in BMI over the follow-up period showed a small negative association ($\beta = -0.19$) with whole-brain and whole-brain gray matter volume change, which was however similar in magnitude in both groups. Moser et al.

(2018) used a multivariate machine approach to examine the effect of BMI on MRI measures from 100 patients with recent-onset schizophrenia (illness duration <5 years) while simultaneously modelling correlations with clinical and cognitive symptoms, substance use, psychological trauma, physical activity, and medication (Fig. 2.4). Even after accounting for these multiple variables, BMI was negatively and significantly associated the cortical thickness (r = −0.28).

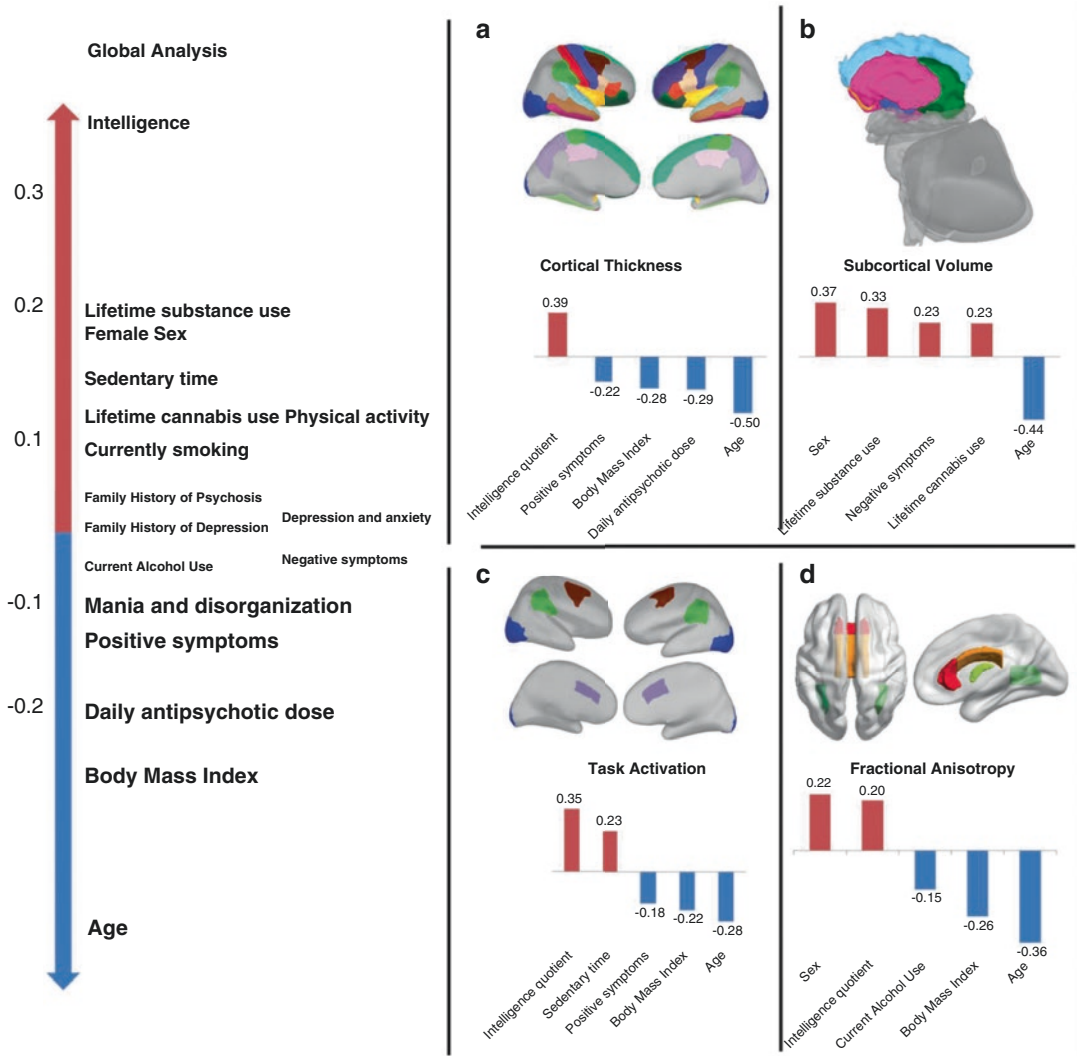

Fig. 2.4 Multivariate associations between behavioral, clinical and multimodal imaging phenotypes in psychosis. Right Panel: Association between neuroimaging and non-imaging variables across all imaging modalities. Left Panel: (**a**): Regional cortical thickness measures correlated most highly with non-imaging variate (top) and correlations between non-imaging variables and cortical thickness variate (bottom). (**b**): Subcortical volumetric measures correlated most highly with non-imaging variate (top) and correlations between non-imaging variables and subcortical volumes variate (bottom). (**c**): Regional task-related brain activation correlated most highly with non-imaging variate (top) and correlations between non-imaging variables and task-related brain activation variate (bottom). (**d**): Regional fractional anisotropy measures correlated most highly with non-imaging variate (top) and correlations between non-imaging variables and fractional anisotropy variate (bottom) Results from sparse canonical correlation analyses from Moser et al. (2018). (From https://www.ncbi.nlm.nih.gov/pubmed/29516092)

2.4 Overview of Findings

The studies presented in the preceding sections provide evidence for the following statements: (1) schizophrenia-related gray matter alterations consist mostly of subtle and widespread reductions in cortical and subcortical gray matter density and volume and in cortical thickness; these gray matter alterations occur in the context of a small but significant reduction in intracranial volume (ICV) in patients with schizophrenia (effect size −0.2) (Haijma et al. 2013); (2) tissue loss is most prominent in the temporal (inferior, middle and superior temporal and parahippocampal gyri), the occipital and the frontal (lateral orbitofrontal and inferior frontal gyrus) cortex, in the posterior ACC, and in the insula; notably regions within the motor (precentral gyrus), somatosensory (postcentral gyrus), and parietal (superior and inferior parietal cortex and paracentral lobule) cortex may show tissue gain; (3) gray matter tissue reductions are largely present at the time of the first psychotic episode and may be greatest early in the course of illness, mirroring the social and occupational deterioration which seems more pronounced in the early stages of psychosis (Häfner and Maurer 2006); (4) after illness onset, the slope of age-related decline in cortical regions appears to be steeper in patients with schizophrenia than in healthy individuals but of small magnitude; it is estimated that the cumulative loss of brain tissue after 20 years of illness is approximately 3% (Hulshoff Pol and Kahn 2008; Wright et al. 2000); (5) the association between gray matter alterations and clinical outcome is complex; the general pattern suggests that whole-brain gray matter reductions are more pronounced in patients that are more symptomatic and have poor clinical and functional outcomes; (6) sex differences in schizophrenia-related gray matter alterations are small, and when present they indicate greater deviance in male patients; (7) antipsychotic drugs, and particularly FGAs, have been associated with progressive striatal and ventricular enlargement and diffuse cortical thinning; (8) several factors including HPA dysregulation, substance abuse, stress, higher BMI, and cardiometabolic risk are likely to contribute to the gray matter alterations observed in schizophrenia (Fig. 2.5).

2.5 Mechanistic Implications and Future Directions

Structural MRI as applied to the studies described above lacks the resolution to inform us about the nature of pathogenetic processes underlying gray matter changes in schizophrenia. Furthermore, the processes involved may not affect all patients in the same fashion. Studies that have applied multivariate clustering techniques to multimodal datasets from patients with schizophrenia (i.e., datasets that include clinical, genetic, cognitive and brain phenotypes) hint at the presence of multiple, partially overlapping syndromes that may be associated with a discrete set of risk factors (Arnedo et al. 2015; Zheutlin et al. 2018). No systematic examination, however, has been undertaken to date to examine the association between gray matter integrity and risk-conferring gene variants or other non-genetic risk factors. A meta-analyses of the limited neuroimaging studies available have implicated a four-marker haplotype in G72, a microsatellite and single nucleotide polymorphism in NRG1, DISC1, CNR1, BDNF, COMT and GAD1; these associations were of small or medium magnitude and were most frequently observed in frontal regions (Harari et al. 2017).

The gray matter changes in patients with schizophrenia should be considered in the context of ICV reduction, a consistent finding in MRI studies of schizophrenia (Haijma et al. 2013). The expansion of the skull, which determines ICV, is driven by brain growth (O'Rahilly and Müller 2001) and reaches its maximum size at approximately 13 years of age (Blakemore 2012). The reduced ICV in patients suggests that the biological process leading to overt disease may be active early in development. As already discussed, there are progressive post-onset changes in brain and gray matter volume that are indicative of on-going disease related mechanisms that lead to further compromise in brain structural integrity.

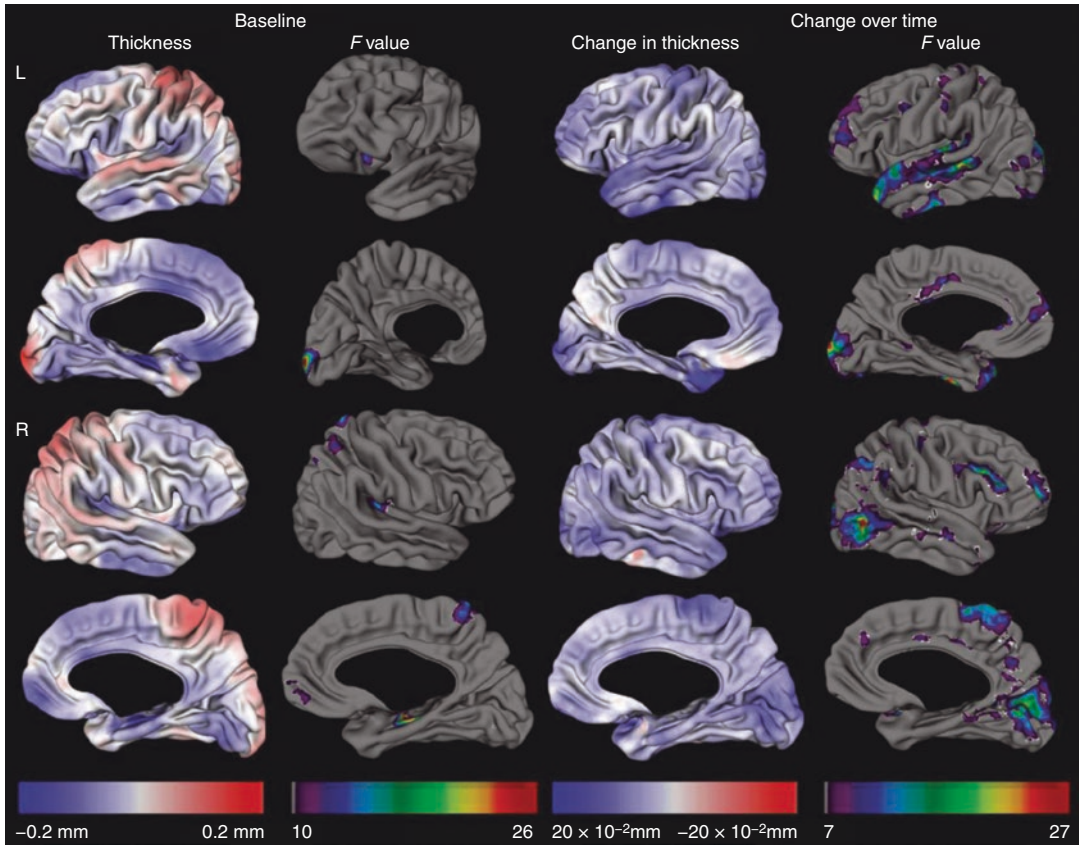

Fig. 2.5 Maps of change in cortical thickness in millimeters and F values, showing reduction (blue) or excess (red) at study entry (patients with schizophrenia = 154, controls = 156) and during the 5-year interval (patients = 96, controls = 113) (van Haren et al., 2011; https://www.ncbi.nlm.nih.gov/pubmed/21893656)

Traditional models of schizophrenia emphasize neurotransmitter abnormalities mostly in the dopaminergic (Howes and Kapur 2009) and glutamatergic systems (Moghaddam and Javitt 2012). According to the dopamine hypothesis, schizophrenia is characterized by hyperactive transmission in the striatal areas and hypoactive transmission in the prefrontal cortex as proposed by Davis and colleagues in 1991 and updated more recently by Howes and Kapur in 2009. In vivo and in vitro studies suggest that excess dopamine can trigger inflammation, oxidative stress, apoptosis, and mitochondrial impairment (Junn and Mouradian 2001). For example, prolonged stimulation of cortical neurons by excessive dopamine can induce calcium-related excitotoxicity and mitochondrial dysfunction through mitochondrial complex I inhibition (Ben-Shachar 2017). With respect to glutamate, the primary excitatory neurotransmitter, gray matter pathology in schizophrenia may be linked to excitotoxic injury through excessive Ca2+ influx via the N-methyl-d-aspartate (NMDA-R) receptor (Moghaddam and Javitt 2012). Further, Ca2+ toxicity targets mitochondria leading to dysfunction, either directly or through oxidative inhibition of mitochondrial complexes I, II and V, ultimately activating death signals (Nicholls 2009; Davis et al. 2014).

Several other mechanisms have been proposed to explain the gray matter alterations observed in schizophrenia with most of the data derived from post-mortem studies. To-date, there is no convincing evidence that schizophrenia is associated with gliosis or neuronal cell loss or other histopathological changes commonly seen in degenerative disorders (Arnold et al. 1998; Baldessarini et al. 1997; Heckers

et al. 1991; Pakkenberg 1993; Thune et al. 2001; Walker et al. 2002). By contrast, decreased cortical neuropil, relative to specimens from psychiatrically-healthy individuals, has been one of the most replicable post-mortem findings in schizophrenia (Selemon and Goldman-Rakic 1999). This reduction has been observed in multiple brain regions including primary sensory and associative cortices (Casanova et al. 2008). In a parallel line of research, replicable reductions have been noted in synaptic protein and mRNA levels in multiple cortical regions, although the precise distribution of these changes cannot be fully evaluated because of limited brain coverage of the available data. The most robust, but modest, reductions have been noted for synaptophysin (a neuron-specific presynaptic protein) particularly within the hippocampus, but also in dorsolateral PFC and ACC as these regions are preferentially sampled in schizophrenia research (Osimo et al. 2018). Additional but smaller reductions in other synaptic proteins (i.e., SNAP-25, PSD-95, synapsin and rab3A) have also been consistently noted in the hippocampus while data for other brain regions are very limited (Osimo et al. 2018). Whether these changes are developmental or whether they occur later in life remains unknown as post-mortem studies are restricted to chronic cases.

Some researchers have proposed that mitochondrial dysfunction (either primary or induced) may contribute to the neuronal, dendritic, and synaptic abnormalities seen in schizophrenia. While the brain comprises less than 2% of the human body mass, it consumes 20% of the energy expensed. ATP production is therefore crucial for cellular homeostasis, electrical conductivity, and synaptic function; neurons are critically dependent on the mitochondria to generate the requisite amounts of ATP. Evidence of abnormal energy generation in schizophrenia has been known since Looney and Childs (1934) who reported increased lactate and decreased glutathione in blood samples from schizophrenic patients. In post-mortem brain tissue from patients with schizophrenia, mitochondria are differentially affected depending on the brain region, cell type, and subcellular location. The overall pattern however indicates that mitochondria, particularly in or near the synapses and neuropil, are functionally compromised (Roberts 2017).

Mitochondrial DNA is susceptible to damage from reactive oxygen species (Corral-Debrinski et al. 1992) while release of mitochondrial DNA during cell stress can trigger inflammatory responses (López-Armada et al. 2013; Naik and Dixit 2011; Oka et al. 2012). There is substantial evidence implicating oxidative/nitrosative stress pathways in the pathophysiology of schizophrenia as recently shown in a meta-analysis of 61 independent cohorts comprising blood samples from 3002 patients with first-episode schizophrenia and 2806 healthy individuals; patients had lower total antioxidant status and docosahexaenoic acid (DHA) levels and higher levels of homocysteine, interleukin-6 (IL-6) and tumor necrosis factor alpha (TNF-α) (Fraguas et al. 2018). Moreover, a recent meta-analysis of post-mortem studies (n = 41; 783 patients and 762 controls) by van Kesteren et al. (2017) confirmed that despite significant inter-study heterogeneity, both microglia density and the concentrations of pro-inflammatory proteins are increased in schizophrenia. These changes were particularly evident in temporal cortical regions. Direct in-vivo evidence that these mechanisms operate centrally is currently lacking. Neuroimaging studies attempting to quantify case-control differences in central pro-inflammatory markers have focused on the activation state of microglia. Activated microglia expresses higher levels of the 18-kDa translocator protein (TSPO) (Cosenza-Nashat et al. 2009) which can be measured in vivo using positron emission tomography (PET) radiotracers. Studies using this methodology have thus far failed to provide consistent support for an increase of TSPO in schizophrenia (Plaven-Sigray et al. 2018; Marques et al. 2018), and the heterogeneity between studies is at least partly attributable to on-going methodological challenges (Plavén-Sigray and Cervenka 2019).

Finally, there is also evidence for myelin-related dysfunction in schizophrenia, which could also account for the observed decreases in brain tissue. Maturational changes in intracortical myelination occur in late adolescence

and early adulthood and coincide with the peak period of risk for schizophrenia (Bartzokis 2002; Paus et al. 2008; Rapoport et al. 2005; Weinberger 1987). Several oligodendrocyte/myelin related genes, such as neuregulin and its receptor ERBB4, are genetically associated with schizophrenia (Karoutzou et al. 2008; Norton et al. 2006). Post-mortem studies in schizophrenia have reported compromised integrity of the myelin sheath (Uranova et al. 2001), abnormal oligodendrocyte density and morphology (Uranova et al. 2004), and expression of genes associated with oligodendrocytes and myelin in multiple brain regions (Dratcheva et al. 2006; Hakak et al. 2001; Katsel et al. 2005). These findings do not seem attributable to antipsychotic exposure (Hakak et al. 2001; Konopaske et al. 2008). In vivo neuroimaging studies of intracortical myelination in schizophrenia have yielded variable results. Nevertheless, reduced intracortical myelin has been found in the prefrontal cortex (Bagary et al. 2003; Bohner et al. 2012; Price et al. 2010), temporal lobes (Foong et al. 2000) and primary/association visual cortex (Bachmann et al. 2011; Palaniyappan et al. 2013). A more recent and larger study reported myelin reduction in patients with schizophrenia compared to controls in the sensorimotor cortex, the transverse temporal gyri, the cuneus, and in the visual cortex (Jørgensen et al. 2016).

The small effect size of case-control differences in gray matter integrity and the multiplicity of potential mechanisms and moderators argue that future research efforts will require adequately powered large-scale projects comprising multiscale measures (e.g., genetic, molecular, neuroimaging, clinical, and cognitive) from patients and healthy individuals. It is widely accepted that adolescent mental health problems arise from complex interactions between these factors. Examination of these interacting influences requires advanced multivariate modelling and significant computing power in order to simultaneously handle high-dimensional datasets. This is an emerging field with multiple groups endeavoring to define optimal statistical algorithms and to test the validity of the resultant models (e.g., Nymberg et al. 2013).

Summary

- Gray matter alterations in schizophrenia comprise subtle and widespread reductions in cortical and subcortical gray matter density and volume and in cortical thickness in the context of reduction in intracranial volume.
- Gray matter tissue reductions seem to occur at the time of the first psychotic episode and may mirror the social and occupational deterioration observed in the early stages of psychosis.
- After illness onset, the slope of age-related decline in cortical regions appears steeper in patients with schizophrenia than in healthy individuals; these age-related changes may be exacerbated by the use of first-generation antipsychotics.
- Factors that may contribute to gray matter abnormalities in schizophrenia also include substance abuse, stress, and cardiometabolic dysregulation.

References

Andreasen NC, Carpenter WT Jr, Kane JM, Lasser RA, Marder SR, Weinberger DR. Remission in schizophrenia: proposed criteria and rationale for consensus. Am J Psychiatry. 2005;162(3):441–9.

Andreasen NC, Nopoulos P, Magnotta V, Pierson R, Ziebell S, Ho BC. Progressive brain change in schizophrenia: a prospective longitudinal study of first-episode schizophrenia. Biol Psychiatry. 2011;70(7):672–9.

Andreasen NC, Liu D, Ziebell S, Vora A, Ho BC. Relapse duration, treatment intensity, and brain tissue loss in schizophrenia: a prospective longitudinal MRI study. Am J Psychiatry. 2013;170(6):609–15.

Arango C, Rapado-Castro M, Reig S, Castro-Fornieles J, González-Pinto A, Otero S, Baeza I, Moreno C, Graell M, Janssen J, Parellada M, Moreno D, Bargalló N, Desco M. Progressive brain changes in children and adolescents with first-episode psychosis. Arch Gen Psychiatry. 2012;69(1):16–26.

Arbabshirani MR, Plis S, Sui J, Calhoun VD. Single subject prediction of brain disorders in neuroimaging: promises and pitfalls. Neuroimage. 2017;145(Pt B):137–65.

Arnedo J, Svrakic DM, Del Val C, Romero-Zaliz R, Hernández-Cuervo H, Molecular Genetics of

Schizophrenia Consortium, Fanous AH, Pato MT, Pato CN, de Erausquin GA, Cloninger CR, Zwir I. Uncovering the hidden risk architecture of the schizophrenias: confirmation in three independent genome-wide association studies. Am J Psychiatry. 2015;172(2):139–53.

Arnold SE, Trojanowski JQ, Gur RE, Blackwell P, Han LY, Choi C. Absence of neurodegeneration and neural injury in the cerebral cortex in a sample of elderly patients with schizophrenia. Arch Gen Psychiatry. 1998;55(3):225–32.

Bachmann S, Haffer S, Beschoner P, Viviani R. Imputation techniques for the detection of microstructural changes in schizophrenia, with an application to magnetization transfer imaging. Schizophr Res. 2011;132(1):91–6.

Bagary MS, Symms MR, Barker GJ, Mutsatsa SH, Joyce EM, Ron MA. Gray and white matter brain abnormalities in first-episode schizophrenia inferred from magnetization transfer imaging. Arch Gen Psychiatry. 2003;60(8):779–88.

Bai O, Chlan-Fourney J, Bowen R, Keegan D, Li XM. Expression of brain-derived neurotrophic factor mRNA in rat hippocampus after treatment with antipsychotic drugs. J Neurosci Res. 2003;71(1): 127–31.

Baldessarini RJ, Hegarty JD, Bird ED, Benes FM. Meta-analysis of postmortem studies of Alzheimer's disease-like neuropathology in schizophrenia. Am J Psychiatry. 1997;154:861–3.

Bartzokis G. Schizophrenia: breakdown in the well-regulated lifelong process of brain development and maturation. Neuropsychopharmacology. 2002;27(4):672–83.

Benes FM, Paskevich PA, Davidson J, Domesick VB. The effects of haloperidol on synaptic patterns in the rat striatum. Brain Res. 1985;329(1–2):265–73.

Ben-Shachar D. Mitochondrial multifaceted dysfunction in schizophrenia; complex I as a possible pathological target. Schizophr Res. 2017;187:3–10.

Blakemore SJ. Imaging brain development: the adolescent brain. Neuroimage. 2012;61:397–406.

Bohner G, Milakara D, Witthaus H, Gallinat J, Scheel M, Juckel G, Klingebiel R. MTR abnormalities in subjects at ultra-high risk for schizophrenia and first-episode schizophrenic patients compared to healthy controls. Schizophr Res. 2012;137(1–3):85–90.

Bora E, Fornito A, Radua J, Walterfang M, Seal M, Wood SJ, Yücel M, Velakoulis D, Pantelis C. Neuroanatomical abnormalities in schizophrenia: a multimodal voxelwise meta-analysis and meta-regression analysis. Schizophr Res. 2011;127(1–3):46–57.

Borges S, Gayer-Anderson C, Mondelli V. A systematic review of the activity of the hypothalamic-pituitary-adrenal axis in first episode psychosis. Psychoneuroendocrinology. 2013;38(5):603–11.

Cahn W, Hulshoff Pol HE, Lems EB, van Haren NE, Schnack HG, van der Linden JA, Schothorst PF, van Engeland H, Kahn RS. Brain volume changes in first-episode schizophrenia: a 1-year follow-up study. Arch Gen Psychiatry. 2002;59(11):1002–10.

Cannon M, Jones P, Huttunen MO, Tanskanen A, Huttunen T, Rabe-Hesketh S, Murray RM. School performance in Finnish children and later development of schizophrenia: a population-based longitudinal study. Arch Gen Psychiatry. 1999;56(5):457–63.

Casanova MF, Kreczmanski P, Trippe J 2nd, Switala A, Heinsen H, Steinbusch HW, Schmitz C. Neuronal distribution in the neocortex of schizophrenic patients. Psychiatry Res. 2008;158(3):267–77.

Chakos MH, Lieberman JA, Bilder RM, Borenstein M, Lerner G, Bogerts B, Wu H, Kinon B, Ashtari M. Increase in caudate nuclei volumes of first-episode schizophrenic patients taking antipsychotic drugs. Am J Psychiatry. 1994;151(10):1430–6.

Chakos MH, Lieberman JA, Alvir J, Bilder R, Ashtari M. Caudate nuclei volumes in schizophrenic patients treated with typical antipsychotics or clozapine. Lancet. 1995;345(8947):456–7.

Chakos MH, Shirakawa O, Lieberman J, Lee H, Bilder R, Tamminga CA. Striatal enlargement in rats chronically treated with neuroleptic. Biol Psychiatry. 1998;44(8):675–84.

Cohen J. Statistical power analysis for the behavioral sciences: Routledge; 1977.

Collinson SL, Mackay CE, James AC, Quested DJ, Phillips T, Roberts N, Crow TJ. Brain volume, asymmetry and intellectual impairment in relation to sex in early-onset schizophrenia. Br J Psychiatry. 2003;183:114–20.

Corral-Debrinski M, Horton T, Lott MT, Shoffner JM, Beal MF, Wallace DC. Mitochondrial DNA deletions in human brain: regional variability and increase with advanced age. Nat Genet. 1992;2(4): 324–9.

Corson PW, Nopoulos P, Miller DD, Arndt S, Andreasen NC. Change in basal ganglia volume over 2 years in patients with schizophrenia: typical versus atypical neuroleptics. Am J Psychiatry. 1999;156(8):1200–4.

Cosenza-Nashat M, Zhao ML, Suh HS, Morgan J, Natividad R, Morgello S, Lee SC. Expression of the translocator protein of 18 kDa by microglia, macrophages and astrocytes based on immunohistochemical localization in abnormal human brain. Neuropathol Appl Neurobiol. 2009;35(3):306–28.

Csernansky JG, Mahmoud R, Brenner R, Risperidone-USA-79 Study Group. A comparison of risperidone and haloperidol for the prevention of relapse in patients with schizophrenia. N Engl J Med. 2002;346(1):16–22.

Davis KL, Kahn RS, Ko G, Davidson M. Dopamine in schizophrenia: a review and reconceptualization. Am J Psychiatry. 1991;148(11):1474–86.

Davis J, Moylan S, Harvey BH, Maes M, Berk M. Neuroprogression in schizophrenia: pathways underpinning clinical staging and therapeutic corollaries. Aust N Z J Psychiatry. 2014;48(6):512–29.

de Leon J, Diaz FJ. A meta-analysis of worldwide studies demonstrates an association between schizophrenia and tobacco smoking behaviors. Schizophr Res. 2005;76(2–3):135–57.

DeLisi LE, Sakuma M, Tew W, Kushner M, Hoff AL, Grimson R. Schizophrenia as a chronic active brain process: a study of progressive brain structural change subsequent to the onset of schizophrenia. Psychiatry Res. 1997;74(3):129–40.

DeLisi LE, Sakuma M, Maurizio AM, Relja M, Hoff AL. Cerebral ventricular change over the first 10 years after the onset of schizophrenia. Psychiatry Res. 2004;130(1):57–70.

Dorph-Petersen KA, Pierri JN, Perel JM, Sun Z, Sampson AR, Lewis DA. The influence of chronic exposure to antipsychotic medications on brain size before and after tissue fixation: a comparison of haloperidol and olanzapine in macaque monkeys. Neuropsychopharmacology. 2005;30(9):1649–61.

Doucet GE, Rasgon N, McEwen BS, Micali N, Frangou S. Elevated body mass index is associated with increased integration and reduced cohesion of sensory-driven and internally guided resting-state functional brain networks. Cereb Cortex. 2018;28(3):988–97.

Dracheva S, Davis KL, Chin B, Woo DA, Schmeidler J, Haroutunian V. Myelin-associated mRNA and protein expression deficits in the anterior cingulate cortex and hippocampus in elderly schizophrenia patients. Neurobiol Dis. 2006;21(3):531–40. https://doi.org/10.1016/j.nbd.2005.08.012.

Ducharme S, Albaugh MD, Nguyen TV, Hudziak JJ, Mateos-Pérez JM, Labbe A, Evans AC, Karama S, Brain Development Cooperative Group. Trajectories of cortical surface area and cortical volume maturation in normal brain development. Data Brief. 2015;5:929–38.

Duncan GE, Miyamoto S, Leipzig JN, Lieberman JA. Comparison of the effects of clozapine, risperidone, and olanzapine on ketamine-induced alterations in regional brain metabolism. J Pharmacol Exp Ther. 2000;293(1):8–14.

Eickhoff SB, Bzdok D, Laird AR, Kurth F, Fox PT. Activation likelihood estimation meta-analysis revisited. Neuroimage. 2012;59(3):2349–61.

Foong J, Maier M, Barker GJ, Brocklehurst S, Miller DH, Ron MA. In vivo investigation of white matter pathology in schizophrenia with magnetisation transfer imaging. J Neurol Neurosurg Psychiatry. 2000;68(1):70–4.

Fornito A, Yücel M, Patti J, Wood SJ, Pantelis C. Mapping grey matter reductions in schizophrenia: an anatomical likelihood estimation analysis of voxel-based morphometry studies. Schizophr Res. 2009;108(1–3):104–13.

Fraguas D, Gonzalez-Pinto A, Micó JA, Reig S, Parellada M, Martínez-Cengotitabengoa M, Castro-Fornieles J, Rapado-Castro M, Baeza I, Janssen J, Desco M, Leza JC, Arango C. Decreased glutathione levels predict loss of brain volume in children and adolescents with first-episode psychosis in a two-year longitudinal study. Schizophr Res. 2012;137(1–3):58–65.

Fraguas D, Díaz-Caneja CM, Pina-Camacho L, Janssen J, Arango C. Progressive brain changes in children and adolescents with early-onset psychosis: a meta-analysis of longitudinal MRI studies. Schizophr Res. 2016;173(3):132–9.

Fraguas D, Díaz-Caneja CM, Ayora M, Hernández-Álvarez F, Rodríguez-Quiroga A, Recio S, Leza JC, Arango C. Oxidative stress and inflammation in first-episode psychosis: a systematic review and meta-analysis. Schizophr Bull. 2018;45:742–51. https://doi.org/10.1093/schbul/sby125.

Frazier JA, Giedd JN, Hamburger SD, Albus KE, Kassen D, Vaituzis AC, Rajapakse JC, Lenane MC, McKenna K, Jacobsen LK, Gordon CT, Breier A, Rapoport JL. Brain anatomic magnetic resonance imaging in childhood-onset schizophrenia. Arch Gen Psychiatry. 1996a;53(7):617–24.

Frazier JA, Giedd JN, Kaysen D, Albus K, Hamburger S, Alaghband-Rad J, Lenane MC, McKenna K, Breier A, Rapoport JL. Childhood-onset schizophrenia: brain MRI rescan after 2 years of clozapine maintenance treatment. Am J Psychiatry. 1996b;153(4):564–6.

Fumagalli F, Molteni R, Roceri M, Bedogni F, Santero R, Fossati C, Gennarelli M, Racagni G, Riva MA. Effect of antipsychotic drugs on brain-derived neurotrophic factor expression under reduced N-methyl-D-aspartate receptor activity. J Neurosci Res. 2003;72(5):622–8.

Fusar-Poli P, Radua J, McGuire P, Borgwardt S. Neuroanatomical maps of psychosis onset: voxel-wise meta-analysis of antipsychotic-naive VBM studies. Schizophr Bull. 2012;38(6):1297–307.

Fusar-Poli P, Smieskova R, Kempton MJ, Ho BC, Andreasen NC, Borgwardt S. Progressive brain changes in schizophrenia related to antipsychotic treatment? A meta-analysis of longitudinal MRI studies. Neurosci Biobehav Rev. 2013;37(8):1680–91.

Gallinat J, Meisenzahl E, Jacobsen LK, Kalus P, Bierbrauer J, Kienast T, Witthaus H, Leopold K, Seifert F, Schubert F, Staedtgen M. Smoking and structural brain deficits: a volumetric MR investigation. Eur J Neurosci. 2006;24(6):1744–50.

Giedd JN, Blumenthal J, Jeffries NO, Castellanos FX, Liu H, Zijdenbos A, Paus T, Evans AC, Rapoport JL. Brain development during childhood and adolescence: a longitudinal MRI study. Nat Neurosci. 1999;2(10):861–3.

Glahn DC, Laird AR, Ellison-Wright I, Thelen SM, Robinson JL, Lancaster JL, Bullmore E, Fox PT. Meta-analysis of gray matter anomalies in schizophrenia: application of anatomic likelihood estimation and network analysis. Biol Psychiatry. 2008;64(9):774–81.

Goff DC, Tsai G, Beal MF, Coyle JT. Tardive dyskinesia and substrates of energy metabolism in CSF. Am J Psychiatry. 1995;152(12):1730–6.

Gogtay N, Giedd JN, Lusk L, Hayashi KM, Greenstein D, Vaituzis AC, Nugent TF 3rd, Herman DH, Clasen LS, Toga AW, Rapoport JL, Thompson PM. Dynamic mapping of human cortical development during childhood through early adulthood. Proc Natl Acad Sci U S A. 2004;101(21):8174–9.

Good CD, Johnsrude IS, Ashburner J, Henson RN, Friston KJ, Frackowiak RS. A voxel-based morphometric study of ageing in 465 normal adult human brains. Neuroimage. 2001;14(1 Pt 1):21–36.

Greenstein D, Lerch J, Shaw P, Clasen L, Giedd J, Gochman P, Rapoport J, Gogtay N. Childhood onset schizophrenia: cortical brain abnormalities as young adults. J Child Psychol Psychiatry. 2006;47(10):1003–12.

Greenstein DK, Wolfe S, Gochman P, Rapoport JL, Gogtay N. Remission status and cortical thickness in childhood-onset schizophrenia. J Am Acad Child Adolesc Psychiatry. 2008;47(10):1133–40.

Gupta CN, Calhoun VD, Rachakonda S, Chen J, Patel V, Liu J, Segall J, Franke B, Zwiers MP, Arias-Vasquez A, Buitelaar J, Fisher SE, Fernandez G, van Erp TG, Potkin S, Ford J, Mathalon D, McEwen S, Lee HJ, Mueller BA, Greve DN, Andreassen O, Agartz I, Gollub RL, Sponheim SR, Ehrlich S, Wang L, Pearlson G, Glahn DC, Sprooten E, Mayer AR, Stephen J, Jung RE, Canive J, Bustillo J, Turner JA. Patterns of gray matter abnormalities in schizophrenia based on an international mega-analysis. Schizophr Bull. 2015;41(5):1133–42.

Guyon I, Weston J, Barnhill S, Vapnik V. Gene selection for cancer classification using support vector machines. Mach Learn. 2002;46(1–3):389–422.

Häfner H, Maurer K. Early detection of schizophrenia: current evidence and future perspectives. World Psychiatry. 2006;5(3):130–8.

Haijma SV, Van Haren N, Cahn W, Koolschijn PCMP, Hulshoff Pol HE, Kahn RS. Brain volumes in schizophrenia: a meta-analysis in over 18 000 subjects. Schizophr Bull. 2013;39(5):1129–38.

Hakak Y, Walker JR, Li C, Wong WH, Davis KL, Buxbaum JD, Haroutunian V, Fienberg AA. Genome-wide expression analysis reveals dysregulation of myelination-related genes in chronic schizophrenia. Proc Natl Acad Sci U S A. 2001;98(8):4746–51.

Halim ND, Weickert CS, McClintock BW, Weinberger DR, Lipska BK. Effects of chronic haloperidol and clozapine treatment on neurogenesis in the adult rat hippocampus. Neuropsychopharmacology. 2004;29(6):1063–9.

Harari JH, Díaz-Caneja CM, Janssen J, Martínez K, Arias B, Arango C. The association between gene variants and longitudinal structural brain changes in psychosis: a systematic review of longitudinal neuroimaging genetics studies. NPJ Schizophr. 2017;3:40. https://doi.org/10.1038/s41537-017-0036-2.

Haukvik UK, Hartberg CB, Nerland S, Jørgensen KN, Lange EH, Simonsen C, Nesvåg R, Dale AM, Andreassen OA, Melle I, Agartz I. No progressive brain changes during a 1-year follow-up of patients with first-episode psychosis. Psychol Med. 2016;46(3):589–98.

Heckers S, Heinsen H, Geiger B, Beckmann H. Hippocampal neuron number in schizophrenia: a stereological study. Arch Gen Psychiatry. 1991;48(11):1002–8.

Hedges L. Distribution theory for Glass's estimator of effect size and related estimators. J Educ Stat. 1981;6(2):107–28.

Ho BC, Andreasen NC, Ziebell S, Pierson R, Magnotta V. Long-term antipsychotic treatment and brain volumes: a longitudinal study of first-episode schizophrenia. Arch Gen Psychiatry. 2011;68(2):128–37.

Howes OD, Kapur S. The dopamine hypothesis of schizophrenia: version III—the final common pathway. Schizophr Bull. 2009;35(3):549–62.

Hulshoff Pol HE, Kahn RS. What happens after the first episode? A review of progressive brain changes in chronically ill patients with schizophrenia. Schizophr Bull. 2008;34(2):354–66.

Hulshoff Pol HE, Schnack HG, Mandl RC, van Haren NE, Koning H, Collins DL, Evans AC, Kahn RS. Focal gray matter density changes in schizophrenia. Arch Gen Psychiatry. 2001;58(12):1118–25.

Hunt GE, Large MM, Cleary M, Lai HMX, Saunders JB. Prevalence of comorbid substance use in schizophrenia spectrum disorders in community and clinical settings, 1990-2017: systematic review and meta-analysis. Drug Alcohol Depend. 2018;191:234–58.

Jacobsen LK, Giedd JN, Vaituzis AC, Hamburger SD, Rajapakse JC, Frazier JA, Kaysen D, Lenane MC, McKenna K, Gordon CT, Rapoport JL. Temporal lobe morphology in childhood-onset schizophrenia. Am J Psychiatry. 1996;153(3):355–61.

Jacobsen LK, Giedd JN, Castellanos FX, Vaituzis AC, Hamburger SD, Kumra S, Lenane MC, Rapoport JL. Progressive reduction of temporal lobe structures in childhood-onset schizophrenia. Am J Psychiatry. 1998;155(5):678–85.

James AC, Crow TJ, Renowden S, Wardell AM, Smith DM, Anslow P. Is the course of brain development in schizophrenia delayed? Evidence from onsets in adolescence. Schizophr Res. 1999;40(1):1–10.

James AC, James S, Smith DM, Javaloyes A. Cerebellar, prefrontal cortex, and thalamic volumes over two time points in adolescent-onset schizophrenia. Am J Psychiatry. 2004;161(6):1023–9.

Jørgensen KN, Nerland S, Norbom LB, Doan NT, Nesvåg R, Mørch-Johnsen L, Haukvik UK, Melle I, Andreassen OA, Westlye LT, Agartz I. Increased MRI-based cortical grey/white-matter contrast in sensory and motor regions in schizophrenia and bipolar disorder. Psychol Med. 2016;46(9):1971–85.

Jørgensen KN, Nesvåg R, Nerland S, Mørch-Johnsen L, Westlye LT, Lange EH, Haukvik UK, Hartberg CB, Melle I, Andreassen OA, Agartz I. Brain volume change in first-episode psychosis: an effect of antipsychotic medication independent of BMI change. Acta Psychiatr Scand. 2017;135(2):117–26.

Junn E, Mouradian MM. Apoptotic signaling in dopamine-induced cell death: the role of oxidative stress, p38 mitogen activated protein kinase, cytochrome c and caspases. J Neurochem. 2001;78(2):374–83.

Juuhl-Langseth M, Rimol LM, Rasmussen IA Jr, Thormodsen R, Holmén A, Emblem KE, Due-Tønnessen P, Rund BR, Agartz I. Comprehensive segmentation of subcortical brain volumes in early onset schizophrenia reveals limited structural abnormalities. Psychiatry Res. 2012;203(1):14–23.

Kambeitz J, Kambeitz-Ilankovic L, Leucht S, Wood S, Davatzikos C, Malchow B, Falkai P, Koutsouleris

N. Detecting neuroimaging biomarkers for schizophrenia: a meta-analysis of multivariate pattern recognition studies. Neuropsychopharmacology. 2015;40(7):1742–51.

Karoutzou G, Emrich HM, Dietrich DE. The myelin-pathogenesis puzzle in schizophrenia: a literature review. Mol Psychiatry. 2008;13(3):245–60.

Katsel P, Davis KL, Haroutunian V. Variations in myelin and oligodendrocyte-related gene expression across multiple brain regions in schizophrenia: a gene ontology study. Schizophr Res. 2005;79(2-3):157–73. https://doi.org/10.1016/j.schres.2005.06.007.

Keller A, Castellanos FX, Vaituzis AC, Jeffries NO, Giedd JN, Rapoport JL. Progressive loss of cerebellar volume in childhood-onset schizophrenia. Am J Psychiatry. 2003;160(1):128–33.

Kempton MJ, Stahl D, Williams SC, DeLisi LE. Progressive lateral ventricular enlargement in schizophrenia: a meta-analysis of longitudinal MRI studies. Schizophr Res. 2010;120(1–3):54–62.

Konopaske GT, Dorph-Petersen KA, Sweet RA, Pierri JN, Zhang W, Sampson AR, Lewis DA. Effect of chronic antipsychotic exposure on astrocyte and oligodendrocyte numbers in macaque monkeys. Biol Psychiatry. 2008;63(8):759–65.

Kumra S, Giedd JN, Vaituzis AC, Jacobsen LK, McKenna K, Bedwell J, Hamburger S, Nelson JE, Lenane M, Rapoport JL. Childhood-onset psychotic disorders: magnetic resonance imaging of volumetric differences in brain structure. Am J Psychiatry. 2000;157(9):1467–74.

Lahti HH, Weiler MA, Medoff DR, Frey KN, Hardin M, Tamminga CA. Clozapine but not haloperidol reestablishes normal task-activated rCBF patterns in schizophrenia within the anterior cingulate cortex. Neuropsychopharmacology. 2004;29(1):171–8.

Lange EH, Nerland S, Jørgensen KN, Mørch-Johnsen L, Nesvåg R, Hartberg CB, Haukvik UK, Osnes K, Melle I, Andreassen OA, Agartz I. Alcohol use is associated with thinner cerebral cortex and larger ventricles in schizophrenia, bipolar disorder and healthy controls. Psychol Med. 2017;47(4):655–68.

Lee WH, Kennedy NI, Bikson M, Frangou S. A computational assessment of target engagement in the treatment of auditory hallucinations with transcranial direct current stimulation. Front Psych. 2018;9:48. https://doi.org/10.3389/fpsyt.2018.00048.

Lidow MS, Song ZM, Castner SA, Allen PB, Greengard P, Goldman-Rakic PS. Antipsychotic treatment induces alterations in dendrite- and spine-associated proteins in dopamine-rich areas of the primate cerebral cortex. Biol Psychiatry. 2001;49(1):1–12.

Lieberman J, Chakos M, Wu H, Alvir J, Hoffman E, Robinson D, Bilder R. Longitudinal study of brain morphology in first episode schizophrenia. Biol Psychiatry. 2001;49(6):487–99.

Lieberman JA, Tollefson GD, Charles C, Zipursky R, Sharma T, Kahn RS, Keefe RS, Green AI, Gur RE, McEvoy J, Perkins D, Hamer RM, Gu H, Tohen M, HGDH Study Group. Antipsychotic drug effects on brain morphology in first-episode psychosis. Arch Gen Psychiatry. 2005;62(4):361–70.

Looney J, Childs H. The lactic acid and glutathione content of the blood of schizophrenic patients. J Clin Invest. 1934;13(6):963–8.

López-Armada MJ, Riveiro-Naveira RR, Vaamonde-García C, Valcárcel-Ares MN. Mitochondrial dysfunction and the inflammatory response? Mitochondrion. 2013;13(2):106–18.

Malchow B, Hasan A, Fusar-Poli P, Schmitt A, Falkai P, Wobrock T. Cannabis abuse and brain morphology in schizophrenia: a review of the available evidence. Eur Arch Psychiatry Clin Neurosci. 2013;263(1):3–13.

Marques TR, Ashok AH, Pillinger T, Veronese M, Turkheimer FE, Dazzan P, Sommer IEC, Howes OD. Neuroinflammation in schizophrenia: meta-analysis of in vivo microglial imaging studies. Psychol Med. 2018;49:1–11. https://doi.org/10.1017/S0033291718003057.

Martín-Santos R, Fagundo AB, Crippa JA, Atakan Z, Bhattacharyya S, Allen P, Fusar-Poli P, Borgwardt S, Seal M, Busatto GF, McGuire P. Neuroimaging in cannabis use: a systematic review of the literature. Psychol Med. 2010;40(3):383–98.

Mathalon DH, Sullivan EV, Lim KO, Pfefferbaum A. Progressive brain volume changes and the clinical course of schizophrenia in men: a longitudinal magnetic resonance imaging study. Arch Gen Psychiatry. 2001;58(2):148–57.

Matsumoto H, Simmons A, Williams S, Pipe R, Murray R, Frangou S. Structural magnetic imaging of the hippocampus in early onset schizophrenia. Biol Psychiatry. 2001;49(10):824–31.

Medic N, Ziauddeen H, Ersche KD, Farooqi IS, Bullmore ET, Nathan PJ, Ronan L, Fletcher PC. Increased body mass index is associated with specific regional alterations in brain structure. Int J Obes (Lond). 2016;40(7):1177–82.

Meshul CK, Janowsky A, Casey DE, Stallbaumer RK, Taylor B. Effect of haloperidol and clozapine on the density of "perforated" synapses in caudate, nucleus accumbens, and medial prefrontal cortex. Psychopharmacology (Berl). 1992;106(1):45–52.

Millan MJ, Fone K, Steckler T, Horan WP. Negative symptoms of schizophrenia: clinical characteristics, pathophysiological substrates, experimental models and prospects for improved treatment. Eur Neuropsychopharmacol. 2014;24(5):645–92.

Miller DD, Andreasen NC, O'Leary DS, Rezai K, Watkins GL, Ponto LL, Hichwa RD. Effect of antipsychotics on regional cerebral blood flow measured with positron emission tomography. Neuropsychopharmacology. 1997;17(4):230–40.

Mitchell AJ, Vancampfort D, Sweers K, van Winkel R, Yu W, De Hert M. Prevalence of metabolic syndrome and metabolic abnormalities in schizophrenia and related disorders—a systematic review and meta-analysis. Schizophr Bull. 2013;39(2):306–18.

Mitelman SA, Canfield EL, Newmark RE, Brickman AM, Torosjan Y, Chu KW, Hazlett EA, Haznedar

M, Shihabuddin L, Buchsbaum MS. Longitudinal assessment of gray and white matter in chronic schizophrenia: a combined diffusion-tensor and structural magnetic resonance imaging study. Open Neuroimaging J. 2009;3:31–47. https://doi.org/10.2174/1874440000903010031.

Miyamoto S, Duncan GE, Marx CE, Lieberman JA. Treatments for schizophrenia: a critical review of pharmacology and mechanisms of action of antipsychotic drugs. Mol Psychiatry. 2005;10(1):79–104.

Moghaddam B, Javitt D. From the revolution to evolution: the glutamate hypothesis of schizophrenia and its implication for treatment. Neuropsychopharmacology. 2012;37(1):4–15.

Molina V, Gispert JD, Reig S, Sanz J, Pascau J, Santos A, Palomo T, Desco M. Cerebral metabolism and risperidone treatment in schizophrenia. Schizophr Res. 2003;60(1):1–7.

Mondelli V, Pariante CM, Navari S, Aas M, D'Albenzio A, Di Forti M, Handley R, Hepgul N, Marques TR, Taylor H, Papadopoulos AS, Aitchison JK, Murray RM, Dazzan P. Higher cortisol levels are associated with smaller left hippocampal volume in first-episode psychosis. Schizophr Res. 2010;119(1–3):75–8.

Moreno D, Burdalo M, Reig S, Parellada M, Zabala A, Desco M, Baca-Baldomero E, Arango C. Structural neuroimaging in adolescents with a first psychotic episode. J Am Acad Child Adolesc Psychiatry. 2005;44(11):1151–7.

Moser DA, Doucet GE, Lee WH, Rasgon A, Krinsky H, Leibu E, Ing A, Schumann G, Rasgon N, Frangou S. Multivariate associations among behavioral, clinical, and multimodal imaging phenotypes in patients with psychosis. JAMA Psychiatry. 2018;75(4):386–95.

Naik E, Dixit VM. Mitochondrial reactive oxygen species drive proinflammatory cytokine production. J Exp Med. 2011;208:417–20.

Nakamura M, Salisbury DF, Hirayasu Y, Bouix S, Pohl KM, Yoshida T, Koo MS, Shenton ME, McCarley RW. Neocortical gray matter volume in first episode schizophrenia and first-episode affective psychosis: a cross-sectional and longitudinal MRI study. Biol Psychiatry. 2007;62(7):773–83.

Nicholls DG. Mitochondrial calcium function and dysfunction in the central nervous system. Biochim Biophys Acta. 2009;1787(11):1416–142.

Nieuwenhuis M, Schnack HG, van Haren NE, Lappin J, Morgan C, Reinders AA, Gutierrez-Tordesillas D, Roiz-Santiañez R, Schaufelberger MS, Rosa PG, Zanetti MV, Busatto GF, Crespo-Facorro B, McGorry PD, Velakoulis D, Pantelis C, Wood SJ, Kahn RS, Mourao-Miranda J, Dazzan P. Multi-center MRI prediction models: predicting sex and illness course in first episode psychosis patients. Neuroimage. 2017;145(Pt B):246–53.

Norton N, Moskvina V, Morris DW, Bray NJ, Zammit S, Williams NM, Williams HJ, Preece AC, Dwyer S, Wilkinson JC, Spurlock G, Kirov G, Buckland P, Waddington JL, Gill M, Corvin AP, Owen MJ, O'Donovan MC. Evidence that interaction between neuregulin 1 and its receptor erbB4 increases susceptibility to schizophrenia. Am J Med Genet B Neuropsychiatr Genet. 2006;141B(1):96–101.

Nymberg C, Jia T, Ruggeri B, Schumann G. Analytical strategies for large imaging genetic datasets: experiences from the IMAGEN study. Ann N Y Acad Sci. 2013;1282:92–106.

O'Rahilly R, Müller F. Human embryology and teratology. 3rd ed. New York: Wiley-Liss; 2001.

Oka T, Hikoso S, Yamaguchi O, Taneike M, Takeda T, Tamai T, Oyabu J, Murakawa T, Nakayama H, Nishida K, Akira S, Yamamoto A, Komuro I, Otsu K. Mitochondrial DNA that escapes from autophagy causes inflammation and heart failure. Nature. 2012;485(7397):251–5.

Okada N, Fukunaga M, Yamashita F, Koshiyama D, Yamamori H, Ohi K, Yasuda Y, Fujimoto M, Watanabe Y, Yahata N, Nemoto K, Hibar DP, van Erp TGM, Fujino H, Isobe M, Isomura S, Natsubori T, Narita H, Hashimoto N, Miyata J, Koike S, Takahashi T, Yamasue H, Matsuo K, Onitsuka T, Iidaka T, Kawasaki Y, Yoshimura R, Watanabe Y, Suzuki M, Turner JA, Takeda M, Thompson PM, Ozaki N, Kasai K, Hashimoto R, COCORO. Abnormal asymmetries in subcortical brain volume in schizophrenia. Mol Psychiatry. 2016;21(10):1460–6.

Olabi B, Ellison-Wright I, McIntosh AM, Wood SJ, Bullmore E, Lawrie SM. Are there progressive brain changes in schizophrenia? A meta-analysis of structural magnetic resonance imaging studies. Biol Psychiatry. 2011;70(1):88–96.

Osimo EF, Beck K, Marques TR, Howes OD. Synaptic loss in schizophrenia: a meta-analysis and systematic review of synaptic protein and mRNA measures. Mol Psychiatry. 2018;24:549–61. https://doi.org/10.1038/s41380-018-0041-5.

Pakkenberg B. Total nerve cell number in neocortex in chronic schizophrenics and controls estimated using optical disectors. Biol Psychiatry. 1993;34(11):768–72.

Palaniyappan L, Al-Radaideh A, Mougin O, Gowland P, Liddle PF. Combined white matter imaging suggests myelination defects in visual processing regions in schizophrenia. Neuropsychopharmacology. 2013;38(9):1808–15.

Plavén-Sigray P, Matheson GJ, Collste K, Ashok AH, Coughlin JM, Howes OD, Mizrahi R, Pomper MG, Rusjan P, Veronese M, Wang Y, Cervenka S.Positron Emission Tomography Studies of the Glial Cell Marker Translocator Protein in Patients With Psychosis: A Meta-analysis Using Individual Participant Data. Biol Psychiatry. 2018;84(6):433–42. https://doi.org/10.1016/j.biopsych.2018.02.1171.

Plavén-Sigray P, Cervenka S. Meta-analytic studies of the glial cell marker TSPO in psychosis - a question of apples and pears? Psychol Med. 2019;49(10):1624–28. https://doi.org/10.1017/S003329171800421X.

Paus T, Keshavan M, Giedd JN. Why do many psychiatric disorders emerge during adolescence? Nat Rev Neurosci. 2008;9(12):947–57.

Price G, Cercignani M, Chu EM, Barnes TR, Barker GJ, Joyce EM, Ron MA. Brain pathology in first-episode psychosis: magnetization transfer imaging provides additional information to MRI measurements of volume loss. Neuroimage. 2010;49(1):185–92.

Puri BK, Hutton SB, Saeed N, Oatridge A, Hajnal JV, Duncan L, Chapman MJ, Barnes TR, Bydder GM, Joyce EM. A serial longitudinal quantitative MRI study of cerebral changes in first-episode schizophrenia using image segmentation and subvoxel registration. Psychiatry Res. 2001;106:141–50.

Radua J, Mataix-Cols D. Voxel-wise meta-analysis of grey matter changes in obsessive-compulsive disorder. Br J Psychiatry. 2009;195(5):393–402.

Radua J, Borgwardt S, Crescini A, Mataix-Cols D, Meyer-Lindenberg A, McGuire PK, Fusar-Poli P. Multimodal meta-analysis of structural and functional brain changes in first episode psychosis and the effects of antipsychotic medication. Neurosci Biobehav Rev. 2012;36(10):2325–33.

Rais M, Cahn W, Van Haren N, Schnack H, Caspers E, Hulshoff Pol H, Kahn R. Excessive brain volume loss over time in cannabis-using first-episode schizophrenia patients. Am J Psychiatry. 2008;165(4):490–6.

Rais M, van Haren NE, Cahn W, Schnack HG, Lepage C, Collins L, Evans AC, Hulshoff Pol HE, Kahn RS. Cannabis use and progressive cortical thickness loss in areas rich in CB1 receptors during the first five years of schizophrenia. Eur Neuropsychopharmacol. 2010;20(12):855–65.

Rapoport JL, Addington AM, Frangou S. The neurodevelopmental model of schizophrenia: update 2005. Mol Psychiatry. 2005;10(5):434–49.

Raz N, Lindenberger U, Rodrigue KM, Kennedy KM, Head D, Williamson A, Dahle C, Gerstorf D, Acker JD. Regional brain changes in aging healthy adults: general trends, individual differences and modifiers. Cereb Cortex. 2005;15(11):1676–89.

Raz N, Ghisletta P, Rodrigue KM, Kennedy KM, Lindenberger U. Trajectories of brain aging in middle-aged and older adults: regional and individual differences. Neuroimage. 2010;51(2):501–11.

Reig S, Moreno C, Moreno D, Burdalo M, Janssen J, Parellada M, Zabala A, Desco M, Arango C. Progression of brain volume changes in adolescent-onset psychosis. Schizophr Bull. 2009;35(1):233–43.

Reig S, Parellada M, Castro-Fornieles J, Janssen J, Moreno D, Baeza I, Bargalló N, González-Pinto A, Graell M, Ortuño F, Otero S, Arango C, Desco M. Multicenter study of brain volume abnormalities in children and adolescent-onset psychosis. Schizophr Bull. 2011;37(6):1270–80.

Roberts RC. Postmortem studies on mitochondria in schizophrenia. Schizophr Res. 2017;187:17–25.

Rosenbaum S, Tiedemann A, Sherrington C, Curtis J, Ward PB. Physical activity interventions for people with mental illness: a systematic review and meta-analysis. J Clin Psychiatry. 2014;75(9):964–74.

Rozycki M, Satterthwaite TD, Koutsouleris N, Erus G, Doshi J, Wolf DH, Fan Y, Gur RE, Gur RC, Meisenzahl EM, Zhuo C, Yin H, Yan H, Yue W, Zhang D, Davatzikos C. Multisite machine learning analysis provides a robust structural imaging signature of schizophrenia detectable across diverse patient populations and within individuals. Schizophr Bull. 2018;44(5):1035–44.

Ryan MC, Collins P, Thakore JH. Impaired fasting glucose tolerance in first-episode, drug-naive patients with schizophrenia. Am J Psychiatry. 2003;160(2):284–9.

Saeys Y, Inza I, Larrañaga P. A review of feature selection techniques in bioinformatics. Bioinformatics. 2007;23(19):2507–17.

Sapolsky RM. Stress and plasticity in the limbic system. Neurochem Res. 2003;28(11):1735–42.

Schaufelberger MS, Lappin JM, Duran FL, Rosa PG, Uchida RR, Santos LC, Murray RM, McGuire PK, Scazufca M, Menezes PR, Busatto GF. Lack of progression of brain abnormalities in first-episode psychosis: a longitudinal magnetic resonance imaging study. Psychol Med. 2011;41(8):1677–89.

Selemon LD, Goldman-Rakic PS. The reduced neuropil hypothesis: a circuit based model of schizophrenia. Biol Psychiatry. 1999;45(1):17–25.

Selemon LD, Lidow MS, Goldman-Rakic PS. Increased volume and glial density in primate prefrontal cortex associated with chronic antipsychotic drug exposure. Biol Psychiatry. 1999;46(2):161–72.

Sporn AL, Greenstein DK, Gogtay N, Jeffries NO, Lenane M, Gochman P, Clasen LS, Blumenthal J, Giedd JN, Rapoport JL. Progressive brain volume loss during adolescence in childhood-onset schizophrenia. Am J Psychiatry. 2003;160(12):2181–9.

Squarcina L, Castellani U, Bellani M, Perlini C, Lasalvia A, Dusi N, Bonetto C, Cristofalo D, Tosato S, Rambaldelli G, Alessandrini F, Zoccatelli G, Pozzi-Mucelli R, Lamonaca D, Ceccato E, Pileggi F, Mazzi F, Santonastaso P, Ruggeri M, Brambilla P, GET UP Group. Classification of first-episode psychosis in a large cohort of patients using support vector machine and multiple kernel learning techniques. Neuroimage. 2017;145(Pt B):238–45.

Steen RG, Mull C, McClure R, Hamer RM, Lieberman JA. Brain volume in first-episode schizophrenia: systematic review and meta-analysis of magnetic resonance imaging studies. Br J Psychiatry. 2006;188:510–8.

Takahashi T, Wood SJ, Soulsby B, McGorry PD, Tanino R, Suzuki M, Velakoulis D, Pantelis C. Follow-up MRI study of the insular cortex in first-episode psychosis and chronic schizophrenia. Schizophr Res. 2009;108(1–3):49–56.

Thompson PM, Vidal C, Giedd JN, Gochman P, Blumenthal J, Nicolson R, Toga AW, Rapoport JL. Mapping adolescent brain change reveals dynamic wave of accelerated gray matter loss in very early-onset schizophrenia. Proc Natl Acad Sci U S A. 2001;98(20):11650–5.

Thompson PM, Stein JL, Medland SE, Hibar DP, Vasquez AA, Renteria ME, Toro R, Jahanshad N, Schumann G, Franke B, Wright MJ, Martin NG, Agartz I, Alda M, Alhusaini S, Almasy L, Almeida J, Alpert K,

Andreasen NC, Andreassen OA, Apostolova LG, Appel K, Armstrong NJ, Aribisala B, Bastin ME, Bauer M, Bearden CE, Bergmann O, Binder EB, Blangero J, Bockholt HJ, Bøen E, Bois C, Boomsma DI, Booth T, Bowman IJ, Bralten J, Brouwer RM, Brunner HG, Brohawn DG, Buckner RL, Buitelaar J, Bulayeva K, Bustillo JR, Calhoun VD, Cannon DM, Cantor RM, Carless MA, Caseras X, Cavalleri GL, Chakravarty MM, Chang KD, Ching CR, Christoforou A, Cichon S, Clark VP, Conrod P, Coppola G, Crespo-Facorro B, Curran JE, Czisch M, Deary IJ, de Geus EJ, den Braber A, Delvecchio G, Depondt C, de Haan L, de Zubicaray GI, Dima D, Dimitrova R, Djurovic S, Dong H, Donohoe G, Duggirala R, Dyer TD, Ehrlich S, Ekman CJ, Elvsåshagen T, Emsell L, Erk S, Espeseth T, Fagerness J, Fears S, Fedko I, Fernández G, Fisher SE, Foroud T, Fox PT, Francks C, Frangou S, Frey EM, Frodl T, Frouin V, Garavan H, Giddaluru S, Glahn DC, Godlewska B, Goldstein RZ, Gollub RL, Grabe HJ, Grimm O, Gruber O, Guadalupe T, Gur RE, Gur RC, Göring HH, Hagenaars S, Hajek T, Hall GB, Hall J, Hardy J, Hartman CA, Hass J, Hatton SN, Haukvik UK, Hegenscheid K, Heinz A, Hickie IB, Ho BC, Hoehn D, Hoekstra PJ, Hollinshead M, Holmes AJ, Homuth G, Hoogman M, Hong LE, Hosten N, Hottenga JJ, Hulshoff Pol HE, Hwang KS, Jack CR Jr, Jenkinson M, Johnston C, Jönsson EG, Kahn RS, Kasperaviciute D, Kelly S, Kim S, Kochunov P, Koenders L, Krämer B, Kwok JB, Lagopoulos J, Laje G, Landen M, Landman BA, Lauriello J, Lawrie SM, Lee PH, Le Hellard S, Lemaître H, Leonardo CD, Li CS, Liberg B, Liewald DC, Liu X, Lopez LM, Loth E, Lourdusamy A, Luciano M, Macciardi F, Machielsen MW, Macqueen GM, Malt UF, Mandl R, Manoach DS, Martinot JL, Matarin M, Mather KA, Mattheisen M, Mattingsdal M, Meyer-Lindenberg A, McDonald C, McIntosh AM, McMahon FJ, McMahon KL, Meisenzahl E, Melle I, Milaneschi Y, Mohnke S, Montgomery GW, Morris DW, Moses EK, Mueller BA, Muñoz Maniega S, Mühleisen TW, Müller-Myhsok B, Mwangi B, Nauck M, Nho K, Nichols TE, Nilsson LG, Nugent AC, Nyberg L, Olvera RL, Oosterlaan J, Ophoff RA, Pandolfo M, Papalampropoulou-Tsiridou M, Papmeyer M, Paus T, Pausova Z, Pearlson GD, Penninx BW, Peterson CP, Pfennig A, Phillips M, Pike GB, Poline JB, Potkin SG, Pütz B, Ramasamy A, Rasmussen J, Rietschel M, Rijpkema M, Risacher SL, Roffman JL, Roiz-Santiañez R, Romanczuk-Seiferth N, Rose EJ, Royle NA, Rujescu D, Ryten M, Sachdev PS, Salami A, Satterthwaite TD, Savitz J, Saykin AJ, Scanlon C, Schmaal L, Schnack HG, Schork AJ, Schulz SC, Schür R, Seidman L, Shen L, Shoemaker JM, Simmons A, Sisodiya SM, Smith C, Smoller JW, Soares JC, Sponheim SR, Sprooten E, Starr JM, Steen VM, Strakowski S, Strike L, Sussmann J, Sämann PG, Teumer A, Toga AW, Tordesillas-Gutierrez D, Trabzuni D, Trost S, Turner J, Van den Heuvel M, van der Wee NJ, van Eijk K, van Erp TG, van Haren NE, van't Ent D, van Tol MJ, Valdés Hernández MC, Veltman DJ, Versace A, Völzke H, Walker R, Walter H, Wang L, Wardlaw JM, Weale ME, Weiner MW, Wen W, Westlye LT, Whalley HC, Whelan CD, White T, Winkler AM, Wittfeld K, Woldehawariat G, Wolf C, Zilles D, Zwiers MP, Thalamuthu A, Schofield PR, Freimer NB, Lawrence NS, Drevets W, Alzheimer's Disease Neuroimaging Initiative, EPIGEN Consortium, IMAGEN Consortium, Saguenay Youth Study (SYS) Group. The ENIGMA Consortium: large-scale collaborative analyses of neuroimaging and genetic data. Brain Imaging Behav. 2014;8(2):153–82.

Thompson PM, Andreassen OA, Arias-Vasquez A, Bearden CE, Boedhoe PS, Brouwer RM, Buckner RL, Buitelaar JK, Bulayeva KB, Cannon DM, Cohen RA, Conrod PJ, Dale AM, Deary IJ, Dennis EL, de Reus MA, Desrivieres S, Dima D, Donohoe G, Fisher SE, Fouche JP, Francks C, Frangou S, Franke B, Ganjgahi H, Garavan H, Glahn DC, Grabe HJ, Guadalupe T, Gutman BA, Hashimoto R, Hibar DP, Holland D, Hoogman M, Pol HEH, Hosten N, Jahanshad N, Kelly S, Kochunov P, Kremen WS, Lee PH, Mackey S, Martin NG, Mazoyer B, McDonald C, Medland SE, Morey RA, Nichols TE, Paus T, Pausova Z, Schmaal L, Schumann G, Shen L, Sisodiya SM, Smit DJA, Smoller JW, Stein DJ, Stein JL, Toro R, Turner JA, van den Heuvel MP, van den Heuvel OL, van Erp TGM, van Rooij D, Veltman DJ, Walter H, Wang Y, Wardlaw JM, Whelan CD, Wright MJ, Ye J. ENIGMA Consortium. ENIGMA and the individual: predicting factors that affect the brain in 35 countries worldwide. Neuroimage. 2017;145(Pt B):389–408.

Thune JJ, Uylings HB, Pakkenberg B. No deficit in total number of neurons in the prefrontal cortex in schizophrenics. J Psychiatr Res. 2001;35(1):15–21.

Tost H, Braus DF, Hakimi S, Ruf M, Vollmert C, Hohn F, Meyer-Lindenberg A. Acute D2 receptor blockade induces rapid, reversible remodeling in human cortical-striatal circuits. Nat Neurosci. 2010;13(8):920–2.

Uranova N, Orlovskaya D, Vikhreva O, Zimina I, Kolomeets N, Vostrikov V, Rachmanova V. Electron microscopy of oligodendroglia in severe mental illness. Brain Res Bull. 2001;55(5):597–610.

Uranova NA, Vostrikov VM, Orlovskaya DD, Rachmanova VI. Oligodendroglial density in the prefrontal cortex in schizophrenia and mood disorders: a study from the Stanley Neuropathology Consortium. Schizophr Res. 2004;67(2–3):269–75.

van Erp TG, Hibar DP, Rasmussen JM, Glahn DC, Pearlson GD, Andreassen OA, Agartz I, Westlye LT, Haukvik UK, Dale AM, Melle I, Hartberg CB, Gruber O, Kraemer B, Zilles D, Donohoe G, Kelly S, McDonald C, Morris DW, Cannon DM, Corvin A, Machielsen MW, Koenders L, de Haan L, Veltman DJ, Satterthwaite TD, Wolf DH, Gur RC, Gur RE, Potkin SG, Mathalon DH, Mueller BA, Preda A, Macciardi F, Ehrlich S, Walton E, Hass J, Calhoun VD, Bockholt HJ, Sponheim SR, Shoemaker JM, van Haren NE, Pol HE, Ophoff RA, Kahn RS, Roiz-Santiañez R, Crespo-Facorro B, Wang L, Alpert KI, Jönsson EG, Dimitrova R, Bois C, Whalley HC, McIntosh AM, Lawrie SM, Hashimoto R, Thompson PM, Turner JA. Subcortical brain volume abnormalities in 2028 individuals with schizophrenia and 2540

healthy controls via the ENIGMA consortium. Mol Psychiatry. 2016;21(4):547–52.

van Erp TGM, Walton E, Hibar DP, Schmaal L, Jiang W, Glahn DC, Pearlson GD, Yao N, Fukunaga M, Hashimoto R, Okada N, Yamamori H, Bustillo JR, Clark VP, Agartz I, Mueller BA, Cahn W, de Zwarte SMC, Hulshoff Pol HE, Kahn RS, Ophoff RA, van Haren NEM, Andreassen OA, Dale AM, Doan NT, Gurholt TP, Hartberg CB, Haukvik UK, Jørgensen KN, Lagerberg TV, Melle I, Westlye LT, Gruber O, Kraemer B, Richter A, Zilles D, Calhoun VD, Crespo-Facorro B, Roiz-Santiañez R, Tordesillas-Gutiérrez D, Loughland C, Carr VJ, Catts S, Cropley VL, Fullerton JM, Green MJ, Henskens FA, Jablensky A, Lenroot RK, Mowry BJ, Michie PT, Pantelis C, Quidé Y, Schall U, Scott RJ, Cairns MJ, Seal M, Tooney PA, Rasser PE, Cooper G, Shannon Weickert C, Weickert TW, Morris DW, Hong E, Kochunov P, Beard LM, Gur RE, Gur RC, Satterthwaite TD, Wolf DH, Belger A, Brown GG, Ford JM, Macciardi F, Mathalon DH, O'Leary DS, Potkin SG, Preda A, Voyvodic J, Lim KO, McEwen S, Yang F, Tan Y, Tan S, Wang Z, Fan F, Chen J, Xiang H, Tang S, Guo H, Wan P, Wei D, Bockholt HJ, Ehrlich S, Wolthusen RPF, King MD, Shoemaker JM, Sponheim SR, De Haan L, Koenders L, Machielsen MW, van Amelsvoort T, Veltman DJ, Assogna F, Banaj N, de Rossi P, Iorio M, Piras F, Spalletta G, McKenna PJ, Pomarol-Clotet E, Salvador R, Corvin A, Donohoe G, Kelly S, Whelan CD, Dickie EW, Rotenberg D, Voineskos AN, Ciufolini S, Radua J, Dazzan P, Murray R, Reis Marques T, Simmons A, Borgwardt S, Egloff L, Harrisberger F, Riecher-Rössler A, Smieskova R, Alpert KI, Wang L, Jönsson EG, Koops S, Sommer IEC, Bertolino A, Bonvino A, Di Giorgio A, Neilson E, Mayer AR, Stephen JM, Kwon JS, Yun JY, Cannon DM, McDonald C, Lebedeva I, Tomyshev AS, Akhadov T, Kaleda V, Fatouros-Bergman H, Flyckt L, Karolinska Schizophrenia Project, Busatto GF, Rosa PGP, Serpa MH, Zanetti MV, Hoschl C, Skoch A, Spaniel F, Tomecek D, Hagenaars SP, McIntosh AM, Whalley HC, Lawrie SM, Knöchel C, Oertel-Knöchel V, Stäblein M, Howells FM, Stein DJ, Temmingh HS, Uhlmann A, Lopez-Jaramillo C, Dima D, McMahon A, Faskowitz JI, Gutman BA, Jahanshad N, Thompson PM, Turner JA. Biol Psychiatry. 2018;84(9):644–54.

van Haren NE, Hulshoff Pol HE, Schnack HG, Cahn W, Brans R, Carati I, Rais M, Kahn RS. Progressive brain volume loss in schizophrenia over the course of the illness: evidence of maturational abnormalities in early adulthood. Biol Psychiatry. 2008;63(1):106–13.

van Haren NE, Schnack HG, Cahn W, van den Heuvel MP, Lepage C, Collins L, Evans AC, Hulshoff Pol HE, Kahn RS. Changes in cortical thickness during the course of illness in schizophrenia. Arch Gen Psychiatry. 2011;68(9):871–80.

van Haren NE, Schnack HG, Koevoets MGJC, Cahn W, Hulshoff Pol HE, Kahn RS. Trajectories of subcortical volume change in schizophrenia: a 5-year follow-up. Schizophr Res. 2016;173(3):140–5.

van Kesteren CF, Gremmels H, de Witte LD, Hol EH, Van Gool AH, Falkai PH, Kahn RS, Sommer IE. Immune involvement in the pathogenesis of schizophrenia: a meta-analysis on post-mortem brain studies. Transl Psychiatry. 2017;7:e1075. https://doi.org/10.1038/tp.2017.4.

Veijola J, Guo JY, Moilanen JS, Jääskeläinen E, Miettunen J, Kyllönen M, Haapea M, Huhtaniska S, Alaräisänen A, Mäki P, Kiviniemi V, Nikkinen J, Starck T, Remes JJ, Tanskanen P, Tervonen O, Wink AM, Kehagia A, Suckling J, Kobayashi H, Barnett JH, Barnes A, Koponen HJ, Jones PB, Isohanni M, Murray GK. Longitudinal changes in total brain volume in schizophrenia: relation to symptom severity, cognition and antipsychotic medication. PLoS One. 2014;9(7):e101689. https://doi.org/10.1371/journal.pone.0101689.

Vernon AC, Natesan S, Modo M, Kapur S. Effect of chronic antipsychotic treatment on brain structure: a serial magnetic resonance imaging study with ex vivo and postmortem confirmation. Biol Psychiatry. 2011;69(10):936–44.

Vernon AC, Natesan S, Crum WR, Cooper JD, Modo M, Williams SC, Kapur S. Contrasting effects of haloperidol and lithium on rodent brain structure: a magnetic resonance imaging study with postmortem confirmation. Biol Psychiatry. 2012;71(10):855–63.

Veronese E, Castellani U, Peruzzo D, Bellani M, Brambilla P. Machine learning approaches: from theory to application in schizophrenia. Comput Math Methods Med. 2013;2013:867924. https://doi.org/10.1155/2013/867924.

Vita A, De Peri L, Silenzi C, Dieci M. Brain morphology in first-episode schizophrenia: a meta-analysis of quantitative magnetic resonance imaging studies. Schizophr Res. 2006;82(1):75–88.

Vita A, De Peri L, Deste G, Sacchetti E. Progressive loss of cortical gray matter in schizophrenia: a meta-analysis and meta-regression of longitudinal MRI studies. Transl Psychiatry. 2012;2:e190. https://doi.org/10.1038/tp.2012.116.

Vita A, De Peri L, Deste G, Barlati S, Sacchetti E. The effect of antipsychotic treatment on cortical gray matter changes in schizophrenia: does the class matter? A meta-analysis and meta-regression of longitudinal magnetic resonance imaging studies. Biol Psychiatry. 2015;78(6):403–12.

Wakade CG, Mahadik SP, Waller JL, Chiu FC. Atypical neuroleptics stimulate neurogenesis in adult rat brain. J Neurosci Res. 2002;69(1):727–9.

Walker MA, Highley JR, Esiri MM, McDonald B, Roberts HC, Evans SP, et al. Estimated neuronal populations and volumes of the hippocampus and its subfields in schizophrenia. Am J Psychiatry. 2002;159(5):821–8.

Walker E, Mittal V, Tessner K. Stress and the hypothalamic pituitary adrenal axis in the developmental course of schizophrenia. Annu Rev Clin Psychol. 2008;4:189–216.

Walton E, Hibar DP, van Erp TG, Potkin SG, Roiz-Santiañez R, Crespo-Facorro B, Suarez-Pinilla P, Van Haren NE, de Zwarte SM, Kahn RS, Cahn W, Doan NT, Jørgensen KN, Gurholt TP, Agartz I, Andreassen OA, Westlye LT, Melle I, Berg AO, Mørch-Johnsen L, Faerden A, Flyckt L, Fatouros-Bergman H, Karolinska Schizophrenia Project Consortium (KaSP), Jönsson EG, Hashimoto R, Yamamori H, Fukunaga M, Preda A, De Rossi P, Piras F, Banaj N, Ciullo V, Spalletta G, Gur RE, Gur RC, Wolf DH, Satterthwaite TD, Beard LM, Sommer IE, Koops S, Gruber O, Richter A, Krämer B, Kelly S, Donohoe G, McDonald C, Cannon DM, Corvin A, Gill M, Di Giorgio A, Bertolino A, Lawrie S, Nickson T, Whalley HC, Neilson E, Calhoun VD, Thompson PM, Turner JA, Ehrlich S. Positive symptoms associate with cortical thinning in the superior temporal gyrus via the ENIGMA Schizophrenia consortium. Acta Psychiatr Scand. 2017;135(5):439–47.

Walton E, Hibar DP, van Erp TGM, Potkin SG, Roiz-Santiañez R, Crespo-Facorro B, Suarez-Pinilla P, van Haren NEM, de Zwarte SMC, Kahn RS, Cahn W, Doan NT, Jørgensen KN, Gurholt TP, Agartz I, Andreassen OA, Westlye LT, Melle I, Berg AO, Morch-Johnsen L, Færden A, Flyckt L, Fatouros-Bergman H, Karolinska Schizophrenia Project Consortium (KaSP), Jönsson EG, Hashimoto R, Yamamori H, Fukunaga M, Jahanshad N, De Rossi P, Piras F, Banaj N, Spalletta G, Gur RE, Gur RC, Wolf DH, Satterthwaite TD, Beard LM, Sommer IE, Koops S, Gruber O, Richter A, Krämer B, Kelly S, Donohoe G, McDonald C, Cannon DM, Corvin A, Gill M, Di Giorgio A, Bertolino A, Lawrie S, Nickson T, Whalley HC, Neilson E, Calhoun VD, Thompson PM, Turner JA, Ehrlich S. Prefrontal cortical thinning links to negative symptoms in schizophrenia via the ENIGMA consortium. Psychol Med. 2018;48(1):82–94.

Wang HD, Deutch AY. Dopamine depletion of the prefrontal cortex induces dendritic spine loss: reversal by atypical antipsychotic drug treatment. Neuropsychopharmacology. 2008;33(6):1276–86.

Wang HD, Dunnavant FD, Jarman T, Deutch AY. Effects of antipsychotic drugs on neurogenesis in the forebrain of the adult rat. Neuropsychopharmacology. 2004;29(7):1230–8.

Weinberger DR. Implications of normal brain development for the pathogenesis of schizophrenia. Arch Gen Psychiatry. 1987;44(7):660–9.

Whiteford HA, Degenhardt L, Rehm J, Baxter AJ, Ferrari AJ, Erskine HE, Charlson FJ, Norman RE, Flaxman AD, Johns N, Burstein R, Murray CJ, Vos T. Global burden of disease attributable to mental and substance use disorders: findings from the Global Burden of Disease Study 2010. Lancet. 2013;382(9904):1575–86.

Whitworth AB, Kemmler G, Honeder M, Kremser C, Felber S, Hausmann A, Walch T, Wanko C, Weiss EM, Stuppaeck CH, Fleischhacker WW. Longitudinal volumetric MRI study in first- and multiple-episode male schizophrenia patients. Psychiatry Res. 2005;140(3):225–37.

Wood SJ, Velakoulis D, Smith DJ, Bond D, Stuart GW, McGorry PD, Brewer WJ, Bridle N, Eritaia J, Desmond P, Singh B, Copolov D, Pantelis C. A longitudinal study of hippocampal volume in first episode psychosis and chronic schizophrenia. Schizophr Res. 2001;52(1–2):37–46.

Wright AM, Bempong J, Kirby ML, Barlow RL, Bloomquist JR. Effects of haloperidol metabolites on neurotransmitter uptake and release: possible role in neurotoxicity and tardive dyskinesia. Brain Res. 1998;788(1–2):215–22.

Wright IC, Rabe-Hesketh S, Woodruff PW, David AS, Murray RM, Bullmore ET. Meta-analysis of regional brain volumes in schizophrenia. Am J Psychiatry. 2000;157(1):16–25.

Xu L, Groth KM, Pearlson G, Schretlen DJ, Calhoun VD. Source-based morphometry: the use of independent component analysis to identify gray matter differences with application to schizophrenia. Hum Brain Mapp. 2009;30(3):711–24.

Yates KF, Sweat V, Yau PL, Turchiano MM, Convit A. Impact of metabolic syndrome on cognition and brain: a selected review of the literature. Arterioscler Thromb Vasc Biol. 2012;32(9):2060–7.

Yoshihara Y, Sugihara G, Matsumoto H, Suckling J, Nishimura K, Toyoda T, Isoda H, Tsuchiya KJ, Takebayashi K, Suzuki K, Sakahara H, Nakamura K, Mori N, Takei N. Voxel-based structural magnetic resonance imaging (MRI) study of patients with early onset schizophrenia. Ann General Psychiatry. 2008;7:25. https://doi.org/10.1186/1744-859X-7-25.

Zahr NM, Pfefferbaum A. Alcohol's effects on the brain: neuroimaging results in humans and animal models. Alcohol Res. 2017;38(2):183–206.

Zanetti MV, Schaufelberger MS, Doshi J, Ou Y, Ferreira LK, Menezes PR, Scazufca M, Davatzikos C, Busatto GF. Neuroanatomical pattern classification in a population-based sample of first-episode schizophrenia. Prog Neuro-Psychopharmacol Biol Psychiatry. 2013;43:116–25.

Zheutlin AB, Chekroud AM, Polimanti R, Gelernter J, Sabb FW, Bilder RM, Freimer N, London ED, Hultman CM, Cannon TD. Multivariate pattern analysis of genotype-phenotype relationships in schizophrenia. Schizophr Bull. 2018;44(5):1045–52.

Zipursky RB, Reilly TJ, Murray RM. The myth of schizophrenia as a progressive brain disease. Schizophr Bull. 2013;39(6):1363–72.

Microstructure Imaging by Diffusion MRI

3

Filip Szczepankiewicz and Carl-Fredrik Westin

Contents

3.1 Introduction

With the development of advanced forms of diffusion-weighted magnetic resonance imaging (dMRI), it is expected that imaging will elucidate pathological and neuro-developmental changes in brain tissue architecture with potential to provide diagnostic and predictive biomarkers. Hypothesized cellular level microstructural pathologies include demyelination, abnormal dendritic pruning, neuroinflammation and cellular degeneration. It is essential to separately identify these pathologies in order to design better and more focused treatment approaches. Modern dMRI technologies has the potential to provide improved specificity, and thus clearer understanding of the relation between the brain's microstructure and the etiology of different types of pathology. This chapter is a brief introduction to the principles of dMRI and gives examples of analysis methods that are frequently used in the field, as well as more advanced methods for diffusion encoding that are promising venues for future exploration of the brain. Where possible, we refer to articles that give more comprehensive descriptions of subjects that are outside of the scope of this chapter.

F. Szczepankiewicz · C.-F. Westin (✉)
Laboratory for Mathematics in Imaging, Department of Radiology, Harvard Medical School, Brigham and Women's Hospital, Boston, MA, USA
e-mail: fszczepankiewicz@bwh.harvard.edu; westin@bwh.harvard.edu

M. Kubicki, M. E. Shenton (eds.), *Neuroimaging in Schizophrenia*,
https://doi.org/10.1007/978-3-030-35206-6_3

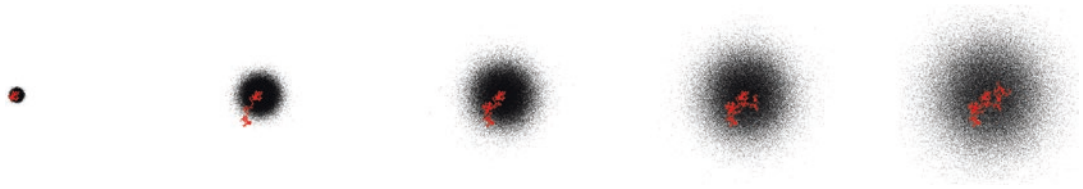

Fig. 3.1 Visualization of an isotropic Gaussian diffusion process. Each plume, from left to right, shows the position of 10^6 particles at five equidistant timepoints. The red line traces the trajectory of a single particle; its path is not straight, but rather stochastic and tortuous. This is the case for all particles, since they are part of a medium within which they constantly collide with each other on a very short time scale. In dMRI, we are not interested in the history of a single particle, but rather in the relevant features of the larger ensemble. At each time point, the black point clouds describes the density of all pathways, and if normalized, they describe the probability of a particle being at a specific location after each time step. In this case, we can say that the diffusion is isotropic, and by measuring the width of the distribution at multiple time points, we may calculate the rate of diffusion, or diffusivity, of the medium

Water is ubiquitous in biological tissues and its thermal motion (diffusion) is vital to all life-sustaining chemical processes—which would halt without it. The diffusing particles interact with each other as well as their surroundings; impermeable membranes restrict the movement to a finite region, and obstacles hinder the motion such that the path between two points becomes more tortuous. Given enough time, the diffusion process will be imprinted with features of the microstructure allowing a carefully designed MRI experiment to serve as an indirect probe of the microstructure.

The phenomenon of diffusion is also named 'Brownian motion' after the botanist Robert Brown, who observed the movement of plant spores floating in the water in 1827. The first theoretical treatment of Brownian motion was not presented until 1905 by Einstein (1905). Einstein's interest in explaining the erratic movement of pollen in water was not directly motivated by a specific interest in diffusion, but by the general interest of proving the existence of the atom. Einstein derived an equation relating the distance travelled by each particle (r) to the time during which the diffusion is observed (t). In the absence of flow, the movement of particles is symmetric with an average displacement of zero. The diffusivity is related to the average over squared distances from the origin (or variance of the distribution of r), expressed

$$\left\langle r^2 \right\rangle = 2nDt \tag{3.1}$$

such that D is the diffusion coefficient and n is the number of spatial dimensions of movement. Interestingly, the mean squared displacement of a particle is not proportional to the time, but rather to its square root; also reflected in the unit of the diffusion coefficient, which is m^2/s. An example of free isotropic diffusion at multiple time points is visualized in Fig. 3.1.

It is a fortunate coincidence that the length scale we can probe with dMRI is approximately the same as the scale of cells, enabling us to probe tissue architecture on a scale of 1–100 μm. An early discovery that propelled MRI as a clinical tool for imaging of brain function demonstrated that DWI was a sensitive tissue alteration in cerebral ischemia at an earlier stage than other imaging techniques such as computed tomography or morphological MRI (Moseley et al. 1990). Soon after, the anisotropy of diffusion was connected to the structural configuration of anisotropic tissue, such as the cylinder-like myelin sheaths that surround axons (Beaulieu 2002), giving rise to quantification of normal and pathological processes in neuronal tissue (Tuch et al. 2003; Assaf and Pasternak 2008; Le Bihan and Iima 2015), and the description of white matter pathways through diffusion tractography (Mori et al. 1999; Farquharson et al. 2013; Jeurissen et al. 2014). Since then, the application of dMRI in clinical research has been explosive (Bodini and Ciccarelli 2014; White and Lim 2010;

Sundgren et al. 2004), and a comprehensive overview of how it is used in psychiatric diseases can be found in Chap. 4.

3.2 Diffusion Weighted Imaging (DWI)

Magnetic resonance diffusion spectroscopy was proposed in the 1960s (Stejskal and Tanner 1965), and later generalized from spectroscopy to imaging in the late 1980s (Le Bihan et al. 1986), which made it an imaging tool with considerable promise in the clinical setting. The underlying principles of diffusion MRI and the history of its first 25 years have been reviewed in detail by Le Bihan and Johansen-Berg (2012).

dMRI employs magnetic field gradients to sensitize the MR signal to incoherent movement of signal carrying particles. For the purposes of this chapter, we consider the hydrogen atoms in water molecules, but other nuclei can be used in much the same way (Konstandin and Schad 2014). The most common DWI sequence is the spin-echo with echo-planar imaging (EPI) readout, although a multitude of alternatives exist (Holdsworth et al. 2019; Le Bihan 1995; Pipe 2014). In a spin-echo, diffusion weighting is achieved by applying a pair of identical pulsed-field gradients one on either side of the refocusing pulse such that the first gradient pulse induces a spatially dependent phase shift for all spin within each voxel, and the second pulse reverts the phase shift in proportion to how far the spin traveled during the experiment (Pipe 2014; Price 1997). Stationary spins are perfectly restored to their original phase, whereas spins that moved exhibit a residual phase shift. Taken over a large number of spins, groups that remained stationary or moved in unison have a high phase coherence (collaborate to create a large signal), whereas groups that moved randomly will have a large dispersion of phases (signal reduced in proportion to the gradient magnitude and rate of diffusion). Mathematically, the normalized diffusion-weighted signal (s) can be described as the average over all spin phases

$$s = \left\langle e^{-i\phi} \right\rangle$$

where ϕ is a distribution of phases and the angle brackets, $\langle\cdot\rangle$, denote averaging over all spins. This signal can be described using an expansion in powers of the natural logarithm of the diffusion-weighted signal.

$$\ln(s) = \ln\left(\left\langle e^{-i\phi} \right\rangle\right) = \sum_{n=1}^{\infty} \frac{i^n}{n!} \left\langle \phi^n \right\rangle_c = -\frac{1}{2}\left\langle \phi^2 \right\rangle_c + \frac{1}{24}\left\langle \phi^4 \right\rangle_c + \ldots$$

where $\langle\cdot\rangle_c$ are the cumulants of which the odd cumulants are zero if we assume that there is no flow, i.e., $\langle\phi\rangle = 0$ This is called the cumulant expansion; a comprehensive introduction can be found in (Kiselev 2010). This expansion is powerful because the cumulants map directly to quantities such as diffusivity and diffusional kurtosis, as discussed below. In the simplest case, we may assume that the diffusion process is approximately Gaussian, retaining only the second cumulant, and resulting in an approximation of the diffusion-weighted signal

$$\ln(s) = -\frac{1}{2}\left\langle \phi^2 \right\rangle_c = -bD \tag{3.2}$$

where b is the b-value, a parameter summarizing the combined effect of the applied diffusion gradient and the diffusion time (Le Bihan et al. 1986). Equation 3.2 is more commonly written as

$$S(b)/S_0 = \mathrm{e}^{-bD}. \tag{3.3}$$

Qualitatively, Eq. 3.3 tells us that strong diffusion encoding (large b-value) and/or fast diffusion (large D) cause a large signal reduction, whereas turning the diffusion encoding off ($b = 0$) or observing particles with negligible random movement ($D = 0$) means that the signal is not affected by diffusion encoding. Since the b-value is controlled as part of the experiment, two unique b-values (here we assume zero and b) are enough to estimate the diffusivity by solving for $D = -\ln(S(b)/S_0)/b$, which is simply the slope of the natural logarithm of the signal-vs-b curve (Fig. 3.2). When measured in complex systems, D is called the *apparent* diffusion coefficient (ADC) to emphasize that it depends on a non-trivial interaction between the experimental parameters and the tissue microstructure.

Imagine that a lesion has a very densely packed cell matrix, such that the diffusing particles are

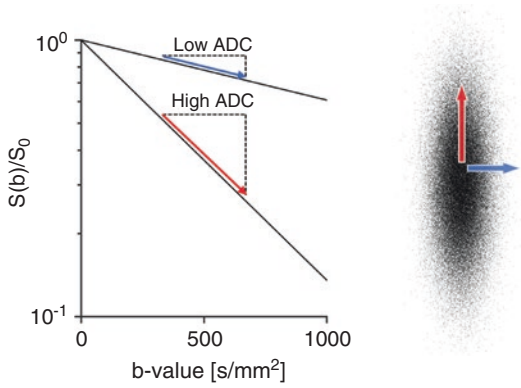

Fig. 3.2 The slope of the diffusion-weighted signal at low b-values defines the apparent diffusion coefficient (ADC). In an isotropic medium, the ADC values are the same in every direction. If, however, the ADC varies as a function of direction, the subject is said to be anisotropic. In this example, the direction indicated by the red arrow exhibits a faster diffusivity compared to the blue direction. Since the dephasing is faster in the red direction, the signal at any given non-zero b-value will be lower along that direction, and a higher ADC is observed compared to the blue direction

highly restricted and exhibit a low ADC. From Eq. 3.3 we can see that such a region would appear hyperintense on diffusion-weighted images, whereas regions with no restrictions attenuate more rapidly, and yield hypointense regions in the image. An overview of studies that investigate the relationship between diffusivity and cell density was presented by (Chen et al. 2013). Even without introducing quantitative analysis, DWI can reveal relevant radiological information (Tang and Zhou 2019). For example, images are hyperintense in regions of abnormally high tissue density, for example, in spinal tumors (Bammer et al. 2000) and in regions affected by acute stroke, where cell swelling is thought to cause a substantial reduction to the ADC (Moseley et al. 1990).

Notably, Eq. 3.3 does not include any information on the direction of the diffusion. It is, however, implicit that the ADC is attributed to the direction along which the diffusion encoding was applied. Since tissue may exhibit anisotropic diffusion characteristics—most prominently in the central nervous system (Beaulieu 2002)—it is useful to create a metric that reflects the apparent diffusivity independent of the direction of the encoding and the orientation of the subject. The most practical approach is to measure the ADC in three mutually orthogonal directions, and calculate the mean diffusivity (MD) as the average, so that $MD = (D_x + D_y + D_z)/3$, where the subscripts indicate the direction in which the ADC was measured. It should be obvious from Fig. 3.2 that neither the ADC nor the MD can provide a metric for how much the diffusivity varies as we measure it along different directions. For this, we require a technique that can capture the *anisotropy* of the diffusion process, as discussed below.

3.3 Diffusion Tensor Imaging (DTI)

Diffusion tensor imaging (DTI) (Basser et al. 1994) refers both to a signal representation as well as to the way that the diffusion process is measured. Unlike measurements that capture only the diffusivity (as described above), DTI also aims to capture the *direction* and *anisotropy* of the diffusion. To do this, the mathematical representation must contain information about how the diffusion depends on the direction in which the encoding is applied, and the measurements must be performed in a way that the model can be inverted. In practice, this means that at least six well-distributed directions at $b > 0$ must be measured along with a non-weighted image. The optimization of sampling schemes for DTI is discussed in (Jones 2010).

The DTI signal model is closely related to Eq. 3.3, but replaces the scalar values D and b, with the tensor-valued diffusion tensor (**D**) (Basser et al. 1994) and b-matrix or b-tensor (**B**) (Westin et al. 2014, 2016), where MD = Trace (**D**)/3 and b = Trace (**B**). The signal representation now incorporates directional information

$$S(\mathbf{B})/S_0 = \mathrm{e}^{-\mathbf{B}:\mathbf{D}}, \tag{3.4}$$

where in the standard Stejskal-Tanner (Stejskal and Tanner 1965) diffusion encoding, $\mathbf{B} = b\mathbf{n}^T\mathbf{n}$, **n** is a unit vector pointing along the diffusion encoding direction and the double inner product is denoted by (:). The diffusion tensor is most commonly written as a 3 × 3 matrix

$$\mathbf{D} = \begin{bmatrix} D_{xx} & D_{xy} & D_{xz} \\ D_{yx} & D_{yy} & D_{yz} \\ D_{zx} & D_{zy} & D_{zz} \end{bmatrix}, \qquad (3.5)$$

where the diagonal elements are the diffusivity along the frame of reference axis, and the off-diagonal elements show their correlations. An extensive description of this formalism can be found in (Kingsley 2006a). The diffusion tensor contains six unique elements (due to the symmetry $D_{ij} = D_{ji}$) that depend on the orientation of the investigated tissue. In order to get a rotation invariant parameterization of the tensor, as well as its shape parameters, we can compute its eigenvectors (e_i) and eigenvalues (λ_i) The eigenvalues describe the apparent diffusivity along three orthonormal axes, where λ_1 is usually chosen to be the largest value. Therefore, in principle, the eigenvalues carry information about the size and shape of the diffusion tensor, and the eigenvectors capture its orientation or direction. In Fig. 3.3, we visualize isotropic and anisotropic diffusion processes and their corresponding diffusion tensors glyphs. When scaled with the square root of its eigenvalues, the diffusion tensor glyphs show a close resemblance to the plume of diffusing particles, assuming their general shape and direction.

From the eigenvalues, we may calculate several rotation invariant scalar quantities (Kingsley 2006b). In Table 3.1, we have stated the definitions of the most frequently used DTI parameters and their values for the diffusion tensors seen in Fig. 3.3. Note that we have also included the 'relative anisotropy' as a complement to the fractional anisotropy, to remind the reader that the derived parameters may have many variants and that there is no general consensus on what parameter definitions are optimal for any particular application.

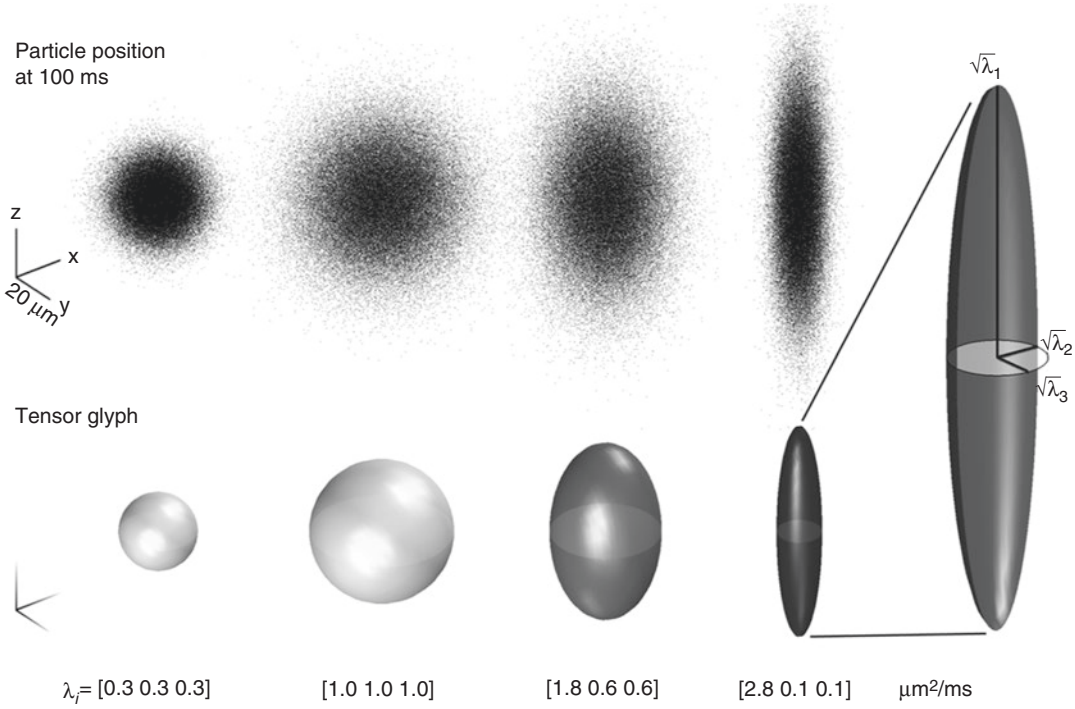

Fig. 3.3 Visualization of distributions of particles for four different microenvironments (top) with varying levels of diffusivity and anisotropy. If these distributions are Gaussian, they can be described (perfectly) by diffusion tensors (bottom). The eigenvalues carry information about the size and shape of the diffusion tensor, and the eigenvectors define its orientation. (The figure was adapted from Szczepankiewicz (2016) with permission, published by Lund University)

Table 3.1 Examples of rotational invariant scalar measures that can be derived from the diffusion tensor (Kingsley 2006b)

Name	Definition from eigenvalues	Values for tensors in Fig. 3.3			
Mean diffusivity	$\mathrm{MD} = \langle\lambda\rangle = (\lambda_1 + \lambda_2 + \lambda_3)/3$	0.30	1.00	1.00	1.00
Radial diffusivity	$\mathrm{RD} = (\lambda_2 + \lambda_3)/2$	0.30	1.00	0.60	0.10
Axial diffusivity	$\mathrm{AD} = \lambda_1$	0.30	1.00	1.80	2.80
Fractional anisotropy	$\mathrm{FA} = \sqrt{\frac{3}{2}\frac{\left(\lambda_1 - \langle\lambda\rangle\right)^2 + \left(\lambda_2 - \langle\lambda\rangle\right)^2 + \left(\lambda_3 - \langle\lambda\rangle\right)^2}{\lambda_1^2 + \lambda_2^2 + \lambda_3^2}}$	0.00	0.00	0.60	0.96
Relative anisotropy	$\mathrm{RA} = \sqrt{\frac{1}{6}\frac{\left(\lambda_1 - \langle\lambda\rangle\right)^2 + \left(\lambda_2 - \langle\lambda\rangle\right)^2 + \left(\lambda_3 - \langle\lambda\rangle\right)^2}{\langle\lambda\rangle^2}}$	0.00	0.00	0.40	0.90

These measures only depend on the shape or size of the diffusion tensor, not its orientation. Note that MD, AD and RD are given in units of $\mu m^2/ms$, whereas FA and RA are unitless. Furthermore, we stress that eigenvalue decomposition is not necessary to calculate these metrics (Kingsley 2006b), although they provide the most transparent definitions

3.4 Limitations of DTI

Although the diffusion tensor is capable of capturing the major features of the diffusion in tissue, it also has several well-known limitations (Jones and Cercignani 2010; Alexander et al. 2001; Szczepankiewicz et al. 2015). These can be broadly described as limited specificity, and limited capability of capturing heterogeneity on the sub-voxel scale. Since DTI is a representation rather than a biophysical model (Novikov et al. 2018a), it is primarily used to describe the diffusion weighted signal as a function of the b-tensor rather than making direct statements about the configuration of the underlying tissue microstructure. The tenuous connection between DTI parameters and the actual tissue microstructure is frequently overinterpreted and has led to inaccurate and misleading terminology. For example, promoting the FA as a metric of "white matter integrity" (Jones et al. 2013). Several papers have stressed that the interpretation of parameters can be challenging (Jones et al. 2013), including confounding effects caused by complex white matter architecture (Douaud et al. 2011; Vos et al. 2012; Jeurissen et al. 2013) and spatial resolution and partial volume effects (Vos et al. 2011; Szczepankiewicz et al. 2013). We illustrate this issue in Fig. 3.4, where particles are traced from two orthogonal anisotropic compartments. In this configuration, a single diffusion tensor is unable to accurately capture the behavior of the system, and the overlapping distributions of particle displacements are prominently non-Gaussian.

DTI is also limited in that it is designed to describe the average behavior of the content of each voxel. The implication of this is that nuances that exist on a sub-voxel scale are lost in the averaging process. For example, DTI cannot capture the presence of multiple diffusion rates within a single voxel. In a voxel that contains a mixture of fast and slow diffusivity, DTI will report an intermediate value depending on the signal fraction of each compartment. The same averaging also causes the observed diffusion anisotropy to depend on the orientation coherence of the tissue that causes it (Pierpaoli et al. 1996). For example, disordered or crossing white matter will exhibit low anisotropy, as will white matter afflicted by disease, making the two underlying mechanisms difficult to distinguish. In fact, there exist many tissue configurations that are dramatically different on the microscopic scale, but that result in identical diffusion tensors as a direct consequence of the signal being averaged across the whole voxel. To visualize this, we may extend the example in Fig. 3.4 from two underlying diffusion tensors to arbitrary distributions of diffusion tensors. Figure 3.5 shows six distributions of diffusion tensors that can not be distinguished by DTI.

Importantly, the limitations stated above should not be taken to mean that DTI produces "true" parameters only on the rare occasion that

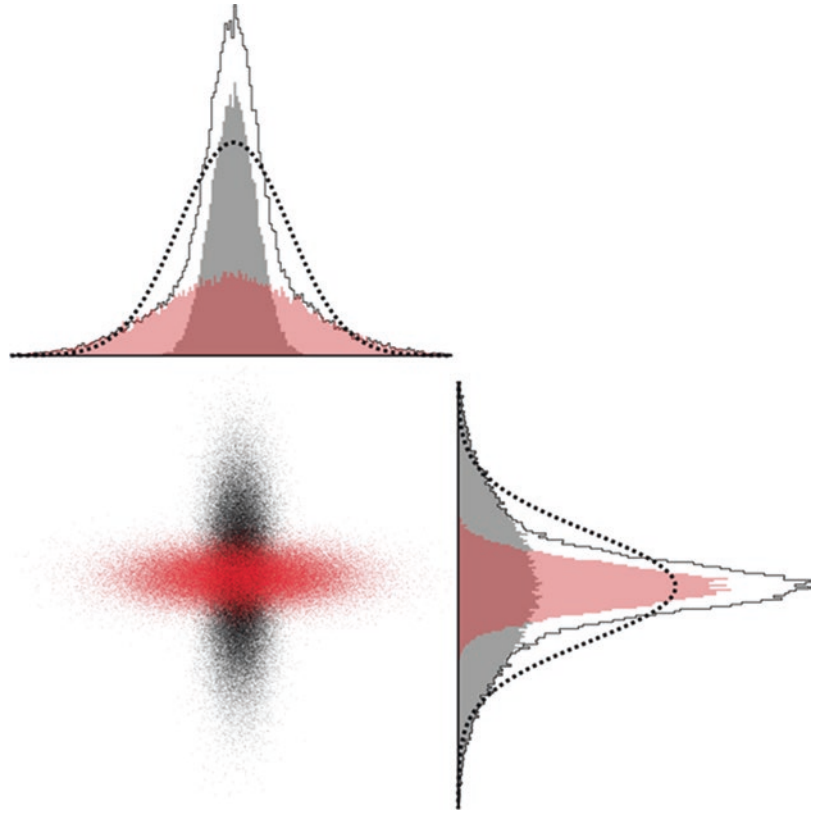

Fig. 3.4 Diffusing particles in two isolated anisotropic compartments (red and black). Each compartment, by itself, exhibits Gaussian diffusion, and could be well-described by a single diffusion tensor. However, if both contribute to the diffusion weighted signal in a voxel, a single diffusion tensor can no longer capture the diffusion process accurately. Furthermore, the total distribution of particles (solid black lines in histograms) differs markedly from the Gaussian distribution (broken line), which means that the distribution is "non-Gaussian" (Jensen et al. 2005) because it is a mixture of multiple Gaussian distributions

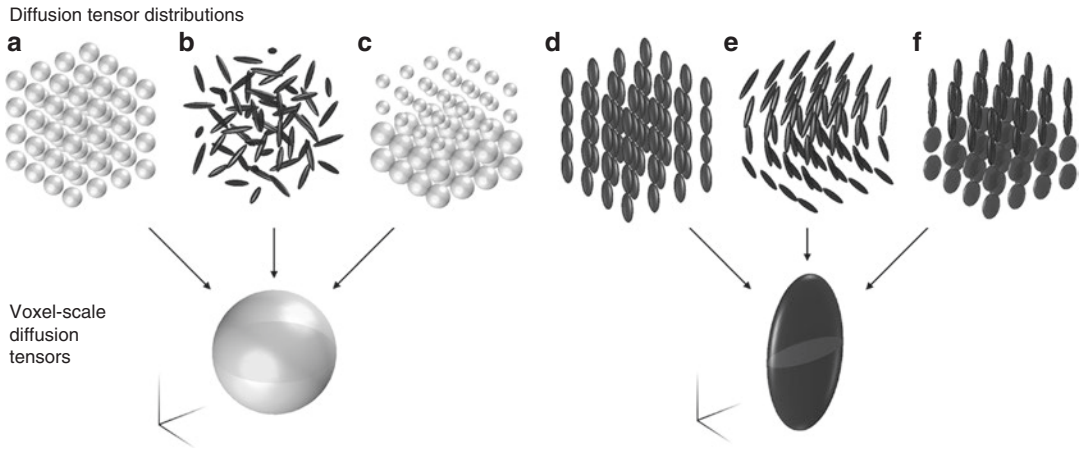

Fig. 3.5 The top row shows six diffusion tensor distributions that represent the content of individual voxels, and the bottom row shows the average (or voxel-scale) diffusion tensor estimated by DTI. Examples A and D are perfectly reproduced by the voxel-scale diffusion tensor since the underlying systems exhibit no heterogeneity (identical tensors) and no orientation dispersion. However, examples B and E show that the diffusion anisotropy on the microscopic scale can be entirely (B), or partially (E), lost in the averaging over multiple directions. Finally, examples C and F show that any information about the heterogeneity within the voxel is lost. (The figure was adapted from Szczepankiewicz (2016) with permission, published by Lund University)

we investigate a homogeneous medium with no orientation dispersion. Instead, DTI is correct when used at sufficiently low b-values, regardless of the complexity of the underlying tissue, but its parameters must be interpreted with its original design in mind! If we aim to uncover more subtle and specific features of the tissue, such as heterogeneity, orientation dispersion, microscopic anisotropy, diffusion time dependence or cell sizes, we must go beyond DTI and use more involved modeling and experimental design.

3.5 Beyond the Diffusion Tensor

Diffusion tensor imaging is capable of capturing the average behavior of diffusion in any one voxel, and is a comprehensive description only of very simple systems. Looking at biological tissues under the microscope often reveals a vast range of subtle features that cannot be captured with this simple approach (Jeurissen et al. 2013; Tuch et al. 2002). The challenge then, is to evolve both the way that diffusion-weighted data is analyzed to capture all the relevant features encoded in the signal (Novikov et al. 2019), as well as to develop diffusion weighting techniques that can probe ever more specific features of the microstructure (Nilsson et al. 2018).

3.6 Advanced Analysis Methods

Diffusion kurtosis imaging (Jensen et al. 2005) is a direct extension of DTI that fully encompasses DTI, and adds to it the capability to probe so-called non-Gaussian diffusion. The concept of kurtosis is used in probability theory and statistics. The word originates from the greek word "kyrtos," or "kurtos," meaning "curved," or "arching," and, in statistics, is a measure of the "tailedness" of a probability distribution. Kurtosis can vaguely be described as the movement of probability mass from the shoulders of a distribution into its center and tails (Balanda and MacGillivray 1988). A Gaussian distribution has zero kurtosis, and with increasing kurtosis, the peak of the distribution gets more pronounced compared to a Gaussian, while the tails get longer and decay slower (Fig. 3.6). We may simplify DKI to one dimension (Jensen et al. 2005; Yablonskiy et al. 2003) to provide some insight into how this representation differs from those that assume monoexponential decay

$$S(b)/S_0 = e^{-bD+b^2D^2K/6}, \qquad (3.6)$$

where the first part of the exponential is identical to that in Eq. (3.3); it differs only by the addition of the apparent kurtosis term (K) The logarithm of the signal is therefore a quadratic function in b. As before, the initial slope captures the ADC, and the kurtosis term captures its curvature. The curvature indicates that the diffusion is non-Gaussian, which can be caused by two main contributions: "multi-Gaussian systems" that contain compartments with varying diffusivity (Fig. 3.6); and "intracompartmental kurtosis" where the movement of water is restricted such that the distribution of particles assumes a non-Gaussian shape (Jensen et al. 2005; Jespersen et al. 2019).

So when can we expect non-Gaussian diffusion in biological tissue? The answer: almost always!

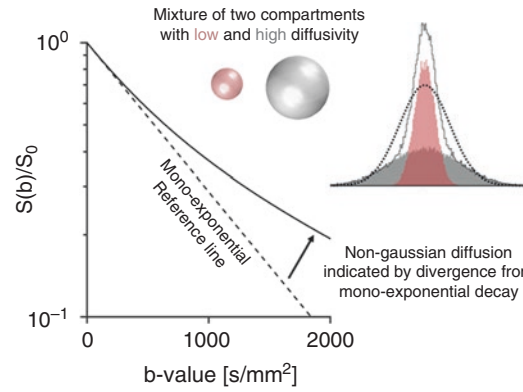

Fig. 3.6 Diffusion weighted signal in substrate that contains equal parts of compartments with low (0.5 μm²/ms) and high (1.5 μm²/ms) apparent diffusivity. As in Fig. 3.2, the initial slope (at b = 0) corresponds to the apparent diffusion coefficient, or average diffusivity along diffusion encoding direction, but the signal-vs-b diverges from the monoexponential line (broken line), which indicates that the content is not purely Gaussian. The histogram shows the distribution of particle positions at an arbitrary time. The distribution of particles is the sum distributions from compartments with low and high diffusivities (solid black line), and is clearly non-Gaussian (compare to broken line showing a Gaussian distribution with the same area)

Although the magnitude of the effect depends on the architecture of the microstructure and the experimental design (Novikov and Kiselev 2010; de Swiet and Mitra 1996), diffusion is generally non-Gaussian (Jensen et al. 2005). In spite of this, the signal detected in the brain parenchyma up to moderate b-values (<1000 s/mm^2 = 1 ms/μm^2) can be remarkably well approximated by a single diffusion tensor. One important exemption is in orientationally dispersed white matter, such as crossing fibers. Although, individually, each fiber may be well-described by a single diffusion tensor, the sum of such components are markedly non-Gaussian (Fig. 3.4). This is another interesting facet of DKI—it captures non-Gaussianity from the local tissue characteristics, but also kurtosis that arises from orientation dispersion. As such, it conflates the presence of multiple average diffusivities and the presence of anisotropic compartments that are orientationally dispersed (Westin et al. 2016; Szczepankiewicz et al. 2015). In fact, examples A and B in Fig. 3.5 are indistinguishable by both DTI *and* DKI.

An alternative approach to representations is to assume that we have a priori knowledge of the tissue composition. For example, we may assume that it is a sum of specific Gaussian compartments, and we estimate how much of each compartment is present in the tissue. This approach is used in biophysical modelling, and its major benefit is that its parameters are relatable to physical quantities—for example, the volume fraction of intracellular water, the axonal diameter, or the density of dendrites. A simple example can be found in free water mapping (Pasternak et al. 2009), where the tissue is modelled by two compartments, each described by a diffusion tensor; the first represents freely diffusing water (D_1), the second represents the remaining tissue (D_2), such that

$$S(\mathbf{B})/S_0 = f_1 e^{-\mathbf{B}:\mathbf{D}_1} + (1-f_1)e^{-\mathbf{B}:\mathbf{D}_2}, \quad (3.7)$$

where the free water fraction (f_1) is the fraction of signal that originates from pools of freely diffusing water. By constraining the relationship between the compartments and signal, the fitting procedure should return e.g. values of the fraction of each tissue type. The obvious benefit of biophysical models is that they instantly generate parameters that appear to have a clear interpretation. However, a major pitfall of biophysical models is that such models are only accurate if the model assumptions are true, which is rarely the case in biological tissue. For example, the biexponential model in Eq. 3.7 may as well capture the behaviour of intra and extracellular water, with no way of telling which interpretation should be used. Therefore, such models are likely to be inaccurate and exceedingly difficult to validate, leading to frequent overinterpretation of their parameters (Lampinen et al. 2019). Simply extending these models to include compartments with all possible characteristics is also not feasible (Mulkern et al. 2017), since the inclusion of more free parameters in the model creates more severe degeneracies (Jelescu et al. 2016). Thus, the model must be parsimonious and contain only relevant features that can be robustly estimated from the available data (Novikov et al. 2018b; Stanisz et al. 1997).

Regardless of what approach is used to translate the measured signal into useful information, certain features of the tissue may remain hidden. For example, cases A from B in Fig. 3.5 are designed to yield identical signal, regardless of the diffusion encoding direction or b-value. It is therefore true that DTI and DKI are both unable to distinguish these cases; what is more striking is that this is true for *all* methods based on conventional diffusion encoding, regardless of the analysis (Mitra 1995). This illustrates a situation in which the underlying truth may be vastly different in two cases, yet it would remain for ever indistinguishable if we were to limit ourselves to use only conventional diffusion encoding. The solution to this problem, and others like it, is to explore alternative modes of performing the diffusion-weighted acquisition, as discussed below.

3.7 Advanced Encoding Methods

The diffusion weighted experiment is most commonly described by the b-value and the diffusion encoding direction. Indeed, these are the default parameters used to design diffusion-weighted

experiments at clinical MRI equipment and they allow the user to adjust the experiment to collect the most relevant data for several applications, even beyond DTI. For example, high b-values at a high directional resolution are beneficial for tractography (Mori et al. 1999; Behrens et al. 2014), whereas low b-values and few directions are preferential for imaging of intravoxel incoherent motion (Le Bihan et al. 1986; Fournet et al. 2018). However, even if directions and b-values are the most prevalent description of the diffusion-weighted experiment, they are by no means comprehensive and should not give users the impression that there is nothing else we can do. In the same sense that we can develop complex signal models, it is possible to design experiments which weight the signal, not only by its diffusivity proportional to the b-value, but rather features that go beyond what is accessible by conventional encoding. In this section, we will briefly survey multidimensional diffusion encoding, variable diffusion times and the inclusion of T1 and T2 relaxation.

A major breakthrough to diffusion encoding was proposed in 1990 by Cory et al. (1990) who showed that the local shape of compartments could be probed, even if the compartments were orientationally disordered. This was achieved by extending the conventional Stejskal-Tanner experiment to include a second pair of pulsed field gradients, or so-called double diffusion encoding. The nomenclature concerning these experiments is described by (Shemesh et al. 2016). By independently varying the direction of the first and second encoding, a correlation between diffusion along multiple spatial dimensions can be probed, and from it the microscopic diffusion anisotropy can be estimated, even if the sample appears to be isotropic on the voxel scale (Shemesh et al. 2010; Lawrenz and Finsterbusch 2011; Jespersen et al. 2013; Avram et al. 2013). This provides a unique tool to probe the anisotropy in tissue such as crossing white matter or gray matter without the confounding effects of orientation dispersion (Szczepankiewicz et al. 2015; Jespersen et al. 2013; Lawrenz and Finsterbusch 2015, 2019). To distinguish this feature from the anisotropy that is observable on the voxel scale (captured by FA), it is frequently called the microscopic anisotropy or compartment eccentricity.

The concept of diffusion encoding along multiple directions in each shot was generalized to arbitrary diffusion weighting waveforms, where the diffusion encoding is described by a diffusion encoding b-tensor (Westin et al. 2016; Szczepankiewicz et al. 2019). The b-tensor carries information on the diffusion encoding direction and b-value, but also the shape of the encoding. At sufficient b-values, the inclusion of b-tensors with multiple shapes can distinguish the problematic cases A and B in Fig. 3.5. The theoretical framework of q-space trajectory imaging (QTI) (Westin et al. 2016) expands on the DKI model to leverage tensor-valued diffusion encoding. By doing so, it can quantify novel parameters such as the microscopic fractional anisotropy (μFA) (Jespersen et al. 2013; Lasič et al. 2014), and it can distinguish between kurtosis caused by variable isotropic diffusivities and anisotropic compartments that are dispersed (Szczepankiewicz et al. 2016) if the tissue is multi-Gaussian and intracompartmental kurtosis is negligible (Jespersen et al. 2019; de Swiet and Mitra 1996). The inclusion of DDE or QTE can therefore improve the interpretability of, for example, DKI parameters in terms of relevant structural characteristics, which has been identified to be a limitation in several studies (Szczepankiewicz et al. 2016; Van Cauter et al. 2012).

Diffusion encoding can also be designed to probe variable diffusion times to access information on the sizes of the microscopic restrictions, for example, by modifying the distance between the diffusion encoding pulses in the Stejskal-Tanner sequence. However, a more efficient and common approach is to use oscillating gradient waveforms (Mallett and Strange 1997; Does et al. 2003) (Fig. 3.7). As seen in Eq. 3.1 and Fig. 3.1, the diffusion time determines the distances probed by diffusing particles. At sufficiently short diffusion times, the particles have yet to interact with surrounding tissue, and therefore appear to be diffusing freely. As the diffusion time increases, the environment hinders or restricts the particles to a larger degree, and the

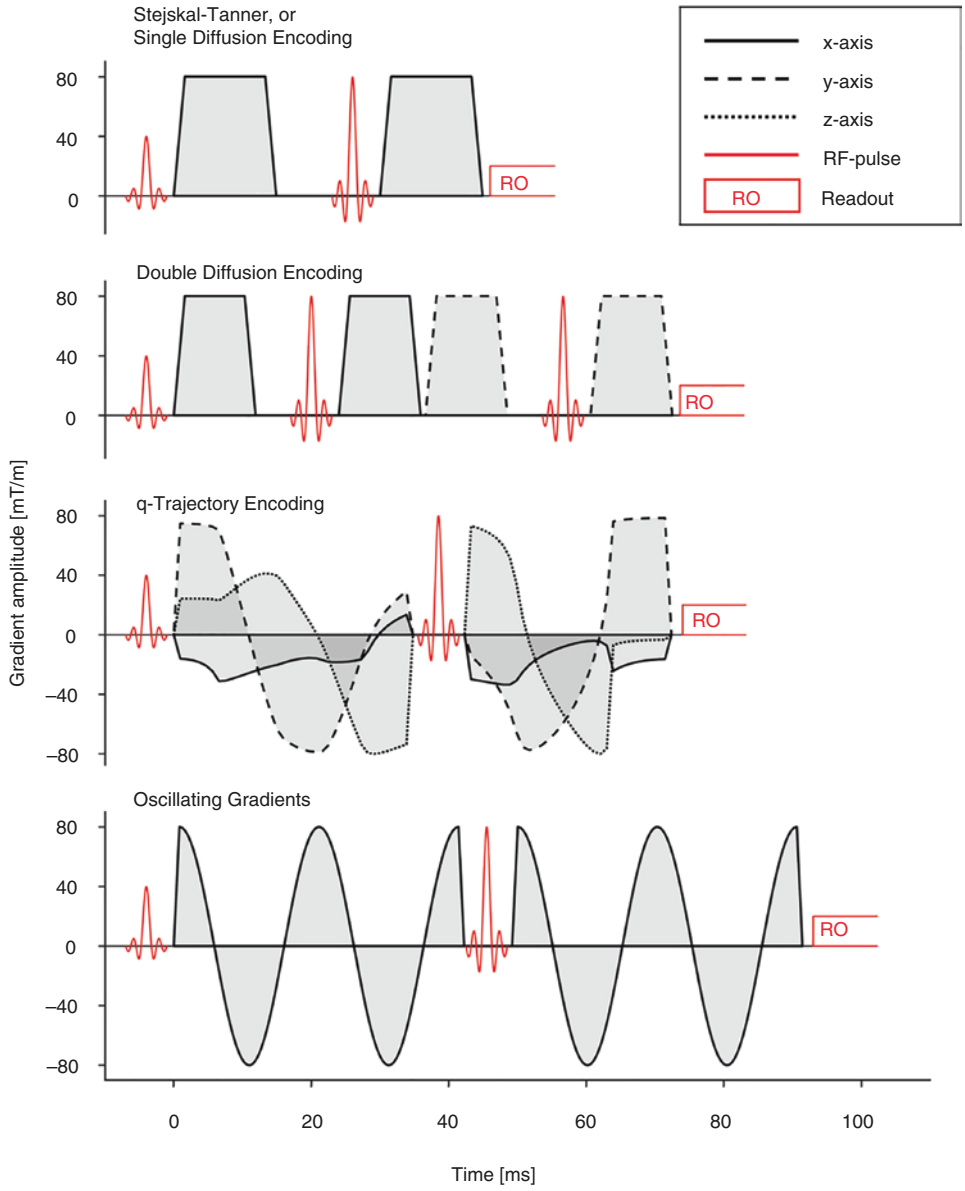

Fig. 3.7 There exist a multitude of gradient waveform designs intended to probe various features of tissue microstructure. The top plot shows the canonical Stejskal-Tanner design from 1965 (Stejskal and Tanner 1965), commonly used in a spin-echo sequence (Pipe 2014). Double diffusion encoding (DDE) was proposed almost three decades later (Cory et al. 1990) to probe the local geometry of compartments, also called microscopic anisotropy, by modulating the orientation of the first and second encoding blocks independently. It is frequently used in a double-spin-echo to avoid artifacts caused by concomitant gradients (Baron et al. 2012). A similar set of experiments can be performed in a single spin-echo by q-trajectory encoding (QTE) where optimized gradient waveforms with arbitrary shapes are used to achieve efficient diffusion encoding in multiple directions per shot (Westin et al. 2016; Eriksson et al. 2013; Sjölund et al. 2015). Both DDE and QTE can be used to render tensor-valued diffusion encoding, and are capable of probing microscopic anisotropy, and can therefore disentangle cases A and B in Fig. 3.5. Oscillating gradients are used to modulate the diffusion time so that the size of restrictions can be estimated from the relation between the ADC and the diffusion time (Mallett and Strange 1997; Does et al. 2003). Notably, oscillating gradients are relatively inefficient (low b-values per unit time), and the example above yields only a tenth of the b-value compared to the other examples

diffusion coefficient appears to be reduced. The transition from free to restricted diffusion can be probed by measuring the ADC at multiple diffusion times, and the size of the restrictions can be estimated (Clark et al. 2001). Modulating the diffusion time also makes the signal sensitive to the rate at which water exchanges over cell membranes (Callaghan and Furó 2004; Lasič et al. 2011; Ning et al. 2018). For example, DDE experiments can be designed to suppress the signal from compartments with high diffusivity, followed by a mixing time during which signal carrying particles can exchange over membranes and re-enter the regions where the diffusion is fast. By measuring the ADC for variable mixing times, the apparent exchange rate can be estimated (Lasič et al. 2011; Nilsson et al. 2013).

So far we have assumed that the effects of relaxation can be ignored. However, it is clear that any tissue in which multiple relaxation times are present will render a signal that depends on the repetition time or echo time. Consider, for example, that we measure the ADC in a sample that contains compartments that have either high diffusivity and high transverse relaxation rates, or low diffusivity and low transverse relaxation rates. In this example, the ADC would decrease with increasing echo times, since the fraction of signal coming from the rapidly relaxing compartment would decrease, and therefore contributes less of its high diffusivity to the average diffusivity. This confounder is present for all methods that do not explicitly address it, but can be remedied by combining the diffusion-weighted experiment with relaxation weighted experiments (Benjamini and Basser 2018; de Almeida Martins and Topgaard 2018). Although the experimental design becomes more involved (Hutter et al. 2018; De Santis et al. 2016), this approach has two major benefits. First, whatever quantification is performed can be related to relative volume fractions, rather than fractions of signal. Second, it allows the separation of compartments that are similar with respect to their diffusion if they show a sufficient difference in relaxation (Lampinen et al. 2019; Veraart et al. 2018). Together, relaxation-diffusion correlation experiments are promising a more comprehensive description of the tissue.

Summary

- Diffusion MRI sensitizes the signal to the random movement of water molecules and serves as a non-invasive probe of the microscopic structure of tissue.
- Methods based on analysis and encoding that go beyond DTI can probe ever more specific features of the tissue.
- The connection between diffusion weighted images and microstructure is indirect. Therefore, parameters and biomarkers rendered by dMRI must be interpreted with their limitations in mind—understanding both the underlying tissue and the experimental design.

Acknowledgements This work was partially funded by grants from the NIH (P41EB015902, R01MH074794, P41EB015898).

References

Alexander AL, Hasan KM, Lazar M, Tsuruda JS, Parker DL. Analysis of partial volume effects in diffusion-tensor MRI. Magn Reson Med. 2001;45(5):770–80.

Assaf Y, Pasternak O. Diffusion tensor imaging (DTI)-based white matter mapping in brain research: a review. J Mol Neurosci. 2008;34(1):51–61.

Avram AV, Özarslan E, Sarlls JE, Basser PJ. In vivo detection of microscopic anisotropy using quadruple pulsed-field gradient (qPFG) diffusion MRI on a clinical scanner. Neuroimage. 2013;64:229–39.

Balanda KP, MacGillivray HL. Kurtosis: a critical review. Am Stat. 1988;42:111. https://doi.org/10.2307/2684482.

Bammer R, Fazekas F, Augustin M, Simbrunner J, Strasser-Fuchs S, Seifert T, et al. Diffusion-weighted MR imaging of the spinal cord. AJNR Am J Neuroradiol. 2000;21(3):587–91.

Baron CA, Lebel RM, Wilman AH, Beaulieu C. The effect of concomitant gradient fields on diffusion tensor imaging. Magn Reson Med. 2012;68:1190–201. https://doi.org/10.1002/mrm.24120.

Basser PJ, Mattiello J, LeBihan D. MR diffusion tensor spectroscopy and imaging. Biophys J. 1994;66(1):259–67.

Beaulieu C. The basis of anisotropic water diffusion in the nervous system—a technical review. NMR Biomed. 2002;15(7–8):435–55.

Behrens TEJ, Sotiropoulos SN, Jbabdi S. MR diffusion tractography. Diffusion MRI. 2014. p. 429–51. https://doi.org/10.1016/b978-0-12-396460-1.00019-6.

Benjamini D, Basser PJ. Towards clinically feasible relaxation-diffusion correlation MRI using MADCO. Microporous Mesoporous Mater. 2018;269:93–6.

Bodini B, Ciccarelli O. Diffusion MRI in neurological disorders. Diffusion MRI. 2014. p. 241–55. https://doi.org/10.1016/b978-0-12-396460-1.00011-1.

Callaghan PT, Furó I. Diffusion-diffusion correlation and exchange as a signature for local order and dynamics. J Chem Phys. 2004;120(8):4032–8.

Chen L, Liu M, Bao J, Xia Y, Zhang J, Zhang L, et al. The correlation between apparent diffusion coefficient and tumor cellularity in patients: a meta-analysis. PLoS One. 2013;8(11):e79008.

Clark CA, Hedehus M, Moseley ME. Diffusion time dependence of the apparent diffusion tensor in healthy human brain and white matter disease. Magn Reson Med. 2001;45(6):1126–9.

Cory DG, Garroway AN, Miller JB. Applications of spin transport as a probe of local geometry. In: Abstracts of Papers of the American Chemical Society. 1990. p. 105.

de Almeida Martins JP, Topgaard D. Multidimensional correlation of nuclear relaxation rates and diffusion tensors for model-free investigations of heterogeneous anisotropic porous materials. Vol. 8. Sci Rep. 2018. https://doi.org/10.1038/s41598-018-19826-9.

De Santis S, Jones DK, Roebroeck A. Including diffusion time dependence in the extra-axonal space improves in vivo estimates of axonal diameter and density in human white matter. Neuroimage. 2016;130:91–103.

de Swiet TM, Mitra PP. Possible systematic errors in single-shot measurements of the trace of the diffusion tensor. J Magn Reson B. 1996;111(1):15–22.

Does MD, Parsons EC, Gore JC. Oscillating gradient measurements of water diffusion in normal and globally ischemic rat brain. Magn Reson Med. 2003;49:206–15. https://doi.org/10.1002/mrm.10385.

Douaud G, Jbabdi S, Behrens TEJ, Menke RA, Gass A, Monsch AU, et al. DTI measures in crossing-fibre areas: increased diffusion anisotropy reveals early white matter alteration in MCI and mild Alzheimer's disease. Neuroimage. 2011;55(3):880–90.

Einstein A. Über die von der molekularkinetischen Theorie der Wärme geforderte Bewegung von in ruhenden Flüssigkeiten suspendierten Teilchen. Ann Phys. 1905;322(8):549–60.

Eriksson S, Lasic S, Topgaard D. Isotropic diffusion weighting in PGSE NMR by magic-angle spinning of the q-vector. J Magn Reson. 2013;226:13–8.

Farquharson S, Tournier J-D, Calamante F, Fabinyi G, Schneider-Kolsky M, Jackson GD, et al. White matter fiber tractography: why we need to move beyond DTI. J Neurosurg. 2013;118(6):1367–77.

Fournet G, Ciobanu L, Le Bihan D. IVIM models: advantages, disadvantages, and analysis pitfalls. Intravoxel incoherent motion (IVIM) MRI. 2018. p. 375–402. https://doi.org/10.1201/9780429427275-19.

Holdsworth SJ, O'Halloran R, Setsompop K. The quest for high spatial resolution diffusion-weighted imaging of the human brain in vivo. NMR Biomed. 2019;32:e4056.

Hutter J, Slator PJ, Christiaens D, Teixeira RPAG, Roberts T, Jackson L, et al. Integrated and efficient diffusion-relaxometry using ZEBRA. Sci Rep. 2018;8(1):15138.

Jelescu IO, Veraart J, Fieremans E, Novikov DS. Degeneracy in model parameter estimation for multi-compartmental diffusion in neuronal tissue. NMR Biomed. 2016;29:33–47. https://doi.org/10.1002/nbm.3450.

Jensen JH, Helpern JA, Ramani A, Lu H, Kaczynski K. Diffusional kurtosis imaging: the quantification of non-gaussian water diffusion by means of magnetic resonance imaging. Magn Reson Med. 2005;53(6):1432–40.

Jespersen SN, Lundell H, Sønderby CK, Dyrby TB. Orientationally invariant metrics of apparent compartment eccentricity from double pulsed field gradient diffusion experiments. NMR Biomed. 2013;26(12):1647–62.

Jespersen SN, Olesen JL, Ianuş A, Shemesh N. Effects of nongaussian diffusion on "isotropic diffusion" measurements: an ex-vivo microimaging and simulation study. J Magn Reson. 2019;300:84–94.

Jeurissen B, Leemans A, Tournier J-D, Jones DK, Sijbers J. Investigating the prevalence of complex fiber configurations in white matter tissue with diffusion magnetic resonance imaging. Hum Brain Mapp. 2013;34(11):2747–66.

Jeurissen B, Tournier J-D, Dhollander T, Connelly A, Sijbers J. Multi-tissue constrained spherical deconvolution for improved analysis of multi-shell diffusion MRI data. Neuroimage. 2014;103:411–26.

Jones DK. Optimal approaches to diffusion MRI acquisition. Diffusion MRI. 2010. p. 250–71. Available from: https://doi.org/10.1093/med/9780195369779.003.0015.

Jones DK, Cercignani M. Twenty-five pitfalls in the analysis of diffusion MRI data. NMR Biomed. 2010;23:803–20. https://doi.org/10.1002/nbm.1543.

Jones DK, Knösche TR, Turner R. White matter integrity, fiber count, and other fallacies: the do's and don'ts of diffusion MRI. Neuroimage. 2013;73:239–54.

Kingsley PB. Introduction to diffusion tensor imaging mathematics: part III. Tensor calculation, noise, simulations, and optimization. Concepts Magn Reson Part A Bridg Educ Res. 2006a;28A(2):155–79.

Kingsley PB. Introduction to diffusion tensor imaging mathematics: part II. Anisotropy, diffusion-weighting factors, and gradient encoding schemes. Concepts Magn Reson Part A. 2006b;28A:123–54. https://doi.org/10.1002/cmr.a.20049.

Kiselev VG. The cumulant expansion: an overarching mathematical framework for understanding diffusion NMR. Diffusion MRI. 2010. p. 152–68. https://doi.org/10.1093/med/9780195369779.003.0010.

Konstandin S, Schad LR. 30 Years of sodium/X-nuclei magnetic resonance imaging. MAGMA. 2014;27(1):1–4.

Lampinen B, Szczepankiewicz F, Novén M, van Westen D, Hansson O, Englund E, et al. Searching for the neurite

density with diffusion MRI: challenges for biophysical modeling. Hum Brain Mapp. 2019;40(8):2529–45. https://doi.org/10.1002/hbm.24542.

Lasič S, Nilsson M, Lätt J, Ståhlberg F, Topgaard D. Apparent exchange rate mapping with diffusion MRI. Magn Reson Med. 2011;66(2):356–65.

Lasič S, Szczepankiewicz F, Eriksson S, Nilsson M, Topgaard D. Microanisotropy imaging: quantification of microscopic diffusion anisotropy and orientational order parameter by diffusion MRI with magic-angle spinning of the q-vector. Vol. 2. Front Phys. 2014. https://doi.org/10.3389/fphy.2014.00011.

Lawrenz M, Finsterbusch J. Detection of microscopic diffusion anisotropy on a whole-body MR system with double wave vector imaging. Magn Reson Med. 2011;66(5):1405–15.

Lawrenz M, Finsterbusch J. Mapping measures of microscopic diffusion anisotropy in human brain white matter in vivo with double-wave-vector diffusion-weighted imaging. Magn Reson Med. 2015;73(2):773–83.

Lawrenz M, Finsterbusch J. Detection of microscopic diffusion anisotropy in human cortical gray matter in vivo with double diffusion encoding. Magn Reson Med. 2019;81(2):1296–306.

Le Bihan D. Molecular diffusion, tissue microdynamics and microstructure. NMR Biomed. 1995;8:375–86. https://doi.org/10.1002/nbm.1940080711.

Le Bihan D, Iima M. Diffusion magnetic resonance imaging: what water tells us about biological tissues. PLoS Biol. 2015;13:e1002203. https://doi.org/10.1371/journal.pbio.1002203.

Le Bihan D, Johansen-Berg H. Diffusion MRI at 25: exploring brain tissue structure and function. Neuroimage. 2012;61(2):324–41.

Le Bihan D, Breton E, Lallemand D, Grenier P, Cabanis E, Laval-Jeantet M. MR imaging of intravoxel incoherent motions: application to diffusion and perfusion in neurologic disorders. Radiology. 1986;161(2):401–7.

Mallett MJD, Strange JH. Diffusion measurements using oscillating gradients. Appl Magn Reson. 1997;12:193–8. https://doi.org/10.1007/bf03162186.

Mitra PP. Multiple wave-vector extensions of the NMR pulsed-field-gradient spin-echo diffusion measurement. Phys Rev B Condens Matter. 1995;51(21):15074–8.

Mori S, Crain BJ, Chacko VP, van Zijl PC. Three-dimensional tracking of axonal projections in the brain by magnetic resonance imaging. Ann Neurol. 1999;45(2):265–9.

Moseley ME, Kucharczyk J, Mintorovitch J, Cohen Y, Kurhanewicz J, Derugin N, et al. Diffusion-weighted MR imaging of acute stroke: correlation with T2-weighted and magnetic susceptibility-enhanced MR imaging in cats. AJNR Am J Neuroradiol. 1990;11(3):423–9.

Mulkern RV, Balasubramanian M, Maier SE. On the perils of multiexponential fitting of diffusion MR data. J Magn Reson Imaging. 2017;45(5):1545–7.

Nilsson M, Lätt J, van Westen D, Brockstedt S, Lasič S, Ståhlberg F, et al. Noninvasive mapping of water diffusional exchange in the human brain using filter-exchange imaging. Magn Reson Med. 2013;69(6):1573–81.

Nilsson M, Englund E, Szczepankiewicz F, van Westen D, Sundgren PC. Imaging brain tumour microstructure. Neuroimage. 2018;182:232–50.

Ning L, Nilsson M, Lasič S, Westin C-F, Rathi Y. Cumulant expansions for measuring water exchange using diffusion MRI. J Chem Phys. 2018;148:074109. https://doi.org/10.1063/1.5014044.

Novikov DS, Kiselev VG. Effective medium theory of a diffusion-weighted signal. NMR Biomed. 2010;23(7):682–97.

Novikov DS, Kiselev VG, Jespersen SN. On modeling. Magn Reson Med. 2018a;79:3172–93. https://doi.org/10.1002/mrm.27101.

Novikov DS, Veraart J, Jelescu IO, Fieremans E. Rotationally-invariant mapping of scalar and orientational metrics of neuronal microstructure with diffusion MRI. Neuroimage. 2018b;174:518–38.

Novikov DS, Fieremans E, Jespersen SN, Kiselev VG. Quantifying brain microstructure with diffusion MRI: theory and parameter estimation. NMR Biomed. 2019;32(4):e3998.

Pasternak O, Sochen N, Gur Y, Intrator N, Assaf Y. Free water elimination and mapping from diffusion MRI. Magn Reson Med. 2009;62(3):717–30.

Pierpaoli C, Jezzard P, Basser PJ, Barnett A, Di Chiro G. Diffusion tensor MR imaging of the human brain. Radiology. 1996;201(3):637–48.

Pipe J. Pulse sequences for diffusion-weighted MRI. Diffusion MRI. 2014. p. 11–34. https://doi.org/10.1016/b978-0-12-396460-1.00002-0.

Price WS. Pulsed-field gradient nuclear magnetic resonance as a tool for studying translational diffusion: part 1. Basic theory. In: Concepts in magnetic resonance. Vol. 9. 1997. p. 299–336. https://doi.org/10.1002/(sici)1099-0534(1997)9:5<299::aid-cmr2>3.3.co;2-2.

Shemesh N, Ozarslan E, Komlosh ME, Basser PJ, Cohen Y. From single-pulsed field gradient to double-pulsed field gradient MR: gleaning new microstructural information and developing new forms of contrast in MRI. NMR Biomed. 2010;23(7):757–80.

Shemesh N, Jespersen SN, Alexander DC, Cohen Y, Drobnjak I, Dyrby TB, et al. Conventions and nomenclature for double diffusion encoding NMR and MRI. Magn Reson Med. 2016;75:82–7. https://doi.org/10.1002/mrm.25901.

Sjölund J, Szczepankiewicz F, Nilsson M, Topgaard D, Westin C-F, Knutsson H. Constrained optimization of gradient waveforms for generalized diffusion encoding. J Magn Reson. 2015;261:157–68.

Stanisz GJ, Szafer A, Wright GA, Henkelman RM. An analytical model of restricted diffusion in bovine optic nerve. Magn Reson Med. 1997;37(1):103–11.

Stejskal EO, Tanner JE. Spin diffusion measurements: spin echoes in the presence of a time-dependent field gradient. J Chem Phys. 1965;42(1):288–92.

Sundgren PC, Dong Q, Gomez-Hassan D, Mukherji SK, Maly P, Welsh R. Diffusion tensor imaging of the

brain: review of clinical applications. Neuroradiology. 2004;46:339–50. https://doi.org/10.1007/s00234-003-1114-x.

Szczepankiewicz F. Imaging diffusional variance by MRI: the role of tensor-valued diffusion encoding and tissue heterogeneity, Ph.D. Thesis. In: Nilsson M, editor. Lund: Lund University; 2016.

Szczepankiewicz F, Lätt J, Wirestam R, Leemans A, Sundgren P, van Westen D, et al. Variability in diffusion kurtosis imaging: impact on study design, statistical power and interpretation. Neuroimage. 2013;76:145–54.

Szczepankiewicz F, Lasič S, van Westen D, Sundgren PC, Englund E, Westin C-F, et al. Quantification of microscopic diffusion anisotropy disentangles effects of orientation dispersion from microstructure: applications in healthy volunteers and in brain tumors. Neuroimage. 2015;104:241–52.

Szczepankiewicz F, van Westen D, Englund E, Westin C-F, Ståhlberg F, Lätt J, et al. The link between diffusion MRI and tumor heterogeneity: mapping cell eccentricity and density by diffusional variance decomposition (DIVIDE). Neuroimage. 2016;142:522–32.

Szczepankiewicz F, Sjölund J, Ståhlberg F, Lätt J, Nilsson M. Tensor-valued diffusion encoding for diffusional variance decomposition (DIVIDE): technical feasibility in clinical MRI systems. PLoS One. 2019;14(3):e0214238.

Tang L, Zhou XJ. Diffusion MRI of cancer: from low to high b-values. J Magn Reson Imaging. 2019;49(1):23–40.

Tuch DS, Reese TG, Wiegell MR, Makris N, Belliveau JW, Wedeen VJ. High angular resolution diffusion imaging reveals intravoxel white matter fiber heterogeneity. Magn Reson Med. 2002;48(4):577–82.

Tuch DS, Reese TG, Wiegell MR, Wedeen VJ. Diffusion MRI of complex neural architecture. Neuron. 2003;40:885–95. https://doi.org/10.1016/s0896-6273(03)00758-x.

Van Cauter S, Veraart J, Sijbers J, Peeters RR, Himmelreich U, De Keyzer F, et al. Gliomas: diffusion kurtosis MR imaging in grading. Radiology. 2012;263(2):492–501.

Veraart J, Novikov DS, Fieremans E. TE dependent Diffusion Imaging (TEdDI) distinguishes between compartmental T relaxation times. Neuroimage. 2018;182:360–9.

Vos SB, Jones DK, Viergever MA, Leemans A. Partial volume effect as a hidden covariate in DTI analyses. Neuroimage. 2011;55:1566–76. https://doi.org/10.1016/j.neuroimage.2011.01.048.

Vos SB, Jones DK, Jeurissen B, Viergever MA, Leemans A. The influence of complex white matter architecture on the mean diffusivity in diffusion tensor MRI of the human brain. Neuroimage. 2012;59(3):2208–16.

Westin C-F, Szczepankiewicz F, Pasternak O, Ozarslan E, Topgaard D, Knutsson H, et al. Measurement tensors in diffusion MRI: generalizing the concept of diffusion encoding. Med Image Comput Comput Assist Interv. 2014;17(Pt 3):209–16.

Westin C-F, Knutsson H, Pasternak O, Szczepankiewicz F, Özarslan E, van Westen D, et al. Q-space trajectory imaging for multidimensional diffusion MRI of the human brain. Neuroimage. 2016;135:345–62.

White T, Lim KO. Diffusion MRI in psychiatric disorders. Diffusion MRI. 2010. p. 608–23. https://doi.org/10.1093/med/9780195369779.003.0037.

Yablonskiy DA, Bretthorst GL, Ackerman JJH. Statistical model for diffusion attenuated MR signal. Magn Reson Med. 2003;50(4):664–9.

White Matter Pathology in Schizophrenia

4

Maria A. Di Biase, Christos Pantelis, and Andrew Zalesky

Contents

M. A. Di Biase
Psychiatry Neuroimaging Laboratory, Brigham and Women's Hospital, Harvard Medical School, Boston, MA, USA

Department of Psychiatry, Melbourne Neuropsychiatry Centre, The University of Melbourne and Melbourne Health, Carlton South, VIC, Australia

Department of Psychiatry, The University of Melbourne, Parkville, VIC, Australia
e-mail: dibiasem@unimelb.edu.au

C. Pantelis (✉)
Department of Psychiatry, Melbourne Neuropsychiatry Centre, The University of Melbourne and Melbourne Health, Carlton South, VIC, Australia

Department of Psychiatry, The University of Melbourne, Parkville, VIC, Australia

Florey Institute for Neuroscience and Mental Health, Parkville, VIC, Australia

North Western Mental Health, Melbourne Health, Parkville, VIC, Australia

Department of Electrical and Electronic Engineering, Centre for Neural Engineering, University of Melbourne, Carlton South, VIC, Australia
e-mail: cpant@unimelb.edu.au

A. Zalesky
Department of Psychiatry, Melbourne Neuropsychiatry Centre, The University of Melbourne and Melbourne Health, Carlton South, VIC, Australia

Department of Psychiatry, The University of Melbourne, Parkville, VIC, Australia

Departments of Psychiatry and Biomedical Engineering, The University of Melbourne and Melbourne Health, Carlton South, VIC, Australia

Department of Biomedical Engineering, The University of Melbourne, Parkville, VIC, Australia
e-mail: azalesky@unimelb.edu.au

M. Kubicki, M. E. Shenton (eds.), *Neuroimaging in Schizophrenia*,
https://doi.org/10.1007/978-3-030-35206-6_4

4.1 The Significance of White Matter Pathology in Schizophrenia

Early neurobiological conceptions of schizophrenia, informed by descriptions of the illness proposed by Kraepelin, Bleuler and other pioneering investigators in the early 1900s, attempted to localize pathology to specific brain cells or sites (Berrios 2003; Collin et al. 2016). However in 1912, Alfred Hoche described this localization approach as the "hunt for phantom" and instead emphasized the synthesis between multiple sites and systems (Hoche et al. 1991). This notion was supported by Geschwind's early work, which demonstrated links between white matter injury and a variety of behavioural deficits (Absher and Benson 1993), providing an impetus for future research.

The emphasis on white matter re-emerged by way of the disconnection hypothesis in the 1990s through the work of Friston and Frith, who elegantly argued that complex symptoms associated with schizophrenia might arise from abnormal functional integration between distinct brain structures (Friston 1998). They pointed to evidence of post-mortem anomalies in myelin and cytoarchitecture, as well as to functional abnormalities shown through electrophysiology and PET imaging (Friston 1998). They further suggested that such alterations may result in associative changes in synaptic efficacy and may also underlie the more complex behavioral and cognitive deficits of schizophrenia, as opposed to disruptions within specific gray matter loci. For example, auditory hallucinations are proposed to arise from deficits in memory, and sensorimotor and imagery processing (Allen et al. 2008), which may reflect a failure to integrate these mental functions. Friston and Frith conceptualized the disconnection hypothesis in terms of abnormal *functional* integration between functionally specialized systems, possibly owing to aberrant, context-dependent regulation of synaptic plasticity (Friston 1998; Friston and Frith 1995). They explicitly dissociated the hypothesis from structural (anatomical) causes of abnormal integration, such as a disruption to cortico-cortical white matter pathways, stating that the evidence for white matter pathology in schizophrenia was not remarkable (Friston 1998). However, white matter pathology is nowadays recognized as a core feature of the disorder, and thus contemporary conceptualizations of the disconnection hypothesis often encompass a lack of both structural and functional integration. Indeed, disrupted white matter architecture, which facilitates integration between gray matter regions, may be integral and even sufficient to produce the characteristic symptoms of schizophrenia. This conceptualization has shifted thinking about the pathophysiology of schizophrenia, away from a localized approach, to a global and circuit-based approach.

Early studies used the size of the white matter compartment (volume or thickness measures) as a way to index the integrity of white matter (Walterfang et al. 2011), and provided important initial findings indicating a disturbance of white matter from before the onset of psychosis, including thinning of the corpus callosum (Walterfang et al. 2008a, b; Haijma et al. 2012). However, the advent of diffusion imaging has propelled this endeavor in new directions allowing for a detailed examination of white matter disturbances across stages of psychosis and schizophrenia.

4.2 Interpreting White Matter Pathology Detected with Diffusion Imaging

Before considering the extent of diffusion imaging studies investigating white matter pathology in schizophrenia, it is first instructive to consider some key factors that impact our interpretation of the findings. Diffusion imaging measures the diffusion of water molecules, which is sensitive to microstructural changes in white matter architecture (Fig. 4.1a). To achieve this, multiple image volumes are acquired, each with a distinct diffusion gradient. Examining any volume in isolation is generally not informative. A mathematical model is required to combine all volumes and yield a single image offering a meaningful contrast. The simplest and earliest model considered in diffusion imaging is the diffusion tensor model (Basser et al. 1994a, b; Basser and Pierpaoli 1998). Diffusion tensor imaging (DTI) fits an ellipsoid (tensor) to each voxel in the brain, where the ellipsoid shape and orientation provides information about the underlying white matter microstructure and the direction of any white matter fibers (See also Chap. 3). Each ellipsoid is parameterized by six components: three eigenvectors and three corresponding eigenvalues (Fig. 4.1b, c). The eigenvector with the largest eigenvalue is called the principal eigenvector and is aligned with the orientation of white matter fibers traversing the voxel. However, in voxels with multiple, intersecting fiber populations, the orientation of the principal eigenvector is ambiguous. This is considered one of the major limitations of the diffusion tensor model (Basser et al. 2000; Alexander et al. 2007), given that a large proportion of white matter voxels comprise intersecting fibers. The shape of the ellipsoid fitted to each voxel is determined by the three eigenvalues and provides insight into white matter microstructure (Fig. 4.1d). Elongated, cigar-shaped ellipsoids indicate constrained diffusion and are associated with a single, well-myelinated fiber population. At the other extreme, spherical ellipsoids indicate unconstrained diffusion and are typical of unmyelinated structures such as gray matter, or white matter regions where multiple fiber populations intersect (Fig. 4.1d).

The three eigenvalues can be combined to yield a variety of scalar measures that quantify the degree of diffusion and enable inference about putative microstructural changes in white matter (See also Table 3.1 in Chap. 3). Fractional anisotropy (FA) is the most commonly used scalar measure derived from the diffusion tensor model. While the precise microstructural corre-

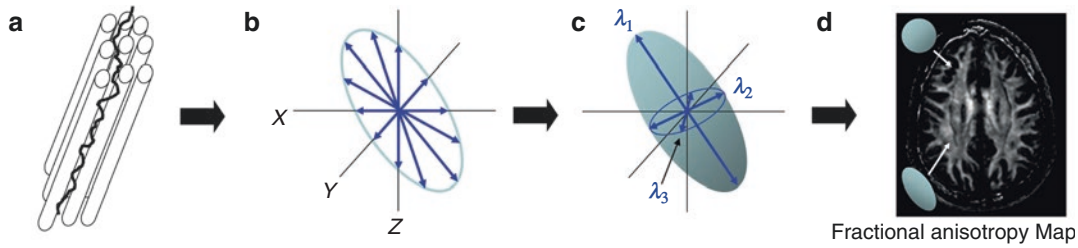

Fig. 4.1 Diffusion tensor imaging. (**a**) Diffusion trajectory of a water molecule (black line) that is parallel to the fiber bundle orientation. Diffusion tensor imaging uses multiple diffusion directions (**b**), to fit a tensor defined by three eigenvectors (lines) and three corresponding eigenvalues (λ_1, λ_2, λ_3). Ellipsoids can be fitted to each voxel to generate an anisotropy map (**d**). Elongated ellipsoids indicate constrained (anisotropic) diffusion and are found within single, well-myelinated fiber populations. Spherical ellipsoids indicate unconstrained (isotropic) diffusion, found in gray matter or white matter regions where multiple fiber populations intersect. [Figure adapted from Fornito and colleagues (2016). Panel (**a**) is from Johansen-Berg and Rushworth (Johansen-Berg and Rushworth 2009) and panels (**b**–**d**) from Mori and Zhang (Mori and Zhang 2006)]

lates of FA remain only partially resolved, abnormally low FA is typically thought to indicate microstructural changes in myelin sheath, microtubules or neurofilaments (Beaulieu 2002). While FA is the most commonly used diffusion metric, other measures, including mean, axial and radial diffusivity enable more nuanced inference and may provide specificity in differentiating between distinct microstructural alterations. In particular, mean (total) diffusivity (MD) is sensitive to myelination (Alexander et al. 2007); axial (parallel) diffusivity to axonal degeneration (Alexander et al. 2007; Song et al. 2003); and radial (perpendicular) diffusivity (RD) to myelin injury (Table 3.1; Alexander et al. 2007; Song et al. 2003).

While these scalar metrics have made it possible to delineate changes in white matter, it is crucial to appreciate the limitations of these techniques, which cannot resolve specific cellular mechanisms. Instead, the variation in diffusion metrics reflects a combination of factors governing these indices, including biological mechanisms (e.g., demyelination or axonal injury), spatial orientation of the fiber population, crossing and other fiber geometries that cannot be well-modeled by the diffusion tensor, partial volume effects, as well as multiple confounding factors that affect diffusivity signals, including body weight, smoking status, drug use and cortisol levels (Keshavan et al. 2011). The interpretation of diffusion studies in schizophrenia is further complicated by different methods used across studies. Four major methods can be identified:

1. Region-of-interest (ROI) analysis involves averaging the diffusion metric of interest across a group of voxels spanning a white matter tract or region and then performing inference on the ROI-averaged metric (Fig. 4.2a). While this is the simplest inference method, the averaging process may conceal focal effects that are circumscribed to a portion of the tract or region of interest.
2. Voxel-based analysis such as tract-based spatial statistics (TBSS; Smith et al. 2006) involves independently testing the same hypothesis about the diffusion metric of interest for each voxel comprising a white matter mask. Cluster-based statistics (Nichols and Holmes 2002) are then used to correct for multiple comparisons, thereby identifying clusters of voxels showing significant effects (Fig. 4.2b). The white matter mask can be confined to a white matter skeleton delineating the core of all fiber bundles

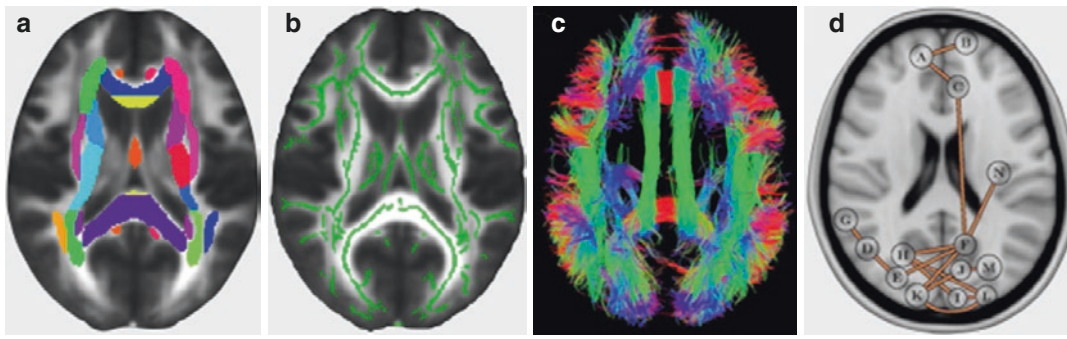

Fig. 4.2 Methods to perform group inference on diffusion MRI data. (**a**) ROI analysis involves averaging the diffusion metric of interest across a group of voxels spanning a white matter tract or region and then performing inference on the ROI-averaged metric. (**b**) Voxel-based analysis involves independently testing the same hypothesis for each voxel comprising a white matter mask, and then using cluster-based statistics to correct for multiple comparisons, thereby identifying clusters of voxels showing significant effects. (**c**) Fiber-tracking or tractography utilizes the fiber orientations estimated for each voxel to infer trajectories of white matter fiber bundles and enables estimation of the putative connectivity strength between cortical and subcortical regions. (**d**) Connectomic analysis involves reconstructing a network representation of white matter connectivity between all pairs of regions comprising a gray matter parcellation and formulating hypotheses about the topological attributes of the network

(Smith et al. 2006) or comprise all white matter voxels (Zalesky et al. 2011).
3. Fiber-tracking or tractography utilizes the fiber orientations estimated for each voxel (e.g., principal eigenvector) to infer trajectories of white matter fiber bundles and enables estimation of the putative connectivity strength between cortical and subcortical regions. Hypotheses can be tested with respect to interregional connectivity strength and fiber geometry (Fig. 4.2c).
4. Connectomic analysis involves reconstructing a network representation of white matter connectivity between all pairs of regions comprising a gray matter parcellation and formulating hypotheses about the topological attributes of the network (Fig. 4.2d).

The regional averaging inherent to the ROI approach produces higher signal-to-noise ratios (SNR), resulting in more robust estimates of diffusion metrics. However, this gain in SNR is at the expense of poorer spatial localization and the possibility of overlooking strong, but spatially circumscribed effects (Friston et al. 1996). In contrast, voxel-based analysis does not require a regional hypothesis and provides improved sensitivity to effects that do not conform to the spatial extent of a predefined ROI. However, the disadvantages of voxel-based analysis are the need for multiple comparison corrections across the set of all voxels tested, and diffusion metrics are inherently noisier for individual voxels than for ROIs (Friston et al. 1996).

Thus, while ROI and voxel-based approaches provide estimates of *local* white matter structure, they do not provide insight into long-range cortico-cortical connectivity. Tractography enables reconstruction of individual fiber trajectories and the investigation of diffusion metrics as a function of a fiber's length (Yeatman et al. 2012). Tractography can also be used to estimate interregional connectivity strength between all pairs of regions comprising a whole-brain gray matter parcellation. This results in a network representation of white matter connectivity called the connectome (Fornito et al. 2016; Sporns et al. 2005).

4.3 Diffusion Tensor Imaging Studies

In the largest, multisite analysis of DTI measures in schizophrenia to date, comprising data for 2359 healthy controls and 1963 schizophrenia patients, Kelly and colleagues (2018) observed significant and widespread reductions in FA (effect size range: 0.04–0.42), in 20 of 25 white matter regions examined using a TBSS-like analysis (See also Chap. 21 for further discussion about this study and other meta-analyses). In addition, no significant effects of age at onset of schizophrenia or medication dosage were detected. This study established robust evidence for white matter pathology in schizophrenia. However, nuances with regard to age (range: 18–86 years), illness duration, symptoms, and medication exposure were not examined in detail. This may reflect incomplete and disparate patient information across the 29 sites included. Therefore, a significant limitation of this multisite study is the heterogeneity in the patient sample with respect to stage of illness, age, medication history, image acquisition and inter-site scanner differences.

In concordance with this study, many earlier DTI studies of smaller but more homogeneous and well-characterized schizophrenia samples have reported reductions in FA and significant abnormalities in other diffusion metrics (Samartzis et al. 2014; Fusar-Poli et al. 2013; Bora et al. 2011). Kubicki and colleagues (2007) provide a review of diffusion tensor imaging studies in schizophrenia and conclude that decreased FA (and increased MD) within prefrontal and temporal lobes, as well as abnormalities within the fiber bundles connecting these regions are the most frequent findings in schizophrenia. More recently, Ellison-Wright and Bullmore (Ellison-Wright and Bullmore 2009) completed a meta-analysis of 15 diffusion tensor imaging studies in schizophrenia (407 patients, 383 healthy comparison subjects) and reported FA reductions in the frontal and temporal cortices in schizophrenia. However, discrepancies among the 15 studies are substantial and the precise location of white matter pathology in

the disorder remains obscured by the inconsistencies across studies. The inconsistency across studies in the loci of white matter pathology may be due to intrinsic heterogeneity within the diagnostic construct of schizophrenia, to differences in image analysis methodologies between studies and/or to spurious heterogeneity introduced by false positive findings owing to small sample sizes and lack of judicious statistical practices. Furthermore, heterogeneity in patient sample characteristics, including stage of illness and chronicity, cannot be underplayed given that white matter microstructure and connectivity changes throughout the lifespan.

4.3.1 Diffusion Tensor Imaging in Chronic Schizophrenia

Most studies have been conducted in chronic schizophrenia patients, with consistent reports of reduced FA and increased MD in patients compared to controls. The most commonly implicated fiber bundles include the superior longitudinal fasciculus (SLF), uncinate fasciculus, cingulum bundle, and corpus callosum (Fitzsimmons et al. 2013; Wheeler and Voineskos 2014). For example, Holleran and colleagues (2014) detected lower FA in 19 individuals with chronic schizophrenia compared to 19 healthy controls in fiber bundles within the genu, body, and splenium of the corpus callosum, as well as in temporal and frontal regions. However, some studies have failed to replicate findings of reduced FA in the corpus callosum (Agartz et al. 2001; Collinson et al. 2014; Foong et al. 2000), whereas other studies identified reduced FA in the anterior portion, but not the body or splenium of the corpus callosum (Shergill et al. 2007; Kong et al. 2011; Lener et al. 2015), whilst a few studies have reported widespread reductions in FA (Bai et al. 2009; Kanaan et al. 2009; Reading et al. 2011; Asami et al. 2014; Fujino et al. 2014; Roalf et al. 2015; Di Biase et al. 2017; Hubl et al. 2004). These findings are interesting given earlier findings of thinning of the anterior portion of the corpus callosum early in the illness with more widespread reduction in chronic schizophrenia (Walterfang et al. 2008b). However, three FA studies were unable to detect any between-group differences (Foong et al. 2002; Boos et al. 2013; Steel et al. 2001). Notably, negative findings were reported in early studies employing ROI approaches compared to voxel-based analyses (such as with TBSS). Hence, voxel-based or whole-brain methods may be more sensitive to diffusion abnormalities in schizophrenia (Snook et al. 2007). While studies in chronic patients have yielded more consistent results than studies at earlier illness stages, they are confounded by epiphenomena unrelated to illness, including stress associated with prolonged or chronic illness, cumulative medication consumption, and normative aging effects (Ozcelik-Eroglu et al. 2014; Hasan et al. 2007). Thus, it is difficult to disambiguate primary white matter changes linked to disease origins from epiphenomena when studying chronic patients.

4.3.2 Diffusion Tensor Imaging in First Episode Psychosis

Studies examining antipsychotic-naïve, first episode patients (Cheung et al. 2008, 2011; Zou et al. 2008; Gasparotti et al. 2009; Guo et al. 2012; Mandl et al. 2013; Filippi et al. 2014; Alvarado-Alanis et al. 2015; Sun et al. 2015) have identified reduced FA, particularly in the callosal fibers and in the cingulum bundle, suggesting that white matter pathology may reflect a primary disease process in schizophrenia. However, treatments with atypical antipsychotic medication may modulate the extent of damage (Szeszko et al. 2014; Marques et al. 2014), which might contribute to the mixed findings.

DTI studies following the initial onset of psychosis in medicated patients (refer to recent reviews: Samartzis et al. 2014; Wheeler and Voineskos 2014) implicate similar fiber bundles affected in chronic illness, however these findings are less consistent. While the majority of studies suggest that white matter pathology emerges early in the illness, little consensus exists regarding specific tracts and regions affected. Furthermore, some studies report no between-group differences

in diffusivity measures (Kong et al. 2011; Price et al. 2005; Peters et al. 2008; Friedman et al. 2008; Mendelsohn et al. 2006; Qiu et al. 2009; Begré et al. 2003). Inconsistencies across studies might reflect methodological discrepancies related to image acquisition and post-processing, limitations of FA as a measure of white matter integrity, inadequate sample sizes leading to underpowered studies (Poldrack et al. 2017), as well as to heterogeneity in the sample population (Pantelis et al. 2009; Cropley and Pantelis 2014). For example, studies reporting negative findings included small sample sizes (≤15 patients; Kong et al. 2011; Peters et al. 2008; Mendelsohn et al. 2006), or applied a ROI approach (Price et al. 2005; Friedman et al. 2008; Qiu et al. 2009). While these studies did not detect differences in FA, some found differences in alternative diffusivity measures (reviewed below; Mendelsohn et al. 2006; Price et al. 2008).

In addition to methodological factors, inconsistencies might reflect different points in illness trajectories between studies such that white matter alterations are less severe or not as widely distributed in earlier illness. In line with this proposition, cross-sectional studies report greater white matter disruption in older patients with longer illness durations, compared to younger patients with schizophrenia (Di Biase et al. 2017; Di Biase et al. 2019; Cropley et al. 2016; Schneiderman et al. 2011), possibly indicating progressive white matter changes or accelerated white matter decline in schizophrenia (Cropley et al. 2016). In addition, it is possible that the timing or age of patients confers selective vulnerability to particular regions or fibers undergoing development or normal aging processes (Kyriakopoulos et al. 2009; Gogtay et al. 2011). For example, the SLF is the most common tract associated with altered FA in individuals at ultra-high risk (UHR) for developing psychosis (Clemm von Hohenberg et al. 2013; Karlsgodt et al. 2009; Carletti et al. 2012). This association fiber tract undergoes accelerated maturation during healthy late adolescence and early adulthood—corresponding to the typical age of UHR patients examined across these studies (Peters et al. 2012). However, previous DTI studies examining the effect of timing and age (Cropley et al. 2016; Schneiderman et al. 2011) have not included patients recently diagnosed with psychosis, thus precluding full characterization of illness course in schizophrenia.

4.3.3 Ultra-High or Clinical Risk of Developing Psychosis

Few studies have examined diffusion metrics prior to psychosis onset (Begré et al. 2003; Clemm von Hohenberg et al. 2013; Karlsgodt et al. 2009; Carletti et al. 2012; Peters et al. 2009; Bloemen et al. 2010; Cho et al. 2016). With the exception of two ROI studies (Peters et al. 2008, 2010), these studies provide preliminary evidence that the UHR state is associated with white matter deficits. While these studies indicate differences, particularly in the SLF and the corpus callosum, precise trajectories of these deficits as a function of illness course and transition to psychosis, remain unclear. For example, Bloemen and colleagues (2010) found decreased FA in UHR patients, who later transitioned to psychosis (UHR-P), compared to UHR individuals who did not develop full-threshold psychosis (UHR-NP) and healthy controls. On the other hand, Carletti and colleagues (2012) did not detect baseline differences between UHR-P and UHR-NP, but rather found longitudinal FA reductions in the internal capsule, corona radiata, fronto-occipital fasciculus and anterior corpus callosum in the UHR-P group, notably localized to regions previously found to be disrupted in first episode patients. The absence of significant baseline reductions in FA may reflect insufficient power, as Carletti and colleagues (2012) studied only eight UHR-P individuals. Alternatively, treatment with antipsychotic medication may have contributed to differences, with some UHR participants treated in Bloemen's cohort, whereas all UHR participants were unmediated in Carletti's cohort at baseline. Longitudinal changes may also relate to the initiation and cumulative effects of antipsychotic medication. However, a previous report found that FA reductions over time occurred in a medication-free subset of UHR patients (Mittal et al. 2013), indicating that illness-related factors influence longitudinal white matter changes.

In particular, they found that neurological soft signs were predictive of white matter integrity after 1 year within cerebellar-thalamic circuits. Interestingly, the normative pattern of white matter development in these tracts was characterized by an increase in FA over time, in contrast to UHR patients who displayed FA decline over time, which may point to progressive white matter deterioration, rather than stunted neurodevelopment, during this prodromal period.

4.3.4 White Matter Trajectories in Schizophrenia

While longitudinal studies are needed to assess the extent to which white matter pathology is progressive in schizophrenia, cross-sectional evidence from different illness stages can provide crucial insight and inform the design of prospective studies. For example, diffusion studies have examined FA in both recently diagnosed and chronic schizophrenia cohorts (Collinson et al. 2014; Kong et al. 2011; Friedman et al. 2008; White et al. 2011). These studies identified widespread FA reductions in chronic illness, while less severe (Friedman et al. 2008) or no alterations (Collinson et al. 2014; Kong et al. 2011; White et al. 2011) in FA were observed at illness onset. Thus, illness onset might be characterized by subtle and regionally localized white matter pathology. These findings accord with a recent study that modelled the influence of age on FA across a wide age range in 326 individuals with a schizophrenia-spectrum disorder and 197 healthy controls (Cropley et al. 2016; Fig. 4.3).

Interestingly, significant FA reductions only emerged after age 35 in schizophrenia relative to controls, and the decline in FA was 60% steeper in the patient group. The findings of this study aligns with an earlier machine learning study, which found that predicted "brain age" was about

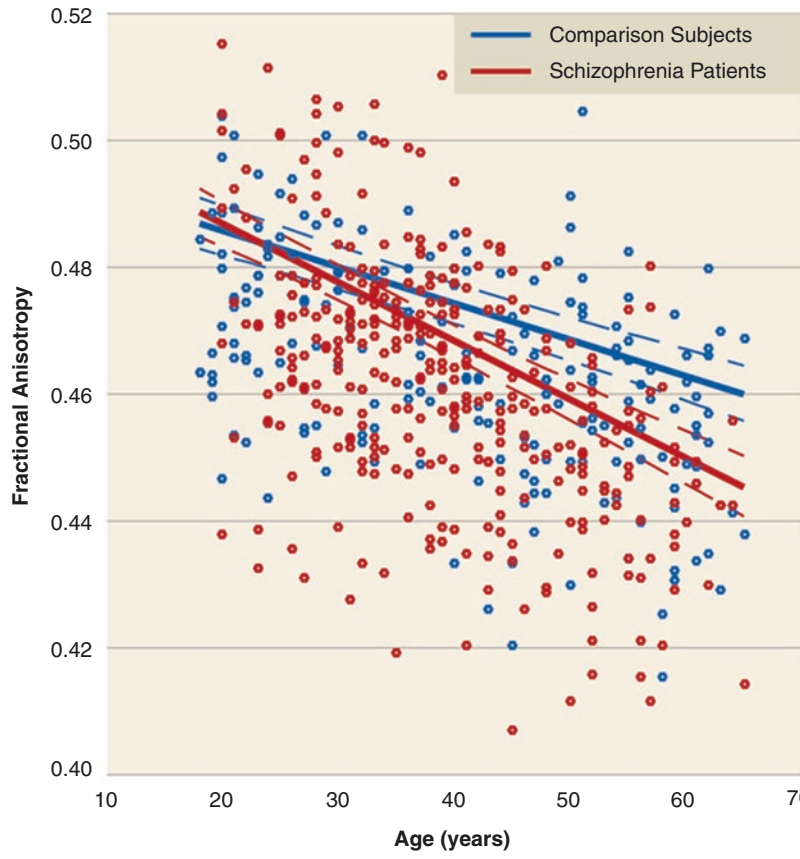

Fig. 4.3 Accelerated white matter deterioration in schizophrenia. Fitted linear curves modeling age-related loss of FA in healthy controls (n = 197; blue curve) and in schizophrenia patients (n = 326; red curve). Dashed lines indicate 95% confidence intervals estimated with bootstrapping. [Figure adapted from Cropley and colleagues (2016)]

3 years greater than a patient's chronological age (Schnack et al. 2016). However, discrepant findings exist. For example, a longitudinal diffusion study identified lower baseline FA in chronic schizophrenia patients within frontoparietal white matter compared to healthy controls, whereas at (~4-year) follow-up, FA, on average, declined faster in *healthy controls* (n = 13) relative to patients (n = 34) (Mitelman et al. 2009). This finding contradicts accelerated white matter ageing in schizophrenia (Kochunov et al. 2013); and rather, suggests that pathological white matter changes are premorbid or confined to the early course of illness, after which the rate of change decelerates with advancing age. As such, little consensus exists regarding the prospective course of pathological white matter changes in schizophrenia. Future longitudinal studies that serially map the timing of anisotropy changes from early to prolonged illness will assist in clarifying white matter trajectories in schizophrenia. Importantly, anomalous white matter trajectories may differ across patient subsets, which could further be addressed by this work.

4.3.5 Summary of Diffusion Tensor Imaging in Schizophrenia

In summary, marked heterogeneity can be found across DTI studies with respect to the spatial extent, loci, topographic distribution and trajectories of white matter pathology in schizophrenia. Aside from patient heterogeneity associated with antipsychotic treatment, illness chronicity, general health, lifestyle and age factors, inconsistent findings across studies likely reflect methodological differences. For example, ROI approaches limit direct comparison across DTI studies due to inconsistency in the choice of ROIs. Furthermore, marked variability in early psychosis may indicate reduced sensitivity of DTI measures to detect subtle pathology, particularly in white matter with complex structure and geometry. Despite variability, a consensus is beginning to emerge: (1) microstructural abnormalities are evident across many schizophrenia populations; (2) at the group-level, white matter pathology is diffuse, widespread and cannot be localized to individual tracts; and (3) white matter pathology may be underpinned by changes in RD rather than AD, pointing to myelin, rather than axonal alterations in schizophrenia.

4.4 Beyond the Tensor: Advanced Diffusion Imaging in Schizophrenia

The information provided by conventional DTI indices measured locally (i.e., voxels or regions), or along the extent of fibers, provide a useful and simple means to detect microstructural changes in white matter. However, these measures cannot distinguish between changes in specific microstructural features such as CSF, axons, myelin, or immunoreactive cells and, therefore, lack specificity. Advanced diffusion imaging approaches attempt to shed new light on the nature of white matter pathology in schizophrenia. These more advanced approaches include free-water imaging (Pasternak et al. 2009), kurtosis imaging, diffusion spectrum imaging (DSI), and neurite orientation dispersion and density imaging (NODDI; Rae et al. 2017). Below we primarily focus on the first three methods, since these have been the most widely studied to date in schizophrenia.

4.4.1 Free-Water Studies

As discussed above, many microstructural features contribute to the signal measured with diffusion imaging. One way of increasing tissue specificity is to minimize non-tissue-related signals. Free-water or partial volume contamination represents one potential source of variance. Free-water constitutes unrestricted water molecules found in CSF, blood, or the extracellular space. A voxel containing free-water would result in lower anisotropy estimates (increased isotropy). Hence, reduced FA, particularly in fibers adjacent to ventricles, may simply reflect increased free-water pools, due to partial volume effects. A recently developed MRI method applies a bi-tensor (two-compartment) model

(Pasternak et al. 2009) to separate the contribution of free-water from that of tissue-specific diffusivity, in order to eliminate partial volume and other free-water effects. This method has been applied to diffusion imaging studies in schizophrenia in order to examine tissue-specific diffusivity (after free water elimination using the tensor model) and free water fractions, which may be linked to atrophy and neuroinflammation (Pasternak et al. 2016).

In the first free-water imaging study, Pasternak and colleagues (2012) compared conventional DTI measures with free-water corrected indices in 18 first episode patients and 20 healthy controls. Widespread FA abnormalities and increased MD were detected with DTI, whereas, free-water-corrected FA (FA_T) revealed a localized decrease in frontal white matter (Fig. 4.4). In contrast, the free-water compartment showed widespread increases in patients compared to controls. This study suggests that most of the FA abnormalities in this FEP group were not associated with changes in the tissue but, rather, were accounted for by increased free-water in the extracellular compartment. Consistent findings were reported in a further study by Lyall and colleagues (2018), which included a larger sample of 63 first episode patients and 70 healthy controls and also found that globally increased free-water values were associated with better cognitive performance after 12 weeks of treatment with antipsychotic medication.

In contrast to these aforementioned studies undertaken in recently diagnosed patients, later studies (Pasternak et al. 2015; Oestreich et al. 2016a, 2017) in chronic patients with schizophrenia found minimal free-water abnormalities, along with a global pattern of decreased FA_T. In particular, Oestreich and colleagues (2017) reported reduced FA_T in the (bilateral) anterior limb of the internal capsule, the (bilateral) posterior thalamic radiation, and the genu of the corpus callosum in 281 chronic schizophrenia patients, compared to 188 controls. In contrast, no significant free-water changes were detected. It is possible that excess free-water parallels acute or exacerbated psychosis, which may explain increased free-water in FEP patients, as they are experiencing, or recently experienced acute psychosis. Consistent with this hypothesis, excess free-water in the left cingulum bundle was specifically found in chronic schizophrenia patients with present (state-related) delusions, compared to chronic patients with remitted delusions and healthy controls (Oestreich et al. 2016b). In this study, FA_T deficits were observed

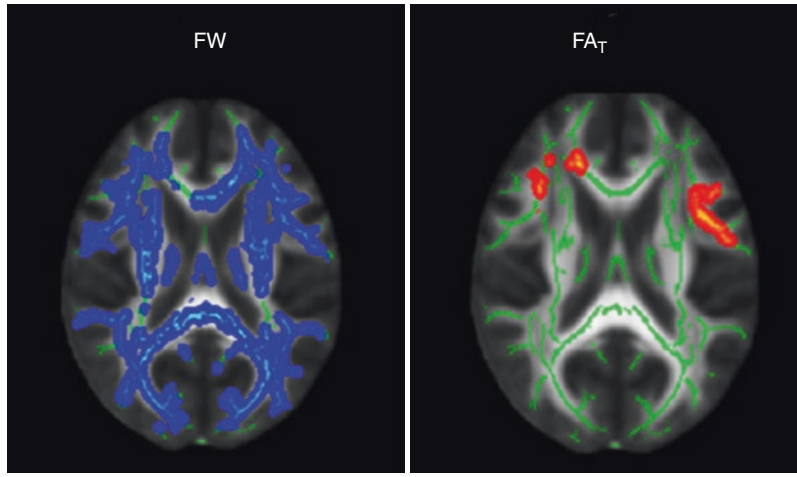

Fig. 4.4 Increased free-water values in first-episode patients. Conventional FA, free-water (FW) and free-water corrected FA (FA_T) were compared between first-episode patients and healthy controls. A widespread increase in free-water values (dark to light blue) was found throughout the white matter skeleton (green), whereas, reduced FA_T (red to yellow) was localized to frontal white matter (Pasternak et al. 2012)

in both patients with present and remitted delusions, compared to healthy controls (Oestreich et al. 2016b).

In summary, free-water imaging enables the differentiation between the contributions of two separate compartments that contribute to DTI indices. These studies indicate widespread increases in extracellular free water in early and acute psychosis, together with localized decreases in tissue-specific FA in chronic schizophrenia. Free-water and tissue-specific components of the diffusion signal potentially enable differentiation of distinct microstructural changes associated with the disorder. However, the microstructural correlates of each compartment remain unclear.

4.4.2 Kurtosis Imaging

Conventional DTI assumes that the surrounding microstructural environments permit free, unrestricted diffusion of water molecules, resulting in a Gaussian (normal) distribution profile. In contrast, it is possible that diffusion is restricted by cell membranes and organelles, for example, within fiber bundles. Furthermore, the underlying white matter structure may not align with the tensor model (e.g., crossing/kissing fibers), even if more than one tensor is modelled, which may obscure resulting signals (Jones et al. 2013). These limitations are overcome to a certain extent by diffusion kurtosis imaging (DKI), which quantifies the non-Gaussian distribution of water molecules, and thus captures molecule displacement where diffusion is restricted. The scalar diffusion metrics derived from kurtosis imaging (mean, axial and radial kurtosis), thus provide measures of microstructural restriction in complex structures.

In an initial study, Zhu and colleagues (2015) compared conventional DTI measures (FA, MD and AD), kurtosis-derived diffusion measures (FA, MD and AD obtained from kurtosis data), and kurtosis-specific parameters (mean, radial and axial kurtosis) in 94 chronic schizophrenia patients, as well as 91 healthy controls. Using TBSS, they identified white matter impairments in patients with diffusion metrics derived from all three models. Conventional DTI and kurtosis-derived diffusion estimates yielded similar findings: widespread reductions in FA (derived from DKI data) and mean kurtosis (derived from DKI), particularly in frontal and temporal regions. Nevertheless, the conventional DTI measures were sensitive to pathology in different white matter regions compared to the kurtosis-specific measures. Specifically, FA and MD abnormalities were found in regions with coherent fiber arrangement (e.g., the corpus callosum), whereas, kurtosis-specific abnormalities, including reduced mean kurtosis, were found in regions with complex fiber arrangement (e.g., corona radiata). Thus, kurtosis-specific and conventional diffusion measures may provide complementary information and may enable differentiation between distinct white matter pathologies in schizophrenia.

A later study compared voxel-wise FA and mean kurtosis metrics in 31 chronic schizophrenia patients and 31 healthy controls (White et al. 2011). These authors identified more widespread mean kurtosis (MK) reductions, compared to FA reductions, which were localized to the corona radiata. These findings would seem to complicate the interpretation offered by Zhu and colleagues (2015) and challenge the suggestion that DTI estimates are more sensitive to pathology in coherent commissural fibers compared to complex, projection fibers. Moreover, reduced MK was also observed in the corona radiata by Narita and colleagues (2016), suggesting that white matter impairments of the corona radiata are detectable with conventional FA, as well as MK measures.

A recent study by Docx and colleagues (2017) compared voxel-wise DTI (FA and MD) to DKI (MK) metrics in 20 schizophrenia patients and 16 healthy controls in terms of their sensitivity to volitional motor activity (a proxy for avolition, which is one of the negative symptoms of schizophrenia). Increasing motor activity was positively correlated with MK in the inferior, medial and superior longitudinal fasciculus, corpus callosum, posterior fronto-occipital fasciculus, and posterior cingulum in patients, but not in controls. Importantly, this association was not found with DTI metrics,

suggesting increased sensitivity of MK to reveal associations with schizophrenia-specific symptomatology. However, in contrast to Zhu and colleagues (2015), Docx and colleagues (2017) did not detect significant differences in MK between patients and healthy controls, but did identify a widespread MD increase in patients. Discrepancies may be explained by the different methods used to analyse the diffusion metrics: Zhu and colleagues (2015) employed TBSS, which examines voxels within a white matter skeleton, whereas Docx and colleagues (2017) employed voxel-based analysis (VBA), which examines all white matter voxels. While these studies differed with respect to case-control findings, both studies point to complementary information provided by tensor and kurtosis metrics. Thus, kurtosis—a measure more sensitive to intracellular restriction and myelin content within complex fibers—may provide supplementary information to DTI metrics regarding microstructural variation in schizophrenia.

4.4.3 Diffusion Spectrum Imaging

Another tensor-free imaging approach used in schizophrenia research is diffusion spectrum imaging (DSI; Pasternak et al. 2015). With DSI, a probability density function (PDF) is fitted to the diffusion signals measured at each voxel. The PDF spatially characterizes the local diffusion profile, without restriction to a particular model such as the tensor. An advantage of this model-free approach is that arbitrarily complex diffusion profiles can be characterized, which are only limited by the angular and spatial resolution of the acquisition. Generalized FA (gFA) is a metric that is commonly used to summarize the isotropy of the PDF fitted to each voxel. In practice, gFA reflects the anisotropy of a voxel (similar to FA). However, it is computed using a model-free framework, and thus results in superior characterization of complex white matter architecture.

Using DSI, Wu and colleagues (2015) found that gFA between first-episode and chronic patients differed only within callosal fibers interconnecting the dorsolateral prefrontal cortices bilaterally. Specifically, gFA in these fibers was significantly decreased in chronic but not in first episode patients compared to controls. They concluded that white matter pathology remained largely static after illness onset. Notably, this contrasts with some DTI studies, which did not detect differences, or which identified subtle differences in first-episode patients. It is therefore possible that advanced, free-model methods provide greater sensitivity to detect subtle pathology occurring in the early stages of psychosis. For example, a pilot study comparing measures derived from a model-free approach (q-ball imaging) to conventional diffusivity measures found an overall decrease in white matter microstructure measured with high b-value DWI in first-episode patients compared to controls, in the absence of any corresponding abnormalities in FA (Mendelsohn et al. 2006).

Taken together, advanced diffusion imaging methods show great potential for addressing the limitations of conventional DTI and for isolating the contribution of distinct biological compartments, including free-water and tissue-specific changes. Furthermore, these distinct biological compartments may provide insight into distinct pathological processes, and thus provide insight into the cellular and microstructural underpinnings of conventional diffusion metrics such as FA. Thus far, these data implicate a predominantly free-water increase in early or acute stages of psychosis, but a predominantly tissue-specific deficit in later or chronic illness stages. Furthermore, advanced diffusion methods may offer greater sensitivity than conventional DTI: DKI for pathology in complex white matter architecture and DSI for subtle or early white matter changes in schizophrenia, since the gFA measure was shown to detect pathology even in the absence of FA deficits.

4.4.4 Using Tractography to Parameterize White Matter Pathology Along the Trajectory of Fiber Bundles

Diffusion indices measured locally cannot identify tract-specific deficits along the trajectory of

fiber bundles and, hence, do not fully account for fiber bundle geometry and connectivity. Tractography-based methods enable measurement of diffusion properties along the course of fiber bundles. To this end, tensor-based (deterministic) or model-free (probabilistic) frameworks can be used to estimate the local orientation of maximum diffusion at each voxel (i.e., the orientation of the fiber bundle), which is used to map coherently oriented fiber bundles.

Most tractography studies have employed deterministic methods in chronic patient cohorts. Once deterministic tractography has been used to reconstruct a fiber bundle of interest, the fiber bundle's trajectory is parameterized, and diffusion measures are then computed for each point along the parameterized trajectory. This enables evaluation and comparison of diffusion measures such as FA for each point along the trajectory, thereby yielding a tract-specific parameterization of diffusion measures (Fig. 4.5).

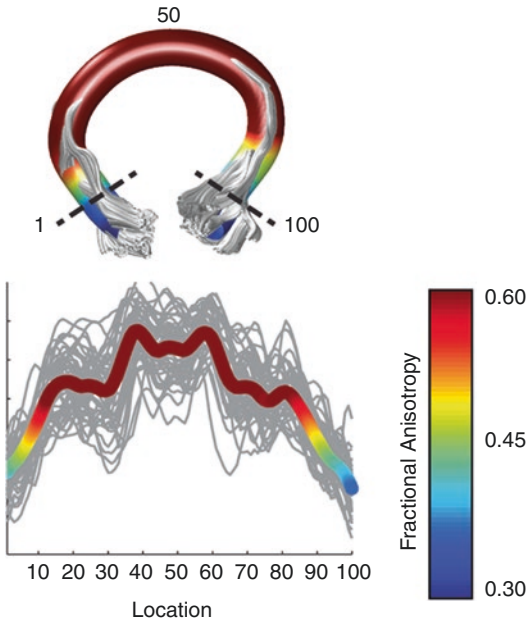

Fig. 4.5 Tract-measured fractional anisotropy of the corpus callosum. After fiber reconstruction, tract FA was measured along the y-axis at each of 100 equidistant points (x-axis). The group mean is shown as a bold line, colored-coded based on the group mean FA value at that point. Gray lines refer to individual FA estimates. Tract FA shows consistent peaks and valleys across individuals (Yeatman et al. 2012)

The most commonly identified tracts showing reduced FA include the cingulum bundle (Voineskos et al. 2010; Nestor et al. 2008, 2010; Rosenberger et al. 2008; Kubicki et al. 2009; Kunimatsu et al. 2012; Whitford et al. 2015), the arcuate (Whitford et al. 2011, 2015; De Weijer et al. 2011; Phillips et al. 2009), the uncinate fasciculus (Voineskos et al. 2010; De Weijer et al. 2011; McIntosh et al. 2008; Singh et al. 2016), the fornix (Kunimatsu et al. 2012; Fitzsimmons et al. 2009; Oestreich et al. 2016c), and the corpus callosum (Whitford et al. 2010, 2015; Kitis et al. 2011; Choi et al. 2011), particularly the anterior corpus callosum. However, discrepancies exist even for the most consistently identified tracts, with negative findings also reported for the cingulum bundle and arcuate fasciculus (Fitzsimmons et al. 2014). For example, Fitzsimmons et al. (Fitzsimmons et al. 2014) found decreased FA in the cingulum bundle in FEP but not chronic schizophrenia patients compared to separate, aged-matched controls, suggesting that diffusivity abnormalities in the cingulum bundle may, in some cases, normalize with illness course. The authors proposed that, given abnormalities involved mean, radial and axial diffusivity, the initial deficit related to an acute process unrelated to myelin or axon abnormalities, but rather an increase in free-water content, which may reflect inflammatory processes. Preliminary free-water studies have since partially supported this hypothesis (as described above), such that first-episode patients display increased free-water content compared to controls (Pasternak et al. 2016). However, other reports have identified widespread tissue-specific deficits in later illness stages (Pasternak et al. 2015), in contrast to Fitzsimmons et al. (Fitzsimmons et al. 2014). Future studies that combine tractography with free-water methods could clarify the contribution of free-water to tract-specific deficits.

Tract-specific FA deficits have been associated with schizophrenia symptomatology: the cingulum bundle with delusions (Whitford et al. 2015), executive functioning, generalized intelligence and visual memory (Nestor et al. 2008; Kubicki et al. 2009); the fornix and uncinate fasciculus with memory (Nestor et al. 2008; Singh

et al. 2016; Fitzsimmons et al. 2009), attention and sensorimotor deficits (Singh et al. 2016); the arcuate fasciculus with positive symptoms (De Weijer et al. 2011; Choi et al. 2011); and the corpus callosum with general psychopathology (Kitis et al. 2011) and positive symptoms (Whitford et al. 2010). Localizing symptoms to particular tracts provides opportunities to personalize therapies such as transcranial magnetic stimulation (TMS; Cocchi and Zalesky 2018) to suit the symptom profile of individual patients.

4.5 Cellular and Molecular Insights into Diffusion Imaging Findings

Cellular and molecular techniques for characterizing neuropathology provide a complementary means to examine white matter pathology in schizophrenia and point to potential sources underlying diffusion related deficits in schizophrenia (Walterfang et al. 2006). To this end, Uranova and colleagues (2014) used electron microscopy and morphometric analysis to reveal similar oligodendrocyte and myelin densities in schizophrenia compared to healthy controls. However, qualitative inspection revealed morphological alterations in oligodendrocytes, characterized by dystrophic changes (e.g., swelling) in the prefrontal white matter of schizophrenia patients (Uranova et al. 2011). A previous study from the same group reported increased volume density of heterochromatin in layer VI and myelin abnormalities in adjacent white matter in a schizophrenia subset with predominantly negative symptoms (Uranova et al. 2011). This study points to links between oligodendrocyte and myelin pathology in schizophrenia, which may contribute to macroscopic diffusion and connectivity deficits through, for example, slowing of the conduction velocity and inducing synaptic changes.

Postmortem and diffusion imaging studies are also consistent with genetic and molecular evidence implicating altered oligodendrocyte and gene expression in schizophrenia. Gene candidate studies have implicated oligodendrocyte and myelin related genes in schizophrenia risk loci, most commonly involving Neuregulin 1 (NRG1) genotypes and haplotypes and the Disrupted-in-schizophrenia 1 (DISC1) gene [For review, refer to Roussos and Haroutunian (Roussos and Haroutunian 2014)]. In addition, microarray and quantitative PCR analyses have shown reduced expression of multiple genes associated with myelin, oligodendrocytes, and integrity of the nodes of Ranvier [For review, refer to Takahashi et al. (Takahashi et al. 2011)]. It is important to note that altered oligodendrocyte function occurs across many neurodevelopmental and psychiatric illnesses, and the functional influences of oligodendrocyte and myelin-related risk genes involve normal developmental processes, including synaptic function and myelination. Thus, oligodendrocyte and myelin deficits may not represent a primary pathological process in schizophrenia (Weinberger 1987).

Irrespective of the pathological origins of white matter deficits in schizophrenia, they appear central to the pathophysiology and symptoms associated with the illness. This conclusion is supported by animal models showing that white matter deficits influence the expression of key neurotransmitter systems involved in schizophrenia. For example, a study by Roy and colleagues (Ramani et al. 2007), revealed that decreased NRG-1-erB signalling not only alters myelin and oligodendrocyte number and morphology, but also increases dopamine receptors and transporters (Ramani et al. 2007). In addition, these transgenic mice displayed behavioural abnormalities consistent with neuropsychiatric conditions (Ramani et al. 2007). The clinical relevance of white matter deficits is further established through evidence that pediatric demyelinating diseases (Sibbitt et al. 2002) and white matter injury (Turkel et al. 2007) are associated with increased risk for developing psychosis (Walterfang et al. 2005). Notably, there is often delay between the initial injury, which may take place at any time during development, and the onset of psychosis (Turkel et al. 2007).

Taken together, data across multiple biological scales converge on a critical role for white matter deficits in schizophrenia. Neuropathological

data point to myelin deficits, which may underlie tissue-specific changes observed in diffusion imaging studies. While the origin of white matter deficits remains unclear, genetic and molecular evidence implicates early developmental biology in white matter disruption. Given the ubiquitous role of oligodendrocytes in supporting myelination, neuronal and synaptic integrity, the functional impact of their disruption is likely dynamic. Cellular and molecular modalities should be considered in conjunction with *in vivo* diffusion imaging studies, which will be crucial to reconcile and expand our knowledge of white matter trajectories, plasticity and treatment in schizophrenia.

4.6 Conclusions and Future Directions

Our understanding of white matter pathology in schizophrenia has dramatically increased in recent years due primarily to advances in diffusion imaging. Unlike two or three decades ago when the evidence for white matter involvement in schizophrenia remained equivocal, there can be no doubt now that white matter abnormalities are a core pathological feature of schizophrenia and may be present before the onset of symptoms. White matter pathology affects widespread networks in chronic patients but may be confined to select callosal and fronto-temporal fibers early in the disorder. These fibers are connected by regions that are also disproportionately affected in the disorder (frontal and temporal regions) and functionally mature in early adulthood, coinciding with the time of peak risk for schizophrenia. Thus, developmental timing may confer increased susceptibility to disruption of particular tracts. Following the initial onset of psychosis, some diffusion tensor imaging studies hint at a pattern of white matter decline over illness at a rate faster than attributable to healthy aging. However, so far, cross-sectional studies have not distinguished primary progressive events from epiphenomena owing to illness chronicity and cumulative treatment. Longitudinal studies that serially map the timing of brain changes will aid in clarifying trajectories in the context of healthy brain maturation and aging factors, as well as illness factors, such as cumulative treatment. Irrespective of the prospective course, the presence of connectivity impairments in early medication naïve cohorts and prior to psychosis points to a central role for white matter pathology in schizophrenia.

Advanced free-water and tensor-free diffusion imaging methods have improved sensitivity to detect these subtle abnormalities early in the course of illness and are, moreover, shedding new light on the nature of these deficits, which may dynamically evolve over the course of illness. In addition, preliminary studies employing DKI and DSI methods may provide complementary information to DTI metrics within complex white matter architecture (e.g., crossing/kissing fibers). These methods have further leveraged tractography approaches to reveal structural connectivity deficits in schizophrenia.

While these advanced models are paving the way forward, it is important to remember that diffusion indices represent mathematical descriptions that are governed by a multitude of variables, and hence cannot be straightforwardly ascribed to specific biological mechanisms. Neuropathological evidence points to a myelin deficit, which may underlie microstructural changes in white matter tissue structure and organization. Furthermore, molecular evidence implicates developmental factors in myelin disruption. Bridging the gap across biological scales and improving characterization of white matter pathology will depend upon validating neuroimaging techniques through concurrent measurement with PET radioligands that pinpoint specific cellular mechanisms, as well as by combining *in vivo* diffusion imaging with histological methods in postmortem and animal studies.

Lastly, it is important to remark that patient heterogeneity complicates the investigation and interpretation of white matter findings across the extent of neuroimaging studies. Thus, future study designs should focus on elucidating links to specific symptoms, general health, lifestyle, as well as illness severity and chronicity factors, rather than examining broad, group-level differences (controls versus all patients), since these

may reflect the combined effect of heterogeneous patient populations. Of course, along with efforts to identify potential therapeutic targets, it is equally important to assess whether white matter biomarkers are clinically valuable in predicting disease progression or outcome, and potentially treatment response.

Summary

- White matter abnormalities are a core pathological feature of schizophrenia and may be present before the onset of symptoms.
- Advanced free-water and tensor-free diffusion imaging methods have improved sensitivity to detect subtle abnormalities early in the course of psychosis and schizophrenia.
- Some diffusion tensor imaging studies indicate a pattern of white matter decline over the course of schizophrenia.
- Patient heterogeneity and variation in image analysis methodologies complicate the interpretation of white matter findings across the extent of neuroimaging studies.
- Neuropathological evidence points to a myelin deficit, which may underlie microstructural changes in white matter tissue structure and organization.

References

Absher JR, Benson DF. Disconnection syndromes: an overview of Geschwind's contributions. Neurology. 1993;43:862–7.

Agartz I, Andersson JL, Skare S. Abnormal brain white matter in schizophrenia: a diffusion tensor imaging study. Neuroreport. 2001;12(10):2251–4.

Alexander AL, Lee JE, Lazar M, Field AS. Diffusion tensor imaging of the brain. Neurotherapeutics. 2007;4(3):316–29.

Allen P, Larøi F, McGuire PK, Aleman A. The hallucinating brain: a review of structural and functional neuroimaging studies of hallucinations. Neurosci Biobehav Rev. 2008;32(1):175–91.

Alvarado-Alanis P, Leon-Ortiz P, Reyes-Madrigal F, Favila R, Rodriguez-Mayoral O, Nicolini H, et al. Abnormal white matter integrity in antipsychotic-naive first-episode psychosis patients assessed by a DTI principal component analysis. Schizophr Res. 2015;162(1–3):14–21.

Asami T, Hyuk Lee S, Bouix S, Rathi Y, Whitford TJ, Niznikiewicz M, et al. Cerebral white matter abnormalities and their associations with negative but not positive symptoms of schizophrenia. Psychiatry Res. 2014;222(1):52–9.

Bai YM, Chou KH, Lin CP, Chen IY, Li CT, Yang KC, et al. White matter abnormalities in schizophrenia patients with tardive dyskinesia: a diffusion tensor image study. Schizophr Res. 2009;109(1–3):167–81.

Basser PJ, Pierpaoli C. A simplified method to measure the diffusion tensor from seven MR images. Magn Reson Med. 1998;39(6):928–34.

Basser PJ, Mattiello J, Le Bihan D. MR diffusion tensor spectroscopy and imaging. Biophys J. 1994a;66(1):259–67.

Basser PJ, Mattiello J, LeBihan D. Estimation of the effective self-diffusion tensor from the NMR spin echo. J Magn Reson B. 1994b;103(3):247–54.

Basser PJ, Pajevic S, Pierpaoli C, Duda J, Aldroubi A. In vivo fiber tractography using DT-MRI data. Magn Reson Med. 2000;44(4):625–32.

Beaulieu C. The basis of anisotropic water diffusion in the nervous system—a technical review. NMR Biomed. 2002;15(7–8):435–55.

Begré S, Federspiel A, Kiefer C, Schroth G, Dierks T, Strik WK. Reduced hippocampal anisotropy related to anteriorization of alpha EEG in schizophrenia. Neuroreport. 2003;14(5):739–42.

Berrios GE. Schizophrenia: a conceptual history. Rev Int Psicol Ter Psicol. 2003;3(2):111–40.

Bloemen OJN, de Koning MB, Schmitz N, Nieman DH, Becker HE, de Haan L, et al. White-matter markers for psychosis in a prospective ultra-high-risk cohort. Psychol Med. 2010;40(08):1297–304.

Boos HB, Mandl RC, van Haren NE, Cahn W, van Baal GC, Kahn RS, et al. Tract-based diffusion tensor imaging in patients with schizophrenia and their non-psychotic siblings. Eur Neuropsychopharmacol. 2013;23(4):295–304.

Bora E, Fornito A, Radua J, Walterfang M, Seal M, Wood SJ, et al. Neuroanatomical abnormalities in schizophrenia: a multimodal voxelwise meta-analysis and meta-regression analysis. Schizophr Res. 2011;127(1):46–57.

Carletti F, Woolley JB, Bhattacharyya S, Perez-Iglesias R, Fusar Poli P, Valmaggia L, et al. Alterations in white matter evident before the onset of psychosis. Schizophr Bull. 2012;38(6):1170–9.

Cheung V, Cheung C, McAlonan GM, Deng Y, Wong JG, Yip L, et al. A diffusion tensor imaging study of structural dysconnectivity in never-medicated, first-episode schizophrenia. Psychol Med. 2008;38(6):877–85.

Cheung V, Chiu CP, Law CW, Cheung C, Hui CL, Chan KK, et al. Positive symptoms and white matter micro-

structure in never-medicated first episode schizophrenia. Psychol Med. 2011;41(8):1709–19.
Cho KI, Shenton ME, Kubicki M, Jung WH, Lee TY, Yun JY, et al. Altered thalamo-cortical white matter connectivity: probabilistic tractography study in clinical-high risk for psychosis and first-episode psychosis. Schizophr Bull. 2016;42(3):723–31.
Choi H, Kubicki M, Whitford TJ, Alvarado JL, Terry DP, Niznikiewicz M, et al. Diffusion tensor imaging of anterior commissural fibers in patients with schizophrenia. Schizophr Res. 2011;130(1–3):78–85.
Clemm von Hohenberg C, Pasternak O, Kubicki M, Ballinger T, Vu MA, Swisher T, et al. White matter microstructure in individuals at clinical high risk of psychosis: a whole-brain diffusion tensor imaging study. Schizophr Bull. 2013;40(4):895–903.
Cocchi L, Zalesky A. Personalized transcranial magnetic stimulation in psychiatry. Biol Psychiatry Cogn Neurosci Neuroimaging. 2018;3(9):731–41.
Collin G, Turk E, van den Heuvel MP. Connectomics in schizophrenia: from early pioneers to recent brain network findings. Biol Psychiatry Cogn Neurosci Neuroimaging. 2016;1(3):199–208.
Collinson SL, Gan SC, Woon PS, Kuswanto C, Sum MY, Yang GL, et al. Corpus callosum morphology in first-episode and chronic schizophrenia: combined magnetic resonance and diffusion tensor imaging study of Chinese Singaporean patients. Br J Psychiatry. 2014;204(1):55–60.
Cropley VL, Pantelis C. Using longitudinal imaging to map the 'relapse signature' of schizophrenia and other psychoses. Epidemiol Psychiatr Sci. 2014;23(03):219–25.
Cropley VL, Klauser P, Lenroot RK, Bruggemann J, Sundram S, Bousman C, et al. Accelerated gray and white matter deterioration with age in schizophrenia. Am J Psychiatry. 2016;174(3):286–95.
Di Biase MA, Cropley VL, Baune BT, Olver J, Amminger P, Phassouliotis C, et al. White matter connectivity disruptions in early and chronic schizophrenia. Psychological Medicine. 2017:1–14. https://doi.org/10.1017/S0033291717001313. PubMed PMID: 28528586.
Di Biase MA, Cropley VL, Cocchi L, Fornito A, Calamante F, Ganella E, et al. Linking cortical and connectional pathology in schizophrenia. Schizophrenia Bulletin. 2019;45(4):911–23. https://doi.org/10.1093/schbul/sby121. PubMed PMID: 30215783; PubMed Central PMCID: PMC6581130.
De Weijer A, Mandl R, Diederen K, Neggers S, Kahn R, Pol HH, et al. Microstructural alterations of the arcuate fasciculus in schizophrenia patients with frequent auditory verbal hallucinations. Schizophr Res. 2011;130(1):68–77.
Docx L, Emsell L, Van Hecke W, De Bondt T, Parizel PM, Sabbe B, et al. White matter microstructure and volitional motor activity in schizophrenia: a diffusion kurtosis imaging study. Psychiatry Res Neuroimaging. 2017;260:29–36.
Ellison-Wright I, Bullmore E. Meta-analysis of diffusion tensor imaging studies in schizophrenia. Schizophr Res. 2009;108(1–3):3–10.
Filippi M, Canu E, Gasparotti R, Agosta F, Valsecchi P, Lodoli G, et al. Patterns of brain structural changes in first-contact, antipsychotic drug-naive patients with schizophrenia. Am J Neuroradiol. 2014;35(1):30–7.
Fitzsimmons J, Kubicki M, Smith K, Bushell G, Estepar RS, Westin CF, et al. Diffusion tractography of the fornix in schizophrenia. Schizophr Res. 2009;107(1):39–46.
Fitzsimmons J, Kubicki M, Shenton ME. Review of functional and anatomical brain connectivity findings in schizophrenia. Curr Opin Psychiatry. 2013;26(2):172–87.
Fitzsimmons J, Schneiderman JS, Whitford TJ, Swisher T, Niznikiewicz MA, Pelavin PE, et al. Cingulum bundle diffusivity and delusions of reference in first episode and chronic schizophrenia. Psychiatry Res Neuroimaging. 2014;224(2):124–32.
Foong J, Maier M, Barker GJ, Brocklehurst S, Miller DH, Ron MA. In vivo investigation of white matter pathology in schizophrenia with magnetisation transfer imaging. J Neurol Neurosurg Psychiatry. 2000;68(1):70–4.
Foong J, Symms MR, Barker GJ, Maier M, Miller DH, Ron MA. Investigating regional white matter in schizophrenia using diffusion tensor imaging. Neuroreport. 2002;13(3):333–6.
Fornito A, Zalesky A, Bullmore E. Fundamentals of brain network analysis. San Diego: Academic; 2016.
Friedman JI, Tang C, Carpenter D, Buchsbaum M, Schmeidler J, Flanagan L, et al. Diffusion tensor imaging findings in first-episode and chronic schizophrenia patients. Am J Psychiatry. 2008;165(8):1024–32.
Friston KJ. The disconnection hypothesis. Schizophr Res. 1998;30(2):115–25.
Friston KJ, Frith CD. Schizophrenia: a disconnection syndrome. Clin Neurosci. 1995;3(2):89–97.
Friston KJ, Holmes A, Poline J-B, Price CJ, Frith CD. Detecting activations in PET and fMRI: levels of inference and power. Neuroimage. 1996;4(3):223–35.
Fujino J, Takahashi H, Miyata J, Sugihara G, Kubota M, Sasamoto A, et al. Impaired empathic abilities and reduced white matter integrity in schizophrenia. Prog Neuropsychopharmacol Biol Psychiatry. 2014;48:117–23.
Fusar-Poli P, Smieskova R, Kempton MJ, Ho BC, Andreasen NC, Borgwardt S. Progressive brain changes in schizophrenia related to antipsychotic treatment? A meta-analysis of longitudinal MRI studies. Neurosci Biobehav Rev. 2013;37(8):1680–91.
Gasparotti R, Valsecchi P, Carletti F, Galluzzo A, Liserre R, Cesana B, et al. Reduced fractional anisotropy of corpus callosum in first-contact, antipsychotic drug-naive patients with schizophrenia. Schizophr Res. 2009;108(1):41–8.

Gogtay N, Vyas NS, Testa R, Wood SJ, Pantelis C. Age of onset of schizophrenia: perspectives from structural neuroimaging studies. Schizophr Bull. 2011;37(3):504–13.

Guo W, Liu F, Liu Z, Gao K, Xiao C, Chen H, et al. Right lateralized white matter abnormalities in first-episode, drug-naive paranoid schizophrenia. Neurosci Lett. 2012;531(1):5–9.

Haijma SV, Van Haren N, Cahn W, Koolschijn PCM, Hulshoff Pol HE, Kahn RS. Brain volumes in schizophrenia: a meta-analysis in over 18 000 subjects. Schizophr Bull. 2012;39(5):1129–38.

Hasan K, Sankar A, Halphen C, Kramer L, Brandt M, Juranek J, et al. Development and organization of the human brain tissue compartments across the lifespan using diffusion tensor imaging. Neuroreport. 2007;18(16):1735–9.

Hoche AE, Denning RG, Denning TR. The significance of symptom complexes in psychiatry. Hist Psychiatry. 1991;2(7):329–43.

Holleran L, Ahmed M, Anderson-Schmidt H, McFarland J, Emsell L, Leemans A, et al. Altered interhemispheric and temporal lobe white matter microstructural organization in severe chronic schizophrenia. Neuropsychopharmacology. 2014;39(4):944–54.

Hubl D, Koenig T, Strik W, Federspiel A, Kreis R, Boesch C, et al. Pathways that make voices: white matter changes in auditory hallucinations. Arch Gen Psychiatry. 2004;61(7):658–68.

Johansen-Berg H, Rushworth MFS. Using diffusion imaging to study human connectional anatomy. Annu Rev Neurosci. 2009;32(1):75–94.

Jones DK, Knösche TR, Turner R. White matter integrity, fiber count, and other fallacies: the do's and don'ts of diffusion MRI. Neuroimage. 2013;73:239–54.

Kanaan R, Barker G, Brammer M, Giampietro V, Shergill S, Woolley J, et al. White matter microstructure in schizophrenia: effects of disorder, duration and medication. Br J Psychiatry. 2009;194(3):236–42.

Karlsgodt KH, Niendam TA, Bearden CE, Cannon TD. White matter integrity and prediction of social and role functioning in subjects at ultra-high risk for psychosis. Biol Psychiatry. 2009;66(6):562–9.

Kelly S, Jahanshad N, Zalesky A, Kochunov P, Agartz I, Alloza C, et al. Widespread white matter microstructural differences in schizophrenia across 4322 individuals: results from the ENIGMA Schizophrenia DTI Working Group. Mol Psychiatry. 2018;23(5):1261–9.

Keshavan MS, Morris DW, Sweeney JA, Pearlson G, Thaker G, Seidman LJ, et al. A dimensional approach to the psychosis spectrum between bipolar disorder and schizophrenia: the Schizo-Bipolar Scale. Schizophr Res. 2011;133(1–3):250–4.

Kitis O, Eker MC, Zengin B, Akyilmaz DA, Yalvac D, Ozdemir HI, et al. The disrupted connection between cerebral hemispheres in schizophrenia patients: a diffusion tensor imaging study. Turk J Psychiatry. 2011;22(4):213–21.

Kochunov P, Glahn DC, Rowland LM, Olvera RL, Winkler A, Yang YH, et al. Testing the hypothesis of accelerated cerebral white matter aging in schizophrenia and major depression. Biol Psychiatry. 2013;73(5):482–91.

Kong X, Ouyang X, Tao H, Liu H, Li L, Zhao J, et al. Complementary diffusion tensor imaging study of the corpus callosum in patients with first-episode and chronic schizophrenia. J Psychiatry Neurosci. 2011;36(2):120–5.

Kubicki M, McCarley R, Westin CF, Park HJ, Maier S, Kikinis R, et al. A review of diffusion tensor imaging studies in schizophrenia. J Psychiatr Res. 2007;41(1–2):15–30.

Kubicki M, Niznikiewicz M, Connor E, Ungar L, Nestor P, Bouix S, et al. Relationship between white matter integrity, attention, and memory in schizophrenia: a diffusion tensor imaging study. Brain Imaging Behav. 2009;3(2):191–201.

Kunimatsu N, Aoki S, Kunimatsu A, Abe O, Yamada H, Masutani Y, et al. Tract-specific analysis of white matter integrity disruption in schizophrenia. Psychiatry Res. 2012;201(2):136–43.

Kyriakopoulos M, Perez-Iglesias R, Woolley JB, Kanaan RA, Vyas NS, Barker GJ, et al. Effect of age at onset of schizophrenia on white matter abnormalities. Br J Psychiatry. 2009;195(4):346–53.

Lener MS, Wong E, Tang CY, Byne W, Goldstein KE, Blair NJ, et al. White matter abnormalities in schizophrenia and schizotypal personality disorder. Schizophr Bull. 2015;41(1):300–10.

Lyall A, Pasternak O, Robinson D, Newell D, Trampush J, Gallego J, et al. Greater extracellular free-water in first-episode psychosis predicts better neurocognitive functioning. Mol Psychiatry. 2018;23(3):701–7.

Mandl RC, Rais M, van Baal GC, van Haren NE, Cahn W, Kahn RS, et al. Altered white matter connectivity in never-medicated patients with schizophrenia. Hum Brain Mapp. 2013;34(9):2353–65.

Marques TR, Taylor H, Chaddock C, Dell'Acqua F, Handley R, Reinders AS, et al. White matter integrity as a predictor of response to treatment in first episode psychosis. Brain. 2014;137(1):172–82.

McIntosh AM, Munoz Maniega S, Lymer GK, McKirdy J, Hall J, Sussmann JE, et al. White matter tractography in bipolar disorder and schizophrenia. Biol Psychiatry. 2008;64(12):1088–92.

Mendelsohn A, Strous RD, Bleich M, Assaf Y, Hendler T. Regional axonal abnormalities in first episode schizophrenia: preliminary evidence based on high b-value diffusion-weighted imaging. Psychiatry Res. 2006;146(3):223–9.

Mitelman M, Canfield EL, Newmark R, Brickman AM, Torosjan Y, Chu K, et al. Longitudinal assessment of gray and white matter in chronic schizophrenia: a combined diffusion-tensor and structural magnetic resonance imaging study. Open Neuroimaging J. 2009;3:31–47.

Mittal VA, Dean DJ, Bernard JA, Orr JM, Pelletier-Baldelli A, Carol EE, et al. Neurological soft signs predict abnormal cerebellar-thalamic tract development and negative symptoms in adolescents at high risk for

psychosis: a longitudinal perspective. Schizophr Bull. 2013;40(6):1204–15.

Mori S, Zhang J. Principles of diffusion tensor imaging and its applications to basic neuroscience research. Neuron. 2006;51(5):527–39.

Narita H, Tha KK, Hashimoto N, Hamaguchi H, Nakagawa S, Shirato H, et al. Mean kurtosis alterations of cerebral white matter in patients with schizophrenia revealed by diffusion kurtosis imaging. Prog Neuropsychopharmacol Biol Psychiatry. 2016;71:169–75.

Nestor PG, Kubicki M, Niznikiewicz M, Gurrera RJ, McCarley RW, Shenton ME. Neuropsychological disturbance in schizophrenia: a diffusion tensor imaging study. Neuropsychology. 2008;22(2):246–54.

Nestor PG, Kubicki M, Nakamura M, Niznikiewicz M, McCarley RW, Shenton ME. Comparing prefrontal gray and white matter contributions to intelligence and decision making in schizophrenia and healthy controls. Neuropsychology. 2010;24(1):121–9.

Nichols TE, Holmes AP. Nonparametric permutation tests for functional neuroimaging: a primer with examples. Hum Brain Mapp. 2002;15(1):1–25.

Oestreich LK, Pasternak O, Shenton ME, Kubicki M, Gong X, Bank ASR, et al. Abnormal white matter microstructure and increased extracellular free-water in the cingulum bundle associated with delusions in chronic schizophrenia. Neuroimage Clin. 2016a;12:405–14.

Oestreich LK, Pasternak O, Shenton ME, Kubicki M, Gong X, McCarthy-Jones S, et al. Abnormal white matter microstructure and increased extracellular free-water in the cingulum bundle associated with delusions in chronic schizophrenia. Neuroimage Clin. 2016b;12:405–14.

Oestreich LK, McCarthy-Jones S, Whitford TJ. Decreased integrity of the fronto-temporal fibers of the left inferior occipito-frontal fasciculus associated with auditory verbal hallucinations in schizophrenia. Brain Imaging Behav. 2016c;10(2):445–54.

Oestreich LK, Lyall AE, Pasternak O, Kikinis Z, Newell DT, Savadjiev P, et al. Characterizing white matter changes in chronic schizophrenia: a free-water imaging multi-site study. Schizophr Res. 2017;189:153–61.

Ozcelik-Eroglu E, Ertugrul A, Oguz KK, Has AC, Karahan S, Yazici MK. Effect of clozapine on white matter integrity in patients with schizophrenia: a diffusion tensor imaging study. Psychiatry Res Neuroimaging. 2014;223(3):226–35.

Pantelis C, Yücel M, Bora E, Fornito A, Testa R, Brewer WJ, et al. Neurobiological markers of illness onset in psychosis and schizophrenia: the search for a moving target. Neuropsychol Rev. 2009;19(3):385–98.

Pasternak O, Sochen N, Gur Y, Intrator N, Assaf Y. Free water elimination and mapping from diffusion MRI. Magn Reson Med. 2009;62(3):717–30.

Pasternak O, Westin C-F, Bouix S, Seidman LJ, Goldstein JM, Woo TU, et al. Excessive extracellular volume reveals a neurodegenerative pattern in schizophrenia onset. J Neurosci. 2012;32(48):17365–72.

Pasternak O, Westin CF, Dahlben B, Bouix S, Kubicki M. The extent of diffusion MRI markers of neuroinflammation and white matter deterioration in chronic schizophrenia. Schizophr Res. 2015;161(1):113–8.

Pasternak O, Kubicki M, Shenton ME. In vivo imaging of neuroinflammation in schizophrenia. Schizophr Res. 2016;173(3):200–12.

Peters BD, de Haan L, Dekker N, Blaas J, Becker HE, Dingemans PM, et al. White matter fibertracking in first-episode schizophrenia, schizoaffective patients and subjects at ultra-high risk of psychosis. Neuropsychobiology. 2008;58(1):19–28.

Peters B, Schmitz N, Dingemans P, Van Amelsvoort T, Linszen D, De Haan L, et al. Preliminary evidence for reduced frontal white matter integrity in subjects at ultra-high-risk for psychosis. Schizophr Res. 2009;111(1):192–3.

Peters BD, Dingemans PM, Dekker N, Blaas J, Akkerman E, van Amelsvoort TA, et al. White matter connectivity and psychosis in ultra-high-risk subjects: a diffusion tensor fiber tracking study. Psychiatry Res. 2010;181(1):44–50.

Peters BD, Szeszko PR, Radua J, Ikuta T, Gruner P, DeRosse P, et al. White matter development in adolescence: diffusion tensor imaging and meta-analytic results. Schizophr Bull. 2012;38(6):1308–17.

Phillips OR, Nuechterlein KH, Clark KA, Hamilton LS, Asarnow RF, Hageman NS, et al. Fiber tractography reveals disruption of temporal lobe white matter tracts in schizophrenia. Schizophr Res. 2009;107(1):30–8.

Poldrack RA, Baker CI, Durnez J, Gorgolewski KJ, Matthews PM, Munafo MR, et al. Scanning the horizon: towards transparent and reproducible neuroimaging research. Nat Rev Neurosci. 2017;18(2):115–26.

Price G, Bagary MS, Cercignani M, Altmann DR, Ron MA. The corpus callosum in first episode schizophrenia: a diffusion tensor imaging study. J Neurol Neurosurg Psychiatry. 2005;76(4):585–7.

Price G, Cercignani M, Parker GJ, Altmann DR, Barnes TR, Barker GJ, et al. White matter tracts in first-episode psychosis: a DTI tractography study of the uncinate fasciculus. Neuroimage. 2008;39(3):949–55.

Qiu A, Zhong J, Graham S, Chia MY, Sim K. Combined analyses of thalamic volume, shape and white matter integrity in first-episode schizophrenia. Neuroimage. 2009;47(4):1163–71.

Rae CL, Davies G, Garfinkel SN, Gabel MC, Dowell NG, Cercignani M, et al. Deficits in neurite density underlie white matter structure abnormalities in first-episode psychosis. Biol Psychiatry. 2017;82(10):716–25.

Ramani A, Jensen J, Szulc K, Ali O, Hu C, Lu H, et al., editors. Assessment of abnormalities in the cerebral microstructure of schizophrenia patients: a diffusional kurtosis imaging study. In: Proceedings of the 15th Annual Meeting of ISMRM, Berlin. 2007.

Reading SA, Oishi K, Redgrave GW, McEntee J, Shanahan M, Yoritomo N, et al. Diffuse abnormality of low to moderately organized white matter in schizophrenia. Brain Connect. 2011;1(6):511–9.

Roalf DR, Gur RE, Verma R, Parker WA, Quarmley M, Ruparel K, et al. White matter microstructure in schizophrenia: associations to neurocognition and clinical symptomatology. Schizophr Res. 2015;161(1):42–9.

Rosenberger G, Kubicki M, Nestor PG, Connor E, Bushell GB, Markant D, et al. Age-related deficits in fronto-temporal connections in schizophrenia: a diffusion tensor imaging study. Schizophr Res. 2008;102(1–3):181–8.

Roussos P, Haroutunian V. Schizophrenia: susceptibility genes and oligodendroglial and myelin related abnormalities. Front Cell Neurosci. 2014;8:5.

Samartzis L, Dima D, Fusar-Poli P, Kyriakopoulos M. White matter alterations in early stages of schizophrenia: a systematic review of diffusion tensor imaging studies. J Neuroimaging. 2014;24(2):101–10.

Schnack HG, van Haren NEM, Nieuwenhuis M, Hulshoff Pol HE, Cahn W, Kahn RS. Accelerated brain aging in schizophrenia: a longitudinal pattern recognition study. Am J Psychiatry. 2016;173(6):607–16.

Schneiderman JS, Hazlett EA, Chu KW, Zhang J, Goodman CR, Newmark RE, et al. Brodmann area analysis of white matter anisotropy and age in schizophrenia. Schizophr Res. 2011;130(1–3):57–67.

Shergill SS, Kanaan RA, Chitnis XA, O'Daly O, Jones DK, Frangou S, et al. A diffusion tensor imaging study of fasciculi in schizophrenia. Am J Psychiatry. 2007;164(3):467–73.

Sibbitt WL, Brandt JR, Johnson CR, Maldonado ME, Patel SR, Ford CC, et al. The incidence and prevalence of neuropsychiatric syndromes in pediatric onset systemic lupus erythematosus. J Rheumatol. 2002;29(7):1536–42.

Singh S, Singh K, Trivedi R, Goyal S, Kaur P, Singh N, et al. Microstructural abnormalities of uncinate fasciculus as a function of impaired cognition in schizophrenia: a DTI study. J Biosci. 2016;41(3):419–26.

Smith SM, Jenkinson M, Johansen-Berg H, Rueckert D, Nichols TE, Mackay CE, et al. Tract-based spatial statistics: voxelwise analysis of multi-subject diffusion data. Neuroimage. 2006;31(4):1487–505.

Snook L, Plewes C, Beaulieu C. Voxel based versus region of interest analysis in diffusion tensor imaging of neurodevelopment. Neuroimage. 2007;34(1):243–52.

Song SK, Sun SW, Ju WK, Lin SJ, Cross AH, Neufeld AH. Diffusion tensor imaging detects and differentiates axon and myelin degeneration in mouse optic nerve after retinal ischemia. Neuroimage. 2003;20(3):1714–22.

Sporns O, Tononi G, Kötter R. The human connectome: a structural description of the human brain. PLoS Comput Biol. 2005;1(4):e42.

Steel RM, Bastin ME, McConnell S, Marshall I, Cunningham-Owens DG, Lawrie SM, et al. Diffusion tensor imaging (DTI) and proton magnetic resonance spectroscopy (1H MRS) in schizophrenic subjects and normal controls. Psychiatry Res Neuroimaging. 2001;106(3):161–70.

Sun H, Lui S, Yao L, Deng W, Xiao Y, Zhang W, et al. Two patterns of white matter abnormalities in medication-naive patients with first-episode schizophrenia revealed by diffusion tensor imaging and cluster analysis. JAMA Psychiatry. 2015;72(7):678–86.

Szeszko PR, Robinson DG, Ikuta T, Peters BD, Gallego JA, Kane J, et al. White matter changes associated with antipsychotic treatment in first-episode psychosis. Neuropsychopharmacology. 2014;39(6):1324–31.

Takahashi N, Sakurai T, Davis KL, Buxbaum JD. Linking oligodendrocyte and myelin dysfunction to neurocircuitry abnormalities in schizophrenia. Prog Neurobiol. 2011;93(1):13–24.

Turkel SB, Tishler D, Tavaré CJ. Late onset psychosis in survivors of pediatric central nervous system malignancies. J Neuropsychiatry Clin Neurosci. 2007;19(3):293–7.

Uranova NA, Vikhreva OV, Rachmanova VI, Orlovskaya DD. Ultrastructural alterations of myelinated fibers and oligodendrocytes in the prefrontal cortex in schizophrenia: a postmortem morphometric study. Schizophr Res Treat. 2011;2011:1–13.

Uranova NA, Vikhreva OV, Rachmanova VI, Orlovskaya DD. Microglial activation in white matter in schizophrenia: findings from a postmortem electron microscopic morphometric study. Neurol Psychiatry Brain Res. 2014;20(1):25.

Voineskos AN, Lobaugh NJ, Bouix S, Rajji TK, Miranda D, Kennedy JL, et al. Diffusion tensor tractography findings in schizophrenia across the adult lifespan. Brain. 2010;133(Pt 5):1494–504.

Walterfang M, Wood SJ, Velakoulis D, Copolov D, Pantelis C. Diseases of white matter and schizophrenia-like psychosis. Aust N Z J Psychiatry. 2005;39(9):746–56.

Walterfang M, Wood SJ, Velakoulis D, Pantelis C. Neuropathological, neurogenetic and neuroimaging evidence for white matter pathology in schizophrenia. Neurosci Biobehav Rev. 2006;30(7):918–48.

Walterfang M, Yung A, Wood AG, Reutens DC, Phillips L, Wood SJ, et al. Corpus callosum shape alterations in individuals prior to the onset of psychosis. Schizophr Res. 2008a;103(1):1–10.

Walterfang M, Wood AG, Reutens DC, Wood SJ, Chen J, Velakoulis D, et al. Morphology of the corpus callosum at different stages of schizophrenia: cross-sectional study in first-episode and chronic illness. Br J Psychiatry. 2008b;192(6):429–34.

Walterfang M, Velakoulis D, Whitford TJ, Pantelis C. Understanding aberrant white matter development in schizophrenia: an avenue for therapy? Expert Rev Neurother. 2011;11(7):971–87.

Weinberger DR. Implications of normal brain development for the pathogenesis of schizophrenia. Arch Gen Psychiatry. 1987;44(7):660–9.

Wheeler AL, Voineskos AN. A review of structural neuroimaging in schizophrenia: from connectivity to connectomics. Front Hum Neurosci. 2014;8:653.

White T, Magnotta VA, Bockholt HJ, Williams S, Wallace S, Ehrlich S, et al. Global white matter abnormalities in schizophrenia: a multisite diffusion tensor imaging study. Schizophr Bull. 2011;37(1):222–32.

Whitford TJ, Kubicki M, Schneiderman JS, O'Donnell LJ, King R, Alvarado JL, et al. Corpus callosum abnormalities and their association with psychotic symptoms in patients with schizophrenia. Biol Psychiatry. 2010;68(1):70–7.

Whitford TJ, Kubicki M, Ghorashi S, Schneiderman JS, Hawley KJ, McCarley RW, et al. Predicting interhemispheric transfer time from the diffusion properties of the corpus callosum in healthy individuals and schizophrenia patients: a combined ERP and DTI study. Neuroimage. 2011;54(3):2318–29.

Whitford TJ, Kubicki M, Pelavin PE, Lucia D, Schneiderman JS, Pantelis C, et al. Cingulum bundle integrity associated with delusions of control in schizophrenia: preliminary evidence from diffusion-tensor tractography. Schizophr Res. 2015;161(1):36–41.

Wu C-H, Hwang T-J, Chen Y-J, Hsu Y-C, Lo Y-C, Liu C-M, et al. Primary and secondary alterations of white matter connectivity in schizophrenia: a study on first-episode and chronic patients using whole-brain tractography-based analysis. Schizophr Res. 2015;169(1):54–61.

Yeatman JD, Dougherty RF, Myall NJ, Wandell BA, Feldman HM. Tract profiles of white matter properties: automating fiber-tract quantification. PLoS One. 2012;7(11):e49790.

Zalesky A, Fornito A, Seal ML, Cocchi L, Westin CF, Bullmore ET, et al. Disrupted axonal fiber connectivity in schizophrenia. Biol Psychiatry. 2011;69(1):80–9.

Zhu J, Zhuo C, Qin W, Wang D, Ma X, Zhou Y, et al. Performances of diffusion kurtosis imaging and diffusion tensor imaging in detecting white matter abnormality in schizophrenia. Neuroimage Clin. 2015;7:170–6.

Zou LQ, Xie JX, Yuan HS, Pei XL, Dong WT, Liu PC. Diffusion tensor imaging study of the anterior limb of internal capsules in neuroleptic-naive schizophrenia. Acad Radiol. 2008;15(3):285–9.

Functional MRI Methods

5

Sheeba Arnold Anteraper, Alfonso Nieto-Castanon, and Susan Whitfield-Gabrieli

Contents

5.1 Introduction

The number of neuroimaging research studies has grown tremendously over the past 20 years, producing over 30,000 papers. In terms of number of publications per year, functional Magnetic Resonance Imaging (fMRI) modality currently dominates the landscape of neuroimaging. Attempts to integrate the results of individual fMRI studies for larger-scale interpretation as well as more recent efforts to aggregate neuroimaging data through public sharing, however, have faced many challenges, due to heterogeneity of this data resulting from the variability in experimental design, data acquisition parameters and data processing. Recognizing the need for the generation of interpretable results and to facili-

S. A. Anteraper · A. Nieto-Castanon
S. Whitfield-Gabrieli (✉)
Department of Psychology, Northeastern University, Boston, MA, USA
e-mail: s.whitfield-gabrieli@northeastern.edu

M. Kubicki, M. E. Shenton (eds.), *Neuroimaging in Schizophrenia*,
https://doi.org/10.1007/978-3-030-35206-6_5

tate the transition of neuroimaging research from individual to large-scale multi-site projects, the Organization for Human Brain Mapping Council has created the Committee on Best Practices in Data Analysis and Sharing (COBIDAS; Nichols et al. 2017) providing guidelines on best practices of data analysis and data sharing in the brain mapping community. Responding to the current need of the neuroimaging community to ensure (1) data quality, (2) the possibility to pool data across several imaging sites (Hibar et al. 2015; Thompson et al. 2014), and (3) the capability to derive neural signatures from fMRI data to aid clinical translation (early detection and prediction), the goal of this chapter is threefold. First, to acquaint the neuroimaging community with the fMRI signal, experimental design and data acquisition methods; then to introduce various data processing strategies with an emphasis on data quality assurance (QA), demonstrating examples of its utility in increasing data validity and sensitivity; and finally, a discussion on advanced topics such as realtime-fMRI neurofeedback, complex networks, early detection and prediction using machine learning approaches to aid clinical translation.

5.1.1 fMRI Contrast

fMRI relies on the intrinsic contrast mechanism called the blood oxygenation level dependent (BOLD) changes elicited during task performance or spontaneously at the resting-state. Whenever there is a local increase in neural activity, there is a local increase in Cerebral Blood Flow (CBF) and Cerebral Blood Volume (CBV) and magnetic properties of hemoglobin (Hb) change when bound with oxygen molecule. In a milestone publication in 1990, Ogawa and colleagues were the first to demonstrate that the BOLD contrast can be maneuvered in rodent brains by changing the oxygen proportion in the air breathed by the animals (Ogawa et al. 1990). Since oxygenated Hb (HbO_2) is diamagnetic and deoxygenated Hb is paramagnetic, T2∗ relaxation time for deoxygenated Hb is shorter (less BOLD signal) than that of HbO_2. Hence increase in neural activity induces reductions in local magnetic field susceptibility changes leading to increases in MR signal. T2∗ weighted MR pulse sequences, gradient-echo echo planar imaging (EPI), has therefore become the workhorse for fMRI. Currently, majority of fMRI research is carried out at 3-T. The field is in a constant chase for improvements in spatiotemporal resolution. Spatial resolution refers to the ability to distinguish elementary units of neuronal activity and temporal resolution refers to the ability to discern time course of various neural events. The former is limited by voxel volume and the latter is limited by repetition time (TR; the time interval between successive acquisition of brain volumes).

5.1.2 Experimental Design

Study design is of utmost importance in fMRI. This is because fMRI BOLD data is only a representation of local changes in neuronal activity and is not absolute neural activity. Neither does fMRI data capture fine-grained temporal information. All study designs must therefore provide the opportunity to statistically contrast the neuronal activity of interest with a suitable rest or baseline condition. Typical types of task-designs are “block design”, “event-related design” and “mixed design”. In all these design scenarios, the percent change in BOLD signal (effect size) is calculated from the differences in BOLD contrast between the two states (“activation” and “baseline”). The BOLD signal changes obtained from local T2∗ changes following a single brief activation event—the Hemodynamic Response Function (HRF)—has to be convolved with the task design vector (a vector containing the onset times of the blocks or events) to derive the regressor of interest that can be modeled and used to test for significant activation in any voxel’s time series. While block designs are optimal for activation detection, event related designs are favored for fMRI time course characterization. Since the resting-state design is task free, it is suited for a wide range of pediatric and clinical population who might not be able to perform the task demands (e.g. low functioning patients with Autism Spectrum Disorder (ASD) or

infants). Furthermore, if clinical populations were able to perform the task there could still be task performance confounds.

Some of the experimental considerations also include what part of the brain to look at (e.g., partial brain coverage vs. whole brain coverage), what head coil to use, and how many times to toggle between conditions within a scan. How to optimize data acquisition protocols that yield a combination of high spatial and temporal resolution is another question of paramount importance. This is because, typically as image resolution increase (smaller voxels), the signal-to-noise ratio (SNR) and functional contrast to noise ratio (CNR) decrease. Using thicker voxels is not an ideal solution to improve SNR because of signal drop out (through-plane dephasing) increase with slice thickness. Furthermore, time-series SNR (tSNR) reach an asymptote at bigger voxel volumes indicating the dominance of physiological noise (cardiac, respiratory, CBF and CBV changes) at big voxel volumes (Kruger and Glover 2001). tSNR increase can be brought about by using multi-channel array coils thereby providing improved sensitivity to BOLD signal and enhanced BOLD CNR (Triantafyllou et al. 2011). It is important to note however that decreasing slice thickness to minimize drop out will require increasing the number of slices to maintain same brain-coverage, again increasing TR and acquisition time (decreasing temporal resolution). There are strategies to address this by adding in-plane parallel imaging schemes, but they come with SNR penalty. A game changer to this has been the implementation of simultaneous multi-slice (SMS) imaging strategies (Setsompop et al. 2012). SMS can improve temporal resolution ($\leq$1 s) in fMRI, is compatible with in-plane acceleration techniques, can provide whole brain coverage at high spatial resolution ($\leq$2.5 mm) and in general there is no SNR penalty for multi-band acceleration (Glasser et al. 2013).

5.1.3 Noise Considerations in fMRI

Noise in fMRI signal arises from multiple sources, including those due to subject motion, such as spin-history effects (Friston et al. 1996) or motion-by-susceptibility interactions (Wu et al. 1997), sources due to physiological variation (Birn et al. 2006; Frank et al. 2001; Kruger and Glover 2001), as well as scanner hardware-related sources. Subject motion, however, is the most prominent source of artifact and the one that has the greatest deleterious impact on fMRI signal. Even small head movements have been shown to cause artifacts in activation maps, particularly when the motion is correlated with the experimental paradigm (Field et al. 2000; Hajnal et al. 1994). Moreover, group differences in the propensity to move (e.g. in young versus older cohorts or psychiatrically disordered versus healthy controls) are well documented (Satterthwaite et al. 2012; Van Dijk et al. 2012). These group differences in motion can and do contribute to erroneously drawn conclusions if not properly controlled (Bullmore et al. 1999).

5.2 Data Processing Strategies

5.2.1 Data Pre-processing

Data Realignment: During motion correction or realignment, a six degrees-of-freedom (three rotation, three translation) rigid body transformation is typically used to align or register volumes from a time series. In performing realignment, one typically assumes that EPI distortion or warping is fixed relative to the head and that the influence of slice-specific de-phasing in proximal slices is not a concern with typical times of repetitions (TR) used to acquire fMRI data. Most realignment algorithms register each scan volume (also referred to as 'time point') independently to a reference volume (typically the first or middle volume of a run) or perform a two-pass operation where they calculate a mean motion-corrected volume and register all time points independently to that volume. Many MRI data acquisition software tools now implement ***prospective*** on-line motion correction (e.g. PACE on Siemens scanners) by estimating the change in position of a participant's head and realign-

ing gradients from time point to time point such that the slice prescription is close to the original (Thesen et al. 2000).

Unwarping/Field-map Correction: Distortion related to susceptibility difference between air and tissue boundaries (medial temporal and orbito-fronal cortices for example) is inevitable in T2∗ weighted funcational images. Unwarping step corrects susceptibility by motion artifacts (plus baseline susceptibility artifacts). Warping in phase-encoding direction caused by scanner inhomogeneity can also be corrected if fieldmaps have been acquired and voxel displacement maps (VDM) computed (Jezzard and Balaban 1995).

Slice-time Correction (STC): Each slice (along slice-select direction; e.g. axial slices) is acquired at a slightly different time, depending on slice-acquisition order (e.g. ascending/descending/interleaved/etc.) within the TR. Temporal changes in BOLD signal can get projected into spatial changes in BOLD signal. The goal of STC is to resample each voxel time-series to compensate for the slice-dependent relative delay of the BOLD signal. STC is recommended especially when the TR is greater than or equal to 2 s.

Coregistration: Structural and functional images do not match in terms of MR contrast, spatial resolution and image distortion. By aligning these between modality volumes from the same individual (within subjects), coregistration allows anatomical localization of single subject activations. The steps involved are:

(1) registration to determine the six parameters of the rigid body transformation between each source image (e.g. structural) and a reference image (e.g. functional), (2) transformation—the actual movement as determined by registration (i.e. rigid body transformation), (3) reslicing—the process of writing the "altered image" according to the transformation ("re-sampling"), (4) interpolation—way of constructing new data points from a set of known data points (i.e. voxels). Reslicing uses interpolation to find the intensity of the equivalent voxels in the current "transformed" data, and changes the position without changing the value of the voxels and give correspondence between voxels. Different methods of interpolation that are typically used include nearest neighbour, linear, and B-spline interpolation.

Spatial Normalization: This step normalizes anatomical differences between subjects with the goal of increasing inter-subject reliability by reducing the influence of anatomical differences between subjects. The goal is to bring individual brains to standard template coordinates so that functional correspondence is established at a voxel-to-voxel level thereby enabling data pooling across subjects to maximize sensitivity. Template fitting is a kind of coregistration during which images are stretched/squeezed/warped to match a standardized template.

Smoothing: This step involves the spatial blurring of functional data by convolution with Gaussian smoothing kernel. The goal is to increase inter-subject reliability by increasing SNR and reducing influence of residual anatomical/functional localization differences between subjects.

There are two important pre-processing steps to be included in addition to the above while processing task-free data: (1) temporal-filtering and (2) de-noising of physiological signal. The former is accomplished by band-pass filtering to remain confined to the frequencies of interest (0.01–0.1 Hz). Successful approaches to denoising appear to be ANATICOR (Jo et al. 2010) and aCompCor (Behzadi et al. 2007), both of which remove non-gray-matter nuisance signals (white matter, CSF and other locations). Also useful are median angle shift, based on the geometric view of the additive global signal (He and Liu 2012), a biophysically-based model called Functional Image Artifact Correction Heuristic (FIACH) (Tierney et al. 2016), and removal of the gray matter global signal (Power et al. 2015; Satterthwaite et al. 2012; Yan et al. 2013).

5.2.2 Data Analysis: fMRI Task

After data pre-processing, the next step is to test the research hypothesis H_1: experimental condition ≠ control condition, against its null

hypothesis H_0: experimental condition = control condition. The General Linear Model (GLM) analysis is commonly used to test how well the experimentally collected data lines up with predicted responses (Friston et al. 1995). Statistical testing that follows estimate how well each voxel's time series is fit by the linear combination of predicted responses. The model definition can be mathematically represented as:

$$Y_{nm} = \sum_k X_{nk} \cdot B_{km} + N_{nm}$$

Y can be considered as a collection of dependent variables, in this case the different timepoints across a scan in the fMRI experiment (observed data). X, the collection of predicted task responses (modeled effects) is scaled by parameter weights B, which are estimated by the linear model to best fit the observed data Y. N represents the *residual values*—difference between observed values (Y) and fitted values (X∗B), and is ideally as small as possible. For hypothesis testing, *t*-, or *F-statistics* is employed to assess the significance of each model factor's contribution to Y (Friston et al. 1995; Worsley and Friston 1995). A likelihood ratio (ratio between likelihood of Y given a reduced "null-hypothesis" model compared to the likelihood of Y given the full model X) test is carried out to derive associated *p*-values. A schematic is presented in Fig. 5.1.

If *p*-value is smaller than a user defined significance level α, the null hypothesis is rejected and the voxel is labeled as 'active'. It is of utmost importance to account for multiple-comparisons in fMRI because a standard analysis involving

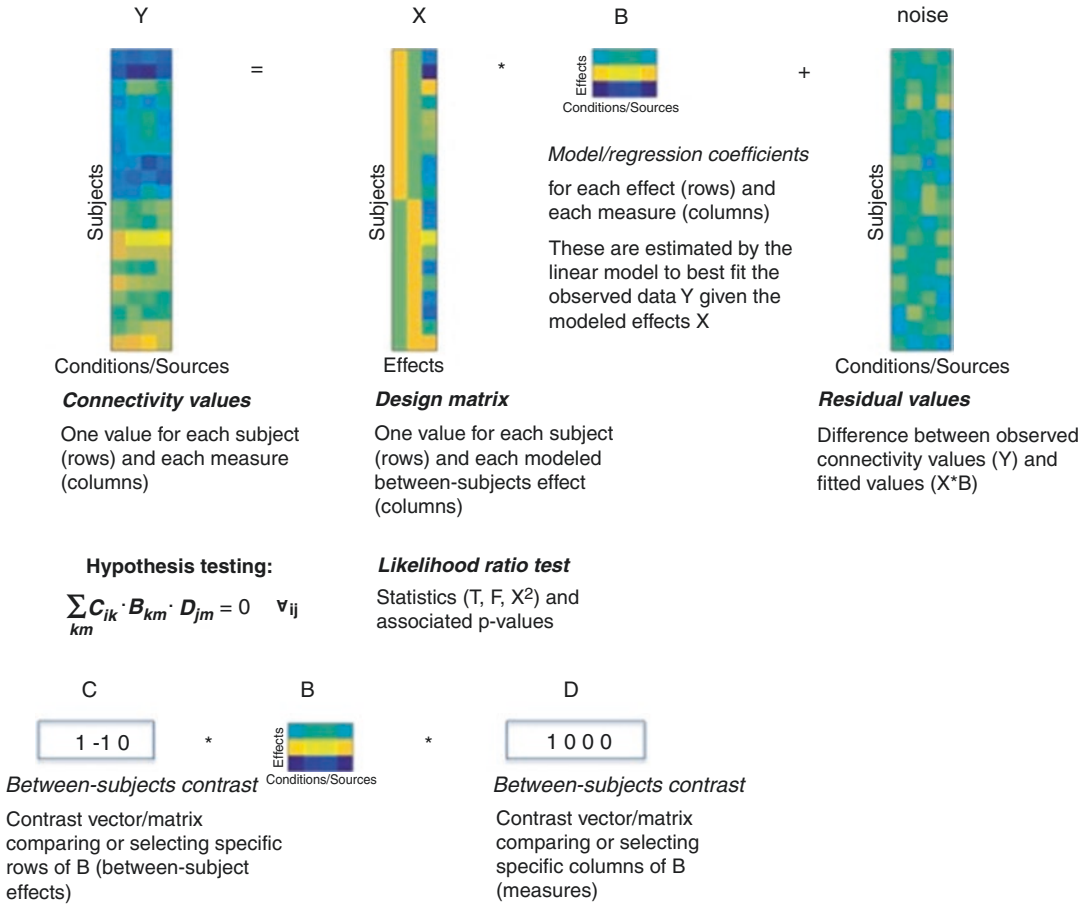

Fig. 5.1 The general linear model: definition, estimation and hypothesis testing

whole-brain 2 mm voxels have about 250,000 voxels. Under the null hypothesis, with $\alpha = 0.05$, ~12,500 voxels may be falsely considered as 'active' by random chance. This reduces to 250 voxels, when $\alpha = 0.001$ (for recommendations on acceptable statistical thresholds see (Eklund et al. 2016)). There are two widely used practices to address such false-positives errors multiple-comparisons (1) Family-wise Error (FWE) correction, (Nichols and Hayasaka 2003) and (2) False Discovery Rate (FDR) correction, (Genovese et al. 2002).

5.2.3 Task-Based Connectivity/ Effective Connectivity

While functional connectivity analysis captures whether signals from ROIs are correlated over time, it provides no information on the causality. To capture notions of causality among time series, effective connectivity analysis can be carried out. Two time signals are causally related if a change in one signal causes a change in the other. Causality can be captured purely in a statistical context, commonly studied based on Granger Causality, or based on assumptions of an underlying model, most commonly studied through Dynamic Causal Modeling (DCM, Friston et al. 2003; Friston et al. 2013). Dynamic Causal Modeling in its most basic form assumes that hidden neuronal states influence each other in a linear fashion, which is dependent on the task being performed by the patient as well as external inputs (Friston et al. 2003). While the original formulation is task dependent, DCM can also be used for resting state data by treating the underlying neuronal system as driven by noise (Razi et al. 2017). The primary limitation of DCM is the relatively small number of ROI's that it can capture for a given model (Stephan et al. 2010), though new techniques have extended the size of DCMs to dozens of ROIs (Razi et al. 2017).

Generalized Psycho-Physiological Interaction (gPPI): gPPI measures represent the level of task-modulated effective connectivity between two ROIs (i.e. changes in functional association strength covarying with the external or experimental factor). gPPI is computed using a separate multiple regression model for each target ROI timeseries (outcome). Each model includes as predictors: (a) all of the selected task effects convolved with a canonical hemodynamic response function (main psychological factor in PPI nomenclature); (b) each seed ROI BOLD timeseries (main physiological factor in PPI nomenclature); and (c) the interaction term specified as the product of (a) and (b) (PPI term). gPPI output is defined as the regression coefficients associated with the interaction term in these model.

5.2.4 Resting State Functional Connectivity Analyses

5.2.4.1 Seed-to-Voxel Analyses

Seed-based correlation (SBC) maps represent the level of functional connectivity between the seed/ROI and every location in the brain. SBC is defined as the Fisher-transformed bivariate correlation coefficients between an ROI BOLD timeseries (averaged across all voxels within an ROI) and an individual voxel BOLD timeseries. The default behavior for functional connectivity analyses is to use a weighted GLM for weighted regression/correlation measures of the condition-specific association between the seed/source BOLD timeseries and each voxel or target ROI BOLD timeseries. In addition to the standard bivariate correlation measure for functional connectivity analyses, one may also select regression measures, as well as define whether one wants to compute bivariate measures—analyzing individual seed/sources separately-, or semipartial/multivariate—where all of the sources/ROIs are entered jointly into the GLM to estimate their unique contributions.

5.2.4.2 ROI-to-ROI Analyses

While whole-brain connectome analysis allow looking at the entire network of functional connectivity, and for effects beyond specific subset of a priori seeds/ROIs, controlling family-wise false positive level on this many connections (connections on the order of 30 billion at 2 mm isotropic) leads to extremely poor sensitivity. One solution is to perform ROI-to-ROI analysis by looking at

larger parcellations of the brain volume such as Brodmann areas (86 ROIs; 3655 connections), AAL atlas (116 ROIs; 6670 connections) Large-voxel parcellations (20–10 mm voxels; 304–2186 ROIs; 46,056–2,388,205 connections).

ROI-to-ROI Correlation (RRC) matrices represent the level of functional connectivity between each pair of ROIs. RRC is defined as the Fisher-transformed bivariate correlation coefficients between two ROIs (Regions Of Interest) BOLD timeseries (ROI BOLD timeseries are computed by averaging voxel timeseries across all voxels within each ROI). Results emerging from such analyses can be reported using clustering algorithm that sorts ROIs so that two ROIs are placed nearby if they show similar effects. For example, hierarchical clustering (ROIs that show similar connectivity effects are contiguous/near), minimum degree algorithm (ROIs that are in same sub network are contiguous), or reverse Cuthill-McKee algorithm (minimize connection lengths) could be employed to group ROIs resulting in meaningful clusters. Inferences could then be made at the connection-level (specific connections between two ROIs e.g. Connectivity between MPFC and PCC is stronger in X compared to controls), seed-level (pattern of connectivity of specific ROIs (not individual connections) e.g. altered MPFC functional connectivity in X compared to controls), or network-level (networks of connected ROIs (not individual ROIs, or individual connections) e.g. Altered functional connectivity network in X compared to controls).

5.2.4.3 Graph Analyses

Functional correlations between all ROIs in the brain can be treated as a network, or functional connectome (Sporns 2010). The study of how network structure affects behavior over that network is commonly referred to as the study of complex networks or network science, (Barabási 2016; Newman 2018), which is based on graph theoretic analysis (Diestel 2018). As it is possible to find a correlation coefficient between the time signals of all ROIs, the analysis of a functional connectome begins with thresholding, which removes edges (which here represent correlations between ROIs) that have a value less than the given threshold. Once the network is thresholded, then it can be analyzed based on a number of measures. These include **degree and cost** (the number (degree) or proportion (cost) of other ROIs that a given ROI has a strong correlation with), **clustering coefficient** (whether ROIs share neighbors), **efficiency** (whether information can move efficiently through the network) and **average path distance** (how many steps it takes between ROIs on average) (Sporns 2010). Definitions of each of these are given below:

Degree and Cost: Number (degree) or proportion (cost) of edges for each node. Degree and Cost represent both measures of network centrality at each node/ROI, characterizing the degree of local connectedness of each ROI within the graph. Network cost represents the proportion of edges among all possible node pairs, and this is typically fixed to allow meaningful between-network comparisons.

Clustering Coefficient: Fraction of edges among all possible edges in the local neighboring sub-graph for each node/ROI. Clustering coefficient represents a measure of local integration, characterizing the degree of inter-connectedness among all nodes within a node neighboring sub-graph. Network clustering coefficient represents a measure of network locality (e.g. grid topologies have comparatively high clustering coefficients).

Global Efficiency: average of inverse-distances between each node and all other nodes in the graph. Global efficiency represents a measure of node centrality within a network, characterizing the degree of global connectedness of each ROI within the graph. Network global efficiency represents a measure of graph inter-connectedness/radius (e.g. random graphs have comparatively high/compact global efficiency).

Local Efficiency: Global efficiency of neighboring sub-graph. Local efficiency represents a measure of local integration, characterizing the degree of inter-connectedness among all nodes within a node neighboring sub-graph. Network local efficiency represents a measure of network locality (e.g. grid topologies have comparatively high local efficiency).

Average path distance: Average minimum path distance between each node and all other nodes in the graph. Average path distance represents a measure of node centrality within a network, characterizing the degree of global connectedness of each ROI within the graph. Network average path distance represents a measure of graph inter-connectedness/radius (e.g. random graphs have comparatively low/compact average path distances).

It is also common to compare brain graphs to canonical random graph models, such as Erdos-Renyi graphs (Erdos and Rényi 1960), scale free networks (Barabasi and Albert 1999), and small world networks (Watts and Strogatz 1998). Past results have found that functional connectomes tend to have short average path length and high clustering, a characteristic of small world networks, as well as having hubs with large degree (Bullmore and Sporns 2012).

5.2.4.4 Multi-voxel Pattern Analysis (MVPA)

These analyses are a type of voxel-to-voxel analyses that create, separately for each voxel, a low-dimensional multivariate representation characterizing the connectivity pattern between this voxel and the rest of the brain (this representation is defined by performing separately for each voxel a Principal Component Analysis (PCA) of the variability in connectivity patterns between this voxel and the rest of the brain across all subjects and conditions). The resulting representation optimally characterizes the observed connectivity patterns across subjects/conditions, and it allows for the investigation of connectivity differences across subjects directly using second-level multivariate analyses. MVPA maps are defined using Singular Value Decomposition, separately for each seed-voxel, of the patterns of seed-based correlations across all subjects (see equations below).

$$r_n(x,y) = \sum_i \rho_{n,i}(x) Q_i(x,y) + \theta_n(x,y)$$

$$\rho_{n,i}(x), Q_i(x,y) \,|\, \min \sum_n \theta_n(x,y)^2$$

$r_n(x,y)$: correlation coefficients between voxels x and y for the n-th subject

$Q_i(x,y)$: group-level i-th orthogonal Principal Component spatial map for seed-voxel x, normalized to unit *norm*

$\rho_{n,i}(x)$: ith Multivariate Connectivity spatial map for seed-voxel x and nth subject

For dimensionality reduction, group-MVPA estimates a multivariate representation of the connectivity pattern by computing the pairwise connectivity pattern between each voxel and the rest of the brain, and using PCA to characterize those patterns using a small number of components in a two-step process. In the first PCA step, separately for each subject, 64 PCA components are retained while characterizing each subject voxel-to-voxel correlation structure. This is a form of subject-level dimensionality reduction typically used in independent component analysis (ICA) applications. In the second PCA step, jointly across all subjects but separately for each voxel, the three strongest components were retained from a principal component decomposition of the between-subjects variability in seed-to-voxel connectivity maps between this voxel and the rest of the brain. An F-test was performed on all three MVPA components (that explain the maximum inter-subject variability) simultaneously in a single second-level analysis to identify the voxels that show significant differences in connectivity patterns between the two groups. This is an omnibus test (equivalent to seed-level F-test in ROI-to-ROI analyses) to identify the abstract multivariate representation.

group-ICA: ICA maps represent a measure of different networks expression and connectivity at each voxel, characterized by the strength and sign

of connectivity between a given network timeseries and the rest of the brain. It is defined as the multivariate regression coefficients between each component/network timeseries and an individual voxel BOLD timeseries. These analyses identify a number of networks of highly functionally-connected areas (Calhoun et al. 2001), with variance normalization pre-conditioning, optional subject-level dimensionality reduction, subject/condition concatenation of BOLD signal data along temporal dimension, group-level dimensionality reduction (to the target number of dimensions/components), fastICA for estimation of independent spatial components, and GICA1 backprojection for individual subject-level spatial map estimation.

group-PCA: These analyses are identical to group-ICA above, but skipping the fastICA reorientation of group-level components and using instead the maximal-variance spatial components determined by the group-level dimensionality reduction step. All other steps, including backprojection, are performed identically to group-ICA.

Intrinsic Connectivity (Intrinsic Connectivity Contrast, ICC, Martuzzi et al. 2011) is a measure of network centrality at each voxel. It characterizes the strength of the connectivity pattern between each voxel and the rest of the brain (root mean square of the correlation coefficient values).

Global Correlation is another measure of network centrality at each voxel. It characterizes the strength and sign of the connectivity pattern between each voxel and the rest of the brain (average of the correlation coefficient values).

Local Correlation (Integrated Local Correlation, ILC, Deshpande et al. 2009) is a measure of local coherence at each voxel. It characterizes the average correlation between each voxel and its neighbors. Neighbourhood is defined as a probabilistic region (isotropic Gaussian with user-defined width).

Radial Correlation Contrast (RCC, Goelman 2004) characterizes the spatial asymmetry of the local connectivity pattern between each voxel and its neighbors (a 3d vector for each voxel).

Radial Similarity characterizes the global similarity (Kim et al. 2010) between the connectivity patterns of neighboring voxels (a 3d vector for each voxel).

5.2.4.5 Dynamic Connectivity Measures

Dynamic connectivity analyses explore dynamic properties (temporal modulation) of the ROI-to-ROI connectivity matrix identifying a number of circuits of similarly-modulated connections.

Sliding window: Every connectivity measure in CONN, including seed-based, ROI-to-ROI, network and graph measures, can also be estimated from windowed BOLD timeseries using a series of sequential sliding windows. Each individual window is treated as a separate condition, and weighted GLM is used to compute the corresponding condition-/time-specific measures. Variability of these measures across time is then computed as the main measure of interest characterizing dynamic connectivity properties. One example of such sliding-window measures of connectivity is dynamic variability in seed-based or ROI-to-ROI connectivity measures:

Dynamic variability in seed-based connectivity (dvSBC): dvSBC maps represent the degree of temporal variability in functional connectivity between a seed/ROI and every location in the brain. They are defined as the standard deviation in bivariate, multivariate, or semipartial correlation or regression measures between seed ROI and each target voxel, computed using weighted Least Squares (WLS) within a discrete set of temporal sliding windows.

Dynamic variability in ROI-to-ROI connectivity (dvRRC): dvRRC matrices represent the degree of temporal variability in functional connectivity between pairs of ROIs. They are defined as the standard deviation in bivariate, multivariate, or semipartial correlation or regression measures between two ROIs, computed using weighted Least Squares (WLS) within a discrete set of temporal sliding windows.

Dynamic Independent Component Analyses (dyn-ICA): ROI-to-ROI connectivity matrix identifying a number of circuits of similarly-modulated connections. Dynamic ICA per-

forms an Independent Component Analysis of the connectivity timeseries (strength of connectivity between each pair of ROIs at any given timepoint), returning a number of independent components/circuits best characterizing the observed functional connectivity modulation across time. Dyn-ICA matrices represent a measure of different modulatory circuits expression and rate of connectivity change between each pair of ROIs, characterized by the strength and sign of connectivity changes covarying with a given component/circuit timeseries. Dyn-ICA matrices are defined as the gPPI interaction terms between each component/circuit timeseries (data-driven gPPI psychologial factors) and a series of ROI BOLD timeseries (user-defined gPPI physiological factors).

An overview of the resting state functional connectivity analysis is summarized in Fig. 5.2.

5.2.5 Quality Assurance, Artifact Detection and Rejection

Although motion correction is a routine step in fMRI preprocessing, there still exists considerable residual motion-related variance in the time series (Friston et al. 1996). The sources of this variance may arise from: (1) interactions between movement, susceptibility and distortion; (2) interactions between movement, susceptibility and signal dropout; (3) spin history effects (residual magnetization effects of previous scans); and (4) intra-volume movement. One accepted approach to mitigating the effect of this residual motion-related variance is to include motion parameter estimates as nuisance regressors in the single-subject GLM analyses (Friston et al. 1996). This approach assumes a linear effect between the amount of subject motion and the fMRI signal,

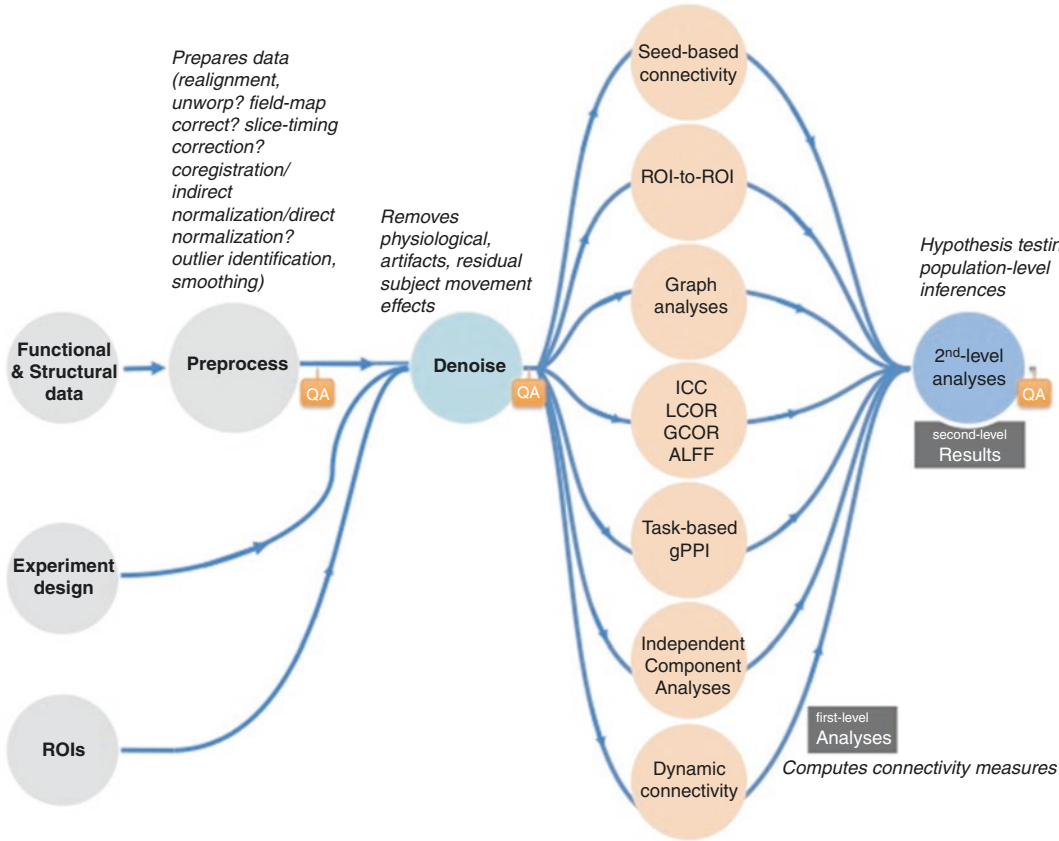

Fig. 5.2 Overview of resting state functional connectivity analysis. *QA* Quality Assurance

which can be expected to offer an acceptable approximation for small levels of motion. Many fMRI studies drop subjects or sessions where the estimated subject motion exceeds a given threshold, under the implicit understanding that this approximation fails in the presence of excessive subject motion. While the approach of dropping sessions and/or subjects due to excessive motion is perfectly valid, an alternative method of omitting, de-weighting or interpolating the time points with excessive motion may be a more appropriate, timely and cost-effective approach towards quality assurance in fMRI. We recommend omitting session specific outliers in the global mean intensity signal and motion, for the reasons outlined below.

While noise is inherent to any measurement process and it is often either explicitly (e.g. motion regression, temporal autocorrelation) or implicitly (e.g. restricted maximum likelihood (ReML) estimation) addressed in standard fMRI analyses, artifactual sources of variability can often also result in isolated outliers in the measured fMRI time series. Individual outliers, or observations that lie outside the overall pattern of a distribution (Moore and McCabe 1999), can have, by their nature, considerable influence in both parameter estimation and statistical inference. The presence of outliers can increase the likelihood of Type II errors (decreasing sensitivity) as well as Type I errors (affecting the validity of the analyses). Some analysis techniques (e.g. functional connectivity analyses) are particularly sensitive to some of the most deleterious effects of outliers, where they can act as confounds affecting both the validity and the interpretability of the fMRI analysis results.

The importance of rigorous artifact detection/rejection and quality assurance has long been noted in the field of Electroencephalography (EEG), in which artifacts are often orders of magnitude larger than the Event-Related Potential (Thompson et al. 2014) signal researchers are attempting to measure. A number of leading ERP experts emphasized the critical role of quality assurance in a paper entitled "Guidelines for using human event-related potentials to study cognition: Recording standards and publication criteria" (Picton et al. 2000). We, and others (Ashby 2011; Luo and Nichols 2003), propose that a similar level of quality assurance (QA) scrutiny is beneficial in fMRI data and analyses. Similar to EEG, fMRI suffers from low SNR. Despite prior work that highlights the importance of QA in fMRI tasks and the availability of tools (e.g., statistical parametric mapping diagnosis (SPMd); (Luo and Nichols 2003)), such methods are not routinely implemented by the imaging community.

It has been demonstrated that motion (Satterthwaite et al. 2012; Van Dijk et al. 2012) and artifacts (Yan et al. 2013) in resting state functional time series may result in substantial and structured changes in functional connectivity data despite standard compensatory spatial registration and regression of motion estimates from the data (Power et al. 2012). In addition to motion related artifact in the global intensity time series, there may be artifacts due to other sources related to the scanner. These findings suggest that rigorous artifact rejection in addition to motion regression is especially prudent for valid interpretation of resting state fMRI (rs-fMRI).

Artifacts in imaging data due to subject motion or scanner problems present a great concern for statistical analysis. Data quality assurance is of paramount importance to the validity of results (Ardekani et al. 2001; Grootoonk et al. 2000; Morgan et al. 2001; Stocker et al. 2005; Ward et al. 2000). Several studies that have been published appeared before attributing head movement for the introduction of spurious correlations, especially in older adults compared to younger adults (Power et al. 2012; Van Dijk et al. 2012). In addition, global signal regression was found to artificially introduce anti-correlations (Murphy et al. 2009) and to alter inter-regional correlations (Saad et al. 2012), leaving open the question of the direction (positive, negative or both) of the correlations. The use of Artifact Detection Tools; ***ART*** [http://www.nitrc.org/projects/artifact_detect] (that is not based on global signal regression) increases the validity of the analysis, preventing false results without obscuring meaningful anti-correlations (Keller et al. 2015). Importantly, using ***ART*** allows one

to investigate anti-correlations (Fox et al. 2009; Weissenbacher et al. 2009), as no global signal regression is performed (Chai et al. 2012).

5.2.6 Quality Assurance for fMRI Task

Quantifying *Stimulus Correlated Motion (SCM),* the degree of stimulus-correlated motion based on the task onsets and motion parameters may be useful when deciding on whether or not to include motion parameters as nuisance regressors in the first level GLM. Including parameters as covariates can increase sensitivity, especially in event related designs. However, if the motion parameters are correlated with the task conditions, including the parameters as covariates could eliminate task activation because one regresses out the variance associated with the task. It has been shown that a modest degree of SCM (e.g. r = 0.2) may result in a significant decrease in spatial extent and T statistics (Johnstone et al. 2006). The SCM is also critical to evaluate between group comparisons regardless of whether or not motion parameters are included in the first level GLM. There may be artifactual between group differences that are merely between group differences in SCM. For example, persons with schizophrenia have been shown to have more SCM than typical participants (Bullmore et al. 1999). One possible solution to this problem would be to invoke a second level ANCOVA, where the amount of SCM for each subject is entered as a nuisance regressor. Another solution would be to match groups based on the degree of SCM. Either solution requires assessing the degree of SCM per subject and between groups.

5.2.7 Quality Assurance for Resting-State fMRI

In the context of resting-state fMRI, the importance of data quality assurance and the necessity to account for motion and other artifacts is recognized in the field (Power et al. 2015). There is, however, less agreement on the methods to adequately deal with artifacts, including ways of ensuring quality control and excluding contaminated trials. Among the available post-hoc correction options, several methods have been suggested to detect nuisance signals, including the realignment estimates and non-gray-matter and gray matter 'scrubbing'/'censoring', i.e. removing motion-contaminated time points and concatenating unaffected volumes. For a detailed discussion of the various methods for dealing with motion artifacts, see the review by Power (Power et al. 2015). Note, however that most of the available correction methods are optimized for resting state data analysis, while rigorous artifact detection is currently not routinely implemented for task related data.

In short, regressing six rigid body realignment parameters has been implemented as a standard in most imaging analysis workflows but recently has been shown to not fully remove motion artifacts (Power et al. 2012; Satterthwaite et al. 2012; Van Dijk et al. 2012). Further expanding the realignment estimates to include the adjacent 2 or 3 time points to remove spin-history related aspects (Friston et al. 1996) of motion-related artifacts has been shown to be insufficient for artifact removal with the additional consequence that expanding the number of motion regressors up to 36 (when 3 time points are included) results in a loss of degrees of freedom. Although deleting preceding and subsequent time points around an artifact is implemented in the commonly used 'scrubbing' method (Power et al. 2015). Alternative and complementary approaches to artifact detection in the past included using Independent Component Analysis (ICA) (Mowinckel et al. 2012; Pruim et al. 2015; Tyszka et al. 2014; Xu et al. 2014) or wavelet despiking (Patel et al. 2014) to identify motion-sensitive variance in the signal. In addition to these methods, removal of individual artifactual time points has been recommended based on the measures of relative displacement of the head, i.e. from one volume

of data to the next volume, often called frame-wise displacement (FD) (Jenkinson et al. 2002; Power et al. 2012; Van Dijk et al. 2012). FD is also recommended as a covariate for group comparisons. However, these approaches have not proven to remove motion artifacts completely either (Power et al. 2015).

The most effective way of removing motion contamination as suggested by Power and colleagues (2015) is global signal regression in combination with scrubbing, in addition to using the differences in FD values as covariates in group analyses (e.g. ANCOVA). This recommended method provides adequate removal of artifacts and as such is a reliable way of performing resting state data analysis. The specifics of data censoring (or time point deletion) implementation (i.e. scrubbing) have been criticized for several reasons. First, removing time points results in the loss of frequency information due to discontinuous data and also introduces concerns about the degrees of freedom. While both of these limitations can be addressed e.g., via the single-time point regression rather than deletion of time points (Power et al. 2015), the main denoising step, i.e., global signal regression, presupposes the removal of the global signal which has been shown to artificially introduce anticorrelations in the data. This limits the possibility of meaningfully interpreting anticorrelations (Murphy et al. 2009) and should not be used when studying rs-fMRI because it biases correlations differently in different regions depending on the underlying true inter-regional correlation structure (Saad et al. 2012).

5.3 Advanced Topics

5.3.1 Realtime-fMRI Neurofeedback

Previous studies have reported the benefits of realtime-fMRI (rt-fMRI) neurofeedback in chronic pain syndrome (deCharms et al. 2005) and chronic tinnitus (Haller et al. 2010).In the context of schizophrenia where aberrations in the default mode network are involved (for review see Whitfield-Gabrieli and Ford 2012), neurofeedback may provide a cognitive intervention that might be used to augment current treatment programs. By explicitly giving feedback by the online monitoring of brain states while performing "mental noting" (Fig. 5.3), the participant can attempt to regulate the connectivity based on meditation excercises such as noting practice (effortless awareness). One simply "notes" what is more predominant in the current experience from moment to moment and based on the neurofeedback they are receiving, the individual learns to adjust or diminish ruminating thoughts.

5.3.2 Simultaneous EEG/fMRI

A strength of fMRI is the spatial localization of activation, which identifies functional neuroanatomy, but a limitation of fMRI is that it has low temporal resolution. EEG has the high temporal resolution (see Chaps. 13 and 14 for more details), but because the scalp EEG signal reflects activity in a multitude of brain areas, an EEG signature of brain networks may best be identified through simultaneous EEG/fMRI recording. There has been substantial progress in overcoming the technical problems of simultaneous EEG/fMRI, so progress can be made in measuring the neural dynamics underlying the brain's spontaneous rhythmic activity (Ford et al. 2016). The infraslow (<0.1 Hz) EEG rhythms (e.g., direct current potentials) are most likely to correlate with slowly changing DMN-spontaneous BOLD fluctuations, but they are not often recorded due to technical issues related to amplifiers and artifacts (Khader et al. 2008). Other EEG frequencies, however, may also provide insight into the more rapidly changing neural activity.

5.3.3 Towards Clinical Translation

Neuroimaging has greatly enhanced the cognitive neuroscience understanding of the human brain

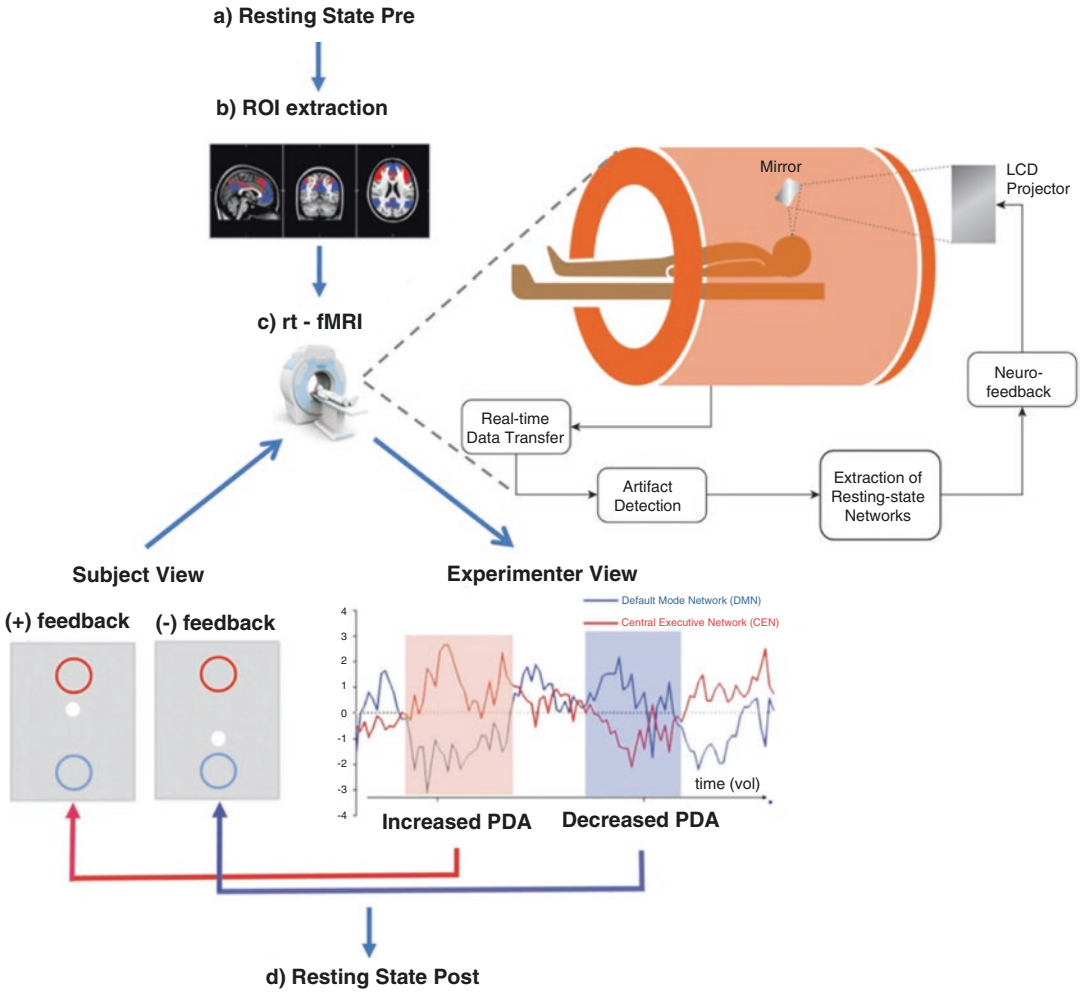

Fig. 5.3 Schematic of a realtime-fMRI (rt-fMRI) neurofeedback system. (A) Baseline resting state (RS-pre) scan. (B) Functional Localization of the default mode network (DMN) and the central executive network (CEN). (C) rt-fMRI feedback process showing the online monitoring of brain states while performing "mental noting". If rt-fMRI analysis resulted in a Positive Diametric Activity (PDA) score (red shadowing) the central white dot of the feedback display moved in the upper direction and towards the red circle. The contrary was the case when a negative PDA score was triggered (blue shadowing). (D) Post rt-fMRI resting state

and its variation across individuals in both health and disease. Neuromarkers often provide better predictions alone or in combination with other measures, than traditional behavioral measures. With further advances in study designs and analyses, neuromarkers may offer opportunities to personalize educational and clinical practices that lead to better outcomes for people. Regardless of the neuropsychiatric condition that is under investigation, prediction, early detection and novel interventions are the three major pathways to accomplish clinical translation. The term prediction can refer to: (1) a correlation between two contemporaneous values, (2) the correlation of one variable in

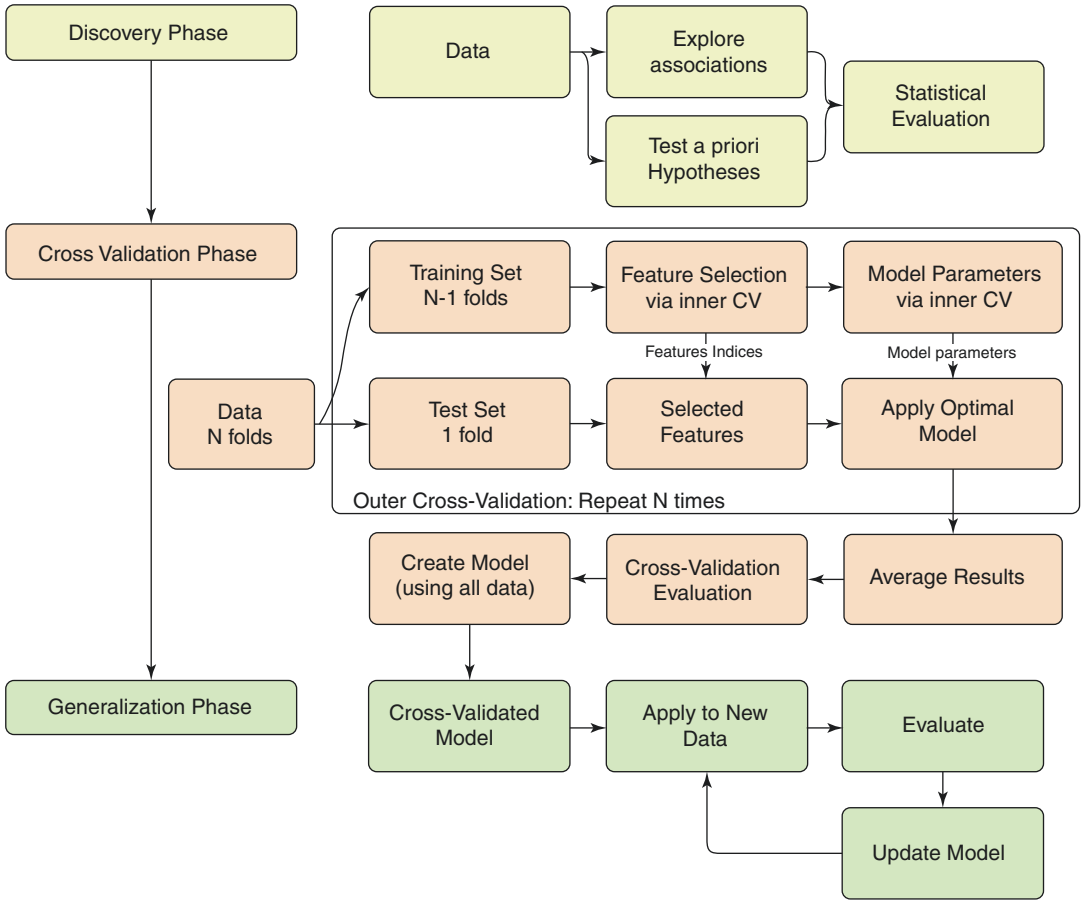

Fig. 5.4 Three stages of predictive model identification. (1) Discovery phase. Explore and evaluate associations between baseline neuromarkers and behavioral outcomes. (2) Cross-validation phase. A cross-validation routine is used to separate data into training and test sets. The model is built using training data and tested on out-of-sample test data. Upon successful evaluation of the performance of the model and features, all data are used to build a prediction model. (3) Generalization phase. A prediction model built via cross-validation is applied to a new data set. The new data are then used to update the model. [From Gabrieli et al. (2015)]

a group at an initial time-point to another variable in the same group at a future time-point (an in-sample correlation) or (3) a generalizable model that applies to out-of-sample individuals. Research geared towards clinical translation can be conceptualized as comprising three stages beginning with within-sample correlations to discover relations of interest, progressing to predictive analyses in which predictions for individuals are derived from data from other in-sample individuals, and culminating in predictive analyses using machine learning approaches in which a model from one sample is used to predict outcomes in an independent sample (Gabrieli et al. 2015). Each stage requires more participants, so that prior stages may justify larger-scale studies. This approach could be extremely useful in the context of schizophrenia where large-scale longitudinal studies may be suitable for gauging disease mechanism, progression, and prognosis (Birur et al. 2017) (Fig. 5.4).

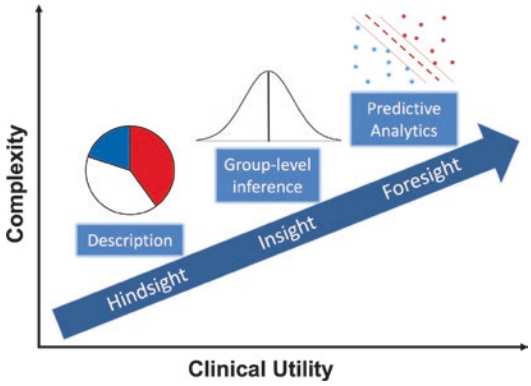

Fig. 5.5 Predictive analytics in mental health is moving from the description of patients (hindsight) and the investigation of statistical group differences or associations (insight) toward models capable of predicting current or future characteristics for individual patients (foresight), thereby allowing for a direct assessment of a model's clinical utility. [From Hahn et al. (2017)]

In contrast to the vast majority of investigations employing group-level statistics, predictive analytics aims to build models which allow for individual (that is, single subject) predictions, thereby moving from the description of patients (hindsight) and the investigation of statistical group differences or associations (insight) toward models capable of predicting current or future characteristics for individual patients ('foresight'), thus allowing for a direct assessment of a model's clinical utility (Fig. 5.5) (Hahn et al. 2017). Key concepts in predicting individual differences in behavior from brain features is illustrated in Fig. 5.6 (Rosenberg et al. 2018). A specific example of how functional changes in brain network organization predicts the onset of psychosis in a clinically high risk-group is provided in Fig. 5.7 (Collin et al. 2018).

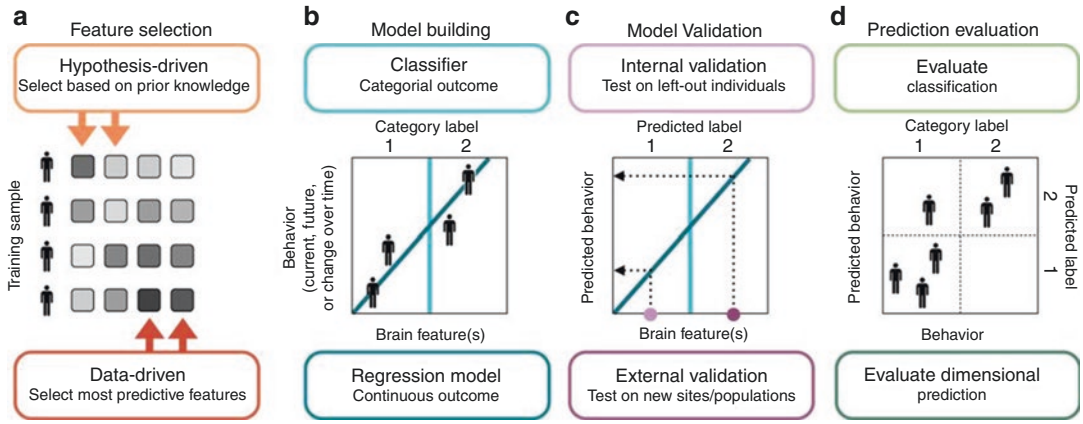

Fig. 5.6 Schema of key concepts in predicting individual differences in behavior from brain features. (**a**) Feature selection. Feature selection techniques: hypothesis-driven (top-down) and data-driven (bottom up) approaches. (**b**) Model building. Machine-learning algorithms can be used to predict categorical measures, such as clinical diagnoses, or dimensional measures, such as task performance or symptom severity. Here, the dark blue line shows the relationship between a single hypothetical brain feature and a behavioral score. The light blue line illustrates a classifier that divides individuals into categories based on this brain feature. (**c**) Model validation. Predictive models are evaluated on previously unseen data—either left-out individuals from the initial data set (internal validation) or individuals from a completely new sample (external validation). (**d**) Prediction evaluation. Continuous predictions (bottom and left axes) are evaluated by comparing observed and predicted behavioral measures. Categorical predictions (top and right axes) are evaluated with percent correct; binary predictions can be assessed with sensitivity and specificity and/or positive and negative predictive value. [From Rosenberg et al. (2018)]

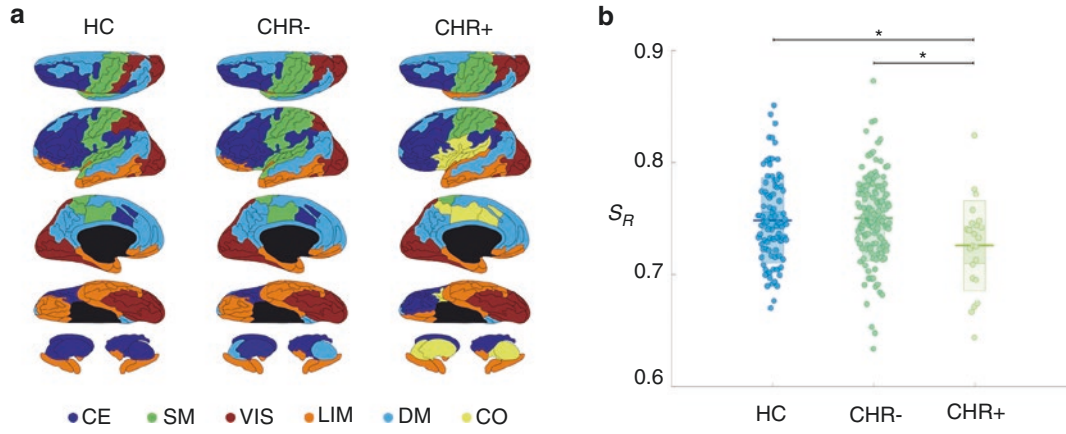

Fig. 5.7 Modular organization of the functional connectome. (**a**) Modular partitions of group-networks, plotted on cortical surface from superior, lateral, medial, and inferior angle, and subcortical structures (top to bottom row respectively). Colors indicate separate modules, with the prefrontal central-executive (CE) module in dark blue, the central sensorimotor (SM) module in green, the posterior visual (VIS) module in red, the (para)limbic (LIM) module in orange, the medial default mode (DM) module in light blue, and the cingulo-opercular (CO) module in yellow. (**b**) Degree of similarity to average healthy network (SR) for individual subjects. Jittered data are plotted for each group, with mean (sd) [95% CI] values represented by the box behind the raw data. ∗ indicates significant group-difference. [From Collin et al. (2018)]

5.4 Conclusions

In this chapter, we reviewed task and resting-state functional MRI data acquisition methods, various data processing strategies with an emphasis on data quality assurance, and suggested some advanced topics that may aid clinical translation. Future studies taking a multi-dimensional approach may improve and complement the behavioral characterization of schizophrenia, and may improve diagnosis, prognosis, and prediction.

Summary

- The primary goal of this chapter was to acquaint the neuroimaging community with the fMRI signal, experimental design and data acquisition methods.
- We have discussed data processing strategies for task-based and resting-state fMRI with an emphasis on data quality assurance, demonstrating examples of its utility in increasing data validity and sensitivity.
- Further advances in study designs and predictive analyses using machine-learning approaches may offer opportunities to personalize educational and clinical practices that lead to better outcomes for people.
- Realtime-fMRI neurofeedback is provided as an example for a behavioral intervention that might be used to augment current treatment programs for schizophrenia.

References

Ardekani BA, Bachman AH, Helpern JA. A quantitative comparison of motion detection algorithms in fMRI. Magn Reson Imaging. 2001;19(7):959–63.

Ashby FG. Statistical analysis of fMRI data. Cambridge: MIT Press; 2011.

Barabási A-L. Network science. Cambridge: Cambridge University Press; 2016.

Barabasi AL, Albert R. Emergence of scaling in random networks. Science. 1999;286(5439):509–12.

Behzadi Y, Restom K, Liau J, Liu TT. A component based noise correction method (CompCor) for BOLD and perfusion based fMRI. Neuroimage. 2007;37(1):90–101. https://doi.org/10.1016/j.neuroimage.2007.04.042.

Birn RM, Diamond JB, Smith MA, Bandettini PA. Separating respiratory-variation-related fluctuations from neuronal-activity-related fluctuations in fMRI. Neuroimage. 2006;31(4):1536–48. https://doi.org/10.1016/j.neuroimage.2006.02.048.

Birur B, Kraguljac NV, Shelton RC, Lahti AC. Brain structure, function, and neurochemistry in schizophrenia and bipolar disorder—a systematic review of the magnetic resonance neuroimaging literature. NPJ Schizophr. 2017;3:15. https://doi.org/10.1038/s41537-017-0013-9.

Bullmore E, Sporns O. The economy of brain network organization. Nat Rev Neurosci. 2012;13(5):336–49. https://doi.org/10.1038/nrn3214.

Bullmore ET, Brammer MJ, Rabe-Hesketh S, Curtis VA, Morris RG, Williams SC, et al. Methods for diagnosis and treatment of stimulus-correlated motion in generic brain activation studies using fMRI. Hum Brain Mapp. 1999;7(1):38–48.

Calhoun VD, Adali T, Pearlson GD, Pekar JJ. Spatial and temporal independent component analysis of functional MRI data containing a pair of task-related waveforms. Hum Brain Mapp. 2001;13(1):43–53.

Chai XJ, Castanon AN, Ongur D, Whitfield-Gabrieli S. Anticorrelations in resting state networks without global signal regression. Neuroimage. 2012;59(2):1420–8. https://doi.org/10.1016/j.neuroimage.2011.08.048.

Collin G, Seidman LJ, Keshavan MS, Stone WS, Qi Z, Zhang T, et al. Functional connectome organization predicts conversion to psychosis in clinical high-risk youth from the SHARP program. Mol Psychiatry. 2018. https://doi.org/10.1038/s41380-018-0288-x.

deCharms RC, Maeda F, Glover GH, Ludlow D, Pauly JM, Soneji D, et al. Control over brain activation and pain learned by using real-time functional MRI. Proc Natl Acad Sci U S A. 2005;102(51):18626–31. https://doi.org/10.1073/pnas.0505210102.

Deshpande G, LaConte S, Peltier S, Hu X. Integrated local correlation: a new measure of local coherence in fMRI data. Hum Brain Mapp. 2009;30(1):13–23. https://doi.org/10.1002/hbm.20482.

Diestel R. Graph theory. Berlin: Springer; 2018.

Eklund A, Nichols TE, Knutsson H. Cluster failure: why fMRI inferences for spatial extent have inflated false-positive rates. Proc Natl Acad Sci U S A. 2016;113(28):7900–5. https://doi.org/10.1073/pnas.1602413113.

Erdos P, Rényi, A. On the evolution of random graphs. Publication of the Mathematical Institute of the Hungarian Academy of Sciences. 1960;5:17–61.

Field AS, Yen YF, Burdette JH, Elster AD. False cerebral activation on BOLD functional MR images: study of low-amplitude motion weakly correlated to stimulus. AJNR Am J Neuroradiol. 2000;21(8):1388–96.

Ford JM, Roach BJ, Palzes VA, Mathalon DH. Using concurrent EEG and fMRI to probe the state of the brain in schizophrenia. Neuroimage Clin. 2016;12:429–41. https://doi.org/10.1016/j.nicl.2016.08.009.

Fox MD, Zhang D, Snyder AZ, Raichle ME. The global signal and observed anticorrelated resting state brain networks. J Neurophysiol. 2009;101(6):3270–83. https://doi.org/10.1152/jn.90777.2008.

Frank LR, Buxton RB, Wong EC. Estimation of respiration-induced noise fluctuations from undersampled multislice fMRI data. Magn Reson Med. 2001;45(4):635–44.

Friston KJ, Holmes AP, Poline JB, Grasby PJ, Williams SC, Frackowiak RS, Turner R. Analysis of fMRI time-series revisited. Neuroimage. 1995;2(1):45–53. https://doi.org/10.1006/nimg.1995.1007.

Friston KJ, Williams S, Howard R, Frackowiak RS, Turner R. Movement-related effects in fMRI time-series. Magn Reson Med. 1996;35(3):346–55.

Friston KJ, Harrison L, Penny W. Dynamic causal modelling. Neuroimage. 2003;19(4):1273–302.

Friston K, Moran R, Seth AK. Analysing connectivity with Granger causality and dynamic causal modelling. Curr Opin Neurobiol. 2013;23(2):172–8. https://doi.org/10.1016/j.conb.2012.11.010.

Gabrieli JDE, Ghosh SS, Whitfield-Gabrieli S. Prediction as a humanitarian and pragmatic contribution from human cognitive neuroscience. Neuron. 2015;85(1):11–26. https://doi.org/10.1016/j.neuron.2014.10.047.

Genovese CR, Lazar NA, Nichols T. Thresholding of statistical maps in functional neuroimaging using the false discovery rate. Neuroimage. 2002;15(4):870–8. https://doi.org/10.1006/nimg.2001.1037.

Glasser MF, Sotiropoulos SN, Wilson JA, Coalson TS, Fischl B, Andersson JL, et al. The minimal preprocessing pipelines for the Human Connectome Project. Neuroimage. 2013;80:105–24. https://doi.org/10.1016/j.neuroimage.2013.04.127.

Goelman G. Radial correlation contrast—a functional connectivity MRI contrast to map changes in local neuronal communication. Neuroimage. 2004;23(4):1432–9. https://doi.org/10.1016/j.neuroimage.2004.07.050.

Grootoonk S, Hutton C, Ashburner J, Howseman AM, Josephs O, Rees G, et al. Characterization and correction of interpolation effects in the realignment of fMRI time series. Neuroimage. 2000;11(1):49–57. https://doi.org/10.1006/nimg.1999.0515.

Hahn T, Nierenberg AA, Whitfield-Gabrieli S. Predictive analytics in mental health: applications, guidelines, challenges and perspectives. Mol Psychiatry. 2017;22(1):37–43. https://doi.org/10.1038/mp.2016.201.

Hajnal JV, Myers R, Oatridge A, Schwieso JE, Young IR, Bydder GM. Artifacts due to stimulus correlated motion in functional imaging of the brain. Magn Reson Med. 1994;31(3):283–91.

Haller S, Birbaumer N, Veit R. Real-time fMRI feedback training may improve chronic tinnitus. Eur Radiol. 2010;20(3):696–703. https://doi.org/10.1007/s00330-009-1595-z.

He H, Liu TT. A geometric view of global signal confounds in resting-state functional MRI. Neuroimage. 2012;59(3):2339–48. https://doi.org/10.1016/j.neuroimage.2011.09.018.

Hibar DP, Stein JL, Renteria ME, Arias-Vasquez A, Desrivieres S, Jahanshad N, et al. Common genetic variants influence human subcortical brain structures. Nature. 2015;520(7546):224–9. https://doi.org/10.1038/nature14101.

Jenkinson M, Bannister P, Brady M, Smith S. Improved optimization for the robust and accurate linear registration and motion correction of brain images. Neuroimage. 2002;17(2):825–41.

Jezzard P, Balaban RS. Correction for geometric distortion in echo planar images from B0 field variations. Magn Reson Med. 1995;34(1):65–73.

Jo HJ, Saad ZS, Simmons WK, Milbury LA, Cox RW. Mapping sources of correlation in resting state FMRI, with artifact detection and removal. Neuroimage. 2010;52(2):571–82. https://doi.org/10.1016/j.neuroimage.2010.04.246.

Johnstone T, Ores Walsh KS, Greischar LL, Alexander AL, Fox AS, Davidson RJ, Oakes TR. Motion correction and the use of motion covariates in multiple-subject fMRI analysis. Hum Brain Mapp. 2006;27(10):779–88. https://doi.org/10.1002/hbm.20219.

Keller JB, Hedden T, Thompson TW, Anteraper SA, Gabrieli JD, Whitfield-Gabrieli S. Resting-state anticorrelations between medial and lateral prefrontal cortex: association with working memory, aging, and individual differences. Cortex. 2015;64:271–80. https://doi.org/10.1016/j.cortex.2014.12.001.

Khader P, Schicke T, Roder B, Rosler F. On the relationship between slow cortical potentials and BOLD signal changes in humans. Int J Psychophysiol. 2008;67(3):252–61. https://doi.org/10.1016/j.ijpsycho.2007.05.018.

Kim JH, Lee JM, Jo HJ, Kim SH, Lee JH, Kim ST, et al. Defining functional SMA and pre-SMA subregions in human MFC using resting state fMRI: functional connectivity-based parcellation method. Neuroimage. 2010;49(3):2375–86. https://doi.org/10.1016/j.neuroimage.2009.10.016.

Kruger G, Glover GH. Physiological noise in oxygenation-sensitive magnetic resonance imaging. Magn Reson Med. 2001;46(4):631–7.

Luo WL, Nichols TE. Diagnosis and exploration of massively univariate neuroimaging models. Neuroimage. 2003;19(3):1014–32.

Martuzzi R, Ramani R, Qiu M, Shen X, Papademetris X, Constable RT. A whole-brain voxel based measure of intrinsic connectivity contrast reveals local changes in tissue connectivity with anesthetic without a priori assumptions on thresholds or regions of interest. Neuroimage. 2011;58(4):1044–50. https://doi.org/10.1016/j.neuroimage.2011.06.075.

Moore DS, McCabe GP. Introduction to the practice of statistics. 3rd ed. New York: W.H. Freeman; 1999.

Morgan VL, Pickens DR, Hartmann SL, Price RR. Comparison of functional MRI image realignment tools using a computer-generated phantom. Magn Reson Med. 2001;46(3):510–4.

Mowinckel AM, Espeseth T, Westlye LT. Network-specific effects of age and in-scanner subject motion: a resting-state fMRI study of 238 healthy adults. Neuroimage. 2012;63(3):1364–73. https://doi.org/10.1016/j.neuroimage.2012.08.004.

Murphy K, Birn RM, Handwerker DA, Jones TB, Bandettini PA. The impact of global signal regression on resting state correlations: are anti-correlated networks introduced? Neuroimage. 2009;44(3):893–905. https://doi.org/10.1016/j.neuroimage.2008.09.036.

Newman M. Networks. New York: Oxford University Press; 2018.

Nichols T, Hayasaka S. Controlling the familywise error rate in functional neuroimaging: a comparative review. Stat Methods Med Res. 2003;12(5):419–46. https://doi.org/10.1191/0962280203sm341ra.

Nichols TE, Das S, Eickhoff SB, Evans AC, Glatard T, Hanke M, et al. Best practices in data analysis and sharing in neuroimaging using MRI. Nat Neurosci. 2017;20(3):299–303. https://doi.org/10.1038/nn.4500.

Ogawa S, Lee TM, Nayak AS, Glynn P. Oxygenation-sensitive contrast in magnetic resonance image of rodent brain at high magnetic fields. Magn Reson Med. 1990;14(1):68–78.

Patel AX, Kundu P, Rubinov M, Jones PS, Vertes PE, Ersche KD, et al. A wavelet method for modeling and despiking motion artifacts from resting-state fMRI time series. Neuroimage. 2014;95:287–304. https://doi.org/10.1016/j.neuroimage.2014.03.012.

Picton TW, Bentin S, Berg P, Donchin E, Hillyard SA, Johnson R Jr, et al. Guidelines for using human event-related potentials to study cognition: recording standards and publication criteria. Psychophysiology. 2000;37(2):127–52.

Power JD, Barnes KA, Snyder AZ, Schlaggar BL, Petersen SE. Spurious but systematic correlations in functional connectivity MRI networks arise from subject motion. Neuroimage. 2012;59(3):2142–54. https://doi.org/10.1016/j.neuroimage.2011.10.018.

Power JD, Schlaggar BL, Petersen SE. Recent progress and outstanding issues in motion correction in resting state fMRI. Neuroimage. 2015;105:536–51. https://doi.org/10.1016/j.neuroimage.2014.10.044.

Pruim RHR, Mennes M, van Rooij D, Llera A, Buitelaar JK, Beckmann CF. ICA-AROMA: a robust ICA-based strategy for removing motion artifacts from fMRI data. Neuroimage. 2015;112:267–77. https://doi.org/10.1016/j.neuroimage.2015.02.064.

Razi A, Seghier ML, Zhou Y, McColgan P, Zeidman P, Park HJ, et al. Large-scale DCMs for resting-state fMRI. Netw Neurosci. 2017;1(3):222–41. https://doi.org/10.1162/NETN_a_00015.

Rosenberg MD, Casey BJ, Holmes AJ. Prediction complements explanation in understanding the developing brain. Nat Commun. 2018;9(1):589. https://doi.org/10.1038/s41467-018-02887-9.

Saad ZS, Gotts SJ, Murphy K, Chen G, Jo HJ, Martin A, Cox RW. Trouble at rest: how correlation patterns and group differences become distorted after global signal regression. Brain Connect. 2012;2(1):25–32. https://doi.org/10.1089/brain.2012.0080.

Satterthwaite TD, Wolf DH, Loughead J, Ruparel K, Elliott MA, Hakonarson H, et al. Impact of in-scanner head motion on multiple measures of functional connectivity: relevance for studies of neurodevelopment in youth. Neuroimage. 2012;60(1):623–32. https://doi.org/10.1016/j.neuroimage.2011.12.063.

Setsompop K, Gagoski BA, Polimeni JR, Witzel T, Wedeen VJ, Wald LL. Blipped-controlled aliasing in parallel imaging for simultaneous multislice echo planar imaging with reduced g-factor penalty. Magn Reson Med. 2012;67(5):1210–24. https://doi.org/10.1002/mrm.23097.

Sporns O. Networks of the brain. Cambridge: MIT Press; 2010.

Stephan KE, Penny WD, Moran RJ, den Ouden HE, Daunizeau J, Friston KJ. Ten simple rules for dynamic causal modeling. Neuroimage. 2010;49(4):3099–109. https://doi.org/10.1016/j.neuroimage.2009.11.015.

Stocker T, Schneider F, Klein M, Habel U, Kellermann T, Zilles K, Shah NJ. Automated quality assurance routines for fMRI data applied to a multicenter study. Hum Brain Mapp. 2005;25(2):237–46. https://doi.org/10.1002/hbm.20096.

Thesen S, Heid O, Mueller E, Schad LR. Prospective acquisition correction for head motion with image-based tracking for real-time fMRI. Magn Reson Med. 2000;44(3):457–65.

Thompson PM, Stein JL, Medland SE, Hibar DP, Vasquez AA, Renteria ME, et al. The ENIGMA Consortium: large-scale collaborative analyses of neuroimaging and genetic data. Brain Imaging Behav. 2014;8(2):153–82. https://doi.org/10.1007/s11682-013-9269-5.

Tierney TM, Weiss-Croft LJ, Centeno M, Shamshiri EA, Perani S, Baldeweg T, et al. FIACH: a biophysical model for automatic retrospective noise control in fMRI. Neuroimage. 2016;124(Pt A):1009–20. https://doi.org/10.1016/j.neuroimage.2015.09.034.

Triantafyllou C, Polimeni JR, Wald LL. Physiological noise and signal-to-noise ratio in fMRI with multi-channel array coils. Neuroimage. 2011;55(2):597–606. https://doi.org/10.1016/j.neuroimage.2010.11.084.

Tyszka JM, Kennedy DP, Paul LK, Adolphs R. Largely typical patterns of resting-state functional connectivity in high-functioning adults with autism. Cereb Cortex. 2014;24(7):1894–905. https://doi.org/10.1093/cercor/bht040.

Van Dijk KR, Sabuncu MR, Buckner RL. The influence of head motion on intrinsic functional connectivity MRI. Neuroimage. 2012;59(1):431–8. https://doi.org/10.1016/j.neuroimage.2011.07.044.

Ward HA, Riederer SJ, Grimm RC, Ehman RL, Felmlee JP, Jack CR Jr. Prospective multiaxial motion correction for fMRI. Magn Reson Med. 2000;43(3):459–69.

Watts DJ, Strogatz SH. Collective dynamics of 'small-world' networks. Nature. 1998;393(6684):440–2. https://doi.org/10.1038/30918.

Weissenbacher A, Kasess C, Gerstl F, Lanzenberger R, Moser E, Windischberger C. Correlations and anticorrelations in resting-state functional connectivity MRI: a quantitative comparison of preprocessing strategies. Neuroimage. 2009;47(4):1408–16. https://doi.org/10.1016/j.neuroimage.2009.05.005.

Whitfield-Gabrieli S, Ford JM. Default mode network activity and connectivity in psychopathology. Annu Rev Clin Psychol. 2012;8:49–76. https://doi.org/10.1146/annurev-clinpsy-032511-143049.

Worsley KJ, Friston KJ. Analysis of fMRI time-series revisited—again. Neuroimage. 1995;2(3):173–81. https://doi.org/10.1006/nimg.1995.1023.

Wu DH, Lewin JS, Duerk JL. Inadequacy of motion correction algorithms in functional MRI: role of susceptibility-induced artifacts. J Magn Reson Imaging. 1997;7(2):365–70.

Xu Y, Tong Y, Liu S, Chow HM, AbdulSabur NY, Mattay GS, Braun AR. Denoising the speaking brain: toward a robust technique for correcting artifact-contaminated fMRI data under severe motion. Neuroimage. 2014;103:33–47. https://doi.org/10.1016/j.neuroimage.2014.09.013.

Yan CG, Cheung B, Kelly C, Colcombe S, Craddock RC, Di Martino A, et al. A comprehensive assessment of regional variation in the impact of head micromovements on functional connectomics. Neuroimage. 2013;76:183–201. https://doi.org/10.1016/j.neuroimage.2013.03.004.

Functional MRI Findings in Schizophrenia

6

Godfrey D. Pearlson

Contents

6.1 Introduction

The construction of DSM-V and the process of assembling the NIH Research Domain Criteria (RDoC) have opened up a number of useful debates in psychiatry. Some of the issues raised include reminders that psychiatry lacks valid diagnostic tests for the majority of its diagnostic entities, in contrast to most of the rest of medicine, including neurology. That restricts us to clinical phenomenology and illness course with which to define the majority of our disorders, including schizophrenia. For major psychiatric illnesses in general we are still startlingly ignorant with regard to etiology, and treatments overlap across diagnoses, as unfortunately do clinical symptoms, risk genes and familial co-occurrence of illnesses. What psychiatrists would like more than anything would be a straightforward biological test that would provide for an individual patient, rather than a group of them, an accurate diagnosis, a prediction of optimal medication response and a prognosis. Since major psychiatric disorders are

G. D. Pearlson (✉)
Yale University School of Medicine,
New Haven, CT, USA

Olin Neuropsychiatry Research Center, Institute of Living, Hartford, CT, USA
e-mail: Godfrey.Pearlson@yale.edu

M. Kubicki, M. E. Shenton (eds.), *Neuroimaging in Schizophrenia*,
https://doi.org/10.1007/978-3-030-35206-6_6

conditions of the brain and involve disordered function, then functional MRI abnormalities would seem suitable candidates for such biological tests. Unfortunately, thus far they are not.

An assumption in the neuroimaging community is that psychotic illnesses in general are disorders of distributed brain circuits. There is certainly little evidence to suggest that functional abnormalities in one particular brain region correspond to any psychiatric syndrome, including schizophrenia. Therefore our focus has been on measures of functional brain connectivity, whether these assess measures from region-to-region within defined neural circuits, across circuits, or how connectivity varies within or across circuits as a function of time. Since Friston's initial 1995 review (Friston and Frith 1995) a leading hypothesis has been that schizophrenia is fundamentally a disorder of abnormal brain connectivity, although what constitutes such "dysconnectivity" or how best to operationalize it are seldom discussed in detail. Some recent papers have probed the concept in more detail (e.g., Scariati et al. 2016). Models of schizophrenia risk hypothesize that abnormal brain connections are determined by schizophrenia risk genes that build deviant brain micro circuitry, in turn underpinned by abnormal cell-to-cell communication, perhaps via unbalanced neurotransmitters. However these presumed precursors and their relationship to what is actually measured inside a functional MRI experiment is not clear. Some of these issues are beginning to be explored, for example by examining consequences of neural pharmacologic probe experiments by computational modeling techniques (Stephan et al. 2015) or by groups using theoretically-derived predictions about functional MRI patterns derived from computational modeling (Anticevic et al. 2015).

Let us begin with a broad, big picture view of a series of caveats and under-addressed issues in the field. One major problem is that currently "schizophrenia" is defined only by symptoms and illness outcome but its underlying pathophysiology is unknown. First, this diagnostic reliability in the absence of valid biological criteria makes it very likely that this is a very *heterogeneous* syndrome, *not meeting criteria for a disease* and thus akin to other broad syndrome entities such as congestive cardiac failure or fever. This state of affairs is indeed suggested by recent structural imaging studies (Wolfers et al. 2018). Second, just as for the known significant overlap of familial co-occurrence, risk genes, treatment response and symptomatology between schizophrenia, bipolar disorder, schizoaffective disorder and autism spectrum cases, it is important to establish the *specificity of functional MRI findings* seen in schizophrenia, to determine whether or not there is significant overlap among these syndromes. For example, findings in multiple domains resulting from the Bipolar-Schizophrenia Network on Intermediate Phenotypes (BSNIP) (Tamminga et al. 2017) have cast considerable doubt on the exclusivity of functional MRI and other biological abnormalities in schizophrenia relative to other psychotic disorders (Khadka et al. 2013; Meda et al. 2014). Also broadly unresolved is whether fMRI findings reported in schizophrenia are *primarily state-or trait-related*, and when they begin relative to overt illness onset versus for example the prodrome or the ultra-high risk state. This latter question is addressed later in the concluding section.

Many functional MRI investigations of schizophrenia have been straightforward comparisons between patients diagnosed with schizophrenia and healthy controls. While some such studies have been primarily motivated by hypotheses such as dysconnection or neurodevelopmental models, the majority have not. If there are indeed "dysconnections," i.e. abnormal connections within and between brain circuits, an important issue is when these first manifest. For example, are they identifiable in some form at birth in high-risk cohorts, and if so can we relate their presence to that of aberrant genes, altered molecular biology, abnormal development/pruning, abnormal structure and diffusion tensor imaging (DTI) in the same individuals? Investigations in adults with the disorder that examined the relationship between polygenic risk scores for schizophrenia and the presence and severity of functional MRI abnormalities would be useful in addressing one of these questions. Another important issue that could bear greater examination is whether the fMRI abnormalities detected in schizophrenia affect all brain circuits equally or are restricted to certain key networks.

Other areas deserving of more clarification are how fMRI changes relate to important clinical symptoms of the disorder, e.g., typical clinical symptomatology (e.g., hallucinations or negative symptoms) versus cognitive or affective abnormalities. Thus, while undoubtedly informative, the majority of fMRI reports often are isolated from these other areas of inquiry, i.e., they center on signals in brain systems/distributed circuits and allied connectivity relationships, but do not probe further into underlying intrinsic causes, whether these be genetic, cellular or physiologic. For example, are circuit abnormalities reflected in function such as compromised synaptic efficiency? The field has just recently been able to address some of these issues using novel approaches such as pharmacologic probes allied with fMRI (Khalili-Mahani et al. 2017; Driesen et al. 2013). Sometimes the studies are allied with computational modeling designs (Joules et al. 2015). Related results suggest that frontal parietal connectivity may be related to NMDA-receptor related plasticity (Schmidt et al. 2015) and the default mode network, strongly influenced by dopaminergic networks.

Another basic question is what constitutes connectivity? Connectivity is most often defined as activity, which is defined as neuronal firing that fluctuates on a millisecond scale and in a predictable manner that is both temporally and spatially correlated. In space, identifiable brain regions constitute networks that synchronize independently, and whose profiles can be distinguished either locally or dispersed. The key measure in fMRI, blood oxygen level dependent (BOLD) signal, represents aspects of both blood flow and metabolism changes on a scale of seconds, differing temporally by several orders of magnitude compared to electrical brain activity, and representing distinctly different physiologic processes. Fundamental introductory concepts for fMRI are detailed in a recent review paper (Pearlson 2017) as well as in Chap. 5. In general, searches employing fMRI in schizophrenia have been directed to quantifying connectional relationships among distributed brain networks. Thus, the focus has been on how these neural systems "talk to each other" under a variety of circumstances. The major measurement approaches include both resting state and task-related studies, some of which have then examined network relationships to common symptoms and other clinical variables.

One difficulty in making straightforward comparisons across different studies is due to wide differences in data analysis approaches. Such diversity is not just a result of different choices in analytic strategy, for example seed voxel versus independent component analysis approaches, but also a result of fundamental differences in analytic design choice such as connectomics, functional connectivity versus functional network connectivity, regional homogeneity, and dynamic/temporal techniques. It is often hard to know how reports in one domain relate to those in another. With these caveats in mind, let us review resting state versus task-based connectivity findings in schizophrenia.

6.2 Resting State (RS) Connectivity Findings in Schizophrenia

RS is defined operationally as an fMRI time-series collected in the absence of a task, while patients are awake and alert. It is believed to reflect intrinsic neural activity and manifests as spontaneous, low-frequency bold signal fluctuations that are correlated at a time scale of seconds. These patterns are unceasing and consume much of the brain's energy. Although the brain's default mode network (DMN) circuitry is most manifest during these resting conditions, and its activity diminished proportionately by cognitive tasks, analysis methods such as independent component analysis reveal that all of the brain's intrinsic connectivity networks are active to some extent and detectable during resting conditions. Such highly reproducible circuits such as a frontoparietal network mediating cognitive control or reward system regions come to the foreground with regard to activity as evoked by specific cognitive or other tasks with proportionate diminution in DMN signal. The brain is not truly "at rest" during RS paradigms but in an unconstrained state of active consciousness. This has both advantages and disadvantages as discussed below.

The usual RS paradigm is to acquire fMRI timeseries over a 5–10 min time period, while the subject remains awake (hopefully with eyes open to help ensure that they are not asleep), but cognitively unengaged except for "mind wandering" or typically looking at an unchanging visual fixation stimulus. Schizophrenia researchers have favored studies of RS fMRI functional connectivity because acquisitions are quick and straightforward and sidestep the issue of needing to administer cognitive paradigms in patients who have challenges remaining relatively immobile and comfortable inside the scanner and whose cognitive issues necessitate careful task design. In addition, analysis of RS timeseries is relatively uncomplicated. Typically either independent component analysis or seed voxel analytic designs are favored. While some investigations have focused primarily on the DMN, others have examined resting relationships within a broader range of independent networks (functional connectivity) or across pairs of such networks. Resting state network analyses have looked beyond simple connectivity within or between brain networks to include such additional measures as regional homogeneity (ReHo), amplitude of low-frequency fluctuations (ALFF) and fractional ALFF, and graph theory-based connectivity and small-world topology measures. Some recent articles (Ding et al. 2019a; Mwansisya et al. 2017; Hu et al. 2017) review these findings in schizophrenia. As summarized comprehensively by Hu et al. (2017), the most frequently reported finding in schizophrenia patients compared to healthy controls is one of default mode functional hyper-connectivity. This observation is reasonably consistent across both different analysis approaches and clinical diagnostic groups, comprising first-episode and chronic patients. It is also reported in individuals at clinical high-risk for psychosis and unaffected first-degree relatives of schizophrenia patients. Another observation is one of disturbed anti-correlation between the DMN and so-called task-positive networks (TPNs) (Whitfield-Gabrieli et al. 2009; Bluhm et al. 2007).

Some authors have used independent component analysis-based approaches (Calhoun et al. 2001) to examine multiple RSNs in schizophrenia compared to other psychotic disorders using both FC and FNC approaches (Khadka et al. 2013; Meda et al. 2014, 2012, 2015). These attempts from the Bipolar-Schizophrenia Network for Intermediate Phenotypes (B-SNIP), aimed to identify whether or not schizophrenia-related RS changes were diagnosis-specific, and their findings are complex to parse. Clearly schizophrenia and psychotic bipolar subjects share common abnormalities, although some RS differences from controls were seen only in schizophrenia probands. Some of the shared abnormalities were also detectable in unaffected first-degree relatives of the study probands. As in several of the studies discussed in the prior paragraph, disrupted relationships between DMN and TPN's were broadly evident in the B-SNIP sample across psychotic disorders.

Ding et al. (2019a), reviewing both structural fMRI and resting state fMRI studies, emphasize the presence of functional abnormalities within multiple cerebellar regions. Mwansisya et al. (2017) examined studies that had assessed both task and RS fMRI in first episode schizophrenia patients and concluded that the two sets of abnormalities overlapped in prefrontal regions including dorsolateral prefrontal and orbitofrontal cortices plus the left superior temporal gyrus. Lo and coworkers (2015) compared directly RS FC measures in schizophrenia versus healthy control comparisons to small-world topology metrics derived from a graph theoretical approach in those subjects. They determined that schizophrenia patients not only manifested reduced FC, but also concominant disruption in all global topology measures assessed. They also found disruption in global topology measures in unaffected close relatives of patients, but to a lesser extent.

Other approaches to resting state analyses have included dynamic functional connectivity, amplitude of low-frequency fluctuations (ALFF) and regional homogeneity measures, as discussed next.

6.2.1 Dynamic FNC (DFNC)

Calhoun and coworkers (2014) varied from the usual analytic approach that averages BOLD signal variation across the entire acquisition period.

However, that approach assumes stable connectivity patterns across time. Instead, using a sliding time window or other approaches, DFNC assesses temporal coordination of large-scale brain networks on a finer time scale of tens of seconds, capturing time-varying fluctuations. Early use of this technique in schizophrenia and bipolar disorder (Du et al. 2017; Rashid et al. 2014) showed that healthy controls enter several correlationally-defined temporary brain configurations or "states" that have their own metrics such as "dwell time," i.e., typical length of time spent in a particular state and "fractional time," i.e., how long an individual spends in a state across the entire measurement epoch. Patients with psychotic disorders clearly differ from healthy controls in a way that was not well explained by current medication status, and to a greater extent than was captured by traditional static FC metrics. Abnormal fractional dwell times in schizophrenia tend to normalize following treatment with antipsychotic medications (Lottman et al. 2017). One recent publication applying similar techniques (Reinen et al. 2018) mapped such cortical dynamic patterns in patients with schizophrenia and psychotic bipolar disorder. Here investigators were able to show convincingly that dynamic profiles remained consistent within individual study participants, and that patients showed "intermittent disruptions within cortical networks previously associated with the disease." Of particular interest was that for patients, within "states," the above-mentioned individual connectivity profiles were clearly correlated temporarily with current psychotic symptoms. The dynamic relationship between the manifestation of such symptoms and of transient cortical network disruptions suggest that dynamic, time-varying relationships underpin syndrome-related features.

6.2.2 Amplitude of Low-Frequency Fluctuations (ALFF)

Amplitude of low-frequency fluctuations and their fractional amplitude (fALFF) constitute a means of quantifying the low-frequency oscillations that are intrinsic to the resting brain. Strictly they are not connectivity estimates, although allied with them. Some initial studies (Meda et al. 2015) have used these measures to compare resting state fMRI studies in the B-SNIP dataset across DSM psychotic disorders and in empirically-derived biologic psychosis classifications known as "Biotypes" (Clementz et al. 2016).

6.2.3 Regional Homogeneity

Finally, among RS fMRI metrics *regional homogeneity* (ReHo) deserves mention. This functional measure assesses local brain connectivity expressed as the synchronization of a particular voxel and its nearest neighbors. The underlying assumption is that such relationships are a proxy for regional integration of information processing or for local synchronization of fMRI signals, and thus more informative regarding finer-grained regional information about local FC imbalances. Abnormal ReHo patterns are reported for schizophrenia, but also in bipolar illness and individuals at risk for psychosis (Liang et al. 2013; Wang et al. 2018, 2016). In one study, drug-naïve, young-onset individuals with schizophrenia showed increased ReHo in medial prefrontal, superior temporal, and inferior parietal regions, and were well discriminated from healthy controls using a support vector machine approach (Wang et al. 2018).

6.2.4 Resting State Studies: Pros and Cons

Advantages of employing RS techniques in schizophrenia include signal that is not made more complex by effects of variable task performance and relative task difficulty, or by subjective task-evoked anxiety or discouragement in the face of a syndrome generally characterized by cognitive deficits, including attentional difficulties. Particularly when challenged by difficult tasks, schizophrenia patients can become disengaged or demoralized, which confounds both performance and the associated brain response. Additionally, cognitive-related responses can be complicated by intrusion of psychotic symptoms and failure to comprehend or retain complex instructions.

Resting state patterns seem consistent within single individuals, and at least for DMN are clearly significantly heritable (Glahn et al. 2010; Richiardi et al. 2015). Some investigations (Meda et al. 2014) used parallel independent component analysis to identify genetic networks that were significantly correlated with fMRI sub-networks within the DMN.

Signal acquisition is quick and straightforward, and analysis generally uncomplicated. Dynamic measures of resting state are now available and informative (Calhoun et al. 2014). Disadvantages, as summarized by Weinberger and Radulescu (2016), include the fact that resting state studies are confounded by variables that differ systematically between patients and controls. Such variables include those attributable to medication, use of tobacco and caffeine, abused substances, environmental-related anxiety, heart and respiration rates, head movement, restlessness and drowsiness (that may be related to prescribed medications). Between-group differences that may be attributed to disease-related abnormalities may in actuality be epi-phenomena of these systematic differences. The degree to which resting state studies are compromised overall by these factors was discussed in a comment on the Weinberger and Radulescu paper by Calhoun et al. (2016). This is not to say however, that task-based paradigms are immune from many of the same potential confounds. Conversely however, task-based designs have their own problems.

6.3 Task-Based Connectivity Findings in Schizophrenia

Tasks induce BOLD changes typically of magnitude around 5% whose functional connectivity patterns differ from those observed at rest. Whether these differences are underpinned by similar event types is uncertain (Gonzalez-Castillo and Bandettini 2018). How to optimize data-gathering choices between task versus resting fMRI paradigms in studying schizophrenia has been the subject of prior reviews (e.g., Pearlson and Calhoun 2009). Typical task-based designs are based on cognitive challenges typically in domains affected by the disorder such as executive functioning or theory of mind. Other designs rely on responses to non-cognitive areas of disease-related impairment such as presentation of emotional, reward, or social stimuli. The cognitive paradigm does not have to be especially challenging to elicit marked differences between patients and controls. For example performance accuracy on straightforward auditory oddball tasks is not typically divergent between schizophrenia patients and healthy controls, yet the associated BOLD signal patterns differ markedly. Although cognitive-based paradigms are essentially designed as stress tests to uncover underlying illness-impacted brain circuitry, it is difficult to disambiguate variant brain responses from different cognitive performance. Various solutions to this include employment of parametrically-based tasks where difficulty level can be manipulated across a wide range, allowing for comparisons between patients and controls at equal performance levels. Other proposed solutions are employment of standardized cognitive tasks or assessment across several cognitive domains within a given study (Sheffield and Barch 2016). These points have much to commend them. Because of the considerable variety of task designs, acquisition parameters, and analysis methods, only very broad general overview statements can be made that capture commonalities across task-based studies in schizophrenia. Generally, and unsurprisingly, patients tend to perform more poorly and to activate task-relevant circuitry differently than healthy controls. Perhaps a more apt question is whether schizophrenia patients show consistent circuit abnormalities across both resting state and task-based paradigms for both FC and FNC, and in the case of task designs whether the abnormalities are of a general rather than task-specific nature. These interlinked issues are addressed both by Sheffield and Barch (2016) and by Mwansisya et al. (2017) with the former stressing a pattern of consistent connectivity disruption across cortical task-positive and task-negative networks and a cortico-cerebellar-striatal-thalamic loop. This pattern is consistent across cognitive domains, and is compatible with the disorder's generalized pattern of cognitive deficits. Sheffield and Barch (2016) further elaborate these observations by

providing evidence that the latter may be underpinned by functional connectivity abnormalities that exist both within and between task-positive and task-negative brain circuits, that proceed from FC disruptions between multiple cortical areas. In some respects this hypothesis is a helpful elaboration of "dysconnection," and one that is consistent with other observations (Mwansisya et al. 2017; Repovs et al. 2011; Unschuld et al. 2014). Some of these studies extend the pattern of disruption to thalamus, cerebellum and striatum, or alternatively restrict it to disturbed fronto-parietal connectivity (Schmidt et al. 2015). Publications from B-SNIP are also consistent with this general hypothesis in showing similar cognitive abnormalities and many common FC and FNC disruptions across multiple psychotic illnesses (Tamminga et al. 2014).

6.3.1 Are "Key Circuits" Involved?

A related question is whether there are "key circuits" at the hub of the FC disruptions. A common hypothetical candidate here is the thalamus, as reviewed in Acsady (2017), Giraldo-Chica and Woodward (2017), Woodward et al. (2012), Anticevic et al. (2014), and Woodward and Heckers (2016). The essential argument is that as a connection hub with multiple connections to and from cortical regions underpinning dozens of sensory, motor, cognitive, and emotional functions, damage to one or more of its numerous nuclei would widely disrupt cortical connectivity. Murray and Anticevic (2017) further complement this discussion of thalamic disorganization with the use of computational modeling and employment of pharmacological probes of the glutamate system (Anticevic et al. 2013).

6.3.2 Are fMRI Findings Specific to Schizophrenia, and are they Linked to Symptoms?

The issue of specificity of task-based fMRI abnormalities to schizophrenia as opposed to other psychoses, particularly psychotic bipolar illness, is important. Outside of the B-SNIP group, pertinent reviews across multiple disorders include that of Birur et al. (2017). As is the case for schizophrenia alone, the wide disparity of tasks and designs interferes with the ability to extract common patterns, but there is supportive evidence for similar abnormalities across schizophrenia and bipolar disorder, as indeed has been shown for resting state studies (Anticevic et al. 2015). Another important strand in the scientific literature explores the links between typical schizophrenia clinical symptoms and FC and FNC disturbances. Conducting such studies adds another layer of difficulty, because considerations of stage of illness, treatment responsiveness, symptom assessment approaches and inclusion criteria make comparison across different reports challenging (Karbasforoushan and Woodward 2012). For verbal hallucinations, symptom capture studies of active hallucinators show increased FC between the basal ganglia and auditory/language regions, while comparisons of patients with and without such symptoms are generally characterized by altered connectivity between language association regions across the two hemispheres (Curcic-Blake et al. 2017). Disturbed left superior temporal gyral FC may be linked to reports of auditory verbal hallucinations across multiple studies (Alderson-Day et al. 2015). Other groups both examined spatial FC and temporal coupling in relation to both clinical and cognitive symptoms in schizophrenia, finding that both relate to globally disturbed ALFF (Northoff and Duncan 2016; Northoff 2018).

6.4 Unaddressed Problems That Future Studies Need to Contend with and Some Recommendations for Improved Design

This section focuses on some of the issues identified above, and reviews recent studies that in one way or another have attempted to address them. The overarching issue to be dealt with is the lack of clarity on exactly how the network

connectional abnormalities identified in fMRI relate to important, superordinate, broader etiologic and functional concepts such as abnormal brain development and impairments in synaptic efficiency and neural plasticity. The current broad hypothesis is that schizophrenia is a neuro-developmental disorder, originating in an interaction between genetic predisposition and environmental abnormalities, that translates into altered molecular biology, which, in turn, has developmental consequences for neural circuitry resulting in a pattern of characteristically disordered behavior. However it is unclear in practice how such hypothesized etiologic events might relate directly to disturbed connections among brain networks, or how those disturbances are related to symptoms. In general, investigators at these different levels of inquiry do not cross disciplines sufficiently to communicate effectively with one another to resolve these issues.

As noted, another major issue is the clear need to establish the uniqueness of reported findings to schizophrenia as opposed narrowly to other psychotic disorders, and more generally to all serious mental illnesses. One useful perspective that addresses this issue is the framework articulated by Craddock and Owen (2010) where major psychiatric disorders are conceived of as arrayed on a continuum, successively from intellectual disability (ID) through autism spectrum disorder, schizophrenia, schizo-affective disorder, psychotic bipolar disorder, non-psychotic bipolar disorder, to major depressive disorder. The underlying hypothesis is that those disorders closest to ID are most developmental in nature, display significant cognitive involvement and are most driven by significant genetic deletions or duplications such as copy number variants. These features diminish as one moves towards MDD. Disorders in the conceptual center of the spectrum such as schizophrenia and psychotic bipolar involve more positive symptoms, while disorders at the furthest end of the spectrum display more affective involvement. In line with this mode of thinking, fMRI abnormalities in schizophrenia would be predicted to display more similarities with other psychotic disorders as has been demonstrated in B-SNIP (Khadka et al. 2013; Meda et al. 2014) and is straightforwardly testable in an adult autism spectrum sample. Some efforts have already been made in this direction (Foss-Feig et al. 2017).

Multi-center group collaborations such as the Enhancing Neuro Imaging Genetics Through Meta Analysis (ENIGMA) consortium (van Erp et al. 2018) demonstrate the power of merging large imaging samples derived from multiple centers in the structural domain. Parallel efforts aimed at functional standardization, e.g., the Human Connectome Project (Barch 2017) that incorporate a standardized analytic pipeline will likely be adopted increasingly over the next 5 years.

The role of machine learning and computational modeling have been mentioned earlier. Both supervised machine learning models (often applied usefully to classification outcome) and unsupervised approaches (that show utility in highlighting subgroups) are effective. Recent useful reviews of this field are these from Murray et al. (2018) and Pinaya et al. (2019).

Individualized prediction/identification is another analytic approach that has received insufficient attention, given its obvious importance to clinical decision-making, and questions asked most often by patients and their families. Other recent approaches have used a variety of the elements above to derive novel techniques that will undoubtedly see increased use in our arena. For example, Yip et al. (2019) employed fully data-driven machine learning approaches such as connectome-based predictive modeling, that use alterations within neural components, to identify brain "fingerprints" that allow actual prediction. For example diagnostic entities, responses to treatment, or other metrics can be theoretically derived from individual differences in whole brain functional connectivity data.

Studies such as North American Prodrome Longitudinal Study (NAPLS) have shown the feasibility of capturing individuals at risk and using functional MRI memory paradigms to help determine who will convert to psychosis (2019). In that publication, the authors compared 155

clinical high-risk individuals 12% of whom later converted to full psychosis and 108 healthy controls on a fMRI paired-associate memory paradigm. Converters 2 years later had shown more marked abnormalities in prefrontal, parietal, and bilateral temporal cortices. Similar study designs are useful as they are potentially uncontaminated by treatment effects. Larger-scale studies of antipsychotic naïve patients with schizophrenia are another important set of investigations; some have explicitly compared first-episode subjects to those at clinical high-risk (Wang et al. 2019; Ding et al. 2019b; Zhu et al. 2019).

In summary, both resting state and task-based fMRI have been informative to the field of schizophrenia research, but many important questions remain to be answered. On the plus side, those questions can now be articulated and many of them can be addressed with larger scale studies of improved design, as I have tried to summarize here.

Summary

- Schizophrenia is widely assumed to be a developmental disorder characterized by cortical dysconnectivity, but fMRI studies have only partially addressed the etiology of this abnormality, it specificity to schizophrenia, and its relationship to treatment effects.
- Both task-based and resting state fMRI abnormalities have been documented in schizophrenia but the relationship of such differences from healthy controls in both relationship to each other and to major features of the disorder, e.g., to symptoms, are hard to summarize easily. In part this state of affairs results from a plethora of both study designs and particularly of analysis methods applied to such data.
- FMRI abnormalities are only beginning to be linked to such superordinate concepts such as synaptic efficiency or neural plasticity.
- As the field moves forward, the role of more focused patient samples (such as ultra-risk and drug-naïve patient populations), more standardized collection and analysis approaches (for example Human Connectome Project), and use of novel analysis methods (including machine learning and individual-level prediction algorithms), will likely prove increasingly important.
- Such approaches will allow for transdiagnostic comparison of findings, reduce over-reliance on small, not necessarily typical patient samples, and address broader disease-related questions including relationships between fMRI findings and relevant underlying risk genes, molecular biology, other physiological abnormalities such as electroencephalography, and clinical expression of the disorder.

References

Acsady L. The thalamic paradox. Nat Neurosci. 2017;20(7):901–2.

Alderson-Day B, McCarthy-Jones S, Fernyhough C. Hearing voices in the resting brain: a review of intrinsic functional connectivity research on auditory verbal hallucinations. Neurosci Biobehav Rev. 2015;55:78–87.

Anticevic A, Cole MW, Repovs G, Savic A, Driesen NR, Yang G, et al. Connectivity, pharmacology, and computation: toward a mechanistic understanding of neural system dysfunction in schizophrenia. Front Psychiatry. 2013;4:169.

Anticevic A, Cole MW, Repovs G, Murray JD, Brumbaugh MS, Winkler AM, et al. Characterizing thalamo-cortical disturbances in schizophrenia and bipolar illness. Cereb Cortex. 2014;24(12):3116–30.

Anticevic A, Murray JD, Barch DM. Bridging levels of understanding in schizophrenia through computational modeling. Clin Psychol Sci. 2015;3(3):433–59.

Barch DM. Resting-state functional connectivity in the human connectome project: current status and relevance to understanding psychopathology. Harv Rev Psychiatry. 2017;25(5):209–17.

Birur B, Kraguljac NV, Shelton RC, Lahti AC. Brain structure, function, and neurochemistry in schizophrenia and bipolar disorder-a systematic review of the

magnetic resonance neuroimaging literature. NPJ Schizophr. 2017;3:15.

Bluhm RL, Miller J, Lanius RA, Osuch EA, Boksman K, Neufeld RW, et al. Spontaneous low-frequency fluctuations in the BOLD signal in schizophrenic patients: anomalies in the default network. Schizophr Bull. 2007;33(4):1004–12.

Calhoun VD, Adali T, Pearlson GD, Pekar JJ. A method for making group inferences from functional MRI data using independent component analysis. Hum Brain Mapp. 2001;14(3):140–51.

Calhoun VD, Miller R, Pearlson G, Adali T. The chronnectome: time-varying connectivity networks as the next frontier in fMRI data discovery. Neuron. 2014;84(2):262–74.

Calhoun V, Glahn D, Pearlson G. Finding the elusive psychiatric "lesion" with twenty-first-century neuroanatomy: a note of caution. In: Weinberger DR, Radulescu E, editors. Online comment ed. Schizophrenia Research Forum. 2016.

Cao H, McEwen SC, Chung Y, Chen OY, Bearden CE, Addington J, et al. Altered brain activation during memory retrieval precedes and predicts conversion to psychosis in individuals at clinical high risk. Schizophr Bull. 2019;45(4):924–33.

Clementz BA, Sweeney JA, Hamm JP, Ivleva EI, Ethridge LE, Pearlson GD, et al. Identification of distinct psychosis biotypes using brain-based biomarkers. Am J Psychiatry. 2016;173(4):373–84.

Craddock N, Owen MJ. The Kraepelinian dichotomy - going, going... but still not gone. Br J Psychiatry. 2010;196(2):92–5.

Curcic-Blake B, Ford JM, Hubl D, Orlov ND, Sommer IE, Waters F, et al. Interaction of language, auditory and memory brain networks in auditory verbal hallucinations. Prog Neurobiol. 2017;148:1–20.

Ding Y, Ou Y, Pan P, Shan X, Chen J, Liu F, et al. Cerebellar structural and functional abnormalities in first-episode and drug-naive patients with schizophrenia: a meta-analysis. Psychiatry Res Neuroimaging. 2019a;283:24–33.

Ding Y, Ou Y, Su Q, Pan P, Shan X, Chen J, et al. Enhanced global-brain functional connectivity in the left superior frontal gyrus as a possible endophenotype for schizophrenia. Front Neurosci. 2019b;13:145.

Driesen NR, McCarthy G, Bhagwagar Z, Bloch M, Calhoun V, D'Souza DC, et al. Relationship of resting brain hyperconnectivity and schizophrenia-like symptoms produced by the NMDA receptor antagonist ketamine in humans. Mol Psychiatry. 2013;18(11):1199–204.

Du Y, Pearlson GD, Lin D, Sui J, Chen J, Salman M, et al. Identifying dynamic functional connectivity biomarkers using GIG-ICA: application to schizophrenia, schizoaffective disorder, and psychotic bipolar disorder. Hum Brain Mapp. 2017;38(5):2683–708.

Foss-Feig JH, Adkinson BD, Ji JL, Yang G, Srihari VH, McPartland JC, et al. Searching for cross-diagnostic convergence: neural mechanisms governing excitation and inhibition balance in schizophrenia and autism spectrum disorders. Biol Psychiatry. 2017;81(10):848–61.

Friston KJ, Frith CD. Schizophrenia: a disconnection syndrome? Clin Neurosci. 1995;3(2):89–97.

Giraldo-Chica M, Woodward ND. Review of thalamocortical resting-state fMRI studies in schizophrenia. Schizophr Res. 2017;180:58–63.

Glahn DC, Winkler AM, Kochunov P, Almasy L, Duggirala R, Carless MA, et al. Genetic control over the resting brain. Proc Natl Acad Sci U S A. 2010;107(3):1223–8.

Gonzalez-Castillo J, Bandettini PA. Task-based dynamic functional connectivity: recent findings and open questions. Neuroimage. 2018;180(Pt B):526–33.

Hu ML, Zong XF, Mann JJ, Zheng JJ, Liao YH, Li ZC, et al. A review of the functional and anatomical default mode network in schizophrenia. Neurosci Bull. 2017;33(1):73–84.

Joules R, Doyle OM, Schwarz AJ, O'Daly OG, Brammer M, Williams SC, et al. Ketamine induces a robust whole-brain connectivity pattern that can be differentially modulated by drugs of different mechanism and clinical profile. Psychopharmacology. 2015;232(21–22):4205–18.

Khadka S, Meda SA, Stevens MC, Glahn DC, Calhoun VD, Sweeney JA, et al. Is aberrant functional connectivity a psychosis endophenotype? A resting state functional magnetic resonance imaging study. Biol Psychiatry. 2013;74(6):458–66.

Karbasforoushan H, Woodward ND. Resting-state networks in schizophrenia. Curr Top Med Chem. 2012;12(21):2404–14.

Khalili-Mahani N, Rombouts SARB, van Osch MJP, Duff EP, Carbonell F, Nickerson LD, et al. Biomarkers, designs, and interpretations of resting-state fMRI in translational pharmacological research: a review of state-of-the-art, challenges, and opportunities for studying brain chemistry. Hum Brain Mapp. 2017;38:2276–325.

Liang MJ, Zhou Q, Yang KR, Yang XL, Fang J, Chen WL, et al. Identify changes of brain regional homogeneity in bipolar disorder and unipolar depression using resting-state FMRI. PLoS One. 2013;8(12):e79999.

Lo CY, Su TW, Huang CC, Hung CC, Chen WL, Lan TH, et al. Randomization and resilience of brain functional networks as systems-level endophenotypes of schizophrenia. Proc Natl Acad Sci U S A. 2015;112(29):9123–8.

Lottman KK, Kraguljac NV, White DM, Morgan CJ, Calhoun VD, Butt A, et al. Risperidone effects on brain dynamic connectivity—a prospective resting-state fMRI study in schizophrenia. Front Psychiatry. 2017;8:14.

Meda SA, Gill A, Stevens MC, Lorenzoni RP, Glahn DC, Calhoun VD, Sweeney JA, Tamminga CA, Keshavan MS, Thaker G, Pearlson GD. Differences in resting-state fMRI functional network connectivity between schizophrenia and psychotic bipolar probands and their unaffected first-degree relatives. Biol Psychiatry. 2012;71(10):881–9.

Meda SA, Ruano G, Windemuth A, O'Neil K, Berwise C, Dunn SM, et al. Multivariate analysis reveals genetic associations of the resting default mode network in psychotic bipolar disorder and schizophrenia. Proc Natl Acad Sci U S A. 2014;111(19):E2066–75.

Meda SA, Wang Z, Ivleva EI, Poudyal G, Keshavan MS, Tamminga CA, et al. Frequency-specific neural signatures of spontaneous low-frequency resting state fluctuations in psychosis: evidence from bipolar-schizophrenia network on intermediate phenotypes (B-SNIP) consortium. Schizophr Bull. 2015;41(6):1336–48.

Murray JD, Anticevic A. Toward understanding thalamocortical dysfunction in schizophrenia through computational models of neural circuit dynamics. Schizophr Res. 2017;180:70–7.

Murray JD, Demirtas M, Anticevic A. Biophysical modeling of large-scale brain dynamics and applications for computational psychiatry. Biol Psychiatry Cogn Neurosci Neuroimaging. 2018;3(9):777–87.

Mwansisya TE, Hu A, Li Y, Chen X, Wu G, Huang X, et al. Task and resting-state fMRI studies in first-episode schizophrenia: a systematic review. Schizophr Res. 2017;189:9–18.

Northoff G. The brain's spontaneous activity and its psychopathological symptoms—"Spatiotemporal binding and integration". Prog Neuropsychopharmacol Biol Psychiatry. 2018;80(Pt B):81–90.

Northoff G, Duncan NW. How do abnormalities in the brain's spontaneous activity translate into symptoms in schizophrenia? From an overview of resting state activity findings to a proposed spatiotemporal psychopathology. Prog Neurobiol. 2016;145–146:26–45.

Pearlson GD. Applications of resting state functional MR imaging to neuropsychiatric diseases. Neuroimaging Clin N Am. 2017;27(4):709–23.

Pearlson GD, Calhoun VD. Convergent approaches for defining functional imaging endophenotypes in schizophrenia. Front Hum Neurosci. 2009;3:37.

Pinaya WHL, Mechelli A, Sato JR. Using deep autoencoders to identify abnormal brain structural patterns in neuropsychiatric disorders: a large-scale multi-sample study. Hum Brain Mapp. 2019;40(3):944–54.

Rashid B, Damaraju E, Pearlson GD, Calhoun VD. Dynamic connectivity states estimated from resting fMRI Identify differences among schizophrenia, bipolar disorder, and healthy control subjects. Front Hum Neurosci. 2014;8:897.

Reinen JM, Chén OY, Hutchison RM, Yeo BT, Anderson KM, Sabuncu MR, et al. The human cortex possesses a reconfigurable dynamic network architecture that is disrupted in psychosis. Nat Commun. 2018;9(1157):1–15.

Repovs G, Csernansky JG, Barch DM. Brain network connectivity in individuals with schizophrenia and their siblings. Biol Psychiatry. 2011;69(10):967–73.

Richiardi J, Altmann A, Milazzo AC, Chang C, Chakravarty MM, Banaschewski T, et al. BRAIN NETWORKS. Correlated gene expression supports synchronous activity in brain networks. Science. 2015;348(6240):1241–4.

Scariati E, Padula MC, Schaer M, Eliez S. Long-range dysconnectivity in frontal and midline structures is associated to psychosis in 22q11.2 deletion syndrome. J Neural Transm (Vienna). 2016;123(8):823–39.

Schmidt A, Diwadkar VA, Smieskova R, Harrisberger F, Lang UE, McGuire P, et al. Approaching a network connectivity-driven classification of the psychosis continuum: a selective review and suggestions for future research. Front Human Neurosci. 2015;8:1047.

Sheffield JM, Barch DM. Cognition and resting-state functional connectivity in schizophrenia. Neurosci Biobehav Rev. 2016;61:108–20.

Stephan KE, Iglesias S, Heinzle J, Diaconescu AO. Translational perspectives for computational neuroimaging. Neuron. 2015;87(4):716–32.

Tamminga CA, Pearlson G, Keshavan M, Sweeney J, Clementz B, Thaker G. Bipolar and schizophrenia network for intermediate phenotypes: outcomes across the psychosis continuum. Schizophr Bull. 2014;40(Suppl 2):S131–7.

Tamminga CA, Pearlson GD, Stan AD, Gibbons RD, Padmanabhan J, Keshavan M, et al. Strategies for advancing disease definition using biomarkers and genetics: the bipolar and schizophrenia network for intermediate phenotypes. Biol Psychiatry Cogn Neurosci Neuroimaging. 2017;2(1):20–7.

Unschuld PG, Buchholz AS, Varvaris M, van Zijl PC, Ross CA, Pekar JJ, et al. Prefrontal brain network connectivity indicates degree of both schizophrenia risk and cognitive dysfunction. Schizophr Bull. 2014;40(3):653–64.

van Erp TGM, Walton E, Hibar DP, Schmaal L, Jiang W, Glahn DC, et al. Cortical brain abnormalities in 4474 individuals with schizophrenia and 5098 control subjects via the enhancing neuro imaging genetics through meta analysis (ENIGMA) consortium. Biol Psychiatry. 2018;84(9):644–54.

Wang S, Wang G, Lv H, Wu R, Zhao J, Guo W. Abnormal regional homogeneity as potential imaging biomarker for psychosis risk syndrome: a resting-state fMRI study and support vector machine analysis. Sci Rep. 2016;6:27619.

Wang S, Zhang Y, Lv L, Wu R, Fan X, Zhao J, et al. Abnormal regional homogeneity as a potential imaging biomarker for adolescent-onset schizophrenia: a resting-state fMRI study and support vector machine analysis. Schizophr Res. 2018;192:179–84.

Wang X, Liao W, Han S, Li J, Zhang Y, Zhao J, et al. Altered dynamic global signal topography in antipsychotic-naive adolescents with early-onset schizophrenia. Schizophr Res. 2019;208:308–16.

Weinberger DR, Radulescu E. Finding the elusive psychiatric "lesion" with 21st-century neuroanatomy: a note of caution. Am J Psychiatry. 2016;173(1):27–33.

Whitfield-Gabrieli S, Thermenos HW, Milanovic S, Tsuang MT, Faraone SV, McCarley RW, et al. Hyperactivity and hyperconnectivity of the default

network in schizophrenia and in first-degree relatives of persons with schizophrenia. Proc Natl Acad Sci U S A. 2009;106(4):1279–84.

Wolfers T, Doan NT, Kaufmann T, Alnaes D, Moberget T, Agartz I, et al. Mapping the heterogeneous phenotype of schizophrenia and bipolar disorder using normative models. JAMA Psychiatry. 2018;75(11):1146–55.

Woodward ND, Heckers S. Mapping thalamocortical functional connectivity in chronic and early stages of psychotic disorders. Biol Psychiatry. 2016;79(12):1016–25.

Woodward ND, Karbasforoushan H, Heckers S. Thalamocortical dysconnectivity in schizophrenia. Am J Psychiatry. 2012;169(10):1092–9.

Yip SW, Scheinost D, Potenza MN, Carroll KM. Connectome-based prediction of cocaine abstinence. Am J Psychiatry. 2019;176(2):156–64.

Zhu F, Liu Y, Liu F, Yang R, Li H, Chen J, et al. Functional asymmetry of thalamocortical networks in subjects at ultra-high risk for psychosis and first-episode schizophrenia. Eur Neuropsychopharmacol. 2019;29(4):519–28.

PET and PET/MRI Methods

7

Cristina Lois, Hasan Sari, Amanda B. Sidwell, and Julie C. Price

Contents

C. Lois
Department of Radiology, Massachusetts General Hospital, Boston, MA, USA

Harvard Medical School, Boston, MA, USA

Gordon Center for Medical Imaging, Boston, MA, USA
e-mail: cloisgomez@mgh.harvard.edu

H. Sari · J. C. Price (✉)
Department of Radiology, Massachusetts General Hospital, Boston, MA, USA

Harvard Medical School, Boston, MA, USA

PET Pharmacokinetic Modeling, Athinoula A. Martinos Center, Charlestown, MA, USA
e-mail: HSARI@mgh.harvard.edu; JCPRICE@mgh.harvard.edu

A. B. Sidwell
Department of Radiology, Massachusetts General Hospital, Boston, MA, USA

PET Pharmacokinetic Modeling, Athinoula A. Martinos Center, Charlestown, MA, USA
e-mail: ASIDWELL@mgh.harvard.edu

M. Kubicki, M. E. Shenton (eds.), *Neuroimaging in Schizophrenia*,
https://doi.org/10.1007/978-3-030-35206-6_7

7.1 Introduction

Positron Emission Tomography (PET) is an imaging tool designed to measure biological processes at the molecular and cellular levels. PET obtains functional information related to the state of a particular physiologic process in a non-invasive manner. PET imaging agents are administered in trace amounts that do not perturb the process under study and make use of a radioactive molecular probe that can be followed, mapped and measured using suitable radiation detectors. Because of the high sensitivity of radioactive assays, PET can measure picomolar concentrations. However, the spatial resolution of PET is limited by physical factors and the difficulty of acquiring sufficient counting statistics. Structural magnetic resonance (MR) imaging (or MRI) is often performed in tandem with PET as this modality provides high resolution anatomical information to guide PET image analysis and interpretation.

Although oncology remains the most frequent clinical application worldwide, PET has been extensively used to study the brain, neurodegeneration and neuropsychiatric disorders. For example, early PET studies provided evidence of dysregulation of the dopaminergic system in patients with schizophrenia and of the association between antipsychotic response and blockade of dopamine D2 receptors (Wong et al. 1986; Farde et al. 1987; Okubo et al. 1997).

This chapter provides an overview of PET imaging principles and methods that are important for its successful application in humans. This review describes PET in terms of its characteristics as a molecular imaging tool, with a particular focus on in vivo imaging of protein targets using PET tracers or radioligands that are relevant to schizophrenia and neuropsychiatric disorders. This includes a brief description of PET methods of data acquisition, data correction, and pharmacokinetic methods that are used to image and quantify radioligand-protein binding. The emergence of simultaneous PET/MR imaging is also reviewed in the context of key advantages and limitations of the individual and combined technologies and examples of research advances in this area.

7.2 Positron Emission Tomography

7.2.1 Basic Principles of PET Imaging

After a positron is emitted from the nucleus of an atom inside the body, it travels a few mm in the surrounding tissue and interacts with an electron. As the positron is an antimatter electron, the pair annihilates emitting two 511 keV photons that move away from the annihilation point in nearly 180° opposing directions (annihilation radiation). PET is based on the detection of the two photons coming from each single radioactive decay. The PET scanner (or tomograph) is typically formed by multiple rings of radiation detectors that encircle the organ under study (e.g., brain) and collect the emitted photons. Only pairs of photons recorded by opposite detectors within a narrow few nanosecond time window are considered as coming from the same radioactive decay and, consequently, considered valid for the purpose of image formation (coincident events). Thus each pair of detectors measures the number of coincident events or positron annihilations that occurred somewhere along the line joining them (line of response).

During a PET study, millions of coincidence events are recorded. Through the application of mathematical algorithms, the distribution of the radionuclide inside the organ under study can be reconstructed. If the distribution changes over time, one can capture this by reconstructing the PET data

into multiple time frames throughout the study (i.e., a dynamic study, see Sect 7.5). In order to obtain quantitatively accurate 3D images, several corrections need to be performed to account for lost photons (e.g. due to photon attenuation and to detector dead time) or photons that do not contribute to the signal but instead create background noise (e.g. scatter and random coincidences). For an in-depth explanation of the principles and technology of PET imaging, see (Townsend 2004; Bailey 2003).

The most common design of PET scanners consists of multiple rings of radiation detectors that encircle the subject under study. The axial coverage of the system depends on the number of detector rings and spans from organ specific coverage, e.g., brain (Grogg et al. 2016) to total body coverage (Badawi et al. 2019). Most PET scanners use scintillator crystals for detecting the 511 keV annihilation photons. Scintillators such as bismuth germinate (BGO) or lutetium oxyorthosilicate (LSO) provide high detection efficiency and good energy resolution. Scintillators convert incident gamma photons (such as those produced by positron annihilation) into visible light. The size of the scintillator crystals is optimized as a trade-off between detector spatial resolution and the collection of sufficient counting statistics. The scintillators are coupled to light-detection devices (photodetectors) that convert the visible scintillation light into an electrical signal that is subsequently processed by the system electronics. Until recently, photomultiplier tubes (PMTs) were generally used. However, their incompatibility with magnetic fields have led to their replacement by solid-state photodetectors in state-of-the-art PET systems.

PET spatial resolution is poor compared to other imaging modalities such as CT or MR imaging, with the spatial resolution of current PET tomographs on the order of 3–6 mm at best (de Jong et al. 2007; Zhang et al. 2018; Rausch et al. 2017; Michopoulou et al. 2019; Pan et al. 2019). This is because of several factors. In PET tomographs that use scintillator-photodetector coupling, the size of the individual crystals generally determines the detector spatial resolution. Another factor is the distance the positron travels in tissue (positron range) prior to annihilation, and this depends on the particular radionuclide. Since PET maps the distribution of annihilation points instead of the distribution of positron emission points, the positron range will result in image blurring. For common PET radionuclides (e.g.: fluorine-18, carbon-11, and oxygen-15), this effect is less than 2.5 mm (Moses 2011). Acolinearity (photons emitted slightly less than 180°) also degrades spatial resolution (typically about 1.5 mm full-width at half-maximum for fluorine-18). Overall, physical effects contribute around 2 mm or less (Townsend 2004).

Photons emitted in the body interact with tissue and this results in photon scatter (introduces noise) and attenuation (causes signal reduction). The PET data must be corrected for these effects. As an example, correction for attenuation has traditionally required measurement of the subject's attenuation characteristics using an external radiation source (transmission source) or X-ray computed tomography (CT). These topics are discussed at length in prior publications (Watson 2000; Zaidi and Montandon 2007).

7.3 Image Processing: Additional Corrections and Applications

7.3.1 Motion Correction

Head motion during long PET acquisitions can degrade image quality and cause artifacts. Interframe motion can cause PET frames to displace over time and lead to errors in generated regional measurements. Several methods have been suggested to correct for motion artifacts before any PET quantification is performed. The simplest of these methods involves registration of individual frames to a reference frame (Picard and Thompson 1997). With the introduction of combined PET/MR scanners, more sophisticated motion correction methods have been proposed that utilize simultaneously acquired MR data to derive motion estimates with high temporal resolution that are then used to correct for motion during image reconstruction (Catana et al. 2011). MR guided motion correction methods were shown to improve the quality of the PET images and to positively impact image quantification in dementia patients (Chen et al. 2018).

7.3.2 Partial Volume Correction

As described above, PET tomographs have limited spatial resolution due to physical factors and the detection process. In addition, PET image reconstruction methods sample an activity distribution into a finite voxel grid that causes a three-dimensional blurring throughout the image. The limited spatial resolution of the tomograph can be characterized using a point spread function (PSF), which represents the response of the PET system to a radioactivity point source (Erlandsson et al. 2012).

As a result, PET images suffer from partial volume (PV) effects that can lead to spill-in or spill-out of the activity in one voxel to neighboring voxels. Spill-in effects from neighboring high activity areas can cause overestimation of the radioactivity in regions of interest (ROI). Similarly, spill-out effects of the radioactivity in the target region to background regions can cause underestimation of the tracer uptake in the target ROI. Therefore, it is often advised to account for these effects using a suitable partial volume correction (PVC) technique before any quantitative PET measurement is performed, particularly when small ROIs are studied.

A number of methods have been proposed to correct for PV effects. Most of these methods rely on anatomical information obtained from co-registered structural MR images to recover the PET radioactivity concentrations in the ROIs. Three common methods are described. The Meltzer method segments the brain into two compartments (Meltzer et al. 1990). One is a combination of grey (GM) and white matter (WM), and the second is cerebrospinal fluid (CSF). No uptake is assumed in the CSF. The PV correction recovers the brain tissue signal by correcting for spill over signal in the CSF. This method is limited to correct for CSF and atrophy-related PV effects. The Muller-Gartner method (Muller-Gartner et al. 1992) extends this method and also accounts for spill-over effects between GM and WM. Here, a co-registered MR image is segmented into GM, WM and CSF. The two latter regions are treated as the background regions. Similar to the Meltzer method, CSF is assumed to be devoid of any uptake and WM is assumed to have a homogeneous tracer distribution. The correction is applied to account for spill out effects from GM to background regions and spill-in effects from WM to GM. Muller-Gartner method is sensitive to GM and WM segmentation errors that can propagate into noise in the corrected images. This correction is restricted to voxels in the target region only.

The Geometric Transfer Matrix (GTM) method (Rousset et al. 1998) utilizes an MR image segmented (or parcellated) into a group of ROIs. Each ROI is assumed to contain uniform activity and is represented by its mean value. Each ROI is convolved with the PSF and the contribution of each region to the neighboring regions is calculated. These data are then used to construct the GTM matrix and its inverse is used to calculate the true regional mean values. The main limitation of the GTM method is that it provides regional mean values rather than a PV corrected image, and hence it is only useful if the analysis is performed on regional basis.

7.3.3 Image Registration and Normalization

Image registration is the process of geometrically aligning two or more images of the same subject that can be obtained at different times or using different imaging modalities. During the registration of two images, an optimization procedure is performed to find the best transformation to spatially align the "input" image to a "reference" image. The types of transformations that are commonly used in intramodal image registration are rigid and affine transformations. Rigid transformation has 6 degrees of freedom and involves translation and rotation of the image around each axis. Application of rigid registration includes PET inter-frame motion correction where PET frames are registered to a reference frame, e.g., the first time frame of the series. Affine transformation has extra parameters to apply scaling and shearing on the input images and is often used to perform inter-modality registrations, such as registering PET images to MR images. Non-rigid transformation is often used to register images obtained from different subjects, where a local warping is applied to image features. An example use of non-rigid transformation is warping of brain images to a common template space, such as the MNI template (Collins et al. 1995), before performing inter-subject com-

parisons. Normalization refers to the spatial transformation of an individual's PET and/or MR image (native space) to an anatomical MR image template (template space). This is often performed to enable automatic regional labeling or parcellation of an MR image using pre-defined template regions and non-rigid registration methods. Region delineation is also possible through manual region tracing or automatic parcellation of the native space MR image. The extracted regions can be then used to sample co-registered PET images to obtain regional PET uptake values or to generate time activity curves (TAC) of the regional uptake collected over several time frames (Fig. 7.1). Software packages such as Freesurfer (Fischl 2012), FSL (Jenkinson et al. 2012) and SPM (Friston 2007) include tools for image registration and normalization.

7.4 Molecular Imaging with PET

7.4.1 Positron-Emitting Radionuclides

The most commonly used positron-emitting radionuclides for PET have short characteristic half-lives ($t_{1/2}$), where $t_{1/2}$ is the time that it takes for a radioactive sample to reduce to half of its original value. The most important positron emitters in PET brain imaging are fluorine-18 ($t_{1/2}$ = 109.8 min), carbon-11 ($t_{1/2}$ = 20.36 min), nitrogen-13 ($t_{1/2}$ = 9.97 min) and oxygen-15 ($t_{1/2}$ = 2.03 min). These radionuclides must be generated using a cyclotron, which is generally located within or near the PET center as a result of the short half-lives of these atoms. Because of the longer half-life of fluorine-18 PET radiotracers, these may be produced by off-site cyclotrons and regionally distributed.

In vivo imaging with PET can be performed at high sensitivity enabling the detection of low in vivo concentrations. With respect to protein targets, PET can also be performed with high molecular specificity and selectivity. A multitude of molecular imaging options that are important targets for the study of schizophrenia and other neuropsychiatric disorders are possible using PET (Table 7.1). Examples include numerous neurore-

Table 7.1 Examples of PET radioligands applied in neuropsychiatric disorders

Neuroreceptor/transporter	
$GABA_A$	[^{11}C]flumazenil, [^{18}F] flumazenil,
Glutamate (mGluR5)	[^{11}C]ABP688, [^{18}F]FPEB
Acetylcholine	
Muscarinic	[^{11}C]NMPB
Nicotinic	2-[^{18}F]-FA-85380 ($\alpha4\beta2$)
Vesicular monoamine transporter-2	[^{11}C]DTBZ, [^{18}F]AV-133
Dopamine	
DA synthesis	[^{18}F]FDOPA
$D_{2/3}$	[^{11}C]FLB 457, [^{18}F]fallypride
	[^{11}C]raclopride
	[^{11}C]NPA, [^{11}C]PHNO (agonists)
Transporter/ reuptake site	[^{11}C]CFT, [^{11}C] methylphenidate, [^{11}C] cocaine, [^{11}C]altropane [^{18}F]FP-CIT, [^{18}F]FECNT
Serotonin	
5-HT_{1A}	[^{11}C]WAY 100635, [^{18}F]MPPF
5-HT_{2A}	[^{11}C]MDL 100907, [^{18}F] altanserin
5-HT_{1B}	[^{11}C]AZ10419369
5-HT_4	[^{11}C]SB207145
Transporter/ reuptake site	[^{11}C]DASB, [^{11}C]McN5652
Norepinephrine transporter	[^{11}C]MeNER, [^{18}F]MeNER, [^{11}C]MRB
Cannabinoid (CB-1)	[^{11}C]OMAR, [^{18}F]MK9470
Purinergic receptor	
$P2X_7$	[^{11}C]A-740003, [^{11}C] SMW139, [^{11}C]JNJ-54173717
Enzyme activity	
Acetylcholinesterase	[^{11}C]PMP
Monoamine oxidase (MAO-A, MAO-B)	[^{11}C]clorgyline (A), [^{11}C] deprenyl (B)
Histone deacetylase	[^{11}C]martinostat
Phosphodiesterase (PDE)	
PDE4	[^{11}C]rolipram
PDE10	[^{11}C]IMA107, [^{11}C]MNI659
Fatty acid amide hydroxylase (FAAH)	[^{11}C]curb
Cyclooygenase	[^{11}C]PS13 (COX-1); [^{11}C] MC1(COX-2)
Microglial activation (TSPO)	
	[^{11}C]PK11195, [^{11}C]PBR28, [^{11}C]ER176,
	[^{11}C]PBR06, [^{18}F]PBR06,
	[^{18}F]DPA-714, [^{18}F]FEPPA

See (Gunn et al. 2015) and (Narayanaswami et al. 2018) for a detailed description of PET protein targets, relevance to disease, and corresponding literature references

ceptor system targets (e.g., presynaptic and postsynaptic sites, transporter/reuptake sites, vesicular transporters, ion channels), enzymes, and translocator proteins (TSPO). Multiple intra-subject PET imaging studies can provide a rich assessment of patient status that can inform on neuroreceptor system status in health and disease, complementary assessments of neuroinflammatory processes (e.g., TSPO, COX-1/COX-2, $P2X_7$), or enzyme activity (e.g., MAO-B, HDAC).

Further detail on PET protein targets relevant to schizophrenia and neuropsychiatric disorders are available in prior publications (Gunn et al. 2015; Narayanaswami et al. 2018).

7.5 PET Pharmacokinetics

7.5.1 Tracer Principle

PET methods enable quantitative in vivo imaging of ligand-binding interactions through application of the tracer principle. As mentioned above, a tracer molecule follows a substance through a process-of-interest (Lassen and Perl 1979). Tracer studies are conducted at high radioligand molar activity (A_m), where A_m is proportional to GBq/μmol (or mCi/μmol). High A_m ensures minimal binding site occupancy by non-radioactive (or unlabeled) mass. The term tracer or radiotracer refers to the general class of PET probes that include blood flow and glucose metabolism, whereas the term radioligand specifically refers to a ligand-protein binding interaction (e.g., neuroreceptor) (Fig. 7.1).

A fully dynamic tracer kinetic PET study follows the tracer behavior from its injection (delivery kinetics) to the end of the study (dominated by process-of-interest), and thus, enables multiple parameters to be studied. Validated simplifications of fully dynamic methods can be more feasible to apply but fewer parameters can be studied (Carson 2003). In a tracer kinetic PET study, the radiotracer is administered to the subject, the radiotracer concentration is measured in blood (or plasma) and in brain over time, and tracer kinetic modeling methods are applied to analyze the kinetic data and obtain estimates of the physiological parameters (Fig. 7.2). There are various methodological assumptions that apply to these studies (Carson 2003; Laruelle et al. 2003). One such assumption is tracer linearity, i.e., the observed kinetics of the tracer are directly related to the dynamics of the process under study (e.g., at high A_m). From this point on, we will assume that radioligand-protein binding is the process-of-interest and studies are conducted at high A_m.

7.5.2 Radiotracer/Radioligand Administration

There are two principal modes of tracer administration commonly used in PET imaging of brain. Bolus injection is the rapid delivery of tracer into the system and the system response is included in the tracer kinetics (Erlandsson et al. 2012). In contrast, bolus plus infusion (B + I) administration is a combination of an initial bolus injection followed by infusion of the radiotracer. The B + I method yields radiotracer concentrations that eventually reach a constant value, consistent with a spatially invariant distribution of tracer (Lassen and Perl 1979; Carson 2003; Huang et al. 1986). When tracer levels in blood and brain become constant, equilibrium conditions are assumed. The bolus method can provide multiple parameters associated with the process-of-interest, while the B + I method generally provides a single equilibrium measure.

7.5.3 Data Collection: Blood/Plasma and PET

For tracer kinetic modeling studies, blood data are commonly collected from a radial artery (arterial blood sampling) in an effort to approximate capillary concentration. The blood collection schedule depends on the particular method (fully quantitative or simplified). Blood data can be collected continuously using a flow-through monitoring system that measures radioactivity concentration or by discrete sampling (e.g., hand-drawn samples) with subsequent assay of plasma samples in a gamma well counter. Radioactivity concentration units are proportional to MBq/mL (or Ci/mL).

After injection, radioligands can be broken down by the body to create radiolabeled metabolic products (radiometabolites). In these cases, additional

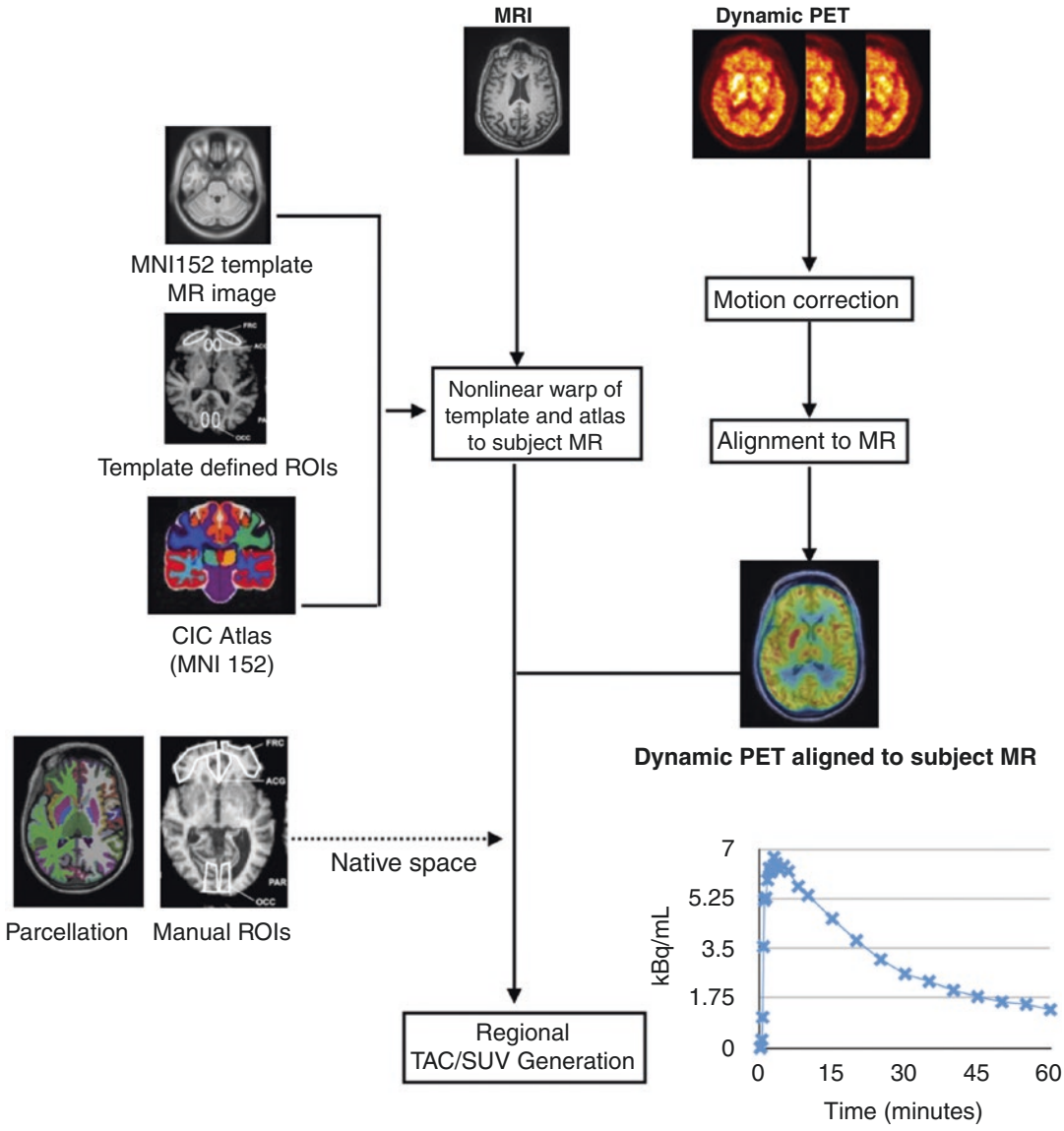

Fig. 7.1 Flowchart representation of ROI delineation and PET sampling methods to derive regional TAC and SUV (standardized uptake value) measurements. ROIs can be defined on a brain image template or in the subject's native image space. ROIs can be defined manually or automatically derived with the help of a brain atlas (e.g., CIC atlas,Tziortzi et al. 2011). ROIs can also be defined using imaging toolboxes to automatically parcellate (e.g. Freesurfer software) the brain into cortical and subcortical regions in the native space. The PET image data (static or dynamic) can be sampled in native space or template/atlas space provided that the MR, PET, and ROIs are in the same space

blood is collected and analyzed using chromatographic methods to determine the fraction of the total radioactivity in blood, or plasma, that corresponds to the parent radioligand (parent fraction) at different times over the study interval. The concentration of parent radioligand in blood or plasma (input function) over time is determined by correcting the total radioactivity concentration for the radiometabolite fraction. It is important also to consider and evaluate whether radiometabolites can be produced in brain or pass into brain. Other measures include the extent that a radioligand may bind to plasma proteins (f_p) and partitioning of the radiotracer in the red cell fraction (Innis et al. 2007).

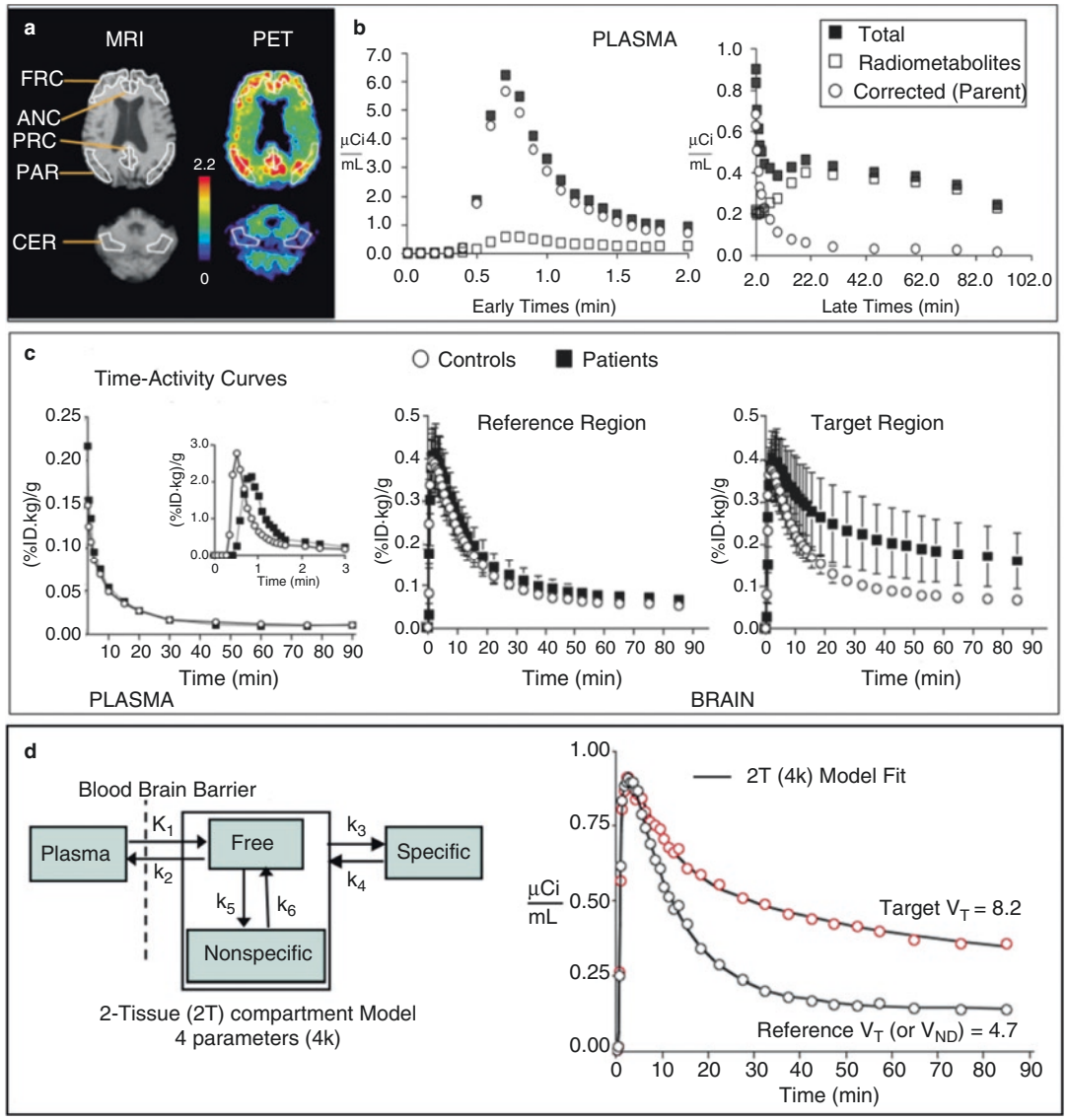

Fig. 7.2 Kinetic analysis steps for a dynamic PET radioligand-protein binding study conducted in control and patient groups. (**a**) Co-registration of anatomical MR and functional PET images with ROI labels. (**b**) Example of the total measured radioactivity concentration in plasma (i.e., unmetabolized parent (decreases over time) + radiolabeled metabolites (increases over time)). The total plasma radioactivity is corrected to yield a metabolite-corrected plasma input function (**c**, left) that is used for kinetic modeling analyses of the TACs with examples shown for target and reference ROIs (**c**, middle and right). (**d**) Application of a 2-tissue 4 parameter model (left) using the metabolite corrected plasma input function results in a curve fit (solid line) to the in vivo kinetics in target and reference ROIs (right) and estimates of the volume of distribution measure, V_T

For a dynamic PET study, data are acquired in multiple time frames. As an example, a 90 min dynamic PET acquisition can consist of 34 time frames (e.g., 4 × 25, 8 × 30, 9 × 60, 2 × 180, 8 × 300, and 3 × 600 s). Short frames at early times can capture rapid changes in radioligand uptake and distribution when counting statistics are high. Longer time frames at later times are appropriate when the kinetics are changing less rapidly and higher counting statistics are sought

to offset the impact of radioactive decay. The units of the PET scanner image data, or voxels, can be basic scanner units (scanner counts/s/pixel) or units of radioactivity concentration kBq/mL, depending on the calibration approach (Geworski et al. 2002, 2003).

7.5.4 Kinetic Modeling Methods: Radioligand-Protein Binding

Mathematical and statistical methods are used to determine parameters-of-interest from the kinetic data. These methods can be generally categorized as compartmental and non-compartmental approaches (Gunn et al. 2015; Carson 2003; Koeppe 2002; Landaw and DiStefano 1984); this section will focus on compartmental modeling techniques. These PET methods have evolved from early studies of blood flow and metabolism.

Compartmental methods involve the formulation of a compartmental model that is configured based on *a priori* knowledge of the chemical and physiological characteristics associated with the process-of-interest. A compartment represents a space, or volume, that the tracer is distributed in that can be of physical (precursor pool) or chemical relevance (metabolized tracer) (Huang and Phelps 1986). Rate constants (internal parameters) link compartments and represent the various rates of inter-compartmental tracer exchange. In this chapter, it is generally assumed that the amount of tracer leaving a compartment is proportional to the total amount in the compartment, all injected tracer exists in one or multiple compartments, and the tracer is uniformly distributed within any given compartment. The validity of a compartmental approach rests on the validity of such assumptions, and others that may involve tracer administration, pharmacological and metabolic properties of the radiotracer, and tracer extraction from vasculature into tissue. Compartmental modeling allows for the study and prediction of process behavior through computer simulation studies that essentially solve the model equations over a series of rate constant values that correspond to different system responses.

PET pharmacokinetic modeling studies provide in vivo outcome measures that are theoretically related to the total concentration of binding sites and inversely related to the affinity of the tracer for the binding site (i.e., B_{max} and K_D, respectively). The nomenclature used herein is that published for reversible radioligand binding (Gunn et al. 2015; Innis et al. 2007). In reality the outcomes are related to the concentration of binding sites not occupied by endogenous ligands and/or freely available for ligand-binding (B_{avail}). The quantitative evaluation of the in vivo kinetics of a novel PET radioligand is generally performed using a bolus injection compartmental modeling approach that requires arterial sampling of the radioligand concentration in plasma to determine the model input (drives in vivo brain kinetics). The most commonly applied model for reversible radioligand binding is a 2-tissue 4-parameter (2T-4k) configuration that describes (1) non-displaceable (ND) uptake of free (FT) and nonspecifically (NS) bound ligand in tissue, with summed concentration of C_{ND} and (2) specifically bound ligand in tissue, with concentration C_S. The concentration of free radioligand in tissue is C_{FT} and $C_{ND} = C_{FT} + C_{NS}$ with compartmental rate constants of K_1 (mL cm^{-3} min^{-1}) and k_2 (min^{-1}) that represent bidirectional blood-brain barrier (BBB) transport of radiotracer, while k_3 (min^{-1}) and k_4 (min^{-1}) are respectively reflective of the bimolecular association to and unimolecular dissociation from the binding site. When $k_4 \approx 0$, the radioligand exhibits irreversible binding. The total radioligand distribution volume is $V_T = V_{ND} + V_S$, defined as the tissue:plasma concentration ratio at equilibrium. A 3-tissue configuration is the most comprehensive approach commonly applied for which FT and NS tracer kinetics are assumed to be distinguishable ($C_T = C_{FT} + C_{NS} + C_S$), while a 2T assumes these are indistinguishable ($C_T = C_{FT+NS} + C_S$), and a 1-tissue model does not distinguish either ($C_{FT+NS+S}$).

Specific binding measures include the total volume of distribution (V_T) and binding potential (BP, unitless). The 2T-4k model $V_T = K_1/k_2*(1 + k_3/k_4)$, $k_3 = f_{ND}\, k_{on}\, B_{avail}$, and $BP_{ND} = k_3/k_4 = f_{ND}\, B_{avail}/K_D$. The f_{ND} parameter, or tissue free fraction, is the fraction of radioligand free from

nonspecific binding. The BP can also be derived from the regional V_T values. Expression of the V_T of binding regions relative to V_{ND} results in a distribution volume ratio, or DVR = V_T/V_{ND}, where BP_{ND} = DVR − 1. The V_{ND} is estimated in a reference region for which specific radioligand binding is assumed to be negligible and concentrations of FT and NS radioligand are representative of other brain regions, e.g., cerebellum is commonly used for neuroreceptor studies. Gunn et al. provide further discussion of reference region applications (Gunn et al. 2015).

7.5.5 Non-compartmental Methods

Non-compartmental methods do not involve specific assumptions as to the internal behavior of the tracer. These techniques include those that mathematically unfold (deconvolve) the input function from the total brain kinetics to obtain the tissue response curve (e.g., spectral analysis). Non-compartmental techniques generally do not require as many assumptions as compartmental methods but are limited if specific information about the kinetic parameters (Gunn et al. 2015; Cunningham and Jones 1993). Graphical analyses offer linear alternatives for neuroreceptor binding studies, using either plasma or reference region data, provided steady-state conditions are established. The Patlak analysis is applied to obtain measures of the overall uptake for an irreversibly binding radioligand, $K_i = K_1k_3/(k_2 + k_3)$ (mL cm^{-3} min^{-1}), but this outcome can be confounded by blood flow. The Logan analysis provides a measure of the total distribution volume (V_T) and is applied to reversible radiotracers to obtain DVR or BP_{ND} measures (Logan 2000). Bias can arise in the outcomes determined using the Logan analysis as a result of noise in the regression variables (Slifstein and Laruelle 2000). Smoothing of the data prior to analysis can address this bias (Logan et al. 2001), although alternative methods that are less vulnerable to noise have been implemented (Ichise et al. 2002). Simple ratios, i.e., tissue:plasma and target:reference, have also been used as outcome measures when strongly related to kinetic binding measures. The SUV, standardized uptake value, is often used in clinical settings and is the average tissue uptake (over a pre-defined post-injection period) normalized to injected dose and body mass (unitless, assuming 1 g cm^{-3} tissue density). The SUV ratio (or SUVR) is simply the target:reference tissue ratio.

7.5.6 Image Derived Input Functions

Kinetic analysis of PET data requires an accurate knowledge of the concentration of the free tracer in the blood plasma, known as the arterial input function (AIF). The current gold standard method to obtain the AIF involves collection of serial blood samples during the course of the PET scan. However, this method's invasiveness makes it not feasible for routine clinical imaging. A non-invasive alternative is the use of an image derived input function (IDIF), which involves extraction of the AIF by measuring the tracer activity in the blood from PET images. This can simply be performed by placing an ROI on a suitable artery and calculating the mean activity within the ROI at each time frame. However, particularly in brain imaging, arteries can be very small in diameter compared to the resolution of the reconstructed PET images and can severely suffer from partial volume effects. Therefore, IDIF methods often utilize registered MR images with higher spatial resolution to obtain an accurate segmentation of the carotid arteries and perform spill-in and spill-out correction based on the geometry of the segmented arteries. See (Fig. 7.3). Fung and Carson (2013) and Su et al. (2013) showed that MR defined carotid arteries could be used to derive an accurate IDIF in [^{15}O]water PET studies. Similarly, a PV corrected IDIF based on MR segmentations may be accurately used to estimate cerebral metabolic rates of glucose (CMRGlc) from [^{18}F]FDG PET images with a comparable accuracy to using AIFs measured from arterial samples (Sari et al. 2017; Sundar et al. 2018). IDIFs might have limited application for a high number of PET radiotracers, particularly when radiolabeled metabolite products are present in

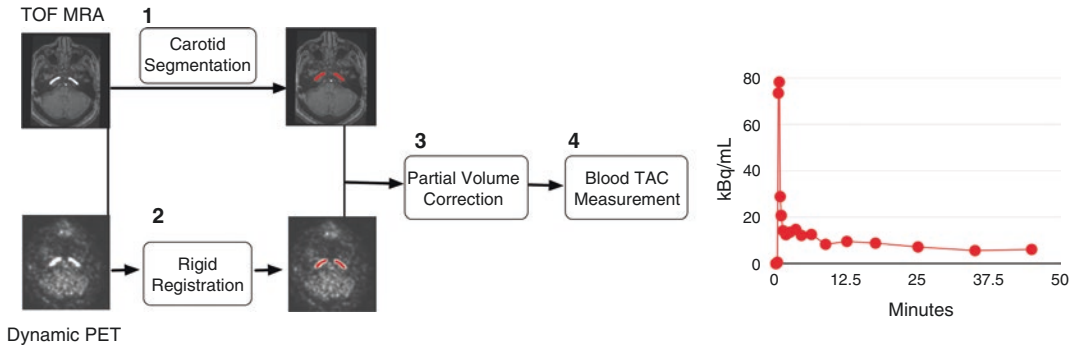

Fig. 7.3 Illustration of a method used to obtain image derived input functions from PV corrected PET images. Carotid arteries are segmented from time-of-flight MR angiography (TOF MRA) images. PV correction is performed on co-registered dynamic PET data using the carotid artery mask as the only region of interest. The mean activity in carotids is computed to derive the IDIF

the blood plasma. One alternative method to obtain the metabolite-free AIF is the simultaneous estimation method (SIME), which models the AIF using a parametric model and tries to estimate the input function while fitting multiple tissue TACs at once (Feng et al. 1997; Ogden et al. 2010). As a result of high number of parameters and its computational complexity, SIME can introduce some bias on the estimated kinetic parameters and is usually complemented with a few arterial samples to aid the AIF estimation (Feng et al. 1997; Wong et al. 2001). More recent work proposed that information from an image derived whole blood measurement can be used as a prior information to improve the accuracy of the estimated AIF and kinetic parameters (Sari et al. 2018).

7.5.7 Challenge Paradigms and Target Engagement

A challenge paradigm may be pharmacological (e.g., amphetamine, agonist or antagonist), task-oriented (e.g., reward to induce increases in extracellular dopamine), or physical (e.g. pain to induce changes in the opioid receptor system (Wey et al. 2014)). As recently reviewed (Gunn et al. 2015), these paradigms usually require a baseline PET study and a challenge PET study that may be performed on the same day (for ^{11}C-labeled radioligands) or within a few days. For studies investigating receptor or protein target engagement (or occupancy), these studies may be conducted over several days, often in non-human primates. These paradigms (Laruelle 2000) have been widely applied to probe the dopamine hypothesis and the monoamine hypothesis of depression which, in the context of schizophrenia, motivated investigations of neuroreceptor system function as PET radioligands became available with sufficient in vivo selectivity and specificity and varying pharmacologic properties (e.g., agonists and antagonists). Radiotracers for monoamine transporters have also been effectively used in drug development for in vivo estimates of the occupancy of therapeutic agents (Gunn et al. 2015; Laruelle 2000; Talbot and Laruelle 2002).

7.6 Multimodal PET/CT and PET/MR Systems

One of the main difficulties in PET imaging is the limited anatomical information, which makes interpretation of the precise location of radiotracer accumulation challenging. Non-specific tracers such as [^{18}F]FDG provide limited anatomical reference from uptake in brain, muscle, etc., but frequently is not enough to differentiate normal from pathological accumulation. This limitation can be overcome by combining PET with another imaging technology able to provide high-

resolution anatomical reference, such as CT or MR imaging.

Multimodal PET/CT scanners were introduced commercially in 2001 and turned into a huge success that led to the cease of production of PET stand-alone systems. In addition to the obvious advantage of precise co-registration of functional and anatomical images, PET/CT provides two other major advantages: reduced scan duration and reduced noise of the PET images (Kinahan et al. 1998; Valk et al. 2003). As mentioned above, a number of annihilation photons lose energy due to scattering or are absorbed in the body before reaching the detectors, resulting in photon attenuation. In stand-alone PET systems, an external 511 keV radiation source is rotated around the subject (transmission scan). By measuring the number of transmission counts both in the presence and absence of the patient, the attenuation can be measured for each line of response and its effect corrected in the PET images. The transmission scan is lengthy and increases the total scan time. This correction is in principle exact, as it employs gamma rays of the same energy (or very similar) as those emitted from positron annihilations. However, as the measurement involves photon counting statistics, the correction introduces additional noise into the PET data. In PET/CT, the attenuation correction is performed by substituting the transmission scan by a CT scan. Although the underlying principles are the same, the CT scan is acquired at lower energy, typically at 120 keV instead of at 511 keV. Because the attenuation of the photons is dependent on their energy, the correction factors obtained with low-energy CT photons must be scaled to 511 keV for accurate correction of the PET images. The scaling is based on piecewise linear functions that cannot account for nonlinear effects, such as those occurring when CT photons are fully absorbed at metal and/or dental implants. On the other hand, the CT produces a very high flux of photons, which in turn dramatically reduces the noise associated with the measurement, and is very fast (Kinahan et al. 1998, 2003).

Even though combined PET/CT systems were introduced almost two decades ago, the technology has undergone continued development with the goal to achieve higher sensitivity and higher resolution capabilities. New scintillator crystals, new solid-state photodetectors and electronics, new detector designs, increased number of detector rings, the introduction of time-of-flight (TOF) information, new reconstruction algorithms, and sophisticated corrections have transformed the technology and led to the achievement of increased signal and exceptional image quality. Some examples of systems incorporating advanced technology are described in (Badawi et al. 2019; Daube-Witherspoon et al. 2010; Jakoby et al. 2011; van Sluis et al. 2019).

However, for brain imaging applications, structural MR offers advantages over CT imaging such as higher gray/white matter contrast. Some MR imaging sequences can, furthermore, provide information about physiology, metabolism, or function by making use of a number of endogenous contrasts and physical properties of matter (Pyatigorskaya et al. 2014). These include sequences to measure water diffusion, blood oxygenation level dependent contrast (BOLD), spectroscopic analysis of brain metabolites, and blood flow/perfusion using dynamic susceptibility contrast (DSC) or arterial spin labeling methods (Catana 2017). As an additional advantage over CT imaging, MR imaging does not employ ionizing radiation thus avoiding risks associated with radiation exposure. Although the combined visualization of PET and MR images acquired separately has been possible for a long time with the aid of co-registration software, the simultaneous acquisition of the two imaging modalities offers additional advantages such as the temporal correlation of the measurements, improved spatial registration, potential for MR-based motion correction of PET data, and improved workflow and patient's comfort.

Simultaneous PET/MR scanners for human imaging were introduced commercially in 2010 by Siemens (Biograph mMR (Delso et al. 2011)), followed more recently by General Electric (SIGNA PET/MR (Levin et al. 2016)). Both system designs include a 60-cm bore 3 tesla (3T) superconductive magnet with the PET components inserted between the body radiofrequency coil and the gradient set. Both PET/MR systems

are based on solid-state photodetectors, but only the SIGNA has TOF capability. Although the incorporation of TOF results in improved signal-to-noise ratio compared to the standard non-TOF images, the benefit is dependent on the size of the object being imaged and is, therefore, limited in the brain compared to other body areas such as the abdomen (Lois et al. 2010).

The development of simultaneous PET/MR systems had to overcome a number of technical challenges comprising both the PET and MR subsystems (Rausch et al. 2017; Catana 2017; Beyer et al. 2010). Traditionally, most PET scanners used photomultiplier tubes (PMTs) to convert the scintillation light into an electrical signal. PMTs are, however, very sensitive to magnetic fields and thus do not work properly inside a MR device. Current simultaneous PET/MR systems have circumvented this issue by substituting PMTs by MR-compatible solid-state photodetectors (Pichler et al. 1977; Catana et al. 2008; Judenhofer et al. 2008; Yamamoto et al. 2011; Hong et al. 2008), such as avalanche photodiodes (APDs) in the Biograph mMR and silicon photomultipliers (SiPMs or Geiger mode APDs) in the Signa PET/MR. In addition, solid-state photodetectors are very small compared to standard PMTs and facilitate the design of compact detector modules. This characteristic is of great importance, as simultaneous PET/MR systems require the placement of the PET detectors in the MR bore. Due to this localization, the PET and MR sub-systems can cause mutual interference if not carefully designed: the PET performance can be affected by the high static magnetic field, gradient fields, and radiofrequency fields; the MR performance can be affected by electromagnetic interference in the radiofrequency by the PET electronics or magnetic field inhomogeneities caused by the PET components. As an additional consideration, the MR radiofrequency coils have to be designed to minimally attenuate the 511 keV PET photons since they are located in the PET field of view.

Finally, a major challenge in combined PET/MR is determining the necessary attenuation correction factors for the PET emission data. Due to lack of space, PET/MR scanners cannot fit the transmission hardware inside the MR bore, and transmission data from a CT is not available either. Therefore, the correction factors have to be derived from the MR data. However, since the MR signal depends on proton density and tissue relaxation and does not provide the information needed for attenuation correction (electron density), the attenuation correction factors have to be derived by other means. Among the different methods proposed to perform attenuation correction in PET/MR, there are algorithms based on segmentation, on atlases, machine learning, and on the simultaneous reconstruction of emission and attenuation data (Izquierdo-Garcia and Catana 2016; Chen and An 2017). Clinical scanners favor segmentation methods: a segmentation of the anatomical MR scan assigns each voxel to a tissue type and each tissue type to a predetermined attenuation value. Current clinical scans use only a few tissue types and often misclassify bone as soft tissue (Martinez-Moller et al. 2009). Ladefoged et al. recently published a comprehensive comparison of different attenuation correction methods in brain PET/MR (Ladefoged et al. 2017). A total of 11 different algorithms, including two used clinically, were compared using CT-based attenuation correction as the reference standard. The authors found that the evaluated methods provided results very similar to a CT-based attenuation correction (within ±5% in about 80% of the brain volume). The authors concluded that the challenge of improving the accuracy of MR-based attenuation correction in adult brains with normal anatomy was solved to a quantitatively acceptable degree.

The potential to leverage the strengths of both PET and MR amid the limitations of each imaging modality is the unique advantage of simultaneous PET/MR imaging, particularly for brain (Fig. 7.4). The combined modality enables a high degree of spatial registration between the PET and MR images and application of advanced MR-guided motion and partial volume correction methods for PET, as mentioned above. Figure 7.5 shows example PET images of the histone deacetylase inhibitor, [^{11}C]martinostat, acquired in a healthy control subject, as part of a study of epigenetics in schizophrenia (Gilbert et al. 2019). The images were acquired on the dedicated

Positron Emission Tomography (PET)

Advantages:

- Sensitivity and molecular specificity of PET coupled with rational radiotracer design and kinetic modeling methods enable quantification of physiological parameters in brain, from BBB transport to specific ligand–protein binding interactions (nM to pM concentrations)

Limitations:

- Limited spatial and temporal resolution (relative to MRI).
- Expense and labor needed to generate positron-emitting radionuclides on-site (mitigated somewhat by radiopharmaceutical distributors)

Magnetic Resonance Imaging (MRI)

Advantages:

- Excellent soft tissue contrast and exquisite spatial resolution for anatomical imaging and capability to assess function, e.g. diffusion-weighted imaging, dynamic contrast-enhanced imaging, fMRI, MR spectroscopy

Limitations:

- Limited sensitivity for direct imaging of physiological processes using basic hydrogen proton MRI contrasts because of the abundance of hydrogen in water in the body (relative to PET)
- Expense of cryogen-based imaging systems

Fig. 7.4 Key advantages and limitations of PET and MR imaging

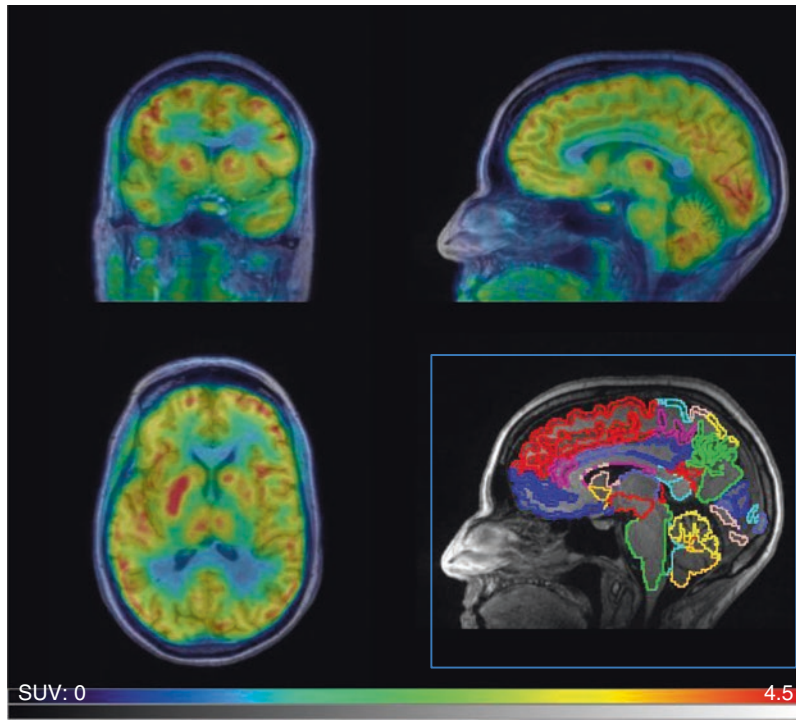

Fig. 7.5 Example of PET/MR imaging of histone deacetylase activity (HDAC) using [^{11}C] martinostat. Orthogonal views of the [^{11}C] martinostat SUV images (averaged 60–90 min post-injection) are overlaid on the T1-weighted 3 T structural MR image (MPRAGE). Also shown are edges of the regional Freesurfer parcellations determined using the MPRAGE image data. The PET and MR images were simultaneously acquired on the Siemens BrainPET that is a dedicated PET/MR system for brain imaging (Schlemmer et al. 2008). The images were acquired in a 57 year old female control study participant. [Courtesy of Dr. Hooker, MGH (Gilbert et al. 2019)]

Siemens BrainPET system (image resolution 3–4 mm).

An early example of innovative simultaneous PET/MR imaging is the work of Sander et al. (2013) to demonstrate relationships between changes in dopamine receptor drug occupancy (with PET) and hemodynamics (with fMRI) in the basal ganglia (Fig. 7.6). This study is one of the earliest demonstrations of the power of simultaneous molecular, functional and structural neuroimaging, in its combined capacity to link neurovascular response to the level of drug binding to dopamine receptors in vivo, with information about temporal dynamics and spatial distribution. These findings were important also for the development of an advanced physiological model for pharmacologic fMRI that described the fMRI response to drug-induced elevations in synaptic dopamine within a multi-receptor framework (Mandeville et al. 2013). This advanced model is innovative and an interesting melding of modeling methodology used in both fMRI and PET research that is potentially extensible to other applications. Other novel work in the simultaneous PET/fMRI field includes imaging of agonist-induced dopamine D_2/D_3 receptor desensitization and internalization using graded doses of a dopamine D_2 receptor agonist (Sander et al. 2016) and studies of the opioid system in pain (Wey et al. 2014). Table 7.2 outlines considerations important in the design of such combined studies whilst other factors, such as relevant timescales for PET and fMRI signal detectability, are discussed by Sander and Hesse (2017).

In summary, PET is a powerful tool when combined with rational radioligand design to target protein sites with high molecular specificity and selectivity. Many targets that range from neuroreceptors to enzymes have been applied for human use and complement the large investigations performed to date applying PET to the study pre- and post-synaptic dopaminergic system changes in schizophrenia. The combination of PET and MR imaging is highly complementary and synergistic, and empowers neuroimaging research. PET has excellent sensitivity and can

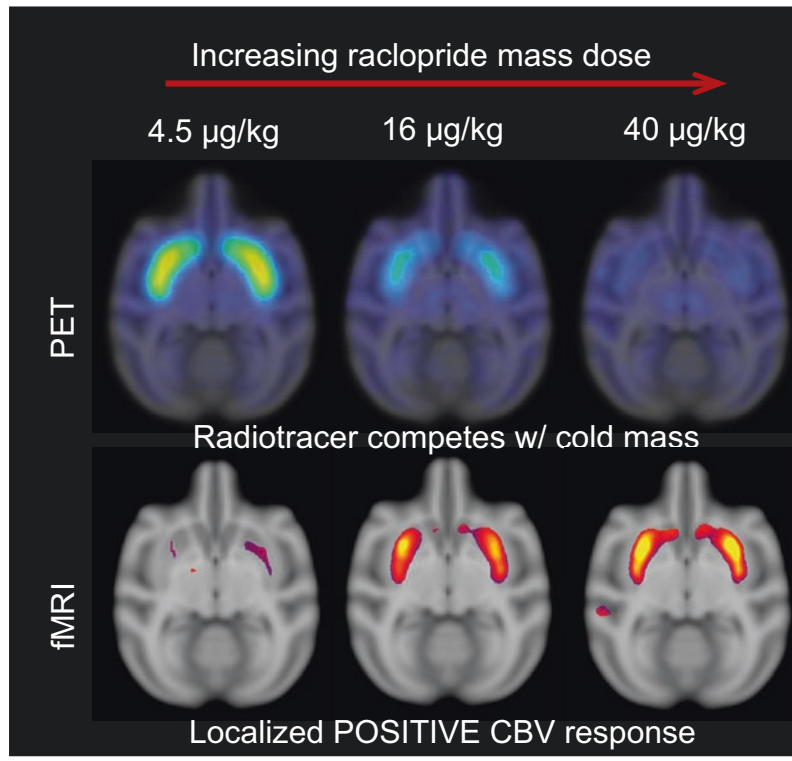

Fig. 7.6 Example of simultaneous PET/MR imaging of dopamine D2/D3 antagonist ([^{11}C] raclopride) drug challenge and its functional response on cerebral blood volume (CBV) are correlated in space. [Reproduced with permission (Sander et al. 2013)]

Table 7.2 Considerations for human PET and MR multimodality brain imaging

	PET (s to min)	BOLD fMRI (ms)
Corrections	Attenuation, dead time, decay, motion	Shim, bias, signal drift, motion
Test-retest	Flow, metabolism, ligand binding (baseline, drug challenge) outcomes	Task response, resting state (baseline, drug challenge)
Experimental design	Bolus or bolus + constant infusion Dynamic or static ROI or voxel level	Block design or event related Complexity of task
Resolution	Scanner limited, detector parameters, spillover HR+ ~6 mm; PET/CT ~5 mm; BrainPET PET/MR ~3 mm; HRRT ~3 mm	Ability to estimate timing of neuronal activity from measured hemodynamic changes ~ 2–3 mm
Timing issues	Half-life Measurement steady state Image over min, hours?	Hemodynamic response Measurement steady state
Confounds	– Age, gender, medication – Atrophy – Endogenous neurotransmitter levels (baseline receptor occupancy—Molar activity)	– Age, gender, medication – Atrophy

measure quantitatively picomolar concentrations but lacks the spatial resolution provided by MR imaging. On the other hand, structural MR imaging provides high-resolution anatomical information but lacks sensitivity and quantification. Compared to CT, MR imaging offers higher gray/white matter contrast and no damage from ionizing radiation. Simultaneous PET/MR enables for novel combinations of PET molecular imaging capabilities with structural and functional MR imaging sequences that together can uniquely inform about in vivo physiology in health and disease.

Summary

- PET imaging measures biological processes at the molecular and cellular levels through the measurement of the spatial and temporal radioactivity distributions of imaging agents labeled with positron-emitting radionuclides.
- PET offers a wide range of molecular probes to image different brain targets such as numerous neuroreceptor systems, translocator proteins, amyloid plaques and glucose metabolism.
- Main strength of PET imaging: allows quantitative in vivo imaging of ligand-binding interactions at low nM to pM concentration levels through application of tracer kinetic principles
- Main limitations of PET imaging: limited spatial resolution, limited anatomical information, scatter/attenuation, partial volume effects
- Simultaneous PET/MR brain imaging offers acquisition of multimodal neuroimaging measures during the same physiologic condition, leverages sensitivity and molecular specificity of PET with exquisite MRI anatomical resolution and fMRI measures of brain activity

References

Badawi RD, Shi H, Hu P, Chen S, Xu T, Price PM, et al. First human imaging studies with the EXPLORER total-body PET scanner. J Nucl Med. 2019;60(3):299–303.

Bailey D. Data acquisition and performance characterization in PET. Positron emission tomography. New York: Springer; 2003. p. 10–31.

Beyer T, Schwenzer N, Bisdas S, Claussen C, Pichler B. MR/PET—hybrid imaging for the next decade. MAGNETOM Flash 3/2010; 2010. http://www.siemens.com/magnetom-world.

Carson R. Tracer kinetic modeling. In: Valk PE, Bailey DL, Townsend DW, Maisey MN, editors. Positron emission tomography basic science and clinical practice. Berlin: Springer; 2003. p. 147–79.

Catana C. Principles of simultaneous PET/MR imaging. Magn Reson Imaging Clin N Am. 2017;25(2):231–43.

Catana C, Procissi D, Wu Y, Judenhofer MS, Qi J, Pichler BJ, et al. Simultaneous in vivo positron emission tomography and magnetic resonance imaging. Proc Natl Acad Sci U S A. 2008;105(10):3705–10.

Catana C, Benner T, van der Kouwe A, Byars L, Hamm M, Chonde DB, et al. MRI-assisted PET motion correction for neurologic studies in an integrated MR-PET scanner. J Nucl Med. 2011;52(1):154–61.

Chen Y, An H. Attenuation correction of PET/MR imaging. Magn Reson Imaging Clin N Am. 2017;25(2):245–55.

Chen KT, Salcedo S, Chonde DB, Izquierdo-Garcia D, Levine MA, Price JC, et al. MR-assisted PET motion correction in simultaneous PET/MRI studies of dementia subjects. J Magn Reson Imaging. 2018;48(5):1288–96.

Collins D, Holmes C, Peters T, Evans A. Automatic 3-D model-based neuroanatomical segmentation. Hum Brain Mapp. 1995;3:190–208.

Cunningham V, Jones T. Spectral analysis of dynamic PET studies. J Cereb Blood Flow Metab. 1993;13:15–23.

Daube-Witherspoon ME, Surti S, Perkins A, Kyba CC, Wiener R, Werner ME, et al. The imaging performance of a LaBr3-based PET scanner. Phys Med Biol. 2010;55(1):45–64.

de Jong H, van Velden FHP, Kloet RW, Buijs FL, Boellaard R, Lammertsma AA. Performance evaluation of the ECAT HRRT: an LSO-LYSO double layer high resolution, high sensitivity scanner. Phys Med Biol. 2007;52(5):1505–26.

Delso G, Furst S, Jakoby B, Ladebeck R, Ganter C, Nekolla SG, et al. Performance measurements of the Siemens mMR integrated whole-body PET/MR scanner. J Nucl Med. 2011;52(12):1914–22.

Erlandsson K, Buvat I, Pretorius PH, Thomas BA, Hutton BF. A review of partial volume correction techniques for emission tomography and their applications in neurology, cardiology and oncology. Phys Med Biol. 2012;57(21):R119–59.

Farde L, Wiesel FA, Hall H, Halldin C, Stone-Elander S, Sedvall G. No D2 receptor increase in PET study of schizophrenia. Arch Gen Psychiatry. 1987;44(7):671–2.

Feng D, Wong KP, Wu CM, Siu WC. A technique for extracting physiological parameters and the required input function simultaneously from PET image measurements: theory and simulation study. IEEE Trans Inf Technol Biomed. 1997;1(4):243–54.

Fischl B. FreeSurfer. Neuroimage. 2012;62(2):774–81.

Friston K. Statistical parametric mapping: the analysis of functional brain. Amsterdam/Boston: Elsevier/Academic Press; 2007. p. 10–31.

Fung EK, Carson RE. Cerebral blood flow with [15O] water PET studies using an image-derived input function and MR-defined carotid centerlines. Phys Med Biol. 2013;58(6):1903–23.

Geworski L, Knoop BO, de Wit M, Ivancevic V, Bares R, Munz DL. Multicenter comparison of calibration and cross calibration of PET scanners. J Nucl Med. 2002;43(5):635–9.

Geworski L, Knoop BO, Hofmann M, Zander A, de Wit M, Bares R, et al. Testing cross-calibration between positron emission tomographs and their peripheral devices. Z Med Phys. 2003;13(2):109–14.

Gilbert TM, Zurcher NR, Wu CJ, Bhanot A, Hightower BG, Kim M, et al. PET neuroimaging reveals histone deacetylase dysregulation in schizophrenia. J Clin Invest. 2019;129(1):364–72.

Grogg KS, Toole T, Ouyang J, Zhu X, Normandin MD, Li Q, et al. National electrical manufacturers association and clinical evaluation of a novel brain PET/CT scanner. J Nucl Med. 2016;57(4):646–52.

Gunn RN, Slifstein M, Searle GE, Price JC. Quantitative imaging of protein targets in the human brain with PET. Phys Med Biol. 2015;60(22):R363–411.

Hong SJ, Song I, Ito M, S Kwon, Lee G, Sim K-S, et al. An investigation into the use of geiger-mode solid-state photomultipliers for simultaneous PET and MRI acquisition. In: IEEE nuclear science symposium conference record; 2008.

Huang S, Phelps M, editors. Principles of tracer kinetic modeling in positron emission tomography and autoradiography. New York: Raven Press; 1986.

Huang S, Barrio J, Phelps M. Neuroreceptor assay with positron emission tomography: equilibrium versus dynamic approaches. J Cereb Blood Flow Metab. 1986;6:515–21.

Ichise M, Toyama H, Innis RB, Carson RE. Strategies to improve neuroreceptor parameter estimation by linear regression analysis. J Cereb Blood Flow Metab. 2002;22(10):1271–81.

Innis RB, Cunningham VJ, Delforge J, Fujita M, Gjedde A, Gunn RN, et al. Consensus nomenclature for in vivo imaging of reversibly binding radioligands. J Cereb Blood Flow Metab. 2007;27(9):1533–9.

Izquierdo-Garcia D, Catana C. MR imaging-guided attenuation correction of PET data in PET/MR imaging. PET Clin. 2016;11(2):129–49.

Jakoby BW, Bercier Y, Conti M, Casey ME, Bendriem B, Townsend DW. Physical and clinical performance of the mCT time-of-flight PET/CT scanner. Phys Med Biol. 2011;56(8):2375–89.

Jenkinson M, Beckmann CF, Behrens TE, Woolrich MW, Smith SM. Fsl. Neuroimage. 2012;62(2):782–90.

Judenhofer MS, Wehrl HF, Newport DF, Catana C, Siegel SB, Becker M, et al. Simultaneous PET-MRI: a new approach for functional and morphological imaging. Nat Med. 2008;14(4):459–65.

Kinahan PE, Townsend DW, Beyer T, Sashin D. Attenuation correction for a combined 3D PET/CT scanner. Med Phys. 1998;25(10):2046–53.

Kinahan PE, Hasegawa BH, Beyer T. X-ray-based attenuation correction for positron emission tomography/computed tomography scanners. Semin Nucl Med. 2003;33(3):166–79.

Koeppe R. Data analysis and image processing. In: Wahl R, Buchanan J, editors. Principles and practice of positron emission tomography. Philadelphia: Lippincott Williams & Wilkins; 2002. p. 65–99.

Ladefoged CN, Law I, Anazodo U, St Lawrence K, Izquierdo-Garcia D, Catana C, et al. A multi-centre evaluation of eleven clinically feasible brain PET/MRI attenuation correction techniques using a large cohort of patients. Neuroimage. 2017;147:346–59.

Landaw E, DiStefano J. Multiexponential, multicompartmental, and noncompartmental modeling. II. Data analysis and statistical considerations. Am J Physiol. 1984;246:R665–R77.

Laruelle M. Imaging synaptic neurotransmission with *in vivo* binding competition techniques: a critical review. J Cereb Blood Flow Metab. 2000;20:423–51.

Laruelle M, Slifstein M, Huang Y. Relationships between radiotracer properties and image quality in molecular imaging of the brain with positron emission tomography. Mol Imaging Biol. 2003;5(6):363–75.

Lassen N, Perl W. Tracer kinetic methods in medical physiology. New York: Raven Press; 1979. p. 104–8.

Levin CS, Maramraju SH, Khalighi MM, Deller TW, Delso G, Jansen F. Design features and mutual compatibility studies of the time-of-flight PET capable GE SIGNA PET/MR system. IEEE Trans Med Imaging. 2016;35(8):1907–14.

Logan J. Graphical analysis of PET data applied to reversible and irreversible tracers. Nucl Med Biol. 2000;27(7):661–70.

Logan J, Fowler JS, Volkow ND, Ding YS, Wang GJ, Alexoff DL. A strategy for removing the bias in the graphical analysis method. J Cereb Blood Flow Metab. 2001;21(3):307–20.

Lois C, Jakoby BW, Long MJ, Hubner KF, Barker DW, Casey ME, et al. An assessment of the impact of incorporating time-of-flight information into clinical PET/CT imaging. J Nucl Med. 2010;51(2):237–45.

Mandeville JB, Sander CYM, Jenkins BG, Hooker JM, Catana C, Vanduffel W, et al. A receptor-based model for dopamine-induced fMRI signal. Neuroimage. 2013;75:46–57.

Martinez-Moller A, Souvatzoglou M, Delso G, Bundschuh RA, Chefd'hotel C, Ziegler SI, et al. Tissue classification as a potential approach for attenuation correction in whole-body PET/MRI: evaluation with PET/CT data. J Nucl Med. 2009;50(4):520–6.

Meltzer C, Leal J, Mayberg H, Wagner H, Frost J. Correction of PET data for partial volume effect in human cerebral cortex by MR imaging. J Comput Assist Tomogr. 1990;14(4):561–70.

Michopoulou S, O'Shaughnessy E, Thomson K, Guy MJ. Discovery molecular imaging digital ready PET/CT performance evaluation according to the NEMA NU2–2012 standard. Nucl Med Commun. 2019;40(3):270–7.

Moses WW. Fundamental limits of spatial resolution in PET. Nucl Instrum Methods Phys Res A. 2011;648(Suppl 1):S236–S40.

Muller-Gartner HW, Links JM, Prince JL, Bryan RN, McVeigh E, Leal JP, et al. Measurement of radiotracer concentration in brain gray matter using positron emission tomography: MRI-based correction for partial volume effects. J Cereb Blood Flow Metab. 1992;12(4):571–83.

Narayanaswami V, Dahl K, Bernard-Gauthier V, Josephson L, Cumming P, Vasdev N. Emerging PET radiotracers and targets for imaging of neuroinflammation in neurodegenerative diseases: outlook beyond TSPO. Mol Imaging. 2018;17:1–25.

Ogden RT, Zanderigo F, Choy S, Mann JJ, Parsey RV. Simultaneous estimation of input functions: an empirical study. J Cereb Blood Flow Metab. 2010;30(4):816–26.

Okubo Y, Suhara T, Suzuki K, Kobayashi K, Inoue O, Terasaki O, et al. Decreased prefrontal dopamine D1 receptors in schizophrenia revealed by PET. Nature. 1997;385(6617):634–6.

Pan T, Einstein S, Kappadath S, Grogg K, Lois C, Alessio A, et al. Performance evaluation of the 5-ring GE discovery MI PET/CT system using the NEMA NU 2–2012 Standard. Med Phys. 2019;46(7):3025–33.

Picard Y, Thompson CJ. Motion correction of PET images using multiple acquisition frames. IEEE Trans Med Imaging. 1997;16(2):137–44.

Pichler B, Lorenz E, Mirzoyan R, Pimpl W, Roder F, Schwaiger M, et al. Performance test of a LSO-APD PET module in a 9.4 Tesla magnet. In: IEEE nuclear science symposium conference record, Albuquerque, NM USA; 1977.

Pyatigorskaya N, Gallea C, Garcia-Lorenzo D, Vidailhet M, Lehericy S. A review of the use of magnetic resonance imaging in Parkinson's disease. Ther Adv Neurol Disord. 2014;7(4):206–20.

Rausch I, Quick HH, Cal-Gonzalez J, Sattler B, Boellaard R, Beyer T. Technical and instrumentational foundations of PET/MRI. Eur J Radiol. 2017;94:A3–A13.

Rousset OG, Ma Y, Evans AC. Correction for partial volume effects in PET: principle and validation. J Nucl Med. 1998;39(5):904–11.

Sander CY, Hesse S. News and views on in-vivo imaging of neurotransmission using PET and MRI. Q J Nucl Med Mol Imaging. 2017;61(4):414–28.

Sander CY, Hooker JM, Catana C, Normandin MD, Alpert NM, Knudsen GM, et al. Neurovascular coupling to D2/D3 dopamine receptor occupancy using simultaneous PET/functional MRI. Proc Natl Acad Sci U S A. 2013;110(27):11169–74.

Sander CY, Hooker JM, Catana C, Rosen BR, Mandeville JB. Imaging agonist-induced D2/D3 receptor desensitization and internalization in vivo with PET/fMRI. Neuropsychopharmacology. 2016;41(5):1427–36.

Sari H, Erlandsson K, Law I, Larsson HB, Ourselin S, Arridge S, et al. Estimation of an image derived input function with MR-defined carotid arteries in FDG-PET human studies using a novel partial volume correction method. J Cereb Blood Flow Metab. 2017;37(4):1398–409.

Sari H, Erlandsson K, Marner L, Law I, Larsson HBW, Thielemans K, et al. Non-invasive kinetic modelling of PET tracers with radiometabolites using a constrained simultaneous estimation method: evaluation with (11)C-SB201745. EJNMMI Res. 2018;8(1):58.

Schlemmer HP, Pichler BJ, Schmand M, Burbar Z, Michel C, Ladebeck R, et al. Simultaneous MR/PET imaging of the human brain: feasibility study. Radiology. 2008;248(3):1028–35.

Slifstein M, Laruelle M. Effects of statistical noise on graphic analysis of PET neuroreceptor studies. J Nucl Med. 2000;41(12):2083–8.

Su Y, Arbelaez AM, Benzinger TL, Snyder AZ, Vlassenko AG, Mintun MA, et al. Noninvasive estimation of the arterial input function in positron emission tomography imaging of cerebral blood flow. J Cereb Blood Flow Metab. 2013;33(1):115–21.

Sundar LK, Muzik O, Rischka L, Hahn A, Rausch I, Lanzenberger R, et al. Towards quantitative [18F] FDG-PET/MRI of the brain: automated MR-driven calculation of an image-derived input function for the non-invasive determination of cerebral glucose metabolic rates. J Cereb Blood Flow Metab. 2018;39(8):1516–30.

Talbot PS, Laruelle M. The role of in vivo molecular imaging with PET and SPECT in the elucidation of psychiatric drug action and new drug development. Eur Neuropsychopharmacol. 2002;12(6):503–11.

Townsend DW. Physical principles and technology of clinical PET imaging. Ann Acad Med Singapore. 2004;33(2):133–45.

Tziortzi AC, Searle GE, Tzimopoulou S, Salinas C, Beaver JD, Jenkinson M, et al. Imaging dopamine receptors in humans with [^{11}C]-(+)-PHNO: Dissection of D3 signal and anatomy. Neuroimage. 2011;54(1):264–77.

Valk PE, Townsend DW, Bailey DB, Maisey MN, editors. Positron emission tomography basic science and clinical practice. Berlin: Springer; 2003.

van Sluis JJ, de Jong J, Schaar J, Noordzij W, van Snick P, Dierckx R, et al. Performance characteristics of the digital Biograph Vision PET/CT system. J Nucl Med. 2019;60(7):1031–6.

Watson C. New, faster, image-based scatter correction for 3D PET. IEEE Trans Nucl Sci. 2000;47(4):1587–94.

Wey HY, Catana C, Hooker JM, Dougherty DD, Knudsen GM, Wang DJ, et al. Simultaneous fMRI-PET of the opioidergic pain system in human brain. Neuroimage. 2014;102(Pt 2):275–82.

Wong DF, Wagner HN Jr, Tune LE, Dannals RF, Pearlson GD, Links JM, et al. Positron emission tomography reveals elevated D2 dopamine receptors in drug-naive schizophrenics. Science. 1986;234(4783):1558–63.

Wong KP, Feng D, Meikle SR, Fulham MJ. Simultaneous estimation of physiological parameters and the input function—in vivo PET data. IEEE Trans Inf Technol Biomed. 2001;5(1):67–76.

Yamamoto S, Watabe H, Kanai Y, Aoki M, Sugiyama E, Watabe T, et al. Interference between PET and MRI sub-systems in a silicon-photomultiplier-based PET/MRI system. Phys Med Biol. 2011;56(13):4147–59.

Zaidi H, Montandon ML. Scatter compensation techniques in PET. PET Clin. 2007;2(2):219–34.

Zhang J, Maniawski P, Knopp MV. Performance evaluation of the next generation solid-state digital photon counting PET/CT system. EJNMMI Res. 2018;8(1):97.

Molecular Imaging

8

Simon Cervenka and Lars Farde

Contents

8.1 Introduction and Background

The dopamine (DA) hypothesis of schizophrenia was first formulated in the 60s and stated that the symptoms are related to an overactivity of dopaminergic neurotransmission (Fog et al. 1967). The hypothesis received strong support from subsequent studies showing markedly elevated striatal density of the D2-dopamine receptor (D2-R) post mortem in brains from patients with schizophrenia. However, it could not be excluded that the elevated density represents an upregulation of D2-R following treatment with antipsychotic drugs. In the early 80s, the prospects of using molecular imaging to study dopamine receptor binding in young neuroleptic-naïve patients with schizophrenia were thus much awaited.

To this date, research on schizophrenia and related psychotic disorders remains the most frequent application of Single Photon Emission Tomography (SPECT) and Positron Emission Tomography (PET) in psychiatry. This chapter

S. Cervenka (✉) · L. Farde
Centre for Psychiatry Research, Department of Clinical Neuroscience, Karolinska Institutet and Stockholm County Council, Stockholm, Sweden
e-mail: simon.cervenka@ki.se; lars.farde@ki.se

M. Kubicki, M. E. Shenton (eds.), *Neuroimaging in Schizophrenia*,
https://doi.org/10.1007/978-3-030-35206-6_8

will focus on studies attempting to measure biochemical markers *in vivo*, with the aim of increasing our understanding of the pathophysiology of schizophrenia, as well as to find biomarkers that can be developed for diagnostic purposes. Imaging studies on brain metabolism and blood flow are beyond the scope of the present review.

A major advantage of PET is that the methodology is quantitative, generating time curves for radioactivity concentration in brain regions (nCi/cc). To obtain biochemical parameters the time curves are interpreted using kinetic compartment models with an arterial input function, or simplified models based on radioactivity in a reference brain region devoid of specific binding (Farde et al. 1989). The concept 'binding potential' was launched as an important outcome parameter and proposed to represent the ratio of receptor density (B_{max}) to affinity (K_D) (Mintun et al. 1984). In an early study using the reversible D2-R radioligand [^{11}C]raclopride, it was possible to mimic test-tube conditions and perform a saturation analysis of D2-R binding in the human brain *in vivo* from two or more PET-measurements in the same subject, thus disentangling B_{max} from K_D-values (Farde et al. 1986) (Fig. 8.1). Important from a validation perspective is that the B_{max} values in this group of healthy control subjects were consistent with levels reported post-mortem. However, instead of an experimentally demanding saturation analysis, the most common approach has been to derive BP from a single PET measurement, and this concept has in a slightly revised form (Innis et al. 2007) remained an endpoint in almost all molecular imaging studies on receptor binding carried out so far.

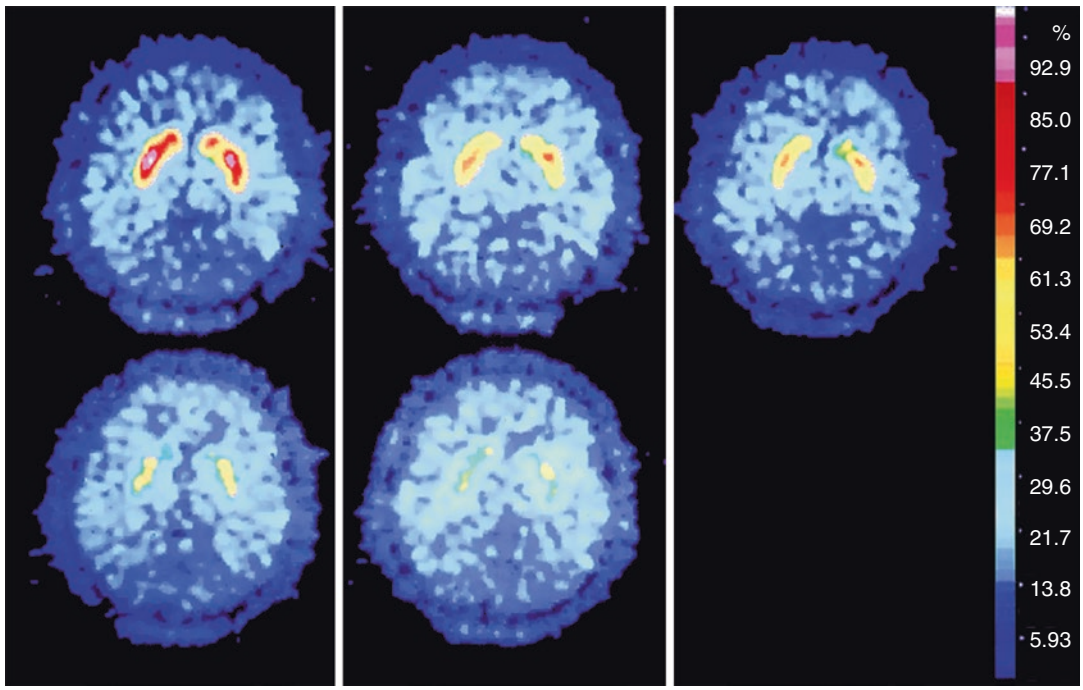

Fig. 8.1 Example of a saturation analysis. Transaxial images of summed radioactive uptake after a series of intravenous injections of the D2-R radioligand [^{11}C]raclopride in a healthy control subject. The total administered mass of radioligand in each experiment was systematically increased, allowing for a saturation analysis. Images were acquired using a Scanditronix PC-384-7B PET system with a spatial resolution of 8.5 mm (full width half maximum, FWHM). (Courtesy of the PET Centre at Karolinska Institutet)

The initial development of suitable radioligands such as [^{11}C]raclopride was the start of a series of investigations whereby PET was used to determine D2-R occupancy in antipsychotic drug treated patients. This work confirmed previous experimental observations that all antipsychotic drugs block D2-R, and provided *in vivo* support for one of the key pharmacological observations underlying the dopamine hypothesis of schizophrenia (Nordstrom et al. 1993a; Nord and Farde 2011). In addition, and perhaps more importantly, the studies on D2-R occupancy revealed distinct occupancy thresholds for antipsychotic effect and side effects (Farde et al. 1992; Kapur et al. 1995). The observation of a therapeutic window of between 70 and 85% D2-R occupancy has since then not only served as a framework for development of new drugs, but also provided clinical guidance, allowing for reduced doses of antipsychotics being administered to patients (Nord and Farde 2011).

In parallel, pioneering studies with the radioligand [^{11}C]N-Methylspiperone ([^{11}C]NMSP) (Wagner et al. 1983) and the aforementioned studies with [^{11}C]raclopride marked the starting point of more than three decades of molecular imaging research into the pathophysiology of schizophrenia. In a consensus workshop in Montreal in 1987, a strong potential was envisaged for this field: "Since we assume that most mental illnesses, and particularly schizophrenia, are due to abnormalities in brain chemistry, PET will clearly be a powerful tool for psychiatric research during the next several decades" (Andreasen et al. 1988). The results of these efforts will be summarized in the present chapter.

8.2 The Dopamine System

8.2.1 The Dopamine D2-R Receptor

Following the development and validation of radioligands for D2-R, a series of studies were initiated to measure differences in receptor levels between patients and control subjects. In a first study published in 1986, Wong and coworkers used [^{11}C]NMSP and found 2.5-fold higher levels of striatal D2-R in both patients previously treated with antipsychotics, as well as a drug-naïve first episode psychosis (FEP) group (Wong et al. 1986). This major difference appeared to confirm post-mortem work showing increases in D2-R in patients (Seeman et al. 1984). However, this result could not be confirmed by an independent center using [^{11}C]raclopride to examine drug naïve FEP patients (Farde et al. 1987). Initially it was suggested that methodological differences were likely to explain these discrepant results, such as different radioligands, PET instrumentation and kinetic modelling (Andreasen et al. 1988). In attempts to resolve the discrepant findings, the question of D2-R changes in schizophrenia has during the following decades been revisited in a series of studies altogether including more than 300 patients and a corresponding number of control subjects. A recent meta-analysis of 22 such studies found a significant elevation in striatum with an effect size of $d = 0.26$, i.e. considerably smaller than the initial report. The effect size was similar when including only studies examining drug-naïve (and not neuroleptic-free) FEP patients, although the difference was not statistically significant in this subpopulation (Howes et al. 2012).

The view that G-protein coupled receptors may exist in a high and low affinity state for agonist ligands has been highlighted by the Nobel Price to Robert Lefkovitz in 2012 and has also attracted attention in schizophrenia research. A subsequent hypothesis is that the fraction of D2-R in a "high-affinity state" is larger in patients with schizophrenia. However, in studies with the agonist radioligands [^{11}C]PHNO and [^{11}C]NPA, which theoretically bind only to the high-affinity D2- R state, there were no clear increases compared to studies with antagonist radioligands, thus failing to provide evidence for this hypothesis (Graff-Guerrero et al. 2009; Frankle et al. 2018).

Patient studies often run with several confounders, such as exposure to medication or environmental stressors associated with being in a

state of disease. To circumvent these issues, an alternative strategy to study the pathophysiology of schizophrenia is to examine individuals at high risk for developing the disorder, with the assumption that these individuals share underlying biological traits with patients. Using this approach, higher D2-R in striatum have been shown in individuals with genetic risk for the disorder (Hirvonen et al. 2005), providing further support for a small increase in striatal D2-R in psychosis.

With the advent of high-affinity radioligands such as [^{11}C]FLB-457 and [^{18}F]fallypride, it became possible to quantify D2-R also in low-density regions outside of the striatum (Mukherjee et al. 2002; Halldin et al. 1995). A handful of studies have been performed using this methodology, on average finding no differences in receptor levels between patients and control subjects in cortical brain regions (Kambeitz et al. 2014), whereas several studies focusing on the thalamus were able to discern a pattern of lower D2-R (Talvik et al. 2003; Talvik et al. 2006; Buchsbaum et al. 2006; Kessler et al. 2009). The thalamus is a region with high functional heterogeneity, with connections to widespread cortical brain regions. This complexity motivates a more detailed analysis of D2-R binding in subregions of the thalamus. One initial study has indeed provided support for such a "compartmentalized" effect, showing specific decreases in D2-R in a thalamic subregion (Yasuno et al. 2004a). However, this finding is in need of replication using currently available high-resolution PET systems.

8.2.2 The Dopamine D1-R Receptor

The D1-R receptor is the most abundant dopamine receptor subtype in the brain. D1-R shows opposing intracellular effects compared to D2-R (Vallone et al. 2000), which in the striatum is balanced by the distribution of cells providing output via the direct nigrostriatal pathway, as opposed to the indirect pathway (Gerfen and Surmeier 2011). In contrast to the D2-R, D1-R has not emerged as a major target for antipsychotic drugs. Occupancy ranges from 0 to 16% for typical antipsycotics (Farde et al. 1992; Reimold et al. 2007) to around 50% for the atypical antipsychotic clozapine (Farde et al. 1992; Farde et al. 1994; Nordström et al. 1995) and drugs specifically targeting D1-R have not shown antipsychotic effects (Karlsson et al. 1995).

In an initial study using the D1-R radioligand [^{11}C]SCH 23390 in a partly drug naïve sample, a decrease in binding was shown in the frontal cortex with a large effect size of around 1. This difference appeared to be region specific since no significant difference was observed in the striatum (Okubo et al. 1997). In a subsequent study using the related radioligand [^{11}C]NNC, and also in a partly drug naïve patient group, a contrasting result was found with increased binding in the frontal cortex (d = 0.87) (Abi-Dargham et al. 2002). Ensuing studies have shown no difference in D1-R B_{max} (Karlsson et al. 2002) or an increase in BP in the frontal cortex in drug-naïve FEP patients (Abi-Dargham et al. 2012). Additional studies in medicated patients have shown large decreases in D1-R binding (Kosaka et al. 2010; Hirvonen and van Erp 2006) however, the interpretation of these results may be uncertain since experimental and post-mortem data has shown a downregulation of D1-R after treatment with antipsychotics (Lidow and Goldman-Rakic 1994; Lidow et al. 1997). In a study in twins discorcordant for schizophrenia, Hirvonen et al. showed increases in frontal D1-R in non-affected twins compared to control twins (Hirvonen and van Erp 2006), providing additional support for a D1-R upregulation in this region as part of the underlying biology of psychosis. More recently however, a study in the largest FEP D1-R psychosis sample to date failed to confirm the hypothesis of higher D1-R in the frontal cortex, instead showing lower binding (Stenkrona et al. 2019). Taken together, the data on D1-R in schizophrenia are inconsistent, failing to show any clear direction. One caveat in these studies is that both [^{11}C]SCH 23390 and [^{11}C]NCC 112 have affinity for the serotonin (5-HT) 5-HT2a receptor (5-HT2a-R), which may account for around 25% of the cortical signal (Ekelund et al. 2007; Slifstein et al. 2007). Although the data on 5- HT2a-R binding in psychosis does not show any clear effects (see

below), it cannot be excluded that binding to this receptor subtype may have influenced the results.

8.2.3 Presynaptic Dopaminergic Markers I: Dopamine Release and Depletion Paradigms

Apart from the effect of D2-R antagonists on psychotic symptoms, another key clinical observation underlying the original dopamine hypothesis was that amphetamine, which increases DA levels, can induce psychotic experiences in healthy subjects, as well as aggravate symptoms in schizophrenia (Angrist and Gershon 1970; Lieberman et al. 1987; Connell 1957). In 1996, Laruelle and co-workers reported an increased amphetamine-induced attenuation of D2-R binding in schizophrenia patients as measured using the SPECT radioligand [^{123}I]IBZM, an observation that was suggested to represent an increased release of endogenous DA (Laruelle et al. 1996). In the patient group, the DA release was associated to positive symptoms. This finding of increased amphetamine-induced release has subsequently been replicated in two independent cohorts (Breier et al. 1997; Abi-Dargham et al. 1998). Moreover, one study has shown increased stress-induced release of DA in both high-risk individuals and schizophrenia patients using the agonist radioligand [^{11}C]PHNO (Mizrahi et al. 2012). However, in a more recent study using an amphetamine challenge and [^{11}C]PHNO, no difference in DA release was observed between patients and control subjects (Frankle et al. 2018).

With regard to the general finding of increased amphetamine-induced reduction in striatal D2-R binding in schizophrenia, it has been suggested that this might in part be explained by an increased agonist-mediated internalisation of D2-R. Although this possibility cannot be fully excluded, a study modelling the change in binding over time found no evidence for such internalisation (Weinstein et al. 2018).

In a recent meta-analysis of studies using an acute dopamine depletion paradigm, it was estimated that around 8–21% of the striatal D2-R population is occupied by endogenous DA in the healthy brain at physiological conditions (Caravaggio et al. 2019). Studies examining the hypothesis of increased basal levels of DA in schizophrenia indeed found higher increases in binding in patients after application of a similar depletion paradigm (Abi-Dargham et al. 2000; Kegeles et al. 2010). However, these observations suggesting higher DA levels are in contrast with an early report by Farde et al. using Scatchard analysis in a group of fully drug naïve patients, showing no difference in apparent affinity (K_D) (Farde et al. 1987).

The initial version of the dopamine hypothesis of schizophrenia postulated elevated striatal DA neurotransmission, generally thought to underlie positive symptoms. A more recent version of the hypothesis also includes DA hypofunction in frontal cortex, a mechanism that could be related to negative and cognitive symptoms. Using PET and the high-affinity D2-R radioligand [^{11}C]FLB-457, Slifstein and coworkers indeed showed a blunting of DA release in a group of FEP patients, most of which were antipsychotic naïve (Slifstein et al. 2015). This deficit was in turn related to cognitive impairment. In a subsequent study, the same radioligand was used to examine the effect of DA release invoked by a cognitive challenge, showing attenuated reductions in binding in patients compared to control subjects (Rao et al. 2018). Additional studies on DA function in frontal regions are warranted to confirm these observations.

8.2.4 Presynaptic Dopaminergic Markers II: Precursor Uptake

An alternative method proposed to indirectly assess the function of the presynaptic dopaminergic neuron is to measure uptake of the radiolabelled dopamine precursor, [^{18}F]dihydroxyphenylalanine ([^{18}F]FDOPA). The first result of such a study in psychosis patients was reported by Hietala and coworkers in Turku, showing an increase of striatal [^{18}F]FDOPA uptake in drug naïve FEP patients (Hietala et al. 1995). This report was followed by a series of studies in both FEP and chronic samples, with a majority of studies confirming an increase (Howes et al.

2012). Moreover, [18F]FDOPA uptake has been shown to associate to reduced prefrontal activity as measured using fMRI (Meyer-Lindenberg et al. 2002), as well as showing increases in at-risk populations (Huttunen et al. 2008; Howes et al. 2009). In a series of studies from the group in London, [18F]FDOPA uptake was shown to increase as high-risk individuals developed psychosis (Howes et al. 2011a), and high levels in high-risk individuals at baseline predicted conversion to psychosis (Howes et al. 2011b). In a meta-analysis the summed effect size of increases in striatal [18F]FDOPA in patients was estimated to d = 0.79 (Howes et al. 2012).

Insterestingly, no elevation of [18F]FDOPA was found in a group of patients who did not respond to antipsychotic treatment (Demjaha et al. 2012; Jahuar et al. 2019). This observation may have implications for treatment by pointing toward a subgroup of "DA-driven" psychosis-although this idea thereby also questions the concept of striatal [18F]FDOPA elevation as a general marker for psychosis.

It should be noted that a direct relationship between [18F]FDOPA uptake and drug challenge induced DA release remains to be shown. So far, the association between uptake of a DA precursor and stimulant-induced changes in DA levels has to our knowledge been evaluated in only one study, showing no relationship between uptake of [18F] Fluoromethyl-tyrosine ([18F]FMT) and methylphenidate-induced decreases of striatal [11C]raclopride binding in healthy control subjects (Berry et al. 2018).

8.2.5 Presynaptic Dopaminergic Markers III: The Dopamine Transporter

The dopamine transporter protein (DAT) is located presynaptically on striatal neurons, and can thus be viewed as another marker of presynaptic DA function. In the first study on DAT in psychosis, researchers from the Turku group examined a small sample of schizophrenia patients and controls, and reported no change in the uptake of the transporter radioligand [18F] CFT (Laakso et al. 2000). A similar result was reported some months later in a larger sample, using the radioligand [123I] beta-CIT (Laruelle et al. 2000). Subsequent studies have not shown any differences, and a metanalysis from 2013 estimated the standardized effect size to be d = −0.07 (Chen et al. 2013).

8.3 Serotonergic Markers

The atypical antipsychotic clozapine has relatively high affinity for the serotonin 5-HT2a-R subtype, which was confirmed in PET occupancy studies in the early 90s (Nordstrom et al. 1993b). High affinity for 5-HT2a-R was also shown for several of the second generation antipsychotics that were introduced in the same period (Nyberg et al. 1997; Gefvert et al. 2001; Kapur et al. 1998). Apart from driving the development of PET radioligands for the 5-HT-R subtypes, these pharmacological observations also re-ignited an interest for the putative role of the serotonin system in the pathophysiology of schizophrenia. Of historical interest is that a serotonin hypothesis of schizophrenia was postulated already in the 50s, even before the dopamine hypothesis, based on effects of hallucinogens on serotonergic function (Woolley and Shaw 1954). The hypothesis received further support when it could be confirmed that hallucinogens have affinity for serotonin receptors, and from post-mortem studies indicating changes in 5-HT2a and 5-HT1a receptor levels in frontal cortex in schizophrenia patients (Lewis et al. 1999; Bantick et al. 2004).

In a series of studies with the 5-HT2A-R radioligands [18F]spiperone or [11C]N-methylspiperone in small samples of antipsychotic naïve or drug free psychosis patients, no differences compared to control subjects were revealed (Lewis et al. 1999; Trichard et al. 1998; Okubo et al. 2000; Verhoeff et al. 2000). In a study using the 5-HT2a-R antagonist radioligand [18F]altanserin there were also no differences in cortical regions, however a marginal increase was observed in nucleus caudatus (Erritzoe et al. 2008), and using the same radioligand lower cortical binding was found in a four unmedicated schizophrenia

patients compared to their non-affected twins (Rasmussen et al. 2016). Finally, [^{18}F]altanserin binding was observed to be lower in small samples of high-risk individuals (Hurlemann et al. 2008; Hurlemann et al. 2005).

With regard to the 5-HT1a-R, the radioligand [^{11}C]WAY-100635 was used in drug naïve patients and control subjects by Tauscher et al., showing increases in binding in temporal regions (Tauscher et al. 2002) whereas another study found decreases in the amygdala in a smaller sample using the same radioligand (Yasuno et al. 2004b). No differences were found in subsequent studies in treated (Bantick et al. 2004) or drug free patients (Frankle et al. 2006). Finally, one study found no differences in serotonin transporter binding between patients and control subjects (Kim et al. 2015). Taken together, although many antipsychotics have affinity for serotonergic receptors, molecular imaging studies do not support a major involvement of the serotonin system in the pathophysiology of schizophrenia.

8.4 Other Neurotransmission Systems

Apart from research on the dopamine and serotonin systems, which was driven by pharmacological observations, a more limited number of studies have explored also other neurotransmittor systems. In the following we will provide some examples of such attempts.

Evidence for an involvement of the gamma butyric acid (GABA) system in schizophrenia comes from post-mortem studies showing reduced expression of key enzymes in the biosynthesis of the molecule (Mitchell et al. 2015). Analyses of GABA-related metabolites in CSF have yielded mixed results although one recent study showed lower GABA levels in FEP patients, most of which were antipsychotic naïve (Orhan et al. 2018). Using SPECT and the GABA-A radioligand [^{123}I] iomazenil in a sample of 25 patients and 24 controls, no group difference in radioligand binding was observed (Verhoeff et al. 1999). The PET radioligand [^{11}C]Ro15-4513, which has high affinity for the alpha5 subunit, has been applied in a smaller sample of drug naïve or drug free patients, also finding no differences (Asai et al. 2008). In a subsequent study, the GABA-A radioligand [^{18}F] fluoroflumazenil was used to show lower binding in the right caudate nucleus in a group of high risk individuals (Kang et al. 2014). Finally, [^{11}C]fluma zenil was used in combination with a GABA membrane transporter blocker to show impaired GABA transmission in a group of unmedicated patients (Frankle et al. 2015). Further studies are required to confirm if GABA system alterations could have a role in early stages of the disease process in schizophrenia.

Given the robust epidemiological association between cannabis use and psychosis, alterations in cannabinoid neurotransmission have been hypothesized to be part of the pathophysiology of schizophrenia. In an initial study using the cannabinoid 1-receptor (CB1-R) radioligand [^{11}C]OMAR, no difference was observed in a sample of nine chronic patients compared to control subjects (Wong et al. 2010). Using the radioligand [^{18}F] MK-9470 in a larger sample, increases in CB1-R binding were found in patients, most of which were on antipsychotic medication (Ceccarini et al. 2013). Quantification was performed using a standardized uptake approach as opposed to full kinetic modelling, owing to the irreversible nature of the radioligand. In a more recent study using [^{11}C]OMAR, decreased binding was observed in a patient group, also with most patients on antipsychotic treatment (Ranganathan et al. 2016). Additional studies in drug free or preferably drug naïve patients are needed to examine a possible involvement of CB1-R in schizophrenia.

Phosphodiesterase 10A (PDE10A) is an enzyme that degrades intracellular second messengers triggered by DA receptor activation in striatal medium spiny neurons. Hence, lower activity in PDE10A could theoretically lead to higher sensitivity to DA. Marques and coworkers examined PDE10A binding in a sample of 12 patients with chronic schizophrenia compared to control subjects, reporting no group difference (Marques et al. 2016). Subsequently, a similarly small number of medicated patients were examined using [^{11}C]Lu AE92686, showing lower binding compared to control subjects, however

confounding effects of age or medication could not be excluded (Bodén et al. 2017).

8.5 Translocator Protein: An In Vivo Glial Cell Marker

An involvement of the immune system in the pathophysiology of schizophrenia has been suggested by genetic and epidemiological research, as well as clinical studies showing increases of inflammatory markers in blood and cerebrospinal fluid (Ripke et al. 2014; Khandaker et al. 2012; Blomström et al. 2016; Upthegrove et al. 2014; Miller et al. 2011). Some studies have shown a positive effect of anti-inflammatory treatment as add-on to antipsychotics, but results have been mixed (Çakici et al. 2019; Deakin et al. 2018). In order to confirm engagement of the brain immune system in patients, molecular imaging tools are needed. The 18 kDa translocator protein (TSPO), previously known as the peripheral bensodiazepine receptor, is present in mitochondria of glial cells in the brain as well as immune cells in the periphery (Braestrup et al. 1977; Canat et al. 1993). Experimental studies have shown increases in TSPO expression in response to inflammatory stimuli (Venneti et al. 2013), and PET radioligands targeting this protein has been the most established method thus far to study brain immune activation.

Initial studies in schizophrenia were performed using the first generation TSPO radioligand [^{11}C]PK11195, which was developed in the 1990s. In the first study by van Berckel et al. in 2008, increased binding was observed in a small sample of medicated patients (van Berckel et al. 2008), with a subsequent study in a similarly small sample also showing elevations (Doorduin et al. 2009). Concerns with low signal-to-noise of [^{11}C]PK11195 led to the development of second generation radioligands with higher brain uptake and specific- to non-specific binding ratios (Imaizumi et al. 2008; Wilson et al. 2008) (Fig. 8.2). One drawback of these tracers is the sensitivity to TSPO genotype, which has to be taken into account in the analysis and also means that around 9% of the (western) population has to be excluded from PET due to insufficient affinity (Owen et al. 2012). Using the second generation TSPO radioligand [^{18}F]FEPPA in a larger group of chronic patients, no difference was found compared to control subjects (Kenk et al. 2014). A subsequent study in high-risk individuals and chronic patients reported increased TSPO levels in grey matter regions relative to whole brain (Bloomfield et al. 2015), however this relative approach has been questioned (Narendran and Frankle 2016; Matheson et al. 2017). Notably, total distribution volume values in grey matter were numerically lower in both groups compared to control subjects in this study, seemingly contradicting the conclu-

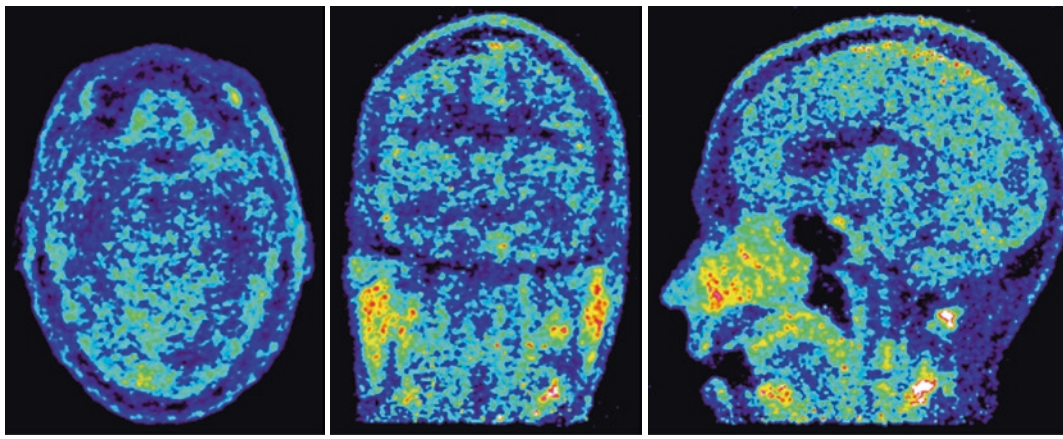

Fig. 8.2 The TSPO radioligand [^{11}C]PBR28. Images of summed radioactive uptake after an intravenous injection of the TSPO radioligand [^{11}C]PBR28 in a healthy control subject in transaxial, coronal and sagittal projections. Images acquired using a High Resolution Research Tomograph (HRRT) with a spatial resolution of 1.5 mm (FWHM) (Varrone et al. 2009). (Courtesy of the PET Centre at Karolinska Institutet)

sions drawn. Subsequent studies in untreated FEP and antipsychotic-naïve cohorts showed no difference and decreases in binding, respectively (Collste et al. 2017; Hafizi et al. 2017a), and additional studies using both and second generation radioligands also failed to yield increases in patients compared to control subjects (Coughlin et al. 2016; Van Der Doef et al. 2016; Holmes et al. 2016; Di Biase et al. 2017; Ottoy et al. 2018), although one [^{11}C]PK11195 study found elevated binding in a small group of medicated patients (Holmes et al. 2016). An additional study in a large group of high-risk individuals, using the second generation TSPO radioligand [^{18}F]FEPPA found no differences in binding (Hafizi et al. 2017b), aligning to the results of Bloomfield et al. when using non-normalised binding measures (Bloomfield et al. 2015).

A challenge in TSPO studies is the large between and within subject variability also after taking TSPO genotype into account, which in combination with the typically small sample sizes in PET research yields limited power. In attempting to overcome this limitation, Plavén-Sigray et al. combined individual participant TSPO data from five studies using second generation TSPO radioligands in schizophrenia or FEP patients, finding strong evidence for a decrease in TSPO in grey matter regions (Plavén-Sigray et al. 2018). Subsequently, a summary-statistics metaanalysis on TSPO in psychosis was published, finding evidence of increases in binding in [^{11}C]PK11195 studies, and no difference in second generation TSPO radioligand studies (Marques et al. 2018). Some methodological limitations have been highlighted in the [^{11}C]PK11195 analyses, including heterogeneous outcome measures and a significant correlation between error and effect size, suggesting that these results should be interpreted with caution (Plavén-Sigray and Cervenka 2019).

Although a decrease or no difference in TSPO at first sight seems to contradict the immune hypothesis of schizophrenia, it should be noted that recent in vitro and experimental evidence has challenged the view of TSPO as an exclusively pro-inflammatory glial marker. TSPO is expressed not only in microglia and astrocytes but also vascular cells and neurons, and down-regulation of TSPO has been observed in pro-inflammatory conditions (Owen et al. 2017; Narayan et al. 2017; Notter et al. 2018). Hence, new markers are needed for reliably assessing brain immune activation in schizophrenia.

8.6 Conclusions and Directions for the Future

The vast majority of PET studies in schizophrenia have focused on the dopamine system, confirming DA receptor blockade as mode of action for antipsychotics, and establishing an overactivity in the striatal DA system as part of the underlying disease mechanism. Arguably, the discovery of a clear therapeutic window of D2-R blockade remains the most important contribution from molecular imaging to clinical psychiatry thus far. These results were important for a dramatic lowering of recommended dosing of antipsychotics, as well as providing a rationale for monotherapy, at least with regard to compounds targeting the D2-R. Another finding emerging from the PET literature in schizophrenia is that of alterations in brain glial cell number or function, although the direction of change warrants further investigation into the underlying biology. In many cases, findings in antipsychotic drug treated patients were not confirmed in drug naïve samples, stressing the need for studies in FEP patients where the confounding effects of medication are avoided.

A general limitation of many clinical PET studies published to date is the low sample size, in relation to the reliability of the outcome measures used. For instance, for the individual studies employing second generation TSPO tracers to study psychosis patients, the power to detect a medium size effect was 23–34% (Plavén-Sigray et al. 2018). Not only does this lead to the failure to detect clinically meaningful effects, as was evident in the case of TSPO studies, but equally increases the risk of false positives that are not replicated in subsequent studies (Button et al. 2013). This is a concern for neuroimaging studies in general, but whereas the magnetic resonance imaging field has followed suit after genetics in

combining datasets from all over the world (ref Chap. 2), the number of multicentre studies within PET are surprisingly low. Although a traditional metaanalysis can be informative, and has for instance helped clarify the nature of the dopminergic alterations in schizophrenia, mega-analyses or individual participant data meta-analyses have the advantage of allowing for control of confounding factors, as well as performing correlational analyses against clinical measures. Moreover, larger samples would facilitate the identification of biologically distinct patient subgroups, such that PET can fulfil its potential in contributing to the development of personalized medicine in psychiatry.

Summary

- Molecular imaging studies have provided support for increased activity of striatal dopaminergic neurons in psychosis or schizophrenia patients.
- Studies of dopamine receptor levels have yielded small increases of D2-R in striatum, whereas reports on D1-R and extrastriatal D2-R levels have been less consistent.
- Serotonin receptor subtypes and transporter levels are not changed in patients with psychosis or schizophrenia.
- Studies of the glial marker TSPO have shown lower levels or no differences, which is in contrast to hypothesized increases.
- Generally, sample sizes have been small, and as such individual studies are often inconclusive.

References

Abi-Dargham A, Gil R, Krystal J, Baldwin RM, Seibyl JP, et al. Increased striatal dopamine transmission in schizophrenia: confirmation in a second cohort. Am J Psychiatry. 1998;155(6):761–7.

Abi-Dargham A, Rodenhiser J, Printz D, Zea-Ponce Y, Gil R, et al. Increased baseline occupancy of D2 receptors by dopamine in schizophrenia. Proc Natl Acad Sci U S A. 2000;97(14):8104–9.

Abi-Dargham A, Mawlawi O, Lombardo I, Gil R, Martinez D, et al. Prefrontal dopamine D1 receptors and working memory in schizophrenia. J Neurosci. 2002;22(9):3708–19.

Abi-Dargham A, Xu X, Thompson JL, Gil R, Kegeles LS, et al. Increased prefrontal cortical D_1 receptors in drug naïve patients with schizophrenia: a PET study with [^{11}C]NNC112. J Psychopharmacol. 2012;26(6):794–805.

Andreasen NC, Carson R, Diksic M, Evans A, Farde L, et al. Workshop on schizophrenia, PET, and dopamine D2 receptors in the human neostriatum. Schizophr Bull. 1988;14(3):471–84.

Angrist BM, Gershon S. The phenomenology of experimentally induced amphetamine psychosis—preliminary observations. Biol Psychiatry. 1970;2(2):95–107.

Asai Y, Takano A, Ito H, Okubo Y, Matsuura M, et al. GABAA/Benzodiazepine receptor binding in patients with schizophrenia using [11C]Ro15-4513, a radioligand with relatively high affinity for alpha5 subunit. Schizophr Res. 2008;99(1–3):333–40.

Bantick RA, Montgomery AJ, Bench CJ, Choudhry T, Malek N, et al. A positron emission tomography study of the 5-HT1A receptor in schizophrenia and during clozapine treatment. J Psychopharmacol. 2004;18(3):346–54.

Berry AS, Shah VD, Furman DJ, White RL, Baker SL, et al. Dopamine synthesis capacity is associated with D2/3 receptor binding but not dopamine release. Neuropsychopharmacology. 2018;43(6):1201–11.

Blomström Å, Karlsson H, Gardner R, Jörgensen L, Magnusson C, Dalman C. Associations between maternal infection during pregnancy, childhood infections, and the risk of subsequent psychotic disorder - a Swedish cohort study of nearly 2 million individuals. Schizophr Bull. 2016;42(1):125–33.

Bloomfield PS, Selvaraj S, Veronese M, Rizzo G, Bertoldo A, et al. Microglial activity in people at ultra high risk of psychosis and in schizophrenia: an [^{11}C]PBR28 PET brain imaging study. Am J Psychiatry. 2015;173(1):44–52.

Bodén R, Persson J, Wall A, Lubberink M, Ekselius L, et al. Striatal phosphodiesterase 10A and medial prefrontal cortical thickness in patients with schizophrenia: a PET and MRI study. Transl Psychiatry. 2017;7(3):e1050.

Braestrup C, Albrechtsen R, Squires RF. High densities of benzodiazepine receptors in human cortical areas. Nature. 1977;269(5630):702–4.

Breier A, Su TP, Saunders R, Carson RE, Kolachana BS, et al. Schizophrenia is associated with elevated amphetamine-induced synaptic dopamine concentrations: evidence from a novel positron emission tomography method. Proc Natl Acad Sci U S A. 1997;94(6):2569–74.

Buchsbaum MS, Christian BT, Lehrer DS, Narayanan TK, Shi B, et al. D2/D3 dopamine receptor binding with [F-18]fallypride in thalamus and cortex of patients with schizophrenia. Schizophr Res. 2006;85(1–3):232–44.

Button KS, Ioannidis JPA, Mokrysz C, Nosek BA, Flint J, et al. Power failure: why small sample size undermines the reliability of neuroscience. Nat Rev Neurosci. 2013;14(5):365–76.

Çakici N, van Beveren NJM, Judge-Hundal G, Koola MM, Sommer IEC. An update on the efficacy of anti-inflammatory agents for patients with schizophrenia: a meta-analysis. Psychol Med. 2019;49(14):2307–19.

Canat X, Carayon P, Bouaboula M, Cahard D, Shire D, et al. Distribution profile and properties of peripheral-type benzodiazepine receptors on human hemopoietic cells. Life Sci. 1993;52(1):107–18.

Caravaggio F, Iwata Y, Kim J, Shah P, Gerretsen P, et al. What proportion of striatal D2 receptors are occupied by endogenous dopamine at baseline? A meta-analysis with implications for understanding antipsychotic occupancy. Neuropharmacology. 2020;163:107591.

Ceccarini J, De Hert M, Van Winkel R, Peuskens J, Bormans G, et al. Increased ventral striatal CB1 receptor binding is related to negative symptoms in drug-free patients with schizophrenia. Neuroimage. 2013;79:304–12.

Chen KC, Yang YK, Howes O, Lee IH, Landau S, et al. Striatal dopamine transporter availability in drug-naive patients with schizophrenia: a case-control SPECT study with [99mTc]-TRODAT-1 and a meta-analysis. Schizophr Bull. 2013;39(2):378–86.

Collste K, Plavén-Sigray P, Fatouros-Bergman H, Victorsson P, Schain M, et al. Lower levels of the glial cell marker TSPO in drug-naive first-episode psychosis patients as measured using PET and [11C]PBR28. Mol Psychiatry. 2017;22(6):850–6.

Connell PH. Amphetamine psychosis. Br Med J. 1957;1(5018):582.

Coughlin JM, Wang Y, Ambinder EB, Ward RE, Minn I, et al. In vivo markers of inflammatory response in recent-onset schizophrenia: a combined study using [^{11}C]DPA-713 PET and analysis of CSF and plasma. Transl Psychiatry. 2016;6:e777.

Deakin B, Suckling J, Barnes TRE, Byrne K, Chaudhry IB, et al. The benefit of minocycline on negative symptoms of schizophrenia in patients with recent-onset psychosis (BeneMin): a randomised, double-blind, placebo-controlled trial. Lancet Psychiatry. 2018;5(11):885–94.

Demjaha A, Murray RM, McGuire PK, Kapur S, Howes OD. Dopamine synthesis capacity in patients with treatment-resistant schizophrenia. Am J Psychiatry. 2012;169(11):1203–10.

Di Biase MA, Zalesky A, O'keefe G, Laskaris L, Baune BT, et al. PET imaging of putative microglial activation in individuals at ultra-high risk for psychosis, recently diagnosed and chronically ill with schizophrenia. Transl Psychiatry. 2017;7(8):e1225.

Doorduin J, de Vries EFJ, Willemsen ATM, de Groot JC, Dierckx RA, Klein HC. Neuroinflammation in schizophrenia-related psychosis: a PET study. J Nucl Med. 2009;50(11):1801–7.

Ekelund J, Slifstein M, Narendran R, Guillin O, Belani H, et al. In vivo DA D1 receptor selectivity of NNC 112 and SCH 23390. Mol Imaging Biol. 2007;9(3):117–25.

Erritzoe D, Rasmussen H, Kristiansen KT, Frokjaer VG, Haugbol S, et al. Cortical and subcortical 5-HT2A receptor binding in neuroleptic-naive first-episode schizophrenic patients. Neuropsychopharmacology. 2008;33(10):2435–41.

Farde L, Hall H, Ehrin E, Sedvall G. Quantitative analysis of D2 dopamine receptor binding in the living human brain by PET. Science. 1986;231(4735):258–61.

Farde L, Wiesel FA, Hall H, Halldin C, Stone-Elander S, Sedvall G. No D2 receptor increase in PET study of schizophrenia. Arch Gen Psychiatry. United States. 1987;44:671–2.

Farde L, Eriksson L, Blomquist G, Halldin C. Kinetic analysis of central [11C]raclopride binding to D2-dopamine receptors studied by PET—a comparison to the equilibrium analysis. J Cereb Blood Flow Metab. 1989;9(5):696–708.

Farde L, Nordström A-L, Wiesel F-A, Pauli S, Halldin C, Sedvall G. Positron emission tomographic analysis of central D1 and D2 dopamine receptor occupancy in Patients treated with classical neuroleptics and clozapine: relation to extrapyramidal side effects. Arch Gen Psychiatry. 1992;49(7):538–44.

Farde L, Nordström AL, Nyberg S, Halldin C, Sedvall G. D1-, D2-, and 5-HT2-receptor occupancy in clozapine-treated patients. J Clin Psychiatry. 1994;55(Suppl B):67–9.

Fog RL, Randrup A, Pakkenberg H. Aminergic mechanisms in corpus striatum and amphetamine-induced stereotyped behaviour. Psychopharmacologia. 1967;11(2):179–83.

Frankle WG, Lombardo I, Kegeles LS, Slifstein M, Martin JH, et al. Serotonin 1A receptor availability in patients with schizophrenia and schizo-affective disorder: a positron emission tomography imaging study with [11C]WAY 100635. Psychopharmacology. 2006;189(2):155–64.

Frankle WG, Cho RY, Prasad KM, Mason NS, Paris J, et al. In vivo measurement of GABA transmission in healthy subjects and schizophrenia patients. Am J Psychiatry. 2015;172(11):1148–59.

Frankle WG, Paris J, Himes M, Mason NS, Mathis CA, Narendran R. Amphetamine-induced striatal dopamine release measured with an agonist radiotracer in schizophrenia. Biol Psychiatry. 2018;83(8):707–14.

Gefvert O, Lundberg T, Wieselgren IM, Bergstrom M, Langstrom B, et al. D(2) and 5HT(2A) receptor occupancy of different doses of quetiapine in schizophrenia: a PET study. Eur Neuropsychopharmacol. 2001;11(2):105–10.

Gerfen CR, Surmeier DJ. Modulation of striatal projection systems by dopamine. Annu Rev Neurosci. 2011;34(1):441–66.

Graff-Guerrero A, Mizrahi R, Agid O, Marcon H, Barsoum P, et al. The dopamine D2 receptors in high-affinity state and D3 receptors in schizophrenia: a clinical [11C]-(+)-PHNO PET study. Neuropsychopharmacology. 2009;34(4):1078–86.

Hafizi S, Tseng H-H, Rao N, Selvanathan T, Kenk M, et al. Imaging microglial activation in untreated first-

episode psychosis: a PET study with [18F]FEPPA. Am J Psychiatry. 2017a;174(2):118–24.

Hafizi S, Gerritsen C, Kiang M, Michael R, Prce I, et al. Imaging microglial activation in individuals at clinical high risk for psychosis: an in-vivo PET study with [18F]FEPPA. Neuropsychopharmacology. 2017b;42(13):2474–81.

Halldin C, Farde L, Högberg T, Mohell N, Hall H, et al. Carbon-11-FLB 457: a radioligand for extrastriatal D2 dopamine receptors. J Nucl Med. 1995;36(7):1275–81.

Hietala J, Syvalahti E, Vuorio K, Rakkolainen V, Bergman J, et al. Presynaptic dopamine function in striatum of neuroleptic-naive schizophrenic patients. Lancet. 1995;346(8983):1130–1.

Hirvonen J, van Erp T. Brain dopamine d1 receptors in twins discordant for schizophrenia. Am J Phychiatry. 2006;163:1747–53.

Hirvonen J, van Erp TGM, Huttunen J, Aalto S, Någren K, et al. Increased caudate dopamine D2 receptor availability as a genetic marker for schizophrenia. Arch Gen Psychiatry. 2005;62(4):371–8.

Holmes SE, Hinz R, Drake RJ, Gregory CJ, Conen S, et al. In vivo imaging of brain microglial activity in antipsychotic-free and medicated schizophrenia: a [11C](R)-PK11195 positron emission tomography study. Mol Psychiatry. 2016;21(12):1672–9.

Howes OD, Montgomery AJ, Asselin M-C, Murray RM, Valli I, et al. Elevated striatal dopamine function linked to prodromal signs of schizophrenia. Arch Gen Psychiatry. 2009;66(1):13–20.

Howes O, Bose S, Turkheimer F, Valli I, Egerton A, et al. Progressive increase in striatal dopamine synthesis capacity as patients develop psychosis: a PET study. Mol Psychiatry. 2011a;16(9):885–6.

Howes OD, Bose SK, Turkheimer F, Valli I, Egerton A, et al. Dopamine synthesis capacity before onset of psychosis: a prospective [18F]-DOPA PET imaging study. Am J Psychiatry. 2011b;168(12):1311–7.

Howes OD, Kambeitz J, Kim E, Stahl D, Slifstein M, et al. The nature of dopamine dysfunction in schizophrenia and what this means for treatment. Arch Gen Psychiatry. 2012;69(8):776–86.

Hurlemann R, Boy C, Meyer PT, Scherk H, Wagner M, et al. Decreased prefrontal 5-HT2A receptor binding in subjects at enhanced risk for schizophrenia. Anat Embryol. 2005;210(5–6):519–23.

Hurlemann R, Matusch A, Kuhn K-U, Berning J, Elmenhorst D, et al. 5-HT2A receptor density is decreased in the at-risk mental state. Psychopharmacology. 2008;195(4):579–90.

Huttunen J, Heinimaa M, Svirskis T, Nyman M, Kajander J, et al. Striatal dopamine synthesis in first-degree relatives of patients with schizophrenia. Biol Psychiatry. 2008;63(1):114–7.

Imaizumi M, Briard E, Zoghbi SS, Gourley JP, Hong J, et al. Brain and whole-body imaging in nonhuman primates of [11C]PBR28, a promising PET radioligand for peripheral benzodiazepine receptors. NeuroImage. 2008;39(3):1289–98.

Innis RB, Cunningham VJ, Delforge J, Fujita M, Gjedde A, et al. Consensus nomenclature for in vivo imaging of reversibly binding radioligands. J Cereb Blood Flow Metab. 2007;27(9):1533–9.

Sameer Jauhar, Mattia Veronese, Matthew M Nour, Maria Rogdaki, Pamela Hathway, Federico E. Turkheimer, James Stone, Alice Egerton, Philip McGuire, Shitij Kapur, Oliver D Howes. Determinants of treatment response in first-episode psychosis: an 18F-DOPA PET study. Mol Psychiatry. 24:1502–1512;2019.

Kambeitz J, Abi-Dargham A, Kapur S, Howes OD. Alterations in cortical and extrastriatal subcortical dopamine function in schizophrenia: systematic review and meta-analysis of imaging studies. Br J Psychiatry. 2014;204(6):420–9.

Kang JI, Park H-J, Kim SJ, Kim KR, Lee SY, et al. Reduced binding potential of GABA-A/benzodiazepine receptors in individuals at ultra-high risk for psychosis: an [18F]-fluoroflumazenil positron emission tomography study. Schizophr Bull. 2014;40(3):548–57.

Kapur S, Remington G, Zipursky RB, Wilson AA, Houle S. The D2 dopamine receptor occupancy of risperidone and its relationship to extrapyramidal symptoms: a PET study. Life Sci. 1995;57(10):103–7.

Kapur S, Zipursky RB, Remington G, Jones C, DaSilva J, et al. 5-HT2 and D2 receptor occupancy of olanzapine in schizophrenia: a PET investigation. Am J Psychiatry. 1998;155(7):921–8.

Karlsson P, Smith L, Farde L, Harnryd C, Sedvall G, Wiesel FA. Lack of apparent antipsychotic effect of the D1-dopamine receptor antagonist SCH39166 in acutely ill schizophrenic patients. Psychopharmacol. 1995;121(3):309–16.

Karlsson P, Farde L, Halldin C, Sedvall G. PET study of D(1) dopamine receptor binding in neuroleptic-naive patients with schizophrenia. Am J Psychiatry. 2002;159(5):761–7.

Kegeles LS, Abi-Dargham A, Frankle WG, Gil R, Cooper TB, et al. Increased synaptic dopamine function in associative regions of the striatum in schizophrenia. Arch Gen Psychiatry. 2010;67(3):231.

Kenk M, Selvanathan T, Rao N, Suridjan I, Rusjan P, et al. Imaging neuroinflammation in gray and white matter in schizophrenia: an in-vivo PET study with [18F]-FEPPA. Schizophr Bull. 2014;41(1):85–93.

Kessler RM, Woodward ND, Riccardi P, Li R, Ansari MS, et al. Dopamine D2 receptor levels in striatum, thalamus, substantia nigra, limbic regions, and cortex in schizophrenic subjects. Biol Psychiatry. 2009;65(12):1024–31.

Khandaker GM, Zimbron J, Dalman C, Lewis G, Jones PB. Childhood infection and adult schizophrenia: a meta-analysis of population-based studies. Schizophr Res. 2012;139(1–3):161–8.

Kim J-H, Son Y-D, Kim J-H, Choi E-J, Lee S-Y, et al. Serotonin transporter availability in thalamic subregions in schizophrenia: a study using 7.0-T MRI with [(11)C]DASB high-resolution PET. Psychiatry Res. 2015;231(1):50–7.

Kosaka J, Takahashi H, Ito H, Takano A, Fujimura Y, et al. Decreased binding of [11C]NNC112 and [11C] SCH23390 in patients with chronic schizophrenia. Life Sci. 2010;86(21–22):814–8.

Laakso A, Vilkman H, Alakare B, Haaparanta M, Bergman J, et al. Striatal dopamine transporter binding in neuroleptic-naive patients with schizophrenia studied with positron emission tomography. Am J Psychiatry. 2000;157(2):269–71.

Laruelle M, Abi-dargham A, Van Dyck CH, Gil R, Souza CDD, et al. Single photon emission computerized tomography imaging of schizophrenic subjects. Psychiatry Interpers Biol Process. 1996;93:9235–40.

Laruelle M, Abi-Dargham A, van Dyck C, Gil R, D'Souza DC, et al. Dopamine and serotonin transporters in patients with schizophrenia: an imaging study with [(123)I]beta-CIT. Biol Psychiatry. 2000;47(5):371–9.

Lewis R, Kapur S, Jones C, DaSilva J, Brown GM, et al. Serotonin 5-HT2 receptors in schizophrenia: a PET study using [18F]setoperone in neuroleptic-naive patients and normal subjects. Am J Psychiatry. 1999;156(1):72–8.

Lidow MS, Goldman-Rakic PS. A common action of clozapine, haloperidol, and remoxipride on D1- and D2-dopaminergic receptors in the primate cerebral cortex. Proc Natl Acad Sci U S A. 1994;91:4353–6.

Lidow MS, Elsworth JD, Goldman-Rakic PS. Down-regulation of the D1 and D5 dopamine receptors in the primate prefrontal cortex by chronic treatment with antipsychotic drugs. J Pharmacol Exp Ther. 1997;281(1):597–603.

Lieberman JA, Kane JM, Alvir J. Provocative tests with psychostimulant drugs in schizophrenia. Psychopharmacology (Berl). 1987;91(4):415–33.

Marques TR, Natesan S, Niccolini F, Politis M, Gunn RN, et al. Phosphodiesterase 10A in schizophrenia: a PET study using [11C]IMA107. Am J Psychiatry. 2016;173(7):714–21.

Marques TR, Ashok AH, Pillinger T, Veronese M, Turkheimer FE, et al. Neuroinflammation in schizophrenia: meta-analysis of in vivo microglial imaging studies. Psychol Med. 2018;49(13):2186–96.

Matheson GJ, Plavén-Sigray P, Forsberg A, Varrone A, Farde L, Cervenka S. Assessment of simplified ratio-based approaches for quantification of PET [11C] PBR28 data. EJNMMI Res. 2017;7:58.

Meyer-Lindenberg A, Miletich RS, Kohn PD, Esposito G, Carson RE, et al. Reduced prefrontal activity predicts exaggerated striatal dopaminergic function in schizophrenia. Nat Neurosci. 2002;5(3):267–71.

Miller BJ, Buckley P, Seabolt W, Mellor A, Kirkpatrick B. Meta-analysis of cytokine alterations in schizophrenia: clinical status and antipsychotic effects. Biol Psychiatry. 2011;70(7):663–71.

Mintun MA, Raichle ME, Kilbourn MR, Wooten GF, Welch MJ. A quantitative model for the in vivo assessment of drug binding sites with positron emission tomography. Ann Neurol. 1984;15(3):217–27.

Mitchell AC, Jiang Y, Peter C, Akbarian S. Transcriptional regulation of GAD1 GABA synthesis gene in the prefrontal cortex of subjects with schizophrenia. Schizophr Res. 2015;167(1–3):28–34.

Mizrahi R, Addington J, Rusjan PM, Suridjan I, Ng A, et al. Increased stress-induced dopamine release in psychosis. Biol Psychiatry. 2012;71(6):561–7.

Mukherjee J, Christian BT, Dunigan KA, Shi B, Narayanan TK, et al. Brain imaging of 18F-fallypride in normal volunteers: blood analysis, distribution, test-retest studies, and preliminary assessment of sensitivity to aging effects on dopamine D-2/D-3 receptors. Synapse. 2002;46(3):170–88.

Narayan N, Mandhair H, Smyth E, Dakin SG. The macrophage marker translocator protein (TSPO) is down-regulated on pro-inflammatory 'M1' human macrophages. PLoS One. 2017;12(10):e0185767.

Narendran R, Frankle WG. Comment on analyses and conclusions of "microglial activity in people at ultra high risk of psychosis and in schizophrenia: an [^{11}C] PBR28 PET brain imaging study". Am J Psychiatry. 2016;173(5):536–7.

Nord M, Farde L. Antipsychotic occupancy of dopamine receptors in schizophrenia. CNS Neurosci Ther. 2011;17(2):97–103.

Nordstrom AL, Farde L, Wiesel FA, Forslund K, Pauli S, et al. Central D2-dopamine receptor occupancy in relation to antipsychotic drug effects: a double-blind PET study of schizophrenic patients. Biol Psychiatry. 1993a;33(4):227–35.

Nordstrom AL, Farde L, Halldin C. High 5-HT2 receptor occupancy in clozapine treated patients demonstrated by PET. Psychopharmacology. 1993b;110(3):365–7.

Nordström AL, Farde L, Nyberg S, Karlsson P, Halldin C, Sedvall G. D1, D2, and 5-HT2 receptor occupancy in relation to clozapine serum concentration: a PET study of schizophrenic patients. Am J Psychiatry. 1995;152(10):1444–9.

Notter T, Coughlin JM, Sawa A, Meyer U. Reconceptualization of translocator protein as a biomarker of neuroinflammation in psychiatry. Mol Psychiatry. 2018;23(1):36–47.

Nyberg S, Farde L, Halldin C. A PET study of 5-HT2 and D2 dopamine receptor occupancy induced by olanzapine in healthy subjects. Neuropsychopharmacology. 1997;16(1):1–7.

Okubo Y, Suhara T, Suzuki K, Kobayashi K, Inoue O, et al. Decreased prefrontal dopamine D1 receptors in schizophrenia revealed by PET. Nature. 1997;385(6617):634–6.

Okubo Y, Suhara T, Suzuki K, Kobayashi K, Inoue O, et al. Serotonin 5-HT2 receptors in schizophrenic patients studied by positron emission tomography. Life Sci. 2000;66(25):2455–64.

Orhan F, Goiny M, Malmqvist A, Piehl F, Schizophrenia K, et al. CSF GABA is reduced in first-episode psychosis and associates to symptom severity. Mol Psychiatry. 2018;23(5):1244–50.

Ottoy J, De Picker L, Verhaeghe J, Deleye S, wyffels L, et al. ^{18}F-PBR111 PET imaging in healthy controls and schizophrenia: test–retest reproducibility and

quantification of neuroinflammation. J Nucl Med. 2018;59(8):1267–74.
Owen DR, Yeo AJ, Gunn RN, Song K, Wadsworth G, et al. An 18-kDa translocator protein (TSPO) polymorphism explains differences in binding affinity of the PET radioligand PBR28. J Cereb Blood Flow Metab. 2012;32(1):1–5.
Owen DR, Narayan N, Wells L, Healy L, Smyth E, et al. Pro-inflammatory activation of primary microglia and macrophages increases 18 kDa translocator protein expression in rodents but not humans. J Cereb Blood Flow Metab. 2017;37(8):2679–90.
Plavén-Sigray P, Cervenka S. Meta-analytic studies of the glial cell marker TSPO in psychosis—a question of apples and pears? Psychol Med. 2019;49(10):1624–8.
Plavén-Sigray P, Matheson GJ, Collste K, Ashok AH, Coughlin JM, et al. Positron emission tomography studies of the glial cell marker translocator protein in patients with psychosis: a meta-analysis using individual participant data. Biol Psychiatry. 2018;84(6):433–42.
Ranganathan M, Cortes-Briones J, Radhakrishnan R, Thurnauer H, Planeta B, et al. Reduced brain cannabinoid receptor availability in schizophrenia. Biol Psychiatry. 2016;79(12):997–1005.
Rao N, Northoff G, Tagore A, Rusjan P, Kenk M, et al. Impaired prefrontal cortical dopamine release in schizophrenia during a cognitive task: a [11C]FLB 457 positron emission tomography study. Schizophr Bull. 2018;45(3):670–9.
Rasmussen H, Frokjaer VG, Hilker RW, Madsen J, Anhøj S, Oranje B, Pinborg LH, Glenthøj B, Knudsen GM, et al. Eur Neuropsychopharmacol. 2016;26(7):1248–50. https://doi.org/10.1016/j.euroneuro.2016.04.008.
Reimold M, Solbach C, Noda S, Schaefer JE, Bartels M, et al. Occupancy of dopamine D1, D2 and serotonin 2A receptors in schizophrenic patients treated with flupentixol in comparison with risperidone and haloperidol. Psychopharmacology. 2007;190(2):241–9.
Ripke S, Neale BM, Corvin A, Walters JTR, Farh K-H, et al. Biological insights from 108 schizophrenia-associated genetic loci. Nature. 2014;511(7510):421–7.
Seeman P, Ulpian C, Bergeron C, Riederer P, Jellinger K, et al. Bimodal distribution of dopamine receptor densities in brains of schizophrenics. Science. 1984;225(4663):728–31.
Slifstein M, Kegeles LS, Gonzales R, Frankle WG, Xu X, et al. [11C]NNC 112 selectivity for dopamine D 1 and serotonin 5-HT 2A receptors: a PET study in healthy human subjects. J Cereb Blood Flow Metab. 2007;27(10):1733–41.
Slifstein M, van de Giessen E, Van Snellenberg J, Thompson JL, Narendran R, et al. Deficits in prefrontal cortical and extrastriatal dopamine release in schizophrenia. JAMA Psychiatry. 2015;10032:1–9.
Stenkrona P, Matheson GJ, Halldin C, Cervenka S, Farde L. D1-dopamine receptor availability in first-episode neuroleptic naive psychosis patients. Int J Neuropsychopharmacol. 2019;22(7):415–25.
Talvik M, Nordström AL, Olsson H, Halldin C, Farde L. Decreased thalamic D2/D3 receptor binding in drug-naive patients with schizophrenia: a PET study with [11C]FLB 457. Int J Neuropsychopharmacol. 2003;6(4):361–70.
Talvik M, Nordström A-L, Okubo Y, Olsson H, Borg J, et al. Dopamine D2 receptor binding in drug-naïve patients with schizophrenia examined with raclopride-C11 and positron emission tomography. Psychiatry Res. 2006;148(2–3):165–73.
Tauscher J, Kapur S, Verhoeff NPLG, Hussey DF, Daskalakis ZJ, et al. Brain serotonin 5-HT(1A) receptor binding in schizophrenia measured by positron emission tomography and [11C]WAY-100635. Arch Gen Psychiatry. 2002;59(6):514–20.
Trichard C, Paillere-Martinot ML, Attar-Levy D, Blin J, Feline A, Martinot JL. No serotonin 5-HT2A receptor density abnormality in the cortex of schizophrenic patients studied with PET. Schizophr Res. 1998;31(1):13–7.
Upthegrove R, Manzanares-Teson N, Barnes NM. Cytokine function in medication-naive first episode psychosis: a systematic review and meta-analysis. Schizophr Res. 2014;155(1–3):101–8.
Vallone D, Picetti R, Borrelli E. Structure and function of dopamine receptors. Neurosci Biobehav Rev. 2000;24(1):125–32.
van Berckel BN, Bossong MG, Boellaard R, Kloet R, Schuitemaker A, et al. Microglia activation in recent-onset schizophrenia: a quantitative (R)-[11C]PK11195 positron emission tomography study. Biol Psychiatry. 2008;64(9):820–2.
Van Der Doef TF, De Witte LD, Sutterland AL, Jobse E, Yaqub M, et al. In vivo (R) - [^{11}C] PK11195 PET imaging of 18kDa translocator protein in recent onset psychosis. NPJ Schizophr. 2016;2:16031.
Varrone A, Sjöholm N, Eriksson L, Gulyás B, Halldin C, Farde L. Advancement in PET quantification using 3D-OP-OSEM point spread function reconstruction with the HRRT. Eur J Nucl Med Mol Imaging. 2009;36(10):1639–50.
Venneti S, Lopresti BJ, Wiley CA. Molecular imaging of microglia/macrophages in the brain. Glia. 2013;61(1):10–23.
Verhoeff NP, Soares JC, D'Souza CD, Gil R, Degen K, et al. [123I]Iomazenil SPECT benzodiazepine receptor imaging in schizophrenia. Psychiatry Res. 1999;91(3):163–73.
Verhoeff NP, Meyer JH, Kecojevic A, Hussey D, Lewis R, et al. A voxel-by-voxel analysis of [18F]setoperone PET data shows no substantial serotonin 5-HT(2A) receptor changes in schizophrenia. Psychiatry Res. 2000;99(3):123–35.
Wagner HN, Burns HD, Dannals RF, Wong DF, Langstrom B, et al. Imaging dopamine receptors in

the human brain by positron tomography. Science. 1983;221(4617):1264–6.

Weinstein JJ, van de Giessen E, Rosengard RJ, Xu X, Ojeil N, et al. PET imaging of dopamine-D2 receptor internalization in schizophrenia. Mol Psychiatry. 2018;23(6):1506–11.

Wilson AA, Garcia A, Parkes J, McCormick P, Stephenson KA, et al. Radiosynthesis and initial evaluation of [18F]-FEPPA for PET imaging of peripheral benzodiazepine receptors. Nucl Med Biol. 2008;35(3):305–14.

Wong DF, Wagner HN, Tune LE, Dannals RF, Pearlson GD, et al. Positron emission tomography reveals elevated D2 dopamine receptors in drug-naive schizophrenics. Science. 1986;234(4783):1558–63.

Wong DF, Kuwabara H, Horti AG, Raymont V, Brasic J, et al. Quantification of cerebral cannabinoid receptors subtype 1 (CB1) in healthy subjects and schizophrenia by the novel PET radioligand [11C] OMAR. Neuroimage. 2010;52(4):1505–13.

Woolley DW, Shaw E. A biochemical and pharmacological suggestion about certain mental disorders. Proc Natl Acad Sci U S A. 1954;40(4):228–31.

Yasuno F, Suhara T, Okubo Y, Sudo Y, Inoue M, et al. Low dopamine D2receptor binding in subregions of the thalamus in schizophrenia. Am J Psychiatry. 2004a;161(6):1016–22.

Yasuno F, Suhara T, Ichimiya T, Takano A, Ando T, Okubo Y. Decreased 5-HT1A receptor binding in amygdala of schizophrenia. Biol Psychiatry. 2004b;55(5):439–44.

9 Magnetic Resonance Spectroscopy Methods

Eduardo Coello, Tyler C. Starr, and Alexander P. Lin

Contents

E. Coello · T. C. Starr · A. P. Lin (✉)
Department of Radiology, Center for Clinical Spectroscopy, Brigham and Women's Hospital, Harvard Medical School, Boston, MA, USA
e-mail: jcoellouribe@bwh.harvard.edu; tstarr@bwh.harvard.edu; aplin@bwh.harvard.edu

M. Kubicki, M. E. Shenton (eds.), *Neuroimaging in Schizophrenia*,
https://doi.org/10.1007/978-3-030-35206-6_9

Abbreviations

13C	Carbon 13
2D COSY	Two-Dimensional COrrelated SpectroscopY
2D JPRESS	Two-Dimensional J-resolved Point RESolved Spectroscopy
Cho	Choline
Cr	Creatine
CRLB	Cramer–Rao lower bounds
CSI	Chemical shift imaging
FT	Fourier transform
FID	Free induction decay
fMRI	functional magnetic resonance imaging
GABA	*gamma*-Aminobutyric acid
Gln	Glutamine
Glu	Glutamate
Glx	Both glutamate and glutamine
GPC	Glycerophosphocholine
GSH	Glutathione
JPRESS	J-resolved Point RESolved Spectroscopy
MCI	Mild cognitive impairment
MEGA PRESS	MEscher-GArwood Point RESolved Spectroscopy
mI	myo-Inositol
MRI	Magnetic resonance imaging
MRS	Magnetic resonance spectroscopy
NAA	*N*-Acetylaspartate
NAAG	*N*-Acetylaspartylglutamate
NMDA	*N*-Methyl-D-aspartic acid
NMR	Nuclear magnetic resonance
PCP	Phencyclidine
PC	Phosphorylcholine
PCr	Phosphocreatine
PET	Positron emission tomography
PRESS	Point RESolved Spectroscopy
RF	Radiofrequency
ROI	Region of interest
ROS	Reactive oxygen species
STEAM	STimulated Echo Acquisition Mode
SVS	Single voxel spectroscopy
TCA	Tricarboxylic acid cycle
TE	Echo time
TI	Inversion time
TR	Relaxation time

9.1 Magnetic Resonance Spectroscopy (MRS)

9.1.1 General Overview

Magnetic Resonance Spectroscopy (MRS) is a non-invasive technique that quantitatively measures the metabolic composition of tissues *in vivo* using conventional magnetic resonance (MR) scanners. This technology is of special interest for clinical applications in psychiatry due to its non-invasive nature. In recent years, studies have demonstrated its diagnostic capability in psychiatric conditions such as schizophrenia, bipolar disorder, depression, as well as in neurodegenerative disorders and neuro-oncology among others (Öz et al. 2014). The most relevant brain chemicals that can be quantified include: N-acetylaspartate (NAA), a neuronal marker; creatine (Cr), involved in energy metabolism; choline (Cho), a key component of myelin; glutamate (Glu), an excitatory neurotransmitter; γ-aminobutyric acid (GABA), an inhibitory neurotransmitter, and glutathione (GSH), an antioxidant involved in neuroinflammation. In this chapter, the biological roles of the primary brain metabolites will be discussed. Moreover, the general principles of MRS and the specialized pulse sequences that enable the detection each of these metabolites will be described. Furthermore, a comprehensive introduction of the most common techniques and examination protocols used in research and clinical applications will be presented.

9.1.2 Physics of MRS

MRS is based in nuclear magnetic resonance (NMR) spectroscopy, which was first introduced in the early 1950s and was typically employed in organic chemistry to define chemical structures (Bloch 1946; Bloch et al. 1946; Purcell et al. 1946). Shortly thereafter, NMR spectroscopy was successfully applied to the human body (Andrew 1980), providing access to quantitative and non-invasive studies of biochemistry.

The physics behind MRS is fundamentally the same as that utilized by NMR. In an MRS experiment, the patient is placed into a uniform static magnetic field such that unbound nuclei precess at

a specific frequency proportional to the field strength, known as the Larmor frequency. Then, a radiofrequency (RF) transmitter coil excites the nuclei by applying electromagnetic radiation in the form of an RF pulse. The nuclei absorb the electromagnetic energy, altering the orientation of the nuclear spins. Finally, as the nuclei relax back to their original state, energy is released and detected by the receiver in the RF coil as a free induction decay (FID) signal. By computing the Fourier transform of the measured FID, its spectral components can be obtained and visualized in a graph (Fig. 9.1). Each molecule in the sample resonates at established frequencies, which appear as a peak at a specific frequency location, or chemical shift, along the x-axis. The chemical shift of a molecule is often expressed in parts per million (ppm) of the Larmor frequency so the scale is independent of the magnetic field strength. In an MRS spectrum, the concentration of a specific metabolite is proportional to the area under the curve of each peak. Higher concentrations result in larger peaks, which enables MRS's use as a quantitative technique. Some pulse sequence parameters that largely influence the robustness and sensitivity of this technique are: echo time (TE), related to the time between the excitation and the signal readout; repetition time (TR), which corresponds to the time between consecutive excitations; number of signal averages and the volume of the excited tissue. The neurometabolites that can be detected with MRS are of great interest as they are tied to metabolic and neurological processes within the brain that directly relate to a physiological, cognitive or neuronal process.

9.1.3 Brain Metabolites

The abundance of hydrogen (^{1}H) in organic molecules and the relatively high sensitivity that it provides in MRS in comparison with other nuclei, allows detecting several characteristic resonances of the central nervous system (CNS). Although up to 18 metabolic components could be identified in a ^{1}H MRS spectrum *in vivo*, their detection is generally limited by different factors related to the hardware sensitivity, field strength, spectral overlap, signal artifacts, and patient stability. The present section presents a detailed description of the most relevant brain metabolites that can be reliably measured and quantified under healthy and disease conditions using clinical MR scanners, typically at 3 T magnetic field strength. In Fig. 9.1, a representative ^{1}H MRS examination is shown together with the measured spectrum and the different metabolic components present in it.

9.1.3.1 N-Acetyl Aspartate (NAA)

NAA is an amino-acid derivative synthesized in neurons and transported down axons (Moffett et al. 1993). In ^{1}H MRS of the brain and under healthy conditions, the primary resonance of NAA appears as the largest peak in the spectrum located at 2.02 ppm. Studies have also correlated the concentration of NAA in the brain with the number of neurons measured. Therefore, it is considered a marker of healthy neurons, axons, and dendrites (Urenjak et al. 1992). A diagnosis can be made using MRS by either comparing the numeric values of NAA concentrations or by recognizing abnormal patterns of peaks in the spectra. This has been shown across a variety of diseases (Lin et al. 2005; Harris et al. 2006; Moffett et al. 2007). Although different studies have shown some of the functions of NAA in the central nervous system, the main role of NAA is not fully understood (Barker 2001).

9.1.3.2 Creatine (Cr)

Creatine (Cr) and its phosphorylated version, phosphocreatine (PCr) appear with their major resonance at 3.02 ppm. The metabolism of Cr and PCr provides the basis of energy metabolism in the brain via the mitochondria where Cr is phosphorylated by the enzyme creatine kinase and adenosine triphosphate (ATP) to form PCr and vice-versa (Ross 2000). As a key metabolite to maintain energy homeostasis, Cr is uniform in different areas of the brain and between subjects. For this reason, the ratio to Cr is often reported as

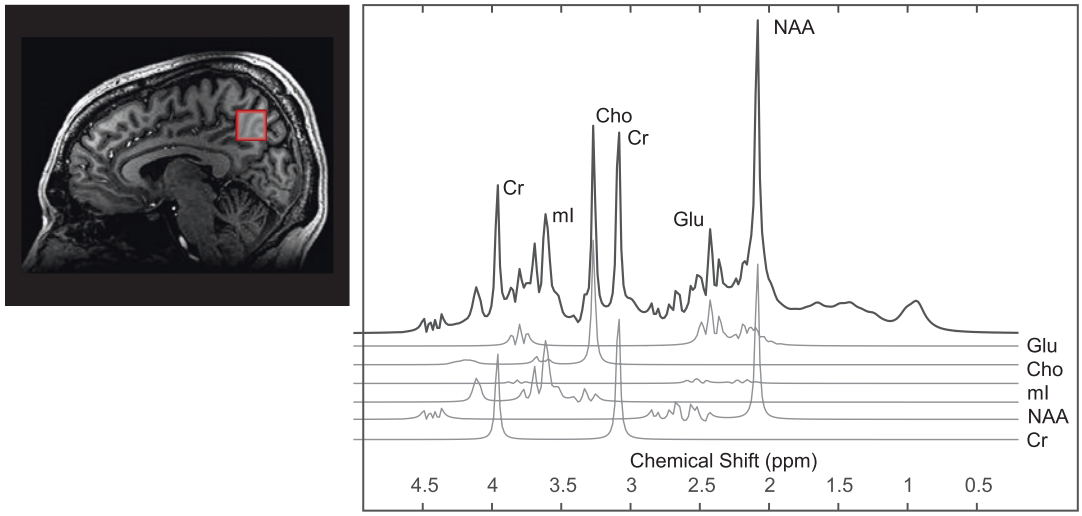

Fig. 9.1 Standard ^{1}H MRS of the brain at short echo time. (left) Selected volume of interest (VOI) within the brain showed together with the anatomical reference. (right) Measured spectrum containing resonances of five metabolites, namely glutamate (Glu), choline (Cho), myo-inositol (mI), N-acetyl-aspartate (NAA) and creatine (Cr)

a normalized concentration between metabolites and subjects. However, in some situations, energy utilization can be affected by disease and other Cr metabolic pathways, thus affecting the reliability of relative concentrations. Mitochondrial dysfunction in the brain would likely cause changes in Cr and PCr and has been implicated across a range of neuropsychiatric disorders including schizophrenia and bipolar disorder (Rezin et al. 2009). Cr can be also affected by osmotic equilibrium in the brain (Bluml et al. 1998). Furthermore, as Cr is synthetized in the liver, a reduction in Cr in the CNS can be caused by liver failure.

9.1.3.3 Choline (Cho)

Choline (Cho) or total Cho (tCho) includes several different metabolites: choline, phosphorylcholine (PC), and glycerophosphorylcholine (GPC), which are the main constituents, as well as phosphorylethanolamine and glycerophosphorylethanolamine, to a lesser extent. The primary resonance can be found at 3.2 ppm. These metabolites are components of the myelin sheath, crucial for the propagation of signals throughout the brain. As a result, an increased Cho level is found in areas of greater myelin and membrane density such as in the white matter. In addition, PC and GPC are involved in the metabolism of phosphatidylcholine and other membrane phospholipids. Thus, the turnover of the membrane of myelin phospholipids, as well as demyelination, are closely tied to increases in Cho as observed by MRS. Due to the involvement of Cho in both membrane turnover and degradation, as well as density, it is a sensitive but not necessarily a specific marker of membrane conditions.

Recent studies in Alzheimer's disease (Kantarci 2007), schizophrenia (Kraguljac et al. 2012), and depression (Caverzasi et al. 2012) have shown conflicting reports on Cho levels in these conditions. In bipolar disorder, however, the literature has shown a consistent elevated choline signal in the basal ganglia (Maddock and Buonocore 2012). The most likely reason for why Cho findings are discordant across different studies even within the same disease is due to the sensitivity of Cho to the gray and white matter volumes in the regions of interest studied. A solution to this problem is to combine image segmentation within the voxel of interest for MRS to account for the relative contributions of gray and white matter to the Cho level.

9.1.3.4 Myo-Inositol (mI)

Myo-inositol (mI) is a cyclic sugar-alcohol only detected at short echo times. Its main observable resonance peak appears at 3.52 ppm. mI is involved in a multitude of different metabolic processes (Ross and Bluml 2001), such as cerebral osmotic regulation and demyelination. While its role may not be well understood, the importance of mI, however, is the broad range of concentrations found across different diseases. For example, mI has nearly zero concentration in hepatic encephalopathy to up to a three-fold increase in newborns compared to nominal adult values. Therefore, it has been found to be highly specific and sensitive within the context of disease diagnosis in patients when compared with controls and therefore provides great clinical value.

Studies of dementia have highlighted the importance of mI. In the early stages of dementia, such as mild cognitive impairment (MCI), mI is elevated long before symptoms of dementia are obvious (Kantarci 2013). Moreover, in combination with NAA, mI predicts the outcome of MCI patients and is also highly sensitive and specific in the diagnosis of Alzheimer's disease (Öz et al. 2014).

9.1.3.5 Glutamate (Glu) and Glutamine (Gln)

Glu is an amino acid with several important roles in the human brain. It is the most abundant excitatory neurotransmitter; therefore, several neurological and psychiatric diseases have an impact upon this molecule. Neuronal dysfunction leads to an accumulation of Glu, which results in excitotoxicity. Additionally, Glu is a key compound in brain energy metabolism via the citric acid cycle. After its release into the synaptic cleft, Glu is taken up by adjoining cells through excitatory amino acid transporters. Astrocytes are responsible for uptake of most extracellular Glu preserving the low extracellular concentration of Glu needed for proper receptor-mediated functions (Schousboe 2003; Schousboe and Waagepetersen 2005). Glu is stored as Gln in the glial cells, and the balanced cycling between these two neurochemicals is essential for the normal functioning of brain cells (Gruetter et al. 1994; Mason et al. 1995).

Gln is the main precursor for neuronal Glu and GABA (Hertz and Zielke 2004). It has been estimated that the cycling between Gln and Glu accounts for more than 80% of cerebral glucose consumption (Sibson et al. 1998; Pellerin and Magistretti 1994). The molecular structures of Glu and Gln are very similar and, consequently, give rise to similar magnetic resonance spectra (Govindaraju et al. 2000). Thus, even though Glu has a relatively higher concentration in the brain, its major resonances are usually contaminated by contributions from Gln, GABA, GSH, and NAA. For this reason, the term Glx is often used to reflect the combined concentrations of Glu and Gln. Section 9.5 details different pulse sequences to achieve the separation of Glu from its neighboring metabolites.

9.1.3.6 γ-Amino Butyric Acid (GABA)

GABA is the major inhibitory neurotransmitter in the brain. In the developing brain, GABA is initially excitatory and later shifts to its inhibitory role as glutamatergic functions develop (Ben-Ari 2002). Moreover, GABA is of interest across a broad range of psychiatric conditions such as anxiety, memory loss, depression, and pain. GABA acts as an inhibitor by binding to specific receptors that open ion channels, creating a negative membrane potential and preventing the further formation of action potentials. Nevertheless, the detection of GABA using MRS is challenging due to a couple of reasons. First, the concentration of GABA in the brain is rather low, ranging from 1.3 to 1.9 mM (Govindaraju et al. 2000), therefore it is difficult to detect accurately and consistently. Additionally, GABA nuclear spins couple with other neighboring spins, causing the molecule to appear as multiple resonances around 1.9 ppm, 2.28 ppm, and 3.0 ppm, that overlap with other major metabolites such as NAA, Glu, and Cr, respectively. Therefore, specialized sequences (see Sects. 9.3.2 and 9.5) are required to reliably estimate GABA concentrations in vivo.

9.1.3.7 Glutathione (GSH)

The primary role of GSH is as an anti-oxidant, providing a defense system against oxidative stress (Dringen et al. 2000), which can cause

damage related to DNA modification, lipid peroxidation, and protein modification, from which the brain is especially vulnerable. Oxidative stress is also strongly associated with neuroinflammatory processes (Agostinho et al. 2010; Mosley et al. 2006). Consequently, GSH metabolism has been found to play an important role in the pathogenesis of neurodegenerative disorders, as well as psychiatric disorders. GSH is synthesized intracellularly and differently between neurons and glial cells, thus providing an interesting specificity to GSH measures to identify inflammatory processes.

GSH is composed of Glu, cysteine, and glycine, therefore its spectrum highly overlaps with all three of those metabolites (Matsuzawa and Hashimoto 2011). Particularly of concern is the overlap with Glu, given that GSH concentrations in the brain are 1–3 mM whereas Glu concentrations are 6–10 mM (Govindaraju et al. 2000). With minor modifications to the methods that will be described in Sects. 9.3.2 and 9.5, resonances of GSH can be effectively separated from Glu.

9.2 Localization Techniques

To detect and to quantify the metabolic components of brain tissue it is necessary to precisely localize the volume of interest (VOI) within the brain. To achieve this, RF pulses combined with magnetic gradients are used to selectively excite the given region of the brain. This effectively isolates the signal from the VOI avoiding overwhelming lipid signals from the skull that can contaminate the signal. In this section, three commonly used localization sequences will be described.

9.2.1 Stimulated Echo Acquisition Mode (STEAM)

STEAM is a method that uses a series of three consecutive slice-selective 90° pulses for localization (Frahm et al. 1989). Since the sequence only yields half as much of the maximum detectable magnetization, the signal-to-noise ratio (SNR) is reduced compared to other localization methods such as PRESS or semi-LASER. Nevertheless, an effective water suppression and shorter echo times (TE; the time between the first two 90° pulses and between the third 90° pulse and the stimulated echo) are more easily accomplished via STEAM (Haase et al. 1986). This provides an advantage when detecting short-T2 metabolites such as GABA, mI, Glu, and Gln.

9.2.2 Point-Resolved Spectroscopy (PRESS)

PRESS is a localization technique that selectively excites a specified volume using a pulse sequence that consists of a slice-selective 90° pulse followed by two slice-selective refocusing 180° pulses (Bottomley 1987). Each RF pulse is applied in conjunction with a perpendicular gradient. The first pulse excites an axial slice, while the other two pulses refocus the proton spins inside the intersection of the three perpendicular slices. In the selected volume, B_0-field homogeneity can be optimized using shim coils to improve the spectral line width and consequently the quality of the measurement. Reduction of contamination by nuisance signals, i.e., water and lipids, is often achieved by additional outer volume suppression (OVS) bands around the localized voxel. While this technique achieves a higher SNR than STEAM, it suffers from chemical shift displacement errors (Andronesi et al. 2010) that reduce the reliability of the localization at high field strengths. Similar to STEAM, metabolites with short T2 are not visible at longer echo times (TE > 80 ms) such that only NAA, Cr, and Cho can be measured.

9.2.3 Semi-Localized by Adiabatic Selective Refocusing (Semi-LASER)

Semi-LASER is an improved localization method that incorporates amplitude- and frequency-

modulated adiabatic full passage (AFP) refocusing pulses. The sequence utilizes an optimized 90° slice-selective pulse followed by a pair of 180° AFP slice selective refocusing pulses (Scheenen et al. 2008a; Scheenen et al. 2008b). The adiabatic pulses achieve an in-plane spin refocusing that is less sensitive to B_1-field inhomogeneities and chemical shift displacement errors, resulting in a more accurate localization. Nevertheless, due to the high energy that AFP pulses deposit in the subject, the minimum repetition time (TR) is limited, thus extending the total acquisition duration.

9.3 Single Voxel Spectroscopy (SVS)

The standard SVS experiment incorporates, at each TR, a water suppression module, a volume localization module and record the resulting FID. To improve SNR, several excitations are recorded and then averaged. Studies have shown that short-TE acquisitions increase the SNR and maximize the number of metabolic components that can be detected (Mlynárik et al. 2006). Details regarding signal reconstruction and processing will be described in Sect. 9.7.

9.3.1 TE-Averaged PRESS

In this method, a series of 1D PRESS spectra are measured with increasing TE value. Then the signals are averaged to produce a 1D spectrum that contains an average of the TE effects in the signal (Bolan et al. 2002; Dreher and Leibfritz 1995). From this 1D spectrum, relatively uncontaminated Glu and Glx peaks can be quantified (Hurd et al. 2004). While TE-averaging is a simple and reliable method for measuring Glu and Gln, it sacrifices spectral information arising from the J-evolution of other metabolites. Moreover, a different T2 effect is present at each TE value, which should be ideally corrected using a basis set with the same experimental parameters as the acquired sequence.

9.3.2 J-Editing

Spectral editing, or J-difference editing, is a method that enables the detection of resonances that overlap with higher-concentration metabolites. Some examples include GABA, which overlaps with Cr, and lactate, which can be obscured by the lipid signal. In general, this method applies the concept of scalar coupling to modify the signal of a single scalar-coupled metabolite and separates it from uncoupled metabolites (Rothman et al. 1984).

9.3.2.1 Meshcher-Garwood PRESS (MEGA-PRESS)

In MEGA-PRESS (Mullins et al. 2014), the J-editing method introduced in the previous section is used in combination with the PRESS excitation scheme. Currently, this technique is widely used as the standard for GABA editing. GABA has two characteristic resonances at 3.0 ppm and 1.9 ppm. Applying a frequency-selective pulse that is on resonance at 1.9 ppm would increase the signal in the 3.0 ppm region if GABA is indeed present. Likewise, a frequency-selective pulse that is off resonance would not influence the 3.0 ppm peak. Subtracting the spectra from these two different acquisitions should preserve the metabolite that only resonates at the characteristic frequencies of GABA. Although this method has shown to successfully estimate GABA concentrations in several brain regions including the anterior cingulate cortex, occipital lobe, and parietal lobe (Terpstra et al. 2002; Öz et al. 2006; Bhattacharyya et al. 2007; Waddell et al. 2007; Kaiser et al. 2007; Edden and Barker 2007), spectral subtraction may lead to artifacts or loss in SNR and undesired off-resonance effects may affect the robustness of the technique.

9.4 Chemical Shift Imaging (CSI)

Chemical shift imaging (CSI), also known as MR spectroscopic imaging (MRSI), allows measuring the spatial distribution of metabolites in the brain. Like in MRI, magnetic gradients are used

to encode the 2D or 3D frequency components of the sample, known as k-space. Like SVS, localization using STEAM, PRESS or semi-LASER and water suppression modules are typically used in combination with the spatial encoding to reduce artifacts related to nuisance signals. For each phase encode, the spectral information is acquired in the form of an FID. Therefore, the signal can be reconstructed following the pipeline described in Fig. 9.2, with the incorporation of an additional 2D or 3D Fourier transform. The reconstructed data can be then visualized as an intensity map showing the spatial distribution of each metabolite. This map is typically interpolated and overlaid with the anatomical MRI image as shown in Fig. 9.3a, b. Alternatively, the reconstructed spectra can be visualized in a grid (Fig. 9.3c) to evaluate its features and detect potential artifacts in the signal, thus avoiding misinterpretation of the data.

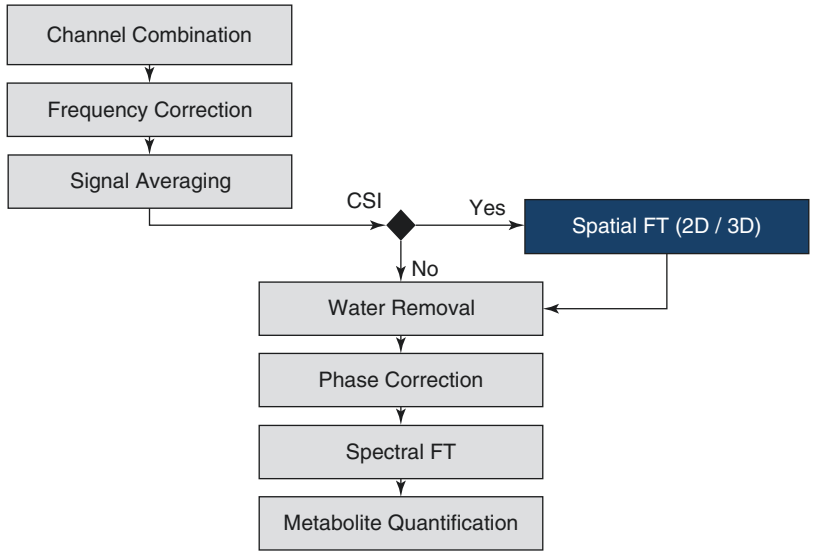

Fig. 9.2 Standard reconstruction and processing pipeline for ^{1}H MRS experiments. Equivalent reconstruction steps can be used for SVS and CSI with only of one extra processing step involved in computing the 2D or 3D spatial Fourier transform (FT) of the data (blue)

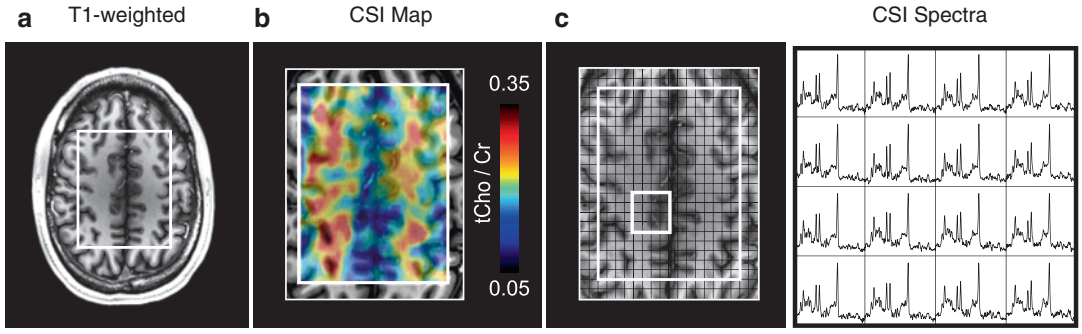

Fig. 9.3 Visualization of 2D CSI reconstructed data. (**a**) The corresponding anatomical T1-weighted image and the localized voxel. (**b**) A representative metabolite map showing the distribution of the total choline to creatine ratio (tCho/Cr). (**c**) Local CSI spectra displayed in every voxel for qualitative assessment. (Modified from Coello et al. 2018)

In CSI acquisitions, the optimization of the B_0-homogeneity is challenging due to the large volume that is measured. This reduces the spectral resolution and may cause spectral overlapping and inaccuracies in metabolite quantification. Moreover, the spatial information measured can extend the acquisition time considerably, limiting the maximum resolution of 2D and 3D-CSI.

9.4.1 Phase Encoded CSI

Phase encoded CSI is the most widely used due to its simplicity and SNR efficiency. It uses magnetic gradients to additionally encode the spatial dimensions of the measured sample. Then the FID signal is recorded in the absence of any gradient to preserve the spectroscopic information. Each voxel in the acquired VOI contains a spectrum that allows for the assessment of the metabolic profile of a specific location or alternatively for the visualization of the spatial distribution of a specific metabolite of interest. This has an advantage over single voxel MRS techniques, as multiple brain regions can be assessed using the CSI technique. However, the acquisition time directly scales with the number of phase encodes, i.e., the number of spatial positions encoded, which limit the maximum matrix size that can be acquired in a clinically feasible time. Several alternatives to phase encoded CSI have been proposed to either reduce scan time or increase the spatial resolution. These include spiral phase encoding, echo-planar sequences, multi-slice sequences, and parallel imaging methods (Posse et al. 2013).

9.4.2 Echo Planar Spectroscopic Imaging (EPSI)

Fast encoding-efficient techniques such as EPSI shorten the acquisition time of CSI scans at the cost of SNR (Posse et al. 1995; Posse et al. 1994). Based on the same principle as echo planar imaging (EPI), this technique simultaneously encodes and acquires the temporal dimension and one spatial dimension. This is achieved using an oscillating gradient that encodes one spatial dimension during the sampling of the FID. Two gradient trajectories commonly used are flyback and symmetric EPSI readouts. In flyback EPSI (Cunningham et al. 2005), sampling takes place only during positive lobes of the oscillating gradient. This has the advantage of being more robust against trajectory imperfections since the flyback gradient causes the sampling points to be well aligned. However, this approach requires a high gradient performance and a significant amount of time is spent on the flyback segment of the trajectory. In symmetric EPSI (Zierhut et al. 2009), on the other hand, the readout takes place during both positive and negative gradient segments. This provides enhanced SNR efficiency and is less gradient demanding. Nonetheless, the bipolar trajectory is prone to spectral ghosting artifacts due to inconsistencies between the odd and even k-space lines, which requires an extra correction step (Coello et al. 2018).

9.5 Two-Dimensional Spectroscopy

Two-dimensional and multi-dimensional spectroscopy methods make it possible to separate scalar coupled and noncoupled metabolites into orthogonal planes (Aue et al. 1976). Despite the longer measurement times compared to 1D MRS, 2D spectroscopic techniques have a great potential for the unambiguous detection of overlapping frequencies. Thus, increasing the number of metabolites that can be reliably quantified.

9.5.1 Correlation Spectroscopy (COSY)

2D correlation spectroscopy (COSY) utilizes a sequence with two 90° pulses separated by a time interval t_1, with variable increments between consecutive excitations, and with a standard readout

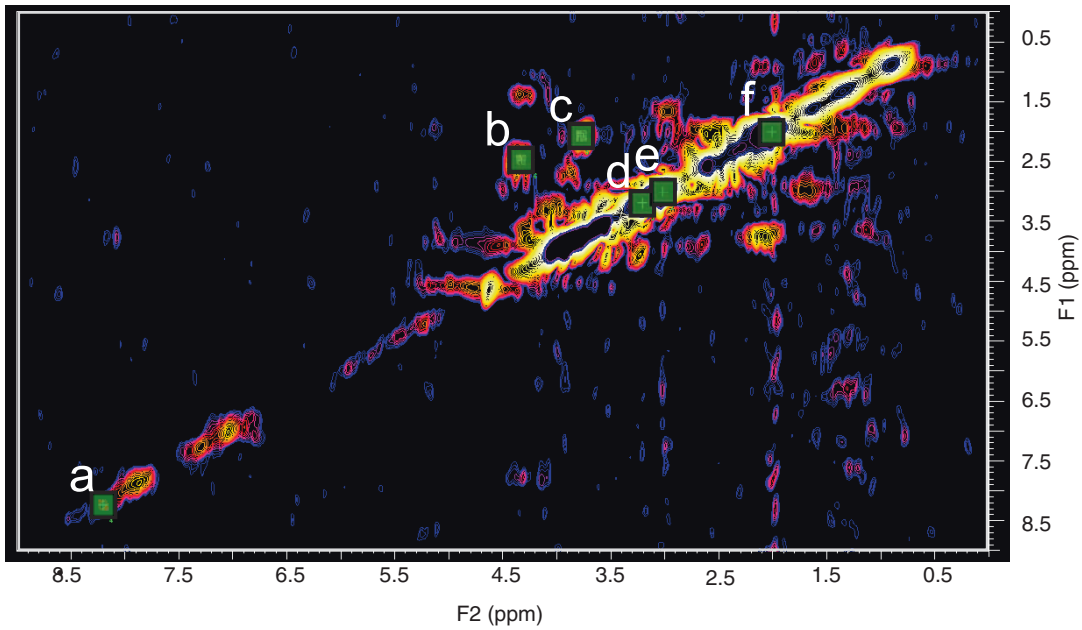

Fig. 9.4 Reconstructed 2D COSY spectrum. Green squares indicate the location of six metabolic components of interest, namely (**a**) GSH, (**b**) NAA, (**c**) Glx, (**d**) Cho, (**e**) Cr, and (**f**) NAA. Quantification can be performed by integration of the area under the peak of interest relative to the area of Cr

time t_2. In this way, a series of 1D spectra is acquired (Jeener et al. 1979). After two-dimensional Fourier transform (FT) of the time dimensions t_1 and t_2, a 2D spectrum is obtained. Figure 9.4 shows a typical reconstructed COSY spectrum, where the x and y axes correspond to the frequencies F2 and F1, respectively. In 2D COSY, scalar-coupling between protons in molecules results in cross-peaks that allow for unambiguous identification of different metabolites (Thomas et al. 2001; Cocuzzo et al. 2011; Ramadan et al. 2011). This technology has been translated to clinical MR scanners and has been applied in vivo (Schulte et al. 2006), demonstrating detection of GABA, Glu, Gln, GSH, among other metabolites (Figs. 9.4 and 9.5).

9.5.2 2D JPRESS

2D JPRESS acquires a series of TE increments to provide a 2D MR spectrum. It differs from 2D COSY in that it utilizes the standard PRESS sequence for each increment with the addition of a maximum echo sampling scheme. This approach increases the sensitivity of the method (Schulte et al. 2006; Ke et al. 2000; Lymer et al. 2007). However, an additional consideration is also necessary to quantify the 2D JPRESS spectra. Unlike COSY where the cross-peak volumes can be measured as an analog of metabolite concentration, 2D JPRESS cross-peaks are not as differentiated and therefore this method does not lend itself as readily for visual analysis. Tools for the quantification of this type of data, like ProFit (Schulte and Boesiger 2006), use prior knowledge, i.e., simulated basis sets of the metabolites, to perform a non-linear fit of the 2D spectrum. In addition, 2D-JPRESS can be combined with the CSI acquisitions described in Sect. 9.4 (Jensen et al. 2005). 2D-JPRESS CSI can sample the distribution of metabolite concentrations throughout the brain. However, this considerably reduces SNR and extends the acquisition time thus making it challenging to obtain reliable estimates for low-concentration metabolites, such as GABA or GSH.

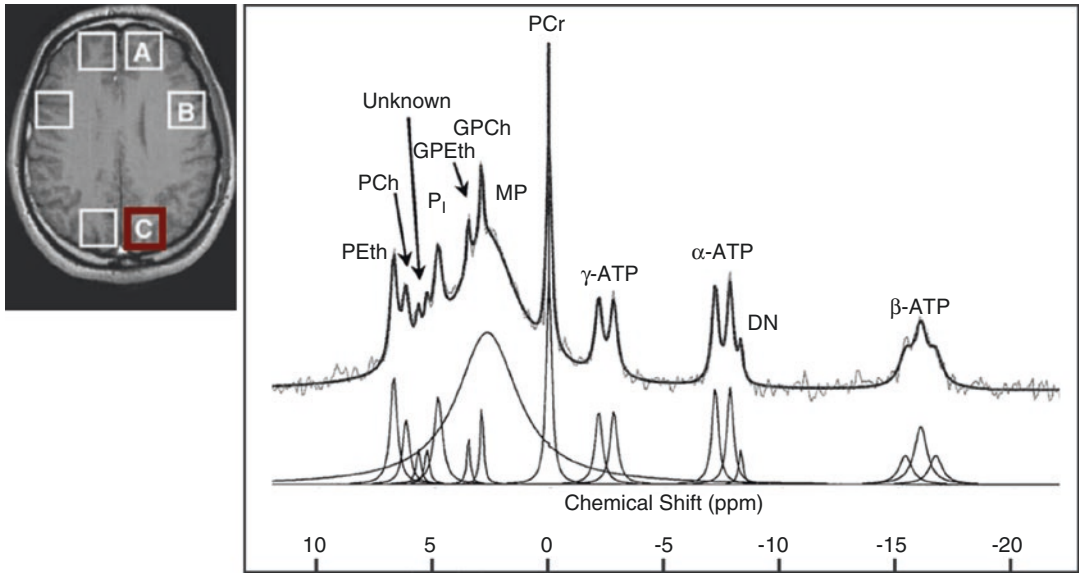

Fig. 9.5 ^{31}P brain spectrum measured with 2D CSI. The location of the plotted spectrum is indicated in red. The right plot shows the measured signal and the spectral fit, where the principal resonances can be identified. (Modified from Potwarka et al. 1999)

9.6 Multi-nuclear Spectroscopy

In addition to ^{1}H MRS, NMR-detectable nuclei that form biomolecules include phosphorous 31, carbon 13 and sodium 23, among others. For several CNS applications, these isotopes are shown to be highly specific and sensitive to changes. Despite the differences in the spectral appearance, resonances that can be found, and measurement challenges that are specific to each of the NMR-detectable nuclei (described in the detail below), the basic principles of the technique, signal acquisition and processing remain unchanged.

9.6.1 Phosphorus-31 (^{31}P) Spectroscopy

^{31}P MRS can be used to qualify brain energetics by measuring the ^{31}P signal from phosphocreatine as well as inorganic phosphate, adenosine triphosphate, and phospholipids such as phosphoethanolamine and phosphocholine, as well as glycerophosphoethanolamine and glycerophosphocholine. ^{31}P studies have focused on reduced PCr in schizophrenia (Blüml et al. 1999; Kegeles et al. 1998), which supports findings from proton MRS studies where reduced Cr has been found using TE-averaged PRESS (Ongür et al. 2009). In the same study, bipolar disorder did not show changes in PCr, however, other studies using both proton MRS (Frey et al. 2007) and ^{31}P MRS (Kato et al. 1994) have shown reductions in Cr and PCr. Findings of changes in Cr in schizophrenia and bipolar disorder are inconsistent. A recent study showed that meta-analysis failed to find significant abnormalities in Cr levels in both diseases (Kraguljac et al. 2012). Other techniques used to measure neurological changes using ^{31}P MRS include diffusion tensor spectroscopy (DTS) (Du et al. 2013) and phosphorus magnetization transfer (MT) (Du et al. 2014).

9.6.2 Carbon (^{13}C) Spectroscopy

Unlike ^{31}P MRS, which focuses on the inherent metabolites within the brain, ^{13}C MRS takes advantage of the low background levels of natural abundance ^{13}C (1.1%) in order to provide

high contrast when ^{13}C-labelled substrates such as ^{13}C-1-glucose or acetate are infused. This allows for the measurement of the metabolites that are subsequently labeled by the metabolism of the substrates. Of particular interest for psychiatry is the ability to measure glutamate and glutamine synthesis rates as a putative measure of neurotransmission. While there have been very limited studies in schizophrenia (Harris et al. 2006), this would prove to be a fascinating area of research.

9.7 MRS Signal Processing

This section outlines data reconstruction and processing as it is generally used for spectroscopic data. Figure 9.2 shows the pipeline of standard data processing applicable to SVS and CSI datasets. Often, a water reference scan is acquired in addition to the water-suppressed metabolite scan, which can be used to further process the spectral data. In the following sections, the processing steps are explained.

9.7.1 SVS Reconstruction

In SVS a complex 1D temporal signal, known as FID, is measured using single- or multi-channel receiver coils in a single TR. Then, the process is repeated to increase SNR via signal averaging. Therefore, several processing steps are required to retrieve a single spectrum from the multi-dimensional signal recorded. Initially, the measurement of each of the coils in the multi-channel receiver is combined. This can be done by simple averaging after signal phasing or using singular value decomposition (SVD) to obtain weighting factors proportional to the signal intensity in each channel, which optimizes the SNR of the combined signal. Then, frequency shifts in the signal, caused by temperature changes or B_0-drifts are corrected through the alignment of the different repetitions before averaging them. This coherently adds the signals and improves the full width at half maximum (FWHM), i.e., the spectral resolution. Finally, the large water signal and zero-order phase are removed from the single 1D temporal signal and the spectrum is obtained via 1D Fourier transform.

9.7.2 CSI Reconstruction

In CSI acquisitions, additional dimensions related to the spatial information of the subject are measured using phase encoding. Analogous to MRI, this spatial information in arranged in a 2D or 3D k-space. In general, the processing steps to reconstruct such a signal are equivalent to the SVS pipeline. However, an additional spatial 2D or 3D FT is necessary to recover the spatial distribution of the signal. Figure 9.2 shows the position in the pipeline where the spatial transform is performed.

9.7.3 Post-processing

MRS data can be post-processed and analyzed in several ways. All major MR platforms have their own methods of reconstructing the data where the details are somewhat different, but the end result is generally an automated or semi-automated fitting of the metabolite peaks and a quantitative measure of major metabolites (NAA, creatine, choline, myo-inositol), usually as a ratio to creatine to provide a normalization factor to account for differences in the peak area or amplitude between subjects, which will differ depending on parameters such as the voxel size, number of averages, transmit/receiver gain, etc.

9.7.3.1 Water Signal Removal

As the metabolites to be detected exist at much lower concentrations, typically 3–4 orders of magnitude, water suppression during data acquisition is a key component of most MRS techniques. However, the intensity of the residual

water peak can still corrupt the baseline of the spectrum. Thus, it is necessary to remove further this unwanted residual water. This can be performed using Hankel singular value decomposition (HSVD). This method decomposes the temporal signal into decaying sinusoids and estimates the components of the water resonance peak (Barkhuijsen et al. 1987). By selecting the spectral range of the water peak, its corresponding FID can be fitted and then subtracted from the initial time domain signal. Finally, after Fourier transform, only the metabolite resonances remain in the spectrum.

9.7.3.2 Eddy Current Correction

Eddy currents are present in every measurement due to the interaction of magnetic field gradients with the scanner hardware components. These can introduce phase distortions in the spectrum and destroy the metabolite resonance peaks, especially in the range from 4.5 to 3.5 ppm. A methodology for correcting eddy current effects has been effectively demonstrated and widely used in vivo (Klose 1990). This method estimates the phase distortions from a water reference acquisition with identical sequence parameters but without water suppression. The estimated phase is then subtracted from the water-suppressed measurement in the time domain and the corrected spectrum is recovered via FT.

9.7.3.3 Frequency Shift Correction

During the acquisition of signal averages, fluctuations in the B_0-field may affect the center frequency of the measurement. This causes the center frequency of the measurement to drift through time and consequently, it blurs the spectral peaks when computing the average. Therefore, the alignment of every individual average is necessary to reduce the effects of the B_0-drifts and improve spatial resolution. It has been shown that when SVS is combined in the same clinical study with other gradient-intense sequences such as diffusion tensor imaging (DTI) this approach reduces the instability artifacts and improves the quantification of metabolites (Rowland et al. 2017).

9.8 Metabolite Quantification

Quantitative MRS is achieved by estimating the relative area of the resonance peaks, which is proportional to their concentration in the tissue. The MRS data can be exported before or after post-processing to be quantified using commercially available packages such as LCModel (Provencher 1993), jMRUI (Naressi et al. 2001), Tarquin (Wilson et al. 2011), AMARES (Vanhamme et al. 1997), etc. These software tools incorporate post-processing routines and prior knowledge to estimate the concentration of metabolites together with other quality measures, such as FWHM, SNR and error estimates.

9.8.1 LCModel Quantification

Fitting algorithms based on prior knowledge have shown superior robustness to non-liner distortions present in the spectra, such as eddy currents, distortions in the baseline, linear and zero-phase effects (de Graaf 2007). Most of these tools are based on modeling the fitting problem as a linear combination of a basis set generated via simulations, signal models or high-quality measurements following identical experimental conditions. LCModel is a widely used tool for used for quantification and reporting of SVS and CSI data. The fitting algorithm estimates the metabolite signal and separates it from the baseline component and the noise. Moreover, a list of the absolute concentrations, relative concentrations and Cramer-Rao Lower Bounds (CRLB) are computed for each metabolite present in the basis set. Finally, a summary of the results is obtained to perform a diagnosis and can be exported for further statistical analysis (Fig. 9.6).

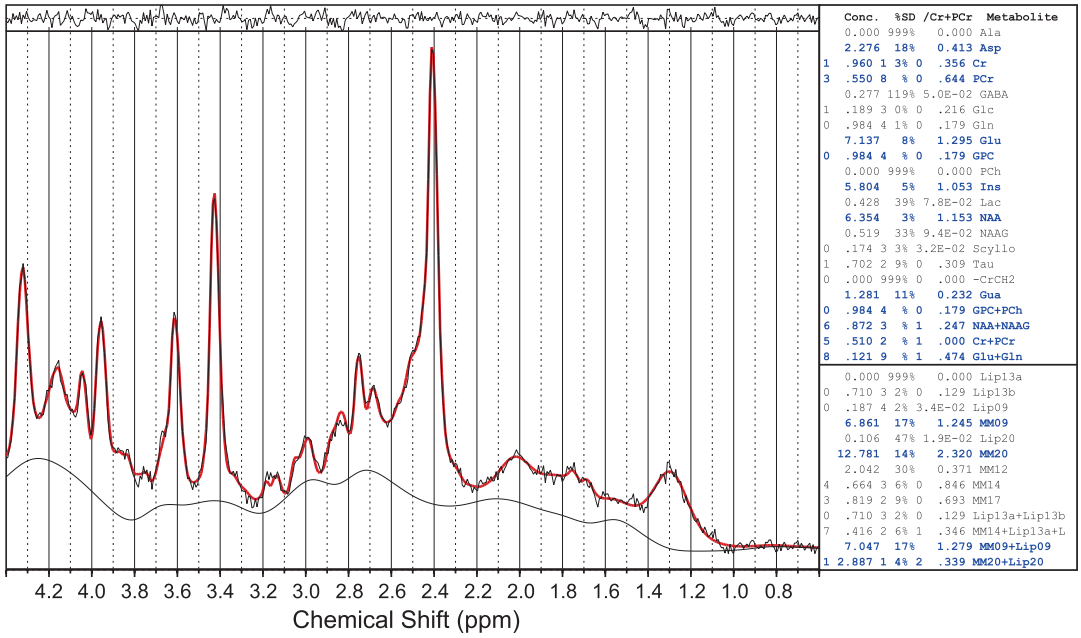

Fig. 9.6 Obtained report using LCModel quantification software (Provencher 1993). The spectral fit using a simulated metabolite basis set estimates the spectral fit (red) of the signal and residual components such as baseline and noise (black). Furthermore, the concentration values, relative concentrations (i.e. Cr ratio) and the CramerRao-Lower Bound (CRLB) are generated for each metabolite in the basis set

Summary

- Magnetic resonance spectroscopy (MRS) can non-invasively measure the concentration of brain metabolites that provide pathophysiological insight into neuropsychiatric diseases such as:
  - N-acetyl aspartate: neuronal marker
  - Creatine: energy marker
  - Choline: membrane marker
  - Myo-inositol: glial marker
  - Glutamate/glutamine: excitatory neurotransmission
  - Gamma-Amino Butyric Acid: inhibitory neurotransmission
  - Glutathione: neuroinflammation marker
- There are several different ways that MRS data can be acquired:
  - Localization methods such as STEAM, PRESS, and semi-LASER
  - Two dimensions providing increased spatial resolution
  - Two dimensions providing increased spectral resolution
  - Multinuclear (i.e., phosphorous) acquisitions
- The methods used for post-processing the MRS data also has an impact on the accuracy of the measurement:
  - Presenting 1D spatial spectral data
  - Presenting 2D spatial spectral data
  - Additional post-processing necessary to correct spectra
  - Quantitation of brain metabolites

References

Agostinho P, Cunha RA, Oliveira C, et al. Curr Pharm Des. 2010;16(25):2766–78.

Andrew ER. N.m.r. imaging of intact biological systems. Philos Trans R Soc Lond B Biol Sci. 1980;289(1037):471–81.

Andronesi OC, Ramadan S, Ratai EM, Jennings D, Mountford CE, Sorensen AG. Spectroscopic imaging with improved gradient modulated constant adiabaticity pulses on high-field clinical scanners. J Magn Reson [Internet]. 2010;203(2):283–93. https://doi.org/10.1016/j.jmr.2010.01.010.

Aue WP, Bartholdi E, Ernst RR. Two-dimensional spectroscopy. Application to nuclear magnetic resonance. J Chem Phys [Internet]. 1976;64(5):2229–46. https://doi.org/10.1063/1.432450.

Barker PB. N-acetyl aspartate--a neuronal marker? Ann Neurol. 2001;49(4):423–4.

Barkhuijsen H, de Beer R, van Ormondt D. Improved algorithm for noniterative time-domain model fitting to exponentially damped magnetic resonance signals. J Magn Reson [Internet]. 1987;73(3):553–7. http://linkinghub.elsevier.com/retrieve/pii/0022236487900230.

Ben-Ari Y. Excitatory actions of gaba during development: the nature of the nurture. Nat Rev Neurosci. 2002;3(9):728–39.

Bhattacharyya PK, Lowe MJ, Phillips MD. Spectral quality control in motion-corrupted single-voxel J-difference editing scans: an interleaved navigator approach. Magn Reson Med. 2007;58(4):808–12.

Bloch F. Nuclear induction. Phys Rev [Internet]. 1946;70(7–8):460–74. https://link.aps.org/doi/10.1103/PhysRev.70.460.

Bloch F, Hansen WW, Packard M. The nuclear induction experiment. Phys Rev [Internet]. 1946;70(7–8):474–85. https://link.aps.org/doi/10.1103/PhysRev.70.474.

Bluml S, Zuckerman E, Tan J, Ross BD. Proton-decoupled 31P magnetic resonance spectroscopy reveals osmotic and metabolic disturbances in human hepatic encephalopathy. J Neurochem. 1998;71(4):1564–76.

Blüml S, Tan J, Harris K, Adatia N, Karme A, Sproull T, et al. Quantitative proton-decoupled 31P MRS of the schizophrenic brain in vivo. J Comput Assist Tomogr. 1999;23(2):272–5.

Bolan PJ, DelaBarre L, Baker EH, Merkle H, Everson LI, Yee D, et al. Eliminating spurious lipid sidebands in 1H MRS of breast lesions. Magn Reson Med. 2002;48:215–22.

Bottomley PA. Spatial localization in NMR spectroscopy in vivo. Ann N Y Acad Sci [Internet]. 1987;508:333–48. https://doi.org/10.1111/j.1749-6632.1987.tb32915.x.

Caverzasi E, Pichiecchio A, Poloni GU, Calligaro A, Pasin M, Palesi F, et al. Magnetic resonance spectroscopy in the evaluation of treatment efficacy in unipolar major depressive disorder: a review of the literature. Funct Neurol. 2012;27(1):13–22.

Cocuzzo D, Lin A, Ramadan S, Mountford C, Keshava N. Algorithms for characterizing brain metabolites in two-dimensional in vivo MR correlation spectroscopy. Conf Proc IEEE Eng Med Biol Soc. 2011;2011:4929–34.

Coello E, Noeske R, Burns BL, Gordon JW, Jakary A, Menze B, et al. High-resolution echo-planar spectroscopic imaging at ultra-high field. NMR Biomed [Internet]. 2018:e3950. https://doi.org/10.1002/nbm.3950.

Cunningham CH, Vigneron DB, Chen AP, Xu D, Nelson SJ, Hurd RE, et al. Design of flyback echo-planar readout gradients for magnetic resonance spectroscopic imaging. Magn Reson Med. 2005;54(5):1286–9.

Dreher W, Leibfritz D. On the use of 2-Dimensional-J NMR measurements for in-vivo proton MRS- measurement of homonuclear decoupled spectra without the need for short echo times. Magn Reson Med. 1995;34(3):331–7.

Dringen R, Gutterer JM, Hirrlinger J. Glutathione metabolism in brain. Eur J Biochem. 2000;267(16):4912–6.

Du F, Cooper AJ, Thida T, Shinn AK, Cohen BM, Öngür D. Myelin and axon abnormalities in schizophrenia measured with magnetic resonance imaging techniques. Biol Psychiatry [Internet]. 2013;74(6):451–7. http://www.ncbi.nlm.nih.gov/pmc/articles/PMC3720707/.

Du F, Cooper AJ, Thida T, Sehovic S, Lukas SE, Cohen BM, et al. In vivo evidence for cerebral bioenergetic abnormalities in schizophrenia measured using 31 P magnetization transfer spectroscopy. JAMA Psychiatry [Internet]. 2014;71(1):19. +.

Edden RAE, Barker PB. Spatial effects in the detection of γ-aminobutyric acid: improved sensitivity at high fields using inner volume saturation. Magn Reson Med. 2007;58(6):1276–82.

Frahm J, Bruhn H, Gyngell ML, Merboldt KD, Hänicke W, Sauter R. Localized high-resolution proton NMR spectroscopy using stimulated echoes: initial applications to human brain in vivo. Magn Reson Med. 1989;9(1):79–93.

Frey BN, Stanley JA, Nery FG, Monkul ES, Nicoletti MA, Chen H-H, et al. Abnormal cellular energy and phospholipid metabolism in the left dorsolateral prefrontal cortex of medication-free individuals with bipolar disorder: an in vivo 1H MRS study. Bipolar Disord. 2007;9(Suppl 1):119–27.

Govindaraju V, Young K, Maudsley AA. Proton NMR chemical shifts and coupling constants for brain metabolites. NMR Biomed [Internet]. 2000;13:129–53. http://www.ncbi.nlm.nih.gov/entrez/query.fcgi?cmd=Retrieve&db=PubMed&dopt=Citation&list_uids=10861994.

de Graaf RA. In vivo NMR spectroscopy - principles and techniques. 2nd ed. Hoboken: Wiley; 2007.

Gruetter R, Novotny EJ, Boulware SD, Mason GF, Rothman DL, Shulman GI, et al. Localized 13C NMR spectroscopy in the human brain of amino acid labeling from d-[1-13C]glucose. J Neurochem. 1994;63(4):1377–85.

Haase A, Frahm J, Matthaei D, Hänicke W, Bomsdorf H, Kunz D, et al. MR imaging using stimulated echoes (STEAM). Radiology. 1986;160(3):787–90.

Harris K, Lin A, Bhattacharya P, Tran T, Wong W, Ross B. Regulation of NAA-synthesis in the human brain in vivo: Canavan's disease, Alzheimer's disease and schizophrenia. In: N-Acetylaspartate [Internet]. New York: Springer; 2006. p. 263–73. http://link.springer.com/10.1007/0-387-30172-0_18.

Hertz L, Zielke HR. Astrocytic control of glutamatergic activity: astrocytes as stars of the show. Trends Neurosci. 2004;27(12):735–43.

Hurd R, Sailasuta N, Srinivasan R, Vigneron DB, Pelletier D, Nelson SJ. Measurement of brain glutamate using TE-averaged PRESS at 3T. Magn Reson Med. 2004;51(3):435–40.

Jeener J, Meier BH, Bachmann P, Ernst RR. Investigation of exchange processes by two-dimensional NMR spectroscopy. J Chem Phys. 1979;71(11):4546.

Jensen JE, Frederick BD, Wang L, Brown J, Renshaw PF. Two-dimensional, J-resolved spectroscopic imaging of GABA at 4 Tesla in the human brain. Magn Reson Med. 2005;54(4):783–8.

Kaiser LG, Young K, Matson GB. Elimination of spatial interference in PRESS-localized editing spectroscopy. Magn Reson Med. 2007;58(4):813–8.

Kantarci K. 1H magnetic resonance spectroscopy in dementia. Br J Radiol. 2007;80 Spec No:S146–52.

Kantarci K. Proton MRS in mild cognitive impairment. J Magn Reson Imaging. 2013;37(4):770–7.

Kato T, Takahashi S, Shioiri T, Murashita J, Hamakawa H, Inubushi T. Reduction of brain phosphocreatine in bipolar II disorder detected by phosphorus-31 magnetic resonance spectroscopy. J Affect Disord. 1994;31(2):125–33.

Ke Y, Cohen BM, Bang JY, Yang M, Renshaw PF. Assessment of GABA concentration in human brain using two-dimensional proton magnetic resonance spectroscopy. Psychiatry Res. 2000;100(3):169–78.

Kegeles LS, Humaran TJ, Mann JJ. In vivo neurochemistry of the brain in schizophrenia as revealed by magnetic resonance spectroscopy. Biol Psychiatry. 1998;44(6):382–98.

Klose U. In vivo proton spectroscopy in presence of eddy currents. Magn Reson Med [Internet]. 1990;14(1):26–30. http://www.ncbi.nlm.nih.gov/pubmed/2161984.

Kraguljac NV, Reid M, White D, Jones R, den Hollander J, Lowman D, et al. Neurometabolites in schizophrenia and bipolar disorder - a systematic review and meta-analysis. Psychiatry Res. 2012;203(2–3):111–25.

Lin A, Ross BD, Harris K, Wong W. Efficacy of proton magnetic resonance spectroscopy in neurological diagnosis and neurotherapeutic decision making. NeuroRx. 2005;2(2):197–214.

Lymer K, Haga K, Marshall I, Sailasuta N, Wardlaw J. Reproducibility of GABA measurements using 2D J-resolved magnetic resonance spectroscopy. Magn Reson Imaging. 2007;25(5):634–40.

Maddock RJ, Buonocore MH. MR spectroscopic studies of the brain in psychiatric disorders. Curr Top Behav Neurosci. 2012;11:199–251.

Mason GF, Gruetter R, Rothman DL, Behar KL, Shulman RG, Novotny EJ. Simultaneous determination of the rates of the TCA cycle, glucose utilization, μ-ketoglutarate/glutamate exchange, and glutamine synthesis in human brain by NMR. J Cereb Blood Flow Metab. 1995;15(1):12–25.

Matsuzawa D, Hashimoto K. Magnetic resonance spectroscopy study of the antioxidant defense system in schizophrenia. Antioxid Redox Signal. 2011;15(7):2057–65.

Mlynárik V, Gambarota G, Frenkel H, Gruetter R. Localized short-echo-time proton MR spectroscopy with full signal-intensity acquisition. Magn Reson Med [Internet]. 2006;56(5):965–70. https://doi.org/10.1002/mrm.21043.

Moffett JR, Namboodiri MA, Neale JH. Enhanced carbodiimide fixation for immunohistochemistry: application to the comparative distributions of N-acetylaspartylglutamate and N-acetylaspartate immunoreactivities in rat brain. J Histochem Cytochem. 1993;41(4):559–70.

Moffett JR, Ross B, Arun P, Madhavarao CN, Namboodiri AMA. N-Acetylaspartate in the CNS: from neurodiagnostics to neurobiology. Prog Neurobiol. 2007;81(2):89–131.

Mosley RL, Benner EJ, Kadiu I, Thomas M, Boska MD, Hasan K, et al. Neuroinflammation, oxidative stress and the pathogenesis of Parkinson's disease. Clin Neurosci Res. 2006;6(5):261–81.

Mullins PG, McGonigle DJ, O'Gorman RL, Puts NAJ, Vidyasagar R, Evans CJ, et al. Current practice in the use of MEGA-PRESS spectroscopy for the detection of GABA. Neuroimage. 2014;86:43–52.

Naressi A, Couturier C, Castang I, de Beer R, Graveron-Demilly D. Java-based graphical user interface for MRUI, a software package for quantitation of in vivo/medical magnetic resonance spectroscopy signals. Comput Biol Med [Internet]. 2001;31(4):269–86. http://www.sciencedirect.com/science/article/pii/S0010482501000063.

Ongür D, Prescot AP, Jensen JE, Cohen BM, Renshaw PF. Creatine abnormalities in schizophrenia and bipolar disorder. Psychiatry Res. 2009;172(1):44–8.

Öz G, Terpstra M, Tkáč I, Aia P, Lowary J, Tuite PJ, et al. Proton MRS of the unilateral substantia nigra in the human brain at 4 tesla: detection of high GABA concentrations. Magn Reson Med. 2006;55(2):296–301.

Öz G, Alger JR, Barker PB, Bartha R, Bizzi A, Boesch C, et al. Clinical proton MR spectroscopy in central nervous system disorders. Radiology [Internet]. 2014;270(3):658–79. http://pubs.rsna.org/doi/10.1148/radiol.13130531.

Pellerin L, Magistretti P. Glutamate uptake into astrocytes stimulates aerobic glycolysis: a mechanism coupling neuronal activity to glucose utilization. Proc Natl Acad Sci U S A. 1994;91:10625–9.

Posse S, DeCarli C, Le Bihan D. Three-dimensional echo-planar MR spectroscopic imaging at short echo times in the human brain. Radiology [Internet]. 1994;192(3):733–8. http://pubs.rsna.org/doi/abs/10.1148/radiology.192.3.8058941.

Posse S, Tedeschi G, Risinger R, Ogg R, Le Bihan D. High speed 1H spectroscopic imaging in human brain by echo planar spatial-spectral encoding. Magn Reson Med. 1995;33(1):34–40.

Posse S, Otazo R, Dager SR, Alger J. MR spectroscopic imaging: principles and recent advances. J Magn Reson Imaging. 2013;37(6):1301–25.

Potwarka JJ, Drost DJ, Williamson PC, Carr T, Canaran G, Rylett WJ, et al. A 1H-decoupled 31P chemical shift imaging study of medicated schizophrenic patients and healthy controls. Biol Psychiatry [Internet]. 1999;45(6):687–93. http://linkinghub.elsevier.com/retrieve/pii/S000632239800136X

Provencher SW. Estimation of metabolite concentrations from localized in vivo proton NMR spectra. Magn Reson Med [Internet]. 1993;30(6):672–9. http://www.ncbi.nlm.nih.gov/pubmed/8139448.

Purcell EM, Torrey HC, Pound RV. Resonance absorption by nuclear magnetic moments in a solid. Phys Rev [Internet]. 1946;69(1–2):37–8. https://link.aps.org/doi/10.1103/PhysRev.69.37.

Ramadan S, Andronesi OC, Stanwell P, Lin AP, Sorensen AG, Mountford CE. Use of in vivo two-dimensional MR spectroscopy to compare the biochemistry of the human brain to that of glioblastoma. Radiology. 2011;259(2):540–9.

Rezin GT, Amboni G, Zugno AI, Quevedo J, Streck EL. Mitochondrial dysfunction and psychiatric disorders. Neurochem Res. 2009;34(6):1021–9.

Ross BD. Real or imaginary? Human metabolism through nuclear magnetism. IUBMB Life. 2000;50(3):177–87.

Ross B, Bluml S. Magnetic resonance spectroscopy of the human brain. Anat Rec. 2001;265(2):54–84.

Rothman DL, Behar KL, Hetherington HP, Shulman RG. Homonuclear 1H double-resonance difference spectroscopy of the rat brain in vivo. Proc Natl Acad Sci [Internet]. 1984;81(20):6330–4. http://www.pnas.org/cgi/doi/10.1073/pnas.81.20.6330.

Rowland BC, Liao H, Adan F, Mariano L, Irvine J, Lin AP. Correcting for frequency drift in clinical brain MR spectroscopy. J Neuroimaging [Internet]. 2017;27(1):23–8. https://doi.org/10.1111/jon.12388.

Scheenen TWJ, Klomp DWJ, Wijnen JP, Heerschap A. Short echo time 1H-MRSI of the human brain at 3T with minimal chemical shift displacement errors using adiabatic refocusing pulses. Magn Reson Med. 2008a;59(1):1–6.

Scheenen TW, Heerschap A, Klomp DW. Towards 1H-MRSI of the human brain at 7T with slice-selective adiabatic refocusing pulses. MAGMA. 2008b;21(1–2):95–101.

Schousboe A. Role of astrocytes in the maintenance and modulation of glutamatergic and GABAergic neurotransmission. Neurochem Res. 2003;28(2):347–52.

Schousboe A, Waagepetersen H. Role of astrocytes in glutamate homeostasis: implications for excitotoxicity. Neurotox Res. 2005;8(3):221–5.

Schulte RF, Boesiger P. ProFit: two-dimensional prior-knowledge fitting of J-resolved spectra. NMR Biomed. 2006;19(2):255–63.

Schulte RF, Lange T, Beck J, Meier D, Boesiger P. Improved two-dimensional J-resolved spectroscopy. NMR Biomed. 2006;19(2):264–70.

Sibson NR, Dhankhar A, Mason GF, Rothman DL, Behar KL, Shulman RG. Stoichiometric coupling of brain glucose metabolism and glutamatergic neuronal activity. Proc Natl Acad Sci U S A. 1998;95(1):316–21.

Terpstra M, Ugurbil K, Gruetter R. Direct in vivo measurement of human cerebral GABA concentration using MEGA-editing at 7 Tesla. Magn Reson Med. 2002;47(5):1009–12.

Thomas MA, Yue K, Binesh N, Davanzo P, Kumar A, Siegel B, et al. Localized two-dimensional shift correlated MR spectroscopy of human brain. Magn Reson Med. 2001;46(1):58–67.

Urenjak J, Williams SR, Gadian DG, Noble M. Specific expression of N-acetylaspartate in neurons, oligodendrocyte-type-2 astrocyte progenitors, and immature oligodendrocytes in vitro. J Neurochem. 1992;59(1):55–61.

Vanhamme L, van den Boogaart A, Van Huffel S. Improved method for accurate and efficient quantification of MRS data with use of prior knowledge. J Magn Reson. 1997;129(1):35–43.

Waddell KW, Avison MJ, Joers JM, Gore JC. A practical guide to robust detection of GABA in human brain by J-difference spectroscopy at 3 T using a standard volume coil. Magn Reson Imaging. 2007;25(7):1032–8.

Wilson M, Reynolds G, Kauppinen RA, Arvanitis TN, Peet AC. A constrained least-squares approach to the automated quantitation of in vivo 1H magnetic resonance spectroscopy data. Magn Reson Med [Internet]. 2011;65(1):1–12. https://onlinelibrary.wiley.com/doi/abs/10.1002/mrm.22579.

Zierhut ML, Ozturk-Isik E, Chen AP, Park I, Vigneron DB, Nelson SJ. 1 H spectroscopic imaging of human brain at 3 Tesla: Comparison of fast three-dimensional magnetic resonance spectroscopic imaging techniques. J Magn Reson Imaging [Internet]. 2009;30(3):473–80. https://doi.org/10.1002/jmri.21834.

Magnetic Resonance Spectroscopy Studies in Schizophrenia

10

Dost Öngür

Contents

10.1 Introduction

MRS is a versatile MR modality that provides a unique window onto brain biochemistry and microstructure. Due to inherent limitations in signal to noise, overlap in metabolite resonances, and difficulty of absolute quantification, this technique has not been utilized as intensively as other MR modalities. However, meaningful progress has been made using MRS in recent years in schizophrenia research due to wider availability of high field MRI scanners and advances in data acquisition and analysis approaches. Chapter 9 covers in detail methods used to obtain and process MRS signals. In this chapter, we review several lines of MRS research in schizophrenia and highlight the contribution made by these efforts to our understanding of this complex disorder.

MRS signal can be obtained from several nuclei. Foremost among these are proton (^{1}H) and phosphorus (^{31}P). These are both naturally abundant and provide biologically relevant information. Several other nuclei can also be studied using MRS, including ^{13}C, ^{23}Na, and ^{17}O, but studies of these nuclei have not made an impact on schizophrenia research to date. Therefore, we have organized this chapter to review ^{1}H and ^{31}P MRS studies in order. For each nucleus, we will review various types of data that can be collected and their interpretations in schizophrenia research.

D. Öngür (✉)
Psychotic Disorders Division, McLean Hospital, Belmont, MA, USA

Harvard Medical School, Boston, MA, USA
e-mail: dongur@partners.org

M. Kubicki, M. E. Shenton (eds.), *Neuroimaging in Schizophrenia*,
https://doi.org/10.1007/978-3-030-35206-6_10

10.2 Proton MRS in Schizophrenia

The proton spectrum is dominated by three large resonances arising from N-acetylaspartate (NAA), total Creatine (Cr), and Choline containing compounds (Cho), respectively. These resonances are the easiest to quantify and have been studied in schizophrenia since the early days of MRS research. NAA is an amino acid found almost exclusively in the neuronal cytosol and mitochondria. It has therefore been considered a marker of neuronal integrity and viability. This interpretation has been supported by the literature in Alzheimer's disease where NAA reductions are commonly observed, and where the degree of progressive reduction is correlated with the degree of neuronal loss (Kantarci et al. 2004; Valenzuela and Sachdev 2001). The Cr signal arises from Creatine and Phosphocreatine in both neurons and non-neuronal elements (glial cells, endothelial cells, etc.). These metabolites provide a storage system for high energy phosphate (HEP) bonds. When energy supplies are available, Creatine is converted to Phosphocreatine by the reversible enzyme Creatine Kinase (CK), and this reaction is reversed to generate energy in times of need (Du et al. 2008). Finally, several choline containing compounds contribute to the Cho signal, which is generally considered a marker of cell membrane synthesis and breakdown. This is because choline stabilized in cell membranes is not MR-visible (Gonzalez-Toledo et al. 2006). To these three metabolites can be added myo-inositol (mI), an intermediate molecule second messenger signaling pathways that happen to be enriched in glial cells. In addition to these four resonances, multiple other metabolites can be quantified using MRS. Of special interest among these are neurotransmission-related metabolites including Glutamate (Glu), Glutamine (Gln), and GABA. Glu is the primary excitatory neurotransmitter in the brain and Gln is its metabolite, while GABA is the primary inhibitory neurotransmitter. Leading theories on the pathophysiology of schizophrenia implicate Glu and GABA dysfunction, making these metabolites of great interest (Lisman et al. 2008). Finally, there are several additional metabolites that are found in lower concentrations in the brain, and therefore can be captured in specialized MRS studies, but are of special physiological interest. These include glutathione (GSH), the brain's primary antioxidant molecule, and lactic acid or lactate (Lac), a metabolic by product that provides information about the state of glycolysis.

10.2.1 NAA/Cr/Cho/mI

There is a large literature of proton MRS studies in schizophrenia reporting on levels of the four metabolites that are most easily quantified. The consensus emerging out of this literature is that NAA levels are reduced in schizophrenia, indicating a reduction in neuronal integrity and function (Steen et al. 2005; Kraguljac et al. 2012). Although this finding is commonly reported, the magnitude of reduction observed is much more modest than that in Alzheimer's Disease, and NAA reduction in schizophrenia likely reflects neuronal damage or atrophy, but not progressive neuronal loss. Measurement of Cr is complicated by the fact that many studies use Cr as an internal reference and do not report Cr levels independently. Nonetheless some studies, including from our group (Ongur et al. 2009), have reported reductions in Cr and interpreted these as reflecting abnormal bioenergetic metabolism in schizophrenia. This finding is not widely replicated, however, and most studies have reported normal Cr levels (Kraguljac et al. 2012). Likewise, Cho levels appear to be normal in schizophrenia, as well (Kraguljac et al. 2012). Because it is enriched in glial cells, some have argued that mI levels may be a marker of glial activation including in neuroinflammation (Rowland et al. 2017). There is no replicated evidence of mI abnormalities in schizophrenia (Schwerk et al. 2014), but mI may be related to specific disease features such as depression (Chiappelli et al. 2015). Normal levels of Cr, Cho, and mI are also seen in younger patients who are antipsychotic naïve (Iwata et al. 2018), indicating that medication effects do not account for these patterns.

10.2.2 Glu/Gln/GABA

There has been intensive MRS research in recent years on what can be termed neurotransmission-related metabolites in schizophrenia. Multiple lines of evidence implicate both glutamatergic and GABAergic abnormalities in this condition. Specifically, it is proposed that in schizophrenia there is a hypofunction of the NMDA receptor, which is critical for learning and memory (Coyle 2012). This hypofunction may arise from genetic or environmental insults and lead to abnormal information processing ultimately presenting as abnormal thought content and cognitive deficits. In addition, abnormal functioning of the GABAergic parvalbumin-containing chandelier neurons has been proposed in schizophrenia that may also lead to abnormal cortical function (Gonzalez-Burgos et al. 2015). MRS research therefore provides an exciting noninvasive *in vivo* opportunity to probe Glu and GABA related measures in schizophrenia to test hypotheses about the involvement of each metabolite in this condition. Two challenges were quickly recognized in this line of work. The first is that the MRS signals arise from all Glu and GABA in the brain parenchyma, and not only those pools that are relevant to synaptic activity. In the case of GABA, this is less of a concern because GABA is primarily (although not exclusively) a neurotransmitter in the brain, but it has long been known that there is a cytosolic pool of Glu in neurons that plays multiple roles in intermediary metabolism and is not related to the synaptic pool (Rothman et al. 1992). At the current time, it is not possible to distinguish these two pools (and possibly a third one in mitochondria) reliably using noninvasive MRS approaches. This challenge has led investigators to consider Glu and Gln measures in conjunction because Glu that is released into the synapse is taken up by glial cells and converted to Gln; thus, the ratio of Gln/Glu may be more closely related to synaptic Glu pools than Glu alone (Ongur et al. 2008; Chowdhury et al. 2012). The second challenge in this line of research has been that these metabolites, and Gln and GABA, in particular, are present at lower concentrations in the brain than NAA, Cr, and Cho. Therefore, the signal to noise ratio is lower for these metabolites and routine MRS approaches such as PRESS do not provide sufficiently reliable Glu/Gln/GABA data. Investigators have used modified MRS data collection approaches of various kinds to quantify these metabolites. The details of these approaches are beyond our scope; it suffices to say that specialized MRS data collection approaches are needed to study Glu/Gln/GABA in human studies with the possible exception of Glu quantified using standard approaches at 3 T or higher field strengths. In settings where such specialized MRS approaches and higher field strength magnets are not available, investigators often quantify a Glx signal which reflects a combination of resonance signals from Glu, Gln, GABA, aspartate, and possibly other metabolites (Govindaraju et al. 2000).

The field has made meaningful progress in the quantification of glutamate and GABA-related metabolites in schizophrenia, despite the challenges described above. This progress has been summarized in several reviews and meta-analyses, and we refer the reader to those publications for more detail (Schwerk et al. 2014; Bustillo 2013; Egerton et al. 2017a; Marsman et al. 2013; Merritt et al. 2016). The emerging picture indicates a replicated finding of elevated glutamate-related metabolites in schizophrenia. This pattern has been seen variably in Glx, Glu, Gln, and the Gln/Glu ratio, and in patients with variable clinical conditions. Although it is not possible to prove that the *in vivo* MRS findings arise from elevated synaptic activity, multiple lines of evidence, including human experimental medicine approaches (Rowland et al. 2005), have suggested this may be the case. Such an interpretation is also consistent with the hypothesized NMDA receptor hypofunction seen in this condition, as Glu signaling is upregulated in this setting in experimental animals (Coyle et al. 2012). There is debate about whether this elevated glutamate-related metabolite signal is restricted to the early phases of illness with a return to normal or below-normal levels in chronic illness

(Marsman et al. 2013), or whether it remains even in chronic illness (Bustillo et al. 2017). The former scenario is intriguing because it may reflect a dynamic change in the glutamatergic system in schizophrenia, with the early phases characterized by elevated neurotransmission and prominent positive symptoms, and the later phases characterized by reduced neurotransmission and prominent negative symptoms and cognitive deficits. The literature in GABA has been much less consistent, with published MRS studies reporting elevated, normal, or reduced GABA levels in various brain regions in schizophrenia. A recent meta-analysis concluded that there is no abnormality in brain GABA concentrations in this condition (Egerton et al. 2017a). This is frustrating because the *a priori* expectation of finding GABA abnormalities in schizophrenia had been strong, and investigators are eager to identify replicable GABA concentration abnormalities, which can be interpreted in the context of the neurobiology of schizophrenia and used to guide treatment development research. Although arguments have been advanced to explain the variable GABA findings on the basis of disease stage, brain region, or medication effects (Kegeles 2016), no set of variables has captured the full range of variability. Of all the MRS-visible metabolites discussed thus far, GABA has the lowest concentration in the healthy human brain, at 0.5–1.0 mM (Govindaraju et al. 2000). This low concentration is indeed at the limit of detection under routine circumstances, even for studies using dedicated GABA-detection approaches such as J-editing. In addition, GABA quantification is hampered by contamination of the GABA resonance from macromolecule and other signals. These technical challenges increase the likelihood that the GABA studies published thus far have been impacted by various kinds of bias and error, and the underlying GABA concentration in schizophrenia is quite possibly in the normal range.

Another line of MRS studies has investigated the impact of antipsychotic drugs (APDs) in schizophrenia patients. This is of interest because normalization of MRS signal abnormalities with adequate treatment can provide significant convergent evidence for the biological significance of the abnormalities reported in patient studies. As in the case-control studies, there is significant variability in disease state, patient clinical condition, brain region, as well as the metabolites reported across APD studies (Bustillo et al. 2014; de la Fuente-Sandoval et al. 2013; Goto et al. 2012). A recent systematic review found that the most consistent finding in this literature is a reduction in glutamate-related metabolites (Glx, Glu, Gln) (Egerton et al. 2017b). This finding is complementary to the elevation seen in the same metabolites in case-control studies, especially early in the course of illness. Thus, the overall picture is that schizophrenia is associated with elevated glutamate function, perhaps as a result of an upstream abnormality in NMDA receptor function, and adequate treatment can normalize this elevation.

10.2.3 GSH/Lac

The two additional proton MRS visible metabolites we will discuss are important for related, but not identical reasons. Like GABA, each is present in the brain in low concentrations and their detection is challenging in human studies. GSH is a tripeptide comprised of glutamate-glycine-cysteine and performs the role of the brain's primary antioxidant defense. GSH can be detected using proton MRS, usually using dedicated data collection approaches such as J-editing. It has attracted attention in recent years due to the growing awareness of the importance of brain redox balance for healthy neuronal function and the potential impact of redox imbalances in schizophrenia. Multiple lines of evidence suggest that neuroinflammation and NMDA receptor hypofunction can both lead to redox imbalance and oxidative stress in the brain (Steullet et al. 2016), which in turn appears to damage GABAergic neuron function (Steullet et al. 2017). Since these processes are all implicated in schizophrenia, investigators have asked whether brain GSH levels may be abnormal in this

condition. Multiple such studies have been conducted and the preponderance of them show no abnormalities in GSH concentration in schizophrenia or clinical high-risk groups when compared with healthy controls (Brandt et al. 2016; Da Silva et al. 2018; Hafizi et al. 2018; Matsuzawa and Hashimoto 2011; Matsuzawa et al. 2008; Terpstra et al. 2005; Xin et al. 2016). One study found a significantly elevated GSH concentration in schizophrenia (Wood et al. 2009). A recent study using an unusual principal analytic components approach has found a reduced "component" in schizophrenia, which includes GSH and Glu levels (Kumar et al. 2018). Because redox abnormalities may be more pronounced in early stages of illness and attenuated in chronic disease after neuronal damage has already taken place, several investigators have studied at-risk subjects and first episode schizophrenia patients (cited above), but these studies have not uncovered any more significant GSH abnormalities than studies in chronic patients.

Lactate is an organic acid which accumulates in conditions where the regular oxidative phosphorylation and mitochondrial energy production pathways are compromised, leading to a compensatory elevation in glycolysis. This is not a desirable circumstance under ordinary conditions because the former pathway provides 36 adenosine triphosphate (ATP) molecules per molecule of glucose metabolized, whereas the latter provides 2–6 ATP molecules. This is commonly observed during anoxia when it is not possible to conduct oxidative phosphorylation and "anaerobic glycolysis" takes over. Measurement of the Lac signal in schizophrenia in vivo has provided a window into the metabolic condition of the brain. There are reports of Lac measures in the schizophrenia literature, but some of these did not use dedicated Lac acquisition approaches. Due to the difficulties in quantifying Lac reliably (Dogan et al. 2018), we mention a single study which did in fact address these issues to a point and reported elevated Lac levels in schizophrenia (Rowland et al. 2016). This finding may indicate that mitochondrial function is compromised in schizophrenia despite the absence of anoxia, and "aerobic glycolysis" may be operative.

10.2.4 Other Results from Proton MRS

So far in this chapter we have focused on studies that reported on metabolite concentrations of various kinds in the brain. Proton MRS can provide additional information about brain structure and function, and alternative approaches have been exploited. One such approach involves diffusion of metabolites. Diffusion-related approaches have been widely used in MRI research, especially water diffusion in the context of diffusion tensor imaging or DTI, but metabolites other than water also have diffusion properties which may be informative. We have described the potential implications of this line of research elsewhere (Du and Ongur 2013) and an expanded discussion of the principles is beyond our scope here. Our work using this approach has provided evidence for both myelin and axon related abnormalities in the white matter in schizophrenia (Du et al. 2013a), and insights on myelin and axon biology separately are not available from DTI studies where results indicate a general problem with white matter integrity.

Another MRS property of metabolites that can be informative about brain biology is T2 relaxation time. T2 relaxation time is determined by the spin-spin interactions of a metabolite resonance, which ultimately reflects the microenvironment in which the metabolite molecules find themselves. For example, NAA, Cr, and Cho T2 relaxation times become shorter with healthy aging, possibly reflecting cellular atrophy and altered intracellular environment (Marjanska et al. 2013). In our studies, we have found prolonged water but shortened metabolite (NAA, Cr, and Cho) T2 relaxation times in schizophrenia numerically (Ongur et al. 2010) and replicated this finding in an independent dataset (Du et al. 2012), although the statistically significant findings across the two studies were not identical. These findings suggest that the brain's intracellular microenvironment is abnormal in schizophrenia and the direction of abnormality is similar to that of aging.

The T2 relaxation time findings provide a potentially important perspective for metabolite

quantification in schizophrenia MRS research. T2 relaxation time determines the rate of signal magnitude decay with echo time (TE) in MRS experiments. If the T2 relaxation time of a metabolite is shorter in Individual #1 than in Individual #2, this will reduce the apparent magnitude of that metabolite measured in Individual #1 even if the concentration of the metabolite is no different; the longer the TE the greater the discrepancy. This raises the concern that shorter metabolite T2 relaxation times may lead to a spurious finding of reduced NAA concentration in people with schizophrenia. This issue has not been directly addressed, but there is some evidence that schizophrenia MRS studies using longer TE have in fact reported greater apparent NAA concentration reductions in this condition (Bracken et al. 2013). It is at least theoretically possible that in schizophrenia the brain NAA concentration is normal, but T2 relaxation time is shortened, leading to apparent NAA concentration reductions.

10.2.5 Studies at 7 T

Recent developments in proton MRS research conducted at 7 T deserve special mention. This is because higher field strength provides greater signal-to-noise, as well as spectral dispersion for MRS studies. These improvements lead to greater ability to resolve smaller metabolite resonances obscured by partially overlapping larger ones. In fact, it is commonly stated that greater field strength differentially benefits MRS over other MR modalities where the greater signal-to-noise advantage is offset by field inhomogeneity challenges. There is understandably hope in the field that 7 T MRS studies may resolve the discrepancies in MRS schizophrenia research discussed above.

At the time of this writing, we are aware of nine 7 T MRS studies of schizophrenia published in peer reviewed journals. Among these, we have already mentioned the glutathione (Brandt et al. 2016; Kumar et al. 2018) and the lactate (Rowland et al. 2016) studies above. These studies also reported results on other metabolites. The remaining studies have generally reported on Glu/Gln/GABA findings, in chronic or first episode patients and in at-risk individuals (Marsman et al. 2014; Taylor et al. 2017, 2015; Thakkar et al. 2017; Posporelis et al. 2018; Reid et al. 2019). Although a systematic review and meta-analysis of this literature is not yet available, the pattern of discrepant findings across studies appears to be continuing at 7 T, with some but not all studies reporting the previously observed elevation in glutamate-related metabolites and some but not all reporting GABA abnormalities.

10.3 Phosphorus MRS in Schizophrenia

The literature reviewed above has focused on the signals coming from proton resonances. Another major set of signals in the brain comes from the ^{31}P nucleus and we will term studies reporting on these signals phosphorus MRS studies. Phosphorus MRS provides windows into the brain's phosphorus containing metabolites including phosphodiesters and phosphomonoesters (PDEs and PMEs), which are involved in cell membrane metabolism, ATP and phosphocreatine (PCr), which are involved in energy production and utilization, and nicotinamide adenine dinucleotides (NAD containing compounds NAD+ and NADH), which form a redox pair and reflect the cell's redox state. In addition to metabolite quantification, phosphorus MRS allows noninvasive quantification of brain parenchymal pH. This is relevant because the shift from oxidative phosphorylation to aerobic glycolysis described above would be expected to generate build-up of Lac and a subsequent pH reduction.

Our group recently reviewed the phosphorus MRS literature in schizophrenia (Yuksel et al. 2015). In this review, we noted that there is a relatively large phosphorus MRS literature on reduced PME and elevated PDE in the brain in schizophrenia. Since PME represents membrane building blocks and PDE represents membrane degradation products, such a pattern would be consistent with greater than normal turnover of cell membrane metabolites in schizophrenia, perhaps reflecting ongoing synaptic remodeling in

the brain (Pettegrew et al. 1993; Keshavan et al. 1994). On the other hand, these studies were typically conducted at lower field strengths in early stages of MRS research. More recent studies, some at higher field strengths, have not found the same pattern in PDE/PME concentrations in the cerebral cortex in schizophrenia e.g. (Shirayama et al. 2004; Du et al. 2014). Thus, we conclude that this is not a well-established finding. In our review, we also did not find a consistent pattern of abnormalities in the concentration of energy-related metabolites ATP and PCr in schizophrenia (Yuksel et al. 2015). Finally, in another review of Lac and pH studies, we noted that only 2 out of 14 studies have reported a reduction in pH in schizophrenia (Dogan et al. 2018). Reduced pH could represent the "footprint" of elevated Lac in this condition, but the finding has not been replicated.

The only reported phosphorus MRS studies of NAD+/NADH in schizophrenia have been from our group. In our first study, conducted at 4 T, we reported a substantial reduction in the NAD+/NADH ratio in schizophrenia and this abnormality was especially pronounced in first episode psychosis patients (Kim et al. 2017). In our second study, we replicated this finding and extended it to siblings of patients with first episode psychosis where the NAD+/NADH ratio was positioned between the healthy control and the patient values (Chouinard et al. 2017). NAD+ and NADH form a redox pair and their ratio reflects the redox status of cells (Zhu et al. 2015). Given the growing interest in brain redox imbalance in schizophrenia, phosphorus MRS has provided a potentially informative window onto this issue. Our findings indicate that the NAD+/NADH ratio abnormality is stronger in earlier stages of the illness, and it is present, but to a lesser degree, in first degree relatives. Both of these features suggest that this index may reflect pathophysiology that is upstream from chronic disease and treatment effects, and perhaps a good target for treatment development. The reduced NAD+/NADH ratio in schizophrenia is consistent with redox imbalance in the direction of excessive reductive power, i.e. not oxidative stress. Oxidative stress is a popular concept at the moment in schizophrenia research (Steullet et al. 2017; Do et al. 2015), and it would arise as a result of oxidative phosphorylation in mitochondria, which leads to generation of reactive oxygen species which then damage DNA, proteins, and, lipids. By contrast, two cellular processes can be associated with reductive stress. One is hyperglycemia, which stimulates intermediary metabolism and elevates NADH levels. The other is slowdown of oxidative phosphorylation and the electron transport chain, which consume NADH and generate NAD+; if these processes are slowed down there would be NADH accumulation, a shift toward glycolysis, and increased reductive stress (Titov et al. 2016). Thus, we interpret our NAD+/NADH results as being consistent with impaired mitochondrial metabolism leading to a shift toward glycolysis and inefficient energy production. Although there are currently no studies focused on correcting the NAD+/NADH abnormality in schizophrenia, some intriguing compounds have recently attracted attention and may be usable in human studies (Martens et al. 2018).

Finally, it is possible to obtain other kinds of information in addition to metabolite concentrations using phosphorus MRS, just as in proton MRS. Our group has recently implemented a dynamic MRS approach that quantifies certain brain enzymatic reaction rates noninvasively (Du et al. 2013b). The approach, which we term phosphorus magnetization transfer (MT) MRS, relies on the chemical exchange of a phosphate moiety from ATP to Cr to generate PCr reversibly catalyzed by the creatine kinase (CK) enzyme. Although ATP is the primary energy currency of life, most high energy phosphate bonds are stored in PCr form by CK within cells. During times of high energy need, the CK reaction is reversed to generate new ATP for utilization; this is indeed the primary source of ATP synthesized in cells, with *de novo* synthesis generating a small minority of ATP. This system maintains ATP concentrations within a narrow range in cells, but the Cr-PCr forms fluctuate in concentration much like a buffer (Du et al. 2008). Phosphorus MT MRS relies on saturation of the ATP signal during the MRS experiment and observation of the PCr resonance magnitude. The PCr magnitude is

reduced over time because phosphates are being transferred to ATP and thereby being saturated, and the rate of reduction of the PCr signal is indeed the rate of the CK enzyme (Du et al. 2007). Using this approach, we reported a significant 22% reduction in the CK reaction rate in the frontal cortex in schizophrenia (Du et al. 2014). This finding suggests that ATP availability may be reduced in schizophrenia during times of high demand, as the primary source of new ATP synthesis is compromised. This may have implications for the brain's response to environmental stressors in schizophrenia, which often require energy-intensive neuronal information processing in time-dependent manner. Although these studies are of interest, there is a need for replication from other research groups in the field.

10.4 Conclusions

Although it is not as well-developed as other MR modalities, MRS research in schizophrenia has now come of age. There is widespread recognition that MRS studies can provide meaningful insight into processes of great interest for schizophrenia research, including neuronal integrity and function, excitatory and inhibitory neurotransmission, redox imbalance, and brain bioenergetics. The literature is broad and deep, with multiple groups of investigators studying various aspects of schizophrenia and its treatment using MRS. Multiple systematic reviews and meta-analyses have already been published with the goal of synthesizing the existing literature and consolidating our insights.

In this chapter we have attempted to provide a high-level overview of the schizophrenia MRS literature. The evidence is clear that NAA abnormalities suggest cortical neuronal dysfunction. Although NAA concentrations are likely reduced in the brain in schizophrenia, the molecular microenvironment is also abnormal as reflected in the NAA T2 relaxation time. Since NAA is exclusively intracellular and primarily in synthesized in mitochondria, these findings may provide biochemical insights into the abnormalities in schizophrenia. The preponderance of evidence also supports the presence of an abnormality in glutamate-related metabolites (quantified as Glx, Glu, or Gln), although this finding is not universal. Glutamate-related metabolite signals, however, cannot be interpreted exclusively in the domain of neurotransmission since Glu plays multiple roles in the brain and in fact only a minority of Glu is in the synaptic pool, with the remainder being localized to the cytosolic metabolic pool. Nonetheless, it is intriguing that these glutamate-related MRS findings have been quite consistent with the NMDA-receptor hypofunction hypothesis of schizophrenia and may ultimately be used in the service of new treatment development or to monitor treatment response. Finally, there is growing evidence from phosphorus MRS studies for abnormal brain bioenergetics and redox balance. Although we don't have replicated robust evidence on each item, the overall picture is one of impaired mitochondrial function, a compensatory shift towards glycolysis, reduced ATP availability, and accumulation of reducing equivalents (NADH) in schizophrenia. Cellular metabolism underlies neuronal integrity as well as healthy neurotransmission (Shulman et al. 2004); thus these energy-related findings may help pull together both the NAA and the Glu findings.

Each of these insights has been useful and moved the field's thinking forward on the pathophysiology of schizophrenia. However, there have been some notable and unexpectedly negative findings in MRS schizophrenia research. These include the apparently normal GABA, GSH, and ATP levels in this condition. It is intriguing that all three of these metabolites (critical for brain function as the key inhibitory neurotransmitter, antioxidant, and energy currency) are present in relatively low concentrations in the brain (each below 5 mM), and have already been implicated in schizophrenia. These features further suggest that these metabolites may be regulated in a particular way, and their concentrations remain within narrow range even in schizophrenia. The brain is an exquisite organ with built-in feedback loops and compensatory mechanisms to defend its homeostasis against disruption. A clue in this direction is our observation of normal ATP

levels despite slowed ATP generation by the CK enzyme. Thus, ATP utilization may be reduced when the system senses that ATP synthesis is lower. From this perspective, the concentration of important metabolites remains in the normal range in schizophrenia precisely because they are important. The system may sacrifice other parameters, e.g. NAD+/NADH to defend the important ones, e.g. ATP. Again, from this perspective the finding of normal GABA or GSH levels does not indicate that these metabolites are not involved in the pathophysiology of schizophrenia. Once we understand the broader context of physiologic compensations, we may understand how these findings fit into the abnormal physiology in schizophrenia. A corollary to this line of argument is that measuring metabolite concentrations is likely to provide an incomplete picture of physiology in schizophrenia. Dynamic methods that quantify how processes behave are more likely to capture meaningful insights. Therefore, we can expect that methods such as "functional MRS," which measure how metabolites respond to pharmacologic or task challenges will be most impactful in the future.

Summary

- MRS studies provide evidence for impaired neuronal integrity and function in schizophrenia
- There is also an abnormality in glutamate-related metabolites, which may implicate glutamate neurotransmission in this condition.
- Finally, phosphorus MRS studies have provided evidence for inefficient mitochondrial function and oxidative phosphorylation and a shift toward glycolysis.
- Future directions include dynamic acquisition of MRS signal, potentially useful in monitoring metabolite changes due to brain activity or pharmacological interventions.

References

Bracken BK, Rouse ED, Renshaw PF, Olson DP. T2 relaxation effects on apparent N-acetylaspartate concentration in proton magnetic resonance studies of schizophrenia. Psychiatry Res. 2013;213:142–53.

Brandt AS, Unschuld PG, Pradhan S, Lim IA, Churchill G, Harris AD, et al. Age-related changes in anterior cingulate cortex glutamate in schizophrenia: a (1)H MRS study at 7 Tesla. Schizophr Res. 2016;172:101–5.

Bustillo JR. Use of proton magnetic resonance spectroscopy in the treatment of psychiatric disorders: a critical update. Dialogues Clin Neurosci. 2013;15:329–37.

Bustillo JR, Chen H, Jones T, Lemke N, Abbott C, Qualls C, et al. Increased glutamine in patients undergoing long-term treatment for schizophrenia: a proton magnetic resonance spectroscopy study at 3 T. JAMA Psychiat. 2014;71:265–72.

Bustillo JR, Jones T, Chen H, Lemke N, Abbott C, Qualls C, et al. Glutamatergic and neuronal dysfunction in gray and white matter: a spectroscopic imaging study in a large schizophrenia sample. Schizophr Bull. 2017;43:611–9.

Chiappelli J, Rowland LM, Wijtenburg SA, Muellerklein F, Tagamets M, McMahon RP, et al. Evaluation of myo-inositol as a potential biomarker for depression in schizophrenia. Neuropsychopharmacology. 2015;40:2157–64.

Chouinard VA, Kim SY, Valeri L, Yuksel C, Ryan KP, Chouinard G, et al. Brain bioenergetics and redox state measured by (31)P magnetic resonance spectroscopy in unaffected siblings of patients with psychotic disorders. Schizophr Res. 2017;187:11–6.

Chowdhury GM, Behar KL, Cho W, Thomas MA, Rothman DL, Sanacora G. (1)H-[(1)(3)C]-nuclear magnetic resonance spectroscopy measures of ketamine's effect on amino acid neurotransmitter metabolism. Biol Psychiatry. 2012;71:1022–5.

Coyle JT. NMDA receptor and schizophrenia: a brief history. Schizophr Bull. 2012;38:920–6.

Coyle JT, Basu A, Benneyworth M, Balu D, Konopaske G. Glutamatergic synaptic dysregulation in schizophrenia: therapeutic implications. Handb Exp Pharmacol. 2012;267–295.

Da Silva T, Hafizi S, Andreazza AC, Kiang M, Bagby RM, Navas E, et al. Glutathione, the major redox regulator, in the prefrontal cortex of individuals at clinical high risk for psychosis. Int J Neuropsychopharmacol. 2018;21:311–8.

de la Fuente-Sandoval C, Leon-Ortiz P, Azcarraga M, Stephano S, Favila R, Diaz-Galvis L, et al. Glutamate levels in the associative striatum before and after 4 weeks of antipsychotic treatment in first-episode psychosis: a longitudinal proton magnetic resonance spectroscopy study. JAMA Psychiat. 2013;70:1057–66.

Do KQ, Cuenod M, Hensch TK. Targeting oxidative stress and aberrant critical period plasticity in the developmental trajectory to schizophrenia. Schizophr Bull. 2015;41:835–46.

Dogan AE, Yuksel C, Du F, Chouinard VA, Ongur D. Brain lactate and pH in schizophrenia and bipolar disorder: a systematic review of findings from magnetic resonance studies. Neuropsychopharmacology. 2018;43:1681–90.

Du F, Ongur D. Probing myelin and axon abnormalities separately in psychiatric disorders using MRI techniques. Front Integr Neurosci. 2013;7:24.

Du F, Zhu XH, Qiao H, Zhang X, Chen W. Efficient in vivo 31P magnetization transfer approach for noninvasively determining multiple kinetic parameters and metabolic fluxes of ATP metabolism in the human brain. Magn Reson Med. 2007;57:103–14.

Du F, Zhu XH, Zhang Y, Friedman M, Zhang N, Ugurbil K, et al. Tightly coupled brain activity and cerebral ATP metabolic rate. Proc Natl Acad Sci U S A. 2008;105:6409–14.

Du F, Cooper A, Cohen BM, Renshaw PF, Ongur D. Water and metabolite transverse T2 relaxation time abnormalities in the white matter in schizophrenia. Schizophr Res. 2012;137:241–5.

Du F, Cooper AJ, Thida T, Shinn AK, Cohen BM, Ongur D. Myelin and axon abnormalities in schizophrenia measured with magnetic resonance imaging techniques. Biol Psychiatry. 2013a;74:451–7.

Du F, Cooper A, Lukas SE, Cohen BM, Ongur D. Creatine kinase and ATP synthase reaction rates in human frontal lobe measured by (3)(1)P magnetization transfer spectroscopy at 4T. Magn Reson Imaging. 2013b;31:102–8.

Du F, Cooper AJ, Thida T, Sehovic S, Lukas SE, Cohen BM, et al. In vivo evidence for cerebral bioenergetic abnormalities in schizophrenia measured using 31P magnetization transfer spectroscopy. JAMA Psychiat. 2014;71:19–27.

Egerton A, Modinos G, Ferrera D, McGuire P. Neuroimaging studies of GABA in schizophrenia: a systematic review with meta-analysis. Transl Psychiatry. 2017a;7:e1147.

Egerton A, Bhachu A, Merritt K, McQueen G, Szulc A, McGuire P. Effects of antipsychotic administration on brain glutamate in schizophrenia: a systematic review of longitudinal (1)H-MRS studies. Front Psychiatry. 2017b;8:66.

Gonzalez-Burgos G, Cho RY, Lewis DA. Alterations in cortical network oscillations and parvalbumin neurons in schizophrenia. Biol Psychiatry. 2015;77:1031–40.

Gonzalez-Toledo E, Kelley RE, Minagar A. Role of magnetic resonance spectroscopy in diagnosis and management of multiple sclerosis. Neurol Res. 2006;28:280–3.

Goto N, Yoshimura R, Kakeda S, Nishimura J, Moriya J, Hayashi K, et al. Six-month treatment with atypical antipsychotic drugs decreased frontal-lobe levels of glutamate plus glutamine in early-stage first-episode schizophrenia. Neuropsychiatr Dis Treat. 2012;8:119–22.

Govindaraju V, Young K, Maudsley AA. Proton NMR chemical shifts and coupling constants for brain metabolites. NMR Biomed. 2000;13:129–53.

Hafizi S, Da Silva T, Meyer JH, Kiang M, Houle S, Remington G, et al. Interaction between TSPO-a neuroimmune marker-and redox status in clinical high risk for psychosis: a PET-MRS study. Neuropsychopharmacology. 2018;43(8):1700–5.

Iwata Y, Nakajima S, Plitman E, Mihashi Y, Caravaggio F, Chung JK, et al. Neurometabolite levels in antipsychotic-naive/free patients with schizophrenia: a systematic review and meta-analysis of (1) H-MRS studies. Prog Neuro-Psychopharmacol Biol Psychiatry. 2018;86:340–52.

Kantarci K, Petersen RC, Boeve BF, Knopman DS, Tang-Wai DF, O'Brien PC, et al. 1H MR spectroscopy in common dementias. Neurology. 2004;63:1393–8.

Kegeles LS. Brain GABA function and psychosis. Am J Psychiatry. 2016;173:448–9.

Keshavan MS, Anderson S, Pettegrew JW. Is schizophrenia due to excessive synaptic pruning in the prefrontal cortex? The Feinberg hypothesis revisited. J Psychiatr Res. 1994;28:239–65.

Kim SY, Cohen BM, Chen X, Lukas SE, Shinn AK, Yuksel AC, et al. Redox dysregulation in schizophrenia revealed by in vivo NAD+/NADH measurement. Schizophr Bull. 2017;43:197–204.

Kraguljac NV, Reid M, White D, Jones R, den Hollander J, Lowman D, et al. Neurometabolites in schizophrenia and bipolar disorder—a systematic review and meta-analysis. Psychiatry Res. 2012;203:111–25.

Kumar J, Liddle EB, Fernandes CC, Palaniyappan L, Hall EL, Robson SE, et al. Glutathione and glutamate in schizophrenia: a 7T MRS study. Mol Psychiatry. 2018.

Lisman JE, Coyle JT, Green RW, Javitt DC, Benes FM, Heckers S, et al. Circuit-based framework for understanding neurotransmitter and risk gene interactions in schizophrenia. Trends Neurosci. 2008;31:234–42.

Marjanska M, Emir UE, Deelchand DK, Terpstra M. Faster metabolite (1)H transverse relaxation in the elder human brain. PLoS One. 2013;8:e77572.

Marsman A, van den Heuvel MP, Klomp DW, Kahn RS, Luijten PR, Hulshoff Pol HE. Glutamate in schizophrenia: a focused review and meta-analysis of (1) H-MRS studies. Schizophr Bull. 2013;39:120–9.

Marsman A, Mandl RC, Klomp DW, Bohlken MM, Boer VO, Andreychenko A, et al. GABA and glutamate in schizophrenia: a 7 T (1)H-MRS study. Neuroimage Clin. 2014;6:398–407.

Martens CR, Denman BA, Mazzo MR, Armstrong ML, Reisdorph N, McQueen MB, et al. Chronic nicotinamide riboside supplementation is well-tolerated and elevates NAD(+) in healthy middle-aged and older adults. Nat Commun. 2018;9:1286.

Matsuzawa D, Hashimoto K. Magnetic resonance spectroscopy study of the antioxidant defense system in schizophrenia. Antioxid Redox Signal. 2011;15:2057–65.

Matsuzawa D, Obata T, Shirayama Y, Nonaka H, Kanazawa Y, Yoshitome E, et al. Negative correlation between brain glutathione level and negative symp-

toms in schizophrenia: a 3T 1H-MRS study. PLoS One. 2008;3:e1944.
Merritt K, Egerton A, Kempton MJ, Taylor MJ, McGuire PK. Nature of glutamate alterations in schizophrenia: a meta-analysis of proton magnetic resonance spectroscopy studies. JAMA Psychiat. 2016;73:665–74.
Ongur D, Jensen JE, Prescot AP, Stork C, Lundy M, Cohen BM, et al. Abnormal glutamatergic neurotransmission and neuronal-glial interactions in acute mania. Biol Psychiatry. 2008;64:718–26.
Ongur D, Prescot AP, Jensen JE, Cohen BM, Renshaw PF. Creatine abnormalities in schizophrenia and bipolar disorder. Psychiatry Res. 2009;172:44–8.
Ongur D, Prescot AP, Jensen JE, Rouse ED, Cohen BM, Renshaw PF, et al. T2 relaxation time abnormalities in bipolar disorder and schizophrenia. Magn Reson Med. 2010;63:1–8.
Pettegrew JW, Keshavan MS, Minshew NJ. 31P nuclear magnetic resonance spectroscopy: neurodevelopment and schizophrenia. Schizophr Bull. 1993;19:35–53.
Posporelis S, Coughlin JM, Marsman A, Pradhan S, Tanaka T, Wang H, et al. Decoupling of brain temperature and glutamate in recent onset of schizophrenia: a 7T proton magnetic resonance spectroscopy study. Biol Psychiatry Cogn Neurosci Neuroimaging. 2018;3:248–54.
Reid MA, Salibi N, White DM, Gawne TJ, Denney TS, Lahti AC. 7T proton magnetic resonance spectroscopy of the anterior cingulate cortex in first-episode schizophrenia. Schizophr Bull. 2019;45(1):180–9.
Rothman DL, Novotny EJ, Shulman GI, Howseman AM, Petroff OA, Mason G, et al. 1H-[13C] NMR measurements of [4-13C]glutamate turnover in human brain. Proc Natl Acad Sci U S A. 1992;89:9603–6.
Rowland LM, Bustillo JR, Mullins PG, Jung RE, Lenroot R, Landgraf E, et al. Effects of ketamine on anterior cingulate glutamate metabolism in healthy humans: a 4-T proton MRS study. Am J Psychiatry. 2005;162:394–6.
Rowland LM, Pradhan S, Korenic S, Wijtenburg SA, Hong LE, Edden RA, et al. Elevated brain lactate in schizophrenia: a 7 T magnetic resonance spectroscopy study. Transl Psychiatry. 2016;6:e967.
Rowland LM, Demyanovich HK, Wijtenburg SA, Eaton WW, Rodriguez K, Gaston F, et al. Antigliadin antibodies (AGA IgG) are related to neurochemistry in schizophrenia. Front Psychiatry. 2017;8:104.
Schwerk A, Alves FD, Pouwels PJ, van Amelsvoort T. Metabolic alterations associated with schizophrenia: a critical evaluation of proton magnetic resonance spectroscopy studies. J Neurochem. 2014;128:1–87.
Shirayama Y, Yano T, Takahashi K, Takahashi S, Ogino T. In vivo 31P NMR spectroscopy shows an increase in glycerophosphorylcholine concentration without alterations in mitochondrial function in the prefrontal cortex of medicated schizophrenic patients at rest. Eur J Neurosci. 2004;20:749–56.
Shulman RG, Rothman DL, Behar KL, Hyder F. Energetic basis of brain activity: implications for neuroimaging. Trends Neurosci. 2004;27:489–95.
Steen RG, Hamer RM, Lieberman JA. Measurement of brain metabolites by 1H magnetic resonance spectroscopy in patients with schizophrenia: a systematic review and meta-analysis. Neuropsychopharmacology. 2005;30:1949–62.
Steullet P, Cabungcal JH, Monin A, Dwir D, O'Donnell P, Cuenod M, et al. Redox dysregulation, neuroinflammation, and NMDA receptor hypofunction: a "central hub" in schizophrenia pathophysiology? Schizophr Res. 2016;176:41–51.
Steullet P, Cabungcal JH, Coyle J, Didriksen M, Gill K, Grace AA, et al. Oxidative stress-driven parvalbumin interneuron impairment as a common mechanism in models of schizophrenia. Mol Psychiatry. 2017;22:936–43.
Taylor R, Neufeld RW, Schaefer B, Densmore M, Rajakumar N, Osuch EA, et al. Functional magnetic resonance spectroscopy of glutamate in schizophrenia and major depressive disorder: anterior cingulate activity during a color-word Stroop task. NPJ Schizophr. 2015;1:15028.
Taylor R, Osuch EA, Schaefer B, Rajakumar N, Neufeld RW, Theberge J, et al. Neurometabolic abnormalities in schizophrenia and depression observed with magnetic resonance spectroscopy at 7 T. BJPsych Open. 2017;3:6–11.
Terpstra M, Vaughan TJ, Ugurbil K, Lim KO, Schulz SC, Gruetter R. Validation of glutathione quantitation from STEAM spectra against edited 1H NMR spectroscopy at 4T: application to schizophrenia. MAGMA. 2005;18:276–82.
Thakkar KN, Rosler L, Wijnen JP, Boer VO, Klomp DW, Cahn W, et al. 7T proton magnetic resonance spectroscopy of gamma-aminobutyric acid, glutamate, and glutamine reveals altered concentrations in patients with schizophrenia and healthy siblings. Biol Psychiatry. 2017;81:525–35.
Titov DV, Cracan V, Goodman RP, Peng J, Grabarek Z, Mootha VK. Complementation of mitochondrial electron transport chain by manipulation of the NAD+/NADH ratio. Science. 2016;352:231–5.
Valenzuela MJ, Sachdev P. Magnetic resonance spectroscopy in AD. Neurology. 2001;56:592–8.
Wood SJ, Berger GE, Wellard RM, Proffitt TM, McConchie M, Berk M, et al. Medial temporal lobe glutathione concentration in first episode psychosis: a 1H-MRS investigation. Neurobiol Dis. 2009;33:354–7.
Xin L, Mekle R, Fournier M, Baumann PS, Ferrari C, Alameda L, et al. Genetic polymorphism associated prefrontal glutathione and its coupling with brain glutamate and peripheral redox status in early psychosis. Schizophr Bull. 2016;42:1185–96.
Yuksel C, Tegin C, O'Connor L, Du F, Ahat E, Cohen BM, et al. Phosphorus magnetic resonance spectroscopy studies in schizophrenia. J Psychiatr Res. 2015;68:157–66.
Zhu XH, Lu M, Lee BY, Ugurbil K, Chen W. In vivo NAD assay reveals the intracellular NAD contents and redox state in healthy human brain and their age dependences. Proc Natl Acad Sci U S A. 2015;112:2876–81.

MEG Methods: A Primer of Basic MEG Analysis

11

Brian A. Coffman and Dean F. Salisbury

Contents

11.1 Introduction

Magnetoencephalography (MEG) was first developed as a neurophysiological recording technique in the 1960s (Cohen 1968). However, the use of MEG increased substantially with the development of high-density sensor arrays in the early 1990s. Since then, MEG has been developed into a major neuroimaging method used by researchers around the globe. In this chapter, we introduce MEG analysis methods. Although not

B. A. Coffman · D. F. Salisbury (✉)
Department of Psychiatry,
University of Pittsburgh School of Medicine,
Pittsburgh, PA, USA
e-mail: salisburyd@upmc.edu

M. Kubicki, M. E. Shenton (eds.), *Neuroimaging in Schizophrenia*,
https://doi.org/10.1007/978-3-030-35206-6_11

exhaustive, we hope this primer for MEG analysis methods will be useful for those new to the field of MEG and particularly those who would like to implement MEG in studies of schizophrenia.

MEG can be classified as either a neurophysiological recording method (when the data are assessed at the sensors or with dipole analysis) or a neuroimaging method (when source activity is mapped across the brain or cortex). MEG data are recorded by an array of approximately 100–300 sensors positioned near the scalp that are sensitive to the magnetic field and temperature of the environment around them. By keeping these sensors at a constant low temperature in a liquid helium bath, temperature no longer factors into this equation, and the sensor activities primarily represent fluctuation of magnetic fields. In MEG, the magnetic fields we are interested in come from the brain and are directly proportional to the intracellular (primary) electric currents generated by post-synaptic potentials in the apical dendrites of cortical pyramidal cells, the primary excitatory neuron in the mammalian brain (Fig. 11.1; also see Hämäläinen et al. 1993). With a constant current, the relationship between magnetic field (B) and electric current (I) can be calculated with Maxwell's equation:

$$B = \frac{\mu_0 I}{2\pi r}$$

where B is the magnetic field, I is the current, r is the distance from the current, and μ_0 is the permeability of free space. These magnetic fields are perpendicular to the velocity of the electric current and the magnetic force and encircle the current flow according to the right-hand rule—point your right thumb in the direction of the current and curl your

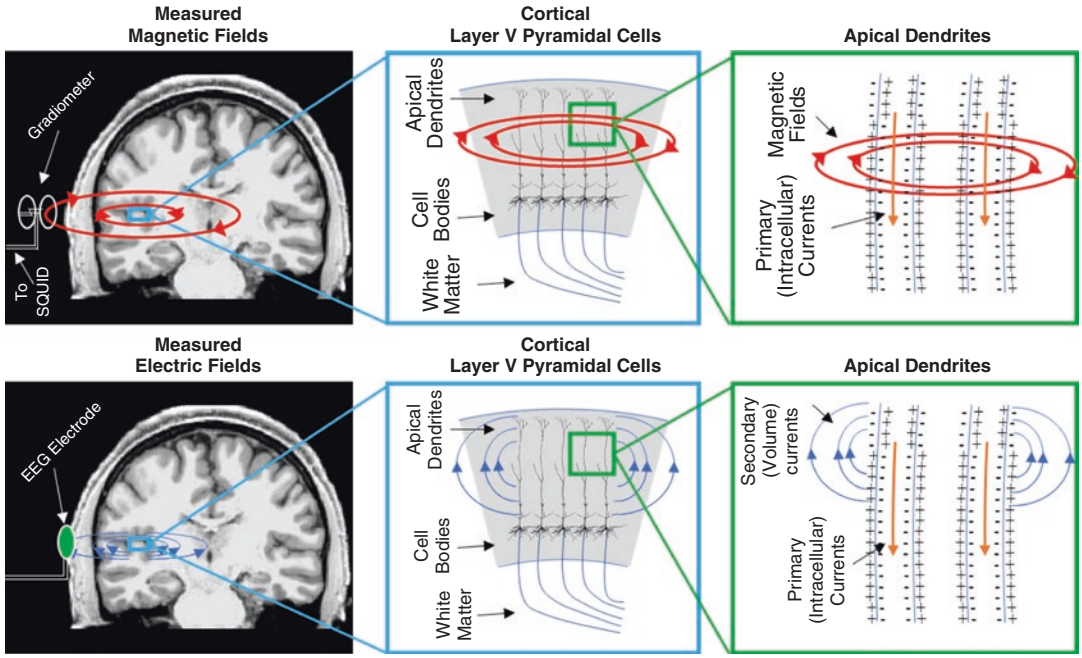

Fig. 11.1 Schematic diagram showing the relationship between primary/intracellular currents in apical dendrites of cortical layer V pyramidal cells and (Upper) magnetic field measured with MEG or (Lower) electric field measured with EEG. MEG measures summed magnetic fields associated with post-synaptic primary (intracellular) currents in apical dendrites of layer V pyramidal cells in the cortex. EEG measures the electric fields generated by summed secondary (volume) currents that are generated in response to the primary currents in apical dendrites of layer V pyramidal cells in the cortex

fingers; your fingers will be curled in the same direction as the magnetic field. In contrast, the electroencephalogram (EEG) reflects the extracellular (volume) currents of post-synaptic potentials, which are also generated primarily by current flow in the apical dendrites of cortical pyramidal cells (Petsche et al. 1984). Thus, EEG and MEG both measure neurophysiological activity of pyramidal cells in the cortex, but the MEG signal is generated mostly by the primary intracellular currents, while the EEG signal is generated mostly from the volume currents that compensate for these primary currents. Measurement of the magnetic component of electrophysiological activity in the brain has another advantage as well. Besides measuring signals more proximal to the neurophysiology of interest, magnetic fields are not impeded or distorted by the boundaries between tissues of differing electrical conductivity, such as soft tissue and bone (Plonsey and Heppner 1967). This means that MEG has greater spatial resolution than EEG for source-level activity, making neuroimaging more feasible. Also, like EEG, MEG can measure brain activity at a very fast rate, usually between 500 and 5000 Hz, making MEG well-suited for neuroimaging at the rate of information transfer in the brain (Hämäläinen et al. 1993).

MEG data analysis is traditionally performed at the source level. That is, comparisons of magnetic fields generated by the brain are usually done by projecting the sensor level data to the brain space where the signals are generated. This contrasts with EEG, where measurements made at the sensors are most often compared with minimal processing applied and inferences about the sources of the measured electric fields are typically made in the discussion section. The primary reason for this discrepancy is the nature of the signals measured. Due to high impedance of the intervening tissues (particularly the skull), the electric fields recorded by EEG are shunted and smoothed at the scalp, making source localization a difficult endeavor. The advantage of measuring these magnetic fields at the scalp is that they are not interrupted by intervening tissues, making source-localization much less burdensome (Plonsey and Heppner 1967). Along with the relative ease of source localization with MEG, the preference for source-level analysis also results from relative difficulty in sensor-level analysis of MEG data compared to EEG data. One of these issues is related to the participant, in that the position of the MEG sensors relative to the head differs between individuals and the head position may even change throughout the session. Although EEG electrodes are fixed to the head and move with the head, MEG sensors are not fixed to the scalp and do not move with the head. Although it is possible to mathematically shift the positions of sensors using Maxwell's equations to artificially align datasets after the data have been acquired, these algorithms are not very robust to issues that may arise along the way and should be used with caution (Medvedovsky et al. 2007; Stolk et al. 2013). The other issue is related to the hardware. Visualization of EEG signals is relatively straightforward and inferences can easily be made regarding the location of signal sources from topographic scalp maps. The same can be said for monopolar magnetometer measurements made with MEG, although the orientations of sources inferred from magnetometers are rotated 90 degrees compared to those inferred from the same patterns in the EEG signal. Many MEG systems incorporate more complex sensors into the array, and some systems may have multiple types of sensors within the same array. For these more complex gradiometer channels, which measure magnetic field gradients between magnetometers, topographic maps may be difficult to interpret, and data are therefore often presented as single-channel waveforms, making source inferences difficult from visualization alone. For these reasons, this chapter focuses on source-level analysis of MEG data.

MEG experiments can be generally separated into two types of designs: *event-related designs*, where a neurophysiological event of interest is correlated in time with a discrete and overtly identifiable event of interest (e.g., the presentation of a sensory stimulus or the execution of a motor event), and *block designs*, where the neurophysiological signal of interest remains constant for a long period of time (e.g., resting-state MEG or

comparison between sustained cognitive/emotional states). In this primer, we focus on event-related designs, but much of the information provided can be applied to block designs, as well. Analysis of event-related MEG signals can be separated into four steps: preprocessing, epoch segmentation and averaging of event related fields and time-frequency representations, forward modeling, and inverse modeling. *Preprocessing* often includes procedures like the removal of unreliable data segments or channels, filtering the data for noise sources, and removal/rejection of artefact signals. Further, some preprocessing methods (i.e., signal space separation) may utilize structural information from magnetic resonance imaging (MRI) for identification and removal of artefacts. Thus, structural MRI data processing is often implemented as the first stage in the MEG data analysis pipeline. *Event-related fields* and *time-frequency representations* are calculated from the preprocessed MEG data to isolate neurophysiological signals of interest from other signals in the data, such as any noise left over after preprocessing or brain signals that are unrelated to the stimuli/events of interest. In this way, we can measure signals much smaller than the background noise that would be invisible when examining data from individual responses. This ratio between the signal of interest and the background noise is called the signal-to-noise ratio (SNR). Structural information from MRI is also used to generate the *forward model*, which models the relationship between activity at the MEG sensors and possible sources of brain activity given estimated physical parameters, such as the electromagnetic properties of the head and of the MEG sensor array. The forward model is then used to generate the *inverse model*, which models the relationship between the signals measured at the MEG sensors and estimated sources. In this chapter, we focus on the most widely-used methods for MEG source localization. However, many inverse modelling methods have been proposed based on different assumptions about the brain responses measured. We present different options at all four MEG data analysis steps, each of which has some advantages and some disadvantages, beginning with MEG data preprocessing.

11.2 Preprocessing MEG Data

Depending on the quality of the data and the dependent variables being assessed, preprocessing can be either simple and quick or computationally demanding and time consuming. As shown in Fig. 11.2, sources of noise can be physiological, such as movement, eye-blinks, and cardiac signals, or artefactual, such as line noise, vibration, or motion of large metal objects (e.g., elevators, cranes, hospital beds). Physiological noise can often be characterized and removed from the data through preprocessing. Eye blinks and eye movements generate DC shifts in the magnetic field, which are usually seen as short (sub-second) deviations in frontal sensors (Hämäläinen et al. 1993). Cardiac signals result from both pulsation and the magnetic counterpart of the QRS complex (Jousmaki and Hari 1996). Conversely, most artefacts are best combatted at data acquisition, as many sources of non-physiological noise cannot be removed once recorded. Thus, the best way to remove these sources from the data is not to record them in the first place. As in the old adage – garbage in, garbage out.

Preprocessing often begins with the identification of unreliable data channels. Removal or interpolation of these noisy channels can aid not only in the eventual estimation of brain activity, but also in some other preprocessing methods. Selection of bad channels can be quite subjective; however, the removal of clear deviations from neighboring channels is straightforward and recommended as a first step. Another simple procedure that often increases signal-to-noise ratio is removing data outside of the frequency-band of interest. Why waste time cleaning data that you won't analyze? If a narrow band of frequencies can explain the signal of interest (e.g., measurement of steady-state evoked responses), then removal of signals outside of these frequencies, through use of a *bandpass filter*, can sometimes be the only preprocessing step needed. Further, just as bandpass filters can be used to filter data outside of a specified frequency band, *high-pass* and *low-pass filters* can be used to filter data below or above a specified frequency, respec-

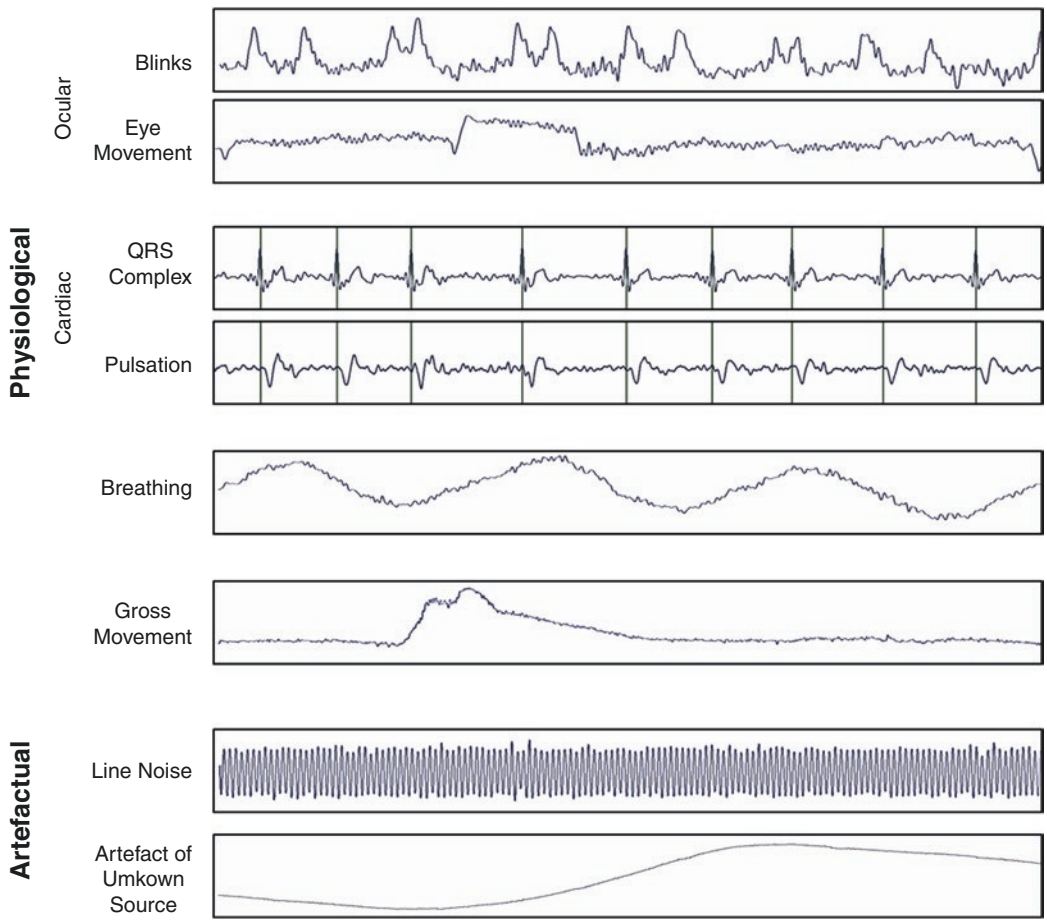

Fig. 11.2 Examples of Common Noise Sources in MEG Data. MEG Data are shown from single channels that exemplify common physiological (upper panels) and artefactual (lower panels) noise sources. All data segments shown are 10 s in duration, although the amplitude scale changes between panels to emphasize the artefact being shown. Vertical lines in the panels showing cardiac noise are centered at the peaks of the R wave of the QRS complex to emphasize relative time differences between the two types of noise. The two cardiac panels are taken from the same dataset; however, all others were taken from independent datasets. All data shown were acquired with the Elekta Neuromag Vectorview

tively. In some cases, rather than passing a set of specific frequencies through the filter, a narrow frequency band is known to contain the noise being removed, such as power line noise. In the Americas and Philippines, this line noise can be identified at 60 Hz and the subsequent harmonics. Elsewhere, it can be explained at 50 Hz and the subsequent harmonics. In most cases, these specific frequencies can be discarded and *notch filters* (filters designed to suppress signals within a narrow frequency band) can be applied to remove the effects of such narrow-band noise.

For noise signals that cannot be simply deleted or filtered from the data, more complicated preprocessing methods are required. These methods, sometimes called *source separation (SS)* methods, are statistical procedures that should be used with caution and diligence. In many cases, these procedures are restricted in their degrees of freedom (which here refers to the number of sources that can be separated from the data), meaning that they can only successfully parse major, large-amplitude components from the data. Further, SS methods vary in computational

demand and overall complexity. We review three SS methods that are most commonly used in MEG research including *signal space projection*, *signal space separation*, and *independent components analysis*.

11.2.1 Signal-Space Projection (SSP)

In the signal-space projection (SSP) method, the measured magnetic field across all sensors is modeled as a time-varying multi-component signal (Ilmoniemi and Williamson 1987; Uusitalo and Ilmoniemi 1997). Each component is defined as a set of elements (sources) whose relative amplitudes and orientations do not change over time. Thus, each source has a consistent and spatially-stereotyped output pattern with variable amplitude, enabling the modeling of various sources of physiological and non-physiological noise sources. In practice, the SSP method has been most commonly used for removing artefacts caused by eye blinks (Hämäläinen et al. 1993), the heart, or by homogeneous gradients that are specific to the location of the device, such as those generated by nearby power sources or ferromagnetic metal. For the latter—sources of noise in the recording room that do not move—the signal space is usually decomposed into individual source components by means of principal components analysis (PCA) of a short segment of data obtained without a subject beneath the sensors, commonly referred to as "empty room" data. Normally three or four source components can be selected to represent the variance associated with homogenous gradients at the site, and these estimates remain stable for many months/years, costing only 3–4 degrees of freedom. SSP solutions have degrees of freedom equal to the number of sensor locations minus one. Thus, removing these components from the data, along with eye-blink and cardiac signals, costs a minimal number of degrees of freedom, given that the magnetic field measurements are usually taken from >100 sensor locations. For physiological artefacts such as eye-blinks and cardiac signals, one can aid the isolation of the source component by increasing the signal-to-noise ratio through response averaging, just as for any event related response (Tesche et al. 1995). For this purpose, electro-oculogram and electrocardiogram are often recorded alongside the MEG data to facilitate automated detection and averaging of these artefact signals. Once the artefact signal of interest has been mostly isolated through averaging, the highest-ranking principal component extracted from the data is likely to explain the artefact signal, and is removed from the data.

11.2.2 Signal Space Separation (SSS) and Spatiotemporal Signal Space Separation (tSSS)

Rather than identifying the individual source components from the measured magnetic field, we can divide the field into two subspaces representing (1) all sources contained within the sensor helmet and (2) all sources beyond the sensor helmet (Taulu et al. 2004, 2005). The subspace representing external noise sources can then be simply dropped from the signal. The temporal extension of the SSS method, spatiotemporal signal space separation (tSSS), was developed to enable the additional rejection of nearby sources of artefact noise, such as vagus nerve stimulators or magnetic dental materials (Taulu and Simola 2006). In this method, SSS is first used to identify the nearby source space; artefacts from nearby sources are then extracted in the time domain and projected out. The subspaces derived by SSS and tSSS typically have about 100 degrees of freedom each, making them more powerful than SSP methods when there are a large number of components needed to fully explain the data.

11.2.3 Independent Components Analysis (ICA)

Over the last 20 years, Independent Components Analysis (ICA) has become a popular method for removal of physiological artefacts such as eye blinks, eye movements, and cardiac signals. ICA is the favored method for artefact rejection in EEG research (Jung et al. 2000), and is slowly

gaining favor in the MEG community, as well. ICA signal decompositions rely on assumptions of orthogonality and linearity. Orthogonality is achieved by the removal of correlations within the data by applying a simple linear transformation, a step called whitening. The linearity assumption is that data measured at sensors (x, a matrix of sensors by time points) are the simultaneous linear mixing of sources (S, a matrix of sources by time points) weighted by a mixing matrix (M, a matrix of sources by channels), plus noise (N, an additive matrix):

$$x = MS + N$$

Based on this principle, ICA algorithms estimate the noisy component matrix (y), where:

$$y = Wx$$

where W is the unmixing matrix, equal to the inverted mixing matrix. Methods for calculation of W differ between ICA methods, which implement different approaches to maximizing independence. There are subtle differences between the algorithms, but they can be roughly grouped into three different types: (1) Natural Gradient Descent algorithms, including Infomax, Extended Infomax, and Adaptive Mixture ICA (AMICA); (2) Cumulant Diagonalization (CD) algorithms, which includes only Joint Approximate Diagonalization of Eigenmatrices (JADE); and (3) Time-Dependent (TD) algorithms, including Second Order Blind Identification (SOBI) and SOBI with Robust Orthogonalization (SOBI-RO).

Natural Gradient Descent algorithms are iterative procedures where maximum entropy (or information content) of the output vectors h(y) is achieved by minimizing the mutual information I(y) shared between them. Entropy within a vector of random data (such as data from an MEG sensor) is given by the equation:

$$h(x) = E\{-log\ p(x)\}$$

where entropy h of the vector x is the expected value of the log transformed probability density function (PDF) for the vector/sensor p(x), which ranges from 0 to 1. In essence, entropy can be described as the area under the curve of the PDF. For a linear transformation Y=BX, entropy of the vector Y can be calculated with the sum of the entropy of vector X and the log determinant of weighting vector B using the formula:

$$h(Y) = log|det\ B| + h(X)$$

Because sensor x and component y have a linear relationship by the factor W, as in (D2), the entropy of component y can be calculated by:

$$h(y) = log|det\ W| + h(x)$$

Pairwise mutual information (I) between two vectors X1 and X2 (which could be two MEG sensors or two ICA components) can be defined as:

$$I(X_{1,2}) = h(X_1) + h(X_2) - h(X_{1,2})$$

where $\boldsymbol{h(X_{1,2})}$ is the joint entropy across the two vectors. Similarly, mutual information I among N components Y derived from a vector/sensor can be defined as:

$$I(Y) = h(Y_1) + \ldots + h(Y_N) - h(Y)$$

Therefore, mutual information between component timecourses $\boldsymbol{y_{1\ldots n}}$ can be defined as:

$$I(y) = h(y_1) + \ldots + h(y_n) - log|det\ W| - h(x)$$

All of the natural gradient descent algorithms effectively work by minimization of $I(y)$. The Infomax ICA algorithm achieves minimization of $I(y)$ based on the information maximization principle (Bell and Sejnowski 1995). Extended Infomax is similar to Infomax, with the additional ability to separate mixed non-Gaussian signal distributions. This is done by a learning rule which adaptively changes the sign of the fourth-order moment of the PDF to fit sub- and super-Gaussian distributions. Adaptive Mixture ICA (AMICA) goes a step further and models adaptive mixtures of Gaussian PDFs fit to individual component time-courses and spatial projections in entropy maximization, rather than a selecting single Gaussian or non-Gaussian PDFs.

The Cumulant Diagonalization algorithm JADE performs mutual information reduction on data transformed to the cumulant of the PDF. In particular, JADE minimizes $\boldsymbol{I}(\boldsymbol{y})$ by rotation and diagonalization of the fourth-order cumulant, which is related mathematically and conceptually to the fourth-order moment (kurtosis). Using the Jacobi technique, JADE reduces mutual information contained in the matrices of the component PDFs by rotating the weighting matrix W until cumulant matrices are maximally diagonal (Cardoso and Donoho 1999).

The Time-Dependent algorithm SOBI takes advantage of the temporal structure in the observed data by comparing time-lagged versions of the PDF. In short, correlations between individual components are expected to exist in time, though instantaneous mutual information content is minimized like the other methods described. SOBI, like JADE, uses the Jacobi technique to achieve diagonalization, though SOBI achieves diagonalization of the correlation matrix of the component PDFs. SOBI-RO is similar to SOBI, but was specifically designed to handle noisy signals by incorporating a robust whitening step (Belouchrani and Cichocki 2000).

11.3 Segmentation and Averaging of Event-Related Fields (ERFs) and Time-Frequency Representations (TFRs)

Event-related fields (ERFs) are the magnetic counterparts of event-related potentials (ERPs) measured with EEG. These signals are sometimes referred to as "evoked responses" because they are generated in response to a stimulus of some type. This contrasts with "spontaneous responses" such as epileptic spikes and endogenous alpha waves. The measurement of ERFs is predominantly dependent on the removal of noise through signal averaging, which is the process of averaging signals across many (usually 100+) trials of the sensory or behavioral event of interest (e.g. presentation of a tone or the onset of a button press response). When neurophysiological events are time-locked to these sensory or behavioral events, the amplitudes of noise signals at any given latency will vary from trial to trial, while the amplitude the underlying signal of interest, the evoked response, will remain (generally) stable with each occurrence. Thus, as the trial count increases, the variable and randomly positive or negative amplitudes of noise signals in the data will cancel one another and approach zero, while the amplitude of the time-locked evoked response will approach its mean. In this way, the magnetic signals generated by neurophysiological events can be elucidated from background noise, even with very small signal-to-noise ratio. In fact, MEG signals as small as 5 fT can be isolated from background noise through the process of event-related signal averaging (Lounasmaa 1989). However, ERFs recorded with MEG typically range between 100 and 400 fT. Particularly for smaller signals or studies with small numbers of trials, it may be important to remove trials that exceed some amplitude threshold prior to averaging to limit the impact of high-amplitude noise on final average response. Similarly, DC shifts between trials can be removed by subtracting pre-stimulus baseline magnetic field strength from each datapoint prior to averaging across trials.

Following event-related averaging, the resulting ERF waveforms, like ERP waveforms, can be characterized by common peaks and troughs observed across studies. For example, the auditory evoked field can be divided into ERFs that have been linked to early auditory brainstem responses (the so-called early ERFs) and those that are thought to arise from cortical auditory processing (the mid-latency and late ERFs). When referring to ERP peaks, it is convention to use the commonly-observed vertex polarity in the label, such as the P50 (a positive ERP that peaks about 50 ms after an auditory stimulus) or the N100 (a negative ERP that peaks around 100 ms post-stimulus). When referring to ERFs, these conventions are no longer appropriate, as the magnetic field representations of these neurophysiological responses obtained with MEG do not have clear and consistent spatial distribution of positivity and negativity at the sensors, primarily due to between-subject differences

in head position relative to the MEG sensors. Thus, ERF peaks are often referred to with a capital "M" in place of the "N" or "P" qualifiers (e.g., M50 and M100), or simply by appending a lower-case "m" suffix to the ERP label (e.g., P50m or N100 m). The latter labeling method has the advantage of facilitating internet search based on single terms; however, the former is far more common in the field. To measure specific ERF peaks, some studies will apply filters at this stage that reduce the signal from other, irrelevant ERFs, this increasing the relative SNR of the ERF peak of interest. For example, auditory evoked ERFs may be band-pass filtered from 10–70 Hz for measurement of the M50, or from 1–40 Hz for measurement of the M100.

11.3.1 Time-Frequency Representations (TFRs)

As we described in the previous section, stimulus averaging increases the SNR for *evoked responses* (responses that occur at the same time relative to event onset at each occurrence), which enables measurement of ERF peak amplitudes, durations, etc., even from signals with low single-trial SNR. Unfortunately, many processes in the brain do not reliably have the same timing on every trial. These variably-timed responses are called *induced responses* (Fig. 11.3). Further, many of the oscillatory responses occur at a rate of 4–100 Hz, meaning that small (≥1 ms) differences in response onset between trials may lead to signal attenuation or even cancellation with trial averaging. However, by using time-frequency representations (TFRs) of the data, one can perform trial-based signal averaging for induced responses (responses that have slightly different onsets from trial-to-trial) as well as evoked responses. Averaging trials in the time-frequency domain allows measurement of amplitude (power) of brain oscillations regardless of shifts in onset time between trials.

TFRs are three-dimensional representations of the spectral power across frequencies and over time. This type of representation differs from power-spectral density (PSD) representations, which depict spectral power over a predefined time range. Rather, TFRs are used to analyze

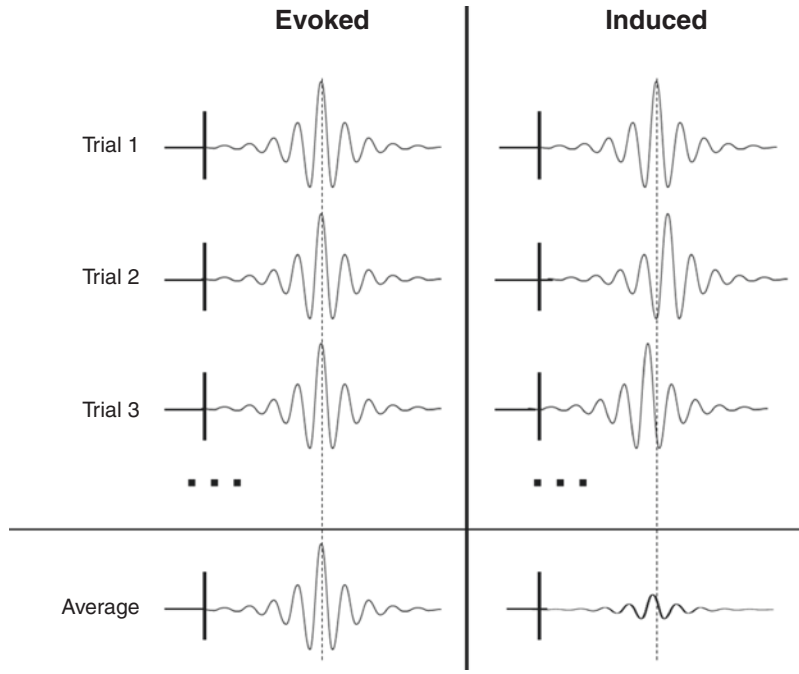

Fig. 11.3 Evoked (Left) and Induced (Right) Event-Related Neurophysiological Activity. With increasing number of trials, the signal of interest is increased relative to the noise when averaging evoked responses, while it is reduced with signal averaging in the case of induced responses. The peak latency of the response (evoked or induced) in the first trial is depicted by dashed lines

nonstationary, or time-varying, oscillatory brain signals. There are many ways to calculate spectral power; however, we will focus on three methods that are most commonly used in MEG research: The Hilbert transform of a band-pass filtered signal, windowed Fourier transform, and wavelet analysis. Each of these three methods will produce a matrix of spectral power by time and frequency, with resolution depending primarily on the sampling rate of the recorded signal. Except for the Hilbert transform, calculating TFRs of power is done using a sliding time window, and power is calculated separately for each time window. This can be done two ways: either the time window has a fixed length independent of frequency, or the time window decreases in length with increased frequency (i.e., a fixed number of oscillatory cycles will change duration as a function of the different wavelength periods). Each of these methods has advantages and disadvantages, and the choice of which method to use often depends on the types of questions being answered. Regardless of the method used, one must also consider how the data will be represented. Will the activity be compared to some baseline? How will this change from baseline be represented (absolute difference, linear ratio, log-linear ratio)? What will be the frequency and time range and the resolution of the resulting TFR? Depicting TFRs that accurately and intuitively display the complete results of an MEG experiment in a simple figure is non-trivial. In most cases, three-dimensional (time x frequency x amplitude/power) TFRs are calculated for different spatial locations, such as MEG sensors or source locations in the brain. This high dimensionality can also lead to statistical power issues when parametric statistics are used. Thus, dependent variables must usually be simplified or distilled in some way by averaging over a window in one or more dimensions. Choosing these windows a priori can sometimes be difficult; however, some methods, such as cluster-based permutation testing, have been proposed for studies in which hypotheses are not so circumscribed (Maris and Oostenveld 2007).

The Hilbert transform method used in generating TFRs is dependent on first band-pass filtering the signal to the frequency band of interest. The nature of these filters is usually the same as those applied to MEG data in other contexts, such as those applied for noise reduction. However, filters used in generating TFRs are often narrower than one would use for noise reduction. The Hilbert transform procedure then represents power at each filtered frequency band using the envelope of the filtered signals (Fig. 11.4). To accomplish this, the MEG signal is transformed to a time series of complex numbers, where the real part is the same as the filtered signal, and the imaginary part is the Hilbert transform. Although the mathematics are a bit more complex than this implies, generating a time series of power from the Hilbert transform can be thought of as a convolution of the band-pass filtered signal of interest with the function $h(t) = 1/(\pi t)$, known as the Cauchy kernel. The Hilbert transform is particularly useful when one would like to generate a quick representation of power with no need for information about the phase of the measured signal. One common use for the Hilbert transform is to investigate cross-frequency phase-amplitude coupling. For example, if one wanted to examine how gamma activity (at 40 Hz) was modulated by theta phase (at 5 Hz), then the envelope of gamma power would have a phase in the alpha range, which can be quantified.

The Fourier transform is one of the most widely-applied methods in signal processing. The Fourier transform is a complex-valued function, whose absolute value represents the amplitude/power of that frequency present in the original signal, and whose complex argument is the phase offset of the basic sinusoid at that frequency. To generate these complex-valued functions for a range of times and frequencies, the signal is often divided into multiple time windows, and the Fourier transform is applied to each window separately. Because of differences in resolution across the frequency spectrum, the Fourier transform method for generating TFRs will include the application of one or multiple tapers, which allow a better control of time and frequency smoothing. A taper is simply a mathematical function that is zero-valued outside of some chosen interval. The most common tapers

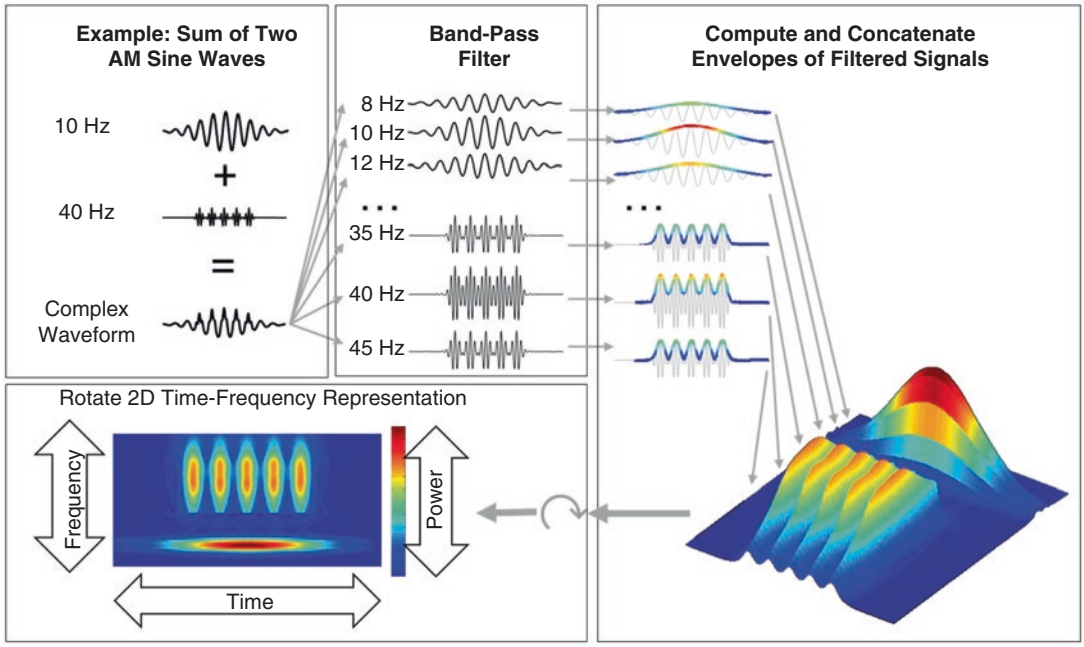

Fig. 11.4 Time Frequency Representation using Hilbert Transform. In this example, the signal of interest is a simple sum of a single burst of 10 Hz oscillations and a series of 4 bursts of 40 Hz oscillations. The first step in the Hilbert transform is to apply multiple narrow band-pass filters to the signal of interest. The envelope of each filtered signal is then taken to represent power at that frequency, which can be used to assemble a three-dimensional time-frequency representation of signal power. By color-mapping signal power, we can rotate the image to see a two-dimensional representation of power by time and frequency. Further, in this example, the 40 Hz (gamma) signal we are measuring is amplitude modulated at 10 Hz (alpha), showing alpha-gamma phase-amplitude coupling

used in MEG research are the Hann/Hanning and Hamming window tapers. Both are cosine functions with similar properties (raised cosine with 18 dB per octave rolloff), with only a small difference between them: The Hann window has an inflection point (a_0) at 0.5, while the Hamming window places a_0 at 0.54 (Harris 1987). This results in a zero value at the edges of the Hann window, but not the Hamming window. The choice of tapers is usually somewhat trivial, but one should use a Hann window if unsure which taper to implement in their study. It is also possible to calculate the TFRs with respect to a time window that varies with frequency. Typically, the time window gets shorter with an increase in frequency. The main advantage of this approach is that the temporal smoothing decreases with higher frequencies; however, this is at the expense of frequency smoothing. The approach is very similar to wavelet analysis, which only differs by applying a Gaussian-shaped taper (Percival and Walden 1993). Wavelet analysis (described below), however, has some advantages over the windowed Fourier transform. Because the Fourier transform deconvolves a complex wave into underlying frequencies, it is very sensitive to abrupt transitions or discontinuities in the complex wave, as can occur at edges of windows. The method introduces a large amount of high frequency artefact at edges in modeling these essentially square waves.

Recently, multitapers have been suggested as a way to improve further on some shortcomings of traditional windowed Fourier analysis methods. The multitaper method utilizes so-called Slepian sequences, which are orthogonal tapers selected to provide better control over the frequency smoothing (Simons et al. 2006). More tapers for a given time window will result in greater smoothing, which is particularly advantageous when dealing with electrophysiological brain signals above 30 Hz. Oscillatory gamma

activity (30–100 Hz), for example, is quite broad band and thus analysis of such signals benefit from multitapering. However, for signals lower than 30 Hz, it is recommended that only a single taper be used. Because wavelet transforms do not deconvolve the complex wave into constituent sinusoids, but rather use specific single frequency sinusoids convolved with a Gaussian function for tapering, these wavelet transforms avoid some of the issues with windowed Fourier transforms, particularly for higher frequencies, thereby providing improved temporal resolution.

The wavelet transform is likely the most common method for generating TFRs from neurophysiological data. In the wavelet transform, a small segment of a sinusoid of a specific frequency tapered by convolution with a Gaussian function, called a wavelet, is convolved with the signal being measured, producing a complex-valued function (as in the Fourier transform), whose absolute value represents the amplitude/power of that frequency present in the original signal, and whose complex argument is the phase offset of the basic sinusoid in that frequency (Percival and Walden 1993). Wavelets come in many types, but the most commonly used wavelet in neuroscience research is the Morlet wavelet. Morlet wavelets have the shape of a sinusoid, weighted by a Gaussian kernel, and they can capture local oscillatory components in the time series. Contrary to the standard Fourier transform, wavelets have variable resolution in time and frequency. For low frequencies, the frequency resolution is high but the time resolution is low. For high frequencies, it's the opposite. As stated above, the approach is equivalent to calculating TFRs with time windows that depend on frequency using a taper with a Gaussian shape.

When designing the wavelet, we basically decide a trade-off between temporal and spectral resolution. We do this by specifying the width of the wavelet, usually given as a number of cycles in the wavelet. For higher temporal resolution, smaller wavelets are preferable, with only 3–5 cycles. This is because more wavelets can be fit into a given time window. For higher spectral resolution, longer wavelets are preferable, with 5–7 cycles. Like the other methods for calculation of spectral power described above, one must be careful when designing MEG research studies to ensure that the trial duration is long enough that the events of interest can be measured effectively, particularly when comparing to some baseline. For example, if one is interested in a 4 Hz oscillation (F) that begins at 200 ms after some event and persists for 200 ms and 6 cycles (C) are to be used, then the wavelet transform must be applied to no later than 550 ms prior to the event (200 – ((C/2) ∗ (1000/F)) and no earlier than 1150 ms after the event (400 + ((C/2) ∗ (1000/F)).

11.4 The Forward Model

Many MEG analysis methods require estimation of geometry and location of the brain relative to the MEG sensors, such as MEG source imaging/analysis and certain artefact filtering methods. As mentioned above, two models are needed for source imaging: the forward model and the inverse model. We will discuss the inverse model later in the chapter. The forward model consists of three components: The source model, the volume conductor model, and the measurement model. The source model for MEG typically assumes that the source of the measured signal (recorded outside the head) comes from electric current dipoles in the brain. More specifically, we usually assume that a complex combination of dipolar currents within gray matter in the brain leads to the magnetic fields observed at the sensors. This model is commonly referred to as the equivalent current dipole model (Brazier 1949). The conductor model explains the relationships between the source model and the measurements and is primarily reliant on Maxwell's equations. Volume conductor models can be solved for a variety of geometries of the volume, such as spherical or ellipsoid volume conductor models. Complex models of the volume conductor, such as boundary element models or finite element models, may include intervening tissue boundaries to estimate conductivity and impedance imposed by tissues such as bone and skin. The measurement model is used to represent the

parameters of the specific measurement system. In MEG, this often incudes parameters such as the type of sensor (i.e., magnetometers or gradiometers) and the location of the head relative to the sensor array. We will skip the discussion of source model options, as there is no currently accepted alternative to the equivalent current dipole model, and we will continue with further discussion of the conductor model and measurement model.

11.4.1 The Conductor Model

Volume Segmentation and Surface Extraction. The simplest model for projecting sensor activity from outside the entire head to specific sources within the brain utilizes a spherical model with dipolar sources assumed to be oriented radially to the surface of the sphere. However, heads are not perfectly round, and the cortical surface is composed of sulci and gyri, meaning that one cannot assume that all dipolar sources will be radial with respect to the scalp or sensor array. Although simple spherical source models do not necessarily rely on measurement of head and brain structure (one can fit a sphere to 3D localizer data representing the surface of the scalp in this case), more complex methods are intimately dependent on good-quality representations of structural geometry. Magnetic resonance imaging (MRI) is the most commonly used method for measuring head and brain structure in MEG research. The specific MR sequences used may differ from one study to the next, but traditionally include a T1-weighted image of some type. The goal of volume segmentation in MEG research is the representation of geometry of the brain (either the volume or cortical mantle) for use in imaging and/or measurement of the neurophysiological responses obtained with MEG. These simple geometric models consider only the brain/cortex and disregard the rest of the head, which is usually appropriate for MEG source analysis. In source imaging of EEG data or combined EEG/MEG data representations of the skull and scalp may be used to model the effects of bone and soft tissue on the recorded EEG signal. These models are more complicated and require high-resolution images, so additional imaging sequences can be implemented (e.g., T2, fat-suppression, contrast) to aid in measurement of the skull, soft tissue, and CSF. Representations of these tissues are traditionally of two varieties – boundary element models (BEMs) or finite element models (FEMs). BEMs identify boundaries between tissue types to represent tissue conductivities between these boundaries, while FEMs represent these tissues as volumes. The advantage of FEMs is the ability to represent each element with a different conductivity, rather than defining conductivity based on the position relative to tissue boundaries. This type of model is particularly useful for assessment of volume currents that propagate through the different tissue types and are restricted and distorted by tissue boundaries. For MEG measurements, since the magnetic field is generated by primary currents, magnetic permeability does not change across layers (actually, it does not change much from what would be observed in a vacuum), and no currents exist outside the head (where the sensors are located), the full magnetic field can be calculated without consideration of volume currents (Mosher et al. 1999). Because FEMs and complex multi-shell BEMs are highly computationally demanding and are seldom used in volume conductor models in MEG research, we will focus on simple geometric models here (Fig. 11.5).

Many MEG analysis programs do not have the capability of performing volume segmentation and surface extraction. This is a time-consuming and non-trivial process that requires the use of specific software, such as FreeSurfer, FSL, or BrainSuite. Although the implementation may differ between software packages, the goal for MEG source analysis is the same; find the brain volume or cortical envelope from within the MRI-based volumetric image. This is accomplished through removal of non-brain tissue from around the brain – a process often referred to as "skull stripping". To solve this problem, we often capitalize on the high T1-weighted image intensity of white matter for identification of the grey/white matter boundary. In region-based approaches, such as the watershed technique, the

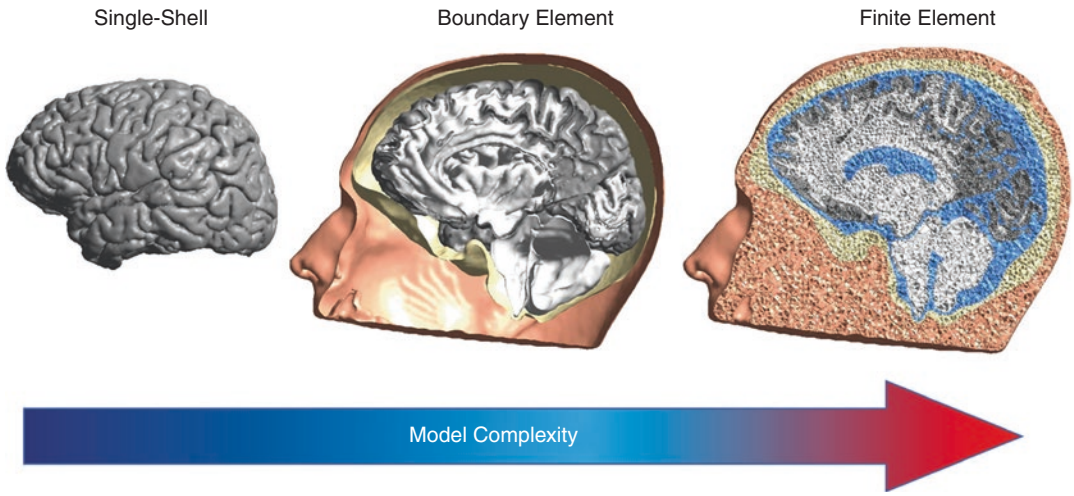

Fig. 11.5 Conductor models commonly used with MEG. Models are shown in increasing complexity from left to right, with the single-shell model at the left, boundary element model in the center, and finite element model at the right. The single shell model does not take into account the intervening tissue boundaries. The boundary element model assumes uniform conductance between each boundary and models the head as a multi-shell volume. The finite element model assigns conductance values to each element when modeling the influence of intervening tissue

brain volume is identified by "flooding" connected voxels within the brain in three dimensions using predefined criteria, such as signal intensity (Mangan and Whitaker 1999). This process often requires user interaction, as thresholding, smoothing, and merging across discontinuities are sometimes required. The brain surface is then calculated as the outer edge of the flooded volume. Other methods rely on gradient information to identify the brain surface directly. In these boundary-based methods, template images are iteratively inflated/deflated and deformed to fit observed intensity gradients. As both methods have strengths and drawbacks, many software packages use a combination of the two for identification of the brain surface.

In both volumetric and surface-based source imaging, the cortical envelope is often identified as the starting point. In volumetric imaging, the entire volume contained within this boundary is subdivided into a grid containing the individual putative dipole locations for use in the forward model. The grid can be sampled in many ways, from evenly-spaced across the brain (most common) to being densely clustered at locations expected to predominantly generate the signals being measured (e.g., auditory cortex in a study of auditory neurophysiology). If the cortical surface is to be used as the source space, the cortical sheet is represented as triangle-tessellated mesh with edge lengths between 1 and 5 mm. The locations of putative dipole sources of the measured MEG signals are often defined at the intersections or vertices. These surface-based models are attractive compared to volumetric models, as the orientations of dipole sources can be fixed to be orthogonal to the cortical surface, as would be expected given that the signals recorded with MEG are thought to predominantly arise from currents in the apical dendrites of pyramidal cells. In other words, the surface-based model places additional biologically-valid constraints onto the model that reduce the model complexity, making the model less prone to error (Fig. 11.6).

11.4.2 The Measurement Model

The measurement model in MEG forward modeling is reliant on two major pieces of information: the physical characteristics of the sensors and the locations of the sensors relative to the sources. The first part of this problem is given by the manufacturer and is simply related to the

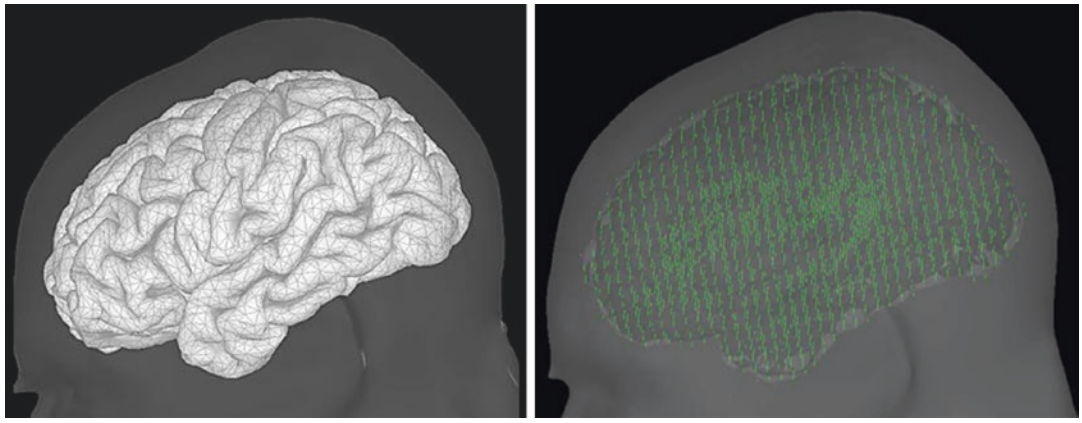

Fig. 11.6 Source spaces commonly used for MEG research. Cortical surface source space is shown on the left, volumetric source space is shown on the right, each with 5 mm isotropic resolution

specific type of sensors being used (magnetometer, planar gradiometer, axial gradiometer, etc.) and (in the case of gradiometers) the orientations of those sensors. Magnetometers are simply sensors that measure magnetic fields, and gradiometers are pairs of magnetometers that measure gradients (spatial differences) in magnetic fields. Unlike EEG electrodes that are fixed directly to the scalp (and so move with the head during recordings), the MEG sensors are in a fixed location and the location of the sensors relative to the head may change during the session. Thus, the exact position of the head (and thus the magnetic sources in the brain inside the head) must be monitored during the session and registered to the positions of the MEG sensors. The relative locations of the sensors are estimated by obtaining and tracking the positions of head-position indicator (HPI) coils attached to the subject at the time of data acquisition. HPI coils are applied to the head prior to MEG data acquisition and the positions of the HPI coils are digitally referenced to landmarks on the surface of the head, such as the nasion and pre-auricular points. These landmarks can then be identified in the MR image used in the conductor model to align the coordinates between the MEG and the source space. In this way, the positions of the sensors can be tracked (in some cases continuously) relative to the brain during MEG recordings. To further increase the accuracy of this coordinate alignment, additional locations are acquired across the scalp and face surface that can be fit to the surface of the head identified in the MR image. In many cases, it may be helpful to create a mesh representing the surface of the head to aid in this process.

11.5 The Inverse Model

As stated previously, analysis of MEG data is most frequently performed at the source level. The specific method used to transform the data measured at the sensors to the space where these signals are thought to be generated differs between studies and can generally be divided into three classes: Dipole modeling methods (i.e., dipole fitting), spatial filters (beamformers and dipole scanning), and minimum-norm solutions (such as minimum-norm estimates, minimum-current estimates, and low-resolution electromagnetic tomography). The methods can also be divided into two general classes based on how inferences about source locations are made: parametric dipole fitting and non-parametric whole-brain imaging. Parametric dipole fitting methods assume that a small set of current dipoles (2–7) can represent the unknown source distribution. The dipole locations and moments then form a set of unknown parameters that are solved with a least-squares fit or maximum likelihood estimation methods. Non-parametric whole-brain imaging includes all other source

analysis methods mentioned above. In this approach, sources are modeled across the entire source space, and the goal is to find a weighting matrix that can best explain the relationship between sources and sensors. These approaches are all implemented in an efficient linear form, where the activity at the sensors is a linear combination of activity at the sources. This has the advantage of representing the relationship with a linear kernel, or multiplicative matrix that can be applied to the timeseries at each point to transform between source and sensor spaces. Each method has advantages and disadvantages, such as the types of questions that can be answered, the constraints placed on the source model, and the computational demand of the method. A major difference between parametric dipole fitting and non-parametric imaging approaches is that non-parametric approaches require separate estimation of the noise and signal components of the data. This necessitates a large number (~(#sensors^2)/2) of independent data observations (samples), which can be taken either from the baseline/stimulus-absent periods (preferred) or the entire dataset. There is usually no correct choice for representing the data at the source, and decisions about which source estimation method to use are most often subjective.

In source estimation from MEG signals, the goal is to estimate the activity of the thousands of dipoles described by our forward model. However, we only have a few hundred spatial measurements as input (the sensors). This problem, called the inverse problem, is ill-posed, meaning there are an infinite number of source activity patterns that could generate the same sensor topography. Inverting the forward model directly is mathematically impossible; however, by making a few assumptions and adding some priors to our model, it becomes tractable. Many solutions to the inverse problem have been proposed based on assumptions about how the brain works and the physics of the signals being measured. These assumptions include things like possible locations of sources, the spatial extent of source activity, the total number of sources, and the source frequency spectrum.

11.5.1 Dipole Fitting

Dipole fitting is the simplest method of source analysis. Parametric dipole localization has been used successfully clinically for pre-surgical mapping of somatosensory and auditory responses, and early sensory peaks can be localized with great precision to primary sensory cortices using dipole fitting. However, there are two major problems with dipole fitting. First, when more than two dipole parameters are estimated, there is an issue with reaching local minima with the non-linear optimization that occurs, meaning that although the result may better fit the data than solutions in the nearby parameter space, a better solution may in fact exist. This can be overcome with stringent parameter search methods, but these methods are computationally demanding and complex. In fact, the computational demand rises exponentially with increasing dipole count. The second problem is that these methods require *a priori* knowledge of the number of dipoles implicated in the process of interest. This information is often not available, particularly for more complex phenomena, and can have a large impact on the result. For example, if the activity of two (or more) "true" dipolar sources are fit into a single dipole, the location of the solution will not properly reflect the true location of the sources, but rather a weighted spatial average location of the multiple sources. In addition to the number of dipoles, the location, orientation, and symmetry across hemispheres of dipoles can also be specified *a priori*. In this way, we can restrict the parameter space to more biologically-valid solutions. This can sometimes be quite impactful, as the pure math of the solution prefers a deep source, sometimes even outside the brain. However, these assumptions may impinge on the validity of the solution if the precise location of the generators are known beforehand (e.g., through invasive depth recordings). Hence, dipole solutions are not optimal for solutions of unknown source configuration. Finally, the locations of resulting dipoles may not match up between participants, making group-level comparisons nearly impossible. For example, in a

study of multisensory integration, although all participants will likely have dipolar sources in primary sensory cortices, some participants may also show dipolar activity in the superior temporal sulcus while others show dipolar activity in middle temporal sulcus. Although mixed-model methods have been proposed to account for this missing data problem, dealing with this issue statistically is less favorable than avoiding the problem altogether.

11.5.2 Spatial Filtering

Spatial filtering is an alternative method to dipole fitting that gets around the issue of predetermining the number of dipolar sources. The goal of spatial filtering methods is to reconstruct an image of source activity by scanning the entire source space with one or two dipoles and computing a spatial filter independently at each source location. These methods compute an estimate of source activity at each location through spatial filtering, such as solving for single-dipole solutions for each possible source location. The spatial data are linearly combined with weights (the spatial filter), which are chosen separately for each location to ensure that the strength of a dipolar source at that location is correctly estimated (assuming a perfect head model). The most common spatial filtering methods are dipole scanning and beamforming. Both methods are similar in the way they estimate source activity; however, additional constraints are placed on the beamformer solution that often make the method preferable over dipole scanning.

Dipole Scanning is the simplest spatial filtering method. In dipole scanning, rather than fitting a few dipoles to undefined or loosely-defined spatial locations, many dipoles are modeled across the cortex, usually with the orientation constrained to be orthogonal to the cortex (as is seen for pyramidal cells, the main generators of the MEG signal). In this way, thousands of dipolar sources are modeled and can be used to image the activity associated with the sensor signal at a specific time point. After fitting each dipolar source, one can compute a linear kernel which, when multiplied by the data, produces a dipole scanning image whose strongest peaks represent the most likely locations of dipolar sources in the brain. This method can even be used prior to dipole fitting to estimate the number of dipoles to be parametrically fit to the data. The most frequently used tools for dipole scanning are the Multiple Signal Classification (MUSIC) toolbox and Brainstorm, both of which can be implemented on MEG data across multiple systems. As implemented in Brainstorm, one can further fit dipolar sources to the local maxima by using the maxima as seed locations for dipole fitting.

Beamformers are increasingly used in MEG research, primarily due to the ability to image time-frequency domain data. There are three types of beamforming methods commonly applied to MEG data. The first two, Linearly Constrained Minimum Variance (LCMV) and Synthetic Aperture Magnetometry (SAM) beamformers, are spatial filtering methods applied to time-domain MEG signals, such as ERFs. This is analogous to dipole scanning procedures. The third type of beamforming, Dynamical Imaging of Coherent Sources (DICS), is used specifically for imaging time-frequency domain data. The main difference between LCMV/SAM beamforming and dipole scanning is that the total output power is minimized with beamforming. This suppresses contributions of sources from other locations to the estimated signal at the location of interest, which may reduce activity estimates for synchronous (without phase lag) or nearby sources. Because of this issue, some have criticized neural synchrony studies based on MEG data localized with beamforming methods; however, recent work shows that this suppression of synchronous activity has little effect on the final connectivity data. In fact, this type of suppression has the opposite result. A distinct advantage of this aspect of beamforming is that it is adaptive and signals that do not originate from the brain (i.e., those signals whose spatial profile at the sensor level cannot be explained by a dipolar source inside the head) are suppressed.

This gives beamforming an interference rejection property, which is not mirrored by non-adaptive algorithms. Using sensor-level analyses, spurious functional connectivity often results from cardiac interference since the artefact affects many sensors. However, correlation between MEG data localized with beamforming methods and the electrocardiogram is small, indicating that cardiac interference is greatly reduced and so unlikely to affect connectivity measurements.

11.5.3 Minimum-Norm Solutions

Minimum norm solutions, like spatial filters, can be considered non-parametric whole brain imaging methods. Data are analyzed across the source space with the goal of calculating the current at each spatial location, regardless of any prior notion about the number of sources that may be involved. This type of non-parametric imaging has a major advantage over dipole fitting procedures. Having data for each spatial location provides the ability to make group level comparisons, as there is no missing data problem like we have with dipole fitting. This is not to say that distributed source models such as minimum norm solutions are superior to parametric dipole fitting. In many cases the number of dipoles is known and a few dipoles can well explain the data, such as the early ERFs in response to a simple sensory stimulus. Unlike spatial filtering methods, minimum-norm solutions model all of the available data. This means that preprocessing is more important, as noise signals can interfere with signal quality to a greater degree than spatial filtering methods of source imaging. Minimum-norm solutions estimate the sources as the solution to a linear imaging problem. The method finds a cortical current source density image that approximately fits the data when mapped through the forward model. As the name implies, all minimum-norm solutions work by minimizing some parameter in the source solution. Minimum-Norm Estimates (MNE) is the most widely-adopted minimum norm solution. MNE, like beamformers, works to minimize the total power across the cortex (L2 norm). Some other types of minimum norm solutions are Minimum-Current Estimates (MCE), which works to minimize the current at the cortex (L1 norm), and Low-Resolution Electromagnetic Tomography (LORETA), which attempts to achieve a maximally smooth source distribution. Minimum-norm solutions are often preferred over spatial filters because of the anatomical validity of the method; however, this is not a fundamental difference between the methods. In both cases, location and orientation of sources can be either constrained to the cortex or not. In fact, minimum-norm and spatial filter methods produce very similar solutions for ERF data. It is in time-frequency representations and connectivity metrics that the methods most significantly diverge. Beamformers perform better than minimum-norm solutions for point-like sources. On the other hand, minimum-norm solutions provide better connectivity estimation than beamformers if the sources are extended cortical patches with highly-coherent time series. Thus, the optimal choice of the inverse solution depends on the spatial and synchronization profile of the interacting cortical sources.

One issue with minimum-norm solutions is that current density values returned by the minimum norm method depend on the signal-to-noise ratio, which may vary significantly between subjects. Amplitude is therefore difficult to interpret directly. Further, current density measures are often artificially greater at the surface, closer to the sensors, than at deeper locations. Normalizing the current density maps with respect to a reference noise level can help with these issues. The most common method for normalization is by the use of dynamic statistical parametric maps (dSPM). In dSPM regularization, the normalizations are computed as part of the inverse routine and based on baseline noise covariances. dSPM regularization produces a Z-score-like map based on the variance observed in the baseline noise covariance. Another common method of regularization is standardized low resolution brain electromagnetic tomography (sLORETA). sLORETA is very similar to dSPM regularization, only sLORETA normalizations are based on the data

covariance during the evoked period, rather than noise covariance in the baseline period. In general, it is best to use non-normalized data to compute time-frequency decompositions or connectivity metrics and normalized solutions (dSPM or sLORETA) for any group-level comparisons of time-domain source data.

11.6 Conclusions

MEG analysis methods, while similar to EEG analysis methods in many ways, are distinct in that source analysis is traditionally the final goal of the methods, rather than measurement of amplitude/latency of brain activity measured at the scalp. MEG source analysis is complicated in many cases and requires not only neurophysiological expertise, but neuroanatomical expertise. New algorithmic approaches are available that not only enable more accurate reconstruction of brain activity, but also enable the measurement of functional connectivity, truly at the speed of thought.

Summary

- Analysis of the brain signals measured with magnetoencephalography (MEG) most often occurs at the source level
- Preprocessing to remove unwanted sources of electromagnetic noise is critical, as MEG signals are dominated by large spatially-stereotyped noise sources
- For modeling sources of the MEG signal, careful considerations must be made when specifying the forward model and inverse model

References

Bell AJ, Sejnowski TJ. An information-maximization approach to blind separation and blind deconvolution. Neural Comput. 1995;7:1129–59.

Belouchrani A, Cichocki A. Robust whitening procedure in blind source separation context. Electron Lett. 2000;36:2050–1.

Brazier M. A study of the electrical fields at the surface of the head. Electroencephalogr Clin Neurophysiol. 1949;2:38–52.

Cardoso JF, Donoho DL. Some experiments on independent component analysis of non-Gaussian processes. Presented at the Higher-Order Statistics, 1999. Proceedings of the IEEE Signal Processing Workshop on, IEEE, 1999; pp. 74–77.

Cohen D. Magnetoencephalography: evidence of magnetic fields produced by alpha-rhythm currents. Science. 1968;161:784–6.

Hämäläinen M, Hari R, Ilmoniemi RJ, Knuutila J, Lounasmaa OV. Magnetoencephalography—theory, instrumentation, and applications to noninvasive studies of the working human brain. Rev Mod Phys. 1993;65:413–97. https://doi.org/10.1103/RevModPhys.65.413.

Harris FJ. On the use of windows for harmonic analysis with the discrete Fourier transform. Proc IEEE. 1987;66:51–83.

Ilmoniemi R, Williamson S. Analysis for the magnetic alpha rhythm in signal space. Presented at the Society for Neuroscience. Abstract, 1987; p. 46.

Jousmaki V, Hari R. Cardiac artifacts in magnetoencephalogram. J Clin Neurophysiol. 1996;13:172–6.

Jung T-P, Makeig S, Humphries C, Lee T-W, Mckeown MJ, Iragui V, Sejnowski TJ. Removing electroencephalographic artifacts by blind source separation. Psychophysiology. 2000;37:163–78.

Lounasmaa OV. Multi-SQUID systems for measurements of cerebral magnetic fields. Phys Scr. 1989; 273.

Mangan AP, Whitaker RT. Partitioning 3D surface meshes using watershed segmentation. IEEE Trans Vis Comput Graph. 1999;5:308–21.

Maris E, Oostenveld R. Nonparametric statistical testing of EEG-and MEG-data. J Neurosci Methods. 2007;164:177–90.

Medvedovsky M, Taulu S, Bikmullina R, Paetau R. Artifact and head movement compensation in MEG. Neurol Neurophysiol Neurosci. 2007;4

Mosher J, Leahy R, Lewis P. EEG and MEG: forward solutions for inverse methods. IEEE Trans Biomed Eng. 1999;46:245–59. https://doi.org/10.1109/10.748978.

Percival DB, Walden AT. Spectral analysis for physical applications. Cambridge: Cambridge University Press; 1993.

Petsche H, Pockberger H, Rappelsberger P. On the search for the sources of the electroencephalogram. Neuroscience. 1984;11:1–27.

Plonsey R, Heppner DB. Considerations of quasi-stationarity in electrophysiological systems. Bull Math Biophys. 1967;29:657–64.. https://doi.org/10.1007/BF02476917

Simons FJ, Dahlen F, Wieczorek MA. Spatiospectral concentration on a sphere. SIAM Rev. 2006;48:504–36.

Stolk A, Todorovic A, Schoffelen J-M, Oostenveld R. Online and offline tools for head movement compensation in MEG. NeuroImage. 2013;68:39–48. https://doi.org/10.1016/j.neuroimage.2012.11.047.

Taulu S, Simola J. Spatiotemporal signal space separation method for rejecting nearby interference in MEG measurements. Phys Med Biol. 2006;51:1759.

Taulu S, Kajola M, Simola J. Suppression of interference and artifacts by the signal space separation method. Brain Topogr. 2004;16:269–75.

Taulu S, Simola J, Kajola M. Applications of the signal space separation method. IEEE Trans Signal Process. 2005;53:3359–72.

Tesche CD, Uusitalo MA, Ilmoniemi RJ, Huotilainen M, Kajola M, Salonen O. Signal-space projections of MEG data characterize both distributed and well-localized neuronal sources. Electroencephalogr Clin Neurophysiol. 1995;95:189–200.

Uusitalo MA, Ilmoniemi RJ. Signal-space projection method for separating MEG or EEG into components. Med Biol Eng Comput. 1997;35:135–40.

12 Magnetoencephalographical Research in Schizophrenia: Current Status and Perspectives

Lingling Hua, Tineke Grent-t'-Jong, and Peter J. Uhlhaas

Contents

12.1 Introduction

Electroencephalography (EEG) and magnetoencephalography (MEG) are both non-invasive techniques to measure the fluctuations in the excitability of neuronal populations with millisecond (ms) resolution. While EEG has been widely applied in the investigation of psychiatric disorders for many decades (Chap. 14), MEG has only been recently introduced as a neuroimaging tool to study circuit anomalies in Schizophrenia (ScZ). Thus, the first MEG studies in ScZ-patients were only conducted in the late 1990s; a Pubmed search identified approxiately 200 papers for MEG studies in Scz, compared with approximately 4000 for EEG studies in ScZ.

Given the widespread use of EEG, the question arises as to why ScZ-reseachers should be interested in MEG. In our view, there are several potential advantages of MEG over EEG that have been reviewed elsewhere in detail (Uhlhaas et al. 2017). These include an increased signal-to-noise-ratio (SNR) for the measurement of high-frequency oscillations, (Muthukumaraswamy and Singh 2013) as well as the improved localisation of generators of neural activity (Hansen et al. 2010). It should also be noted that EEG records signals relative to a reference electrode, the definition of which requires adequate consideration. In contrast, MEG recordings are reference-free. MEG is also less susceptible to contamination by muscle artifacts, particularly those that result from volume conduction across electrodes, including the reference electrode (Mima and Hallett 1999) (See also Chap. 11 for more details).

L. Hua · T. Grent-t'-Jong · P. J. Uhlhaas (✉)
Institute of Neuroscience and Psychology, University of Glasgow, Glasgow, UK
e-mail: peter.uhlhaas@glasgow.ac.uk

M. Kubicki, M. E. Shenton (eds.), *Neuroimaging in Schizophrenia*,
https://doi.org/10.1007/978-3-030-35206-6_12

12.2 MEG-Findings in ScZ

12.2.1 Event-Related Fields in MEG-Data

Similar to EEG, MEG-data can be analysed for fluctuations in response to external and internal stimuli that lead to different waveforms of event-related fields (ERFs). The nomenclature for ERFs follows those observed in EEG-recordings and distinguishes between early sensory components (M50, M100, MMNm, M170) (Liu et al. 2002; Tiitinen et al. 1993; Edgar et al. 2003) and later components involved in attentional selection and executive functions (M300, M400) (Kähkönen et al. 2001; McDonald et al. 2010). As ScZ involves impairments in both early sensory processing (Javitt 2009) and higher cognitive functions (Elvevag and Goldberg 2000), ERFs have been explored across a range of auditory and visual sensory as well as cognitive tasks in ScZ (Rojas 2014; Rivolta et al. 2014; Hayrynen et al. 2016).

12.2.1.1 Sensory Gating

The P/M50 has been investigated in the context of sensory gating (for a review see (Patterson et al. 2008)). Sensory-gating is typically explored by a paired-click paradigm in which two consecutive clicks are presented with an inter-stimulus interval (ISI) of ~500 ms. The duration of the ISI has a significant impact on the magnitude of the P/M50 amplitude (Boutros and Belger 1999). The difference in amplitude between the first click (S1) and the second click, (S2) or the S2/S1 ratio, provides an index of pre-attentive sensory gating. In addition to the P/M50, the P/M100 component suppression during sensory gating may related to an attentional filter mechanism (Lijffijt et al. 2009).

Several MEG-studies have replicated dysfunctions in sensory gating in ScZ (for a review see (Rojas 2014)) in both first-episode (FEP) as well as chronic ScZ-patients, as well as identified the brain regions that give rise to impaired M50/M100 responses (Thoma et al. 2003, 2005; Hanlon et al. 2005; Schubring et al. 2018; Ahveninen et al. 2006; Hirano et al. 2010). Specifically, the contributions of reduced activity in the left superior temporal cortex towards reduced M50 amplitudes in ScZ have been highlighted (Thoma et al. 2003; Hanlon et al. 2005; Schubring et al. 2018; Hirano et al. 2010). In addition, there is evidence for correlations between reductions in the M50 and clinical symptoms, in particular with auditory hallucinations (Hirano et al. 2010) and negative symptoms (Thoma et al. 2005).

Sources for the M50 and M100 gating have been most consistently found in the superior temporal gyrus (STG), however, several studies, including one EEG study (Boutros et al. 2013), have suggested other contributing generators in the (pre)frontal, parietal and cingulate cortex (Boutros et al. 2013, 2018; Williams et al. 2011; Grunwald et al. 2003; Garcia-Rill et al. 2008). Some of these regions have been shown to have been shown to be differentially affected between deficit and non-deficit ScZ-patients (Boutros et al. 2018).

12.2.1.2 Neuromagnetic Magnetic Mismatch Negativity (MMNm)

The MMN/MMNm-potential is obtained during an auditory oddball paradigm in which a series of repetitive standard stimuli is interspersed by a rare deviant stimulus, such as frequency, intensity, or duration deviants (Näätänen 1995). A robust reduced amplitude of MMN has been consistently observed in ScZ patients for duration, pitch, and intensity variants, (for reviews see (Umbricht and Krljes 2005; Yáñez-Téllez and Rodríguez-Agudelo 2011)) and relationships with cognitive deficits and functioning have been established (Baldeweg and Hirsch 2015; Light and Braff 2005).

Several MEG-studies have replicated reduced MMNm amplitudes in ScZ-patients for duration, amplitude and frequency deviants (for a review see (Näätänen and Kähkönen 2009)). In addition, MMNm impairments have been observed in response to speech sounds in ScZ-patients (Kasai et al. 2003; Yamasue et al. 2004), as well as in bipolar disorder (Shimano et al. 2014; Takei et al. 2010; Braeutigam et al. 2018). Similar to EEG-findings (Light and Näätänen 2013), impaired MMNm amplitudes have also been demonstrated

in participants at clinical high-risk (CHR) for psychosis (Shin et al. 2011).

An important issue concerns the question whether responses to standard sounds is intact in ScZ. Consistent with EEG-findings (Rosburg et al. 2008), similar amplitude and latency of M100 responses were observed during MMN-paradigms in ScZ compared to controls (Sauer et al. 2017). This contrasts with findings during auditory paradigms that have reported reduced M100 responses in ScZ (Wang et al. 2014) as well as in CHR-participants (Shin et al. 2012).

Recent MEG-studies have provided novel insights into the underlying generators and mechanisms of MMNm deficits in ScZ. One model to explain the occurrence of MMN-potentials is the predictive coding framework (Friston 2008). From this perspective, the MMN is thought to reflect the prediction error response that occurs when the input differs from an expected sensory input (Garrido et al. 2008; Wacongne et al. 2012). In line with the idea of a hierarchy of internal models that transmit predictions in a top-down fashion to lower sensory areas (Friston 2008), empirical evidence shows the existence of several auditory MMN generators, localized in primary and secondary auditory cortices, as well as in temporal, parietal, and frontal regions (Recasens et al. 2015; Deouell 2007; Giard et al. 1990). MEG is well-suited to study interactions between these regions due to its superior ability to localize primary auditory cortex contributions and its ability to separate generators in left/right hemispheres (Wang et al. 2014).

To test this framework, (Sauer et al. (2017)) employed a hierarchical auditory novelty paradigm that involved unexpected omissions in 16 medicated ScZ-patients and 16 controls. A critical test of the predictive coding account of MMN-responses is the use of experimental conditions that include the unexpected omission of an auditory stimulus in a sequence of standard tones, as omission responses are more difficult to accommodate within a passive adaption model of MMN responses (Wacongne et al. 2012). ScZ-patients showed reduced responses to omitted tones, which overlapped both in latency and generators with the MMNm sources, supporting the hypothesis of impaired sensory predictions in ScZ patients (Shergill et al. 2005).

Several MEG-studies contributed towards the identification of the underlying brain regions involved in MMNm deficits. Evidence from MEG in combination with high spatial-resolution MRI supported the involvement of secondary as well as superior temporal cortex MMNm deficits in ScZ (Yamasue et al. 2004; Kircher et al. 2004). Furthermore, reductions in grey matter (GM) volume of the left planum temporal in ScZ patients may underlie reduced MMNm amplitudes in ScZ, especially in the left hemisphere (Yamasue et al. 2004).

12.2.1.3 M300/M400

The M300 has been related to attention and memory-updating, (Polich and Kok 1995) and can be further differentiated into two components: (1) the P3a is associated with the capture of the deviance detection (novel or unexpected stimuli) and (2) the P3b is related to attentional processing (Friedman et al. 2001). A consistent finding in the EEG-literature is the reduced amplitude and/or delayed latency of the P300 in ScZ (Jeon and Polich 2003).

Hayrynen et al. (2016) examined the processing of relevant vs. irrelevant information during an oddball auditory task that involved auditory steady state (ASS) stimulation at 24, 40, or 80 Hz. In comparison to controls, ScZ-patients displayed reduced M100 and M300 amplitudes, regardless of the different frequency background noise as well as a reduction in spectral power, suggesting that ScZ patients were characterized by a deficit in the amplification of salient stimuli.

Furthermore, there is preliminary evidence for abnormalities in the M400 during semantic processing in ScZ. Vistoli et al. (2011a) showed that ScZ-patients did not show increased activation in the left temporal and anterior cingulate cortices between 200 and 450 ms in response to semantic incongruity, indicating a functional disturbance in brain regions that gave rise to the M400 component, which has been found to be impaired in EEG-studies in ScZ. Moreover, the same group (Vistoli et al. 2011b) also examined MEG-responses during a theory-of mind

(ToM) task in 19 ScZ-patients and 21 controls. The experimental conditions involved (a) attribution of intentions to others (AI) (b) physical causality with human characters (PCCH) and (c) physical causality with objects (PCOB). Source-localization with a minimum norm approach in bilateral temporal and parietal regions identified significant ToM-related activations in controls. In contrast, reduced cortical activation within a 200 to 600 ms time-window was observed in ScZ-patients during attribution of intentions.

12.2.1.4 Visual ERFs

One aspect of visual dysfunctions that has received prominent attention in the ScZ-field are abnormalities in the perception of facial information, which can be linked to distinct ERP-components (McCleery et al. 2015). Rivolta et al. (2014) examined face processing in a sample of 14 medication-naive FEP ScZ-patients, and 17 healthy control participants during perception of Mooney faces. At sensor-level, M100 and M170 amplitude were intact while the FEP-group showed a decrease in the M250 responses. Source-level analysis revealed, however, elevated M100/170 amplitudes in the occipital-temporal areas in FEP-patients. Moreover, ScZ-patients were characterized by impaired perceptual learning as indexed by decreased repetition suppression of the M170. These findings suggest that neural circuits in FEP-patients may be characterized by a failure to gate information flow and abnormal spreading of activity, which is compatible with proposed dysfunctional glutamatergic neurotransmission in ScZ.

12.2.2 Neural Oscillations

Neural oscillations are a fundamental mechanism to establish synchronization between and within distributed neuronal ensembles (Singer 1999; Fries 2005) and can be divided into distinct frequency-bands that subserve different cognitive and perceptual functions (Siegel et al. 2012). More recently, evidence has emerged that rhythmic activity may be fundamentally altered in ScZ and related syndromes, which could provide novel insights into the pathophysiology of the disorder (Uhlhaas and Singer 2010).

12.2.2.1 Auditory Steady-State Responses (ASSRs)

ASSRs are evoked oscillatory responses that are entrained to the frequency and phase of temporally modulated auditory stimuli. Kwon et al. (1999) provided the first evidence for a deficit in EEG-recorded 40 Hz ASSRs in ScZ. This finding has been replicated in several studies (for a meta-analysis see (Thuné et al. 2016)) and deficits at lower ASSRs frequencies have also been demonstrated (O'Donnell et al. 2013).

Similar to EEG studies, several MEG-studies have also demonstrated reduced 40 Hz ASSR power and phase-locking in chronic-ScZ patients, (Teale et al. 2008; Vierling-Claassen et al. 2008; Hamm et al. 2011; Maharajh et al. 2010; Edgar et al. 2018) as well as early-onset psychosis (Wilson et al. 2007). Hamm et al. (2011) examined ASSRs at 5, 20, 40, 80 and 160 Hz in a sample of ScZ-patients. ScZ-patients showed reduced entrainment bilaterally at low 5-Hz and 80-Hz modulation frequencies, while 40 Hz ASSR was only reduced in the right auditory cortex, suggesting that ASSR-impairments are not specific to 40 Hz stimulation. Similar findings were also obtained by Tsuchimoto et al. (2011).

Importantly, MEG-studies have furthermore provided insights into the underlying generators of the ASSR-deficit in ScZ. During normal brain functioning, generators of the 40 Hz ASSR encompass auditory cortices (Gutschalk et al. 1999; Herdman et al. 2003; Pantev et al. 1996) as well as subcortical areas, such as the brainstem (Farahani et al. 2017; Herdman et al. 2002). In ScZ, impaired 40 Hz ASSRs have been localized to the primary auditory cortex (Teale et al. 2008) and superior temporal cortex (Edgar et al. 2014). In addition, there is evidence that left-hemisphere generators are more strongly impaired in ScZ than on the right (Hayrynen et al. 2016; Teale et al. 2008; Tsuchimoto et al. 2011; Edgar et al. 2014) (but see (Hamm et al. 2011). Finally, there is preliminary evidence to suggest that the amplitude reduction of the 40Hz-ASSR in ScZ-patients is related to reduced cortical thickness of the left superior temporal cortex (Edgar et al. 2014).

12.2.2.2 Oscillatory Correlates of Auditory Sensory Gating

Oscillatory substrates of sensory gating in patients with ScZ have been investigated in chronic- and FEP-ScZ patients (Popov et al. 2011a; Carolus et al. 2014). ScZ-patients displayed smaller evoked alpha (8–12 Hz) and gamma activity (60–80 Hz), as well as induced 10–15 Hz alpha desynchronization in response to the auditory paired stimuli (Popov et al. 2011a; Carolus et al. 2014). Interestingly, there is preliminary evidence to suggest that impaired evoked 60–80 Hz and induced 8–12 Hz desynchronization could be normalized after 4-week auditory cognitive training (Popov et al. 2011b, 2012, 2015).

12.2.2.3 Visual Perception

A large body of EEG studies have examined the relationship between neural oscillations and visual processing in ScZ (for a review see (Tan et al. 2013)), especially at beta/gamma-band ranges (Spencer et al. 2003, 2004; Uhlhaas and Silverstein 2005). Recent MEG-studies have examined, in particular, the role of so-called high gamma-band oscillations (60–120 Hz) during visual perception in ScZ-patients (Grützner et al. 2013; Sun et al. 2013).

Uhlhaas and colleagues (Grützner et al. 2013; Sun et al. 2013) explored the role of high-frequency oscillations during perception of Mooney faces (Mooney and Ferguson 1951). Both unmedicated FEP and chronic ScZ-patients were characterized by a pronounced deficit in high gamma-band power while low gamma-band power (25–60 Hz activity) was intact, suggesting that MEG-measured gamma-band oscillations provide a novel insight into the role of high-frequency oscillations in ScZ.

To further identify the contribution of ventral vs. dorsal stream deficits towards dysfunctions in visual processing, Grent-´t-Jong et al. (2016) employed a visual grating task that robustly elicits gamma-band oscillations during normal brain functioning with a high SNR (Hoogenboom et al. 2006). At sensor level, chronic ScZ-patients showed a reduction at 47–67 Hz while alpha-band activity was intact. A beamforming analysis localized gamma-band deficits to ventral steam areas, including the fusiform and lingual gyrus. Importantly, differences in task-related gamma-band activity were not due to differences in baseline activity between controls and ScZ-patients, highlighting that neural circuits in ScZ are characterized by an impairment in the generation of gamma-band oscillations.

The role of neural oscillations during facial affect recognition was examined by Popova et al. (2014). MEG-activity was recorded during videos that showed human faces with dynamic emotional expressions (Popov et al. 2014). Controls exhibited an alpha-power increase prior to full recognition, followed by a 10–15 Hz power decrease during the post-recognition phase. In contrast, ScZ-patients did not show this pattern (Hirvonen et al. 2017) and were characterized by abnormal connectivity during the prestimulus period. Accordingly, these data provide evidence for the potential role of aberrant oscillations for social-cognitive impairments in ScZ. In a follow-up study, preliminary data indicated that targeted cognitive remediation could potentially improve both behavioural and oscillatory dysfunctions in ScZ (Popova et al. 2014).

It is well established that ScZ involves aberrant connectivity between brain areas, leading to a disconnection syndrome, (Friston and Frith 1995) which could be mediated by an impairment in long-range synchronization (Uhlhaas and Singer 2010). Despite preliminary EEG evidence for this hypothesis (Spencer et al. 2003; Uhlhaas and Silverstein 2005), EEG-investigation of such phenomena, especially at electrode-level, remain problematic because of unsolved methodological issues, especially due to the contribution of volume conduction (Maran et al. 2016). Accordingly, MEG approaches that combine advanced source-modelling with estimates of functional connectivity (Schoffelen and Gross 2009) could provide a novel perspective on alterations in large-scale interactions in ScZ.

In a recent study by Hirvonen et al. (2017), large-scale phase synchronization was examined during Mooney faces in chronic ScZ-patients using large-scale networks from source reconstructed MEG data (Fig. 12.1). Oscillation amplitudes and interareal phase-synchronization in the 3–120 Hz frequency range were estimated for 400 cortical parcels and correlated with clinical

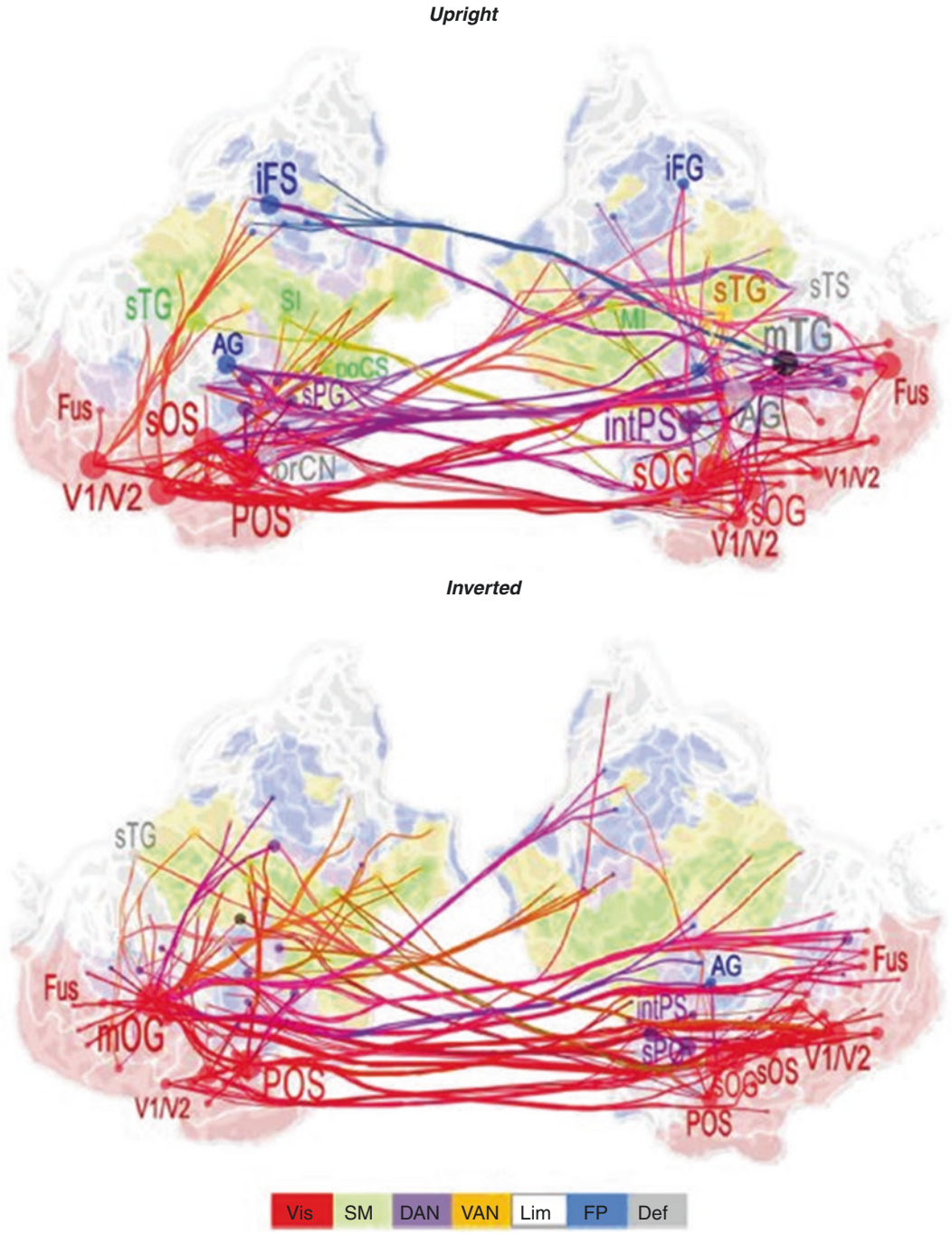

Fig. 12.1 Large-Scale Phase-Synchronization in ScZ. Large-scale networks from source reconstructed MEG data were identified using data-driven analyses of neuronal synchronization. Oscillation amplitudes and interareal phase-synchronization in the 3–120 Hz frequency range were estimated for 400 cortical parcels during presentation of upright and inverted Mooney faces. Top panel: Cortical networks of low-γ-synchronization (30–40 Hz) that differ between controls and ScZ for upright Mooney faces. Bottom Panel: Cortical networks for responses to inverted Mooney faces. Graphs display 200 strongest connections on an inflated and flattened cortical surface. Abbreviation: angular gyrus, *iFS/G* inferior frontal sulcus/gyrus, *MI* primary motor cortex, *mOG* middle occipital gyrus, *mTG* middle temporal gyrus, *Fus* fusiform gyrus, *POS* parieto-occipital sulcus, *prCN* precuneus, *SI* primary somatosensory cortex, *sTG* superior temporal gyrus. [Adapted from (Hirvonen et al. 2017)]

symptoms and neuropsychological scores. ScZ-patients were characterized by a reduction in gamma-band (30–120 Hz) power that was accompanied by a pronounced deficit in large-scale synchronization at gamma-band frequencies. Synchronization was reduced within visual regions, as well as between visual and frontal cortex. The reduction of synchronization correlated with elevated clinical disorganization.

Moreover, large-scale connectivity in thalamo-cortical (TC) circuits in both FEP and chronic ScZ was examined in MEG by Grent-t'-Jong et al. (2018). Results were compared with the effects of ketamine in healthy volunteers. In the ScZ-groups, gamma-band activity was reduced, while TC-connectivity, as assessed through a granger-causality approach, was upregulated at both low and high frequencies. In contrast, ketamine induced a downregulation of TC-connectivity, while the amplitude of gamma-band oscillations was increased. Accordingly, the current novel MEG-recorded findings have implications for theories of cognitive dysfunctions and circuit impairments in the disorder, suggesting that acute NMDAR-hypofunction does not recreate alterations in neural oscillations during visual processing observed in both chronic- and FEP- ScZ.

12.2.2.4 Higher Cognitive Processes

Working memory (WM) impairments are one of the most prominent cognitive deficits in ScZ patients (Barch and Ceaser 2012). During normal brain functioning, WM-processes are supported by the distinct contribution of theta, alpha and gamma-band oscillations (Roux and Uhlhaas 2014). Preliminary evidence for a potential role of aberrant MEG-measured neural oscillations was provided by Kang et al. (2018), who showed impaired desynchronization at low and high frequency ranges. However, these findings need to be replicated in a larger sample and in an experimental task that induces robust oscillatory activity during the WM-delay period.

Further evidence for the involvement of neural oscillations in executive deficits in ScZ was reported by Kissler et al. (2000). The authors examined gamma-band activity at sensor-level during rest and during a mental arithmetic task. ScZ-patients failed to upregulate 30–45 Hz activity and were characterized by reversed lateralization. Moreover, the relationship between selective attention and oscillations in a sample of CHR-participants (n = 17) and in ScZ-patients (n = 10) was examined by Koh et al. (2011). The authors examined alpha-band activity during an auditory oddball task to investigate selective attention to target stimuli and selective inhibition of irrelevant stimuli. The ScZ-group showed diminished alpha-band desynchronization and inter-trial phase coherence relative to controls, while CHR-participants were characterized by intermediate values between controls and ScZ-patients.

12.2.3 Resting-State Activity

In addition to task-related oscillations, MEG has been employed to examine alterations in resting-state activity in ScZ. This work builds on recent evidence suggesting that MEG allows the characterisation of the lay-out and frequencies involved in resting-state networks during normal brain functioning, which overlap with those disclosed by fMRI (Brookes et al. 2011).

In line with previous EEG-data (Boutros et al. 2008; Howells et al. 2018), MEG-studies suggest increased low frequency power (delta and theta) in ScZ-patients, particularly in temporal lobes (Fehr et al. 2001, 2003; Sperling et al. 2002; Wienbruch et al. 2003; Canive et al. 1998; Chen et al. 2016). Aberrant slow-wave activity in temporal cortex has been shown to be correlated with negative symptoms (Fehr et al. 2001, 2003; Wienbruch et al. 2003; Canive et al. 1998; Chen et al. 2016), as well as with auditory hallucinations (Van Lutterveld et al. 2011; Ishii et al. 2000).

Alpha-band oscillations, a key feature of resting-state activity (Barry et al. 2007), have been investigated in several MEG-studies. Evidence for both a reduction and increase in spectral power has been reported (Ikezawa et al. 2011; Kim et al. 2014; Zeev-Wolf et al. 2018), as well as for aberrant connectivity (Kim et al. 2014; Hinkley et al. 2011). Similarly, there is mixed evidence for alterations in beta-band activity (see (Siekmeier and Stufflebeam 2010; van Lutterveld et al. 2012).

Rutter et al. (2009) identified reduced gamma-band power in a sample of chronic ScZ-patients in the posterior region of the medial parietal cortex, which extended into unaffected siblings. However, there is emerging evidence that fluctuations in resting-state gamma-band power may be different across illness-stages in ScZ. Grent-t'-Jong et al. (2018) examined alterations in in resting-state gamma-band activity in a group of CHR-participants, FEP-, and chronic ScZ-patients (Fig. 12.2). Furthermore, MRS-data were obtained in CHR-participants to establish relations with GABA and Glutamate-levels. CHR-participants were characterized by increased 64–90 Hz power. In contrast, FEP-patients showed a mixture of both elevated as well as decreased spectral power at both low- and high gamma-band frequencies, while chronic ScZ-patients showed a pronounced reduction. MRS-data showed increased Glx-levels in CHR-participants (Fig. 12.3), which correlated with increased occipital gamma-band power of gamma-band across cortical regions. Accordingly, these findings highlight the possibility that resting-state gamma-band activity is increased at illness-onset, which is in agreement with current theories implicating a shift in E/I-balance parameters across illness stages in ScZ.

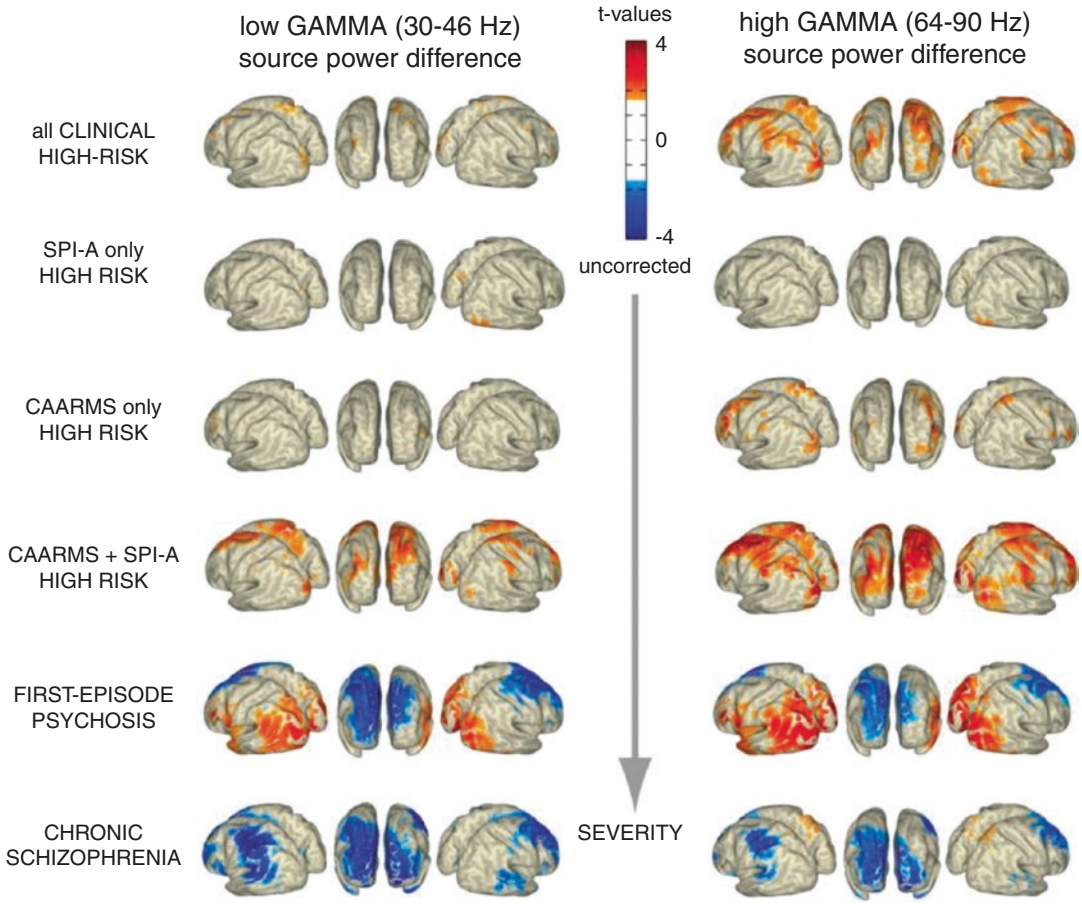

Fig. 12.2 Resting-State Gamma-Band Activity across Illness-Stages in ScZ: MEG resting-state gamma-band activity in participants meeting clinical high-risk (CHR) criteria (n = 88), first episode (FEP) patients (n = 21) and chronic ScZ-patients (n = 34) were investigated. Top-Panel: Surface-projected statistical group differences in low gamma (30–46 Hz; left column) and high gamma-band (64–90 Hz; right column) for all main and the three CHR-subgroups contrasts. Values represent t-values corresponding to significant voxels ($p<0.05$; uncorrected, masked at critical t-values of non-parametric, Monte-Carlo permutation independent t-tests). [Adapted from (Grent et al. 2018)]

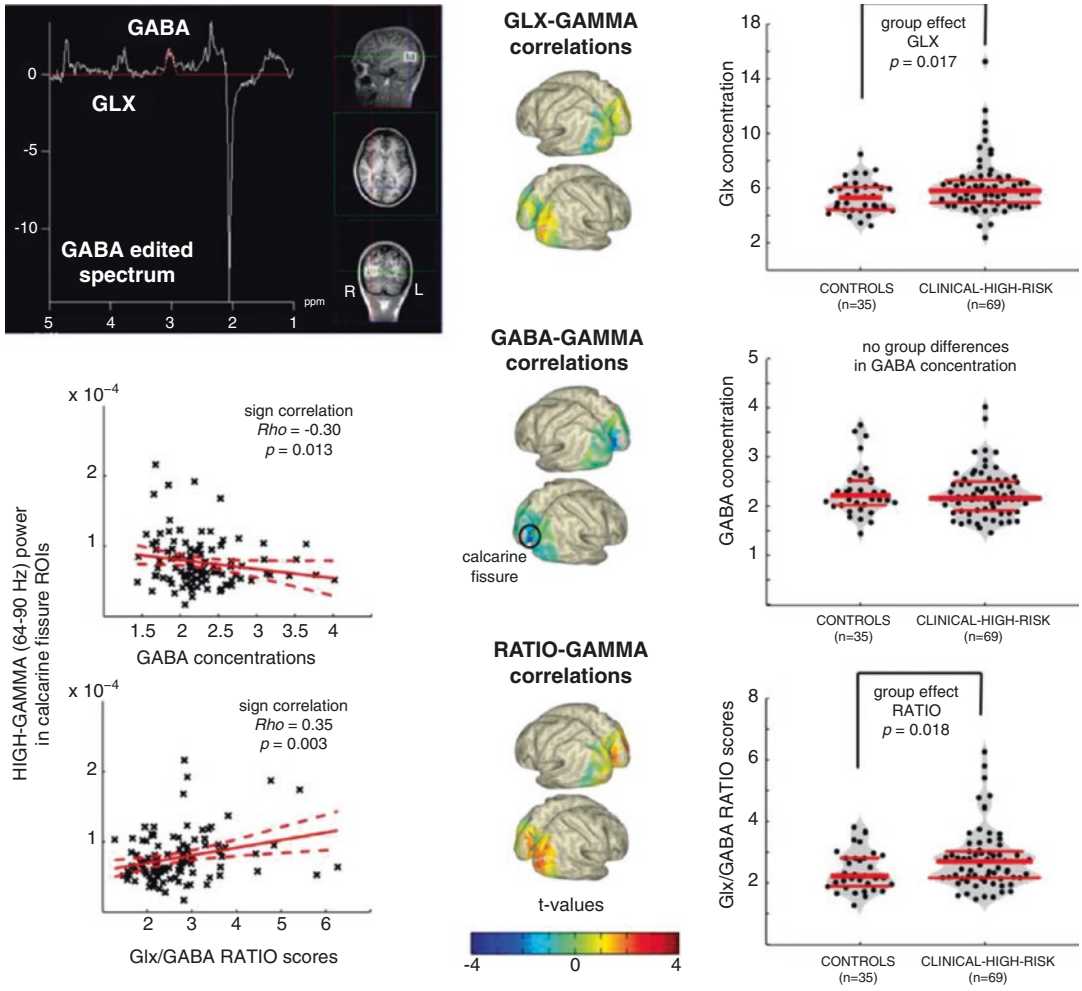

Fig. 12.3 Bottom-Panel: Aberrant Gamma band activity is linked to changes in E/I balance. Upper Left Panel: Data from a 2 × 2 × 2 cm voxel placed in the right middle occipital gyrus (RMOG) during 1H-MRS of GABA and Glx (Glutamate/Glutamine) concentrations (MEGAPRESS GABA editing sequence). Right Column: dot-violin distribution plots showing concentration of each metabolite (or ratio between them) for each individual participant (black dots), separately for controls (n = 35) and CHR (n = 69) participants. Red lines indicate median concentration (middle line) and 1st and 3rd quartiles of the distribution. Data was tested for statistical group differences, using one-way repeated-measures ANOVAs, followed up by post-hoc Welch t-tests (bootstrapping: n = 1000, LSD corrected for multiple comparisons). Significant increases were found for CHRs, compared to controls, in both Glx concentration and Glx/GABA ratio scores. Middle Column: Surface-projected t-values representing linear-regression based correlations between MRS variables and high gamma-band (64–90Hz) power from all 104 participants (35 controls plus 69 CHR). Both Glx and ratio scores correlate positively with increased occipital gamma-band power (uncorrected), whereas GABA concentrations correlate negatively with increased gamma-band power in calcarine areas (FDR corrected), resulting in a significantly increased ratio score in the same regions. Lower Left Panel: Correlation plots for the two strongest effects in calcarine regions. [Adapted from (Grent et al. 2018)]

12.3 Conclusion and Outlook

There has been a recent increase in the application of MEG towards identifying electrophysiological abnormalities in ScZ during a range of experimental protocols. The most consistent evidence for impaired circuit functions comes from studies into sensory processing, especially experimental tasks using MMN, ASSR, and visual stimulation protocols. The findings on resting-state activity

in ScZ provide conflicting findings on alterations across different frequencies, and further studies are required with larger sample sizes and standardized analysis protocols.

While MEG-studies have replicated many findings obtained through EEG in ScZ, there are several areas where we feel MEG has gone significantly beyond the existing EEG-literature, providing a potentially powerful tool for future studies to identify circuit dysfunctions in ScZ and related disorders. One is the improved identification of the underlying generators that allow insights into the brain regions that give rise to aberrant neural responses. While source reconstruction techniques can also be applied to EEG-data, MEG is characterized by improved localization accuracy (Vorwerk et al. 2014), especially when combined with individual anatomical information. There is evidence to suggest that even mm localization accuracy may be feasible (Troebinger et al. 2014). Challenges for source-localisation with MEG-data are, however, highly correlated sources as well as generators in frontal regions that may not always be reliably detected (Schoffelen and Gross 2009; Herrmann et al. 2009).

Until recently, source-localization of MEG data was largely confined to cortical sources. However, emerging data suggests that deep sources, such as the thalamus (Roux et al. 2013) and hippocampus (Recasens et al. 2018) can be reliably detected given that certain conditions, such as trial numbers, are met, significantly extending the application of MEG to the investigation of subcortical networks.

This approach is particularly relevant for the implementation of connectivity measures that provide important insights into the functional architecture of large-scale networks. Analysis of measures, such as coherence and phase-locking, on surface electrode/sensor data is complicated by several methodological challenges (Maran et al. 2016; Van Diessen et al. 2015). While the implementation of analytic routines at source-level in MEG is not trivial, analysis of source-reconstructed time-courses provides more physiologically realistic insights into functional interactions between distributed neuronal ensembles.

A second major improvement in our view of MEG over EEG is the ability to measure high-frequency oscillations. This is because MEG-recordings are hardly affected by different tissues and are less susceptible to artifacts, resulting in increased signal to noise (Muthukumaraswamy and Singh 2013), especially for gamma band oscillations above 60 Hz, which may be important for cortical computations (Uhlhaas et al. 2011). Given the importance of gamma-band oscillations for the understanding of cognitive deficits in ScZ and certain symptoms of the disorder (Uhlhaas and Singer 2010), MEG is likely to play a crucial role in translational research in this area.

At the same time, there are several significant challenges that remain to be addressed before MEG can be more widely employed in clinical studies. The most obvious is the availability of MEG-systems and associated running costs, as MEG systems require regular helium supplies. Recent advances in helium recycling technology have led to dramatic reductions in helium costs, however, and novel MEG sensors have been developed that can operate at room temperatures and thus do not require helium for cooling (Boto et al. 2018). These developments offer the promise of conducting MEG measurements without the confines of elaborate dewar and cooling systems that could increase the availability of MEG-systems significantly.

Summary

- Electrophysiological abnormalities are a crucial aspect of the pathophysiology of ScZ. However, MEG has only been recently applied to investigate circuit anomalies in the disorder.
- Consistent with EEG studies, impaired event-related fields (ERFs) during sensory processing and cognitive processes in ScZ have been demonstrated in MEG-data.
- There is consistent evidence for impaired high gamma-band (>60 Hz) oscillations in ScZ that can be disclosed with MEG.

- MEG is a promising tool for translational research in ScZ and discovery of biomarkers.

References

Ahveninen J, Jääskeläinen IP, Osipova D, Huttunen MO, Ilmoniemi RJ, Kaprio J, et al. Inherited auditory-cortical dysfunction in twin pairs discordant for schizophrenia. Biol Psychiatry. 2006;60(6):612–20.

Baldeweg T, Hirsch SR. Mismatch negativity indexes illness-specific impairments of cortical plasticity in schizophrenia: a comparison with bipolar disorder and Alzheimer's disease. Int J Psychophysiol. 2015;95(2):145–55.

Barch DM, Ceaser A. Cognition in schizophrenia: core psychological and neural mechanisms. Trends Cogn Sci. 2012;16(1):27–34.

Barry RJ, Clarke AR, Johnstone SJ, Magee CA, Rushby JA. EEG differences between eyes-closed and eyes-open resting conditions. Clin Neurophysiol. 2007;118(12):2765–73.

Boto E, Holmes N, Leggett J, Roberts G, Shah V, Meyer SS, et al. Moving magnetoencephalography towards real-world applications with a wearable system. Nature. 2018;555(7698):657.

Boutros NN, Belger A. Midlatency evoked potentials attenuation and augmentation reflect different aspects of sensory gating. Biol Psychiatry. 1999;45(7):917–22.

Boutros NN, Arfken C, Galderisi S, Warrick J, Pratt G, Iacono W. The status of spectral EEG abnormality as a diagnostic test for schizophrenia. Schizophr Res. 2008;99(1-3):225–37.

Boutros NN, Gjini K, Eickhoff SB, Urbach H, Pflieger ME. Mapping repetition suppression of the P50 evoked response to the human cerebral cortex. Clin Neurophysiol. 2013;124(4):675–85.

Boutros NN, Gjini K, Wang F, Bowyer SM. Evoked potentials investigations of deficit versus nondeficit schizophrenia: EEG-MEG preliminary data. Clin EEG Neurosci. 2018:1550059418797868.

Braeutigam S, Dima D, Frangou S, James A. Dissociable auditory mismatch response and connectivity patterns in adolescents with schizophrenia and adolescents with bipolar disorder with psychosis: a magnetoencephalography study. Schizophr Res. 2018;193:313–8.

Brookes MJ, Woolrich M, Luckhoo H, Price D, Hale JR, Stephenson MC, et al. Investigating the electrophysiological basis of resting state networks using magnetoencephalography. Proc Natl Acad Sci. 2011;108(40):16783–8.

Canive JM, Lewine JD, Edgar JC, Davis JT. Spontaneous brain magnetic activity in schizoprenia patients treated with aripiprazole. Psychopharmacol Bull. 1998;34(1):101–5.

Carolus AM, Schubring D, Popov TG, Popova P, Miller GA, Rockstroh BS. Functional cognitive and cortical abnormalities in chronic and first-admission schizophrenia. Schizophr Res. 2014;157(1-3):40–7.

Chen Y-H, Stone-Howell B, Edgar JC, Huang M, Wootton C, Hunter MA, et al. Frontal slow-wave activity as a predictor of negative symptoms, cognition and functional capacity in schizophrenia. Br J Psychiatry. 2016;208(2):160–7.

Deouell LY. The frontal generator of the mismatch negativity revisited. J Psychophysiol. 2007;21(3-4):188–203.

Edgar J, Huang M, Weisend M, Sherwood A, Miller G, Adler L, et al. Interpreting abnormality: an EEG and MEG study of P50 and the auditory paired-stimulus paradigm. Biol Psychol. 2003;65(1):1–20.

Edgar JC, Chen Y-H, Lanza M, Howell B, Chow VY, Heiken K, et al. Cortical thickness as a contributor to abnormal oscillations in schizophrenia? NeuroImage Clin. 2014;4:122–9.

Edgar J, Fisk IVCL, Chen YH, Stone-Howell B, Liu S, Hunter MA, et al. Identifying auditory cortex encoding abnormalities in schizophrenia: the utility of low-frequency versus 40 Hz steady-state measures. Psychophysiology. 2018:e13074.

Elvevag B, Goldberg TE. Cognitive impairment in schizophrenia is the core of the disorder. Crit Rev Neurobiol. 2000;14(1).

Farahani ED, Goossens T, Wouters J, van Wieringen A. Spatiotemporal reconstruction of auditory steady-state responses to acoustic amplitude modulations: potential sources beyond the auditory pathway. Neuroimage. 2017;148:240–53.

Fehr T, Kissler J, Moratti S, Wienbruch C, Rockstroh B, Elbert T. Source distribution of neuromagnetic slow waves and MEG-delta activity in schizophrenic patients. Biol Psychiatry. 2001;50(2):108–16.

Fehr T, Kissler J, Wienbruch C, Moratti S, Elbert T, Watzl H, et al. Source distribution of neuromagnetic slow-wave activity in schizophrenic patients—effects of activation. Schizophr Res. 2003;63(1-2):63–71.

Friedman D, Cycowicz YM, Gaeta H. The novelty P3: an event-related brain potential (ERP) sign of the brain's evaluation of novelty. Neurosci Biobehav Rev. 2001;25(4):355–73.

Fries P. A mechanism for cognitive dynamics: neuronal communication through neuronal coherence. Trends Cogn Sci. 2005;9(10):474–80.

Friston K. Hierarchical models in the brain. PLoS Comput Biol. 2008;4(11):e1000211.

Friston KJ, Frith CD. Schizophrenia: a disconnection syndrome. Clin Neurosci. 1995;3(2):89–97.

Garcia-Rill E, Moran K, Garcia J, Findley W, Walton K, Strotman B, et al. Magnetic sources of the M50 response are localized to frontal cortex. Clin Neurophysiol. 2008;119(2):388–98.

Garrido MI, Friston KJ, Kiebel SJ, Stephan KE, Baldeweg T, Kilner JM. The functional anatomy of the MMN: a DCM study of the roving paradigm. Neuroimage. 2008;42(2):936–44.

Giard MH, Perrin F, Pernier J, Bouchet P. Brain generators implicated in the processing of auditory stimulus deviance: a topographic event-related potential study. Psychophysiology. 1990;27(6):627–40.

Grent T, Rivolta D, Sauer A, Grube M, Singer W, Wibral M, et al. MEG-measured visually induced gamma-band oscillations in chronic schizophrenia: evidence for impaired generation of rhythmic activity in ventral stream regions. Schizophr Res. 2016;176(2):177–85.

Grent T, Gross J, Goense J, Wibral M, Gajwani R, Gumley AI, et al. Resting-state gamma-band power alterations in schizophrenia reveal E/I-balance abnormalities across illness-stages. Elife. 2018;7:e37799.

Grent-t'-Jong T, Rivolta D, Gross J, Gajwani R, Lawrie SM, Schwannauer M, et al. Acute ketamine dysregulates task-related gamma-band oscillations in thalamo-cortical circuits in schizophrenia. Brain. 2018;141(8):2511–26.

Grunwald T, Boutros NN, Pezer N, von Oertzen J, Fernández G, Schaller C, et al. Neuronal substrates of sensory gating within the human brain. Biol Psychiatry. 2003;53(6):511–9.

Grützner C, Wibral M, Sun L, Rivolta D, Singer W, Maurer K, et al. Deficits in high-(> 60 Hz) gamma-band oscillations during visual processing in schizophrenia. Front Hum Neurosci. 2013;7:88.

Gutschalk A, Mase R, Roth R, Ille N, Rupp A, Hähnel S, et al. Deconvolution of 40 Hz steady-state fields reveals two overlapping source activities of the human auditory cortex. Clin Neurophysiol. 1999;110(5):856–68.

Hamm JP, Gilmore CS, Picchetti NA, Sponheim SR, Clementz BA. Abnormalities of neuronal oscillations and temporal integration to low-and high-frequency auditory stimulation in schizophrenia. Biol Psychiatry. 2011;69(10):989–96.

Hanlon FM, Miller GA, Thoma RJ, Irwin J, Jones A, Moses SN, et al. Distinct M50 and M100 auditory gating deficits in schizophrenia. Psychophysiology. 2005;42(4):417–27.

Hansen P, Kringelbach M, Salmelin R. MEG: an introduction to methods. Oxford: Oxford University Press; 2010.

Hayrynen LK, Hamm JP, Sponheim SR, Clementz BA. Frequency-specific disruptions of neuronal oscillations reveal aberrant auditory processing in schizophrenia. Psychophysiology. 2016;53(6):786–95.

Herdman AT, Lins O, Van Roon P, Stapells DR, Scherg M, Picton TW. Intracerebral sources of human auditory steady-state responses. Brain Topogr. 2002;15(2):69–86.

Herdman AT, Wollbrink A, Chau W, Ishii R, Ross B, Pantev C. Determination of activation areas in the human auditory cortex by means of synthetic aperture magnetometry. Neuroimage. 2003;20(2):995–1005.

Herrmann B, Maess B, Hasting AS, Friederici AD. Localization of the syntactic mismatch negativity in the temporal cortex: an MEG study. Neuroimage. 2009;48(3):590–600.

Hinkley LB, Vinogradov S, Guggisberg AG, Fisher M, Findlay AM, Nagarajan SS. Clinical symptoms and alpha band resting-state functional connectivity imaging in patients with schizophrenia: implications for novel approaches to treatment. Biol Psychiatry. 2011;70(12):1134–42.

Hirano Y, Hirano S, Maekawa T, Obayashi C, Oribe N, Monji A, et al. Auditory gating deficit to human voices in schizophrenia: a MEG study. Schizophr Res. 2010;117(1):61–7.

Hirvonen J, Wibral M, Palva JM, Singer W, Uhlhaas P, Palva S. Whole-brain source-reconstructed MEG-data reveal reduced long-range synchronization in chronic schizophrenia. eNeuro. 2017;4:ENEURO.0338-17.

Hoogenboom N, Schoffelen J-M, Oostenveld R, Parkes LM, Fries P. Localizing human visual gamma-band activity in frequency, time and space. Neuroimage. 2006;29(3):764–73.

Howells FM, Temmingh HS, Hsieh JH, van Dijen AV, Baldwin DS, Stein DJ. Electroencephalographic delta/alpha frequency activity differentiates psychotic disorders: a study of schizophrenia, bipolar disorder and methamphetamine-induced psychotic disorder. Transl Psychiatry. 2018;8(1):75.

Ikezawa K, Ishii R, Iwase M, Kurimoto R, Canuet L, Takahashi H, et al. Decreased alpha event-related synchronization in the left posterior temporal cortex in schizophrenia: a magnetoencephalography-beamformer study. Neurosci Res. 2011;71(3):235–43.

Ishii R, Shinosaki K, Ikejiri Y, Ukai S, Yamashita K, Iwase M, et al. Theta rhythm increases in left superior temporal cortex during auditory hallucinations in schizophrenia: a case report. Neuroreport. 2000;11(14):3283–7.

Javitt DC. Sensory processing in schizophrenia: neither simple nor intact. Schizophr Bull. 2009;35(6):1059–64.

Jeon YW, Polich J. Meta-analysis of P300 and schizophrenia: patients, paradigms, and practical implications. Psychophysiology. 2003;40(5):684–701.

Kähkönen S, Ahveninen J, Jääskeläinen IP, Kaakkola S, Näätänen R, Huttunen J, et al. Effects of haloperidol on selective attention a combined whole-head MEG and high-resolution EEG study. Neuropsychopharmacology. 2001;25(4):498.

Kang SS, MacDonald AW, Chafee MV, Im C-H, Bernat EM, Davenport ND, et al. Abnormal cortical neural synchrony during working memory in schizophrenia. Clin Neurophysiol. 2018;129(1):210–21.

Kasai K, Yamada H, Kamio S, Nakagome K, Iwanami A, Fukuda M, et al. Neuromagnetic correlates of impaired automatic categorical perception of speech sounds in schizophrenia. Schizophr Res. 2003;59(2):159–72.

Kim JS, Shin KS, Jung WH, Kim SN, Kwon JS, Chung CK. Power spectral aspects of the default mode network in schizophrenia: an MEG study. BMC Neurosci. 2014;15(1):104.

Kircher TT, Rapp A, Grodd W, Buchkremer G, Weiskopf N, Lutzenberger W, et al. Mismatch negativity responses in schizophrenia: a combined fMRI and whole-head MEG study. Am J Psychiatry. 2004;161(2):294–304.

Kissler J, Müller MM, Fehr T, Rockstroh B, Elbert T. MEG gamma band activity in schizophrenia patients and

healthy subjects in a mental arithmetic task and at rest. Clin Neurophysiol. 2000;111(11):2079–87.

Koh Y, Shin KS, Kim JS, Choi J-S, Kang D-H, Jang JH, et al. An MEG study of alpha modulation in patients with schizophrenia and in subjects at high risk of developing psychosis. Schizophr Res. 2011;126(1):36–42.

Kwon JS, O'donnell BF, Wallenstein GV, Greene RW, Hirayasu Y, Nestor PG, et al. Gamma frequency–range abnormalities to auditory stimulation in schizophrenia. Arch Gen Psychiatry. 1999;56(11):1001–5.

Light GA, Braff DL. Mismatch negativity deficits are associated with poor functioning in schizophrenia patients. Arch Gen Psychiatry. 2005;62(2):127–36.

Light GA, Näätänen R. Mismatch negativity is a breakthrough biomarker for understanding and treating psychotic disorders. Proc Natl Acad Sci. 2013;110(38):15175–6.

Lijffijt M, Lane SD, Meier SL, Boutros NN, Burroughs S, Steinberg JL, et al. P50, N100, and P200 sensory gating: relationships with behavioral inhibition, attention, and working memory. Psychophysiology. 2009;46(5):1059–68.

Liu J, Harris A, Kanwisher N. Stages of processing in face perception: an MEG study. Nat Neurosci. 2002;5(9):910.

Maharajh K, Teale P, Rojas DC, Reite ML. Fluctuation of gamma-band phase synchronization within the auditory cortex in schizophrenia. Clin Neurophysiol. 2010;121(4):542–8.

Maran M, Grent T, Uhlhaas PJ. Electrophysiological insights into connectivity anomalies in schizophrenia: a systematic review. Neuropsychiatr Electrophysiol. 2016;2(1):6.

McCleery A, Lee J, Joshi A, Wynn JK, Hellemann GS, Green MF. Meta-analysis of face processing event-related potentials in schizophrenia. Biol Psychiatry. 2015;77(2):116–26.

McDonald CR, Thesen T, Carlson C, Blumberg M, Girard HM, Trongnetrpunya A, et al. Multimodal imaging of repetition priming: using fMRI, MEG, and intracranial EEG to reveal spatiotemporal profiles of word processing. Neuroimage. 2010;53(2):707–17.

Mima T, Hallett M. Electroencephalographic analysis of cortico-muscular coherence: reference effect, volume conduction and generator mechanism. Clin Neurophysiol. 1999;110(11):1892–9.

Mooney C, Ferguson GA. A new closure test. Can J Psychol. 1951;5(3):129–33.

Muthukumaraswamy SD, Singh KD. Visual gamma oscillations: the effects of stimulus type, visual field coverage and stimulus motion on MEG and EEG recordings. Neuroimage. 2013;69:223–30.

Näätänen R. The mismatch negativity: a powerful tool for cognitive neuroscience. Ear Hear. 1995;16(1):6–18.

Näätänen R, Kähkönen S. Central auditory dysfunction in schizophrenia as revealed by the mismatch negativity (MMN) and its magnetic equivalent MMNm: a review. Int J Neuropsychopharmacol. 2009;12(1):125–35.

O'Donnell BF, Vohs JL, Krishnan GP, Rass O, Hetrick WP, Morzorati SL. The auditory steady-state response (ASSR): a translational biomarker for schizophrenia. Supplements to Clinical neurophysiology, vol. 62. Amsterdam: Elsevier; 2013. p. 101–12.

Pantev C, Roberts LE, Elbert T, Roβ B, Wienbruch C. Tonotopic organization of the sources of human auditory steady-state responses. Hear Res. 1996;101(1-2):62–74.

Patterson JV, Hetrick WP, Boutros NN, Jin Y, Sandman C, Stern H, et al. P50 sensory gating ratios in schizophrenics and controls: a review and data analysis. Psychiatry Res. 2008;158(2):226–47.

Polich J, Kok A. Cognitive and biological determinants of P300: an integrative review. Biol Psychol. 1995;41(2):103–46.

Popov T, Jordanov T, Weisz N, Elbert T, Rockstroh B, Miller GA. Evoked and induced oscillatory activity contributes to abnormal auditory sensory gating in schizophrenia. Neuroimage. 2011a;56(1):307–14.

Popov T, Jordanov T, Rockstroh B, Elbert T, Merzenich MM, Miller GA. Specific cognitive training normalizes auditory sensory gating in schizophrenia: a randomized trial. Biol Psychiatry. 2011b;69(5):465–71.

Popov T, Rockstroh B, Weisz N, Elbert T, Miller GA. Adjusting brain dynamics in schizophrenia by means of perceptual and cognitive training. PLoS One. 2012;7(7):e39051.

Popov TG, Rockstroh BS, Popova P, Carolus AM, Miller GA. Dynamics of alpha oscillations elucidate facial affect recognition in schizophrenia. Cogn Affect Behav Neurosci. 2014;14(1):364–77.

Popov TG, Carolus A, Schubring D, Popova P, Miller GA, Rockstroh BS. Targeted training modifies oscillatory brain activity in schizophrenia patients. NeuroImage Clin. 2015;7:807–14.

Popova P, Popov TG, Wienbruch C, Carolus AM, Miller GA, Rockstroh BS. Changing facial affect recognition in schizophrenia: effects of training on brain dynamics. NeuroImage Clin. 2014;6:156–65.

Recasens M, Leung S, Grimm S, Nowak R, Escera C. Repetition suppression and repetition enhancement underlie auditory memory-trace formation in the human brain: an MEG study. Neuroimage. 2015;108:75–86.

Recasens M, Gross J, Uhlhaas PJ. Low-frequency oscillatory correlates of auditory predictive processing in cortical-subcortical networks: a MEG-study. Sci Rep. 2018;8(1):14007.

Rivolta D, Castellanos NP, Stawowsky C, Helbling S, Wibral M, Grützner C, et al. Source-reconstruction of event-related fields reveals hyperfunction and hypofunction of cortical circuits in antipsychotic-naive, first-episode schizophrenia patients during Mooney face processing. J Neurosci. 2014;34(17):5909–17.

Rojas DC. Review of schizophrenia research using MEG. In: Magnetoencephalography. Berlin: Springer; 2014. p. 849–74.

Rosburg T, Boutros NN, Ford JM. Reduced auditory evoked potential component N100 in schizophrenia—a critical review. Psychiatry Res. 2008;161(3):259–74.

Roux F, Uhlhaas PJ. Working memory and neural oscillations: alpha–gamma versus theta–gamma codes for distinct WM information? Trends Cogn Sci. 2014;18(1):16–25.

Roux F, Wibral M, Singer W, Aru J, Uhlhaas PJ. The phase of thalamic alpha activity modulates cortical gamma-band activity: evidence from resting-state MEG recordings. J Neurosci. 2013;33(45):17827–35.

Rutter L, Carver FW, Holroyd T, Nadar SR, Mitchell-Francis J, Apud J, et al. Magnetoencephalographic gamma power reduction in patients with schizophrenia during resting condition. Hum Brain Mapp. 2009;30(10):3254–64.

Sauer A, Zeev-Wolf M, Grent-t'-Jong T, Recasens M, Wacongne C, Wibral M, et al. Impairment in predictive processes during auditory mismatch negativity in Scz: evidence from event-related fields. Hum Brain Mapp. 2017;38(10):5082–93.

Schoffelen JM, Gross J. Source connectivity analysis with MEG and EEG. Hum Brain Mapp. 2009;30(6):1857–65.

Schubring D, Popov T, Miller GA, Rockstroh B. Consistency of abnormal sensory gating in first-admission and chronic schizophrenia across quantification methods. Psychophysiology. 2018;55(4):e13006.

Shergill SS, Samson G, Bays PM, Frith CD, Wolpert DM. Evidence for sensory prediction deficits in schizophrenia. Am J Psychiatry. 2005;162(12):2384–6.

Shimano S, Onitsuka T, Oribe N, Maekawa T, Tsuchimoto R, Hirano S, et al. Preattentive dysfunction in patients with bipolar disorder as revealed by the pitch-mismatch negativity: a magnetoencephalography (MEG) study. Bipolar Disord. 2014;16(6):592–9.

Shin KS, Kim JS, Kim SN, Koh Y, Jang JH, An SK, et al. Aberrant auditory processing in schizophrenia and in subjects at ultra-high-risk for psychosis. Schizophr Bull. 2011;38(6):1258–67.

Shin KS, Jung WH, Kim JS, Jang JH, Hwang JY, Chung CK, et al. Neuromagnetic auditory response and its relation to cortical thickness in ultra-high-risk for psychosis. Schizophr Res. 2012;140(1-3):93–8.

Siegel M, Donner TH, Engel AK. Spectral fingerprints of large-scale neuronal interactions. Nat Rev Neurosci. 2012;13(2):121–34.

Siekmeier PJ, Stufflebeam SM. Patterns of spontaneous magnetoencephalographic activity in schizophrenic patients. J Clin Neurophysiol. 2010;27(3):179–90.

Singer W. Neuronal synchrony: a versatile code for the definition of relations? Neuron. 1999;24(1):49–65.

Spencer KM, Nestor PG, Niznikiewicz MA, Salisbury DF, Shenton ME, McCarley RW. Abnormal neural synchrony in schizophrenia. J Neurosci. 2003;23(19):7407–11.

Spencer KM, Nestor PG, Perlmutter R, Niznikiewicz MA, Klump MC, Frumin M, et al. Neural synchrony indexes disordered perception and cognition in schizophrenia. Proc Natl Acad Sci. 2004;101(49):17288–93.

Sperling W, Martus P, Kober H, Bleich S, Kornhuber J. Spontaneous, slow and fast magnetoencephalographic activity in patients with schizophrenia. Schizophr Res. 2002;58(2-3):189–99.

Sun L, Castellanos N, Grützner C, Koethe D, Rivolta D, Wibral M, et al. Evidence for dysregulated high-frequency oscillations during sensory processing in medication-naïve, first episode schizophrenia. Schizophr Res. 2013;150(2-3):519–25.

Takei Y, Kumano S, Maki Y, Hattori S, Kawakubo Y, Kasai K, et al. Preattentive dysfunction in bipolar disorder: a MEG study using auditory mismatch negativity. Progr Neuro-Psychopharmacol Biolsychiatry. 2010;34(6):903–12.

Tan H-RM, Lana L, Uhlhaas PJ. High-frequency neural oscillations and visual processing deficits in schizophrenia. Front Psychol. 2013;4:621.

Teale P, Collins D, Maharajh K, Rojas DC, Kronberg E, Reite M. Cortical source estimates of gamma band amplitude and phase are different in schizophrenia. Neuroimage. 2008;42(4):1481–9.

Thoma RJ, Hanlon FM, Moses SN, Edgar JC, Huang M, Weisend MP, et al. Lateralization of auditory sensory gating and neuropsychological dysfunction in schizophrenia. Am J Psychiatry. 2003;160(9):1595–605.

Thoma RJ, Hanlon FM, Moses SN, Ricker D, Huang M, Edgar C, et al. M50 sensory gating predicts negative symptoms in schizophrenia. Schizophr Res. 2005;73(2-3):311–8.

Thuné H, Recasens M, Uhlhaas PJ. The 40-Hz auditory steady-state response in patients with schizophrenia: a meta-analysis. JAMA Psychiat. 2016;73(11):1145–53.

Tiitinen H, Alho K, Huotilainen M, Ilmoniemi RJ, Simola J, Näätänen R. Tonotopic auditory cortex and the magnetoencephalographic (MEG) equivalent of the mismatch negativity. Psychophysiology. 1993;30(5):537–40.

Troebinger L, López JD, Lutti A, Bradbury D, Bestmann S, Barnes G. High precision anatomy for MEG. Neuroimage. 2014;86:583–91.

Tsuchimoto R, Kanba S, Hirano S, Oribe N, Ueno T, Hirano Y, et al. Reduced high and low frequency gamma synchronization in patients with chronic schizophrenia. Schizophr Res. 2011;133(1-3):99–105.

Uhlhaas PJ, Silverstein SM. Perceptual organization in schizophrenia spectrum disorders: empirical research and theoretical implications. Psychol Bull. 2005;131(4):618–32.

Uhlhaas PJ, Singer W. Abnormal neural oscillations and synchrony in schizophrenia. Nat Rev Neurosci. 2010;11(2):100–13.

Uhlhaas PJ, Pipa G, Neuenschwander S, Wibral M, Singer W. A new look at gamma? High-(> 60 Hz) γ-band activity in cortical networks: function, mechanisms and impairment. Prog Biophys Mol Biol. 2011;105(1-2):14–28.

Uhlhaas PJ, Liddle P, Linden DE, Nobre AC, Singh KD, Gross J. Magnetoencephalography as a tool in psychiatric research: current status and perspective. Biol Psychiatry Cognit Neurosci Neuroimaging. 2017;2(3):235–44.

Umbricht D, Krljes S. Mismatch negativity in schizophrenia: a meta-analysis. Schizophr Res. 2005;76(1):1–23.

Van Diessen E, Numan T, Van Dellen E, Van Der Kooi A, Boersma M, Hofman D, et al. Opportunities and methodological challenges in EEG and MEG resting state functional brain network research. Clin Neurophysiol. 2015;126(8):1468–81.

Van Lutterveld R, Sommer IE, Ford JM. The neurophysiology of auditory hallucinations–a historical and contemporary review. Front Psych. 2011;2:28.

van Lutterveld R, Hillebrand A, Diederen KM, Daalman K, Kahn RS, Stam CJ, et al. Oscillatory cortical network involved in auditory verbal hallucinations in schizophrenia. PLoS One. 2012;7(7):e41149.

Vierling-Claassen D, Siekmeier P, Stufflebeam S, Kopell N. Modeling GABA alterations in schizophrenia: a link between impaired inhibition and altered gamma and beta range auditory entrainment. J Neurophysiol. 2008;99(5):2656–71.

Vistoli D, Passerieux C, Houze B, Hardy-Baylé M-C, Brunet-Gouet E. Neural basis of semantic priming in schizophrenia during a lexical decision task: a magneto-encephalography study. Schizophr Res. 2011a;130(1-3):114–22.

Vistoli D, Brunet-Gouet E, Lemoalle A, Hardy-Baylé M-C, Passerieux C. Abnormal temporal and parietal magnetic activations during the early stages of theory of mind in schizophrenic patients. Soc Neurosci. 2011b;6(3):316–26.

Vorwerk J, Cho J-H, Rampp S, Hamer H, Knösche TR, Wolters CH. A guideline for head volume conductor modeling in EEG and MEG. Neuroimage. 2014;100:590–607.

Wacongne C, Changeux J-P, Dehaene S. A neuronal model of predictive coding accounting for the mismatch negativity. J Neurosci. 2012;32(11):3665–78.

Wang Y, Jia Y, Feng Y, Zhong S, Xie Y, Wang W, et al. Overlapping auditory M100 and M200 abnormalities in schizophrenia and bipolar disorder: a MEG study. Schizophr Res. 2014;160(1):201–7.

Wienbruch C, Moratti S, Elbert T, Vogel U, Fehr T, Kissler J, et al. Source distribution of neuromagnetic slow wave activity in schizophrenic and depressive patients. Clin Neurophysiol. 2003;114(11):2052–60.

Williams TJ, Nuechterlein KH, Subotnik KL, Yee CM. Distinct neural generators of sensory gating in schizophrenia. Psychophysiology. 2011;48(4):470–8.

Wilson TW, Hernandez OO, Asherin RM, Teale PD, Reite ML, Rojas DC. Cortical gamma generators suggest abnormal auditory circuitry in early-onset psychosis. Cereb Cortex. 2007;18(2):371–8.

Yamasue H, Yamada H, Yumoto M, Kamio S, Kudo N, Uetsuki M, et al. Abnormal association between reduced magnetic mismatch field to speech sounds and smaller left planum temporale volume in schizophrenia. Neuroimage. 2004;22(2):720–7.

Yáñez-Téllez G, Rodríguez-Agudelo Y. Mismatch negativity (MMN) and schizophrenia: a revision. Actas Esp Psiquiatr. 2011;39(6):363–73.

Zeev-Wolf M, Levy J, Jahshan C, Peled A, Levkovitz Y, Grinshpoon A, et al. MEG resting-state oscillations and their relationship to clinical symptoms in schizophrenia. NeuroImage Clin. 2018;20:753–61.

13 EEG Connectivity Pattern: A Window into the Schizophrenia Mind?

Saskia Steinmann, Guido Nolte, and Christoph Mulert

Contents

13.1 Introduction

Schizophrenia (SZ) is a chronic and severe mental disorder that affects approximately 1% of the general population and is characterized by a set of symptoms, including positive/psychotic symptoms (e.g., hallucinations and delusions), negative symptoms (e.g., thought disorder and loss of motivation), and cognitive symptoms (e.g., impairment of memory and attention). Since 1980, advances in neuroimaging and neurophysiological techniques have led to tremendous progress in understanding SZ associated neurophysiological alterations of several cortical and subcortical regions. Evidence of such studies has shown that the brain—as one of the most complex organs in the human body—is a self-organized, highly-connected neuronal network, where different specialized brain regions have to communicate

S. Steinmann
Psychiatry Neuroimaging Branch, Department of Psychiatry and Psychotherapy, University Medical Center Hamburg-Eppendorf, Hamburg, Germany
e-mail: s.steinmann@uke.de

G. Nolte
Department of Neurophysiology and Pathophysiology, University Medical Center Hamburg-Eppendorf, Hamburg, Germany
e-mail: g.nolte@uke.de

C. Mulert (✉)
Centre for Psychiatry and Psychotherapy, Justus-Liebig-University, Giessen, Germany

Psychiatry Neuroimaging Branch, Personality Disorder Unit, Department of Psychiatry and Psychotherapy, University Medical Center Hamburg-Eppendorf, Hamburg, Germany
e-mail: Christoph.Mulert@psychiat.med.uni-giessen.de, c.mulert@uke.de

M. Kubicki, M. E. Shenton (eds.), *Neuroimaging in Schizophrenia*,
https://doi.org/10.1007/978-3-030-35206-6_13

and interact to enable every cognitive, emotional, motivational, and perceptual behaviour. As a consequence, a growing literature has focused on the so-called disconnection hypothesis (Friston 1998), suggesting that a disturbed interaction and integration among these neuronal dynamic systems (Uhlhaas 2013) lead to altered information processing, and to the occurrence of SZ symptoms (Spencer 2009).

In particular, EEG—a non-invasive electrophysiological monitoring method with a millisecond-range temporal resolution—provides, through placing electrodes on the scalp, a direct measurement of whole-brain electrical activity, known as oscillations. These oscillations are periodic components of time series characterized by their frequency, amplitude, and phase (see glossary in Table 13.1). Traditionally, neural oscillations have been clustered into frequency bands, including delta (1–3 Hz), theta (4–7 Hz), alpha (8–12 Hz), beta (13–30 Hz), and gamma (>30 Hz), as well as finer subdivisions within each band (Buzsaki and Watson 2012). Such coordinated brain oscillations are considered to play key roles in neural communication, integration, and computation, and therefore offer an exceptional window into the dynamics of healthy and disturbed brain function. In recent years, a substantial effort has been directed toward elucidating the role of coherence and synchronization of oscillations for estimation of functional connectivity between neural populations. For instance, long-distance connectivity preferentially has been observed at slower rhythms (theta, alpha, and beta), while short-distance connectivity tends to occur at higher frequencies (gamma) (Uhlhaas et al. 2010). The kind of measure applied to estimate such patterns depends on the data and the question of interest. A multitude of methods have been incorporated, varying from linear and non-linear, bivariate and multivariate, phase and amplitude, to directed and undirected measures. Throughout this review, measures of neuronal interactions are described using the terms *connectivity, coupling*, and *synchronization,* interchangeably.

The purpose of this chapter is to introduce the reader to the state-of-the-art EEG tools used to measure dynamical connectivity in both sensory/cognitive tasks and the resting-state, with an emphasis on those approaches applied in psychiatric research elucidating the pathophysiological mechanism underlying SZ symptoms. The chapter starts with the most common analytical approaches used for examining functional brain connectivity, followed by the presentation of those approaches addressing the direction of information flow between neural systems, without claim to completeness (see Table 13.1). This chapter concludes by a short résumé of the current state-of-knowledge of altered connectivity pattern in SZ.

Table 13.1 Glossary and most popular measures to assess connectivity in schizophrenia research

Measure	Description
Frequency	The number of cycles of a wave per second, measured in Hertz (Hz)
Amplitude	The magnitude of an oscillation in a signal, measured in microvolts (μV)
Phase	The periodic angle of the oscillatory cycle, measured in degrees from 0 to 360 or radians (rad)
Resting-state microstates	A measure of prototypical topographies (states) of electric field potentials recorded from all electrodes over the scalp
Coherence (Coh)	A measure of covariation in the amplitude and phase of two signals
Phase Locking Value (PLV)	A measures of the covariation in the phase of two signals
Phase Lag Index (PLI)	A measure of the asymmetric distribution of phase differences between two signals
Phase-Amplitude Coupling (PAC)	A measure of statistical dependence between the phase of a low-frequency oscillation and the amplitude (or power) of a high-frequency oscillation
Lagged Phase Synchronization (LPS)	A measure of phase synchrony between two time series related to coherence
Granger Causality (GC)	Estimates the directed information flow between two time series through predicting the course of activation in another cortical area

13.2 Functional Connectivity

13.2.1 Microstate Analysis

One analytical approach to extract information from the EEG signal is termed ***Microstate Analysis***, in which distinct states are defined by prototypical topographies of electric field potentials recorded from all electrodes over the scalp (Lehmann et al. 1987). Such microstates remain stable for 60–120 ms before rapidly transitioning into another microstate, and are considered to reflect the momentary functional state with its millisecond by millisecond interactions of large-scale neuronal networks (Koenig et al. 2002). Accordingly, it is assumed that specific microstate time series are generated by coordinated activity of neural ensembles, and thus different microstates presumably organize different brain functions—leading to the hypothesis that they constitute the "atoms of thought" (Lehmann et al. 1998). Technically, microstates are calculated as the global field power (GFP), which is the root of the mean of the squared potential differences at all *K* electrodes (i.e. *Vi(t)*) from the mean of instantaneous potentials across all electrodes over the scalp (i.e. *Vmean(t)*) (Lehmann and Skrandies 1980).

In the past, analysis was focussed on the alpha frequency band (8–12 Hz), while nowadays larger frequency bands from 2 to 20 Hz (Koenig et al. 2002), 1 to 40 Hz (Van de Ville et al. 2010), or 1 to 50 Hz (Khanna et al. 2014) are used. The parameters of interest considered to influence the frequency, the duration, and the syntax (i.e., chronological order) of microstates have been, for instance, age, medication, and specific neurocognitive or neuropsychiatric conditions. Microstate topographies are mostly clustered into four typical resting-state configurations (labelled a–d, see Fig. 13.1), which are very reliable within and between healthy subjects across the entire life span (Andreou et al. 2014b; Kindler et al. 2011; Koenig et al. 2002). Using simultaneous EEG-fMRI, it has been shown that those classes correspond to well-known fMRI resting-state networks (Britz et al. 2010; Musso et al. 2010; Yuan et al. 2012): [A] a network consisting of superior and middle temporal areas involved in phonological processing, [B] a visual network consisting of bilateral extrastriate areas, [C] an insular-cingulate network thought to be involved in own-body representation, and [D] a right-lateralized fronto-parietal network associated with attention.

Interestingly, deviances from these four classes have been described in drug–naive patients with SZ, in those who experience their first episode (FES) (Irisawa et al. 2006; Kikuchi et al. 2007; Lehmann et al. 2005; Merrin et al. 1990; Nishida et al. 2013; Strelets et al. 2003), in individuals with an at-risk mental state (ARMS) (Andreou et al. 2014a; Tomescu et al. 2014), as well as in patients with specific symptoms such as auditory-verbal hallucinations (AVH) (Kindler et al. 2011). In particular, shortened duration of the microstate B and D and increased occurrence of A and C were reported in acutely ill patients compared to healthy controls (Andreou et al. 2014a; Koenig et al. 1999; Lehmann et al. 2005; Nishida et al. 2013; Rieger et al. 2016; Strelets et al. 2003). It is suggested that such abnormal microstates in patients reflect a breakdown of normal network activities in the brain, leading to psychotic experiences. In line with that, successful antipsychotic treatment has been shown to normalize the pattern of microstate C and D (Kikuchi et al. 2007), while intensive repetitive Transcranial Magnet Stimulation (TMS) over the left dorsolateral prefrontal cortex (DLPFC) decreased the occurrence of C in patients who responded to treatment (Sverak et al. 2017). However, it is not clear whether these deviant microstates mirror the state of the brain during the psychotic experience, or a trait that predispose the individual to such experiences. Moreover, questions such as the number of microstate and how to define them are still a matter of research and debate.

13.2.2 Coherence and 1:1 Phase Locking Value (PLV)

Among the most frequently used functional connectivity measures defined in the frequency domain, ***Coherence*** between two EEG-channels

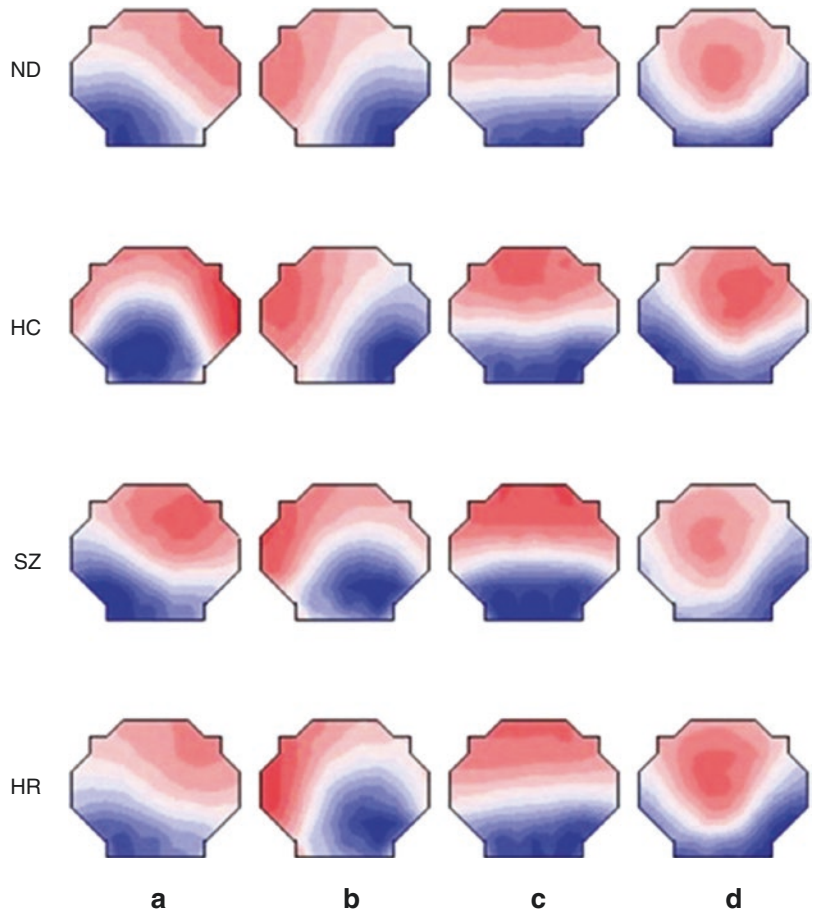

Fig. 13.1 Spatial configuration of the four microstate classes (**a**–**d**) in normative data (ND), in patients with schizophrenia (SZ), in high-risk individuals (HR), and healthy controls (HC). Head seen from above, nose up; red positive, blue negative potential areas. (After Andreou et al. 2014a)

is probably the simplest and most popular approach (Nunez et al. 1997). Oscillations are defined though their frequency, phase and amplitude. Coherence essentially measures the phase coupling of two channels. If $x_{nk}(f)$ is the Fourier transforms of the time series k of n channels, then

$$S_{nm}(f) = \frac{1}{K}\sum_{k=1}^{K} x_{nk}(f)\, x^{*}_{mk}(f)$$

is the (estimated) cross-spectrum, which is calculated analogously to a covariance matrix, but here in the frequency domain. The (complex) coherence $C_{nm}(f)$ corresponds to a correlation and is defined as

$$C_{nm}(f) = \frac{S_{nm}(f)}{\left(S_{nn}(f) S_{mm}(f)\right)^{1/2}}$$

Another related method of detecting frequency-specific phase coupling between two signals is called ***1:1 Phase Locking Value (PLV)*** (Lachaux et al. 1999). In this case, for each time segment, the signals are first windowed (for example with a Hanning window) and then Fourier-transformed. If the phase of the Fourier coefficients at the frequency f denotes the signal n of the segment k, then 1:1 PLV is defined as

$$PLV_{nm}(f) = \frac{1}{K}\sum_{k=1}^{K} \exp\left(i\left(\Phi_{nk}(f) - \Phi_{mk}(f)\right)\right)$$

Thus, while coherence measures both the dependence of the amplitude and the phase, PLV only estimates variations of the phase differences, regardless of amplitude. However, despite the conceptual differences between coherence and PLV, there are hardly any differences within the

results. Both measures determine values between zero and 1, with a value of zero indicating that the processes are linearly independent, and a value of 1 means a complete connection. The only difference between coherence and PLV is the meaning of a 'complete connection'. While for PLV a value of 1 indicates a constant phase difference across the segments, coherence assumes the same value if the frequency-specific signals are linearly related, thus, $x_{ik}(f) = ax_{jk}(f)$ for two channels i, j with a complex constants a.

A considerable body of work using EEG over the last 20 years has identified altered coherence and PLV at both low and high frequencies in SZ (Bachiller et al. 2015; Olejarczyk and Jernajczyk 2017; Spencer et al. 2009; Thune et al. 2016; Uhlhaas and Singer 2010), emphasizing that cognitive deficits and certain clinical symptoms arise from a disturbance of neuronal dynamics. For instance, patients with SZ showed reduced delta and theta coherence over left frontal lobes during resting-state (Tauscher et al. 1998), a reduction of interhemispheric alpha coherence during frontal lobe tasks (Morrison-Stewart et al. 1996), as well as reduced fronto-temporal theta coherence during talking in particularly hallucinating patients (Ford et al. 2002).

Furthermore, frontal theta oscillations—consistently found to originate in the anterior cingulate cortex (ACC) (Tsujimoto et al. 2006)—have been repeatedly shown to be associated with working memory (WM) processing, and thus are sensitive to task difficulty and prominent during maintenance and manipulation of information (Cavanagh and Frank 2014; Sauseng et al. 2005, 2010). In particular, it is suggested that a distinctive fronto-parietal theta network is substantially involved in executive control and manipulation of WM processes. Notably, WM deficits are among the first cognitive signs and the most common symptoms in the course of SZ (Forbes et al. 2009), and have been repeatedly seen in individuals prior to psychotic symptoms, in chronic patients (Reichenberg et al. 2010), and in first-degree relatives (Conklin et al. 2000). In line with that, PLV in the theta frequency range between a specific fronto-parietal network (i.e., executive control network/ACC—posterior parietal cortex) has been repeatedly found to be reduced in patients compared to healthy controls during performance of WM tasks (Berger et al. 2016; Griesmayr et al. 2014).

13.2.3 Cross-Frequency-Coupling (CFC)

Cross-frequency coupling (CFC) refers to the coupling between two oscillations of distinct frequencies and can be assessed as phase-amplitude coupling, phase-phase coupling, phase-frequency coupling, and amplitude-amplitude coupling (Hyafil et al. 2015). Most commonly used in research is the calculation of ***Phase-Amplitude Coupling (PAC),*** as it has been related to various functional roles including decision making, motivation, and memory (Schroeder and Lakatos 2009), and is based on plausible physiological mechanisms; low frequency phase reflects local neuronal excitability, while high frequency power increases reflect either a general increased number of coherently active neurons or the selective activation of a connected neuronal sub-network (Canolty and Knight 2010).

Briefly, PAC (also known as "nested oscillations") describes the statistical dependence between the phase of a low-frequency oscillation and the amplitude (or power) of a high-frequency oscillation of electrical brain activity. With the corresponding Hilbert transform of the bandpass filtered signals $x_\gamma(t)$ with the amplitude $A(t) = |x_\gamma(t)|$ or rather $x_\alpha(t) = |x_\alpha(t)| \exp(i\Phi_\varepsilon(t))$, the PAC can be defined as

$$PAC = \frac{\left| A(t) \exp\left(i\Phi_\alpha(t) \right)_t \right|}{N}$$

where N is a normalization. Thus, the phase of the lower frequency oscillation (e.g., theta band) is coupled to the power of the coupled higher frequency oscillation (e.g., gamma band), resulting in synchronization of the amplitude envelopes of faster rhythms with the phases of slower rhythms.

PAC has, in general, a poor frequency resolution and its calculation can be very time

consuming, in particular when calculated for all combinations of high and low frequencies, because for each choice of frequency pairs the raw data have to be filtered with a different filter. This can be avoided using bispectral analysis (Shahbazi Avarvand et al. 2018), which was shown to be formally equivalent to PAC if the amplitude of the high frequency signal is squared and the phase of the low frequency signal is weighted by its amplitude.

One of the best known examples occurs in the rodent hippocampus between the theta phase (4–7 Hz) and the gamma amplitude (30–100 Hz) (Buhl et al. 2003), and has also been demonstrated in humans (Canolty et al. 2006). Several studies of humans and animals have reported that the theta/gamma PAC plays an important role for information processing and integration (Demiralp et al. 2007; Kendrick et al. 2011; Voytek et al. 2010), for learning and memory formation (Mormann et al. 2005; Xu et al. 2013), and for multi-item WM performance (Axmacher et al. 2010; Rajji et al. 2017).

Notably, compared to healthy controls, reduced theta/gamma PAC has been observed in SZ patients during a Stroop colour interference task (Popov et al. 2015) and during WM performance (Barr et al. 2017). A more recent study demonstrated an impaired PAC of left-hemispheric auditory lateralization, consistent with the well-known abnormalities of the left hemispheric auditory cortex of SZ patients (Hirano et al. 2018). In contrast, one study revealed increased theta/gamma PAC during resting-state in drug-naïve patients, and suggested this deficit might be related to the compensatory hyper-arousal patterns of a dysfunctional default mode network (Won et al. 2017). Moreover, PAC has been shown to be intact during a 40-Hz auditory-steady-state stimulation, denoting it may contribute to higher-order cognitive tasks but not necessarily for passive tasks (Kirihara et al. 2012). While the above mentioned studies points toward altered theta/gamma PAC as a potential pathophysiological mechanism of disparate cognitive and functional impairments of SZ, future studies are necessary to assess the predictive utility of this approach.

While microstate-type connectivity, coherence, PLV, as well as CFC assumes simultaneity of activity among the involved signals without taking potential confounders of volume conduction into account, the next paragraph presents connectivity approaches with a solution to this problem.

13.2.4 Connectivity Measures with Correction for Volume Conduction

In recent years, a number of functional connectivity measures have been proposed that are all based on the same principle of addressing the so-called volume conduction (electric spread) effects. This approach is based on the notion that volume conduction of any active source contributes to the signals at all sensors and give rise to artificial signal correlations and, thus, to false conclusions of brain coupling. As a possible solution to this problem, the imaginary part of coherence can be analysed, which, if significant, cannot be explained by volume conduction (Nolte et al. 2004). The measures of ***Lagged Phase Synchronization (LPS)*** (Pascual-Marqui 2007b; Pascual-Marqui et al. 2011) and the ***Phase Lag Index (PLI)*** (Stam et al. 2007) are based upon the idea that the existence of consistent, nonzero phase lag between two time series cannot be explained by volume conduction from a single strong source, and therefore, renders true interactions between the underlying systems. Both LPS and PLI assume values between zero and 1, where zero indicates no coupling or coupling with phase difference centred at zero, and 1 indicates complete phase coupling.

If *C (f)* is the complex-valued coherence, ***Lagged Phase Synchronization (LPS)*** is defined as

$$LPS(f) = \frac{\left|Im\left(C(f)\right)\right|}{\sqrt{1-\left(\mathrm{Re}\left(C(f)\right)\right)^2}}$$

where *Re[C]* and *Im[C]* denote the real and imaginary parts of a complex number, *C*. We emphasize that the imaginary part of coherence is robust

to artifacts of volume conduction in the sense that a non-vanishing value cannot be explained as a mixing artifact of independent sources, and must be caused by coupled sources. However, the actual value still depends on how these sources are mapped into sensors. LPS has the nice features that for two coupled sources and in the absence of noise, the value is independent of the mixing. We consider this is a conceptual advantage, even though in practice the result are very similar.

LPS is provided by the LORETA software package, which is a discrete, three-dimensional (3D) distributed, linear, weighted minimum norm inverse solution that has the property of exact localization to test point sources (Pascual-Marqui 2007a). LPS measures the similarity between signals in the frequency domain based on normalized (unit module) Fourier transforms; thus it is related to nonlinear functional connectivity. The LPS measure represents the connectivity between two time series after the instantaneous, zero-lag contribution has been excluded. As mentioned above, such a correction is necessary when using scalp EEG signals or estimated intracranial signals (EEG tomography), because zero-lag connectivity in a given frequency band is often due to non-physiological effects or intrinsic physical artifacts, in particular volume conduction and low spatial resolution. Thus, this measure removes this confounding factor considerably and is thought to contain only physiological connectivity information.

Several EEG studies using LORETA source estimation and the LPS approach identified pathophysiological coupling mechanism across small-scale and large-scale brain networks in ARMS subjects (Ramyead et al. 2015), in drug-naïve FES (Ramyead et al. 2016), in chronic SZ patients (Di Lorenzo et al. 2015), and in those who experience AVH (Mulert et al. 2011; Steinmann et al. 2017). For instance, reduced resting-state functional connectivity was repeatedly found within the beta and the gamma frequency range, and further, either linked to illness duration (Di Lorenzo et al. 2015) or to high risk for SZ (Ramyead et al. 2015).

Furthermore, this approach was used to investigate the interhemispheric miscommunication theory suggesting that AVH occur due to disturbed functional and structural interhemispheric connectivity between bilateral speech-relevant brain areas (Curcic-Blake et al. 2017). Indeed, it has been shown that particularly those patients who suffer from AVH demonstrated increased interhemispheric gamma band synchrony between bilateral primary auditory cortices/Heschl's gyri (Mulert et al. 2011; Steinmann et al. 2017). Another pharmacological study used the LPS approach and Ketamine—an N-Methyl-D-Aspartate receptor (NMDAR) antagonist—to evaluate the effects of Ketamine on glutamate-related mechanisms underlying interhemispheric gamma band connectivity, conscious auditory perception during dichotic listening and the emergence of AVH, or auditory distortions in healthy volunteers (Thiebes et al. 2018). Gamma rhythms are dependent on the activity of parvalbumin (PV)-positive GABAergic cortical inhibitory interneurons, which are subject to glutamate NMDAR modulation from excitatory pyramidal cells (Traub et al. 1996). It is hypothesized that an excitatory-to-inhibitory (E/I) imbalance related to disturbed NMDAR functioning might be a possible mechanism underlying altered gamma band oscillations and the occurrence of AVH. In particular, as it has been shown that ketamine induce SZ-like symptoms in healthy controls (Krystal et al. 1994). In line with that, the results showed that ketamine induced positive symptoms such as hallucinations in a subgroup of healthy subjects. In addition, interhemispheric gamma band synchrony was found to be altered under ketamine compared to placebo, and particularly the subjects with auditory distortions under ketamine showed significantly higher interhemispheric gamma band connectivity than subjects without such distortions. This finding offered important insights into a relationship between NMDAR functioning, interhemispheric auditory gamma band synchrony, and the emergence of altered auditory perception, and argues for a possible role of glutamate in AVH.

The ***Phase Lag Index (PLI)*** approach, for two channels with Fourier coefficients $x(f,k)$ and $y(f,k)$ at frequency f in the kth segment, is defined as

$$PLI(f) = \left\langle sign\left(Im\left(x(f,k)\,y^{*}(f,k)\right)\right)\right\rangle_{k}$$

where *sign* denotes the sign of the argument and $\langle\cdot\rangle_k$ the average over all segments. The idea is to make the result as independent as possible of the size of the phase difference, by merely including the sign of the phase difference in the calculation. This is only partially accessible. Phases do disperse in the individual segments, and if the average phase difference is close to zero, relatively more single phases have the 'wrong' sign than with a large phase difference. Also, reducing the information for each trial to a sign leads to estimates which are statistically less stable than for related measures.

The PLI approach has also been selected to investigate disturbed functional connectivity pattern in SZ, albeit less frequently (Krukow et al. 2018; Takahashi et al. 2018; Yan et al. 2017). For instance, altered resting-state connectivity of the beta band across frontal regions and of the gamma band throughout the scalp has been described in drug–naive patients with SZ (Takahashi et al. 2018), while disturbed theta connectivity within the left PFC or within sensorimotor areas was found in FES, and related to impaired cognitive speed (Krukow et al. 2018). Summing up, the LPS, and to a lesser extent also the PLI, approach that estimate connectivity on the basis of source activity delivered converging evidence that oscillatory synchrony across several brain regions in different frequency bands is disturbed in SZ and linked to altered neurotransmission as well as specific cognitive and positive symptoms.

13.3 Causality: Effective/Directed Connectivity

While all connectivity measures presented so far were undirected and quantified with measures of statistical dependencies, such as correlations and coherence, effective/directed connectivity refers explicitly to the influence that one neural system exerts over another, either at a synaptic or population level (Friston 2011). The most widely accepted definition for directionality is based on the Granger's causality (G-causality) principle stating that the cause must both precede and help to predict the effect. The most popular approaches to effective connectivity are ***Granger Causality (GC)*** and ***Dynamic Causal Modelling (DCM)*** (Friston et al. 2003)**.**

The idea behind ***GC*** is that *X* causes *Y* if *X* contains information that helps to predict the future of *Y* better than information already in the past of *Y* (and in the past of other variables *Z*). In general, when this condition is satisfied one can say that information flows from *X* to *Y. GC* is based on linear vector autoregressive (VAR) models with the ability to characterize oscillatory and multivariate time series data, either at the source or sensor level (Barrett et al. 2010, 2012). Thus, GC determines the frequency-specific synchronization between neural populations and the directed propagation of their electrical activity. Although GC provides a powerful tool for describing observed data in terms of effective connectivity, only one study has examined neural circuity in SZ patients. The well-known WM deficits have been associated with reduced hemodynamic and electromagnetic activity and altered network connectivity spanning DLPFC, ACC, and the superior temporal cortex (STG) to the posterior cortex (Van Snellenberg et al. 2016). Based on this knowledge, effective connectivity was estimated via GC in a fronto-parietal network normally supporting WM performance in SZ patients compared to healthy controls (Kustermann et al. 2018). Results confirmed that SZ patients were characterized by a theta-specific temporal-to-posterior information flow, in contrast to bidirectional temporal-posterior communication in healthy controls.

Over the past decade, ***Dynamic Causal Modelling (DCM)***—originally developed for fMRI (Friston et al. 2003) and subsequently generalised to EEG (David et al. 2006; Kiebel et al. 2007)—has become the predominant way of characterising effective connectivity within networks of distributed neuronal responses. DCM can be defined by the following key features: first, DCMs use (linear or non-linear) differential equations for describing how dynamics in one

neuronal population cause dynamics in another, and how these interactions are modulated by experimental manipulations or endogenous brain activity. Second, DCMs use a biophysically informed and parameterized forward model to link the modelled neuronal dynamics to observed EEG responses. Third, DCMs are an explicit generative (Bayesian) autoregressive model; each parameter is constrained by a prior distribution, which reflects empirical knowledge about the range of possible parameter values, or principled considerations.

In contrast to GC, an increasing number of EEG studies used DCM to quantify the effective connectivity within and between specific networks in FES patients (Zheng et al. 2017), as well as in chronic SZ patients and their first-degree unaffected relatives (Diez et al. 2017; Fogelson et al. 2014; Ranlund et al. 2016). For example, a DCM analysis of medicated and unmediated FES patients during resting-state EEG revealed a reduced information flow from right medial frontal gyrus (MFG) to left STG in unmedicated FES relative to that in medicated FES. Notably, patients in the medicated group showed no difference with healthy controls. Moreover, the effective connections accompanied with modulation were improved when AVH diminished at early response of routine medication, indicating early drug response-related alterations in effective brain connectivity. Fogelson et al. (2014) used DCM of EEG responses of predictable and unpredictable visual targets to quantify the effective connectivity within and between cortical sources in the visual hierarchy. A striking loss of intrinsic connectivity modulation by stimulus predictability was found in occipital, temporal and parietal sources in patients during visual oddball detection. While controls were able to modulate ascending prediction errors, patients failed to adjust predictability in a context-dependent fashion, processing both predictable and unpredictable stimuli in the same way.

While GC models dependency among observed EEG responses, DCM models coupling among the hidden neural states generating observations. Despite this fundamental difference, the two approaches could be complementary, with GC detecting candidate models that could finally be verified via DCM analysis. Such a combination could facilitate the characterisation of brain circuits that may hold promise for the understanding and treatment of SZ pathophysiological circuits.

13.4 Conclusion

While it is impossible to describe all of the functional and effective connectivity measures in this review, we focussed on the methods that have been repeatedly used to investigate the pathophysiological coupling mechanism underlying SZ. The above body of work broadly supports the disconnectivity hypothesis of SZ (Friston 1998) stating that cognitive deficits (i.e., WM) and psychotic symptoms (i.e., AVH) emerge due to a disturbed interaction between distributed brain areas and corresponding altered coherence, and/or synchronization of oscillatory rhythms in neuronal large-scale networks.

Important achievements over the years were gained by studies that described higher cognitive deficits and developmental abnormalities already in childhood preceding adult schizophrenia (Reichenberg et al. 2010) and in first-degree unaffected relatives (Conklin et al. 2000). Hence, increasing evidence point out that SZ—as a neurodevelopmental disorder—is linked to neurophysiological alterations that are detectable before first manifestation of severe psychotic symptoms. Such a valuable biomarker for SZ are the well-known WM deficits which have been observed in all stages of SZ; the performance on WM tasks is regulated by NMDAR glutamatergic and GABAergic neurotransmission and depends on dopamine function in DLPFC. Given the numerous dopaminergic abnormalities found in SZ (Abi-Dargham et al. 2002; Slifstein et al. 2015) and the emerging evidence for a disruption in PFC (Zhou et al. 2015), in glutamate (Javitt 2007) as well as in GABA (Gonzalez-Burgos and Lewis 2012), altered WM representations in the DLPFC of patients with SZ seems clear, although the precise pathophysiological mechanism are still unknown.

In recent years, several EEG studies demonstrated that theta coupling between prefrontal and parietal brain regions plays a crucial role for memory functions, specifically for encoding and retrieval (Sato and Yamaguchi 2007; Sauseng et al. 2004; Summerfield and Mangels 2005), retention (Sarnthein et al. 1998), and executive control (Sauseng et al. 2005). It is said that this long-range communication underlies (top–down) executive control from frontal areas interacting with posterior information processing. There is also evidence for phase coupling between theta and gamma (around 40 Hz) during short-term memory processing (Schack et al. 2002). According to the theta/gamma coding hypothesis, it is suggested that a theta/gamma coding scheme may be used in the hippocampus and other cortical regions to encode multi-item short-term memory (Lisman and Buzsaki 2008). In detail, it is hypothesized that gamma oscillations encode items of information and theta phase order these items through modulation of gamma amplitude providing a "coding scheme" for WM.

Notably, decreased fronto-parietal theta coupling and impaired theta/gamma PAC was found in SZ patients and associated with impaired performance in WM tasks (Barr et al. 2017; Griesmayr et al. 2014). Furthermore, Berger et al. (2016) examined the fronto-parietal theta communication during a WM task with high central executive load in patients with predominantly negative symptoms, patients with predominantly positive symptoms, and healthy controls. Again, reduced theta coupling between a fronto-parietal executive network (ACC and posterior parietal regions) was found in all patients. Moreover, the negative symptomatic patient group displayed significantly stronger gamma power than the positive symptomatic group in the ACC during high-load conditions. This finding denotes that local frontal information processing represented by gamma oscillatory activity seems to be aberrant in SZ and might be a crucial indicator for different neural underpinnings of specific symptoms.

This is further supported by converging evidence of the crucial role of a microcircuit involving PV-positive GABAergic interneurons and glutamatergic pyramidal cells for the generation of gamma band oscillations (Sohal et al. 2009). Pharmacological or genetic models of SZ have shown that an NMDAR hypofunction of GABAergic interneurons produce an E/I imbalance that is thought to underlie prefrontal gamma band alterations (Gandal et al. 2012; Lisman et al. 2008). Further, subanestetic doses of ketamine—an NMDAR antagonist—elicit in healthy volunteers SZ-like symptoms, including some of the attentional and memory problems, (Krystal et al. 1994) as well as auditory verbal distortions, and AVH (Thiebes et al. 2018). Conversely, agents that modulate the glycine modulatory site on the NMDAR have been reported to reduce some of the cognitive deficits. Hence, an optimal balance of E/I in cortical circuits seems to be crucial for maintaining normal information processing. Today, the neurochemical view of SZ comprise both the dopamine and the glutamate hypothesis (Coyle 2006). Although we are still unravelling the mechanisms of information representation in the PFC, targeting glutamatergic transmission might be one potential key mechanism responsible for many of the PFC-dependant symptoms seen in SZ (Lisman 2012).

Summing up, the longitudinal monitoring of the brain's neurophysiological processes from risk, to prodrome, to first episode, to chronic SZ offer a promising diagnostic and disease treatment strategy. To achieve this goal, we further have to improve the applied methods to finally identify and establish reliable neurophysiological biomarkers that have potential for translation into clinical practice. So far, no "gold standard" of EEG connectivity approaches has yet emerged; each metric has different advantages and disadvantages, depending on the question of the research. However, the idea that synchronised temporal patterns between different neural populations carries information above and beyond the isolated activity of these groups has led to tremendous progress in understanding healthy and disturbed brain functions.

Summary

- Schizophrenia is characterized by deficits in local and long-range connectivity.
- Brain oscillations and their synchronization play a key role for neural communication and offer an exceptional window into the dynamics of healthy and disturbed brain function.
- EEG metrics hold promise for establishment of reliable neurophysiological biomarkers that have potential for translation into clinical practice.

References

Abi-Dargham A, Mawlawi O, Lombardo I, Gil R, Martinez D, Huang Y, Hwang DR, Keilp J, Kochan L, Van Heertum R, Gorman JM, Laruelle M. Prefrontal dopamine D1 receptors and working memory in schizophrenia. J Neurosci. 2002;22:3708–19.

Andreou C, Faber PL, Leicht G, Schoettle D, Polomac N, Hanganu-Opatz IL, Lehmann D, Mulert C. Resting-state connectivity in the prodromal phase of schizophrenia: insights from EEG microstates. Schizophr Res. 2014a;152:513–20.

Andreou C, Nolte G, Leicht G, Polomac N, Hanganu-Opatz IL, Lambert M, Engel AK, Mulert C. Increased resting-state gamma-band connectivity in first-episode schizophrenia. Schizophr Bull. 2014b;41:930–9.

Axmacher N, Henseler MM, Jensen O, Weinreich I, Elger CE, Fell J. Cross-frequency coupling supports multi-item working memory in the human hippocampus. Proc Natl Acad Sci U S A. 2010;107:3228–33.

Bachiller A, Poza J, Gomez C, Molina V, Suazo V, Hornero R. A comparative study of event-related coupling patterns during an auditory oddball task in schizophrenia. J Neural Eng. 2015;12:016007.

Barr MS, Rajji TK, Zomorrodi R, Radhu N, George TP, Blumberger DM, Daskalakis ZJ. Impaired theta-gamma coupling during working memory performance in schizophrenia. Schizophr Res. 2017;189:104–10.

Barrett AB, Barnett L, Seth AK. Multivariate Granger causality and generalized variance. Phys Rev E Stat Nonlin Soft Matter Phys. 2010;81:041907.

Barrett AB, Murphy M, Bruno MA, Noirhomme Q, Boly M, Laureys S, Seth AK. Granger causality analysis of steady-state electroencephalographic signals during propofol-induced anaesthesia. PLoS One. 2012;7:e29072.

Berger B, Minarik T, Griesmayr B, Stelzig-Schoeler R, Aichhorn W, Sauseng P. Brain oscillatory correlates of altered executive functioning in positive and negative symptomatic schizophrenia patients and healthy controls. Front Psychol. 2016;7:705.

Britz J, Van De Ville D, Michel CM. BOLD correlates of EEG topography reveal rapid resting-state network dynamics. Neuroimage. 2010;52:1162–70.

Buhl DL, Harris KD, Hormuzdi SG, Monyer H, Buzsaki G. Selective impairment of hippocampal gamma oscillations in connexin-36 knock-out mouse in vivo. J Neurosci. 2003;23:1013–8.

Buzsaki G, Watson BO. Brain rhythms and neural syntax: implications for efficient coding of cognitive content and neuropsychiatric disease. Dialogues Clin Neurosci. 2012;14:345–67.

Canolty RT, Knight RT. The functional role of cross-frequency coupling. Trends Cogn Sci. 2010;14:506–15.

Canolty RT, Edwards E, Dalal SS, Soltani M, Nagarajan SS, Kirsch HE, Berger MS, Barbaro NM, Knight RT. High gamma power is phase-locked to theta oscillations in human neocortex. Science. 2006;313:1626–8.

Cavanagh JF, Frank MJ. Frontal theta as a mechanism for cognitive control. Trends Cogn Sci. 2014;18:414–21.

Conklin HM, Curtis CE, Katsanis J, Iacono WG. Verbal working memory impairment in schizophrenia patients and their first-degree relatives: evidence from the digit span task. Am J Psychiatry. 2000;157:275–7.

Coyle JT. Glutamate and schizophrenia: beyond the dopamine hypothesis. Cell Mol Neurobiol. 2006;26:365–84.

Curcic-Blake B, Ford JM, Hubl D, Orlov ND, Sommer IE, Waters F, Allen P, Jardri R, Woodruff PW, David O, Mulert C, Woodward TS, Aleman A. Interaction of language, auditory and memory brain networks in auditory verbal hallucinations. Prog Neurobiol. 2017;148:1–20.

David O, Kiebel SJ, Harrison LM, Mattout J, Kilner JM, Friston KJ. Dynamic causal modeling of evoked responses in EEG and MEG. Neuroimage. 2006;30:1255–72.

Demiralp T, Bayraktaroglu Z, Lenz D, Junge S, Busch NA, Maess B, Ergen M, Herrmann CS. Gamma amplitudes are coupled to theta phase in human EEG during visual perception. Int J Psychophysiol. 2007;64:24–30.

Di Lorenzo G, Daverio A, Ferrentino F, Santarnecchi E, Ciabattini F, Monaco L, Lisi G, Barone Y, Di Lorenzo C, Niolu C, Seri S, Siracusano A. Altered resting-state EEG source functional connectivity in schizophrenia: the effect of illness duration. Front Hum Neurosci. 2015;9:234.

Diez A, Ranlund S, Pinotsis D, Calafato S, Shaikh M, Hall MH, Walshe M, Nevado A, Friston KJ, Adams RA, Bramon E. Abnormal frontoparietal synaptic gain mediating the P300 in patients with psychotic disorder and their unaffected relatives. Hum Brain Mapp. 2017;38:3262–76.

Fogelson N, Litvak V, Peled A, Fernandez-del-Olmo M, Friston K. The functional anatomy of schizophrenia: a dynamic causal modeling study of predictive coding. Schizophr Res. 2014;158:204–12.

Forbes NF, Carrick LA, McIntosh AM, Lawrie SM. Working memory in schizophrenia: a meta-analysis. Psychol Med. 2009;39:889–905.

Ford JM, Mathalon DH, Whitfield S, Faustman WO, Roth WT. Reduced communication between frontal and temporal lobes during talking in schizophrenia. Biol Psychiatry. 2002;51:485–92.

Friston KJ. The disconnection hypothesis. Schizophr Res. 1998;30:115–25.

Friston KJ. Functional and effective connectivity: a review. Brain Connect. 2011;1:13–36.

Friston KJ, Harrison L, Penny W. Dynamic causal modelling. Neuroimage. 2003;19:1273–302.

Gandal MJ, Edgar JC, Klook K, Siegel SJ. Gamma synchrony: towards a translational biomarker for the treatment-resistant symptoms of schizophrenia. Neuropharmacology. 2012;62:1504–18.

Gonzalez-Burgos G, Lewis DA. NMDA receptor hypofunction, parvalbumin-positive neurons, and cortical gamma oscillations in schizophrenia. Schizophr Bull. 2012;38:950–7.

Griesmayr B, Berger B, Stelzig-Schoeler R, Aichhorn W, Bergmann J, Sauseng P. EEG theta phase coupling during executive control of visual working memory investigated in individuals with schizophrenia and in healthy controls. Cogn Affect Behav Neurosci. 2014;14:1340–55.

Hirano S, Nakhnikian A, Hirano Y, Oribe N, Kanba S, Onitsuka T, Levin M, Spencer KM. Phase-amplitude coupling of the electroencephalogram in the auditory cortex in schizophrenia. Biol Psychiatry Cogn Neurosci Neuroimaging. 2018;3:69–76.

Hyafil A, Giraud AL, Fontolan L, Gutkin B. Neural cross-frequency coupling: connecting architectures, mechanisms, and functions. Trends Neurosci. 2015;38:725–40.

Irisawa S, Isotani T, Yagyu T, Morita S, Nishida K, Yamada K, Yoshimura M, Okugawa G, Nobuhara K, Kinoshita T. Increased omega complexity and decreased microstate duration in nonmedicated schizophrenic patients. Neuropsychobiology. 2006;54:134–9.

Javitt DC. Glutamate and schizophrenia: phencyclidine, N-methyl-D-aspartate receptors, and dopamine-glutamate interactions. Int Rev Neurobiol. 2007;78:69–108.

Kendrick KM, Zhan Y, Fischer H, Nicol AU, Zhang X, Feng J. Learning alters theta amplitude, theta-gamma coupling and neuronal synchronization in inferotemporal cortex. BMC Neurosci. 2011;12:55.

Khanna A, Pascual-Leone A, Farzan F. Reliability of resting-state microstate features in electroencephalography. PLoS One. 2014;9:e114163.

Kiebel SJ, Garrido MI, Friston KJ. Dynamic causal modelling of evoked responses: the role of intrinsic connections. Neuroimage. 2007;36:332–45.

Kikuchi M, Koenig T, Wada Y, Higashima M, Koshino Y, Strik W, Dierks T. Native EEG and treatment effects in neuroleptic-naive schizophrenic patients: time and frequency domain approaches. Schizophr Res. 2007;97:163–72.

Kindler J, Hubl D, Strik WK, Dierks T, Koenig T. Resting-state EEG in schizophrenia: auditory verbal hallucinations are related to shortening of specific microstates. Clin Neurophysiol. 2011;122:1179–82.

Kirihara K, Rissling AJ, Swerdlow NR, Braff DL, Light GA. Hierarchical organization of gamma and theta oscillatory dynamics in schizophrenia. Biol Psychiatry. 2012;71:873–80.

Koenig T, Lehmann D, Merlo MC, Kochi K, Hell D, Koukkou M. A deviant EEG brain microstate in acute, neuroleptic-naive schizophrenics at rest. Eur Arch Psychiatry Clin Neurosci. 1999;249:205–11.

Koenig T, Prichep L, Lehmann D, Sosa PV, Braeker E, Kleinlogel H, Isenhart R, John ER. Millisecond by millisecond, year by year: normative EEG microstates and developmental stages. Neuroimage. 2002;16:41–8.

Krukow P, Jonak K, Karakula-Juchnowicz H, Podkowinski A, Jonak K, Borys M, Harciarek M. Disturbed functional connectivity within the left prefrontal cortex and sensorimotor areas predicts impaired cognitive speed in patients with first-episode schizophrenia. Psychiatry Res Neuroimaging. 2018;275:28–35.

Krystal JH, Karper LP, Seibyl JP, Freeman GK, Delaney R, Bremner JD, Heninger GR, Bowers MB Jr, Charney DS. Subanesthetic effects of the noncompetitive NMDA antagonist, ketamine, in humans. Psychotomimetic, perceptual, cognitive, and neuroendocrine responses. Arch Gen Psychiatry. 1994;51:199–214.

Kustermann T, Popov T, Miller GA, Rockstroh B. Verbal working memory-related neural network communication in schizophrenia. Psychophysiology. 2018;55:e13088.

Lachaux JP, Rodriguez E, Martinerie J, Varela FJ. Measuring phase synchrony in brain signals. Hum Brain Mapp. 1999;8:194–208.

Lehmann D, Skrandies W. Reference-free identification of components of checkerboard-evoked multichannel potential fields. Electroencephalogr Clin Neurophysiol. 1980;48:609–21.

Lehmann D, Ozaki H, Pal I. EEG alpha map series: brain micro-states by space-oriented adaptive segmentation. Electroencephalogr Clin Neurophysiol. 1987;67:271–88.

Lehmann D, Strik WK, Henggeler B, Koenig T, Koukkou M. Brain electric microstates and momentary conscious mind states as building blocks of spontaneous thinking: I. Visual imagery and abstract thoughts. Int J Psychophysiol. 1998;29:1–11.

Lehmann D, Faber PL, Galderisi S, Herrmann WM, Kinoshita T, Koukkou M, Mucci A, Pascual-Marqui RD, Saito N, Wackermann J, Winterer G, Koenig T. EEG microstate duration and syntax in acute, medication-naive, first-episode schizophrenia: a multi-center study. Psychiatry Res. 2005;138:141–56.

Lisman J. Excitation, inhibition, local oscillations, or large-scale loops: what causes the symptoms of schizophrenia? Curr Opin Neurobiol. 2012;22:537–44.

Lisman J, Buzsaki G. A neural coding scheme formed by the combined function of gamma and theta oscillations. Schizophr Bull. 2008;34:974–80.

Lisman JE, Coyle JT, Green RW, Javitt DC, Benes FM, Heckers S, Grace AA. Circuit-based framework for understanding neurotransmitter and risk gene interactions in schizophrenia. Trends Neurosci. 2008;31:234–42.

Merrin EL, Meek P, Floyd TC, Callaway E 3rd. Topographic segmentation of waking EEG in medication-free schizophrenic patients. Int J Psychophysiol. 1990;9:231–6.

Mormann F, Fell J, Axmacher N, Weber B, Lehnertz K, Elger CE, Fernandez G. Phase/amplitude reset and theta-gamma interaction in the human medial temporal lobe during a continuous word recognition memory task. Hippocampus. 2005;15:890–900.

Morrison-Stewart SL, Velikonja D, Corning WC, Williamson P. Aberrant interhemispheric alpha coherence on electroencephalography in schizophrenic patients during activation tasks. Psychol Med. 1996;26:605–12.

Mulert C, Kirsch V, Pascual-Marqui R, McCarley RW, Spencer KM. Long-range synchrony of gamma oscillations and auditory hallucination symptoms in schizophrenia. Int J Psychophysiol. 2011;79:55–63.

Musso F, Brinkmeyer J, Mobascher A, Warbrick T, Winterer G. Spontaneous brain activity and EEG microstates. A novel EEG/fMRI analysis approach to explore resting-state networks. Neuroimage. 2010;52:1149–61.

Nishida K, Morishima Y, Yoshimura M, Isotani T, Irisawa S, Jann K, Dierks T, Strik W, Kinoshita T, Koenig T. EEG microstates associated with salience and frontoparietal networks in frontotemporal dementia, schizophrenia and Alzheimer's disease. Clin Neurophysiol. 2013;124:1106–14.

Nolte G, Bai O, Wheaton L, Mari Z, Vorbach S, Hallett M. Identifying true brain interaction from EEG data using the imaginary part of coherency. Clin Neurophysiol. 2004;115:2292–307.

Nunez PL, Srinivasan R, Westdorp AF, Wijesinghe RS, Tucker DM, Silberstein RB, Cadusch PJ. EEG coherency. I. Statistics, reference electrode, volume conduction, Laplacians, cortical imaging, and interpretation at multiple scales. Electroencephalogr Clin Neurophysiol. 1997;103:499–515.

Olejarczyk E, Jernajczyk W. Graph-based analysis of brain connectivity in schizophrenia. PLoS One. 2017;12:e0188629.

Pascual-Marqui RD. Discrete, 3D distributed, linear imaging methods of electric neuronal activity. Part 1: exact, zero error localization. arXiv: First published on 17 October 2007; 2007a. http://arxiv.org/pdf/0710.3341.

Pascual-Marqui RD. Instantaneous and lagged measurements of linear and nonlinear dependence between groups of multivariate time series: frequency decomposition. [arXiv: 0711.1455 [stat.ME]; 2007b.

Pascual-Marqui RD, Lehmann D, Koukkou M, Kochi K, Anderer P, Saletu B, Tanaka H, Hirata K, John ER, Prichep L, Biscay-Lirio R, Kinoshita T. Assessing interactions in the brain with exact low-resolution electromagnetic tomography. Philos Trans A Math Phys Eng Sci. 2011;369:3768–84.

Popov T, Wienbruch C, Meissner S, Miller GA, Rockstroh B. A mechanism of deficient interregional neural communication in schizophrenia. Psychophysiology. 2015;52:648–56.

Rajji TK, Zomorrodi R, Barr MS, Blumberger DM, Mulsant BH, Daskalakis ZJ. Ordering information in working memory and modulation of gamma by theta oscillations in humans. Cereb Cortex. 2017;27:1482–90.

Ramyead A, Kometer M, Studerus E, Koranyi S, Ittig S, Gschwandtner U, Fuhr P, Riecher-Rossler A. Aberrant current source-density and lagged phase synchronization of neural oscillations as markers for emerging psychosis. Schizophr Bull. 2015;41:919–29.

Ramyead A, Studerus E, Kometer M, Heitz U, Gschwandtner U, Fuhr P, Riecher-Rossler A. Neural oscillations in antipsychotic-naive patients with a first psychotic episode. World J Biol Psychiatry. 2016;17:296–307.

Ranlund S, Adams RA, Diez A, Constante M, Dutt A, Hall MH, Maestro Carbayo A, McDonald C, Petrella S, Schulze K, Shaikh M, Walshe M, Friston K, Pinotsis D, Bramon E. Impaired prefrontal synaptic gain in people with psychosis and their relatives during the mismatch negativity. Hum Brain Mapp. 2016;37:351–65.

Reichenberg A, Caspi A, Harrington H, Houts R, Keefe RS, Murray RM, Poulton R, Moffitt TE. Static and dynamic cognitive deficits in childhood preceding adult schizophrenia: a 30-year study. Am J Psychiatry. 2010;167:160–9.

Rieger K, Diaz Hernandez L, Baenninger A, Koenig T. 15 years of microstate research in schizophrenia—where are we? A meta-analysis. Front Psych. 2016;7:22.

Sarnthein J, Petsche H, Rappelsberger P, Shaw GL, von Stein A. Synchronization between prefrontal and posterior association cortex during human working memory. Proc Natl Acad Sci U S A. 1998;95:7092–6.

Sato N, Yamaguchi Y. Theta synchronization networks emerge during human object-place memory encoding. Neuroreport. 2007;18:419–24.

Sauseng P, Klimesch W, Doppelmayr M, Hanslmayr S, Schabus M, Gruber WR. Theta coupling in the human electroencephalogram during a working memory task. Neurosci Lett. 2004;354:123–6.

Sauseng P, Klimesch W, Schabus M, Doppelmayr M. Fronto-parietal EEG coherence in theta and upper alpha reflect central executive functions of working memory. Int J Psychophysiol. 2005;57:97–103.

Sauseng P, Griesmayr B, Freunberger R, Klimesch W. Control mechanisms in working memory: a possible function of EEG theta oscillations. Neurosci Biobehav Rev. 2010;34:1015–22.

Schack B, Vath N, Petsche H, Geissler HG, Moller E. Phase-coupling of theta-gamma EEG rhythms during short-term memory processing. Int J Psychophysiol. 2002;44:143–63.

Schroeder CE, Lakatos P. Low-frequency neuronal oscillations as instruments of sensory selection. Trends Neurosci. 2009;32:9–18.

Shahbazi Avarvand F, Bartz S, Andreou C, Samek W, Leicht G, Mulert C, Engel AK, Nolte G. Localizing

bicoherence from EEG and MEG. Neuroimage. 2018;174:352–63.
Slifstein M, van de Giessen E, Van Snellenberg J, Thompson JL, Narendran R, Gil R, Hackett E, Girgis R, Ojeil N, Moore H, D'Souza D, Malison RT, Huang Y, Lim K, Nabulsi N, Carson RE, Lieberman JA, Abi-Dargham A. Deficits in prefrontal cortical and extrastriatal dopamine release in schizophrenia: a positron emission tomographic functional magnetic resonance imaging study. JAMA Psychiat. 2015;72:316–24.
Sohal VS, Zhang F, Yizhar O, Deisseroth K. Parvalbumin neurons and gamma rhythms enhance cortical circuit performance. Nature. 2009;459:698–702.
Spencer KM. The functional consequences of cortical circuit abnormalities on gamma oscillations in schizophrenia: insights from computational modeling. Front Hum Neurosci. 2009;3:33.
Spencer KM, Niznikiewicz MA, Nestor PG, Shenton ME, McCarley RW. Left auditory cortex gamma synchronization and auditory hallucination symptoms in schizophrenia. BMC Neurosci. 2009;10:85.
Stam CJ, Nolte G, Daffertshofer A. Phase lag index: assessment of functional connectivity from multi channel EEG and MEG with diminished bias from common sources. Hum Brain Mapp. 2007;28:1178–93.
Steinmann S, Leicht G, Andreou C, Polomac N, Mulert C. Auditory verbal hallucinations related to altered long-range synchrony of gamma-band oscillations. Sci Rep. 2017;7:8401.
Strelets V, Faber PL, Golikova J, Novototsky-Vlasov V, Koenig T, Gianotti LR, Gruzelier JH, Lehmann D. Chronic schizophrenics with positive symptomatology have shortened EEG microstate durations. Clin Neurophysiol. 2003;114:2043–51.
Summerfield C, Mangels JA. Coherent theta-band EEG activity predicts item-context binding during encoding. Neuroimage. 2005;24:692–703.
Sverak T, Albrechtova L, Lamos M, Rektorova I, Ustohal L. Intensive repetitive transcranial magnetic stimulation changes EEG microstates in schizophrenia: a pilot study. Schizophr Res. 2017;
Takahashi T, Goto T, Nobukawa S, Tanaka Y, Kikuchi M, Higashima M, Wada Y. Abnormal functional connectivity of high-frequency rhythms in drug-naive schizophrenia. Clin Neurophysiol. 2018;129:222–31.
Tauscher J, Fischer P, Neumeister A, Rappelsberger P, Kasper S. Low frontal electroencephalographic coherence in neuroleptic-free schizophrenic patients. Biol Psychiatry. 1998;44:438–47.
Thiebes S, Steinmann S, Curic S, Polomac N, Andreou C, Eichler I, Eichler L, Zöllner C, Gallinat J, Leicht G, Mulert C. Alterations in interhemispheric gamma-band connectivity are related to the emergence of auditory verbal hallucinations in healthy subjects during NMDA-receptor blockade. Neuropsychopharmacology. 2018;43(7):1608–1615.
Thune H, Recasens M, Uhlhaas PJ. The 40-Hz auditory steady-state response in patients with schizophrenia: a meta-analysis. JAMA Psychiat. 2016;73:1145–53.
Tomescu MI, Rihs TA, Becker R, Britz J, Custo A, Grouiller F, Schneider M, Debbane M, Eliez S, Michel CM. Deviant dynamics of EEG resting state pattern in 22q11.2 deletion syndrome adolescents: a vulnerability marker of schizophrenia? Schizophr Res. 2014;157:175–81.
Traub RD, Whittington MA, Stanford IM, Jefferys JG. A mechanism for generation of long-range synchronous fast oscillations in the cortex. Nature. 1996;383:621–4.
Tsujimoto T, Shimazu H, Isomura Y. Direct recording of theta oscillations in primate prefrontal and anterior cingulate cortices. J Neurophysiol. 2006;95:2987–3000.
Uhlhaas PJ. Dysconnectivity, large-scale networks and neuronal dynamics in schizophrenia. Curr Opin Neurobiol. 2013;23:283–90.
Uhlhaas PJ, Singer W. Abnormal neural oscillations and synchrony in schizophrenia. Nat Rev Neurosci. 2010;11:100–13.
Uhlhaas PJ, Roux F, Rodriguez E, Rotarska-Jagiela A, Singer W. Neural synchrony and the development of cortical networks. Trends Cogn Sci. 2010;14:72–80.
Van de Ville D, Britz J, Michel CM. EEG microstate sequences in healthy humans at rest reveal scale-free dynamics. Proc Natl Acad Sci U S A. 2010;107:18179–84.
Van Snellenberg JX, Girgis RR, Horga G, van de Giessen E, Slifstein M, Ojeil N, Weinstein JJ, Moore H, Lieberman JA, Shohamy D, Smith EE, Abi-Dargham A. Mechanisms of working memory impairment in schizophrenia. Biol Psychiatry. 2016;80:617–26.
Voytek B, Canolty RT, Shestyuk A, Crone NE, Parvizi J, Knight RT. Shifts in gamma phase-amplitude coupling frequency from theta to alpha over posterior cortex during visual tasks. Front Hum Neurosci. 2010;4:191.
Won GH, Kim JW, Choi TY, Lee YS, Min KJ, Seol KH. Theta-phase gamma-amplitude coupling as a neurophysiological marker in neuroleptic-naive schizophrenia. Psychiatry Res. 2017;260:406–11.
Xu X, Zheng C, Zhang T. Reduction in LFP cross-frequency coupling between theta and gamma rhythms associated with impaired STP and LTP in a rat model of brain ischemia. Front Comput Neurosci. 2013;7:27.
Yan T, Wang W, Liu T, Chen D, Wang C, Li Y, Ma X, Tang X, Wu J, Deng Y, Zhao L. Increased local connectivity of brain functional networks during facial processing in schizophrenia: evidence from EEG data. Oncotarget. 2017;8:107312–22.
Yuan H, Zotev V, Phillips R, Drevets WC, Bodurka J. Spatiotemporal dynamics of the brain at rest--exploring EEG microstates as electrophysiological signatures of BOLD resting state networks. Neuroimage. 2012;60:2062–72.
Zheng L, Liu W, He W, Yu S, Zhong G. Altered effective brain connectivity at early response of antipsychotics in first-episode schizophrenia with auditory hallucinations. Clin Neurophysiol. 2017;128:867–74.
Zhou Y, Fan L, Qiu C, Jiang T. Prefrontal cortex and the dysconnectivity hypothesis of schizophrenia. Neurosci Bull. 2015;31:207–19.

14 Event Related Potential Studies and Findings: Schizophrenia as a Disorder of Cognition

Yingying Tang and Margaret A. Niznikiewicz

Contents

14.1 Introduction

Event related potentials are post-synaptic potentials that reflect neuronal activation associated with cognitive events. They can index sensory, pre-attentive, attentional processes, memory operations, language processes, emotional processes, as well as interactions between these cognitive operations. Most ERPs show sensitivity to certain medications and to illness stage, making them useful and powerful probes of the nature of cognitive dysfunction in schizophrenia.

In inquiries into the neurophysiological underpinnings of schizophrenia, ERP methodology preceded functional magnetic imaging (fMRI) in firmly linking abnormal cognition to abnormal neural function. Since schizophrenia is an illness that impacts several cognitive systems, ERP methodology has been an ideal tool to unlock its underlying cognitive mechanisms. Furthermore, ERP studies have provided important evidence for several theories regarding the nature of this

Y. Tang
Shanghai Key Laboratory of Psychotic Disorders, Shanghai Mental Health Center, School of Medicine, Shanghai Jiao Tong University, Shanghai, China

Brain Science and Technology Research Center, Shanghai Jiao Tong University, Shanghai, China

M. A. Niznikiewicz (✉)
Laboratory of Neuroscience, Clinical Neuroscience Division, VA Boston Healthcare System, Brockton Division, Department of Psychiatry, Harvard Medical School, Brockton, MA, USA
e-mail: Margaret_niznikiewicz@hms.harvard.edu

M. Kubicki, M. E. Shenton (eds.), *Neuroimaging in Schizophrenia*,
https://doi.org/10.1007/978-3-030-35206-6_14

devastating illness. These include the hypothesis that schizophrenia cognitive and clinical symptomatology is a result of sensory impairments whose faulty outputs impact further, more complex processes, the hypothesis that schizophrenia is a disease of pre-attentive and attentional systems, as well as the hypothesis that schizophrenia is a disorder of higher order cognition including language and memory. ERP studies have provided critical evidence in support of all these hypotheses. Finally, schizophrenia has been proposed to be a disorder of abnormal connectivity with evidence supported by EEG based connectivity studies, as discussed in the Chapter on connectivity patterns (Chap. 13).

In reviewing the research, we address two major conceptualizations of schizophrenia: as a disease of sensory processing, as well as a disease of higher order cognition. Evidence derived from ERP studies has played a major role in shaping these arguments. Finally, while early studies focused on isolated cognitive processes, more recent studies recognize the fact that schizophrenia is a disease that involves neural systems and networks that interact, and that these interactions and interdependencies, when abnormal, result in what is ultimately experienced as schizophrenia symptoms. Again, studies using ERP and EEG methodology have contributed to this understanding, and recently the focus has been more on neural systems and networks as the direction for research studies, as opposed to a focus on local brain regions in isolation.

14.2 Event Related Potential Evidence for Schizophrenia as a Disorder of Sensory Processes

The hypothesis that clinical symptoms and cognitive impairments observed in schizophrenia are associated with abnormalities in sensory processes, which in turn impact higher cognitive operations, has garnered a great deal of support from the numerous ERP studies that have examined early, pre-attentive processes, and from studies examining ERP correlates of processing relatively simple auditory and visual stimuli. The questions raised in these studies have sought not only to identify which aspects of sensory processes are impaired in schizophrenia, but also the extent to which these impairments might be biomarkers or endophenotypes for schizophrenia.

14.2.1 Mismatch Negativity and Pre-attentive Processes

Mismatch negativity (MMN) is a negative potential with a latency of about 150 ms post-stimulus onset. It is generated in experimental paradigms where a series of stimuli characterized by identical sensory features are interspersed with stimuli, which deviate from the standard stimuli in one or two dimensions. In schizophrenia research, most MMN studies have focused on the auditory modality, but some visual MMN have also been conducted. The subject's task in MMN experiments is typically to listen to tones, or to watch simple images, without paying attention to them, which is achieved with a variety of experimental manipulations. It is thus believed that MMN reflects pre-attentive processes in the short-term sensory memory. In spite of the apparent simplicity of the experimental set up, MMN has been used successfully to study an array of operations related to the processing of stimulus properties within sensory memory. Accordingly, MMN has been elicited by deviations in frequency (f-MMN), duration (d-MMN), intensity, by gaps in an expected sequence of stimulus presentation (Salisbury and McCathern 2016), as well as by a combination of these features (Salisbury et al. 2018), suggesting that each of these physical sensory attributes is associated with a somewhat unique neural signature. Recently, it has been pointed out that MMN is also sensitive to sensory context and expectations developed about such contexts (e.g., Schmidt et al. 2012). Therefore, in addition to indexing sensory operations, MMN has recently been associated with prediction error detection.

14.2.1.1 MMN and Its Neural Generators

Studies focusing on neural sources of MMN suggest a network of regions that encompass temporal, parietal, and frontal regions (Fulham et al. 2014; Kasai et al. 2002; Takahashi et al. 2013). For example, a recent study suggests a link between reduced left hippocampal volume and MMN reduction in schizophrenia (Huang et al. 2018). Furthermore, Kim et al. (2019) reported that cortical thinning in frontal and temporal regions in schizophrenia patients, especially those with auditory hallucinations, was associated with reduced MMN, while in bipolar patients reduced MMN was associated with cortical thinning in emotion-related brain regions. Similar results in terms of cortical thinning in schizophrenia patients and its association with MMN have been reported by Seol et al. (2017). Likewise, reductions in cortical gray matter in the temporal regions (e.g., Heschl's gyrus) and in frontal regions were associated with MMN amplitude reductions (Rasser et al. 2011). A recent study using MMN paradigm as well as using a resting state connectivity approach identified a network of regions involving both cortico-cortical and thalamo-cortical connectivity, which contributed to auditory dysfunction in schizophrenia (Lee et al. 2017).

Overall, these studies suggest that structural abnormalities in both temporal and frontal brain regions contribute to MMN abnormalities in schizophrenia. It is of interest that bipolar patients, in keeping with a clinical profile of this disorder, seem to present with cortical thinning in limbic brain regions, which is also associated with MMN reductions (Kim et al. 2019).

14.2.1.2 MMN as an Index of Sensory Processing Abnormalities and Its Functional Consequences

One of the major questions addressed in MMN paradigms is the nature of sensory, mostly auditory, abnormalities in schizophrenia and their cognitive and clinical consequences, with some studies suggesting that MMN may be a better predictor of functional outcomes than neurocognition (Lee et al. 2014).

Leitman et al. (2010) outlined a hierarchical model of auditory sensory abnormalities where early sensory abnormalities contribute to abnormalities in higher order cognition. In support of this thesis, using structural equation modeling, P300 abnormalities indexing attentional deficits were predicted by MMN deficits (Leitman et al. 2010). According to this model of schizophrenia dysfunction, low level sensory abnormalities associated with the processing of a variety of sensory features result in a host of higher order cognitive impairments (Javitt 2015; Leitman et al. 2010).

Baldeweg and Hirsch (2015) used MMN in a roving paradigm where the number of standard tones presented between one deviant tone and another varied, and thus allowed for the examination of MMN as a function of a memory trace for the deviant tone. An impairment was found in chronic schizophrenia and was interpreted in terms of abnormal modulation of NMDA receptor dependent plasticity. The MMN reduction was correlated with memory impairment. A similar conclusion was reached in a review devoted to this topic by Bartha-Doering et al. (2015). Deficits in the memory trace were also reported by Javitt et al. (2000), Minami and Kirino (2005), and Todd et al. (2000, 2003).

Some studies suggest that MMN's most robust association is with real-world function disability rather than with specific, discrete cognitive processes (Hamilton et al. 2018a, b; Kaur et al. 2013; Kim et al. 2014a, b; Light and Braff 2005a, b; Taylor et al. 2017; Thomas et al. 2017). D-MMN amplitude reduction has also been associated with reductions in global function in early schizophrenia (Koshiyama et al. 2018).

The majority of MMN studies suggest that impairments in the analysis of auditory sensory features are widespread in schizophrenia. These impairments seem to be related to laying down an effective sensory memory trace, which in turn makes it harder to effectively analyze auditory sensory information. It also appears that while MMN correlations with memory function have been reported, sensory level deficits indexed by MMN most reliably impact real world functioning in schizophrenia.

14.2.1.3 MMN and Prediction Error

A more recent theoretical interpretation of MMN deficits points to MMN's role as an index of the encoding prediction error. However, this interpretation of MMN deficits is far from fully agreed upon. For example, recent meta-analysis (Erickson et al. 2017) of a predictive coding error impairment in schizophrenia suggested that MMN deficits in such paradigms were not associated with symptoms severity but rather with lower education and older age, indicating that this impairment may be more closely related to premorbid function. A somewhat similar conclusion was reached by Salisbury et al. (2017), who reported that reduced d- and f-MMN amplitude was related to estimates of premorbid intellectual function in all participants in a study that compared schizophrenia spectrum participants tested 1 year following their first hospitalization for psychosis. The relationship between MMN and premorbid function was also reported by Friedman et al. (2012), but here both function and illness duration correlates of MMN were interpreted as support for both neurodevelopmental and neurodegenerative contributions to pre-attentive impairment in schizophrenia.

On the other hand, the review of MMN as an index of predictive error signaling suggests that these types of impairments exist across schizophrenia spectrum severity (Randeniya et al. 2018), and thus may be an illness biomarker rather than solely a measure of premorbid function. Impairments in the prediction error mechanism have been proposed as an overarching framework for auditory dysfunction reported across studies in schizophrenia (Retsa et al. 2018; Sauer et al. 2017; Todd et al. 2012).

Todd et al. (2018) couched MMN impairments in terms of higher-order pattern recognition related to temporal sequencing and hierarchical pattern learning. Schmidt et al. (2012) explicitly associated the NMDAR system with prediction error deficits in schizophrenia in a study that contrasted both ketamine (NMDA antagonist) and psilocybin (5-HT(2A)R antagonist) in a group of healthy controls in a double blind cross-over design. Finally, McCleery et al. (2018) reported a relationship between prediction error signaling and auditory hallucinations in a roving MMN paradigm in schizophrenia patients.

The introduction of MMN as a measure of prediction error deficits is an appealing theoretical development in schizophrenia research. While this model of MMN is different from the model of MMN as an index of pre-attentive processes, the two models are not necessarily mutually exclusive. It is likely that the debate on how these two models fit together will continue.

14.2.1.4 MMN as an Index of Neurochemical Imbalance in Schizophrenia

Questions about the relationship between MMN and neurotransmitters are aimed at understanding how brain neurochemistry impacts cognition. At the neurochemical level, MMN abnormalities in schizophrenia are believed to be mediated by N-methyl-D-aspartate receptor (NMDAR) glutamatergic hypofunction (Javitt 2015; Kantrowitz et al. 2016, 2018; Umbricht et al. 2000), but the contribution of other neuro-transmitters needs to also be considered.

NMDAR abnormality in relation to MMN has been assessed across several studies. Javitt et al. (2018) proposed that MMN reflects activity primarily in theta band frequency, which is supported by the interplay between cortical pyramidal neurons and local circuit GABA interneurons. Greenwood et al. (2018) examined the effects of glycine, which increases NMDAR mediated glutamatergic function, and the authors reported that acute glycine administration improves d-MMN in schizophrenia, in support of the glutamatergic model of schizophrenia dysfunction.

Taking a different approach, several studies examined the effects of ketamine, which is an NMDA antagonist, to test whether its administration would bring cognitive and neural impairments similar to those observed in schizophrenia if used in healthy volunteers. In most of such studies, ketamine induced psychotic-like positive symptoms, and abnormalities in working memory and attention, along with reductions in MMN, have been reported, (Gunduz-Bruce et al. 2012; Hamilton et al. 2018a, b) suggesting that indeed

deficits in NMDA receptors can contribute to schizophrenia symptomatology. These effects have been recently confirmed in a meta-analysis (Haaf et al. 2018), where ketamine has been consistently found to produce deficits in MMN, in support of the glutamatergic model of schizophrenia abnormality. In a study that directly assessed the association between glutamate and MMN (Nagai et al. 2017), fasting plasma levels of glutamate were higher in first episode schizophrenia and associated with lower MMN amplitude in both first episode patients and in their healthy comparison subjects. Rosch et al. (2019), using an MMN roving paradigm, examined the effects of ketamine in healthy volunteers and concluded that its effects may be due to ketamine induced reduction of inhibitory interneuron connectivity in the frontal sources compared with temporal MMN sources. In a study that used both MMN assessment and spectroscopy assessment of glutamate and GABA contributions to both MMN and working memory in schizophrenia, (Rowland et al. 2016) it was suggested that both glutamatergic and GABA-ergic function contribute to MMN and working memory impairments in schizophrenia.

Bravermanova et al. (2018) examined the role of serotonin in psychosis using psilocybin, a psychedelic with 5-HT2A/C properties, in a group of healthy volunteers within the context of the MMN paradigm and concluded that pre-attentive processes are not affected by altered serotonergic levels. In contrast Heekeren et al. (2008) found additive and distinct effects of both glutamatergic and serotonergic contributions to schizophrenia pre-attentive dysfunction. Similarly, Oranje et al. (2008) used escilatopram in a double blind placebo controlled cross-over study and found enhanced MMN in a group receiving escilatopram.

The results of the studies on the role of nicotine in the generation of MMN, and especially on its role in the improvement of MMN amplitude in the patient group, are mixed, with some studies suggesting that d-MMN amplitude can be normalized by nicotine (Dulude et al. 2010), while others find this effect weak at most (Fisher et al. 2012a, b; Hamilton et al. 2018a, b; Mathalon et al. 2014). Inami et al. (2007) showed both latency and amplitude MMN improvements in healthy subjects but not in a schizophrenia group, suggesting that this effect may be due to low nicotinic receptor function in schizophrenia.

Knott et al. (2012) examined an issue of ketamine (which mimics NMDA hypofunction) and nicotine (targeting the nicotinic acetylcholine receptor) interactions in a group of healthy individuals prone to auditory hallucinatory experiences in a visual rapid information processing task while auditory stimuli were simultaneously delivered. The study reported longer latencies and reduced MMN amplitude in a high dose ketamine condition, which was prevented by co-administration of nicotine, suggesting a role for both glutamatergic and nicotinic receptors in schizophrenia symptomatology.

Finally, the contribution of dopamine to MMN generation was not confirmed in healthy subjects by Leung et al. (2007).

Overall, this group of studies points to a complex relationship between MMN, the processes that it indexes, and neurotransmitter systems. While the role of glutamate and GABA are well established in contributing to MMN abnormality in schizophrenia, the role of serotonin as contributing to MMN abnormality received less support. Similarly, the evidence for the contribution of nicotinic receptor hypofunction in schizophrenia is equivocal.

14.2.1.5 MMN as a Biomarker and Endophenotype

Another important issue addressed in MMN studies has been the extent to which MMN can be used as a biomarker for schizophrenia or an endophenotype for the disease (Light and Swerdlow 2015a; Light and Naatanen 2013; Light et al. 2015b; Michie et al. 2016; Turetsky et al. 2007).

Auditory sensory processes indexed with MMN were found impaired in both first episode (Brockhaus-Dumke et al. 2005; Hay et al. 2015; Hermens et al. 2010; Kaur et al. 2011) and chronic schizophrenia patients (Hamilton et al. 2018a, b; Kiang et al. 2009; Michie et al. 2000; Salisbury et al. 2002; Umbricht et al. 2003, Umbricht and Krljes 2005). A study by Fisher

et al. (2018) using a multi-feature MMN where several dimensions of the auditory signal are varied including pitch, duration, intensity and location, suggested that MMN impairment existed more robustly in the chronic than in the early phase of schizophrenia.

A series of studies examined MMN abnormalities across different groups of subjects to test whether MMN is reduced as a function of a genetic risk. Recent meta-analysis (Haigh et al. 2017) suggests that d-MMN is a more robust biomarker for pre-attentive sensory memory abnormalities than frequency MMN (f-MMN). Ahveninen's et al. (2006) study compared mono- and dizygotic twins discordant for schizophrenia and matched healthy controls. Abnormal MMN was found in the schizophrenia group but not in the unaffected twin group, suggesting that MMN does not index genetic vulnerability for psychosis. Similar conclusions were reached in other studies focusing on the familiar risk for schizophrenia using MMN as a dependent measure (Bramon et al. 2004a, b; Kim et al. 2014a, b). On the other hand, a recent meta-analysis (Earls et al. 2016) suggested more circumscribed MMN deficits limited to the frontal site Fz in the relatives of schizophrenia patients relative to controls. Also, Michie et al. (2002) found reduced d-MMN, but not f-MMN, in the unaffected relatives of schizophrenia patients.

On the other hand, most studies examining MMN in clinical (CHR) and ultra-high risk groups (UHR), especially using duration MMN (d-MMN) paradigm, found MMN impairment, suggesting that sensory abnormalities probed with MMN mark at risk state and can be regarded a biomarker for psychosis (Atkinson et al. 2012; Bodatsch et al. 2011; Brockhaus-Dumke et al. 2005; Carrion et al. 2015; Higuchi et al. 2013, 2014; Hong et al. 2012; Jahshan et al. 2012a, b; Kim et al. 2018b; Murphy et al. 2013; Naatanen et al. 2016; Niznikiewicz et al. 2009; Pantlin and Davalos 2016; Rydkjaer et al. 2017; Shin et al. 2009; Solis-Vivanco et al. 2014), including the transition to psychosis (Lavoie et al. 2018; Perez et al. 2014; Shaikh et al. 2012; Sumiyoshi et al. 2013). Similarly, Koshiyama et al. (2017) reported reduced d-MMN and f-MMN in both early psychosis and UHR individuals with no indication of progression at follow up.

Recent meta-analysis of CHR studies focusing on MMN as a predictor of psychosis supported the conclusion that MMN can be regarded as a predictor of conversion to psychosis, with d-MMN achieving the highest effect size (Bodatsch et al. 2015; Erickson et al. 2016; Nagai et al. 2013). The presence of MMN abnormalities in CHR was also confirmed by the recent review by Lepock et al. (2018). Lee et al. (2018) also suggested that dMMN is a more robust indicator of auditory sensory abnormalities, while f-MMN was found to be abnormal in more chronic and with worse functional outcome patient groups.

However, not all studies support the finding of early presence of sensory auditory abnormalities in schizophrenia. Magno et al. (2008) reported on the reduced d-MMN and f-MMN in the chronic, but not in the first episode schizophrenia patients, in a relatively large study cohort.

Thus, a clear majority of MMN studies support the idea that pre-attentive abnormalities indexed by MMN, especially by d-MMN, appear well in advance of psychotic symptoms in individuals at high risk for psychosis, and that MMN can be regarded a biomarker for risk for psychosis. However, the evidence that this risk is genetically mediated is weaker, with several studies not finding MMN deficits in unaffected relatives of schizophrenia patients.

14.2.1.6 MMN and Symptoms

A specific association between MMN and symptoms was reported in several studies. Kargel et al. (2014) reported an association between d-MMN and severity of positive symptoms. Fisher et al. (2011) suggested that the impairment indexed by MMN may be related to auditory hallucinations, especially the auditory impairment marked by d-MMN (Fisher et al. 2008, 2012a, b, 2014). Perrin et al. (2018) associated auditory hallucinations with MMN impairments to location deviants, i.e., rare sounds that appear to be delivered from a different location than frequent sounds, and suggested that they may be related to source monitoring abnormalities.

14.2.1.7 MMN and Illness Specificity

Several studies looked at the degree to which MMN is similar and different across major psychiatric diagnoses, especially in terms of its profile of similarities between schizophrenia and bipolar disorder. A study contrasting healthy controls and bipolar patients found reduced magnetic f-MMN in the patients' group (Shimano et al. 2014). A recent meta-analysis (Erickson et al. 2016) suggests that MMN abnormalities exist in both schizophrenia and bipolar disease, although they are attenuated in bipolar disorder (Jahshan et al. 2012a, b).

14.2.1.8 MMN in Visual Modality

A handful of studies examined MMN in the visual modality, including a recent meta-analysis (Kremlacek et al. 2016). The results of these studies suggest that MMN impairments reported in the auditory modality also exist in the visual modality. Farkas et al. (2015) found reduced MMN in a paradigm that examined visual predictive coding of unattended low level sensory visual features. Javitt et al. (2000) reported abnormal MMN related to forming an effective memory trace. Reduced visual MMN was also reported in Urban et al. (2008) and in Neuhaus's et al. (2013) study, where it was interpreted as an index of prediction error.

14.2.1.9 Summary

The MMN paradigm has been used effectively to ask several specific questions about early, sensory driven cognitive deficits in schizophrenia. It provides important insights about the nature of these sensory abnormalities, including identifying defective formation of a memory trace, and likely impaired processes of error prediction as some of the fundamental deficits found in schizophrenia. These findings have also been tied to both structural and neurochemical abnormalities. Within structural abnormalities, cortical thinning in the frontal and temporal regions was associated with MMN reductions. Within neurochemical abnormalities, abnormalities of glutamatergic and GABA-ergic systems have received the most robust support as contributing to MMN deficits in schizophrenia. Several studies associated MMN deficits with auditory hallucinations, and functionally, with reduced global functioning. More pronounced MMN deficits have also been found in schizophrenia relative to bipolar disorder (Table 14.1).

Table 14.1 Mismatch negativity (MMN) in schizophrenia

Citation	Subjects	Deviants	Main findings
Javitt et al. (2000)	17 ChSZ, 13 recent-onset SZ and 20 HC	Duration, pitch	ChSZ and recent-onset SZ showed decreased MMN amplitude but normal latency and topography
Michie et al. (2000)	14 SZ and 19 HC	Low/large frequency, duration	SZ showed reduced duration MMN and a similar trend for frequency MMN
Todd et al. (2000)	22 SZ and 25 HC	Duration	SZ showed a reduction of duration MMN
Umbricht et al. (2000)	20 HC	Pitch, duration	An infusion with subanesthetic doses of ketamine led to decreased amplitudes of pitch MMN and duration MMN by 27% and 21% respectively
Kasai et al. (2002)	23 SZ and 28 HC	Duration (pure-tone), duration (Japanese vowel A), differences between vowels a and O	MMN amplitude for across-phoneme boundary change was lower than for change of tone or vowel duration in SZ; Bilateral MMN amplitude for across-phoneme change was lower in SZ than HC; SZ had a weaker left temporal combination of current sink and current source, and a weaker right frontal/temporal current sink than HC

(continued)

Table 14.1 (continued)

Citation	Subjects	Deviants	Main findings
Michie et al. (2002)	22 medicated SZ, 17 SZ first-degree relatives and 21 HC	Duration	SZ and SZ relatives showed reduced duration MMN amplitude compared with HC; Duration MMN amplitude did not differ between SZ and SZ relatives, but P3a was larger in SZ relatives than SZ
Salisbury et al. (2002)	16 ChSZ and 13 older HC; 21 FESZ and 27 younger controls	Pitch	ChSZ showed a reduction of pitch MMN by approximately 47% relative to controls, while FESZ did not show MMN reduction; All groups showed larger pitch MMN over the right hemisphere than over the left hemisphere
Davalos et al. (2003)	10 SZ and 11 HC	Interval	SZ showed a reduction of MMN amplitude for the temporal deviance compared with HC
Todd et al. (2003)	20 SZ and 22 HC	Duration	SZ produced smaller MMN amplitude to temporally deviant stimuli; SZ who showed the highest temporal thresholds for discrimination between two different sounds produced the smallest MMN response
Umbricht et al. (2003)	26 SZ, 16 BP, 22 MDD and 25 HC	Duration, frequency	SZ showed smaller duration and frequency MMN than HC; The reduction of frequency MMN in SZ was not significant in the comparison across all groups; MMN topography did not differ among groups; No consistent correlations with clinical, psychopathologic, or treatment variables were observed
Bramon et al. (2004a, b)	25 SZ, 37 SZ first-degree relatives and 20 HC	Duration	SZ showed smaller MMN amplitudes at Fz and F3 relative to SZ relatives and HC; MMN amplitude in SZ relatives did not differ from that in HC; No between-group differences in MMN amplitude at F4 were observed
Brockhaus-Dumke et al. (2005)	43 prodromal subjects, 31 neuroleptic-free SZ and 33 HC	Duration, frequency	SZ showed reduced duration MMN amplitudes in SZ compared to controls; Prodromal subjects showed MMN amplitude intermediate between HC and SZ
Light et al. (2005a)	10 ChSZ and 10 HC	Duration	SZ had MMN deficits with large effect sizes that were reliable over time; MMN deficits were associated with poor functional status at both the first and second testing time
Light et al. (2005b)	25 SZ and 25 HC	Duration	SZ showed reduced MMN; Greater levels of MMN impairment, in particular at fronto-central sites, were associated with lower GAF; SZ with greater MMN impairments were more likely to live in highly structured than independent settings; MMN deficits were not associated with symptom severity or performance on laboratory-based tasks
Minami et al. (2005)	Experiment 1: 12 SZ and 12 HC; Experiment 2: 11 SZ and 10 HC	Frequency	SZ showed MMN amplitude reductions when stimuli were presented at longer inter-trial intervals compared to the shorter ones, while little difference in MMN was observed in HC as a function of inter-trial differences

Table 14.1 (continued)

Citation	Subjects	Deviants	Main findings
Ahveninen et al. (2006)	23 SZ, 23 twins (10 discordant monozygotic pairs and 13 discordant dizygotic pairs) and 40 HC	Frequency	SZ but not unaffected SZ relatives showed reduced MMN, reflecting state-dependent neurodegeneration
Inami et al. (2007)	10 non-smoking SZ and 10 HC	Frequency	Nicotine administration shortened the MMN latencies at Fz in HC; No significant differences in MMN latencies were observed in SZ
Leung et al. (2007)	15 HC	Duration	Neither D(2) receptor stimulation with bromocriptine nor simultaneous D(1) and D(2) receptor stimulation with pergolide had effects on MMN
Fisher et al. (2008)	12 hallucinating SZ, 12 non-hallucinating SZ and 12 HC	Frequency, duration, intensity, location, gap	Hallucinating SZ showed smaller duration MMNs compared to HC and non-hallucinating SZ, and smaller intensity MMN compared to HC; Scalp regional differences between HC and each of SZ groups were observed in frequency MMN; No between-group effects were observed in location or gap MMN, or in MMN latency
Heekeren et al. (2008)	15 HC	Frequency-respective duration	The reduction in MMN activity was more pronounced after S-ketamine intake, and only S-ketamine had a significant impact on the frontal source of MMN
Oranje et al. (2008)	18 HC	Frequency	Escitalopram increased MMN compared to placebo
Urban et al. (2008)	24 SZ/SA and HC	Downward motion	SZ had smaller visual MMN, MMN reductions were associated with higher dose of medication, lower level of functioning and the presence of deficit syndrome
Kiang et al. (2009)	253 SZ and 147 HC	Duration	SZ showed smaller MMN than HC over the entire age range; MMN amplitude declined with age in both groups, slightly less steeply in SZ than in HC
Niznikiewicz et al. (2009)	23 SPD and 26 HC	Pitch	Reduced MMN amplitude was found in SPD relative to HC
Shin et al. (2009)	16 UHR and 18 HC	Duration	UHR showed a smaller right MMNm dipole moment than HC; Group difference was observed in MMNm dipole latency; The left MMNm dipole moment was negatively correlated with positive symptoms scores
Dulude et al. (2010)	12 smokers with SZ and 12 smoker HC	Duratin, frequency	SZ smokers showed reduced frequency and duration MMN amplitudes compared with HC smokers. Nicotine prolonged duration MMN latency and increased duration MMN amplitude in SZ
Hermens et al. (2010)	17 FEP and 17 HC	Duration	FEP showed reduced MMN amplitudes compared to HC; Fronto-central MMN peak amplitude was associated with cognitive/psychosocial functioning

(continued)

Table 14.1 (continued)

Citation	Subjects	Deviants	Main findings
Leitman et al. (2010)	50 SZ and 21 HC	Pitch	SZ showed MMN deficits of large effect size (d>1.26) relative to HC in the standard fixed-deviance condition; SZ required elevated tone-matching thresholds relative to HC; SZ and HC no longer differed in MMN amplitude when tone differences were individually adjusted to equate tone-matching performance across groups; MMN generation was explained by dipoles seeded within the bilateral auditory cortex
Bodatsch et al. (2011)	62 antipsychotic-naïve at-risk subjects, 33 FEP and 67 HC	Duration	Fronto-central duration MMN amplitude in at-risk subjects who later converted to psychosis was smaller than in HC, and comparable with FEP; Duration MMN in at-risk subjects who later did not convert to psychosis was comparable to HC and larger than in FES
Fisher et al. (2011)	12 SZ with AH and 12 HC	Frequency, duration, intensity	SZ showed a significantly smaller duration MMN compared to HC; Attenuated duration MMN amplitudes were correlated with increased PSYRATS scores, PANSS positive symptom, hallucination and general psychoticism ratings; Attenuated intensity MMN amplitudes were correlated with increased PSYRATS scores
Kaur et al. (2011)	17 FEP affective-spectrum, 18 FEP SZ-spectrum and 18 HC	Duration	FEP SZ- and FEP affective-spectrum showed reduced fronto-central MMN and reduced central P3a compared to HC; The combined FEP sample showed correlations between fronto-central MMN amplitudes and cognitive measures
Rasser et al. (2011)	18 Sz and 18 HC	Duration, frequency, intensity	MMN amplitude reduced in SZ and correlated with their impaired day-to-day function; Reduced frequency MMN amplitude was correlated with bilateral gray matter reduction in Heschl's gyrus in SZ, while reduced duration MMN amplitude correlated with reduced gray matter in right Heschl's gyrus
Atkinson et al. (2012)	30 UHR, 10 FEP and 20 HC	Duration, intensity	Both FEP and UHR showed reduced duration MMN; MMN and P3a reductions were unrelated in both UHR and FEP groups
Friedman et al. (2012)	26 SZ and 19 HC	Pitch, duration, intensity	SZ exhibited reduced MMN to all deviant types; MMN amplitude was correlated with premorbid educational achievement, cognitive symptoms, global function, and illness duration; Duration MMN related to MMN by other deviants was differentially reduced in individuals with poor premorbid function
Fisher et al. (2012a)	12 SZ with persistent AH	Duration, frequency and intensity	Nicotine administration shortened latency for intensity MMN; Nicotine-related change in MMN amplitude was correlated with nicotine-related change in subjective measures of hallucinatory state

Table 14.1 (continued)

Citation	Subjects	Deviants	Main findings
Fisher et al. (2012b)	12 SZ with AH and 15 HC	Duration, frequency, gap, intensity, location	SZ exhibited reduced duration, gap, intensity and location MMNs compared to HC; Gap MMN amplitudes were correlated with measures of hallucinatory state and AH frequency, while location MMN was correlated with perceived AH locations
Gunduz-Bruce et al. (2012)	16 HC	Frequency, intensity	Ketamine produced amplitude reductions for the frequency and intensity MMN; NAC pretreatment reduced frequency-MMN amplitude; The decrements in frequency MMN amplitude produced by ketamine and NAC were not additive
Hong et al. (2012)	95 SZ, 75 SZ first-degree relatives, 87 HC, and 34 community subjects with schizophrenia spectrum personality traits	Duration, duration/pitch	Both SZ and community subjects with schizophrenia spectrum personality traits showed reduced MMN, but SZ relatives did not; Theta-alpha (5–12 Hz) oscillations were strongly correlated with MMN in HC and SZ relatives, while delta (<5 Hz) was strongly correlated with MMN in SZ and community subjects with schizophrenia spectrum personality traits
Jahshan et al. (2012a, b)	26 at-risk for psychosis, 31 recent-onset SZ, 33 ChSZ and 28 HC	Duration	At-risk for psychosis subjects had intermediate MMN amplitudes relative to those in HC and recent-onset SZ; MMN was associated with psychosocial functioning in ChSZ
Knott et al. (2012)	24 HC	Frequency	Ketamine induced prolongation of MMN latency and MMN amplitude reduction in HC with ketamine induced higher AH/delusions, with amplitude attenuation being blocked by the co-administration of nicotine
Schmidt et al. (2012)	39 HC	Roving paradigm	S-ketamine, but not psilocybin showed a frontally disrupted MMN memory trace effect in HC
Shaikh et al. (2012)	41 at-risk subjects and 50 HC	Duration	At-risk subjects showed reduced duration MMN amplitude compared to HC; At-risk subjects who subsequently developed psychosis had smaller MMN amplitude than at-risk individuals who did not become psychotic
Shin et al. (2012)	16 UHR subjects, 15 SZ and 18 HC	Duration	MMNm dipole moment was reduced in both UHR and SZ compared with HC; MMN did not differ between UHR and SZ
Higuchi et al. (2013)	17 at-risk subjects, 31 SZ (20 FEP, 11 ChSZ) and 20 HC	Duration	FEP showed smaller frontal MMN amplitudes than HC, and ChSZ showed smaller frontal and central MMN amplitudes; Four at-risk subjects who later transitioned to SZ showed smaller duration MMN than HC, but at-risk subjects who did not transition to SZ did not differ from HC; At-risk subjects showed a positive correlation between frontal duration MMN amplitudes and verbal fluency

(continued)

Table 14.1 (continued)

Citation	Subjects	Deviants	Main findings
Kaur et al. (2013)	60 young SZ/SA and 30 HC	Duration	SZ showed impaired temporal MMN at baseline; MMN measures in SZ did not differ from those in SA; Reduced temporal MMN amplitude at baseline was significantly associated with greater levels of occupational disability, and showed trend-level associations with general and social disability at follow-up; Centro-midline MMN amplitudes were reduced in SZ/SA over time
Murphy et al. (2013)	14 adolescents with psychotic symptoms and 22 adolescents without psychotic symptoms	Duration	Adolescents with psychotic symptoms showed a reduction in MMN amplitude at frontal and temporal regions relative to those without psychotic symptoms
Neuhaus et al. (2013)	22 SZ and 24 HC	Visual letter of "x"	SZ showed a reduced visual MMN compared to HC with a large effect size
Takahashi et al. (2013)	410 SZ and 247 HC	Duration	MMN deficit found in SZ and was associated with reduced activations in discrete medial frontal regions
Fisher et al. (2014)	10 SZ with AH and 13 HC	Frequency (non-novel), environmental sounds (novel)	SZ exhibited reduced MMN amplitudes to both non-novel and novel deviants relative to HC; Novelty MMN amplitudes were correlated with measures of hallucinatory traits
Fulham et al. (2014)	16 recent-onset SZ, 19 ChSZ and HC	Duration	Frontal MMN and its hemispheric asymmetry reduced in both patient groups and was correlated with GAF and negative symptom ratings
Higuchi et al. (2014)	19 At-risk subjects, 38 SZ (19 FEP and 19 ChSZ) and 19 HC.	Duration	At-risk subjects who later transitioned to psychosis showed smaller frontal and central duration MMN amplitudes relative to those at-risk subjects who did not transition and HC; At-risk subjects who did not transition had comparable duration MMN amplitudes with those of HC
Kargel et al. (2014)	40 SZ and 16 HC	Frequency, duration	SZ showed diminished MMN amplitude and shorter MMN latency to both deviants than HC; Decreased duration MMN amplitude was associated with severity of positive symptoms, and prolonged frequency MMN latency was related to enhanced verbal memory performance in SZ
Kim et al. (2014)	26 SZ, 20 GHR and 48 HC	Duration	SZ showed a reduction of peak MMN amplitude, but GHR did not. MMN amplitude at Fz and Cz was correlated with GAF scores in SZ
Lee et al. (2014)	25 SZ, 21 SZ first-degree relatives and 29 HC	Duration	MMN amplitudes decreased in order of SZ, then SZ relatives, then HC; MMN amplitude was correlated with measures of neurocognition, theory of mind, and functional outcome measurements in SZ; Hierarchical regression analysis revealed that functional outcomes constituted the most powerful predictor of MMN

Table 14.1 (continued)

Citation	Subjects	Deviants	Main findings
Mathalon et al. (2014)	17 HC	Duration	Nicotine reduced MMN amplitude, but ketamine did not
Perez et al. (2014)	19 early-onset SZ, 38 CHR (15 CHR-C and 16 CHR-NC) and 44 HC	Duration, frequency, duration + frequency	MMN was reduced in ESZ and CHR for all deviants relative to HC. CHR-C had a smaller MMN relative to CHR-NC; MMN did not differ between early-onset SZ and CHR; Duration + frequency MMN, but not duration MMN or frequency MMN predicted the time to psychosis onset in CHR
Solis-Vivanco et al. (2014)	20 FEP, 20 UHR and 23 HC	Duration	FEP and UHR showed reduced MMN compared to controls, especially in the left middle regions
Baldeweg and Hirsch (2015)	49 SZ, 25 BP, 15 AD and 49 HC	Duration, frequency	The reduction of the MMN memory trace effect and its correlation with memory impairment was only found in SZ
Carrion et al. (2015)	34 CHR and 33 HC	Pitch, duration, intensity	CHR showed impairments in MMN generation relative to HC; Lower MMN amplitude was correlated with worse reading ability, slower processing speed, and poorer social and role functioning
Farkas et al. (2015)	28 SZ and 27 HC	Horizontal stripes of Gabor patches versus vertical stripes	HC showed MMN effect but SZ did not in the prefrontal and occipital-parietal regions; SZ showed decreased deviant minus standard difference waveforms relative to HC with moderate to large effect sizes
Hay et al. (2015)	24 SZ and 21 HC	Duration, frequency, duration + frequency and intensity	SZ showed significantly reduced MMN relative to HC for all deviant types; No correlations between MMN and clinical symptoms were observed
Light et al. (2015b)	966 SZ, 824 HC	Duration	MMN recorded across 5 recording sites in SZ showed highly reduced amplitude, comparable with the MMN reduction observed in single-lab studies; Demographically-adjusted MMN was related to medication status as well as several clinical, cognitive, and functional characteristics in SZ
Kantrowitz et al. (2016)	Cohort 1: 40 SZ/SA and 42 HC; Cohort 2: 21 SZ/SA and 13 HC	Pitch	Repeated administration of d-serine led to improvements in MMN generation to trained versus untrained tones
Pantlin and Davalos (2016)	72 HC and 49 HR	Duration	HC showed more negative MMN amplitudes than HR
Rowland et al. (2016)	45 SZ and 53 HC	Duration	MMN amplitude and glutamate were reduced in SZ; Smaller MMN amplitude was associated with lower GABA level, lower glutamate level, and higher ratio of glutamine to glutamate; Reduced MMN amplitude was associated with poor verbal working memory in schizophrenia
Salisbury and McCathern (2016)	14 SZ and 16 HC	Missing 4th or 6th tones	HC generated a robust response to a missing but expected tone; SZ were impaired in activating the missing stimulus MMN, generating no significant activity

(continued)

Table 14.1 (continued)

Citation	Subjects	Deviants	Main findings
Coffman et al. (2017)	26 SZ and 26 HC	Pitch, duration	SZ showed a reduction of pitch and duration MMN; Pitch and duration MMN were correlated with repetition suppression of auditory-evoked potentials
Koshiyama et al. (2017)	14 FEP, 16 UHR and 16 HC	Frequency, duration	FEP and UHR had smaller duration MMN amplitude than HC and did not show a progressive decrease over time; No between-group differences of frequency MMN amplitude were observed
Lee et al. (2017)	MMN: 69 SZ and 38 HC;fMRI: 38 SZ and 23 HC	Frequency, intensity and duration	MMN amplitude reduced in SZ across deviants types; Independent deficits in schizophrenia were observed in both the theta response to deviants and the alpha-response to standards
Nagai (2017)	19 FEP, 21 UHR and 16 HC	Duration, frequency	FEP and UHR showed reduced duration MMN amplitudes compared to HC; FEP had higher plasma levels of glutamate than HC; Higher plasma levels of glutamate were associated with smaller duration MMN amplitudes in FEP and HC
Rydkjaer et al. (2017)	27 FEP, 28 ADHD and 43 HC	Frequency, duration, combination of frequency and duration	FES showed reduced frequency and duration MMN compared to HC; MMN amplitude in ADHD did not differ from that in FEP or HC
Salisbury et al. (2017)	29 SZ under 1 year from their first hospitalization and 40 HC	Pitch, duration	SZ and HC did not differ in pitch MMN or duration MMN amplitudes; Smaller pitch and duration MMN amplitudes were associated with lower estimates of premorbid intellect in SZ
Sauer et al. (2017)	16 SZ and 16 HC	A fifth different tone, a fifth omission	SZ showed a reduction in the MMNm amplitude during both local (within trials) and global (across trials) conditions; Responses to sound omissions were reduced in SZ both in terms of MMN latency and in terms of its generators
Seol et al. (2017)	16 SZ and 18 HC	Duration	Frontal and temporal current source density reduced in SZ; The current source density was positively correlated with cortical thickness of frontal and temporal regions in HC, but negatively correlated with cortical thickness of the bilateral inferior gyri in SZ
Taylor et al. (2017)	21 SZ and 22 HC	Duration, monaural gap, inter-aural timing	Regression analysis revealed that MMN predicted GAF scores
Bravermanova et al. (2018)	20 HC	Frequency	Psilocybin did not affect MMN. A negative correlation between P300 and MMN amplitude was observed
Fisher et al. (2018)	14 early-phase SZ and 17 HC	Duration, frequency, gap, intensity, location	No between-group differences of MMN were observed between early-phase SZ and HC; Intensity MMN latency was correlated with PANSS positive symptom scores

Table 14.1 (continued)

Citation	Subjects	Deviants	Main findings
Greenwood et al. (2018)	22 SZ receiving stable antipsychotic medication and 21 HC; 12 SZ added glycine and 10 SZ with palcebo	Duration, frequency	SZ had smaller duration MMN compared to HC at baseline; Acute glycine increased duration MMN (compared to placebo), but this difference was absent after 6-weeks glycine treatment; Smaller baseline duration MMN was associated with greater PANSS-Negative symptoms and with a trend level of PANSS-Negative symptom improvement after 6-weeks
Hamilton et al. (2018a)	24 SZ and 30 HC	Intensity, frequency, duration, frequency + duration	Ketamine decreased intensity, frequency and frequency+duration MMN amplitudes, but nicotine increased intensity and frequency+duration MMN amplitudes. Nicotine did not attenuate the MMN decrease associated with ketamine
Hamilton et al. (2018b)	20 high-functioning SZ, 17 low-functioning SZ and 35 HC	Duration, pitch	Low-functioning SZ had diminished MMN compared to High functioning SZ and HC, and High-functioning SZ had comparable MMN to HC; Logistic regression suggested independent sensitivity of MMN to functioning in SZ over and above P300 measures; Neither MMN nor P300 were associated with positive or negative symptom severity
Huang et al. (2018)	36 SZ and 14 HC	MMN paradigm	MMN amplitude was significantly lower in SZ. In SZ, MMN was positively correlated with age and negatively correlated with left hippocampal and right pars opercularis volumes. The association between left hippocampal volume and MMN in schizophrenia remained significant after controlling for potential confounders
Kantrowitz et al. (2018)	14 SZ for double-blind group, 19 SZ for open-label group	Duration, pitch, intensity	Double-blind d-serine treatment improved MMN frequency generation and clinical symptoms; MMN frequency was correlated with symptoms changes following co-variation for treatment type; No significant effects of bitopertin were observed for symptoms or MMN
Kim et al. (2018b)	48 CHR and 47 HC	Duration	CHR non-remitters showed reduced MMN amplitudes at baseline compared to CHR remitters and HC; Frontal baseline MMN amplitude was the only significant predictor of remission; The MMN amplitude, antipsychotic use, and years of education predicted an improvement in attenuated positive symptoms
Kim et al. (2019)	38 SZ, 37 BP and 32 HC	Duration	MMN amplitude reduced in both SZ and BP as compared with HC; MMN amplitude in BP was intermediate among groups; Average MMN amplitude was negatively correlated with cortical thickness of the right STG in SZ, and of the left anterior cingulate cortex and left STG in BP

(continued)

Table 14.1 (continued)

Citation	Subjects	Deviants	Main findings
Koshiyama et al. (2018)	26 recent-onset SZ, 30 UHR and 20 HC	Duration, frequency	Duration MMN amplitude was impaired in recent-onset SZ compared to HC and was correlated with GAF in recent-onset SZ and UHR. Frequency MMN amplitude showed between-group differences and was correlated with working memory only in recent-onset SZ
Lavoie et al. (2018)	42 UHR and 29 HC	Frequency	UHR showed reduced frequency MMN amplitude relative to HC; UHR-T individuals showed a significant decrease in frequency MMN amplitude from baseline to post-transition, but UHR-NT did not
Lee et al. (2018)	NKI site: 67 SZ and 38 HC; Columbia site: 29 SZ and 28 HC	Duration, frequency	SZ showed reduced duration MMN at both sites relative to HC; Frequency MMN deficit was highly correlated with impairments in tone matching ability across sites and impairments in verbal learning; Deficits in alpha inter-trail coherence were observed across sites, deficits in alpha power were observed at the inpatient but not outpatient site
McCleery et al. (2018)	16 SZ with recent AH, 14 SZ without AH and 20 HC	Roving paradigm	SZ with recent AH exhibited an abnormal roving MMN profile, reduced prediction error signaling, and a trend for diminished short-term neuroplasticity
Perrin et al. (2018)	20 SZ with persistent AH and 20 HC	Spatial-location, pitch, duration	SZ showed impaired location and pitch MMN generation. Hallucinating and non-hallucinating SZ showed similar deficits in location MMN to left-hemifield stimuli. Non-hallucinating SZ differed from HC and hallucinating SZ for MMN to right-lateral hemifield stimuli
Salisbury et al. (2018)	Experiment 1: 20 SZ and 22 HC; Experiment 2: 24 SZ and 21 HC, 21 FESZ.	Tone pairs	Complex MMN reduced in SZ but was not reduces in FESZ as compared to HC

AD Alzheimer's disease, *ADHD* attention-deficit/hyperactivity disorder, *AH* auditory hallucination, *BP* bipolar disorder, *CHR* clinical high-risk for psychosis, *CHR-C* CHR subjects who converted to psychosis, *CHR-NC* CHR subjects who did not converted to psychosis, *ChSZ* chronic schizophrenia, *CPT* continuous performance test, *FESZ* patients with first-episode schizophrenia, *GAF* Global Assessment of Functioning, *GHR* genetic high risk for psychosis, *MDD* major depressive disorder, *NAC* N-acetylcysteine, *PANSS* the Positive and Negative Syndrome Scale, *SA* schizoaffective disorder, *SPD* schizotypal personality disorder, *STG* superior temporal gyrus, *SZ* schizophrenia, *UHR* ultra-high risk for psychosis

14.2.2 Sensory Analyses and N100/P200/N200

Sensory-driven analyses are indexed by early ERP components of N100, P200, and N200, which represent different aspects of neuronal responses involved in the processing of sensory data, their initial categorization, and assigning salience/relevance in the context of a task. Furthermore, these processes have been demonstrated to interact with early attentional and short-term memory processes. Since these ERP components are stimulus bound, their neural sources depend on the modality of the information to be processed, i.e., on whether it is auditory or visual information. All three components have been extensively studied in schizophrenia, with most studies reporting reductions in their

amplitude. Early studies focused on documenting abnormal sensory processes in schizophrenia (e.g., Alain et al. 2001), leading to the hypothesis that clinical symptoms and cognitive impairments seen in this disorder stem from faulty initial processes (e.g., Javitt and Sweet 2015; Shin et al. 2012), with N100 and P200 regarded as genetic endophenotypes and quantitative biological markers of response outcome (Rissling and Light 2010; Salisbury et al. 2010).

However, some studies point out a lack of association between N100 reduction and a risk of developing schizophrenia. For example, van Tricht et al. (2010) reported a lack of N100 and P200 reduction in ultra high risk individuals, but a reduction in the P300 amplitude. A recent study by Morales-Munoz et al. (2017) also suggested that the model of complex cognitive deficits inexorably arising from impairments in simple sensory processes may not capture the complicated nature of schizophrenia pathology. In that study, using a three-stimulus auditory paradigm, deficits were found in first episode schizophrenia in the P2 and P3 components, but not in N1 and P1. Furthermore, the P2 and P3, but not the early components, correlated with the MATRICS Consensus Cognitive Battery (MCCB) attentional and speed of processing measures. A somewhat similar conclusion has been reached for the visual modality by Oribe et al. (2013), who found abnormalities in prodromal individuals in P300 but not in the N1.

Thus, overall, while there is strong evidence that sensory abnormalities exist in schizophrenia, there is some debate as to whether sensory deficits are first harbingers of a schizophrenia disease process, as will be discussed in more detail in later parts of this review.

14.2.2.1 Early Sensory Components and Neurochemical Imbalance

Similar to the MMN impairments discussed above, impairments in early sensory processes have been proposed to be associated with deficits in neurotransmission at N-methyl-d-aspartate (NMDARs) glutamate receptors. Holliday et al. (2017) tested the effects of ketamine in monkeys and suggested the abnormal excitatory/inhibitory balance contributing to the reductions of N100. NMDAR has been also implicated in predictive coding that was suggested to contribute to cognitive dysfunction in schizophrenia and is discussed in greater detail in Sect. 14.2.2.2. The role of NMDAR in predictive coding has been examined in the paradigm with two conditions: talk and passive listen: 34 schizophrenia patients and 31 healthy controls participated in the study. N100 suppression was reduced both in schizophrenia patients, and by ketamine in HC (Kort et al. 2017) suggesting that indeed NMDA receptors play a role in predictive coding and its abnormalities in schizophrenia.

A role of serotonin in sensory abnormalities indexed by N1/P2 has been examined in a group of studies using auditory stimuli focusing on the loudness dependence auditory evoked potentials (LDAEP), as expressed by N1/P2 ratio (e.g., Gudlowski et al. 2009; Juckel et al. 2003, 2008; Wyss et al. 2013) as indicators of serotonergic contribution to schizophrenia dysfunction. Based on both human and animal studies, weak LDAEP is associated with high serotonergic activity, whereas strong LDAEP is associated with low serotonergic activity (Kayser et al. 2001; Gudlowski et al. 2009). This association is quite helpful since another valid indicator of serotonergic transmission does not exist. In the Gudlowski et al. (2009) study in 60 high risk for developing psychosis individuals, 34 first episode, 28 chronic schizophrenia patients, and 57 healthy controls, weak LDAEP was found in all clinical groups including prodromal individuals relative to healthy controls, suggesting that higher serotonergic tone may exist before psychosis onset and be one of vulnerability markers. This upregulated serotonergic tone seems to remain high in all groups of subjects (Juckel et al. 2008; Gudlowski et al. 2009).

Overall, these studies suggest that unlike MMN, N1/P2 abnormalities may depend on both glutamate and serotonergic system abnormalities, including the fact that these abnormalities may precede psychosis onset.

14.2.2.2 Early Sensory Components as Indices of Specific Auditory Sensory Impairments

In addition to several early studies that examined auditory sensory abnormalities (e.g., Salisbury et al. 2010), more recent studies have focused on two processes: auditory predictive coding and categorization processes as they relate to pathophysiology of schizophrenia. Predictive coding refers to the ability of an organism to predict consequences of its own actions and has been demonstrated to exist across several species. Predictive coding is critical to being able to flexibly adjust motor programs such that they would result in desired behavioral consequences (Kort et al. 2017). In schizophrenia, predictive coding has been studied in the context of corollary discharge mechanism, most extensively in designs probing speech perception.

Since corollary discharge allows for distinguishing between self-generated actions and externally generated information, it has been hypothesized that abnormalities here may lead to positive symptoms, most notably auditory hallucinations. N100 has been used as a marker of auditory corollary discharge, as it has been demonstrated to be sensitive to auditory cortex responses during talking and during listening to self-generated speech; it is reduced when subjects engage in talking relative to when they are engaged in listening.

Accordingly, all studies that have examined this phenomenon in schizophrenia report that this N100 reduction was diminished in schizophrenia patients (Ford 2016; Ford et al. 2001a, b, c, d, 2004, 2007, 2013, 2014), with most studies suggesting an association with positive symptoms. In some of these studies correlations with auditory hallucinations have also been found (Ford et al. 2004), while in other studies they have not (Ford et al. 2001a, b, c, d). Randeniya et al. (2018), in their review of the corollary discharge mechanism, couch it in terms of the theory of prediction errors and fundamental to the disease. Recently, Kort et al. (2017) explicitly tested the hypothesis that NMDA hypofunction is associated with predictive coding impairment in schizophrenia as described in Sect. 14.2.2.1. In addition, Whitford et al. (2011, 2018) associated the abnormal N100 suppression with structural abnormalities in the arcuate fasciculus, a fiber bundle connecting the frontal and temporal regions. This result dovetails nicely with the concept of inefficient corollary discharge mechanism, as the arcuate fasciculus carries auditory sensory information from the temporal to the premotor frontal regions, and thus its compromised integrity could contribute to abnormalities in corollary discharge.

Finally, deficits in automatic stimulus classification using a phonetic task were found to be associated with reductions in N100 and N200 (Kayser et al. 2001). Diminished ability to process sound complexity as expressed by reduced N100 and P200 was reported by Wu et al. (2013). Such deficits can contribute to sound misattribution and be another contributing factor to auditory hallucinations.

Overall, most studies using auditory paradigms that tap into processes indexed by N100 and P200 were focused on elucidating neurocognitive mechanisms that contribute to positive symptoms and auditory hallucinations. Most of these studies pointed to abnormal predictive coding as an underlying cause of both positive symptoms and auditory hallucinations in schizophrenia. Further, deficits in predictive coding have been associated with NMDAR hypofunction and with structural abnormalities in the arcuate fasciculus.

14.2.2.3 Early Sensory Components as Endophenotypes

Several other studies supported the idea of N100 as an endophenotype. The Foxe et al. study (2011) used an auditory simple tone paradigm to examine N100 as an endophenotype. This study reported reduced N100 in chronic and first episode patients, but also in their relatives. High genetic heritability was shown for both N100 and P200 in a large group of monozygotic and dizygotic twin studies (Anokhin et al. 2007). Further support for N100 as a marker of genetic vulnerability comes from the Force et al. (2008) study in a dichotic listening paradigm, in which N100

reductions were observed in both schizophrenia patients and their relatives, but not in bipolar patients or their relatives.

Thus, while a number of studies suggest N100 to be an endophenotype for schizophrenia, this is more limited relative to the number of studies in support of MMN as an endophenotype.

14.2.2.4 Early Visual Sensory Components as Indices of Specific Early Visual Impairments

In addition to auditory processes, the N1/P2 components have been used in the study of the visual system and its abnormalities in schizophrenia. As in the case of MMN and of N1/P2 auditory studies, the questions posed by these studies were aimed at understanding what specific processes were abnormal in schizophrenia and what their functional consequences were. The studies have focused on two major topics: the relative contribution of subcortical magnocellular and parvocellular pathways—which project to dorsal and ventral cortical streams—and on visual working memory impairment. Most of the studies suggest that the deficit is in the magnocellular pathway, as indexed by the early N1/P2 potentials, and may be a trait biomarker for psychosis (e.g., Koychev et al. 2011). Across studies, several different designs have been used to bias visual processing either towards the magnocellular or parvocellular pathway. The examples include using low special frequency (magnocellular), or high spatial frequency (parvocellular) stimuli (e.g., Butler et al. 2007), or stimuli contrast sensitivity (Dias et al. 2011). Magnocellular impairment at the subcortical level, found in most of these studies, leads to impairment at the cortical level that, in turn, impacts dorsal and ventral processing streams (e.g., Butler et al. 2007; Schechter et al. 2005). The ERP indices of these impairments have been both N1 and P2 components. For example, Doniger et al. (2002) probed the function of the dorsal and ventral visual stream with the study of closure perception in patients with chronic schizophrenia, and concluded, based on the reduced P1 amplitude over dorsal sites, that the dorsal processing pathway was a major contributor to visual impairments and to visual distortions sometimes reported in schizophrenia. A similar conclusion has been reached by Foxe et al. (2001), who reported the P2 but not N1 impairment over dorsal sites in a task that required line drawing processing in a group of schizophrenia and healthy control individuals.

A handful of studies have focused on visual working memory contribution as one more source of visual impairment in schizophrenia. For example, Lynn et al. (2016) used a delayed visuospatial working memory task to examine N1 responses in a memory retrieval task. N1 responses related to the retrieval process were impaired in chronic schizophrenia patients relative to healthy controls and unaffected patients' relatives, with N1 responses in the relatives falling between SZ and HC. Similarly, Zhao et al. (2011) suggested that visual working memory impairments in schizophrenia may be related to early processes associated both with encoding and with retrieval, as evidenced by reduced N1 and P2 at both the encoding and retrieval stages.

Kayser et al. (2012) examined early N1and P2 potentials in the working memory paradigm for words and faces in both auditory hallucination (AH) and non-AH schizophrenia patients and found deficits in the visual N1 in the hallucinating vs. non-hallucinating group. The authors linked these early deficits with deficits in perceptual integration, which they suggested may be present in both visual and auditory modalities leading to the hallucinatory experience. The interaction between bottom up and top down deficits in schizophrenia was examined by Neuhaus et al. (2011a, b), who employed a visual attention paradigm where both cue and target N1 were analyzed. Both types of N1 were reduced in schizophrenia, with both partially localized to the posterior parietal cortex. At the same time, bottom up N1 was associated with the right parietal lobe while target, top down N1 was associated with the anterior cingulate cortex, in keeping with the role of parietal cortex in mediating sensory-driven processes, and of anterior cingulate cortex in mediating selective attention.

Together, studies that examined N1 and P2 abnormalities in visual modality suggest that

the magnocellular subcortical pathway, is abnormal in schizophrenia and that this abnormality leads to cortical dorsal visual stream abnormalities, which, in turn, contribute to visual distortions and visual hallucinations in schizophrenia. Furthermore, some studies suggest that visual working memory processes may further contribute to visual impairment in schizophrenia.

14.2.2.5 Early Olfactory Sensory Components

There have also been efforts to use N1 and P2 components to examine olfactory processes and their deficits as predictors of psychosis. While reduced ERPs to odors have been found in chronic schizophrenia (e.g., Kayser et al. 2010; Turetsky et al. 2003), Kayser et al. (2013) did not find group differences in N1/P2 in a clinical high risk group (CHR). However, CHR showed less N1/P2 sensitivity to odor intensity and lower amplitude of these potentials was associated with more negative symptoms in this clinical group, suggesting that early sensory processes in the olfactory domain are also affected in CHR individuals. Turetsky et al. (2008) found reduced N1 in the unaffected relatives of schizophrenia patients and suggested that this deficit may be a genetically mediated vulnerability marker.

14.2.2.6 Summary

Studies that used paradigms examining N1 and P2 responses in both the auditory and visual modality have focused on the nature of cognitive sensory processes that are abnormal in schizophrenia and their relationships to symptoms, especially to auditory and visual hallucinations. Studies in the auditory modality point to an abnormality in predictive coding as a probable mechanism that can lead to attributing internally generated signals to outside causes, and thus to auditory hallucinations. In addition, both glutamatergic and serotonergic systems' impairments have been implicated in abnormalities of N1 and P2 in schizophrenia. Studies in visual modality have examined the two major processing streams: the magnocellular and parvocellular pathways, and have concluded that it is the magnocellular processing pathway that plays a major role in abnormal visual experiences, including visual hallucinations, in those diagnosed with schizophrenia (Table 14.2).

Table 14.2 Early sensory components in schizophrenia

Citation	Subjects	Paradigm	ERP measures	Main findings
Ford et al. (2001a)	7 SZ and 7 HC	A task with vowels spoken and played-back (listen)	N1	The reduction of N1 elicited by spoken vowels observed in HC but not in SZ
Ford et al. (2001b)	24 SZ, 32 HC, 6 EPI-SZ and 16 EPI-nSZ	Visual and auditory oddball tasks	N1	N1 reduced only in SZ, but not in EPI
Ford et al. (2001c)	15 SZ and 15 HC	Visual and auditory task with three conditions: (1) inner speech; (2) directed inner speech with repeating a statement silently; (3) listening to recorded speech	N1	N1 elicited by acoustic stimuli, but not by visual stimuli, was lower during directed inner speech than during the silent baseline condition in HC but not in SZ
Ford et al. (2001d)	12 SZ and 10 HC	Visual and auditory task during talking aloud, listening to one's speech played back, and silent baseline	N1	Acoustic N1 was affected by talking and listening, but visual N1 was not Acoustic N1 was reduced during talking compared with baseline in HC, but not in SZ; N1 was reduced during listening in both SZ and HC

Table 14.2 (continued)

Citation	Subjects	Paradigm	ERP measures	Main findings
Foxe et al. (2001)	14 ChSZ and 16 HC	A visual task with line drawings of animate and inanimate objects	N1, P1	P1 amplitudes were reduced across all conditions for ChSZ vs. HC; No between-group differences in N1 amplitude
Kayser et al. (2001)	66 SZ / SA and 32 HC	Two oddball tasks using consonant-vowel syllables or complex tones	N1, N2	The reduction of N1 and N2 amplitude was task-independent in SZ
Doniger et al. (2002)	16 ChSZ and 16 HC	A visual reorganization task	P1, N1, N(cl)	Visual N1 was intact in SZ; Visual P1 reduced in SZ and N(cl) impaired in SZ
Juckel et al. (2003)	25 medication-free SZ and 25 HC	An auditory task using increasing tone loudness	LDAEP	Primary auditory cortex but not the secondary auditory cortex reflected by LDAEP source analysis was weaker in SZ relative to HC; LDAEP in the right hemisphere tended to be increased after 5-HT(2) antagonists treatment in SZ
Turetsky et al. (2003)	21 SZ and 20 HC	An olfactory detection task	N1	Olfactory N1 amplitude was abnormal in SZ and related to odor detection threshold sensitivity
Ford et al. (2004)	Study 1 & 4: 12 SZ and 10 HC; Study 2: 7 SZ and 7 Hc; Study 3: 15 SZ and 15 HC	Auditory tasks during salient baseline, speaking out loud, listening to played-back speech and inner speech	N1	N1 was reduced during talking and inner speech in HC but not in SZ
Schechter et al. (2005)	74 SZ/SA and 59 HC	A visual task with low (M), chromatic (P) and high (mixed M/P) contrasts	N1, P1	The reduction of P1 and N1 amplitudes across conditions observed in SZ; but only reduction of P1 amplitude survived covariation for between group differences in visual acuity
Anokhin et al. (2007)	54 monozygotic and 55 dizygotic twin pairs	A dual-click auditory task	N1, P2	Heritability of N1 and P2 gating was high and significant
Butler et al. (2007)	23 SZ/SA and 19 HC	Two visual tasks	C1, P1, N1	Visual P1 in response to magnocellular-biased checker stimuli decreased more in SZ than HC; The reduction of C1, P1 and N1 amplitude to magnocellular-biased low spatial frequency stimuli observed in SZ, but not to parvocellular-biased high spatial frequency stimuli
Ford et al. (2007)	27 SZ/SA, and 26 HC	Talking, agency and expectancy experiments	N1	N1 suppression was greatest when elicited by talking in HC, but not in SZ. Modest N1 suppression by agency and expectancy observed only in HC

(continued)

Table 14.2 (continued)

Citation	Subjects	Paradigm	ERP measures	Main findings
Force et al. (2008)	19 SZ, 37 first-degree SZ relative, 18 BP, 35 first-degree BP relatives and 36 HC	A dichotic listening task	N1	The N1 reduction observed in SZ and SZ relatives, but not in BP or BP relatives; No significant augmentation of N1 amplitude with attention observed in SZ or in BP
Juckel et al. (2008)	36 male SZ and 26 HC	An auditory task with five-intensity tones	LDAEP	LDAEP was weaker in SZ than in HC
Turetsky et al. (2008)	14 first-degree SZ relatives and 20 HC	An olfactory detection task	N1	N1 amplitudes reduced in SZ relatives to stimuli presented in the left nostril
Gudlowski et al. (2009)	60 at-risk for schizophrenia, 34 FESZ, 28 ChSZ and 57 HC	An auditory task with five-intensity tones	LDAEP	LDAEP was weaker in prodromal patients than in HC, but similar to FESZ and chronic SZ; In a subsample of prodromal patients, LDAEP values remained the same after retesting 10 months later
Kayser et al. (2010)	32 SZ and 35 HC	An olfactory detection task	N1	Olfactory ERPs in detection of high and low odor intensities were similar in SZ and HC; However, N1 current source density sink localized to bilateral fronto-temporal regions was reduced in SZ for high odor intensity stimuli
Koychev et al. (2011)	18 schizotypes and 20 HC	A computerized delayed matching to sample working memory task	P1, N1, P2	The reduction of cue-evoked P1 amplitude observed in high schizotypy group vs. HC; N1 and P2 amplitudes didn't differ between the two groups
Salisbury et al. (2010)	55 FHSZ, 56 ChSZ, 55 younger HC and 53 older HC	Two active auditory oddball tasks	N1, P2, the vertex potentials in response to standard stimuli	N1 and P2 were reduced in ChSZ and FHSZ
van Tricht et al. (2010)	61 UHR and 28 HC; 18 UHR+T and 43 UHR+NT	An auditory oddball task	N1, P2	N1 and P2 didn't differ between UHR and HC
Dias et al. (2011)	30 SZ and 17 HC	The AX version of the visual continuous performance task (AX-CPT)	P1, N1	The reduction of P1 and N1 amplitude observed in SZ; N1 deficits contributed independently to impaired behavioral performance
Foxe et al. (2011)	35 SZ, 30 first-degree relatives, 13 FESZ, and 22 HC	An auditory oddball task	N1	N1 amplitude decreased in both SZ and FESZ relative to HC; First-degree relatives also showed a N1 deficit

Table 14.2 (continued)

Citation	Subjects	Paradigm	ERP measures	Main findings
Neuhaus et al. (2011a, b)	33 SZ and 61 HC	A visual selective attention task	N1	Both cue and target N1 amplitude reduced in SZ; Bottom-up and top-down N1 deficits in SZ were associated with partially overlapping current density deficits in posterior cortex, while differential deficits were observed in the right parietal lobe for bottom-up N1 and in anterior cingulate cortex for top-down N1
Whitford et al. (2011)	ERP: 21 SZ and 25 HC; DTI: 15 SZ and 17 HC	A button-press auditory task	N1	N1 suppression to not delayed, self-generated auditory stimuli was subnormal in SZ, and was eliminated by imposing a 50-ms, but not a 100-ms, delay between the button-press and the evoked stimulus; The 50-ms delay normalized a patient's level of N1 suppression, which was linearly related to the FA of their arcuate fasciculus
Kayser et al. (2012)	26 SZ with AV, 49 SZ without AV and 46 HC	Recognition working memory tasks with words or faces	N1	In both word and face recognition tasks, N1 reduced in SZ with AVH relative to SZ without AVH and HC; N1 difference between SZ with and without AVH was not due to overall symptom severity or performance accuracy
Perez et al. (2012)	75 SZ, 77HC; 39 ESZ, 35 CHR and 36 HC	An auditory task during vocalizations (talking) and listening to played-back speech	N1	Speech-related N1 suppression was attenuated in SZ and ESZ vs. HC N1 suppression values in CHR were intermediate to HC and ESZ and not statistically distinguishable; Age-corrected N1 Talk-Listen difference z scores were not correlated with illness duration in SZ
Shin et al. (2012)	16 UHR, 15 SZ and 18 HC	A passive auditory oddball task	N1m	N1m adaptation occurred in HCs, but not in either UHR or SZ; UHR had values between those for HCs and SZ
Kayser et al. (2013)	21 CHR and 20 HC	An olfactory detection task	N1	N1 varied monotonically with odor intensity and did not differ across groups. N1 reduced in three CHR patients who developed psychosis, and was associated with poorer odor detection and thresholds in these patients

(continued)

Table 14.2 (continued)

Citation	Subjects	Paradigm	ERP measures	Main findings
Ford et al. (2013)	30 SZ, 19 SA, 30 BP, 30 SZ relatives, 23 SA relatives, 50 BP relatives, and 43 HC	An auditory speech task during talking and listening	N1	N1 was suppressed during talking compared to N1 during listening; N1 suppression was significantly reduced in SZ and BPP patients, with a similar trend in the smaller N SA group. Unaffected relatives did not differ from HC or probands
Oribe et al. (2013)	23 prodromal patients, 17 FESZ and 31 HC	A visual oddball task	N1	N1 amplitude was significantly reduced only in FESZ but not in prodromal patients
Wu et al. (2013)	12 SZ and 12 HC	An auditory task	N1, P2	The reduction of N1 and P2 to musical stimuli was significant in SZ; The differences between interval and chord stimuli were not perceived by SZ as compared with HC
Wyss et al. (2013)	13 SZ with predominant negative symptoms and 13 HC	An auditory task with five-intensity tones	LDAEP	LDAEP in both hemispheres was higher in SZ than HC; LDAEP in the right hemisphere in SZ was related to higher scores of negative symptoms, but not to scores of positive symptoms
Ford et al. (2014)	26 SZ/SA and 22 HC	An auditory task with three conditions: button tone, play tone and button alone	N1, the lateralized readiness potential (LRP)	N1 suppression was larger in HC than in SZ; N1 suppression was correlated with LRP amplitude in both groups
Zhao et al. (2014)	20 SZ and 22 HC	A self-referential memory task	P2, N2	P2 elicited in both self- and other-reflection conditions was smaller in SZ; N1 amplitude differed between self- and other-reflection conditions in SZ but not in HC
Oestreich et al. (2015)	37 individuals with high SPQ scores and 37 with low SPQ scores	A task with three conditions: vocalizing syllables (Talk), passively listening (Listen), and Cued listen	N1	N1 amplitude was reduced in the Talk condition than in both the Listen and Cued Listen conditions in low SPQ group; High SPQ group exhibited significantly lower levels of N1-suppression relative to low SPQ group. The Cued Listen condition induced significantly lower N1-amplitudes compared to the Listen condition in the low SPQ group, but not in the high SPQ group
Lynn et al. (2016)	23 SZ, 30 SZ relatives and 37 HC	A delayed response visuospatial working memory task	N1	N1 response to probes during retrieval differentiated between the type and locations of stimuli presented during encoding in HC and SZ relatives, but not in SZ

Table 14.2 (continued)

Citation	Subjects	Paradigm	ERP measures	Main findings
Oestreich et al. (2016)	39 individuals with high SPQ scores and 41 with low SPQ scores	An auditory task with two conditions: actively and passively listening to tones	N1	The low SPQ group exhibited significantly higher N1-suppression to un-delayed tones than the high SPQ group N1-suppression decreased linearly with increasing delays between the button press and the tone in the low SPQ group, but not in the high SPQ group
Holliday et al. (2017)	4 macaque monkeys	A passive auditory oddball task	N1	Peak N1 amplitude was reduced by ketamine, MK-801 and midazolam in the longest SOA condition
Kort et al. (2017)	Study1: 34 SZ and 33 HC; Study 2: 31 HC	A speech-sound vocalization (talk) and passive playback (listen) task	N1	N1 suppression to self-produced vocalizations was significantly reduced in SZ, and similarly reduced by ketamine in HC
Morales-Munoz et al. (2017)	38 FEP and 38 HC	An auditory three-stimulus oddball paradigm	P1, N1, MMN, P2	FEP had lower P2 amplitude; P2 amplitude was associated with MCCB scores on tests of attention and speed of processing in FEP; No group differences in P1, N1 and MMN
Whitford et al. (2018)	51 ESZ, 40 CHR and 59 HC	An auditory task with speech spoken and listened to	N1	N1 suppression to self-generation speech was reduced in ESZ relative to HC, with CHR exhibiting intermediate N1 suppression levels; Fractional anisotropy in the arcuate fasciculus decreased and radial diffusivity increased in ESZ relative to both in HC and CHR. Structural integrity of the pyramidal tract did not differ between groups; Level of N1-suppression was linearly related to the structural integrity of the arcuate fasciculus, but not the pyramidal tract, across groups

AV auditory hallucination, *BP* bipolar disorder, *CHR* clinical high-risk for psychosis, *ChSZ* chronic schizophrenia, *EPI-SZ* epilepsy patients with schizophrenia-like features, *EPI-nSZ* epilepsy patients without schizophrenia-like features, *ESZ* early illness schizophrenia, *FEP* first-episode psychosis, *FHSZ* first-hospitalized schizophrenia patients, *LDAEP* loudness dependence of auditory evoked potentials, *N(cl)* closure negativity, *SA* schizoaffective patients, *SOA* stimulus-onset asynchrony, *SZ* patients with schizophrenia, *SPQ* the Schizotypal Personality Questionnaire, *UHR* ultra high-risk for psychosis individuals

14.3 Event Related Potential Evidence for Schizophrenia as a Disorder of Higher Order Cognition

While studies focusing on early sensory abnormalities in schizophrenia emphasize the pivotal role that these early impairments have in cognitive abnormalities and symptom development in schizophrenia, studies focusing on impairments in attention, memory processes, and language processes view these latter deficits as central to schizophrenia pathology. Furthermore, in many of these studies, the ERPs regarded as indices of higher order cognition are found to be abnormal, but the earlier ERP components indexing sensory

operations are not. The theoretical tension created by these two sets of findings regarding the origins of schizophrenia neuropathology has not been seriously addressed in most of the published studies, with only some of them attempting to resolve this apparent controversy. In the sections below, we focus on studies that probed higher order cognition including memory function, attentional, and executive functions, as well as different aspects of language operations.

14.3.1 P300 and the Study of Schizophrenia

A positive component of a waveform with a peak amplitude around 300 ms, post stimulus, P300, is typically generated by rare stimuli presented within a series of frequent stimuli in either auditory or visual modality in a task that requires participants to pay attention to rare stimuli. P300 abnormalities are one of the best documented impairments in schizophrenia (see meta-analyses Jeon and Polich 2001, 2003; Qiu et al. 2014). The P300 component with a parietal scalp distribution, or P300b, is believed to index attention and working memory processes, while frontally distributed P300a is believed to index orienting and salience processes. Within these two broad categories, studies using P300 as a dependent variable have addressed several important issues. Such studies have attempted to establish what brain generators underly scalp recorded P300, they have examined correlations between schizophrenia symptoms and cognitive impairments, they have used the P300 as an index of specific cognitive operations, and they have tested the utility of P300 as an endophenotype and biomarker, as well as the role of medication in improving the P300 response.

14.3.1.1 P300 and Its Neural Generators

Studies focusing on P300 generators point to the fronto-temporo-parietal network of brain regions associated with attention, attentional control, and working memory. While there exist differences among specific studies depending on the methodology used, most of them report structural and/or functional abnormalities, which span these regions. For example, Bachiller et al. (2015) conducted a low resolution brain electromagnetic tomography study of P300a and P300b neural sources and their distribution in schizophrenia. The authors found different sets of sources for the P300a and P300b, with P300a generators impacted by schizophrenia disease processes in the right superior, medial, and middle frontal gyrus, and P300b generators showing lower activity in bilateral frontal structures and in the cingulate. A study of Heschl's gyrus volume and its resting state connectivity found these two measures to be correlated with P300 amplitude, suggesting that both Heschl's gyrus volumetric reduction and its abnormal connectivity contribute to P300 abnormalities in schizophrenia. Takahashi et al. (2013) associated P300a deficits with the reduction in neural activity within the fronto-temporo-parietal networks, reflecting impaired attentional shifting to rare stimuli. A similar conclusion was reached by an fMRI study of attentional re-orienting (Pae et al. (2003), which used a paradigm typically employed to generate P300a. The results suggest an underactivation to novel stimuli in a patient group in a network of regions, involving amygdala-hippocampus, right frontal operculum, and posterior cingulate cortex, as well as the association cortex of temporo-parietal junction, bilateral intraparietal sulcus, and dorsal frontal cortex.

Some studies have examined P300 generators in relation to symptoms. For example, Shim et al. (2014) evaluated P300 as well as the small-world functional connectivity network in the auditory oddball paradigm and showed that patients had lower clustering coefficients and increased path length, suggesting that the small-world network functional network is disrupted in schizophrenia. Both measures correlated with indices of symptoms severity. Kawasaki et al. (2007) associated P300 generators located in the left superior temporal gyrus (STG) with positive symptoms, and those localized to both left STG and medial frontal region with negative symptoms. In turn, Kim et al. (2014a, b) suggested negative symptoms are related to the reduced source activation in the

fronto-temporo-parietal network. A similar conclusion was reached by Pae et al. (2003), who also reported an abnormal current density in fronto-temporal regions in schizophrenia patients. In addition, Iwanami et al. (2002) suggested that the left lateralized deficit in P300 may be related to chronicity and more severe symptoms.

Finally, a few studies suggest that reduction in P300 amplitude may be due to the temporal jitter in the neural circuits involved in P300 generation (e.g., Ergen et al. 2008).

In summary, the evidence accumulated thus far, across several approaches to identifying neural generators for P300a and P300b, suggests that these two ERP components are associated with a widely distributed set of neural generators that include both auditory regions of the temporal lobe and association areas of the frontal and parietal lobes. Not surprisingly, these brain regions are involved in attentional, working memory, and executive functions, which are indexed by the P300 component as reported in numerous studies discussed below.

14.3.1.2 P300 as an Index of Memory, Attentional, and Executive Functions

While there is broad agreement that P300 indexes attentional and working memory processes (e.g., Galletly et al. 2007), several studies have used designs to examine specific aspects of these processes. For example, Gaspar et al. (2011) showed how working memory load impairment impacts attentional processing in schizophrenia. The authors demonstrated that increased working memory load reduced P300 amplitude in HC, while in the patient group, P300 amplitude did not reduce further with increasing load, but remained low and unchanged regardless of the load. These results suggest that there exists a ceiling effect for attentional resources in schizophrenia: patients use all their attentional resources at a low working memory load, and thus P300 cannot be reduced any further.

Several recent studies examined an inhibitory function, an aspect of the executive process, in schizophrenia patients using a Go/NoGo paradigm where P300 is recorded to two types of stimuli: one requiring a response, and another requiring an inhibition of a response. Results have been mixed. Some studies have reported an impairment in the inhibitory function while other did not. For example, Araki et al. (2016) reported intact P300 amplitudes to both Go and NoGo conditions in schizophrenia, but individual differences in P300 amplitude were associated with a level of Global functioning. Similarly, Ford et al. (2004) found that inhibiting a response was easier for schizophrenia patients than for HC. However, HC used a more complex system of brain regions relative to the patient group to complete the task.

In contrast, several studies have found reduced P300, especially in the NoGo inhibitory condition (Ertekin et al. 2017; Weisbrod et al. 2000). In addition, in a visual task of inhibition and conflict resolution (attentional network test (ANT)), P300 amplitude was reduced and latency prolonged in the conflict condition only (Neuhaus et al. 2007). Overall, it appears that inhibitory function is compromised in schizophrenia, with patients finding it either more difficult to inhibit the response or using a less efficient set of neural processes to achieve the goal.

A handful of studies have used the P300 paradigm to examine the allocation of attentional resources. For example, Kogoj et al. (2005) suggested that patients with schizophrenia have impairments in the flexible allocation of attention between target and distractor stimuli. Accordingly, reduced P300 novelty has been associated with distractibility in chronic schizophrenia (Cortinas et al. 2008).

Another group of studies has used the P300 paradigm to examine executive processes of integrating information across levels of analysis and brain regions. For example, Vianin et al. (2002) used a gestalt figure task where geometrical shapes were recognized in either figure or non-figure conditions. The authors reported that the P300 was significantly reduced in the figure condition, suggesting a failure to integrate information across frontal and parietal regions. Top down attentional processes have been also found impacted in a visual task that manipulated early visual processes and focused attention

(Berkovitch et al. 2018). In a somewhat different approach, Johnson et al. (2005) used stimuli that tested local and global processes, with results suggesting a primarily global visual deficit in schizophrenia, again pointing to difficulties with information integration.

The study of reward anticipation by Vignapiano et al. (2016) further supports the idea of inability to integrate relevant information in the service of task demands. Schizophrenia patients did not show a larger P300 in anticipation of reward, in contrast to healthy controls. Furthermore, the P300 in patients was larger to a larger loss, while in healthy controls it was larger to a larger reward. In addition, P300 to large magnitude incentives was inversely related to social anhedonia.

Finally, Zhao et al. (2014) examined P300 response in the context of a self-referential task where stimuli either refer to the subject or to another person. In healthy controls, self-referential items were better remembered than those that were not self-referential. This bias was absent in the patient group and, importantly, parietal P300 correlated with the self-referential memory score in the patient group only.

Overall, P300 studies that examined what cognitive processes are impaired in schizophrenia point to reduced working memory capacity, impairments in inhibitory function, flexible allocation of attentional resources, integrating information across different levels of analysis in the service of goals, and impaired memory processes associated with self-referential thinking.

14.3.1.3 P300 as an Endophenotype and a Biomarker

Several studies, including several reviews of the literature and meta-analyses, have suggested that P300 can be regarded as a biomarker of vulnerability for schizophrenia. Evidence of P300 amplitude reduction has been found in unaffected relatives of schizophrenia and in clinical high risk (CHR) samples (Bharath et al. 2000; Bramon et al. 2004a, b, 2005; Earls et al. 2016; Groom et al. 2008; Hall et al. 2007; Hoshino et al. 2005; Kim et al. 2018a; Lee et al. 2010; Ozgurdal et al. 2008; Turetsky et al. 2015; van der Stelt et al. 2005). P300 latency prolongation has also been found in the group of unaffected relatives (Karoumi et al. 2000), and P300 functional connectivity has been found reduced in both schizophrenia patients and their siblings (Winterer et al. 2003). Tang et al. (2019) found evidence that P300 novel distinguishes between those CHR who converted to psychosis and those who do not in a large CHR study. Likewise, Jahshan et al. (2012a, b) found that P300a abnormality exists across the entire schizophrenia spectrum, including individuals at high risk for psychosis.

However, not all studies have endorsed P300 as an endophenotype. For example, Chen et al. (2014) found no differences in P300 amplitude or latency between first episode drug naïve schizophrenia patients and healthy controls, suggesting that P300 remains intact even as first rank symptoms of psychosis develop. Similarly, De Wilde et al. (2008) found that P300 deficits were present in patients with first episode schizophrenia, but not in their unaffected relatives, in contrast to evidence of both genetic and phenotypic vulnerability suggested by studies discussed above. Similar results have been reported by Sumich et al. (2008) and Winterer et al. (2001). Sharma et al. (2011) examined twins discordant and concordant for schizophrenia: while concordant twins showed lower P300 amplitude relative to affected discordant twins, discordant affected and unaffected twins did not differ significantly from each other or from control twins, suggesting different degrees to which schizophrenia can be mediated genetically. Studies examining P300 as an index of attentional and orienting responses have found that attentional processes in unaffected relatives of schizophrenia were impaired, while orienting and novelty detection remained intact (Andersen et al. 2016).

Chronicity versus first episode status has been associated with differences in P300a in the study by Del Re et al. (2015). In contrast, Devrim-Ucok et al. (2006) found that it was P300b that distinguished between chronic and first episode patients with P300a being intact. However, Devrim-Ucok et al. (2016) reported a lack of progressive reduction in P300b in first episode

patients over a 6 year period, suggesting that it does not track chronicity.

While there is some disagreement about the status of P300 as an endophenotype, most well powered studies and meta-analyses suggest that P300 indexes both abnormalities at the clinical high risk stage and in individuals at genetic risk for psychosis.

14.3.1.4 P300 as an Index of Symptom Profiles and Severity

Yet another group of studies examined the relationship between P300 and symptoms. An association between symptoms and P300 amplitude was tested by Mathalon et al. (2000a). The authors analyzed both auditory and visual P300 in a design that tracked both P300 and symptoms measured with Brief Psychiatric Rating Scale (BPRS) over multiple occasions. The study found that P300 amplitude changed as a function of symptom severity: getting larger with symptom improvement and smaller with symptom exacerbation.

Most robust results were obtained for the relationship between P300 and positive symptomatology. For example, Fisher et al. (2010) reported that reduced P300a was associated with auditory hallucinations, especially in the context of exacerbation of symptoms (Fisher et al. 2014). Frodl et al. (2002) and Kirihara et al. (2005, 2009) reported that the extent of P300 reductions was associated with more severe thought disorder symptoms. Furthermore, higher scores on thought disorder indices have been correlated with reduced P300 at the left temporal region, relative to the right temporal region. A similar conclusion was reached by Iwanami et al. (2000), who found that P300 in patients with thought disorder was significantly reduced compared to those without thought disorder. Similarly, Meisenzahl et al. (2004) and Higashima et al. (2003) reported that P300 in the left hemisphere correlated with positive symptoms both in cross-sectional and longitudinal data.

Some studies have reported a relationship between P300 and negative symptoms. For example, negative symptoms have been associated with more reduced and prolonged P300 (Liu et al. 2004). Turetsky et al. (2009) reported that reduced P300a and P300b were associated with avolition, attentional disturbances, and delusions.

A group of studies examined a relationship between P300 and age of onset as well as illness duration. Mathalon et al. (2000b) reported that P300 amplitude correlated positively with the age of illness onset and negatively with illness duration, while P300 latency correlated positively and strongly with age in the patient group and weakly in the control group. Thus, most severe P300 abnormality was observed in patients with early age of illness onset and its longest duration. Similarly, Mori et al. (2007) reported an association between P300 latency and illness duration. In contrast, Neuhaus et al. (2011a, b) reported that visual P300 was independent of illness duration, since it was found similarly impacted in recent onset and chronic schizophrenia in a visual Attention Network Test.

Finally, Van der Stelt et al. (2004) examined P300 auditory and P300 visual in patients at different stages of illness and found impairments in both of these components but not in the earlier sensory ones across all stages of illness chronicity. Therefore, the authors made a case for schizophrenia being associated primarily with deficits in cognitive integrative functions that make it difficult to engage in behaviors guided by the context of previously presented information.

Together these studies suggest that cognitive impairments indexed by P300 contribute primarily to positive symptoms, even though sensitivity to overall symptom severity was also noted. In addition, it appears that auditory P300 is influenced by both age of onset and illness duration such that the lowest P300 amplitudes are found in patients with early onset and long illness duration.

14.3.1.5 P300 and Diagnostic Specificity

Several studies examined P300 in the context of diagnostic specificity. Two types of questions have been asked in these type of studies: whether there are differences in cognitive impairments

indexed by P300 within major psychiatric disorders, and whether the P300 impairments found in schizophrenia are also found in other disorders that are characterized by attentional deficits.

Accordingly, some studies that examined differences in attentional processes between schizophrenia and bipolar disorder suggested less impairment in bipolar disorder than in schizophrenia (Bestelmeyer 2012; Bestelmeyer et al. 2009; Kaur et al. 2013). Similarly, Mathalon et al. (2010a, b) reported that patients with schizoaffective disorder, relative to schizophrenia patients, had larger P300 amplitude, which were comparable to healthy controls, but P300 latency was delayed in both groups. The distinction between P300b in schizophrenia patients and patients with affective psychosis was also reported by McCarley et al. (2002) with less impairment found in affective psychosis. However, some studies found comparable P300 deficits in both clinical groups (Ethridge et al. 2012; Johannesen et al. 2013; O'Donnell et al. 2004). Kaur et al. (2011) tested first episode schizophrenia and schizoaffective patients and concluded that auditory attentional impairments as expressed with P300a are common to both subject groups

Differences in inhibitory processes impairments between bipolar, schizophrenia, and schizoaffective disorder were probed with a Go/NoGo task (Chun et al. 2013), with results suggesting significant differences on this task between bipolar and schizophrenia patients, but not between schizophrenia and schizoaffective patients.

Among studies that compared schizophrenia to other disorders, Itagaki et al. (2011) compared attentional deficits in ADHD and schizophrenia and concluded that while both groups had reduced P300 amplitude, the schizophrenia group also showed increased P300 latency, suggesting that the attentional impairment in schizophrenia is more severe.

Another comparison has been made between obsessive compulsive disorder (OCD) and schizophrenia in terms of the extent of cognitive impairment, especially as related to attentional function (Kim et al. 2003). The results suggested wide spread attentional deficits in schizophrenia, with OCD patients showing more limited deficits of controlled attention and self-guided flexible behavior.

Overall, it appears that schizophrenia patients are more impacted by attentional/working memory deficits relative to both schizoaffective and bipolar patients, and that in spite of some similarities between schizophrenia and ADHD and OCD individuals, more severe attentional deficits exist in schizophrenia relative to the two other disorders.

14.3.1.6 P300 and Medication Effects

A handful of studies examined a role of medication in ameliorating cognitive symptoms as indexed by the P300. Several studies examined the effect of olanzapine, reporting inconsistent results. Gonul et al. (2003) reported that olanzapine used in previously unmedicated patients contributed to P300 improvement after 6-week treatment, with greater effect observed for the P300a than P300b whose amplitude remained below HC. Similarly, Higuchi et al. (2008) reported that 6-month treatment with olanzapine improved P300 source density only in the left STG, along with improvements in both positive and negative symptoms and verbal learning memory. However, some studies did not find the effect of olanzapine on either P300 amplitude or latency in spite of clinical and cognitive improvement (Molina et al. 2004).

Modest improvements of P300 amplitude after clozapine were reported by Niznikiewicz et al. (2005). Park et al. (2010) reported improvements in both P300 amplitude and latency after treatment with quentiapine. Su et al. (2012) conducted a meta-analysis of antipsychotic treatment effects in China and concluded that both P300 amplitude and latency improve after treatment.

On balance, it appears that medication, both olanzapine and clozapine, may have some beneficial effects on attentional/working memory function as probed with P300.

14.3.1.7 Summary

Studies using P300 as an index of attentional and working memory operations in schizophrenia

have identified several specific operations, which are abnormal in this disorder. These include compromised working memory capacity, lack of flexibility in deploying attentional resources, abnormal inhibitory function, and difficulty in integrating information across different levels of cognitive analysis. The P300 generators have been localized to a distributed network of fronttemporo-parietal sources, with some studies associating particular symptom profiles with volume reductions in specific brain regions, with positive symptoms being associated with the temporal lobe reductions. Overall, most studies associate P300 reductions with positive symptoms, including auditory hallucinations and thought disorder. There is also evidence of the relationship between P300 reductions and age of onset and illness duration. In terms of distinctions between P300 abnormalities in schizophrenia relative to other psychiatric disorders, and relative to clinical conditions characterized by deficits in attention, schizophrenia seems to be associated with more severe P300 abnormalities, and thus with more severe attentional and working memory deficits, relative to other disorders. Most studies suggest that P300 can be considered to be a biomarker and endophenotype for schizophrenia. Finally, it appears that some antipsychotic medications may improve P300 response (Table 14.3).

Table 14.3 P300 in schizophrenia

Citation	Subjects	Task	Main findings
Iwanami et al. (2000)	29 ChSZ	A standard oddball task	P300 amplitude was negatively correlated with the severity of thought disorder; SZ with thought disorder showed smaller P300 amplitude than those without
Karoumi et al. (2000)	21 SZ, 21 SZ siblings and 21 HC	An auditory oddball task	SZ exhibited reduced P300 amplitude relative to HC; SZ siblings showed prolonged P300 latency
Mathalon et al. (2000a)	36 male SZ and 34 male HC	An auditory oddball task and a visual oddball task	Amplitudes of auditory P3a and P3b but not visual P3b were smaller in SZ than in HC; Auditory and visual P3b amplitudes tracked negative symptoms, while auditory P3a tracked depression-anxiety symptoms in SZ
Weisbrod et al. (2000)	16 SZ and 16 HC	An auditory Go/Nogo task	Both SZ and HC showed similar pattern of a fronto-central P3 in the Go condition; In the NoGo (inhibitory) condition, HC showed a left lateralization of P3 but SZ did not
Winterer et al. (2001)	42 SZ, 62 SZ siblings and 34 HC	An auditory oddball task	SZ showed a reduction of P300 amplitude in the range of 54%-58% over the left parieto-temporal area relative to HC but SZ siblings did not; P300 latencies were not prolonged in both SZ and SZ siblings relative to HC
Frodl et al. (2002)	50 SZ	An auditory oddball task	SZ with more thought disorder showed a smaller P300 amplitude which remained reduced after stabilization on medication; Reduced P300 was correlated with illness duration in SZ with a later age of onset
Iwanami et al. (2002)	57 SZ and 33 HC	An auditory oddball task	P300 amplitude at T3 was not smaller than at T4 in SZ; Lateral topographical distribution of P300 amplitude did not differ between SZ and HC; SZ patients with lower P300 at T3 were older and received higher doses of antipsychotic medicine than those with high P300 at T3

(continued)

Table 14.3 (continued)

Citation	Subjects	Task	Main findings
McCarley et al. (2002)	15 FESZ, 18 patients with affective psychosis and 18 HC	A standard oddball task	FESZ showed a smaller P300 in the left hemisphere than in the right, and smaller gray matter volume of the left posterior STG, left planum temporale and Heschl's gyrus than HC and patients with affective psychosis; Gray matter volume loss in the left posterior STG and left planum temporale were positively correlated with left temporal P300 amplitude only in FESZ
Vianin et al. (2002)	10 SZ and 14 HC	A gestalt recognition task	SZ showed smaller P300 amplitudes than HC during correct figure detection trials; HC showed an earlier, more positive and widely distributed P300 than SZ in the analyses of the differences between the figure and non-figure conditions
Gonul et al. (2003)	26 unmedicated SZ and 20 HC	An auditory oddball task	Unmedicated SZ showed attenuated and delayed P300 before the treatment compared to HC; After 6-week treatment with olanzapine, frontal P300 amplitude was normalized, parietal P300 amplitude remained below that of HC and P300 latency was not affected; No correlation between P300 and symptoms was observed either before or after treatment
Higashima et al. (2003)	93 SZ and 36 HC in the cross-sectional study and 20 of SZ in the longitudinal study	An auditory oddball task	P300 amplitude was negatively correlated with the positive but not with the negative syndrome scale score in SZ; Changes in P300 amplitude and in positive syndrome scores between the first and second test were negatively correlated; These correlations were found in P300 amplitude in the left, but not in right, posterior temporal region
Pae et al. (2003)	20 right-handed SZ and 21 HC	An auditory oddball task	The sources of P300 were consistently localized to the left superior parietal area in HC, while they were more distributed in SZ; SZ showed a significant P300 current density reduction in the left medial temporal area and left inferior parietal area, and current density increases in the left prefrontal and right orbitofrontal areas; The left parietotemporal area was negatively correlated with PANSS total scores in SZ
Winterer et al. (2003)	64 SZ, 79 SZ siblings, 88 HC	An auditory oddball task	Both SZ and SZ siblings showed a reduction of frontotemporal coherence; During P300 peak time-window, HC showed a negative fronto-temporal path coefficient, whereas SZ showed a positive coefficient and SZ siblings showed an intermediate coefficient
Ford et al. (2004)	11 SZ and 11 HC	A simple No/NoGo task	HC showed a relationship between NoGo P300 and activation in the anterior cingulate cortex, dorsal lateral prefrontal cortex, and right inferior parietal lobule and caudate nucleus; SZ showed a modest relationship between NoGo P300 and activation in the anterior cingulate cortex
Liu et al. (2004)	22 SZ with positive profile, 27 SZ with negative profile and 30 HC	An auditory oddball task	SZ exhibited reduced P300 amplitude relative to HC; SZ with negative symptoms profile showed decreased P300 amplitude and longer latencies

Table 14.3 (continued)

Citation	Subjects	Task	Main findings
Meisenzahl et al. (2004)	50 male SZ and 50 male HC	An auditory oddball task	The symptoms of thought disorder in SZ were correlated with the P300 reduction at T3 and with the gray matter of the left posterior STG; but no reduction of P300 amplitude or left STG gray matter volume, and no association between P300 and gray matter volume was observed in SZ
Molina et al. (2004)	11 SZ and 30 HC	An auditory oddball task	SZ showed overall improvement in positive and negative symptoms, but no changes of P300 amplitude or latency at Pz and Fz after 6-month treatment with olanzapine; there was an association between P300 amplitude increase with olanzapine and the improvement in negative symptoms
O'Donnell et al. (2004)	12 SZ, 13 manic or BP and 24 HC	An auditory discrimination task	Both BP and SZ showed reduced P300 amplitude and prolonged latency
van der Stelt et al. (2004)	22 SZ and 22 HC	A visual and auditory oddball task	SZ showed smaller P3 amplitudes to visual novel and auditory target stimuli than HC; P3 in the left hemisphere was smaller than in the right in SZ; P3 amplitude was negatively correlated with illness duration
Hoshino et al. (2005)	13 neuroleptic-naïve SZ	An auditory oddball task	P300 amplitude was highly correlated with the anxiety/depression factor score and with the positive factor score
Johnson et al. (2005)	24 SZ and 29 HC	A global-local visual task	SZ failed to show an augmented P300 in response to local stimuli
Kirihara et al. (2005)	55 SZ	An auditory oddball task	SZ showed a negative correlation between P300 amplitude and scores on TDI, which was more pronounced in the left temporal region than in the right
Kogoj et al. (2005)	25 ChSZ and 12 HC	An auditory target-detection task	ChSZ showed reduced P300 responses to all target stimuli but equal P300 responses to distractors compared to HC. P300 amplitudes to distractors were reduced in both groups, but only HC showed enlargement of P300 amplitude when the distractors became the target stimuli
Molina et al. (2005)	17 SZ and 25 HC	An attentional task	SZ exhibited lower metabolic activity in the DLPFC but no cortical atrophy, and a reduction of P300 amplitude compared with HC. Right DLPFC metabolic activity was correlated with P300 amplitude
Niznikiewicz et al. (2005)	10 SZ	An auditory oddball task	SZ treated with clozapine showed increased P300 amplitude compared to baseline, off-medication status, but SZ treated with chlorpromazine did not show P300 improvement
van der Stelt et al. (2005)	10 CHR, 10 recent-onset SZ, 14 ChSZ, 14 young HC and 14 older HC	An auditory oddball task	CHR showed smaller P300 amplitudes at the parietal, centro-parietal and central locations than HC; The P300 reduction of P300 in CHR was severe and comparable to that in recent-onset and ChSZ. P300 abnormality was larger over the left temporal sites in SZ, but bilaterally symmetrical in CHR
Devrim-Ucok et al. (2006)	31 FESZ, 36 younger HC, 26 ChSZ and 35 older HC	An auditory oddball task	Both FESZ and ChSZ showed reduced P3b amplitudes vs. HC; ChSZ also showed reduced novelty P3 amplitude relative to HC, but FESZ showed novelty P3 amplitude comparable to HC

(continued)

Table 14.3 (continued)

Citation	Subjects	Task	Main findings
Galletly et al. (2007)	25 SZ and 25 HC	An auditory target detection task	SZ showed a P3 parietal reduction when required to remember a new stimulus, which was correlated with symptom measures of preoccupation and poor volition
Hall et al. (2007)	16 monozygotic twin pairs concordant for SZ, 9 monozygotic twin pairs discordant for SZ and 78 HC	An auditory task	Significant phenotypic correlation with schizophrenia was found for P300 amplitude and latency
Kawasaki et al. (2007)	26 SZ	An auditory oddball task	P300 current density in the left STG and that in the right medial frontal region were negatively correlated with the BPRS total score; The Positive subscale score was correlated with the mean current density in the left STG, while the Negative subscale score was correlated with the mean current densities in the medial frontal region and left STG
Mori et al. (2007)	60 SZ and 70 HC	An auditory oddball task	P300 latency was positively correlated with age in both SZ and HC, and positively correlated with illness duration in SZ; The prolonged latency of P300, associated with age or illness duration, was more prominent in male than in female SZ
Neuhaus et al. (2007)	16 SZ and 16 HC	An attention network test	P300 amplitude was reduced at Pz and P300 latency was increased at Cz for the conflict condition; SZ showed a difference in P300 latency at Cz during late conflict processing, together with a deficit in anterior cingulate cortex
Cortinas et al. (2008)	19 SZ and 19 HC	A visual classification task with auditory stimuli ignored	SZ showed a reduction of novelty P3 in the attention orienting toward distractors task relative to HC
de Wilde et al. (2008)	53 SZ, 27 unaffected siblings, 28 HC	An auditory oddball task	SZ showed a reduction of P300 amplitude but unaffected SZ siblings did not; P300 latency did not differ among three groups
Ergen et al. (2008)	ChSZ and HC	A visual oddball task	SZ showed a reduction of both evoked delta activity and P3 amplitude to target stimuli, but no such difference for the total delta activity
Groom et al. (2008)	30 early-onset SZ, 36 non-psychotic siblings, 36 HC and 36 ADHD	Auditory oddball and visual Go/NoGo tasks	SZ and SZ siblings showed reduced auditory P3 amplitude relative to HC; SZ also showed reduced visual P3 amplitude for NoGo stimuli, but SZ siblings showed reduced visual P3 amplitude for both Go and NoGo stimuli; ADHD showed no P3 reduction in either paradigm
Higuchi et al. (2008)	16 SZ and 16 HC	An auditory oddball task	SZ showed smaller LORETA values on the left side including STG, middle frontal gyrus and precentral gyrus than HC. SZ treated with olanzapine for 5 months had increased P300 source density only in the left STG; The increase in LORETA values in left STG was correlated with improvements of negative symptoms and verbal learning memory, while those in middle frontal gyrus were correlated with improvements in the quality of life scores
Ozgurdal et al. (2008)	54 prodromal patients, 31 FESZ, 27 ChSZ and 54 HC	An auditory oddball task	P300 amplitudes in non-medicated prodromal patients, FESZ and ChSZ were lower than in HC

Table 14.3 (continued)

Citation	Subjects	Task	Main findings
Sumich et al. (2008)	18 SZ and unafftective siblings and HC	An auditory oddball task	SZ had lower P300 than HC and reduced P300 parietal amplitude relative to SZ siblings; No-Go P300 amplitude was associated with executive function measures; There were intraclass correlations between SZ and siblings for centro-midline No-Go P300 amplitude; Fronto-central P300 amplitude was positively correlated with anxiety-related aspects of schizotypy
Bestelmeyer et al. (2009)	14 monozygotic twins and 14 dizygotic twins	Auditory and visual oddball tasks	The auditory, but not visual P300 amplitude at centro-parietal regions was genetically influenced; In addition, auditory and to a lesser extent visual P300 amplitude were decreased in SZ and BP
Kirihara et al. (2009)	60 SZ and 58 HC	An auditory oddball task	The correlation between P3b amplitude and thought disorder was replicated; No correlation between the P3a subcomponent and thought disorder was observed
Fisher et al. (2010)	12 hallucinating SZ, 12 non-hallucinating SZ and 12 HC	A passive two-tone auditory oddball task using vowel phonemes	Hallucinating SZ exhibited smaller P3a amplitudes than non-hallucinating SZ and HC; P3a amplitude was negatively correlated with hallucinating trait scores in hallucinating SZ
Lee et al. (2010)	16 UHR, 21 FESZ and 16 HC	A visuospatial oddball task	UHR and FESZ showed reduced P300 amplitudes vs. HC; P300 amplitudes were negatively correlated with severity of negative symptoms in both UHR and FESZ
Mathalon et al. (2010a, b)	22 SZ, 15 SA and 22 HC	Auditory and visual oddball tasks	SZ showed reduced P300 amplitude and delayed latency relative to HC, independent of stimulus type or modality; P300 amplitude in SA was larger than in SZ and comparable with HC, but P300 latency was delayed in SA
Park et al. (2010)	20 SZ	Two-stimulus auditory and two-stimulus visual oddball tasks	SZ showed increased P300 amplitudes and shorter P300 latencies after 3-month treatment with quetiapine; Baseline visual P300 amplitude was negatively correlated with the severity of positive symptoms at FZ; No correlation between visual P300 amplitude and severity of positive or negative symptoms was observed after treatment
Gaspar et al. (2011)	13 SZ and 13 HC	N-back working memory task	HC showed highest P300 amplitude in the low working-memory load condition and lowest P300 amplitude in both the attentional control condition and the high working-memory load condition; However SZ showed low P300 amplitude in all conditions; SZ showed smaller P300 amplitude than HC only in the 1-back (low memory load) working memory condition
Itagaki et al. (2011)	54 adult ADHD, 43 SZ and 40 HC	An attentional task and an auditory task	Both SZ and ADHD exhibited a lower peak P300 amplitude than HC; SZ had a longer P300 latency than HC and ADHD
Kaur et al. (2011)	17 FEP affective-spectrum, 18 FEP SZ-spectrum and 18 HC	A two-tone auditory task	FEP SZ-spectrum and FEP affective-spectrum showed reduced fronto-central MMN, central P3a amplitudes and poorer cognitive and psychosocial functioning than HC; The combined FEP sample showed correlations between fronto-central MMN amplitudes and cognitive measures

(continued)

Table 14.3 (continued)

Citation	Subjects	Task	Main findings
Neuhaus et al. (2011a, b)	18 recent-onset SZ,18 ChSZ and 36 HZ	The attention network test	SZ showed lower mean visual P3 than HC; Parietal P3 amplitude was less modulated in both recent-onset SZ and ChSZ compared to HC; P3 modulation was not correlated with clinical or demographic variables
Sharma et al. (2011)	36 monozygotic twins (6 concordant for SZ/SA, 11 discordant and 19 HC pairs)	An auditory oddball task	Affected concordant twins showed a lower P300 amplitude than affected discordant and HC twins; Discordant affected and unaffected twins did not differ from each other or from HC twins; P300 was not correlated with the BPRS
Bestelmeyer et al. 2012	21 SZ, 19 BP and 19 HC	A cognitively demanding visual oddball task	SZ showed reduced P300 amplitude to targets, distractors and frequent stimuli relative to HC; The P300 in BP did not differ from either group
Ethridge et al. (2012)	60 SZ, 60 BP with psychosis and 60 HC	An auditory oddball task	In linear discriminant analysis, five variables were best to differentiate between groups, including late beta activity to standard stimuli, late beta/gamma activity to targets, mid-latency theta/alpha activity to standards, late N2 amplitude to targets and early N2 amplitude to targets
Horan et al. (2012)	35 SZ and 26 HC	A modified visual P300 oddball detection task	SZ and HC showed larger ERP and LPP for both pleasant and unpleasant versus neutral pictures; SZ and HC showed comparable P300 differentiation between target versus non-target stimuli
Jahshan et al. (2012a, b)	26 individuals at risk for psychosis, 31 recent-onset SZ, 33 ChSZ and 28 HC	An auditory oddball task	The at-risk group showed intermediate P3a amplitudes relative to those of HC and recent-onset SZ; P3a deficits were associated with psychosocial functioning in ChSZ, while they were associated with higher levels of negative symptoms in at-risk subjects
Chun et al. (2013)	SZ, BP, SA and HC	A lateralized Go/No-Go task	SZ showed reduced P300 when stimuli were presented to the right visual field; BP exhibited prolonged P300 latency for NoGo trials; Six selected NoGo P300 variables correctly classified SZ (79%), SA (64%) in Study 1 and seven variables selected in Study 2 classified HC (80%), and SZ (61%), BP (67%) and HC (68%) with higher than chance level accuracy
Johannesen et al. (2013)	88 SZ, 52 BP and 83 HC	A paired-click and a 2-stimulus auditory discrimination task	P50 and P300 endophenotypes distinguished SZ from HC with 71% accuracy but did not differentiate SZ from BP above chance level
Kaur et al. (2013)	60 young SZ/SA and 30 HC	An auditory oddball task	SZ/SA showed a trend-level deficit in central P3a amplitudes at baseline; SZ showed reduced P3a amplitudes compared to SA. SZ who did not return for follow-up showed reduced fronto-central P3a amplitudes vs. SZ who returned
Takahashi et al. (2013)	410 SZ and 247 HC	An auditory oddball task	SZ had robust deficits in P3a responses, associated with widespread reductions in the activation of attentional networks (frontal, temporal, parietal regions)
Chen et al. (2014)	36 drug-naïve SZ and 138 HC	An auditory oddball task	No difference in mean P300 amplitude or latency was observed between SZ and HC; Females showed greater P300 amplitude than males, while P300 latency was correlated with aging and increased at a steeper slope in SZ; No effect of dopamine transporter availability on P300 latency or amplitude was observed

Table 14.3 (continued)

Citation	Subjects	Task	Main findings
Fisher et al. (2014)	10 SZ with persistent AH and 13 HC	A passive auditory oddball task	SZ showed reduced novelty P3 amplitudes relative to HC; Novelty P3 amplitudes were correlated with measures of hallucinatory state
Kim et al. (2014a, b)	34 SZ and 34 HC	An auditory oddball task	SZ showed decreased P300 vs. HC; SZ showed decreased source activation predominantly over the left hemisphere, including the cingulate, inferior occipital gyrus, middle occipital gyrus, middle temporal gyrus, posterior cingulate, precuneus, and superior occipital gyrus; The decreased activation in the middle temporal gyrus, posterior cingulate, precuneus, and superior occipital gyrus was negatively correlated with PANSS negative symptom scores
Shim et al. (2014)	34 SZ and 34 HC	An auditory oddball task	SZ showed reduced clustering coefficients and increased path lengths; The negative and cognitive symptom components of PANSS were negatively correlated with the clustering coefficients and positively with path lengths
Zhao et al. (2014)	22 SZ and 22 HC	A self-referential memory (SRM) task	Parietal P3 amplitudes were correlated with the SRM bias score in SZ
Bachiller et al. (2015)	31 SZ and 38 HC	An auditory 3-stimulus oddball paradigm	Differences in source localization between SZ and HC were observed; SZ showed lower P3b source activity in the bilateral frontal structures and the cingulate and less widespread P3a source activity in the right superior, medial and middle frontal gyrus than HC
del Re et al. (2015)	21 CHR, 20 FESZ and 25 HC	An auditory oddball and novelty task	P3a and P3b were affected in CHR and in FESZ compared with controls with similar effect sizes; Only the P3a and N100 distinguished CHR and FESZ from HC
Turetsky et al. (2015)	587 SZ and 649 HC	An auditory oddball task	SZ showed robust P300 amplitude reduction; Each site independently observed between-group difference of P300 amplitude with effect size ranging from 0.36 to 0.94; Smoking, race, cognitive status and real-life functional capacity were factors modulating P300 amplitudes
Andersen et al. (2016)	31 SZ, 28 SZ first-degree relatives and 47 HC	An auditory oddball task	SZ and SZ relatives had intact P3a, but attenuated target-P3b vs. HC; SZ relatives revealed a unique enhancement of the late-LPP response; Reduced target-P3b amplitudes were associated with enhanced symptom severity
Araki et al. (2016)	21 SZ and 22 HC	A visual Go/No-Go paradigm	P3 amplitudes were influenced by the Go/No-go conditions, but not reduced in SZ; No-Go P3 amplitudes were correlated with global functioning in SZ
Devrim-Ucok et al. (2016)	14 FESZ and 22 HC	An auditory oddball task	P3 amplitudes were smaller in FESZ than in HC; Over the 6-year interval, the P3 amplitudes were reduced in HC, but did not change in SZ
Vignapiano (2016)	30 SZ and 23 HC	A Monetary Incentive Delay task	HC showed larger early P3 for large magnitude incentives and larger late P3 for large reward; Early P3 did not discriminate the incentive magnitude and the late P3 was larger for large losses in SZ; Early P3 amplitude for large magnitude incentives was negatively related to trait social anhedonia but not to negative symptoms dimensions

(continued)

Table 14.3 (continued)

Citation	Subjects	Task	Main findings
Ertekin et al. (2017)	46 SZ and 29 HC	A Go/No-Go task	SZ had an overall P3 amplitude reduction that was more prominent on NoGo compared with Go trials, which was present in central and parietal regions but absent in the frontal region. Frontal P3 reduction was comparable on NoGo and Go trials
Berkovitch et al. (2018)	17 SZ and 16 HC	A visual attentional task	Under top down attentional condition, the P3 component was reduced in SZ; But SZ had essentially normal attentional amplification of the P1 and N2 components
Kim et al. (2018a, b)	45 SZ, 32 GHR, 32 CHR and 52 HC	An auditory oddball task	Average P300 amplitude was reduced in GHR, CHR and SZ compared with HC; P300 inter-trial variability was elevated in the CHR and SZ but relatively normal in GHR and HC; P300 inter-trial variability was related to negative symptom severity and neurocognitive performance in SZ
Tang et al. (2019)	P300 oddball task: 104 CHR and 69 HC; P300 novelty task: 131 CHR and 69 HC	An auditory oddball task and an auditory novelty task	CHR converters had lower fronto-central P300 novel amplitude as well as marginally lower P300 oddball amplitude relative to HC; P300 novel amplitude in remitted CHR subjects was comparable to HC, and it was higher than in CHR subjects who converted to psychosis or who did not remit

ADHD attention-deficit/hyperactivity disorder, *AH* auditory hallucination, *BP* bipolar disorder, *BPRS* the Brief Psychiatric Rating Scale, *CHR* clinical high-risk for psychosis, *ChSZ* chronic schizophrenia, *EPN* early posterior negativity, *FEP* first-episode psychosis, *FESZ* patients with first-episode schizophrenia, *GHR* genetic high risk, *HC* healthy controls, *LPP* late positive potential, *PANSS* the Positive and Negative Syndrome Scale, *LORETA* low resolution electromagnetic tomography, *SA* Schizoaffective disorder, *SZ* patients with schizophrenia, *STG* superior temporal gyrus, *TDI* thought disorder index, *UHR* ultra high-risk

14.3.2 Language and N400/P600

Schizophrenia has been associated with language abnormalities, and thus language processes have been studied in schizophrenia using ERPs. The questions asked in these studies are related to semantic memory structure, processes that operate within this structure as well as syntactic processes. The two ERP components used as indices of these processes have been N400 and P600. N400 is a negative, or negative going, potential whose latency peaks around 400 ms after the onset of a stimulus and is sensitive to semantic relationships between words and concepts. P600 has been associated with meaning integration processes and examined most often in paradigms using sentences as stimuli.

Accordingly, N400 has been used to probe priming processes, or the ease with which a target word is processed if preceded by a related word or concept. Such studies typically address the questions of a semantic structure of memory, but also initial processes of activation if words/concepts are presented in close temporal sequence (under 500 ms onset to onset), and of later processes of inhibition and context utilization if stimuli are presented at longer onset to onset times (over 500 ms).

In addition, N400 has been used to examine context and semantic memory operations. A recent meta-analysis of the N400 effect across studies probing both early processes of activation and late processes of context utilization and predictive processes (Wang et al. (2011) suggested that both types of processes are abnormal in schizophrenia. Several early studies demonstrated that semantic processes in schizophrenia are abnormal (Adams et al. 1993; Andrews et al. 1993; Bobes et al. 1996; Condray et al. 1999).

14.3.2.1 N400 and Structure and Function of Semantic Networks in Schizophrenia

Questions about the structure of semantic memory and processes within semantic memory networks have been addressed by several studies, with most suggesting impairments in context utilization (Hokama et al. 2003; Iakimova et al. 2005). In several studies, the distinction between automatic semantic access and controlled processes has been addressed. It is assumed that initial activation within semantic networks is fast and automatic and it spreads to related concepts along the gradient of similarly. The more an item is related to the initial word, the faster it is activated, with items that are not related not receiving any activation. Most studies examining the issues of the structure of semantic networks and processes within them used word pair priming paradigms, where the first presented word (prime) is followed by another word (target) that is either related or not related to the prime. The subject's task is most often a lexical decision where participants decide if the target word is a word or a non-word. In such studies the distance between the prime and a target, or stimulus onset asynchrony (SOAs), is manipulated to either test initial processes of activation, which are observed at SOAs less than about 500 ms, or the later 'controlled' processes of context utilization and inhibition which arise at SOAs longer than 500 ms, post-stimulus.

Several studies have examined both the processes of initial semantic activation and later processes of local context utilization. Studies using priming paradigms at short SOAs (e.g., Mathalon et al. 2002, 2010a, b) proposed that overly broad activation of concepts exists in schizophrenia. Niznikiewicz et al. (2010) also suggested the presence of abnormally broad activation and inefficient early inhibitory processes. Condray et al. (2008) conducted a semantic priming study of both automatic activation and controlled semantic processes in which the frequency of word stimuli was varied. In the healthy control group, N400 increased as word frequency decreased, while patients did not show this effect, suggesting that in the patient group semantic access to words is not ruled by their semantic distance, which may be due to abnormal connectivity within semantic networks. Kiang et al. (2012) examined priming using both semantic and repetition priming at both short and long SOAs in schizophrenia. The patient group had abnormal priming at the short SOA for semantic priming only, suggesting that functional connections between concepts are abnormal, but not the ability to activate access to the prime. Kiang et al. (2011) also tested the connections among semantic concepts using N400 in a depth of processing task. Both patients and healthy controls showed more robust N400 effect in the semantic task relative to the detection of a letter task, suggesting that while connections among concepts are abnormal in schizophrenia, this abnormality is subtle. One aspect of such an abnormality may be a lack of sensitivity to low and high category exemplars, supporting the idea of abnormal organization of conceptual networks (Kiang et al. 2008). Salisbury et al. (2010) also suggested that the organization of conceptual networks may be abnormal in schizophrenia.

In a somewhat dissenting view, Kuperberg et al. (2019) suggested that abnormal processes observed within semantic lexicon may be related to the disrupted connections between the meaning of words and their form. Such an interpretation may be especially relevant for visual language processing. The thesis of looser lexical-semantic associations described above was pursued in an fMRI study, which found evidence for enhanced indirect priming in schizophrenia with the effect localized to fusiform gyrus involved in mapping word form to meaning.

Overall, N400 studies using priming paradigms suggest abnormalities in both the structure of semantic networks and in the processes that operate on these networks. A recent study by Kuperberg et al. (2019) opens the possibility that the abnormalities observed at the semantic level may have their origins in disrupted connections between a physical form of a word and its meaning representation.

14.3.2.2 N400/P600 and Semantic Memory

N400 and P600 components, with their sensitivity to meaning representation, lend themselves to examining semantic memory operations in schizophrenia. Battal Merlet et al. (2018) examined the effects of internal semantic coherence (defined as a relational bond between two words of a word-pair) and external semantic coherence (defined as a word pair belonging to a specific semantic category) in schizophrenia. At encoding, both groups showed external coherence effects, but only healthy controls showed internal coherence effect. At retrieval, the external semantic coherence effect was associated with old/new effect at parietal sites, but in the patient group it was associated with frontal N400. These results suggest that while both groups may be able to use context, they use different strategies to achieve better memory performance. Green et al. (2017) examined both encoding and memory recognition in the patient group and found abnormal N400 and late positive component at the encoding stage, but not at the recognition stage in the patient group (Guillem et al. 2001).

While the results of these studies differ somewhat from each other given the different designs used to address the research questions, all of them point to abnormalities in both encoding semantic information and in retrieving this information in schizophrenia patients.

14.3.2.3 N400/P600 and Context Utilization

In addition to abnormalities within semantic networks described above, several N400 studies focused on language abnormalities related to meaning construction from sentences and paragraphs. For example, discourse level comprehension was tested in Sitnikova's et al. (2009), study which found that semantic processing was more difficult for schizophrenia patients in contextually more ambiguous scenarios and was associated with an enhanced N400, while P600 indexing integration processes was reduced signaling greater difficulties in constructing a semantic model of discourse.

Ditman and Kuperberg (2007) examined the use of context in building a model of discourse in schizophrenia and healthy control groups. While behaviorally both groups showed sensitivity to context, the N400 in the patient group did not differentiate between different levels of relatedness across context and discourse, suggesting at the very least that context is used differently, and less efficiently, in schizophrenia relative to healthy control populations.

The Pinheiro et al. (2015) study showed that processes of context utilization interact with affective processes and that these interactions are abnormal, especially in the negative mood in schizophrenia. The results of this study also lent support for the abnormal semantic memory structure in schizophrenia.

Finally, Ruchsow et al. (2003) used sentences to examine schizophrenia patients' sensitivity to syntactic violations and suggested that the integration processes indexed by P600 are abnormal in this population.

Studies devoted to language processes related to meaning construction from sentences and paragraphs clearly show that these processes are abnormal both in terms of semantic and syntactic operations. In addition, as the Pinheiro et al. (2015) study demonstrated, interactions between semantic and emotional processes are also impaired in schizophrenia.

14.3.2.4 N400 as a Biomarker

Some studies have examined the presence of language related abnormalities across the spectrum of schizophrenia development and chronicity. Most of these studies have been conducted in schizotypal personality disorder (SPD), which is believed to be on the schizophrenia spectrum, with some studies conducted in unaffected relatives of schizophrenia patients.

These studies recapitulate results reported in studies of schizophrenia patients in terms of the types of abnormalities identified in this subject group. However, the N400 effects found in SPD tended to be less severe (e.g., Niznikiewicz et al. 1999, 2004). N400 effects in unaffected relatives present a more complex picture with some studies finding an N400 impairment and other studies not reporting such a finding in this subject group.

For example, Kimble et al. (2000) tested both SPD and unaffected relatives of schizophrenia patients and reported reduced N400 effect in high schizotypy, but not in the relatives' group. De Loye et al. (2013) found that SPD subjects were not effective in using inhibition to exclude inappropriate sentence endings but could use context to process sentences that ended with congruent final words. Similarly, Del Goleto et al. (2016) found that the use of context in the processing of irony was impaired in high SPD relative to low SPD individuals. The reduced use of context was also found in Kiang and Kutas (2005) in SPD. Overall, it appears that while language impairment in SPD exists, it is milder than in schizophrenia.

Among studies that have examined N400 deficits in unaffected relatives, Kiang et al. (2014) conducted a study of semantic associations processing at both short and long SOAs in a group of patients, unaffected relatives, and healthy controls. In all conditions, N400 in unaffected relatives was similar to that found in healthy controls and different from the patient group, suggesting that N400 may be an illness biomarker but not endophenotype. A similar conclusion was reached by Sharma's et al. (2017) study, which showed that twins discordant for schizophrenia had N400 effect similar to healthy controls, while the N400 effect in the affected twins was reduced.

In contrast, Guerra et al. (2009) used a picture matching task to examine semantic processes in unaffected relatives of schizophrenia patients and found both N400 amplitude and latency abnormalities in the relatives comparable to those found in the schizophrenia group, suggesting that N400 can be regarded an endophenotype for schizophrenia. A similar conclusion was reached by Longenecker et al. (2018). This study used late positive component (LPC) to examine encoding accuracy, and found that the LPC was reduced in both the patient and in the relatives' group.

Thus, the evidence for N400 deficits in unaffected relatives in schizophrenia is mixed with some studies supporting the presence of N400 abnormalities in this subject group and suggesting N400 to be an endophenotype for schizophrenia and other studies not finding this evidence. Since all these studies tend to have relatively low subjects N, it is possible that disease heterogeneity contributes to these different results.

Finally, a handful of studies tested a utility of N400 as a stable biomarker of semantic impairment in schizophrenia. Besche-Richard et al. (2014) tested patients with schizophrenia on two occasions in a semantic priming paradigm. While behavioral indices of impaired semantic priming remained the same on both occasions, N400 semantic priming effect improved on retesting, suggesting that it may not be a stable index of semantic memory problems in schizophrenia.

Boyd et al. (2014) reached an opposite conclusion using a semantic priming task at two SOAs, 350 ms tapping into automatic processing of semantic activation, and 750 SOA tapping into controlled processes and testing schizophrenia subjects at two occasions. N400s to both related and unrelated words and at both SOAs were highly correlated, suggesting its utility as a biomarker of semantic abnormalities in schizophrenia. Similarly, Guillem et al. (2003) examined schizophrenia patients with both high and low reality distortion scores in a task of memory recognition for faces and concluded that the N400 abnormalities in this study were associated with knowledge integration, and seemed to be related to an illness trait as similar impairments were found in both low and high reality distortion groups.

Overall, it appears that N400 can be regarded as a biomarker for language abnormalities in schizophrenia with some but not all studies, suggesting that it can also be regarded as an endophenotype. As for previously discussed ERP components, large, well-powered and carefully designed studies may be able to resolve the discussion in the field on the status of N400 as biomarker and endophenotype.

14.3.2.5 N400 and Symptoms

A handful of studies have linked N400 to positive symptomatology in schizophrenia. For example, Kostova et al. (2005) reported the relationship between thought disorder index score and reduced N400 effect in the patient group, and a similar conclusion was reached by Laurent et al. (2010). Debruille et al. (2007) examined N400 in the context of delusions in schizophrenia and

proposed that they are related to an abnormal processing of context.

Jackson et al. (2014) conducted a longitudinal study of the N400 changes as a function of recovery and symptoms, where the patients were followed over the span of 15 years. The results were somewhat reminiscent of the Mathalon et al. (2000a) study where P300 amplitude was found to fluctuate with symptom severity. In the Jackson et al. study, patients who did not recover had reduced N400 amplitude, while those who did recover had N400 amplitude comparable to healthy controls. The authors suggested the N400 is sensitive to symptoms but should not be regarded as endophenotype.

14.3.2.6 N400/P600 and Illness Specificity

A comparison between manic and schizophrenic patients in a study of syntactic violations revealed no difference between the two groups, with both showing reduced P600 relative to healthy controls (Lee et al. 2016). In turn, Ryu et al. (2012) examined priming in a word relatedness paradigm in both manic and schizophrenia patients and concluded that while the N400 was abnormal in both groups, the two groups differed in the type of abnormalities, with manic patients showing larger N400 to related words and schizophrenic patients showing reduced N400 to unrelated words.

Too few N400/P600 studies have been conducted to make clear conclusions regarding the extent to which N400/P600 impairments are unique in each psychiatric diagnosis. The initial studies suggest that there may be differences between how syntactic and semantic processes are impacted by different diagnoses. Furthermore, there may be differences in the type of abnormalities that exist in the processes of semantic activation in manic and schizophrenia patients.

14.3.2.7 N400 and Medication Effects

A handful of studies have looked at the impact of medications on language impairment in schizophrenia. For example, Condray et al. (2008) examined automatic and controlled processes in semantic networks in schizophrenia patients either on haloperidol or on placebo replacement therapy at two time points, the beginning and the end of the trial. While N400 was abnormal at both time points, a larger N400 priming effect was observed at the frontal sites in the automatic semantic activation condition in patients in the haloperidol group. These results support both the idea that N400 can be regarded as a trait marker for schizophrenia, as well as the idea that medications may modulate this abnormality.

In another study, Condray et al. (2008) examined the association between semantic memory processes in schizophrenia and polyunsaturated fatty acids (PUFAs) and dopamine in both unmedicated and medicated with haloperidol patient groups. The results suggested that levels of PUFAs were associated with semantic memory and language in schizophrenia, but only N400 was associated with clinical symptoms.

Guillem et al. (2006) examined the effects of a cholinergic enhancer, rivastigmine, on semantic memory function in schizophrenia with N400 recorded during the recognition memory phase. The results suggested that patients who were assigned to the rivastigmine intervention improved in both posterior and frontal N400 relative to patients who did not take this medication.

Overall, studies that have examined an impact of antipsychotic medications on the N400 response have found that some aspects of language function can be improved by pharmacological treatment. Haloperidol has been found to improve processes of semantic activation, while a cholinergic agent has been associated with semantic memory improvement.

14.3.2.8 N400 and Societal Perception of Schizophrenia

Finally, one study used N400 to examine how the general public views individuals who carry a diagnosis of schizophrenia. Best and Bowie (2015) presented healthy participants with sentences that either ended with a typical ending, neologism, or word approximation and the subjects were told that sentences were produced either by university students or by schizophrenia patients. The large N400 was recorded to atypical sentence endings only when the participants

thought the sentences were produced by university students, but not when they thought they were produced by schizophrenia patients, suggesting bias in terms of how schizophrenia individuals are perceived; it appears that the perception exists that patients with schizophrenia produce incoherent and poorly constructed speech (Table 14.4).

14.4 Overall Summary

The use of ERP methodology in schizophrenia has produced a wealth of information on cognitive processes affected by this disease process. Nearly all ERP components discussed in this chapter have been proposed to be biomarkers for schizophrenia, and MMN, N100/P200, and P300

Table 14.4 Language related N400 and P600 in schizophrenia

Citation	Subjects	Task	ERP measures	Main findings
Adams et al. (1993)	12 ChSZ and 12 HC	Semantically incongruent words and phrases	N400, LPC	N400 amplitude reduced and latency to semantically anomalous endings increased in SZ; Amplitude of late positive component reduced in SZ; N400 topographical distribution did not differ between SZ and HC
Andrews et al. (1993)	SZ and HC	Reading congruous and incongruous sentences in anticipation of a memory test	N400, LPC	N400 amplitude did not differ between SZ and HC, but differences between the ERPs to congruous and incongruous sentences persisted longer in SZ; Amplitude of late positive component reduced in SZ; Amplitude of N400 and late positive component correlated with attentional impairment and positive thought disorder in SZ
Bobes et al. (1996)	SZ and HC	A picture semantic-matching task	N400	N400 latency was delayed and amplitude of N400 in the difference waveform was reduced in SZ; N400 amplitude in response to congruent trials was more negative in SZ than in HC
Condray et al. (1999)	37 male SZ and 34 male HC	A lexical decision task	N400	N400 priming effect was absent in SZ; overall mean N400 amplitude did not differ between SZ and HC
Niznikiewicz et al. (1999)	17 SPD and 16 HC	A sentence task presented both visually and aurally	N400	N400 amplitude in congruent condition was more negative in SPD than in HC in both visual and auditory modalities; SPD had prolonged N400 latency in the visual modality
Guillem et al. (2001)	15 SZ and 15 HC	Implicit and explicit memory tasks	N400, LPC	SZ showed a reduced modulation of an N400-like component in both the implicit and explicit tasks; SZ also displayed an enhanced frontally distributed N400 in the explicit task; the modulation of the LPC did not differ between groups in both implicit and explicit tasks
Mathalon et al. (2002)	18 SZ and 18 HC	A picture-word matching task	N400	N400 amplitude to unprimed words was smaller in SZ, while N400 to primed words was similar in SZ and in HC

(continued)

Table 14.4 (continued)

Citation	Subjects	Task	ERP measures	Main findings
Guillem et al. (2003)	17 RD+, 21 RD- and 22 HC	A recognition memory task for face	P2a, N400, P600	P2a and N400 effect reduced in RD+ and RD−; Larger N300 and fronto-central effect occurred in RD+; RD+ showed a comparable P600 effect with HC, but larger than RD−
Hokama et al. (2003)	18 unmedicated SZ and 18 HC	A lexical decision task	N350, N400, LPC	N350 latency was prolonged in SZ; N400 amplitude from the difference waveforms was smaller in SZ; Peak amplitude of late positive component was reduced and latency was delayed in SZ
Ruchsow et al. (2003)	19 SZ and 19 HC	A sentence processing task	ELAN, N400, LPC	Syntactic mismatch elicited an ELAN component and semantic mismatch elicited a larger N400 in both SZ and HC; HC exhibited a P600 syntactic mismatch effect, but SZ did not
Niznikiewicz et al. (2004)	17 female SPD and 16 female HC	A classical N400 sentence task	N400	Female SPD had a more negative N400 to auditory congruent sentences than female HC
Kiang et al. (2005)	24 healthy participants with SPQ assessments	A category-verification task	N400	N400 amplitude was largest for non-exemplars, intermediate for low-typicality exemplars, and smallest for high-typicality exemplars; SPQ score was negatively correlated with the N400 amplitude difference between non-exemplars and low/high-typicality exemplars, but not correlated with N400 amplitude difference between low- and high-typicality exemplars
Kostova et al. (2005)	50 SZ and 40 HC	A lexical decision task with semantic priming	N400	SZ showed greater N400 amplitude than HC; N400 amplitude to related and unrelated words differed in HC but not in SZ; lower N400 effect was correlated with higher formal thought disorder scores
Lakimova et al. (2005)	20 SZ and 20 HC	Reading metaphorical, literal and incongruous sentences and judging their meaningfulness	N400, LPC	A more negative N400 amplitude was evoked by incongruous endings to sentences in both SZ and HC; SZ exhibited a more negative N400 amplitude for all sentences, reduced amplitude of late positive component and delayed latency for both components
Guillem et al. (2006)	18 SZ	A recognition memory task	N2b, P2a, N400, FN400	Posterior N2b was reduced and frontal P2a was enhanced by a rivastigmine adjuvant therapy; posterior N400 and frontal FN400 were also enhanced
Ditman et al. (2007)	15 SZ and 18 HC	Reading sentences with highly causal, intermediate related or no relationship with preceding contexts	N400	SZ did not show N400 differences across conditions, and this failure was correlated with positive thought disorder

Table 14.4 (continued)

Citation	Subjects	Task	ERP measures	Main findings
Debruille et al. (2007)	35 SZ and 26 HC	A category-verification task	N400	N400 amplitude to target words was negatively correlated with delusion severity; N400 to category-discrepant targets was smaller in SZ with more delusions than those with fewer delusions
Condray et al. (2008)	37 male SZ and 34 male HC	A semantic priming-lexical decision task	N400	N400 was associated with cognition in SZ and HC; N400 was associated with levels of total PUFAs (polyunsaturated fatty acids) and arachidonic acid in unmedicated SZ; N400 was also associated with clinical symptoms of paranoia and thought disturbance
Kiang et al. (2008)	16 SZ and 16 HC	A lexical decision task	N400	HC exhibited largest N400 amplitude to unrelated targets, intermediate after indirectly related targets and smallest after directly related targets, but SZ did not show N400 differences among these target types; SZ showed larger N400 amplitudes to both directly and indirectly related targets at the longer SOA, which was correlated with positive psychotic symptoms
Guerra et al. (2009)	21 SZ first-degree relatives, 21 SZ probands and 21 HC	A picture semantic matching task	N400	SZ relatives and probands showed reduced N400 amplitude to congruent categories and delayed N400 latency as compared with HC
Sitnikova et al. (2009)	16 SZ and 16 HC	A novel video task	N400, P600	N400 was abnormally enhanced to less comprehensible incongruous scenes in SZ, and was associated with disorganization severity; P600 was abnormally attenuated in SZ and associated with the SANS ratings of impersistence at work or school
Kimble et al. (2000)	15 SZ relatives and 15 HC with schizotypy assessments	An auditory oddball task and a sentence processing task	N400	HC higher in schizotypy showed a reduced N400, but SZ relatives did not
Laurent et al. (2010)	10 SZ and 10 HC	A lexical decision task and a physical task	N400, P300	HC, but not SZ, showed an N400 effect in the lexical decision task; Both groups showed a P300 effect for either related or unrelated targets in the physical task
Mathalon et al. (2010a, b)	26 SZ and 29 HC	A picture-word verification task	N400	N400 amplitudes in both SZ and HC were sensitive to the difference between primed and unprimed words and the subtler difference between classes of unprimed words, but SZ are less sensitive than HC
Niznikiewicz et al. (2010)	20 male ChSZ and 20 male HC	A word-pair priming task with short SOA	N400	HC and SZ groups differed in the unrelated condition with a less negative N400 amplitude in SZ but did not differ in the related condition; HC showed a N400 priming effect, but SZ did not

(continued)

Table 14.4 (continued)

Citation	Subjects	Task	ERP measures	Main findings
Salisbury et al. (2010)	20 SZ and 20 HC	Presenting short 4 word sentences	N400	N400 amplitude in SZ was smaller to congruent and dominant endings and larger to subordinate and incongruous endings
Kiang et al. (2011)	16 SZ and 16 HC	A semantic priming task and a non-semantic task	N400	Both groups exhibited greater N400 semantic priming in the semantic task than in the orthographic task; N400 semantic priming effect in SZ was smaller than that in HC
Kiang et al. (2012)	16 SZ and 16 HC	A lexical decision task	N400	N400 amplitude was largest for unrelated, intermediate for related and smallest for repeated targets in both groups; SZ exhibited subnormal N400 semantic relatedness priming at the 300-ms SOA, but normal repetition priming at both SOAs
Ryu et al. (2012)	20 SZ, 20 manic patients and 20 HC	A word-matching task	N400	N400 amplitude to congruent words was larger in manic patients; N400 to incongruent words was smaller in SZ than in other groups; N400 was not correlated with symptom severity in patient groups
de Loye et al. (2013)	17 high-SPQ individuals and 14 low-SPQ individuals	Semantic judgement of sentence pairs	N400	N400 amplitude was reduced for expected words versus unrelated violations in both groups; High-SPQ group had less negative N400 for unrelated violations in both hemispheres
Besche-Richard et al. (2014)	15 SZ and 10 HC	A semantic priming task	N400	SZ exhibited a semantic priming deficit indexed with N400 amplitude, which was improved after 1 year
Boyd et al. (2014)	16 SZ	A semantic priming task	N400	SZ showed no differences between N400 amplitude for related and unrelated targets at each SOA; N400 amplitudes at FZ across timepoints had significant test-retest reliability for both target types at each SOA
Jackson et al. (2014)	41 SZ, 48 other psychotic disorders and 35 HC	A picture-word priming task	N400	SZ showed reduced N400 to semantically incongruent stimuli relative to HC; SZ and other psychoses did not differ on N400; Patients who remained ill had a blunted N400, and those who recovered did not differ from HC; Reduced N400 was correlated with greater psychotic symptoms, worse global assessment of functioning scores, unemployment, and impaired social functioning
Kiang et al. (2014)	12 SZ, 12 SZ relatives and 12 HC	A lexical decision task	N400	SZ relatives and HC showed smaller N400 amplitude to related than to unrelated targets; SZ showed larger N400 amplitude for related targets than HC and SZ relatives, but comparable N400 amplitude for unrelated targets

Table 14.4 (continued)

Citation	Subjects	Task	ERP measures	Main findings
Best et al. (2015)	73 healthy participants	Listening to conversation segments	N400	Centro-parietal N400 was observed in response to word approximations and neologisms if subjects believed that the sentences were produced by university students but not when the subjects thought the sentences were produced by SZ
Pinheiro et al. (2015)	17 male ChSZ and 15 HC	Reading sentence pairs after positive, negative or neutral mood induction	N400	SZ showed N400 reduction to sentences ended with expected words relative to both within-category violations and between-category violations; N400 abnormalities were enhanced under a negative mood in SZ
Del Goleto et al. (2016)	20 high-SPQ individuals and 20 low-SPQ individuals	Reading short stories ending with a literal, ironic or incompatible statement	N400, P600	Low-SPQ group showed a less negative N400 amplitude for literal targets compared to incompatible targets and a greater P600 amplitude for ironic targets than literal targets; High SPQ group showed neither an N400 or P600 effect
Lee et al. (2016)	26 SZ, 21 manic patients and 20 HC	Auditory sentences processing with syntactic violations or non-violations	P600	Manic patients and SZ showed smaller P600 amplitudes associated with syntactic violations compared with HC. There was no difference in P600 amplitude between SZ and manic patients
Green et al. (2017)	24 SZ and 19 HC	A forced-choice recognition memory task	N400, LPC	During encoding: SZ had reduced N400 and LPC amplitudes vs. HC; LPC amplitude was correlated with task performance
Sharma et al. (2017)	6 monozygotic twin pairs concordant for SZ, 11 discordant pairs and 19 HC pairs	A lexical decision task	N400	N400 effect observed only in the direct priming condition; N400 effect was reduced in affected concordant twins and tended to be reduced in discordant affected twins compared to controls; Reduced N400 effect tended to be correlated with higher BPRS scores, and the N400 effect did not differ between medicated and unmedicated patients
Battal Merlet et al. (2018)	18 SZ and 15 HC	A recognition memory task	N400, FN400	During encoding: both groups exhibited an N400 external semantic coherence effect; HC also showed an N400 internal semantic coherence effect while SZ did not During memory test: FN400 old/new effect was associated with the related stimuli in both groups; SZ showed an association between fN400 and external semantic coherence

(continued)

Table 14.4 (continued)

Citation	Subjects	Task	ERP measures	Main findings
Kuperberg et al. (2019)	18 SZ and 20 HC	A highly automatic indirect semantic priming task	N400	SZ showed a larger automatic indirect priming effect than HC; MEG localized the enhanced effect to the N400 time window while fMRI localized the effect to the left temporal fusiform cortex
Longenecker et al. (2018)	23 SZ, 17 SZ relatives and 32 HC	Encoding of verbal material	N1, LPC	N1 was abnormal at encoding in SZ and differentially accounted for by later memory performance

ChSZ chronic schizophrenia, *ELAN* early left anterior negativity, *FN400* the early midfrontally-distributed difference between ERPs elicited by old and new items, *LPC* late positive component, *RD+* schizophrenia patients with high reality distortion, *RD-* RD+, schizophrenia patients with low (RD-) or high (RD+) reality distortions, *SAPS/SANS* the assessment of positive and negative symptoms, *SOA* stimulus-onset asynchrony, *SPD* schizotypal personality disorder, *SPQ* the Schizotypal Personality Questionnaire, *SZ* patients with schizophrenia

have also been suggested to be endophenotypes, which can track psychosis development. ERP methodology has also been used to probe the integrity of specific cognitive processes in schizophrenia and has produced results that served to inform theories of schizophrenia.

More specifically, MMN studies have highlighted the involvement of glutamatergic and GABA-ergic systems in the development of schizophrenia, while N100 and P200 studies point to the role of the serotonergic system, in addition to the glutamatergic system. In terms of processes impacted by schizophrenia pathophysiology, each class of studies has contributed to a better understanding of specific cognitive impairments. MMN studies have suggested abnormalities in forming a memory trace, and in processes of error prediction. N100/P200 studies, on the other hand, have provided evidence for impairments in predictive coding and corollary discharge mechanisms, as well as in early categorical stimulus classification in the auditory modality, while in the visual modality, impairments in the magnocellular pathway have been identified along with deficits in early encoding and retrieval mechanisms.

P300 studies have demonstrated impairments in working memory and attentional processes, including inhibitory function, efficient use of context, and its integration in the service of flexibly pursued goals. Finally, N400/P600 studies have demonstrated abnormalities in the structure and function within semantic memory networks, and in the efficient use of context to guide meaning construction. Several of these impairments have been associated with symptoms, especially positive symptoms of delusions and auditory hallucinations.

As mentioned above, the two dominating theories of schizophrenia offer somewhat opposite views regarding the root causes of cognitive dysfunction in schizophrenia and its accompanying symptomatology: one has focused on sensory deficits (Javitt 2015) while the other has focused on impairments in higher order cognition (Brown and Kuperberg 2015). Few studies have offered a way to reconcile these views. Brown and Kuperberg (2015) in their work are one of the few exceptions in which these authors outline a hierarchical generative framework for broadly defined language dysfunction in schizophrenia. In their paper they attempt to bring together perceptual and abstract cognitive processes that impinge on both language understanding and on its production, and whose abnormalities they view as resulting in a unique set of language related impairments observed in schizophrenia patients.

It also appears that recent proposals on cognitive architecture outlined within graph theory may offer interesting approaches to understand how higher order cognitions arise from sensory data, how the sensory and the abstract interact with each other, as well as what would be the consequences of abnormalities in such processes.

Summary

- ERPs index cognitive impairment in schizophrenia spectrum disorders in both sensory based cognitive processes and in higher order cognition.
- MMN indexes pre-attentive deficits in schizophrenia; it has recently been linked to impaired error prediction mechanism. MMN has been associated with faulty NMDA receptor mechanism and its abnormalities have been found in chronic, first episode schizophrenia, and in individuals at high risk for psychosis development, but not consistently in individuals at genetic risk for psychosis.
- N100/P200 abnormalities in schizophrenia index impairments in early sensory and categorization processes and have been found in both auditory, visual, and olfactory modalities, with some studies suggesting that these abnormalities, in addition to being found in chronic and first episode schizophrenia, are also found in genetic high risk individuals.
- P300 abnormalities index impairments in attentional, context updating and attentional orienting responses in schizophrenia and have been found in individuals at high risk for psychosis.
- N400 indexes processes within semantic networks as well as the use of semantic context and its abnormalities exist in both first episode and chronic schizophrenia with attenuated abnormalities found in schizotypal personality disorder.

References

Adams J, Faux SF, Nestor PG, Shenton M, Marcy B, Smith S, McCarley RW. ERP abnormalities during semantic processing in schizophrenia. Schizophr Res. 1993;10(3):247–57.

Ahveninen J, Jaaskelainen IP, Osipova D, Huttunen MO, Ilmoniemi RJ, Kaprio J, Lonnqvist J, Manninen M, Pakarinen S, Therman S, Naatanen R, Cannon TD. Inherited auditory-cortical dysfunction in twin pairs discordant for schizophrenia. Biol Psychiatry. 2006;60(6):612–20.

Alain C, Cortese F, Bernstein LJ, He Y, Zipursky RB. Auditory feature conjunction in patients with schizophrenia. Schizophr Res. 2001;49(1-2):179–91.

Andersen EH, Campbell AM, Schipul SE, Bellion CM, Donkers FC, Evans AM, Belger A. Electrophysiological correlates of aberrant motivated attention and salience processing in unaffected relatives of schizophrenia patients. Clin EEG Neurosci. 2016;47(1):11–23.

Andrews S, Shelley AM, Ward PB, Fox A, Catts SV, McConaghy N. Event-related potential indices of semantic processing in schizophrenia. Biol Psychiatry. 1993;34(7):443–58.

Anokhin AP, Vedeniapin AB, Heath AC, Korzyukov O, Boutros NN. Genetic and environmental influences on sensory gating of mid-latency auditory evoked responses: a twin study. Schizophr Res. 2007;89(1-3):312–9.

Araki T, Kirihara K, Koshiyama D, Nagai T, Tada M, Fukuda M, Kasai K. Intact neural activity during a Go/No-go task is associated with high global functioning in schizophrenia. Psychiatry Clin Neurosci. 2016;70(7):278–85.

Atkinson RJ, Michie PT, Schall U. Duration mismatch negativity and P3a in first-episode psychosis and individuals at ultra-high risk of psychosis. Biol Psychiatry. 2012;71(2):98–104.

Bachiller A, Romero S, Molina V, Alonso JF, Mananas MA, Poza J, Hornero R. Auditory P3a and P3b neural generators in schizophrenia: an adaptive sLORETA P300 localization approach. Schizophr Res. 2015;169(1-3):318–25.

Baldeweg T, Hirsch SR. Mismatch negativity indexes illness-specific impairments of cortical plasticity in schizophrenia: a comparison with bipolar disorder and Alzheimer's disease. Int J Psychophysiol. 2015;95(2):145–55.

Bartha-Doering L, Deuster D, Giordano V, am Zehnhoff-Dinnesen A, Dobel C. A systematic review of the mismatch negativity as an index for auditory sensory memory: from basic research to clinical and developmental perspectives. Psychophysiology. 2015;52(9):1115–30.

Battal Merlet L, Blanchet A, Lockman H, Kostova M. An event related potentials study of semantic coherence effect during episodic encoding in schizophrenia patients. Schizophr Res Treat. 2018;2018:8501973.

Berkovitch L, Del Cul A, Maheu M, Dehaene S. Impaired conscious access and abnormal attentional amplification in schizophrenia. Neuroimage Clin. 2018;18:835–48.

Besche-Richard C, Iakimova G, Hardy-Bayle MC, Passerieux C. Behavioral and brain measures (N400) of semantic priming in patients with schizophrenia: test-retest effect in a longitudinal study. Psychiatry Clin Neurosci. 2014;68(5):365–73.

Best MW, Bowie CR. Neurophysiological evidence for a processing bias towards schizophrenia-associated communication abnormalities. Schizophr Res. 2015;169(1-3):334–9.

Bestelmeyer PE. The visual P3a in schizophrenia and bipolar disorder: effects of target and distractor stimuli on the P300. Psychiatry Res. 2012;197(1-2):140–4.

Bestelmeyer PE, Phillips LH, Crombie C, Benson P, St Clair D. The P300 as a possible endophenotype for schizophrenia and bipolar disorder: evidence from twin and patient studies. Psychiatry Res. 2009;169(3):212–9.

Bharath S, Gangadhar BN, Janakiramaiah N. P300 in family studies of schizophrenia: review and critique. Int J Psychophysiol. 2000;38(1):43–54.

Bobes MA, Lei ZX, Ibanez S, Yi H, Valdes-Sosa M. Semantic matching of pictures in schizophrenia: a cross-cultural ERP study. Biol Psychiatry. 1996;40(3):189–202.

Bodatsch M, Ruhrmann S, Wagner M, Muller R, Schultze-Lutter F, Frommann I, Brinkmeyer J, Gaebel W, Maier W, Klosterkotter J, Brockhaus-Dumke A. Prediction of psychosis by mismatch negativity. Biol Psychiatry. 2011;69(10):959–66.

Bodatsch M, Brockhaus-Dumke A, Klosterkotter J, Ruhrmann S. Forecasting psychosis by event-related potentials-systematic review and specific meta-analysis. Biol Psychiatry. 2015;77(11):951–8.

Boyd JE, Patriciu I, McKinnon MC, Kiang M. Test-retest reliability of N400 event-related brain potential measures in a word-pair semantic priming paradigm in patients with schizophrenia. Schizophr Res. 2014;158(1-3):195–203.

Bramon E, Croft RJ, McDonald C, Virdi GK, Gruzelier JG, Baldeweg T, Sham PC, Frangou S, Murray RM. Mismatch negativity in schizophrenia: a family study. Schizophr Res. 2004a;67(1):1–10.

Bramon E, Rabe-Hesketh S, Sham P, Murray RM, Frangou S. Meta-analysis of the P300 and P50 waveforms in schizophrenia. Schizophr Res. 2004b;70(2-3):315–29.

Bramon E, McDonald C, Croft RJ, Landau S, Filbey F, Gruzelier JH, Sham PC, Frangou S, Murray RM. Is the P300 wave an endophenotype for schizophrenia? A meta-analysis and a family study. Neuroimage. 2005;27(4):960–8.

Bravermanova A, Viktorinova M, Tyls F, Novak T, Androvicova R, Korcak J, Horacek J, Balikova M, Griskova-Bulanova I, Danielova D, Vlcek P, Mohr P, Brunovsky M, Koudelka V, Palenicek T. Psilocybin disrupts sensory and higher order cognitive processing but not pre-attentive cognitive processing-study on P300 and mismatch negativity in healthy volunteers. Psychopharmacology (Berl). 2018;235(2):491–503.

Brockhaus-Dumke A, Tendolkar I, Pukrop R, Schultze-Lutter F, Klosterkotter J, Ruhrmann S. Impaired mismatch negativity generation in prodromal subjects and patients with schizophrenia. Schizophr Res. 2005;73(2-3):297–310.

Brown M, Kuperberg GRA. Hierarchical generative framework of language processing: linking language perception, interpretation, and production abnormalities in schizophrenia. Front Hum Neurosci. 2015;9:643.

Butler PD, Martinez A, Foxe JJ, Kim D, Zemon V, Silipo G, Mahoney J, Shpaner M, Jalbrzikowski M, Javitt DC. Subcortical visual dysfunction in schizophrenia drives secondary cortical impairments. Brain. 2007;130(Pt 2):417–30.

Carrion RE, Cornblatt BA, McLaughlin D, Chang J, Auther AM, Olsen RH, Javitt DC. Contributions of early cortical processing and reading ability to functional status in individuals at clinical high risk for psychosis. Schizophr Res. 2015;164(1-3):1–7.

Chen KC, Lee IH, Yang YK, Landau S, Chang WH, Chen PS, Lu RB, David AS, Bramon E. P300 waveform and dopamine transporter availability: a controlled EEG and SPECT study in medication-naive patients with schizophrenia and a meta-analysis. Psychol Med. 2014;44(10):2151–62.

Chun J, Karam ZN, Marzinzik F, Kamali M, O'Donnell L, Tso IF, Manschreck TC, McInnis M, Deldin PJ. Can P300 distinguish among schizophrenia, schizoaffective and bipolar I disorders? An ERP study of response inhibition. Schizophr Res. 2013;151(1-3):175–84.

Coffman BA, Haigh SM, Murphy TK, Salisbury DF. Impairment in mismatch negativity but not repetition suppression in schizophrenia. Brain Topogr. 2017;30(4):521–30.

Condray R, Steinhauer SR, Cohen JD, van Kammen DP, Kasparek A. Modulation of language processing in schizophrenia: effects of context and haloperidol on the event-related potential. Biol Psychiatry. 1999;45(10):1336–55.

Condray R, Yao JK, Steinhauer SR, van Kammen DP, Reddy RD, Morrow LA. Semantic memory in schizophrenia: association with cell membrane essential fatty acids. Schizophr Res. 2008;106(1):13–28.

Cortinas M, Corral MJ, Garrido G, Garolera M, Pajares M, Escera C. Reduced novelty-P3 associated with increased behavioral distractibility in schizophrenia. Biol Psychol. 2008;78(3):253–60.

Davalos DB, Kisley MA, Polk SD, Ross RG. Mismatch negativity in detection of interval duration deviation in schizophrenia. Neuroreport. 2003;14(9):1283–6.

de Loye C, Beaucousin V, Bohec AL, Blanchet A, Kostova M. An event-related potential study of predictive and integrative semantic context processing in subjects with schizotypal traits. Psychophysiology. 2013;50(11):1109–19.

de Wilde OM, Bour LJ, Dingemans PM, Koelman JH, Boeree T, Linszen DH. P300 deficits are present in young first-episode patients with schizophrenia and not in their healthy young siblings. Clin Neurophysiol. 2008;119(12):2721–6.

Debruille JB, Kumar N, Saheb D, Chintoh A, Gharghi D, Lionnet C, King S. Delusions and processing of dis-

crepant information: an event-related brain potential study. Schizophr Res. 2007;89(1-3):261–77.
Del Goleto S, Kostova M, Blanchet A. Impaired context processing during irony comprehension in schizotypy: an ERPs study. Int J Psychophysiol. 2016;105:17–25.
del Re EC, Spencer KM, Oribe N, Mesholam-Gately RI, Goldstein J, Shenton ME, Petryshen T, Seidman LJ, McCarley RW, Niznikiewicz MA. Clinical high risk and first episode schizophrenia: auditory event-related potentials. Psychiatry Res. 2015;231(2):126–33.
Devrim-Ucok M, Keskin-Ergen HY, Ucok A. Novelty P3 and P3b in first-episode schizophrenia and chronic schizophrenia. Prog Neuropsychopharmacol Biol Psychiatry. 2006;30(8):1426–34.
Devrim-Ucok M, Keskin-Ergen Y, Ucok A. Lack of progressive reduction in P3 amplitude after the first-episode of schizophrenia: a 6-year follow-up study. Psychiatry Res. 2016;243:303–11.
Dias EC, Butler PD, Hoptman MJ, Javitt DC. Early sensory contributions to contextual encoding deficits in schizophrenia. Arch Gen Psychiatry. 2011;68(7):654–64.
Ditman T, Kuperberg GR. The time course of building discourse coherence in schizophrenia: an ERP investigation. Psychophysiology. 2007;44(6):991–1001.
Doniger GM, Foxe JJ, Murray MM, Higgins BA, Javitt DC. Impaired visual object recognition and dorsal/ventral stream interaction in schizophrenia. Arch Gen Psychiatry. 2002;59(11):1011–20.
Dulude L, Labelle A, Knott VJ. Acute nicotine alteration of sensory memory impairment in smokers with schizophrenia. J Clin Psychopharmacol. 2010;30(5):541–8.
Earls HA, Curran T, Mittal V. A meta-analytic review of auditory event-related potential components as endophenotypes for schizophrenia: perspectives from first-degree relatives. Schizophr Bull. 2016;42(6):1504–16.
Ergen M, Marbach S, Brand A, Basar-Eroglu C, Demiralp T. P3 and delta band responses in visual oddball paradigm in schizophrenia. Neurosci Lett. 2008;440(3):304–8.
Erickson MA, Ruffle A, Gold JM. A meta-analysis of mismatch negativity in schizophrenia: from clinical risk to disease specificity and progression. Biol Psychiatry. 2016;79(12):980–7.
Erickson MA, Albrecht M, Ruffle A, Fleming L, Corlett P, Gold J. No association between symptom severity and MMN impairment in schizophrenia: a meta-analytic approach. Schizophr Res Cogn. 2017;9:13–7.
Ertekin E, Ucok A, Keskin-Ergen Y, Devrim-Ucok M. Deficits in Go and NoGo P3 potentials in patients with schizophrenia. Psychiatry Res. 2017;254:126–32.
Ethridge LE, Hamm JP, Shapiro JR, Summerfelt AT, Keedy SK, Stevens MC, Pearlson G, Tamminga CA, Boutros NN, Sweeney JA, Keshavan MS, Thaker G, Clementz BA. Neural activations during auditory oddball processing discriminating schizophrenia and psychotic bipolar disorder. Biol Psychiatry. 2012;72(9):766–74.
Farkas K, Stefanics G, Marosi C, Csukly G. Elementary sensory deficits in schizophrenia indexed by impaired visual mismatch negativity. Schizophr Res. 2015;166(1-3):164–70.
Fisher DJ, Labelle A, Knott VJ. The right profile: mismatch negativity in schizophrenia with and without auditory hallucinations as measured by a multi-feature paradigm. Clin Neurophysiol. 2008;119(4):909–21.
Fisher DJ, Labelle A, Knott VJ. Auditory hallucinations and the P3a: attention-switching to speech in schizophrenia. Biol Psychol. 2010;85(3):417–23.
Fisher DJ, Grant B, Smith DM, Borracci G, Labelle A, Knott VJ. Effects of auditory hallucinations on the mismatch negativity (MMN) in schizophrenia as measured by a modified 'optimal' multi-feature paradigm. Int J Psychophysiol. 2011;81(3):245–51.
Fisher DJ, Grant B, Smith DM, Borracci G, Labelle A, Knott VJ. Nicotine and the hallucinating brain: effects on mismatch negativity (MMN) in schizophrenia. Psychiatry Res. 2012a;196(2-3):181–7.
Fisher DJ, Labelle A, Knott VJ. Alterations of mismatch negativity (MMN) in schizophrenia patients with auditory hallucinations experiencing acute exacerbation of illness. Schizophr Res. 2012b;139(1-3):237–45.
Fisher DJ, Smith DM, Labelle A, Knott VJ. Attenuation of mismatch negativity (MMN) and novelty P300 in schizophrenia patients with auditory hallucinations experiencing acute exacerbation of illness. Biol Psychol. 2014;100:43–9.
Fisher DJ, Campbell DJ, Abriel SC, Ells EML, Rudolph ED, Tibbo PG. Auditory mismatch negativity and P300a elicited by the "optimal" multi-feature paradigm in early schizophrenia. Clin EEG Neurosci. 2018;49(4):238–47.
Force RB, Venables NC, Sponheim SR. An auditory processing abnormality specific to liability for schizophrenia. Schizophr Res. 2008;103(1-3):298–310.
Ford JM. Studying auditory verbal hallucinations using the RDoC framework. Psychophysiology. 2016;53(3):298–304.
Ford JM, Mathalon DH, Heinks T, Kalba S, Faustman WO, Roth WT. Neurophysiological evidence of corollary discharge dysfunction in schizophrenia. Am J Psychiatry. 2001a;158(12):2069–71.
Ford JM, Mathalon DH, Kalba S, Marsh L, Pfefferbaum A. N1 and P300 abnormalities in patients with schizophrenia, epilepsy, and epilepsy with schizophrenialike features. Biol Psychiatry. 2001b;49(10):848–60.
Ford JM, Mathalon DH, Kalba S, Whitfield S, Faustman WO, Roth WT. Cortical responsiveness during talking and listening in schizophrenia: an event-related brain potential study. Biol Psychiatry. 2001c;50(7):540–9.
Ford JM, Mathalon DH, Kalba S, Whitfield S, Faustman WO, Roth WT. Cortical responsiveness during inner speech in schizophrenia: an event-related potential study. Am J Psychiatry. 2001d;158(11):1914–6.
Ford JM, Gray M, Whitfield SL, Turken AU, Glover G, Faustman WO, Mathalon DH. Acquiring and inhibiting prepotent responses in schizophrenia: event-related brain potentials and functional magnetic resonance imaging. Arch Gen Psychiatry. 2004;61(2):119–29.

Ford JM, Roach BJ, Faustman WO, Mathalon DH. Synch before you speak: auditory hallucinations in schizophrenia. Am J Psychiatry. 2007;164(3):458–66.

Ford JM, Mathalon DH, Roach BJ, Keedy SK, Reilly JL, Gershon ES, Sweeney JA. Neurophysiological evidence of corollary discharge function during vocalization in psychotic patients and their nonpsychotic first-degree relatives. Schizophr Bull. 2013;39(6):1272–80.

Ford JM, Palzes VA, Roach BJ, Mathalon DH. Did I do that? Abnormal predictive processes in schizophrenia when button pressing to deliver a tone. Schizophr Bull. 2014;40(4):804–12.

Foxe JJ, Doniger GM, Javitt DC. Early visual processing deficits in schizophrenia: impaired P1 generation revealed by high-density electrical mapping. Neuroreport. 2001;12(17):3815–20.

Foxe JJ, Yeap S, Snyder AC, Kelly SP, Thakore JH, Molholm S. The N1 auditory evoked potential component as an endophenotype for schizophrenia: high-density electrical mapping in clinically unaffected first-degree relatives, first-episode, and chronic schizophrenia patients. Eur Arch Psychiatry Clin Neurosci. 2011;261(5):331–9.

Friedman T, Sehatpour P, Dias E, Perrin M, Javitt DC. Differential relationships of mismatch negativity and visual P1 deficits to premorbid characteristics and functional outcome in schizophrenia. Biol Psychiatry. 2012;71(6):521–9.

Frodl T, Meisenzahl EM, Muller D, Holder J, Juckel G, Moller HJ, Hegerl U. P300 subcomponents and clinical symptoms in schizophrenia. Int J Psychophysiol. 2002;43(3):237–46.

Fulham WR, Michie PT, Ward PB, Rasser PE, Todd J, Johnston PJ, Thompson PM, Schall U. Mismatch negativity in recent-onset and chronic schizophrenia: a current source density analysis. PLoS One. 2014;9(6):e100221.

Galletly CA, McFarlane AC, Clark CR. Impaired updating of working memory in schizophrenia. Int J Psychophysiol. 2007;63(3):265–74.

Gaspar PA, Ruiz S, Zamorano F, Altayo M, Perez C, Bosman CA, Aboitiz F. P300 amplitude is insensitive to working memory load in schizophrenia. BMC Psychiatry. 2011;11:29.

Gonul AS, Suer C, Coburn K, Ozesmi C, Oguz A, Yilmaz A. Effects of olanzapine on auditory P300 in schizophrenia. Prog Neuropsychopharmacol Biol Psychiatry. 2003;27(1):173–7.

Green AE, Fitzgerald PB, Johnston PJ, Nathan PJ, Kulkarni J, Croft RJ. Evidence for a differential contribution of early perceptual and late cognitive processes during encoding to episodic memory impairment in schizophrenia. World J Biol Psychiatry. 2017;18(5):369–81.

Greenwood LM, Leung S, Michie PT, Green A, Nathan PJ, Fitzgerald P, Johnston P, Solowij N, Kulkarni J, Croft RJ. The effects of glycine on auditory mismatch negativity in schizophrenia. Schizophr Res. 2018;191:61–9.

Groom MJ, Bates AT, Jackson GM, Calton TG, Liddle PF, Hollis C. Event-related potentials in adolescents with schizophrenia and their siblings: a comparison with attention-deficit/hyperactivity disorder. Biol Psychiatry. 2008;63(8):784–92.

Gudlowski Y, Ozgurdal S, Witthaus H, Gallinat J, Hauser M, Winter C, Uhl I, Heinz A, Juckel G. Serotonergic dysfunction in the prodromal, first-episode and chronic course of schizophrenia as assessed by the loudness dependence of auditory evoked activity. Schizophr Res. 2009;109(1-3):141–7.

Guerra S, Ibanez A, Martin M, Bobes MA, Reyes A, Mendoza R, Bravo T, Dominguez M, Sosa MV. N400 deficits from semantic matching of pictures in probands and first-degree relatives from multiplex schizophrenia families. Brain Cogn. 2009;70(2):221–30.

Guillem F, Bicu M, Hooper R, Bloom D, Wolf MA, Messier J, Desautels R, Debruille JB. Memory impairment in schizophrenia: a study using event-related potentials in implicit and explicit tasks. Psychiatry Res. 2001;104(2):157–73.

Guillem F, Bicu M, Pampoulova T, Hooper R, Bloom D, Wolf MA, Messier J, Desautels R, Todorov C, Lalonde P, Debruille JB. The cognitive and anatomo-functional basis of reality distortion in schizophrenia: a view from memory event-related potentials. Psychiatry Res. 2003;117(2):137–58.

Guillem F, Chouinard S, Poulin J, Godbout R, Lalonde P, Melun P, Bentaleb LA, Stip E. Are cholinergic enhancers beneficial for memory in schizophrenia? An event-related potentials (ERPs) study of rivastigmine add-on therapy in a crossover trial. Prog Neuropsychopharmacol Biol Psychiatry. 2006;30(5):934–45.

Gunduz-Bruce H, Reinhart RM, Roach BJ, Gueorguieva R, Oliver S, D'Souza DC, Ford JM, Krystal JH, Mathalon DH. Glutamatergic modulation of auditory information processing in the human brain. Biol Psychiatry. 2012;71(11):969–77.

Haaf M, Leicht G, Curic S, Mulert C. Glutamatergic deficits in schizophrenia - biomarkers and pharmacological Interventions within the ketamine model. Curr Pharm Biotechnol. 2018;19(4):293–307.

Haigh SM, Coffman BA, Salisbury DF. Mismatch negativity in first-episode schizophrenia: a meta-analysis. Clin EEG Neurosci. 2017;48(1):3–10.

Hall MH, Rijsdijk F, Picchioni M, Schulze K, Ettinger U, Toulopoulou T, Bramon E, Murray RM, Sham P. Substantial shared genetic influences on schizophrenia and event-related potentials. Am J Psychiatry. 2007;164(5):804–12.

Hamilton HK, D'Souza DC, Ford JM, Roach BJ, Kort NS, Ahn KH, Bhakta S, Ranganathan M, Mathalon DH. Interactive effects of an N-methyl-D-aspartate receptor antagonist and a nicotinic acetylcholine receptor agonist on mismatch negativity: implications for schizophrenia. Schizophr Res. 2018a;191:87–94.

Hamilton HK, Perez VB, Ford JM, Roach BJ, Jaeger J, Mathalon DH. Mismatch negativity but not P300 is

associated with functional disability in schizophrenia. Schizophr Bull. 2018b;44(3):492–504.

Hay RA, Roach BJ, Srihari VH, Woods SW, Ford JM, Mathalon DH. Equivalent mismatch negativity deficits across deviant types in early illness schizophrenia-spectrum patients. Biol Psychol. 2015;105:130–7.

Heekeren K, Daumann J, Neukirch A, Stock C, Kawohl W, Norra C, Waberski TD, Gouzoulis-Mayfrank E. Mismatch negativity generation in the human 5HT2A agonist and NMDA antagonist model of psychosis. Psychopharmacology (Berl). 2008;199(1):77–88.

Hermens DF, Ward PB, Hodge MA, Kaur M, Naismith SL, Hickie IB. Impaired MMN/P3a complex in first-episode psychosis: cognitive and psychosocial associations. Prog Neuropsychopharmacol Biol Psychiatry. 2010;34(6):822–9.

Higashima M, Nagasawa T, Kawasaki Y, Oka T, Sakai N, Tsukada T, Koshino Y. Auditory P300 amplitude as a state marker for positive symptoms in schizophrenia: cross-sectional and retrospective longitudinal studies. Schizophr Res. 2003;59(2-3):147–57.

Higuchi Y, Sumiyoshi T, Kawasaki Y, Matsui M, Arai H, Kurachi M. Electrophysiological basis for the ability of olanzapine to improve verbal memory and functional outcome in patients with schizophrenia: a LORETA analysis of P300. Schizophr Res. 2008;101(1-3):320–30.

Higuchi Y, Sumiyoshi T, Seo T, Miyanishi T, Kawasaki Y, Suzuki M. Mismatch negativity and cognitive performance for the prediction of psychosis in subjects with at-risk mental state. PLoS One. 2013;8(1):e54080.

Higuchi Y, Seo T, Miyanishi T, Kawasaki Y, Suzuki M, Sumiyoshi T. Mismatch negativity and P3a/reorienting complex in subjects with schizophrenia or at-risk mental state. Front Behav Neurosci. 2014;8:172.

Hokama H, Hiramatsu K, Wang J, O'Donnell BF, Ogura C. N400 abnormalities in unmedicated patients with schizophrenia during a lexical decision task. Int J Psychophysiol. 2003;48(1):1–10.

Holliday WB, Gurnsey K, Sweet RA, Teichert T. A putative electrophysiological biomarker of auditory sensory memory encoding is sensitive to pharmacological alterations of excitatory/inhibitory balance in male macaque monkeys. J Psychiatry Neurosci. 2017;43(1):170093.

Hong LE, Moran LV, Du X, O'Donnell P, Summerfelt A. Mismatch negativity and low frequency oscillations in schizophrenia families. Clin Neurophysiol. 2012;123(10):1980–8.

Horan WP, Foti D, Hajcak G, Wynn JK, Green MF. Intact motivated attention in schizophrenia: evidence from event-related potentials. Schizophr Res. 2012;135(1-3):95–9.

Hoshino KY, Takeuchi S, Jodo E, Suzuki Y, Kayama Y, Niwa S. Tripartite relationship among P300, clinical features and brain structure in neuroleptic-naive schizophrenia. Psychiatry Clin Neurosci. 2005;59(4):410–7.

Huang WL, Liu CY, Liu CM, Liu HM, Yang CY, Hwang TJ, Hsieh MH, Hwu HG. Association between mismatch negativity and voxel-based brain volume in schizophrenia. Clin Neurophysiol. 2018;129(9):1899–906.

Iakimova G, Passerieux C, Laurent JP, Hardy-Bayle MC. ERPs of metaphoric, literal, and incongruous semantic processing in schizophrenia. Psychophysiology. 2005;42(4):380–90.

Inami R, Kirino E, Inoue R, Suzuki T, Arai H. Nicotine effects on mismatch negativity in nonsmoking schizophrenic patients. Neuropsychobiology. 2007;56(2-3):64–72.

Itagaki S, Yabe H, Mori Y, Ishikawa H, Takanashi Y, Niwa S. Event-related potentials in patients with adult attention-deficit/hyperactivity disorder versus schizophrenia. Psychiatry Res. 2011;189(2):288–91.

Iwanami A, Okajima Y, Kuwakado D, Isono H, Kasai K, Hata A, Nakagome K, Fukuda M, Kamijima K. Event-related potentials and thought disorder in schizophrenia. Schizophr Res. 2000;42(3):187–91.

Iwanami A, Kato N, Kasai K, Kamio S, Furukawa S, Fukuda M, Nakagome K, Araki T, Okajima Y, Isono H, Kamijima K. P300 amplitude over temporal regions in schizophrenia. Eur Arch Psychiatry Clin Neurosci. 2002;252(1):1–7.

Jackson F, Foti D, Kotov R, Perlman G, Mathalon DH, Proudfit GH. An incongruent reality: the N400 in relation to psychosis and recovery. Schizophr Res. 2014;160(1-3):208–15.

Jahshan C, Cadenhead KS, Rissling AJ, Kirihara K, Braff DL, Light GA. Automatic sensory information processing abnormalities across the illness course of schizophrenia. Psychol Med. 2012a;42(1):85–97.

Jahshan C, Wynn JK, Mathis KI, Altshuler LL, Glahn DC, Green MF. Cross-diagnostic comparison of duration mismatch negativity and P3a in bipolar disorder and schizophrenia. Bipolar Disord. 2012b;14(3):239–48.

Javitt DC. Neurophysiological models for new treatment development in schizophrenia: early sensory approaches. Ann N Y Acad Sci. 2015;1344:92–104.

Javitt DC, Sweet RA. Auditory dysfunction in schizophrenia: integrating clinical and basic features. Nat Rev Neurosci. 2015;16(9):535–50.

Javitt DC, Shelley AM, Silipo G, Lieberman JA. Deficits in auditory and visual context-dependent processing in schizophrenia: defining the pattern. Arch Gen Psychiatry. 2000;57(12):1131–7.

Javitt DC, Lee M, Kantrowitz JT, Martinez A. Mismatch negativity as a biomarker of theta band oscillatory dysfunction in schizophrenia. Schizophr Res. 2018;191:51–60.

Jeon YW, Polich J. P300 asymmetry in schizophrenia: a meta-analysis. Psychiatry Res. 2001;104(1):61–74.

Jeon YW, Polich J. Meta-analysis of P300 and schizophrenia: patients, paradigms, and practical implications. Psychophysiology. 2003;40(5):684–701.

Johannesen JK, O'Donnell BF, Shekhar A, McGrew JH, Hetrick WP. Diagnostic specificity of neurophysi-

ological endophenotypes in schizophrenia and bipolar disorder. Schizophr Bull. 2013;39(6):1219–29.

Johnson SC, Lowery N, Kohler C, Turetsky BI. Global-local visual processing in schizophrenia: Evidence for an early visual processing deficit. Biol Psychiatry. 2005;58(12):937–46.

Juckel G, Gallinat J, Riedel M, Sokullu S, Schulz C, Moller HJ, Muller N, Hegerl U. Serotonergic dysfunction in schizophrenia assessed by the loudness dependence measure of primary auditory cortex evoked activity. Schizophr Res. 2003;64(2-3):115–24.

Juckel G, Gudlowski Y, Muller D, Ozgurdal S, Brune M, Gallinat J, Frodl T, Witthaus H, Uhl I, Wutzler A, Pogarell O, Mulert C, Hegerl U, Meisenzahl EM. Loudness dependence of the auditory evoked N1/P2 component as an indicator of serotonergic dysfunction in patients with schizophrenia—a replication study. Psychiatry Res. 2008;158(1):79–82.

Kantrowitz JT, Epstein ML, Beggel O, Rohrig S, Lehrfeld JM, Revheim N, Lehrfeld NP, Reep J, Parker E, Silipo G, Ahissar M, Javitt DC. Neurophysiological mechanisms of cortical plasticity impairments in schizophrenia and modulation by the NMDA receptor agonist D-serine. Brain. 2016;139(Pt 12):3281–95.

Kantrowitz JT, Epstein ML, Lee M, Lehrfeld N, Nolan KA, Shope C, Petkova E, Silipo G, Javitt DC. Improvement in mismatch negativity generation during d-serine treatment in schizophrenia: correlation with symptoms. Schizophr Res. 2018;191:70–9.

Kargel C, Sartory G, Kariofillis D, Wiltfang J, Muller BW. Mismatch negativity latency and cognitive function in schizophrenia. PLoS One. 2014;9(4):e84536.

Karoumi B, Laurent A, Rosenfeld F, Rochet T, Brunon AM, Dalery J, d'Amato T, Saoud M. Alteration of event related potentials in siblings discordant for schizophrenia. Schizophr Res. 2000;41(2):325–34.

Kasai K, Nakagome K, Itoh K, Koshida I, Hata A, Iwanami A, Fukuda M, Kato N. Impaired cortical network for preattentive detection of change in speech sounds in schizophrenia: a high-resolution event-related potential study. Am J Psychiatry. 2002;159(4):546–53.

Kaur M, Battisti RA, Ward PB, Ahmed A, Hickie IB, Hermens DF. MMN/P3a deficits in first episode psychosis: comparing schizophrenia-spectrum and affective-spectrum subgroups. Schizophr Res. 2011;130(1-3):203–9.

Kaur M, Lagopoulos J, Lee RS, Ward PB, Naismith SL, Hickie IB, Hermens DF. Longitudinal associations between mismatch negativity and disability in early schizophrenia- and affective-spectrum disorders. Prog Neuropsychopharmacol Biol Psychiatry. 2013;46:161–9.

Kawasaki Y, Sumiyoshi T, Higuchi Y, Ito T, Takeuchi M, Kurachi M. Voxel-based analysis of P300 electrophysiological topography associated with positive and negative symptoms of schizophrenia. Schizophr Res. 2007;94(1-3):164–71.

Kayser J, Bruder GE, Tenke CE, Stuart BK, Amador XF, Gorman JM. Event-related brain potentials (ERPs) in schizophrenia for tonal and phonetic oddball tasks. Biol Psychiatry. 2001;49(10):832–47.

Kayser J, Tenke CE, Malaspina D, Kroppmann CJ, Schaller JD, Deptula A, Gates NA, Harkavy-Friedman JM, Gil R, Bruder GE. Neuronal generator patterns of olfactory event-related brain potentials in schizophrenia. Psychophysiology. 2010;47(6):1075–86.

Kayser J, Tenke CE, Kroppmann CJ, Alschuler DM, Fekri S, Gil R, Jarskog LF, Harkavy-Friedman JM, Bruder GE. A neurophysiological deficit in early visual processing in schizophrenia patients with auditory hallucinations. Psychophysiology. 2012;49(9):1168–78.

Kayser J, Tenke CE, Kroppmann CJ, Alschuler DM, Ben-David S, Fekri S, Bruder GE, Corcoran CM. Olfaction in the psychosis prodrome: Electrophysiological and behavioral measures of odor detection. Int J Psychophysiol. 2013;90(2):190–206.

Kiang M, Kutas M. Association of schizotypy with semantic processing differences: an event-related brain potential study. Schizophr Res. 2005;77(2-3):329–42.

Kiang M, Kutas M, Light GA, Braff DL. An event-related brain potential study of direct and indirect semantic priming in schizophrenia. Am J Psychiatry. 2008;165(1):74–81.

Kiang M, Braff DL, Sprock J, Light GA. The relationship between preattentive sensory processing deficits and age in schizophrenia patients. Clin Neurophysiol. 2009;120(11):1949–57.

Kiang M, Christensen BK, Zipursky RB. Depth-of-processing effects on semantic activation deficits in schizophrenia: an electrophysiological investigation. Schizophr Res. 2011;133(1-3):91–8.

Kiang M, Christensen BK, Kutas M, Zipursky RB. Electrophysiological evidence for primary semantic memory functional organization deficits in schizophrenia. Psychiatry Res. 2012;196(2-3):171–80.

Kiang M, Christensen BK, Zipursky RB. Event-related brain potential study of semantic priming in unaffected first-degree relatives of schizophrenia patients. Schizophr Res. 2014;153(1-3):78–86.

Kim MS, Kang SS, Youn T, Kang DH, Kim JJ, Kwon JS. Neuropsychological correlates of P300 abnormalities in patients with schizophrenia and obsessive-compulsive disorder. Psychiatry Res. 2003;123(2):109–23.

Kim DW, Shim M, Kim JI, Im CH, Lee SH. Source activation of P300 correlates with negative symptom severity in patients with schizophrenia. Brain Topogr. 2014a;27(2):307–17.

Kim M, Kim SN, Lee S, Byun MS, Shin KS, Park HY, Jang JH, Kwon JS. Impaired mismatch negativity is associated with current functional status rather than genetic vulnerability to schizophrenia. Psychiatry Res. 2014b;222(1-2):100–6.

Kim M, Lee TH, Kim JH, Hong H, Lee TY, Lee Y, Salisbury DF, Kwon JS. Decomposing P300 into correlates of genetic risk and current symptoms in schizophrenia: an inter-trial variability analysis. Schizophr Res. 2018a;192:232–9.

Kim M, Lee TH, Yoon YB, Lee TY, Kwon JS. Predicting remission in subjects at clinical high risk for psy-

chosis using mismatch negativity. Schizophr Bull. 2018b;44(3):575–83.

Kim S, Jeon H, Jang KI, Kim YW, Im CH, Lee SH. Mismatch negativity and cortical thickness in patients with schizophrenia and bipolar disorder. Schizophr Bull. 2019;45(2):425–35.

Kimble M, Lyons M, O'Donnell B, Nestor P, Niznikiewicz M, Toomey R. The effect of family status and schizotypy on electrophysiologic measures of attention and semantic processing. Biol Psychiatry. 2000;47(5):402–12.

Kirihara K, Araki T, Kasai K, Maeda K, Hata A, Uetsuki M, Yamasue H, Rogers MA, Kato N, Iwanami A. Confirmation of a relationship between reduced auditory P300 amplitude and thought disorder in schizophrenia. Schizophr Res. 2005;80(2-3):197–201.

Kirihara K, Araki T, Uetsuki M, Yamasue H, Hata A, Rogers MA, Iwanami A, Kasai K. Association study between auditory P3a/P3b event-related potentials and thought disorder in schizophrenia. Brain Imaging Behav. 2009;3(3):277–83.

Knott V, Shah D, Millar A, McIntosh J, Fisher D, Blais C, Ilivitsky V. Nicotine, auditory sensory memory, and sustained attention in a human ketamine model of schizophrenia: moderating influence of a hallucinatory trait. Front Pharmacol. 2012;3:172.

Kogoj A, Pirtosek Z, Tomori M, Vodusek DB. Event-related potentials elicited by distractors in an auditory oddball paradigm in schizophrenia. Psychiatry Res. 2005;137(1-2):49–59.

Kort NS, Ford JM, Roach BJ, Gunduz-Bruce H, Krystal JH, Jaeger J, Reinhart RM, Mathalon DH. Role of N-methyl-D-aspartate receptors in action-based predictive coding deficits in schizophrenia. Biol Psychiatry. 2017;81(6):514–24.

Koshiyama D, Kirihara K, Tada M, Nagai T, Koike S, Suga M, Araki T, Kasai K. Duration and frequency mismatch negativity shows no progressive reduction in early stages of psychosis. Schizophr Res. 2017;190:32–8.

Koshiyama D, Kirihara K, Tada M, Nagai T, Fujioka M, Koike S, Suga M, Araki T, Kasai K. Association between mismatch negativity and global functioning is specific to duration deviance in early stages of psychosis. Schizophr Res. 2018;195:378–84.

Kostova M, Passerieux C, Laurent JP, Hardy-Bayle MC. N400 anomalies in schizophrenia are correlated with the severity of formal thought disorder. Schizophr Res. 2005;78(2-3):285–91.

Koychev I, El-Deredy W, Deakin JF. New visual information processing abnormality biomarker for the diagnosis of Schizophrenia. Expert Opin Med Diagn. 2011;5(4):357–68.

Kremlacek J, Kreegipuu K, Tales A, Astikainen P, Poldver N, Naatanen R, Stefanics G. Visual mismatch negativity (vMMN): a review and meta-analysis of studies in psychiatric and neurological disorders. Cortex. 2016;80:76–112.

Kuperberg GR, Weber K, Delaney-Busch N, Ustine C, Stillerman B, Hamalainen M, Lau E. Multimodal neuroimaging evidence for looser lexico-semantic connections in schizophrenia: evidence from masked indirect semantic priming. Neuropsychologia. 2019;124:337–49.

Laurent JP, Kostova M, Passerieux C. N400 and P300 modulation as functions of processing level in schizophrenia patients exhibiting formal thought disorder. Int J Psychophysiol. 2010;75(2):177–82.

Lavoie S, Jack BN, Griffiths O, Ando A, Amminger P, Couroupis A, Jago A, Markulev C, McGorry PD, Nelson B, Polari A, Yuen HP, Whitford TJ. Impaired mismatch negativity to frequency deviants in individuals at ultra-high risk for psychosis, and preliminary evidence for further impairment with transition to psychosis. Schizophr Res. 2018;191:95–100.

Lee SY, Namkoong K, Cho HH, Song DH, An SK. Reduced visual P300 amplitudes in individuals at ultra-high risk for psychosis and first-episode schizophrenia. Neurosci Lett. 2010;486(3):156–60.

Lee SH, Sung K, Lee KS, Moon E, Kim CG. Mismatch negativity is a stronger indicator of functional outcomes than neurocognition or theory of mind in patients with schizophrenia. Prog Neuropsychopharmacol Biol Psychiatry. 2014;48:213–9.

Lee CW, Kim SH, Shim M, Ryu V, Ha RY, Lee SJ, Cho HS. P600 alteration of syntactic language processing in patients with bipolar mania: Comparison to schizophrenic patients and healthy subjects. J Affect Disord. 2016;201:101–11.

Lee M, Sehatpour P, Hoptman MJ, Lakatos P, Dias EC, Kantrowitz JT, Martinez AM, Javitt DC. Neural mechanisms of mismatch negativity dysfunction in schizophrenia. Mol Psychiatry. 2017;22(11):1585–93.

Lee M, Sehatpour P, Dias EC, Silipo GS, Kantrowitz JT, Martinez AM, Javitt DC. A tale of two sites: differential impairment of frequency and duration mismatch negativity across a primarily inpatient versus a primarily outpatient site in schizophrenia. Schizophr Res. 2018;191:10–7.

Leitman DI, Sehatpour P, Higgins BA, Foxe JJ, Silipo G, Javitt DC. Sensory deficits and distributed hierarchical dysfunction in schizophrenia. Am J Psychiatry. 2010;167(7):818–27.

Lepock JR, Mizrahi R, Korostil M, Bagby RM, Pang EW, Kiang M. Event-related potentials in the clinical high-risk (CHR) state for psychosis: a systematic review. Clin EEG Neurosci. 2018;49(4):215–25.

Leung S, Croft RJ, Baldeweg T, Nathan PJ. Acute dopamine D(1) and D(2) receptor stimulation does not modulate mismatch negativity (MMN) in healthy human subjects. Psychopharmacology (Berl). 2007;194(4):443–51.

Light GA, Braff DL. Stability of mismatch negativity deficits and their relationship to functional impairments in chronic schizophrenia. Am J Psychiatry. 2005a;162(9):1741–3.

Light GA, Braff DL. Mismatch negativity deficits are associated with poor functioning in schizophrenia patients. Arch Gen Psychiatry. 2005b;62(2):127–36.

Light GA, Naatanen R. Mismatch negativity is a breakthrough biomarker for understanding and treating psychotic disorders. Proc Natl Acad Sci U S A. 2013;110(38):15175–6.

Light GA, Swerdlow NR. Future clinical uses of neurophysiological biomarkers to predict and monitor treatment response for schizophrenia. Ann N Y Acad Sci. 2015a;1344:105–19.

Light GA, Swerdlow NR, Thomas ML, Calkins ME, Green MF, Greenwood TA, Gur RE, Gur RC, Lazzeroni LC, Nuechterlein KH, Pela M, Radant AD, Seidman LJ, Sharp RF, Siever LJ, Silverman JM, Sprock J, Stone WS, Sugar CA, Tsuang DW, Tsuang MT, Braff DL, Turetsky BI. Validation of mismatch negativity and P3a for use in multi-site studies of schizophrenia: characterization of demographic, clinical, cognitive, and functional correlates in COGS-2. Schizophr Res. 2015b;163(1-3):63–72.

Liu Z, Tam WC, Xue Z, Yao S, Wu D. Positive and negative symptom profile schizophrenia and abnormalities in the P300 component of the event-related potential: a longitudinal controlled study. Psychiatry Res. 2004;132(2):131–9.

Longenecker JM, Venables NC, Kang SS, McGuire KA, Sponheim SR. Brain responses at encoding predict limited verbal memory retrieval by persons with schizophrenia. Arch Clin Neuropsychol. 2018;33(4):477–90.

Lynn PA, Kang SS, Sponheim SR. Impaired retrieval processes evident during visual working memory in schizophrenia. Schizophr Res Cogn. 2016;5:47–55.

Magno E, Yeap S, Thakore JH, Garavan H, De Sanctis P, Foxe JJ. Are auditory-evoked frequency and duration mismatch negativity deficits endophenotypic for schizophrenia? High-density electrical mapping in clinically unaffected first-degree relatives and first-episode and chronic schizophrenia. Biol Psychiatry. 2008;64(5):385–91.

Mathalon DH, Ford JM, Pfefferbaum A. Trait and state aspects of P300 amplitude reduction in schizophrenia: a retrospective longitudinal study. Biol Psychiatry. 2000a;47(5):434–49.

Mathalon DH, Ford JM, Rosenbloom M, Pfefferbaum A. P300 reduction and prolongation with illness duration in schizophrenia. Biol Psychiatry. 2000b;47(5):413–27.

Mathalon DH, Faustman WO, Ford JM. N400 and automatic semantic processing abnormalities in patients with schizophrenia. Arch Gen Psychiatry. 2002;59(7):641–8.

Mathalon DH, Hoffman RE, Watson TD, Miller RM, Roach BJ, Ford JM. Neurophysiological distinction between schizophrenia and schizoaffective disorder. Front Hum Neurosci. 2010a;3:70.

Mathalon DH, Roach BJ, Ford JM. Automatic semantic priming abnormalities in schizophrenia. Int J Psychophysiol. 2010b;75(2):157–66.

Mathalon DH, Ahn KH, Perry EB Jr, Cho HS, Roach BJ, Blais RK, Bhakta S, Ranganathan M, Ford JM, D'Souza DC. Effects of nicotine on the neurophysiological and behavioral effects of ketamine in humans. Front Psych. 2014;5:3.

McCarley RW, Salisbury DF, Hirayasu Y, Yurgelun-Todd DA, Tohen M, Zarate C, Kikinis R, Jolesz FA, Shenton ME. Association between smaller left posterior superior temporal gyrus volume on magnetic resonance imaging and smaller left temporal P300 amplitude in first-episode schizophrenia. Arch Gen Psychiatry. 2002;59(4):321–31.

McCleery A, Wynn JK, Mathalon DH, Roach BJ, Green MF. Hallucinations, neuroplasticity, and prediction errors in schizophrenia. Scand J Psychol. 2018;59(1):41–8.

Meisenzahl EM, Frodl T, Muller D, Schmitt G, Gallinat J, Zetzsche T, Marcuse A, Juckel G, Leinsinger G, Hahn K, Moller HJ, Hegerl U. Superior temporal gyrus and P300 in schizophrenia: a combined ERP/structural magnetic resonance imaging investigation. J Psychiatr Res. 2004;38(2):153–62.

Michie PT, Budd TW, Todd J, Rock D, Wichmann H, Box J, Jablensky AV. Duration and frequency mismatch negativity in schizophrenia. Clin Neurophysiol. 2000;111(6):1054–65.

Michie PT, Innes-Brown H, Todd J, Jablensky AV. Duration mismatch negativity in biological relatives of patients with schizophrenia spectrum disorders. Biol Psychiatry. 2002;52(7):749–58.

Michie PT, Malmierca MS, Harms L, Todd J. The neurobiology of MMN and implications for schizophrenia. Biol Psychol. 2016;116:90–7.

Minami Y, Kirino E. Schizophrenic patients are impaired in memory reinstatement underlying mismatch negativity system. Clin Neurophysiol. 2005;116(1):120–8.

Molina V, Munoz F, Martin-Loeches M, Casado P, Hinojosa JA, Iglesias A. Long-term olanzapine treatment and P300 parameters in schizophrenia. Neuropsychobiology. 2004;50(2):182–8.

Molina V, Sanz J, Munoz F, Casado P, Hinojosa JA, Sarramea F, Martin-Loeches M. Dorsolateral prefrontal cortex contribution to abnormalities of the P300 component of the event-related potential in schizophrenia. Psychiatry Res. 2005;140(1):17–26.

Morales-Munoz I, Jurado-Barba R, Fernandez-Guinea S, Alvarez-Alonso MJ, Rodriguez-Jimenez R, Jimenez-Arriero MA, Rubio G. Cognitive impairments in patients with first episode psychosis: the relationship between neurophysiological and neuropsychological assessments. J Clin Neurosci. 2017;36:80–7.

Mori Y, Kurosu S, Hiroyama Y, Niwa S. Prolongation of P300 latency is associated with the duration of illness in male schizophrenia patients. Psychiatry Clin Neurosci. 2007;61(5):471–8.

Murphy JR, Rawdon C, Kelleher I, Twomey D, Markey PS, Cannon M, Roche RA. Reduced duration mismatch negativity in adolescents with psychotic symptoms: Further evidence for mismatch negativity as a possible biomarker for vulnerability to psychosis. BMC Psychiatry. 2013;13:45.

Naatanen R, Todd J, Schall U. Mismatch negativity (MMN) as biomarker predicting psychosis in clinically at-risk individuals. Biol Psychol. 2016;116:36–40.

Nagai T, Tada M, Kirihara K, Araki T, Jinde S, Kasai K. Mismatch negativity as a “translatable” brain

marker toward early intervention for psychosis: a review. Front Psych. 2013;4:115.

Nagai T, Kirihara K, Tada M, Koshiyama D, Koike S, Suga M, Araki T, Hashimoto K, Kasai K. Reduced mismatch negativity is associated with increased plasma level of glutamate in first-episode psychosis. Sci Rep. 2017;7(1):2258.

Neuhaus AH, Koehler S, Opgen-Rhein C, Urbanek C, Hahn E, Dettling M. Selective anterior cingulate cortex deficit during conflict solution in schizophrenia: an event-related potential study. J Psychiatr Res. 2007;41(8):635–44.

Neuhaus AH, Hahn E, Hahn C, Ta TM, Opgen-Rhein C, Urbanek C, Dettling M. Visual P3 amplitude modulation deficit in schizophrenia is independent of duration of illness. Schizophr Res. 2011a;130(1-3):210–5.

Neuhaus AH, Karl C, Hahn E, Trempler NR, Opgen-Rhein C, Urbanek C, Hahn C, Ta TM, Dettling M. Dissection of early bottom-up and top-down deficits during visual attention in schizophrenia. Clin Neurophysiol. 2011b;122(1):90–8.

Neuhaus AH, Brandt ES, Goldberg TE, Bates JA, Malhotra AK. Evidence for impaired visual prediction error in schizophrenia. Schizophr Res. 2013;147(2-3):326–30.

Niznikiewicz MA, Voglmaier M, Shenton ME, Seidman LJ, Dickey CC, Rhoads R, Teh E, McCarley RW. Electrophysiological correlates of language processing in schizotypal personality disorder. Am J Psychiatry. 1999;156(7):1052–8.

Niznikiewicz MA, Friedman M, Shenton ME, Voglmaier M, Nestor PG, Frumin M, Seidman L, Sutton J, McCarley RW. Processing sentence context in women with schizotypal personality disorder: an ERP study. Psychophysiology. 2004;41(3):367–71.

Niznikiewicz MA, Patel JK, McCarley R, Sutton J, Chau DT, Wojcik J, Green AI. Clozapine action on auditory P3 response in schizophrenia. Schizophr Res. 2005;76(1):119–21.

Niznikiewicz MA, Spencer KM, Dickey C, Voglmaier M, Seidman LJ, Shenton ME, McCarley RW. Abnormal pitch mismatch negativity in individuals with schizotypal personality disorder. Schizophr Res. 2009;110(1-3):188–93.

Niznikiewicz MA, Mittal MS, Nestor PG, McCarley RW. Abnormal inhibitory processes in semantic networks in schizophrenia. Int J Psychophysiol. 2010;75(2):133–40.

O'Donnell BF, Vohs JL, Hetrick WP, Carroll CA, Shekhar A. Auditory event-related potential abnormalities in bipolar disorder and schizophrenia. Int J Psychophysiol. 2004;53(1):45–55.

Oestreich LK, Mifsud NG, Ford JM, Roach BJ, Mathalon DH, Whitford TJ. Subnormal sensory attenuation to self-generated speech in schizotypy: electrophysiological evidence for a 'continuum of psychosis'. Int J Psychophysiol. 2015;97(2):131–8.

Oestreich LK, Mifsud NG, Ford JM, Roach BJ, Mathalon DH, Whitford TJ. Cortical suppression to delayed self-initiated auditory stimuli in schizotypy: neurophysiological evidence for a continuum of psychosis. Clin EEG Neurosci. 2016;47(1):3–10.

Oranje B, Jensen K, Wienberg M, Glenthoj BY. Divergent effects of increased serotonergic activity on psychophysiological parameters of human attention. Int J Neuropsychopharmacol. 2008;11(4):453–63.

Oribe N, Hirano Y, Kanba S, del Re EC, Seidman LJ, Mesholam-Gately R, Spencer KM, McCarley RW, Niznikiewicz MA. Early and late stages of visual processing in individuals in prodromal state and first episode schizophrenia: an ERP study. Schizophr Res. 2013;146(1-3):95–102.

Ozgurdal S, Gudlowski Y, Witthaus H, Kawohl W, Uhl I, Hauser M, Gorynia I, Gallinat J, Heinze M, Heinz A, Juckel G. Reduction of auditory event-related P300 amplitude in subjects with at-risk mental state for schizophrenia. Schizophr Res. 2008;105(1-3):272–8.

Pae JS, Kwon JS, Youn T, Park HJ, Kim MS, Lee B, Park KS. LORETA imaging of P300 in schizophrenia with individual MRI and 128-channel EEG. Neuroimage. 2003;20(3):1552–60.

Pantlin LN, Davalos D. Neurophysiology for detection of high risk for psychosis. Schizophr Res Treat. 2016;2016:2697971.

Park EJ, Han SI, Jeon YW. Auditory and visual P300 reflecting cognitive improvement in patients with schizophrenia with quetiapine: a pilot study. Prog Neuropsychopharmacol Biol Psychiatry. 2010;34(4):674–80.

Perez VB, Ford JM, Roach BJ, Loewy RL, Stuart BK, Vinogradov S, Mathalon DH. Auditory cortex responsiveness during talking and listening: early illness schizophrenia and patients at clinical high-risk for psychosis. Schizophr Bull. 2012;38(6):1216–24.

Perez VB, Woods SW, Roach BJ, Ford JM, McGlashan TH, Srihari VH, Mathalon DH. Automatic auditory processing deficits in schizophrenia and clinical high-risk patients: forecasting psychosis risk with mismatch negativity. Biol Psychiatry. 2014;75(6):459–69.

Perrin MA, Kantrowitz JT, Silipo G, Dias E, Jabado O, Javitt DC. Mismatch negativity (MMN) to spatial deviants and behavioral spatial discrimination ability in the etiology of auditory verbal hallucinations and thought disorder in schizophrenia. Schizophr Res. 2018;191:140–7.

Pinheiro AP, Del Re E, Nestor PG, Mezin J, Rezaii N, McCarley RW, Goncalves OF, Niznikiewicz M. Abnormal interactions between context, memory structure, and mood in schizophrenia: an ERP investigation. Psychophysiology. 2015;52(1):20–31.

Qiu YQ, Tang YX, Chan RC, Sun XY, He J. P300 aberration in first-episode schizophrenia patients: A meta-analysis. PLoS One. 2014;9(6):e97794.

Randeniya R, Oestreich LKL, Garrido MI. Sensory prediction errors in the continuum of psychosis. Schizophr Res. 2018;191:109–22.

Rasser PE, Schall U, Todd J, Michie PT, Ward PB, Johnston P, Helmbold K, Case V, Soyland A, Tooney PA, Thompson PM. Gray matter deficits, mismatch

negativity, and outcomes in schizophrenia. Schizophr Bull. 2011;37(1):131–40.

Retsa C, Knebel JF, Geiser E, Ferrari C, Jenni R, Fournier M, Alameda L, Baumann PS, Clarke S, Conus P, Do KQ, Murray MM. Treatment in early psychosis with N-acetyl-cysteine for 6months improves low-level auditory processing: pilot study. Schizophr Res. 2018;191:80–6.

Rissling AJ, Light GA. Neurophysiological measures of sensory registration, stimulus discrimination, and selection in schizophrenia patients. Curr Top Behav Neurosci. 2010;4:283–309.

Rosch RE, Auksztulewicz R, Leung PD, Friston KJ, Baldeweg T. Selective prefrontal disinhibition in a roving auditory oddball paradigm under N-methyl-D-aspartate receptor blockade. Biol Psychiatry Cogn Neurosci Neuroimaging. 2019;4(2):140–50.

Rowland LM, Summerfelt A, Wijtenburg SA, Du X, Chiappelli JJ, Krishna N, West J, Muellerklein F, Kochunov P, Hong LE. Frontal glutamate and gamma-aminobutyric acid levels and their associations with mismatch negativity and digit sequencing task performance in schizophrenia. JAMA Psychiat. 2016;73(2):166–74.

Ruchsow M, Trippel N, Groen G, Spitzer M, Kiefer M. Semantic and syntactic processes during sentence comprehension in patients with schizophrenia: evidence from event-related potentials. Schizophr Res. 2003;64(2-3):147–56.

Rydkjaer J, Mollegaard Jepsen JR, Pagsberg AK, Fagerlund B, Glenthoj BY, Oranje B. Mismatch negativity and P3a amplitude in young adolescents with first-episode psychosis: a comparison with ADHD. Psychol Med. 2017;47(2):377–88.

Ryu V, An SK, Ha RY, Kim JA, Ha K, Cho HS. Differential alteration of automatic semantic processing in treated patients affected by bipolar mania and schizophrenia: an N400 study. Prog Neuropsychopharmacol Biol Psychiatry. 2012;38(2):194–200.

Salisbury DF, McCathern AG. Abnormal complex auditory pattern analysis in schizophrenia reflected in an absent missing stimulus mismatch negativity. Brain Topogr. 2016;29(6):867–74.

Salisbury DF, Shenton ME, Griggs CB, Bonner-Jackson A, McCarley RW. Mismatch negativity in chronic schizophrenia and first-episode schizophrenia. Arch Gen Psychiatry. 2002;59(8):686–94.

Salisbury DF, Collins KC, McCarley RW. Reductions in the N1 and P2 auditory event-related potentials in first-hospitalized and chronic schizophrenia. Schizophr Bull. 2010;36(5):991–1000.

Salisbury DF, Polizzotto NR, Nestor PG, Haigh SM, Koehler J, McCarley RW. Pitch and duration mismatch negativity and premorbid intellect in the first hospitalized schizophrenia spectrum. Schizophr Bull. 2017;43(2):407–16.

Salisbury DF, McCathern AG, Coffman BA, Murphy TK, Haigh SM. Complex mismatch negativity to tone pair deviants in long-term schizophrenia and in the first-episode schizophrenia spectrum. Schizophr Res. 2018;191:18–24.

Sauer A, Zeev-Wolf M, Grent-'t-Jong T, Recasens M, Wacongne C, Wibral M, Helbling S, Peled A, Grinshpoon A, Singer W, Goldstein A, Uhlhaas PJ. Impairment in predictive processes during auditory mismatch negativity in ScZ: evidence from event-related fields. Hum Brain Mapp. 2017;38(10):5082–93.

Schechter I, Butler PD, Zemon VM, Revheim N, Saperstein AM, Jalbrzikowski M, Pasternak R, Silipo G, Javitt DC. Impairments in generation of early-stage transient visual evoked potentials to magno- and parvocellular-selective stimuli in schizophrenia. Clin Neurophysiol. 2005;116(9):2204–15.

Schmidt A, Bachmann R, Kometer M, Csomor PA, Stephan KE, Seifritz E, Vollenweider FX. Mismatch negativity encoding of prediction errors predicts S-ketamine-induced cognitive impairments. Neuropsychopharmacology. 2012;37(4):865–75.

Seol JJ, Kim M, Lee KH, Hur JW, Cho KIK, Lee TY, Chung CK, Kwon JS. Is there an association between mismatch negativity and cortical thickness in schizophrenia patients? Clin EEG Neurosci. 2017;48(6):383–92.

Shaikh M, Valmaggia L, Broome MR, Dutt A, Lappin J, Day F, Woolley J, Tabraham P, Walshe M, Johns L, Fusar-Poli P, Howes O, Murray RM, McGuire P, Bramon E. Reduced mismatch negativity predates the onset of psychosis. Schizophr Res. 2012;134(1):42–8.

Sharma A, Sauer H, Smit DJ, Bender S, Weisbrod M. Genetic liability to schizophrenia measured by P300 in concordant and discordant monozygotic twins. Psychopathology. 2011;44(6):398–406.

Sharma A, Sauer H, Hill H, Kaufmann C, Bender S, Weisbrod M. Abnormal N400 semantic priming effect may reflect psychopathological processes in schizophrenia: a twin study. Schizophr Res Treat. 2017;2017:7163198.

Shim M, Kim DW, Lee SH, Im CH. Disruptions in small-world cortical functional connectivity network during an auditory oddball paradigm task in patients with schizophrenia. Schizophr Res. 2014;156(2-3):197–203.

Shimano S, Onitsuka T, Oribe N, Maekawa T, Tsuchimoto R, Hirano S, Ueno T, Hirano Y, Miura T, Kanba S. Preattentive dysfunction in patients with bipolar disorder as revealed by the pitch-mismatch negativity: a magnetoencephalography (MEG) study. Bipolar Disord. 2014;16(6):592–9.

Shin KS, Kim JS, Kang DH, Koh Y, Choi JS, O'Donnell BF, Chung CK, Kwon JS. Pre-attentive auditory processing in ultra-high-risk for schizophrenia with magnetoencephalography. Biol Psychiatry. 2009;65(12):1071–8.

Shin KS, Kim JS, Kim SN, Koh Y, Jang JH, An SK, O'Donnell BF, Chung CK, Kwon JS. Aberrant auditory processing in schizophrenia and in subjects at ultra-high-risk for psychosis. Schizophr Bull. 2012;38(6):1258–67.

Sitnikova T, Goff D, Kuperberg GR. Neurocognitive abnormalities during comprehension of real-world goal-directed behaviors in schizophrenia. J Abnorm Psychol. 2009;118(2):256–77.

Solis-Vivanco R, Mondragon-Maya A, Leon-Ortiz P, Rodriguez-Agudelo Y, Cadenhead KS, de la Fuente-Sandoval C. Mismatch Negativity reduction in the left cortical regions in first-episode psychosis and in individuals at ultra high-risk for psychosis. Schizophr Res. 2014;158(1-3):58–63.

Su L, Cai Y, Shi S, Wang L. Meta-analysis of studies in China about changes in P300 latency and amplitude that occur in patients with schizophrenia during treatment with antipsychotic medication. Shanghai Arch Psychiatry. 2012;24(4):200–7.

Sumich A, Kumari V, Dodd P, Ettinger U, Hughes C, Zachariah E, Sharma T. N100 and P300 amplitude to Go and No-Go variants of the auditory oddball in siblings discordant for schizophrenia. Schizophr Res. 2008;98(1-3):265–77.

Sumiyoshi T, Miyanishi T, Seo T, Higuchi Y. Electrophysiological and neuropsychological predictors of conversion to schizophrenia in at-risk subjects. Front Behav Neurosci. 2013;7:148.

Takahashi H, Rissling AJ, Pascual-Marqui R, Kirihara K, Pela M, Sprock J, Braff DL, Light GA. Neural substrates of normal and impaired preattentive sensory discrimination in large cohorts of nonpsychiatric subjects and schizophrenia patients as indexed by MMN and P3a change detection responses. Neuroimage. 2013;66:594–603.

Tang Y, Wang J, Zhang T, Xu L, Qian Z, Cui H, Tang X, Li H., Whitfield-Gabrieli S, Shenton ME, Seidman LJ, McCarley RW, Keshavan MS, Stone WS, Wang J, Niznikiewicz MA. P300 as an index of transition to psychosis and of remission: data from a clinical high risk for psychosis study and review of literature. Schizophr Res. 2019; pii: S0920-9964(19)30074-X. https://doi.org/10.1016/j.schres.2019.02.014.

Taylor JA, Matthews N, Michie PT, Rosa MJ, Garrido MI. Auditory prediction errors as individual biomarkers of schizophrenia. Neuroimage Clin. 2017;15:264–73.

Thomas ML, Green MF, Hellemann G, Sugar CA, Tarasenko M, Calkins ME, Greenwood TA, Gur RE, Gur RC, Lazzeroni LC, Nuechterlein KH, Radant AD, Seidman LJ, Shiluk AL, Siever LJ, Silverman JM, Sprock J, Stone WS, Swerdlow NR, Tsuang DW, Tsuang MT, Turetsky BI, Braff DL, Light GA. Modeling deficits from early auditory information processing to psychosocial functioning in schizophrenia. JAMA Psychiat. 2017;74(1):37–46.

Todd J, Michie PT, Budd TW, Rock D, Jablensky AV. Auditory sensory memory in schizophrenia: inadequate trace formation? Psychiatry Res. 2000;96(2):99–115.

Todd J, Michie PT, Jablensky AV. Association between reduced duration mismatch negativity (MMN) and raised temporal discrimination thresholds in schizophrenia. Clin Neurophysiol. 2003;114(11):2061–70.

Todd J, Michie PT, Schall U, Ward PB, Catts SV. Mismatch negativity (MMN) reduction in schizophrenia-impaired prediction—error generation, estimation or salience? Int J Psychophysiol. 2012;83(2):222–31.

Todd J, Petherbridge A, Speirs B, Provost A, Paton B. Time as context: the influence of hierarchical patterning on sensory inference. Schizophr Res. 2018;191:123–31.

Turetsky BI, Moberg PJ, Owzar K, Johnson SC, Doty RL, Gur RE. Physiologic impairment of olfactory stimulus processing in schizophrenia. Biol Psychiatry. 2003;53(5):403–11.

Turetsky BI, Calkins ME, Light GA, Olincy A, Radant AD, Swerdlow NR. Neurophysiological endophenotypes of schizophrenia: the viability of selected candidate measures. Schizophr Bull. 2007;33(1):69–94.

Turetsky BI, Kohler CG, Gur RE, Moberg PJ. Olfactory physiological impairment in first-degree relatives of schizophrenia patients. Schizophr Res. 2008;102(1-3):220–9.

Turetsky BI, Bilker WB, Siegel SJ, Kohler CG, Gur RE. Profile of auditory information-processing deficits in schizophrenia. Psychiatry Res. 2009;165(1-2):27–37.

Turetsky BI, Dress EM, Braff DL, Calkins ME, Green MF, Greenwood TA, Gur RE, Gur RC, Lazzeroni LC, Nuechterlein KH, Radant AD, Seidman LJ, Siever LJ, Silverman JM, Sprock J, Stone WS, Sugar CA, Swerdlow NR, Tsuang DW, Tsuang MT, Light G. The utility of P300 as a schizophrenia endophenotype and predictive biomarker: clinical and sociodemographic modulators in COGS-2. Schizophr Res. 2015;163(1-3):53–62.

Umbricht D, Krljes S. Mismatch negativity in schizophrenia: a meta-analysis. Schizophr Res. 2005;76(1):1–23.

Umbricht D, Schmid L, Koller R, Vollenweider FX, Hell D, Javitt DC. Ketamine-induced deficits in auditory and visual context-dependent processing in healthy volunteers: implications for models of cognitive deficits in schizophrenia. Arch Gen Psychiatry. 2000;57(12):1139–47.

Umbricht D, Koller R, Schmid L, Skrabo A, Grubel C, Huber T, Stassen H. How specific are deficits in mismatch negativity generation to schizophrenia? Biol Psychiatry. 2003;53(12):1120–31.

Urban A, Kremlacek J, Masopust J, Libiger J. Visual mismatch negativity among patients with schizophrenia. Schizophr Res. 2008;102(1-3):320–8.

van der Stelt O, Frye J, Lieberman JA, Belger A. Impaired P3 generation reflects high-level and progressive neurocognitive dysfunction in schizophrenia. Arch Gen Psychiatry. 2004;61(3):237–48.

van der Stelt O, Lieberman JA, Belger A. Auditory P300 in high-risk, recent-onset and chronic schizophrenia. Schizophr Res. 2005;77(2-3):309–20.

van Tricht MJ, Nieman DH, Koelman JH, van der Meer JN, Bour LJ, de Haan L, Linszen DH. Reduced parietal P300 amplitude is associated with an increased risk for a first psychotic episode. Biol Psychiatry. 2010;68(7):642–8.

Vianin P, Posada A, Hugues E, Franck N, Bovet P, Parnas J, Jeannerod M. Reduced P300 amplitude in a visual recognition task in patients with schizophrenia. Neuroimage. 2002;17(2):911–21.

Vignapiano A, Mucci A, Ford J, Montefusco V, Plescia GM, Bucci P, Galderisi S. Reward anticipation and trait anhedonia: an electrophysiological investigation in subjects with schizophrenia. Clin Neurophysiol. 2016;127(4):2149–60.

Wang K, Cheung EF, Gong QY, Chan RC. Semantic processing disturbance in patients with schizophrenia: a meta-analysis of the N400 component. PLoS One. 2011;6(10):e25435.

Weisbrod M, Kiefer M, Marzinzik F, Spitzer M. Executive control is disturbed in schizophrenia: evidence from event-related potentials in a Go/NoGo task. Biol Psychiatry. 2000;47(1):51–60.

Whitford TJ, Kubicki M, Ghorashi S, Schneiderman JS, Hawley KJ, McCarley RW, Shenton ME, Spencer KM. Predicting inter-hemispheric transfer time from the diffusion properties of the corpus callosum in healthy individuals and schizophrenia patients: a combined ERP and DTI study. Neuroimage. 2011;54(3):2318–29.

Whitford TJ, Oestreich LKL, Ford JM, Roach BJ, Loewy RL, Stuart BK, Mathalon DH. Deficits in cortical suppression during vocalization are associated with structural abnormalities in the arcuate fasciculus in early illness schizophrenia and clinical high risk for psychosis. Schizophr Bull. 2018;44(6):1312–22.

Winterer G, Egan MF, Radler T, Coppola R, Weinberger DR. Event-related potentials and genetic risk for schizophrenia. Biol Psychiatry. 2001;50(6):407–17.

Winterer G, Coppola R, Egan MF, Goldberg TE, Weinberger DR. Functional and effective frontotemporal connectivity and genetic risk for schizophrenia. Biol Psychiatry. 2003;54(11):1181–92.

Wu KY, Chao CW, Hung CI, Chen WH, Chen YT, Liang SF. Functional abnormalities in the cortical processing of sound complexity and musical consonance in schizophrenia: evidence from an evoked potential study. BMC Psychiatry. 2013;13:158.

Wyss C, Hitz K, Hengartner MP, Theodoridou A, Obermann C, Uhl I, Roser P, Grunblatt E, Seifritz E, Juckel G, Kawohl W. The loudness dependence of auditory evoked potentials (LDAEP) as an indicator of serotonergic dysfunction in patients with predominant schizophrenic negative symptoms. PLoS One. 2013;8(7):e68650.

Zhao YL, Tan SP, Yang FD, Wang LL, Feng WF, Chan RC, Gao X, Zhou DF, Li BB, Song CS, Fan FM, Tan YL, Zhang JG, Wang YH, Zou YZ. Dysfunction in different phases of working memory in schizophrenia: evidence from ERP recordings. Schizophr Res. 2011;133(1-3):112–9.

Zhao Y, Zhang D, Tan S, Song C, Cui J, Fan F, Zhu X, Zou Y, Luo Y. Neural correlates of the abolished self-referential memory effect in schizophrenia. Psychol Med. 2014;44(3):477–87.

Part II

Recent Applications of Neuroimaging to Schizophrenia

15 Early Childhood Brain Development and Schizophrenia: An Imaging Perspective

John H. Gilmore

Contents

15.1 Introduction

It has been over 30 years since it was first hypothesized that schizophrenia was a neurodevelopmental disorder (Murray and Lewis 1987; Weinberger 1987). Since that time, the case for the neurodevelopmental origins of schizophrenia has become much stronger. Recent genetic studies implicate neurodevelopment influences (Birnbaum and Weinberger 2017), as many of the genes of risk for schizophrenia play a role in multiple processes important for brain development and plasticity, and may be preferentially expressed during fetal and perinatal brain development (Birnbaum et al. 2015; Jaffe et al. 2018). Schizophrenia is also associated with copy number variants that are non-specific and overlap with risk for other neurodevelopmental disorders (Marshall et al. 2017), also implicating early neurodevelopmental processes. Abnormalities in early childhood brain development are apparent from studies of at risk children and in children who go on to development schizophrenia. These children have abnormal cognitive and motor development that is evident in very early in childhood (Fish et al. 1992; Sorensen et al. 2010; Hameed and Lewis 2016; Filatova et al. 2017). Finally, schizophrenia is associated with a variety of pre- and perinatal obstetric complications, including maternal infection, hypoxia and other

J. H. Gilmore (✉)
Department of Psychiatry, CB# 7160, University of North Carolina School of Medicine, University of North Carolina at Chapel Hill, Chapel Hill, NC, USA
e-mail: jgilmore@med.unc.edu, john_gilmore@med.unc.edu

M. Kubicki, M. E. Shenton (eds.), *Neuroimaging in Schizophrenia*,
https://doi.org/10.1007/978-3-030-35206-6_15

complications (Cannon et al. 2002; Matheson et al. 2011; Estes and McAllister 2017). These studies strongly implicate prenatal and early postnatal brain development in the pathogenesis of schizophrenia.

There has been great interest in the neurodevelopmental processes of adolescence and how they contribute to the clinical onset of symptoms (Cannon et al. 2015). Most studies have focused on the normal elimination or pruning of cortical synapses thought to be reflected, at least in part, by cortical thinning on MRI. For example, individuals with prodromal symptoms of schizophrenia who convert to psychosis have reductions in cortical thickness in the right superior frontal, middle frontal, and medial orbitofrontal regions (Cannon et al. 2015). Alterations in adolescent white matter maturation and in oscillatory networks (Uhlhaas and Singer 2011) have also been implicated (Kochunov and Hong 2014; von Hohenberg et al. 2014). More recent conceptualizations of the pathogenesis of schizophrenia have begun to emphasize the understudied period of early brain development, especially when considering early identification and early interventions that may prevent or ameliorate the severity of schizophrenia (Insel 2010; Millan et al. 2016). Of note, impaired synaptic plasticity, and related theoretical abnormalities in excitatory and inhibitory balance thought to be a fundamental aspect of schizophrenia, likely have consequences at all stages of development (Forsyth and Lewis 2017; Krystal et al. 2017).

The hypothesis that aberrant brain development during adolescence contributes to the onset of clinical symptoms in adolescence and in early adulthood has been widely promoted and studied (Paus et al. 2008). From a theoretical standpoint, the structural and functional brain abnormalities associated with schizophrenia may arise during adolescence, and there is some evidence that gray matter abnormalities progress during the prodromal period. However, it is also likely, given the genetic and pre- and perinatal risk factors for schizophrenia, that brain abnormalities arise much earlier in brain development, when the basic architecture of the brain is being formed. For example, cognitive abnormalities associated with schizophrenia are evident in very early childhood and tend to progress throughout childhood and adolescence (Fuller et al. 2002; Woodberry et al. 2008; Reichenberg et al. 2010; Dickson et al. 2012; Gur et al. 2014; Meier et al. 2014; Hameed and Lewis 2016; Mollon et al. 2018). Cognitive dysfunction is a major cause of disability in schizophrenia (Rajji et al. 2014; Green 2016), so interventions to improve cognitive dysfunction may need to be targeted in early childhood. It is therefore critical that the field develop a better knowledge base about normal and abnormal brain development in early childhood, its relationship to cognitive and behavioral development, as well as risk for schizophrenia and other psychiatric disorders. This will ultimately allow us to identify periods of development that can be optimally targeted for early identification and intervention to ameliorate risk and improve outcomes. There is also a growing interest in the identification of endophenotypes in the perinatal period, such as P50 sensory gating (Ross and Freedman 2015). Additionally, there is a growing interest in early interventions that may reduce ultimate risk for schizophrenia, such as social support and cognitive remediation for children at risk (Liu et al. 2015), as well as micronutrient primary prevention in the prenatal period (Freedman et al. 2018).

A variety of abnormalities in brain structure have been identified in persons with schizophrenia, including reductions in gray matter, white matter, and subcortical volumes (Olabi et al. 2011; Shepherd et al. 2012; Vita et al. 2012; Haijma et al. 2013; van Erp et al. 2016, 2018), as well as alterations in white matter integrity assessed with diffusion weighted imaging (Kubicki et al. 2007; Wheeler and Voineskos 2014; Kelly et al. 2018). More recent network approaches have also revealed abnormalities in gray and white matter and functional networks networks/connectomes in schizophrenia (Narr and Leaver 2015; van den Heuvel and Fornito 2014; Wheeler and Voineskos 2014). Many of these structural and functional abnormalities are present in the first episode and prodromal phases of the illness, suggesting that they precede the clinical onset of symptoms (Fitzsimmons et al.

2013; Gong et al. 2016; Dietsche et al. 2017). In addition, brain abnormalities have been identified in unaffected siblings and in older children at genetic high risk (Boos et al. 2007; Ordonez et al. 2016; Collin et al. 2017), suggesting that some structural brain abnormalities represent an endophenotype of risk and may be useful as an early imaging biomarker (Figs. 15.1 and 15.2).

The main question about structural and functional brain abnormalities observed in the various stages of schizophrenia is when in development they arise. An answer to this question would provide important insights into the nature and timing of developmental processes that deviate from normal in a way that increases risk for schizophrenia. It would also determine whether it is possible to identify early imaging biomarkers of risk, potentially allowing for early identification and intervention. While there have been very few studies of early childhood brain development in children at risk for schizophrenia, studies in normal children are beginning to shed light on how early childhood brain development may contribute to brain abnormalities observed in schizophrenia. Most prior imaging studies of human brain development have focused on the period spanning older childhood, adolescence, and early adulthood. Studies have started to chart postnatal brain development in early childhood, a period of very rapid and dynamic growth. Finally, more recent studies are beginning to investigate fetal brain development (Jakab et al. 2015; Makropoulos et al. 2018; Vasung et al. 2018). A review of what these imaging studies tell us about how various components of brain structure and function that have been identified as abnormal in schizophrenia develop will likely provide new insights into the origins of schizophrenia (Gilmore et al. 2018).

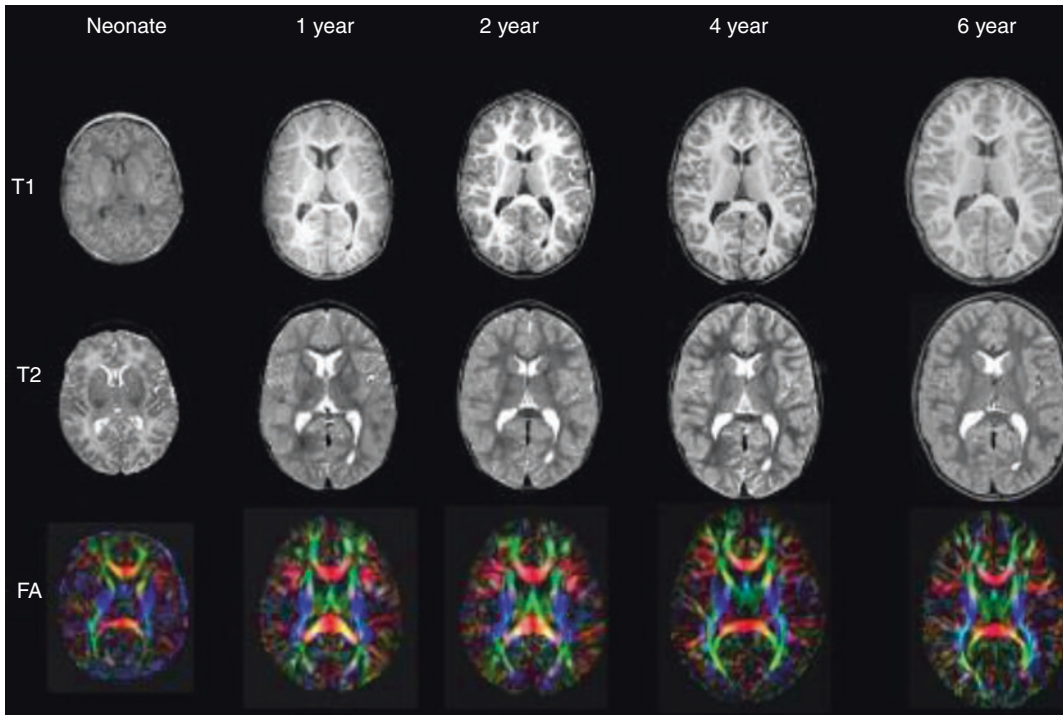

Fig. 15.1 Representative MRI scans from birth to 6 years. There is rapid volume growth between birth and 1 year with more gradual growth after that. After birth, most white matter is not myelinated (T1 scans), at 1 year and older, myelination has occurred and white matter assumes the typical white appearance seen in adults. Cortical gray matter is relatively thin in neonate scans and reaches adult-like thickness by year 1. In the FA images, note that most major white matter tracts are present in neonates

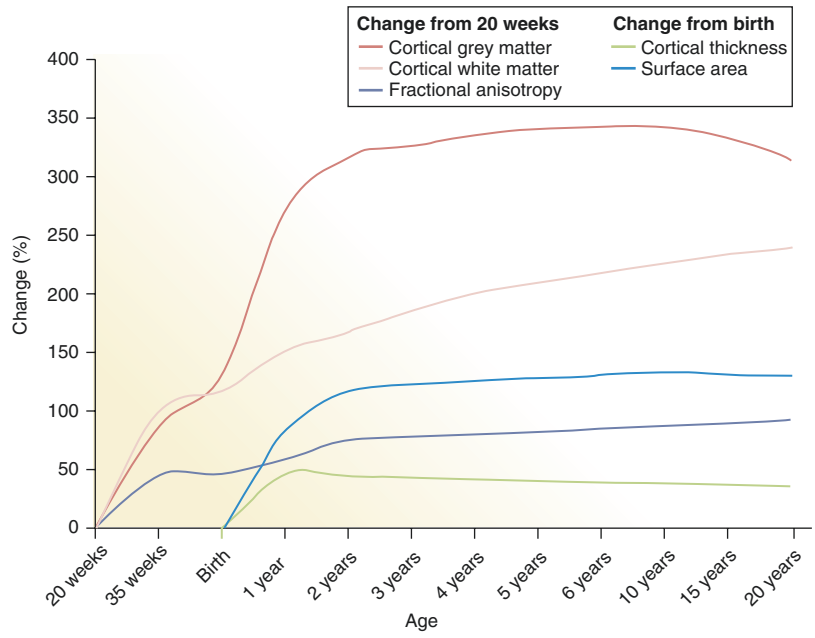

Fig. 15.2 Relative developmental changes in brain structure. (From Gilmore et al. 2018)

15.2 Fetal Brain Development

Growth of the fetal brain is especially rapid in the second half of pregnancy. Overall cerebral volume increases exponentially by 20-fold from 18 weeks until birth (Andescavage et al. 2017). Interestingly, white and gray matter exhibit different trajectories, with white matter volume increasing more rapidly than gray matter until roughly 30 weeks gestational age; after that gray matter volumes begin to increase rapidly, while white matter growth begins to slow (Andescavage et al. 2017; Kyriakopoulou et al. 2017). Cortical folding also proceeds rapidly from about 25 weeks until birth (Rajagopalan et al. 2011; Wright et al. 2014), with adult patterns of gyrification present at birth (White et al. 2010; Li et al. 2014).

Diffusion weighted imaging is also being applied to fetal imaging (Jakab et al. 2015). White matter tracts develop very early in fetal brain development, with the fornix emerging at 13 weeks, the corpus callosum and uncinate fibers becoming evident at about 15 weeks (Jakab et al. 2015; Ouyang et al. 2019), and other projection and association fibers appearing by 23–28 weeks (Vasung et al. 2018). Most major white matter tracts are present at birth (Geng et al. 2012; Qiu et al. 2015c).

Recent studies have even begun to apply functional imaging to the fetal stage of brain development (Hykin et al. 1999; Anderson and Thomason 2013; van den Heuvel and Thomason 2016). Early results indicate that hubs of both primary and association functional networks form before birth (van den Heuvel et al. 2018). Interestingly, fetal functional connectivity is associated with subsequent premature birth (Thomason et al. 2017) and infant motor development (Thomason et al. 2018), suggesting that alterations in the functional connectome in fetal life can have long lasting consequences and may serve as predictive biomarkers.

15.3 Early Childhood Brain Development

The rapid growth trajectory of fetal brain development continues after birth, especially in the first year of life (Holland et al. 2014; Gilmore et al. 2018). Brain volume is about 35% that of adults after birth, and increases 100% by age 1 year, and another 15% by age 2, to 80% of adult size

(Knickmeyer et al. 2008). Brain volume growth in the first year of life is driven mainly by gray matter, which expands rapidly in the first year of life, while white matter volume grows much more slowly (Matsuzawa et al. 2001; Knickmeyer et al. 2008). Subcortical gray matter structures including the amygdala, thalamus, and caudate grow with rates similar to cortical gray matter, while the hippocampus grows somewhat slower (Knickmeyer et al. 2008; Gilmore et al. 2012; Uematsu et al. 2012; Choe et al. 2013). After age 2, volume growth is much more gradual. Lateral ventricle volume expands by over 100% in the first year of life, and decreases somewhat by age 2 (Knickmeyer et al. 2008; Gilmore et al. 2012; Bompard et al. 2014).

At birth, overall gyrification patterns in the cortex are similar to those observed in adults and the gyrification index increases in the first 2 years of life (Hill et al. 2010; Li et al. 2013; Li et al. 2015). Cortical gray matter growth is mainly driven by surface area expansion, which increases by 76% at age 1, and an additional 22% by year 2 to about 69% of adult values (Li et al. 2013; Lyall et al. 2015). Interestingly, cortical thickness has a different developmental trajectory, increasing an average of 31% in year 1 and remaining stable or even decreasing between 1 and 2 years (Lyall et al. 2015; Remer et al. 2017). It appears that cortical thickness reaches maximum values at 1–2 years and decreases thereafter. It is also important to note that the regional heterogeneity of cortical thickness observed in adults is well established at birth (Li et al. 2015; Lyall et al. 2015). Because cortical thickness is stable or decreasing after age 1 year, surface area expansion is the main driver of cortical volume expansion after year 1.

As noted above, most white matter tracts develop during fetal life and are present at the time of birth (Qiu et al. 2015c). White matter microstructure, determined with quantitative diffusion tensor imaging (DTI), matures rapidly in the first year of life and more gradually thereafter (Dubois et al. 2014). Increasing organization and myelination of white matter tracts result in robust decreases of axial diffusivity (AD) and radial diffusivity (RD), and increases of fractional anisotropy (FA) with age (Gao et al. 2009b; Geng et al. 2012; Sadeghi et al. 2013; Dubois et al. 2014). Multicomponent relaxometry, which provides a more direct assessment of myelination, indicates that myelination occurs rapidly in the first year of life and proceeds more gradually after the age of 2 (Deoni et al. 2011, 2014, 2015).

Studies of structural and functional networks in early childhood are beginning to fill in gaps in knowledge about how these networks develop (Cao et al. 2016). At birth, the white-matter connectome is highly organized and many hubs and connections present are similar to those observed in adults (Yap et al. 2011; Huang et al. 2015; van den Heuvel et al. 2015). White-matter networks at birth and in premature infants at 30 weeks gestational age already exhibit a rich club property of highly connected modules (Ball et al. 2014). In the first years after birth, networks mature (Yap et al. 2011; Huang et al. 2015), with many major hubs and modules present by 2 years (Hagmann et al. 2010).

Structural covariance networks (SCNs) are regions of highly correlated variation of gray matter volume or cortical thickness that are altered in schizophrenia and other neuropsychiatric disorders (Evans 2013; Alexander-Bloch et al. 2013) SCNs demonstrate small-world properties and modular organization at birth (Fan et al. 2011) and at 3 years of age (Nie et al. 2013). Primary sensorimotor SCNs are fairly mature at birth, while higher-order association SCNs mature and become increasingly distributed after birth (Zielinski et al. 2010).

Resting state networks also develop rapidly in the first years after birth. At birth, the functional connectome already exhibits small-worldness, high global efficiency, and clustering coefficients (Grayson and Fair 2017). Primary sensorimotor networks develop first and have relatively mature topologies in premature and term infants (Fransson et al. 2007; Gao et al. 2009a, 2015a, b; Doria et al. 2010; Smyser et al. 2010; Fransson et al. 2011). The default-mode (Shulman et al. 1997; Raichle et al. 2001; Anderson and Thomason 2013), dorsal attention (Corbetta and Shulman 2002; Fox et al. 2005) and salience networks (Seeley et al. 2007) establish distrib-

uted network-like topologies by 2 years of age (Gao et al. 2013; Gao et al. 2015a, b), while the executive control networks tend to mature later in childhood (Seeley et al. 2007; Gao et al. 2015a). Many inter-network relationships also mature in early childhood; the inverse correlation between the dorsal attention network and the default-mode network becomes apparent in the first year of life (Gao et al. 2013).

15.4 Late Childhood and Adolescent Brain Development

Structural and functional brain development after 6 years progresses at a much more gradual pace compared to the first years of life. Gray matter volumes increase very slowly until adolescence and then decrease; interestingly, white matter volumes continue to have a different trajectory, increasing through adolescence and early adulthood until about until age 30, and decreasing thereafter (Matsuzawa et al. 2001; Groeschel et al. 2010; Mills et al. 2016). Most studies find that cortical thickness decreases gradually through late childhood, adolescence, and early adulthood, after peaking in early childhood (Sowell et al. 2004; Brown et al. 2012; Ducharme et al. 2016; Walhovd et al. 2017); earlier studies that found cortical thickness peaking in early adolescence may have been confounded by motion (Shaw et al. 2008; Raznahan et al. 2011). Surface area tends to increase until about age 10–12 years and then decreases.

White matter tract microstructure, reflected though diffusion values, changes gradually through later childhood and adolescence, with AD and RD decreasing, and FA increasing (Faria et al. 2010; Uda et al. 2015; Cohen et al. 2016; Krogsrud et al. 2016; Oyefiade et al. 2018). Neurite orientation dispersion and density imaging (NODDI) finds that the neurite density index increases in late childhood and adolescence, suggesting that axon density and myelination are increasing in this age range (Chang et al. 2015; Genc et al. 2017; Mah et al. 2017). Interestingly, a recent study of first episode psychosis found regions of decreased neurite density (Rae et al. 2017), suggesting that axon density and myelination are contributing to the pathophysiology of schizophrenia.

As noted above, the white matter connectome appears to be fairly mature in early childhood, with major hubs and a "rich club" structure present. One study found no differences in the rich club structure of 7–11 year olds and adults (Grayson et al. 2014). Overall, studies suggest that after early childhood, the white matter connectome becomes more distributed and integrated, with increasing global efficiency and decreasing local connectivity, though there are conflicting reports (Tymofiyeva et al. 2014; Richmond et al. 2016). There have been limited studies of gray matter structural covariance though development (Zielinski et al. 2010; Khundrakpam et al. 2013; Richmond et al. 2016). Structural covariance in later childhood appears to be the result of coordinated maturation of gray matter networks (Alexander-Bloch et al. 2013). SCNs and maturational networks are not related in the first 2 years of life (Geng et al. 2017), suggesting that the fine tuning of cortical SCNs, especially high-order SCNs, occurs later in childhood (Khundrakpam et al. 2013).

Developmental trends of resting state networks evident in early childhood are generally maintained throughout later childhood and adolescent development (Grayson and Fair 2017). Resting state maturation was initially thought to be characterized by a weakening of short range connections and strengthening of longer range connections (Dosenbach et al. 2010), though more recent studies that control for head motion suggest that functional networks are similar in children and adults, and that network maturation is much more subtle and complex (Grayson and Fair 2017).

Overall, it appears that much of the fundamental structural and functional architecture of the human brain is in place at birth, and becomes well established by age 2. At birth, most white matter tracts are present, cortical gyrification is adult-like and adult patterns of regional cortical thickness are present, major hubs of the white matter connectome are in place, and

sensorimotor functional networks are adult-like. By age 1–2 years, cortical thickness has reached its peak, the bulk of myelination has occurred, and higher order association functional networks are adult-like. Brain development after the age of 2 years is characterized by surface area expansion, gradual reduction of cortical thickness, slow and continued myelination of white matter tracts, and refinement of resting state functional networks. There is clearly significant behavioral and cognitive development that occurs after the age of 2 years, though it appears that development is based mainly on the "fine tuning" of and plasticity within structural and functional networks that are already well developed.

15.5 Genetic and Environmental Influences

Early studies suggest that some of the genetic and environmental risk factors for schizophrenia do influence early childhood brain development (Gao et al. 2019). Common variants in psychiatric risk genes such as *DISC1* (disrupted-in schizophrenia 1) of *COMT* (catechol-O-methyltransferase) are associated with individual differences in brain tissue volumes in neonates (Knickmeyer et al. 2014). Interestingly, neonates carrying the ε4 allele of *APOE* (which encodes apolipoprotein E), a major susceptibility allele for late-onset Alzheimer disease, have reduced volumes in the temporal cortex, similar to the association in adults. There is also evidence of gene-environment interactions in early childhood. For example, antenatal maternal anxiety and infant *COMT* genotypes interact to influence neonatal cortical thickness (Qiu et al. 2015b). *BDNF* genotype may also interact with maternal anxiety, influencing amygdala and hippocampal volume (Chen et al. 2015). Finally, the common variant encoding postsynaptic density protein 95 is associated with significant differences in white-matter microstructure in preterm infants (Krishnan et al. 2017).

There is evidence that maternal depression or stress during pregnancy increases risk for schizophrenia and other psychiatric disorders (Maki et al. 2010; Van den Bergh et al. 2017). Our understanding of how maternal stress influences the developing brain is beginning to improve. For example, maternal depression during pregnancy is associated with reduced cortical thickness and white-matter diffusivity in children aged 2.5–5 years (Lebel et al. 2016), as well as altered microstructure and functional connectivity of the amygdala in 6-month-olds (Rifkin-Graboi et al. 2013; Qiu et al. 2015a). Maternal interleukin 6 (IL-6) levels during pregnancy, a marker of inflammation and stress, alters neonatal white matter (Rasmussen et al. 2018), amygdala volume (Graham et al. 2018), and functional connectivity (Rudolph et al. 2018). These studies suggest that prenatal genetic and environmental risk factors for schizophrenia can significantly alter infant brain structure and function.

15.6 Imaging Biomarkers in Early Childhood

Given that much of the fundamental structural and functional architecture of the human brain is well established by early childhood, a major question is whether it is possible to identify imaging biomarkers of risk for schizophrenia and other neuropsychiatric disorders. This would allow for early identification and intervention, potentially normalizing developmental trajectories during periods of rapid development and plasticity in early childhood. There is increasing recognition that biomarkers derived from the most current imaging approaches in adults and children have small effect sizes with limited clinical utility, and that clinical and demographic variables typically have stronger correlations with outcomes than imaging biomarkers (Gabrieli et al. 2015; Reddan et al. 2017; Woo et al. 2017; Batalle et al. 2018). The wide distribution of specific cognitive functions or disease risk across networks in the brain is also a significant limitation (Woo et al. 2017). In young children, studies of white matter, including DTI-derived individual white matter tracts (Short et al. 2013; Keunen et al. 2017) or principle components (Lee et al. 2017), and

myelin water fraction (O'Muircheartaigh et al. 2014; Deoni et al. 2016) have found only modest relationships to cognitive outcomes. Newer machine-learning approaches find that the neonatal white matter connectome can also be predictive of later cognitive development, though correlations were still relatively low (0.23–0.31) (Ball et al. 2016; Keunen et al. 2017).

There have been a few initial studies of infants at risk for schizophrenia and autism. Male neonates with high genetic risk for schizophrenia have increased gray-matter volumes compared with controls (Gilmore et al. 2010) and young children who develop autism have altered white matter (Wolff et al. 2012) and cortical surface area development (Hazlett et al. 2017). A machine learning approach was able to predict future autism in high risk 6 month olds with high accuracy (Emerson et al. 2017). Finally, white matter networks at birth may be predictive of internalizing and externalizing behavior at 2 and 4 years (Wee et al. 2017).

Combining advanced machine learning with whole brain network approaches may prove to be more fruitful at identifying imaging biomarkers than current techniques that focus on specific regions or connections. This makes intuitive sense as cognitive functions are highly complex and widely distributed across the brain. Analyses that combine multiple components of brain structure and functional connectivity may also provide better predictive ability in young children (Braun et al. 2018; Seidlitz et al. 2018).

15.7 Conclusion

Schizophrenia is the most human of brain diseases, its symptoms and pathophysiology reflecting the remarkable complexity of the human brain – its genetic underpinnings, its responses to environmental factors during development, and its functional complexity. Schizophrenia is also a very heterogeneous illness, the result of multiple genetic and environmental risk factors, each one with very small and non-specific contributions to overall risk. This causal heterogeneity is the likely basis for the broad heterogeneity of symptoms and cognitive deficits observed in schizophrenia. While there are some commonalities in risk and symptoms across individuals with schizophrenia, it is becoming more and more likely that each person with schizophrenia develops the illness in a unique way, with a unique and diverse set of genetic and environmental risk factors that results in a unique and diverse set of symptoms and cognitive deficits.

Can early childhood imaging identify useful biomarkers that reflect the common impact of multiple genetic and environmental risk factors on the developmental trajectories of the brain and its networks that increase risk for schizophrenia? Many of the structural and functional brain abnormalities observed in schizophrenia may have origins in very early brain development. Studies in this period of rapid brain development suggest that genetic and environmental factors that contribute to risk for schizophrenia do alter development in a way that is detectable early in life. Much work needs to be done, and future studies will tell us whether imaging during early childhood will be informative. Currently, two projects are underway that will provide important basic imaging in this period – the NIH Baby Connectome Study (Howell et al. 2019), and the European Research Council's Developing Human Connectome Project (Bastiani et al. 2019). The hope is that understanding how risk factors influence brain development when the basic architecture of the brain is being set up will ultimately allow us to identify children at risk early enough to intervene and mitigate risk.

Summary

- Schizophrenia is associated with fetal and early childhood risk factors.
- Imaging studies have begun to elucidate fetal and infant brain development.
- By birth, cortical morphology is well developed, white matter tracts are in place, and sensorimotor functional networks are mature.
- In the first 2 years of life, higher order functional networks are well developed,

the bulk of myelination has occurred, and cortical thickness has peaked.
- Early studies indicate that maternal stress and depression, as well as genetic risk factors, can influence brain structure and function in early childhood.

References

Alexander-Bloch A, Raznahan A, Bullmore E, Giedd J. The convergence of maturational change and structural covariance in human cortical networks. J Neurosci. 2013;33(7):2889–99.

Anderson AL, Thomason ME. Functional plasticity before the cradle: a review of neural functional imaging in the human fetus. Neurosci Biobehav Rev. 2013;37(9 Pt B):2220–32.

Andescavage NN, du Plessis A, McCarter R, Serag A, Evangelou I, Vezina G, Robertson R, Limperopoulos C. Complex trajectories of brain development in the healthy human fetus. Cereb Cortex. 2017;27(11):5274–83.

Ball G, et al. Rich-club organization of the newborn human brain. Proc Natl Acad Sci U S A. 2014;111:7456–61.

Ball G, Aljabar P, Arichi T, Tusor N, Cox D, Merchant N, Nongena P, Hajnal JV, Edwards AD, Counsell SJ. Machine-learning to characterise neonatal functional connectivity in the preterm brain. Neuroimage. 2016;124(Pt A):267–75.

Bastiani M, Andersson JLR, Cordero-Grande L, Murgasova M, Hutter J, Price AN, Makropoulos A, Fitzgibbon SP, Hughes E, Rueckert D, Victor S, Rutherford M, Edwards AD, Smith SM, Tournier JD, Hajnal JV, Jbabdi S, Sotiropoulos SN. Automated processing pipeline for neonatal diffusion MRI in the developing Human Connectome Project. Neuroimage. 2019;185:750–63.

Batalle D, Edwards AD, O'Muircheartaigh J. Annual research review: not just a small adult brain: understanding later neurodevelopment through imaging the neonatal brain. J Child Psychol Psychiatry. 2018;59(4):350–71.

Birnbaum R, Weinberger DR. Genetic insights into the neurodevelopmental origins of schizophrenia. Nat Rev Neurosci. 2017;18(12):727–40.

Birnbaum R, Jaffe AE, Chen Q, Hyde TM, Kleinman JE, Weinberger DR. Investigation of the prenatal expression patterns of 108 schizophrenia-associated genetic loci. Biol Psychiatry. 2015;77(11):e43–51.

Bompard L, Xu S, Styner M, Paniagua B, Ahn M, Yuan Y, Jewells V, Gao W, Shen D, Zhu H, Lin W. Multivariate longitudinal shape analysis of human lateral ventricles during the first twenty-four months of life. PLoS One. 2014;9(9):e108306.

Boos HB, Aleman A, Cahn W, Hulshoff Pol H, Kahn RS. Brain volumes in relatives of patients with schizophrenia: a meta-analysis. Arch Gen Psychiatry. 2007;64(3):297–304.

Braun U, Schaefer A, Betzel RF, Tost H, Meyer-Lindenberg A, Bassett DS. From maps to multi-dimensional network mechanisms of mental disorders. Neuron. 2018;97(1):14–31.

Brown TT, Kuperman JM, Chung Y, Erhart M, McCabe C, Hagler DJ Jr, Venkatraman VK, Akshoomoff N, Amaral DG, Bloss CS, Casey BJ, Chang L, Ernst TM, Frazier JA, Gruen JR, Kaufmann WE, Kenet T, Kennedy DN, Murray SS, Sowell ER, Jernigan TL, Dale AM. Neuroanatomical assessment of biological maturity. Curr Biol. 2012;22(18):1693–8.

Cannon M, Jones PB, Murray RM. Obstetric complications and schizophrenia: historical and meta-analytic review. Am J Psychiatry. 2002;159(7):1080–92.

Cannon TD, Chung Y, He G, Sun D, Jacobson A, van Erp TG, McEwen S, Addington J, Bearden CE, Cadenhead K, Cornblatt B, Mathalon DH, McGlashan T, Perkins D, Jeffries C, Seidman LJ, Tsuang M, Walker E, Woods SW, Heinssen R, North American Prodrome Longitudinal Study C. Progressive reduction in cortical thickness as psychosis develops: a multisite longitudinal neuroimaging study of youth at elevated clinical risk. Biol Psychiatry. 2015;77(2):147–57.

Cao M, Huang H, Peng Y, Dong Q, He Y. Toward developmental connectomics of the human brain. Front Neuroanat. 2016;10:25.

Chang YS, Owen JP, Pojman NJ, Thieu T, Bukshpun P, Wakahiro ML, Berman JI, Roberts TP, Nagarajan SS, Sherr EH, Mukherjee P. White matter changes of neurite density and fiber orientation dispersion during human brain maturation. PLoS One. 2015;10(6):e0123656.

Chen L, Pan H, Tuan TA, Teh AL, MacIsaac JL, Mah SM, McEwen LM, Li Y, Chen H, Broekman BF, Buschdorf JP, Chong YS, Kwek K, Saw SM, Gluckman PD, Fortier MV, Rifkin-Graboi A, Kobor MS, Qiu A, Meaney MJ, Holbrook JD, Gusto Study G. Brain-derived neurotrophic factor (BDNF) Val66Met polymorphism influences the association of the methylome with maternal anxiety and neonatal brain volumes. Dev Psychopathol. 2015;27(1):137–50.

Choe MS, Ortiz-Mantilla S, Makris N, Gregas M, Bacic J, Haehn D, Kennedy D, Pienaar R, Caviness VS Jr, Benasich AA, Grant PE. Regional infant brain development: an MRI-based morphometric analysis in 3 to 13 month olds. Cereb Cortex. 2013;23(9):2100–17.

Cohen AH, Wang R, Wilkinson M, MacDonald P, Lim AR, Takahashi E. Development of human white matter fiber pathways: From newborn to adult ages. Int J Dev Neurosci. 2016;50:26–38.

Collin G, Scholtens LH, Kahn RS, Hillegers MHJ, van den Heuvel MP. Affected anatomical rich club and structural-functional coupling in young offspring of schizophrenia and bipolar disorder patients. Biol Psychiatry. 2017;82(10):746–55.

Corbetta M, Shulman GL. Control of goal-directed and stimulus-driven attention in the brain. Nat Rev Neurosci. 2002;3(3):201–15.

Dean DC III, O'Muircheartaigh J, Dirks H, Waskiewicz N, Lehman K, Walker L, Han M, Deoni SC. Modeling healthy male white matter and myelin development: 3 through 60 months of age. Neuroimage. 2014;84:742–52.

Dean DC III, O'Muircheartaigh J, Dirks H, Waskiewicz N, Walker L, Doernberg E, Piryatinsky I, Deoni SC. Characterizing longitudinal white matter development during early childhood. Brain Struct Funct. 2015;220(4):1921–33.

Deoni SC, Mercure E, Blasi A, Gasston D, Thomson A, Johnson M, Williams SC, Murphy DG. Mapping infant brain myelination with magnetic resonance imaging. J Neurosci. 2011;31(2):784–91.

Deoni SC, O'Muircheartaigh J, Elison JT, Walker L, Doernberg E, Waskiewicz N, Dirks H, Piryatinsky I, Dean DC 3rd, Jumbe NL. White matter maturation profiles through early childhood predict general cognitive ability. Brain Struct Funct. 2016;221(2):1189–203.

Dickson H, Laurens KR, Cullen AE, Hodgins S. Meta-analyses of cognitive and motor function in youth aged 16 years and younger who subsequently develop schizophrenia. Psychol Med. 2012;42(4):743–55.

Dietsche B, Kircher T, Falkenberg I. Structural brain changes in schizophrenia at different stages of the illness: a selective review of longitudinal magnetic resonance imaging studies. Aust N Z J Psychiatry. 2017;51(5):500–8.

Doria V, Beckmann CF, Arichi T, Merchant N, Groppo M, Turkheimer FE, Counsell SJ, Murgasova M, Aljabar P, Nunes RG, Larkman DJ, Rees G, Edwards AD. Emergence of resting state networks in the preterm human brain. Proc Natl Acad Sci U S A. 2010;107(46):20015–20.

Dosenbach NU, Nardos B, Cohen AL, Fair DA, Power JD, Church JA, Nelson SM, Wig GS, Vogel AC, Lessov-Schlaggar CN, Barnes KA, Dubis JW, Feczko E, Coalson RS, Pruett JR Jr, Barch DM, Petersen SE, Schlaggar BL. Prediction of individual brain maturity using fMRI. Science. 2010;329(5997):1358–61.

Dubois J, Dehaene-Lambertz G, Kulikova S, Poupon C, Huppi PS, Hertz-Pannier L. The early development of brain white matter: a review of imaging studies in fetuses, newborns and infants. Neuroscience. 2014;276:48–71.

Ducharme S, Albaugh MD, Nguyen TV, Hudziak JJ, Mateos-Perez JM, Labbe A, Evans AC, Karama S, Brain Development Cooperative G. Trajectories of cortical thickness maturation in normal brain development—the importance of quality control procedures. Neuroimage. 2016;125:267–79.

Emerson RW, Adams C, Nishino T, Hazlett HC. Functional neuroimaging of high-risk 6-month-old infants predicts a diagnosis of autism at 24 months of age. Sci Transl Med. 2017;9(393).

Estes ML, McAllister AK. Maternal immune activation: implications for neuropsychiatric disorders. Science. 2017;353(6301):772–7.

Evans AC. Networks of anatomical covariance. Neuroimage. 2013;80:489–504.

Fan Y, et al. Brain anatomical networks in early human brain development. Neuroimage. 2011;54:1862–71.

Faria AV, Zhang J, Oishi K, Li X, Jiang H, Akhter K, Hermoye L, Lee SK, Hoon A, Stashinko E, Miller MI, van Zijl PC, Mori S. Atlas-based analysis of neurodevelopment from infancy to adulthood using diffusion tensor imaging and applications for automated abnormality detection. Neuroimage. 2010;52(2):415–28.

Filatova S, Koivumaa-Honkanen H, Hirvonen N, Freeman A, Ivandic I, Hurtig T, Khandaker GM, Jones PB, Moilanen K, Miettunen J. Early motor developmental milestones and schizophrenia: a systematic review and meta-analysis. Schizophr Res. 2017;188:13–20.

Fish B, Marcus J, Hans SL, Auerbach JG, Perdue S. Infants at risk for schizophrenia: sequelae of a genetic neurointegrative defect. A review and replication analysis of pandysmaturation in the Jerusalem Infant Development Study. Arch Gen Psychiatry. 1992;49(3):221–35.

Fitzsimmons J, Kubicki M, Shenton ME. Review of functional and anatomical brain connectivity findings in schizophrenia. Curr Opin Psychiatry. 2013;26(2):172–87.

Forsyth JK, Lewis DA. Mapping the consequences of impaired synaptic plasticity in schizophrenia through development: an integrative model for diverse clinical features. Trends Cogn Sci. 2017;21(10):760–78.

Fox MD, Snyder AZ, Vincent JL, Corbetta M, Van Essen DC, Raichle ME. The human brain is intrinsically organized into dynamic, anticorrelated functional networks. Proc Natl Acad Sci U S A. 2005;102(27):9673–8.

Fransson P, Skiold B, Horsch S, Nordell A, Blennow M, Lagercrantz H, Aden U. Resting-state networks in the infant brain. Proc Natl Acad Sci U S A. 2007;104(39):15531–6.

Fransson P, Aden U, Blennow M, Lagercrantz H. The functional architecture of the infant brain as revealed by resting-state fMRI. Cereb Cortex. 2011;21(1):145–54.

Freedman R, Hunter SK, Hoffman MC. Prenatal primary prevention of mental illness by micronutrient supplements in pregnancy. Am J Psychiatry. 2018;175(7):607–19.

Fuller R, Nopoulos P, Arndt S, O'Leary D, Ho BC, Andreasen NC. Longitudinal assessment of premorbid cognitive functioning in patients with schizophrenia through examination of standardized scholastic test performance. Am J Psychiatry. 2002;159(7):1183–9.

Gabrieli JD, Ghosh SS, Whitfield-Gabrieli S. Prediction as a humanitarian and pragmatic contribution from human cognitive neuroscience. Neuron. 2015;85(1):11–26.

Gao W, Zhu H, Giovanello KS, Smith JK, Shen D, Gilmore JH, Lin W. Evidence on the emergence of the brain's default network from 2-week-old to 2-year-old healthy pediatric subjects. Proc Natl Acad Sci U S A. 2009a;106(16):6790–5.

Gao W, Lin W, Chen Y, Gerig G, Smith JK, Jewells V, Gilmore JH. Temporal and spatial development of axonal maturation and myelination of white mat-

ter in the developing brain. Am J Neuroradiol. 2009b;30(2):290–6.
Gao W, Gilmore JH, Shen D, Smith JK, Zhu H, Lin W. The synchronization within and interaction between the default and dorsal attention networks in early infancy. Cereb Cortex. 2013;23(3):594–603.
Gao W, Alcauter S, Elton A, Hernandez-Castillo CR, Smith JK, Ramirez J, Lin W. Functional network development during the first year: relative sequence and socioeconomic correlations. Cereb Cortex. 2015a;25(9):2919–28.
Gao W, Alcauter S, Smith JK, Gilmore JH, Lin W. Development of human brain cortical network architecture during infancy. Brain Struct Funct. 2015b;220(2):1173–86.
Gao W, Grewen K, Knickmeyer RC, Qiu A, Salzwedel A, Lin W, Gilmore JH. A review on neuroimaging studies of genetic and environmental influences on early brain development. Neuroimage. 2019;185:802–12.
Genc S, Malpas CB, Holland SK, Beare R, Silk TJ. Neurite density index is sensitive to age related differences in the developing brain. Neuroimage. 2017;148:373–80.
Geng X, Gouttard S, Sharma A, Gu H, Styner M, Lin W, Gerig G, Gilmore JH. Quantitative tract-based white matter development from birth to age 2 years. Neuroimage. 2012;61(3):542–57.
Geng X, Li G, Lu Z, Gao W, Wang L, Shen D, Zhu H, Gilmore JH. Structural and maturational covariance in early childhood brain development. Cereb Cortex. 2017;27(3):1795–807.
Gilmore JH, Kang C, Evans DD, Wolfe HM, Smith JK, Lieberman JA, Lin W, Hamer RM, Styner M, Gerig G. Prenatal and neonatal brain structure and white matter maturation in children at high risk for schizophrenia. Am J Psychiatry. 2010;167(9):1083–91.
Gilmore JH, Shi F, Woolson SL, Knickmeyer RC, Short SJ, Lin W, Zhu H, Hamer RM, Styner M, Shen D. Longitudinal development of cortical and subcortical gray matter from birth to 2 years. Cereb Cortex. 2012;22(11):2478–85.
Gilmore JH, Knickmeyer RC, Gao W. Imaging structural and functional brain development in early childhood. Nat Rev Neurosci. 2018;19(3):123–37.
Gong Q, Lui S, Sweeney JA. A selective review of cerebral abnormalities in patients with first-episode schizophrenia before and after treatment. Am J Psychiatry. 2016;173(3):232–43.
Graham AM, Rasmussen JM, Rudolph MD, Heim CM, Gilmore JH, Styner M, Potkin SG, Entringer S, Wadhwa PD, Fair DA, Buss C. Maternal systemic interleukin-6 during pregnancy is associated with newborn amygdala phenotypes and subsequent behavior at 2 years of age. Biol Psychiatry. 2018;83(2):109–19.
Grayson DS, Fair DA. Development of large-scale functional networks from birth to adulthood: a guide to the neuroimaging literature. Neuroimage. 2017;160:15–31.
Grayson DS, Ray S, Carpenter S, Iyer S, Dias TG, Stevens C, Nigg JT, Fair DA. Structural and functional rich club organization of the brain in children and adults. PLoS One. 2014;9(2):e88297.
Green MF. Impact of cognitive and social cognitive impairment on functional outcomes in patients with schizophrenia. J Clin Psychiatry. 2016;77(Suppl 2):8–11.
Groeschel S, Vollmer B, King MD, Connelly A. Developmental changes in cerebral grey and white matter volume from infancy to adulthood. Int J Dev Neurosci. 2010;28(6):481–9.
Gur RC, Calkins ME, Satterthwaite TD, Ruparel K, Bilker WB, Moore TM, Savitt AP, Hakonarson H, Gur RE. Neurocognitive growth charting in psychosis spectrum youths. JAMA Psychiatry. 2014;71(4):366–74.
Hagmann P, Sporns O, Madan N, Cammoun L, Pienaar R, Wedeen VJ, Meuli R, Thiran JP, Grant PE. White matter maturation reshapes structural connectivity in the late developing human brain. Proc Natl Acad Sci U S A. 2010;107(44):19067–72.
Haijma SV, Van Haren N, Cahn W, Koolschijn PC, Hulshoff Pol HE, Kahn RS. Brain volumes in schizophrenia: a meta-analysis in over 18 000 subjects. Schizophr Bull. 2013;39(5):1129–38.
Hameed MA, Lewis AJ. Offspring of parents with schizophrenia: a systematic review of developmental features across childhood. Harv Rev Psychiatry. 2016;24(2):104–17.
Hazlett HC, Gu H, Munsell BC, Kim SH, Styner M, Wolff JJ, Elison JT, Swanson MR, Zhu H, Botteron KN, Collins DL, Constantino JN, Dager SR, Estes AM, Evans AC, Fonov VS, Gerig G, Kostopoulos P, McKinstry RC, Pandey J, Paterson S, Pruett JR, Schultz RT, Shaw DW, Zwaigenbaum L, Piven J, Network I, Clinical S, Data Coordinating C, Image Processing C, Statistical A. Early brain development in infants at high risk for autism spectrum disorder. Nature. 2017;542(7641):348–51.
Hill J, Dierker D, Neil J, Inder T, Knutsen A, Harwell J, Coalson T, Van Essen D. A surface-based analysis of hemispheric asymmetries and folding of cerebral cortex in term-born human infants. J Neurosci. 2010;30(6):2268–76.
Holland D, Chang L, Ernst TM, Curran M, Buchthal SD, Alicata D, Skranes J, Johansen H, Hernandez A, Yamakawa R, Kuperman JM, Dale AM. Structural growth trajectories and rates of change in the first 3 months of infant brain development. JAMA Neurol. 2014;71(10):1266–74.
Howell BR, Styner MA, Gao W, Yap PT, Wang L, Baluyot K, Yacoub E, Chen G, Potts T, Salzwedel A, Li G, Gilmore JH, Piven J, Smith JK, Shen D, Ugurbil K, Zhu H, Lin W, Elison JT. The UNC/UMN Baby Connectome Project (BCP): an overview of the study design and protocol development. Neuroimage. 2019;185:891–905.
Huang H, Shu N, Mishra V, Jeon T, Chalak L, Wang ZJ, Rollins N, Gong G, Cheng H, Peng Y, Dong Q, He Y. Development of human brain structural networks through infancy and childhood. Cereb Cortex. 2015;25(5):1389–404.

Hykin J, Moore R, Duncan K, Clare S, Baker P, Johnson I, Bowtell R, Mansfield P, Gowland P. Fetal brain activity demonstrated by functional magnetic resonance imaging. Lancet. 1999;354(9179):645–6.

Insel TR. Rethinking schizophrenia. Nature. 2010;468(7321):187–93.

Jaffe AE, Straub RE, Shin JH, Tao R, Gao Y, Collado-Torres L, Kam-Thong T, Xi HS, Quan J, Chen Q, Colantuoni C, Ulrich WS, Maher BJ, Deep-Soboslay A, BrainSeq C, Cross AJ, Brandon NJ, Leek JT, Hyde TM, Kleinman JE, Weinberger DR. Developmental and genetic regulation of the human cortex transcriptome illuminate schizophrenia pathogenesis. Nat Neurosci. 2018;21(8):1117–25.

Jakab A, Pogledic I, Schwartz E, Gruber G, Mitter C, Brugger PC, Langs G, Schopf V, Kasprian G, Prayer D. Fetal cerebral magnetic resonance imaging beyond morphology. Semin Ultrasound CT MR. 2015;36(6):465–75.

Kelly S, Jahanshad N, Zalesky A, Kochunov P, Agartz I, Alloza C, Andreassen OA, Arango C, Banaj N, Bouix S, Bousman CA, Brouwer RM, Bruggemann J, Bustillo J, Cahn W, Calhoun V. Widespread white matter microstructural differences in schizophrenia across 4322 individuals: results from the ENIGMA Schizophrenia DTI Working Group. Mol Psychiatry. 2018;23(5):1261–9.

Keunen K, Benders MJ, Leemans A, Fieret-Van Stam PC, Scholtens LH, Viergever MA, Kahn RS, Groenendaal F, de Vries LS, van den Heuvel MP. White matter maturation in the neonatal brain is predictive of school age cognitive capacities in children born very preterm. Dev Med Child Neurol. 2017;59(9):939–46.

Khundrakpam BS, Reid A, Brauer J, Carbonell F, Lewis J, Ameis S, Karama S, Lee J, Chen Z, Das S, Evans AC, Brain Development Cooperative G. Developmental changes in organization of structural brain networks. Cereb Cortex. 2013;23(9):2072–85.

Knickmeyer RC, Gouttard S, Kang C, Evans D, Wilber K, Smith JK, Hamer RM, Lin W, Gerig G, Gilmore JH. A structural MRI study of human brain development from birth to 2 years. J Neurosci. 2008;28(47):12176–82.

Knickmeyer RC, Wang J, Zhu H, Geng X, Woolson S, Hamer RM, Konneker T, Lin W, Styner M, Gilmore JH. Common variants in psychiatric risk genes predict brain structure at birth. Cereb Cortex. 2014;24(5):1230–46.

Kochunov P, Hong LE. Neurodevelopmental and neurodegenerative models of schizophrenia: white matter at the center stage. Schizophr Bull. 2014;40(4):721–8.

Krishnan ML, Van Steenwinckel J, Schang AL, Yan J, Arnadottir J, Le Charpentier T, Csaba Z, Dournaud P, Cipriani S, Auvynet C, Titomanlio L, Pansiot J, Ball G, Boardman JP, Walley AJ, Saxena A, Mirza G, Fleiss B, Edwards AD, Petretto E, Gressens P. Integrative genomics of microglia implicates DLG4 (PSD95) in the white matter development of preterm infants. Nat Commun. 2017;8(1):428.

Krogsrud SK, Fjell AM, Tamnes CK, Grydeland H, Mork L, Due-Tonnessen P, Bjornerud A, Sampaio-Baptista C, Andersson J, Johansen-Berg H, Walhovd KB. Changes in white matter microstructure in the developing brain—a longitudinal diffusion tensor imaging study of children from 4 to 11years of age. Neuroimage. 2016;124(Pt A):473–86.

Krystal JH, Anticevic A, Yang GJ, Dragoi G, Driesen NR, Wang XJ, Murray JD. Impaired tuning of neural ensembles and the pathophysiology of schizophrenia: a translational and computational neuroscience perspective. Biol Psychiatry. 2017;81(10):874–85.

Kubicki M, McCarley R, Westin CF, Park HJ, Maier S, Kikinis R, Jolesz FA, Shenton ME. A review of diffusion tensor imaging studies in schizophrenia. J Psychiatr Res. 2007;41(1-2):15–30.

Kyriakopoulou V, Vatansever D, Davidson A, Patkee P, Elkommos S, Chew A, Martinez-Biarge M, Hagberg B, Damodaram M, Allsop J, Fox M, Hajnal JV, Rutherford MA. Normative biometry of the fetal brain using magnetic resonance imaging. Brain Struct Funct. 2017;222(5):2295–307.

Lebel C, Walton M, Letourneau N, Giesbrecht GF, Kaplan BJ, Dewey D. Prepartum and postpartum maternal depressive symptoms are related to children's brain structure in preschool. Biol Psychiatry. 2016;80(11):859–68.

Lee SJ, Steiner RJ, Yu Y, Short SJ, Neale MC, Styner MA, Zhu H, Gilmore JH. Common and heritable components of white matter microstructure predict cognitive function at 1 and 2 y. Proc Natl Acad Sci U S A. 2017;114(1):148–53.

Li G, Nie J, Wang L, Shi F, Lin W, Gilmore JH, Shen D. Mapping region-specific longitudinal cortical surface expansion from birth to 2 years of age. Cereb Cortex. 2013;23(11):2724–33.

Li G, Wang L, Shi F, Lyall AE, Lin W, Gilmore JH, Shen D. Mapping longitudinal development of local cortical gyrification in infants from birth to 2 years of age. J Neurosci. 2014;34(12):4228–38.

Li G, Lin W, Gilmore JH, Shen D. Spatial patterns, longitudinal development, and hemispheric asymmetries of cortical thickness in infants from birth to 2 years of age. J Neurosci. 2015;35(24):9150–62.

Liu WJ, Yin DZ, Cheng WH, Fan MX, You MN, Men WW, Zang LL, Shi DH, Zhang F. Abnormal functional connectivity of the amygdala-based network in resting-state FMRI in adolescents with generalized anxiety disorder. Med Sci Monit. 2015;21:459–67.

Lyall AE, Shi F, Geng X, Woolson S, Li G, Wang L, Hamer RM, Shen D, Gilmore JH. Dynamic development of regional cortical thickness and surface area in early childhood. Cereb Cortex. 2015;25(8):2204–12.

Mah A, Geeraert B, Lebel C. Detailing neuroanatomical development in late childhood and early adolescence using NODDI. PLoS One. 2017;12(8):e0182340.

Maki P, Riekki T, Miettunen J, Isohanni M, Jones PB, Murray GK, Veijola J. Schizophrenia in the offspring of antenatally depressed mothers in the northern Finland 1966 birth cohort: relationship to family history of psychosis. Am J Psychiatry. 2010;167(1):70–7.

Makropoulos A, Counsell SJ, Rueckert D. A review on automatic fetal and neonatal brain MRI segmentation. Neuroimage. 2018;170:231–48.

Marshall CR, Howrigan DP, Merico D, Thiruvahindrapuram B, Wu W, Greer DS, Antaki D, Shetty A, Holmans PA, Pinto D. Contribution of copy number variants to schizophrenia from a genome-wide study of 41,321 subjects. Nat Genet. 2017;49(1):27–35.

Matheson SL, Shepherd AM, Laurens KR, Carr VJ. A systematic meta-review grading the evidence for non-genetic risk factors and putative antecedents of schizophrenia. Schizophr Res. 2011;133(1-3):133–42.

Matsuzawa J, Matsui M, Konishi T, Noguchi K, Gur RC, Bilker W, Miyawaki T. Age-related volumetric changes of brain gray and white matter in healthy infants and children. Cereb Cortex. 2001;11(4):335–42.

Meier MH, Caspi A, Reichenberg A, Keefe RS, Fisher HL, Harrington H, Houts R, Poulton R, Moffitt TE. Neuropsychological decline in schizophrenia from the premorbid to the postonset period: evidence from a population-representative longitudinal study. Am J Psychiatry. 2014;171(1):91–101.

Millan MJ, Andrieux A, Bartzokis G, Cadenhead K, Dazzan P, Fusar-Poli P, Gallinat J, Giedd J, Grayson DR, Heinrichs M, Kahn R, Krebs MO, Leboyer M, Lewis D, Marin O, Marin P, Meyer-Lindenberg A, McGorry P, McGuire P, Owen MJ, Patterson P, Sawa A, Spedding M, Uhlhaas P, Vaccarino F, Wahlestedt C, Weinberger D. Altering the course of schizophrenia: progress and perspectives. Nat Rev Drug Discov. 2016;15(7):485–515.

Mills KL, Goddings AL, Herting MM, Meuwese R, Blakemore SJ, Crone EA, Dahl RE, Guroglu B, Raznahan A, Sowell ER, Tamnes CK. Structural brain development between childhood and adulthood: convergence across four longitudinal samples. Neuroimage. 2016;141:273–81.

Mollon J, David AS, Zammit S, Lewis G, Reichenberg A. Course of cognitive development from infancy to early adulthood in the psychosis spectrum. JAMA Psychiatry. 2018;75(3):270–9.

Murray RM, Lewis SW. Is schizophrenia a neurodevelopmental disorder? British Medical Journal (Clinical research ed). 1987;295(6600):681–2.

Narr KL, Leaver AM. Connectome and schizophrenia. Curr Opin Psychiatry. 2015;28(3):229–35.

Network and Pathway Analysis Subgroup of Psychiatric Genomics Consortium. Psychiatric genome-wide association study analyses implicate neuronal, immune and histone pathways. Nat Neurosci. 2015;18(2):199–209.

Nie J, Li G, Shen D. Development of cortical anatomical properties from early childhood to early adulthood. Neuroimage. 2013;76:216–24.

Olabi B, Ellison-Wright I, McIntosh AM, Wood SJ, Bullmore E, Lawrie SM. Are there progressive brain changes in schizophrenia? A meta-analysis of structural magnetic resonance imaging studies. Biol Psychiatry. 2011;70(1):88–96.

O'Muircheartaigh J, et al. White matter development and early cognition in babies and toddlers. Hum Brain Mapp. 2014;35:4475–87.

Ordonez AE, Luscher ZI, Gogtay N. Neuroimaging findings from childhood onset schizophrenia patients and their non-psychotic siblings. Schizophr Res. 2016;173(3):124–31.

Ouyang M, Dubois J, Yu Q, Mukherjee P, Huang H. Delineation of early brain development from fetuses to infants with diffusion MRI and beyond. Neuroimage. 2019;185:836–50.

Oyefiade AA, Ameis S, Lerch JP, Rockel C, Szulc KU, Scantlebury N, Decker A, Jefferson J, Spichak S, Mabbott DJ. Development of short-range white matter in healthy children and adolescents. Hum Brain Mapp. 2018;39(1):204–17.

Paus T, Keshavan M, Giedd JN. Why do many psychiatric disorders emerge during adolescence? Nat Rev Neurosci. 2008;9(12):947–57.

Qiu A, Anh TT, Li Y, Chen H, Rifkin-Graboi A, Broekman BF, Kwek K, Saw SM, Chong YS, Gluckman PD, Fortier MV, Meaney MJ. Prenatal maternal depression alters amygdala functional connectivity in 6-month-old infants. Transl Psychiatry. 2015a;5:e508.

Qiu A, Tuan TA, Ong ML, Li Y, Chen H, Rifkin-Graboi A, Broekman BF, Kwek K, Saw SM, Chong YS, Gluckman PD, Fortier MV, Holbrook JD, Meaney MJ. COMT haplotypes modulate associations of antenatal maternal anxiety and neonatal cortical morphology. Am J Psychiatry. 2015b;172(2):163–72.

Qiu A, Mori S, Miller MI. Diffusion tensor imaging for understanding brain development in early life. Annu Rev Psychol. 2015c;66:853–76.

Rae CL, Davies G, Garfinkel SN, Gabel MC, Dowell NG, Cercignani M, Seth AK, Greenwood KE, Medford N, Critchley HD. Deficits in neurite density underlie white matter structure abnormalities in first-episode psychosis. Biol Psychiatry. 2017;82(10):716–25.

Raichle ME, MacLeod AM, Snyder AZ, Powers WJ, Gusnard DA, Shulman GL. A default mode of brain function. Proc Natl Acad Sci U S A. 2001;98(2):676–82.

Rajagopalan V, Scott J, Habas PA, Kim K, Corbett-Detig J, Rousseau F, Barkovich AJ, Glenn OA, Studholme C. Local tissue growth patterns underlying normal fetal human brain gyrification quantified in utero. J Neurosci. 2011;31(8):2878–87.

Rajji TK, Miranda D, Mulsant BH. Cognition, function, and disability in patients with schizophrenia: a review of longitudinal studies. Can J Psychiatry. 2014;59(1):13–7.

Rasmussen JM, Graham AM, Entringer S, Gilmore JH, Styner M, Fair DA, Wadhwa PD, Buss C. Maternal Interleukin-6 concentration during pregnancy is associated with variation in frontolimbic white matter and cognitive development in early life. Neuroimage. 2018;185:825–35.

Raznahan A, Shaw P, Lalonde F, Stockman M, Wallace GL, Greenstein D, Clasen L, Gogtay N, Giedd JN. How does your cortex grow? J Neurosci. 2011;31(19):7174–7.

Reddan MC, Lindquist MA, Wager TD. Effect size estimation in neuroimaging. JAMA Psychiatry. 2017;74(3):207–8.

Reichenberg A, Caspi A, Harrington H, Houts R, Keefe RS, Murray RM, Poulton R, Moffitt TE. Static and dynamic cognitive deficits in childhood preceding adult schizophrenia: a 30-year study. Am J Psychiatry. 2010;167(2):160–9.

Remer J, Croteau-Chonka E, Dean DC, D'Arpino S, Dirks H, Whiley D, Deoni SCL. Quantifying cortical development in typically developing toddlers and young children, 1-6 years of age. NeuroImage. 2017;153:246–61.

Richmond S, Johnson KA, Seal ML, Allen NB, Whittle S. Development of brain networks and relevance of environmental and genetic factors: a systematic review. Neurosci Biobehav Rev. 2016;71:215–39.

Rifkin-Graboi A, Bai J, Chen H, Hameed WB, Sim LW, Tint MT, Leutscher-Broekman B, Chong YS, Gluckman PD, Fortier MV, Meaney MJ, Qiu A. Prenatal maternal depression associates with microstructure of right amygdala in neonates at birth. Biol Psychiatry. 2013;74(11):837–44.

Ross RG, Freedman R. Endophenotypes in schizophrenia for the perinatal period: criteria for validation. Schizophr Bull. 2015;41(4):824–34.

Rudolph MD, Graham AM, Feczko E, Miranda-Dominguez O. Maternal IL-6 during pregnancy can be estimated from newborn brain connectivity and predicts future working memory in offspring. Nat Neurosci. 2018;21(5):765–72.

Sadeghi N, Prastawa M, Fletcher PT, Wolff J, Gilmore JH, Gerig G. Regional characterization of longitudinal DT-MRI to study white matter maturation of the early developing brain. Neuroimage. 2013;68:236–47.

Schizophrenia Working Group of the Psychiatric Genomics Consortium. Biological insights from 108 schizophrenia-associated genetic loci. Nature. 2014;511(7510):421–7.

Seeley WW, Menon V, Schatzberg AF, Keller J, Glover GH, Kenna H, Reiss AL, Greicius MD. Dissociable intrinsic connectivity networks for salience processing and executive control. J Neurosci. 2007;27(9):2349–56.

Seidlitz J, Vasa F, Shinn M, Romero-Garcia R, Whitaker KJ, Vertes PE, Wagstyl K, Kirkpatrick Reardon P, Clasen L, Liu S, Messinger A, Leopold DA, Fonagy P, Dolan RJ, Jones PB, Goodyer IM, Consortium N, Raznahan A, Bullmore ET. Morphometric similarity networks detect microscale cortical organization and predict inter-individual cognitive variation. Neuron. 2018;97(1):231–247 e237.

Shaw P, Kabani NJ, Lerch JP, Eckstrand K, Lenroot R, Gogtay N, Greenstein D, Clasen L, Evans A, Rapoport JL, Giedd JN, Wise SP. Neurodevelopmental trajectories of the human cerebral cortex. J Neurosci. 2008;28(14):3586–94.

Shepherd AM, Laurens KR, Matheson SL, Carr VJ, Green MJ. Systematic meta-review and quality assessment of the structural brain alterations in schizophrenia. Neurosci Biobehav Rev. 2012;36(4):1342–56.

Short SJ, Elison JT, Goldman BD, Styner M, Gu H, Connelly M, Maltbie E, Woolson S, Lin W, Gerig G, Reznick JS, Gilmore JH. Associations between white matter microstructure and infants' working memory. Neuroimage. 2013;64:156–66.

Shulman GL, Fiez JA, Corbetta M, Buckner RL, Miezin FM, Raichle ME, Petersen SE. Common blood flow changes across visual tasks: II. Decreases in cerebral cortex. J Cogn Neurosci. 1997;9(5):648–63.

Smyser CD, Inder TE, Shimony JS, Hill JE, Degnan AJ, Snyder AZ, Neil JJ. Longitudinal analysis of neural network development in preterm infants. Cereb Cortex. 2010;20(12):2852–62.

Sorensen HJ, Mortensen EL, Schiffman J, Reinisch JM, Maeda J, Mednick SA. Early developmental milestones and risk of schizophrenia: a 45-year follow-up of the Copenhagen Perinatal Cohort. Schizophr Res. 2010;118(1-3):41–7.

Sowell ER, Thompson PM, Leonard CM, Welcome SE, Kan E, Toga AW. Longitudinal mapping of cortical thickness and brain growth in normal children. J Neurosci. 2004;24(38):8223–31.

Thomason ME, Scheinost D, Manning JH, Grove LE, Hect J, Marshall N, Hernandez-Andrade E, Berman S, Pappas A, Yeo L, Hassan SS, Constable RT, Ment LR, Romero R. Weak functional connectivity in the human fetal brain prior to preterm birth. Sci Rep. 2017;7:39286.

Thomason ME, Hect J, Waller R, Manning JH, Stacks AM, Beeghly M, Boeve JL, Wong K, van den Heuvel MI, Hernandez-Andrade E, Hassan SS, Romero R. Prenatal neural origins of infant motor development: associations between fetal brain and infant motor development. Dev Psychopathol. 2018;30(3):763–72.

Tymofiyeva O, Hess CP, Xu D, Barkovich AJ. Structural MRI connectome in development: challenges of the changing brain. Br J Radiol. 2014;87(1039):20140086.

Uda S, Matsui M, Tanaka C, Uematsu A, Miura K, Kawana I, Noguchi K. Normal development of human brain white matter from infancy to early adulthood: a diffusion tensor imaging study. Dev Neurosci. 2015;37(2):182–94.

Uematsu A, Matsui M, Tanaka C, Takahashi T, Noguchi K, Suzuki M, Nishijo H. Developmental trajectories of amygdala and hippocampus from infancy to early adulthood in healthy individuals. PLoS One. 2012;7(10):e46970.

Uhlhaas PJ, Singer W. The development of neural synchrony and large-scale cortical networks during adolescence: relevance for the pathophysiology of schizophrenia and neurodevelopmental hypothesis. Schizophr Bull. 2011;37(3):514–23.

Van den Bergh BRH, van den Heuvel MI, Lahti M, Braeken M, de Rooij SR, Entringer S, Hoyer D, Roseboom T, Raikkonen K, King S, Schwab M. Prenatal developmental origins of behavior and mental health: the influence of maternal stress in pregnancy. Neurosci Biobehav Rev. 2017.

van den Heuvel MP, Fornito A. Brain networks in schizophrenia. Neuropsychol Rev. 2014;24(1):32–48.

van den Heuvel MI, Thomason ME. Functional connectivity of the human brain in utero. Trends Cogn Sci. 2016;20(12):931–9.

van den Heuvel MP, Kersbergen KJ, de Reus MA, Keunen K, Kahn RS, Groenendaal F, de Vries LS, Benders MJ. The neonatal connectome during preterm brain development. Cereb Cortex. 2015;25(9):3000–13.

van den Heuvel MI, Turk E, Manning JH, Hect J, Hernandez-Andrade E, Hassan SS, Romero R, van den Heuvel MP, Thomason ME. Hubs in the human fetal brain network. Dev Cogn Neurosci. 2018;30:108–15.

van Erp TG, Hibar DP, Rasmussen JM, Glahn DC, Pearlson GD, Andreassen OA, Agartz I, Westlye LT, Haukvik UK, Dale AM, Melle I, Hartberg CB, Gruber O, Kraemer B, Zilles D, Donohoe G, Kelly S, McDonald C, Morris DW, Cannon DM, Corvin A, Machielsen MW, Koenders L, de Haan L, Veltman DJ, Satterthwaite TD, Wolf DH, Gur RC, Gur RE, Potkin SG, Mathalon DH, Mueller BA, Preda A, Macciardi F, Ehrlich S, Walton E, Hass J, Calhoun VD, Bockholt HJ, Sponheim SR, Shoemaker JM, van Haren NE, Pol HE, Ophoff RA, Kahn RS, Roiz-Santianez R, Crespo-Facorro B, Wang L, Alpert KI, Jonsson EG, Dimitrova R, Bois C, Whalley HC, McIntosh AM, Lawrie SM, Hashimoto R, Thompson PM, Turner JA. Subcortical brain volume abnormalities in 2028 individuals with schizophrenia and 2540 healthy controls via the ENIGMA consortium. Mol Psychiatry. 2016;21(4):585.

van Erp TG, Walton EH, Derrek P, Schmaal L, Jiang W, Glahn DC, Pearlson GD, Yao N, Fukunaga M, Hashimoto R, et al. Cortical brain abnormalities in 4474 individuals with schizophrenia and 5098 control subjects via the enhancing neuro imaging genetics through meta analysis (ENIGMA) consortium. Biol Psychiatry. 2018;84:644–54.

Vasung L, Abaci Turk E, Ferradal SL, Sutin J, Stout JN, Ahtam B, Lin PY, Grant PE. Exploring early human brain development with structural and physiological neuroimaging. Neuroimage. 2018;187:226–54.

Vita A, De Peri L, Deste G, Sacchetti E. Progressive loss of cortical gray matter in schizophrenia: a meta-analysis and meta-regression of longitudinal MRI studies. Transl Psychiatry. 2012;2:e190.

von Hohenberg CC, Pasternak O, Kubicki M, Ballinger T, Vu MA, Swisher T, Green K, Giwerc M, Dahlben B, Goldstein JM, Woo TU, Petryshen TL, Mesholam-Gately RI, Woodberry KA, Thermenos HW, Mulert C, McCarley RW, Seidman LJ, Shenton ME. White matter microstructure in individuals at clinical high risk of psychosis: a whole-brain diffusion tensor imaging study. Schizophr Bull. 2014;40(4):895–903.

Walhovd KB, Fjell AM, Giedd J, Dale AM, Brown TT. Through thick and thin: a need to reconcile contradictory results on trajectories in human cortical development. Cereb Cortex. 2017;27(2):1472–81.

Wee CY, Tuan TA, Broekman BF, Ong MY, Chong YS, Kwek K, Shek LP, Saw SM, Gluckman PD, Fortier MV, Meaney MJ, Qiu A. Neonatal neural networks predict children behavioral profiles later in life. Hum Brain Mapp. 2017;38(3):1362–73.

Weinberger DR. Implications of normal brain development for the pathogenesis of schizophrenia. Arch Gen Psychiatry. 1987;44(7):660–9.

Wheeler AL, Voineskos AN. A review of structural neuroimaging in schizophrenia: from connectivity to connectomics. Front Hum Neurosci. 2014;8:653.

White T, Su S, Schmidt M, Kao CY, Sapiro G. The development of gyrification in childhood and adolescence. Brain Cogn. 2010;72(1):36–45.

Wolff JJ, Gu H, Gerig G, Elison JT, Styner M, Gouttard S, Botteron KN, Dager SR, Dawson G, Estes AM, Evans AC, Hazlett HC, Kostopoulos P, McKinstry RC, Paterson SJ, Schultz RT, Zwaigenbaum L, Piven J, Network I. Differences in white matter fiber tract development present from 6 to 24 months in infants with autism. Am J Psychiatry. 2012;169(6):589–600.

Woo CW, Chang LJ, Lindquist MA, Wager TD. Building better biomarkers: brain models in translational neuroimaging. Nat Neurosci. 2017;20(3):365–77.

Woodberry KA, Giuliano AJ, Seidman LJ. Premorbid IQ in schizophrenia: a meta-analytic review. Am J Psychiatry. 2008;165(5):579–87.

Wright R, Kyriakopoulou V, Ledig C, Rutherford MA, Hajnal JV, Rueckert D, Aljabar P. Automatic quantification of normal cortical folding patterns from fetal brain MRI. Neuroimage. 2014;91:21–32.

Yap PT, Fan Y, Chen Y, Gilmore JH, Lin W, Shen D. Development trends of white matter connectivity in the first years of life. PLoS One. 2011;6(9):e24678.

Zielinski BA, Gennatas ED, Zhou J, Seeley WW. Network-level structural covariance in the developing brain. Proc Natl Acad Sci U S A. 2010;107(42):18191–6.

Genetics and Neuroimaging in Schizophrenia

16

Grace R. Jacobs and Aristotle N. Voineskos

Contents

16.1 Introduction

Schizophrenia is a complex disorder affecting approximately 1% of the population (McGrath et al. 2008) and found to have a heritability as high as 85% (Sullivan et al. 2003; Wray and Gottesman 2012). However, genetic underpinnings and the widespread polygenic contributions to risk are far from fully understood (Sullivan et al. 2012). Accumulating evidence

G. R. Jacobs · A. N. Voineskos (✉)
Kimel Family Translational Imaging-Genetics Laboratory, Campbell Family Mental Health Research Institute, Centre for Addiction and Mental Health, Toronto, ON, Canada

University of Toronto, Toronto, ON, Canada
e-mail: aristotle.voineskos@camh.ca

M. Kubicki, M. E. Shenton (eds.), *Neuroimaging in Schizophrenia*,
https://doi.org/10.1007/978-3-030-35206-6_16

demonstrates that individuals with schizophrenia have disruptions on the molecular, cellular, and neural circuit level that lead to the behaviors and cognitive impairments associated with the illness. Although a person's genetic profile can predispose them to have increased vulnerability for developing schizophrenia, there are also environmental factors and external stressors that may be the tipping point for illness onset or symptom severity. Neuroimaging is an important tool to understand better the neurobiological and genetically mediated risk mechanisms associated with this debilitating brain disorder.

There has been an increased focus in the literature on identifying biomarkers of schizophrenia and indicators of vulnerability, instead of examining the illness only as a clinical phenotype (Schmitt et al. 2016). Studies integrating genetic and imaging approaches can aid in the identification of endophenotypes or intermediate biomarkers between genotype and risk for disorders, such as quantifiable brain measures. If intermediate phenotypes capture a middle point in the pathway towards pathology, and are closer biologically to mechanisms underlying schizophrenia than clinical measures, then focusing on them may increase power for genetic studies. However, this approach assumes that the genetic architecture underlying brain structures will be less complex than that involved in neuropsychiatric disorders. Despite initial hopes for increased effect sizes, recent larger studies show that effect sizes of SNPs on imaging phenotypes are quite small (<1%), and similar to those of schizophrenia risk variants (Hibar et al. 2017; Franke et al. 2016).

Two main approaches exist for studying genetic risk and imaging phenotypes. The first, and more bottom-up, is to examine the effect of a single or group of genetic risk variants on neural systems and circuitry. Alternatively, a top-down data-driven approach can be used to begin with an altered pattern of neural circuitry, and then find both novel genetic variants, as well as confirm existing knowledge of variants. Some challenges with beginning first with an imaging phenotype is that one to one mapping in relation to the presentation of symptoms is challenging. However, it is a less biased approach and has the potential for discovery regarding biological pathways associated with the illness.

A common strategy to understand the contribution of genetics to risk for schizophrenia is to study patients and their unaffected family members. Investigating brain structure and functional abnormalities in healthy family members allows for analyses of genetic contribution of risk, without complications introduced by confounds such as illness duration, treatment, or symptom severity. This approach however, cannot infer specificities of which risk variants contribute to associated brain alterations, or how such contributions are made. It does not take into account the heterogeneity in genetic risk factors that can lead to schizophrenia. Nevertheless, family and twin studies have importantly indicated high heritability across neuroimaging phenotypes in relation to schizophrenia and have been reviewed in depth elsewhere (Lancaster et al. 2016a, b; Blokland et al. 2012; Jansen et al. 2015; Polderman et al. 2015).

The field of imaging genetics is gaining momentum, specifically in psychiatry, as multimodal approaches are increasingly used to study elevated vulnerability and the underlying pathophysiology of mental health and illnesses (Arslan 2015, 2018a, b; Bogdan et al. 2017; Lancaster et al. 2016a, b; Dima and Breen 2015; Carter et al. 2017; Meyer-Lindenberg 2010). Advances in neuroimaging methodologies and the increasing number of publically available datasets with multimodal data are contributing factors. Sample sizes for psychiatric populations are growing exponentially through large-scale collaborative consortiums such as Enhancing Neuro Imaging Genetics through Meta-Analysis (ENIGMA, Chap. 21) (Thompson et al. 2014), the Cohorts for Heart and Aging Research in Genomics Epidemiology (CHARGE) (Psaty et al. 2009), IMAGEN (Schumann et al. 2010), Alzheimer's Disease Neuroimaging Initiative (ADNI) (Petersen et al. 2010), and recently specifically targeted at schizophrenia Genetics of Endophenotypes of Neurofunction to Understand Schizophrenia (GENUS) (Blokland et al. 2018), and have become accessible to a wide range of researchers.

In this chapter, we will focus on studies combining the use of neuroimaging and genetic

approaches to review what is currently known about the genetic architecture underlying imaging phenotypes of schizophrenia. Work that has been done in healthy subjects, schizophrenia patients, as well as youth at clinically high-risk for psychosis is included.

16.2 Types of Genetic Variation

Genetic risk for schizophrenia is highly polygenic and heterogeneous, with no single factor associated with the guaranteed development of schizophrenia in an individual. The most well-known variations in the genome associated with schizophrenia are single nucleotide polymorphisms (SNPs), more rare mutations such as copy number variants (CNVs), and larger structural chromosomal abnormalities. The majority of rare mutations involve several genes and have greater functional and more deleterious effects as compared to common variants (Sebat et al. 2009; Sebat and Malhotra 2013). They also often are not inherited and occur *de novo*, perhaps explaining their enduring prevalence despite reduced fitness of carriers (Van Dongen and Boomsma 2013). There has been a surge in studies and shift towards focusing on rare variants and their contribution to genetic risk for schizophrenia, alongside the variance explained by common variants (Bustamante et al. 2017). Studies of effect sizes have shown that the 16p11.2 duplication has an Odds Ratio (OR) for psychosis of 14.4 (Giaroli et al. 2014), the 3q29 deletion is above 40 (Mulle 2015), and the 22q11.2 deletion increases risk for schizophrenia roughly 30-fold (Schneider et al. 2014). Implicated rare variants like 22q11.2 increase risk for multiple neural pathologies in addition to schizophrenia, such as Autism Spectrum Disorder and intellectual disability. Imaging genetic studies have begun determining brain structure and functional abnormalities associated with rare variants. Additionally, with the recent emergence of a 22q11.2 deletion ENGIMA working group, there is promise moving forward for large meta-analyses with the power to build on our understanding of developmental trajectories associated with this condition. However, further in-depth discussion of imaging studies focusing on rare mutations is beyond the scope of this chapter, and moving forward, the focus will be on studies involving common variants.

16.3 Moving from a Candidate Gene Approach to the Era of GWAS

A substantial portion of imaging-genetic studies thus far have been dominated by investigations of candidate genes pre-selected for studies based on *a priori* knowledge. These initial studies were important in creating neurobiological models of schizophrenia risk and validating hypotheses of the involvement of these genes in specific biological systems. Candidate genes such as catechol-O-methyltransferase (COMT; Witte and Flöel 2012; Gonzalez-Castro et al. 2016), brain-derived neurotrophic factor (BDNF; Hong et al. 2011; Harrisberger et al. 2015), dopamine 2-receptor (DRD2; Luykx et al. 2017), and 5-HTTLPR (Raab et al. 2016; Murphy et al. 2013). Their effects have been reviewed and found to be associated with a variety of brain changes from altered activation to structure (Arslan 2015; Hashimoto et al. 2015; Rasetti and Weinberger 2011). However, the strategy of investigating a single gene at a time has not been overly successful, as effects of single variants are quite small and statistical power is often low (Meyer-Lindenberg 2010; Farrell et al. 2015).

Recently, growth in sample sizes has provided the opportunity to use GWAS to study genetic risk variants associated with schizophrenia. The largest GWAS of risk for schizophrenia currently published by the PGC includes 36,989 cases and 113,075 controls, scanned for 9.5 million variants, and has identified 125 genetic loci (of which 108 are independent) associated with this mental disorder (Schizophrenia Working Group of the Psychiatric Genomics Consortium 2014). This un-biased data-driven alternative to studying candidate genes has been able to identify novel genetic variants and polymorphisms linked to schizophrenia because of the large study power. Although GWAS findings have increased support for some candidate risk variants such

as zinc-finger protein 804A (ZNF804A), calcium voltage-gated channel subunit alpha1 C (CACNA1C), glutamate receptor mgluR3 (GRM3), and DRD2, they have also found unexpected negative results for others such as COMT and BDNF, and questioned previous effect size findings of others such as 5-HTTLPR (serotonin transporter–linked polymorphic region; Hariri et al. 2002; Flint and Munafò 2013).

There are many hypotheses about the mechanisms underlying schizophrenia development, such as the dysregulation of the dopamine (Howes et al. 2017; Meltzer and Stahl 1976), glutamate (Moghaddam and Javitt 2012), or GABAnergic systems (Nakazawa et al. 2012), disruption in myelin and axons (Stedehouder and Kushner 2017; Cassoli et al. 2015), calcium imbalance (Berridge 2014; Lidow 2003), or inflammation (Howes and Mccutcheon 2017). These have traditionally been investigated separately and as more is discovered about the genetic architecture and polygenic nature of schizophrenia through GWAS, evidence has emerged that supports each of these theories instead of narrowing down possible mechanisms or pathophysiological processes (Devor et al. 2017). However, recent analyses are converging on the involvement of biological pathways to unify many of these theories into a general hypothesis of disrupted intracellular signaling pathways, communication across fast (voltage-gated ionic channels) and slow (G-protein coupled receptors) neurotransmission (Devor et al. 2017), as well as on excitatory and inhibitory synaptic neurotransmission and plasticity (Hall et al. 2015).

16.4 Targeted GWAS Risk Variant Studies

As a result of GWAS findings, a great deal of work has been done to target identified risk genes or specific variants and to examine their relationship with imaging phenotypes. These structural and functional studies involving genes implicated in the schizophrenia GWAS have found associated alterations in brain volume, density, white and gray matter, cortical folding and thickness, as well as regional activation and connectivity during executive tasks (Gurung and Prata 2015; Harrison 2015).

Genes containing loci that were implicated in the most recent PGC GWAS include dopaminergic system related gene DRD2, glutamatergic transmission genes GRM3 and GRIN2A, and calcium signalling genes CACNA1C and NRG1, in addition to other genes of interest such as ZNF804A, DISC1, MIR137, and ANK3, to name a few.

GWAS have been important for the identification of novel variants to target for further investigation. Results have inspired follow up imaging and molecular studies to try to understand the relationship between common variants and effects on functioning that might be related to psychosis symptoms. These multimodal explorations are especially important for identifying the actual susceptibility gene and mechanism conferring risk. Only 10 of the identified variants exist in exonic regions of the genome and result in amino acid changes in proteins. Many of the others are most likely located in regulatory regions and lead to functional effects through changes in splicing, gene expression, or other molecules involved in these processes. Considering the high linkage disequilibrium that can occur across many variants and span regions that encompass multiple genes, it is also possible that identified risk variants are merely in high define with the actual variant that confers risk through altered functioning (Bray and Hill 2015).

A recent large study by Erk et al. (2017) examined all of the significant GWAS schizophrenia risk alleles (Schizophrenia Working Group of the Psychiatric Genomics Consortium 2014) and their effects across RDoC neurocognitive domains and brain activation. Only a single SNP rs9607782 near EP300 survived significance after correcting for multiple comparisons and was associated with amygdala activation during emotional processing, indicating that the schizophrenic risk may be mediated by amygdala functioning. There were also findings regarding ZNF804A and CACNA1C, but these only reached subthreshold significance and did not survive correction. It is possible that other mean-

ingful links were lost because of the multiple tests and stringent corrections applied to address false positives. There have also been negative findings in another smaller study looking at associations between identified GWAS schizophrenia risk variants and both cortical thickness and white matter FA neuroimaging phenotypes across the lifespan (Voineskos et al. 2015).

However, significant progress has been made in smaller studies with more a narrowed focus on one or a few risk variants in elucidating functioning. A highly implicated risk allele and one of the first to be identified by GWAS is ZNF804A rs1344706, an intron of a zinc-finger gene coding for a transcription factor. This gene is thought to regulate other genes (Donohoe et al. 2011), including other candidate genes associated with schizophrenia: PRSS16, COMT, PDE4B and DRD2 (Girgenti et al. 2012), and to impact cell adhesion among other functions (Hill et al. 2012). The effect of ZNF804A on structural white matter fractional anisotropy (FA) remains unclear, with both positive (Mallas et al. 2017; Kuswanto et al. 2015; Ikuta et al. 2014) and negative findings (Voineskos et al. 2011; Fernandes et al. 2014; Sprooten et al. 2012; Wei et al. 2015). A recent study showed more widespread effects on white matter FA (Mallas et al. 2017). The ZNF804A risk allele also has mixed effects on gray matter volume in schizophrenia and healthy controls (Donohoe et al. 2011; Cousijn et al. 2012; Voineskos et al. 2011).

Functional imaging studies of the ZNF804A risk allele have replicated findings related to working memory and modulation of connectivity between the hippocampus and dorsolateral PFC (Esslinger et al. 2009, 2011; Rasetti and Weinberger 2011), as well as altered regional activity during social theory of mind tasks and emotional processing (Esslinger et al. 2011; Walter et al. 2011; Mohnke et al. 2014), as well as cognitive control (Thurin et al. 2013).

Investigations have shown that rs1344706 reduces the expression of ZNF804A during the fetal stage, a critical period in neurodevelopment (Hill and Bray 2012; Tao et al. 2014). However, the mechanism by which this risk variant alters expression remains unknown. There is also evidence from animal models that ZNF804A is involved in neurite growth and elongation in the hippocampus and frontal cortex, areas also implicated in imaging studies, and that the rs1344706 allele reduces dendritic spine density, which is consistent with the clinical presentation of schizophrenia (Deans et al. 2016). Overall, compelling findings indicate that this risk variant is a significant factor relating to the onset of schizophrenia that affects the brain early in life and may be involved in white matter structure, connectivity, and cognition (Chang et al. 2017).

It is clear that although GWAS studies have identified novel risk variants, the underlying functioning of these variants and their involvement in molecular pathways leading to their effect on the brain is far from understood. A combination of basic science and molecular genetic studies are needed to move forward in disentangling how genetics contribute to the risk for mental illnesses (Bogdan et al. 2017). A recent study by Sekar et al. (2016) investigated the possible mechanisms of C4 risk alleles located in the dense major histocompatibility complex (MHC), the area most highly associated with schizophrenia through GWAS. Through post-mortem, animal, and population studies, these investigators reported that structural variants altered C4A and C4B expression in the brain that were related to risk for schizophrenia. In combination with findings that C4 mediated synaptic pruning in mice during neuronal maturation, this research suggests that alterations in C4 expression may be related to the reduced number of synapses in the brains of individuals with schizophrenia. These findings have triggered studies of C4 expression and the complement system, although neuroimaging studies have not been done to elucidate how expression relates to imaging phenotypes in humans.

16.5 Polygenic Risk Scores and Imaging Phenotypes

Examining the role of each GWAS identified risk variant or groups of variants is important for understanding the specificities of how they are involved in schizophrenia risk. However, individ-

ual GWAS SNPs capture little of the phenotypic variance observed in schizophrenia (often much less than 1%) and do not address the possible polygenic, additive, or synergistic contributions thought to be involved in illness development. Using an accumulated polygenic risk score (PRS), created by aggregating the effects of many risk variants based on odds ratios, increases the amount of explained variance to as much as a third, and can be a useful tool for applying findings from large GWAS to small samples (Dima and Breen 2015). PRS is thus advantageous as it can incorporate the effects of all or a portion of SNPs, which can extend beyond the few that reach genome-wide significance as determined by a corrected statistical threshold. This approach most likely introduces false positives for the effects of some SNPs, but it also overcomes biases associated with a relatively arbitrary cut-off threshold for significance. Recently, studies have begun to investigate the overlap between polygenic risk for schizophrenia and brain abnormalities linked with the disorder as a complementary bottom-up approach to studying individual common variants. Effect sizes from the PGC GWAS are typically used to construct scores, although not universally (Ohi et al. 2014), and studies often use all SNPs under a certain p-value significance threshold. Importantly, even in healthy youth, an increased polygenic risk score (PRS) for schizophrenia has been found to be correlate with impairments in social cognition and verbal reasoning, demonstrating that relationships emerge early in development (Germine et al. 2016). Additionally, a higher PRS is linked to a family history of psychotic illnesses (Bigdeli et al. 2016). However, there are variations in how studies define PRS and the number of variants included, which has led to challenges related to comparing and replicating results.

As genetic testing of massive numbers of an individual's SNPs continues to quickly become more inexpensive and accessible, it is increasingly becoming an attractive option for quickly determining an individual's risk load for a mental illness that is consistent across a lifespan. A recent growth of studies examining PRS and their associations with cognition, behavior, and neuroimaging phenotypes are improving our understanding of the implications of this aggregated score and its possible utility in health care and clinical practice. As research accumulates to improve specificity and sensitivity, it is possible that one day a PRS may be used for more personalized and preventative medicine, resulting in early identification and more individually targeted interventions.

16.6 Findings from PRS Imaging Studies

Despite the well-established structural alterations prevalent in schizophrenia, larger studies examining overlap between PRS and these abnormalities have found mixed results. Some earlier studies identified direct relationships between PRS and total brain and white matter volume using a range of significance cut-offs for PRS (Terwisscha van Scheltinga et al. 2013), although this has not been consistently replicated and there have been predominantly negative findings for total GM volume (Papiol et al. 2014; Van der Auwera et al. 2015; Reus et al. 2017; Lancaster et al. 2018). One study did support an association between reductions in total white matter and PRS in psychosis, as well as familial genetic risk using a 7 SNP white matter targeted score (Oertel-knöchel et al. 2015).

Studies looking at regional volume differences associated with PRS have found a negative relationship with globus pallidus volume and a trending negative relationship with thalamic volume, both with a range of schizophrenia PRS and a shared PRS between schizophrenia and bipolar disorder (Caseras et al. 2015). This trending association with thalamic volume has been replicated (Reus et al. 2017). Additionally, when a range of PRS are examined using effect sizes from a Japanese GWAS (Ikeda et al. 2011), a negative relationship was found with the left superior temporal gyrus volume (Ohi et al. 2014).

Findings related to the hippocampus show that a higher PRS based on 108 loci is negatively associated with volume (Harrisberger et al. 2016). Additionally, higher scores for a range of

PRS have been related to reduced neuroplasticity in response to an aerobic exercise intervention for schizophrenia, specifically in the left CA4/DG region of the hippocampus (Papiol et al. 2017). Another study with a discovery Chinese sample and European replication sample found negative results for hippocampus volumes, intracranial volume (ICV), and total volumes when both a mixture of GWAS significant and previously found variants associated with candidate genes were included in a PRS (Li et al. 2015). Additionally, when PRS scores based on the 108 identified variants were broken down into biological systems such as calcium signalling, neurodevelopment, and glutamatergic neurotransmission, findings of volume changes were negative across the brain (Van der Auwera et al. 2017). Further, there were no associations found between white matter tract measures FA and MD with a PRS based on the 108 loci (Voineskos et al. 2015), or a range of PRS (Reus et al. 2017). Of note, replicated findings show evidence for lower cortical gyrification in the inferior parietal lobes associated with a range of PRS (Liu et al. 2017). Global cortical thinning has also been associated with a range of higher PRS in individuals with schizophrenia (Neilson et al. 2017).

In a large study by French et al. (2015), a negative relationship was discovered between cannabis use and cortical thickness in adolescent boys with high PRS determined by the significant 108 loci. This relationship was replicated in three samples and was not present in any of the adolescent girls or the boys with low PRS, although a higher PRS in girls was associated with elevated cortical thinning. This finding demonstrates possible useful applications of PRS in elucidating neurobiological mechanisms of risk factors for schizophrenia development, such as cannabis use during adolescence (Manrique-Garcia et al. 2012).

There have been fewer functional neuroimaging studies involving PRS, but with more consistently positive results. A novel study by Erk et al. (2017) investigated schizophrenia risk PRS and its impact on brain activation during the five neurocognitive domains outlined by the RDoc in healthy controls using two thresholds from the PGC study—5×10^{-8} and 0.05. Findings showed activation of the perigenual anterior cingulate during an emotion recognition task, and posterior cingulate during a theory of mind task, which were both associated with PRS.

Altered activation and inefficiency of the dorsolateral and middle superior PFC during WM related tasks has been found to be related to a variety of differently chosen PRS (Walton et al. 2013, 2014; Kauppi et al. 2014). A recent study also showed a positive association between a PRS created from 418 genes from the CREBS and BDNF family, with deviation in the variability in resting-state networks and functional network connectivity predominantly related to the thalamus, parahippocampal gyrus, visual, and/or sensorimotor areas compared to cohort-common patterns (Chen et al. 2018).

Multiple studies have found a relationship between PRS and alterations in ventral striatal activity. The first examined a monetary incentive delay task and found that higher scores across a range of PRS thresholds were associated with lower IQ and striatal activity, indicating that it may be related to different reward processing in higher risk individuals (Lancaster et al. 2016b). The second study found increased BOLD signal in the ventral striatum, extended reward-related areas, and cortical networks, including posterior regions, occurred during a reversal learning task in individuals with a higher PRS thresholded at 0.05 (Lancaster et al. 2018).

These findings overall support a lack of genetic overlap between this disorder and subcortical volumes, but larger overlap with cognition and altered neural circuitry (Hubbard et al. 2016; Hagenaars et al. 2016). However, the success of studies focusing on specific variants and targeted PRS including variants previously implicated in structural abnormalities may indicate that a subgroup of variants are involved in structural changes related to risk, and that the use of more complex PRS dilute effects. Evidence points to the hypothesis that common genetic variants associated with schizophrenia are involved in altering cognition (especially emotion processing) and motivational circuitry predominantly, which may influence the volu-

metric abnormalities observed in schizophrenia. The varied findings may also be related to the fact that the relationships observed between neuroimaging phenotypes and a continuous PRS are not as linear as expected, especially in functional imaging (Birn and Bandettini 2005).

16.7 Successes and Failures of Collaborative Imaging Genetic Efforts

In the last decade, multiple large-scale consortiums have worked to combine impressive quantities of imaging and genetic data internationally into meta-analyses. One of the largest efforts has been by ENIGMA, which had as its initial aim to use GWAS to identify common variants underlying variation in brain structure, function, and connectivity. This work now extends to identifying factors that reliably affect brain features and can be used for individual prediction of risk and deviations from normal development (Thompson et al. 2014). Although individually common variants have small effects, collaborative efforts use the strategy of collecting large samples and increasing power to identify enough variants that, when aggregated, explain a substantial portion of imaging phenotype variance. This increase in power through meta-analysis can also be used to study diseased populations and build upon our knowledge of intermediate phenotypes to clarify mechanisms involved in how these abnormalities relate to the development of mental illnesses such as schizophrenia. Thus far, over 20 psychiatric, neurodegenerative and neurodevelopmental disorders have been studied as part of ENIGMA, and publications have followed from the largest structural MRI studies for multiple mental illnesses (Schmaal et al. 2015; Hibar et al. 2017; Boedhoe et al. 2017; Hoogman et al. 2017). Initiatives have also led to the identification of the first genome-wide variants associated with subcortical structures (Hibar et al. 2015, 2017; Stein et al. 2012). However, this large-scale approach has met with both successes and failures, and there are many challenges to offering insight into pathology related to schizophrenia.

Findings to date have shown that there is little overlap between GWAS identified risk variants for schizophrenia and those associated with subcortical volume (Hibar et al. 2015, 2017). A large population study by (Hibar et al. 2015), including both healthy and mentally ill individuals, examined ICV and seven subcortical volumes in 13,171 subjects of European ancestry, and a replication sample of 17,546. Findings showed significant and suggestive findings for ICV, hippocampus, putamen, amygdala and caudate, but not the nucleus accumbens, pallidum or thalamus. A single significant SNP rs2909457 is also associated with schizophrenia risk, and was found to be correlated with hippocampus volume. A similar correlation with a SNP in high LD emerged in a following study (Hibar et al. 2017). Contrary to what was expected based on changes commonly seen in schizophrenia (Adriano et al. 2012), hippocampal volume increased with increasing risk.

A study by Franke et al. (2016) examined the overlap between genetic variants related to these same structural measures and those associated with schizophrenia to further confirm null results. These results are perhaps even more surprising as the use of the same methodology has found large overlaps in common variants between schizophrenia and both bipolar disorder and major depressive disorder (Cross-Disorder Group of the PGC 2013a, b). Overall, converging evidence does not support the hypothesis that alterations in brain structure are causally associated with schizophrenia risk, or that there are pleiotropic effects of common variants on structural phenotypes and schizophrenia. Limited progress has forced the reassessment of the potential for this approach to assist with constructing new or improved hypotheses about how the brain is involved in the onset and course of schizophrenia.

Little overlap in associated common variants suggest that alternative hypotheses independent of genetic causes regarding structural abnormalities seen in schizophrenia may need to be considered. Other possible contributing factors are rare

mutations, epigenetics (Cariaga-Martinez and Alelú-Paz 2017), gene interactions, environmental interactions (Davis et al. 2016), course of illness (Mathalon et al. 2001), or treatments (Ho et al. 2011). More consistent findings of altered cognitive and behavioral alterations associated with common variants may be related to downstream effects or reverse causation of volume changes (Owens et al. 2012; Toulopoulou et al. 2015).

Alternatively, it is possible that the effect sizes of genetic overlap between brain structure and schizophrenia are quite small and that GWAS are either underpowered or methodology is insufficient to find results. The higher the number of participants in a study, the larger the power to discover variants contributing small effects that may be overshadowed by heterogeneity within the sample. This is supported by a more recent focused study with increased power that examined only the overlap between schizophrenia and subcortical structures genetic risk, and had positive findings in loci such as FOXO3 and ITIH4, associated with ICV, SLC4A10 and SPATS2L with the hippocampus, as well as DCC, and DLG2 with the putamen (Smeland et al. 2017). Additionally, the use of a newer method called partitioning-based heritability analysis demonstrated that schizophrenia risk variants significantly modulate normal variation in cortical thickness and surface area in multiple brain regions (Lee et al. 2016).

16.8 Combining Gene Expression, Risk Variants and Imaging Phenotypes

A similar approach to beginning with imaging phenotypes as continuous quantitative traits and determining genetic associations is to begin with gene expression and discover genetic variation contributing to changes. Variants that affect expression levels are considered expression quantitative trait loci (eQTL) and provide a possible mechanism by which common variants may influence imaging phenotypes and confer risk for schizophrenia. Many genes have altered expression in schizophrenia, and a significant portion of variants associated with schizophrenia (Schizophrenia Working Group of the Psychiatric Genomics Consortium 2014) have been found to be eQTL and to alter the expression of at least one gene (Richards et al. 2012; Fromer et al. 2016).

However, another aspect not commonly captured is the wide-ranging effects these risk variants sometimes have spatially across the brain. It is known that the majority of gene expression varies both by brain region and temporally across the lifespan, as well as that SNPs can impact expression (Kang et al. 2012). Post-mortem studies have shown that gene expression disturbances in schizophrenia patients exist across and vary by brain region (Horváth et al. 2011). Recent studies are beginning to highlight the importance of regional expression of specifically schizophrenia related risk genes associated with abnormalities observed in the brain that may improve understanding of why brain changes are concentrated in certain areas or along specific pathways in schizophrenia. This strategy also provides the opportunity to study the relationships between genetic risk and more complex imaging phenotypes, such as network connectivity.

In the same way that similar co-expression networks of multiple genes indicate a common regulatory pathway (Weirauch 2011), overlapping gene expression and brain connectivity networks may indicate common underlying mechanisms and influence. Further, areas where risk variants have increased expression may indicate increased influence on neural functioning of that region and greater effect on local imaging phenotypes.

With increasing accessibility through publically available resources such as the Allen Human Brain Atlas, BrainCloud, BrainSpan, and CommonMind Consortium (providing maps of gene specific transcription across the brain), it is possible to examine genetic risk with regionally specific gene expression patterns throughout the brain. Examining the spatial expression of schizophrenia risk variants together with brain abnormalities may provide insight into the complex relationships between them and the pathogenic mechanisms involved in psychosis development (French et al. 2015).

16.9 Structural and Functional Connectivity Overlapping with Networks of Gene Expression

A recent study by Romme et al. (2016) cross-correlated connectivity networks determined using diffusion-weight imaging with spatial expression of schizophrenia GWAS identified genes (Schizophrenia Working Group of the Psychiatric Genomics Consortium 2014) from post-mortem microarray data in the Allen Human Brain Atlas (Hawrylycz et al. 2012). Results showed that increased differences in structural connectivity between schizophrenia and healthy controls across the brain overlapped with areas of the cortex where there was heightened expression of risk genes. Further breakdown of schizophrenia risk genes into classes of function, as specified by PGC, showed that genes involved in neuronal calcium signaling (including CACNA1C) were most closely associated with connectivity differences. Additionally, findings were specific to schizophrenia and there was no association between expression of schizophrenia risk genes and structural connectivity in individuals with bipolar disorder. This differentiation between these illnesses may be key, particularly given the strong overlaps in genetic risk of approximately 65% (Cross-Disorder Group of the Psychiatric Genomics Consortium 2013a, b) in brain abnormalities and symptomology that exist.

As well as investigating previously associated genes found through GWAS of schizophrenia, Romme et al. (2016) linked novel genes, as well as supported previous findings, in a data driven approach examining all available gene expression networks and the most highly correlated with networks of altered connectivity in schizophrenia. Many of the identified top 100 and 500 genes (the second most highly correlated being C4A) have already been associated with psychiatric disorders, and investigation of the remaining genes may assist with the identification of risk genes involved in pathophysiology specifically related to altered neural connectivity observed in schizophrenia.

Another study examined the relationship between white matter network organization and local gene expression across age in schizophrenia (Powell et al. 2017). Declining network integrity across age was delayed in individuals with schizophrenia compared to controls. Additionally, when the spatial expression of six top schizophrenia associated genes were examined, DISC1, DRD2, DTNBP1, and GRM3 were associated with age-dependent changes in white matter network modularity, with DISC1 additionally associated with local efficiency. There were no significant associations between white matter network measures and regional expression of the COMT and BDNF genes.

A study by Pergola et al. (2017) focused on the commonly implicated dopamine molecular pathway and DRD2 gene expression across the PFC. SNPs associated with co-expression of specifically the D2 long dopamine receptor were identified to create a Polygenic Co-expression Index (PCI). An increased PCI was found to predict working memory performance, greater BOLD signal in the PFC indicating inefficiency during this task, as well as a better clinical course. This approach demonstrates that investigating gene co-expression can be used to investigating gene co-expression can be used to better understand the role of risk genes in biological pathways that relate to behavioral and clinical phenotypes.

There is also evidence that resting-state networks are heritable (Glahn et al. 2010; Fu et al. 2015), signifying that genetic risk associated with schizophrenia may underlie alterations observed in the disorder. Furthermore, resting-state functional connectivity networks correspond with networks of correlated gene expression, and polymorphisms in these identified genes, which alters resting-state connectivity in healthy adolescents (Richiardi et al. 2015). It has also been shown that spatial patterns of gene expression have a high correspondence with cortico-striatal pathways involved in limbic and somatomotor functional networks (Anderson et al. 2018), which are pathways strongly associated with schizophrenia pathology.

16.10 At Risk Youth and Discovering Predictors for Psychosis

Schizophrenia is considered a neurodevelopmental disorder involving altered neural maturation and connectivity (Insel 2010; Marenco and Weinberger 2000). Numerous studies have examined and found alterations in brain circuitry and functioning in youth at all stages of psychosis development, from subthreshold symptoms (Satterthwaite et al. 2016) to clinically high-risk groups and genetic high-risk groups (Fusar-Poli et al. 2012), to the emergence of first-episode psychosis. There is support that increased genetic risk based on family history increases risk of transition and is associated with symptom severity and with brain abnormalities (Fusar-Poli et al. 2015; Seidman et al. 2010).

Imaging-genetic studies in neurodevelopmental samples as well as adult samples provide the opportunity to study changes across the emergence of symptoms and answer the question of when, in addition to how, genetic factors confer risk by affecting brain structure and function. The early detection and treatment of psychosis at prodromal stages is an important and widely accepted goal to move towards reducing the burden of schizophrenia (Pettersson-Yeo et al. 2013). If biomarkers are identified, they can be integrated into predictive models to distinguish better high risk youth that will later transition to full psychosis or schizophrenia so that they can be targeted for preventative early interventions (Millan et al. 2016).

Despite this surge in studies examining high-risk youth, the majority of imaging-genetics studies focus on neuroimaging phenotypes and increased risk in the context of familial or genetic risk, with fewer studies addressing specifics in the heterogeneity of genetic vulnerability (Fusar-Poli et al. 2015). Additionally, there are challenges with methodology and reporting of studies aimed at predicting transition to psychosis in CHR (Studerus and Ramyead 2017). For example, a study reviewing brain abnormalities in genetic high-risk groups and clinical high-risk groups found that clinical high risk groups had more severe structural and functional differences, including abnormalities associated with transition to psychosis. This is most likely related to the higher symptom severity seen in this high-risk group (Smieskova et al. 2013).

A promising finding from multiple studies is the association of risk variants in the 5′ region of neuroregulin 1 (NRG1) and rates of transition to schizophrenia in high-risk psychosis groups. This gene is involved in regulating myelination processes (Ortega et al. 2012; Wood et al. 2009) and is important for cortico-cortical myelination during neurodevelopment (Chen et al. 2016). It has been marginally associated with total brain FA, and together with other genes involved in myelination, it is significantly associated with schizophrenia and FA, perhaps indicating that it works by affecting oligodendrocyte-expressed specific genes (Chavarria-siles et al. 2015).

Studies have also found a 100% transition rate in both genetic and clinical high-risk cohorts associated with the NRG1 rs6994992 SNP (Hall et al. 2006; Keri et al. 2009). Another larger study by Bousman et al. (2013) did not replicate these findings, but did discover that nearby rs4281084 and rs12155594 risk alleles increased the risk for transition. A recent follow-up imaging-genetics study by Bousman et al. (2018), looked at the neurobiological effect of having a high allelic risk load based on these identified SNPs in the NRG1 gene. Individuals who had an early age of onset and developed schizophrenia before the age of 26 had increased left and right ventricles. Further, all carriers of high risk alleles had reduced FA, elevated RA, and stable AD in the frontal cortex, but no differences in cortical thickness, gray matter volume, and surface area.

In another study, higher schizophrenia PRS has been associated with decreasing hippocampal volume in at-risk mental state youth, and with a higher rate of transition to first episode psychosis (Harrisberger et al. 2016).

Recent initiatives, such as the publically available Philadelphia Neurodevelopmental

Cohort (PNC), hold promise for improving our understanding of factors involved in psychosis risk. This large-scale population sample study began with just genetics data, but now has approximately 1600 participants aged 8–21 with multimodal neuroimaging, cognitive, and psychopathology data, with an enrichment for youth with psychosis spectrum symptoms. Further, a portion of the participants have data from multiple follow up assessments 2 years apart. Studies to date have shown structural and functional brain abnormalities associated with youth experiencing psychosis spectrum symptoms (Wolf et al. 2015; Satterthwaite et al. 2016). An investigation by Voineskos et al. (2015) examining the relationship between schizophrenia risk variants, cortical thickness, and white matter tract measures included PNC participants but showed negative findings. A recent paper by Cordova-Palomera et al. (2018) examined a wide range of PGR, as well as brain thickness, surface and volume in the PNC. A higher risk score was associated with reduced cortical surface area and thalamic volume. This study also found an apparent suppressing effect, in that altered brain features compensated for the effect of PGR on cognition. Although there are only a few PNC studies integrating imaging and genetics as of yet, this sample's large numbers and range of data present exciting possibilities for elucidating mechanisms associated with psychosis development in adolescence.

There is also accumulating evidence that genetic factors and epigenetic mechanisms are involved in hormonal responses causing brain changes during adolescent development, and that these are linked to underlying pathophysiological mechanisms of psychosis development (Trotman et al. 2013; Walker et al. 2013). Further work is needed to better understand the relationship between hormones and their role during this key neurodevelopmental period when symptoms being to emerge. Revealing these mechanisms may also explain sex differences in cognition and brain abnormalities occurring in schizophrenia in adulthood that may be tied to hormonal divergences that begin in adolescence (Mendrek and Mancini-Marïe 2016).

16.11 The Challenge of High Dimensionality of Imaging and Genetic Data

Mixed findings of genetic overlap between schizophrenia risk and brain structure, but replicated positive findings from studies examining individual SNPs and neuroimaging phenotypes indicate that the problem may lie in the methodology for discovering GWAS common variants, and not that there truly is no overlap in genetic underpinnings. There are a number of evolving statistical methods to address the challenge of the high-dimensionality of imaging and genetic data (Schork et al. 2016). In GWAS, each SNP is independently tested using regression models for association with a scalar measure such as clinical diagnosis. This results in huge numbers of pairwise univariate tests that need to have statistical corrections applied to reduce the prevalence of false positives. The number of tests increases when multiple neuroimaging phenotypes, especially voxel-wise measures, are investigated, and leads to reductions in power and elevated computational costs. Additionally, applied corrections may be too stringent, ignoring the possibility that SNPs may have high LD and that regions of imaging phenotypes such as cortical thickness, FA, and volume tend to be highly co-varied across the brain, and not actually independent. Alternative strategies such as controlling for false discovery rate (FDR) instead of family-wise error rates, or prioritizing genes based on ontology in combination with stratified corrections have been proposed (Patel et al. 2016).

Other approaches such as set-based association tests can reduce the number of comparisons, as well as detect small effects from rare variants that GWAS currently does not have the power to take into account. By looking at whether a group of variants collectively affect a phenotype, their accumulated effect may be large enough to be identified. Different set-based association tests are more appropriate depending on whether or not genetic variants within a set are heterogeneous or homogeneous in their effects (Lee et al. 2014). This approach has been successfully extended for analyses of gene-environment interactions on

neuroimaging phenotypes, taking into account both fixed and random effects (Wang et al. 2017). Bayesian approaches with mixed models have also been a sophisticated multivariate strategy to select variables and reduce dimensionality, while ensuring that variables are more likely to correspond to SNPs within the same gene and across different neuroimaging phenotypes (Greenlaw et al. 2016; Stingo et al. 2014; Chekouo et al. 2016). Parallel independent component analysis is also an option for a multivariate method to associate groups of common variants with neuroimaging phenotypes (Pearlson et al. 2015). Additionally, the use of machine learning is an important way forward with both approaches based on pre-selected risk variants and more data-driven analyses (Yang et al. 2010).

16.12 Other Limitations and Future Directions

Although, substantive progress has been made in understanding the pathology of schizophrenia and how risk is conferred genetically using imaging genetic studies, there are many limitations that need to be considered (Blokland et al. 2017). In general, there has been an overall lack of replication of many candidate findings and effect sizes in structural and functional imaging genetic studies (Button et al. 2013, Ioannidis from Thompson et al. 2014), including in the large meta-analyses that have been done by ENIGMA.

One of the reasons that there has been little success in linking imaging phenotypes such as subcortical structure to genetic risk for schizophrenia in meta-analyses may be that these simplistic phenotypes are not complex enough to capture relationships bridging genetic risk with a multifaceted illness such as schizophrenia. More promising progress may be made by examining networks of structure and function to represent the polygenic and clinical diversity of schizophrenia. Additionally, continuing to move towards combining multiple levels of data such as risk variants, gene expression, and more intricate brain features holds promise for disentangling convoluted causal mechanisms. Further, methodology is being developed to integrate factors such as gene-environment interactions and epistatic effects of genes into imaging genetic studies (Kang et al. 2015).

Some limitations on imaging genetic studies targeting a single or groups of variants often include small samples, inconsistencies choosing phenotypes, demographic differences, as well as a range of symptom severity, course of illness, comorbidities, medication confounds, and a publication bias that may lead to false positives (Nickl-Jockschat et al. 2015). However, smaller samples can provide the opportunity for more homogeneity to discern aspects of altered biological processes that affect subgroups of individuals with schizophrenia. In combination with larger studies, it is important to further dissect potentially meaningful differences in studies when findings are not uniform.

The GWAS and collaborative approach has and continues to contribute greatly to our understanding of genetic architecture. However, there are disadvantages and limitations to using simple phenotypes such as binary categorizations for cases and controls. This method relies on sample size to address heterogeneity within cases, as well as controls. It allows genetic variants with small effects to be identified, but it also forces the creation of national and sometimes international norms that may or may not exist. By grouping everyone together, signals from important risk factors that affect subgroups of the cases may be drowned out. This is important considering our knowledge of the heterogeneity in schizophrenia, as well as the effects from factors such as environment and ethnicity. It is becoming apparent that the same disorder, schizophrenia, can develop from a range of differently implicated genetic alterations and impaired biological systems, and that the key to moving towards meaningful understanding of this illness and the ability to aid in treatment is to acknowledge and accept these subtypes of pathophysiological mechanisms instead of studying the disorder as a whole. Moving forward we can take advantage of larger samples to find subgroups within meta-analyses, and instead of trying to remove the effect of influential factors, we can strive to integrate them meaningfully into the analytic models used.

There are also specific limitations associated with bringing together studies in large meta-analyses, such as the heterogeneity between samples in scanners, protocols, participant inclusion criteria, and recruitment location. Substantial work by groups such as ENIGMA are creating a shift towards standardized procedures of data collection and analysis to address these differences. A general challenge with collaborations though, is how to define accurate measurements and models that are both consistent and relevant across the studies being brought together. There are many confounds that interact with measurements and impact results. Additionally, many individuals have co-morbidities and potentially subtypes of illnesses that cause variation in their classification and inclusion in studies. As more information is gathered and modelling approaches are developed to take these variables and their complex interactions into account, predictive models relevant to an individual or cohort are likely to become more valuable in the variance they describe.

Another consideration is the timing of many studies in the context of brain maturation and development. Large changes in volume, cortical thickness, growth, and maturation occur across late childhood and adolescence (Sussman et al. 2016). Investigations using GWAS at earlier ages may better capture genetic underpinnings of structural function and development. The aspect of development across time is underutilized in imaging genetic studies, especially considering our knowledge of how temporally dependent gene expression, brain changes, and clinical presentation are. Studying younger samples may be particularly helpful for elucidating disease risk, as opposed to studying adults who may be more indicative of disease progression or course. The increasing number of large youth multimodal datasets such as the PNC hold promise for pursuing these key questions.

Additionally, longitudinal studies provide the opportunity to investigate timing of changes. Thus far, longitudinal imaging genetics findings in adults have varied results, although predominantly declines in gray matter are observed, but this may be partially explained by the genetic effect on variation (Olabi et al. 2011; Vita et al. 2012). A systematic review by Harari and Díaz-caneja (2017) uncovered the few studies analyzing the longitudinal structural changes associated with gene variants. Progressive brain changes were most commonly observed in frontal regions, with small or intermediate effect sizes. None of the findings were replicated, and for the two risk variants with multiple studies there were heterogeneous results, indicating that further work is needed for concrete conclusions.

A further limitation that may affect consistency of imaging genetic findings is that many studies were done with healthy controls, and not individuals with schizophrenia. Studying healthy samples has the advantage of minimizing confounding factors associated with clinical diagnoses. However, there is evidence that results can differ between these populations (Lett et al. 2013), and it is important to consider that effects might be observed only once vulnerability for schizophrenia development has progressed to full illness onset. Although there is support that disease risk lies along a continuum, there may still be a tipping point leading to illness onset and a cascade of risk mechanisms and emerging effects.

A final limitation of imaging genetic studies is that the use of MRI cannot capture whether genetic variants are influencing specific cell types within the brain, which may be contributing to a lessened signal strength for association with imaging phenotypes. The use of both imaging and genetics methods to study schizophrenia need to be interpreted within the context of their methodology and limitations.

16.13 Conclusion

As the field evolves rapidly in terms of technology, method development, collaborative initiatives, sample sizes, and statistical power, there is no doubt that new discoveries will continue to be made regarding the genetic risk and neural circuit disruptions underlying schizophrenia. Huge progress has been made that can inform new initiatives and redirect focus moving forward. A

recent project, the Adolescent Brain Cognitive Development (ABCD), is a massive longitudinal study with well characterized phenotyping and multimodal assessments of a population sample (Casey et al. 2018). This rigorous multi-site study includes over 11,000 American children ages 9–10 who will receive follow up assessments every year for the next 10 years. As a publically available resource, there is immense potential for improving our understanding of the development of mental illnesses, cognition, and overall neurodevelopment across adolescence including the effect of environmental and genetic influences.

Another opportunity is the integration of multiple data types, such as structural and functional imaging, clinical, cognitive, and genetic risk measures into models that can capture complex patterns across individuals. Further, clustering algorithms able to integrate these diverse data, such as Similarity Network Fusion (Wang et al. 2014), can be used to group participants into more biologically and functionally homogeneous groups in a way that is agnostic to diagnostic labels. These subgroups within schizophrenia or psychosis may be useful for developing and targeting treatments and interventions in a more personalized way that takes into account specific biological alterations and genetic risk, instead of just inferences from symptomology.

Summary

- Schizophrenia is highly heritable and has heterogeneous and polygenic contributions to risk.
- Studies integrating genetic and imaging approaches can improve our understanding of pathophysiology and aid in the identification of endophenotypes or intermediate biomarkers between genotype and disorder risk.
- Hypothesis driven studies focusing on single candidate genes complement data-driven GWAS that identify novel variants in improving our understanding of mechanisms underlying schizophrenia development.
- Polygenic risk scores that aggregate the effects of many risk variants increases the amount of explained variance and has potential for an accessible, inexpensive, and effective method for determining individualized risk.
- There has been a surge in collaborative efforts that increase sample sizes and power with meta-analyses, but results have been mixed in terms of overlapping with previous findings and hypotheses.
- Examining genetic variants that affect gene expression levels (eQTL) and regional gene expression across the brain provide a possible mechanism by which variants may influence imaging phenotypes, confer risk for schizophrenia, and provide insight into why brain changes are concentrated in certain areas or along specific pathways in schizophrenia.
- Studying youth at all stages of psychosis development provides the opportunity to evaluate changes across the emergence of symptoms and answer the question of when, in addition to how, genetic factors confer risk by affecting brain structure and function, in addition to aiding with early detection and treatment of psychosis at prodromal stages.
- Although imaging genetic studies face challenges such as the high dimensionality of data, lack of findings replication, and heterogeneity in samples, there has been progress in developing strategies to overcome these obstacles.

References

Adriano F, Caltagirone C, Spalletta G. Hippocampal volume reduction in first-episode and chronic schizophrenia. Neuroscientist. 2012;18(2):180–200.

Anderson KM, Holmes AJ, Krienen FM, Choi EY, Reinen JM, Yeo BTT. Gene expression links func-

tional networks across cortex and striatum. Nat Commun. 2018;9:1428. https://doi.org/10.1038/s41467-018-03811-x.

Arslan A. Genes, brains, and behavior: imaging genetics for neuropsychiatric disorders. J Neuropsychiatry Clin Neurosci. 2015;27:81–92. https://doi.org/10.1176/appi.neuropsych.13080185.

Arslan A. Progress in neuropsychopharmacology & biological psychiatry imaging genetics of schizophrenia in the post-GWAS era. Prog Neuropsychopharmacol Biol Psychiatry. 2018a;80:155–65. https://doi.org/10.1016/j.pnpbp.2017.06.018.

Arslan A. Mapping the schizophrenia genes by neuroimaging: the opportunities and the challenges. Int J Mol Sci. 2018b;19:E219. https://doi.org/10.3390/ijms19010219.

Berridge MJ. Calcium signalling and psychiatric disease: bipolar disorder and schizophrenia. Cell Tissue Res. 2014;357:477–92. https://doi.org/10.1007/s00441-014-1805-z.

Bigdeli TB, Ripke S, Bacanu SA, Lee SH, Wray NR, Gejman PV, et al. Genome-wide association study reveals greater polygenic loading for schizophrenia in cases with a family history of illness. Am J Med Genet. 2016;171B:276–89. https://doi.org/10.1002/ajmg.b.32402.

Birn RM, Bandettini PA. The effect of stimulus duty cycle and "off" duration on BOLD response linearity. Neuroimage. 2005;27:70–82. https://doi.org/10.1016/j.neuroimage.2005.03.040.

Blokland GA, Zubicaray GI, McMahon KL, Wright MJ. Genetic and environmental influences on neuroimaging phenotypes: a meta-analytical perspective on twin imaging studies. Twin Res Hum Genet. 2012;15:351–71. https://doi.org/10.1017/thg.2012.11.Genetic.

Blokland GAM, del Re EC, Mesholam-Gately RI, Jovicich J, Trampush JW, Keshavan MS, DeLisi LE, Walters JTR, Turner JA, Malhotra AK, Lencz T, Shenton ME, Voineskos AN, Rujescu D, Giegling I, Kahn RS, Roffman JL, Holt DJ, Ehrlich S, Kikinis Z, Dazzan P, Murray RM, Di Forti M, Lee J, Sim K, Lam M, Wolthusen RPF, de Zwarte SMC, Walton E, Cosgrove D, Kelly S, Maleki N, Osiecki L, Picchioni MM, Bramon E, Russo M, David AS, Mondelli V, Reinders AATS, Aurora Falcone M, Hartmann AM, Konte B, Morris DW, Gill M, Corvin AP, Cahn W, Ho NF, Liu JJ, Keefe RSE, Gollub RL, Manoach DS, Calhoun VD, Charles Schulz S, Sponheim SR, Goff DC, Buka SL, Cherkerzian S, Thermenos HW, Kubicki M, Nestor PG, Dickie EW, Vassos E, Ciufolini S, Marques TR, Crossley NA, Purcell SM, Smoller JW, van Haren NEM, Toulopoulou T, Donohoe G, Goldstein JM, Seidman LJ, McCarley RW, Petryshen TL. The genetics of endophenotypes of neurofunction to understand schizophrenia (GENUS) consortium: a collaborative cognitive and neuroimaging genetics project. Schizophr Res. 2018;195:306–17.

Boedhoe PS, Schmaal L, Abe Y, Ameis SH, Arnold PD, Batistuzzo MC, et al. Distinct subcortical volume alterations in pediatric and adult OCD: a worldwide meta- and mega-analysis. Am J Psychiatry. 2017;174:60–9. https://doi.org/10.1176/appi.ajp.2016.16020201.

Bogdan R, Salmeron BJ, Carey CE, Agrawal A, Calhoun VD, Garavan H, et al. Review imaging genetics and genomics in psychiatry: a critical review of progress and potential. Biol Psychiatry. 2017;82:165–75. https://doi.org/10.1016/j.biopsych.2016.12.030.

Bousman CA, Yung AR, Pantelis C, Ellis JA, Chavez RA, Nelson B, Lin A, Wood SJ, Amminger GP, Velakoulis D, Mcgorry PD, Everall IP, Foley DL. Effects of NRG1 and DAOA genetic variation on transition to psychosis in individuals at ultra-high risk for psychosis. Transl Psychiatry. 2013;3:e251. https://doi.org/10.1038/tp.2013.23.

Bousman CA, Cropley V, Klauser P, Hess JL, Pereira A, Idrizi R, Bruggemann J. Neuregulin-1 (NRG1) polymorphisms linked with psychosis transition are associated with enlarged lateral ventricles and white matter disruption in schizophrenia. Psychol Med. 2018;48:801–9. https://doi.org/10.1017/S0033291717002173.

Bray NJ, Hill MJ. Translating genetic risk loci into molecular risk mechanisms for schizophrenia. Schizophr Bull. 2015;42:5–8. https://doi.org/10.1093/schbul/sbv156.

Bustamante ML, Herrera L, Gaspar PA, Nieto R, Maturana A, Villar MJ, et al. Shifting the focus toward rare variants in schizophrenia to close the gap from genotype to phenotype. Am J Med Genet. 2017;174B:663–70. https://doi.org/10.1002/ajmg.b.32550.

Button KS, Ioannidis JP, Mokrysz C, Nosek BA, Flint J, Robinson ES, Munafò MR. Power failure: why small sample size undermines the reliability of neuroscience. Nat Rev Neurosci. 2013;14(5):365–76. https://doi.org/10.1038/nrn3475.

Cariaga-Martinez A, Alelú-Paz R. Rethinking the epigenetic framework to unravel the molecular pathology of schizophrenia. Int J Mol Sci. 2017;18(4):790. https://doi.org/10.3390/ijms18040790.

Carter CS, Bearden CE, Bullmore ET, Geschwind DH, Glahn DC, Gur RE, et al. Review enhancing the informativeness and replicability of imaging genomics studies. Biol Psychiatry. 2017;82:157–64. https://doi.org/10.1016/j.biopsych.2016.08.019.

Caseras X, Tansey K, Foley S, Linden D. Association between genetic risk scoring for schizophrenia and bipolar disorder with regional subcortical volumes. Transl Psychiatry. 2015;5:e692. https://doi.org/10.1038/tp.2015.195.

Casey BJ, Cannonier T, Conley MI, Cohen AO, Barch DM, Heitzeg MM, et al. The Adolescent Brain Cognitive Development (ABCD) study: imaging acquisition across 21 sites. Dev Cogn Neurosci. 2018;32:43–54. https://doi.org/10.1016/j.dcn.2018.03.001.

Cassoli JS, Guest PC, Malchow B, Schmitt A, Falkai P, Martins-de-Souza D. Disturbed macro-connectivity in schizophrenia linked to oligodendrocyte dysfunction: from structural findings to molecules. NPJ Schizophr. 2015;1:15034. https://doi.org/10.1038/npjschz.2015.34.

Chang H, Xiao X, Li M. The schizophrenia risk gene ZNF804A: clinical associations, biological mechanisms and neuronal functions. Mol Psychiatry. 2017;22(7):944–53.

Chavarria-siles I, White T, De Leeuw C, Goudriaan A, Lips E, Ehrlich S, et al. Myelination-related genes are associated with decreased white matter integrity in schizophrenia. Eur J Hum Genet. 2015;24(3):381–6. https://doi.org/10.1038/ejhg.2015.120.

Chekouo T, Stingo FC, Guindani M, Do K-A. A Bayesian predictive model for imaging genetics with application to schizophrenia. Ann Appl Stat. 2016;10(3):1547–71. https://doi.org/10.1214/16-AOAS948.

Chen S, Velardez MO, Warot X, Yu ZX, Miller SJ, Cros D, Corfas G. Neuregulin 1-erbB signaling is necessary for normal myeli- nation and sensory function. J Neurosci. 2016;26:3079–86. https://doi.org/10.1523/JNEUROSCI.3785-05.2006.

Chen J, Rashid B, Yu Q, Liu J, Lin D, Du Y. Variability in resting state network and functional network connectivity associated with schizophrenia genetic risk: a pilot study. Front Neurosci. 2018;12:114. https://doi.org/10.3389/fnins.2018.00114.

Cordova-Palomera A, Kaufmann T, Bettella F, Wang Y, Doan NT, Van Der Meer D, Westlye LT, et al. Effects of autozygosity and schizophrenia polygenic risk on cognitive and brain developmental trajectories. Eur J Hum Genet. 2018;26:1049–59. https://doi.org/10.1101/159939.

Cousijn H, Rijpkema M, Harteveld A, et al. Schizophrenia risk gene ZNF804A does not influence macroscopic brain structure: an MRI study in 892 volunteers. Mol Psychiatry. 2012;17(12):1155–7. https://doi.org/10.1038/mp.2011.181.

Cross-Disorder Group of the Psychiatric Genomics Consortium. Genetic relationship between five psychiatric disorders estimated from genome-wide ANPs. Nat Genet. 2013a;45:984–94. https://doi.org/10.1038/ng.2711.

Cross-Disorder Group of the Psychiatric Genomics Consortium. Identification of risk loci with shared effects on five major psychiatric disorders: a genome-wide analysis. Lancet. 2013b;381(9875):1371–9. https://doi.org/10.1016/S0140-6736(12)62129-1.

Davis J, Eyre H, Jacka FN, Dodd S, Dean O, McEwen S, et al. A review of vulnerability and risks for schizophrenia: beyond the two hit hypothesis. Neurosci Biobehav Rev. 2016;65:185–94. https://doi.org/10.1016/j.neubiorev.2016.03.017.

Deans MPJ, Raval P, Sellers JK, Gatford JFN, Halai S, Duarte RRR, et al. Psychosis risk candidate ZNF804A localizes to synapses and regulates neurite formation and dendritic spine structure. Biol Psychiatry. 2016;82(1):49–61. https://doi.org/10.1016/j.biopsych.2016.08.038.

Devor A, Andreassen O, Wang Y, Mäki-Marttunen T, Smeland O, Fan C-C, et al. Genetic evidence for role of integration of fast and slow neurotransmission in schizophrenia. Mol Psychiatry. 2017;22(6):792–801. https://doi.org/10.1038/mp.2017.33.

Dima D, Breen G. Polygenic risk scores in imaging genetics: usefulness and applications. J Psychopharmacol. 2015;29(8):867–71. https://doi.org/10.1177/0269881115584470.

Donohoe G, Rose E, Frodl T, et al. ZNF804A risk allele is associated with relatively intact gray matter volume in patients with schizophrenia. Neuroimage. 2011;54(3):2132–7. https://doi.org/10.1016/j.neuroimage.2010.09.089.

Erk S, Mohnke S, Ripke S, Lett TA, Veer IM, Wackerhagen C, et al. Functional neuroimaging effects of recently discovered genetic risk loci for schizophrenia and polygenic risk profile in five RDoC subdomains. Transl Psychiatry. 2017;27(1):e997. https://doi.org/10.1038/tp.2016.272.

Esslinger C, Walter H, Kirsch P, Erk S, Schnell K, Arnold C, et al. Neural mechanisms of a genome-wide supported psychosis variant. Science. 2009;324:605. https://doi.org/10.1126/science.1167768.

Esslinger C, Kirsch P, Haddad L, Mier D, Sauer C, Erk S, et al. NeuroImage cognitive state and connectivity effects of the genome-wide significant psychosis variant in ZNF804A. Neuroimage. 2011;54(3):2514–23. https://doi.org/10.1016/j.neuroimage.2010.10.012.

Farrell MS, Werge T, Sklar P, Owen MJ, Ophoff RA, O'Donovan MC, Corvin A, Cichon S, Sullivan PF. Evaluating historical candidate genes for schizophrenia. Mol Psychiatry. 2015;20:555–62. https://doi.org/10.1038/mp.2015.16.

Fernandes CP, Westlye LT, Giddaluru S, Christoforou A, Kauppi K, Adolfsson R, Nilsson LG, Nyberg L, Lundervold AJ, Reinvang I, Steen VM, Le Hellard S, Espeseth T. Lack of association of the rs1344706 ZNF804A variant with cognitive functions and DTI indices of white matter microstructure in two in- dependent healthy populations. Psychiatry Res. 2014;222(1–2):60–6. https://doi.org/10.1016/j.pscychresns.2014.02.009.

Flint J, Munafò MR. Candidate and non-candidate genes in behavior genetics. Curr Opin Neurobiol. 2013;23:57–61. https://doi.org/10.1016/j.conb.2012.07.005.

Franke B, Stein JL, Ripke S, Anttila V, Hibar DP, van Hulzen KJ, et al. Genetic influences on schizophrenia and subcortical brain volumes: large-scale proof of concept. Nat Neurosci. 2016;19:420–31. https://doi.org/10.1038/nn.4228.

French L, Gray C, Leonard G, et al. Early cannabis use, polygenic risk score for schizophrenia and brain maturation in adolescence. JAMA Psychiat. 2015;72:1002–11. https://doi.org/10.1001/jamapsychiatry.2015.1131.

Fromer M, Roussos P, Sieberts SK, Johnson JS, Kavanagh DH, Perumal TM, et al. Gene expression elucidates functional impact of polygenic risk for schizophrenia. Nat Neurosci. 2016;19(11):1442–53. https://doi.org/10.1038/nn.4399.

Fu Y, Ma Z, Hamilton C, Liang Z, Hou X, Ma X, et al. Genetic influences on resting-state functional networks: a twin study. Hum Brain Mapp. 2015;36:3959–72. https://doi.org/10.1002/hbm.22890.

Fusar-Poli P, Mcguire P, Borgwardt S. Mapping prodromal psychosis: a critical review of neuroimaging studies. Eur Psychiatry. 2012;27(3):181–91. https://doi.org/10.1016/j.eurpsy.2011.06.006.

Fusar-Poli P, Borgwardt S, Bechdolf A, Addington J, Riecher-Rössler A, Schultze-Lutter F, et al. The psychosis high-risk state: a comprehensive state-of-the-art review. JAMA Psychiat. 2015;70(1):107–20. https://doi.org/10.1001/jamapsychiatry.2013.269.The.

Germine L, Robinson EB, Smoller JW, Calkins ME, Moore TM, Hakonarson H, et al. Association between polygenic risk for schizophrenia, neurocognition and social cognition across development. Transl Psychiatry. 2016;6(10):e924–7. https://doi.org/10.1038/tp.2016.147.

Giaroli G, Bass N, Strydom A, Rantell K, McQuillin A. Does rare matter? Copy number variants at 16p11.2 and the risk of psychosis: a systematic review of literature and meta-analysis. Schizophr Res. 2014;159:340–6. https://doi.org/10.1016/j.schres.2014.09.025.

Girgenti MJ, LoTurco JJ, Maher BJ. ZNF804a regulates expression of the schizophrenia-associated genes PRSS16, COMT, PDE4B, and DRD2. PLoS One. 2012;7(2):e32404. https://doi.org/10.1371/journal.pone.0032404.

Glahn DC, Winkler A, Kochunov P, Almasy L, Duggirala R, Carless M, et al. Genetic control over the resting brain. Proc Natl Acad Sci U S A. 2010;107:1223–8. https://doi.org/10.1073/pnas.0909969107.

Gonzalez-Castro TB, Hernandez-Diaz Y, Juarez-Rojop IE, Lopez-Narvaez ML, Tovilla-Zarate CA, Fresan A. The role of a catechol-O-methyltransferase (COMT) Val158Met genetic polymorphism in schizophrenia: A systematic review and updated meta-analysis on 32,816 subjects. Neuromolecular Med. 2016;18:216–23. https://doi.org/10.1007/s12017-016-8392-z.

Greenlaw K, Szefer E, Graham J, Lesperance M, Nathoo FS. A Bayesian group sparse multi-task regression model for imaging genetics arXiv: 1605. 02234v2 [stat. ME]; 2016.

Gurung R, Prata DP. What is the impact of genome-wide supported risk variants for schizophrenia and bipolar disorder on brain structure and function? A systematic review. Psychol Med. 2015;45(12):2461–80. https://doi.org/10.1017/S0033291715000537.

Hagenaars SP, Harris SE, Davies G, et al. Shared genetic aetiology between cognitive functions and physical and mental health in UK biobank (N = 112 151) and 24 GWAS consortia. Mol Psychiatry. 2016;21:1624–32. https://doi.org/10.1038/mp.2015.225.

Hall J, Whalley HC, Job DE, Baig BJ, Mcintosh AM, Evans KL, Thomson PA, Porteous DJ, Cunningham-Owens DG, Johnstone EC, Lawrie SM. A neuregulin 1 variant associated with abnormal cortical function and psychotic symptoms. Nat Neurosci. 2006;9:1477–8. https://doi.org/10.1038/nn1795.

Hall J, Trent S, Thomas KL, O'Donovan MC, Owen MJ. Genetic risk for schizophrenia: convergence on synaptic pathways involved in plasticity. Biol Psychiatry. 2015;77:52–8. https://doi.org/10.1016/j.biopsych.2014.07.011.

Harari JH, Díaz-caneja CM. The association between gene variants and longitudinal structural brain changes in psychosis: a systematic review of longitudinal neuroimaging genetics studies. NPJ Schizophr. 2017;3:40. https://doi.org/10.1038/s41537-017-0036-2.

Hariri AR, Mattay VS, Tessitore A, et al. Serotonin transporter genetic variation and the response of the human amygdala. Science. 2002;297:400–3. https://doi.org/10.1126/science.1071829.

Harrisberger F, Smieskova R, Schmidt A, Lenz C, Walter A, Wittfeld K. Neuroscience and biobehavioral reviews BDNF Val66Met polymorphism and hippocampal volume in neuropsychiatric disorders: a systematic review and meta-analysis. Neurosci Biobehav Rev. 2015;55:107–18. https://doi.org/10.1016/j.neubiorev.2015.04.017.

Harrisberger F, Smieskova R, Vogler C, et al. Impact of polygenic schizophrenia-related risk and hippocampal volumes on the onset of psychosis. Transl Psychiatry. 2016;6(8):e868. https://doi.org/10.1038/tp.2016.143.

Harrison PJ. Recent genetic findings in schizophrenia and their therapeutic relevance. J Psychopharmacol. 2015;29(2):85–96. https://doi.org/10.1177/0269881114553647.

Hashimoto R, Ohi K, Yamamori H, Yasuda Y, Fujimoto M. Imaging genetics and psychiatric disorders. Curr Mol Med. 2015;15(2):168–75.

Hawrylycz M, Lein E, Guillozet-Bongaarts A, Shen E, Ng L, Miller J, et al. An anatomically comprehensive atlas of the adult human brain transcriptome. Nature. 2012;489:391–9. https://doi.org/10.1038/nature11405.

Hibar DP, Stein JL, Renteria ME, Arias-Vasquez A, Desrivières S, Jahanshad N, Toro R, Wittfeld K, Abramovic L, Andersson M, Aribisala BS, Armstrong NJ, Bernard M, Bohlken MM, Boks MP, Bralten J, Brown AA, Mallar Chakravarty M, Chen Q, Ching CRK, Cuellar-Partida G, den Braber A, Giddaluru S, Goldman AL, Grimm O, Guadalupe T, Hass J, Woldehawariat G, Holmes AJ, Hoogman M, Janowitz D, Jia T, Kim S, Klein M, Kraemer B, Lee PH, Olde Loohuis LM, Luciano M, Macare C, Mather KA, Mattheisen M, Milaneschi Y, Nho K, Papmeyer M, Ramasamy A, Risacher SL, Roiz-Santiañez R, Rose EJ, Salami A, Sämann PG, Schmaal L, Schork AJ, Shin J, Strike LT, Teumer A, van Donkelaar MMJ, van Eijk KR, Walters RK, Westlye LT, Whelan CD, Winkler AM, Zwiers MP, Alhusaini S, Athanasiu L, Ehrlich S, Hakobjan MMH, Hartberg CB, Haukvik UK, Heister AJGAM, Hoehn D, Kasperaviciute D, Liewald DCM, Lopez LM, Makkinje RRR, Matarin M, Naber MAM, McKay DR, Needham M, Nugent AC, Pütz B, Royle NA, Shen L, Sprooten E, Trabzuni D, van der Marel SSL, van Hulzen KJE, Walton E, Wolf C, Almasy L, Ames D, Arepalli S, Assareh AA, Bastin ME, Brodaty H, Bulayeva KB, Carless MA, Cichon S, Corvin A, Curran JE, Czisch M, de Zubicaray GI, Dillman A,

Duggirala R, Dyer TD, Erk S, Fedko IO, Ferrucci L, Foroud TM, Fox PT, Fukunaga M, Gibbs JR, Göring HHH, Green RC, Guelfi S, Hansell NK, Hartman CA, Hegenscheid K, Heinz A, Hernandez DG, Heslenfeld DJ, Hoekstra PJ, Holsboer F, Homuth G, Hottenga J-J, Ikeda M, Jack CR, Jenkinson M, Johnson R, Kanai R, Keil M, Kent JW, Kochunov P, Kwok JB, Lawrie SM, Liu X, Longo DL, McMahon KL, Meisenzahl E, Melle I, Mohnke S, Montgomery GW, Mostert JC, Mühleisen TW, Nalls MA, Nichols TE, Nilsson LG, Nöthen MM, Ohi K, Olvera RL, Perez-Iglesias R, Pike GB, Potkin SG, Reinvang I, Reppermund S, Rietschel M, Romanczuk-Seiferth N, Rosen GD, Rujescu D, Schnell K, Schofield PR, Smith C, Steen VM, Sussmann JE, Thalamuthu A, Toga AW, Traynor BJ, Troncoso J, Turner JA, Valdés Hernández MC, van't Ent D, van der Brug M, van der Wee NJA, van Tol M-J, Veltman DJ, Wassink TH, Westman E, Zielke RH, Zonderman AB, Ashbrook DG, Hager R, Lu L, McMahon FJ, Morris DW, Williams RW, Brunner HG, Buckner RL, Buitelaar JK, Cahn W, Calhoun VD, Cavalleri GL, Crespo-Facorro B, Dale AM, Davies GE, Delanty N, Depondt C, Djurovic S, Drevets WC, Espeseth T, Gollub RL, Ho B-C, Hoffmann W, Hosten N, Kahn RS, Le Hellard S, Meyer-Lindenberg A, Müller-Myhsok B, Nauck M, Nyberg L, Pandolfo M, Penninx BWJH, Roffman JL, Sisodiya SM, Smoller JW, van Bokhoven H, van Haren NEM, Völzke H, Walter H, Weiner MW, Wen W, White T, Agartz I, Andreassen OA, Blangero J, Boomsma DI, Brouwer RM, Cannon DM, Cookson MR, de Geus EJC, Deary IJ, Donohoe G, Fernández G, Fisher SE, Francks C, Glahn DC, Grabe HJ, Gruber O, Hardy J, Hashimoto R, Hulshoff Pol HE, Jönsson EG, Kloszewska I, Lovestone S, Mattay VS, Mecocci P, McDonald C, McIntosh AM, Ophoff RA, Paus T, Pausova Z, Ryten M, Sachdev PS, Saykin AJ, Simmons A, Singleton A, Soininen H, Wardlaw JM, Weale ME, Weinberger DR, Adams HHH, Launer LJ, Seiler S, Schmidt R, Chauhan G, Satizabal CL, Becker JT, Yanek L, van der Lee SJ, Ebling M, Fischl B, Longstreth WT, Greve D, Schmidt H, Nyquist P, Vinke LN, van Duijn CM, Xue L, Mazoyer B, Bis JC, Gudnason V, Seshadri S, Ikram MA, Martin NG, Wright MJ, Schumann G, Franke B, Thompson PM, Medland SE. Common genetic variants influence human subcortical brain structures. Nature. 2015;520(7546):224–9.

Hibar DP, Adams HHH, Jahanshad N, Chauhan G, Stein JL, Hofer E, et al. Novel genetic loci associated with hippocampal volume. Nat Commun. 2017;8:13624. https://doi.org/10.1038/ncomms13624.

Hill MJ, Bray NJ. Evidence that schizophrenia risk variation in the ZNF804A gene exerts its effects during fetal brain development. Am J Psychiatry. 2012;169:1301–8. https://doi.org/10.1176/appi.aip.2012.11121845.

Hill MJ, Jeffries AR, Dobson RJ, Price J, Bray NJ. Knockdown of the psychosis susceptibility gene ZNF804A alters expression of genes involved in cell adhesion. Hum Mol Genet. 2012;21(5):1018–24. https://doi.org/10.1093/hmg/ddr532.

Ho BC, Andreasen NC, Ziebell S, Pierson R, Magnotta V. Long-term antipsychotic treatment and brain volumes: a longitudinal study of first-episode schizophrenia. Arch Gen Psychiatry. 2011;68:128–37. https://doi.org/10.1001/archgenpsychiatry.2010.199.

Hong CJ, Liou YJ, Tsai SJ. Effects of BDNF polymorphisms on brain function and behavior in health and disease. Brain Res Bull. 2011;86:287–97. https://doi.org/10.1016/j.brainresbull.2011.08.019.

Hoogman M, Bralten J, Hibar DP, Mennes M, Zwiers MP, Schweren LS, van Hulzen KJ, Medland SE, Shumskaya E, Jahanshad N, et al. Subcortical brain volume differences of participants with ADHD across the lifespan: an ENIGMA collaboration. Lancet Psychiatry. 2017;4:310–9. https://doi.org/10.1016/S2215-0366(17)30049-4.

Horváth S, Janka Z, Mirnics K. Analyzing schizophrenia by DNA microarrays. Biol Psychiatry. 2011;69:157–62. https://doi.org/10.1016/j.biopysch.2010.07.017.

Howes OD, Mccutcheon R. Inflammation and the neural diathesis-stress hypothesis of schizophrenia: a reconceptualization. Transl Psychiatry. 2017;7(2):e1024–11. https://doi.org/10.1038/tp.2016.278.

Howes OD, McCutcheon R, Owen MJ, Murray R. The role of genes, stress and dopamine in the development of schizophrenia. Biol Psychiatry. 2017;81(1):9–20. https://doi.org/10.1016/j.biopsych.2016.07.014.

Hubbard L, Tansey KE, Rai D, et al. Evidence of common genetic overlap between schizophrenia and cognition. Schizophr Bull. 2016;42:832–42. https://doi.org/10.1093/schbul/sbv168.

Ikeda M, Aleksic B, Kinoshita Y, Okochi T, Kawashima K, Kushima I, et al. Genome-wide association study of schizophrenia in a Japanese population. Biol Psychiatry. 2011;69:472–8. https://doi.org/10.1016/j.biopsych.2010.07.010.

Ikuta T, Peters BD, Guha S, John M, Karlsgodt KH, Lencz T, et al. A schizophrenia risk gene, ZNF804A, is associated with brain white matter microstructure. Schizophr Res. 2014;155(1–3):15–20. https://doi.org/10.1016/j.schres.2014.03.001.

Insel TR. Rethinking schizophrenia. Nature. 2010;468:187–93.

Jansen AG, Mous SE, White T, Posthuma D, Polderman TJ. What twin studies tell us about the heritability of brain development, morphology, and function: a review. Neuropsychol Rev. 2015;25:27–46.

Kang HJ, et al. Spatio-temporal transcriptome of the human brain. Nature. 2012;478:483–9.

Kang M, Zhang C, Chun H-W, Ding C, Liu C, Gao J. eQTL epistasis: detecting epistatic effects and inferring hierarchical relationships of genes in biological pathways. Bioinformatics. 2015;31(5):656–64.

Kauppi K, Westlye LT, Tesli M, et al. Polygenic risk for schiz- ophrenia associated with working memory-related prefrontal brain activation in patients with schizophrenia and healthy controls. Schizophr Bull. 2014;41:736–43.

Keri S, Kiss I, Kelemen O. Effects of a neuregulin 1 variant on conversion to schizophrenia and schizophreni-

form disorder in people at high risk for psychosis. Mol Psychiatry. 2009;14:118–9.

Kuswanto CN, Sum MY, Qiu A, Sitoh Y, Liu J, Sim K. The impact of genome wide supported MicroRNA- 137 (MIR137) risk variants on frontal and striatal White matter integrity, neurocognitive functioning, and negative symptoms in schizophrenia. Am J Med Genet B Neuropsychiatr Genet. 2015;168B(5):317–26. https://doi.org/10.1002/ajmg.b.32314.

Lancaster T, Doherty J, Linden DE, Hall J. Imaging genetics of schizophrenia. In: Bigos KL, Hariri AR, Weinberger DR, editors. Neuroimaging genetics: principles and practices. Oxford, New York: Oxford University Press; 2016a.

Lancaster TM, Ihssen N, Brindley LM, et al. Associations between polygenic risk for schizophrenia and brain function during probabilistic learning in healthy individuals. Hum Brain Mapp. 2016b;37:491–500.

Lancaster TM, Dimitriadis SL, Tansey KE, Perry G, Ihssen N, Jones DK, et al. Structural and functional neuroimaging of polygenic risk for schizophrenia: a recall-by-genotype—based approach. Schizophr Bull. 2018;(April):1–3. https://doi.org/10.1093/schbul/sby037.

Lee S, Abecasis GR, Boehnke M, Lin X. Rare-variant association analysis: study designs and statistical tests. Am J Hum Genet. 2014;95:5–23. https://doi.org/10.1016/j.ajhg.2014.06.009.

Lee PH, Baker JT, Holmes AJ, Jahanshad N, Ge T, Jung J, et al. Partitioning heritability analysis reveals a shared genetic basis of brain anatomy and schizophrenia. 2016;(August):1680–9. https://doi.org/10.1038/mp.2016.164.

Lett TA, Chakavarty MM, Felsky D, Brandl EJ, Tiwari AK, Gonçalves VF, Rajji TK, Daskalakis ZJ, Meltzer HY, Lieberman JA, Lerch JP, Mulsant BH, Kennedy JL, Voineskos AN. The genome-wide supported microRNA-137 variant predicts phenotypic heterogeneity within schizophrenia. Mol Psychiatry. 2013;18(4):443–50.

Li M, Huang L, Wang J, Su B, Luo X-J. No association between schizophrenia susceptibility variants and macroscopic structural brain volume variation in healthy subjects. Am J Med Genet B Neuropsychiatr Genet. 2015;171B(2):160–8.

Lidow MS. Calcium signaling dysfunction in schizophrenia: a unifying approach. Brain Res Brain Res Rev. 2003;43:70–84.

Liu B, Zhang X, Cui Y, Qin W, Tao Y, Li J. Polygenic risk for schizophrenia influences cortical gyrification in 2 independent general populations. Schizophr Bull. 2017;43(3):673–80. https://doi.org/10.1093/schbul/sbw051.

Luykx JJ, Broersen JL, Leeuw MD. Neuroscience and biobehavioral reviews the DRD2 rs1076560 polymorphism and schizophrenia-related intermediate phenotypes: a systematic review and meta-analysis. Neurosci Biobehav Rev. 2017;74:214–24. https://doi.org/10.1016/j.neubiorev.2017.01.006.

Mallas E, Carletti F, Chaddock CA, Kalidindi S, Bramon E, Murray R, Barker GJ (2017) The impact of CACNA1C gene, and its epistasis with ZNF804A, on white matter microstructure in health, schizophrenia and bipolar disorder, vol 1, pp. 479–488. https://doi.org/10.1111/gbb.12355.

Manrique-Garcia E, Zammit S, Dalman C, Hemmingsson T, Andreasson S, Allebeck P. Cannabis, schizophrenia and other non-affective psychoses: 35 years of follow-up of a population-based cohort. Psychol Med. 2012;42(6):1321–8.

Marenco S, Weinberger DR. The neurodevelopmental hypothesis of schizophrenia: following a trail of evidence from cradle to grave. Dev Psychopathol. 2000;12:501–27.

Mathalon DH, Sullivan EV, Lim KO, Pfefferbaum A. Progres- sive brain volume changes and the clinical course of schizophrenia in men: a longitudinal magnetic resonance imaging study. Arch Gen Psychiatry. 2001;58:148–57.

McGrath J, Saha S, Chant D, Welham J. Schizophrenia: a concise overview of incidence, prevalence, and mortality. Epidemiol Rev. 2008;30:67–76.

Meltzer HY, Stahl SM. The dopamine hypothesis of schizophrenia: a review. Schizophrenia bulletin. Bethesda: National Institute of Mental Health; 1976. https://doi.org/10.1093/schbul/2.1.19.

Mendrek A, Mancini-Marïe A. Sex/gender differences in the brain and cognition in schizophrenia. Neurosci Biobehav Rev. 2016;67:57–78. https://doi.org/10.1016/j.neubiorev.2015.10.013.

Meyer-Lindenberg A. Imaging genetics of schizophrenia. Transl Res. 2010:449–56.

Millan MJ, Andrieux A, Bartzokis G, Cadenhead K, Dazzan P. Altering the course of schizophrenia: progress and perspectives. Nat Publ Group. 2016;15(7):485–515. https://doi.org/10.1038/nrd.2016.28.

Moghaddam B, Javitt D. From revolution to evolution: the glutamate hypothesis of schizophrenia and its implication for treatment. Neuropsychopharmacology. 2012;37:4–15.

Mohnke S, Erk S, Schnell K, Schutz C, Romanczuk-Seiferth N, Grimm O, et al. Further evidence for the impact of a genome-wide-supported psychosis risk variant in ZNF804A on the Theory of Mind Network. Neuropsychopharmacology. 2014;39:1196–205.

Mulle JG. The 3q29 deletion confers >40-fold increase in risk for schizophrenia. Mol Psychiatry. 2015;20:1028–9.

Murphy SE, Norbury R, Godlewska BR, Cowen PJ, Mannie ZM, Harmer CJ, et al. The effect of the serotonin transporter polymorphism (5-HTTLPR) on amygdala function: a meta-analysis. Mol Psychiatry. 2013;18:512–20.

Nakazawa K, Zsiros V, Jiang Z, Nakao K, Kolata S, Zhang S, et al. GABAergic interneuron origin of schizophrenia pathophysiology. Neuropharmacology. 2012;62:1574–83.

Neilson E, Bois C, Gibson J, Duff B, Watson A, Roberts N, et al. Effects of environmental risks and polygenic loading for schizophrenia on cortical thickness. Schizophr Res. 2017;184:128–36. https://doi.org/10.1016/j.schres.2016.12.011.

Oertel-knöchel V, Lancaster TM, Knöchel C, Stäblein M, Storchak H, Reinke B, et al. Clinical Schizophrenia risk variants modulate white matter volume across the psychosis spectrum: evidence from two independent cohorts YNICL. Neuroimage. 2015;7:764–70. https://doi.org/10.1016/j.nicl.2015.03.005.

Ohi K, Hashimoto R, Ikeda M, et al. Genetic risk variants of schizophrenia associated with left superior temporal gyrus volume. Cortex. 2014;58:23–6.

Olabi B, et al. Are there progressive brain changes in schizophrenia? A meta-analysis of structural magnetic resonance imaging studies. Biol Psychiatr. 2011;70:88–96.

Ortega MC, Bribian A, Peregrin S, Gil MT, Marin O, de Castro F. Neuregulin-1/ErbB4 signaling controls the migration of oligodendrocyte precursor cells during development. Exp Neurol. 2012;235:610–20.

Owens SF, Picchioni MM, Ettinger U, et al. Prefrontal deviations in function but not volume are putative endophenotypes for schizophrenia. Brain. 2012;135:2231–44.

Papiol S, Mitjans M, Assogna F, et al. Polygenic determinants of white matter volume derived from GWAS lack reproducibility in a replicate sample. Transl Psychiatry. 2014;4:e362.

Papiol S, Popovic D, Keeser D, Hasan A, Degenhardt F, Rossner MJ, et al. Polygenic risk has an impact on the structural plasticity of hippocampal sub fi elds during aerobic exercise combined with cognitive remediation in multi-episode schizophrenia. Nat Publ Group. 2017;7(6):e1159. https://doi.org/10.1038/tp.2017.131.

Patel S, Park MTM, The Alzheimer's Disease Neuroimaging Initiative, Chakravarty MM, Knight J. Gene prioritization for imaging genetics studies using gene ontology and a stratified false discovery rate approach. Front Neuroinform. 2016;10:14. https://doi.org/10.3389/fninf.2016.00014.

Pearlson GD, Calhoun VD, Liu J. An introductory review of parallel independent component analysis (p-ICA) and a guide to applying p- ICA to genetic data and imaging phenotypes to identify disease-associated biological pathways and systems in common complex disorders. Front Genet. 2015;6:276. https://doi.org/10.3389/fgene.2015.00276.

Pergola G, Di Carlo P, Ambrosio ED, Gelao B, Fazio L, Papalino M, et al. DRD2 co-expression network and a related polygenic index predict imaging, behavioral and clinical phenotypes linked to schizophrenia. Nat Publ Group. 2017;7(1):e1006–8. https://doi.org/10.1038/tp.2016.253.

Petersen RC, Aisen PS, Beckett LA, Donohue MC, Gamst AC, Harvey DJ, Jack CR, Jagust WJ, Shaw LM, Toga AW, Trojanowski JQ, Weiner MW. Alzheimer's disease neuroimaging initiative (ADNI): clinical characterization. Neurology. 2010;74(3):201–9.

Pettersson-Yeo W, Benetti S, Marquand AF, Dell'acqua F, Williams SC, Allen P, et al. Using genetic, cognitive and multi-modal neuroimaging data to identify ultra-high-risk and first-episode psychosis at the individual level. Psychol Med. 2013;43(12):2547–62. https://doi.org/10.1017/S003329171300024X.

Polderman TJ, Benyamin B, de Leeuw CA, Sullivan PF, van Bochoven A, Visscher PM, et al. Meta-analysis of the heritability of human traits based on fifty years of twin studies. Nat Genet. 2015;47:702–9.

Powell F, LoCastro E, Acosta D, Ahmed M, O'Donoghue S, Forde N, Cannon D, Scanlon C, Rao T, McDonald C, Raj A. Age-related changes in topological degradation of white matter networks and gene expression in chronic schizophrenia. Brain Connect. 2017;7(9):574–89.

Psaty BM, O'Donnell CJ, Gudnason V, et al. Cohorts for heart and aging research in genomic epidemiology (CHARGE) consortium: design of prospective meta-analyses of genome-wide association studies from 5 cohorts. Circ Cardiovasc Genet. 2009;2:73–80.

Raab K, Kirsch P, Mier D. Neuroscience and biobehavioral reviews understanding the impact of 5-HTTLPR, antidepressants, and acute tryptophan depletion on brain activation during facial emotion processing: a review of the imaging literature. Neurosci Biobehav Rev. 2016;71:176–97. https://doi.org/10.1016/j.neubiorev.2016.08.031.

Rasetti R, Weinberger DR. Intermediate phenotypes in psychiatric disorders. Curr Opin Genet Dev. 2011;21:340–8.

Reus LM, Shen X, Gibson J, et al. Association of polygenic risk for major psychiatric illness with subcortical vol- umes and white matter integrity in UK biobank. Sci Rep. 2017;7:42140.

Richards AL, Jones L, Moskvina V, Kirov G, Gejman PV, Levinson DF, et al. Schizophrenia susceptibility alleles are enriched for alleles that affect gene expression in adult human brain. Mol Psychiatry. 2012;17(2):193–201. https://doi.org/10.1038/mp.2011.11.

Richiardi J, Altmann A, Milazzo A-C, Chang C, Mallar Chakravarty M, Banaschewski T, et al. Correlated gene expression supports synchronous activity in brain networks. Science. 2015;348:1241–4. https://doi.org/10.1126/science.1255905.

Romme IAC, De Reus MA, Ophoff RA, Kahn RS, Van Den Heuvel MP. Connectome disconnectivity and cortical gene expression in patients with schizophrenia. Biol Psychiatry. 2016;81(6):495–502. https://doi.org/10.1016/j.biopsych.2016.07.012.

Satterthwaite TD, Wolf DH, Calkins ME, Vandekar SN, Erus G, Ruparel K, et al. Structural brain abnormalities in youth with psychosis spectrum symptoms. JAMA Psychiat. 2016;73(5):515–24. https://doi.org/10.1001/jamapsychiatry.2015.3463.

Schizophrenia Working Group of the Psychiatric Genomics Consortium. Biological insights from 108 schizophrenia- associated genetic loci. Nature. 2014;511:421–7.

Schmaal L, Veltman DJ, van Erp TG, Sämann PG, Frodl T, Jahanshad N, Loehrer E, Tiemeier H, Hofman A, Niessen WJ, Vernooij MW, Ikram MA, Wittfeld K, Grabe HJ, Block A, Hegenscheid K, Völzke H, Hoehn D, Czisch M, Lagopoulos J, Hatton SN, Hickie IB, Goya-Maldonado R, Krämer B, Gruber O, Couvy-Duchesne B, Rentería ME, Strike LT, Mills NT, de Zubicaray GI, McMahon KL, Medland

SE, Martin NG, Gillespie NA, Wright MJ, Hall GB, MacQueen GM, Frey EM, Carballedo A, van Velzen LS, van Tol MJ, van der Wee NJ, Veer IM, Walter H, Schnell K, Schramm E, Normann C, Schoepf D, Konrad C, Zurowski B, Nickson T, McIntosh AM, Papmeyer M, Whalley HC, Sussmann JE, Godlewska BR, Cowen PJ, Fischer FH, Rose M, Penninx BW, Thompson PM, Hibar DP. Subcortical brain alterations in major depressive disorder: findings from the ENIGMA major depressive disorder working group. Mol Psychiatry. 2015;21(6):806–12. https://doi.org/10.1038/mp.2015.69.

Schmitt A, Rujescu D, Gawlik M, Hasan A, Hashimoto K, Iceta S. Consensus paper of the WFSBP Task Force on Biological Markers: criteria for biomarkers and endophenotypes of schizophrenia part II: cognition, neuroimaging and genetics. World J Biol Psychiatry. 2016;17(6):406–28.

Schneider M, Debbané M, Bassett AS, Chow EWC, Fung WLA, van den Bree MBM, et al. Psychiatric disorders from childhood to adulthood in 22q11.2 deletion syndrome: results from the international consortium on brain and behavior in 22q11.2 deletion syndrome. Am J Psychiatry. 2014;171:627–39.

Schork AJ, Wang Y, Thompson WK, Dale AM, Andreassen OA. New statistical approaches exploit the polygenic architecture of schizophrenia—implications for the underlying neurobiology. Curr Opin Neurobiol. 2016;50:89–98. https://doi.org/10.1016/j.conb.2015.10.008.New.

Schumann G, Loth E, Banaschewski T, et al. The IMAGEN study: reinforcement-related behavior in normal brain function and psychopathology. Mol Psychiatry. 2010;15:1128–39.

Sebat J, Malhotra D. CNVs: harbinger of a rare variant revolution in psychiatric genetics. Cell. 2013;148:1223–41.

Sebat J, Levy DL, McCarthy SE. Rare structural variants in schizophrenia: one disorder, multiple mutations; one mutation, multiple disorders. Trends Genet. 2009;25:528–35.

Seidman LJ, Giuliano AJ, Meyer EC, Addington J, Cadenhead KS, Cannon TD, McGlashan TH, Perkins DO, Tsuang MT, Walker EF, Woods SW, Bearden CE, Christensen BK, Hawkins K, Heaton R, Keefe RS, Heinssen R, Cornblatt BA, North American Prodrome Longitudinal Study (NAPLS) Group. Neuropsychology of the prodrome to psychosis in the NAPLS consortium: relationship to family history and conversion to psychosis. Arch Gen Psychiatry. 2010;67(6):578–88.

Sekar A, Bialas AR, de Rivera H, Davis A, Hammond TR, Kamitaki N, et al. Schizophrenia risk from complex variation of complement component 4. Nature. 2016;530(7589):177–83. https://doi.org/10.1038/nature16549.

Smeland OB, Wang Y, Frei O, Li W, Hibar DP, Franke B, Bettella F, Witoelar A, Djurovic S, Chen CH, Thompson PM, Dale AM, Andreassen OA. Genetic overlap between schizophrenia and volumes of hippocampus, putamen, and intracranial volume indicates shared molecular genetic mechanisms. Schizophr Bull. 2017;sbx148. https://doi.org/10.1093/schbul/sbx148

Smieskova R, Marmy J, Schmidt A, Bendfeldt K, Walter M, Lang UE. Do subjects at clinical high risk for psychosis differ from those with a genetic high risk?—a systematic review of structural and functional brain abnormalities; 2013. pp. 467–481.

Sprooten E, McIntosh AM, Lawrie SM, et al. An investigation of a genomewide supported psychosis variant in ZNF804A and white matter integrity in the human brain. Magn Reson Imaging. 2012;30(10):1373–80.

Stedehouder J, Kushner SA. Myelination of parvalbumin interneurons: a parsimonious locus of pathophysiological convergence in schizophrenia. Mol Psychiatry. 2017;22(1):4–12. https://doi.org/10.1038/mp.2016.147.

Stein JL, Medland SE, Vasquez AA, et al. Identification of common variants associated with human hippocampal and intracranial volumes. Nat Genet. 2012;44:552–61.

Stingo FC, Guindani M, Vannucci M, Calhoun VD. An integrative Bayesian modeling approach to imaging genetics. J Am Stat Assoc. 2014;108(503):876–91. https://doi.org/10.1080/01621459.2013.804409.

Studerus E, Ramyead A. Prediction of transition to psychosis in patients with a clinical high risk for psychosis: a systematic review of methodology and reporting. 2017. pp. 1163–1178. https://doi.org/10.1017/S0033291716003494.

Sullivan PF, Kendler KS, Neale MC. Schizophrenia as a complex trait: evidence from a meta-analysis of twin studies. Arch Gen Psychiatry. 2003;60:1187–92. https://doi.org/10.1001/archpsyc.60.12.1187.

Sullivan PF, Daly MJ, O'Donovan M. Genetic architectures of psychiatric disorders: the emerging picture and its implications. Nat Rev Genet. 2012;13:537–51.

Sussman D, Leung RC, Chakravarty MM, Lerch JP, Taylor MJ. Developing human brain: age-related changes in cortical, subcortical, and cerebellar anatomy. Brain Behav. 2016;6(4):e00457. https://doi.org/10.1002/brb3.457.

Tao R, Cousijn H, Jaffe AE, Burnet PW, Edwards F, Eastwood SL, et al. Expression of ZNF804A in human brain and alterations in schizophrenia, bipolar disorder, and major depressive disorder: a novel transcript fetally regulated by the psychosis risk variant rs1344706. JAMA Psychiat. 2014;71:1112–20.

Terwisscha van Scheltinga AF, Bakker SC, van Haren NE, et al. Genetic schizophrenia risk variants jointly modulate total brain and white matter volume. Biol Psychiatry. 2013;73(6):525–31.

Thompson PM, Stein JL, Medland SE, Hibar DP, Vasquez AA, Renteria ME, Toro R, Jahanshad N, Schumann G, Franke B, Wright MJ, Martin NG, Agartz I, Alda M, Alhusaini S, Almasy L, Almeida J, Alpert K, Andreasen NC, Andreassen OA, Apostolova LG, Appel K, Armstrong NJ, Aribisala B, Bastin ME, Bauer M, Bearden CE, Bergmann Ø, Binder EB, Blangero J, Bockholt HJ, Bøen E, Bois C, Boomsma DI, Booth

T, Bowman IJ, Bralten J, Brouwer RM, Brunner HG, Brohawn DG, Buckner RL, Buitelaar J, Bulayeva K, Bustillo JR, Calhoun VD, Cannon DM, Cantor RM, Carless MA, Caseras X, Cavalleri GL, Mallar Chakravarty M, Chang KD, Ching CRK, Christoforou A, Cichon S, Clark VP, Conrod P, Coppola G, Crespo-Facorro B, Curran JE, Czisch M, Deary IJ, de Geus EJC, den Braber A, Delvecchio G, Depondt C, de Haan L, de Zubicaray GI, Dima D, Dimitrova R, Djurovic S, Dong H, Donohoe G, Duggirala R, Dyer TD, Ehrlich S, Ekman CJ, Elvsåshagen T, Emsell L, Erk S, Espeseth T, Fagerness J, Fears S, Fedko I, Fernández G, Fisher SE, Foroud T, Fox PT, Francks C, Frangou S, Frey EM, Frodl T, Frouin V, Garavan H, Giddaluru S, Glahn DC, Godlewska B, Goldstein RZ, Gollub RL, Grabe HJ, Grimm O, Gruber O, Guadalupe T, Gur RE, Gur RC, Göring HHH, Hagenaars S, Hajek T, Hall GB, Hall J, Hardy J, Hartman CA, Hass J, Hatton SN, Haukvik UK, Hegenscheid K, Heinz A, Hickie IB, Ho B-C, Hoehn D, Hoekstra PJ, Hollinshead M, Holmes AJ, Homuth G, Hoogman M, Hong LE, Hosten N, Hottenga J-J, Hulshoff Pol HE, Hwang KS, Jack CR, Jenkinson M, Johnston C, Jönsson EG, Kahn RS, Kasperaviciute D, Kelly S, Kim S, Kochunov P, Koenders L, Krämer B, Kwok JBJ, Lagopoulos J, Laje G, Landen M, Landman BA, Lauriello J, Lawrie SM, Lee PH, Le Hellard S, Lemaître H, Leonardo CD, Li C-s, Liberg B, Liewald DC, Liu X, Lopez LM, Loth E, Lourdusamy A, Luciano M, Macciardi F, Machielsen MWJ, MacQueen GM, Malt UF, Mandl R, Manoach DS, Martinot J-L, Matarin M, Mather KA, Mattheisen M, Mattingsdal M, Meyer-Lindenberg A, McDonald C, McIntosh AM, McMahon FJ, McMahon KL, Meisenzahl E, Melle I, Milaneschi Y, Mohnke S, Montgomery GW, Morris DW, Moses EK, Mueller BA, Maniega SM, Mühleisen TW, Müller-Myhsok B, Mwangi B, Nauck M, Nho K, Nichols TE, Nilsson L-G, Nugent AC, Nyberg L, Olvera RL, Oosterlaan J, Ophoff RA, Pandolfo M, Papalampropoulou-Tsiridou M, Papmeyer M, Paus T, Pausova Z, Pearlson GD, Penninx BW, Peterson CP, Pfennig A, Phillips M, Pike GB, Poline J-B, Potkin SG, Pütz B, Ramasamy A, Rasmussen J, Rietschel M, Rijpkema M, Risacher SL, Roffman JL, Roiz-Santiañez R, Romanczuk-Seiferth N, Rose EJ, Royle NA, Rujescu D, Ryten M, Sachdev PS, Salami A, Satterthwaite TD, Savitz J, Saykin AJ, Scanlon C, Schmaal L, Schnack HG, Schork AJ, Schulz SC, Schür R, Seidman L, Shen L, Shoemaker JM, Simmons A, Sisodiya SM, Smith C, Smoller JW, Soares JC, Sponheim SR, Sprooten E, Starr JM, Steen VM, Strakowski S, Strike L, Sussmann J, Sämann PG, Teumer A, Toga AW, Tordesillas-Gutierrez D, Trabzuni D, Trost S, Turner J, van den Heuvel M, van der Wee NJ, van Eijk K, van Erp TGM, van Haren NEM, van't Ent D, van Tol M-J, Valdés Hernández MC, Veltman DJ, Versace A, Völzke H, Walker R, Walter H, Wang L, Wardlaw JM, Weale ME, Weiner MW, Wen W, Westlye LT, Whalley HC, Whelan CD, White T, Winkler AM, Wittfeld K, Woldehawariat G, Wolf C, Zilles D, Zwiers MP, Thalamuthu A, Schofield PR, Freimer NB, Lawrence NS, Drevets W. The ENIGMA Consortium: large-scale collaborative analyses of neuroimaging and genetic data. Brain Imaging Behav. 2014;8(2):153–82.

Thurin K, Rasetti R, Sambataro F, Safrin M, Chen Q, Callicott JH, et al. Effects of ZNF804A on neurophysiologic measures of cognitive control. Mol Psychiatry. 2013;18:852–4.

Toulopoulou T, van Haren N, Zhang X, et al. Reciprocal causation models of cognitive vs volumetric cerebral intermediate phenotypes for schizophrenia in a pan-European twin cohort. Mol Psychiatry. 2015;20:1482.

Trotman HD, Holtzman CW, Ryan AT, Shapiro DI, MacDonald AN, Goulding SM, et al. The development of psychotic disorders in adolescence: a potential role for hormones. Horm Behav. 2013;64(2):411–9. https://doi.org/10.1016/j.yhbeh.2013.02.018.

Van der Auwera S, Wittfeld K, Homuth G, Teumer A, Hegenscheid K, Grabe HJ. No association between polygenic risk for schizophrenia and brain volume in the general population. Biol Psychiatry. 2015;78:e41–2.

Van der Auwera S, Wittfeld K, Shumskaya E, Bralten J, Zwiers MP, Onnink AMH, et al. Predicting brain structure in population-based samples with biologically informed genetic scores for schizophrenia; 2017. pp. 324–32. https://doi.org/10.1002/ajmg.b.32519.

Van Dongen J, Boomsma DI. The evolutionary paradox and the missing heritability of schizophrenia. Am J Med Genet B Neuropsychiatr Genet. 2013;162B:122–36.

Vita A, De Peri L, Deste G, Sacchetti E. Progressive loss of cortical gray matter in schizophrenia: a meta-analysis and meta-regression of longitudinal MRI studies. Transl Psychiatry. 2012;2:e190.

Voineskos AN, Lerch JP, Felsky D, et al. The ZNF804A gene: characterization of a novel neural risk mechanism for the major psychoses. (2011). Neuropsychopharmacology. 2011;36:1871–8.

Voineskos AN, Felsky D, Wheeler AL, Rotenberg DJ, Levesque M, Patel S, et al. Limited evidence for association of genome-wide schizophrenia risk variants on cortical neuroimaging phenotypes. Schizophr Bull. 2015:sbv180. https://doi.org/10.1093/schbul/sbv180.

Walker EF, Trotman HD, Goulding SM, et al. Developmental mechanisms in the prodrome to psychosis. Dev Psychopathol. 2013;25(4 Pt 2):1585–600. https://doi.org/10.1017/S0954579413000783.

Walter H, Schnell K, Erk S, Arnold C, Kirsch P, Esslinger C, et al. Effects of a genome-wide supported psychosis risk variant on neural activation during a theory-of-mind task. Mol Psychiatry. 2011;16:462–70.

Walton E, Turner J, Gollub RL, et al. Cumulative genetic risk and prefrontal activity in patients with schizophrenia. Schizophr Bull. 2013;39:703–11.

Walton E, Geisler D, Lee PH, et al. Prefrontal inefficiency is associated with polygenic risk for schizophrenia. Schizophr Bull. 2014;40:1263–71.

Wang B, Mezlini AM, Demir F, Fiume M, Tu Z, Brudno M, et al. Similarity network fusion for aggregating data

types on a genomic scale. Nat Methods. 2014;11:333. https://doi.org/10.1038/nmeth.2810.

Wang C, Jianping S, Bryan G, Tian G, Hibar Derrek P, Greenwood Celia MT, Qiu A, The Alzheimer's Disease Neuroimaging Initiative. A set-based mixed effect model for gene-environment interaction and its application to neuroimaging phenotypes. Front Neurosci. 2017;11:191. https://doi.org/10.3389/fnins.2017.00191.

Wei Q, Li M, Kang Z, Li L, Diao F, Zhang R, et al. ZNF804A rs1344706 is associated with cortical thickness, surface area, and cortical volume of the Unmedicated first episode schizophrenia and healthy controls. Am J Med Genet B Neuropsychiatr Genet. 2015;168B(4):265–73. https://doi.org/10.1002/ajmg.b.32308.

Weirauch MT. Gene coexpression networks for the analysis of DNA microarray data. Applied statistics for network biology: methods in systems biology; 2011.

Witte AV, Flöel A. Effects of COMT polymorphisms on brain function and behavior in health and disease. Brain Res Bull. 2012;88:418–28.

Wolf DH, Satterthwaite TD, Calkins ME, Ruparel K, Elliott MA, Hopson RD, et al. Functional neuroimaging abnormalities in psychosis spectrum youth. JAMA Psychiat. 2015;72:456–65. https://doi.org/10.1001/jamapsychiatry.2014.3169.

Wood JD, Bonath F, Kumar S, Ross CA, Cunliffe VT. Disrupted-in-schizophrenia 1 and neuregulin 1 are required for the specification of oligodendrocytes and neurones in the zebrafish brain. Hum Mol Genet. 2009;18:391–404.

Wray NR, Gottesman II. Using summary data from the danish national registers to estimate heritabilities for schizophrenia, bipolar disorder, and major depressive disorder. Front Genet. 2012;3:118. https://doi.org/10.3389/fgene.2012.00118.

Yang H, Liu J, Sui J, Pearlson G, Calhoun VD. A hybrid machine learning method for fusing fMRI and genetic data: combining both improves classification of schizophrenia. Front Hum Neurosci. 2010;4:192.

17 Predicting Outcome in Schizophrenia: Neuroimaging and Clinical Assessments

Nancy C. Andreasen and Thomas Nickl-Jockschat

Contents

17.1 Introduction

Schizophrenia is a debilitating neuropsychiatric disorder that typically begins during adolescence or young adulthood and leads to grave personal, familial, and socioeconomic consequences. Due to the early manifestation and the comparatively high prevalence, the disease results in an enormous global burden of disease (Whiteford et al. 2013). Symptoms are heterogeneous and are usually categorized into three groups: positive symptoms, such as delusions and hallucinations, that occur most severely during psychotic episodes; negative symptoms, such as affective flattening and avolition; and disorganized symptoms, such as bizarre behavior (Andreasen 1995). Cognitive impairments, which may worsen during the course of the disease, may also be important early prognosticators. Despite ongoing efforts to improve outcomes for these patients, many symptoms, especially negative symptoms, and cognitive

N. C. Andreasen (✉)
Andrew H Woods Chair of Psychiatry, Mental Health Clinical Research Center, The University of Iowa College of Medicine, Iowa City, IA, USA
e-mail: nancy-andreasen@uiowa.edu

T. Nickl-Jockschat
Department of Psychiatry, Iowa Neuroscience Institute, The University of Iowa College of Medicine, Iowa City, IA, USA
e-mail: thomas-nickl-jockschat@uiowa.edu

M. Kubicki, M. E. Shenton (eds.), *Neuroimaging in Schizophrenia*,
https://doi.org/10.1007/978-3-030-35206-6_17

impairments remain largely nonresponsive to current pharmaceutical approaches.

When patients and their families are first confronted with this diagnosis, they often want to know the prognosis and a prediction of the future disease trajectory. However, while there is consensus that affected individuals may face increasing cognitive and psychosocial deficits over the course of the disease (Owen et al. 2016), clinicians and researchers also acknowledge a considerable heterogeneity of individual disease trajectories (Joyce and Roiser 2007). This heterogeneity confronts clinicians with several problems: first, prospective planning of care and treatment is significantly limited due to prognostic uncertainty; second, patients and their relatives naturally have high interest in how to plan the future; third, it is unknown whether this clinical diversity reflects different pathophysiologies, and if so, whether individual treatments could be optimized when the approach is based on individual disease mechanisms.

The latter problem points to another unsolved riddle: whether clinical or neurobiological parameters are better suited for prognostic use. The neuroanatomical changes in schizophrenia are likely the best characterized biomarkers of disease (Fig. 17.1). Brain volume loss in a fronto-temporo-thalamo-basal ganglia network has been robustly identified in patients (Andreasen et al. 2011; Francis et al. 2012; Nickl-Jockschat et al. 2011). Importantly, these changes are not static, but appear to be progressive throughout the disease course and are linked, at least in retrospective studies, to symptom severity (Andreasen et al. 2011; Ho et al. 2003). However, there is a high heterogeneity of findings regarding regional brain volume decreases in patients (van Erp et al. 2016). While neuroanatomical heterogeneity apparently renders neuroimaging unsuitable for diagnostic purposes, it may reflect the neurobiological basis for the heterogeneous disease trajectories. However, it remains uncertain whether neuroanatomical changes can serve as predictors of disease outcomes, thus, the quest for powerful outcome predictors remains largely incomplete.

17.2 Early Predictors of Conversion into Psychosis: Clinical Measures

Schizophrenia is increasingly perceived as a neurodevelopmental disorder, with ongoing pathophysiological processes occurring long

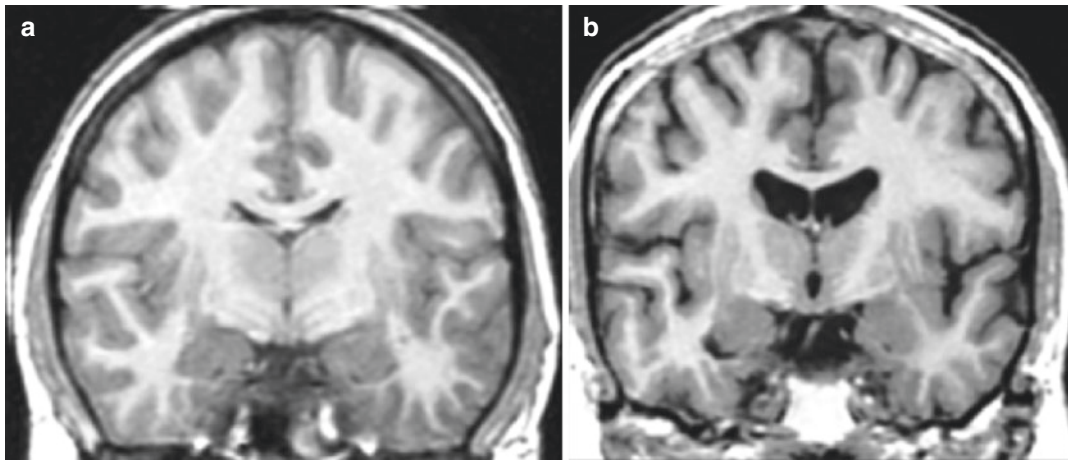

Fig. 17.1 Patients have evidence of brain tissue loss at the onset of the illness. Exemplary comparison of the MR images of a 21 year old healthy subject (**a**) and a schizophrenia patient at first hospital admission of the same age (**b**) with prominent enlargement of the lateral ventricles

before the actual onset of the disorder (Andreasen 2010; Insel 2010). Children who will later manifest with schizophrenia may have impairments in standardized scholastic tests across all domains as early as fourth grade. These deficits show a rapidly accelerated decline around 11th grade, before the actual onset of illness (Ho et al. 2005). Nonspecific prodromal syndromes, such as affective or attenuated psychotic symptoms, can sometimes be observed over several years prior to the first psychotic episode (Häfner et al. 1992; Schultze-Lutter et al. 2007). As only a minority of all subjects with prodromal symptoms actually convert into the full-blown disease, an important question to be addressed is whether early clinical signs and neurobiological parameters can be used to distinguish later patients from non-converters.

Studies on *clinical predictors* of conversion into psychosis have highlighted the importance of prodromal psychopathology. Of note especially, the severity of positive symptoms, such as unusual thought content and suspiciousness, have been identified to predict conversion into psychosis (Carrión et al. 2017; Perkins et al. 2015). The negative symptom cluster, in contrast, appears to be a weaker predictor, although individual negative symptoms, namely anhedonia and reduced concentration, indicate transition to psychosis (Azar et al. 2018; Flückiger et al. 2019; Perkins et al. 2015, reviewed in: Riecher-Rössler and Studerus 2017).

Besides distinct symptom patterns, a poor baseline level of functioning indicates an increased risk for conversion to psychosis (Fusar-Poli et al. 2015). Analogous to this, global cognitive measures, such as general IQ, may also be predictive (Metzler et al. 2016). More specific cognitive measures seem to have the potential to identify later converters: high-risk subjects who manifest schizophrenia later have been described as performing worse in classical cognitive domains implicated in schizophrenia, such as attention, working memory, processing speed, and verbal fluency (Carrión et al. 2015; Metzler et al. 2016; Seidman et al. 2016).

17.3 Early Predictors of Conversion into Psychosis: Neuroimaging

Comparing neuroimaging patterns of converters and non-converters within a high-risk sample promises two major benefits:

1. A better understanding of the pathophysiology that underlies the manifestation of schizophrenia;
2. A potential way to identify subjects prior to their conversion for early intervention.

Most neuroimaging studies have utilized structural magnetic resonance imaging (sMRI) to identify later converters. In the following, we will focus on them, but also briefly discuss findings from studies using diffusion tensor imaging (DTI) and other imaging methods to identify changes in neurotransmission.

Longitudinal studies have demonstrated that the onset of psychosis is actually marked by a structural remodeling of the brain. A major hallmark is volume loss in fronto-temporal regions that has been consistently demonstrated across different studies. Orbitofrontal regions, for example, have been consistently implicated in this remodeling during the onset of disease across different studies and analysis methods (Cannon et al. 2015; Pantelis et al. 2003). Along with longitudinal findings in patients with schizophrenia (see below), these studies paint the picture of dynamic, rather than stable, neuroanatomical changes that emerge long before and still progress significantly after, the onset of disease. Given their dynamic nature, these brain structural processes might be a suitable biomarker to identify converters.

This hope has sparked several studies that analyzed baseline MRIs from subjects at risk that compared converters to non-converters. These studies have the huge advantage that they do not necessarily need longitudinal MRI scans, but only a clinical follow-up to determine which subjects actually converted and which did not. This goes along with the challenge to choose the right

observation interval. As depicted above, the prodrome can last for several years before the disease actually manifests. Consequently, subjects that are considered as non-converters might present with schizophrenia later, if the observation duration is too short, while longer observation is oftentimes challenging for researchers. Adding to this, some researchers have suggested that different lengths of the prodromal interval might reflect different neurobiological subtypes of schizophrenia (Lappin et al. 2007). Consequently, commonly accepted standards for the duration of the observation interval would be highly desirable; however, they do not exist at this time.

These challenges might explain some of the heterogeneous findings in prodromal prediction studies. However, despite different observation intervals, methods, and cohorts, some results have been replicated across studies. Lower volumes of the prefrontal cortex have been consistently reported in subjects at risk that indeed later converted to psychosis (Borgwardt et al. 2008; Cannon et al. 2015; Pantelis et al. 2003); however, it should be noted that the exact anatomical locations did differ between studies. The same holds true for the second hotspot that differentiates between converters and non-converters: the temporal lobe (Borgwardt et al. 2008; Cannon et al. 2015; Mechelli et al. 2011; Pantelis et al. 2003). Of particular note here, the parahippocampal gyrus seems to discriminate well between converters and non-converters, but structures of the lateral temporal lobe, such as the superior temporal gyrus, have also been reported as differentiating between these two groups (Cannon et al. 2015; Mechelli et al. 2011; Pantelis et al. 2003). Finally, the cingulate cortex appears as the third hotspot, in which lower volumes might be distinctive of those converting into full-blown disease (Cannon et al. 2015; Pantelis et al. 2003).

It should be noted that these three hubs are canonical regions that also show progressive volume loss in later stages of schizophrenia (Andreasen et al. 2011; see below). The idea that accelerated volume loss in these key regions is a marker for conversion to psychosis therefore seems plausible. Current research actually aims to identify whether these structural changes are not only discriminative at a group level, but also for individual prediction (see below).

Fewer data exist on structural changes of white matter structures, and these are less convergent. Subjects who later converted into the full-blown disease have been reported to show changed connectivity, e.g., in the superior longitudinal fasciculus and the corpus callosum (Carletti et al. 2012; Saito et al. 2017). Functional MRI studies also are comparatively scarce, but indicate dysfunctional fronto-thalamic networks in converters (Anticevic et al. 2014).

Antipsychotic agents rely upon the modulation of dopaminergic signaling. This basic finding in biological psychiatry has inspired studies to focus on dopaminergic and related neurotransmission with different imaging methods in prodromal subjects. These studies have found, e.g., higher striatal glutamate levels (using magnetic resonance spectroscopy (MRS)) and greater striatal dopamine synthesis capacity (using positron emission tomography (PET)) in converters (de la Fuente-Sandoval et al. 2011; Howes et al. 2011).

In sum, various lines of evidence point to progressive gray matter changes in a fronto-temporal network that may discriminate between later converters and non-converters. Studies on changes in white matter structures and neurotransmission are still scarce. More of these studies are warranted to corroborate these results.

17.4 Predictors of Long-Term Outcome in Schizophrenia: General Considerations and Challenges

Schizophrenia is usually a life-long disorder. Hence, identifying factors at early stages of the disease that correlate with long-term outcome is critical to improving the planning of treatment and care for patients. However, compared to studies investigating predictors of conversion from prodromal stages to the fully manifested disease, research in this field is confronted with still additional challenges. Given the life-long course of schizophrenia, observation intervals for patient samples should span several years to capture true

long-term trajectories and not only short-term effects. During that time, clinical and/or neurobiological assessments need to be fairly frequent to reliably capture the disease trajectory.

The disease trajectory can also be modified by a large range of additional factors. Substance use disorders, access to healthcare, homelessness, and adherence/non-compliance with antipsychotic therapy, e.g., can be reasonably expected to alter long-term outcome. These factors need to be reliably identified and to be corrected in order to provide meaningful results.

These challenges might explain why comparatively few studies exist in that field. We will discuss these findings in the following two sections.

17.5 Predictors of Long-Term Outcome in Schizophrenia: Clinical Measures

Symptom patterns in schizophrenia are often perceived as unstable and quick to change (Nickl-Jockschat and Abel 2016). Because of their seemingly elusive nature, the idea that symptoms can be used to identify stable subtypes of schizophrenia has been discussed critically in the literature (Tandon et al. 2013). Thus, the question arises as to whether or not symptom patterns or cognitive measures at the onset of disease be informative about later disease trajectories.

Despite these concerns, various lines of evidence consistently highlight negative symptoms as predictors of a negative long-term outcome. Most importantly, several prospective studies have identified negative symptoms at baseline as robust predictors for a high frequency of relapses, poor remissions, and a course towards disability (Fenton and McGlashan 1991; Kurihara et al. 2011). A higher load of negative symptoms at disease onset was also associated with poorer cognitive performance (Gold et al. 1999). Results from the much larger Iowa Longitudinal Study (ILS) cohort, which followed the disease trajectories of more than 380 patients for a mean interval of more than 11 years, also identified negative symptoms as a major predictor of the disease trajectory (Nickl-Jockschat et al. 2019).

These findings are well in line with studies that report negative symptoms as strongly associated with deficits in various independent living skills, such as occupational impairments, financial dependence on others, and global functional deficits, highlighting this symptom cluster as a key player in the emergence of schizophrenia-associated disability (Ho et al. 1998; Hunter and Barry 2012; Milev et al. 2005; Owen et al. 2016; Patel et al. 2015). Unfortunately, the pivotal impact of negative symptoms on global outcome measures is further aggravated by their minimal response to pharmacological interventions: of the three basic symptom dimensions, negative symptoms are the least improved by antipsychotic agents or other psychotropic medications, such as antidepressants (Aleman et al. 2017; Helfer et al. 2016). These findings support a stronger research focus specifically on negative symptoms (Andreasen 1982; Bijanki et al. 2015). Clinicians should thoroughly assess this symptom dimension in their first-episode patients; at present it tends to be neglected even by experienced providers (Hunter and Barry 2012).

Besides symptom patterns, neuropsychological parameters at first episode have also been implicated in long-term outcome. A study surveying schizophrenia patients for more than 15 years, for example, found that impairments of verbal memory at baseline were associated with poorer long-term functioning, while executive function impairments were correlated with time spent as in-patients (Fujii and Wylie 2003). However, it should be pointed out that this study only monitored 26 patients. Also in the much larger ILS cohort, three major cognitive domains (IQ scores, verbal abilities, and attention) at baseline predicted time in relapse. Impairments in these domains are typically perceived as hallmarks of schizophrenia, namely attention, language ability, and IQ (Boudewyn et al. 2017; Hoonakker et al. 2017a, b; Kendler et al. 2015; Kim et al. 2015; Toulopoulou et al. 2017). These findings suggest that first-episode patients might benefit from baseline neuropsychological testing, although this is not currently recommended as standard of care.

While these predictors can hardly be modified by treatment, duration of untreated psychosis (DUP) is a factor that can be addressed by an earlier initiation of treatment. Several studies have identified a longer duration of psychosis (DUP) as a negative predictor of long-term outcome. These findings have been corroborated by a recent meta-analysis (Penttilä et al. 2014). Thus, an earlier identification of first episode patients might help to improve their long-term outcome.

17.6 Predictors of Long-Term Outcome in Schizophrenia: Neuroimaging

Since the days of Emil Kraepelin and Alois Alzheimer, psychiatric research has tried to identify neurobiological correlates of schizophrenia (Alzheimer 1913). The introduction of modern neuroimaging methods, especially MRI, has led to tremendous advances in this field of research, which have reshaped our perception of psychiatric disorders in general, and of schizophrenia in particular (Andreasen 1982).

It is now well-recognized that schizophrenia is a brain disease that is associated with dynamic changes of neuroanatomy. Patients suffer from a volume loss, mainly in frontal, temporal, and subcortical brain regions, but also rather global measures, such as total cerebral volume. Brain volume loss is most pronounced during the first year of the illness and closely related to the disease trajectory (Andreasen et al. 2011). Neuroanatomical changes have been shown to be associated with relapse patterns and psychopathology (Andreasen et al. 2013; Ho et al. 2003). Specifically, a progressive decrement in frontal lobe white matter and enlargement in frontal lobe cerebrospinal fluid volume were associated with greater negative symptom severity. Given this obviously close relationship between brain structural changes and psychopathology, neuroanatomical patterns at first episode might also be predictive for long-term outcome. However, it should be noted that neuroimaging studies on long-term outcome face many more challenges than purely clinical assessments. MRI scans are labor- and cost-intensive, and scanners are not necessarily available at every psychiatric institution. Consequently, large samples are rather hard to acquire, and continuous funding is an indispensible prerequisite. These additional hurdles alone might explain why prospective studies, especially on the relationship between brain measures and long-term outcome, are still scarce.

Thus, most publications report observation intervals of 1 year or less (Dazzan et al. 2015). Reported relationships between brain structure at baseline and the reported outcomes have been inconsistent. A study using a whole-brain approach on 39 patients found an association between striatothalamic volumes and response to antipsychotics (Fung et al. 2014). Remarkably, such a relationship was found only in female, not male, patients. Another study, however, did not report a gender relationship, but rather implicated lateral and third ventricle abnormalities as a predictor of relapse status after 1 year (Lieberman et al. 1993). The volume of the internal capsule has also been reported as a predictor of outcome after the first year (Wobrock et al. 2009).

These inconsistencies between studies might in part be explained by methodical challenges. Study designs that assess symptom levels at only two time points, baseline and a 1 year follow-up, for example, will not capture variance in symptom levels over the rest of the observation period.

Data from the ILS cohort implicates variations of regional brain volumes in frontal and temporal regions at baseline as predictive of long-term general relapse patterns. It should be noted that these are classical brain regions implicated in schizophrenia. Remarkably, while there was a negative correlation between these regional brain volumes and general relapse, striatal volumes showed a positive correlation with time spent in psychotic relapse (i.e., episodes with predominantly positive symptoms) (unpublished data). While these results are certainly encouraging, since they show that brain structural variation at

baseline is correlated with long-term outcome per se, it remains to be determined whether neuroimaging data sets are better suited than clinical or cognitive parameters.

17.7 Novel Approaches: Machine Learning

All the approaches described above rely upon *univariate statistics* to characterize *average differences* between groups, e.g., between prodromal subjects that convert into psychosis and those who do not. This identification of group differences is certainly helpful for identifying underlying neurobiological processes. However, it does not allow the assignment of an *individual patient's data set* to one of these groups, a major obstacle for using neuroimaging data in psychiatric clinical routine diagnostics in general, and for predictive purposes specifically.

To address these limitations, researchers have developed new *multivariate approaches* that are usually subsumed under the term *machine learning*. They are based on statistical methods that are designed to detect robust patterns in a data set in a first step (e.g., what patterns distinguish the MRI data sets of patients vs. controls or converters vs. non-converters). Once these patterns are identified, they are used for prediction in a second step (in this example, whether a yet unknown MRI data set belongs to a converter or not). It is important to notice that machine learning approaches are therefore all based on the assumption that "the truth lies within the data," thus, respective algorithms pick up patterns that are distinctive in a certain data set, but that does not necessarily mean that such a distinction is based on causal criteria (Bzdok and Eickhoff 2016).

Machine learning is a comparatively new and rapidly evolving field in psychiatric research. Up to now, studies using prospective methods to predict long-term outcome based on baseline MR imaging still are scarce and replication is still lacking. Given this, we will depict the use of support vector machines (SVMs) as the most widely applied method in the field, and briefly discuss potential options to use this for our research questions.

SVMs belong to the so-called *supervised* methods. This means that an algorithm is automatically learning certain patterns in a labeled data set (i.e., in our example the information about whether a certain data set belongs to a converter or a non-converter), the so-called *training phase*. In a second step, the success of the learning is quantified in the *testing phase*. The algorithm is now used to assign a classification of data sets based on the previously detected patterns (out-of-sample performance). The latter step provides an estimate about how successfully the algorithm can perform in future settings. (In contrast to that, *unsupervised* forms of machine learning are usually based on clustering algorithms, such as k-means or hierarchical clustering). SVMs, specifically, are based on finding the most representative data points for each class ("support vectors") to define a boundary between samples (in our example converters and non-converters) (Fig. 17.2).

Based on their ability to detect patterns within data sets and to develop classifiers accordingly, machine learning approaches have the potential to individualize diagnosis and prognosis in a data-driven way. However, they will have to prove in large samples that they are indeed robustly useful for prediction of outcome in schizophrenia.

17.8 Summary and Conclusion

Identifying predictors of long-term outcome in schizophrenia is highly warranted, but studies confront several important challenges. So far, a set of clinical and cognitive parameters at baseline—mainly the manifestation of negative symptoms and IQ impairments—appear as robust predictors of a malignant disease trajectory. Volume reductions in the frontal and temporal lobe at first episode also seem to indicate a negative outcome, but it remains to be determined

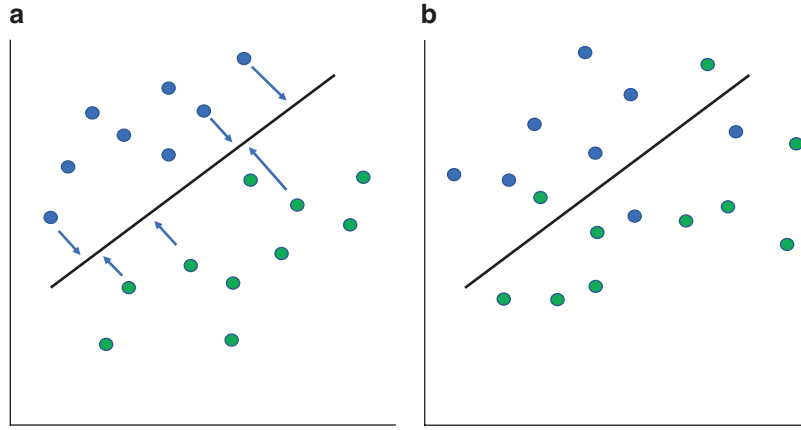

Fig. 17.2 Schematic overview over the basic mode of operation of an SVM. (**a**) In an initial step, the algorithm is automatically learning certain patterns in a labeled data set. In this example, the algorithm has to distinguish between two data sets (green and blue dots) according to two variables (here symbolized by the x and y axis). The algorithm aims to detect patterns of the distribution of the two data sets and establishes a decision boundary accordingly (here depicted as the thick diagonal line that separates the two data sets). This is done by finding the most representative data points for each class. This step is called the *training phase*. (**b**) In a second step, the success of the learning is quantified in the *testing phase*. The algorithm is now used to assign a classification of data sets based on the previously detected patterns. In other words, it uses the previously established decision boundary to predict whether a certain data set belongs to the "green" or the "blue" cohort. The ratio of correct vs. incorrect assignments provides a measure of how reliable the algorithm actually is

whether these changes are reliable and better suited than clinical parameters to predict the course of the disorder. Machine learning approaches are a thriving new field of research in this regard that raise hopes for individualized treatment.

Summary

- Parameters that can predict the clinical course of schizophrenia are highly warranted, as this will help to optimize prospective planning of care and treatment.
- Negative symptoms and cognitive impairments at baseline are robust clinical predictors of an unfavorable long-term outcome.
- Neuroimaging studies have hinted at volume reductions in fronto-temporal regions to predict a negative long-term outcome, but it remains to be determined whether those are better suited for predictive purposes than clinical markers.
- Machine learning is a promising, but novel field, that develops computational approaches to detect robust patterns in a data set and to use these patterns for individual predictions

References

Aleman A, Lincoln TM, Bruggeman R, Melle I, Arends J, Arango C, Knegtering H. Treatment of negative symptoms: where do we stand, and where do we go? Schizophr Res. 2017;186:55–62.

Alzheimer A. Beitraege zur pathologischen Anatomie der Dementia praecox. Zeitschrift fuer die gesamte Neurologie und Psychiatrie. 1913;7:621.

Andreasen NC. Negative symptoms in schizophrenia. Definition and reliability. Arch Gen Psychiatry. 1982;39(7):789–94.

Andreasen NC. Symptoms, signs, and diagnosis of schizophrenia. Lancet. 1995;346(8973):477–81.

Andreasen NC. The lifetime trajectory of schizophrenia and the concept of neurodevelopment. Dialogues Clin Neurosci. 2010;12(3):409–15.

Andreasen NC, Nopoulos P, Magnotta V, Pierson R, Ziebell S, Ho BC. Progressive brain change in schizophrenia: a prospective longitudinal study of first-episode

schizophrenia. Biol Psychiatry. 2011;70(7):672–9. https://doi.org/10.1016/j.biopsych.2011.05.017.

Andreasen NC, Liu D, Ziebell S, Vora A, Ho BC. Relapse duration, treatment intensity, and brain tissue loss in schizophrenia: a prospective longitudinal MRI study. Am J Psychiatry. 2013;170(6):609–15.

Anticevic A, Tang Y, Cho YT, Repovs G, Cole MW, Savic A, et al. Amygdala connectivity differs among chronic, early course, and individuals at risk for developing schizophrenia. Schizophr Bull. 2014;40(5):1105–16. https://doi.org/10.1093/schbul/sbt165.

Azar M, Pruessner M, Baer LH, Iyer S, Malla AK, Lepage M. A study on negative and depressive symptom prevalence in individuals at ultra-high risk for psychosis. Early Interv Psychiatry. 2018;12(5):900–6. https://doi.org/10.1111/eip.12386.

Bijanki KR, Hodis B, Magnotta VA, Zeien E, Andreasen NC. Effects of age on white matter integrity and negative symptoms in schizophrenia. Schizophr Res. 2015;161(1):29–35.

Borgwardt SJ, McGuire PK, Aston J, Gschwandtner U, Pflüger MO, Stieglitz RD, et al. Reductions in frontal, temporal and parietal volume associated with the onset of psychosis. Schizophr Res. 2008;106(2–3):108–14. https://doi.org/10.1016/j.schres.2008.08.007.

Boudewyn MA, Carter CS, Long DL, Traxler MJ, Lesh TA, Mangun GR, Swaab TY. Language context processing deficits in schizophrenia: the role of attentional engagement. Neuropsychologia. 2017;96:262–73.

Bzdok D, Eickhoff SB. Statistical learning of the neurobiology of schizophrenia: neuroimaging meta-analyses and machine-learning in schizophrenia research. In: Abel T, Nickl-Jockschat T, editors. The neurobiology of schizophrenia. San Diego: Elsevier; 2016.

Cannon TD, Chung Y, He G, Sun D, Jacobson A, van Erp TG, et al. Progressive reduction in cortical thickness as psychosis develops: a multisite longitudinal neuroimaging study of youth at elevated clinical risk. Biol Psychiatry. 2015;77(2):147–57. https://doi.org/10.1016/j.biopsych.2014.05.023.

Carletti F, Woolley JB, Bhattacharyya S, Perez-Iglesias R, Fusar Poli P, Valmaggia L, et al. Alterations in white matter evident before the onset of psychosis. Schizophr Bull. 2012;38(6):1170–9. https://doi.org/10.1093/schbul/sbs053.

Carrión RE, McLaughlin D, Auther AM, Olsen R, Correll CU, Cornblatt BA. The impact of psychosis on the course of cognition: a prospective, nested case-control study in individuals at clinical high-risk for psychosis. Psychol Med. 2015;45(15):3341–54. https://doi.org/10.1017/S0033291715001233.

Carrión RE, Correll CU, Auther AM, Cornblatt BA. A severity-based clinical staging model for the psychosis prodrome: longitudinal findings from the New York Recognition and Prevention Program. Schizophr Bull. 2017;43(1):64–74. https://doi.org/10.1093/schbul/sbw155.

Dazzan P, Arango C, Fleischacker W, Galderisi S, Glenthøj B, Leucht S, et al. Magnetic resonance imaging and the prediction of outcome in first-episode schizophrenia: a review of current evidence and directions for future research. Schizophr Bull. 2015;41(3):574–83. https://doi.org/10.1093/schbul/sbv024.

de la Fuente-Sandoval C, León-Ortiz P, Favila R, Stephano S, Mamo D, Ramírez-Bermúdez J, Graff-Guerrero A. Higher levels of glutamate in the associative-striatum of subjects with prodromal symptoms of schizophrenia and patients with first-episode psychosis. Neuropsychopharmacology. 2011;36(9):1781–91. https://doi.org/10.1038/npp.2011.65.

Fenton WS, McGlashan TH. Natural history of schizophrenia subtypes. II. Positive and negative symptoms and long-term course. Arch Gen Psychiatry. 1991;48(11):978–86.

Flückiger R, Michel C, Grant P, Ruhrmann S, Vogeley K, Hubl D, et al. The interrelationship between schizotypy, clinical high risk for psychosis and related symptoms: cognitive disturbances matter. Schizophr Res. 2019. pii: S0920-9964(18)30734-5. https://doi.org/10.1016/j.schres.2018.12.039.

Francis AN, Seidman LJ, Jabbar GA, Mesholam-Gately R, Thermenos HW, Juelich R, et al. Alterations in brain structures underlying language function in young adults at high familial risk for schizophrenia. Schizophr Res. 2012;141(1):65–71. https://doi.org/10.1016/j.schres.2012.07.015.

Fujii DE, Wylie AM. Neurocognition and community outcome in schizophrenia: long-term predictive validity. Schizophr Res. 2003;59(2–3):219–23.

Fung G, Cheung C, Chen E, Lam C, Chiu C, Law CW, et al. MRI predicts remission at 1 year in first-episode schizophrenia in females with larger striato-thalamic volumes. Neuropsychobiology. 2014;69(4):243–8. https://doi.org/10.1159/000358837.

Fusar-Poli P, Rocchetti M, Sardella A, Avila A, Brandizzi M, Caverzasi E, et al. Disorder, not just state of risk: meta-analysis of functioning and quality of life in people at high risk of psychosis. Br J Psychiatry. 2015;207(3):198–206. https://doi.org/10.1192/bjp.bp.114.157115.

Gold S, Arndt S, Nopoulos P, O'Leary DS, Andreasen NC. Longitudinal study of cognitive function in first-episode and recent-onset schizophrenia. Am J Psychiatry. 1999;156(9):1342–8.

Häfner H, Riecher-Rössler A, Maurer K, Fätkenheuer B, Löffler W. First onset and early symptomatology of schizophrenia. A chapter of epidemiological and neurobiological research into age and sex differences. Eur Arch Psychiatry Clin Neurosci. 1992;242(2–3):109–18.

Helfer B, Samara MT, Huhn M, Klupp E, Leucht C, Zhu Y, et al. Efficacy and safety of antidepressants added to antipsychotics for schizophrenia: a systematic review and meta-analysis. Am J Psychiatry. 2016;173(9):876–86.

Ho BC, Nopoulos P, Flaum M, Arndt S, Andreasen NC. Two-year outcome in first-episode schizophrenia: predictive value of symptoms for quality of life. Am J Psychiatry. 1998;155(9):1196–201.

Ho BC, Andreasen NC, Nopoulos P, Arndt S, Magnotta V, Flaum M. Progressive structural brain abnormalities and their relationship to clinical outcome: a longitudinal magnetic resonance imaging study early in schizophrenia. Arch Gen Psychiatry. 2003;60(6):585–94.

Ho BC, Andreasen NC, Nopoulos P, Fuller R, Arndt S, Cadoret RJ. Secondary prevention of schizophrenia: utility of standardized scholastic tests in early identification. Ann Clin Psychiatry. 2005;17(1):11–8.

Hoonakker M, Doignon-Camus N, Marques-Carneiro JE. Sustained attention ability in schizophrenia: investigation of conflict monitoring mechanisms. Clin Neurophysiol. 2017a;128(9):1599–607.

Hoonakker M, Doignon-Camus N, Bonnefond A. Sustaining attention to simple visual tasks: a central deficit in schizophrenia? A systematic review. Ann N Y Acad Sci. 2017b;1408(1):32–45.

Howes O, Bose S, Turkheimer F, Valli I, Egerton A, Stahl D, et al. Progressive increase in striatal dopamine synthesis capacity as patients develop psychosis: a PET study. Mol Psychiatry. 2011;16(9):885–6. https://doi.org/10.1038/mp.2011.20.

Hunter R, Barry S. Negative symptoms and psychosocial functioning in schizophrenia: neglected but important targets for treatment. Eur Psychiatry. 2012;27(6):432–6.

Insel TR. Rethinking schizophrenia. Nature. 2010;468(7321):187–93. https://doi.org/10.1038/nature09552.

Joyce EM, Roiser JP. Cognitive heterogeneity in schizophrenia. Curr Opin Psychiatry. 2007;20(3):268–72.

Kendler KS, Ohlsson H, Sundquist J, Sundquist K. IQ and schizophrenia in a Swedish national sample: their causal relationship and the interaction of IQ with genetic risk. Am J Psychiatry. 2015;172(3):259–65.

Kim SJ, Shim JC, Kong BG, Kang JW, Moon JJ, Jeon DW, et al. The relationship between language ability and cognitive function in patients with schizophrenia. Clin Psychopharmacol Neurosci. 2015;13(3):288–95.

Kurihara T, Kato M, Reverger R, Tirta IG. Seventeen-year clinical outcome of schizophrenia in Bali. Eur Psychiatry. 2011;26(5):333–8. https://doi.org/10.1016/j.eurpsy.2011.04.003.

Lappin JM, Dazzan P, Morgan K, Morgan C, Chitnis X, Suckling J, et al. Duration of prodromal phase and severity of volumetric abnormalities in first-episode psychosis. Br J Psychiatry Suppl. 2007;51:s123–7. https://doi.org/10.1192/bjp.191.51.s123.

Lieberman J, Jody D, Geisler S, Alvir J, Loebel A, Szymanski S, et al. Time course and biologic correlates of treatment response in first-episode schizophrenia. Arch Gen Psychiatry. 1993;50(5):369–76.

Mechelli A, Riecher-Rössler A, Meisenzahl EM, Tognin S, Wood SJ, Borgwardt SJ, et al. Neuroanatomical abnormalities that predate the onset of psychosis: a multicenter study. Arch Gen Psychiatry. 2011;68(5):489–95. https://doi.org/10.1001/archgenpsychiatry.2011.42.

Metzler S, Dvorsky D, Wyss C, Nordt C, Walitza S, Heekeren K, et al. Neurocognition in help-seeking individuals at risk for psychosis: prediction of outcome after 24 months. Psychiatry Res. 2016;246:188–94. https://doi.org/10.1016/j.psychres.2016.08.065.

Milev P, Ho BC, Arndt S, Andreasen N. Predictive values of neurocognition and negative symptoms on functional outcome in schizophrenia: a longitudinal first-episode study with 7-year follow-up. Am J Psychiatry. 2005;162(3):495–506.

Nickl-Jockschat T, Schneider F, Pagel AD, Laird AR, Fox PT, Eickhoff SB. Progressive pathology is functionally linked to the domains of language and emotion: meta-analysis of brain structure changes in schizophrenia patients. Eur Arch Psychiatry Clin Neurosci. 2011;261(Suppl 2):S166–71. https://doi.org/10.1007/s00406-011-0249-8.

Nickl-Jockschat T, Abel T. Historical and clinical overview—implications for schizophrenia research. In: Abel T, Nickl-Jockschat T, editors. The neurobiology of schizophrenia. San Diego: Elsevier Academic Press; 2016.

Nickl-Jockschat T, Ho BC, Andreasen NC. Clinical and neurobiological predictors of long-term outcome in schizophrenia; 2019, submitted for publication.

Owen MJ, Sawa A, Mortensen PB. Schizophrenia. Lancet. 2016;388(10039):86–97. https://doi.org/10.1016/S0140-6736(15)01121-6.

Pantelis C, Velakoulis D, McGorry PD, Wood SJ, Suckling J, Phillips LJ, et al. Neuroanatomical abnormalities before and after onset of psychosis: a cross-sectional and longitudinal MRI comparison. Lancet. 2003;361(9354):281–8.

Patel R, Jayatilleke N, Broadbent M, Chang CK, Foskett N, Gorrell G, et al. Negative symptoms in schizophrenia: a study in a large clinical sample of patients using a novel automated method. BMJ Open. 2015;5(9):e007619.

Penttilä M, Jääskeläinen E, Hirvonen N, Isohanni M, Miettunen J. Duration of untreated psychosis as predictor of long-term outcome in schizophrenia: systematic review and meta-analysis. Br J Psychiatry. 2014;205(2):88–94. https://doi.org/10.1192/bjp.bp.113.127753.

Perkins DO, Jeffries CD, Cornblatt BA, Woods SW, Addington J, Bearden CE, et al. Severity of thought disorder predicts psychosis in persons at clinical high-risk. Schizophr Res. 2015;169(1–3):169–77. https://doi.org/10.1016/j.schres.2015.09.008.

Riecher-Rössler A, Studerus E. Prediction of conversion to psychosis in individuals with an at-risk mental state: a brief update on recent developments. Curr Opin Psychiatry. 2017;30(3):209–19. https://doi.org/10.1097/YCO.0000000000000320.

Saito J, Hori M, Nemoto T, Katagiri N, Shimoji K, Ito S, et al. Longitudinal study examining abnormal white matter integrity using a tract-specific analysis in individuals with a high risk for psychosis. Psychiatry Clin

Neurosci. 2017;71(8):530–41. https://doi.org/10.1111/pcn.12515.

Schultze-Lutter F, Ruhrmann S, Hoyer C, Klosterkötter J, Leweke FM. The initial prodrome of schizophrenia: different duration, different underlying deficits? Compr Psychiatry. 2007;48(5):479–88.

Seidman LJ, Shapiro DI, Stone WS, Woodberry KA, Ronzio A, Cornblatt BA, et al. Association of neurocognition with transition to psychosis: baseline functioning in the second phase of the North American Prodrome Longitudinal Study. JAMA Psychiat. 2016;73(12):1239–48. https://doi.org/10.1001/jamapsychiatry.2016.2479.

Tandon R, Gaebel W, Barch DM, Bustillo J, Gur RE, Heckers S, et al. Definition and description of schizophrenia in the DSM-5. Schizophr Res. 2013;150(1):3–10. https://doi.org/10.1016/j.schres.2013.05.028.

Toulopoulou T, Picchioni M, Mortensen PB, Petersen L. IQ, the urban environment, and their impact on future schizophrenia risk in men. Schizophr Bull. 2017;43(5):1056–63.

van Erp TG, Hibar DP, Rasmussen JM, Glahn DC, Pearlson GD, Andreassen OA, Agartz I, et al. Subcortical brain volume abnormalities in 2028 individuals with schizophrenia and 2540 healthy controls via the ENIGMA consortium. Mol Psychiatry. 2016;21(4):585. https://doi.org/10.1038/mp.2015.118.

Whiteford HA, Degenhardt L, Rehm J, Baxter AJ, Ferrari AJ, Erskine HE, et al. Global burden of disease attributable to mental and substance use disorders: findings from the Global Burden of Disease Study 2010. Lancet. 2013;382(9904):1575–86. https://doi.org/10.1016/S0140-6736(13)61611-6.

Wobrock T, Gruber O, Schneider-Axmann T, Wölwer W, Gaebel W, Riesbeck M, et al. Internal capsule size associated with outcome in first-episode schizophrenia. Eur Arch Psychiatry Clin Neurosci. 2009;259(5):278–83. https://doi.org/10.1007/s00406-008-0867-y.

18 Structural and Functional Neuroimaging Biomarkers of Antipsychotic Treatment Response in Early-Course and Chronic Schizophrenia

Deepak K. Sarpal and Anil K. Malhotra

Contents

18.1 Introduction

Schizophrenia spectrum disorders typically emerge during adolescence and early adulthood, severely altering an individual's natural life course (Millan et al. 2016). Characteristic to these disorders are episodes of psychosis that include hallucinations of various modalities, delusional thought processes, and disorganized behavior. Numerous antipsychotic drugs exist to treat these symptoms and primarily target the dopamine D2 receptor, though response to their administration is variable and cannot be predicted (Kapur and Mamo 2003; Carbon and Correll 2014). Treatment decisions are based on trial and error, with no quantitative guidance, unlike in other areas of medicine where precision medicine strategies are integrated. Poor response to antipsychotic treatment, occurring in up to 40% of patients, accounts for a disproportionate amount of disability and health care expenditure (Kennedy et al. 2014).

Outcome trajectories coalesce over time and are unknown at illness onset. Heterogeneity of outcomes in individuals diagnosed with schizophrenia has been described for many decades. Early longitudinal studies, predating the availability of antipsychotic drugs, showed several

D. K. Sarpal
Department of Psychiatry, University of Pittsburgh, Pittsburgh, PA, USA
e-mail: sarpaldk@upmc.edu

A. K. Malhotra (✉)
Psychiatry Research, Zucker Hillside Hospital, Glen Oaks, NY, USA

Department of Psychiatry, The Zucker School of Medicine at Hofstra/Northwell, Hempstead, NY, USA

Center for Psychiatric Neuroscience, The Feinstein Institute of Medical Research, Manhasset, NY, USA
e-mail: amalhotra@northwell.edu

M. Kubicki, M. E. Shenton (eds.), *Neuroimaging in Schizophrenia*,
https://doi.org/10.1007/978-3-030-35206-6_18

illness courses following the emergence of psychotic symptoms (Bleuler 1968). Subsequent to the advent of antipsychotic drugs, Huber et al. demonstrated 12 treatment trajectories, ranging from persistent and refractory to monophasic illnesses in patients with schizophrenia (Huber et al. 1980). More recent evidence supports this vast degree of variation in outcome (Carbon and Correll 2014).

Many studies have sought to understand the neural mechanisms underlying variation of outcomes in schizophrenia. Neuroimaging methods have emerged as key contributors in this effort (See Chaps. 1, 3 and 5 for more details). Numerous studies have applied both structural and functional neuroimaging to examine the complex phenotypic manifestations and illness trajectories observed in disorders such as schizophrenia (See Chaps. 2, 4 and 6 for more details). While ongoing neuroimaging methods have the capacity to follow and predict treatment outcomes in a noninvasive and applicable manner, the gap between existing findings and clinical practice remains significant.

The following chapter focuses on these efforts by reviewing findings from both structural and functional neuroimaging studies. Both early-course and chronic patients with schizophrenia will be considered, given the importance of markers at both onset and in chronic illness. We will also discuss the potential for structural and functional neuroimaging-related measures to be used as prognostic biomarkers of outcomes. Within this text, various definitions of outcomes and response will be considered. Of note, we emphasize and concentrate on measures associated with efficacy and outcomes to treatment, rather than the effect of medications on brain structure and function.

18.2 Structural Studies of Early-Course Schizophrenia

Structural neuroimaging methods have been used to examine treatment response in individuals with first-episode psychosis or early-course schizophrenia. Patients early in the course of illness offer the advantages of no or limited prior treatment and reduced durations of illness, resulting in potentially less environmental confounds that may serve to decrease study power. Collectively, structural neuroimaging measures, particularly assessments of cortical folding patterns, may reflect developmentally mediated abnormalities that contribute to treatment response.

Initial neuroimaging studies in first-episode and early-course patients with schizophrenia focused on ventricular-brain ratios versus clinical outcomes with magnetic resonance imaging (MRI). Longitudinal studies, using serial MRIs during treatment, reported that in patients with poor outcome to treatment, significant ventricular enlargement was observed over time, whereas the patients with better treatment outcomes and healthy control subjects did not show ventricular enlargements (Lieberman et al. 2001; Ho et al. 2003). Subsequent work focused on ventricular enlargement in relation to antipsychotic type. Lieberman et al. (Lieberman et al. 2005) compared ventricular enlargement between treatment with olanzapine and haloperidol, and found that treatment response, measured by ratings of global psychopathology, correlated with lower increases in ventricular volume in the olanzapine treated group. In a more recently published study, increases in ventricular volume correlated with less reductions of negative symptoms in first-episode psychosis patients during treatment with the second-generation antipsychotic, quetiapine (Ebdrup et al. 2011).

Along with changes in ventricular size, structural neuroimaging studies have shown response-related morphological findings in the prefrontal cortex. Reductions in negative symptoms were found to be related to increased thickness of middle frontal gyrus following treatment with atypical antipsychotics (Goghari et al. 2013). Poorer overall functioning after 1 year of treatment in a small cohort of patients with first-episode schizophrenia was associated with reduced prefrontal grey matter volume (Kasparek et al. 2009). Prasad and colleagues demonstrated that a larger

dorsolateral prefrontal cortex volume after 1 year of treatment predicted better functional outcome based on a score that incorporated social contacts, employment, and symptomatology (Prasad et al. 2005).

Multiple findings related to treatment outcome have been reported in medial temporal regions. In a study where first-episode psychosis patients were categorized as responders or non-responders by the Schizophrenia Working Group remission criteria, responders were found to have larger parahippocampal cortex volumes in both left and right hemisphere (Bodnar et al. 2011; 2012a). An analysis of cortical gyrification in first-episode psychosis revealed that non-response to antipsychotic treatment was associated with decreased gyrification in regions of the insula, frontal, and temporal cortices (Palaniyappan et al. 2013). Moreover, responders to antipsychotic treatment displayed more asymmetry between left and right frontal cortices and greater thickness of temporal regions relative to patients with poor response to antipsychotic treatment (Szeszko et al. 2012).

Structural neuroimaging findings associated with treatment response have also been reported outside of fronto-temporal areas. Greater total cortical grey matter was shown to be associated with a percent reduction in psychotic symptoms following antipsychotic treatment (Zipursky et al. 1980). Likewise, a greater decrease in total grey matter volume after 1 year of treatment was associated with a greater need for psychosocial support after long term follow-up 5 years later (Cahn et al. 2006). Findings have been described in non-cortical regions as well. In white matter, a smaller baseline volume of the left anterior limb of the internal capsule was noted in patients with first-episode psychosis who showed a greater clinical deterioration after 1 year of treatment relative to those with more stable measures of psychopathology (Wobrock et al. 2009). In the basal ganglia, increased striatal volume was observed in relation to treatment efficacy after 6 weeks of medications (Li et al. 2012). Sex differences have also been noted in the striatum and thalamus. Larger volumes of these structures at baseline predicted remission after 1 year of treatment in females, but not males (Fung et al. 2014). Recent work has combined structural neuroimaging with graph theoretical measures to examine response to antipsychotic treatment. In a large cohort of patients undergoing treatment for 12 weeks, patterns of structural covariance across the brain were examined that focused on gyrification (Palaniyappan et al. 2016). Treatment non-responders showed increased segregation and impaired integration of structural relationships, possibly resulting in unstable information flow throughout the brain. It should be noted that relationships between structure and treatment response are not universally described, with several non-significant results reported (Molina et al. 2014; van Haren et al. 2003; Robinson et al. 1999).

In addition to studies of grey matter and volumetric analyses, efficacy of antipsychotic treatment has been examined along with white matter integrity. Diffusion tensor imaging (DTI) allows for the measurement of fractional anisotropy (FA), which characterizes water diffusion to provide a proxy measure of the white matter myelination. While most published studies examine changes in DTI measures in relation to antipsychotic exposure (Szeszko et al. 2014; Bartzokis et al. 2011; Samartzis et al. 2014), a few report state-dependent changes in white matter related to the amelioration of psychotic symptoms in early-course patients with schizophrenia. Reduced FA was reported within the uncinate and superior longitudinal fasciculi in first-episode psychosis patients who were characterized by poor treatment outcomes (Luck et al. 2011). Consistent with this report, FA increase in the superior longitudinal fasciculi was associated with more efficacious treatment over the course of 8 weeks of antipsychotic treatment (Zeng et al. 2016). Reis Marques et al. (2014) reported findings from a longitudinal study of 63 first-episode psychosis patients with stringent response criteria (Andreasen et al. 2005). While no change was observed in FA following 12 weeks of antipsychotic treatment, a negative correlation was observed between baseline psychopathology and

FA. Other studies in first-episode psychosis patients reported whole-brain increases in fractional anisotropy in patients with greater reductions in ratings of psychopathology (Serpa et al. 2017). More recent work has merged DTI tractography with network-based statistics to examine antipsychotic treatment in a cohort of first-episode patients. Responders to 12 weeks of treatment had more efficient DTI-derived connectomes at baseline, reflecting a higher capacity for information flow throughout the brain (Crossley et al. 2017).

18.3 Functional Studies of Early-Course Schizophrenia

Task-based functional neuroimaging has been used to examine treatment outcomes in patients with schizophrenia. While some studies describe negative findings relating treatment outcome and neural activation (Snitz et al. 2005; Blasi et al. 2009), others reported treatment-related findings, primarily in decreased engagement of prefrontal and striatal regions with poor response. In treatment-naive first-episode psychosis patients, nonresponse to a 10-week trial of antipsychotic treatment was associated with greater dysfunction of dorsolateral prefrontal activation during a working memory task (van Veelen et al. 2011). Supporting this finding, decreased engagement of executive regions and increased activation of the default mode network has been reported in non-remitters relative to patients who responded to treatment during memory encoding (Bodnar et al. 2012b). Two studies examined longitudinal changes in activation of the striatum during treatment with second-generation antipsychotic drugs. One reported that recruitment of the ventral striatum during reward processing was normalized only in first-episode patients who responded to treatment (Nielsen et al. 2012), while the second study found that activation of the striatum corresponded with drug-related weight gain, suggesting a link between neural engagement and metabolic outcomes to treatment (Nielsen et al. 2016).

Along with activation studies, findings show changes in resting-state functional connectivity during antipsychotic treatment. Resting-state scans are a convenient method for examining the intrinsic functional architecture of the brain. Analytic approaches to resting-state connectivity range from hypothesis-driven inter-regional assessments to more data-driven global connectivity measure that capture small-world network clustering throughout the brain. Recent work, including resting-state findings, has conceptualized schizophrenia as a 'dysconnectivity' syndrome, consisting of abnormalities in large-scale functional networks (van den Heuvel and Fornito 2014; Nejad et al. 2012). Supporting this theory, multiple reports characterize functional interactions between subcortical and prefrontal regions across antipsychotic treatment. Treatment-induced increases in functional connectivity of the striatum with important limbic and prefrontal regions, including the hippocampus, the anterior cingulate, and the dorsolateral prefrontal cortex, corresponded with efficacy of treatment in a randomized controlled trial between two second-generation drugs in a cohort of patients with first-episode schizophrenia (Sarpal et al. 2015). In addition, an index of striatal connectivity at treatment initiation predicted ultimate response to treatment in two independent cohorts (Sarpal et al. 2016). Functional interactions of brain regions including the striatum, hippocampus, and the anterior cingulate cortex are additionally implicated in the mechanism of response by other longitudinal, treatment-based studies (Anticevic et al. 2015; Kraguljac et al. 2016a).

Together, the fMRI studies described above suggest that when antipsychotic treatment works, there is an associated increase in either activation or synchronization of neural activity in brain regions important for cognition and emotional processing. Additional studies use more novel connectivity methods and report either negative findings or normalization of fMRI signals with treatment response (Lui et al. 2010; Guo et al. 2017, 2018; Wang et al. 2017). It is worth noting that analytic approaches vary

across these fMRI studies, introducing heterogeneity in reported findings. Multisite studies with a uniform analytic approach may yield more conclusive results.

18.4 Structural Studies of Chronic Schizophrenia

In addition to studies focused on patients early in the course of illness, multiple studies have assessed more chronically ill subjects. These study groups, though perhaps more heterogeneous that early phase patients, represent the vast majority of patients seen in treatment settings, and therefore predictors of response in this group of patients would be of potentially enormous clinical utility.

The first studies to use neuroimaging to examine treatment response examined ventricular-brain ratios with computed tomography imaging (CT scans). Larger ventricles were observed in patients who were poorer responders to treatment (Weinberger et al. 1980; Schroder et al. 1993; Kaplan et al. 1990). Later studies continued to examine ventricular volumes with MRI scans. In a comparison of percent time hospitalized in the previous year and ventricular-brain ratios, smaller frontal lobe volumes and larger ventricles were observed in patients who spent more time hospitalized (Staal et al. 2001). Supporting this finding that gross measures of outcome and structure may be useful markers, Jääskeläinen and colleagues showed that in a large voxel based morphological analysis, individuals with better functional and clinical outcomes following treatment had "denser" frontal and limbic grey matter, relative to those with worse treatment outcomes (Jaaskelainen et al. 2014).

Across analyses, larger volumes of various structures have been associated with response to antipsychotic treatment in chronic patients with schizophrenia. This includes hippocampal volumes in both cross-sectional and longitudinal studies (Savas et al. 2002; Panenka et al. 2007), temporal grey matter volumes compared with reductions of psychotic symptoms (McClure et al. 2006), the thalamic volume after 4 weeks of treatment (Strungas et al. 2003), and cerebellar volume after a 7 year follow-up (Wassink et al. 1999). In addition, a decline in social and occupational functioning was associated with a corresponding decrease in supramarginal gyrus volume (Guo et al. 2015).

Studies focused on white matter in chronic patients with schizophrenia are limited. As with early-course patients, most studies concentrate on the effect of antipsychotic drugs on DTI-based measures, rather than correlates of treatment efficacy. Mitelman et al. (2006) reported widespread increases in FA, driven by treatment response. One additional report found an increase in DTI-based mean diffusivity in patients who demonstrated reduced psychotic symptoms following 1 month of antipsychotic treatment (Garver et al. 2008).

Neuroimaging findings of chronic patients with schizophrenia have also centered on treatment-refractory patients who are often treated with clozapine. Non-responders to clozapine treatment showed reduced grey matter volumes in the middle frontal gyrus, bilaterally, and in the medial temporal cortex (Quarantelli et al. 2014; Arango et al. 2003). In a comparison with cohort of responders, treatment-resistant patients, many treated with clozapine, showed reduced cortical thickness in the dorsolateral prefrontal cortex, perhaps suggesting a neurobiological marker for illness severity (Zugman et al. 2013).

Despite this pattern of larger brain volumes in responders, several structural studies with negative findings have also been reported (Friedman et al. 1992; Lawrie et al. 1995; Roiz-Santianez et al. 2012; Scheepers et al. 2001). Likewise, meta-analyses of treatment-associated changes in both grey matter and ventricular volume did not replicate the results described in individual studies, including ones outlined above (Fusar-Poli et al. 2013). Reasons for this may be due to a lack of overlapping results secondary to variation in treatment approaches and definitions of response, as well as disparate neuroimaging and analytic approaches.

18.5 Functional Studies of Chronic Schizophrenia

Functional neuroimaging has been used to examine treatment response in chronic patients with schizophrenia spectrum disorders, largely reporting findings in the prefrontal cortex and striatum. Significantly increased activation of the dorsolateral prefrontal cortex, anterior cingulate cortex, and striatum was reported during passive viewing of stimuli with a negative emotional valance in the context of successful antipsychotic treatment over 22 weeks (Fahim et al. 2005). Refractory patients who responded to clozapine showed increased activation of dorsomedial prefrontal regions (Potvin et al. 2015). Furthermore, increased dorsolateral prefrontal activity during working memory paradigm was also noted to predict successful response to cognitive behavioral therapy for psychotic symptoms (Kumari et al. 2009). In addition to prefrontal findings, reward paradigms have been applied in chronic patients. Vanes et al. (2018) reported that responders to treatment failed to functionally engage the striatum during reward processing, compared to both treatment-resistant patients and healthy volunteers. This work differentiates antipsychotic treatment response by a reward-related mechanism, supporting the hypothesis that nonresponders to treatment may exhibit a non-dopaminergic pathophysiology.

Functional connectivity analyses have also been applied to capture treatment response in chronic schizophrenia. The connectivity strength between dopaminergic regions, such as the ventral tegmental area and midbrain to the anterior cingulate cortex, positively correlated with good response to a 6-week course of risperidone (Hadley et al. 2014). Moreover, successful treatment with olanzapine was associated with increases in connectivity within the default mode network (Sambataro et al. 2010), and aberrant intra-network connectivity within the dorsal attention network was normalized with successful antipsychotic treatment (Kraguljac et al. 2016b). Like the early-course literature, novel methods for examining large-scale functional connectivity shows both normalization of functional networks with antipsychotic treatment, as well as negative findings (Lottman et al. 2017; Bai et al. 2016).

18.6 Discussion

In the studies described above, there is evidence that neuroimaging parses the heterogeneity of response to treatment of psychotic symptoms with antipsychotic medications while elucidating potential mechanisms. Relatedly, neuroimaging may assist in clinical treatment by serving as a prognostic assay.

Some important clinical considerations should be noted. Across studies, definitions of response vary. An assortment of outcomes and groupings of patients are represented by the studies described, reflecting the complexity of schizophrenia and the various methods for characterizing outcomes to treatment. Standardization of response criteria has been suggested (Andreasen et al. 2005; Emsley et al. 2007), including a rigorous and uniform definition of nonresponse (Howes et al. 2017). In addition, it should be noted that antipsychotic treatments do not significantly impact the negative and cognitive symptoms of schizophrenia, which may result in the severe functional and social impairments characteristic of the illness (Remington et al. 2016; Kane and Correll 2010). As described above, some studies examined response to clozapine or focused on treatment refractory illness. Clozapine is uniquely efficacious for patients who have failed other antipsychotic drugs and plays an important role in treatment algorithms. For ultra-refractory patients who fail clozapine, electroconvulsive therapy is often delivered, which has long demonstrated efficacy for psychotic symptoms (Petrides et al. 2015). The classification of patients based on responsiveness to these therapies may become standard of care as our knowledge of the neurobiology underlying treatment improves, and if replicable biomarkers are identified (Remington et al. 2015).

Results described in this chapter show that there is an overall convergence of findings from neuroimaging studies in both early-course patients and chronic patients. These results suggest that variation in neural circuitry may encode

the potential for response to treatment, preceding the onset of psychosis, and may have its roots in neurodevelopment. Structural neuroimaging findings suggest that non-responders to treatment exhibit greater ventricular volumes, along with decreased grey matter density in regions important for cognitive functioning, including frontal and medial temporal regions, as well as other limbic and subcortical structures. Greater dysfunction within these regions that confer importance for cognition is also observed in functional MRI studies, though the variance of reported results is considerable. Though some evidence suggests that non-responders to antipsychotic treatment display overall decreased white matter integrity, DTI studies are limited in numbers, and distinct conclusions cannot be drawn for early-course and chronic illness. Of note, it is unknown how findings from structural and functional imaging modalities are related to each other and whether neurodevelopmentally encoded structural deficits in patients with poor outcomes precede functional observations.

Existing studies also indicate that the heterogeneity in clinical outcomes to antipsychotic treatment in patients with schizophrenia may be driven by neurobiologically distinct subtypes of illness. The development of novel therapeutic approaches may depend on stratifying our approaches to clinical trials on subgroupings of patients with distinct biological profiles. This approach may maximize the efficacy of therapeutic interventions. Progress in this effort may lead to more efficacious and personalized treatments. Efforts will require consistency across study designs, stringent and uniform outcome criteria, as well as consolidation of neuroimaging datasets via multisite studies. In addition, further integration of clinical trials with neuroimaging will bridge clinical care with neurobiology. Future work may also integrate neuroimaging-derived markers with combinations of demographic, neurocognitive, and pharmacogenomic markers to enhance our prognostic capabilities. While this chapter focuses on antipsychotic drugs, other treatment modalities for psychosis should be examined with neuroimaging, including electroconvulsive therapy, transcranial magnetic stimulation, and evidence-based psychosocial interventions. Future directions for the field include the incorporation of neuroimaging with data-driven, machine learning approaches to transition, from descriptions of differences between groups of patients, to prognostic inferences that can be made for individuals, to usher the field in the direction of precision medicine approaches for schizophrenia treatment.

Summary

- Overall, there is convergence of findings from studies of treatment response in both early-course and chronic patients with schizophrenia.
- Early studies focused on ventricular enlargement in first-episode psychosis found greater ventricular size in patients with poorer outcomes to treatment.
- Morphologic findings in patients with schizophrenia, ranging from first-episode psychosis to chronic, treatment-refractory illness, largely report decreased frontal and temporal gray matter volumes.
- Functional studies of treatment response via task and resting-state imaging report abnormalities in regions important for cognition within the prefrontal cortex and the striatum.
- DTI studies suggest that non-response to antipsychotic treatment is associated with overall decreased white matter integrity.

Acknowledgements This work was funded by K23MH110661, and a NARSAD Young Investigator Grant from the Brain & Behavior Research Foundation awarded to D.K.S.

References

Andreasen NC, Carpenter WT Jr, Kane JM, Lasser RA, Marder SR, Weinberger DR. Remission in schizophrenia: proposed criteria and rationale for consensus. Am J Psychiatry. 2005;162(3):441–9. https://doi.org/10.1176/appi.ajp.162.3.441.

Anticevic A, Hu X, Xiao Y, Hu J, Li F, Bi F, Cole MW, Savic A, Yang GJ, Repovs G, Murray JD, Wang XJ,

Huang X, Lui S, Krystal JH, Gong Q. Early-course unmedicated schizophrenia patients exhibit elevated prefrontal connectivity associated with longitudinal change. J Neurosci. 2015;35(1):267–86. https://doi.org/10.1523/jneurosci.2310-14.2015.

Arango C, Breier A, McMahon R, Carpenter WT Jr, Buchanan RW. The relationship of clozapine and haloperidol treatment response to prefrontal, hippocampal, and caudate brain volumes. Am J Psychiatry. 2003;160(8):1421–7. https://doi.org/10.1176/appi.ajp.160.8.1421.

Bai Y, Wang W, Xu J, Zhang F, Yu H, Luo C, Wang L, Chen X, Shan B, Xu L, Xu X, Cheng Y. Altered resting-state regional homogeneity after 13 weeks of paliperidone injection treatment in schizophrenia patients. Psychiatry Res. 2016;258:37–43. https://doi.org/10.1016/j.pscychresns.2016.10.008.

Bartzokis G, Lu PH, Amar CP, Raven EP, Detore NR, Altshuler LL, Mintz J, Ventura J, Casaus LR, Luo JS, Subotnik KL, Nuechterlein KH. Long acting injection versus oral risperidone in first-episode schizophrenia: differential impact on white matter myelination trajectory. Schizophr Res. 2011;132(1):35–41. https://doi.org/10.1016/j.schres.2011.06.029.

Blasi G, Popolizio T, Taurisano P, Caforio G, Romano R, Di Giorgio A, Sambataro F, Rubino V, Latorre V, Lo Bianco L, Fazio L, Nardini M, Weinberger DR, Bertolino A. Changes in prefrontal and amygdala activity during olanzapine treatment in schizophrenia. Psychiatry Res. 2009;173(1):31–8. https://doi.org/10.1016/j.pscychresns.2008.09.001.

Bleuler M. A 23-year longitudinal study of 208 schizophrenics and impressions in regard to the nature of schizophrenia. J Psychiatr Res. 1968;6(Suppl 1):3–12.

Bodnar M, Harvey PO, Malla AK, Joober R, Lepage M. The parahippocampal gyrus as a neural marker of early remission in first-episode psychosis: a voxel-based morphometry study. Clin Schizophr Relat Psychoses. 2011;4(4):217–28. https://doi.org/10.3371/csrp.4.4.2.

Bodnar M, Malla AK, Joober R, Lord C, Smith E, Pruessner J, Lepage M. Neural markers of early remission in first-episode schizophrenia: a volumetric neuroimaging study of the parahippocampus. Psychiatry Res. 2012a;201(1):40–7. https://doi.org/10.1016/j.pscychresns.2011.07.012.

Bodnar M, Achim AM, Malla AK, Joober R, Benoit A, Lepage M. Functional magnetic resonance imaging correlates of memory encoding in relation to achieving remission in first-episode schizophrenia. Br J Psychiatry. 2012b;200(4):300–7. https://doi.org/10.1192/bjp.bp.111.098046.

Cahn W, van Haren NE, Hulshoff Pol HE, Schnack HG, Caspers E, Laponder DA, Kahn RS. Brain volume changes in the first year of illness and 5-year outcome of schizophrenia. Br J Psychiatry. 2006;189:381–2. https://doi.org/10.1192/bjp.bp.105.015701.

Carbon M, Correll CU. Clinical predictors of therapeutic response to antipsychotics in schizophrenia. Dialogues Clin Neurosci. 2014;16(4):505–24.

Crossley NA, Marques TR, Taylor H, Chaddock C, Dell'Acqua F, Reinders AA, Mondelli V, DiForti M, Simmons A, David AS, Kapur S, Pariante CM, Murray RM, Dazzan P. Connectomic correlates of response to treatment in first-episode psychosis. Brain. 2017;140(2):487–96. https://doi.org/10.1093/brain/aww297.

Ebdrup BH, Skimminge A, Rasmussen H, Aggernaes B, Oranje B, Lublin H, Baare W, Glenthoj B. Progressive striatal and hippocampal volume loss in initially antipsychotic-naive, first-episode schizophrenia patients treated with quetiapine: relationship to dose and symptoms. Int J Neuropsychopharmacol. 2011;14(1):69–82. https://doi.org/10.1017/s1461145710000817.

Emsley R, Rabinowitz J, Medori R. Remission in early psychosis: rates, predictors, and clinical and functional outcome correlates. Schizophr Res. 2007;89(1–3):129–39. https://doi.org/10.1016/j.schres.2006.09.013.

Fahim C, Stip E, Mancini-Marie A, Gendron A, Mensour B, Beauregard M. Differential hemodynamic brain activity in schizophrenia patients with blunted affect during quetiapine treatment. J Clin Psychopharmacol. 2005;25(4):367–71.

Friedman L, Lys C, Schulz SC. The relationship of structural brain imaging parameters to antipsychotic treatment response: a review. J Psychiatry Neurosci. 1992;17(2):42–54.

Fung G, Cheung C, Chen E, Lam C, Chiu C, Law CW, Leung MK, Deng M, Cheung V, Qi L, Nailin Y, Tai KS, Yip L, Suckling J, Sham P, McAlonan G, Chua SE. MRI predicts remission at 1 year in first-episode schizophrenia in females with larger striato-thalamic volumes. Neuropsychobiology. 2014;69(4):243–8. https://doi.org/10.1159/000358837.

Fusar-Poli P, Smieskova R, Kempton MJ, Ho BC, Andreasen NC, Borgwardt S. Progressive brain changes in schizophrenia related to antipsychotic treatment? A meta-analysis of longitudinal MRI studies. Neurosci Biobehav Rev. 2013;37(8):1680–91. https://doi.org/10.1016/j.neubiorev.2013.06.001.

Garver DL, Holcomb JA, Christensen JD. Compromised myelin integrity during psychosis with repair during remission in drug-responding schizophrenia. Int J Neuropsychopharmacol. 2008;11(1):49–61. https://doi.org/10.1017/s1461145707007730.

Goghari VM, Smith GN, Honer WG, Kopala LC, Thornton AE, Su W, Macewan GW, Lang DJ. Effects of eight weeks of atypical antipsychotic treatment on middle frontal thickness in drug-naive first-episode psychosis patients. Schizophr Res. 2013;149(1–3):149–55. https://doi.org/10.1016/j.schres.2013.06.025.

Guo JY, Huhtaniska S, Miettunen J, Jaaskelainen E, Kiviniemi V, Nikkinen J, Moilanen J, Haapea M, Maki P, Jones PB, Veijola J, Isohanni M, Murray GK. Longitudinal regional brain volume loss in schizophrenia: relationship to antipsychotic medication and change in social function. Schizophr Res.

2015;168(1–2):297–304. https://doi.org/10.1016/j.schres.2015.06.016.

Guo W, Liu F, Chen J, Wu R, Li L, Zhang Z, Chen H, Zhao J. Olanzapine modulates the default-mode network homogeneity in recurrent drug-free schizophrenia at rest. Aust N Z J Psychiatry. 2017;51(10):1000–9. https://doi.org/10.1177/0004867417714952.

Guo W, Liu F, Chen J, Wu R, Li L, Zhang Z, Chen H, Zhao J. Treatment effects of olanzapine on homotopic connectivity in drug-free schizophrenia at rest. World J Biol Psychiatry. 2018;19(Suppl 3):S106–14. https://doi.org/10.1080/15622975.2017.1346280.

Hadley JA, Nenert R, Kraguljac NV, Bolding MS, White DM, Skidmore FM, Visscher KM, Lahti AC. Ventral tegmental area/midbrain functional connectivity and response to antipsychotic medication in schizophrenia. Neuropsychopharmacology. 2014;39(4):1020–30. https://doi.org/10.1038/npp.2013.305.

Ho BC, Andreasen NC, Nopoulos P, Arndt S, Magnotta V, Flaum M. Progressive structural brain abnormalities and their relationship to clinical outcome: a longitudinal magnetic resonance imaging study early in schizophrenia. Arch Gen Psychiatry. 2003;60(6):585–94. https://doi.org/10.1001/archpsyc.60.6.585.

Howes OD, McCutcheon R, Agid O, de Bartolomeis A, van Beveren NJ, Birnbaum ML, Bloomfield MA, Bressan RA, Buchanan RW, Carpenter WT, Castle DJ, Citrome L, Daskalakis ZJ, Davidson M, Drake RJ, Dursun S, Ebdrup BH, Elkis H, Falkai P, Fleischacker WW, Gadelha A, Gaughran F, Glenthoj BY, Graff-Guerrero A, Hallak JE, Honer WG, Kennedy J, Kinon BJ, Lawrie SM, Lee J, Leweke FM, MacCabe JH, McNabb CB, Meltzer H, Moller HJ, Nakajima S, Pantelis C, Reis Marques T, Remington G, Rossell SL, Russell BR, Siu CO, Suzuki T, Sommer IE, Taylor D, Thomas N, Ucok A, Umbricht D, Walters JT, Kane J, Correll CU. Treatment-resistant schizophrenia: treatment response and resistance in psychosis (TRRIP) working group consensus guidelines on diagnosis and terminology. Am J Psychiatry. 2017;174(3):216–29. https://doi.org/10.1176/appi.ajp.2016.16050503.

Huber G, Gross G, Schuttler R, Linz M. Longitudinal studies of schizophrenic patients. Schizophr Bull. 1980;6(4):592–605.

Jaaskelainen E, Juola P, Kurtti J, Haapea M, Kyllonen M, Miettunen J, Tanskanen P, Murray GK, Huhtaniska S, Barnes A, Veijola J, Isohanni M. Associations between brain morphology and outcome in schizophrenia in a general population sample. Eur Psychiatry. 2014;29(7):456–62. https://doi.org/10.1016/j.eurpsy.2013.10.006.

Kane JM, Correll CU. Past and present progress in the pharmacologic treatment of schizophrenia. J Clin Psychiatry. 2010;71(9):1115–24. https://doi.org/10.4088/JCP.10r06264yel.

Kaplan MJ, Lazoff M, Kelly K, Lukin R, Garver DL. Enlargement of cerebral third ventricle in psychotic patients with delayed response to neuroleptics. Biol Psychiatry. 1990;27(2):205–14.

Kapur S, Mamo D. Half a century of antipsychotics and still a central role for dopamine D2 receptors. Prog Neuropsychopharmacol Biol Psychiatry. 2003;27(7):1081–90. https://doi.org/10.1016/j.pnpbp.2003.09.004.

Kasparek T, Prikryl R, Schwarz D, Kucerova H, Marecek R, Mikl M, Vanicek J, Ceskova E. Gray matter morphology and the level of functioning in one-year follow-up of first-episode schizophrenia patients. Prog Neuropsychopharmacol Biol Psychiatry. 2009;33(8):1438–46. https://doi.org/10.1016/j.pnpbp.2009.07.025.

Kennedy JL, Altar CA, Taylor DL, Degtiar I, Hornberger JC. The social and economic burden of treatment-resistant schizophrenia: a systematic literature review. Int Clin Psychopharmacol. 2014;29(2):63–76. https://doi.org/10.1097/YIC.0b013e32836508e6.

Kraguljac NV, White DM, Hadley N, Hadley JA, Ver Hoef L, Davis E, Lahti AC. Aberrant hippocampal connectivity in unmedicated patients with schizophrenia and effects of antipsychotic medication: a longitudinal resting state functional MRI study. Schizophr Bull. 2016a;42(4):1046–55. https://doi.org/10.1093/schbul/sbv228.

Kraguljac NV, White DM, Hadley JA, Visscher K, Knight D, ver Hoef L, Falola B, Lahti AC. Abnormalities in large scale functional networks in unmedicated patients with schizophrenia and effects of risperidone. Neuroimage Clin. 2016b;10:146–58. https://doi.org/10.1016/j.nicl.2015.11.015.

Kumari V, Peters ER, Fannon D, Antonova E, Premkumar P, Anilkumar AP, Williams SC, Kuipers E. Dorsolateral prefrontal cortex activity predicts responsiveness to cognitive-behavioral therapy in schizophrenia. Biol Psychiatry. 2009;66(6):594–602. https://doi.org/10.1016/j.biopsych.2009.04.036.

Lawrie SM, Ingle GT, Santosh CG, Rogers AC, Rimmington JE, Naidu KP, Best JJ, O'Carroll R, Goodwin GM, Ebmeier KP, et al. Magnetic resonance imaging and single photon emission tomography in treatment-responsive and treatment-resistant schizophrenia. Br J Psychiatry. 1995;167(2):202–10.

Li M, Chen Z, Deng W, He Z, Wang Q, Jiang L, Ma X, Wang Y, Chua SE, Cheung C, McAlonan GM, Sham PC, Collier DA, Gong Q, Li T. Volume increases in putamen associated with positive symptom reduction in previously drug-naive schizophrenia after 6 weeks antipsychotic treatment. Psychol Med. 2012;42(7):1475–83. https://doi.org/10.1017/s0033291711002157.

Lieberman J, Chakos M, Wu H, Alvir J, Hoffman E, Robinson D, Bilder R. Longitudinal study of brain morphology in first episode schizophrenia. Biol Psychiatry. 2001;49(6):487–99.

Lieberman JA, Tollefson GD, Charles C, Zipursky R, Sharma T, Kahn RS, Keefe RS, Green AI, Gur RE, McEvoy J, Perkins D, Hamer RM, Gu H, Tohen M. Antipsychotic drug effects on brain morphology in first-episode psychosis. Arch Gen Psychiatry.

2005;62(4):361–70. https://doi.org/10.1001/archpsyc.62.4.361.

Lottman KK, Kraguljac NV, White DM, Morgan CJ, Calhoun VD, Butt A, Lahti AC. Risperidone effects on brain dynamic connectivity—a prospective resting-state fMRI study in schizophrenia. Front Psychiatry. 2017;8:14. https://doi.org/10.3389/fpsyt.2017.00014.

Luck D, Buchy L, Czechowska Y, Bodnar M, Pike GB, Campbell JS, Achim A, Malla A, Joober R, Lepage M. Fronto-temporal disconnectivity and clinical short-term outcome in first episode psychosis: a DTI-tractography study. J Psychiatr Res. 2011;45(3):369–77. https://doi.org/10.1016/j.jpsychires.2010.07.007.

Lui S, Li T, Deng W, Jiang L, Wu Q, Tang H, Yue Q, Huang X, Chan RC, Collier DA, Meda SA, Pearlson G, Mechelli A, Sweeney JA, Gong Q. Short-term effects of antipsychotic treatment on cerebral function in drug-naive first-episode schizophrenia revealed by "resting state" functional magnetic resonance imaging. Arch Gen Psychiatry. 2010;67(8):783–92. https://doi.org/10.1001/archgenpsychiatry.2010.84.

McClure RK, Phillips I, Jazayerli R, Barnett A, Coppola R, Weinberger DR. Regional change in brain morphometry in schizophrenia associated with antipsychotic treatment. Psychiatry Res. 2006;148(2–3):121–32. https://doi.org/10.1016/j.pscychresns.2006.04.008.

Millan MJ, Andrieux A, Bartzokis G, Cadenhead K, Dazzan P, Fusar-Poli P, Gallinat J, Giedd J, Grayson DR, Heinrichs M, Kahn R, Krebs MO, Leboyer M, Lewis D, Marin O, Marin P, Meyer-Lindenberg A, McGorry P, McGuire P, Owen MJ, Patterson P, Sawa A, Spedding M, Uhlhaas P, Vaccarino F, Wahlestedt C, Weinberger D. Altering the course of schizophrenia: progress and perspectives. Nat Rev Drug Discov. 2016;15(7):485–515. https://doi.org/10.1038/nrd.2016.28.

Mitelman SA, Newmark RE, Torosjan Y, Chu KW, Brickman AM, Haznedar MM, Hazlett EA, Tang CY, Shihabuddin L, Buchsbaum MS. White matter fractional anisotropy and outcome in schizophrenia. Schizophr Res. 2006;87(1–3):138–59. https://doi.org/10.1016/j.schres.2006.06.016.

Molina V, Taboada D, Aragues M, Hernandez JA, Sanz-Fuentenebro J. Greater clinical and cognitive improvement with clozapine and risperidone associated with a thinner cortex at baseline in first-episode schizophrenia. Schizophr Res. 2014;158(1–3):223–9. https://doi.org/10.1016/j.schres.2014.06.042.

Nejad AB, Ebdrup BH, Glenthoj BY, Siebner HR. Brain connectivity studies in schizophrenia: unravelling the effects of antipsychotics. Curr Neuropharmacol. 2012;10(3):219–30. https://doi.org/10.2174/157015912803217305.

Nielsen MO, Rostrup E, Wulff S, Bak N, Broberg BV, Lublin H, Kapur S, Glenthoj B. Improvement of brain reward abnormalities by antipsychotic monotherapy in schizophrenia. Arch Gen Psychiatry. 2012;69(12):1195–204. https://doi.org/10.1001/archgenpsychiatry.2012.847.

Nielsen MO, Rostrup E, Wulff S, Glenthoj B, Ebdrup BH. Striatal reward activity and antipsychotic-associated weight change in patients with schizophrenia undergoing initial treatment. JAMA Psychiat. 2016;73(2):121–8. https://doi.org/10.1001/jamapsychiatry.2015.2582.

Palaniyappan L, Marques TR, Taylor H, Handley R, Mondelli V, Bonaccorso S, Giordano A, McQueen G, DiForti M, Simmons A, David AS, Pariante CM, Murray RM, Dazzan P. Cortical folding defects as markers of poor treatment response in first-episode psychosis. JAMA Psychiat. 2013;70(10):1031–40. https://doi.org/10.1001/jamapsychiatry.2013.203.

Palaniyappan L, Marques TR, Taylor H, Mondelli V, Reinders A, Bonaccorso S, Giordano A, DiForti M, Simmons A, David AS, Pariante CM, Murray RM, Dazzan P. Globally efficient brain organization and treatment response in psychosis: a connectomic study of gyrification. Schizophr Bull. 2016;42(6):1446–56. https://doi.org/10.1093/schbul/sbw069.

Panenka WJ, Khorram B, Barr AM, Smith GN, Lang DJ, Kopala LC, Vandorpe RA, Honer WG. A longitudinal study on the effects of typical versus atypical antipsychotic drugs on hippocampal volume in schizophrenia. Schizophr Res. 2007;94(1–3):288–92. https://doi.org/10.1016/j.schres.2007.05.002.

Petrides G, Malur C, Braga RJ, Bailine SH, Schooler NR, Malhotra AK, Kane JM, Sanghani S, Goldberg TE, John M, Mendelowitz A. Electroconvulsive therapy augmentation in clozapine-resistant schizophrenia: a prospective, randomized study. Am J Psychiatry. 2015;172(1):52–8. https://doi.org/10.1176/appi.ajp.2014.13060787.

Potvin S, Tikasz A, Lungu O, Dumais A, Stip E, Mendrek A. Emotion processing in treatment-resistant schizophrenia patients treated with clozapine: an fMRI study. Schizophr Res. 2015;168(1–2):377–80. https://doi.org/10.1016/j.schres.2015.07.046.

Prasad KM, Sahni SD, Rohm BR, Keshavan MS. Dorsolateral prefrontal cortex morphology and short-term outcome in first-episode schizophrenia. Psychiatry Res. 2005;140(2):147–55. https://doi.org/10.1016/j.pscychresns.2004.05.009.

Quarantelli M, Palladino O, Prinster A, Schiavone V, Carotenuto B, Brunetti A, Marsili A, Casiello M, Muscettola G, Salvatore M, de Bartolomeis A. Patients with poor response to antipsychotics have a more severe pattern of frontal atrophy: a voxel-based morphometry study of treatment resistance in schizophrenia. Biomed Res Int. 2014;2014:325052. https://doi.org/10.1155/2014/325052.

Reis Marques T, Taylor H, Chaddock C, Dell'Acqua F, Handley R, Reinders AA, Mondelli V, Bonaccorso S, Diforti M, Simmons A, David AS, Murray RM, Pariante CM, Kapur S, Dazzan P. White matter integrity as a predictor of response to treatment in first episode psychosis. Brain. 2014;137(Pt 1):172–82. https://doi.org/10.1093/brain/awt310.

Remington G, Agid O, Foussias G, Fervaha G, Takeuchi H, Lee J, Hahn M. What does schizophrenia teach us

about antipsychotics? Can J Psychiatry. 2015;60(3 Suppl 2):S14–8.

Remington G, Foussias G, Fervaha G, Agid O, Takeuchi H, Lee J, Hahn M. Treating negative symptoms in schizophrenia: an update. Curr Treat Options Psychiatry. 2016;3:133–50. https://doi.org/10.1007/s40501-016-0075-8.

Robinson DG, Woerner MG, Alvir JM, Geisler S, Koreen A, Sheitman B, Chakos M, Mayerhoff D, Bilder R, Goldman R, Lieberman JA. Predictors of treatment response from a first episode of schizophrenia or schizoaffective disorder. Am J Psychiatry. 1999;156(4):544–9. https://doi.org/10.1176/ajp.156.4.544.

Roiz-Santianez R, Tordesillas-Gutierrez D, Ortiz-Garcia de la Foz V, Ayesa-Arriola R, Gutierrez A, Tabares-Seisdedos R, Vazquez-Barquero JL, Crespo-Facorro B. Effect of antipsychotic drugs on cortical thickness. A randomized controlled one-year follow-up study of haloperidol, risperidone and olanzapine. Schizophr Res. 2012;141(1):22–8. https://doi.org/10.1016/j.schres.2012.07.014.

Samartzis L, Dima D, Fusar-Poli P, Kyriakopoulos M. White matter alterations in early stages of schizophrenia: a systematic review of diffusion tensor imaging studies. J Neuroimaging. 2014;24(2):101–10. https://doi.org/10.1111/j.1552-6569.2012.00779.x.

Sambataro F, Blasi G, Fazio L, Caforio G, Taurisano P, Romano R, Di Giorgio A, Gelao B, Lo Bianco L, Papazacharias A, Popolizio T, Nardini M, Bertolino A. Treatment with olanzapine is associated with modulation of the default mode network in patients with schizophrenia. Neuropsychopharmacology. 2010;35(4):904–12. https://doi.org/10.1038/npp.2009.192.

Sarpal DK, Robinson DG, Lencz T, Argyelan M, Ikuta T, Karlsgodt K, Gallego JA, Kane JM, Szeszko PR, Malhotra AK. Antipsychotic treatment and functional connectivity of the striatum in first-episode schizophrenia. JAMA Psychiat. 2015;72(1):5–13. https://doi.org/10.1001/jamapsychiatry.2014.1734.

Sarpal DK, Argyelan M, Robinson DG, Szeszko PR, Karlsgodt KH, John M, Weissman N, Gallego JA, Kane JM, Lencz T, Malhotra AK. Baseline striatal functional connectivity as a predictor of response to antipsychotic drug treatment. Am J Psychiatry. 2016;173(1):69–77. https://doi.org/10.1176/appi.ajp.2015.14121571.

Savas HA, Unal B, Erbagci H, Inaloz S, Herken H, Canan S, Gumusburun E, Zoroglu SS. Hippocampal volume in schizophrenia and its relationship with risperidone treatment: a stereological study. Neuropsychobiology. 2002;46(2):61–6. https://doi.org/10.1159/000065413.

Scheepers FE, de Wied CC, Hulshoff Pol HE, van de Flier W, van der Linden JA, Kahn RS. The effect of clozapine on caudate nucleus volume in schizophrenic patients previously treated with typical antipsychotics. Neuropsychopharmacology. 2001;24(1):47–54. https://doi.org/10.1016/s0893-133x(00)00172-x.

Schroder J, Geider FJ, Sauer H. Can computerised tomography be used to predict early treatment response in schizophrenia? Br J Psychiatry Suppl. 1993;21:13–5.

Serpa MH, Doshi J, Erus G, Chaim-Avancini TM, Cavallet M, van de Bilt MT, Sallet PC, Gattaz WF, Davatzikos C, Busatto GF, Zanetti MV. State-dependent microstructural white matter changes in drug-naive patients with first-episode psychosis. Psychol Med. 2017;47(15):2613–27. https://doi.org/10.1017/s0033291717001015.

Snitz BE, MacDonald A 3rd, Cohen JD, Cho RY, Becker T, Carter CS. Lateral and medial hypofrontality in first-episode schizophrenia: functional activity in a medication-naive state and effects of short-term atypical antipsychotic treatment. Am J Psychiatry. 2005;162(12):2322–9. https://doi.org/10.1176/appi.ajp.162.12.2322.

Staal WG, Hulshoff Pol HE, Schnack HG, van Haren NE, Seifert N, Kahn RS. Structural brain abnormalities in chronic schizophrenia at the extremes of the outcome spectrum. Am J Psychiatry. 2001;158(7):1140–2. https://doi.org/10.1176/appi.ajp.158.7.1140.

Strungas S, Christensen JD, Holcomb JM, Garver DL. State-related thalamic changes during antipsychotic treatment in schizophrenia: preliminary observations. Psychiatry Res. 2003;124(2):121–4.

Szeszko PR, Narr KL, Phillips OR, McCormack J, Sevy S, Gunduz-Bruce H, Kane JM, Bilder RM, Robinson DG. Magnetic resonance imaging predictors of treatment response in first-episode schizophrenia. Schizophr Bull. 2012;38(3):569–78. https://doi.org/10.1093/schbul/sbq126.

Szeszko PR, Robinson DG, Ikuta T, Peters BD, Gallego JA, Kane J, Malhotra AK. White matter changes associated with antipsychotic treatment in first-episode psychosis. Neuropsychopharmacology. 2014;39(6):1324–31. https://doi.org/10.1038/npp.2013.288.

Vanes LD, Mouchlianitis E, Collier T, Averbeck BB, Shergill SS. Differential neural reward mechanisms in treatment-responsive and treatment-resistant schizophrenia. Psychol Med. 2018;48(14):2418–27.

van den Heuvel MP, Fornito A. Brain networks in schizophrenia. Neuropsychol Rev. 2014;24(1):32–48. https://doi.org/10.1007/s11065-014-9248-7.

van Haren NE, Cahn W, Hulshoff Pol HE, Schnack HG, Caspers E, Lemstra A, Sitskoorn MM, Wiersma D, van den Bosch RJ, Dingemans PM, Schene AH, Kahn RS. Brain volumes as predictor of outcome in recent-onset schizophrenia: a multi-center MRI study. Schizophr Res. 2003;64(1):41–52.

van Veelen NM, Vink M, Ramsey NF, van Buuren M, Hoogendam JM, Kahn RS. Prefrontal lobe dysfunction predicts treatment response in medication-naive first-episode schizophrenia. Schizophr Res. 2011;129(2–3):156–62. https://doi.org/10.1016/j.schres.2011.03.026.

Wang Y, Tang W, Fan X, Zhang J, Geng D, Jiang K, Zhu D, Song Z, Xiao Z, Liu D. Resting-state functional connectivity changes within the default mode network and the salience network after antipsychotic treatment

in early-phase schizophrenia. Neuropsychiatr Dis Treat. 2017;13:397–406. https://doi.org/10.2147/ndt.s123598.

Wassink TH, Andreasen NC, Nopoulos P, Flaum M. Cerebellar morphology as a predictor of symptom and psychosocial outcome in schizophrenia. Biol Psychiatry. 1999;45(1):41–8.

Weinberger DR, Bigelow LB, Kleinman JE, Klein ST, Rosenblatt JE, Wyatt RJ. Cerebral ventricular enlargement in chronic schizophrenia. An association with poor response to treatment. Arch Gen Psychiatry. 1980;37(1):11–3.

Wobrock T, Gruber O, Schneider-Axmann T, Wolwer W, Gaebel W, Riesbeck M, Maier W, Klosterkotter J, Schneider F, Buchkremer G, Moller HJ, Schmitt A, Bender S, Schlosser R, Falkai P. Internal capsule size associated with outcome in first-episode schizophrenia. Eur Arch Psychiatry Clin Neurosci. 2009;259(5):278–83. https://doi.org/10.1007/s00406-008-0867-y.

Zeng B, Ardekani BA, Tang Y, Zhang T, Zhao S, Cui H, Fan X, Zhuo K, Li C, Xu Y, Goff DC, Wang J. Abnormal white matter microstructure in drug-naive first episode schizophrenia patients before and after eight weeks of antipsychotic treatment. Schizophr Res. 2016;172(1–3):1–8. https://doi.org/10.1016/j.schres.2016.01.051.

Zipursky RB, Zhang-Wong J, Lambe EK, Bean G, Beiser M. MRI correlates of treatment response in first episode psychosis. Schizophr Res. 1980;30(1):81–90.

Zugman A, Gadelha A, Assuncao I, Sato J, Ota VK, Rocha DL, Mari JJ, Belangero SI, Bressan RA, Brietzke E, Jackowski AP. Reduced dorso-lateral prefrontal cortex in treatment resistant schizophrenia. Schizophr Res. 2013;148(1–3):81–6. https://doi.org/10.1016/j.schres.2013.05.002.

19 Omega-3 Polyunsaturated Fatty Acids and Antioxidants for the Treatment of Schizophrenia: A Role for Magnetic Resonance Imaging

Rosarito Clari, Robert K. McNamara, and Philip R. Szeszko

Contents

19.1 Introduction

Although antipsychotics are considered the main treatment for schizophrenia, they are associated with significant side effects including weight gain, cardiometabolic effects, and sexual dysfunction. Because of these side effects, many patients often relapse due to nonadherence. There is therefore a critical need to understand whether alternative pharmacologic treatments can be used to assist in the clinical management of schizophrenia. In this chapter we discuss a potential role for omega-3 polyunsaturated fatty acids (PUFAs) and antioxidants in the treatment of schizophrenia and how neuroimaging may assist in understanding their mechanisms of action.

R. Clari
Department of Psychiatry, Icahn School of Medicine at Mount Sinai, New York, NY, USA

R. K. McNamara
Department of Psychiatry and Behavioral Neuroscience, Lipidomics Research Program, University of Cincinnati College of Medicine, Cincinnati, OH, USA

P. R. Szeszko (✉)
Department of Psychiatry, Icahn School of Medicine at Mount Sinai, New York, NY, USA

James J. Peters VA Medical Center, Mental Illness Research Education Clinical Center (MIRECC), Bronx, NY, USA
e-mail: philip.szeszko@va.gov, philip.szeszko@mssm.edu

M. Kubicki, M. E. Shenton (eds.), *Neuroimaging in Schizophrenia*,
https://doi.org/10.1007/978-3-030-35206-6_19

The membrane hypothesis of schizophrenia posits that abnormalities in the metabolism and/or structure of membrane phospholipids are involved in the pathophysiology of schizophrenia, and may be caused, in part, by alterations in brain fatty acid composition (Horrobin et al. 1994; Horrobin 1998). We examine the evidence for this hypothesis by first describing PUFAs and their physiological functions. Given their strong association with neuropsychiatric disorders, we focus on omega-3 PUFAs, including eicosapentaenoic acid (EPA), docosapentaenoic acid (DPA), and docosahexaenoic acid (DHA).

Oxidation is a chemical process that occurs in the brain, which is associated with the production of free radicals and deleterious effects on brain structure and function. Antioxidants are compounds that can inhibit the process of oxidation. In this chapter, we discuss abnormal oxidation in the brains of individuals with psychosis and emphasize a role for manganese superoxide dismutase (MnSOD) and glutathione peroxidase-1 (GPX1) in this process.

Limitations associated with a postmortem approach to understanding how fatty acids and antioxidants impact the brain in both healthy aging and neuropsychiatric disorders warrant alternative methods (McNamara 2013). Magnetic resonance (MR) imaging is well-suited to provide insight into the role that fatty acids and antioxidants play in brain structure and function *in vivo*. MR imaging techniques, such as phosphorous magnetic resonance spectroscopy (^{31}P MRS), can yield information regarding the neurochemical composition of the brain, including phosphomonoesters, which are important in the biosynthesis and degradation of neuronal membranes, cellular energetics, and pH level. Additionally, because myelin is formed from oligodendrocyte membranes that are comprised in part by fatty acids, techniques such as diffusion tensor imaging (DTI) may elucidate the nature of the associations between omega-3 PUFAs and putative white matter microstructural integrity. We therefore discuss how these and other MR imaging techniques could shed light onto the role of omega-3 PUFAs and antioxidants in the pathophysiology and treatment of schizophrenia in an effort to guide future research.

19.2 Polyunsaturated Fatty Acids

PUFAs account for approximately 35% of all cell membrane phospholipids (Benatti et al. 2004). The phospholipid composition of membranes is involved in the activation of ion channels and other enzyme functions (e.g., regulation of sodium/potassium channels and cAMP) that are critical to cellular neurotransmission. Depending on the position of the first double bond in the carbon chain, PUFAs can be classified into omega-3 (*n*-3) or omega-6 (*n*-6) fatty acids. In the case of omega-3, the first double bond occurs between the third and fourth carbon atoms, and for omega-6, the bond is between the sixth and seventh carbon atoms (Youdim et al. 2000). Linoleic acid (LA, 18:2; *n*-6) and alpha-linoleic acid (ALA, 18:3; *n*-3), the respective short-chain precursors of the omega-6 and omega-3 PUFAs, are considered "essential" because the body cannot synthesize them and they therefore must be obtained from the diet. Marine organisms such as fatty fish and fish oils are the primary dietary sources of preformed EPA (C20:5; *n*-3), DHA (C22:6; *n*-3), and to a lesser extent, DPA (C22:5; *n*-3) (Youdim et al. 2000).

PUFAs have several important physiological functions in the brain, including, but not limited to, energy storage and production, gene expression, and cell signaling (Liu et al. 2015; Luchtman and Song 2013). Both EPA and DHA take part in the synthesis of bioactive metabolites (i.e., eicosanoids), which have inflammation-resolving properties and are protective against oxidative stress. For example, omega-3 PUFAs can reduce inflammatory responses by enhancing glutathione-related antioxidant pathways (Smesny et al. 2015). Additionally, several studies indicate that DPA is bioactive (Skulas-Ray et al. 2015; Dangi et al. 2009; Dalli et al. 2013) and plays a role in lipid metabolism and inflammatory processes (Kaur et al. 2016).

As a potential therapeutic agent, omega-3 PUFAs have generated considerable enthusiasm given their relative safety, minimal side effects, and low cost. Clinical studies utilizing omega-3 PUFAs have focused on a number of medical conditions, including the primary and secondary prevention

of cardiovascular disease. The question of whether omega-3 PUFAs can aid in the treatment of brain disorders such as schizophrenia, and how neuroimaging can assist in this regard, represents an important goal of research. Over the last decade there has been a substantial increase in the number of studies investigating the relationship between PUFA intake, or biostatus, and indices of MR imaging in healthy humans (McNamara et al. 2018a). In a recent review, Bos et al. (2016) summarized the effects of omega-3 PUFAs from 24 published studies focusing on brain structure and function. This review suggested that naturalistic studies and clinical trials in healthy subjects provide evidence that PUFA supplementation may increase functional activity in the prefrontal cortex of children and enhance gray matter volume and white matter integrity during aging. In contrast, fewer studies have examined the relationship between PUFA levels and/or their manipulation in relationship to indices of brain structure and function in schizophrenia and associated psychotic disorders.

There is growing evidence that omega-3 PUFAs may be relevant to the pathophysiology and progression of schizophrenia. Specifically, cross-sectional studies have reported low PUFA levels in red blood cell membranes (erythrocytes) (Yao et al. 1994; Peet et al. 1995; Arvindakshan et al. 2003a; van der Kemp et al. 2012) and postmortem brain tissue (Yao et al. 2000; Horrobin et al. 1991; McNamara et al. 2007) of patients with schizophrenia. Abnormalities in PUFA levels are present in the early stages of schizophrenia, including individuals who are antipsychotic drug naïve (Reddy et al. 2004) and at high risk for developing a psychotic disorder (Rice et al. 2015). Results from rodent studies further suggest that developmental omega-3 insufficiency leads to enduring abnormalities in neurochemical systems associated with the pathophysiology of schizophrenia, including glutamate (McNamara et al. 2017a) and dopamine (Zimmer et al. 2002). In the context of the membrane phospholipid hypothesis of schizophrenia (Horrobin et al. 1994), these findings have generated interest in the administration of PUFAs as an alternative or add-on treatment for schizophrenia symptomatology.

19.2.1 Omega-3 PUFA Treatment in Chronic Schizophrenia

Initial studies that investigated omega-3 PUFAs used patients with chronic schizophrenia. In a case report, Puri and Richardson (1998) described an antipsychotic-drug naïve patient with schizophrenia who exhibited a reduction in positive and negative symptoms following treatment with ethyl-EPA (2 g/day). EPA administration was also associated with a correction of membrane fatty acid levels and a reduction of neuronal membrane phospholipid turnover (Puri et al. 2000). In an open label study by Mellor et al. (1995), 20 patients with schizophrenia were given EPA (10 g/day) fish oil for 6 weeks, in addition to their antipsychotic medication. Study results revealed that PUFA supplementation had a remarkable effect on positive symptoms as well as tardive dyskinesia, and were accompanied by an increase in erythrocyte EPA levels. In contrast to the aforementioned studies, Fenton et al. (2001) found no effect on positive or negative symptoms, mood, or cognition following supplementation of 3 g/day of ethyl-EPA to patients with schizophrenia or schizoaffective disorder treated for 16 weeks.

In treatment-resistant schizophrenia, Emsley et al. (2002) reported a significant improvement in positive and negative symptoms and tardive dyskinesia after a 12-week placebo-controlled intervention of ethyl-EPA (3 g/day). Emsley and colleagues (2006) later failed to demonstrate the beneficial effect of 12 weeks of EPA (2 g/day) supplementation on tardive dyskinesia in a different sample of schizophrenia or schizoaffective patients. Peet and Horrobin (2002) performed a dose-ranging study of 1, 2, or 4 g/day with ethyl-EPA or placebo for 12 weeks in a large sample of treatment-resistant patients taking different antipsychotic medications. The authors described only a 2 g/day EPA positive effect on psychotic symptoms in patients treated with clozapine, but not in those treated with other antipsychotic medications.

In another study, patients received EPA/DHA (180:120 mg) and antioxidants (vitamins E and C, 400 IU:500 mg) for 16 weeks as adjunctive

therapy (Arvindakshan et al. 2003b). Patients' PUFA levels in erythrocytes and plasma lipid peroxides were assessed prior to and following the intervention. Post-intervention erythrocyte levels were significantly higher than pre-intervention levels and compared to healthy controls. Importantly, patients showed improvement in psychotic symptoms and overall quality of life. Sivrioglu et al. (2007) administered omega-3 PUFAs and vitamins E and C to haloperidol-treated patients with schizophrenia and similarly demonstrated a reduction in symptoms.

In a double-blind, placebo-controlled clinical trial with chronic schizophrenia patients, Peet et al. (2001) supplemented antipsychotic treatment with 2 g/day of EPA, DHA, or placebo for 3 months. EPA was more effective compared to DHA and placebo in attenuating psychotic symptoms. In another randomized, double-blind clinical trial (Jamilian et al. 2014), patients with schizophrenia were treated with 1000 mg/day of omega-3 or placebo for 8 weeks in addition to their antipsychotic medication. Although the omega-3 group showed a reduction in psychotic symptoms at weeks 4 and 6, the PUFA intervention was not found to be significantly more effective than placebo. In a study by Bentsen et al. (2013), patients with schizophrenia or related psychoses currently taking psychotropic medication were randomized into four groups: double placebo, active vitamins E (364 mg/day) and C (1000 mg/day), active ethyl-EPA (2 g/day), or double active. In patients with high erythrocyte PUFAs, none of the interventions affected psychotic symptoms. In patients with low PUFA levels, EPA alone was associated with greater psychotic symptoms. Vitamins alone were associated with greater severity of psychotic symptoms. Interestingly, adding vitamins to EPA neutralized this negative effect on symptoms. The authors suggested that the beneficial effect of PUFA and vitamins E and C might only be observed during a stabilized phase of the disorder in those patients with low PUFA levels.

19.2.2 Omega-3 PUFA Treatment in First-Episode Psychosis

There have been fewer clinical trials evaluating the effectiveness of omega-3 in first-episode schizophrenia and associated psychotic disorders. Peet et al. (2001) conducted a study with 30 antipsychotic-naïve first-episode psychosis or newly relapsed patients. Patients were given 2 g/day of EPA or placebo as the sole treatment for 3 months, unless it became necessary to prescribe antipsychotic drugs during the trial. By the end of the study, all patients on placebo, but only half of the patients on EPA, were taking antipsychotic medications. Overall, patients in the EPA group reported less psychotic symptoms than those in the placebo group. In a study by Berger et al. (2007), patients experiencing their first episode of psychosis received 2 g/day of ethyl-EPA or placebo for 12 weeks, in addition to traditional antipsychotics. Although patients showed improvement in the first 4–6 weeks of treatment, there was no sustained symptomatic benefit from supplementation of PUFA, which was attributed to a ceiling effect caused by the concurrent use of antipsychotic medications. Nonetheless, EPA coupled with antipsychotics was found to be effective, safe, and tolerable.

Emsley and colleagues (2014) conducted one of the first randomized, placebo-controlled clinical trials that focused specifically on the impact of PUFAs and a metabolic antioxidant in relapse prevention in schizophrenia. The administration consisted of 1 g/day of DHA, 2 g/day of EPA, and 300 mg/day of alpha-lipoic acid or placebo in recently relapsed first-episode psychosis patients for whom antipsychotic therapy was tapered and discontinued. Relapse rates were very high (and severe in some cases) in both groups, including those receiving active treatment (90%) and those receiving placebo (75%), which led to the premature termination of the study. The authors concluded that based on their findings, omega-3 PUFAs and antioxidants together do not seem to be an effective alternative to antipsychotic treat-

ment in relapse prevention. Pawelczyk et al. (2016) reported positive results after a 26-week intervention in first-episode psychosis involving 2.2 g/day of omega-3 PUFAs, 1.32 g/day of EPA and 0.88 g/day of DHA, or placebo as adjunctive therapy. Omega-3 supplementation was associated with a reduction in psychotic and depressive symptoms, and an increase in overall level of functioning.

In a study recently completed by our group (Robinson et al. 2019), we examined adjunctive omega-3 treatment for individuals experiencing recent-onset psychosis. Patients were treated for 16 weeks with risperidone and either omega-3 (EPA 740 mg/day and DHA 400 mg/day daily) or placebo. Longitudinal analysis of the total Brief Psychiatric Rating Scale (BPRS) score revealed trend level effects in favor of the omega-3 treatment. Among the subgroup of individuals who did not receive lorazepam, the omega-3 treatment effect on BPRS total scores was significant with the most pronounced effects evident in depression/anxiety, but no change with placebo. These data suggest that omega-3 supplementation may be one option for the treatment of depression and anxiety among individuals with recent-onset psychosis.

19.2.3 Omega-3 PUFA Treatment in Clinical High Risk and Ultra-High Risk for Psychosis

It is widely acknowledged that psychotic disorders are preceded by a prodromal phase in which functional decline and attenuated positive and negative symptoms can be observed (Bošnjak et al. 2016; Yung and Nelson 2011). Individuals that exhibit these symptoms are considered to be at clinical high-risk (CHR) or ultra-high risk for psychosis (UHR). The intensity of prodromal symptoms, coupled with additional risk factors, can accurately predict general functional outcome and clinical severity (Cannon et al. 2016). In addition, duration of untreated psychosis (DUP), the time between the onset of psychotic symptoms and initiation of treatment, is associated with poor outcome (Marshall et al. 2005). Therefore, interventions targeting the early phase of psychotic illness may not only attenuate symptoms, but might also assist in delaying or preventing the onset of frank psychosis.

An initial study by Amminger et al. (2010) raised the exciting possibility of delaying the transition to psychosis with omega-3 treatment. Eighty-one UHR adolescents and young adults were recruited for this 12-week study. Subjects were treated with either 1.2 g/day of EPA/DHA or placebo, in addition to their psychological and/or pharmacological treatment (i.e., antidepressants). The researchers monitored subjects for a 40-week period after omega-3 administration and reported that 4.9% in the PUFA group and 27.5% in the placebo group developed a psychotic disorder, respectively. There was also a concomitant reduction in overall psychotic symptoms and improvement in functioning in the group treated with PUFAs compared with placebo.

Follow-up studies carried out by Amminger and colleagues, using the same or part of the initial sample, confirmed the positive effect of omega-3 and shed light on the physiological profile of UHR individuals (Amminger et al. 2015a, b; Mossaheb et al. 2018). A follow-up study performed almost 7 years after the intervention revealed omega-3 supplementation had significantly reduced the risk of progression to psychosis (Amminger et al. 2015b). Baseline fatty acid levels were found to predict treatment response in the PUFA group in a very specific way. Individuals with high levels of erythrocyte membrane ALA and severe negative symptoms at baseline were more likely to show subsequent functional improvement than their counterparts (Amminger et al. 2015a). Moreover, changes in EPA levels throughout the study were the most significant predictors of outcome, even after controlling for baseline psychosocial functioning and overall psychopathology (Mossaheb et al. 2018). A secondary analysis of the 7-year longitudinal data (Berger et al. 2017)

demonstrated that a higher omega-6/omega-3 PUFA ratio in erythrocyte membranes is a risk biomarker for mood disorders, but not any other psychiatric disorder. Kim et al. (2014) examined biological correlates of cognitive symptoms and functioning in UHR individuals. They found that omega-9 eicosenoic and erucic acid levels were significantly higher, but omega-3 DHA levels were significantly lower, in those with cognitive and functional impairments.

More recent studies, however, have not replicated Amminger's et al. (2010) original findings. Cadenhead and colleagues (2017) recruited 127 clinical high risk individuals for a randomized, double-blind, placebo-controlled 6 month study where individuals were assigned to a combination of 740 mg of EPA and 400 mg of DHA or placebo. Although functional and symptomatic improvement was observed, the authors reported no significant differences between the transition rates to psychosis of the omega-3 (13%) and placebo (8%) groups. Interestingly, those who converted to psychosis were more likely to report low omega-3 PUFA daily consumption. Similarly, McGorry et al. (2017) conducted a multisite clinical trial in which 304 UHR individuals were randomly assigned to receive omega-3 (EPA 840 mg + DHA 560 mg) or placebo. In addition, participants received up to 20 sessions of cognitive behavioral case management (CBCM) over the 6-month study period and, if necessary, the 6-month follow-up. The only medications allowed during the study were antidepressants and benzodiazepines. The rates of psychotic conversion did not differ in the omega-3 versus placebo groups at 6 months (6.7% vs. 5.1%) or at 12 months (11.5% vs. 11.2%), respectively. In fact, both arms showed low transition rates and symptomatic remission. The authors attributed their negative findings to a possible ceiling effect caused by the other treatments received (i.e., CBCM and antidepressants/benzodiazepines).

19.2.4 Omega-3s and Magnetic Resonance Imaging

There is evidence that PUFAs cross the blood brain barrier in animal studies assessed using positron emission tomography (PET) [1-(11)C] DHA (Umhau et al. 2009). In that same study, healthy volunteers who underwent PET using [1-(11)C]DHA following intraveneous injection of DHA showed that the net rate of human brain DHA uptake was 3.8 ± 1.7 mg/day, implying that the half-life of DHA in the human brain is approximately 2.5 years. Preclinical studies, however, suggest that the half-life of DHA in rat brain is approximately 30 days with a constant dietary supply of omega-3 fatty acids, and that omega-*3* fatty acid deficiency robustly decreases the half-life of DHA (DeMar et al. 2004).

Several animal studies investigated the relationship between omega-3 deficits or enrichment on MR imaging measures. Using a mouse model, Li et al. (2015) reported that omega-3 PUFA dietary enrichment early in life provided a safe approach to limit the potentially deleterious behavioral and biochemical consequences of prenatal exposure to inflammation. These investigators reported that mice with prenatal exposure to maternal immune activation fed a standard diet had greater N-acetylaspartate/creatine (Cr) and lower *myo*-inositol/Cr levels within the cingulate cortex *in vivo* compared to those fed an omega-3 enriched diet. More recently, McNamara and colleagues (2018b) investigated the effects of altering brain DHA accrual during adolescence on white matter integrity in young adulthood. Periadolescent rats were randomized to one of three diets: a diet deficient in omega-3 PUFAs, a diet rich in DHA, or a control diet. DTI showed that omega-3 PUFA-deficient rats exhibited right-lateralized reductions in radial diffusivity and mean diffusivity in the external capsule, and increased axial diffusivity within the left corpus callosum and external capsule. The authors interpreted these findings to suggest the presence of demyelination and a disturbance in axonal pruning.

Cutuli et al. (2014) showed that aged mice receiving omega-3 PUFAs exhibited improved "hippocampal-dependent amnesic functions," and concomitant improvements in cellular plasticity and dampened neurodegeneration. In a follow-up study, Cutuli et al. (2016) investigated the effects of 8 weeks of omega-3 PUFA supplementation on cognitive (discriminative, spatial

and social) and emotional (anxiety and coping skills) abilities of aged C57B6/J mice in relationship to gray matter analyses assessed using high resolution voxel-based morphometry. Results indicated that following omega-3 treatment, the aged mice demonstrated better memory performance and coping skills that were associated with larger hippocampal, retrosplenial, and prefrontal gray matter volumes, and also greater omega-3 levels post-mortem. It should be noted that a study by Ahmad et al. (2004) used MR imaging to compute gray and white matter volumes in brains of older rats that were raised on an omega-3 deficient diet for three generations. The authors did not report any differences in the total or regional gray and white matter volumes of brains of older rats fed an omega-3 deficient or supplemented diet.

McNamara et al. (2019) examined the relationship between repeated amphetamine exposure and alterations in brain DHA levels on brain activity assessed using BOLD signal in male rats fed a diet without omega-3 fatty acids, one that included fish oil, or a control diet consisting of ALA. During the adolescent period one-half of each group received daily amphetamine injections that increased weekly, or provided drug vehicle. BOLD response was then assessed following a period of abstinence and amphetamine challenge. Among the rats who were amphetamine naïve, the challenge increased BOLD activity in the substantia nigra and basal forebrain. The amphetamine challenge increased BOLD activation in the bilateral caudate putamen, thalamus, and motor and cingulate cortex among amphetamine pre-treated control and rats fed fish oil. In contrast, amphetamine pretreated omega-3 deficient rats demonstrated less frontostriatal BOLD signal activation compared to rats administered amphetamine prior to treatment with control or fish oil diet. The authors interpreted their findings to indicate that frontostriatal recruitment is associated with escalating amphetamine treatment and that deficits in DHA accrual during peri-adolescence development impairs this neuroplastic response.

In a study that investigated the effects of dietary-induced alterations in brain DHA accrual on cortical glutamate in adult rats, McNamara et al. (2017a) fed them a control diet, an omega-3 fatty acid-deficient diet, or a fish oil-fortified diet. Using proton magnetic resonance spectroscopy (^{1}H MRS), they examined glutamate in the prefrontal cortex and thalamus. Findings indicated that erythrocyte, prefrontal cortex, and thalamus DHA levels were significantly lower in rats fed an omega-3 deficient diet, and significantly higher in rats fed a fish oil-fortified diet compared to the control rats. In the prefrontal cortex, glutamate was found to be significantly elevated in the omega-3 deficient rats compared to the control and fish oil rats. Moreover, across all groups, prefrontal DHA levels correlated inversely with prefrontal glutamate levels. The authors concluded that during adolescence, cortical DHA accrual plays a role in glutamate homeostasis in the adult prefrontal cortex. A recent animal study using ^{31}P MRS did not identify a relationship between brain DHA accrual and indices of bioenergetics (e.g., adenosine triphosphate and phosphocreatine level), or indices of phospholipid metabolism (e.g., phosphodiesters) (Lindquist et al. 2017).

Recent clinical studies indicate that omega-3 PUFAs are associated with healthy brain white matter integrity across late childhood and adolescence. Using DTI, McNamara and colleagues (McNamara et al. 2017b) assessed white matter in 30 healthy subjects along with erythrocyte membrane PUFA levels and plasma intracellular phospholipase A_2 activity (inPLA_2). Plasma inPLA_2 activity showed a significant U-curved association with white matter radial diffusivity, and an inverted U-curved association with white matter fractional anisotropy. They also found a significant positive linear association between DHA levels and axial diffusivity in the corpus callosum. Higher DHA and lower LA levels in preterm infants are linked to decreased intraventricular hemorrhage, lower diffusivity in white matter, and improved developmental outcomes (Tam et al. 2016). Almaas et al. (2016) measured white matter microstructure after an 8-year follow-up of a randomized clinical trial, in which preterm infants with low birth weight were given 32 mg of DHA and 31 mg of arachidonic acid in human milk. The intervention started 1 week after birth and lasted approximately 9 weeks (corresponding to the

time of hospital discharge). The authors reported no significant differences in cerebral white matter between the PUFA group and the placebo group, but there was a non-significant finding of higher fractional anisotropy in the PUFA treated group within the corpus callosum.

Several studies investigated the link between memory, PUFAs, and white matter integrity in cognitively intact older adults. Zamroziewicz et al. (2017) found that memory is dependent upon a combination of plasma phospholipid omega-3 and omega-6 PUFAs, and that fornix fractional anisotropy mediates this relationship. In a study by Witte et al. (2014), 65 healthy subjects received 2.2 g/day of omega-3 PUFA or placebo for 26 weeks. At the end of the intervention, the group receiving PUFA scored significantly higher on measures of executive functioning compared to the placebo group. PUFA administration also increased fractional anisotropy and gray matter volume in multiple left hemisphere brain regions. It is noteworthy that improved executive functioning was correlated positively with changes in erythrocyte membrane PUFA levels. In addition, cross-sectional and longitudinal MR imaging studies conducted in healthy subjects demonstrate that PUFA intake and/or biostatus are related to more gray matter in temporal lobe structures, including the hippocampus and amygdala (McNamara et al. 2018a). For example, a 5-year prospective study of cognitively healthy elderly subjects reported that dietary consumption of PUFAs (i.e., EPA and DHA) at baseline was positively correlated with gray matter volume, but not white matter volume, and enhanced cognitive performance 5 years later (Titova et al. 2013).

19.3 Antioxidants

Gray matter subcortical and cortical abnormalities are commonly observed in premature aging (Rosenblum et al. 1996) and psychiatric disorders such as schizophrenia (Szeszko et al. 2003; Narr et al. 2005a, b). One key factor that has been considered to play a role in these effects relates to stress (Betensky et al. 2008). Specifically, reactive oxygen species (ROS) are created as a natural byproduct of the normal metabolism of oxygen within the cell and are important for cell signaling and homeostasis. During mitochondrial respiration, there is a normal buildup of superoxide that can be potentially deleterious. The cell's primary defense against ROS damage is from enzymes such as superoxide dismutase and glutathione, which are antioxidants that protect against free radicals. ROS levels can increase significantly during periods of considerable environmental stress, which can damage cellular structures within the gray matter, and thus may be more susceptible to the effects of oxidative stress compared to the white matter (Yousef et al. 2003). There is therefore increasing interest in the identification of interventions that may restore this oxidative balance.

A gene believed to be critical for the protection of mitochondria from superoxide radicals that are released normally as a byproduct of respiration is manganese superoxide dismutase (MnSOD), *SOD2*. A polymorphism within the mitochondrial targeting sequence (MTS) of MnSOD resulting in an alanine (Ala) to valine (Val) substitution has been linked to 40% greater MnSOD *in vitro* activity after import into isolated mitochondria (Sutton et al. 2003), and has been one of the most widely studied polymorphisms to date in this gene. Specifically, the Ala16 variant is able to enter the matrix quickly in contrast to the Val16 variant, which stays embedded within the inner matrix. Animal studies indicate that MnSOD deficient mice show evidence of CNS abnormalities, motor disturbances, and mitochondrial injury (Li et al. 1995; Lebovitz et al. 1996). There is some data indicating that alterations in SOD activity occur in patients with schizophrenia, but results have been highly inconsistent (Wang et al. 2015). Other data indicate that lower MnSOD activity may play a role in the risk of chronic schizophrenia, but not in tardive dyskinesia (Wang et al. 2015).

Another antioxidant, glutathione peroxidase-1 (GPX1), is a critical enzyme that is known to prevent cell damage caused by free radicals. In contrast to omega-3s, glutathione is not considered to be essential for humans, given that it may be synthesized in the body from amino acids such as glutamate, cysteine and glycine. It plays a criti-

cal role in the detoxification of hydrogen peroxide by catalyzing it into water. The GPX1 Pro198Leu polymorphism has been demonstrated to be functional, with a proline to leucine change at codon 198 located on chromosome 3, and its activation is associated with selenium concentration that is located within the enzyme itself. Gao et al. (2017) did not find evidence, however, for an association between elevated risk for schizophrenia and polymorphisms within the rs1050450 single nucleotide polymorphism in a large study of Han Chinese individuals that included 323 healthy controls and 210 patients with schizophrenia.

A comprehensive review examining the efficacy of antioxidants in the treatment of psychosis was completed recently by Magalhães et al. (2016) using the Cochrane Database. This study included 22 randomized clinical trials investigating antioxidants such as Ginkgo biloba, N-acetyl cysteine (NAC), allopurinol, dehydroepiandrosterone (DHEA), vitamin C, vitamin E, or selegiline as add-on treatments to antipsychotics to improve long-term care and prevent relapse in psychosis. The authors concluded that there was limited evidence for their efficacy (possibly due to inadequate statistical power), and that the information was likely not relevant to consumers or clinicians. There was, however, a low risk of attrition and the authors concluded there was a greater need for safety data, tolerability, longer follow-up periods, and the inclusion of measures of improvement and relapse. Of note, a double-blind, placebo-controlled study reported that the addition of NAC, which is a precursor of glutathione, to antipsychotic treatment was associated with negative symptom improvement and reduction of akathisia in patients with chronic schizophrenia (Berk et al. 2008).

19.4 Applications in Schizophrenia

19.4.1 Omega-3 PUFAs

While there is increasing evidence that a diet consisting of omega-3 PUFAs may be associated with beneficial effects on cortical structure and function in healthy humans, there is a relative dearth of studies investigating the relationship between fatty acids in psychiatric disorders coupled with the use of MR imaging. Such studies are critically needed to identify potential mechanistic pathways for these interventions to assist in the design of future controlled treatment trials. In a recent study, Pawełczyk and colleagues (Pawelczyk et al. 2018) examined cortical thickness changes associated with the administration of omega-3 adjuvant treatment in patients experiencing a first-episode of schizophrenia. They conducted a 26-week, double-blind, randomized study involving concentrated fish oil containing 2.2 g/day of EPA and DHA or placebo. Individuals received MR imaging exams prior to and following treatment. Findings revealed less cortical gray matter thickness loss in left parieto-occipital regions among the omega-3 treated patients compared to the placebo group, supporting the hypothesis that omega-3s may be protective against neurodegenerative processes.

Wood et al. (2010) used MR imaging to examine the effects of ethyl-EPA on T(2) transverse relaxation time within the hippocampus in patients experiencing a first-episode of psychosis at baseline and then again following 12 weeks of treatment. T(2) is a constant defined by the time at which 63% of the transverse magnetization that is associated with dephasing from local field disturbances has decayed. It thus provides a potential index of the water that is present within neuronal tissue, such that T(2) reductions may be associated with better neuronal integrity. These investigators reported no change in T(2) relaxation time in the ethyl-EPA group in contrast to the placebo group, which demonstrated an increase in T(2). Findings were interpreted to suggest that ethyl-EPA may have a neuroprotective effect, especially given that smaller increases in T(2) were associated with more negative symptom improvement.

Proton MRS is another technique that can be used to understand the neurophysiological effects of omega-3 treatment in individuals with schizophrenia (Sota et al. 2007). In one of the first studies to use MRS, Berger et al. (2008) investigated the effects of ethyl-EPA on brain metabolism in 24 patients experiencing a first-episode of psychosis prior to and then following

12 weeks of treatment as part of a larger double-blind, placebo-controlled augmentation study. The investigators performed MRS at 3 T using the temporal lobe as the region-of-interest. They reported group treatment effects for glutathione, as well as a hemisphere-by-group interaction for glutamine/glutamate. Post-hoc analyses revealed an increase in glutathione bilaterally and an increase in glutamate/glutamine within the left hemisphere following omega-3 administration. These findings are consistent with the hypothesis that augmentation with ethyl-EPA in the treatment of psychosis alters glutathione availability within the brain and can alter the glutamine/glutamate cycle early in the course of the disorder.

The use of phosphorus MRS (^{31}P MRS) may also provide information about phosphomonoesters, which are the building blocks of neuronal membranes that are relevant to schizophrenia (Reddy et al. 2004). Using this technique, Keshavan and colleagues (2003) quantified phosphomonoester and phosphodiester levels and the concomitant signals underlying these peaks in 16 nonpsychotic CHR offspring of parents with schizophrenia or schizoaffective disorder, and 37 age-matched healthy volunteers. Findings indicated that CHR subjects had reduced phosphomonoester compared to controls. In addition, high-risk subjects with an Axis I disorder demonstrated increases in the signal for phosphomonoester and phosphodiester levels. These findings are consistent with the membrane hypothesis of schizophrenia and suggest that these abnormalities may be evident before the frank onset of psychosis and potentially useful to predict psychosis.

The use of ^{31}P MRS can be an important tool for the treatment of schizophrenia using omega-3s. Visualization of an individual's phospholipid spectrum conveys information regarding membrane integrity, intracellular PH, cellular energetics, and neurotransmitter activity (Cox and Puri 2004) that has direct relevance to omega-3 treatment. In one of the first applications of this technique, Puri et al. (2000) reported lower neuronal membrane phospholipid turnover following treatment with EPA to a drug-naive patient with schizophrenia. Puri et al. (2008) investigated differences in membrane phospholipids in 16 patients with schizophrenia who presented with mild to moderate negative symptoms compared to 16 healthy volunteers using ^{31}P MRS. The authors did not identify any differences between groups in either phosphomonoesters or phosphodiesters signals. Subsequently, Puri et al. (2009) used the same imaging technique in 54 human subjects, including healthy volunteers and patients with schizophrenia. Results indicated a significant positive correlation between the phosphomonoester resonances and broad resonance signal, suggesting that the former may be an index of cell membrane phospholipid anabolism.

Emerging evidence from neuroimaging studies using diffusion tensor imaging (DTI) has identified white matter abnormalities that support the hypothesis for a disruption in brain myelination and connectivity in schizophrenia (Kubicki et al. 2007; Wheeler and Voineskos 2014; Karlsgodt 2016). Although there is no clear consensus regarding the precise location of white matter abnormalities in schizophrenia, most often the superior longitudinal fasciculus, uncinate fasciculus, cingulum, and corpus callosum appear to be involved (Parnanzone et al. 2017). There is evidence that DHA, and to a lesser extent EPA <0.1%, are important structural lipids that are abundant in the brain, especially in the prefrontal cortex (i.e., ~15% of total fatty acids). It is known that myelin is formed from the membranes of oligodendrocytes and that the phospholipid bilayers of all cell membranes in myelin sheath contain PUFAs (Ozgen et al. 2016). It is therefore conceivable that the administration of omega-3s may promote the expression of myelin proteins, thus enhancing brain plasticity, synaptic connections, and anti-inflammatory effects (Silva et al. 2017).

In one of the first studies to examine the relationship between brain white matter and cell membrane fatty acids in schizophrenia, Peters et al. (2009) reported a significant relationship between total PUFA concentration and fractional anisotropy within a fronto-temporal white matter tract. In a more recent study with a larger sample, Peters et al. (2013) found that lower total PUFA concentration was associated with lower fractional anisotropy throughout the corpus callosum

and bilateral parietal, occipital, temporal and frontal white matter in patients with early-phase psychosis. Investigation of the individual PUFAs revealed that lower arachidonic acid concentration, and to a lesser extent, lower nervonic acid, LA, and DPA concentration were the fatty acids driving these results. Findings were interpreted to suggest that PUFAs are needed to preserve myelin formation and/or to maintain oligodendrocytes.

19.4.2 Antioxidants

Several animal studies utilizing glutathione paradigms have shed light on its possible role in the neurobiology of psychosis. Using high-resolution MRS at 14.1 T, das Neves Duarte et al. (2012) used a mouse model with chronic glutathione deficit induced by knockout of a glutathione enzyme, glutamate-cysteine ligase modulatory subunit (GCLM-KO). They investigated the chemical composition of GCLM-KO, heterozygous, and wild-type mice with a focus on the anterior cingulate and identified glutathione deficits accompanied by an elevation of glutamine. Particularly noteworthy is that changes were mostly evident at prepubertal ages, which may have strong relevance to neurodevelopmental models of schizophrenia, and that treatment with N-acetylcysteine normalized these abnormalities to wild-type level.

It is acknowledged that there are technical challenges regarding the estimation of oxidative stress-related brain changes leading to the use of peripheral glutathione as a potential proxy measure. In a study by Sedlak et al. (2018), these authors identified an association between whole brain and peripheral glutathione levels using 7 T MRS. Specifically, they reported effects of sulforaphane on brain glutathione levels in multiple brains regions. Following 7 days of daily oral administration of isothiocyanate sulforaphane, these investigators identified increased blood glutathione levels in healthy humans and thalamic glutathione post- and pre-sulforaphane treatment ratios. This study therefore provides a model for examining peripheral glutathione as a proxy for changes occurring within the brain and the influence of sulforaphane on these measures.

Using 7 T MRS, Kumar et al. (2018) measured glutathione, glutamate, and glutamine concentration in the anterior cingulate cortex (ACC), left insula, and visual cortex in 28 patients with chronic schizophrenia and 45 healthy participants. Principal components analysis revealed: (1) an ACC glutathione-glutamate component; (2) an insula-visual glutathione-glutamate component; and a (3) glutamine component. Notably, stabilized patients with schizophrenia had lower scores on the ACC glutathione-glutamate component, which was driven primarily by a subgroup of patients with residual schizophrenia. In addition, the three metabolite concentrations within the ACC were significantly reduced in this subgroup. The authors interpreted their findings to suggest that excitotoxicity during the acute phase of illness predicts lower glutathione and glutamate during the residual illness phase.

Langbein et al. (2018) used high resolution 3 T MRI to examine the relationship between glutathione and brain abnormalities in drug-naïve patients with first-episode psychosis. These investigators focused on brain abnormalities between glutathione metabolites and gray matter density. They reported that glutathione reductase activity was lower in patients compared to controls. Moreover, plasma glutathione reductase activity was inversely correlated with depression symptoms. In addition, there was an interaction between glutathione reductase activity and gray matter in the left orbitofrontal cortex. This study thus highlights abnormal glutathione reductase activity as a potential factor in brain abnormalities in unmedicated acute psychosis patients.

Magnetic resonance imaging can quantitatively assess bioactive chemicals, such as glutathione, in-vivo. Matsuzawa et al. (2011) investigated 4 MR imaging sequences including double quantum coherence (DQC) filtering, MEscher-Garwood Point-RESolved Spectroscopy (MEGA-PRESS), Stimulated Echo Acquisition Mode (STEAM), and PRESS to investigate the 1H-MRS measurement of glutathione in schizophrenia. Findings revealed a negative correlation between brain glutathione levels and negative symptom severity in patients, indicating that higher glutathione levels may be

beneficial for a subgroup of patients with prominent negative symptoms.

Some data indicate that antioxidant administration may play a role in the progression of brain changes associated with the clinical high-risk phenotype (Jung et al. 2012). In one of the first studies focusing on oxidative stress and neuroimmune functioning in the development of psychosis, Hafizi et al. (2018) investigated the relationship between translocator protein 18 kDa (TSPO) expression and glutathione in the medial prefrontal cortex. The sample included 27 antipsychotic-naïve CHR individuals and 21 healthy volunteers who were scanned using positron emission tomography with the TSPO radioligand, [18F]FEPPA, along with 1H MRS. The authors reported that in healthy volunteers, but not in CHR individuals, there was a significant negative association between glutathione levels and [18F]FEPPA total distribution volume, suggesting it may be involved in the clinical phenomenology of schizophrenia.

19.5 Conclusions and Future Directions

Given recent negative findings regarding the efficacy of omega-3s and/or antioxidants to prevent the transition to psychosis in clinical high-risk samples, coupled with mixed results from clinical trials in patients with first-episode or chronic schizophrenia, a potentially more relevant question may be whether there are characteristics of patients who may derive maximal benefit from these compounds (Chen et al. 2015). For example, some data suggest that omega-3s may be effective in the treatment of symptoms of depression and that antioxidants may be useful in the treatment of negative symptoms. In addition, it is also possible that omega-3s and antioxidants are most effective when administered together with psychological treatment and/or antidepressants. More research is required to understand factors that may play a role in the successful treatment of schizophrenia and associated psychotic disorders using these compounds.

In addition, when conceptualized as a neurodevelopmental disorder, it is plausible that a subgroup of individuals at high risk for psychosis (or even those with early-phase psychosis) may demonstrate an aberrant white matter trajectory and be most receptive to intervention with omega-3s or antioxidants. Such studies will also require examining genetic factors that contribute to metabolism of omega-3s. For example, the protein encoded by the fatty acid desaturase (FADS) gene family is involved in the desaturation of omega-3s that catalyzes the formation of EPA. Single nucleotide polymorphisms (e.g., rs174583) in the FADS gene may influence the metabolism of PUFAs, and thus have significance for psychiatric disorders that have a white matter pathogenesis of neurodevelopmental origin, such as schizophrenia. Similarly, single nucleotide polymorphisms in the GPX1 and MnSOD genes may play a part in the mitigation of free radicals, and therefore be relevant to the gray matter alterations often observed in patients with psychosis. Thus, imaging-genetics paradigms should be an important focus of future studies investigating omega-3s and antioxidants in schizophrenia.

Although there is some support for the membrane hypothesis of schizophrenia, neuroimaging studies in both humans and animals may hold promise for developing a better understanding of the effect of omega-3s and antioxidants on brain structure and function to potentially guide treatment strategies. In particular, the use of MR imaging sequences such as ^{31}P MRS and DTI may provide much needed information regarding the mechanism of action of omega-3s and antioxidants in the brain. Additionally, the use of techniques such as positron emission tomography using [1-^{11}C]DHA could reveal information about DHA metabolism and how it is regulated by calcium-independent iPLA$_2\beta$ (Rapoport 2013). An additional quantitative technique to image PUFA in the brain may be provided from PET of unesterified plasma DHA incorporation, which can then be used as a biomarker of brain PUFA metabolism and neurotransmission (Basselin et al. 2012). Similarly, PET could yield valuable information regarding the relationship between translocator protein expression and glutathione within the cortex, both in healthy and disease-state individuals.

In sum, despite mixed findings from clinical treatment trials of omega-3s and antioxidants, we believe their role in the pathophysiology and treatment of schizophrenia warrants additional investigation. The use of noninvasive techniques such as MR imaging will be important to guide our understanding of their mechanism(s) of action using both animal and human studies to elucidate possible targets for treatment intervention that can benefit patients.

Summary

- Clinical trials investigating the efficacy of omega-3 PUFAs and antioxidants in patients with psychosis have yielded mixed findings.
- Omega-3 PUFAs and antioxidants might be most effective when combined with psychological treatment and/or antidepressants.
- Neuroimaging studies may provide information about whether there are subgroups of individuals with psychosis who may be responsive to intervention with omega-3 PUFAs and/or antioxidants.
- Novel neuroimaging techniques hold promise for developing a better understanding regarding how omega-3 PUFAs and antioxidants affect brain structure and function to potentially guide treatment strategies.

References

Ahmad A, Momenan R, van Gelderen P, Moriguchi T, Greiner RS, Salem N Jr. Gray and white matter brain volume in aged rats raised on n-3 fatty acid deficient diets. Nutr Neurosci. 2004;7(1):13–20. https://doi.org/10.1080/1028415042000202009.

Almaas AN, Tamnes CK, Nakstad B, Henriksen C, Grydeland H, Walhovd KB, et al. Diffusion tensor imaging and behavior in premature infants at 8 years of age, a randomized controlled trial with long-chain polyunsaturated fatty acids. Early Hum Dev. 2016;95:41–6. https://doi.org/10.1016/j.earlhumdev.2016.01.021.

Amminger GP, Schafer MR, Papageorgiou K, Klier CM, Cotton SM, Harrigan SM, et al. Long-chain omega-3 fatty acids for indicated prevention of psychotic disorders: a randomized, placebo-controlled trial. Arch Gen Psychiatry. 2010;67(2):146–54. https://doi.org/10.1001/archgenpsychiatry.2009.192.

Amminger GP, Mechelli A, Rice S, Kim SW, Klier CM, McNamara RK, et al. Predictors of treatment response in young people at ultra-high risk for psychosis who received long-chain omega-3 fatty acids. Transl Psychiatry. 2015a;5:e495. https://doi.org/10.1038/tp.2014.134.

Amminger GP, Schafer MR, Schlogelhofer M, Klier CM, McGorry PD. Longer-term outcome in the prevention of psychotic disorders by the Vienna omega-3 study. Nat Commun. 2015b;6:7934. https://doi.org/10.1038/ncomms8934.

Arvindakshan M, Sitasawad S, Debsikdar V, Ghate M, Evans D, Horrobin DF, et al. Essential polyunsaturated fatty acid and lipid peroxide levels in never-medicated and medicated schizophrenia patients. Biol Psychiatry. 2003a;53(1):56–64.

Arvindakshan M, Ghate M, Ranjekar PK, Evans DR, Mahadik SP. Supplementation with a combination of omega-3 fatty acids and antioxidants (vitamins E and C) improves the outcome of schizophrenia. Schizophr Res. 2003b;62(3):195–204.

Basselin M, Ramadan E, Rapoport SI. Imaging brain signal transduction and metabolism via arachidonic and docosahexaenoic acid in animals and humans. Brain Res Bull. 2012;87(2–3):154–71. https://doi.org/10.1016/j.brainresbull.2011.12.001.

Benatti P, Peluso G, Nicolai R, Calvani M. Polyunsaturated fatty acids: biochemical, nutritional and epigenetic properties. J Am Coll Nutr. 2004;23(4):281–302.

Bentsen H, Osnes K, Refsum H, Solberg DK, Bohmer T. A randomized placebo-controlled trial of an omega-3 fatty acid and vitamins E+C in schizophrenia. Transl Psychiatry. 2013;3:e335. https://doi.org/10.1038/tp.2013.110.

Berger GE, Proffitt TM, McConchie M, Yuen H, Wood SJ, Amminger GP, et al. Ethyl-eicosapentaenoic acid in first-episode psychosis: a randomized, placebo-controlled trial. J Clin Psychiatry. 2007;68(12):1867–75.

Berger GE, Wood SJ, Wellard RM, Proffitt TM, McConchie M, Amminger GP, et al. Ethyl-eicosapentaenoic acid in first-episode psychosis. A 1H-MRS study. Neuropsychopharmacology. 2008;33(10):2467–73. https://doi.org/10.1038/sj.npp.1301628.

Berger ME, Smesny S, Kim SW, Davey CG, Rice S, Sarnyai Z, et al. Omega-6 to omega-3 polyunsaturated fatty acid ratio and subsequent mood disorders in young people with at-risk mental states: a 7-year longitudinal study. Transl Psychiatry. 2017;7(8):e1220. https://doi.org/10.1038/tp.2017.190.

Berk M, Copolov D, Dean O, Lu K, Jeavons S, Schapkaitz I, et al. N-acetyl cysteine as a glutathione precursor for schizophrenia—a double-blind, randomized, placebo-controlled trial. Biol Psychiatry. 2008;64(5):361–8. https://doi.org/10.1016/j.biopsych.2008.03.004.

Betensky JD, Robinson DG, Gunduz-Bruce H, Sevy S, Lencz T, Kane JM, et al. Patterns of stress in schizophrenia. Psychiatry Res. 2008;160(1):38–46. https://doi.org/10.1016/j.psychres.2007.06.001.

Bos DJ, van Montfort SJT, Oranje B, Durston S, Smeets PAM. Effects of omega-3 polyunsaturated fatty acids on human brain morphology and function: what is the evidence? Eur Neuropsychopharmacol. 2016;26(3):546–61. https://doi.org/10.1016/j.euroneuro.2015.12.031.

Bošnjak D, Kekin I, Hew J, Kuzman MR. Early interventions for prodromal stage of psychosis. Cochrane Database Syst Rev. 2016;(6). https://doi.org/10.1002/14651858.CD012236.

Cadenhead K, Addington J, Cannon T, Cornblatt B, Mathalon D, McGlashan T, et al. Omega-3 fatty acid versus placebo in a clinical high-risk sample from the North American Prodrome Longitudinal Studies (Napls) Consortium. Schizophr Bull. 2017;43:S16.

Cannon TD, Yu C, Addington J, Bearden CE, Cadenhead KS, Cornblatt BA, et al. An individualized risk calculator for research in prodromal psychosis. Am J Psychiatry. 2016;173(10):980–8. https://doi.org/10.1176/appi.ajp.2016.15070890.

Chen AT, Chibnall JT, Nasrallah HA. A meta-analysis of placebo-controlled trials of omega-3 fatty acid augmentation in schizophrenia: possible stage-specific effects. Ann Clin Psychiatry. 2015;27(4):289–96.

Cox IJ, Puri BK. In vivo MR spectroscopy in diagnosis and research of neuropsychiatric disorders. Prostaglandins Leukot Essent Fatty Acids. 2004;70(4):357–60. https://doi.org/10.1016/j.plefa.2003.12.010.

Cutuli D, De Bartolo P, Caporali P, Laricchiuta D, Foti F, Ronci M, et al. n-3 polyunsaturated fatty acids supplementation enhances hippocampal functionality in aged mice. Front Aging Neurosci. 2014;6:220. https://doi.org/10.3389/fnagi.2014.00220.

Cutuli D, Pagani M, Caporali P, Galbusera A, Laricchiuta D, Foti F, et al. Effects of omega-3 fatty acid supplementation on cognitive functions and neural substrates: a voxel-based morphometry study in aged mice. Front Aging Neurosci. 2016;8:38. https://doi.org/10.3389/fnagi.2016.00038.

Dalli J, Colas RA, Serhan CN. Novel n-3 immunoresolvents: structures and actions. Sci Rep. 2013;3:1940. https://doi.org/10.1038/srep01940.

Dangi B, Obeng M, Nauroth JM, Teymourlouei M, Needham M, Raman K, et al. Biogenic synthesis, purification, and chemical characterization of anti-inflammatory resolvins derived from docosapentaenoic acid (DPAn-6). J Biol Chem. 2009;284(22):14744–59. https://doi.org/10.1074/jbc.M809014200.

das Neves Duarte JM, Kulak A, Gholam-Razaee MM, Cuenod M, Gruetter R, Do KQ. N-acetylcysteine normalizes neurochemical changes in the glutathione-deficient schizophrenia mouse model during development. Biol Psychiatry. 2012;71(11):1006–14. https://doi.org/10.1016/j.biopsych.2011.07.035.

DeMar JC Jr, Ma K, Bell JM, Rapoport SI. Half-lives of docosahexaenoic acid in rat brain phospholipids are prolonged by 15 weeks of nutritional deprivation of n-3 polyunsaturated fatty acids. J Neurochem. 2004;91(5):1125–37. https://doi.org/10.1111/j.1471-4159.2004.02789.x.

Emsley R, Myburgh C, Oosthuizen P, van Rensburg SJ. Randomized, placebo-controlled study of ethyl-eicosapentaenoic acid as supplemental treatment in schizophrenia. Am J Psychiatry. 2002;159(9):1596–8. https://doi.org/10.1176/appi.ajp.159.9.1596.

Emsley R, Niehaus DJ, Koen L, Oosthuizen PP, Turner HJ, Carey P, et al. The effects of eicosapentaenoic acid in tardive dyskinesia: a randomized, placebo-controlled trial. Schizophr Res. 2006;84(1):112–20. https://doi.org/10.1016/j.schres.2006.03.023.

Emsley R, Chiliza B, Asmal L, du Plessis S, Phahladira L, van Niekerk E, et al. A randomized, controlled trial of omega-3 fatty acids plus an antioxidant for relapse prevention after antipsychotic discontinuation in first-episode schizophrenia. Schizophr Res. 2014;158(1–3):230–5. https://doi.org/10.1016/j.schres.2014.06.004.

Fenton WS, Dickerson F, Boronow J, Hibbeln JR, Knable M. A placebo-controlled trial of omega-3 fatty acid (ethyl eicosapentaenoic acid) supplementation for residual symptoms and cognitive impairment in schizophrenia. Am J Psychiatry. 2001;158(12):2071–4. https://doi.org/10.1176/appi.ajp.158.12.2071.

Gao H, Liu C, Song S, Zhang C, Ma Q, Li X, et al. GPX1 Pro198Leu polymorphism and GSTP1 Ile105Val polymorphisms are not associated with the risk of schizophrenia in the Chinese Han population. Neuroreport. 2017;28(15):969–72. https://doi.org/10.1097/WNR.0000000000000870.

Hafizi S, Da Silva T, Meyer JH, Kiang M, Houle S, Remington G, et al. Interaction between TSPO-a neuroimmune marker-and redox status in clinical high risk for psychosis: a PET-MRS study. Neuropsychopharmacology. 2018;43(8):1700–5. https://doi.org/10.1038/s41386-018-0061-5.

Horrobin DF. The membrane phospholipid hypothesis as a biochemical basis for the neurodevelopmental concept of schizophrenia. Schizophr Res. 1998;30(3):193–208. https://doi.org/10.1016/S0920-9964(97)00151-5.

Horrobin DF, Manku MS, Hillman H, Iain A, Glen M. Fatty acid levels in the brains of schizophrenics and normal controls. Biol Psychiatry. 1991;30(8):795–805.

Horrobin DF, Glen AI, Vaddadi K. The membrane hypothesis of schizophrenia. Schizophr Res. 1994;13(3):195–207.

Jamilian H, Solhi H, Jamilian M. Randomized, placebo-controlled clinical trial of omega-3 as supplemental treatment in schizophrenia. Glob J Health Sci. 2014;6(7 Spec No):103–8. https://doi.org/10.5539/gjhs.v6n7p103.

Jung WH, Borgwardt S, Fusar-Poli P, Kwon JS. Gray matter volumetric abnormalities associated with the onset of psychosis. Front Psychiatry. 2012;3:101. https://doi.org/10.3389/fpsyt.2012.00101.

Karlsgodt KH. Diffusion imaging of white matter in schizophrenia: progress and future directions.

Biol Psychiatry Cogn Neurosci Neuroimaging. 2016;1(3):209–17. https://doi.org/10.1016/j.bpsc.2015.12.001.

Kaur G, Guo XF, Sinclair AJ. Short update on docosapentaenoic acid: a bioactive long-chain n-3 fatty acid. Curr Opin Clin Nutr Metab Care. 2016;19(2):88–91. https://doi.org/10.1097/MCO.0000000000000252.

Keshavan MS, Stanley JA, Montrose DM, Minshew NJ, Pettegrew JW. Prefrontal membrane phospholipid metabolism of child and adolescent offspring at risk for schizophrenia or schizoaffective disorder: an in vivo 31P MRS study. Mol Psychiatry. 2003;8(3):316–23., , 251. https://doi.org/10.1038/sj.mp.4001325.

Kim SW, Schafer MR, Klier CM, Berk M, Rice S, Allott K, et al. Relationship between membrane fatty acids and cognitive symptoms and information processing in individuals at ultra-high risk for psychosis. Schizophr Res. 2014;158(1–3):39–44. https://doi.org/10.1016/j.schres.2014.06.032.

Kubicki M, McCarley R, Westin CF, Park HJ, Maier S, Kikinis R, et al. A review of diffusion tensor imaging studies in schizophrenia. J Psychiatr Res. 2007;41(1–2):15–30. https://doi.org/10.1016/j.jpsychires.2005.05.005.

Kumar J, Liddle EB, Fernandes CC, Palaniyappan L, Hall EL, Robson SE, et al. Glutathione and glutamate in schizophrenia: a 7T MRS study. Mol Psychiatry. 2018. https://doi.org/10.1038/s41380-018-0104-7.

Langbein K, Hesse J, Gussew A, Milleit B, Lavoie S, Amminger GP, et al. Disturbed glutathione antioxidative defense is associated with structural brain changes in neuroleptic-naive first-episode psychosis patients. Prostaglandins Leukot Essent Fatty Acids. 2018;136:103–10. https://doi.org/10.1016/j.plefa.2017.10.005.

Lebovitz RM, Zhang H, Vogel H, Cartwright J Jr, Dionne L, Lu N, et al. Neurodegeneration, myocardial injury, and perinatal death in mitochondrial superoxide dismutase-deficient mice. Proc Natl Acad Sci U S A. 1996;93(18):9782–7.

Li Y, Huang TT, Carlson EJ, Melov S, Ursell PC, Olson JL, et al. Dilated cardiomyopathy and neonatal lethality in mutant mice lacking manganese superoxide dismutase. Nat Genet. 1995;11(4):376–81. https://doi.org/10.1038/ng1295-376.

Li Q, Leung YO, Zhou I, Ho LC, Kong W, Basil P, et al. Dietary supplementation with n-3 fatty acids from weaning limits brain biochemistry and behavioural changes elicited by prenatal exposure to maternal inflammation in the mouse model. Transl Psychiatry. 2015;5:e641. https://doi.org/10.1038/tp.2015.126.

Lindquist DM, Asch RH, Schurdak JD, McNamara RK. Effects of dietary-induced alterations in rat brain docosahexaenoic acid accrual on phospholipid metabolism and mitochondrial bioenergetics: an in vivo(31)P MRS study. J Psychiatr Res. 2017;95:143–6. https://doi.org/10.1016/j.jpsychires.2017.08.014.

Liu JJ, Green P, John Mann J, Rapoport SI, Sublette ME. Pathways of polyunsaturated fatty acid utilization: implications for brain function in neuropsychiatric health and disease. Brain Res. 2015;1597:220–46. https://doi.org/10.1016/j.brainres.2014.11.059.

Luchtman DW, Song C. Cognitive enhancement by omega-3 fatty acids from child-hood to old age: findings from animal and clinical studies. Neuropharmacology. 2013;64:550–65. https://doi.org/10.1016/j.neuropharm.2012.07.019.

Magalhaes PV, Dean O, Andreazza AC, Berk M, Kapczinski F. Antioxidant treatments for schizophrenia. Cochrane Database Syst Rev. 2016;2:CD008919. https://doi.org/10.1002/14651858.CD008919.pub2.

Marshall M, Lewis S, Lockwood A, Drake R, Jones P, Croudace T. Association between duration of untreated psychosis and in cohorts of first-episode outcome patients—a systematic review. Arch Gen Psychiatry. 2005;62(9):975–83. https://doi.org/10.1001/archpsyc.62.9.975.

Matsuzawa D, Hashimoto K. Magnetic resonance spectroscopy study of the antioxidant defense system in schizophrenia. Antioxid Redox Signal. 2011;15(7):2057–65. https://doi.org/10.1089/ars.2010.3453.

McGorry PD, Nelson B, Markulev C, Yuen HP, Schafer MR, Mossaheb N, et al. Effect of omega-3 polyunsaturated fatty acids in young people at ultrahigh risk for psychotic disorders: the NEURAPRO randomized clinical trial. JAMA Psychiat. 2017;74(1):19–27. https://doi.org/10.1001/jamapsychiatry.2016.2902.

McNamara RK. Deciphering the role of docosahexaenoic acid in brain maturation and pathology with magnetic resonance imaging. Prostaglandins Leukot Essent Fatty Acids. 2013;88(1):33–42. https://doi.org/10.1016/j.plefa.2012.03.011.

McNamara RK, Jandacek R, Rider T, Tso P, Hahn CG, Richtand NM, et al. Abnormalities in the fatty acid composition of the postmortem orbitofrontal cortex of schizophrenic patients: gender differences and partial normalization with antipsychotic medications. Schizophr Res. 2007;91(1–3):37–50. https://doi.org/10.1016/j.schres.2006.11.027.

McNamara RK, Asch RH, Schurdak JD, Lindquist DM. Glutamate homeostasis in the adult rat prefrontal cortex is altered by cortical docosahexaenoic acid accrual during adolescence: an in vivo(1)H MRS study. Psychiatry Res Neuroimaging. 2017a;270:39–45. https://doi.org/10.1016/j.pscychresns.2017.10.003.

McNamara RK, Szeszko PR, Smesny S, Ikuta T, DeRosse P, Vaz FM, et al. Polyunsaturated fatty acid biostatus, phospholipase A2 activity and brain white matter microstructure across adolescence. Neuroscience. 2017b;343:423–33. https://doi.org/10.1016/j.neuroscience.2016.12.007.

McNamara RK, Asch RH, Lindquist DM, Krikorian R. Role of polyunsaturated fatty acids in human brain structure and function across the lifespan: an update on neuroimaging findings. Prostaglandins Leukot Essent Fatty Acids. 2018a;136:23–34. https://doi.org/10.1016/j.plefa.2017.05.001.

McNamara RK, Schurdak JD, Asch RH, Peters BD, Lindquist DM. Deficits in docosahexaenoic acid accrual during adolescence reduce rat forebrain white

matter microstructural integrity: an in vivo diffusion tensor imaging study. Dev Neurosci. 2018b;40(1):84–92. https://doi.org/10.1159/000484554.

McNamara RK, Schurdak JD, Asch RH, Lindquist DM. Omega-3 fatty acid deficiency impairs frontostriatal recruitment following repeated amphetamine treatment in rats: a 7 Tesla in vivo phMRI study. Nutr Neurosci. 2019;22(8):587–95. https://doi.org/10.1080/1028415X.2017.1419550.

Mellor JE, Laugharne JD, Peet M. Schizophrenic symptoms and dietary intake of n-3 fatty acids. Schizophr Res. 1995;18(1):85–6.

Mossaheb N, Schafer MR, Schlogelhofer M, Klier CM, Smesny S, McGorry PD, et al. Predictors of longer-term outcome in the Vienna omega-3 high-risk study. Schizophr Res. 2018;193:168–72. https://doi.org/10.1016/j.schres.2017.08.010.

Narr KL, Bilder RM, Toga AW, Woods RP, Rex DE, Szeszko PR, et al. Mapping cortical thickness and gray matter concentration in first episode schizophrenia. Cereb Cortex. 2005a;15(6):708–19. https://doi.org/10.1093/cercor/bhh172.

Narr KL, Toga AW, Szeszko P, Thompson PM, Woods RP, Robinson D, et al. Cortical thinning in cingulate and occipital cortices in first episode schizophrenia. Biol Psychiatry. 2005b;58(1):32–40. https://doi.org/10.1016/j.biopsych.2005.03.043.

Ozgen H, Baron W, Hoekstra D, Kahya N. Oligodendroglial membrane dynamics in relation to myelin biogenesis. Cell Mol Life Sci. 2016;73(17):3291–310. https://doi.org/10.1007/s00018-016-2228-8.

Parnanzone S, Serrone D, Rossetti MC, D'Onofrio S, Splendiani A, Micelli V, et al. Alterations of cerebral white matter structure in psychosis and their clinical correlations: a systematic review of diffusion tensor imaging studies. Riv Psichiatr. 2017;52(2):49–66. https://doi.org/10.1708/2679.27441.

Pawelczyk T, Grancow-Grabka M, Kotlicka-Antczak M, Trafalska E, Pawelczyk A. A randomized controlled study of the efficacy of six-month supplementation with concentrated fish oil rich in omega-3 polyunsaturated fatty acids in first episode schizophrenia. J Psychiatr Res. 2016;73:34–44. https://doi.org/10.1016/j.jpsychires.2015.11.013.

Pawelczyk T, Piatkowska-Janko E, Bogorodzki P, Gebski P, Grancow-Grabka M, Trafalska E, et al. Omega-3 fatty acid supplementation may prevent loss of gray matter thickness in the left parieto-occipital cortex in first episode schizophrenia: a secondary outcome analysis of the OFFER randomized controlled study. Schizophr Res. 2018;195:168–75. https://doi.org/10.1016/j.schres.2017.10.013.

Peet M, Laugharne J, Rangarajan N, Horrobin D, Reynolds G. Depleted red cell membrane essential fatty acids in drug-treated schizophrenic patients. J Psychiatr Res. 1995;29(3):227–32.

Peet M, Brind J, Ramchand CN, Shah S, Vankar GK. Two double-blind placebo-controlled pilot studies of eicosapentaenoic acid in the treatment of schizophrenia. Schizophr Res. 2001;49(3):243–51.

Peet M, Horrobin DF, E-E Multicentre Study Group. A dose-ranging exploratory study of the effects of ethyl-eicosapentaenoate in patients with persistent schizophrenic symptoms. J Psychiatr Res. 2002;36(1):7–18. https://doi.org/10.1016/S0022-3956(01)00048-6.

Peters BD, Duran M, Vlieger EJ, Majoie CB, den Heeten GJ, Linszen DH, et al. Polyunsaturated fatty acids and brain white matter anisotropy in recent-onset schizophrenia: a preliminary study. Prostag Leukotr Ess. 2009;81(1):61–3. https://doi.org/10.1016/j.plefa.2009.04.007.

Peters BD, Machielsen MWJ, Hoen WP, Caan MWA, Malhotra AK, Szeszko PR, et al. Polyunsaturated fatty acid concentration predicts myelin integrity in early-phase psychosis. Schizophr Bull. 2013;39(4):830–8. https://doi.org/10.1093/schbul/sbs089.

Puri BK, Richardson AJ. Sustained remission of positive and negative symptoms of schizophrenia following treatment with eicosapentaenoic acid. Arch Gen Psychiatry. 1998;55(2):188–9.

Puri BK, Treasaden IH. A human in vivo study of the extent to which 31-phosphorus neurospectroscopy phosphomonoesters index cerebral cell membrane phospholipid anabolism. Prostaglandins Leukot Essent Fatty Acids. 2009;81(5–6):307–8. https://doi.org/10.1016/j.plefa.2009.10.003.

Puri BK, Richardson AJ, Horrobin DF, Easton T, Saeed N, Oatridge A, et al. Eicosapentaenoic acid treatment in schizophrenia associated with symptom remission, normalisation of blood fatty acids, reduced neuronal membrane phospholipid turnover and structural brain changes. Int J Clin Pract. 2000;54(1):57–63.

Puri BK, Counsell SJ, Hamilton G. Brain cell membrane motion-restricted phospholipids: a cerebral 31-phosphorus magnetic resonance spectroscopy study of patients with schizophrenia. Prostaglandins Leukot Essent Fatty Acids. 2008;79(6):233–5. https://doi.org/10.1016/j.plefa.2008.08.002.

Rapoport SI. Translational studies on regulation of brain docosahexaenoic acid (DHA) metabolism in vivo. Prostaglandins Leukot Essent Fatty Acids. 2013;88(1):79–85. https://doi.org/10.1016/j.plefa.2012.05.003.

Reddy RD, Keshavan MS, Yao JK. Reduced red blood cell membrane essential polyunsaturated fatty acids in first episode schizophrenia at neuroleptic-naive baseline. Schizophr Bull. 2004;30(4):901–11.

Rice SM, Schafer MR, Klier C, Mossaheb N, Vijayakumar N, Amminger GP. Erythrocyte polyunsaturated fatty acid levels in young people at ultra-high risk for psychotic disorder and healthy adolescent controls. Psychiatry Res. 2015;228(1):174–6. https://doi.org/10.1016/j.psychres.2015.04.036.

Robinson DG, Gallego JA, John M, Hanna LA, Zhang J, Birnbaum ML, et al. A potential role for adjunctive omega-3 polyunsaturated fatty acids for depression and anxiety symptoms in recent onset psychosis: results from a 16 week randomized placebo-controlled trial for participants concurrently treated with risperidone. Schizophr Res. 2019;204:295–303.

Rosenblum JS, Gilula NB, Lerner RA. On signal sequence polymorphisms and diseases of distribution. Proc Natl Acad Sci U S A. 1996;93(9):4471–3.

Sedlak TW, Nucifora LG, Koga M, Shaffer LS, Higgs C, Tanaka T, et al. Sulforaphane augments glutathione and influences brain metabolites in human subjects: a clinical pilot study. Mol Neuropsychiatry. 2018;3(4):214–22. https://doi.org/10.1159/000487639.

Silva RV, Oliveira JT, Santos BLR, Dias FC, Martinez AMB, Lima CKF, et al. Long-chain omega-3 fatty acids supplementation accelerates nerve regeneration and prevents neuropathic pain behavior in mice. Front Pharmacol. 2017;8:723. https://doi.org/10.3389/fphar.2017.00723.

Sivrioglu EY, Kirli S, Sipahioglu D, Gursoy B, Sarandol E. The impact of omega-3 fatty acids, vitamins E and C supplementation on treatment outcome and side effects in schizophrenia patients treated with haloperidol: an open-label pilot study. Prog Neuropsychopharmacol Biol Psychiatry. 2007;31(7):1493–9. https://doi.org/10.1016/j.pnpbp.2007.07.004.

Skulas-Ray AC, Flock MR, Richter CK, Harris WS, West SG, Kris-Etherton PM. Red blood cell docosapentaenoic acid (DPA n-3) is inversely associated with triglycerides and C-reactive protein (CRP) in healthy adults and dose-dependently increases following n-3 fatty acid supplementation. Nutrients. 2015;7(8):6390–404. https://doi.org/10.3390/nu7085291.

Smesny S, Milleit B, Schaefer MR, Hipler UC, Milleit C, Wiegand C, et al. Effects of omega-3 PUFA on the vitamin E and glutathione antioxidant defense system in individuals at ultra-high risk of psychosis. Prostag Leukotr Ess. 2015;101:15–21. https://doi.org/10.1016/j.plefa.2015.07.001.

Sota M, Allegri C, Cortesi M, Barale F, Politi P, Fusar-Poti P. Targeting the effects of omega-3 and omega-6 fatty acid supplementation on schizophrenic spectrum disorders: role of neuroimaging. Med Hypotheses. 2007;69(2):466–7. https://doi.org/10.1016/j.mehy.2006.12.034.

Sutton A, Khoury H, Prip-Buus C, Cepanec C, Pessayre D, Degoul F. The Ala16Val genetic dimorphism modulates the import of human manganese superoxide dismutase into rat liver mitochondria. Pharmacogenetics. 2003;13(3):145–57. https://doi.org/10.1097/01.fpc.0000054067.64000.8f.

Szeszko PR, Goldberg E, Gunduz-Bruce H, Ashtari M, Robinson D, Malhotra AK, et al. Smaller anterior hippocampal formation volume in antipsychotic-naive patients with first-episode schizophrenia. Am J Psychiatry. 2003;160(12):2190–7. https://doi.org/10.1176/appi.ajp.160.12.2190.

Tam EWY, Chau V, Barkovich AJ, Ferriero DM, Miller SP, Rogers EE, et al. Early postnatal docosahexaenoic acid levels and improved preterm brain development. Pediatr Res. 2016;79(5):723–30. https://doi.org/10.1038/pr.2016.11.

Titova OE, Sjogren P, Brooks SJ, Kullberg J, Ax E, Kilander L, et al. Dietary intake of eicosapentaenoic and docosahexaenoic acids is linked to gray matter volume and cognitive function in elderly. Age (Dordr). 2013;35(4):1495–505. https://doi.org/10.1007/s11357-012-9453-3.

Umhau JC, Zhou WY, Carson RE, Rapoport SI, Polozova A, Demar J, et al. Imaging incorporation of circulating docosahexaenoic acid into the human brain using positron emission tomography. J Lipid Res. 2009;50(7):1259–68. https://doi.org/10.1194/jlr.M800530-JLR200.

van der Kemp WJ, Klomp DW, Kahn RS, Luijten PR, Hulshoff Pol HE. A meta-analysis of the polyunsaturated fatty acid composition of erythrocyte membranes in schizophrenia. Schizophr Res. 2012;141(2–3):153–61. https://doi.org/10.1016/j.schres.2012.08.014.

Wang DF, Cao B, Xu MY, Liu YQ, Yan LL, Liu R, et al. Meta-analyses of manganese superoxide dismutase activity, gene Ala-9Val polymorphism, and the risk of schizophrenia. Medicine (Baltimore). 2015;94(36):e1507. https://doi.org/10.1097/MD.0000000000001507.

Wheeler AL, Voineskos AN. A review of structural neuroimaging in schizophrenia: from connectivity to connectomics. Front Hum Neurosci. 2014;8:653. https://doi.org/10.3389/fnhum.2014.00653.

Witte AV, Kerti L, Hermannstadter HM, Fiebach JB, Schreiber SJ, Schuchardt JP, et al. Long-chain omega-3 fatty acids improve brain function and structure in older adults. Cereb Cortex. 2014;24(11):3059–68. https://doi.org/10.1093/cercor/bht163.

Wood SJ, Cocchi L, Proffitt TM, McConchie M, Jackson GD, Takahashi T, et al. Neuroprotective effects of ethyl-eicosapentaenoic acid in first episode psychosis: a longitudinal T2 relaxometry pilot study. Psychiatry Res. 2010;182(2):180–2. https://doi.org/10.1016/j.pscychresns.2009.12.003.

Yao JK, van Kammen DP, Welker JA. Red blood cell membrane dynamics in schizophrenia. II. Fatty acid composition. Schizophr Res. 1994;13(3):217–26.

Yao JK, Leonard S, Reddy RD. Membrane phospholipid abnormalities in postmortem brains from schizophrenic patients. Schizophr Res. 2000;42(1):7–17.

Youdim KA, Martin A, Joseph JA. Essential fatty acids and the brain: possible health implications. Int J Dev Neurosci. 2000;18(4–5):383–99.

Yousef N, Pistorius EK, Michel KP. Comparative analysis of idiA and isiA transcription under iron starvation and oxidative stress in Synechococcus elongatus PCC 7942 wild-type and selected mutants. Arch Microbiol. 2003;180(6):471–83. https://doi.org/10.1007/s00203-003-0618-4.

Yung AR, Nelson B. Young people at ultra high risk for psychosis: research from the PACE clinic. Rev Bras Psiquiatr. 2011;33(Suppl 2):s143–60.

Zamroziewicz MK, Paul EJ, Zwilling CE, Barbey AK. Predictors of memory in healthy aging: polyunsaturated fatty acid balance and fornix white matter integrity. Aging Dis. 2017;8(4):372–83. https://doi.org/10.14336/AD.2017.0501.

Zimmer L, Vancassel S, Cantagrel S, Breton P, Delamanche S, Guilloteau D, et al. The dopamine mesocorticolimbic pathway is affected by deficiency in n-3 polyunsaturated fatty acids. Am J Clin Nutr. 2002;75(4):662–7.

20 Impact of Non-pharmacological Interventions on Brain Structure and Function in Schizophrenia

Rachal Hegde, Sinead Kelly, Synthia Guimond, and Matcheri Keshavan

Contents

R. Hegde
Department of Psychiatry, Beth Israel Deaconess Medical Center, Massachusetts Mental Health Center, Boston, MA, USA
e-mail: rhegde@bidmc.harvard.edu

S. Kelly
Department of Psychiatry, Beth Israel Deaconess Medical Center, Massachusetts Mental Health Center, Boston, MA, USA

Department of Psychiatry, Brigham and Women's Hospital, Boston, MA, USA
e-mail: skelly8@bidmc.harvard.edu

S. Guimond
Department of Psychiatry, The Royal's Institute of Mental Health Research, The University of Ottawa Brain and Mind Research Institute, University of Ottawa, Ottawa, ON, Canada
e-mail: sguimond@uottawa.ca

M. Keshavan (✉)
Department of Psychiatry, Beth Israel Deaconess Medical Center, Massachusetts Mental Health Center, Boston, MA, USA
e-mail: mkeshava@bidmc.harvard.edu

M. Kubicki, M. E. Shenton (eds.), *Neuroimaging in Schizophrenia*,
https://doi.org/10.1007/978-3-030-35206-6_20

20.1 Introduction

Schizophrenia is a complex psychiatric disorder associated with an array of symptoms, including delusions, hallucinations, anhedonia, social withdrawal, and impaired cognition. The disorder affects approximately 1% of the population and is considered one of the most debilitating psychiatric disorders, significantly affecting the lives of patients and their families (e.g., Saha et al. 2005). The first-line treatment of schizophrenia is antipsychotic medications (e.g., Lehman et al. 2004). The treatment of schizophrenia involves alleviating symptoms, preventing relapse, and improving adaptive functioning so the patient can be integrated back into the community (e.g., Patel et al. 2014). However, antipsychotics are often associated with adverse side-effects, including extrapyramidal symptoms, weight gain, and diabetes. Furthermore, as antipsychotics are unable to treat the full spectrum of symptoms, including negative symptoms (e.g., apathy, anhedonia, social withdrawal), cognitive deficits (e.g., memory and attention impairments), and functional recovery, psychosocial and other nonpharmacological treatments are also important for long-term outcome (e.g., Patel et al. 2014). This has led to a major increase in the development of non-pharmacological interventions for schizophrenia (Andreou and Moritz 2016).

20.2 Non-pharmacological Treatments and Associated Brain Mechanisms

The non-pharmacological treatments discussed in this chapter include physical activity, Cognitive Remediation Therapy (CRT), Cognitive Behavioral Therapy (CBT), Transcranial Magnetic Stimulation (TMS), and Transcranial Direct Current Stimulation (TDCS). We will discuss the impact of these interventions on brain structure and function in schizophrenia based on findings in the neuroimaging literature. Neuroimaging and related techniques can potentially provide a platform for studying the mechanisms underlying the effects of non-pharmacological treatments on schizophrenia, which in turn may reveal key biological targets for treatment and predictors of treatment response.

20.3 Physical Activity

Sedentary behavior is highly prevalent in schizophrenia and is associated with poor outcome (Vancampfort et al. 2017). Studies have shown that regular physical activity is beneficial for people with schizophrenia and has been associated with improvements in metabolic responses, reductions in psychopathological symptoms, and increases in overall quality of life (Knöchel et al. 2012). Moderate to vigorous exercise has also been shown to reduce clinical symptoms in schizophrenia (Firth et al. 2015). Additionally, physical activity such as aerobic exercise and resistance training have been shown to increase levels of neurotrophic factors, which are thought to influence brain plasticity. Furthermore, exercise has been shown to significantly improve cognitive functioning, predominantly in the domains of working memory, attention, and social cognition (Firth et al. 2017a, b).

Previous neuroimaging studies of exercise intervention in schizophrenia indicate that physical activity is associated with increases in brain volume, although there are some inconsistent findings of its effects on specific brain regions (see Table 20.1). For example, two studies investigating the effects of aerobic exercise three times a week over a period of 12 weeks suggest evidence for greater increases in hippocampal gray matter volume in schizophrenia over other conditions such as yoga, table football, and wait list control. Furthermore, increased hippocampal volume in schizophrenia following physical activity has been associated with an increase in working memory performance (Lin et al. 2015; Pajonk et al. 2010). However, other similar studies have found no changes in hippocampal areas after physical exercise, despite improvements in short-term memory and reductions in clinical symptom severity (Falkai et al. 2013; Malchow et al. 2016). Malchow et al.

Table 20.1 Effects of physical activity on brain structure and functioning: structural MRI and fMRI studies

Physical activity								
Study	Country	Population	Active condition	Control condition	Dose/duration	Targeted outcomes	Brain imaging method/task	Main findings
Pajonk et al. (2010)	Germany	Schizophrenia (males)	Aerobic exercise training: cycling (n = 8)	Table football (n = 8)	Both: 36 sessions (30 min each)/12 weeks	1. Working memory 2. Verbal learning	MRI: SPM99 segmentation of hippocampal volumes	↑ in hippocampal gray matter volume in aerobic exercise compared to table football
Takahashi et al. (2012)	Japan	Schizophrenia	Exercise module: aerobic exercise (walking and jogging), muscle-stretching exercise, and basketball (n = 13)	Treatment as usual (n = 10)	Active: 60 sessions (60–120 min each)/12 weeks	1. Attention	fMRI: Exercise video clips of basketball-related motions and basketball-unrelated motions	↑ brain activation in extrastriate body area (EBA) of posterior temporal cortex while watching basketball clips for exercise intervention; ↓ in clinical symptoms associated with ↑ EBA activation
Falkai et al. (2013)	Germany	Schizophrenia (males)	Aerobic exercise training: cycling (n = 8)	Schizophrenia control: Table football (n = 8) Healthy control: Aerobic exercise (n = 8)	Both: 36 sessions (30 min each)/12 weeks	1. Working memory	MRI: Cortical pattern matching for gray matter density	No exercise related changes in cortical regions; ↑ in short-term memory and ↓ negative symptoms after exercise
Lin et al. (2015)	China	Schizophrenia or schizoaffective disorder (females)	Aerobic exercise group: walking and cycling (n = 17) Yoga group (n = 20)	Treatment as usual (n = 11)	Both: 36 sessions (60 min each)/12 weeks	1. Working memory 2. Attention 3. Verbal acquisition	MRI: Freesurfer pipeline segmentation of hippocampal volume	↑ hippocampal gray matter volume for aerobic exercise group and ↑ in left hippocampus. No significant changes in total hippocampal volume for yoga group; Exercise and yoga ↑ working memory and overall symptoms
Lin et al. (2017)	China	Schizophrenia or schizoaffective disorder (females)	Aerobic exercise group: walking and cycling (n = 23) Yoga group (n = 23)	Treatment as usual (n = 12)	Both: 36 sessions (60 min each)/12 weeks	1. Clinical symptoms	fMRI: Resting-state	Amplitude of low frequency fluctuations (ALFF) changes in precuneus associated with changes in negative symptoms for yoga group

(continued)

Table 20.1 (continued)

Physical activity								
Study	Country	Population	Active condition	Control condition	Dose/duration	Targeted outcomes	Brain imaging method/task	Main findings
Malchow et al. (2016)	Germany	Schizophrenia	Endurance training: cycling (n = 20)	Schizophrenia control: Table football (n = 19) Healthy controls: endurance training (n = 21)	Both: 36 sessions (30 min each)/12 weeks	1. Working memory 2. Verbal learning 3. Processing speed	MRI: Voxel-based morphometry and Freesurfer pipeline segmentation of hippocampal volume	↑ gray matter volume in left anterior temporal lobe compared to baseline
Svatkova et al. (2015)	Netherlands	Schizophrenia	Aerobic exercise training: cycling (n = 16)	Schizophrenia control: Treatment as usual (n = 17) Healthy controls: Aerobic exercise (n = 24) and treatment as usual (n = 24)	Both: 48 sessions (1 h each)/24 weeks	1. Global IQ	MRI: Diffusion tensor imaging (DTI) using tract-based spatial statistics (TBSS)	↑ in white matter integrity in fiber tracts for motor functioning; ↓ positive symptoms correlated with ↑ white matter integrity

(2016) found significant increases in gray matter volume in the left anterior temporal lobe after 3 months of endurance training specifically in people with schizophrenia. This is interesting to note as the left temporal lobe is considered to be a key region associated with volumetric abnormalities in early stages of schizophrenia, as well as for those at high risk for developing schizophrenia (Malchow et al. 2016).

Changes in white matter associated with physical exercise have also been reported in schizophrenia. Svatkova et al. (2015) examined a combination of aerobic exercise and resistance training from stationary bicycling and found significant increases in white matter integrity in fiber tracts after a period of 6 months, particularly in tracts associated with motor functioning in individuals with schizophrenia. Moreover, increased white matter integrity was significantly correlated with reductions in positive symptoms. However, there was no significant associations between aerobic exercise and improvements in cognitive functioning (Svatkova et al. 2015).

Takahashi et al. (2012) examined changes in brain activation from physical activity in schizophrenia using fMRI analysis. An intervention including aerobic exercise and basketball led to increased activation of the extrastriate body area (EBA) in the posterior temporal-occipital cortex while watching sports-related videos (basketball clips) during fMRI 3 months afterwards, whereas no changes in brain activation were observed in patients in the control condition (i.e., no intervention). Greater EBA activation was associated with improvements in the general clinical symptoms subscale, but was not observed for the positive and negative symptom subscales (Takahashi et al. 2012). Additionally, Lin et al. (2017) investigated the effects of aerobic exercise and yoga in female patients. The study observed local spontaneous neuronal fluctuations during resting state, measuring the amplitude of low-frequency fluctuations (ALFF). In the yoga group, ALFF reductions in the precuneus were significantly correlated with improvements in negative symptoms in schizophrenia.

Overall, results from physical activity studies have shown promising effects on enhanced cognitive performance, reduced clinical symptom severity, as well as improvements in brain structure and function. Physical activity appears to have the greatest brain effects in the temporal regions, mostly in the hippocampus, and has further been associated with improved cognition. However, inconsistent results across hippocampal studies and the lack of studies investigating other neural correlates, and the neural mechanisms underlying behavioral improvements, highlight the need for additional studies. Furthermore, there is currently a limited understanding of the neurobiological mechanisms through which exercise may improve cognitive functioning and clinical symptoms in people with schizophrenia. Preliminary evidence from biomarker studies in schizophrenia indicate that exercise interventions are associated with upregulation of brain-derived neurotrophic factor (BDNF) levels and cognitive enhancement (Kimhy et al. 2015; Nuechterlein et al. 2016; Vakhrusheva et al. 2016). This is important as BDNF is associated with neurogenesis and neuroplasticity, and is shown to facilitate memory and cognitive function (Wang and Holsinger 2018). As exercise has emerged as a promising intervention for schizophrenia, prospective research should assess the effects of induced BDNF expression on neurocognition as well as the potential role of other neurotrophic factors. Future studies are nonetheless still needed to gain further insight into the biological mechanisms of exercise, with the hopes of developing beneficial interventions for reducing clinical symptoms and cognitive deficits in schizophrenia.

20.4 Cognitive Remediation Therapy

Cognitive remediation therapy (CRT) is a behavioral training-based intervention which aims to improve cognitive functioning and

behavior (e.g., Keshavan et al. 2014). CRT focuses on teaching skills and tactics to enhance cognition with the hopes that improvements in cognitive domains will enrich community functioning. Cognitive domains targeted by CRT include attention/vigilance, working memory, verbal learning and memory, visual learning and memory, reasoning and problem solving, processing speed, and social cognition (Nuechterlein et al. 2014; Wykes et al. 2011). CRT studies indicate overall improvements in the majority of cognitive domains with the exception of visual learning and memory (McGurk et al. 2007; Wykes et al. 2011). The majority of CRT treatment approaches separately target neurocognitive or sociocognitive factors, but some cognitive therapies such as cognitive enhancement therapy (CET) utilize an integrated approach of both neurocognitive and social cognitive factors for maximal treatment outcomes (Eack et al. 2009; Hogarty et al. 2004).

CRT is known to be an effective non-pharmacological intervention for cognitive impairments and daily functioning in schizophrenia. CRT treatment programs focus on teaching effective strategies to improve community functioning in patients (Wykes et al. 2011). Recently, CRT has also been suggested as having a small to moderate positive effect on reducing negative symptoms of schizophrenia (Cella et al. 2017). Evidence from neuroimaging studies have also reported both structural and functional changes in major prefrontal brain regions (Keshavan et al. 2014; Thorsen et al. 2014). There is, however, limited knowledge of the neural mechanisms through which CRT effects are mediated. Cognitive strategies may directly reverse neural circuitry deficits and/or preserve cognitive function by strengthening compensatory neuroplasticity (Minzenberg et al. 2009). A greater understanding of neural substrates that are susceptible to CRT is warranted to help identify target mechanisms for the development of effective treatments for schizophrenia.

20.4.1 Neural Correlates: Evidence from Various Brain Imaging Modalities

CRT has been associated with changes in several brain regions including major prefrontal regions, as well as parietal and limbic areas (Thorsen et al. 2014). Abnormal prefrontal cortex activity has been linked to cognitive deficits in multiple cognitive domains (Keshavan et al. 2014; Thorsen et al. 2014). Over the years, researchers have utilized various neuroimaging techniques to investigate the impact of CRT in individuals with schizophrenia.

20.4.1.1 Functional Magnetic Resonance Imaging

Several functional magnetic resonance imaging (fMRI) studies have shown associations between increased activation in various prefrontal cortex regions and improvements in cognition after CRT in schizophrenia (see Table 20.2) (Guimond et al. 2018; Haut et al. 2010; Keshavan et al. 2017; Ramsay et al. 2017a; Subramaniam et al. 2012). Specifically, increased PFC activity has been associated with improvements in cognitive control, affect recognition, and semantic encoding strategies in associative memory (Guimond et al. 2018; Habel et al. 2010; Hooker et al. 2013; Keshavan et al. 2017). Guimond et al. (2018) showed positive associations between increases in PFC activity and semantic encoding strategies in associative memory, indicating novel evidence for the potential to treat episodic memory deficits in schizophrenia. Additionally, resting-state functional connectivity analysis after CRT demonstrates increased activation in numerous regions, including lateral and medial prefrontal cortices, and enhanced amplitude of low-frequency fluctuations in the medial prefrontal cortex and the anterior cingulate cortex (Donohoe et al. 2018; Fan et al. 2017). Overall, results from neuroimaging studies highlight the role of the PFC as possibly mediating the positive CRT response. Nonetheless, other regions also seem to be involved, but their implication may depend on CRT methods, patient populations, and imaging paradigms.

Table 20.2 Effects of CRT on brain functioning: fMRI studies

Functional magnetic resonance imaging: cognitive remediation therapy								
Study	Country	Population	Active condition	Control condition	Dose/duration	Targeted outcomes	Brain imaging method/ task	Main findings
Wykes et al. (2002)	England	Chronic schizophrenia	Individualized paper and pencil neurocognitive tasks and strategies teaching (n = 6)	Occupational therapy activities (n = 6)	Both: 40 sessions (1 h each)/12 weeks	1. Cognitive flexibility 2. Working memory 3. Planning	fMRI: N-back task	↑ activity in right inferior frontal gyrus
Edwards et al. (2010)	USA	Schizophrenia or schizoaffective disorder	Focused computer-based strategies training (n = 22)	No patient control condition	Active: 1 session (20 min)/1 day	1. Cognitive control	fMRI: AX-CPT cognitive control task	↑ activity in inferior frontal junction
Habel et al. (2010)	Germany	Schizophrenia (males)	Focused computer-based facial affect recognition training (n = 10)	Treatment as usual (n = 12)	Active: 12 sessions (45 min each)/6 weeks	1. Affect recognition	fMRI: Facial emotion recognition task	↑ activity in the left middle and superior occipital lobe, right inferior and superior parietal cortex, and inferior frontal cortex bilateral
Haut et al. (2010)	USA	Chronic schizophrenia	Focused computer-based neurocognitive training in group (n = 9)	Social skills training (n = 9)	Both: 25 sessions (1 h each)/4–6 weeks	1. Working memory	fMRI: (1) word N-back task (2) Picture N-back task (3) Non-targeted lexical decision task	↑ activity in dorsolateral prefrontal cortex, anterior cingulate, and frontopolar cortex
Bor et al. (2011)	France	Schizophrenia	Individualized computer-based neurocognitive exercises (n = 8)	Treatment as usual (n = 9)	Active: 14 sessions (2 h each)/7 weeks	1. Attention/ concentration 2. Working memory 3. Logical thinking 4. Executive functions	fMRI: (1) verbal N-back task (2) Spatial N-back task	↑ activity in left inferior/ middle frontal gyrus, cingulate gyrus, and inferior parietal lobule
Hooker et al. (2012)	USA	Chronic schizophrenia or schizoaffective disorder	Computer-based cognitive remediation with neurocognitive and sociocognitive exercises (n = 11)	Computer games (n = 11)	Active: 50 computerized auditory-based sessions (1 h each) + 50 sessions of emotion recognition exercises (5–15 min each)/10 weeks Control: 50 sessions (1 h each)/10 weeks	1. Auditory and verbal information processing 2. Working memory 3. Verbal learning and memory 4. Affect recognition	fMRI: Facial emotion recognition task	↑ right postcentral gyrus activity
Subramaniam et al. (2012)	USA	Schizophrenia	Computer-based cognitive remediation with neurocognitive and sociocognitive exercises (n = 15)	Computer games (n = 14)	Active: 50 auditory exercise sessions (1 h each) + 30 visual exercise sessions (1 h each) + 40 sessions of emotion identification exercises (15 min each)/16 weeks Control: 80 sessions (1 h each)/16 weeks	1. Working memory 2. Affect recognition	fMRI: Reality monitoring task	↑ left medial prefrontal cortex activity

(continued)

Table 20.2 (continued)

Functional magnetic resonance imaging: cognitive remediation therapy								
Study	Country	Population	Active condition	Control condition	Dose/duration	Targeted outcomes	Brain imaging method/ task	Main findings
Hooker et al. (2013)	USA	Chronic schizophrenia or schizoaffective disorder	Computer-based cognitive remediation with neurocognitive and sociocognitive exercises (n = 11)	Computer games (n = 11)	Active: 50 computerized auditory-based sessions (1 h each) + 50 sessions of emotion recognition exercises (5–15 min each)/10 weeks Control: 50 sessions (1 h each)/10 weeks	1. Auditory and verbal information processing 2. Working memory 3. Verbal learning and memory 4. Affect recognition	fMRI: Facial emotion recognition task	↑ activity in the bilateral amygdala, right putamen, and right medial prefrontal cortex
Penadés et al. (2013)	Spain	Schizophrenia	Individualized paper and pencil neurocognitive tasks and strategies teaching (n = 17)	Social skills training (n = 18)	Active: 80–120 sessions (1 h each)/4 months Control: 40 sessions (1 h each)/4 months	1. Cognitive flexibility 2. Working memory 3. Planning	fMRI: N-back task	↓ activity in central executive network (normalized) and ↑ deactivation in default mode network
Subramaniam et al. (2014)	USA	Schizophrenia	Computer-based cognitive remediation with neurocognitive and sociocognitive exercises (n = 15)	Computer games (n = 14)	Active: 50 auditory exercise sessions (1 h each) + 30 visual exercise sessions (1 h each) + 40 sessions of emotion identification exercises (15 min each)/16 weeks Control: 80 sessions (1 h each)/16 weeks	1. Working memory 2. Affect recognition	fMRI: N-back task	↑ activity in the left middle frontal gyrus and left inferior frontal gyrus
Vianin et al. (2014)	Switzerland	Schizophrenia	Individualized computer-based neurocognitive exercises and exercises at home (n = 8)	Treatment as usual (n = 8)	Active: 28 computer sessions (1 h each) + exercises at home (total of 14 h)/14 weeks	1. Selective attention 2. Verbal memory 3. Visuo-spatial attention and memory 4. Working memory 5. Reasoning 6. Speed of processing	fMRI: Verbal fluency task	↑ activity in the left Broca's area (BA45)
Eack et al. (2016)	USA	Early course schizophrenia or schizoaffective disorder	Computer-based neurocognitive exercises in pair + sociocognitive group sessions + individual meeting with coach (n = 17)	Enriched supportive therapy (n = 8)	Active: 60 computer-based neurocognitive sessions (1 h each) + 45 sociocognitive group sessions (60–90 min each) + 45 individual meeting sessions (30–60 min each)/18 months Control: 45 individual meeting sessions (30–60 min each)/18 months	1. Attention 2. Memory 3. Problem solving 4. Social cognition	fMRI: Pseudo resting-state	↓ functional connectivity loss between posterior cingulate cortex and left dorsolateral prefrontal cortex, ↑ functional connectivity between posterior cingulate cortex and right insular cortex

Fan et al. (2017)	China	Schizophrenia	Computer-based neurocognitive exercises in group (n = 12)	Treatment as usual (n = 11)	Active: 40 sessions (45 min each)/8 weeks	1. Working memory 2. Cognitive flexibility 3. Planning 4. Affect recognition 5. Emotion management	fMRI: Resting-state using amplitude of low-frequency fluctuation (ALFF)	↑ALFF in the medial prefrontal cortex/anterior cingulate cortex
Keshavan et al. (2017)	USA	Early course schizophrenia or schizoaffective disorder	Computer-based neurocognitive exercises in pair + sociocognitive group sessions + individual meeting with coach (n = 17)	Enriched supportive therapy (n = 8)	Active: 60 computer-based neurocognitive sessions (1 h each) + 45 sociocognitive group sessions (60–90 min each) + 45 individual meeting sessions (30–60 min each)/18 months Control: 45 individual meeting session (30–60 min each)/18 months	1. Attention 2. Memory 3. Problem solving 4. Social cognition	fMRI: Preparing to overcome prepotency task	↑ activity in the right dorsolateral prefrontal cortex and ↓connectivity between dorsolateral prefrontal cortex and anterior cingulate cortex
Ramsay et al. (2017a, b, c)	USA	Schizophrenia or schizoaffective disorder	Focused computer-based neurocognitive exercises in group and bridging group (n = 14)	Active computer skills training and bridging group (n = 12)	Both: 48 sessions (1 h each)/16 weeks	1. Working memory	fMRI: (1) resting state (2) N-back	↑ thalamocortical connectivity with middle frontal gyrus and anterior cingulate cortex
Ramsay et al. (2017a, b, c)	USA	Schizophrenia or schizoaffective disorder	Focused computer-based neurocognitive exercises in group and bridging group (n = 14)	Active computer skills training and bridging group (n = 12)	Both: 48 sessions (1 h each)/16 weeks	1. Working memory	fMRI: (1) word N-back task (2) Picture N-back task	↑ activity in left prefrontal cortex
Donohoe et al. (2018)	Ireland	Schizophrenia, schizoaffective, bipolar disorder, or major depressive disorder	Focused auditory and visual computer-based neurocognitive and sociocognitive exercises + individual meeting with study therapist (n = 25)	General computer-based neurocognitive exercises + sociocognitive group sessions + individual meeting with study therapist (n = 30)	Both: 40 sessions (30–40 min)/8 weeks + 8 individual meeting with study therapist (45 min)/8 weeks	1. Auditory working memory 2. Visual working memory	fMRI: (1) N-back task (2) Resting state	↑ connectivity between right precuneus and left inferior parietal lobule and between left anterior cingulate and right midcingulate
Guimond et al. (2018)	Canada	Schizophrenia or schizoaffective disorder	Focused computer-based strategies training and assignments (n = 15)	No patient control condition	Active: 2 sessions (1 h each)/2 weeks	1. Semantic encoding strategies in associative memory	fMRI: Semantic encoding memory task	↑ activity in the left dorsolateral prefrontal cortex

Adapted from Guimond et al. (2019)

20.4.1.2 Structural Magnetic Resonance Imaging

Structural imaging studies of CRT have reported neuroprotective and neuroplasticity effects in gray matter indicating significant increases in gray matter volume in the left amygdala and right hippocampus, as well as greater preservation of gray matter volume in the left hippocampus, left thalamus, parahippocampal gyrus, and fusiform gyrus in relation to working memory improvements (see Table 20.3) (Eack et al. 2010; Morimoto et al. 2018; Ramsay et al. 2017a). Eack et al. (2010) found greater preservation in gray matter volume over 2 years in brain regions such as the left hippocampus, in addition to increases in the left amygdala gray matter after CET. Results from the study indicate the potential for CET to offer neuroprotective effects in early schizophrenia, as well as improvements in both social cognition and neurocognition. In addition, Morimoto et al. (2018) found evidence for hippocampal plasticity in schizophrenia following CRT intervention. Twelve weeks of CRT resulted in significant increases in right hippocampal gray matter volume and a significant positive correlation with verbal fluency scores. However, as both studies report hippocampal plasticity in different hemispheres, future studies are necessary to address these inconsistent findings. Penadés et al. (2013) is the only study to date to examine the effects of CRT on white matter changes in schizophrenia using diffusion tensor imaging analysis. This study observed increased fractional anisotropy in the anterior part of the genu of the corpus callosum and in the right posterior thalamic radiations after 4 months of CRT treatment. Evidence of structural changes after CRT provide preliminary evidence for neuroprotection and neuroplasticity, thus supporting the beneficial effects of CRT to potentially reduce the progression of degradative brain changes in schizophrenia. However, as these findings have not as yet been replicated, more studies are needed to validate these findings.

20.4.1.3 Electrophysiology and Magnetoencephalography

Findings from electrophysiology (EEG) and magnetoencephalography (MEG) studies investigating the effects of CRT are listed in Table 20.4. CRT has been associated with improvements in frontal theta and gamma power and reduced posterior alpha power during computerized cognitive tasks after training (Best et al. 2019; Popova et al. 2018). Additionally, studies focusing on the effects of sociocognitive CRT indicate changes in neuronal activity of prefrontal and frontoparietal regions (Luckhaus et al. 2013; Mazza et al. 2010; Stroth et al. 2015).

Recently, Best et al. (2019) conducted the first EEG study to examine the neurophysiological effects of CRT on executive functioning and suggest greater frontal theta frequency power and reduced posterior alpha frequency power as potential neurophysiological markers to consider in CRT studies. Additionally, the study showed evidence for neurophysiological and neurocognitive changes after executive functioning training. Alpha and theta frequency band oscillations in EEG have been associated with attentional and working memory capabilities respectively (Klimesch 1999).

MEG studies focusing on auditory discrimination and working memory have shown increases of M100 amplitude and reduction of M50 gating ratio, as well as improvements in alpha and gamma signals (Dale et al. 2016; Popov et al. 2011, 2012). Specifically, Popov et al. (2011) applied MEG to investigate neuronal effects of auditory-focused CRT by measuring auditory gating ratios and overall performance on verbal memory and fluency tests before and after 4 weeks of training. Results showed cognitive training improved both auditory-verbal discrimination and working memory, in addition to normalized M50 sensory gating ratio in schizophrenia. In another study, Popov et al. (2012) examined if training effects on task performance and M50 ratio are mediated by brain

Table 20.3 Effects of CRT on brain structure: MRI studies

Brain structure (MRI): cognitive remediation therapy								
Study	Country	Population	Active condition	Control condition	Dose/duration	Targeted outcomes	Brain imaging method	Main findings
Eack et al. (2010)	USA	Early course schizophrenia or schizoaffective disorder	Computer-based neurocognitive exercises in pair + sociocognitive group sessions + individual meeting with coach (n = 30)	Enriched supportive therapy (n = 23)	Active: 60 computer-based neurocognitive sessions (1 h each) + 45 sociocognitive group sessions (60–90 min each) + 45 individual meeting sessions (30–60 min each)/18 months control: 45 individual meeting sessions (30–60 min each)/18 months	1. Attention 2. Memory 3. Problem solving 4. Social cognition	MRI: Voxel-based morphometry (VBM)	↑ preservation of gray matter volume in the left hippocampus parahippocampal gyrus, and fusiform gyrus; ↑ gray matter increases in the left amygdala
Penadés et al. (2013)	Spain	Schizophrenia	Individualized paper and pencil neurocognitive tasks and strategies teaching (n = 17)	Social skills training (n = 18)	Active: 80–120 sessions (1 h each)/4 months Control: 40 sessions (1 h each)/4 months	1. Cognitive flexibility 2. Working memory 3. Planning	MRI: Diffusion tensor imaging (DTI) using tract-based spatial statistics (TBSS)	↑ fractional anisotropy index in the anterior part of the genu of the corpus callosum
Ramsay et al. (2017a, b, c)	USA	Early course schizophrenia or schizoaffective disorder	Focused auditory computer-based neurocognitive training at home (n = 22)	Computer games at home (n = 22)	Both: 40 sessions (1 h each)/8 weeks	1. Auditory and verbal information processing 2. Working memory	MRI: Freesurfer longitudinal pipeline segmentation of the left and right thalamic regions	No significant treatment condition interaction but ↑ left thalamic volume in active condition related to ↑ global cognition scores
Morimoto et al. (2018)	Japan	Schizophrenia	Computer-based Japanese Cognitive Rehabilitation Program for Schizophrenia (Jcores) training (n = 16)	Treatment as usual (n = 15)	Active: 24 sessions (1 h each) + 24 (1 h) group sessions/12 weeks Control: 24 sessions (1 h each)/12 weeks	1. Attention 2. Psychomotor speed 3. Learning 4. Verbal fluency 5. Memory 6. Executive function	MRI: Voxel-based morphometry (VBM)	↑ right hippocampal gray matter volume and improvements in verbal fluency and global cognitive scores for CRT group

Table 20.4 Effects of CRT on brain function: EEG and MEG studies

Electrophysiology and magnetoencephalography: cognitive remediation therapy								
Study	Country	Population	Active condition	Control condition	Dose/duration	Targeted outcomes	Brain imaging method/task	Main findings
Mazza et al. (2010)	Italy	Schizophrenia	Group based emotion and theory of mind imitation training and "in vivo" practice assignments (n = 16)	Problem solving training group (n = 17)	Both: 24 sessions (50 min each)/12 weeks	1. Social cognition	EEG: Emotion recognition event-related potential	↑ electroactivity of medio-frontal areas
Popov et al. (2011)	Germany	Paranoid-hallucinatory schizophrenia	Focused auditory computer-based neurocognitive training (n = 20)	General computer-based neurocognitive exercises (n = 19)	Active: 20 sessions (1 h each)/4 weeks control: 12 sessions (60–90 min each)/4 weeks	1. Auditory verbal discrimination 2. Working memory	MEG: Auditory sensory gating task	↓ gating M50 ratios (normalized)
Popov et al. (2012)	Germany	Paranoid-hallucinatory schizophrenia	Focused auditory computer-based neurocognitive training (n = 18)	General computer-based neurocognitive exercises (n = 18)	Active: 20 sessions (1 h each)/4 weeks control: 12 sessions (60–90 min each)/4 weeks	1. Auditory verbal discrimination 2. Working memory	MEG: Auditory sensory gating task	↑ time-locked gamma-band response and ↑ non-time-locked alpha-band desynchronization associated with normalized M50 ratio
Rass et al. (2012)	USA	Schizophrenia or schizoaffective disorder	Computer-based neurocognitive exercises (n = 17)	Watching TV (n = 17) Treatment as usual (n = 10)	Both: 20 sessions (2 h each)/10 weeks	1. Speed of processing 2. Attention and vigilance 3. Memory	EEG: Auditory steady state response and P300 event-related potential	No significant differences
Luckhaus et al. (2013)	Germany	Violent male offenders with schizophrenia	Focused computer-based facial affect recognition training in pair and assignments (n = 16)	No patient control condition	Active: 12 sessions (1 h each)/6 weeks	1. Affect recognition	EEG: Event-related potential and low-resolution brain electromagnetic tomography (LORETA) during affect recognition task (LORETA), during affect recognition task	LORETA: ↓ activation in the left-hemispheric parietal–temporal–occipital regions at 172 ms and ↑ activation in the right dorsolateral prefrontal cortex and anterior cingulate at 250 ms No significant changes on ERPs
Popova et al. (2014)	Germany	Paranoid-hallucinatory schizophrenia	Focused computer-based facial affect recognition training (n = 19)	Treatment as usual (n = 19) Focused computerized auditory-verbal training (n = 19)	Both: 20 sessions (1 h each)/4 weeks	1. Affect recognition	MEG: Dynamic facial affect recognition task	↑ alpha power (10–13 Hz) = perceptual–cognitive training > treatment-as-usual
Popov et al. (2015)	Germany	Chronic schizophrenia	Focused auditory computer-based neurocognitive training (n = 19)	Treatment as usual (n = 19) Focused computer-based facial affect discrimination training (n = 19)	Both: 20 sessions (1 h each)/4 weeks	1. Auditory verbal discrimination 2. Working memory	MEG: Auditory paired-click task	↑ click-induced posterior alpha power modulation

Stroth et al. (2015)	Germany	Schizophrenia	Focused computer-based facial affect recognition training in pair and assignments (n = 12)	No patient control condition	Active: 12 sessions (1 h each)/6 weeks	1. Affect recognition	EEG: Event-related potential and low-resolution brain electromagnetic tomography (LORETA) during affect recognition task	↑ activation in the superior parietal and the inferior parietal lobes
Dale et al. (2016)	USA	Chronic schizophrenia	Focused auditory computer-based neurocognitive training (n = 18)	Computer games (n = 18)	Both: 50 sessions (1 h each)/10 weeks	1. Auditory verbal discrimination 2. Working memory	MEG: Auditory syllable identification task	↑ M100 responses, ↑ induced high gamma band activity within left dorsolateral prefrontal cortex immediately after stimulus presentation and later in bilateral temporal cortices
Kärgel et al. (2016)	Germany	Schizophrenia or schizoaffective disorder	Focused auditory computer-based neurocognitive training (n = 14) Focused visuo-spatial computer-based neurocognitive training (n = 14)	Treatment as usual (n = 14)	Active: 10 sessions (50 min each)/2 weeks	1. Discrimination and identification of auditory stimuli 2. Discrimination and identification of visual stimuli	EEG: Event-related potential MMN	No significant differences
Best et al. (2019)	Canada	Schizophrenia, schizoaffective, bipolar disorder, or major depressive disorder	Computer-based neurocognitive executive function training (n = 13)	General computer-based neurocognitive exercises (n = 12)	Both: 6 training sessions (1 h each) + 14 home training sessions (40 min each)/2 weeks	1. Executive functioning 2. Working memory	EEG: Cognitive training exercises	↑ in frontal theta power and reduced posterior alpha power
Perez et al. (2017)	USA	Schizophrenia	Focused auditory computer-based neurocognitive training (n = 28)	No patient control condition	Active: 2 training sessions (1 h each)	1. Discrimination of auditory stimuli	EEG: Event-related potential MMN	↑ MMN amplitude
Popova et al. (2018)	Germany	Paranoid-hallucinatory schizophrenia, schizoaffective disorder, or transient schizophrenia	Computer-based targeted neurocognitive training (n = 40)	General treatment of cognitive remediation and social and work activities (n = 21)	Active: 20 sessions (1 h each)/4 weeks; control: 8 sessions (30 min each)/4 weeks	1. Perceptual discrimination acuity 2. Working memory 3. Attention	MEG: Resting state task (5 min)	↑ in gamma power of 40–90 Hz after training in frontoparietal network

oscillatory activity changes. They found increases in both time-locked gamma-band activity, (60–80 Hz) as well as in non-time-locked alpha-band desynchronization (8–12 Hz) in association with M50 and improvements in verbal memory.

Kärgel et al. (2016) examined the effects of auditory and visual training on mismatch negativity (MMN), yet found no significant changes. However, Perez et al. (2017) found that enhanced auditory perceptual learning was associated with larger MMN amplitudes before and after training, demonstrating MMN amplitude as an EEG biomarker of enhanced auditory perceptual learning in schizophrenia. Conflicting findings suggest that future trials of MMN as a biomarker for predicting patients' treatment response to cognitive interventions in schizophrenia are needed.

Overall, electrophysiological studies indicate cognitive changes toward normalization after CRT and suggest potential neurophysiological markers to consider in CRT studies.

20.4.2 Structural Biomarkers of Positive Response to CRT

Studies utilizing CRT suggest potential structural biomarkers for predicting treatment response (see Table 20.2). Structural biomarkers such as left frontal cortical thickness and left thalamic volume preservation can positively predict treatment response and improvements in cognition (Guimond et al. 2018; Ramsay et al. 2017a). Keshavan et al. (2011) was the first study to investigate the impact of cortical reserve as a neural predictor of improvement after CRT intervention. The study found that baseline cortical surface area and gray matter volume predicted enhanced social cognition improvements 1 year after CRT treatment. Guimond et al. (2018) showed relations between greater cortical reserve in the left DLPFC at baseline to greater improvements in semantic encoding after CRT. Additionally, Ramsay et al. (2017a, b, c) demonstrated that improvements in cognition after CRT are positively correlated to lower baseline symptoms, as well as volumetric increases in the left thalamic region over a 4-month period in early schizophrenia.

In summary, neuroimaging studies of CRT have observed significant findings of neuronal changes accompanied by improvements in neurocognition and social cognition in schizophrenia. Evidence from research studies have supported the beneficial application of CRT to improve cognitive deficits in schizophrenia. Future investigations on the longitudinal effects of CRT post-treatment are warranted for assessing durability and the long-term effects of CRT on brain structure and function in schizophrenia.

20.5 Cognitive Behavioral Therapy

Cognitive behavioral therapy (CBT) is a psychological intervention that aims to improve mental health by establishing links between thoughts, emotions, and behavior to help with emotional regulation and coping strategies. CBT serves as a beneficial treatment strategy for effectively reducing the severity of positive symptoms in schizophrenia (Habel et al. 2010). Furthermore, CBT aims to establish a strong therapeutic alliance by incorporating cognitive and behavioral interventions to reduce occurrence and distress associated with schizophrenia, to target comorbid affect states, and to reduce potential relapse (Patterson and Leeuwenkamp 2008; Rector and Beck 2001). Patients learn to recognize the nature of psychosis within a biopsychosocial model and develop beneficial techniques to reduce stress and learn effective coping strategies and cognitive restructuring to help alleviate their positive and negative symptoms (Patterson and Leeuwenkamp 2008). While CBT has shown positive effects on clinical symptoms in schizophrenia, little is known about the brain mechanisms underlying positive response to this type of treatment.

An fMRI study using an N-back working memory task by Kumari et al. (2009) showed increased DLPFC activity, as well as strengthened DLPFC-cerebellum connectivity during the highest memory load condition (2-back vs. 0-back) post-CBT treatment (see Table 20.5).

Table 20.5 Effects of CBT on brain structure: MRI studies

Cognitive behavioral therapy								
Study	Country	Population	Active condition	Control condition	Dose/duration	Targeted outcomes	Brain imaging method/task	Main findings
Kumari et al. (2009)	England	Schizophrenia	CBT with treatment as usual (n = 19)	Schizophrenia controls: Treatment as usual (n = 17) Healthy controls (n = 20)	Active: 16 sessions of CBT (1 h each)/6–8 months	1. Executive functioning	fMRI: N-back task	↑ dorsolateral prefrontal cortex activity and DLPFC-cerebellum connectivity during highest memory load condition (2-back)
Premkumar et al. (2009)	England	Schizophrenia	CBT with treatment as usual (n = 25)	Schizophrenia controls: Treatment as usual (n = 19) Healthy controls: (n = 25)	Active: 16 sessions of CBT (1 h each)/6–8 months	1. Clinical symptoms	MRI: SPM2 modulated segmentation	↑ gray matter volume in the frontal, temporal, parietal, and cerebellar areas related to ↑ in CBT responsiveness
Premkumar et al. (2018)	England	Schizophrenia	CBT with treatment as usual (n = 24)	Schizophrenia controls: Treatment as usual (n = 16) Healthy controls: (n = 30)	Active: 16 sessions of CBT (1 h each)/6–8 months	1. Verbal learning and memory	MRI: Pituitary volumetry with MEASURE program	↓ pituitary volume correlated with pre-CBT verbal learning

The positive DLPFC-cerebellum connectivity was strongly associated with a favorable response to CBT during the 2-back vs. 0-back condition and suggests the brain's default mode network plays a role in the effectiveness of CBT in schizophrenia. Additionally, a reduction in general symptom severity was related to greater bilateral activity in the inferior-middle frontal gyrus, primarily in the DLPFC post-CBT treatment.

Premkumar et al. (2009) aimed to determine whether improvements in clinical symptoms following CBT were correlated with pre-CBT gray matter volume in brain regions involved in cognitive processing. The authors focused on frontal, temporal, parietal, and cerebellar gray matter volume associated with coordination of mental activity, cognitive flexibility, and verbal learning and memory. Specifically, improvements in positive symptoms were associated with greater right cerebellar gray matter volume, and negative symptoms were associated with the left precentral gyrus and right inferior parietal lobule volume. General psychopathology was associated with the right superior temporal gyrus (STG), right cuneus, and right cerebellum volume, and total symptoms were associated with the right STG and right cuneus. As one of the main goals of CBT is to lower the stress of psychotic symptoms, Premkumar et al. (2018) went on to investigate the relation between CBT and pituitary volumetric changes in schizophrenia. The study observed reductions in pituitary volume in CBT post-treatment, and further observed that pre-therapy verbal learning memory performance was strongly correlated with baseline-to-follow-up pituitary volumetric changes. The authors suggest that CBT reduces pituitary volume by enhancing stress regulation and reducing distress caused by psychotic symptoms.

Currently, there is a limited understanding of the outcomes of CBT on brain structure and function and further studies are warranted for investigating the efficacy of CBT on cognition and clinical symptoms in schizophrenia.

20.6 Neuromodulation: Transcranial Magnetic Stimulation (TMS) and Transcranial Direct-Current Stimulation (TDCS)

20.6.1 Transcranial Magnetic Stimulation (TMS)

Transcranial magnetic stimulation (TMS) is a type of neuromodulation providing a new frontier in potential effective treatment options for schizophrenia (Cole et al. 2015). TMS is a noninvasive neurostimulation technique that induces an electrical current in the cortex by using alternating magnetic fields. The United States Food and Drug Administration (FDA) has approved TMS for the treatment of adult major depression for individuals who have not responded to medication. The procedure involves the placement of an electromagnetic coil on the scalp which transforms electrical activity to pulsed magnetic energy to induce an electrical field in the cortex causing neurons to depolarize and generate action potentials (Ji et al. 1998). TMS has an inhibitory effect (through GABAergic effects or long-term neuronal depression (LTD)) if the frequency of the pulse is low (i.e., 1 Hz or less) (Chen et al. 1997), while high pulse frequency will generate an excitatory effect (through glutamatergic effects or long term potentiation (LTP)). Pulses can be administered as single, paired, or in a series, called a train. TMS delivered in a train is referred to as repetitive *TMS* (rTMS). No anesthesia is required when administering TMS and patients can usually leave immediately following their session.

A 2015 review of 21 studies by Cole et al. concluded that TMS in schizophrenia has been effective in treating auditory hallucinations. They found that targeting low frequency TMS to Wernicke's area in the left temporoparietal cortex may reduce the frequency and severity of auditory hallucinations. However, they suggested that

further studies of both inpatient and outpatient populations are needed. They also noted that negative symptoms can be alleviated using high frequency TMS to the dorso-lateral prefrontal cortex (DLPFC) and there are also some positive findings regarding cognitive symptoms. Furthermore, Osoegawa et al. (2018) conducted a systematic review of non-invasive brain stimulation for negative symptoms in randomized clinical trials and found that rTMS was superior to sham for treating negative symptoms but concluded that further clinical trials with larger sample sizes are needed.

In an attempt to explain how the technique may be contributing to improvements in symptoms, a handful of studies have used neuroimaging techniques to identify the underlying neural mechanisms associated with the application of rTMS in schizophrenia (see Table 20.6). Dlabac-de Lange et al. (2015) examined whether or not 3 weeks of high frequency rTMS of the DLPFC would improve frontal brain activation in patients with negative symptoms of schizophrenia, during an executive functioning task. After rTMS treatment, brain activity increased in the right DLPFC and in the right medial frontal gyrus compared to the sham group. In addition, the rTMS group showed decreased brain activation in the left posterior cingulate compared to increased activation in the sham group. These findings suggest that treatment with rTMS over the DLPFC may have the potential for increasing task-related activation in frontal areas in patients with schizophrenia. A recent study by Brady et al. (2019) identified a functional brain network between the cerebellum and right dorsolateral prefrontal cortex that was associated with negative symptoms in 44 schizophrenia patients. They found that restoration of this functional connectivity with rTMS was significantly associated with a reduction in negative symptoms.

A number of studies have also examined the effects of rTMS on cognitive symptoms in schizophrenia. A recent study by Francis et al. (2018) examined cognitive function in early psychosis before and after high frequency rTMS targeting the DLPFC. They found that individuals receiving rTMS for 2 weeks showed improvement on a standardized cognitive battery compared to individuals in the sham condition. These improvements remained apparent at a 2-week follow-up post-treatment completion. They also revealed that thickness of the left frontal cortex at baseline was correlated with treatment response, indicating that MRI measures may provide biomarkers to predict response to treatment (Senkowski and Gallinat 2015). Farzan et al. (2012) also investigated the effects of rTMS on the DLPFC using EEG and gamma oscillations. These findings revealed that patients with schizophrenia have selective gamma inhibition deficits in the DLPFC and that rTMS targeting the DLPFC can normalize excessive gamma oscillations, as well as cognitive performance. Similarly, Barr et al. (2011) revealed that patients with schizophrenia had significantly reduced frontal gamma oscillatory activity following rTMS to the DLPFC. However, for healthy controls, rTMS significantly increased oscillatory activity as N-back cognitive demand increased, suggesting that rTMS may have differential effects on oscillatory activity depending on differences at baseline. Using a TMS-EEG paradigm of short interval intracortical inhibition (SICI) and facilitation (ICF) of the DLPFC, Noda et al. (2017) found that patients showed reductions in P60 inhibition by SICI as well as reduced facilitation in P60 and N100 by ICF. Furthermore, the modulation of P60 by SICI was correlated with the longest span of the Letter-Number Span Test, while the modulation of N100 by ICF was correlated with the clinical symptom total score. These findings suggest that deficits in schizophrenia may be associated with prefrontal $GABA_A$ and glutamatergic dysfunctions. The authors suggest that restoring gamma impairments in the DLPFC may be a potential strategy for improving cognitive deficits in schizophrenia.

Table 20.6 Effects of neuromodulation on brain function: EEG and fMRI studies

Transcranial magnetic stimulation (TMS) and Transcranial direct-current stimulation (TDCS)								
Study	Country	Population	Active condition	Control condition	Dose/duration	Targeted outcomes	Brain imaging method/task	Main findings
Barr et al. (2011)	Canada	Schizophrenia	High frequency rTMS stimulation to dorsolateral prefrontal cortex (n = 24)	High frequency rTMS (n = 22)	Active: 1 session of bilateral dorsolateral prefrontal cortex stimulation at 90% resting motor threshold of 20 Hz for 25 trains comprising 30 pulses per train, inter-train interval of 30 s for 750 total pulses (25 min)/1 day	1. Working memory	TMS-EEG: N-back task	↓ excessive power of gamma oscillations significantly in prefrontal cortex for rTMS in schizophrenia group
Guse et al. (2013)	Germany	Schizophrenia	High frequency rTMS stimulation to left posterior middle frontal gyrus (n = 25)	Sham rTMS with one wing angulated 45° away from skull (n = 22)	Active: 15 sessions of dorsolateral prefrontal cortex stimulation at 110% resting motor threshold of 10 Hz, inter-train interval of 30 s with 1000 stimuli per session/3 weeks Control: 15 sessions of sham rTMS/3 weeks	1. Working memory	fMRI: Verbal working memory task	No significant differences were found over time
Dlabac-de Lange et al. (2015)	Netherlands	Schizophrenia	High frequency rTMS stimulation to dorsolateral prefrontal cortex (n = 11)	Sham rTMS with coil tilted 90° off scalp with two wings of coil touching scalp (n = 13)	Active: 30 sessions of bilateral dorsolateral prefrontal cortex stimulation at 90% motor threshold for 10 Hz for 10 s trains with inter-train interval of 50 s (20 min)/3 weeks Control: 30 sessions of sham rTMS/2 weeks	1. Verbal working memory	fMRI: Tower of London task	↑ right dorsolateral prefrontal cortex and right medial frontal gyrus for active rTMS
Noda et al. (2017)	Canada	Schizophrenia	Monophasic TMS pulses to left primary motor cortex (n = 12)	Healthy controls (n = 12)	SICI and ICF paradigms administered to DLPFC	1. Working memory	TMS-EEG	↓ inhibition in P60 by SICI and ↓ facilitation and N100 by ICF for patients
Francis et al. (2018)	USA	Schizophrenia, schizophreniform disorder, schizoaffective, or bipolar disorder	High frequency rTMS stimulation to dorsolateral prefrontal cortex (n = 9)	Sham rTMS without tactile sensation (n = 10)	Active: 10 sessions of bilateral dorsolateral prefrontal cortex stimulation at 110% motor threshold of 20 Hz, for 30 trains comprising 20 pulses per train, inter-train interval of 30 s for 1200 total pulses/2 weeks Control: 10 sessions of sham rTMS/2 weeks	1. Working memory	MRI: Freesurfer pipeline segmentation of cortical thickness measurements	Left frontal cortical thickness after rTMS administration is associated with overall improvement in cognitive function

Orlov et al. (2017)	England	Schizophrenia	TDCS of medial frontal cortex (n = 13)	Sham tDCS stimulation to medial frontal cortex (n = 11)	Active: 8 sessions of medial frontal cortex stimulation continuously for 30 min (real) or 30 s (sham) at 2 mA using an Edith stimulator and magnetic field compatible electrodes pre-gelled with EEG paste. The anode (35 cm^2) was placed over the F3 [Brodmann area (BA) 10/46], and the cathode (35 cm^2) over the right supraorbital area, according to the 10–20 electrode placement system.	1. Working memory	fMRI: (1) N-back task	TDCS of the medial frontal cortex was associated with ↑ functional activation of this region was also positively associated with consolidation of working memory performance 24 h post-stimulation.
					Control: 8 sessions of sham tCDS for 30 s at 2 mA	2. Executive function	(2) Stroop task	
Mondino et al. (2016)	France	Schizophrenia	TDCS of medial frontal cortex (n = 11)	Sham tDCS stimulation of medial frontal cortex (n = 12)	Active: 10 sessions (2× daily) with an Eldith DC stimulator (NeuroConn, GmbH). The anode was positioned over left dorsolateral prefrontal cortex and the cathode over left temporo-parietal junction. Active TDCS consisted in delivering a constant current of 2 mA for 20 min/5 consecutive days	1. Auditory verbal hallucinations	fMRI: Resting state	Active TDCS significantly reduced auditory verbal hallucinations as well as negative symptoms. Reduction of auditory verbal hallucination severity was correlated with reduction of resting state connectivity between the left temporo-parietal junction and the left anterior insula
					Control: 10 sessions (2× daily) with sham TDCS. The 2-mA current was delivered only during the first 30 s of the 20-min stimulation period/5 consecutive days	2. Negative symptoms		

Finally, an fMRI study by Guse et al. (2013) to investigate the effect of 3-week high frequency rTMS over the left posterior middle frontal gyrus on working memory found no significant activation differences over time for patients or controls in either the rTMS or sham conditions. The authors concluded that although TMS can alter BOLD responses, the long-lasting effects of the treatment may be more subtle and therefore more difficult to detect. They suggest that other imaging methodologies such as EEG or MEG may be more sensitive to detect subtle changes in brain activity.

20.6.2 Transcranial Direct-Current Stimulation (TDCS)

TDCS is a form of neuromodulation using constant, low direct current via electrodes. A few studies suggest that TDCS may be a potential treatment to alter frontal cortical activity and enhance pro-cognitive effects. In a double-blind randomized sham-controlled study in 28 patients with schizophrenia, Orlov et al. (2017) found that TDCS of the medial frontal cortex was associated with increased functional activation of this region and was also positively associated with consolidation of working memory performance 24 h post-stimulation. Mondino et al. (2016) investigated the effect of TDCS on the resting-state functional connectivity of the left temporoparietal junction (TPJ) in 23 patients with schizophrenia and treatment-resistant auditory verbal hallucinations (AVH). They found that active TDCS significantly reduced AVH as well as negative symptoms and further found that the reduction of AVH severity was correlated with the reduction of resting state connectivity between the left TPJ and left anterior insula. Single case studies have also found cerebral blood flow changes after TDCS in schizophrenia (Shiozawa et al. 2014), as well as changes in negative symptoms and functional connectivity in a treatment resistant case (Palm et al. 2013), but more studies are needed.

A major challenge of neuromodulation is designing an effective and consistent protocol between studies. Many studies use a variety of protocols, involving stimulation of various regions of the brain, making it difficult to compare results across studies. Nonetheless, while further rTMS and TDCS studies are needed, along with larger sample sizes and additional imaging modalities, the findings thus far provide insights into the neurophysiological mechanisms underlying clinical symptoms and cognitive deficits in schizophrenia, and demonstrate that such interventions may modulate abnormal brain activity associated with these deficits.

20.7 Conclusion

This chapter outlines the effects of non-pharmacological treatments on brain structure and function in schizophrenia. Findings from the neuroimaging literature suggest that the treatment modalities discussed, in conjunction with traditional pharmacological treatments, have potential benefits not only on clinical and cognitive symptoms, but also on brain structure and function in individuals with schizophrenia. The impact of CRT on the brain is the most widely studied, showing improvements in cognitive functioning and brain measures, in addition to alleviating symptoms associated with schizophrenia. However, the neuroimaging literature to date is more limited in terms of findings from other non-pharmacological treatment modalities, including CBT, rTMS, TDCS, and physical activity. Furthermore, there are few studies examining the effects of these treatments using alternative imaging modalities, including diffusion tensor imaging (DTI) and MR spectroscopy. Such investigations are required to determine whether or not these treatments result in changes to white matter, metabolite concentrations, and additional brain measures.

Neuroimaging studies are critical to better understand the impact of non-pharmacological treatments on the brain, but also to determine brain markers that could predict response to treatment. Future studies need to be carefully designed, taking into consideration the treatment approach, as well as baseline cross-sectional

measures of brain structure and function. Additionally, imaging studies may also be useful for monitoring change in pathophysiology in relation to non-response to treatment. Lewandowski et al. (2018) suggest three key steps to consider when assessing experimental therapeutics for developing novel psychological interventions, including: target identification (is there a specific treatable target mechanism?), target engagement (can the target mechanism be modified?), and target clinical testing (is this target engagement clinically effective?). At this time, the imaging literature in non-pharmacological treatment studies is promising, however, further studies are warranted to understand the underlying neurobiological mechanisms of these interventions and their improvements on cognition and functional outcomes in schizophrenia.

Summary

- Neuroimaging methods such as structural MRI, fMRI, DTI, EEG, and MEG provide a promising platform for studying the mechanisms underlying the effects of non-pharmacological treatments in schizophrenia.
- Neuroimaging studies of non-pharmacological treatments (such as intervention based on physical activity, CRT, CBT, TMS, and TDCS) support preliminary evidence toward improvements in clinical symptoms, neurocognitive functioning, and brain function.
- Physical activity interventions, which improve metabolic responses, psychopathological symptoms, cognition, and overall quality of life, may influence brain structure and function, perhaps by impacting plasticity.
- Neuroimaging studies of CRT have shown significant neuronal changes in major prefrontal regions accompanied by improvements in neurocognition and social cognition. Structural imaging studies of CRT have reported preliminary evidence of neuroprotective and neuroplastic effects in gray matter. Additionally, EEG and MEG studies focusing on the effects of sociocognitive CRT indicate changes in neuronal activity of prefrontal and frontoparietal regions.
- Relatively little is known about the brain effects of CBT, an effective psychological intervention in schizophrenia.
- rTMS is a novel and potential neuromodulation treatment option for schizophrenia as it potentially modulates abnormal brain activity associated with clinical symptoms and cognitive deficits.
- Structural brain markers can be used to predict non-pharmacological treatment response in addition to improvements in cognition and clinical symptom outcomes.
- Several neuroimaging studies have examined the effects of CRT on the brain, but there is a limited understanding of the effects of other treatment modalities, such as CBT, neuromodulation, and physical activity. Further research will provide greater insight into the neural mechanisms of non-pharmacological interventions in concurrence with traditional medication treatment for patients.

References

Andreou C, Moritz S. Editorial: Non-pharmacological interventions for schizophrenia: how much can be achieved and how? Front Psychol. 2016;7:1289. https://doi.org/10.3389/fpsyg.2016.01289.

Barr MS, Farzan F, Arenovich T, Chen R, Fitzgerald PB, Daskalakis ZJ. The effect of repetitive transcranial magnetic stimulation on gamma oscillatory activity in schizophrenia. PLoS One. 2011;6(7):e22627. https://doi.org/10.1371/journal.pone.0022627.

Best MW, Gale D, Tran T, Haque MK, Bowie CR. Brief executive function training for individuals with severe mental illness: effects on EEG synchronization and

executive functioning. Schizophr Res. 2019;203:32–40. https://doi.org/10.1016/j.schres.2017.08.052.

Bor J, Brunelin J, d'Amato T, Costes N, Suaud-Chagny M-F, Saoud M, Poulet E. How can cognitive remediation therapy modulate brain activations in schizophrenia?: An fMRI study. Psychiatry Res Neuroimaging. 2011;192(3):160–6. https://doi.org/10.1016/j.pscychresns.2010.12.004.

Brady RO, Gonsalvez I, Lee I, Öngür D, Seidman LJ, Schmahmann JD, Keshavan MS, Pascual-Leone A, Halko MA. Cerebellar-prefrontal network connectivity and negative symptoms in schizophrenia. Am J Psychiatry. 2019;176(7):512–20. https://doi.org/10.1176/appi.ajp.2018.18040429.

Cella M, Preti A, Edwards C, Dow T, Wykes T. Cognitive remediation for negative symptoms of schizophrenia: a network meta-analysis. Clin Psychol Rev. 2017;52:43–51. https://doi.org/10.1016/j.cpr.2016.11.009.

Chen R, Classen J, Gerloff C, Celnik P, Wassermann EM, Hallett M, Cohen LG. Depression of motor cortex excitability by low-frequency transcranial magnetic stimulation. Neurology. 1997;48(5):1398–403. https://doi.org/10.1212/WNL.48.5.1398.

Cole JC, Green Bernacki C, Helmer A, Pinninti N, O'Reardon JP. Efficacy of transcranial magnetic stimulation (TMS) in the treatment of schizophrenia: a review of the literature to date. Innov Clin Neurosci. 2015;12(7–8):12–9.

Dale CL, Brown EG, Fisher M, Herman AB, Dowling AF, Hinkley LB, Subramaniam K, Nagarajan SS, Vinogradov S. Auditory cortical plasticity drives training-induced cognitive changes in schizophrenia. Schizophr Bull. 2016;42(1):220–8. https://doi.org/10.1093/schbul/sbv087.

Dlabac-de Lange JJ, Liemburg EJ, Bais L, Renken RJ, Knegtering H, Aleman A. Effect of rTMS on brain activation in schizophrenia with negative symptoms: a proof-of-principle study. Schizophr Res. 2015;168(1):475–82. https://doi.org/10.1016/j.schres.2015.06.018.

Donohoe G, Dillon R, Hargreaves A, Mothersill O, Castorina M, Furey E, Fagan AJ, Meaney JF, Fitzmaurice B, Hallahan B, McDonald C, Wykes T, Corvin A, Robertson IH. Effectiveness of a low support, remotely accessible, cognitive remediation training programme for chronic psychosis: cognitive, functional and cortical outcomes from a single blind randomised controlled trial. Psychol Med. 2018;48(5):751–64. https://doi.org/10.1017/S0033291717001982.

Eack SM, Greenwald DP, Hogarty SS, Cooley SJ, DiBarry AL, Montrose DM, Keshavan MS. Cognitive enhancement therapy for early-course schizophrenia: effects of a two-year randomized controlled trial. Psychiatr Serv. 2009;60(11):1468–76. https://doi.org/10.1176/ps.2009.60.11.1468.

Eack SM, Hogarty GE, Cho RY, et al. Neuroprotective effects of cognitive enhancement therapy against gray matter loss in early schizophrenia: results from a 2-year randomized controlled trial. Arch Gen Psychiatry. 2010;67(7):674–82. https://doi.org/10.1001/archgenpsychiatry.2010.63.

Eack SM, Newhill CE, Keshavan MS. Cognitive enhancement therapy improves resting-state functional connectivity in early course schizophrenia. J Soc Soc Work Res. 2016;7(2):211–30. https://doi.org/10.1086/686538.

Edwards BG, Barch DM, Braver TS. Improving prefrontal cortex function in schizophrenia through focused training of cognitive control. Front Hum Neurosci. 2010;4:32.

Falkai P, Malchow B, Wobrock T, Gruber O, Schmitt A, Honer WG, Pajonk FG, Sun F, Cannon TD. The effect of aerobic exercise on cortical architecture in patients with chronic schizophrenia: a randomized controlled MRI study. Eur Arch Psychiatry Clin Neurosci. 2013;263(6):469–73. https://doi.org/10.1007/s00406-012-0383-y.

Fan F, Zou Y, Tan Y, Hong LE, Tan S. Computerized cognitive remediation therapy effects on resting state brain activity and cognition in schizophrenia. Sci Rep. 2017;7(1):4758. https://doi.org/10.1038/s41598-017-04829-9.

Farzan F, Barr MS, Sun Y, Fitzgerald PB, Daskalakis ZJ. Transcranial magnetic stimulation on the modulation of gamma oscillations in schizophrenia. Ann N Y Acad Sci. 2012;1265(1):25–35. https://doi.org/10.1111/j.1749-6632.2012.06543.x.

Firth J, Cotter J, Elliott R, French P, Yung AR. A systematic review and meta-analysis of exercise interventions in schizophrenia patients. Psychol Med. 2015;45(7):1343–61. https://doi.org/10.1017/S0033291714003110.

Firth J, Cotter J, Carney R, Yung AR. The pro-cognitive mechanisms of physical exercise in people with schizophrenia. Br J Pharmacol. 2017a;174(19):3161–72. https://doi.org/10.1111/bph.13772.

Firth J, Stubbs B, Rosenbaum S, Vancampfort D, Malchow B, Schuch F, Elliott R, Nuechterlein KH, Yung AR. Aerobic exercise improves cognitive functioning in people with schizophrenia: a systematic review and meta-analysis. Schizophr Bull. 2017b;43(3):546–56. https://doi.org/10.1093/schbul/sbw115.

Francis MM, Hummer TA, Vohs JL, Yung MG, Visco AC, Mehdiyoun NF, Kulig TC, Um M, Yang Z, Motamed M, Liffick E, Zhang Y, Breier A. Cognitive effects of bilateral high frequency repetitive transcranial magnetic stimulation in early phase psychosis: a pilot study. Brain Imaging Behav. 2018;13:852–61. https://doi.org/10.1007/s11682-018-9902-4.

Guimond S, Béland S, Lepage M. Strategy for semantic association memory (SESAME) training: effects on brain functioning in schizophrenia. Psychiatry Res Neuroimaging. 2018;271:50–8. https://doi.org/10.1016/j.pscychresns.2017.10.010.

Guse B, Falkai P, Gruber O, Whalley H, Gibson L, Hasan A, Obst K, Dechent P, McIntosh A, Suchan B, Wobrock T. The effect of long-term high frequency repetitive transcranial magnetic stimulation on work-

ing memory in schizophrenia and healthy controls—a randomized placebo-controlled, double-blind fMRI study. Behav Brain Res. 2013;237:300–7. https://doi.org/10.1016/j.bbr.2012.09.034.

Habel U, Koch K, Kellermann T, Reske M, Frommann N, Wölwer W, Zilles K, Shah NJ, Schneider F. Training of affect recognition in schizophrenia: neurobiological correlates. Soc Neurosci. 2010;5(1):92–104. https://doi.org/10.1080/17470910903170269.

Haut KM, Lim KO, MacDonald A III. Prefrontal cortical changes following cognitive training in patients with chronic schizophrenia: effects of practice, generalization, and specificity. Neuropsychopharmacology. 2010;35:1850–9.

Hogarty GE, Flesher S, Ulrich R, et al. Cognitive enhancement therapy for schizophrenia: effects of a 2-year randomized trial on cognition and behavior. Arch Gen Psychiatry. 2004;61(9):866–76. https://doi.org/10.1001/archpsyc.61.9.866.

Hooker CI, Bruce L, Fisher M, Verosky SC, Miyakawa A, Vinogradov S. Neural activity during emotion recognition after combined cognitive plus social cognitive training in schizophrenia. Schizophr Res. 2012;139(1–3):53–9. https://doi.org/10.1016/j.schres.2012.05.009.

Hooker CI, Bruce L, Fisher M, Verosky SC, Miyakawa A, D'Esposito M, Vinogradov S. The influence of combined cognitive plus social-cognitive training on amygdala response during face emotion recognition in schizophrenia. Psychiatry Res Neuroimaging. 2013;213(2):99–107. https://doi.org/10.1016/j.pscychresns.2013.04.001.

Ji RR, Schlaepfer TE, Aizenman CD, Epstein CM, Qiu D, Huang JC, Rupp F. Repetitive transcranial magnetic stimulation activates specific regions in rat brain. Proc Natl Acad Sci U S A. 1998;95(26):15635–40.

Kärgel C, Sartory G, Kariofillis D, Wiltfang J, Müller BW. The effect of auditory and visual training on the mismatch negativity in schizophrenia. Int J Psychophysiol. 2016;102:47–54. https://doi.org/10.1016/j.ijpsycho.2016.03.003.

Keshavan MS, Eack SM, Wojtalik JA, Prasad KMR, Francis AN, Bhojraj TS, Greenwald DP, Hogarty SS. A broad cortical reserve accelerates response to cognitive enhancement therapy in early course schizophrenia. Schizophr Res. 2011;130(1-3):123–9.

Keshavan MS, Vinogradov S, Rumsey J, Sherrill J, Wagner A. Cognitive training in mental disorders: update and future directions. Am J Psychiatr. 2014;171(5):510–22. https://doi.org/10.1176/appi.ajp.2013.13081075.

Keshavan MS, Eack SM, Prasad KM, Haller CS, Cho RY. Longitudinal functional brain imaging study in early course schizophrenia before and after cognitive enhancement therapy. Neuroimage. 2017;151:55–64. https://doi.org/10.1016/j.neuroimage.2016.11.060.

Kimhy D, Vakhrusheva J, Bartels MN, Armstrong HF, Ballon JS, Khan S, Chang RW, Hansen MC, Ayanruoh L, Lister A, Castrén E, Smith EE, Sloan RP. The impact of aerobic exercise on brain-derived neurotrophic factor and neurocognition in individuals with schizophrenia: a single-blind, randomized clinical trial. Schizophr Bull. 2015;41(4):859–68. https://doi.org/10.1093/schbul/sbv022.

Klimesch W. EEG alpha and theta oscillations reflect cognitive and memory performance: a review and analysis. Brain Res Rev. 1999;29(2):169–95. https://doi.org/10.1016/S0165-0173(98)00056-3.

Knöchel C, Oertel-Knöchel V, O'Dwyer L, Prvulovic D, Alves G, Kollmann B, Hampel H. Cognitive and behavioural effects of physical exercise in psychiatric patients. Prog Neurobiol. 2012;96(1):46–68. https://doi.org/10.1016/j.pneurobio.2011.11.007.

Kumari V, Peters ER, Fannon D, Antonova E, Premkumar P, Anilkumar AP, Williams SC, Kuipers E. Dorsolateral prefrontal cortex activity predicts responsiveness to cognitive–behavioral therapy in schizophrenia. Biol Psychiatry. 2009;66(6):594–602. https://doi.org/10.1016/j.biopsych.2009.04.036.

Lehman AF, Lieberman JA, Dixon LB, McGlashan TH, Miller AL, Perkins DO, Kreyenbuhl J, American Psychiatric Association, Steering Committee on Practice Guidelines. Practice guideline for the treatment of patients with schizophrenia, second edition. Am J Psychiatry. 2004;161(2 Suppl):1–56.

Lewandowski KE, Ongur D, Keshavan MS. Development of novel behavioral interventions in an experimental therapeutics world: challenges, and directions for the future. Schizophr Res. 2018;192:6–8. https://doi.org/10.1016/j.schres.2017.06.010.

Lin J, Chan SK, Lee EH, Chang WC, Tse M, Su WW, Sham P, Hui CL, Joe G, Chan CL, Khong PL, So KF, Honer WG, Chen EY. Aerobic exercise and yoga improve neurocognitive function in women with early psychosis. NPJ Schizophr. 2015;1:15047.

Lin J, Geng X, Lee EH, Chan SK, Chang WC, Hui CL, Tse M, Chan CL, Khong PL, Honer WG, Chen EY. Yoga reduces the brain's amplitude of low-frequency fluctuations in patients with early psychosis results of a randomized controlled trial. Schizophr Res. 2017;184:141–2. https://doi.org/10.1016/j.schres.2016.11.040.

Luckhaus C, Frommann N, Stroth S, Brinkmeyer J, Wölwer W. Training of affect recognition in schizophrenia patients with violent offences: behavioral treatment effects and electrophysiological correlates. Soc Neurosci. 2013;8(5):505–14. https://doi.org/10.1080/17470919.2013.820667.

Malchow B, Keeser D, Keller K, Hasan A, Rauchmann B-S, Kimura H, Schneider-Axmann T, Dechent P, Gruber O, Ertl-Wagner B, Honer WG, Hillmer-Vogel U, Schmitt A, Wobrock T, Niklas A, Falkai P. Effects of endurance training on brain structures in chronic schizophrenia patients and healthy controls. Schizophr Res. 2016;173(3):182–91. https://doi.org/10.1016/j.schres.2015.01.005.

Mazza M, Lucci G, Pacitti F, Pino MC, Mariano M, Casacchia M, Roncone R. Could schizophrenic subjects improve their social cognition abilities only with observation and imitation of social situations? Neuropsychol Rehabil. 2010;20(5):675–703. https://doi.org/10.1080/09602011.2010.486284.

McGurk SR, Twamley EW, Sitzer DI, McHugo GJ, Mueser KT. A meta-analysis of cognitive remediation in schizophrenia. Am J Psychiatr. 2007;164(12):1791–802. https://doi.org/10.1176/appi.ajp.2007.07060906.

Minzenberg MJ, Laird AR, Thelen S, Carter CS, Glahn DC. Meta-analysis of 41 functional neuroimaging studies of executive function in schizophrenia. Arch Gen Psychiatry. 2009;66(8):811–22. https://doi.org/10.1001/archgenpsychiatry.2009.91.

Mondino M, Jardri R, Suaud-Chagny M-F, Saoud M, Poulet E, Brunelin J. Effects of Fronto-temporal transcranial direct current stimulation on auditory verbal hallucinations and resting-state functional connectivity of the left temporo-parietal junction in patients with schizophrenia. Schizophr Bull. 2016;42(2):318–26. https://doi.org/10.1093/schbul/sbv114.

Morimoto T, Matsuda Y, Matsuoka K, Yasuno F, Ikebuchi E, Kameda H, Taoka T, Miyasaka T, Kichikawa K, Kishimoto T. Computer-assisted cognitive remediation therapy increases hippocampal volume in patients with schizophrenia: a randomized controlled trial. BMC Psychiatry. 2018;18(1):83. https://doi.org/10.1186/s12888-018-1667-1.

Noda Y, Barr MS, Zomorrodi R, Cash RFH, Farzan F, Rajji TK, Chen R, Daskalakis ZJ, Blumberger DM. Evaluation of short interval cortical inhibition and intracortical facilitation from the dorsolateral prefrontal cortex in patients with schizophrenia. Sci Rep. 2017;7(1):17106. https://doi.org/10.1038/s41598-017-17052-3.

Nuechterlein KH, Ventura J, Subotnik KL, Hayata JN, Medalia A, Bell MD. Developing a cognitive training strategy for first-episode schizophrenia: integrating bottom-up and top-down approaches. Am J Psychiatr Rehabil. 2014;17(3):225–53. https://doi.org/10.1080/15487768.2014.935674.

Nuechterlein KH, Ventura J, McEwen SC, Gretchen-Doorly D, Vinogradov S, Subotnik KL. Enhancing cognitive training through aerobic exercise after a first schizophrenia episode: theoretical conception and pilot study. Schizophr Bull. 2016;42(Suppl 1):S44–52. https://doi.org/10.1093/schbul/sbw007.

Orlov ND, O'Daly O, Tracy DK, Daniju Y, Hodsoll J, Valdearenas L, Rothwell J, Shergill SS. Stimulating thought: a functional MRI study of transcranial direct current stimulation in schizophrenia. Brain. 2017;140(9):2490–7. https://doi.org/10.1093/brain/awx170.

Osoegawa C, Gomes JS, Grigolon RB, Brietzke E, Gadelha A, Lacerda ALT, Dias ÁM, Cordeiro Q, Laranjeira R, de Jesus D, Daskalakis ZJ, Brunelin J, Cordes J, Trevizol AP. Non-invasive brain stimulation for negative symptoms in schizophrenia: an updated systematic review and meta-analysis. Schizophr Res. 2018;197:34–44. https://doi.org/10.1016/j.schres.2018.01.010.

Pajonk F, Wobrock T, Gruber O, et al. Hippocampal plasticity in response to exercise in schizophrenia. Arch Gen Psychiatry. 2010;67(2):133–43. https://doi.org/10.1001/archgenpsychiatry.2009.193.

Palm U, Keeser D, Blautzik J, Pogarell O, Ertl-Wagner B, Kupka MJ, Reiser M, Padberg F. Prefrontal transcranial direct current stimulation (tDCS) changes negative symptoms and functional connectivity MRI (fcMRI) in a single case of treatment-resistant schizophrenia. Schizophr Res. 2013;150(2):583–5. https://doi.org/10.1016/j.schres.2013.08.043.

Patel KR, Cherian J, Gohil K, Atkinson D. Schizophrenia: overview and treatment options. P T. 2014;39(9):638–45.

Patterson TL, Leeuwenkamp OR. Adjunctive psychosocial therapies for the treatment of schizophrenia. Schizophr Res. 2008;100(1):108–19. https://doi.org/10.1016/j.schres.2007.12.468.

Penadés R, Pujol N, Catalán R, Massana G, Rametti G, García-Rizo C, Bargalló N, Gastó C, Bernardo M, Junqué C. Brain effects of cognitive remediation therapy in schizophrenia: a structural and functional neuroimaging study. Biol Psychiatry. 2013;73(10):1015–23. https://doi.org/10.1016/j.biopsych.2013.01.017.

Perez VB, Tarasenko M, Miyakoshi M, Pianka ST, Makeig SD, Braff DL, Swerdlow NR, Light GA. Mismatch negativity is a sensitive and predictive biomarker of perceptual learning during auditory cognitive training in schizophrenia. Neuropsychopharmacology. 2017;42:2206–13.

Popov T, Jordanov T, Rockstroh B, Elbert T, Merzenich MM, Miller GA. Specific cognitive training normalizes auditory sensory gating in schizophrenia: a randomized trial. Biol Psychiatry. 2011;69(5):465–71. https://doi.org/10.1016/j.biopsych.2010.09.028.

Popov T, Rockstroh B, Weisz N, Elbert T, Miller GA. Adjusting brain dynamics in schizophrenia by means of perceptual and cognitive training. PLoS One. 2012;7(7):e39051. https://doi.org/10.1371/journal.pone.0039051.

Popov TG, Carolus A, Schubring D, Popova P, Miller GA, Rockstroh BS. Targeted training modifies oscillatory brain activity in schizophrenia patients. Neuroimage Clinical. 2015;7:807–14. https://doi.org/10.1016/j.nicl.2015.03.010.

Popova P, Popov TG, Wienbruch C, Carolus AM, Miller GA, Rockstroh BS. Changing facial affect recognition in schizophrenia: effects of training on brain dynamics. Neuroimage Clin. 2014;6:156–65. https://doi.org/10.1016/j.nicl.2014.08.026.

Popova P, Rockstroh B, Miller GA, Wienbruch C, Carolus AM, Popov T. The impact of cognitive training on spontaneous gamma oscillations in schizophrenia. Psychophysiology. 2018;55(8):e13083. https://doi.org/10.1111/psyp.13083.

Premkumar P, Fannon D, Kuipers E, Peters ER, Anilkumar APP, Simmons A, Kumari V. Structural magnetic resonance imaging predictors of responsiveness to cognitive behaviour therapy in psychosis. Schizophr Res. 2009;115(2):146–55. https://doi.org/10.1016/j.schres.2009.08.007.

Premkumar P, Bream D, Sapara A, Fannon D, Anilkumar AP, Kuipers E, Kumari V. Pituitary volume reduction in schizophrenia following cognitive behavioural

therapy. Schizophr Res. 2018;192:416–22. https://doi.org/10.1016/j.schres.2017.04.035.

Ramsay IS, Fryer S, Boos A, Roach BJ, Fisher M, Loewy R, Vinogradov S, Mathalon DH. Response to targeted cognitive training correlates with change in thalamic volume in a randomized trial for early schizophrenia. Neuropsychopharmacology. 2017a;43:590.

Ramsay IS, Nienow TM, MacDonald AW 3rd. Increases in intrinsic thalamocortical connectivity and overall cognition following cognitive remediation in chronic schizophrenia. Biol Psychiatry Cogn Neurosci Neuroimaging. 2017b;2(4):355–62. https://doi.org/10.1016/j.bpsc.2016.11.001.

Ramsay IS, Nienow TM, Marggraf MP, MacDonald AW. Neuroplastic changes in patients with schizophrenia undergoing cognitive remediation: triple-blind trial. Br J Psychiatry. 2017c;210(3):216–22. https://doi.org/10.1192/bjp.bp.115.171496.

Rass O, Forsyth JK, Bolbecker AR, Hetrick WP, Breier A, Lysaker PH, O'Donnell BF. Computer-assisted cognitive remediation for schizophrenia: a randomized single-blind pilot study. Schizophr Res. 2012;139(1–3):92–8. https://doi.org/10.1016/j.schres.2012.05.016.

Rector NA, Beck AT. Cognitive behavioral therapy for schizophrenia: an empirical review. J Nerv Ment Dis. 2001;189:278–87. The Journal of Nervous and Mental Disease, 2012;200(10). Retrieved from https://journals.lww.com/jonmd/Fulltext/2012/10000/Cognitive_Behavioral_Therapy_for_Schizophrenia__.2.aspx.

Saha S, Chant D, Welham J, McGrath J. A systematic review of the prevalence of schizophrenia. PLoS Med. 2005;2(5):e141. https://doi.org/10.1371/journal.pmed.0020141.

Senkowski D, Gallinat J. Dysfunctional prefrontal gamma-band oscillations reflect working memory and other cognitive deficits in schizophrenia. Biol Psychiatry. 2015;77(12):1010–9. https://doi.org/10.1016/j.biopsych.2015.02.034.

Shiozawa P, Santos MMSA, Piovesan FX, Pellegrinelli A, Enokibara da Silva M, Bocato MQ, Cordeiro Q, Fregni F, Brunoni AR. Cerebral blood flow changes after transcranial direct current stimulation for a patient with schizophrenia: a case report. J Neuropsychiatry Clin Neurosci. 2014;26(2):E03–5. https://doi.org/10.1176/appi.neuropsych.13020039.

Stroth S, Kamp D, Drusch K, Frommann N, Wölwer W. Training of affect recognition impacts electrophysiological correlates of facial affect recognition in schizophrenia: analyses of fixation-locked potentials. World J Biol Psychiatry. 2015;16(6):411–21. https://doi.org/10.3109/15622975.2015.1051110.

Subramaniam K, Luks TL, Fisher M, Simpson GV, Nagarajan S, Vinogradov S. Computerized cognitive training restores neural activity within the reality monitoring network in schizophrenia. Neuron. 2012;73(4):842–53. https://doi.org/10.1016/j.neuron.2011.12.024.

Subramaniam K, Luks TL, Garrett C, Chung C, Fisher M, Nagarajan S, Vinogradov S. Intensive cognitive training in schizophrenia enhances working memory and associated prefrontal cortical efficiency in a manner that drives long-term functional gains. NeuroImage. 2014;99:281–92. https://doi.org/10.1016/j.neuroimage.2014.05.057.

Svatkova A, Mandl RCW, Scheewe TW, Cahn W, Kahn RS, Hulshoff Pol HE. Physical exercise keeps the brain connected: biking increases white matter integrity in patients with schizophrenia and healthy controls. Schizophr Bull. 2015;41(4):869–78. https://doi.org/10.1093/schbul/sbv033.

Takahashi H, Sassa T, Shibuya T, Kato M, Koeda M, Murai T, Matsuura M, Asai K, Suhara T, Okubo Y. Effects of sports participation on psychiatric symptoms and brain activations during sports observation in schizophrenia. Transl Psychiatry. 2012;2:e96.

Thorsen AL, Johansson K, Løberg E-M. Neurobiology of cognitive remediation therapy for schizophrenia: a systematic review. Front Psych. 2014;5:103. https://doi.org/10.3389/fpsyt.2014.00103.

Vakhrusheva J, Marino B, Stroup TS, Kimhy D. Aerobic exercise in people with schizophrenia: neural and neurocognitive benefits. Curr Behav Neurosci Rep. 2016;3(2):165–75. https://doi.org/10.1007/s40473-016-0077-2.

Vancampfort D, Firth J, Schuch FB, Rosenbaum S, Mugisha J, Hallgren M, Probst M, Ward PB, Gaughran F, De Hert M, Carvalho AF, Stubbs B. Sedentary behavior and physical activity levels in people with schizophrenia, bipolar disorder and major depressive disorder: a global systematic review and meta-analysis. World Psychiatry. 2017;16(3):308–15. https://doi.org/10.1002/wps.20458.

Vianin P, Urben S, Magistretti P, Marquet P, Fornari E, Jaugey L. Increased activation in Broca's area after cognitive remediation in schizophrenia. Psychiatry Res Neuroimaging. 2014;221(3):204–9. https://doi.org/10.1016/j.pscychresns.2014.01.004.

Wang R, Holsinger RMD. Exercise-induced brain-derived neurotrophic factor expression: therapeutic implications for Alzheimer's dementia. Ageing Res Rev. 2018;48:109–21. https://doi.org/10.1016/j.arr.2018.10.002.

Wykes T, Brammer M, Mellers J, Bray P, Reeder C, Williams C, Corner J. Effects on the brain of a psychological treatment: cognitive remediation therapy: functional magnetic resonance imaging in schizophrenia. Br J Psychiatry. 2002;181(2):144–52. https://doi.org/10.1192/bjp.181.2.144.

Wykes T, Huddy V, Cellard C, McGurk SR, Czobor P. A meta-analysis of cognitive remediation for schizophrenia: methodology and effect sizes. Am J Psychiatr. 2011;168(5):472–85. https://doi.org/10.1176/appi.ajp.2010.10060855.

Big Data Initiatives in Psychiatry: Global Neuroimaging Studies

21

Paul M. Thompson, Christopher R. K. Ching, Emily L. Dennis, Lauren E. Salminen, Jessica A. Turner, Theo G. M. van Erp, and Neda Jahanshad

Contents

P. M. Thompson (✉) · C. R. K. Ching · L. E. Salminen N. Jahanshad
Imaging Genetics Center, Mark and Mary Stevens Neuroimaging and Informatics Institute, Keck School of Medicine, University of Southern California, Los Angeles, CA, USA
e-mail: thompson@loni.usc.edu

E. L. Dennis
Department of Neurology, TBI and Concussion Center, University of Utah, Salt Lake City, UT, USA

J. A. Turner
Psychology Department and Neuroscience Institute, Georgia State University, Atlanta, GA, USA

T. G. M. van Erp
Clinical Translational Neuroscience Laboratory, Department of Psychiatry and Human Behavior, University of California Irvine, Irvine, CA, USA

Center for the Neurobiology of Learning and Memory, University of California Irvine, Irvine, CA, USA

M. Kubicki, M. E. Shenton (eds.), *Neuroimaging in Schizophrenia*,
https://doi.org/10.1007/978-3-030-35206-6_21

21.1 Big Data, Rigor, and Reproducibility

Big data and large-scale biobanks offer the potential to answer new types of questions, as well as address older questions with greater confidence and rigor. In the last decade, attention has been drawn to a 'crisis of reproducibility' in the neurosciences, in which findings from small datasets were often not replicated in independent samples (Button et al. 2013; Ioannidis 2017; Dumas-Mallet et al. 2017). The large cost of data collection in neuroimaging meant that many studies assessed fewer than a hundred subjects and were thus not well powered to detect the sometimes subtle effects of psychiatric disease on the brain, or to consistently identify the effects of disease modulators in the genome or environment (Turner 2014). In the early days of psychiatric genetics, assertions were often made about candidate genes and their effects on the brain that later did not replicate when tested in independent samples (Farrell et al. 2015). A recent paradigm shift has led to the formation of large-scale consortia that pool resources from around the world and significantly improve the power to screen the genome for variants that consistently affect disease risk. In much the same way, large-scale imaging consortia have recently formed to establish the effects of a large range of psychiatric disorders on the brain in populations worldwide (Thompson et al. 2017; Okada et al. 2016; Satizabal et al. 2017). The availability of diverse datasets from people with different ethnic and cultural backgrounds now allows researchers to determine common and distinct patterns of brain structure and function in different psychiatric disorders, as well as factors that modulate them by combining data across research centers. While some researchers remain skeptical about the aggregation of imaging data across multiple centers and scanners, replicated imaging and imaging genetics findings across consortia provide clear evidence for the validity of this approach. As a result, it is now possible to combine evidence across collaborative studies to determine the robust brain signatures of disorders such as schizophrenia. In this chapter, we describe some of the efforts underway internationally to analyze mental health data in a coordinated way, as well as some of the challenges in comparing data from different studies.

21.2 Advantages of Big Data Analyses

Large scale data sets and big data analyses offer many advantages for psychiatric research, although they are not without limitations (which we discuss at the end of this chapter). On the positive side, the sheer size of large-scale data often allows us to test hypotheses about nuanced effects of disease or interventions on the brain-effects that may not be detectable in smaller datasets. A second advantage is that many imaging datasets from around the world can be processed using harmonized analysis protocols, making it efficient to apply advanced computational methods to the derived data. In particular, machine learning methods have begun to combine information from imaging, clinical, and genetic sources to make predictions about patient outcomes and discover new patterns that further elucidate the neurobiology of disease. A third advantage of big data is that consortia have emerged that have become highly efficient in coordinating analyses of ever-larger datasets, guided by the collective expertise of neuroscientists, psychiatrists, data scientists, and geneticists (Guglielmi 2018). The opportunity to work cohesively on similar research questions, bringing diverse sources of information to bear on the same problem, often leads to new hypotheses about the origin of disease outcomes and resolves controversies from previously conflicting studies.

21.3 Big Data in Imaging Genetics: A Case Study

Many loci in the human genome have been identified that are statistically associated with increased risk for disorders such as schizophrenia, bipolar disorder, and major depression. The Psychiatric Genomics Consortium (PGC), in par-

ticular, is an example of a 'big data' study in psychiatric genetics. It has screened millions of loci in the human genome for associations with disease, discovering hundreds of common variants that are over-represented in patients compared to controls (Bipolar Disorder and Schizophrenia Working Group of the Psychiatric Genomics Consortium et al. 2018; Wray et al. 2018; Schizophrenia Working Group of the Psychiatric Genomics Consortium 2014). These large scale genomics approaches have also been used to examine genetic overlap between disorders (Brainstorm Consortium 2018). Until recently, however, it was not possible to understand which aspects of brain structure and function were influenced by these risk loci in the genome. In the field of biological psychiatry, neuroimaging research has been proposed as a means to identify biological measures of disease that may be directly influenced by genetic variation—the so-called 'endophenotype' approach (Gottesman and Gould 2003).

With the possible exception of *APOE4*—a major risk factor for Alzheimer's disease—very few of the candidate genes in psychiatry have been found to have reproducible effects on brain measures (Jahanshad et al. 2017). Adapting the multi-site model of the PGC to analyze measures derived from brain images, information from individual imaging genetics datasets have been aggregated to perform genome-wide meta-analysis studies to identify loci that are consistently associated with brain structure and function. Recently, the Enhancing Neuro Imaging Genetics through Meta-Analysis (ENIGMA) consortium has published large-scale genetic screens for loci associated with hippocampal volume (Stein et al. 2012; Hibar et al. 2017), other subcortical structures (Hibar et al. 2015), and total intracranial volume (Adams et al. 2016), discovering a number of common variants associated with the structure volume (Fig. 21.1; Hibar et al. 2015). Driven by a common interest in discovering robust genetic effects on the brain, these were among the first neuroimaging studies to assess brain scans from over 10,000 individuals.

One major strength of ENIGMA over previous meta-analyses was the implementation of ENIGMA-harmonized image analysis protocols across all cohorts worldwide. These procedures made it possible to derive measures from images consistently and to perform robust statistical modeling to reliably identify associations with genetic loci not always detected within individual cohorts (see Fig. 21.2). Both ENIGMA and the PGC initially used a meta-analysis approach to combine evidence from multiple cohorts worldwide, weighing the evidence for effects by the size of the cohort, and allowing direct testing of the heterogeneity of the results and their reproducibility.

Figure 21.2 shows an example Forest plot of the effect of a common genetic variant on the volume of the hippocampus in different cohorts from around the world. Carriers of a single nucleotide variant at this location in the genome have, on average, lower hippocampal volume than non-carriers. Although the effect is not found universally in all cohorts, in aggregate, the meta-analyzed effect is clear. To date, using this 'big data' approach to imaging genetics, over 40 loci have been discovered that are associated with subcortical volumes (Satizabal et al. 2017), and over a hundred loci have been found that are associated with regional cortical thickness and surface area. Work is ongoing to identify the overlap between genetic loci that influence both neuroimaging measures and risk for psychiatric disease (Franke et al. 2016; Mufford et al. 2017). According to initial data, some of the genetic loci that affect risk for schizophrenia, bipolar disorder, Tourette syndrome, OCD, and ADHD also affect the brain in specific locations (Mufford et al. 2019; Hibar et al. 2018a; Lee et al. 2016), offering new clues to the mechanisms that may confer risk for these psychiatric disorders.

In one such study of the overlap between schizophrenia risk loci and loci associated with regional brain volumes, Lee et al. (2016) reported that schizophrenia-associated genetic variants explained a significantly enriched proportion of trait heritability for eight brain phenotypes; in particular, intracranial volume and left superior frontal gyrus thickness showed significant and robust associations with schizophrenia genetic risk. Using a related enrichment approach that

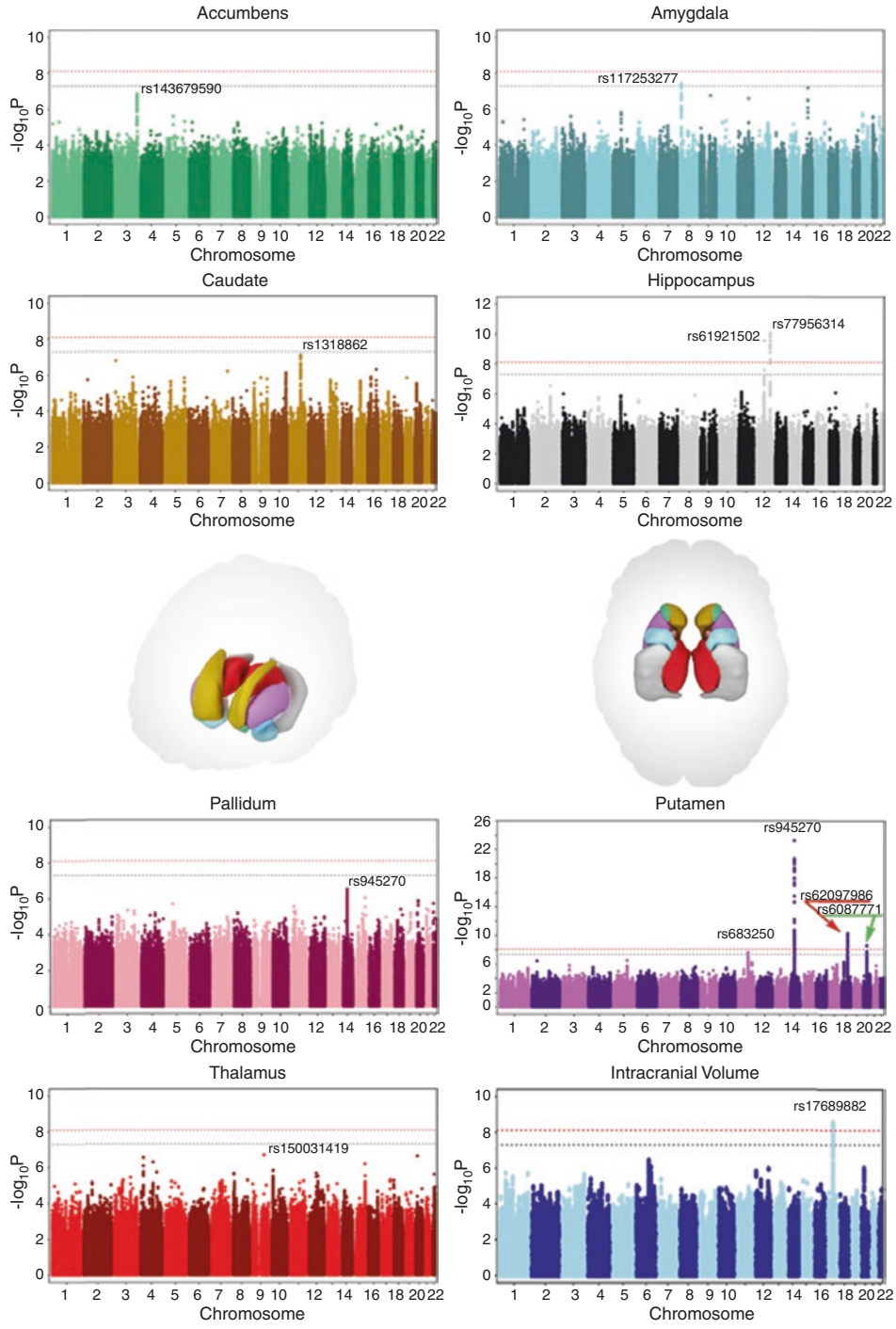

Fig. 21.1 Worldwide genomic screening discovered multiple genetic variants that are associated with the volumes of subcortical brain regions that are implicated in psychiatric and neurological illness. Color-coded plots show the evidence (on a $-\log_{10}$ scale) that common variants in the genome affect the volume of the structure shown. Consistent effects were found in 48 cohorts across the world, showing that single nucleotide changes in DNA can be identified that influence brain structure, by screening MRI data worldwide. [Reproduced with permission, from Hibar et al., *Nature*, 2015.] ENIGMA also recently published large-scale GWAS of EEG measures of functional brain synchrony (Smit et al. 2018)

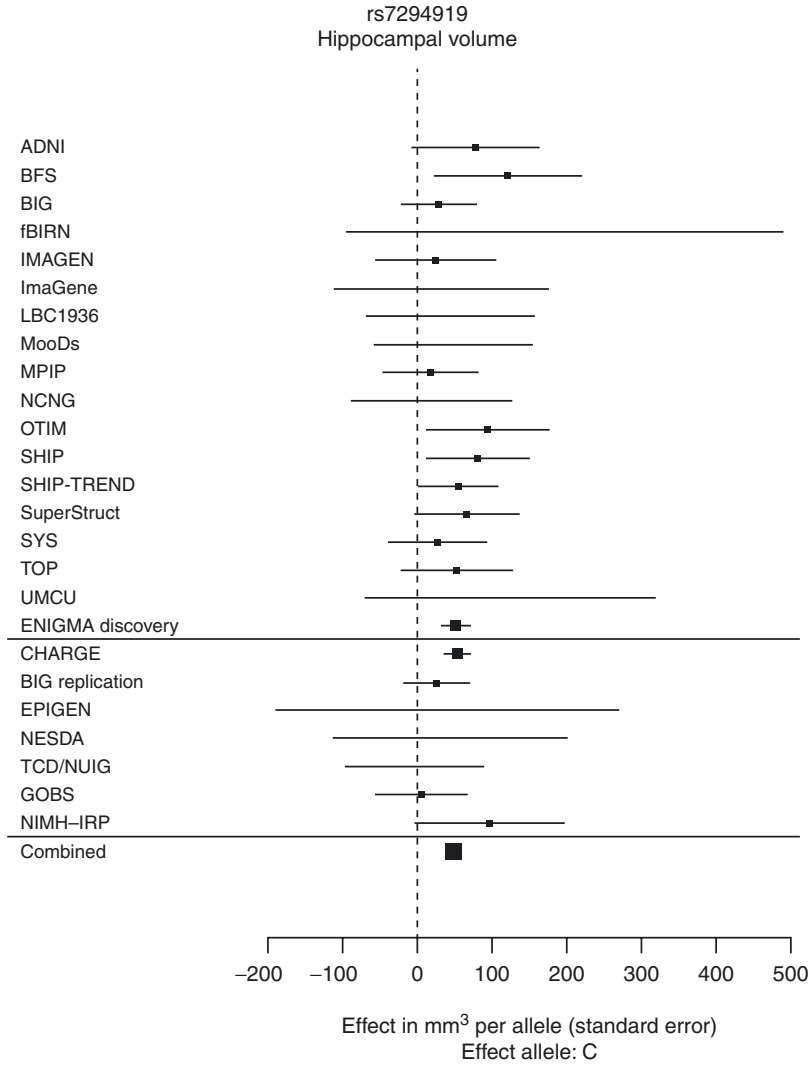

Fig. 21.2 Large scale analysis of the genetics of hippocampal volume. This Forest plot shows the result from a genome-wide association meta-analysis of mean bilateral hippocampal volume, from a large multinational consortium, ENIGMA, in partnership with another consortium, CHARGE. The analysis involved computing hippocampal volumes from 21,151 brain MRI scans, from multiple cohorts, and aggregating the evidence for an effect at over a million common variants in the genome. The intergenic variant rs7294919 was associated with hippocampal volume (12q24.22; $N = 21{,}151$; $P = 6.70 \times 10^{-16}$). The value of the "big data" approach is evident—the individual cohorts contributed to the detection of this subtle effect, but most lacked sufficient data to reject the null hypothesis. The effect size for the genetic marker on hippocampal volume is shown, with a 95% confidence interval, for each cohort in the study. [Reproduced with permission, from Stein et al. (2012), *Nature Genetics*]

partitioned the genome into different functional categories, Smeland et al. (2018) identified two loci shared between SCZ and intracranial volume—implicating genes *FOXO3* and *ITIH4*—and four additional loci shared between SCZ and either hippocampal or putamen volume, implicating the genes *DCC* and *DLG2*. The continual refinement of genome-wide association studies (GWAS) for brain metrics, and for schizophrenia and related disorders, is likely to allow the direct

mapping of key schizophrenia risk loci to profiles of functional and structural abnormalities in the brain.

21.4 ENIGMA and Global Neuroimaging Consortia

Following these initial successes, imaging consortia, such as ENIGMA, started to analyze independently collected neuroimaging datasets to find common trends. Genetic variants explaining as little as 0.5–1% of the variance in key brain measures were detected; this demonstrates that data collection heterogeneity did not obscure the signals of interest. ENIGMA, in particular, began large-scale international studies of a variety of psychiatric and neurological disorders, and recently published the largest neuroimaging studies of schizophrenia (van Erp et al. 2016; Kelly et al. 2018; Walton et al. 2017, 2018; van Erp et al. 2018), bipolar disorder (Hibar et al. 2016, 2018b; Pauling et al. 2017), major depressive disorder (Schmaal et al. 2016, 2017; Rentería et al. 2017; Frodl et al. 2017; Gerritsen et al. 2015), PTSD, and a range of disorders that are also more prevalent in children, including OCD (Boedhoe et al. 2017), autism spectrum disorders (van Rooij et al. 2018), and ADHD (Hoogman et al. 2017). In studies of brain asymmetry in over 17,141 healthy individuals, long standing controversies were resolved regarding the scope and consistency of brain asymmetries in 99 cohorts worldwide (Kong et al. 2018; Guadalupe et al. 2017). Figure 21.3 shows the range of psychiatric disorders that ENIGMA currently studies with large-scale neuroimaging.

Below we summarize some of the major findings regarding schizophrenia and other disorders, along with caveats and limitations of the big data approach. The initial goal of each of these studies was to understand whether there were common anatomical differences between patients and matched healthy controls, and whether these differences are consistent across cohorts from around the world.

21.5 Large Scale MRI Studies of Schizophrenia

One of the first studies conducted by ENIGMA's Schizophrenia Working Group assessed the volumes of subcortical structures on MRI across a broad range of international cohorts (van Erp et al. 2016). In a study of data from 2028 individuals with schizophrenia and 2540 healthy controls from 15 centers worldwide, the working group identified subcortical brain volumes that differentiated cases from controls, and ranked them according to their effect sizes (Fig. 21.4). Compared to healthy controls, patients with schizophrenia had, on average, a smaller hippocampus (Cohen's $d = -0.46$), amygdala ($d = -0.31$), thalamus ($d = -0.31$), accumbens ($d = -0.25$), and intracranial volumes ($d = -0.12$), as well as larger pallidum (d = 0.21), and lateral ventricle volumes ($d = 0.37$). Putamen and pallidum volume enlargements were positively associated with duration of illness, and hippocampal deficits scaled with the proportion of unmedicated patients in each cohort. In an independent validation of these analyses, researchers from the COCORO Consortium in Japan analyzed an additional set of independent data—from 1680 healthy individuals and 884 individuals with schizophrenia, assessed with 15 imaging protocols across 11 sites—and found strong agreement in the ranking of brain metrics, and the order of their effect sizes for distinguishing patients versus controls (Okada et al. 2016; van Erp et al. 2016).

In a follow-up meta-analysis of cortical thickness and surface area abnormalities, the ENIGMA Schizophrenia Working group performed a coordinated analysis of data from 4474 individuals with schizophrenia (mean age, 32.3 years; range, 11–78 years; 66% male) and 5098 healthy volunteers (mean age, 32.8 years; range, 10–87 years; 53% male) assessed with standardized methods at 39 centers worldwide. Compared to healthy volunteers, individuals with schizophrenia had widespread thinner cortex (left/right hemisphere: Cohen's $d = -0.530/-0.516$) and smaller cortical surface area (left/right hemisphere: Cohen's

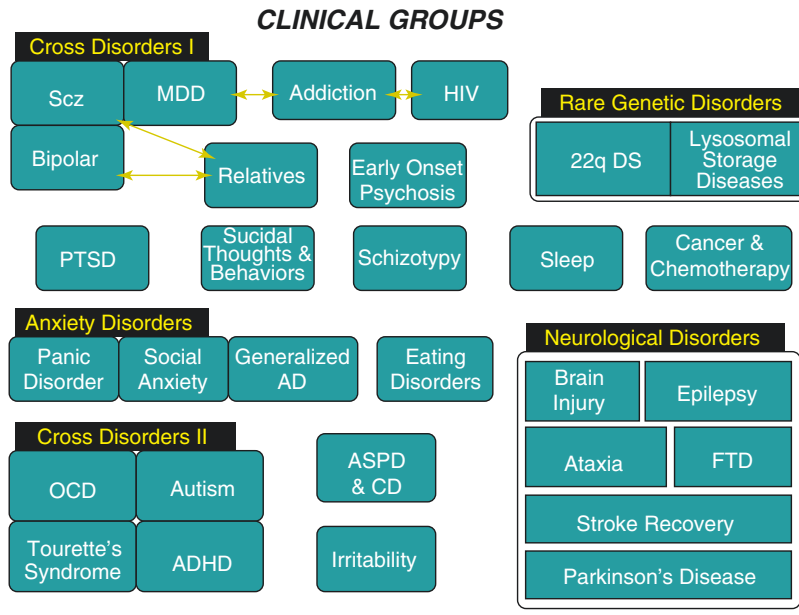

Fig. 21.3 ENIGMA's clinical working groups have completed the largest neuroimaging analyses to date for schizophrenia (van Erp et al. 2018)], bipolar disorder, major depressive disorder, PTSD, substance use disorders, and several disorders that are prevalent in children, including ADHD, OCD, and autism spectrum disorders. There are also active working groups for a range of neurological disorders, including the largest neuroimaging study of epilepsy (Whelan et al. 2018), and a separate set of technical working groups (not shown here) that support harmonized analyses of different data types. The coordinated analysis of brain MRI metrics along with other clinical and 'omics' data allows for the testing of hypothesis about brain differences between patients and controls, enabling cross-disorder and transdiagnostic studies

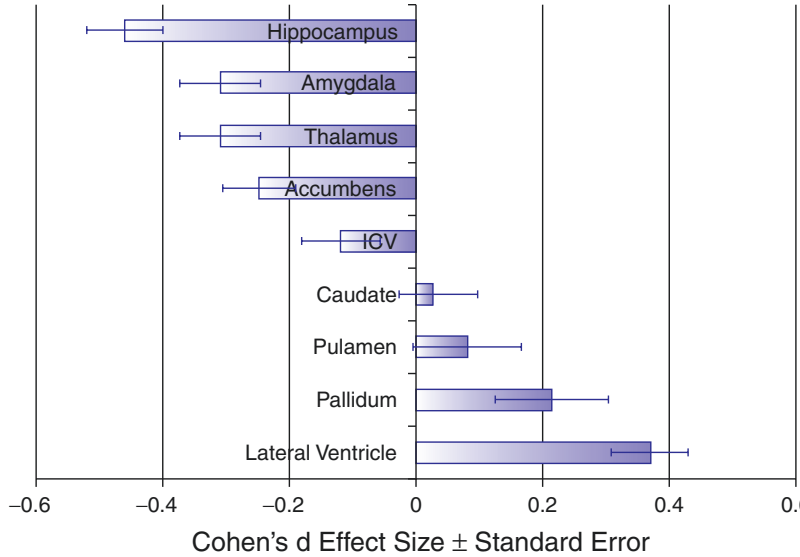

Fig. 21.4 Subcortical volumes in schizophrenia. Cohen's *d* effect sizes (±s.e.) are shown for regional brain volume differences between groups of individuals with schizophrenia and matched healthy controls, based on data from 2028 individuals with schizophrenia and 2540 healthy controls from 15 centers worldwide. Effect sizes for all subcortical volumes depicted were corrected for sex, age and intracranial volume (ICV). The effect size for ICV was corrected for sex and age. [Reproduced, with permission, from van Erp et al. (2015), *Molecular Psychiatry*]

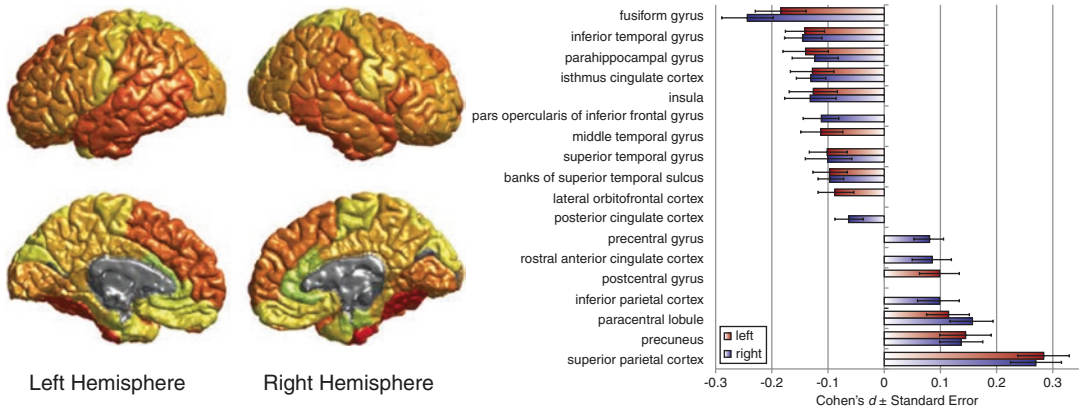

Fig. 21.5 Cortical thickness deficits in schizophrenia. Cortical map of regional Cohen's *d* effect sizes for subjects with schizophrenia vs. healthy volunteers' cortical thickness, after statistically controlling for age and sex. [Reproduced, with permission, from van Erp et al. (2018), *Biological Psychiatry*]

$d = -0.251/-0.254$); the largest effect sizes were found, for both, in frontal and temporal lobe regions (see Fig. 21.5).

These effects are mapped in Fig. 21.5. Three key features are evident. First, with the possible exception of the primary visual (pericalcarine) cortex, there were no cortical regions in which differences were *not* detected between patients and controls. By contrast with many early studies—in which reported effects were inconsistent or controversial—these maps show the broad anatomical impact of the disease and the power of the study to pick up even subtle differences. Second, frontal and temporal lobe regions long implicated in the disorder were among the most strongly affected. Third, and perhaps surprisingly, the fusiform gyrus showed the greatest group differences among all of the *cortical* regions examined, although the subcortical effects in the hippocampus were even greater.

Two follow-up papers by Esther Walton and colleagues (Walton et al. 2017, 2018) assessed the relation between these brain metrics and positive and negative symptom severity. In a total of 1985 individuals with schizophrenia from 17 research groups worldwide, meta-analysis of case-control differences showed that left, but not right, medial orbitofrontal cortical (MOFC) thickness was significantly associated with negative symptom severity (β std = −0.075; $p = 0.019$) after accounting for age, sex, and study site. This effect remained significant ($p = 0.036$) in a model including overall disease severity. While the link between lower prefrontal thickness and negative symptom severity has been reported previously, the reliability of the effect across so many international cohorts provides insight into the consistency of the effects.

Some caveats are warranted regarding the meta-analysis approach. Studies vary in their goals, and thus in their design and patient composition. For example, Walton et al. faced the problem that some studies used the PANSS (Positive and Negative Syndrome Scale), while others used the SAPS (Schedule for the Assessment of Positive Symptoms) and SANS (Schedule for the Assessment of Negative Symptoms) to assess symptom severity; they had to leverage work done by another study, which collected both assessments on the same subjects, to develop a translational calculation from one to the other (van Erp et al. 2014). Clearly, schizophrenia is a clinically heterogeneous disorder, and study cohorts differ in terms of demographic composition, the duration of illness, treatment effects, the mean age of onset, and the prevalence of other risk factors for schizophrenia. When identifying common patterns of brain abnormalities in schizophrenia, there may be important subtypes within these overall patterns. Given the large individual variance in anatomy in both patients and controls, individual patients typically will

not exhibit the exact distribution of abnormalities seen in the group averages.

In an effort to resolve important distinctions, the ENIGMA Schizophrenia Working Group has supported the development of specific ENIGMA working groups to perform parallel large-scale analyses of brain differences in early-onset psychosis, schizotypy, and in first-degree relatives of patients. Pioneering work by Judith Rapoport and colleagues at the U.S. National Institute of Mental Health in the late 1990s revealed that children with childhood-onset psychosis tended to demonstrate cortical thickness deficits that gradually spread into the frontal lobes as adolescence proceeds. Decades of work in discordant twins and first-degree relatives of patients also suggests that some component of the anatomical abnormalities seen in patients might not be specific to those with the illness, and may also be evident, to some degree, in first-degree relatives (de Zwarte et al. 2018). Medication effects also influence the degree of difference, while the degree of medication each patient receives is not independent of their duration or severity of illness. Large-scale meta-analyses in the future may shed light on which interventions resist the progression of brain changes, by comparing groups of patients in whom other factors can be equalized; future work will also help to determine how early and how consistently brain changes can be detected in people at heightened risk of psychosis.

A unique perspective on the development of schizophrenia is afforded by the analysis of patients with the 22q11 deletion syndrome—a chromosomal abnormality that leads to heightened risk for schizophrenia. In the largest analysis of brain structural alterations in 22q11DS to date, Sun et al. (2018) analyzed imaging data from 10 centers worldwide, including 474 subjects with 22q11DS (age = 18.2 ± 8.6 years; 46.9% female) and 315 typically developing, matched controls (age = 18.0 ± 9.2 years; 45.9% female). Compared to controls, 22q11DS individuals showed thicker cortical gray matter overall, but focal thickness reduction in temporal and cingulate cortex. Cortical surface area (SA), however, showed pervasive reductions in 22q11DS ($d = -1.01/-1.02$ for left/right hemispheres). Analysis of 22q11DS individuals with psychosis found cortical alterations that significantly overlapped with those from the ENIGMA schizophrenia study, particularly in fronto-temporal cortex, lending further evidence that 22q11DS is a powerful tool for studying the development of idiopathic psychosis.

21.6 Diffusion MRI and White Matter Microstructure in Schizophrenia

In a further extension of this work, Kelly et al. (2018) studied the regional distribution of white matter (WM) abnormalities in schizophrenia in 2359 healthy controls and 1963 individuals with schizophrenia from 29 independent international studies; unlike many prior meta-analyses, the group harmonized the processing and statistical analyses of diffusion tensor imaging (DTI) data across sites and meta-analyzed effects across studies (Fig. 21.6). Effect sizes varied by region, peaking at ($d = 0.42$) for the entire WM skeleton. The anterior *corona radiata* ($d = 0.40$) and corpus callosum ($d = 0.39$), specifically its body ($d = 0.39$) and genu ($d = 0.37$), showed greatest effects. Larger effect sizes were observed for FA (fractional anisotropy) than diffusivity measures, and mean and radial diffusivity were higher, on average, in individuals with schizophrenia compared to controls. No significant effects of age at onset of schizophrenia or medication dosage were detected.

21.7 Large Scale MRI Studies of Other Psychiatric Disorders

A key question in psychiatric neuroimaging research is the extent to which brain variations may differentiate and overlap across disorders. A series of papers were published by ENIGMA's working groups focusing on schizophrenia, bipolar disorder, major depressive disorder, substance use disorders, as well as disorders that are prevalent in childhood and adolescence, including

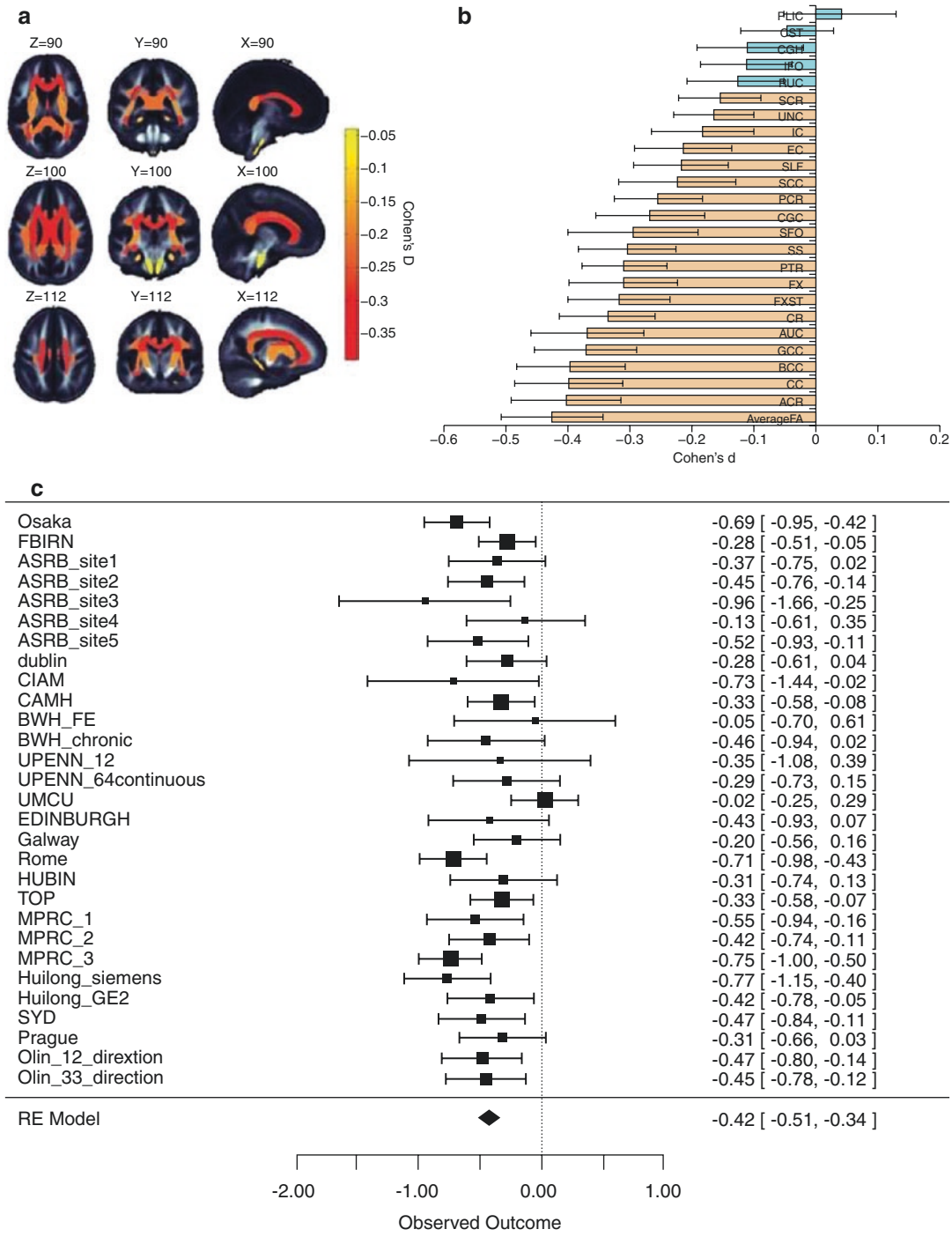

Fig. 21.6 White matter microstructural abnormalities in schizophrenia. In this study by the ENIGMA Schizophrenia DTI Working Group (Kelly et al. 2018), widespread abnormalities were observed in fractional anisotropy (FA) between individuals with schizophrenia and healthy controls for 25 white matter (WM) regions representing major fasciculi. The color bar indicates Cohen's *d* effect sizes after meta-analysis, sorted in increasing magnitude, after including age, sex, age × sex, age^2 and age^2 × sex as covariates. Error bars represent 95% confidence intervals. [Reproduced, with permission, from Kelly et al. (2018), *Molecular Psychiatry*]

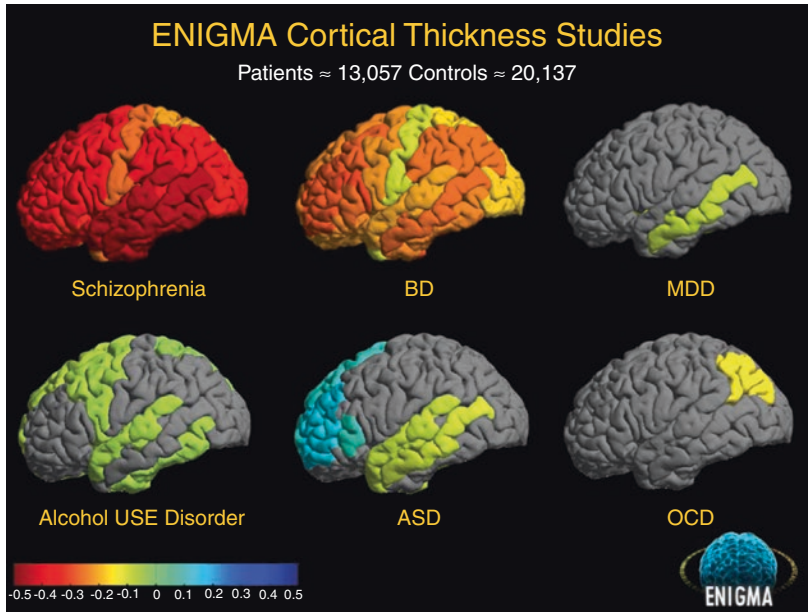

Fig. 21.7 Large-scale analysis of cortical gray matter thickness shows profiles of abnormalities in six brain disorders. In a series of large-scale analyses, ENIGMA's working groups examined the profile of cortical thickness and surface area abnormalities across a broad range of disorders. Maps of Cohen's *d* effect sizes show the magnitude of differences between patients and controls, with *warmer colors* denoting deficits in patients and *cooler colors* denoting relative enlargement. [Data adapted with permission from the authors]

autism spectrum disorders, OCD, and ADHD. Figure 21.7 shows the maps of case-control differences for each disorder. Among the most striking findings from these studies is the observation that the schizophrenia effects were more widespread and greater in degree than those found in bipolar disorder and major depressive disorders. In line with prior hypotheses about the anatomical correlates of bipolar disorder versus major depressive disorder, frontal lobe systems showed greater deficits in bipolar patients, whereas limbic regions tended to show greater deficits in major depressive disorder. A key finding across a diverse set of psychiatric disorders is the volumetric deficit in the hippocampus; in the psychiatric disorders studied to date, hippocampal volume deficits are found in highest degree in PTSD. Ongoing efforts to refine these results include the examination of hippocampal subfield volumes and shape analysis of subcortical structures.

Large-scale analyses such as these offer some benefits not afforded by smaller studies. Subtle abnormalities not detectable in smaller studies may be identified as robust effects when data are aggregated from multiple centers. The geographic, ethnic, and cultural diversity of the cohorts assessed also makes it possible to assert that the abnormalities found are somewhat invariant to specifics of the cohort such as their educational level, socioeconomic status, and ethnic composition.

Meta-analyses also have some limitations, however. When an effect size is analyzed across multiple cohorts, it may be easy to overlook important or influential factors that operate only in certain contexts. One example of this is the different profile of brain abnormalities seen in adult versus pediatric patients for several of the disorders studied. Meta-analyses may also not detect the effects of factors that are strongly age-dependent. For instance, the effect on hippocampal volume of the major Alzheimer's risk allele, *APOE4*, is not the strongest locus in the genome-wide analysis of common variants that affect hippocampal volume. This limitation is important to

keep in mind because some rarer risk factors for illness may not be efficiently detected in a meta-analysis. To address some of these limitations, several of the ENIGMA working groups are now performing 'mega-analysis' of individual level data in which brain measures derived from MRI scans are centralized and analyzed jointly in an overall statistical model. Search analyses allow for the detection of effects of subtle modulatory factors such as medication, sex differences, and environmental risk factors.

Another limitation of the first round of ENIGMA analyses was the assessment of diagnostic categories rather than dimensional measures of specific symptom domains. As exemplified by the National Institutes of Health Research Domain Criteria (NIH RDoC) (Insel 2014) and other ongoing initiatives, there is a general trend in psychiatry towards the examination of dimensional measures of cognitive and behavioral symptoms which may be expressed to different degrees in different psychiatric disorders. A major challenge in the aggregation and comparison of data across cohorts is the fact that different symptom and cognitive measures have been collected from the various cohorts. Before direct comparisons can be made of data from the different disease working groups—and even across cohorts within them—a dedicated effort is needed to assemble a dictionary of common data elements containing factors that might influence brain development and disease. In this way, it is possible to distinguish the effects of common risk factors—as well as common co-morbidities, such as major depression and alcohol use—on the expression of various psychiatric disorders.

21.8 Technical Challenges for Large-Scale Imaging Consortia

As imaging studies in psychiatry and neurology grow from hundreds of subjects to tens of thousands of subjects, several considerations arise that affect the feasibility of performing the studies. Many of the algorithms that derive measures from MRI scans segment the brain into distinct regions, but this segmentation process is never perfect—typically requiring an expert rater to identify segmentation failures and outliers. Early studies in ENIGMA 'crowd-sourced' the quality control process, so that anatomically trained raters at each site curated their own datasets, while reporting summary measures of quality control. Some recent innovations have involved the use of machine learning approaches—in particular deep learning—to expedite the quality control of imaging data sets. Petrov et al. (2017) used computational shape models of a variety of brain structures across 19 cohorts in over 7500 human-rated subjects, to train kernelized support vector machine classifiers to detect anatomical segmentations of poor quality. This step reduced human workload by 30–70% in inspecting and verifying data quality, or equivalently hundreds of human rater hours for datasets of comparable size, with accuracy rates approaching human inter-rater reliability. Nevertheless, designing similar quality control procedures for more complex data types in neuroimaging will require significant skill, as well as consensus and coordination. Diffusion imaging in particular can give rise to maps of anatomical brain connectivity via the use of fiber tracking methods. A major challenge in aggregating connectivity maps for large-scale statistical inference is making the analyses invariant to the image acquisition protocols and parameters of the fiber tracking methods.

21.9 Large Scale Functional Imaging Studies

21.9.1 Functional MRI

For many years, task-related functional MRI has been used to understand spatial and temporal patterns of brain activation associated with behavioral and cognitive processes, including alterations in these activation patterns in schizophrenia and other psychiatric disorders. The variety of possible tasks and the complexity of administering them made it difficult to integrate findings across cohorts for task-based functional

MRI. In the last decade, there has been an increasing use of resting-state functional MRI to understand the functional synchrony among brain regions at rest. The relative ease of collecting resting-state versus task-based functional data has meant that it can be readily applied in patient populations and large databases of normative data can also be collected.

Resting-state functional MRI can be analyzed with a diverse range of approaches, including methods that assess the synchrony among regions using seed-based methods, independent components analysis, and graph theory. In one approach to harmonizing metrics across datasets, Adhikari et al. (2018) assessed both anatomical and functional connectivity in a total of 261 patients with schizophrenia (161M/100F; age = 18–63 years) and 327 controls (146M/211F; age = 18–65 years) using a mega-analytical aggregation of three cohorts. Patients showed consistent structural, functional, and cognitive deficits with robust effect sizes (Cohen's d = 0.2–0.9) in the three cohorts; structural and functional connectivity contributed to the intersubject variance on processing speed and working memory, and individuals with schizophrenia showed abnormalities in areas and networks that serve these cognitive domains. When ranking the functional connectivity measures for degree of deficit in patients, one of the top metrics was the functional connectivity between auditory network ROIs, consistent with the known patterns of auditory dysfunction in schizophrenia. In follow-up studies, Adhikari et al. (2018) found that the intersubject variance in functional connectivity within several functional networks was moderately heritable in two independent studies (HCP and GOBS), suggesting the feasibility of performing multi-cohort analyses of genetic risk and disease effects using the same measures.

A major goal of ENIGMA and other neuroimaging consortia is to develop a set of functional connectivity phenotypes that can be reliably extracted and compared across diverse datasets. The initial approach being taken is to rank phenotypes for case-control effect sizes to determine the suitability for studies of modulators of disease. A second round of screening is now underway, using the structural and functional connectivity measures together to examine relationships to cognition.

21.10 Future Opportunities and Challenges

Big data analyses and large-scale neuroimaging datasets offer great potential in psychiatric research. Most of the analyses described in this chapter describe relatively simple, 'mass univariate' analysis of individual imaging features. Even so, clear benefits are expected if features from multiple imaging modalities are combined to make predictions about diagnosis and prognosis. In addition to classical multivariate approaches (Lorenzi et al. 2018), machine learning models are being applied to neuroimaging data across a variety of brain disorders to predict outcomes, treatment response, or to begin to identify and characterize subtypes or clusters within highly heterogeneous diagnostic categories.

Recently, there has been great interest in the application of machine learning, and more recently deep learning, to multi-site neuroimaging data, given the advantages of scale shown for other applications when large amounts of training data are available. Imaging consortia that collect data from patients at multiple sites offer an opportunity for fair validation and evaluation of machine learning models. Initial efforts in the diagnostic classification of affective disorders show promise (Zhu et al. 2017), but their accuracy is likely to improve as more advanced metrics are added, including structural, functional, and even activity or geospatial data from mobile sensors.

In the near future, it is likely that new connections will be made between neuroimaging measures and other types of "omics" data—such as plasma markers, metabolomic data, epigenetic data, gene expression data, and other biological assays. Big data methods have been proposed that use information theory to extract clusters and patterns in high dimensional data; in initial tests, these have identified both hypothesized and unexpected predictors of disease (Madsen et al. 2015).

An ever-present challenge for big data methods in psychiatry involves the quest to relate imaging findings to cellular and molecular measures seen in histologic data, including molecular markers that can be influenced with drug treatment. A major barrier in understanding the significance of neuroimaging changes in psychiatry is the relative lack of histologic or molecular markers of these psychiatric conditions.

It is now possible to efficiently screen very large databases of phenotypes, and it will be increasingly important to use brain imaging biobanks to identify new correlates of genetic risk, and other molecular markers.

The ongoing effort to bridge molecular findings and neuroimaging is likely to lead to improvements in imaging as well, by identifying features that are more tightly linked with cellular processes, such as markers of inflammation and immune response. In the meantime, however, even before the cellular basis of these imaging signatures is fully understood, the imaging markers can provide valuable proxies for understanding the effects of risk factors and treatment in psychiatric disorders.

Summary

- The 'crisis of reproducibility' in the neurosciences can be addressed with large-scale international efforts.
- International collaborations have helped identify factors with small effect sizes, such as single genetic variations, that contribute to risk for a neuropsychiatric disease, as well as those that affect the brain.
- The ENIGMA Consortium is a large, international initiative for studying brain health, disease, and factors that modulate the brain's structure and function.
- The ENIGMA Consortium has many working groups dedicated to understanding specific psychiatric disorders and conditions, many with data from thousands of patients from around the world.
- Data harmonization remains a challenge for several clinical and imaging data types when aggregating data from around the world.

Acknowledgments This work is supported in part by NIH grant U54 EB020403 from the BD2K Initiative. Additional support was provided by R01 MH116147, P41 EB015922, RF1 AG051710, and RF1 AG041915. We also thank the many scientists and participants worldwide who contributed to the studies reviewed here.

References

Adams HHH, et al. Novel genetic loci underlying human intracranial volume identified through genome-wide association. Nat Neurosci. 2016;19:1569–82.

Adhikari BM, et al. Comparison of heritability estimates on resting state fMRI connectivity phenotypes using the ENIGMA analysis pipeline. Hum Brain Mapp. 2018;39(12):4893–902. https://doi.org/10.1002/hbm.24331.

Bipolar Disorder and Schizophrenia Working Group of the Psychiatric Genomics Consortium, Electronic address: douglas.ruderfer@vanderbilt.edu, Bipolar Disorder and Schizophrenia Working Group of the Psychiatric Genomics Consortium. Genomic dissection of bipolar disorder and schizophrenia, including 28 subphenotypes. Cell. 2018;173:1705–1715.e16.

Boedhoe PSW, et al. Distinct subcortical volume alterations in pediatric and adult OCD: a worldwide meta- and mega-analysis. Am J Psychiatry. 2017;174:60–9.

Brainstorm Consortium, et al. Analysis of shared heritability in common disorders of the brain. Science. 2018;360(6395)

Button KS, et al. Power failure: why small sample size undermines the reliability of neuroscience. Nat Rev Neurosci. 2013;14:365–76.

de Zwarte S, et al. T235. Brain abnormalities in cotwins, siblings, offspring and parents of schizophrenia and bipolar patients: an ENIGMA Collaboration. Biol Psychiatry. 2018;83(9):S220.

Dumas-Mallet E, Button KS, Boraud T, Gonon F, Munafò MR. Low statistical power in biomedical science: a review of three human research domains. R Soc Open Sci. 2017;4:160254.

Farrell MS, et al. Evaluating historical candidate genes for schizophrenia. Mol Psychiatry. 2015;20:555–62.

Franke B, et al. Genetic influences on schizophrenia and subcortical brain volumes: large-scale proof of concept. Nat Neurosci. 2016;19:420–31.

Frodl T, et al. Childhood adversity impacts on brain subcortical structures relevant to depression. J Psychiatr Res. 2017;86:58–65.
Gerritsen L, et al. Childhood maltreatment modifies the relationship of depression with hippocampal volume. Psychol Med. 2015;45:3517–26.
Gottesman II, Gould TD. The endophenotype concept in psychiatry: etymology and strategic intentions. Am J Psychiatry. 2003;160:636–45.
Guadalupe T, et al. Human subcortical brain asymmetries in 15,847 people worldwide reveal effects of age and sex. Brain Imaging Behav. 2017;11:1497–514.
Guglielmi, G. The world's largest set of brain scans are helping reveal the workings of the mind and how diseases ravage the brain. Science; 2018. https://doi.org/10.1126/science.aat0994.
Hibar DP, et al. Common genetic variants influence human subcortical brain structures. Nature. 2015;520:224–9.
Hibar DP, et al. Subcortical volumetric abnormalities in bipolar disorder. Mol Psychiatry. 2016;21:1710–6.
Hibar DP, et al. Novel genetic loci associated with hippocampal volume. Nat Commun. 2017;8:13624.
Hibar DP, et al. Significant concordance of genetic variation that increases both the risk for obsessive–compulsive disorder and the volumes of the nucleus accumbens and putamen. Br J Psychiatry. 2018a;213:430–6.
Hibar DP, et al. Cortical abnormalities in bipolar disorder: an MRI analysis of 6503 individuals from the ENIGMA Bipolar Disorder Working Group. Mol Psychiatry. 2018b;23:932–42.
Hoogman M, et al. Subcortical brain volume differences in participants with attention deficit hyperactivity disorder in children and adults: a cross-sectional mega-analysis. Lancet Psychiatry. 2017;4:310–9.
Insel TR. The NIMH Research Domain Criteria (RDoC) Project: precision medicine for psychiatry. Am J Psychiatry. 2014;171:395–7.
Ioannidis JPA. Acknowledging and overcoming nonreproducibility in basic and preclinical research. JAMA. 2017;317:1019–20.
Jahanshad N, et al. Do candidate genes affect the brain's white matter microstructure? Large-scale evaluation of 6,165 diffusion MRI scans; 2017. https://doi.org/10.1101/107987.
Kelly S, et al. Widespread white matter microstructural differences in schizophrenia across 4322 individuals: results from the ENIGMA Schizophrenia DTI Working Group. Mol Psychiatry. 2018;23:1261–9.
Kong X-Z, et al. Mapping cortical brain asymmetry in 17,141 healthy individuals worldwide via the ENIGMA Consortium. Proc Natl Acad Sci U S A. 2018;115:E5154–63.
Lee PH, et al. Partitioning heritability analysis reveals a shared genetic basis of brain anatomy and schizophrenia. Mol Psychiatry. 2016;21:1680–9.
Lorenzi M, et al. Susceptibility of brain atrophy toTRIB3in Alzheimer's disease, evidence from functional prioritization in imaging genetics. Proc Natl Acad Sci. 2018;115:3162–7.
Madsen SK, et al. Information-theoretic characterization of blood panel predictors for brain atrophy and cognitive decline in the elderly. Proc IEEE Int Symp Biomed Imaging. 2015;2015:980–4.
Mufford MS, et al. Neuroimaging genomics in psychiatry—a translational approach. Genome Med. 2017;9(1):102.
Mufford MS, et al. Concordance of genetic variation that increases risk for Tourette syndrome and that influences its underlying neurocircuitry. Transl Psychiatry. 2019;9(1):120. https://doi.org/10.1101/366294.
Okada N, et al. Abnormal asymmetries in subcortical brain volume in schizophrenia. Mol Psychiatry. 2016;21:1460–6.
Pauling M, et al. Bipolar disorder and white matter microstructure: ENIGMA bipolar disorder fractional anisotropy DTI results. Eur Neuropsychopharmacol. 2017;27:S839–40.
Petrov D, et al. Machine learning for large-scale quality control of 3D shape models in neuroimaging. Mach Learn Med Imaging. 2017;10541:371–8.
Rentería ME, et al. Subcortical brain structure and suicidal behaviour in major depressive disorder: a meta-analysis from the ENIGMA-MDD working group. Transl Psychiatry. 2017;7:e1116.
Satizabal CL, et al. Genetic architecture of subcortical brain structures in over 40,000 individuals worldwide. bioRxiv; 2017.
Schizophrenia Working Group of the Psychiatric Genomics Consortium. Biological insights from 108 schizophrenia-associated genetic loci. Nature. 2014;511:421–7.
Schmaal L, et al. Subcortical brain alterations in major depressive disorder: findings from the ENIGMA Major Depressive Disorder working group. Mol Psychiatry. 2016;21:806–12.
Schmaal L, et al. Cortical abnormalities in adults and adolescents with major depression based on brain scans from 20 cohorts worldwide in the ENIGMA Major Depressive Disorder Working Group. Mol Psychiatry. 2017;22:900–9.
Smeland OB, et al. Genetic overlap between schizophrenia and volumes of hippocampus, putamen, and intracranial volume indicates shared molecular genetic mechanisms. Schizophr Bull. 2018;44:854–64.
Smit DJA, et al. Genome-wide association analysis links multiple psychiatric liability genes to oscillatory brain activity. Hum Brain Mapp. 2018;39(11):4183–95. https://doi.org/10.1002/hbm.24238.
Stein JL, et al. Identification of common variants associated with human hippocampal and intracranial volumes. Nat Genet. 2012;44:552–61.
Sun D, et al. Large-scale mapping of cortical alterations in 22q11.2 deletion syndrome: convergence with idiopathic psychosis and effects of deletion size. Mol Psychiatry. 2018; https://doi.org/10.1038/s41380-018-0078-5.
Thompson PM, et al. ENIGMA and the individual: predicting factors that affect the brain in 35 countries worldwide. Neuroimage. 2017;145:389–408.

Turner JA. The rise of large-scale imaging studies in psychiatry. Gigascience. 2014;3:29.

van Erp TGM, et al. Converting positive and negative symptom scores between PANSS and SAPS/SANS. Schizophr Res. 2014;152:289–94.

van Erp TGM, et al. Subcortical brain volume abnormalities in 2028 individuals with schizophrenia and 2540 healthy controls via the ENIGMA consortium. Mol Psychiatry. 2016;21:547–53.

van Erp TGM, et al. Cortical brain abnormalities in 4474 individuals with schizophrenia and 5098 control subjects via the Enhancing Neuro Imaging Genetics Through Meta Analysis (ENIGMA) Consortium. Biol Psychiatry. 2018;84(9):644–54. https://doi.org/10.1016/j.biopsych.2018.04.023.

van Rooij D, et al. Cortical and subcortical brain morphometry differences between patients with autism spectrum disorder and healthy individuals across the lifespan: results from the ENIGMA ASD Working Group. Am J Psychiatry. 2018;175:359–69.

Walton E, et al. Positive symptoms associate with cortical thinning in the superior temporal gyrus via the ENIGMA Schizophrenia consortium. Acta Psychiatr Scand. 2017;135:439–47.

Walton E, et al. Prefrontal cortical thinning links to negative symptoms in schizophrenia via the ENIGMA consortium. Psychol Med. 2018;48:82–94.

Whelan CD, et al. Structural brain abnormalities in the common epilepsies assessed in a worldwide ENIGMA study. Brain. 2018;141:391–408.

Wray NR, et al. Genome-wide association analyses identify 44 risk variants and refine the genetic architecture of major depression. Nat Genet. 2018;50:668–81.

Zhu D, Thompson PM, Schmaal L, Veltman D. 757. Machine learning insights from enigma's studies of major depressive disorder: classification via distributed analysis. Biol Psychiatry. 2017;81:S307.

22 Towards an Integration of Information Gleaned from Neuroimaging in Schizophrenia

Amanda E. Lyall, Martha E. Shenton, and Marek Kubicki

Contents

A. E. Lyall (✉)
Psychiatry Neuroimaging Laboratory, Department of Psychiatry, Brigham and Women's Hospital, Harvard Medical School, Boston, MA, USA

Department of Psychiatry, Massachusetts General Hospital, Harvard Medical School, Boston, MA, USA
e-mail: alyall@bwh.harvard.edu

M. E. Shenton
Psychiatry Neuroimaging Laboratory, Department of Psychiatry, Brigham and Women's Hospital, Harvard Medical School, Boston, MA, USA

Department of Psychiatry, Massachusetts General Hospital, Harvard Medical School, Boston, MA, USA

Department of Radiology, Brigham and Women's Hospital, Harvard Medical School, Boston, MA, USA

VA Boston Healthcare System, Brockton, MA, USA
e-mail: shenton@bwh.harvard.edu

M. Kubicki
Psychiatry Neuroimaging Laboratory, Department of Psychiatry, Brigham and Women's Hospital, Harvard Medical School, Boston, MA, USA

Department of Psychiatry, Massachusetts General Hospital, Harvard Medical School, Boston, MA, USA

Department of Radiology, Brigham and Women's Hospital, Harvard Medical School, Boston, MA, USA
e-mail: kubicki@bwh.harvard.edu

M. Kubicki, M. E. Shenton (eds.), *Neuroimaging in Schizophrenia*,
https://doi.org/10.1007/978-3-030-35206-6_22

22.1 Introduction

Since its inception, neuroimaging in schizophrenia research has proven to be a very useful tool for the interrogation of both the biological nature and the trajectory of the illness, *in vivo,* as well as more clearly establishing schizophrenia as a "brain disorder." The inherent complexity of schizophrenia's underlying pathophysiology has been a key motivator for the continued use and development of sophisticated neuroimaging tools and analytic approaches. These approaches have made possible the *in vivo* exploration of the neuroanatomy, neurophysiology, neurobiology, and neurochemistry of this debilitating, sometimes lifelong, psychiatric illness.

For years, the field of schizophrenia research in general, and neuroimaging, in particular, has been an experimental incubator where new ideas are first tested, and later adapted for use in other neuropsychiatric illnesses. The chapters in this book document this process further—from the development of methods to parcellate the brain better, to measuring the smallest anatomical brain structures (Chaps. 1 and 2), to visualizing and quantifying large brain connections (Chaps. 2, 3, and 4), to investigating the nature and timing of neuronal firing and connectivity (Chaps. 5, 6, 11, 12, 13 and 14), and to understanding brain chemistry and neurotransmission (Chaps. 7, 8, 9 and 10).

Part 1 of ***Neuroimaging in Schizophrenia*** provides comprehensive summaries of both the methods that have been used in schizophrenia, as well as the findings that describe how changes in the brain structure and/or function may contribute to schizophrenia illness presentation. Part 2 then identifies a few representative examples where the application of neuroimaging has made a significant impact on our understanding of this disorder. These include: (a) providing imaging biomarkers for the assessment of traditional (Chap. 18) and/or novel intervention and treatment paradigms (Chaps. 19 and 20); (b) re-characterizing diagnoses by introducing imaging-based biotypes and "Big Data"-driven classifications (Chap. 21); (c) proposing predictors based on imaging (Chap. 17), or imaging-derived developmental trajectories (Chap. 15); and, finally, (d) understanding the interaction between imaging measures and genetics (Chap. 16). In addition to highlighting all of these advances, the goal of **Neuroimaging in Schizophrenia** is to point to the limitations extant in the neuroimaging field, and to discuss them within the context of future directions for schizophrenia research. Neuroimaging promises to provide the field of psychiatry with objective observations for diagnosis and patient management, and yet, sadly, this goal has yet to be achieved. Moreover, despite the large number of imaging studies, across an equally impressive number of modalities available to the modern-day schizophrenia researcher, the field has yet to produce clinically relevant or diagnostic "biomarkers of schizophrenia." Of note here, within almost all other fields of medicine, diagnostic evaluations can be carried out upon entry into a hospital. However, psychiatry remains limited in this regard, as many of the decisions made in psychiatric care are still based on the observation or report of symptoms and patient illness history, which can vary significantly between and within individuals. This is in contrast to other areas of medicine where laboratory tests can be performed as part of a diagnostic evaluation of the patient. In addition, the majority of neuroimaging research studies continue to rely upon case-control comparisons, many of which can be under-powered and therefore lack generalizability to the entire population. Thus, despite significant contributions towards a greater understanding of schizophrenia, many of the imaging methods employed in research paradigms today have yet to provide sufficient diagnostic information that is clinically relevant to a given individual.

Thus, while imaging tools are valuable in research studies, reliable biomarkers remain allusive and the field may need to change both conceptually and methodologically with respect to how we approach the study of schizophrenia. In this chapter, we identify possible obstacles within the field, and we highlight advances currently being made to address these obstacles. We recognize two general approaches that we believe could have the greatest impact for overcoming these obstacles moving forward: (1) reconceptualizing the way we

think about schizophrenia, i.e., *Reconciling Schizophrenia Hypotheses*, *Studying Schizophrenia as a Lifespan Disorder*, and *Clinical versus Biological Classification Paradigms* (see below), and (2) methodological considerations related to how we ask important scientific and clinical questions, i.e., *Implementation of Multimodal Imaging Paradigms*, *Big-Data Versus Precision Medicine*, and *Biological Validation of Imaging Measures* (see below). This is then followed by *A Look to the Future*.

22.2 Reconceptualizing Schizophrenia

22.2.1 Reconciling Schizophrenia Hypotheses

Imaging studies, over several different modalities, have been used to characterize an array of pathological alterations in both brain structure and function. Over the course of the last few decades, there have been a number of well-founded and widely accepted hypotheses about brain structure and function that are strongly supported by findings from neuroimaging studies in schizophrenia. These include the neuropil hypothesis (1), the neurodevelopmental hypothesis (2), the dopamine hypothesis (3), the glutamate hypothesis (4), the dysconnection hypothesis (5), the accelerated aging hypothesis (6), the inflammation hypothesis (7), (Selemon & Goldman-Rakic 1999); (Howes et al. 2015); (Egerton & Stone 2012); (Koutsouleris et al. 2014); (Feigenson et al. 2014) and the list continues. Each of these hypotheses have sufficient confirmatory evidence from a diverse number of neuroimaging experts across the globe and many are discussed at length by these same experts throughout the course of this book. Yet, very little has been done to reconcile these disparate hypotheses into a more coherent theory. Instead, scientists who use diffusion or functional connectivity methods tend to test the hypothesis that schizophrenia is a "disconnection disorder," while researchers utilizing electroencephalography (EEG) or magnetoencephalography (MEG) are more likely to contend that schizophrenia symptoms are related to abnormalities in neuronal synchrony, or to information-processing deficits, while those using magnetic resonance spectroscopy tend to test theories of mitochondrial or glutamatergic dysfunction, while those using positron emission tomography imaging may lean towards dopamine-centric or inflammatory hypotheses. In the end, despite the very best of intentions, it can be argued that the individual imaging fields cultivate "modality-specific" and "modality-driven" hypotheses. The intrinsic advantages and disadvantages of each modality to study particular aspects of the illness do, understandably, create research niches. However, these niches are analogous to studying the natural history and/or physical properties of one specific star, say Betelgeuse, within a much larger and potentially more complex constellation, like Orion. To make progress, there still remains a crucial need to integrate the information that has been collected into more synthesized hypotheses that can begin to appreciate all of the stars that comprise the entire constellation. This necessitates conceptual changes that would begin to appreciate the complexity of this illness and how each of the puzzle pieces fit together.

A first step toward meeting this goal would be to design studies aimed at understanding the interactions between and among the aforementioned hypotheses. We have already clearly demonstrated within the preceding chapters that we possess the tools and methods to test many of these hypotheses. To start, it is important to understand to the full extent what individual imaging modalities can accomplish. For example, diffusion imaging has been predominantly used to test hypotheses centered on dysconnectivity or white matter aberrations (Friston et al. 2016; Pettersson-Yeo et al. 2011). Advances in diffusion modeling have produced novel metrics that are proposed to be sensitive to both tissue-related properties and extracellular water, a proposed proxy for neuroinflammation (Pasternak et al. 2016). Similar types of discoveries are being made within other modalities, each of which will widen further our scientific scope. In the future, the key to progress will be to leverage

the unique capabilities of an individual imaging modality (e.g., diffusion MRI) and combine it with complementary information generated from another imaging modality (e.g., structural MRI) and/or from non-imaging data (e.g., peripheral blood markers). Multi-modal approaches, which will be discussed in greater detail later in this chapter, are a powerful way to capture the many dimensions of schizophrenia illness.

22.2.2 Studying Schizophrenia as a Lifespan Disorder

When thinking about schizophrenia, we must also be cognizant that it is not a static disorder, but more likely an intricate constellation of biological pathologies that evolve over time (Oribe et al. 2015; Kempton et al. 2010; Whitford et al. 2006; Andreasen et al. 2011). Thus, we need to be asking questions about how the changes or alterations occurring in one system over time interact, interfere, or influence other systems in the brain and body, as well as what effect these changes may have on the presentation of illness. It has been posited that as a neurodevelopmental disorder with identified genetic and environmental risk factors, schizophrenia is likely the end result of a disease state interacting with development (Rapoport et al. 2012; Kochunov and Hong 2014). This means that studying the nature of illness trajectory is critical to our understanding of this disorder. While cross-sectional studies have been the bedrock of schizophrenia research, this developmental perspective highlights the limitations of using a single-time point in data collection, which is akin to inferring a person's life story from a single photo. The latter approach is too simplistic for an illness that is as heterogenous and complex as schizophrenia. Further, with only a single time point it is difficult to be certain that we have not missed a critical window in time in which a pathology may be present. It is thus much more likely that the amount of change occurring in any particular neuroimaging feature over time will prove to be more informative than a static data point. By mapping trajectories across different imaging modalities and different non-imaging markers, we can understand better the roles that distinct biological systems may play at different stages of the disorder. A clearer picture of how schizophrenia develops can also strongly impact the way we will ultimately identify, treat, and some day, hopefully, prevent this illness.

To address these concerns, there needs to be a continued focus on effective and well-powered longitudinal studies that collect multiple types of imaging and non-imaging data. Examples of non-imaging data that could be important to look at over the course of the illness might include the collection of peripheral blood, cerebrospinal fluid, genetic information, behavioral assessments, and qualitative information regarding a person's lifestyle (Agerbo et al. 2015). With this information, we may be able to elucidate further the role of dynamic brain changes and their relationship to environmental elements, such as stress or nutrition and/or genetic, epigenetic, or sex-specific factors in the context of schizophrenia illness trajectory (Do et al. 2015; Bale et al. 2010). Ultimately, deeply phenotyping individuals with schizophrenia over time will be critical to increasing our knowledge regarding the interplay that may occur between biological systems in the natural progression of disease states from prodromal periods, to illness onset, and beyond.

22.2.3 Clinical Versus Biological Classification Paradigms

Finally, it is becoming increasingly more widely accepted that the phenomenologically defined disorder of schizophrenia may be a collection of more nuanced biological changes ranging along an illness spectrum. In fact, the term "psychosis spectrum disorders" has begun to supersede the use of more discrete illnesses such as "schizoaffective disorder" or "schizophrenia" in the research world (e.g., (Roalf et al. 2017; Gur et al. 2014; van Dellen et al. 2016)). The recognition of a model in which psychiatric illnesses are characterized as a set of potentially overlapping biological pathologies is shaping the way the field has begun to progress. Initiatives such as the National Institute of Mental Health's Research Domain Criteria (RDoC)

framework (Insel 2014) have recognized the critical need for more biologically-based approaches to the study of psychiatric illnesses. Imaging techniques are uniquely suited to address this need as they are presently the only avenue to investigate human brain structure and function *in vivo*.

This shift in perspective is historically consistent with changes previously made within the Diagnostic and Statistical Manual. In earlier editions (DSM-III), psychoses were characterized as "organic" versus "functional," yet this was recast in later editions as "primary" versus "secondary to another medical illness" (DSM-IV). Early applications of magnetic resonance imaging (MRI) and computerized tomography (CT) were pivotal in the identification of neurobiological factors, such as space occupying lesions, tumors, or degenerative illnesses that lead to the presentation of psychosis symptoms. In many instances, the identification of the pathology led to a more targeted treatment plan resulting in better outcomes for the individual. Thus, it can be argued that neuroimaging has had a significant and direct effect on the evolution of the definition of primary versus secondary psychosis. Moreover, the evolution of these definitions provides motivation for future generations of scientists as there is the hope that we will be able to classify all presentations of psychosis as the result of an identified biological illness.

22.3 Methodological Considerations

22.3.1 Implementation of Multimodal Imaging Paradigms

As stated previously, many of the current neuroimaging approaches to the study of schizophrenia involve the application of a single neuroimaging modality with the aim of testing a specific hypothesis. Yet, as discussed earlier, in order to reconcile disparate biological hypotheses in the field, it will be very important to develop more elegant and powerful multimodal imaging paradigms. Since any single modality might not be sufficiently powered to explain all of the variability within the clinical or cognitive phenotypes observed in schizophrenia, the use of complementary imaging modalities may assist in providing new and interesting perspectives. However, this is not a trivial task. At present, data are being acquired separately for each modality and then combined during the analysis stage. For example, combinations of diffusion imaging with structural MRI, resting state/task functional MRI, magnetic resonance spectroscopy (MRS), and/or EEG (Isobe et al. 2016) have already been employed. Such studies, in general, demonstrate that alterations in one modality are associated with abnormalities in the other (Schultz et al. 2012). These studies also suggest the added value of multimodal imaging in developing measures that could improve the prediction of clinical groups (Venkataraman et al. 2012; Kempton and McGuire 2015) or cognitive abilities (Sui et al. 2015), response to pharmacological treatment (Kempton and McGuire 2015), or further our understanding of the biological processes underlying psychotic symptoms (e.g., (Assaf et al. 2008; Du et al. 2013; Chiappelli et al. 2016)).

While the present multi-modal approaches add valuable information to the field, the simultaneous acquisition of multimodal data will prove to be even more powerful. Simultaneous acquisition allows for direct *in vivo* observations, allowing for the integration of information regarding brain biology, physiology, chemistry, neuronal coupling, and connectivity. The development of scanners capable of simultaneous acquisition of PET and MRI data, or EEG and MRI, and even PET-MR-EEG data have only just begun to emerge (Herzog et al. 2010). Similarly, there are emergent technologies that could allow for novel combinations of imaging modalities, such as measuring the diffusion of MRS metabolites, also known as diffusion-weighted spectroscopy (Döring et al. 2018), or observing functional signal fluctuations through measuring water cellular exchange, also known as functional diffusion tensor imaging (Mandl et al. 2013). As the field marches onward, we will continue to strive for these kinds of innovations so that we can increase the specificity and sensitivity of our imaging measures.

22.3.2 Big Data Versus Precision Medicine

The recruitment of psychotic populations for research studies is a non-trivial task. As a result, many imaging experiments ultimately use small sample sizes that lack power, thereby leading to studies with restricted generalizability to the larger population. This is why of all the limitations currently facing the field of neuroimaging in schizophrenia, one of the largest confounders is sample size. Small effect sizes paired with a high level of variability in imaging and non-imaging measures require significant statistical power to ascertain a clear picture of the underlying pathology, thus necessitating large populations. Meta-analyses utilizing "big data" approaches, introduced in several chapters in this book, allow for increased knowledge regarding general trends within a field. An example of a "Big Data" approach that was showcased in Chap. 21 is for multiple sites to apply the same post-processing techniques to their imaging data in order to increase sample size through data pooling (e.g., the Enhanced Neuroimaging Genetics Through Meta-Analysis (ENIGMA) consortium (Thompson et al. 2014)). The number of multisite consortia utilizing this, or other alternative data pooling approaches, is growing exponentially and represents an important step forward.

Additionally, it is worth noting that many large-scale databases have already been created and several are freely available to the public (e.g., fBIRN, NAPLS, PRONIA, Australian Schizophrenia Research Bank, BSNIP, Human Connectome Project, SchizConnect, etc.). The compilation of these resources has also made it possible for research teams around the world to employ another important emergent group of analysis tools: machine learning. As we have already discussed, because traditional definitions of psychiatric illness may not accurately represent the underlying biological cause(s), many researchers have decided to use data-driven approaches that can generate subgroups of psychiatric patients based on objective imaging phenotypes. Such an approach leverages the combined strength of the large sample sizes of these consortia and the high-dimensionality of the data that can be acquired on an individual subject. There are two generalized classes of approaches: (1) supervised methods, such as support vector machines and neural-networks, which are usually best for outcome prediction, and (2) unsupervised methods, such as principal component analysis, which can be used for identifying patterns in data without *a priori* knowledge, also known as data clustering (Bzdok and Meyer-Lindenberg 2018). As we start to build these large repositories of data, investigators can have access to larger, and potentially more representative samples from a wider definition of psychosis. Thus, machine learning approaches using Big Data may offer an opportunity to identify, in a data-driven way, a collection of biological features that may underly schizophrenia pathophysiology.

One critique of the data pooling approach is that the methodological heterogeneity (scanner type, pre-processing pipelines, etc.) across sites can be a considerable limitation that even the most sophisticated statistical methods cannot adequately address. Moving forward, one way to tackle this problem is to combine the power of coordinated efforts over multiple sites using the same data acquisition protocols (for both imaging and non-imaging variables). Universal or standardized data acquisition protocols, like those employed by the Human Connectome Project (HCP), where independent groups utilize the same scanner, the same acquisition protocol, and the same image post-processing steps, have been welcomed in the field (Van Essen et al. 2013). Similarly, the development of a "minimum dataset," whereby groups agree to collect specific, similarly-defined pieces of data (e.g., duration of illness, treatment responses, NIH Toolbox, etc.) may become increasingly important for team science approaches to flourish. Yet, even with these types of protocols implemented, there are still methodological confounds not accounted for. For example, it is difficult to combine imaging data acquired from different scanners (even if they are the same make, model, and imaging sequence such as in the case of HCP mentioned above) due to inherent hardware and

software inhomogeneities (Cetin Karayumak et al. 2019; Shinohara et al. 2017; Yu et al. 2018). This is why researchers have focused on developing new tools which can remove site- and scanner-specific effects from imaging data (Cetin Karayumak et al. 2019). These methods harmonize, or adjust the imaging data at the signal level, while still maintaining individual variability so that all of the imaging data, regardless of site or scanner, appears as if it all comes from the same scanner. Methods such as these, across different modalities (imaging and non-imaging), are important moving forward because they open the door for more complex questions to be asked.

Complementary to the Big Data approach is precision medicine. Where Big Data attempts to leverage statistical power to probe overarching hypotheses regarding schizophrenia etiology, precision medicine approaches are centered around the life of an individual. These approaches incorporate individual patient information such as illness history, medication history, family history, symptom changes, trauma exposure, nutrition, genetic information, and much more to develop detailed profiles that can be investigated in the context of specific questions. The advantage of this approach is that it recognizes the individual nature of the illness. Thus instead of large studies in which a patient is a single data-point, precision medicine encourages the development of "small and smart" studies, which conduct targeted hypothesis-driven research. If successful, outcomes from these studies may have a higher likelihood of making a substantial impact on an individual's life, and will also be more likely to be applied in the clinic. However, the lack of generalizability to a larger population of individuals with the same illness, as well as the significant resources that it takes, can make these approaches difficult.

Despite representing two ends of a methodological spectrum, "Big Data" and precision medicine work best when used together (Bzdok and Meyer-Lindenberg 2018; Thompson et al. 2017; Serretti 2018). As mentioned earlier, one of the limitations of precision medicine is the potential lack of generalizability to a larger population, which is paired with a complementary limitation of Big Data, that there is limited applicability to the individual. Interestingly, machine learning approaches, discussed earlier, in which a model is trained on a large set of data and then tested with an individual subject's data, have yielded promising results (Bzdok and Meyer-Lindenberg 2018; Thompson et al. 2017; Woo et al. 2017). In fact, a recent study suggests that the identification of biological patient subgroups may be useful in predicting which patients might benefit from neuromodulation treatment paradigms (Drysdale et al. 2017). With increased access of the imaging community to larger repositories of high-resolution and high-dimensional data, it will be possible in the future to develop new hypotheses in smaller groups of patients generated from precision medicine approaches that can then be tested in a larger samples that may be more representative of a clinical population, and vice versa.

22.3.3 Biological Validation of Imaging Measures

From their initial use in schizophrenia research, the greatest benefit of all neuroimaging techniques discussed in **Neuroimaging of Schizophrenia** is their ability to probe brain structure and/or function in living individuals. This is a significant advantage over earlier methods which relied almost entirely on histological techniques of post-mortem tissue (e.g., (Harrison 2000)). The initial goal of neuroimaging studies was to test hypotheses pertaining to structure-function relationships and how these relationships may be altered in psychiatry disorders. Yet, one central problem for many of the metrics employed in imaging studies is that they have not as yet been biologically validated. For example, fractional anisotropy, a widely accepted and commonly-used metric derived from diffusion tensor imaging, has been posited to be a marker of "white matter integrity" (Karlsgodt et al. 2009; Reis Marques et al. 2014; Bijanki et al. 2015). However, this imaging metric has been shown to be affected by a number of different underlying biological alterations, including axonal degeneration, edema, demyelination, fiber packing, and

more, suggesting that while fractional anisotropy is a highly sensitive measure, it ultimately lacks biological specificity (Jones et al. 2013). More simply put, it is not just a marker of white matter. The BOLD response in fMRI is another example. Widely believed to be a marker of aggregated neuronal activity, there are those who are uncertain what specific aspect of neuronal processing the BOLD signal represents (Logothetis 2008; Ekstrom 2010). And while both metrics have been integral to novel discoveries about brain structure and function, they are among a number of imaging measures that lack biological specificity.

One current limitation is the resolution of the images that we are able to attain with present day imaging hardware. Structural MR and diffusion imaging approaches can generally achieve a resolution of about 1 × 1 × 1 mm; functional and neurochemical approaches, including fMRI, PET, and MRS, achieve a resolution of up to a few millimeters (e.g., PET resolution is ~4 × 4 × 4 mm). A single voxel in a traditional structural scan has been estimated to contain approximately 5.5 million neurons, with potentially just as many glial cells and cellular process (Bennett 2011). Thus, the signal that we are measuring is being generated by diverse populations of cell types, each with distinct physical properties and functions. Novel innovations in the imaging field such as the development of cell-type specific PET ligands (Narayanaswami et al. 2018), as well as advanced MRI and dMRI acquisition paradigms, such as multi-slice or multi-shell protocols, will allow for higher-resolution data to be acquired (Lüsebrink et al. 2013; Westin et al. 2014). Similarly, increased clinical use of high-field MR, such as 7T (Chap. 10), offers improved signal-to-noise ratios which can lead to an augmented ability to resolve smaller metabolite resonances that were obscured when using lower-field strengths. Thus, there should continue to be concentrated efforts to biologically validate neuroimaging measures, or, at the very least, to understand better all possible biological influences on the imaging signal(s) so that the field can more accurately interpret findings.

Multi-level studies, or so-called "bench-to-bedside" approaches, will also be a valuable source of information for this venture. Unlike imaging studies which are still limited in their ability to establish causal relationships, preclinical models can offer ways to directly test biological schizophrenia hypotheses (Nestler and Hyman 2010). Thus compared to human studies, animal models offer very attractive advantages. First, animals can be maintained in a controlled environment, which minimizes various confounding factors. Second, anatomical variability of brain regions in animals is usually less than in humans. Third, reasonably large sample sizes can be obtained that have complete behavioral assessments, neuroimaging, and optimal brain tissue preparation within a short period of time. Integrating findings from the bench will also help in the development of biological targets of interest that could be developed into novel imaging measures in the future.

22.4 A Look Toward the Future

In the past decades, neuroimaging approaches have revolutionized our understanding of the biological factors that are contributing to psychiatric illness, particularly schizophrenia. Across imaging modalities, there have been significant discoveries that have provided promising leads, yet despite the wealth of knowledge that has been generated by the schizophrenia neuroimaging community, the etiology of this illness remains unclear. The lack of reliable "biomarkers of schizophrenia" is an acknowledged short-coming in the field that many are very passionate to address. In this chapter, we have identified several conceptual and methodological challenges that we believe are hindering progress. We then propose several approaches that will likely be most effective in resolving these hinderances so that we can move closer to understanding the pathophysiological mechanisms underlying of schizophrenia.

The conceptual changes proposed in this chapter focus predominantly on the way schizo-

phrenia, as an illness, should be viewed in a research setting moving forward. In many ways, imaging approaches have taken a "reductionist" view of schizophrenia by attempting to study various facets of an intricate biological system in isolation. This contradicts the phenomenological definitions of schizophrenia utilized in a psychiatric care setting, which are based upon observations of behavioral phenotypes, such as hallucinations, lack of affect, or cognitive deficits, to name a few. These behaviors are likely the manifestation of an assemblage of neurobiological mechanisms arising from a coordinated set of brain regions. And yet, the field has predominantly attempted to study these complex behaviors with unimodal or unidimensional study designs. Still, neuroimaging methodologies have proven to be critical in the identification of measurable phenotypes that could be useful as future "biomarkers of schizophrenia." We believe, however, that our progress here will continue to be hampered unless conceptual and methodological changes are made in the way in which we approach the study of this illness.

The proposed methodological changes discussed in this chapter highlight the need for cross-modality integration, complementary analysis pipelines, increased biological specificity of imaging measures, validation, and continued innovation. While the underlying principles of many neuroimaging techniques have remained the same, the face of neuroimaging is constantly changing. Intricately tied to physics, computer science, engineering, and mathematics, clinical neuroimaging has reaped the benefits of the tremendous synergy generated from discoveries within each of these fields. In fact, many of the hypotheses discussed above regarding schizophrenia would not have been testable in humans had it not been for the advent of neuroimaging. In this chapter we highlighted the need for the concerted efforts of both large-scale data analyses and smaller, patient-centered studies. The complementary nature of these two approaches will ensure that we focus on methodologically rigorous approaches without losing sight of the people who are afflicted with this illness. Also, the adoption of novel imaging methods with biologically validated measures will be key to providing a road map for asking more detailed questions about the underlying etiology of schizophrenia illness.

In conclusion, we propose a more holistic and integrative approach to the study of schizophrenia, in which the interactions between multiple systems be considered. More importantly, we believe that utilizing this holistic approach over the course of the lifespan will be critical to the identification of biological constructs that will be most effective for use in novel treatment paradigms. Finally, we believe that the identification of more biologically-based, objective markers of illness will be critical to more precisely diagnosing, treating, and monitoring individual patients in psychiatric care environments. Movement away from the present reliance on a classification system characterized by self-report and subjective observations will not only improve the research community's ability to parse the biological natures of a spectrum of illnesses, but will also likely lead to better outcomes for those being treated. Imaging will be central to this process not only because of its unparalleled ability to interrogate the brain *in vivo* but because of the unwavering dedication and creativity of the researchers who choose to work in this field and the altruism demonstrated by the patients who volunteer their time to make all of this work possible.

Summary

- Neuroimaging approaches have revolutionized our understanding of the biological factors that are contributing to psychiatric illness, particularly schizophrenia.
- The lack of reliable "biomarkers of schizophrenia" is an acknowledged short-coming of the field. In this chapter, we identify several hindrances within the schizophrenia neuroimaging field and we then propose conceptual and methodological changes that would allow us to make progress toward the

identification of clinically-relevant imaging-based biomarkers.

- The conceptual changes proposed in this chapter focus primarily upon the way schizophrenia, as an illness, should be reconceptualized in a research setting moving forward. We also discuss the need to: (1) focus on reconciling the multiple hypotheses within the field of schizophrenia, (2) recognize that schizophrenia illness trajectories are important components of the illness, and (3) move away from the use of phenomenological, as opposed to biological, classification paradigms.
- The methodological changes discussed in this chapter also highlight the increased need for cross-modality integration, complementary analysis pipelines (e.g., Big Data versus precision medicine), increased biological specificity of imaging measures, validation studies, and continued technical innovation.

References

Agerbo E, Sullivan PF, Vilhjálmsson BJ, Pedersen CB, Mors O, Borglum AD, et al. Polygenic risk score, parental socioeconomic status, family history of psychiatric disorders, and the risk for schizophrenia: a Danish population-based study and meta-analysis. JAMA Psychiatry. 2015;72(7):635–41.

Andreasen NC, Nopoulos P, Magnotta V, Pierson R, Ziebell S, Ho B-C. Progressive brain change in schizophrenia: a prospective longitudinal study of first-episode schizophrenia. Biol Psychiatry. 2011;70(7):672–9.

Assaf Y, Blumenfeld-Katzir T, Yovel Y, Basser PJ. AxCaliber: a method for measuring axon diameter distribution from diffusion MRI. Magn Reson Med. 2008;59(6):1347–54.

Bale TL, Baram TZ, Brown AS, Goldstein JM, Insel TR, McCarthy MM, et al. Early life programming and neurodevelopmental disorders. Biol Psychiatry. 2010;68(4):314–9.

Bennett MR. The prefrontal-limbic network in depression: a core pathology of synapse regression. Prog Neurobiol. 2011;93(4):457–67.

Bijanki KR, Hodis B, Magnotta VA, Zeien E, Andreasen NC. Effects of age on white matter integrity and negative symptoms in schizophrenia. Schizophr Res. 2015;161(1):29–35.

Bzdok D, Meyer-Lindenberg A. Machine learning for precision psychiatry: opportunities and challenges. Biol Psychiatry Cogn Neurosci Neuroimaging. 2018;3(3):223–30.

Cetin Karayumak S, Bouix S, Ning L, James A, Crow T, Shenton M, et al. Retrospective harmonization of multi-site diffusion MRI data acquired with different acquisition parameters. NeuroImage. 2019;184:180–200.

Chiappelli J, Postolache TT, Kochunov P, Rowland LM, Wijtenburg SA, Shukla DK, et al. Tryptophan metabolism and white matter integrity in schizophrenia. Neuropsychopharmacology. 2016;41(10):2587–95.

Do KQ, Cuenod M, Hensch TK. Targeting oxidative stress and aberrant critical period plasticity in the developmental trajectory to schizophrenia. Schizophr Bull. 2015;41(4):835–46. https://doi.org/10.1093/schbul/sbv065.

Döring A, Adalid V, Boesch C, Kreis R. Diffusion-weighted magnetic resonance spectroscopy boosted by simultaneously acquired water reference signals. Magn Reson Med. 2018;80(6):2326–38.

Drysdale AT, Grosenick L, Downar J, Dunlop K, Mansouri F, Meng Y, et al. Resting-state connectivity biomarkers define neurophysiological subtypes of depression. Nat Med. 2017;23(1):28–38.

Du F, Cooper AJ, Thida T, Shinn AK, Cohen BM, Ongür D. Myelin and axon abnormalities in schizophrenia measured with magnetic resonance imaging techniques. Biol Psychiatry. 2013;74(6):451–7.

Egerton A, Stone JM. The glutamate hypothesis of schizophrenia: neuroimaging and drug development. Curr Pharm Biotechnol. 2012;13(8):1500–12.

Ekstrom A. How and when the fMRI BOLD signal relates to underlying neural activity: the danger in dissociation. Brain Res Rev. 2010;62(2):233–44.

Feigenson KA, Kusnecov AW, Silverstein SM. Inflammation and the two-hit hypothesis of schizophrenia. Neurosci Biobehav Rev. 2014;38:72–93.

Friston K, Brown HR, Siemerkus J, Stephan KE. The dysconnection hypothesis (2016). Schizophr Res. 2016;176(2–3):83–94.

Gur RC, Calkins ME, Satterthwaite TD, Ruparel K, Bilker WB, Moore TM, et al. Neurocognitive growth charting in psychosis spectrum youths. JAMA Psychiatry. 2014;71(4):366–74.

Harrison PJ. Postmortem studies in schizophrenia. Dialogues Clin Neurosci. 2000;2(4):349–57.

Herzog H, Pietrzyk U, Shah NJ, Ziemons K. The current state, challenges and perspectives of MR-PET. Neuroimage. 2010;49(3):2072–82.

Howes O, McCutcheon R, Stone J. Glutamate and dopamine in schizophrenia: an update for the 21st century. J Psychopharmacol. 2015;29(2):97–115.

Insel TR. The NIMH Research Domain Criteria (RDoC) Project: precision medicine for psychiatry. Am J Psychiatry. 2014;171(4):395–7.

Isobe M, Miyata J, Hazama M, Fukuyama H, Murai T, Takahashi H. Multimodal neuroimaging as a window into the pathological physiology of schizophrenia: current trends and issues. Neurosci Res. 2016;102:29–38.

Jones DK, Knösche TR, Turner R. White matter integrity, fiber count, and other fallacies: the do"s and don"ts of diffusion MRI. NeuroImage. 2013;73:239–54.

Karlsgodt KH, Niendam TA, Bearden CE, Cannon TD. White matter integrity and prediction of social and role functioning in subjects at ultra-high risk for psychosis. Biol Psychiatry. 2009;66(6):562–9.

Kempton MJ, McGuire P. How can neuroimaging facilitate the diagnosis and stratification of patients with psychosis? Eur Neuropsychopharmacol. 2015;25(5):725–32.

Kempton MJ, Stahl D, Williams SCR, DeLisi LE. Progressive lateral ventricular enlargement in schizophrenia: a meta-analysis of longitudinal MRI studies. Schizophr Res. 2010;120(1–3):54–62.

Kochunov P, Hong LE. Neurodevelopmental and neurodegenerative models of schizophrenia: white matter at the center stage. Schizophr Bull. 2014;40(4):721–8.

Koutsouleris N, Davatzikos C, Borgwardt S, Gaser C, Bottlender R, Frodl T, et al. Accelerated brain aging in schizophrenia and beyond: a neuroanatomical marker of psychiatric disorders. Schizophrenia Bull. 2014;40(5):1140–53.

Logothetis NK. What we can do and what we cannot do with fMRI. Nature. 2008;453(7197):869–78.

Lüsebrink F, Wollrab A, Speck O. Cortical thickness determination of the human brain using high resolution 3T and 7T MRI data. NeuroImage. 2013;70:122–31.

Mandl R, Schnack HG, Zwiers MP, Kahn RS, Hulshoff Pol HE. Functional diffusion tensor imaging at 3 Tesla. Front Hum Neurosci. 2013;7:817.

Narayanaswami V, Dahl K, Bernard-Gauthier V, Josephson L, Cumming P, Vasdev N. Emerging PET radiotracers and targets for imaging of neuroinflammation in neurodegenerative diseases: outlook beyond TSPO. Mol Imaging. 2018;17(7203):1536012118792317.

Nestler EJ, Hyman SE. Animal models of neuropsychiatric disorders. Nat Neurosci. 2010;13(10):1161–9.

Oribe N, Hirano Y, Kanba S, Del Re EC, Seidman L, Mesholam-Gately R, et al. Progressive reduction of visual P300 amplitude in patients with first-episode schizophrenia: an ERP study. Schizophr Bull. 2015;41(2):460–70.

Pasternak O, Kubicki M, Shenton ME. In vivo imaging of neuroinflammation in schizophrenia. Schizophr Res. 2016;173(3):200–12.

Pettersson-Yeo W, Allen P, Benetti S, McGuire P, Mechelli A. Dysconnectivity in schizophrenia: where are we now? Neurosci Biobehav Rev. 2011;35(5):1110–24.

Rapoport JL, Giedd JN, Gogtay N. Neurodevelopmental model of schizophrenia: update 2012. Mol Psychiatry. 2012;17(12):1228–38.

Reis Marques T, Taylor H, Chaddock C, Dell'Acqua F, Handley R, Reinders AA, et al. White matter integrity as a predictor of response to treatment in first episode psychosis. Brain. 2014;137(Pt 1):172–82.

Roalf DR, Nanga RPR, Rupert PE, Hariharan H, Quarmley M, Calkins ME, et al. Glutamate imaging (GluCEST) reveals lower brain GluCEST contrast in patients on the psychosis spectrum. Mol Psychiatry. 2017;22(9):1298–305.

Schultz CC, Fusar Poli P, Wagner G, Koch K, Schachtzabel C, Gruber O, et al. Multimodal functional and structural imaging investigations in psychosis research. Eur Arch Psychiatry Clin Neurosci. 2012;262(Suppl 2):S97–106.

Selemon LD, Goldman-Rakic PS. The reduced neuropil hypothesis: a circuit based model of schizophrenia. Biol Psychiatry. 1999;45(1):17–25.

Serretti A. The present and future of precision medicine in psychiatry: focus on clinical psychopharmacology of antidepressants. Clin Psychopharmacol Neurosci. 2018;16(1):1–6.

Shinohara RT, Oh J, Nair G, Calabresi PA, Davatzikos C, Doshi J, et al. Volumetric analysis from a harmonized multisite brain MRI study of a single subject with multiple sclerosis. Am J Neuroradiol. 2017;38(8):1501–9.

Sui J, Pearlson GD, Du Y, Yu Q, Jones TR, Chen J, et al. In search of multimodal neuroimaging biomarkers of cognitive deficits in schizophrenia. Biol Psychiatry. 2015;78(11):794–804.

Thompson PM, Stein JL, Medland SE, Hibar DP, Vasquez AA, Renteria ME, et al. The ENIGMA Consortium: large-scale collaborative analyses of neuroimaging and genetic data. Brain Imaging Behav. 2014;8(2):153–82.

Thompson PM, Andreassen OA, Arias-Vasquez A, Bearden CE, Boedhoe PS, Brouwer RM, et al. ENIGMA and the individual: predicting factors that affect the brain in 35 countries worldwide. NeuroImage. 2017;145(Pt B):389–408.

van Dellen E, Bohlken MM, Draaisma L, Tewarie PK, van Lutterveld R, Mandl R, et al. Structural brain network disturbances in the psychosis spectrum. Schizophr Bull. 2016;42(3):782–9.

Van Essen DC, Smith SM, Barch DM, Behrens TEJ, Yacoub E, Ugurbil K. The WU-Minn Human Connectome Project: an overview. NeuroImage. 2013;80:62–79.

Venkataraman A, Rathi Y, Kubicki M, Westin C, Golland P. Joint modeling of anatomical and functional connectivity for population studies. IEEE Trans Med Imaging. 2012;31(2):164–82.

Westin C-F, Knutsson H, Pasternak O, Szczepankiewicz F, Özarslan E, van Westen D, et al. Q-space trajectory imaging for multidimensional diffusion MRI of the human brain. NeuroImage. 2016;135:345–62.

Whitford TJ, Grieve SM, Farrow TFD, Gomes L, Brennan J, Harris AWF, et al. Progressive grey matter atrophy over the first 2-3 years of illness in first-episode schizophrenia: a tensor-based morphometry study. NeuroImage. 2006;32(2):511–9.

Woo C-W, Chang LJ, Lindquist MA, Wager TD. Building better biomarkers: brain models in translational neuroimaging. Nat Neurosci. 2017;20(3):365–77.

Yu M, Linn KA, Cook PA, Phillips ML, McInnis M, Fava M, et al. Statistical harmonization corrects site effects in functional connectivity measurements from multi-site fMRI data. Hum Brain Mapp. 2018;39(11):4213–27.